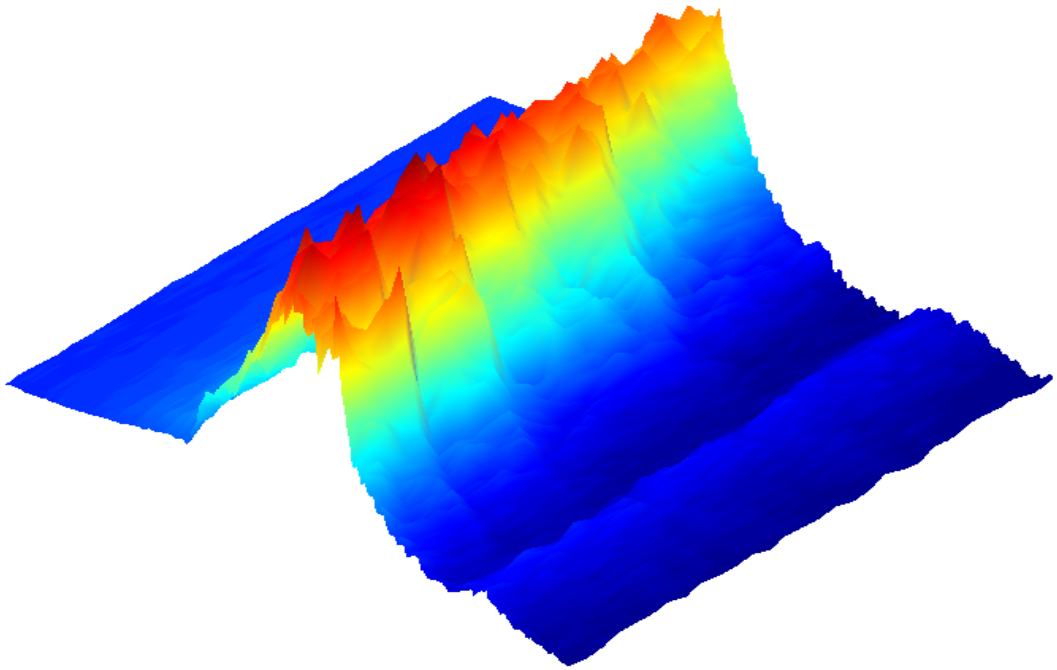
# RESPONSIBLE PACKAGING FOR A GLOBAL MARKET

**Proceedings of the 19th IAPRI World Conference on Packaging**
**Melbourne, Australia**
**15 – 18 June 2014**

Editors: M.A. Sek, V. Rouillard and S.W. Bigger



hosted by Victoria University, Melbourne
under the auspices of
the International Association of Packaging Research Institutes

VICTORIA UNIVERSITY
MELBOURNE AUSTRALIA

iapri

# RESPONSIBLE PACKAGING FOR A GLOBAL MARKET

Proceedings of the 19th IAPRI World Conference on Packaging
Melbourne, Australia, 15 – 18 June 2014,

Editors:

M.A. Sek, V. Rouillard and S.W. Bigger
Victoria University, Melbourne, Australia

Published by:

Victoria University PO Box 14428 Melbourne
Victoria 8001, Australia
*www.vu.edu.au*

All rights reserved
© 2014 Victoria University, Melbourne, Australia

No part of this work may be reproduced,
stored in a retrieval system, or transmitted in
any form or by any means, electronic,
mechanical, photocopying, microfilming,
recording or otherwise without written
permission from the Publisher.

ISBN: 978-1-86272-699-4

**Cover picture**
3D spectrogram showing the evolution of damage in a paperboard container subjected to sustained random loads. The spectrogram is an example of research at Victoria University aimed at developing data analysis techniques for detecting progression of damage through monitoring small changes in the dynamic characteristics (Frequency Response Function) of packaging structures subjected to sustained random loading akin to those experienced during road transport.

# Contents

**ORGANISING COMMITTEE ..... vi**

**SCIENTIFIC COMMITTEE ..... vi**

**PREFACE ..... vii**

**ACTIVE & INTELLIGENT PACKAGING .....1**

Controlled Release of Mangiferin using Ethylene Vinyl Acetate Matrix for Antioxidant Packaging....3

Reduced Liquid Loss and Extended Shelf Life of Chicken Filets by the use of Carbon Dioxide Emitters and Modified Atmosphere Packaging .....4

Microwaveable Packaging for Heating and Crisping a Food Product.....14

Development of an Intelligent Packaging Device for the Monitoring of Ready to Eat Salad Spoilage .....23

Development and Properties of High Density Polyethylene (HDPE) and Ethylene-Vinyl Acetate Copolymer (EVA) Blend Antioxidant Active Packaging Films Containing Quercetin .....30

Nanoiron Based Composite Oxygen Scavengers.....40

Effect of Storage Conditions and Sulphur Compounds on the Activity of Palladium Based Oxygen Scavenging Films.....43

Possibility of Electric Devices and Devices with Drug Packaging in Medical and Health Care .....49

Effects of Active Packaging on the Physico-Chemical Properties of Fresh-Cut Cantaloupe (*Cucumis Melo* L. Var. *Glamour*) .....53

Release of Oregano Essential Oil and Green Tea Extract from Ethylene Vinyl Alcohol Copolymer Films .....60

Methodology to Evaluate the Performance of Active Ingredients as Oxygen Scavengers.....65

Developments in Antimicrobial Food Packaging Research.....72

Biodegradable Cross-Linked Gliadin Films with Antifungal Activity for Active Packaging of Bread .....80

Effect of Nano-Semiconductors and Sacrificial Electron Donors on Color Transition of a Novel UV-Activated Oxygen Bio-Indicator.....88

Effect of Photoinitiator and Binder Concentration on Color of Methylene Blue-Based Oxygen Indicator .....98

**DISTRIBUTION PACKAGING.....107**

Issues with Combining Road Elevation Spectral Models and Vehicle Vibration Response to Estimate Vehicle Dynamic Characteristics.....109

Reduced-Order Modeling of the Linear Vibration Response of Expanded Polymer Cushion Material .....110

Estimation of the Dynamic Properties of Nonlinear Packaging Materials Using an Optimised Reverse Multiple Input/single Output Based Approach ..... 111

Future Demands in Distribution Dynamics Research ..... 112

The Application of Computational Methods to the Analysis of Unitized Load Performance ..... 118

Vibration Transmissibility of Packaging in Three-Substructures Coupled Product Transport System ..... 132

Measurement and Analysis of Vibration Levels in 2 and 3 Wheel Delivery Vehicles in South East Asia ..... 144

New Standardized Package System for Imported Fresh Mangos to the United States from Mexico and Guatemala ..... 145

An Introduction to Next-Generation Loggers for Measuring Distribution Hazards on the Product and Package ..... 153

Indirect Inverse Sub-structuring Theory for Coupling Dynamic Stiffness Identification of Complex Interface between Packaged Product and Vehicle Transport System ..... 165

Carton Clamp Test Methodologies and the Effects on Load Containment and Retention ..... 166

Combination Cushioning Pad Design and Drop Simulation ..... 167

Damage to Carton Board Packages Subjected to Concentrated Loads ..... 172

Evaluation Method of Abrasion Damage on Corrugated Board ..... 183

Comparison of Two Vibration Recording Methods Depending on the Data Recorder Position ..... 203

Transport Simulation Testing for Stretch Wrap Film Optimisation and Palletised Load Safety (DUOPLAST Business Case) ..... 213

Vibration Performance for Biocushion Materials ..... 231

How to Choose the Resistance to Vertical Crushing of Stacked Cardboard Box Suitable for your Trip. ..... 237

Influence of Corrugated Cardboard Corners in Shock Damping: Case of a 100% Cardboard Packaging. ..... 243

Impact of Liquid Nitrogen Dosing on Application and Removal Torque of Wine Bottle ..... 249

**LOGISTICS & SUPPLY CHAIN ..... 255**

The Sacks of Rome? ..... 257

RFID Tags Characterization by Studying Their Backscattering Response ..... 258

Elastic Modulus of Corrugating Medium under Different Temperature and Relative Humidity ..... 263

A Method Review and a Case Study of Packaging Design Difference of Automobile KD Parts and After-Sale Parts with an Application on Transport ..... 271

The Status of Wood Pallet Repair Operations in the United States: A Survey Study ..... 284

**MEDICAL, COSMETICS & PHARMACEUTICAL PACKAGING.....293**

Microbiological Stability of Shampoo Stored in Polymeric Packaging Modified with Nanosilver ...295

Evaluation of Opening Status of PTPs with Three Element from Push to Go Out from Package .....301

**PACKAGING DESIGN, ERGONOMICS & HUMAN FACTORS.....307**

The Study of Uncertainty Elements Related to Heat Seal Strength by Comparison of Standard Testing Methods .....309

An Empirical Study for Exploring Reusable Packaging Attributes.....321

Relationship between Peel Angle and Peel Force in Peelable Semi-Rigid Packaging Comprising Tyvek® and PETG .....322

A Review of Thermoplastic Composites Vapour Permeability Models: Applicability for Barrier Dispersion Coatings.....323

The Functional Analysis Methodology for Environmentally Conscious Packaging Design.....335

Easy Opening or a Lost 16% Sale.....347

Packaging for Personalized Food for Nutrition of Elderly Consumers Made using Rapid Manufacturing.....358

Attention Grabbing Power of Branded vs Unbranded Packaging .....368

The Design Development of Perforation Rule for Retail Ready Packaging.....380

Is Your Package Pro-LOHAS? – Findings of the Finnish LOHASPACK Study 2011-2014.....388

Material Identity in a Packaging Context .....396

Crumpling of Paper Sheet and Packaging .....404

**PACKAGING FOR FOOD & AGRICULTURE .....409**

Migration of Plasticizers from Paper and Board into Food Simulant Tenax and Olive Oil during Microwave Cooking .....411

The Effect of Packaging on Consumer Food Quality Perception in Quick-Service Restaurants .....424

Determination of Ti in Nano/Submicro-$TiO_2$-Plastic Composite Food Packaging by Microwave Digestion and Inductively Coupled Plasma Atomic Emission Spectrometry or Inductively Coupled Plasma Mass Spectrometry .....425

Determination of Four Types of Hazardous Chemicals in Food Contact Materials by UHPLC-MS/MS .....434

Modelling of Migration from Printing Inks on Paper Packaging and its Verification.....446

Glucoamylase Time-Temperature Indicators Based on Fat Oxidation of Chilled Pork .....447

The Flexible Packaging Line – PickNPack.....455

Sulfide Black in Canned Meat .....467

Packaging for Controlling Texture of Frozen Microwaveable Sandwiches .....476

Effect of Propolis Extract on Physical and Antioxidant Properties of Chitosan Film .....485

Effects of In-Package Atmosphere on Temporal Changes in the Fractionation of Oxygen Isotopes during Respiration in Tomatoes ..... 490

An Innovative Corrugated Shipper to Improve Palletized Load Airflow for Fresh Produce ..... 496

Development of a Freshness Indicator for Monitoring Chicken Meat Freshness ..... 506

If at First You Don't Succeed: Older Consumers and Hospital Food & Beverage Packaging – a Matter of Try, Try and Try Again! ..... 512

Equilibrium Modified Atmosphere Packaging for Preserving Quality and Extending Shelf-Life of Longan ..... 524

Development of Time-Temperature Indicator Based on Polydiacetylene/Silica Nanocomposite for Monitoring Fresh Skinless Chicken Breast Quality ..... 533

Response Modelling of Time-Temperature Indicator Based on Polydiacetylene/Silica Nanocomposite ..... 539

Development of a Biodegradable Coating based on Seaweed Extracts and Starch for Food Packaging Applications. ..... 545

**PACKAGING MATERIALS ..... 553**

Evaluation of Static and Dynamic Cushioning Properties of Polyethylene Foam for Determining its Cushion Curves ..... 555

Outdoor Weathering of HDPE Containers Filled with Nitric Acid ..... 556

The Effect of a Vibration Force Field on the Crystallization and Barrier Properties of Polymer Nanocomposites ..... 561

The Effect of Heating Speed on the Expression of Heat Seal Strength in Plastics Packaging Materials. ..... 572

Maximum Gauge Pressure in Dangerous Goods Packaging under Normal Conditions of Carriage - Comparison of Direct Measurement and Calculations ..... 573

Preparation and Characterization of Low Methoxyl Pectin/Carboxymethyl Cellulose-Based MMT Composite Films ..... 574

New Bio-Based Plastics, from a Non-Edible Plant Oil Side-Stream, for Film Extrusion ..... 586

Degradation of Steel Packages in Tropical Environments – Results after 10 Years of Discarding ..... 591

Characteristics of Poly(lactic Acid) Composites Reinforced with Natural Fibres ..... 603

Properties of Corrugated Liner Made from Musa Sapientum Linn Banana Pulp and Recycled Kraft Pulp ..... 609

Effect of Compatibilizer on Physical and Rheological Properties of PLLA/PPC Binary Blends ..... 615

Influence of Reprocessing on Mechanical Properties of SAN Copolymers in Injection Moulding ..... 625

Development of Biodegradable-Starch-Based Cushions with High Shock Absorption ..... 628

Evaluating the Dynamic Characteristics of Starch Based Loose-Fill ..... 631

Designing Polypropylene Lidding Film with Combined Peelable and Antifogging Properties for Food Packaging ..... 640

Microperforation of Three Common Plastic Films by Laser and their Enhanced Oxygen Transmission for Fresh Produce Packaging ..... 648

**PACKAGING PRINTING & GRAPHICS ..... 649**

Qualitative Analysis of Coverage Value Transfer in Modern Packaging Printing Workflow ..... 651

A Method for General Printing Anti-Counterfeiting by Moiré Patterns ..... 661

The Study on Symbol Contrast of Inks and Paper Liners for Barcode Printing on Corrugated Box . 667

**PACKAGING SUSTAINABILITY ..... 675**

Implementing Packaging Sustainability Metrics in a Developing Economy ..... 677

ULab© Cloud Testing System for Flexible Plastic Packages ..... 687

Green Fibre Bottles ..... 696

Plasma Enhanced Surfaces for Sustainable Fiber Based Packaging ..... 704

The Greenhouse Gas Profile of a "Hungry Planet"; Quantifying the Impacts of the Weekly Food Purchases Including Associated Packaging and Food Waste of Three Families ..... 709

Film Performance of Poly(lactic Acid) Blends for Packaging Applications ..... 721

Trends and Drivers Influencing Papermaking and its Products Towards the Future ..... 728

**AUTHOR INDEX ..... 739**

## ORGANISING COMMITTEE

**Chairs**

A/Professor Michael Sek, Engineered Packaging and Distribution Research Group, Victoria University
A/Professor Vincent Rouillard, Engineered Packaging and Distribution Research Group, Victoria University
Professor Stephen Bigger, College of Engineering and Science, Victoria University

**Committee Members**

Dr Matthew Lamb, Engineered Packaging and Distribution Research Group, Victoria University
Dr Anthony Parker, Engineered Packaging and Distribution Research Group, Victoria University
Dr Marlene Cran, Engineered Packaging and Distribution Research Group, Victoria University
A/Professor Karli Verghese, Program Director, Sustainable Products, RMIT University
Gavin Williams, CEO, Packaging Council of Australia
Stan Moore, CEO, Australian Packaging Covenant
Adele Elice-Invaso, Executive Director, Australasian Pulp and Paper Industry Technical Association (APPITA)
Professor Gil Garnier, Australian Paper and Pulp Institute, Monash University

**Conference Secretariat**

Luba Schnitzer, Victoria University
Sue Davies, Victoria University

**Conference Ambassador**

Dr Mervyn Minett

## SCIENTIFIC COMMITTEE

| | | |
|---|---|---|
| Rafael Auras | Michigan State University | USA |
| Greg Batt | Clemson University, NC | USA |
| Carlos Bernad | Instituto Tecnologico de Aragon | Spain |
| Stephen Bigger | Victoria University | Australia |
| Wanee Chinsirikul | National Metal and materials Technology Centre | Thailand |
| Vanee Chonkenchob | Kasetsart University | Thailand |
| Marlene Cran | Victoria University | Australia |
| Damian Erre | Reims University | France |
| Mikael Gallstedt | Innventia | Sweden |
| Manuel Garcia-Romeu | ITENE | Spain |
| Rafael Gavara | IATA-CSIC | Spain |
| Changfeng Ge | Rochester Institute of Technology (RIT) | USA |
| Thomas Goedecke | BAM Federal Institute for Materials Research and Testing | Germany |
| Dan Goodwin | Rochester Institute of Technology (RIT) | USA |
| Qian Jing | Jiangnan University | China |
| Kennert Johansson | Innventia AB | Sweden |
| Robert Kimmel | Clemson University | USA |
| Takamasa Nakajima | Technology Research Institute, Osaka | Japan |
| Cristina Nerin | University of Zaragoza | Spain |
| Soren Ostergaard | Danish Technological Institute (DTI) | Denmark |
| Roman Popil | Georgia Tech | USA |
| Vincent Rouillard | Victoria University | Australia |
| Katsuhito Saito | Kobe University | Japan |
| Panuwat Suppakul | Kasetsart University | Thailand |
| Michael Sek | Victoria University (Chair) | Australia |
| Jay Singh | Cal Poly State University | USA |
| Thomas Trost | Innventia AB | Sweden |
| Diane Twede | Michigan State University | USA |
| Mika Vaha-Nissi | VTT, Technical Research Centre | Finland |
| Karli Verghese | RMIT University | Australia |
| Jun Wang | Jiangnan University | China |
| Fredrik Wikstrom | Karlstad University | Sweden |
| Yves Wyser | Nestle Research Centre | Switzerland |
| Zhi-Wei Wang | Jinan University | China |

# PREFACE

The IAPRI conferences and symposia have become an important and prestigious international forum where leading researchers and global experts gather to share their research findings in the field of packaging and distribution. The International Association of Packaging Research Institutes is the global peak body for packaging research and is responsible for fostering packaging research and for promoting packaging as a global science. The IAPRI was established in 1971 and has evolved into a unique global network which allows organisations to exchange research ideas and results, develop new research initiatives and engage in collaborative work. Today the IAPRI consists of 86 member institutes, universities and corporations across 30 countries. The IAPRI conferences are held biennially and are open to general participation, while the IAPRI symposia, held in the years between conferences, are restricted to researchers from member organisations only. Membership of the IAPRI offers a unique access to the packaging research community. Since 2012 the IAPRI offers competitive travel scholarships to foster quality among early career researchers. It is an excellent opportunity for research students from the IAPRI member organisations to gain international experience by being able to working at another member organisation.

This 19th IAPRI World Conference on Packaging 2014 coincides with the 25th anniversary of Victoria University's involvement in multidisciplinary packaging research initiated in 1989 with the establishment of the Transportation Simulation and Packaging Dynamics Laboratory, and the Packaging Research and Training Centre. Since then the University's research capabilities in packaging have expanded to include expertise in environmental shock and vibration and distribution dynamics, material characterisation, optimisation of protective packaging, product and fragility analysis, polymer and analytical chemistry, biodegradable polymers, and modified atmosphere antimicrobial active/intelligent food packaging.

This is the second occasion that an IAPRI conference has been hosted by Victoria University. VicUni was the host of the 10th IAPRI Conference in 1997.

Abstracts of submitted papers have been reviewed by the International Scientific Committee to judge their suitability. These proceedings contain 84 full papers as well as 15 abstracts of papers which have been subjected to independent peer review process, and are to be published in Wiley's Journal of Packaging Technology and Science. All these papers, presented over three days in three parallel and one poster sessions, involved 278 authors and co-authors who are associated with 109 organisations from 25 countries on five continents.

In these Proceedings the papers are placed in submission order and are grouped within nine sections:

1. Active & intelligent packaging
2. Distribution packaging
3. Logistics & supply chain
4. Medical, cosmetics & pharmaceutical packaging
5. Packaging design, ergonomics & human factors
6. Packaging for food & agriculture
7. Packaging materials
8. Packaging printing & graphics
9. Packaging sustainability

On behalf of the Organising Committee we thank all participants for their involvement.

M.A. Sek, V. Rouillard and S.W. Bigger
Chairs, IAPRI-2014 Organising Committee
June 2014

# ACTIVE & INTELLIGENT PACKAGING

# Controlled Release of Mangiferin using Ethylene Vinyl Acetate Matrix for Antioxidant Packaging[#]

**Vanee Chonhenchob[1*], Rungkan Boonnattakorn[1], Muhammad Siddiq[2] and Sher Paul Singh[3]**

[1] *Department of Packaging and Materials Technology, Kasetsart University, Thailand*
[2] *Department of Food Science and Human Nutrition, Michigan State University, United States*
[3] *Packaging Forensic Associates Inc, United States*

[*]*Corresponding author. Email: vanee.c@ku.ac.th*

**Abstract:** This study investigated the use of ethylene vinyl acetate (EVA) matrix in controlled release packaging. Mangiferin, a rich source of antioxidant activity, was incorporated into the EVA matrix with different vinyl acetate (VA) contents. Mangiferin release rate increased with increasing VA content (decreasing crystallinity). Linear relationship between mangiferin release rate and VA content was observed in the range of 18% to 40% VA. The diffusion coefficients of mangiferin released from the EVA matrices containing 12, 18, 25 and 40% VA were 0.005, 0.079, 0.281 and 5.87 ($\times 10^{-14}$ $m^2.s^{-1}$), respectively. Partition coefficients decreased with increasing VA content. The enhancement factors of 22.32-fold and 7.22-fold were observed in the 12 and 18% VA matrices, respectively when using triethyl citrate as a plasticizer. EVA film containing 40% VA had the highest antioxidant activity (81.90 % RSC) since the highest amount of mangiferin was released in the food simulant (84.66 $\mu g.mL^{-1}$). Plasticizer and mangiferin had no significant effect ($p > 0.05$) on mechanical and barrier properties of the films. The results of this study demonstrated that EVA matrices with different degree of crystallinity, could potentially be used to control mangiferin release rate for antioxidant packaging.

Keywords: active packaging; mangiferin; antioxidant; controlled release; EVA matrix; release kinetic.

[#] This is the abstract of a peer-reviewed paper to appear in a Special Edition of Wiley's journal *Packaging Technology and Science* dedicated to the 19th IAPRI World Conference on Packaging 2014 hosted by Victoria University, Melbourne, Australia.

# Reduced liquid loss and extended shelf life of chicken filets by use of Modified atmosphere and active packaging

**Marit Kvalvåg Pettersen[1*], Oddvin Sørheim[1], Marie H. Moen[2] and Askild L. Holck[1]**

[1] *Nofima- Norwegian Institute of Food, Fisheries and Aquaculture Research, Norway*

[2] *Nortura SA, Norway*

[*] *Corresponding author. Email: marit.kvalvag.pettersen@nofima.no*

**Abstract:** The consumption of poultry meat has increased over the last decades in many countries, and is nowadays a very popular food commodity around the world. Fresh chicken meat is a highly perishable product due to its high content of nutrients and water.

Modified atmosphere packaging (MAP) is widely used for extending shelf life of fresh meat. High concentrations of $CO_2$ in the headspace of meat packages inhibit or reduce microbial growth. Active packaging by adding $CO_2$ emitter sachets to packages of meat is an alternative to traditional MAP.

The purpose of the study was to investigate the effects of different $CO_2$ concentrations on the shelf-life of chicken filets, at 4 ºC storage. The inhibition of microbial growth was proportional the $CO_2$ concentration. Storage in 100 % $CO_2$ resulted in a microbial shelf life of approximately 25 days that is a 6-7 days extension compared to 60 % $CO_2$. The dominating species were *Carnobacterium divergens*, *Carnobacterium* sp. and *Lactococcus* sp. Drip loss was highly affected by the gas atmosphere in the packages. $CO_2$ dissolved in the meat during storage, and storage in pure $CO_2$ caused collapse of the packages. The resulting so called vacuum –effect or squeeze of the packages lead to a severe increase in liquid loss. The liquid loss was reduced profoundly by using a $CO_2$ emitting sachet in the packages. Addition of $CO_2$ emitters can easily be implemented at industrial packaging lines without reductions in production efficiency.

Keywords: Active packaging, Carbon dioxide emitter, Chicken breast, Drip loss, Extended shelf- life, Modified atmosphere packaging

# 1 Introduction

During the last decades the consumption of poultry meat has increased in many countries and is a very popular food commodity [1, 2]. Poultry meat is a perishable food due to its high content of nutrients and water and undergoes numerous changes during storage. Product shelf-life is controlled by factors like product characteristics and initial quality, as well as storage and distribution conditions. Deterioration is mainly due to bacterial growth and off-odour [3] oxidative damage and enzymatic activity, leading to discoloration, nutrient loss, texture changes and pathogenicity. In addition to external parameters like packaging material, storage atmosphere and storage temperature, internal factors like type of chicken cut, presence of skin and the initial bacterial load affect the development of unwanted odorous compounds [4-5] With the increasing demand for high quality, convenience, safety and fresh appearance there is a great interest in technologies aimed at extending shelf-life of meat [6].

Modified atmosphere packaging (MAP) is often used to prolong the microbiological shelf life of foods [4, 7, 8]. Introduction of MAP of meat has led to reduced product losses and hence to diminished environmental impact of meat production and consumption [9]. The gas-mixture commonly consists of carbon dioxide ($CO_2$), nitrogen ($N_2$) and oxygen ($O_2$). The antimicrobial effect of $CO_2$ in modified atmosphere packaging (MAP) of fish and meat is well known. Microbial sensitivity to $CO_2$ varies substantially between different microorganisms. Many Gram-negative organisms such as Pseudomonas and *Enterobacteriaceae* are inhibited in their growth by $CO_2$, while many Gram-positive organisms such as lactic acid bacteria and *Brochothrix*, are less affected by the presence of $CO_2$ [5,10]. Storage in modified atmosphere with high $N_2$ (70 % $N_2$, 30 % $CO_2$) has been reported to resulting in lactic acid bacteria being the dominant flora after 15 days of storage, with some growth of *Enterobacteriaceae* and *Pseudomonas* [11]. *(24)*. In contrast, the dominant flora of broiler products stored at 6 ºC in high $CO_2$ atmosphere (80 % $CO_2$, 20 % $N_2$) were *Carnobacterium maltaromaticum* and *C. divergens* together with different *Lactococcus* species [12].

The absorption of $CO_2$ and the microbial inhibition increases with increased $CO_2$ concentration in the head space [13-15]. Thus, relative high gas volume to product volume ratio is needed in order to obtain optimal antimicrobial effect of $CO_2$. The optimal gas/product ratio can be reduced and compensated by the use of $CO_2$-emitters due to their production of $CO_2$ after sealing. $CO_2$ emitters have been tested on salmon filet packaging [16] and cod packaging[17], resulting in similar or longer microbiological shelf life than vacuum packaging and reduced gas volume to product volume ratio compared to optimal MAP.

Commercial chicken filets in Norway are packaged in 70 % $CO_2$, 30 % $N_2$, stored at 4 ºC and have a shelf-life of approximately 19 days. Chicken filets are prone to drip loss during storage, and drip loss may give undesirable packages with a pool of fluid surrounding the meat. This also affects the economic value of the packages. The aim of the study was to investigate the shelf-life of MAP chicken filets under different $CO_2$ concentrations. In particular, we wanted to see if the use of 100% $CO_2$ and the use of active packaging ($CO_2$-emitter) would lead to extended shelf-life.

# 2 Materials and methods

## 2.1 Packaging Methods and Storage Conditions

Fresh chicken breast fillets were obtained from a commercial processing plant (Nortura, Hærland, Norway). The filets were mixed to achieve an equal number of CFU/$cm^2$ on the surface. The chicken filets were stored in thermoformed trays using a Multivac R145 thermoforming machine (Multivac, Wolfertschwenden, Germany), The base web consisted of amorphous-polyethylene terephthalate/polyethylene (APET/PE) (Wipak, Nastola, Finland)) with oxygen transmission rate (OTR) 10 $cm^3/m^2$/24 h at 23 ºC, 50 % RH, and with a top web consisting of polyethylene terephthalate/polyethylene/ethylene vinyl alcohol/ polyethylene (PET/PE/EVOH/PE) (Wipak, Nastola, Finland) with OTR 5 $cm^3/m^2$/24 h at 23 ºC, 50 % RH.

Packaging was performed at Nofima on the day of slaughtering. The modified atmosphere consisted of 0, 30, 60 and 100% $CO_2$ supplemented with N2, and one sample was added a $CO_2$-emitter. Two filets (total 295 - 310 g) were placed in each package resulting in initial gas volume to product volume ratio of 2.5. In addition, a liquid absorber, Boundi 70 ml (Bjarne Johnsen AS, Bergen, Norway) was used in each package except where the $CO_2$ emitter was used. The $CO_2$ emitters were prepared by adding $NaHCO_3$ and citric acid to a liquid absorber (Ny-Tek, Tønsberg, Norway). The added amount of the $CO_2$ emitter ingredients in order to obtain appropriate $CO_2$ production were based on the results from earlier studies with $CO_2$ [16, 18]. The samples were stored at 4ºC for 8, 14, 20, 26 and 30 days. Six packages were analysed for each series and sampling day.

## 2.2 Analyses

**Gas composition, pH and drip loss**
The packages were analyzed for gas composition and drip loss. The $CO_2$ and $O_2$ level in the headspace were monitored directly after packaging and at each sampling time by a CheckMate 9900 $O_2/CO_2$ analyser (PBI Dansensor, Ringsted, Denmark). Samples were analysed for pH directly in the meat with an Ingold Xerolyt gel electrode (Mettler-Toledo A.G., Greifensee, Switzerland) on days 0 and 20, except for meat samples stored in 100 % $N_2$, which were measured at days 0 and 14. The drip loss from the samples was measured as the increased weight of the liquid absorber pads during storage. Results are given as % of initial muscle weight.

**Microbiology**
Microbiological analyses were performed on the chicken breasts fillets at the time of packaging and at each sampling time. Samples of 10 $cm^2$ and 1 cm thick were cut from the surface of each filet with a sterile scalpel, and diluted in 90 ml peptone water. Each sample was macerated in a stomacher for 1 min. Serial 10-fold dilutions of each stomacher bag were prepared, and plated on the following media directly or using a Whitley automatic spiral plater (Don Whitley Scientific Ltd., West Yorkshire, UK):

- For total anaerobic counts : plate count agar (PCA; Difco, Difco Laboratories, Detroit, MI, USA) (incubation temperature 30 ºC, 3 days, anaerobic incubation);
- Lactic acid bacteria: de Man, Sharpe and Rogosa agar (MRS; Oxoid, Unipath Ltd., Basingstoke, Hampshire, UK,) adjusted to pH 5.7 (20 ºC, 3 days, anaerobic incubation);
- *Brochothrix thermosphacta:* streptomycin thallous acetate actidione agar base (STAA; CM 881 with selective supplement SR 151; Oxoid, Hampshire, UK) (25 ºC, 2 days, aerobic incubation);
- Pseudomonads : pseudomonads agar base (CFC; CM 559 with selective supplement SR 103; Oxoid) (20 ºC, 2 days, aerobic incubation);
- *Enterobacteriaceae:* Violet Red Bile Glucose Agar (VRBGA, Oxoid, Hampshire, UK) (37 ºC, 1 day, semi-aerobic conditions, cells embedded in agar with sterile overlay).

Microbial counts were expressed as colony forming units (CFU) per $cm^2$. For each sampling day and each gas mixture 6 parallel samples from different packages were used.
DNA was isolated from single colonies and 16S rDNA was amplified by PCR and sequenced by a 3130xl Genetic Analyzer (Applied Biosystems). Sequences were compared with those found in the RDP database (Ribosomal database project, release 10 update 32) [19].

**Statistics** Calculations were done in Excel 2010. Statistical analyses were carried out using SAS ver. 9.4 (SAS Institute, Cary, North Carolina, USA) and SYSTAT ver. 12 (Systat Software Inc., San Jose, Calif., USA) and Minitab ver. 16.1.1 Statistical software (Minitab Inc., State College, PA, USA).

# 3 Results and discussions

## 3.1 Gas Composition

The shelf-life of products depends on several factors such as the gas composition in the modified atmosphere, the amount of headspace, the storage temperature and the type and amount of microorganisms on the meat on the onset of storage, pH of the meat and use of additives [20-21]. The $CO_2$ and $O_2$ level in the headspace were monitored at each sampling time. Monitoring gas composition in modified atmosphere storage experiments of meat is important in order to detect defect packages /leakage in addition to the evaluation of pigment oxidation and microbial growth.

The average $O_2$ concentration in all packages was 0.17 % (range 0.05 – 0.48 %) immediately after packaging. From day 8 and onwards no $O_2$ was found in the packages. The changes in $CO_2$ during the storage are presented in Figure 1. The $CO_2$ content in the packages had as expected different profile due to both original gas composition and the use of $CO_2$-emitter. Some $CO_2$ is produced during storage as is evident from samples packed in 100 % $N_2$. The initial reduction of $CO_2$ for samples packaged in both 30 and 60 % $CO_2$ was attributed to the $CO_2$ absorption by the meat [8, 21-23].

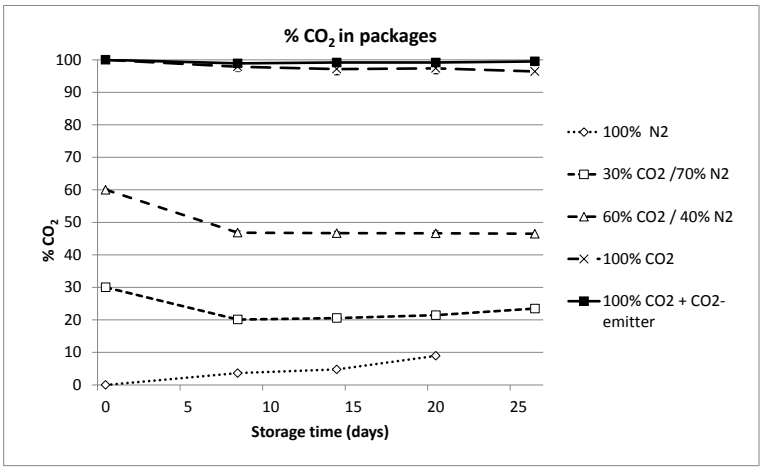



**Figure 1**: Changes in concentration of $CO_2$ (%) during storage of chicken filets stored in different initial packaging atmospheres at 4°C.

## 3.2 pH and Drip Loss

Increasing the $CO_2$ concentration in the packages leads to a slight decrease in pH of the meat. For example chicken filets stored at 100 % $N_2$ showed a pH of 6.27 while samples stored at 100 % $CO_2$ were 5.88-6.08 on day 0 (Figure 2). During storage, the pH had a tendency to drop a little further, but still ending in the same range as samples stored at 60 - 100 % $CO_2$. Samples stored at 100 % $N_2$ had a markedly shorter shelf-life (see below) and pH was here measured at day 14 instead of day 20. For these samples no changes in pH were observed during storage and pH remained at around 6.27.

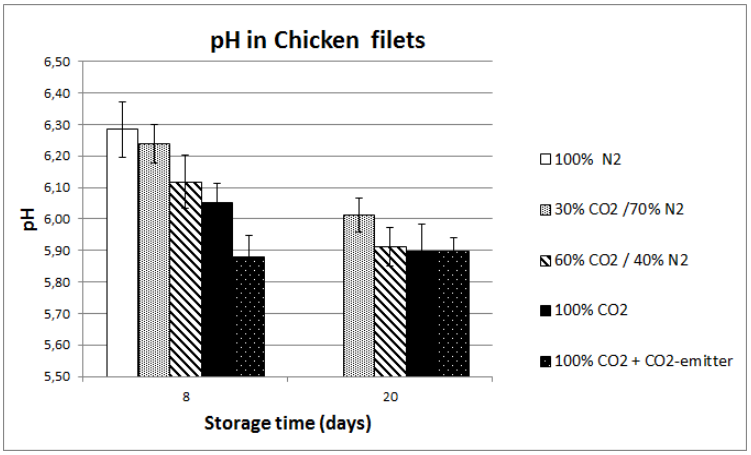



**Figure 2**: pH of the chicken filets stored for 8 and 20 days in different initial packaging atmospheres at 4°C.

The water binding abilities of meat is lowered as the pH of the meat drops. The pH drop during storage may be caused by a combination of production of lactic acid from the carnobacteria and by $CO_2$ reacting with water to form carbonic acid.

The gas composition had impact on appearance of the packages in addition to the drip loss. The problem related to use of high amounts of $CO_2$ in the headspace is that $CO_2$ is absorbed in the meat and causes collapse of the packages This absorption appears to induce a squeeze or suction on the meat which leads to a substantial increase in drip loss (Figure 3).When the chicken was stored in 100 % $CO_2$ the packages collapsed and appeared squeezed These packages showed a weight loss of around 7.3 %.The packaging series with 100 % $CO_2$ and $CO_2$ emitter, however, had no squeezed appearance In the samples with $CO_2$ emitter the drip loss was reduced to 2.5

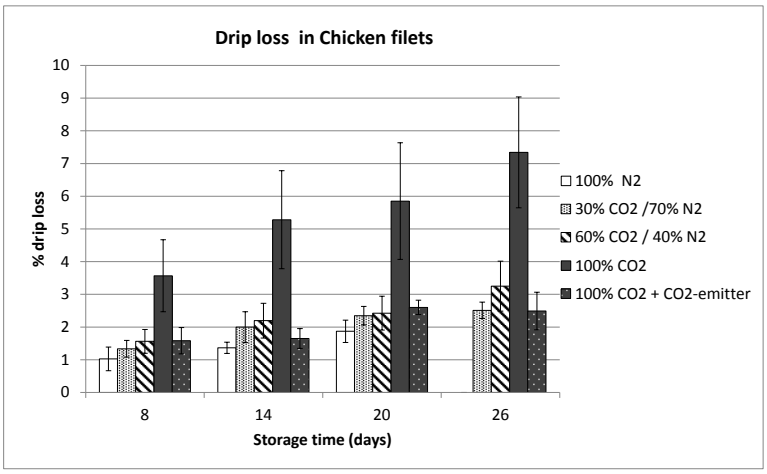



**Figure 3**: Drip loss in Chicken filets stored at 4°C in different initial gas compositions

Drip loss from chicken meat can have economical and sensory effects. Excessive loss can make the meat become dry upon cooking. Different effects on drip loss due to different gas composition have been reported in previous survey of studies on drip loss of meat stored under different percentages of $CO_2$ or vacuum. These studies have shown that $CO_2$ can increase, decrease or not change drip loss compared to vacuum, probably depending on packaging and storage conditions [24].

It has been suggested that one of the mechanisms for increased drip loss [25] could be due to the reduction of pH in meat exposed to $CO_2$. However, chicken stored in 60 % $CO_2$ showed the same pH and had a low drip loss in our study, thus slight reduction in pH of the meat by using 100 % $CO_2$ in the packages appeared not to be important for the drip loss.

Handling and pressure changes on the meat surface may be expected to increase drip losses [21]. In addition, the ratio of surface area to volume of the meat, and longitudinal, rather than transverse, cutting of muscle fibers will also have impact on the drip loss [21].

## 3.3 Bacterial Growth

Although spoilage is not always of microbial origin, microorganisms generally play an important role in this defect. The microbial spoilage point of a food has been defined as the time at which the activities of the microbes present in a product become offensively evident to the senses. As a general rule, meat acquires an offensive odor when the bacterial flora reaches about $10^7$ CFU/cm$^2$ of meat surface. When the numbers have reached $10^8$ CFU/cm$^2$, the meat surface becomes slimy [26-27]. In addition to microbial spoilage, oxidative damages may cause rancidity, off-odors, off-flavors and color defects. Oxidative damage is strongly reduced by removing oxygen from the headspace gas.

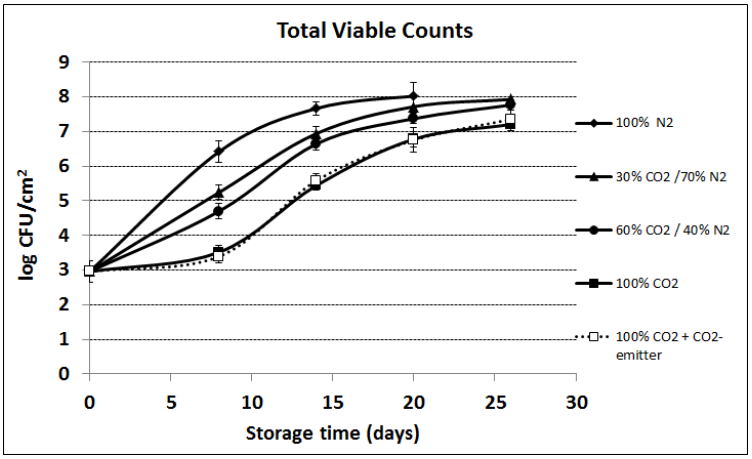



**Figure 4**: Bacterial growth of total viable counts of anaerobic colony forming units during storage of chicken filets packed in different gas compositions. The detection limit was 10 CFU/ cm$^2$.

The microbial growth was investigated by plating on PCA and growing bacteria anaerobically determine total anaerobic cell count (Figure 4)... Different microorganisms are selected on the meat depending on the composition of modified atmosphere used during storage. The growth rate of total viable counts was progressively reduced when the partial pressure of $CO_2$ in the gas increased. Most conspicuous was the growth retardation when increasing the $CO_2$ in the gas mixture from 60 % to 100 %. Relatively high level of bacteria, level of $10^7$ CFU/cm$^2$ was obtained 6 -7 days later when growing in 100 % $CO_2$, with or without $CO_2$ emitter compared to the 60 % $CO_2$ samples.

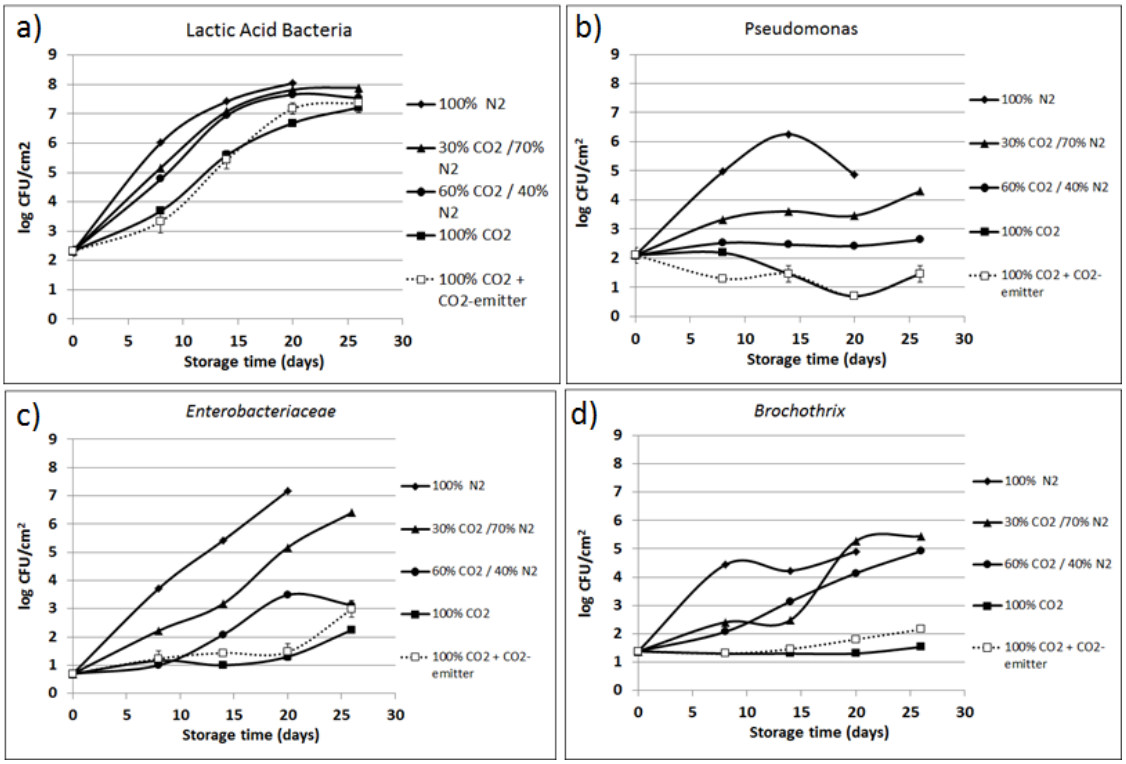



**Figure 5**: Bacterial growth on selective petri dishes of a) lactic acid bacteria, b) Pseudomonads, c) *Enterobacteriaceae* and d) *Brochothrix* during storage of chicken filets packed in different gas compositions. The detection limit was 10 CFU/ cm$^2$. For samples below the detection limit the CFU/cm$^2$ was arbitrarily set at 50 % of the detection limit

The same patterns as with PCA dishes were observed for counts of lactic acid bacteria, Pseudomonads, *Enterobacteriaceae* and *Brochothrix* sp., (Figure 5). , increasing concentrations of $CO_2$ increasingly retarded or totally inhibited growth, so that at 100 % $CO_2$ both CFU/ cm$^2$ counts from the *Brochothrix* sp., Pseudomonads, *Enterobacteriaceae* selective dishes remained very low. Also the onset of growth of lactic acid bacteria was delayed in the 100 % $CO_2$ samples, although the growth rate during the linear log phase appeared similar to those of the 30 % and 60 % $CO_2$ samples. When meat is stored without oxygen bacteria that can grow anaerobically and are only partly inhibited by high $CO_2$ concentrations have a selective advantage. Generally pseudomonads are inhibited when oxygen is removed, while *Enterobacteriaceae* and *B. thermospacta* may dominate in gas mixtures at around 50 % $CO_2$, 50 % $N_2$ [28]. Lactic acid bacteria will often dominate when using pure $CO_2$. Our results were in accordance with these general findings. The higher the $CO_2$ conc., the lower the growth rate of both *Brochothrix*, Pseudomonads and *Enterobacteriaceae*. Very little growth of these groups was detected at 100% $CO_2$. The effect of packaging atmosphere were more pronounced for the growth of *Brochothrix*, Pseudomonads and *Enterobacteriaceae* compared to lactic acid bacteria and for total viable counts which can be seen in the main effects plot for TVC and *Enterobacteriaceae* in Figure 6).

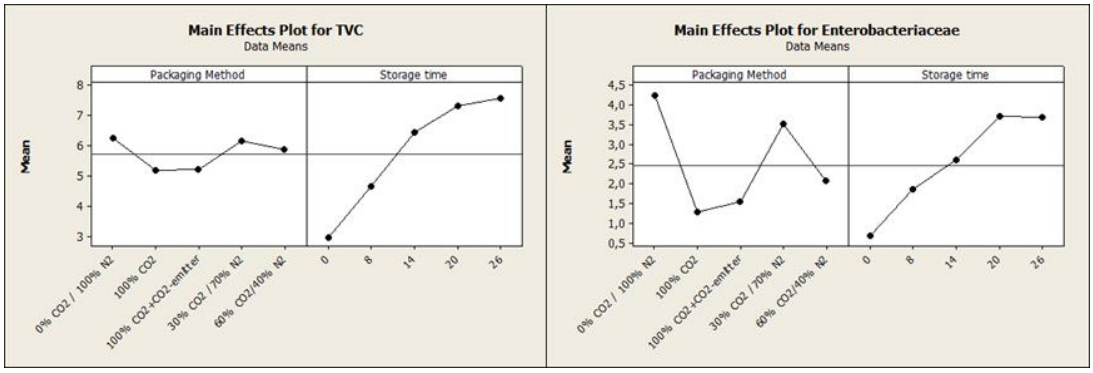



**Figure 6**: Main effects Plots of packaging method (packaging gas composition) and storage time on total viable counts of anaerobic colony forming units and growth on selective selective petri dishes *of Enterobacteriaceae* of chicken filets.

The identity of 333 selected colonies from different petri dishes from the 100 % $CO_2$ samples, both with and without emitter, and from the 60 % $CO_2$ samples, were determined by isolating DNA from single colonies and carrying out 16S rDNA sequencing (Table 1). Similar results were obtained for the three series, which could be expected as conditions with high level of CO2 strongly selected for growth of lactic acid bacteria. These dominated both on the PCA dishes and on the dishes selective for lactic acid bacteria.

**Table 1**. *Identity of the bacteria after storage as determined by 16S rDNA analysis*

| Growth medium[a] | Species | % of analyzed colonies | | |
|---|---|---|---|---|
| | | 60% $CO_2$ / 40% $N_2$ | 100% $CO_2$ | 100% $CO_2$ + $CO_2$-emitter |
| Total count, PCA, 30 °C | *C. divergens* | 45 | 28 | 72 |
| | *Carnobacterium* sp. | 52 | 53 | 23 |
| | *Hafnia alvei* | 0 | 13 | 0 |
| | Others | 3 | 6 | 5 |
| | | | | |
| Lactic acid bacteria, MRS | *C. divergens* | 100 | 93 | 75 |
| | *Carnobacterium* sp. | 0 | 7 | 15 |
| | *Serratia* sp. | 0 | 0 | 5 |
| | Others | 0 | 0 | 5 |
| | | | | |
| *Brochothrix* , STAA | *B. thermospacta* | 20 | 0 | 0 |
| | *Brochothrix* sp. | 80 | 100 | 100 |
| | | | | |
| Pseudomonads, CFC | *Serratia* sp. | 22 | 75 | ND |
| | *Morganella psykrotolerans* | 45 | 25 | ND |
| | *Morganella* sp. | 11 | 0 | ND |
| | Others | 22 | 0 | ND |
| | | | | |
| *Enterobacteriaceae* , VRBGA | *C. divergens* | 100 | 83 | 80 |
| | *C. maltaromaticum* | 0 | 17 | 20 |

[a]Colonies picked from different petri dishes.
ND, not determined.

*Brochothrix* selective dishes detected both *B. thermospacta* and other *Brochothrix* species present. *B. thermospacta* produces different hydrolases which participate in spoilage of meat. Some strains of *B. thermospacta* also produce proteinase [29]. Furthermore, pseudomonads selective dishes detected primarily *Serratia* sp. and *Morganella* species at very low numbers. According to Sade et al. (2013) [30], Serratia are implicated in meat spoilage.

However, the levels detected in our experiment were much too low to cause problems. The *Enterobacteriaceae* selective dishes revealed only growth of *C. divergens* and *Carnobacterium maltaromaticum*, and these were, by far, dominating species in our experiments using pure $CO_2$. Carnobacteria are often the dominating floras in MAP seafood and constitute the dominating lactic acid bacteria in meat during storage. Meat spoilage by carnobacteria is strain dependent and often high numbers have little influence on the sensory attributes of foods

## 4 Conclusions

Chicken filets stored in pure $CO_2$ showed an enhanced shelf-life in terms of microbiology compared to the lower concentrations of $CO_2$ used commercially as storage in 100 % $CO_2$ resulted in a microbial shelf life of approximately 25 days, that is a 6-7 days extension compared to 60 % $CO_2$. The dominating species were *Carnobacterium divergens*, *Carnobacterium* sp. and *Lactococcus* sp. Drip loss was highly affected by the gas atmosphere within the packages. $CO_2$ dissolved in the meat during storage, and storage in pure $CO_2$ caused collapse of the packages. The resulting so called vacuum –effect or squeeze of the packages lead to a severe increase in drip loss. By including a $CO_2$ emitter, collapse of the packages was avoided and the drip loss was reduced profoundly. Addition of $CO_2$ emitters can easily be implemented at industrial packaging lines without reductions in production efficiency.

## Acknowledgement

We thank Janina Berg, Signe Marie Drømtorp, Aud Espedal, Karin Solgaard and Anette Wold Åsli for skillful technical assistance. The research was partially financed the Research Council of Norway, through the project "Prevention of food waste in a value chain approach", project number 199761.

## References

1. W.R. Cortez-Vega. S. Pizato and C. Prentice, 2012, "Quality of raw chicken breast stored at 5C and packaged under different modified atmospheres, *Journal of Food Safety*, vol. 32, pp. 360-368.
2. E. Chouliara. A. Karatapanis. I.N. Savvaidis and M.G. Kontominas, 2007, "Combined effect of oregano essential oil and modified atmosphere packaging on shelf-life extension of fresh chicken breast meat, stored at 4°C", *Food Microbiology* , vol. 24, pp. 607–617.
3. E. Tsigarida and G.J.E. Nychas, 2001, "Ecophysiological attributes of a Lactobacillus sp and a Pseudomonas sp on sterile beef fillets in relation to storage temperature and film permeability", *Journal of Applied Microbiology*, vol. 10, pp. 696-705, DOI: 10.1046/j.1365-2672.2001.01292.x.
4. M.K. Pettersen. H. Nissen. T. Eie and A. Nilsson, 2004, "Effect of packaging materials and storage conditions on bacterial growth, off-odour, pH and colour in chicken breast fillets", *Packaging Technology and Science*, vol. 17, pp. 165-174, DOI**:** 10.1016/S0924-2244(99)00019-9.
5. S.M.Jimeneze. M.S. Salsi. M.C. Tiburzi. R.C. Rafaghelli. M.A. Tessi and V.R. Coutaz, 1997, "Spoilages microflora in fresh chicken breast stored at 4C; influence of packaging methods", *Journal of Applied Microbiology* , vol. 83, pp. 613-618, DOI**:** 10.1046/j.1365-2672.1997.00276.x.
6. G.H. Zhou. X. L. Xu and Y. Liu. 2010, "Preservation technologies for fresh meat - A review", *Meat Science*, vol. 86, pp. 119-128.
7. S. Rousset and M. Renerre, 1991, "Effect of $CO_2$ or vacuum packaging on normal and high pH meat shelf-life", *International Journal of Food Science and Technology*, vol. 26, pp. 641-652.
8. M.K. Pettersen. S. Bardet. J. Nilsen and S.B. Fredriksen, 2011, "Evaluation and suitability of biomaterials for modified atmosphere packaging of fresh salmon fillets", *Packaging Technology and Science*, vol. 24, pp. 237–248, DOI: 10.1002/pts.931.
9. E.U.T. van Velzen and A. R. Linnemann, 2008," Modified atmosphere packaging of fresh meats - Sudden partial adaptation caused an increase in sustainability of Dutch supply chains of fresh meats", *Packaging Technology and Science*, vol. 21, pp. 37-46.

10. Y. Zhao. J.H. Wells and K.W. McMillin, 1995, "Dynamic changes of headspace gases in $CO_2$ and $N_2$ packaged fresh beef", *Journal of Food Science*, vol. 60, no. 3, pp. 571-575. DOI: 10.1111/j.1365-2621.1995.tb09829.x.

11. A.A. Patsias. V. Badeka. I. N. Savvaidis and M. G. Kontominas. 2008. "Combined effect of freeze chilling and MAP on quality parameters of raw chicken fillets", *Food Microbiol.* vol. 25, pp.575-581.

12. E. Vihavainen. H.-S. Lundstrom, T. Susiluoto, J. Koort, L. Paulin, P. Auvinen, and K. J. Bjorkroth, 2007, "Role of broiler carcasses and processing plant air in contamination of modified-atmosphere-packaged broiler products with psychrotrophic lactic acid bacteria", *Appl. Environ. Microbiol.* vol. 73, pp. 136-1145.

13. F. Devlieghere and J. Debevere, 2000, "Influence of dissolved carbon dioxide on the growth of spoilage bacteria", *Lebensmittel-Wissenschaft Und-Technologie-Food Science and Technology*, vol. 33, no. 8, pp. 531-537, DOI: 10.1006/fstl.2000.0705.

14. M. Jakobsen and G. Bertelsen, 2004, "Predicting the amount of carbon dioxide absorbed in meat", *Meat Science*, vol. 68, no. 4, pp. 603-610, DOI: 10.1016/j.meatsci.2004.05.012

15. G.L. Robertson, 1993, *Packaging of flesh foods, in Food Packaging Principles and Practice*, Ed., Marcel Dekker Inc, New York. pp. 431-469

16. A.A. Hansen. T. Morkore. K. Rudi. M. Rodbotten. F. Bjerke, and T. Eie, 2009, "Quality changes of prerigor filleted atlantic salmon (*Salmo salar* L.) packaged in modified atmosphere using $CO_2$ emitter, traditional map, and vacuum", *Journal of Food Science.* vol. 74, pp. M242-M249.

17. A.A. Hansen. T. Morkore. K. Rudi. E. Olsen and T. Eie, 2007, "Quality changes during refrigerated storage of MA-packaged pre-rigor fillets of farmed Atlantic cod (*Gadus morhua* L.) using traditional MAP, $CO_2$ emitter, and vacuum", *Journal of Food Science,* vol. 72, pp. M423-M430.

18. A.A.Hansen. M. Hoy and M. K. Pettersen, 2009, "Prediction of optimal $CO_2$ emitter capacity developed for modified atmosphere packaging of fresh salmon fillets (*Salmo salar* l.)", *Packaging Technology and Science*, vol. 22, pp. 199-208.

19. J.R. Cole. Q. Wang. E. Cardenas. J. Fish. B. Chai. R.J. Farris. A.S. Kulam-Syed-Mohideen. D.M. McGarrell. T. Marsh. G.M. Garrity and J.M. Tiedje, 2009. "The Ribosomal Database Project: improved alignments and new tools for rRNA analysis", *Nucl. Acids Res.* vol. 37, pp. D141-D145.

20. R.H. Dainty, 1996, "Chemical/biochemical detection of spoilage", *Int. J. Food Microbiol.* vol. 33, pp. 19-33.

21. K.W. McMillin, 2008, "Where is MAP going? A review and future potential of modified atmosphere packaging for meat", *Meat Science*, vol. 80, no. 1, pp. 43-65, DOI: 10.1016/j.meatsci.2008.05.028.

22. G.O. Gill, 1988, "The solubility of carbon dioxide in meat", *Meat Science*, vol. 22, no. 1, pp. 65-71, DOI: 10.1016/0309-1740(88)90027-7.

23. L.M. McMullen and M.E. Stiles, 1991, "Changes in microbial parameterse and gas-composition during modified atmosphere storage of fresh pork loin cuts", *Journal of Food Protection*, vol. 54, no. 10, pp. 778-783

24. I.S. Arvanitoyannis and A. C. Stratakos, 2012, "Application of modified atmosphere packaging and active/smart technologies to red meat and poultry: A review". *Food and Bioproc. Technol*. vol. 5, pp.1423-1446.

25. M. Jakobsen and G. Bertelsen, 2002, "The use of $CO_2$ in packaging of fresh red meats and its effect on chemical quality changes in the meat: A review", *J. Muscle Foods*, vol. 13, pp. 143-168.

26. E. Borch. M.L. KantMuermans and Y. Blixt, 1996, "Bacterial spoilage of meat and cured meat products", *Int. J. Food Microbiol.* vol. 33, pp.103-120.

27. G. Molin, 2000, "Modified atmospheres", *In* B.M. Lund, T.C. Baird-Parker, and G.W. Gould (eds.), *The Microbiological safety and quality of food*, vol. 1, Aspen Publishers, Gaithersburg, Maryland, USA, . pp. 214-234.

28. M.A. Nadkarni. F.E. Martin. N.A. Jacques and N. Hunter, 2002, "Determination of bacterial load by real-time PCR using a broad-range (universal) probe and primers set", *Microbiol.-SGM*. vol.148, pp. 257-266.

29. O.S.Papadopoulou. A.I. Doulgeraki. C.Botta. L. Cocolin and G.-J. E. Nychas, 2012, "Genotypic characterization of *Brochothrix thermosphacta* isolated during storage of minced pork under aerobic or modified atmosphere packaging conditions", *Meat Sci.* vol. 92, pp. 735-738.

30. E. Sade. A. Murros and J. Bjorkroth, 2013, "Predominant enterobacteria on modified-atmosphere packaged meat and poultry", *Food Microbiol*, vol. 34, pp. 252-258.

# Microwaveable Packaging for Heating and Crisping a Food Product

**Eric Martine[1*], Didier Louvier[1]**

[1] *University of Applied Sciences Western Switzerland (HEIG-VD), Packaging Laboratory, Switzerland*
[*] *Corresponding author. Email: eric.martine@heig-vd.ch*

**Abstract:**
The susceptor is widely used since about 15 years ago to package convenience foods such as French fries, pop-corn, hamburgers, pizzas, etc. A susceptor is an artificial film slightly vacuum-metallized (the thickness of the metal layer is in the order of the nanometer). The susceptor, placed around the food, concentrates the microwave energy onto the product surface, crisping it. Its main role is to transform the microwaves into infrared waves, able to crisp or even brown-crisp the food.

One of the most appreciated swiss food is the "Raclette" a special hot cheese meal. Usually, this cheese is heated inside a special oven by an electrical resistance, whose heat first melts the cheese and then crisps the surface of the melted cheese.

The aim of this project is to study and develop a "food product cheese / packaging" couple in order to melt an individual raclette cheese portion in a microwave oven with crispy surface. The development of the packaging involved the use of two technologies: susceptor and micro-rite™. To develop the appropriate packaging, different types of raclette cheeses (17) and several different packaging designs have been tested.

Moreover, to avoid the occurrence of a hot spot during the cooking of the cheese in the microwave oven, a secondary packaging has to be developed.

To assess the potential of the microwaveability of the cheese, the level of satisfaction of potential clients is evaluated by organizing two separate public organoleptic tastings in Swiss supermarkets. Criteria such as color, separation of fats, formation of strings, consistency and aroma are considered to perform the assessment. Both tastings give satisfactory results on all organoleptic criteria concerning the microwaveable "raclette" cheese portion.

Keywords: susceptor, aluminized container, active packaging, "raclette" cheese, microwaveable food, convenience food.

## 1. Introduction

The aim of this project is to study and develop a "food product cheese / microwaveable packaging" couple allowing to heat and to brown / to crisp in surface the food product.

To reach the optimal packaging to cook foodstuff by using a microwave oven, the following steps have been realized:

- Characterize the properties of the food products: define properties, what desired results after cooking…
- Acquire the competences about the microwave thermal properties as well as the use and the assessment of the thermal and electromagnetically properties of the packaging materials used in microwave oven
- Define and choose the susceptor for an optimal heating and browning of the food product
- Define and choose nature and structure of the primary and secondary packaging
- Produce and optimize the microwaveable packaging / food product couple

In a microwave oven, the active packaging (such as the susceptor…) is involved in the conversion of microwave energy into infrared energy.

The materials properties as regard to the microwave energy make it possible to conceive a packaging that defrosts, heats and crisps a food product.

## 2. Materials and Methods

### 2.1. Definition of the susceptor

A susceptor is a flexible synthetic film PET (around 12µm) slightly vacuum metallized (from 25Å to 2000Å thick), which, placed under or around the food, will concentrate the microwave energy onto the product surface. This film is generally laminated on a paperboard or cardboard. It exists various kind of susceptors on the market whose the difference is due to the drawn patterns on the metallized layer (uniform layer, cross pattern…) chosen in function of the characteristics of the food products.

The susceptor transform the microwaves into infrared allowing to brown and to make crispy the food product. Moreover, thicker the metallized layer is, less the electro-magnetical energy will be transform in heat.

The energy of the microwaves coming on the susceptor is split in 3 energies and the proportion altered in function of exposure time to the microwaves:

- Reflected energy = energy reflected by the susceptor
- Absorbed energy = energy transformed in IR to brown and to make crispy the food product
- Transmitted energy = energy which goes across the susceptor and heat the product under microwave shape

### 2.2. Materials

The materials used in this project must have an impact on the microwaves that means it must not disrupt the action of the microwaves and allow an optimal cook of the food product.

It is generally transparent to the microwaves and must not be sensitive to the temperature elevation of the product.

Then in our project, we have used an active packaging mixing the susceptor technology and the fields modification technology (micro-rite™).

The fields of modification allow to heat the food product uniformly up to the center of the product thank to the conduction of the energy and to reduce the temperature of the heating of the product.

The materials used for our packaging (primary and secondary packaging) are defined in the table 1.

**Table 1:** Materials

| Materials | Characteristics | Supplier |
|---|---|---|
| Aluminized container | Composition : PET / Aluminum / Cardboard<br>Dimensions : 150 x 120 x 7 [mm], for the preparation of one raclette portion, 60g | Graphic Packaging Corporation, Canada |
| Lid | Composition: Safety Susceptor / cardboard.<br>Safety Susceptor type Tiny Crosses (=fused susceptor) | A.D. Tech, USA<br>Trick Pack A/S, Denmark |
| Secondary packaging | Coated board 320 g/m$^2$ | Saüberlin & Pfeiffer S.A., Switzerland |
| Microwave oven | Domestic Microwave oven, Power : from 130 to 800W ; Cooking time: from 1s to 35min | - |
| Cheese | 17 different “raclette” cheeses.<br>Cf. table 2. Different cheese characteristics. | Valcrème S.A., Switzerland |

## 2.3. Different raclette cheeses

Different raclette cheeses (table 2) made with unpasturized milk, taken at different maturing and with variable fat and water contents are conditioned in the primary packaging.

The different tests have been made with an approximate mass of 60g which simulate one raclette portion.

The aim is to obtain a mass of creamy cheese with a crispy surface.

**Table 2:** Different raclette cheeses

| Cheese # | Maturing [months] | Fat content [%] | Water content [%] | Cheese # | Maturing [months] | Fat content [%] | Water content [%] |
|---|---|---|---|---|---|---|---|
| 1 | 4 | 50.55 | 41.83 | 10 | 2 | 55.10 | 40.11 |
| 2 | 3 | 50.00 | 41.85 | 11 | 3 | 56.94 | 39.94 |
| 3 | 2 | 52.37 | 41.77 | 12 | 3 | 53.22 | 40.82 |
| 4 | 3 ½ | 55.53 | 40.76 | 13 | 2 | 55.16 | 41.09 |
| 5 | 3 ½ | 53.60 | 40.86 | 14 | 3 | 56.93 | 42.39 |
| 6 | 3 ½ | 56.90 | 42.01 | 15 | 4 | 55.33 | 40.36 |
| 7 | 4 | 53.85 | 42.86 | 16 | 4 | 55.47 | 39.97 |
| 8 | 4 | 55.19 | 38.04 | 17 | 4 | 53.79 | 39.59 |
| 9 | 3 | 50.79 | 40.93 | | | | |

The behavior of the different cheese after microwave preparation differs according to several criteria such as:

- fat separation,
- creaminess,
- unctuousness,
- consistency (“gummy”),
- crispness.

### 2.4. Sensory analysis

2 general public tastings (table 3) have been realized to test the feasibility demonstrator and quantify the quality criteria of the defined micro waved food product.

The criteria for the assessment of the final product are:

- Color
- Separation of fats
- Formation of string
- Consistency
- Aroma
- Overall impression

**Table 3:** Tasting data

| | Tasting 1 | Tasting 2 |
|---|---|---|
| Tasted cheese | Cheese # 16 | Cheese # 17 |
| Tasters | Hypermarket consumers. Number = 67 | Hypermarket consumers. Number = 91 |
| Method | In an isolated box, the subjects taste:<br>- one raclette prepared in a microwave oven,<br>- one raclette prepared with an specific electric infrared grill ( raclonnette).<br>The consumers ignore the way the raclettes have been prepared. | In an isolated box, the subjects taste only one raclette prepared in a microwave oven.<br>The consumers ignore the way the raclette has been prepared. |

The method to treat the results is an interval test realized on a 7 level scale.

## 3. Results and Discussion

To obtain a performant packaging in order to prepare a delicious food product, we have worked on the following parameters:

- Primary packaging
- Secondary packaging
- Cheese product
- Sensory analysis

### 3.1. Primary packaging

The choice of the design for the primary packaging has been done following the criteria:

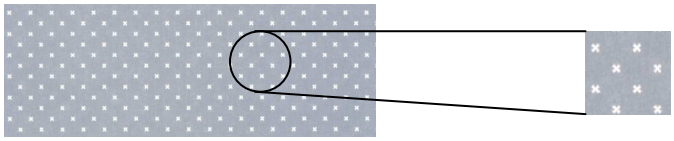
- No heating of the product through the tray: too much heat coming from this part of the packaging could overheat the product (heat regulation)
- Generate an uniform heating into the product
- Transform the microwaves into infrared to brown and crisp partially the product in surface
- Avoid the separation of the cheese into 2 phases: oil and residual cheese
- Avoid the cheese to become a gummy product, overheating spot

Concerning the tray, we have tested various materials such as cardboard, PETG, PP/EVOH/PP, PP, cardboard laminated PET. From all tests, this one which gives bet result is the structure cardboard / aluminium / PET.

The aluminium foil included between the cardboard and the PET of the container avoids the overheating and subsequently the food product degradation. From a thickness of one micrometer or so, aluminium reflects the microwaves which then can't reach the food product. This technology not only enables to modify the properties of the heating of the product but also to influence the distribution of energy inside the product.

Concerning the lid, we have also tested several design and structures such as Seifert susceptor, membrane susceptor, safety susceptor. Concerning the choice of the susceptor patterns, our choice has been done on namely on the safety susceptor shown in picture 3.

So, thanks to the « barrier » effect of aluminum on microwaves, the energy supply to the food product mainly comes from the susceptor/lid (photo 3) allowing to heat longer the food product without degrading it and to help the crispness appearance.



**Picture 1**. Safety Suscepteur (type fused susceptor). *Source AD Tech*.

To make the primary packaging, the Safety Susceptor lid/ cardboard (picture 3) is thermally sealed on the aluminized container (picture 2).



**Picture 2:** Aluminized tray

+



**Picture 3.** Safety Susceptor cardboard

In order to get the complete primary packaging, the aluminized tray and the safety susceptor cardboard have been thermally welded together (picture 4).

**Primary packaging**



**Picture 4:** Container and Safety Susceptor lid.

## 3.2. Secondary packaging

The face of the product (bottom) into contact with the microwave oven plate shown hot spot and the product is locally modified.

In order to cut down the heat transfer by conduction between the bottom of the oven and the bottom of the tray and so to prevent the appearance of hot spots at the center of the product, the packaging is raised from the microwave oven.

Then we will use a secondary packaging on which the primary packaging will be laid. The raising of the primary packaging is important:

- Isolating the food product of the microwave oven plate in order to avoid the heating of the product by conduction and then the overheating of the product
- Increasing the rate of absorbed waves by the susceptor in order to have an optimal efficiency of the transformation of the microwaves in infra-red heat.

Moreover, the secondary packaging (picture 4) will use both to pack the primary packaging and to give sale unit.



**Picture 5**: Secondary packaging

### 3.3. Cheese and conclusions packaging/cheese

The study allows:

- to specify the type of cheese used in our application: cheese 4, 5, 16 and 17 from 3 to 4 months maturing (cf. table 2.). Even though cheese 15 presents similar characteristics as the retained cheeses, the result after heating is not acceptable : important separation of the fat and gummy consistency,
- to define the primary packaging made of an aluminized container as deep as the cheese thickness and a Safety Tiny Crosses type susceptor-lid on a cardboard support with weldings,
- to define the secondary packaging as a raising agent,
- to define the cooking time ranging from 150 and 180s for a power of 600 W. By working on the cooking time it is possible to obtain a crispness gradient. The longer the heating the more « religieuse » (crispness) is obtained.

### 3.4. Sensory analysis

After preliminary tests and many corrective actions, the primary packaging is produced and used during 2 general public sensory analyses in hypermarket.

These tests show that (cf. figures 1, 2 and 3):

* For **testing 1**:

- the microwaved raclette is approved in comparison to the raclonnette oven (=Electric infrared grill) mainly because of the fat separation, thread formation and flavor,

- the flavors are more intense for the microwaved raclette ,

- the product appetizer is reinforced compared to the product obtained with a raclonnette oven.

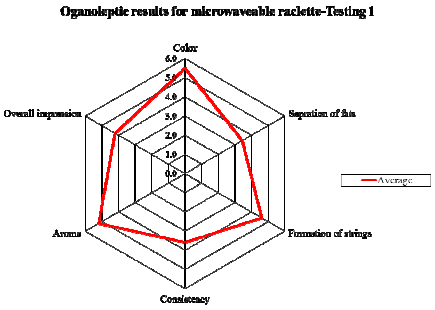



**Figure 1**: Organoleptic results for microwaveable raclette-Testing 1

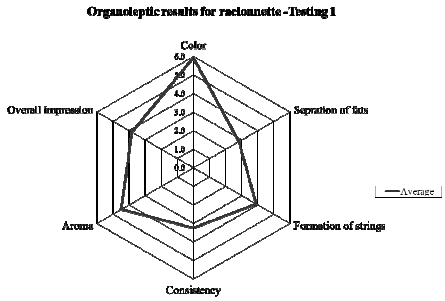



**Figure 2**: Organoleptic results for raclonnette system-Testing 1

* For **testing 2** :

- 89% of the consumers appreciated the crispy surface when using the microwave oven,

- general impression criteria, we note that:

  ↳ 5.5% (5 consumers) consider the microwaveable raclette as a bad product,

  ↳ 94.5% (86 subjects) consider the microwaveable raclette as a good or excellent product.

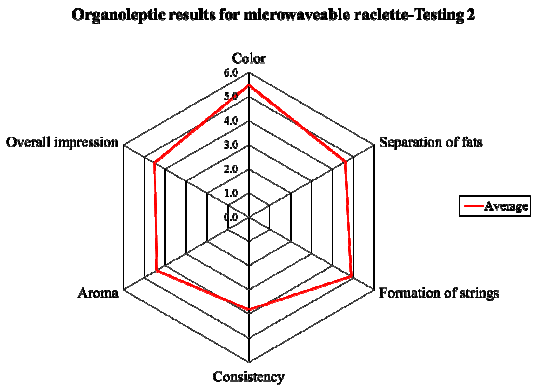



**Figure 3**: Organoleptic results for microwaveable raclette-Testing 2

## 4. Conclusion

In this study, to develop the optimal packaging in order to cook a perfect “raclette” cheese, the following parameters have been taken into account:

- Distance susceptor / food product: to obtain a browning and crispy food product, the distance between the susceptor and the product must be lower than 3mm.
- Protection of the food product against the overheating
- Distance between the primary packaging / microwave oven
- Behavior of the food product in function of the temperature (oil separation)
- Cheese and browning product: To crisp and brown some food, the surface temperature must be higher than 150°C. The maximal temperature of the susceptor must be reached very quickly without creating a thermal boom, thus allowing the susceptor to play its role before the food product overheated.

Finally, using an active packaging (aluminized container and susceptor) enables to obtain a crispy product in a microwave oven is approved by the consumer. However, one must not forget that the food product must be optimized for this conditioning technology.

## Acknowledgements

The authors want to thank:

- the Innovation Promotion Agency Switzerland (CTI), the School of Business and Engineering Vaud Switzerland (HEIG-VD) and Valcrème S.A. for their financial backing,

- our research partners, the University of applied sciences Valais, Food department

- their associated research partners A.D. Tech and Graphic Packaging Corp. for samples and stimulating discussions.

**References**


1. P. Harrison, 1989, "The Role of Packaging in Achieving Microwave Browning & Crisping", *Packaging Technology & Science*, vol. 2 pp 5-10
2. K. Woods, 2000, "Microwave packaging-susceptors, current and future", Paper 6 (i), *FoodPack* 2000.
3. K. Woods, 1997, "Developing packaging systems for heating microwave snacks & recipe meals", Paper 7, Packed, wrapped and microzapped III, Leatherhead Food Research Association
4. T. Russell, F. James, Beckett Technologies Corporation, 1997, "The next stage – an update on microwave-active packaging systems", Paper 8, Packed, wrapped and microzapped III, Leatherhead Food Research Association
5. M. Audhuy-Peaudecerf, 1997, « Contribution de l'emballage à la maîtrise du chauffage d'un aliment dans un four micro-onde », *Revue Industrie Alimentaire Agr.*
6. R. Roberts, Technical Consultancy PIRA International, 1996 "Packaging for Consumer Convenience", Paper 4, Pira International
7. J. A. McCormick, AD Tech, 1993, "Membrane susceptor-A patented active microwave packaging structure", FuturePack´ 93, The tenth annual Ryder conference on food packaging innovations.

# Development of an Intelligent Packaging Device for the Monitoring of Ready to Eat Salad Spoilage

**Anne Maltais[1*] and Mina Zitouni[2]**

[1] *Institut de Technologie des Emballages et du Génie Alimentaire (ITEGA), Collège de Maisonneuve, Canada*
[2] *Department de biologie, Université de Sherbrooke, Canada*

[*] *Corresponding author. Email: amaltais@cmaisonneuve.qc.ca*

**Abstract:** An intelligent packaging prototype to detect freshness level of ready-to-eat lettuce was developed in this study. In order to create such a system, the first step was to investigate quality index markers in lettuce. Ethanol and total volatile basic nitrogen (TVBN) were found to slightly increase in ready-to-eat romaine lettuce as a function of time when packed in polyethylene (PE) bags conditioned with 100% nitrogen. In ventilated PET packages with atmospheric oxygen conditions, no ethanol accumulation was detected in salad mix containing baby lettuce leaves (arugula, spinach and chicory). However, in the same packaging conditions, TVBN reached 35 mg nitrogen equivalents (N) per 100 g of salad mix after 11 days at 5°C in response to aerobic spoilage flora. These findings were used to developed colorimetric devices responsive to the accumulation of such metabolites. The device developed was based on color change as a response to accumulation of basic pH molecules (TVBN) in package headspace. Bromocresol purple (BCP) was chosen as the active molecule for the freshness detection in the prototype developed. In presence of TVBN vapors corresponding to concentrations found in salad mix after days of storage, BCP color changed from yellow to purple. Different strategies were tested to increase sensitivity to TVBN of the intelligent device and to limit leaching of the active molecules. The final prototype developed showed the ability to successfully detect TVBN levels as low as 5 mg N/100 g of salad, which corresponds to mid-shelf life of this specific produce. Smart packaging device developed in this study represents a great alternative to 'best before' labels which cannot precisely inform the consumer as to freshness level of ready to eat vegetables.

Keywords: intelligent packaging, freshness indicator, color indicator, food spoilage, ready-to-eat salad, volatile amines.

## 1 Introduction

The spoilage of perishable foods with time is a recurring problem encounter by consumers. To overcome this problem, several strategies can be applied to the products to extend their shelf-life. Among them, the use of low temperature, modified atmosphere packaging, sanitizing solutions and others all contribute to significantly delay food spoilage of foods. Depending on the techniques used, initial quality of product, temperature fluctuations during handling and transport and other parameters, variable shelf lives of the same product can be found from one lot to another. Hence, the 'best before' date applied to food products may not always represent their real freshness state. This situation can either lead to consumption of expired food or wasting good quality food.

Food quality level has traditionally been monitored by microbiological or chemical laboratory methods. These techniques are time consuming, expensive and cause food waste since they imply the opening of package and sampling of food. In regards of these drawbacks, there is great interest among the food industry, retailers and consumers in developing accurate, cost-effective, rapid, reliable and non-destructive devices to evaluate real-time freshness of food products. Prototypes of intelligent packaging have recently been developed to monitor freshness status of a different kind of food [1]. Intelligent packaging includes all surveillance devices that, once applied to the packaging, give information on the product during handling, transport and storage [2-3]. Among the prototypes developed, quality and food safety indicators (time-temperature indicators, metabolites and gas detectors, traceability devices (radio-frequency identification) and leak detectors are some of the most promising ones [4-7]. Quality and food spoilage detectors represent an interesting alternative to sensory and microbiological analyses [8]. It can also prevent food poisoning and waste of food through 'best before' date specific to each product and its own quality.

A limited number of scientific papers on the development of food spoilage indicator exist. Some prototypes based on the detection of volatile compounds resulting from microbial growth have proved their efficiency on poultry [9], fish [10] and prepared desserts [1]. In the first two cases, the detection system is based on the pH change through basic volatile amine accumulation in packaging, while the latter is based on the colorimetric

detection through $CO_2$ accumulation. In all case, the gases and metabolites detected are produced by microbial flora specific to the food tested. Even though efficiency of the prototypes developed has been proven, some parameters still need to be improved. For example, labels developed were only tested at higher temperature than their usual storage temperature (4°C) to enhance the spoiling effect and facilitate vaporization of metabolites. Moreover, leaching of colorimetric detectors in contact with food or humidity in packaging was previously reported [10].

Ready to eat vegetables such as mixed salad are good candidates for the development of spoilage indicator for many reasons. They are highly perishable produces given their high water content, neutral pH and high concentration in nutrients [11]. All these conditions are very favorable to contamination by spoilage microbial flora such as *Enterobacteriaceae*, *Erwinia and Pseudomonas* species [12-13]. They also go through a long travelling before reaching their final destination, which make them prone to temperature elevation [11]. Moreover, their initial quality is variable depending on the season and where they were harvested. For all these reasons, ready to eat salad has highly variable shelf-life. Determining its quality from one unit to another instead of general 'best before' dates would be beneficial for this kind of produce.

As previously evocated, the development of a quality indicator must be based on the production of spoilage metabolites. Fermentation of ready to eat vegetables by microorganisms in certain conditions is one of the most important causes of quality loss [13]. Molecules produced throughout this mechanism can potentially be measured and be the basics of freshness detection prototypes for salad. Among these molecules, ethanol, acetaldehyde and organic acids are produced by spoilage microorganisms naturally found in vegetables.

Proteolytic bacterias such as *Pseudomonas* have the ability to transform proteins and enzymes into volatile basic nitrogen molecules. These specific molecules, if present in sufficient quantity, could also be used in the development of freshness indicator of ready to eat salad. The presence of such molecules in package headspace can potentially modify the surrounding pH atmosphere [10]. This pH change can be measured qualitatively by colorimetric indicators specifically chosen as to their transition pH range. This technique was previously used to detect basic nitrogen molecules in poultry and fish, which contains high ratios of proteins [9-10]. No such indicators were developed for real-time spoilage detection of low protein content food such as salad.

The objective of this work is to first investigate the production of specific spoilage metabolites in ready to eat salad when stored at refrigeration temperature and to use it in the development of a quality index prototype for this category of food product.

## 2 Materials and methods

### 2.1 Processing and packaging

Fresh romaine lettuce heads were bought from the market, brought to the lab and kept at 5°C. The same day, lettuce was cut (5 cross-section cuts per head), washed in tap water and spin-dried. Samples of 100 g of salad were packed in sterile low density polyethylene (LDPE) bags (18 X 24 cm, thickness = 75 µm, oxygen transmission rate = 2650 cc/$m^2$.24h). Bags were then flushed with 100% nitrogen and sealed using a Sipromac II model 350 packaging machine (Sipromac, St-Germain, Canada). Mixed ready to eat salad containing baby lettuce leaves (arugula, spinach and chicory) packed in ventilated PET clamshells were also bought from the market. All packages were kept at 5°C until analyses.

### 2.2 Headspace analysis

The $O_2$ and $CO_2$ concentrations in both kinds of salad packages were measured periodically over time using a Checkpoint $O_2$/$CO_2$ analyzer (PBI-Dansensor). One headspace determination was taken from five different packages for each treatment.

### 2.3 Ethanol concentration

Ethanol content in packed salads was determined periodically over time. A mass of 60 g of salad was homogenized with 80 mL of distilled water using a glass blender. The homogenized sample was then centrifuged for 10 minutes at 9000 rpm. Supernatant was re-centrifuged in the same conditions. A volume of 500 µL of the liquid extract was diluted in $H_2SO_4$ 0.01 N to get a final dilution of 0.1 and filtrated through 0.2 µm filter. A volume of 2 mL was transferred to a 3 mL vial for HPLC analysis. The quantification of ethanol was performed by HPLC using a Shimadzu LC-600 HPLC pump coupled to a refractive index detector (Shimadzu RID-10A). The HPLC was equipped with an Aminex HPX 87H column (300 x 7.8 mm, Bio-Rad). A 20 µL sample volume was injected in a Shimadzu SIL-9A injector into the HPLC at an oven temperature of 65°C (isocratic) and a flow of 0.4 mL/min. using $H_2SO_4$ 0.1 N as mobile phase. Analyses were carried out in duplicate for 45 min. Ethanol concentration was calculated using the Equation 1:

$$\textbf{[EtOH] (mg/100g salad) = \% EtOH (mL/100g)*10*2.5*788.5 mg/mL} \quad (1)$$

where:

2.5: dilution factor salad;
10: mobile phase dilution factor;
788.5 mg/mL: EtOH density (at 21.5°C).

## 2.4 TVBN determination

TVBN (ammoniac, dimethylamine and trimethylamine) was determined periodically on romaine salad packed in bags and on mixed salad packed in ventilated clamshells. Conway microdiffusion method was used to ensure determination of low TVBN concentrations expected. In brief, 4 samples of 4 g of salad were withdrawn from the packages, shredded and mixed with 8 mL trichloroacetic acid (TCA) 4% (w/v) in centrifuge tubes. Samples were then sonicated for 1 minute and let at room temperature for 30 minutes with occasional grinding. Filtration of samples was carried out using filter paper (Whatman #41) and supernatants were kept in the freezer until analysis. A thin grease coat was applied to the edges of Conway cell caps. After thawing, 1 mL of each filtrate was placed in the outer ring of a Conway cell. 1 mL of TCA 4% was used as blank. 1 mL of the Conway reagent (4% (w/v) bromocresol green + 4% (w/v) methyl red in boric acid 2% (w/v)) was pipetted into the inner ring of the cell. To initiate the reaction, 1 mL of saturated carbonate potassium solution ($K_2CO_3$) was added to the outer ring and the cell was immediately closed. Gentle shaking of cells allowed mixing of reagents in outer ring. After 3h of incubation at 30°C, cells were opened and the inner ring solution was titrated with 0.02 N HCl until a pink color appeared (as found for the blank). TVBN of each sample was calculated using Equation 2:

$$\textbf{TVBN (mg nitrogen/100g salad)} = V_{HCl}*(N_{HCl}*A_N)*V_E*100/W_S \quad (2)$$

where:

$\mathbf{V_{HCl}}$: HCl 0.02 N volume added for titration (mL);
$\mathbf{N_{HCl}}$: HCl normality (0.02);
$\mathbf{A_N}$: Nitrogen atomic weight (14);
$\mathbf{V_E}$: TCA 4% volume used for extraction (mL);
$\mathbf{W_S}$: salad weight used for extraction (g).

## 2.5 Prototypes fabrication

Indicator solution used was bromocresol purple (BCP) 0.04% (w/v) in ethanol/water (50:50). 30 µL of indicator solution was absorbed on 5 mm diameter Whatman filter paper #41 and allowed to dry. In order to prevent leaching of the indicator in presence of humidity, different strategies were tested:

1. Indicators were sealed between 2 layers of thin adhesive LDPE film (thickness: 15 µm; oxygen transmission rate: 12550 cc/$m^2$.24h);
2. Indicators were sprayed with polytetrafluoroethylene (PTFE) and sealed between 2 layers of the LDPE film micro perforated 5 times with a needle tip;
3. Indicators were coated with a thin layer (thickness =1 mm) of silicone rubber and allowed to dry at room temperature for 24 h.

## 2.6 Performance testing

Prototypes developed were first tested in closed system with ammoniac ($NH_3$) standards solutions which mimic TVBN concentrations found after different storage time in mixed ready to eat salad packed in ventilated clamshells (at 5°C). 5 mL of 0, 0.0005, 0.001, 0.005 and 0.01 M $NH_3$ solutions were placed in 20 mL glass vials covered with parafilm and equilibrated at 4°C for 3h. Prototypes were suspended in the vials by fixing them on disposable pipette tip so that standard solutions are not in direct contact with the sensors. Vials were sealed and stored at 4°C for 72h. Final experiment consisted in fixing coated prototypes in the inside cover of clamshells containing mixed ready to eat mix salad and store them at 5°C. Color change of the indicators from the initial color was evaluated and quantified using a colorimeter (CR-10, Minolta, Japan) using L, *a* and *b* parameters. Global color change (ΔE) was obtained from Equation 3 [14]:

$$\Delta E = [(\Delta L)^2 + (\Delta a)^2 + (\Delta b)^2]^{1/2} \quad (3)$$

# 3 Results and discussion

## 3.1 Headspace gas analysis

Figure 1 presents headspace gas composition in fresh-cut romaine salad in bags stored at 5°C. Oxygen and carbon dioxide concentrations are both at 0% on the first day of storage due to the initial gas flush conditioning (100% $N_2$). $CO_2$ tends to increase with time, while $O_2$ stays very close to 0% in response to the equilibrium created between respiration rate of salad and the gas permeability of the film. While a large proportion of the oxygen entering the bag is consumed by salad as a respiration substrate, $CO_2$ produced through respiration accumulates into the bag. Moreover, the very low oxygen concentration in bags may also lead to fermentation metabolism for which by-products such as ethanol are produced. Gas headspace for ventilated clamshells remained at atmospheric concentrations (oxygen: 20.8% and $CO_2$ 0.03%) due to high gas exchange rate with the surrounding atmosphere (results not shown).

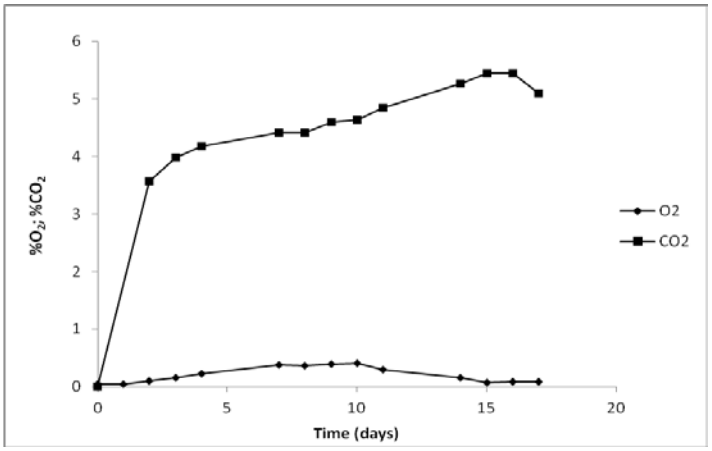



**Figure 1**: $O_2$ and $CO_2$ concentrations in romaine salad packed in bags stored at 5°C.

## 3.2 Ethanol production in salad

Figure 2 presents the evolution of ethanol accumulation in fresh-cut romaine salad. There is no ethanol accumulation in salad mix packed in clamshell (results not shown). Ethanol is a by-product resulting of anaerobic metabolism when low oxygen concentrations are available for respiration metabolism. This condition occurs in bags which results in the accumulation of ethanol. However, ethanol is already present in salad tissues at the initial stage. This early accumulation was already observed for other pre-cut vegetables and is associated with a wound response to cutting [15]. Hence, ethanol might not be the ideal metabolite to be detected for freshness indicator device. It would only be applicable for low oxygen packages and could also lead to false positives due to early detection of high ethanol concentration.

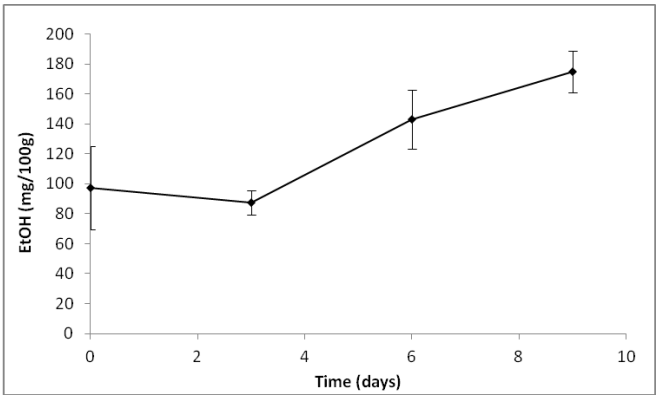



**Figure 2**: Ethanol production in romaine salad packed in bags stored at 5°C.

## 3.3 TVBN production in salad

TVBN accumulation in romaine salad packed in bags and in mixed lettuce packed in clamshell was recorded as a function of time of storage at 5°C. Figure 3 clearly demonstrates that for both kinds of products, there is no TVBN accumulation at the initial stage. For romaine salad, low levels of TVBN were accumulated over time. At the end of its shelf life (15 days), a total of 12 mg TVBN/100g of salad was reached. A higher rate of TVBN production was found for mixed baby salad in clamshell, where 35 mg/100g was reached at the end of its shelf life (11 days). Mixed baby lettuce seems to be more prone to the microbial spoilage responsible of TVBN

production. Moreover, knowing that proteolytic bacteria such as *Pseudomonas* grow in presence of oxygen, they can develop more easily in ventilated clamshell than bags.

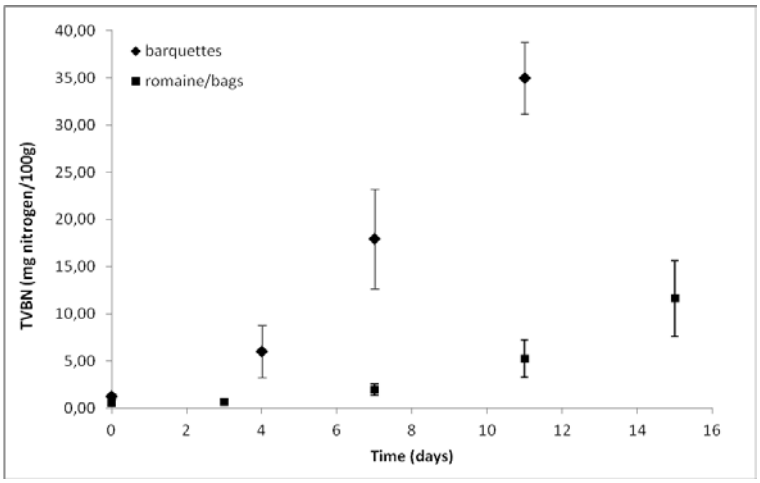



**Figure 3**: TVBN accumulation in romaine salad packed in bags and in mixed lettuce packed in clamshell (atmospheric gas conditions) stored at 5°C.

The absence of TVBN at initial stage, their high accumulation as a function of time at refrigeration temperature and their good correlation with mixed salad freshness level when stored in atmospheric gas conditions, make these specific metabolites good candidates to develop real time freshness indicator prototypes.

### 3.4 Prototype performance

Prototype developed is meant to be in contact with atmospheric conditions in the package and not in direct contact with the tissues. For this reason, the device was suspended in a closed system and not in direct contact with the simulated TVBN conditions. Figure 4 shows the colour of the uncoated indicator after 72h of indirect contact with simulated conditions at 4°C. It can be observed that at conditions where no TVBN is found (which correspond to initial condition in salad clamshell), indicator is yellow. The colour turns into burgundy and then purple as the $NH_3$ concentration is increased at concentrations corresponding to middle and end of shelf life of mixed lettuce in packed in atmospheric conditions. $NH_3$ vapours in the vials create a pH change in the headspace which reacts with BCP and causes a colour change. The same mechanism is believed to happen within the salad packages.




**Figure 4**: Uncoated indicator prototypes in indirect contact with varying $NH_3$ concentration solutions after 72h stored at 4°C.

Due to the presence of humidity within salad packages, the coating of the prototype with a water barrier and non gas barrier material was necessary to prevent leaching of the device. Coatings described in the section 2.5 were applied to the prototypes and tested in real conditions with mixed baby salad packed in clamshell. Figure 5 shows the colour of the indicators at different stages of salad shelf-life. Figure 6 quantifties the colour change

using the ΔE values. The colour slightly changes at day 4 for the coating #2, which is the most permeable to gases. The purple color gets more intense on day 7 for coating #2 and appears slightly for coating #3. At day 11, prototypes with coatings #2 and 3 are completly purple, while de prototype with coating #1, which is the most gas impermeable, shows a minimal colour change. Knowing that the end of shelf life of the salad corresponds to day 9 according to manufacturer, prototypes with coatings #2 and #3 would be suitable for detecting adequate freshness level of this kind of salad packed in ventilated clamshells. Moreover, the devices do not show apparent leaching, which confirms the efficiency of the coatings used. The coating #1 is too gas impermeable to allow contact of TVBN vapours with the active indicator. It can be noticed that there is a direct relationship between gas permeability of coatings and sensitivity of the prototypes to TVBN.

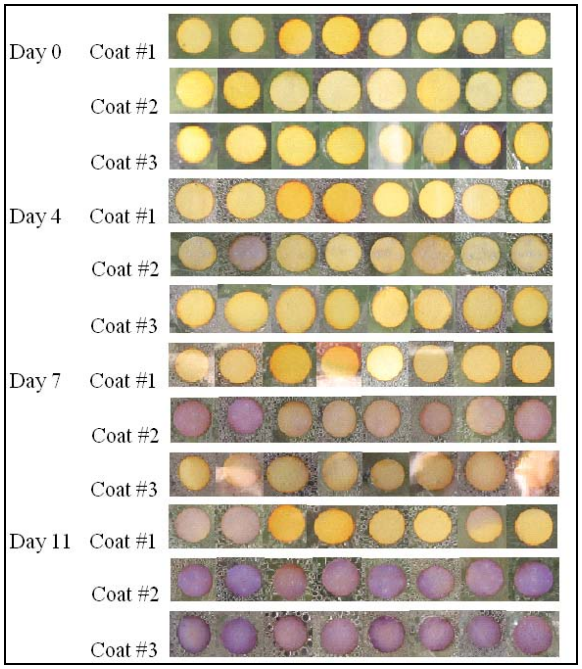



**Figure 5**: Evolution of coated prototypes colour at different stage of mixed baby salad shelf-life stored at 5°C.

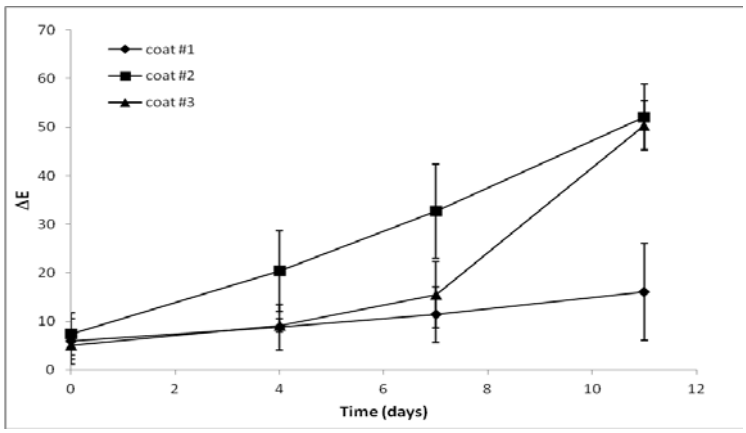



**Figure 6**: Evolution of ΔE for indicator prototypes using 3 different coatings when put in contact with mixed baby salad packed in clamshell and stored at 5°C.

## 4 Conclusion

The results presented in this study indicated that different kinds of metabolites were produced in ready-to-eat salad depending on its nature and the package used. In low oxygen concentration packages, ethanol is produced in response to fermentation metabolism. However, ventilated clamshells, generally used to pack fragile ready-to-eat baby lettuce, allow high oxygen concentration which promotes spoilage by microorganisms responsible for TVBN production. The constant increase of basic metabolites was used to develop a colorimetric indicator for freshness level of mixed baby lettuce salad. Bromocresol purple was chosen as the active compound owing its ability to change colour from yellow to purple when in contact with TVBN vapours. Anti-leaching coatings were

tested as to their TVBN permeability and humidity resistance. PTFE and silicone coatings showed the most sensitive results and allowed successful colour change of indicators at mid-end of salad mix shelf life packed in ventilated clamshell. The intelligent label developed in this study is a promising tool that could easily be used by the consumers to assess quality level of ready to eat salad.

## Acknowledgements

This research was supported by the Ministère de l'Enseignement Supérieur, Recherche, Science et Technologie (MESRST) through its funding program 'Programme d'Aide à la Recherche et au Transfert' (PART).

## References

1. A. Nopwinyuwong S. Trevanich and P. Suppakul, 2010. "Development of a novel colorimetric indicator label for monitoring freshness of intermediate-moisture dessert spoilage", *Talanta*, vol. 81, pp. 1126-1132.
2. R. Ahvenainen, 2003. "Active and intelligent packaging: an introduction", In: R. Ahvenainen (ed.), *Novel food packaging techniques*, Woodhead Publishing Ltd., Cambridge, pp. 5-21.
3. K.L. Yam P.T. Takhistov and J. Miltz, 2005. "Intelligent packaging: Concept and Applications", *Journal of Food Science*, vol. 70, pp. R1-R10.
4. H. Vaikousi C.G. Biliaderis K.P. Koutsoumanis, 2009. "Applicability of a microbial time–temperature Indicator (TTI) for monitoring spoilage of modified atmosphere packed minced meat", *International Journal of Food Microbiology*, vol. 133, pp. 272-278.
5. M. Smolander E. Hurme K. Latva-Kala T. Luoma H.L. Alakomi and R. Ahvenainen, 2002. "Myoglobin-based indicators for the evaluation of freshness of unmarinated broiler cuts", *Innovative Food Science and Emerging Technologies*, vol. 3, pp. 279-288.
6. F.C. O'Mahony T.C. O'Riordan N. Papkovskaia V.I. Ogurtsov JP Kerry and DB Papkovsky, 2004. "Assessment of oxygen levels in convenience-style muscle-based sous vide products through optical means and impact on shelf-life stability", *Packaging Technology and Science*, vol. 17, pp. 225-234.
7. J.P. Kerry M.N. O'Grady and S.A Hogan, 2006. "Past, current and potential utilisation of active and intelligent packaging systems for meat and muscle-based products: a review", *Meat Science*, vol. 74, pp. 113-130.
8. R.H. Dainty, 1996. "Chemical/biochemical detection of spoilage". *International Journal of Food Microbiology*, vol. 33, pp. 19-33.
9. C. Rukchon S. Trevanich T. Jinkarn and P. Suppakul, 2011. "Volatile compounds as quality indicators of fresh chicken and possible application in intelligent packaging", *Proceedings of the 12th Asean Food Conference*, Bankok, Thailand, 16-18 juin, pp. 287-294.
10. A. Pacquit J. Frisby D. Diamond K. Tong Lau A. Farrell B. Quilty and D. Diamond, 2007. "Development of a smart packaging for the monitoring of fish spoilage", *Food Chemistry*, vol. 102, pp. 466-470.
11. L. Jacxsen F. Devlieghere and J. Debevere, 2002. "Predictive modeling for packaging design: equilibrium modified atmosphere packages of fresh-cut vegetables subjected to a simulated distribution chain", *International Journal of Food Microbiology*, vol. 73, pp. 331-341.
12. A. Allende E. Aguayo and F. Artes, 2004. "Microbial and sensory quality of commercial fresh processed red lettuce throughout the production chain and shelf life", *International Journal of Food Microbiology*, vol. 91, pp. 109-117.
13. M. Barth T.R. Hankinson H. Zhuang and F. Breidt, 2009. "Microbiological spoilage of fruits and vegetables", In: W.H. Sperber, M.P. Doyle (eds), *Compendium of the Microbiological Spoilage of Foods and Beverages, Food Microbiology and Food Safety*, Springer, New York, pp. 135-183.
14. R.W.G. Hunt, 1991. Measuring color, 2nd Ed., Ellis Horwood Ltd, Chichester, UK.
15. A.B. Smith P.C. Talasila and A.C. Cameron, 1999. "An ethanol biosensor can detect low-oxygen injury in modified atmosphere packages of fresh-cut produce", *Postharvest Biology and Technology*, vol. 15, pp. 127-134.

# Development and Properties of High Density Polyethylene (HDPE) and Ethylene-vinyl Acetate Copolymer (EVA) Blend Antioxidant Active Packaging Films Containing Quercetin

**Tiantian Han[1], Lixin Lu[1,2*], Changfeng Ge[3] and Yali Tang[1,2]**

*[1]Department of Packaging Engineering, Jiangnan University,Wuxi 214122, China*
*[2]Jiangsu Province Key Laboratory of Advanced Food Manufacturing Equipment and Technology, Wuxi 214122, China*
*[3]Department of MMET/Packaging Science, Rochester Institute of Technology, 78 Lomb Memorial Drive, Rochester, NY 14623, USA*

*[*]Corresponding author. Email:lulx@jiangnan.edu.cn*

**Abstract:** Antioxidant active packaging is a promising technology for extending shelf life of lipid-rich food products.In order to secure the safety of the active package, the using of natural antioxidants is the trend.In this study,high Density Polyethylene (HDPE) and ethylene-vinyl Acetate Copolymer (EVA) bend films incorporated with quercetin as the bioactive antioxidant were successfully developed by the method of flat compression. The mass ratio of HDPE/EVA was 65:35.The addition percentages of quercetin were 0.74% and 1.23%, respectively. This film making method could keep the quercetin retention percentage in a higher level which was 96.75% in this study. The addition of quercetin did not modify greatly the film’ s thermal stability. In addition, the barrier performance for water vapor and oxygen of the active films were kept well with the presence of quercetin. Release quantity of quercetin from the active antioxidant films into 50% (simulant for high alcohol containing products and milk and some dairy products) and 95% ethanol (simulant for fatty food products) at 37 ℃ was periodically measured by HPLC system for 45 days. In 50% ethanol and 95% ethanol, the release extent and kinetics of quercetin differed largely. The ultimate release content of quercetin in 50% ethanol and 95% ethanol were 70% and 10%, respectively. The diffusion of antioxidant showed a Fick's behavior with its diffusion coefficient (D) falling in $10^{-13}$ and $10^{-15}$ $m^2/s$ and partition coefficient in 44 and 5863.The obtained films showed good release profiles. Packaging applications of these films can improve food stability and provide another method for adding bioactive compounds and making films.

Keywords:HDPE, EVA, quercetin, antioxidant, food packaging, simulant.

## INTRODUCTION

In various nutrients that can maintain sustainable growth and development for humanity and animals, lipid is the primary nutrient for storage and supply of energy and plays an important role in the sensorial quality of foods. However, the lipid is susceptible to the effects of external environment. Lipid oxidation is one of the major factors that determine food quality loss and shelf-life reduction. Therefore, delaying lipid deterioration is vitally important for food manufacturer[1]. Oxidative process in food products lead to the degradation of lipids and pr-

oteins[2], flavour and color changes[3], enzymatic and nonenzymatic affect[4,5], even food poisoning, which all of these will finally results in not acceptable of the foods by consumers.

Oxidative rancidity of lipid is the main reason for the off-flavors and metamorphism which decrease nutritional and sensory qualities[1]. In order to prevent or retard the oxidative rancidity of foodstuffs, there are mainly two kinds of methods. The one is adding antioxidants in the production process of foods. For instance, Sesamol, tocopherol and their mixture were added into vegetable oils to retard oxidative deterioration[6]. Lipid oxidation of raw turkey meatballs were studied with the addition of oil-soluble rosemary extract and BHT[7]. Other Effects of antioxidant plant extracts and synthetic antioxidants on oxidative stability was studied[4,8,9,10].

The other method is active packaging. Compared with traditional package forms, active packaging is an innovative concept which can be defined as a mode of packaging in which the package, the product, and the environment interact to prolong shelf life or enhance safety or sensory properties, while maintaining the quality of the product[11~13]. Antioxidant (AO) packaging technology belongs to the categories of this new packaging. So AO packaging can be defined as a version of active packaging in which the package, the product and the environment interact to limit or prevent lipid oxidation by donating electrons or hydrogens, quenching oxygen and/or scavenging free radicals[1]. By incorporating antioxidants into packaging materials[1,13~22] or coating antioxidants on the surface of the materials[23~25], the packaged food can be effectively protected and the oxidative rancidity can be retarded.

As a natural antioxidant, quercetin is a kind of polyphenols widely existed in edible and nonedible with high antioxidant activity[4,26,27]. Apart from its antioxidant property, the addition of quercetin can also protect the polymer from degradation. High density polyethylene (HDPE) possesses high degree of crystallinity which makes the release of quercetin difficult and slow. Whereas, Ethylene-vinyl acetate copolymer (EVA) with a low crystallinity can makes the release of quercetin easy and fast. So the blending of these two materials can reach the goal of appropriate release of quercetin.

The aim of the present work was to a)characterize the blending properties of HDPE/EVA as food packaging film;b)study the effect of quercetin on the blending film;c)determine the release kinetics of quercetin from the blending film into two different food simulants.

## MATERIALS AND METHODS

### Chemicals and reagents

HDPE (DGDA6098) was purchased from China Petroleum & Chemical Corporation (Zibo, Shandong, China). EVA with a 14% vinyl acetate content was from Beijing Eastern Petrochemical Co.,Ltd(Beijing, China). Quercetin standard was purchased from Chinese Inspection Institute of Pharmaceutical and Biological Products. Quercetin, methanol (HPLC grade), phosphate (AR) was purchased from Sinopharm Chemical Reagent Co., Ltd(Shanghai, China). Water was obtained from Wahaha Ltd(Hangzhou, Zhejiang, China).

### Film manufacturing

Three formulations of HDPE/EVA blend films, containing 0% quercetin(blank), 0.74% quercetin(Q 0.74%), and 1.23% quercetin(Q 1.23%) in which the HDPE/EVA mass ratio is 65:35. Table 1 shows the composition of each sample and the extractable mass of quercetin. The films were obtained with the following steps: the melt blending with a two roll mixing mill for Plastics (Shanghai Rubber Machinery Factory,Shanghai,China), the flat compression with a flat vulcanizing machine, shaping with a Pressure Forming Machine (Wenlin Chemical Machinery Factory,Jiangyin,Jiangsu,China).

Film thickness was determined with a micrometer. Five replicates were taken and the data were expressed in micrometers.

**Table 1:** Composition of each sample and the extractable mass of quercetin

| Film | HDPE(g) | EVA(g) | Initial loading of Quercetin | Extractable quercetin(g) |
|---|---|---|---|---|
| blank | 130 | 70 | 0 | 0 |
| Q 0.74% | 130 | 70 | 1.5 | 1.45 |
| Q 1.23% | 130 | 70 | 2.5 | 2.42 |

The film samples obtained through the above method were kept in aluminum/LDPE bags at room temperature before analysis . In this paper, thermal properties, oxygen and water vapor barrier properties and the release properties of quercetin from the films were analyzed.

The quercetin retention content in the films was determined by extraction two times in ethanol at 65℃ for 5h. The concentration was then measured by HPLC.

## Thermal Analysis

Thermogravimetric analyses were carried out using a TA Q500 thermal analyzer(New Castle, USA). Square parts were cut from the testing samples and then the small parts (ca. 5mg) were heated from 30℃ to 550℃ with a heating rate of 10℃/min under a nitrogen protection atmosphere of 40 mL/min. Then the mass changes of different samples with the growth of time were obtained from which the degradation temperatures of the antioxidant blend films. All thermal analyses were done in triplicate.

## Barrier properties

*Water vapor permeability(WVP)*.WVP tests were carried out at 90% RH using a water vapor permeability tester (Model:TSY-T, Labthink, Jinan, Shandong, China).The samples to be tested were cut into round pieces by a metal sampler. Each sample was tested in triplicate.

*Oxygen permeability*.The oxygen permeability were determined at 50% RH and 23℃ by using an oxygen permeability tester (Model: BTY-B1, Labthink, Jinan, Shandong, China). The samples to be tested were cut into round pieces by a metal sampler. Before on-machine testing, it was necessary for the sample conditioning in the dryer to remove the moisture in the packaging material for at least 24h. Each sample was tested in triplicate.

## Antioxidant release tests

To simplify and standardize the release test procedure, the European union (EU) has defined the simulants that can be used (Commission Directive 2007/19/EC,2007).The regulation about the simulants were as follows: water was used for aqueous foodstuffs; 3% acetic acid was used for acidic foodstuffs with pH＜4.5; 10% ethanol was used for alcoholic foodstuffs; 50% ethanol was used for high alcohol containing products and milk and some dairy products; and 95% ethanol was used for fatty food products[28].

The quercetin migration studies were conducted at 37℃. Film Q 0.74% was cut into rectangle pieces (~20mm×150mm) and then accurately weighed and determined the thicknesses. One rectangle piece and 40mL food stimulant (95% ethanol or 50% ethanol) were then together placed in a borosilicate glass vial (12.5 cm high×4.3 cm diameter) with PTEF septum and PP lid. The glasses containing films were put in an incubator (Nuoji, Changzhou, Jiangsu, China) without illumination. All the vials were shook manually two times every day to minimize mass-transfer resistance of quercetin from the films. Periodically, 1 mL liquid was taken from each

vial for test and then 1mL same simulants was added into the vials to make the volume of the simulant keep stationary.

## Quantification of quercetin in simulants

HPLC was used for determining the concentration of quercetin in different food simulants. The HPLC measurements were performed by a Dionex HPLC system (USA) equipped with a binary pump, an auto-injector (SIL-20AC HT), a UV detector, and a column (Acclaim 120-C18). The quercetin concentrations in different food simulants were analyzed using isocratic mode of methanol: 0.2% phosphate(v/v, 50:50) at a flow rate of 1.0 mL $min^{-1}$. 10 μL of the simulants were injected into an AcclaimTM 120-C18 (250mm×4.6mm, 5μm) column. The detection wavelength was 360 nm and the detection temperature was 30℃. The quercetin standard was used for making the standard curve. Precision of the HPLC method was evaluated by measuring one sample six times (RSD=0.37%). Stability was evaluated by measuring one sample at 0, 2, 4, 8, 12and 24 h respectively (RSD=0.34%). Repeatability was evaluated by taking 6 samples from one extraction and quantifying the quercetin concentration in each sample (RSD=1.08%). Recovery tests were accomplished by adding quercetin standard to samples in which the quercetin concentration was already known and then determining the total concentration in the sample(RSD=1.77%). Linear regression analysis showed a linear relationship between peak area and concentration of quercetin standard. The linear range was from 1.6 $\mu g \cdot mL^{-1}$ to 400 $\mu g \cdot mL^{-1}$, and the correlation coefficient ($R^2$) was 0.9995. At the end of each detection, the whole chromatographic system was rinsed with water/methanol 90:10 (v/v) for 0.5 h and then with methanol for 1h.

## Determination of partition and diffusion coefficients

*Estimation of partition coefficient.* After a lengthy exposure time, the antioxidant quercetin would reach equilibrium. The extent of release at equilibrium is always characterized by the partition coefficient (*K*) which is calculated as

$$K = \frac{C_{P,\infty}}{C_{F,\infty}} \tag{1}$$

where $C_{P,\infty}$ and $C_{F,\infty}$ are the concentrations of antioxidant in the package material and in food at equilibrium respectively. When the release appears, the *K* can be calculated by $C_{P,\infty}$ and $C_{F,\infty}$ so as to evaluate the release extent.

*Estimation of diffusion coefficient.*The diffusion coefficients (D) of antioxidants were determined from the curve of release versus time. There were some assumptions in consideration: (1) mass-transfer resistance of antioxidants from the film surface into the food simulant was negligible; (2) initial concentration of antioxidants in the food simulant was zero; (3) there was no concentration gradient of antioxidants in the food simulant; (4) partition coefficient and diffusion coefficient were constant at a given temperature; (5) the volume of food simulant is much larger than that of the film (food simulant volume: film volume=333); (6)interactions between the food simulant and the film were not considered. With these consumptions, the following equation (Equation (2)) which is based on Fick's second law can be used[29]:

$$\frac{M_t}{M_\infty} = 1 - \frac{8}{\pi^2}\sum_{m=0}^{\infty}\frac{1}{(2m+1)^2} exp\left\{- D((2\mathrm{m}+1)^2\pi^2\mathrm{t}/l^2)\right\} \tag{2}$$

where $M_t$ is the amount of antioxidant in food stimulant at time *t*, $M_\infty$ is the amount of antioxidant in food

stimulant at equilibrium, $l$ is the thickness of the film, and $D$ is the diffusion coefficient.

When antioxidant release was too slow ($M_t/M_\infty \leq 0.6$) to reach equilibrium after a lengthy contact time, equation (2) can be simplified to equation (3) which is also widely used[30]:

$$\frac{M_t}{M_\infty} = 4\left(\frac{Dt}{4l^3\pi}\right)^{\frac{1}{2}} \tag{3}$$

If the antioxidant diffusion is Fickian, then a plot of $M_t/M_\infty$ versus $t^{1/2}$ ($M_t/M_\infty \leq 0.6$) should yield a straight line, and the diffusion coefficient (D) can be estimated from the slope of the straight line according to the following equation (4):

$$D = \pi\left(\frac{Sl}{2}\right)^2 \tag{4}$$

where S is the slope of one straight line for $M_t/M_\infty$ versus $t^{1/2}$.

### Statistical analysis

One-way analyses of variance were carried out. The SPSS computer programme (SPSS Inc., version 19) was used. Differences in paries of mean values were evaluated by the Tukey test for a confidence interval of 95%. Data are represented as means±standard deviation.

## RESULTS AND DISCUSSION

By flat compression, the antioxidant blending packaging films of HDPE/EVA incorporated in quercetin were successfully developed. The advantages of this method are: (a) development process is simple; (b) the temperature during film preparation is not very high and thus the retention of quercetin can keep a higher level; The developed transparent film with quercetin are slightly yellow, the surface is smooth, soft, and there are no voids and cracks. The thicknesses of the antioxidant films are 0.200~0.250mm.

By extracted in ethanol two times for 10h in 60℃, the quercetin quantities in antioxidant films were determined by HPLC.And the average retention rate was 96.75±0.8%.

### Thermal characterization

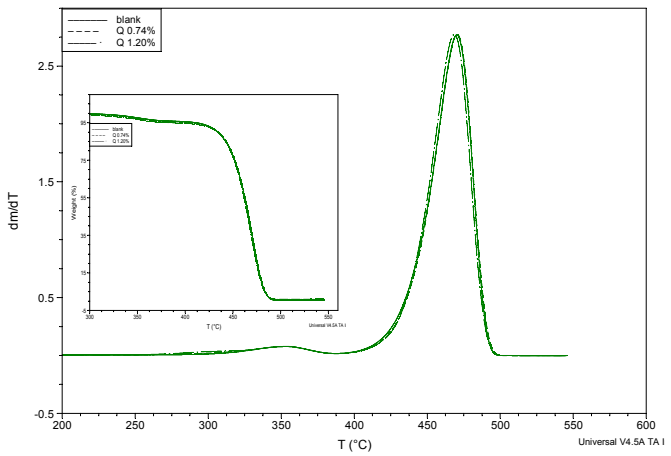


**Figure 1:** Weight loss and derivative of the weight of the developed materials

TGA test were conducted to study the addition influence of quercetin on the thermal stability of the polymer. The results of TGA analysis can determine degradation temperature of the tested materials. Figure 1 shows that the thermal stability of the polymer containing quercetin was not modified greatly by the addition of the natural antioxidant, because of the degradation of the obtained films occurring at the temperature near to the blank sample. As can be seen in Figure 1, the degradation temperatures of the films containing quercetin are near to that of the blank HDPE/EVA sample, which degrade at 368.71℃, compared to 368.36 and 369.47℃ for 0.74% and 1.23% quercetin. The degradation temperature is a reflection on the thermal stability of materials. From the analysis, slight effects of quercetin on the HDPE/EVA blend films can be concluded. This may be the result of the weak interaction between quercetin and polymer substrate.

## Barrier properties

**Table 2**: Oxygen and water vapor permeability values determined at 50% RH and 23℃ for the films developed by flat compression

| | oxygen permeability ($\times 10^{-13}$)/($cm^3 \cdot cm/(m^2 \cdot s \cdot Pa)$) | water vapor permeability ($\times 10^{-15}$)/($g \cdot cm/cm^2 \cdot s \cdot Pa$) |
|---|---|---|
| Blank | $2.39 \pm 0.08^a$ | $8.97 \pm 0.61^b$ |
| Q 0.74% | $2.45 \pm 0.06^a$ | $10.33 \pm 0.55^c$ |
| Q 1.23% | $2.82 \pm 0.02^b$ | $3.54 \pm 0.12^a$ |

*Water vapour permeability.* The water vapor permeability (WVP) values were determined for all samples at 90% RH and 23℃. Table 2 shows that the incorporation of quercetin effects the water vapor permeability of the antioxidant films greatly. When the quercetin addition was 0.74%, the WVP of the film can be raised to some extent, which may be a consequence of the crystal defects caused by the addition of quercetin. And when the addition is 1.23%, the WVP is reduced sharply, which might be the results of the hydrophobicity of quercetin[31].

*Oxygen permeability.* Table 2 also shows the oxygen permeability values for antioxidant films with different addition of quercetin at 50% RH and 23 ℃. As the addition of quercetin increased, the oxygen permeability coefficients are raised. When the addition is 0.74%, the barrier capability for oxygen of the films are not modified significantly. When it is 1.23%, the barrier capability are changed markedly. The presence of antioxidant quercetin may result in more crystal defects so that the passing of oxygen molecular through the films gets easier[31].

From the water and oxygen measured results, it can be concluded that the addition of quercetin did not modify the barrier properties of the HDPE/EVA blend films. The films containing quercetin present a medium permeability.

## Antioxidant release from the film

Figure 2 shows the release profile of quercetin from HDPE/EVA blend polymer films. In Figure 2A, 95% ethanol was chosen as the fatty simulant for fats, oil and fatty foods based on the similar hydrophobicity between 95% ethanol and lipid. Ethanol can be fully miscible in water, and can provide a more hydrophobic environment[32].

In Figure 2B, 50% ethanol was used as the simulant for dairy products which is recommended by the European commission.

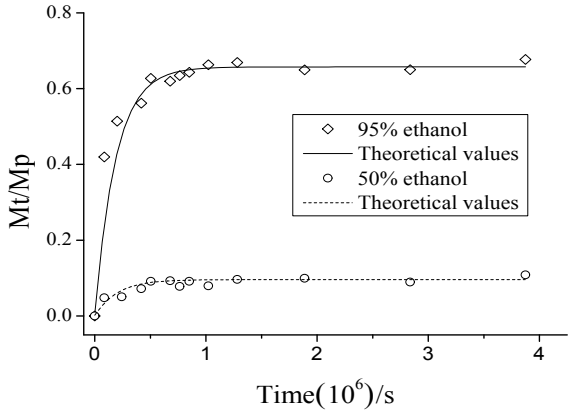



**Figure 2:** Release of quercetin from HDPE/EVA blend packaging films in different simulants

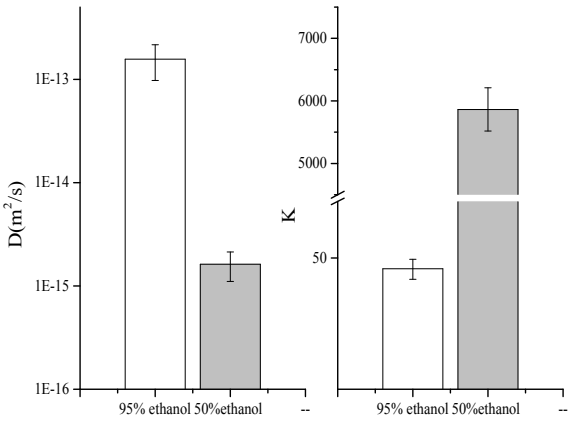



**Figure 3:** Diffusion (D) and Partition (K) coefficient values for the migration of quercetin from HDPE/EVA based packaging films into different food simulants

The release of quercetin from the films into different food simulants was measured by HPLC at 37 ℃. As showed in Figure 2, the cumulation of quercetin from films into simulants follows an "exponential growth to a maximum" type of file with the release extent and kinetics differs from each other greatly. From Figure 2, same release equilibration time for quercetin can be concluded--about 11 days.

By comparing Mt/Mp in equilibrium, notable differences between release extent of quercetin into 95% ethanol and 50% ethanol can be seen easily. Release of quercetin from 95% ethanol is much more complete than that from 50% ethanol. The final release of quercetin from films into 95% ethanol and 50% ethanol are 70% and 10%, respectively. The release extent at equilibrium is determined largely by the compatibility between the antioxidant and the simulant. The partition coefficient (K) can be used to characterize the release extent intuitively, which is defined as the ratio of the concentration of quercetin in the package to that in the simulant at equilibrium. The K values are showed in Figure 3. Quercetin are highly soluble in ethanol so that the release of quercetin into 95% ethanol reach almost full extraction with a K below 100[31,33]. In opposite, the solubility quercetin can hardly dissolve in water so that the release of quercetin into 50% ethanol is limited greatly compared with that into 95% ethanol with a K of 103.

Figure 2 also reveals that the kind of simulant can also change the kinetics of the release. Diffusion (D) coefficient which is defined in Fick's laws is usually used to characterize the kinetics of migrant releasing from

polymer materials. From the release of quercetin during storage, the D values is calculated according to Equation (4). The D values of different samples are shown in Figure 3. There is a big difference of two orders of magnitude between D values in 95% ethanol and 50% ethanol. The smooth curves in Figure 2 are the theoretical values of release which depict the experimental data quite well, indicating that releases of quercetin are in accordance with Fick's laws.

For different simulants, the releases of quercetin possess different release properties. Apart from different solubility of quercetin, the plasticization effect of low molecular weight alcohols on polymer bases may be another important factor. When plastizing in presence, the chains of polymer can be more flexible, which can accelerate the release rate of antioxidant.

## CONCLUSIONS

The results stand for that antioxidant food films having been successfully developed through the method of flat compression by incorporating quercetin into HDPE/EVA blend matrix. With the presence of quercetin, the thermal and barrier properties of the materials maintain the major properties of HDPE/EVA film. Because of difference of concentrations existing between package films and simulants, quercetin releases from the polymer materials to simulants, which is also applicable to the contact with real foods and reaches the goal of protecting foods from going bad quickly. The release of quercetin into 95% ethanol and 50% ethanol follows Fick's law. Therefore, the HDPE/EVA films with quercetin are proved to be effective for fatty and dairy products. Further studies could put more efforts on the controlled release of antioxidant from the package films into foods.

## ACKNOWLEDGEMENTS

This work was supported by the Achievements Industrialization Prospective Research Project of Jiangsu Province (Grant No. BY2013025-26), by the Innovation and Technology Fund of Jiangnan University (Grant No. 2009CXTD01), and by the Fundamental Research Funds for the Central Universities (Grant No. JUSRP51403A).

## REFERENCES

1. P Phoopuritham. M Thongngam and R Yoksan et al, 2012, "Antioxidant Properties of Selected Plant Extracts and Application in Packaging as Antioxidant Cellulose-Based Films for Vegetable Oil", *Packaging Technology and Science*, vol. 25, no. 3, pp. 125-136.

2. E.A. Decker. W.K.M. Chan and S.A. Livisay et al, 1995, "Interactions Between Carnosine and the Different Redox States of Myoglobin", *Journal of Food Science*, vol. 60, no. 6, pp.1201-1204.

3. E.A. Decker and A.D. Crum, 1991,"Inhibition of Oxidative Rancidity in Salted Ground Pork by Carnosine", *Journal of Food Science*, vol. 56, no. 5, pp. 1179-1181.

4. D.S. Waterhouse. D Xue and S Wadhwa, 2013, "Effects of Added Phenolics on the Lipid Deterioration and Antioxidant Content of Deep-Fried Potato Fritter", *Food and Bioprocess Technology*, vol. 6, no. 11, pp. 3256-3265.

5. A.F. Doblado-Maldonado. O.A. Pike and J.C. Sweley et al, 2012, "Key issues and challenges in whole wheat flour milling and storage", *Journal of Cereal Science*, vol. 56, no. 2, pp.119-126.

6. H. Yoshida and S.Takagi, 1999, "Antioxidative effects of sesamol and tocopherols at various concentrations in oils during microwave heating", *Journal of the Science of Food and Agriculture*, vol. 79, no. 2, pp. 220-226.

7. M.K. Tymoszczyk, 2014, “The effect of antioxidants, packaging type and frozen storage time on the quality of cooked turkey meatballs”, *Food Chemistry*, vol. 148, pp.276-283.

8. M. Pateiro. J.M. Lorenzo and I.R. Amado et al, 2014, “Effect of addition of green tea, chestnut and grape extract on the shelf-life of pig liver pate”, *Food Chemistry*, vol. 147, pp.386-394.

9. M. Estevez. R. Ramirez and S. Ventanas et al, 2007, “Sage and rosemary essential oils versus BHT for the inhibition of lipid oxidative reactions in liver pate”, *LWT-Food Science and Technology*, vol. 40, no. 1, pp.58-65.

10. A.A. Wani. D.S. Sogi and P Singh et al, 2013, “Impacts of Refining and Antioxidants on the Physico-Chemical Characteristics and Oxidative Stability of Watermelon Seed Oil”, *Journal of the American Oil Chemists Society*, vol. 90, no. 9, pp.1423-1430.

11. A Lopez-Rubio. J.M. Lagaron, 2011, “Improved incorporation and stabilisation of beta-carotene in hydrocolloids using glycerol”, *Food Chemistry*, vol. 125, no. 3, pp. 997-1004.

12. S Quintavalla. L. Vicini, 2002, “Antimicrobial food packaging in meat industry”, *Meat Science*,vol. 62, no. 3, pp.373-380.

13. P. Suppakul, J. Miltz and K. Sonneveld et al, 2003, “Active Packaging Technologies with an Emphasis on Antimicrobial Packaging and its Applications”, *Journal of Food Science*, vol. 68, no. 2, pp.408-420.

14. C. Lopez-de-Dicastillo. D. Pezo and C. Nerin et al, 2012, “Reducing Oxidation of Foods Through Antioxidant Active Packaging Based on Ethyl Vinyl Alcohol and Natural Flavonoids”, *Packaging Technology and Science*, vol. 25, no. 8, pp.457-466.

15. X .Zhu. K. Schaich and X. Chen et al, 2013, “Antioxidant Effects of Sesamol Released from Polymeric Films on Lipid Oxidation in Linoleic Acid and Oat Cereal”, *Packaging Technology and Science*, vol. 26, no. 1, pp.31-38.

16. S. Gemili. A. Yemenicioglu and S.A. Altınkaya, 2010, “Development of antioxidant food packaging materials with controlled release properties”, *Journal of Food Engineering*, vol.96, no. 3, pp.325-332.

17. M. Jamshidian. E.A. Tehrany and M. Imran et al, 2012, “Structural, mechanical and barrier properties of active PLA-antioxidant films”, *Journal of Food Engineering*, vol. 110, no. 3, pp.380-389.

18. C. Colin-Chavez. H. Soto-Valdez and E. Peralta et al, 2013, “Fabrication and Properties of Antioxidant Polyethylene-based Films Containing Marigold (Tagetes erecta) Extract and Application on Soybean Oil Stability”, *Packaging Technology and Science*, vol. 26, no. 5, pp. 267-280.

19. D.G. Granda-Restrepo. E. Peralta and R. Troncoso-Rojas, 2009, “Release of antioxidants from co-extruded active packaging developed for whole milk powder”, *International Dairy Journal*, vol. 19, no. 8, pp. 481-488.

20. K. Norajit. K.M. Kim and G.H. Ryu, 2010, “Comparative studies on the characterization and antioxidant properties of biodegradable alginate films containing ginseng extract”, *Journal of Food Engineering*, vol. 98, no. 3, pp.377-384.

21. F. Manzanarez-Lopez. H. Soto-Valdez and R. Auras et al, 2011, “Release of alpha-Tocopherol from Poly(lactic acid) films, and its effect on the oxidative stability of soybean oil”, *Journal of Food Engineering*, vol. 104, no. 4, pp. 508-517.

22. L. Boragno. P. Stagnaro and S. Losio et al, 2012, "LDPE-Based Blends and Films Stabilized with Nonreleasing Polymeric Antioxidants for Safer Food Packaging", *Journal of Applied Polymer Science*, vol. 124, no. 5, pp. 3912-3920.

23. D.A. Pereira de Abreu. P.P. Losada and J. Maroto et al, 2011, "Natural antioxidant active packaging film and its effect on lipid damage in frozen blue shark (Prionace glauca)", *Innovative Food Science & Emerging Technologies*, vol. 124, no. 5, pp.50-55.

24. D.A. Pereira de Abreu. K.V. Rodriguez and J.M. Cruz, 2012, "Extraction, purification and characterization of an antioxidant extract from barley husks and development of an antioxidant active film for food package", *Innovative Food Science and Emerging Technologies*, vol. 13, pp.134-141.

25. D.A. Pereira de Abreu. P.P. Losada and J. Maroto, 2010, "Evaluation of the effectiveness of a new active packaging film containing natural antioxidants (from barley husks) that retard lipid damage in frozen Atlantic salmon (Salmo salar L.)", *Food Research International*, vol. 43, no. 5, pp.1277-1282.

26. D. Prochazkova. I. Bousova and N. Wilhelmova, 2011, "Antioxidant and prooxidant properties of flavonoids", *Fitoterapia*, vol. 82, no. 4, pp. 513-523.

27. A.W. Boots. G.R.M.M. Haenen and A. Bast,2008, "Health effects of quercetin: From antioxidant to nutraceutical", *European Journal of Pharmacology*, vol. 585, no. 2-3, pp.325-337.

28. Directive 2007/19/EC Commission Directive of 2 April 2007 amending Directive 2002/72/EC related to plastic materials and articles intended to come into contact with food and Council Directive 85/572/EEC laying down the list of simulants to be used for testing migration of constituents of plastic materials and articles intended to come into contact with foodstuffs.

29. J.M. Krochta, 2007, *Handbook of food engineering*, 2nd Ed., Taylor & Francis Group, New York, pp. 847-927.

30. M. Hamdani. A. Feigenbaum and J.M. Vergnaud, 1997, "Prediction of worst case migration from packaging to food using mathematical models", *Food Additives and Contaminants*, vol. 14, no. 5, pp. 499-506.

31. C. Lopez-de-Dicastillo. J.M. Alonso and R. Catala et al, 2010, "Improving the antioxidant protection of packaged food by incorporating natural flavonoids into ethylene-vinyl alcohol copolymer (EVOH) films", *Journal of Agricultural and Food Chemistry*, vol. 58, no. 20, pp. 10958-10964.

32. M. Jamshidian. E.A. Tehrany EA and S. Desobry, 2012, "Release of synthetic phenolic antioxidants from extruded poly lactic acid (PLA) film", *Food Control*, vol. 28, no. 2, pp. 445-455.

33. X. Chen. D.S. Lee and X. Zhu et al, 2012, "Release Kinetics of Tocopherol and Quercetin from Binary Antioxidant Controlled-Release Packaging Films", *Journal of Agricultural and Food Chemistry*, vol. 60, no. 13, pp. 3492-3497.

# Nanoiron Based Composite Oxygen Scavengers

**Zenon Foltynowicz*, Wojciech Kozak**

*Faculty of Commodity Science, Department of Product Quality and Ecology,*
*Poznan University of Economics, Poland*

*Corresponding author. Email: zenon.foltynowicz@ue.poznan.pl*

**Abstract:** Man has grappled with the problem of food spoilage since the beginning of time. Thanks to serendipitous observations and methodical research, we have known for more than a century that the presence of oxygen is one of the key factor effecting food quality. The amount of oxygen in the packaging can be reduced by increasing the concentration of carbon dioxide and/or another gas (e.g. nitrogen), using modified atmosphere packaging, vacuum packaging, or active packaging with oxygen scavengers. Traditional commercial oxygen scavengers are based mainly on iron or its compounds. So far known oxygen absorbents based on iron and its compounds may be used only when at least small amounts of water are present in the packaging, what is limiting factor of their application. In this study new type of oxygen scavengers based on nanoiron will be presented. Why nanoiron? Nanoscale particles have a much larger surface area available for interaction with reagents than bulky particles leading to higher surface reactivity.
The iron nanoparticles were synthesized by reducing the iron salts with the reducing agent, e.g. sodium tetraborohydride. As results of investigation shows water or humidity as well as activators are not necessary for oxygen fixation by nanoiron. The simultaneous presence of CO2 and moisture has no negative influence of the oxygen absorption process.
The study also shows that nanoiron can be an active component of oxygen scavenging composites based on polymers commonly applied in packaging industry.

Keywords: oxygen scavenger, nanoiron based oxygen scavenger, nanoiron composites oxygen scavenger.

## 1 Introduction

The presence of oxygen is one of the key factor effecting food quality. Basically, oxygen can spoil food in several ways. First of all it causes oxidation of fats and oils and growth of aerobic microorganisms such as moulds. Even small amounts of residual oxygen in a food packaging can result in loss of freshness, discoloration, decomposition, unpleasant flavor, as well as in nutritional degradation of the product. The ascorbic acid content can be significantly affected by the level of dissolved oxygen in the juice as well as browning over the whole period of storage was significantly correlated to the level of dissolved oxygen [1]. Oxygen within the sealed package can reduce the quality of liquid-based food products with high oil content such as hot-filled meal-ready-to-eat (MRE) cheese spread, a component of military operational rations [2].
In other cases the oxygen presence in the packaging may cause corrosion, spoilage of medicaments, degradation of archive materials, etc.
Many degradation processes caused in foods by oxygen can be commonly delayed with the application of antioxidant agents. Even though antioxidants added directly into the food protect them from oxidizing, however, they do not meet consumers' preference for pure and natural food products.
Removing the oxygen from the packaging interior and from the liquid food and drinks is a way of extending their shelf-life and protection from the negative effects of contact with the oxygen.
The amount of oxygen in the packaging can be reduced by increasing the concentration of carbon dioxide and/or another gas (e.g. nitrogen), using modified atmosphere packaging, vacuum packaging, or active packaging with oxygen scavengers. However, vacuum and modified atmosphere packaging technologies common in the food industry do not remove oxygen completely. Small amounts of oxygen always remain in the package headspace and in food pores or permeate the barrier packaging film. In order to remove the oxygen residues from the gas filling the packaging and penetrating through the packaging material, as well as the oxygen produced inside the packaging during the processes taking place in the packed product the oxygen absorbents are used, i.e. the substances fixing the oxygen or reacting with it, creating the permanent compounds, neutral for the packed product [3].

Traditional commercial oxygen scavengers are based mainly on iron or its compounds. In such absorbents the iron compounds are used, like powdered ferrous oxide, ferrous carbonate and other ferrous compounds, which for inducing the reaction are connected with various catalysts, and also fine powdered iron[4].

So far known oxygen absorbents based on iron and its compounds may be used only when at least small amounts of water are present in the packaging, what is limiting factor of their application.

The aim of this study was to evaluate the effectiveness of composite oxygen scavengers based on defined nanoiron, working irrespective of the presence of moisture in the packaging or water activity of the product as well as in the absence of activators.
Why nanoiron? Nanoscale particles have a much larger surface area available for interaction with reagents than bulky particles leading to higher surface reactivity. According to Zhang, zero valent iron nanoparticles of a diameter 1-100 nm and with a surface area in the range 20-40 $m^2/g$, provide 10-1,000 times greater reactivity than granular iron, which has a surface area < 1 $m^2/g$ [5].

## 2 Materials and methods

The iron nanoparticles were synthesized by reducing the iron salts with the reducing agent, e.g. sodium tetraborohydride [5, 6].

The investigation of oxygen sorption capacity was based on determination of oxygen amount, which was absorbed by known amount of nanoiron from packaging of known volume, filled with air (containing 20.9% of oxygen). In the typical experiment the nanoiron and nanocomposite samples, of weight approx 1 g, have been placed in the glass vials of $260\pm1cm^3$ volume, similar to the one applied in [7]. Then each vial was tide closed. The closure was equipped with two valves enabling gas introduction and connection to apparatus. All operation were conducted in the oxygen free atmosphere warranted by the dry-box Lab Master 130 (M.Braun). . The gas samples for determining the oxygen content have been collected every day, from the first day to 30 days. The oxygen concentration inside them was measured using the O*xygen Analyzer* 9070 made by Teledyne Analytical Instruments. Determination of simultaneous influence of moisture and $CO_2$ on the sorption activity of nanoiron was made using the same procedure was as above, but the packaging was filled with the mixture of gases (20.95% of oxygen + 20% of carbon dioxide + 49.05% of nitrogen) instead of air and contained also the tampon soaked with 2 ml of water.

## 3 Results

The results of the tests of oxygen sorption in the packaging after a given time of nanoiron action are shown in Table 1. As results of investigation shows water or humidity as well as activators are not necessary for oxygen fixation by nanoiron. The simultaneous presence of $CO_2$ and moisture has no negative influence of the oxygen absorption process.

**Table 1.** The results of the tests of oxygen sorption in the packaging after a given time of nanoiron action.

| test day | Absorption from air | | Absorption in the presence of moisture and $CO_2$ | |
|---|---|---|---|---|
| | oxygen concentration after absorption [%] | amount of absorbed oxygen [%] | oxygen concentration after absorption [%] | amount of absorbed oxygen [%] |
| 0 | 20.95 | 0 | 20.95 | 0 |
| 1 | 9.45 | 54.89 | 6.62 | 68.4 |
| 2 | 6.08 | 70.98 | 3.46 | 83.48 |
| 3 | 4.51 | 78.47 | 1.97 | 90.6 |
| 4 | 0.71 | 96.61 | 0.000001 | 100 |
| 5 | 0.051 | 99.76 | 0.000001 | 100 |
| 6 | 0.0011 | 99.99 | 0.000001 | 100 |
| 30 | 0.000001 | 100.00 | 0.000001 | 100 |

## 3 Conclusions

The present study shows that nanoiron can be an active component of oxygen scavenging composites. Unlike absorbents so far applied on the basis of iron it doesn't require the presence of water in order to be active. It is creating new opportunities of using absorbents of this type in the case of dry food packaging or where water presence in the packaging is undesirable.
Scavengers based on the invention can be used in the form of sachets filled with the active material or in another form preventing the contact of nanoiron with the packaged product.
It is a well known fact that nanometals behave totally different from their ordinary counterparts. Depending on the need and the predicted application in packaging, nanoiron can be encased for example into such polymers as: polysiloxanes, modified cellulose acetate butyrate (CAB), polyamide, polyethylene, polyterephthalate ethylene (PET), cellulose derivatives, modified starch and biodegradable polymers, including, e.g., polylactic acid, polyhydroxybutyrate (PHB), polyoxymethylene (POM) or mixtures of these polymers what is outlined in a recently published our patent applications [6, 8].

## References


1. O. Solomon. U. Svanberg and A. Sahlström, "Effect of oxygen and fluorescent light on the quality of orange juice during storage at 8°C", *Food Chemistry* ; vol. 53 no.4, pp. 363–368.
2. C. Gomes. M.E. Castell-Perez. E. Chimbombi. F. Barros. D. Sun. J.D. Liu. H.J. Sue. P. Sherman. P. Dunne and A.O. Wright, 2009, "Effect of oxygen-absorbing packaging on the shelf life of a liquid-based component of military operational rations", *J Food Sci*.; vol.74, no. 4, pp.E167-76.
3. M.L. Rooney,1995, *Active Food Packaging*, Blackie Acadmic & Professional.
4. A.L. Brody. E.R. Strupinsky and L.R. Kline, 2001, *Active Packaging for Food Applications*, CRC Press, Boca Raton, Fla.
5. C.B. Wang and W.X.Zhang, 1997, "Synthesizing Nanoscale Iron Particles for Rapid and Complete Dechlorination of TCE and PCBs", *Environ. Sci. Technol.* Vol. 31, pp. 2154-2156.
6. Z. Foltynowicz. W. Kozak. J. Stoinska. M. Urbanska. K. Muc. A. Dominiak and K. Kublicka, 2011, *Nanoiron-based oxygen scavengers*, PCT/PL2011/050055.
7. S. Sängerlaub. D. Gibis. E. Kirchhoff. M. Tittjung. M. Schmid and K. Müller, 2013, "Compensation of Pinhole Defects in Food Packages by Application of Iron-based Oxygen Scavenging Multilayer Films" *Packaging Technology and Science*; vol. 26, pp. 17–30.
8. Z. Foltynowicz. W. Kozak. J. Stoinska. M. Urbanska. K. Muc. A. Dominiak and K. Kublicka, 2012, *Nanoiron-based oxygen scavengers*, WO 2012/091587 A1.

# Effect of Storage Conditions and Sulphur Compounds on the Activity of Palladium Based Oxygen Scavenging Films

**Selcuk Yildirim[*] and Nadine Renke**

*Institute of Food and Beverage Innovation, Zurich University of Applied Sciences, Switzerland*

[*]*Corresponding author. Email: selcuk.yildirim@zhaw.ch*

**Abstract:** Palladium acts a catalyst for the oxidation of hydrogen in the presence of oxygen. In a previous work, palladium was coated on a film using magnetron sputtering technology and the oxygen scavenging activity of the film was tested. In this study the influence of temperature and relative humidity on the scavenging activity of palladium coated films was evaluated. Oxygen scavenging rates increased from 145 ± 20 to 2653 ± 172 ml/(m2*h) as the temperature increased from -10°C to 60°C. However, an increase in relative humidity from 15% to 90% did not have a significant influence on the oxygen scavenging rates of the films. A very significant reduction in oxygen scavenging activity was observed when the active films were introduced into the packaging of different foodstuffs. Storing oxygen scavenging films in the presence of sulphur containing foods such as wine, coffee beans, grains of corn, sauerkraut and onion resulted in a reduction in the oxygen scavenging activity of the active films. The influence of different thiols, dimethyl sulfide (DMS) and sulphur dioxide (SO2) (that are naturally found in tested foods) on the oxygen scavenging activity were evaluated. Ethanetiol, and furylmethanethiol resulted in very fast deactivation of the catalyst at concentrations above 0.1 mmol/L. Propanethiol and DMS had a similar effect at concentrations above 0.01 mmol/L. Thiol and DMS concentrations of 1 µmol/L did not have a significant effect on the oxygen scavenging activity of the films. Wine containing 30 mg free SO2 also deactivated the catalyst, whereas SO2 free wine did not show any significant influence on the activity.

Keywords: active packaging, oxygen scavenger, palladium, sulphur inhibition.

## 1 Introduction

Active packaging is an innovative technology designed to enhance the shelf life of food while improving its quality, safety and integrity [1, 2]. During the last decades there has been a lot of research done to develop different active packaging technologies. Among these active packaging technologies, oxygen scavengers have vast potential, since the quality or safety of several packaged foods is influenced by the presence of oxygen in the packaging [3-6]. Food packers employ methods such as vacuum packaging, modified atmosphere packaging or gas flushing to remove the oxygen in the headspace of packages. However, a certain amount of residual oxygen remains in the packages due to insufficient evacuation of the headspace gases and the fact that oxygen that is dissolved in the food itself is subsequently released into the headspace. Oxygen scavengers can complement modified atmosphere packaging by removing the residual oxygen that remains in the headspace after the packaging process and/or the oxygen that permeates the packaging material during storage.

Typically oxygen scavenger technology is based on the oxidation of iron powder by chemical means, or the scavenging of oxygen through the use of enzymes [1, 7, 8]. In previous studies we developed an oxygen scavenging technology for food packaging applications based on palladium catalysis that removes the residual oxygen remaining in the packages after modified atmosphere packaging [9]. Palladium functions by acting as a catalyst for the oxidation of hydrogen in the presence of oxygen. The packaging material as well as the thickness of the palladium coating were optimized to increase the oxygen scavenging activity of the active film. The activity of the oxygen scavenging films was also tested in the presence of various foodstuffs. PET/SiOx films coated with palladium significantly inhibited vitamin C degradation in orange juice and orange segments and preserved the colour of ham [9]. These oxygen scavenging films also prolonged the microbiological shelf life of part baked bread [10].

The catalytic activity of metal catalysts can be influenced by environmental conditions such as relative humidity and temperature. It may also be inhibited by the presence of certain chemical compounds such as sulphur or chlorine compounds that degrade the performance of palladium based compounds [11, 12]. In this study, we evaluated the influence of storage conditions (relative humidity and temperature) and the influence of sulphur

compounds (naturally found in different foodstuffs) on the oxygen scavenging activity of palladium coated films.

# 2 Materials

## 2.1 Oxygen Scavenging film

The palladium based oxygen scavenging film (PET/SiOx/Pd) used in this study was produced using magnetron sputtering technology, as previously described [9].

## 2.2 Food systems

The following foodstuffs were used in this study: coffee beans (roasted, Max Havelaar, Zurich); grains of corn (Coop, Zurich); sauerkraut (cooked, Schöni, Oberbipp), 5 $cm^3$ pieces of onion (freshly sliced); red wine, 13% alcohol (with and without sulphur dioxide). The coffee beans, grains of corn and sauerkraut were removed from their packaging, weighed and then tested without performing any subsequent processing steps.

## 2.3 Chemicals

The following chemicals were used in this study: ethanethiol, 97% (Sigma Aldrich); 2-Furylmethanethiol, ≥97% (Sigma Aldrich); 1-Propanethiol, 99% (Sigma Aldrich); dimetyhyldisulfide; ≥98% (Fluka); hydrogen sulfide; ≥98% (Fluka); L-Cysteine ≥98.5% (Fluka); sodium acetate, ≥99% (Sigma Aldrich); acetic acid ≥99.7% (Sigma Aldrich)

# 3 Methods

## 3.1 Determination of the effect of temperature on oxygen scavenging activity

Airtight steel chambers with a total volume of 86.2 cm3 was used for oxygen scavenging measurements. The chamber contained two valves for gas flushing and a plexiglass lid. An oxygen-sensitive sensor spot (PSt6 sensor, 5 mm diameter, Presens, Regensburg, Germany) was fixed to the inner side of the plexiglass lid to measure the oxygen concentration. A section of palladium coated film was cut (5 cm x 5 cm) and placed in the chamber. Additionally, a temperature datalogger was placed in one steel chamber to record temperature changes inside. All the steel chambers were placed in a temperature controlled climatic chamber until the internal temperature reached the same temperature as the climatic chamber (at constant relative humidity of 57%). Afterwards, the steel chamber was flushed with a gas mixture containing 1% oxygen, 3% hydrogen and 96% nitrogen (PanGas AG, Dagmarsellen). When the gas in the chamber reached equilibrium, the valves were closed and measurement of the oxygen began. The oxygen scavenging test at -10°C was performed in a cold room. The oxygen concentration in the chamber was measured by a non-destructive measurement method using fiber optic optodes (Fibox 3 LCD, Presens, Regensburg, Germany). Oxygen concentrations were measured by linking a light-emitting (600–660 nm) optical fiber to the sensor spot (from the outside of the plexiglass). The sensor emits more or less luminescence depending on the oxygen concentration in the sample.

## 3.2 Determination of the effect of relative humidity on oxygen scavenging activity

The effect of relative humidity on oxygen scavenging activity was measured in a similar way to that described in section 3.1. However, temperature in the climatic chamber was kept constant at 40°C and the relative humidity in the climatic chamber varied (15-90%). A relative humidity data logger was placed in one steel chamber to measure the internal relative humidity of the chamber. The measurement of oxygen concentrations in the steel chamber was started when the relative internal humidity reached the adjusted relative humidity of the climatic chamber.

## 3.3 Measurement of oxygen scavenging activity in the presence of foodstuffs

50 g of the foodstuff listed in section 2.2 were placed in glass petri dishes. Afterwards the petri dishes were placed in a tray (APET/PE, Staeger Co AG, Muri) and packaged under a modified atmosphere (1% oxygen, 3% hydrogen, 96% nitrogen) with scavenger film (5 x 15 cm). The trays were sealed with a PETP/PE/EVOH/PE lid (Hawa, Sulzbach) using a tray sealer (Multivac, T200, Hünenberg, CH). The headspace volume was approximately 203 ml. The packaged foods were stored at room temperature and changes in the oxygen concentration in the packages were recorded using the non-destructive measurement method described in section 3.1.

### 3.4 Measurement of oxygen scavenging activity in the presence of sulphur compounds

The sulphur compounds listed in section 2.3 were diluted with a buffer solution (sodium acetate – acetic acid buffer with a pH of 5). 50 ml of the diluted solution was transferred into a glass petri dish. Afterwards the petri dish was packaged as described in section 3.3, stored at room temperature and the changes in oxygen concentration in the package were recorded using the non-destructive measurement method described in section 3.1.

## 4. Results & Discussion

### 4.1 Influence of temperature on the oxygen scavenging activity of palladium based oxygen scavengers

To elucidate the influence of temperature on the oxygen scavenging kinetics of palladium based oxygen scavenging film, films were stored at different temperatures (-10°C to 60°C) and the oxygen scavenging kinetics were recorded. At -10°C the oxygen scavenging rate (OSR) was 145 ± 20 (ml/$m^2$*h). At 5°C, which is of interest for refrigerated products, an OSR of 350 ± 25 (ml/$m^2$*h) was recorded. As can be seen in Figure 1, as the temperature increased the also OSR increased to 2653 ± 172 (ml/$m^2$*h).

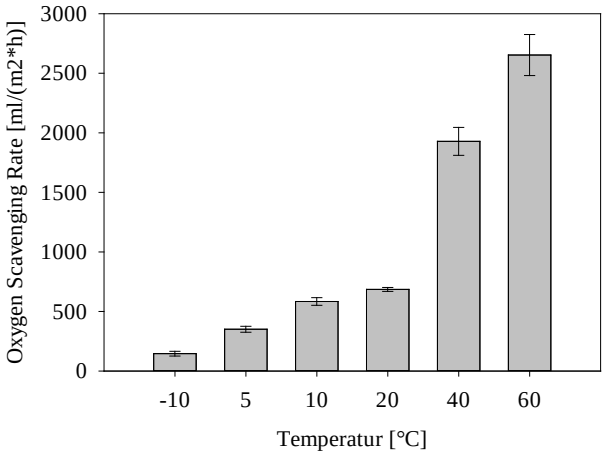



**Figure 1.** Oxygen scavenging rates of palladium based oxygen scavenging films at different temperatures

### 4.2 Influence of relative humidity on the oxygen scavenging activity of palladium based oxygen scavengers

The effect of relative humidity on the oxygen scavenging activity of palladium based oxygen scavengers was tested by storing the oxygen scavenging films at different relative humidities (15-90%) and tracking the oxygen concentration. As can be seen in Figure 2, oxygen scavenging activity was not significantly affected by the relative humidity of the environment. In all cases, it was possible to remove the oxygen within 10-16 minutes.

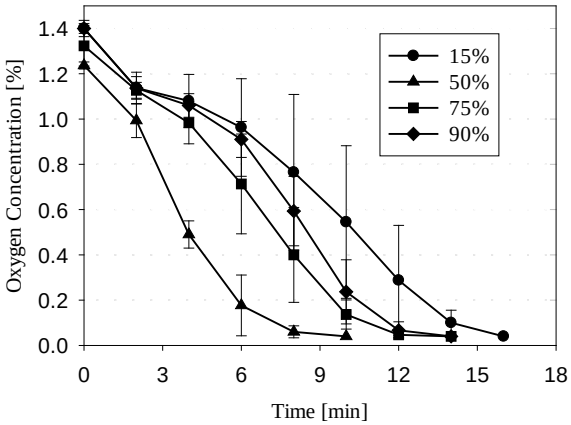



**Figure 2.** Oxygen scavenging rates of active films at different temperatures

### 4.3 Effect of the presence of food on the oxygen scavenging activity of palladium based oxygen scavengers

In order to elucidate the effect of foods containing sulphur compounds on the oxygen scavenging activity of palladium based oxygen scavengers, coffee beans, grains of corn, sauerkraut and onions were packaged using scavenging films and the oxygen concentrations in the packages were tracked. Coffee beans had the strongest inhibitory effect (Figure 3). The oxygen concentration in the headspace of the package decreased to 0.87% within 3 minutes and subsequently remained constant. When sauerkraut, was packaged using oxygen scavenging films, the oxygen concentration decreased to 0.7% within four minutes and subsequently remained almost constant. Grains of corn and onion showed similar inhibitory patterns, however the oxygen concentrations were reduced by up to 0.56 %.

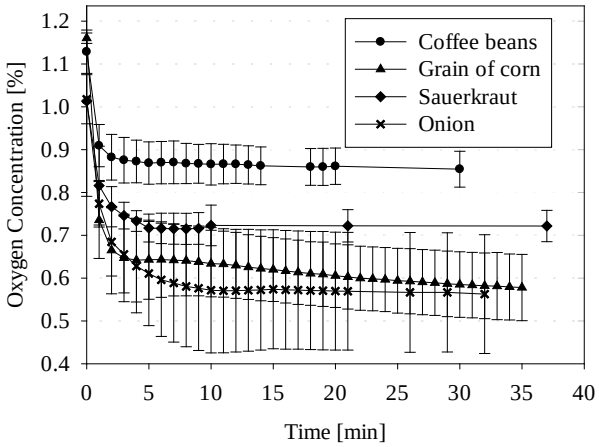



**Figure 3.** Oxygen scavenging activities of palladium based oxygen scavenging films in the presence of different foodstuffs containing sulphur compounds

### 4.4 Effect of sulphur compounds on the oxygen scavenging activity of palladium based oxygen scavengers

To evaluate the effect of sulphur compounds on the oxygen scavenging activity of palladium based scavengers, buffer solutions containing different sulphur compounds at various concentrations were packaged using active films and the oxygen scavenging kinetics were tracked. Propanethiol and hydrogen sulfide showed the strongest inhibitory effects (Figure 4). Concentrations of 0.1 and 1 mmol/L inhibited the activity almost completely. At a concentration of 0.01 mmol/L, the residual oxygen concentrations after 30 minutes were 0.62 and 0.67%, respectively. At a concentration of 1 µmol/L, the oxygen concentrations decreased to less than 0.1%. Hydrogen

sulphide is found in grains of corn [13] and sauerkraut [14] which also showed a strong inhibitory effect on the scavenging activity. Furylmethanethiol showed only a slightly lower inhibitory effect compared to propanethiol and hydrogen sulphide at concentrations of 0.1 and 1 mmol/L. However at a concentration of 0.01 mmol/L, oxygen concentrations decreased to 0.24, which is significantly lower. Furylmethanethiol is found in coffee [15] and could be the component responsible for the inhibition of scavenging activity in the presence of coffee beans. Ethanethiol showed a similar inhibitory effect at 1 mmol/L. At lower concentrations the inhibitory effect was lower than for the other compounds. Besides hydrogen sulphide, grains of corn also contain ethanethiol.

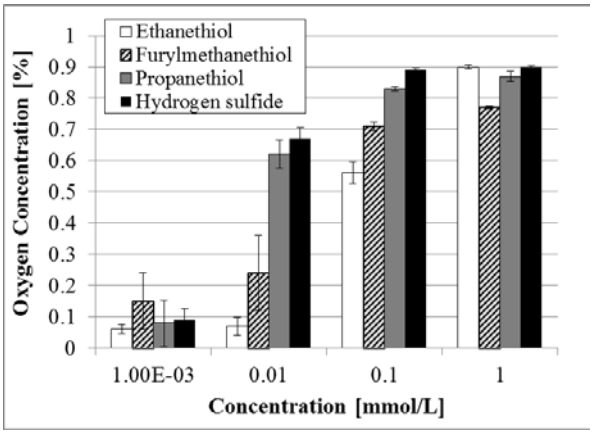



**Figure 4.** Oxygen concentrations in the headspace of packages using oxygen scavenging film (5x15 cm) and containing buffer solutions with different concentrations of sulphur compounds. The initial oxygen concentration is 1 %, the data shows oxygen concentrations after 30 minutes

Additional to the sulphur compounds presented above, the inhibitory effect of dimethyldisulfide in buffer solutions and sulphur dioxide in wine was also evaluated. Dimethyldisulfide at concentrations of 16 mmol/L and 0.1 mmol/L inhibited the oxygen scavenging activity and after 30 minutes resulted in oxygen concentrations of 0.8 and 0.59%, respectively. Sauerkraut [14] and onion [16] contain dimethyldisulfide. To evaluate the effect of sulphur dioxide in wine, wine without sulphur dioxide and wine with 30 mg/L of sulphur dioxide were both tested. As a control a 13% ethanol solution was used. Ethanol and wine without sulphur dioxide did not exhibit a major effect on the scavenging activity and it was possible to reduce the oxygen concentrations within 30 minutes to 0.05 and 1.7 %, respectively. However wine with sulphur dioxide inhibited the scavenging activity after 4 minutes from which point the oxygen concentrations remained constant at 0.7%.

## 5 Conclusions

Palladium based oxygen scavengers are inhibited by coffee beans, grains of corn, sauerkraut, onion and wine in packages. It was shown that the sulphur compounds found in these foodstuffs could be responsible for this inhibitory effect since such compounds also exhibited inhibitory effects when exposed to buffer solutions. The inhibitory effect of sulphur compounds is concentration dependent. The volatility of such compounds in foodstuff is likely to play an important role in inhibiting the scavenger. EFSA panel on food contact materials, enzymes, flavourings and processing aids recently published that the active substances palladium and hydrogen do not raise a safety concern for the consumer when used as an oxygen scavenger in packages for foods and beverages at room temperatures or below [17]. Palladium should not be in direct contact with food and should be incorporated in a passive structure impermeable to liquids which prevents the migration at detectable levels. Such scavenger concepts with different food contact layers are being evaluated.

## References

1. D.A.P. de Abreu.J.M. Cruz, and P.P. Losada, 2012, “Active and intelligent packaging for the food industry”, *Food Reviews International*, vol. 28, no. 2, pp. 146-187.

2. S. Yildirim 2011,“Active packaging for food biopreservation”, In C. Lacroix, *Protective cultures, antimicrobial metabolites and bacteriophages for food and beverage biopreservation*, Woodhead Publishing, Cambridge, pp. 460-489.

3. D.S. Lee 2010,“Packaging and the microbial shelf life of food”, In G.L. Robertson, *Food packaging and shelf life*, CRC Press, Boca Raton, pp. 55-79.

4. E. Choe and D.B. Min, 2006, “Chemistry and reactions of reactive oxygen species in foods”, *Critical Reviews in Food Science and Nutrition*, vol. 46, no. 1, pp. 1-22.

5. M.R.-C. Antonio Lopez-Gomez 2010,“Packaging and shelf life of orange juice”, In G.L. Robertson, *Food pacakging and shelf life*, CRC Press, Boca Raton, pp. 179-198.

6. J.K.S. Moller, et al., 2000, “Effect of residual oxygen on colour stability during chill storage of sliced, pasteurised ham packaged in modified atmosphere”, *Meat Science*, vol. 54, no. 4, pp. 399-405.

7. M.J. Galotto.S.A. Anfossi, and A. Guarda, 2009, “Oxygen absorption kinetics of sheets and films containing a commercial iron-based oxygen scavenger”, *Food Science and Technology International*, vol. 15, no. 2, pp. 159-168.

8. G. Tewari.D.S. Jayas.L.E. Jeremiah, and R.A. Holley, 2002, “Absorption kinetics of oxygen scavengers”, *International Journal of Food Science and Technology*, vol. 37, no. 2, pp. 209-217.

9. S. Yildirim, et al., *Development of palladium based oxygen scavenging film for food packaging*, in *Eighteenth IAPRI World Packaging Conference*, J. Singh, Editor. 2012, DEStech Publications, Inc: Pennsylvania. p. 7-14.

10. R. Kündig, et al., 2013,“*Use of an oxygen scavenger to prolong the shelf life of part baked bread*”. in *26th IAPRI Symposium on Packaging 2013 Book of Abstracts*, Espoo VTT Technical Research Center of Finland.

11. P.A. Gravil and H. Toulhoat, 1999, “Hydrogen, sulphur and chlorine coadsorption on pd(111): A theoretical study of poisoning and promotion”, *Surface Science*, vol. 430, no. 1–3, pp. 176-191.

12. P.A. Gravil and H. Toulhoat, 1999, “Ethylene, sulphur, and chlorine coadsorption on pd(111): A theoretical study of poisoning and promotion”, *Surface Science*, vol. 430, no. 1–3, pp. 192-198.

13. J.A. Maga and I. Katz, 1976, “The role of sulfur compounds in food flavor part iii: Thiols”, *C R C Critical Reviews in Food Science and Nutrition*, vol. 7, no. 2, pp. 147-192.

14. G.P. Dateo, et al., 1957, “Identification of the volitile sulfur componens of cooked cabbage and the nature of the precursurs in the fresh vegetable”, *Food Research*, vol. 22, no. 5, pp. 440-447.

15. D.-D. Belitz.W. Grosch, and P. Schieberle, 2009,“Food chemistry”. Heidelberg: Springer verlag.

16. H. Schulz.H. Kruger.J. Liebmann, and H. Peterka, 1998, “Distribution of volatile sulfur compounds in an interspecific hybrid between onion (allium cepa l) and leek (allium porrum l)”, *Journal of Agricultural and Food Chemistry*, vol. 46, no. 12, pp. 5220-5224.

17. EFSA, 2014, “Scientific opinion on the safety assessment of the active substances, palladium metal and hydrogen gas, for use in active food contact materials.”, *EFSA Journal* vol. 12, no. 2.

# Possibility of electric devices and devices with drug packaging in medical and health care

**Kiyomi Sadamoto[1*], Mikio Murata [1], Takaharu Sadamoto[2] and Hiroko Takamori[3]**

[1] *Yokohama College of Pharamacy*
[2] *Sadamoto Clinic*
[3] *Dainippon Printing Co.Ltd(DNP)*

[*] *Corresponding author. Email: k.sadamoto@hamayaku.ac.jp*

**Abstract:** We have developed electronic devices which are used for supporting drug taking and monitoring disease symptom[1) 2)]. It is innovative that the card also play a role of drug packaging. Since the electronic card is flexible in arrangement of button and item design, there is a lot of possibility of usage in medical care including drug taking, symptom change, appearing side effects. In addition, it can be used not only disease therapy but also preventive medicine such as health check for elderly, check of food taking, situation of evacuation and some body conditions. So we considering several sample design which has different usage in medical and health care. First one is the card for monitoring mental status for patients with depression, second one is monitoring condition of body for elderly people in the community, and third one is monitoring drug taking with card with packaging type (drug in). To see the potential in using devices, we also tried questionnaire which include usability study of electric devices and their hope to use packaging for patients and pharmacists. Patients are able to understand how to use the card devices in every generation (more than 85%), and evaluated that it can show their situation of drug taking and symptom just pushing button without difficult instruction. As for the pharmacists, it is highly evaluated that they can monitor accurate drug taking data with referring basic symptom and vital sign which are difficult to collect with ordinary pharmacist activities. Both patients and pharmacists understand simplicity of usage and usability of electric cards for evidence-based drug therapy. We confirm the possibility of usage in several ways, so that it is necessary to consider the reasonable design and easily open packaging in practical use.

Keywords: electric devices, monitoring, drug taking, symptom, evidence based drug therapy

## 1 Introduction

Considering accurate drug therapy and cost-effective medical care, monitoring both adherence of drug and symptom of disease are essential things[3)]. However, since information from patients are limited with ordinary ways, real situation that elder patients tend to ship drug taking and hardly remember their symptom change during the time until they visit next out patients' clinic is not enough under consideration for therapy. On the other hand, pharmacists have a role to monitor drug therapy and give advice for not only drug rerated information but symptom of side effects and appropriate life style. Under ordinary style pharmacist activities, collecting these information are difficult. From former study, medical care givers including pharmacist evaluated that some supporting devices for drug therapy in the community are essential.

## 2 Methods

To study the usability of electric devices and searching possibility of usage in the area of monitoring disease and life style, we made sample of 5 different electric devices including drug taking monitoring ones and symptom and life style monitoring ones (Fig1). Using these devices, we have done questionnaire study both for patients and pharmacists. Some item in questionnaire are same both patients version and pharmacists one. And other item of questionnaire are different depend on patients and pharmacists. Observation and use samples, patients and pharmacists evaluate the devices. The data of questionnaire are studied with Excel2012.

Fig1 The sample of electric devices




## 3 Results

Table1 shows usability evaluation of electric devices by patients and pharmacists. It is obvious that both patients and pharmacists evaluated that the electric cards is easy to understand, and there is no difficulty to use it.

## Table1. Usability Evaluation of electric devices (patients & pharmacists)

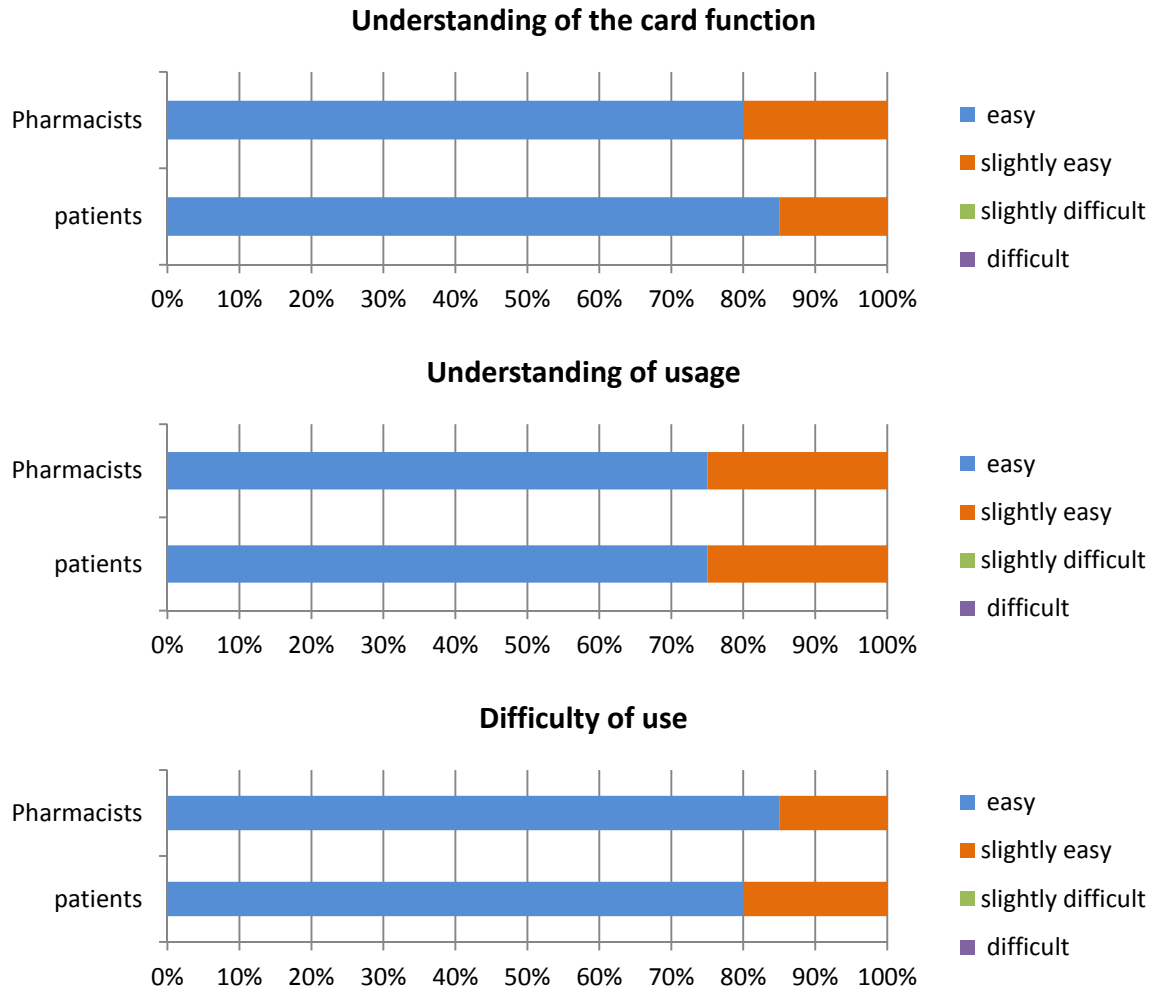


Table2 shows Drug and related needs from patients. They are very much conscious of their disease and it's monitoring. On the other hand, it is difficult to note situation of drug taking. Only 40% of them take note it.

## Table2 Drug & Disease related needs (patients)

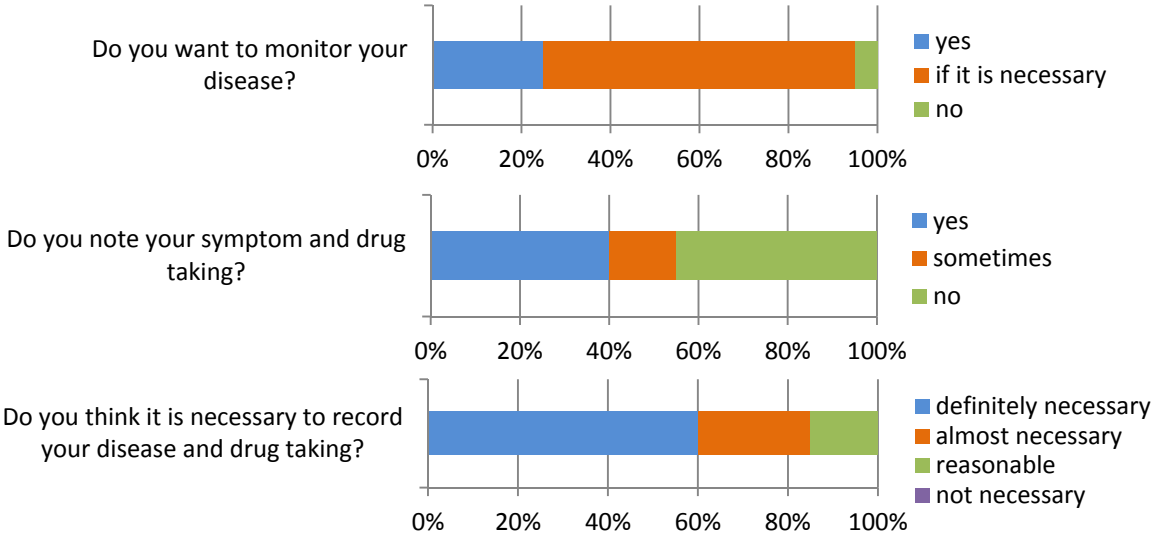



Table3 shows how much and what kind of information which pharmacists can get with ordinary ways. Only 30% of them thought they get information from patients with ordinary way. However, the contents of information is mainly drug and one dose pack. As for the life and symptom related information, only 10% of pharmacists get them with ordinary way.

## Table3 Pharmacists' current information taking

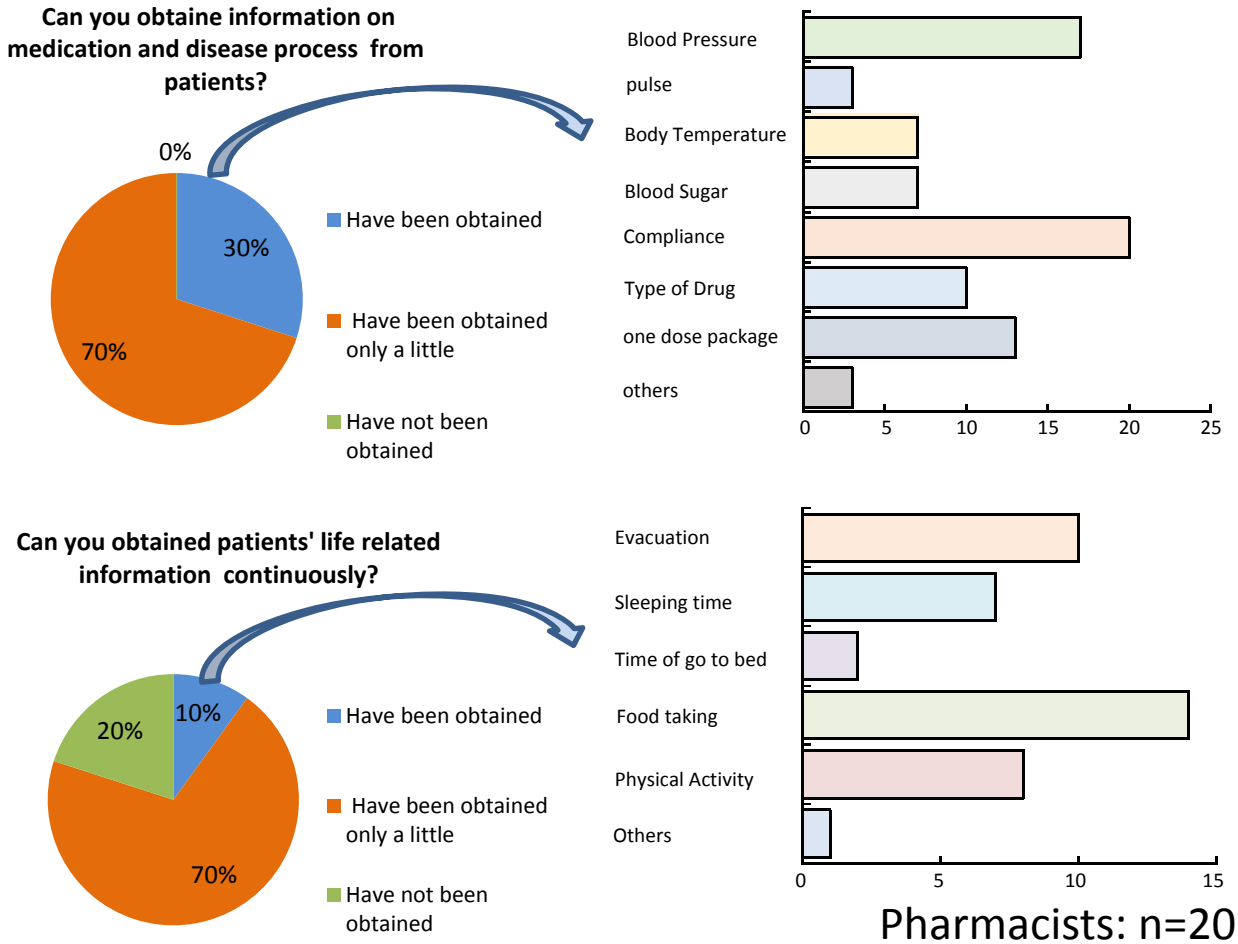


Table4 shows pharmacists' free comments including needs and possibility of information using electric devices. Currently, pharmacist does not have ways to get disease and life related information which is listed, and they hope to know a lot of medical and physical information for appropriate drug therapy monitoring with using electronic.

## Table4 Pharmacists' needs and possibility of information using electric devices

What kind of information is necessary in pharmacist' activities?

1. Medical examination, Electro cardio graph, XP
2. Dr' way of thinking for therapy including drug use, and education for patients.
3. Who is the key parson in elderly patients' care, and life style including drug management in the house.
   (living style information)
4. Patients' real compliance and life situation such as meal, sleeping status, activity.
5. Common disease existence (DM、CKD)
6. Situation of food and drug taking
7. Patients' understanding and will for their therapy
8. Diagnosis
9. Real drug taking and side effects
10. Frequency of misuse and forget to take drug
11. Real disease and direction of therapy
12. Detail of timing of drug taking in a day
13. Situation of evacuation

## 4 Discussion

It is obvious that both patients and pharmacists are able to use electric devices without difficulty (Table1). Both patients and pharmacists evaluated the simple usage and flexibility of devices. As for patients, they can recognized that using devices enable for monitoring not only drug taking but also disease and symptoms. As for pharmacists, they are recognized importance of monitoring not only drug use but also life rerated information such as food, sleep, activity. In the health care area, monitoring of drug use and life rerated information are essential for effective therapy. The simple paper made electronic devices have possibility for various setting use in health care

## 5 Conclusions

The paper made electronic devices have possibility to extend monitoring disease and life rerated information. It is innovative packaging devices for flexible use.


## Acknowledgements

We acknowledged for all cooperate people for the study.


## References


1. Hiroko Takamori, Takaharu Sadamoto, Takakazu Himeno, Kiyomi Sadamoto,2013, "PTP with electric card devices suport adherence and therapy", *26th IAPRI Sympojium on Packaging*, pp. 586-588.
2. Kiyomi sadamoto, Takaharu sadamoto, Manami Yoshikai, Hiroko Takamori, Takakazu Himeno, Masaru Mizoguchi, 2012, "Drug therapy supporting tool for patients with RA and Osteopolosis", *IAPRI world packaging*, pp. 6-7.
3. Sally W. Wade, Aalok Nadkar, David Macarios, Anna N.A. Tosteson, 2011, "Impact of Medication adhere nce on Health Care Utilization and Productivity: Self-Reported Data From a Cohort of Postmenopausal Wo men on Osteoporosis Therapy", *Clin. Ther.*, vol. 33, no. 12, pp. 2006-2015.

# Effects of Active Packaging on the Physico-Chemical Properties of Fresh-Cut Cantaloupe (*Cucumis Melo* L. Var. *Glamour*)

**Syahidah K.[1], Rosnah S. [1*], Ahmedov A.[1], Zaulia O.[2], Noranizan M.A. [3], M.Z.M Nor[1]**

[1] *Department of Process and Food Engineering, Faculty of Engineering, Universiti Putra Malaysia, 43400 Serdang Selangor, Malaysia*
[2]*Horticulture Research Centre, Persiaran MARDI-UPM, MARDI Headquarters, 43400 Serdang, Selangor, Malaysia*
[3]*Department of Food Technology, Faculty of Food Science and Technology, Universiti Putra Malaysia, 43400 Serdang Selangor, Malaysia*

**Corresponding author. Email: rosnahs@upm.edu.my*

**Abstract:** One of the most well-known active packaging concepts is gas absorbers or scavengers. In this study, modified atmosphere packaging was developed to investigate the physico-chemical properties of fresh-cut cantaloupe (*Cucumis Melo L. Var. Glamour*) fruit during storage by using oxygen and ethylene absorbers. The fresh-cut cantaloupes were cut into small cubes and immersed in a calcium lactate solution (1%) prior to packing in polypropylene (PP) container that contained ethylene and oxygen absorbers and sealed with low-density polyethylene (LDPE) films. The changes in physico-chemical properties of the packed fruits were determined in terms of colour, pH, texture and total soluble solid (TSS) during storage for 18 days at 2 ºC with 87% relative humidity (RH). No overall significant changes ($p<0.05$) were observed on the colour and pH properties of the fresh-cut cantaloupes in all packages. The fresh-cut cantaloupes packed with ethylene absorber in the PP container demonstrated better firmness than ethylene/oxygen absorbers and control packages. The total soluble solid (TSS) of the fruits in the ethylene and ethylene-oxygen absorbers packages were well preserved compare to the control package. These findings indicate that the shelf life of fresh-cut cantaloupes was extended to a certain period of time due to the presence of the gas absorbers.

Keywords: active packaging, physico-chemical properties, quality, fresh-cut cantaloupe, gas absorber.

## 1 Introduction

Nowadays, fresh-cut fruit products, also known as minimally processed fruits [1], offer high demand due to the modern lifestyle of its consumers. Besides, these fresh and ready-to-eat fruits have a wide potential to be commercialized and marketed in hotels, restaurants and retail food stores in the form of sliced, slabs diced and peeled fresh-cut. However, the fresh-cut fruits processes which involve cutting, slicing and trimming will lead to damage of the fruit's tissue and affect the perishability of the products [2]. Hence, the introduction of active packaging can give better alternative in controlling the fruit-perishability issue. Active packaging system, in particular, modified atmosphere packaging (MAP) helps to develop a gas composition in the package in order to maintain the quality and extends the shelf life of products [3].

Cantaloupe (*Cucumis Melo L. Var. Glamour*) is a well-known fruit that contains high vitamins and minerals. In this study, the beneficial effects of using the active packaging for fresh-cut cantaloupes were investigated with the intention to extend the shelf life and reduce the deterioration rate of the fruits. Nevertheless, it is important to note that the quality of the fresh-cut fruits depends not only to the type of packaging used but to the storage temperature too [4]. Previous studies demonstrated that the optimum storage temperature of the fresh cut cantaloupe was at 2ºC [5-7]. Accordingly, this study was aimed to determine the effectiveness of active packaging containing fresh-cut cantaloupes by monitoring the changes in colour, texture, pH and TSS at 2°C in 18 days.

## 2 Materials and Methods

### 2.1 Preparation of fresh-cut cantaloupe

Cantaloupe melons (*Cucumis Melo* L. Var. *Reticulatus*) cultivar Glamour was purchased from a commercial grower farm, Selangor, Malaysia at maturity of 3/4 of full slip, transported to the laboratory and temporary stored at an optimum temperature of 10°C with 90% relative humidity (RH) for 48 hours. The fruits were selected based on uniform sizes, defect-free and full netted. The cantaloupe fruits were then cut into small cubes (2cmx2cmx2cm) and were immersed in a calcium lactate solution (1%) prior to packaging and storage study.

### 2.2 Packaging procedure

In this study, the application of active packaging was done by the inclusion of gas absorbers in the fruit packages. Approximately 200g of the fresh-cut cantaloupe cubes were weighed and packed in PP container and sealed with LDPE film (40µm of thickness) in three different conditions, namely control (without absorber), S1 (with ethylene absorber) and S2 (with ethylene and oxygen absorbers) as in Figure 1. Ethylene and oxygen absorbers used were commercially purchased in small sachets from Bioconservacion Australia Pty. Ltd., Australia and MGC America, USA, respectively. All packages were then stored for 18 days at 2°C with 87% RH. The physico-chemical properties were analyzed at 0, 4, 7, 11, 14 and 18 days.




**Figure 1**: Diagram of the three different packages of the fresh-cut cantaloupe fruits. (All samples were packed in polypropylene (PP) container and sealed with LDPE film in three different conditions; Control - without any gas absorber; S1 - with the inclusion of the ethylene absorber; and S2 - with the inclusion of ethylene and oxygen absorbers).

### 2.3 Physico-chemical analyses

#### *2.3.1 Firmness*

A TA.XTPlus Texture Analyser (Stable Micro Systems, Surrey, UK) with a 5 mm diameter (P/5) cylindrical probe attached was used to determine tissue firmness of the fresh-cut cantaloupe. Initially, a 5kg load was set on the equipment for calibration. A two-cycle compression test was performed with the settings as follows: preset speed, 2 mm/s; test speed 1 mm/s; post-test speed 2 mm/s; distance as 30% strain; time 1 s; trigger force 20 g [7,8]. The result was recorded as maximum load in Newtons (N). Results of three replications were averaged to acquire a single value.

#### *2.3.2 Total Soluble Solid (TSS) and pH*

The stored fruits were initially extracted with juice extractor to obtain juice. A drop of each fruit juice was pipetted onto a screen panel of digital Abbe refractometer (AR2008, KRUESS, Germany) to determine its soluble solids content. The results were recorded as degree Brix.

As for the determination of pH, 10 ml of the fruit juice was added with 40 ml distilled water to form a mixture solution and was titrated (Model 785 DMP Titrino, Metrohm, Switzerland) with 0.1 mol/L NaOH until the pH reached 8.5.

#### *2.3.3 Colour*

Colour was measured by using colour reader (CR 10 Tristimulus Colorimeter Konica Minolta, Japan). The fruits which were cut into standardized cubic shapes (2cmx2cmx2cm) were measured. The measurement simply measures the target. After one second the colour difference is expressed as L*a*b*. Luminosity (L*), greenness (a*) and yellowness (b*) values were recorded while chromaticity (C*) and hue angle ($h_{ab}$) were calculated by following the given equations, respectively.

$$C^* = [(a^*)^2 + (b^*)^2]^{0.5} \quad (1)$$

$$h_{ab} = \tan^{-1}[(b^*) \times (a^*)^{-1}] \quad (2)$$

### 2.4 Statistical analysis

The experiment was conducted with a completely randomized design of three replicates per treatment. Statistical software of SAS 9.2 system (SAS Institute Inc., Cary, NC, USA) was used to analyse the mean, standard error and variance (ANOVA). Least significant difference test (t-test) ($P<0.05$) was used to compare differences among treatment and sample storage time.

## 3 Results and Discussion

### 3.1 Firmness

The shelf life of fruits will normally be affected by the softening process. Previous studies have reported that firmness is one of the main factors related to the quality of the fresh-cut Cantaloupe [9-10]. Figure 2 shows the firmness of fresh-cut cantaloupes during 18 days of storage at 2ºC. The values of firmness for the control, S1 and S2 samples were reduced significantly throughout the storage ($p \leq 0.05$) from 12.30N to 7.57N for control, 12.04N to 8.57N for S1 and 12.11N to 7.09N for S2, respectively. This firmness reduction may probably happen due to the enzymatic activity, in particular by solubilization of pectin in cell walls [10]. Among all samples, fresh-cut cantaloupe packaged in S2 package showed the highest reduction of firmness value from day 0 to day 18 in contrary with S1 samples that exhibited the highest firmness values in overall. High firmness in S1 package indicates that the samples were well preserved, probably because the ethylene absorber used had reduced the respiration rate resulting in the prevention of water loss, cell rupture and starch to sugar conversion [11].

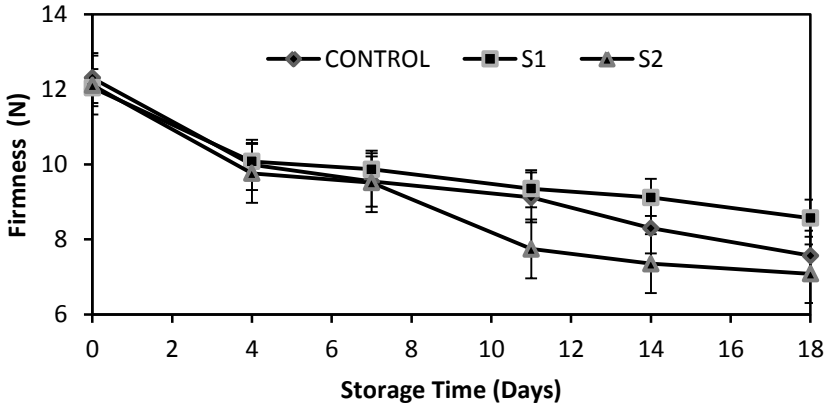



**Figure 2**: Means for firmness of fresh-cut cantaloupes stored for 18 days (2 °C with 87 % RH). (All samples were packed in polypropylene (PP) container and sealed with LDPE film in three different conditions; Control - without any gas absorber; S1 - with the inclusion of the ethylene absorber; and S2 - with the inclusion of ethylene and oxygen absorbers).

## 3.2 Colour

An important issue in fresh-cut processing is discoloration which is due to the browning process that usually occurs on cut surfaces [12]. Figure 3, 4 and 5 display the colour parameters of luminosity (L*), hue angle ($h_{ab}$) and chroma (C*) of the fresh-cut cantaloupe throughout 18 days of storage at 2ºC, respectively. The mean values of L* for all the samples were increased from day 0 to day 4 although they were not statistically significant ($P<0.05$). At this stage, the ripening process of the fruit's flesh may increase its lightness colour. Nevertheless, the luminosity values remained constant during storage for all the packaged samples after day 7. The same observations were found for $h_{ab}$ and C* values of the fresh-cut cantaloupe in Figure 4 and 5 with no significantly changes ($P<0.05$) throughout the 18 days of storage period at 2ºC. By referring to the trend from these figures, it can be concluded that no discoloration of fresh-cut cantaloupe had occurred during the 18 days storage in the packages. This is in agreement with Arruda et al. [13] which reported no development of translucency on fresh-cut cantaloupe stored under refrigeration. By considering that colour deterioration in fruit is due to increase in respiration rate and enzymatic process [14], the existence of ethylene and oxygen absorbers in the packages might have had further prevented these processes from occuring.

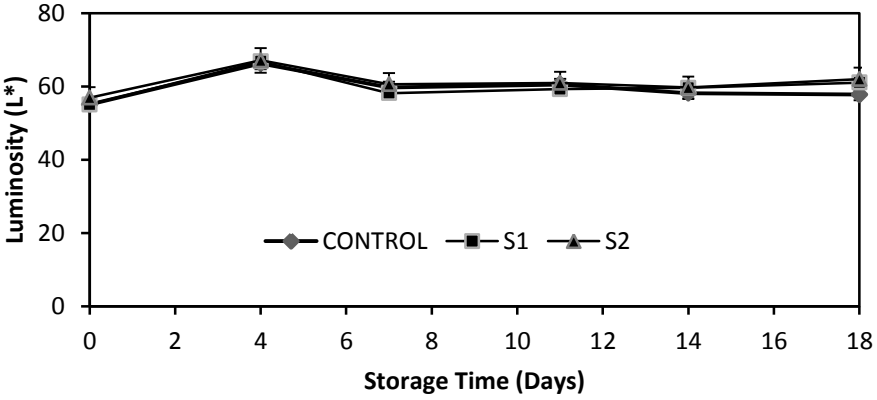



**Figure 3**: Means for luminosity (L*) of fresh-cut cantaloupes stored for 18 days (2 °C with 87 % RH). (All samples were packed in polypropylene (PP) container and sealed with LDPE film in three different conditions; Control - without any absorber; S1 - with the inclusion of the ethylene absorber; and S2 - with the inclusion of ethylene and oxygen absorbers).

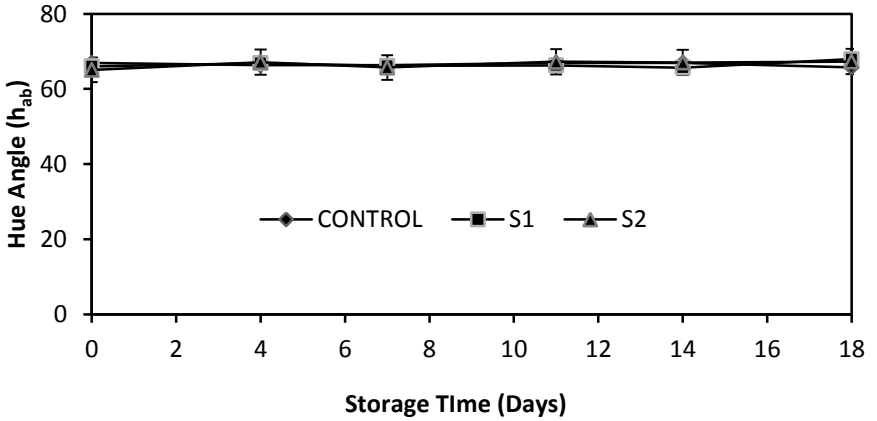



**Figure 4**: Means for hue angle ($h_{ab}$) of fresh-cut cantaloupes stored for 18 days (2 °C with 87 % RH). (All samples were packed in polypropylene (PP) container and sealed with LDPE film in three different conditions; Control - without any absorber; S1 - with the inclusion of the ethylene absorber; and S2 - with the inclusion of ethylene and oxygen absorbers).

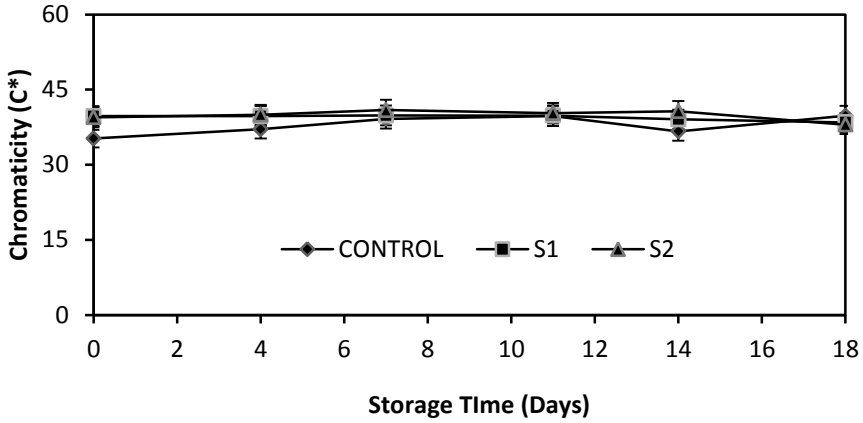



**Figure 5**: Means for chromaticity (C*) of fresh-cut cantaloupes stored for 18 days (2 °C with 87 % RH). (All samples were packed in polypropylene (PP) container and sealed with LDPE film in three different conditions; Control - without any absorber; S1 - with the inclusion of the ethylene absorber; and S2 - with the inclusion of ethylene and oxygen absorbers).

## 3.3Total Soluble Solid (TSS) and pH

Total soluble solid is an important aspect of fruit quality [15]. Table 1 shows that the TSS values of the control, S1 and S2 samples were the same on day 0 (9.98 ºBrix). Initial TSS values were found high because of high $CO_2$ concentration in the package due to respiration process. Thus, it leads to anaerobic metabolism with an accumulation of organic acids [16]. For the control sample, the level of TSS has increased slightly from 9.98 ºBrix to 10.00 ºBrix from day 0 to day 4 and was maintained within 18 days of storage (Table 1). In contrary, the total soluble solid values decreased significantly ($p<0.05$) for S1 and S2 samples, on day 0 until day 7. This is may be due to the low $O_2$ and high $CO_2$ content in the packages which can reduce the rates of ripening and senescence [17]. In addition, changes in sugars, starch and cell wall can occur by eliminating the $O_2$ and ethylene atmosphere [18]. However, it was also noticeable that after day 7, the TSS values of the samples were increased back similarly to their initial values. Nevertheless, the result indicates that the TSS values of the fruits can be retained with the existence of ethylene and oxygen absorbers in the packages.

**Table 1**: Means for total soluble solids (TSS) and pH of fresh-cut cantaloupes stored for 18 days (2 °C with 87 % RH). (All samples were packed in polypropylene (PP) container and sealed with LDPE film in three different conditions; Control - without any gas absorber; S1 - with inclusion of the ethylene absorber; and S2 - with inclusion of ethylene and oxygen absorbers).

| Samples | Storage Time (Days) | Total Soluble Solids (TSS) (ºBrix) | pH |
|---|---|---|---|
| Control | 0 | 9.98±0.06[a] | 7.00±0.01[b] |
| S1 | | 9.98±0.10[a] | 7.02±0.04[c] |
| S2 | | 9.98±0.06[b] | 7.03±0.01[a] |
| Control | 4 | 10.00±0.11[a] | 6.77±0.13[a] |
| S1 | | 8.80±0.10[b] | 6.74±0.01[b] |
| S2 | | 8.00±0.10[c] | 6.65±0.01[b] |
| Control | 7 | 10.07±0.05[a] | 6.47±0.02[b] |
| S1 | | 8.87±0.20[a] | 6.57±0.01[c] |
| S2 | | 7.43±0.06[b] | 6.60±0.03[a] |
| Control | 11 | 10.73±0.06[a] | 7.02±0.01[a] |
| S1 | | 9.97±0.12[b] | 6.97±0.01[a] |
| S2 | | 9.30±0.06[c] | 6.89±0.01[b] |
| Control | 14 | 10.70±0.00[a] | 7.01±0.06[a] |
| S1 | | 10.00±0.00[b] | 6.99±0.02[a] |
| S2 | | 9.30±0.06[c] | 6.79±0.01[b] |

| | | | |
|---|---|---|---|
| Control | | 10.70±0.06[a] | 7.03±0.02[a] |
| S1 | 18 | 9.97±0.20[b] | 7.00±0.02[a] |
| S2 | | 9.53±0.06[c] | 6.77±0.04[b] |

*Means followed by the same letter are not significantly different at P<0.05 for each column

The pH measures the acidity and alkalinity of the food product. The pH for cantaloupe ranges from 6.1 to 6.6 [19-20]. Table 1 shows the results from the analysis of pH that was carried out. The pH values for the control, S1 and S2 samples decreased significantly at (P<0.05) from day 0 until day 7, respectively. These decrements might be due to the utilization of organic acids and their conversion to sugar during respiration [21]. Nevertheless, the value of pH was maintained among all the samples for the remaining storage days. Lamikanra *et al*. [22] and Portela and Cantwell [23] reported that the pH level of fresh-cut cantaloupe fruits were stable if they were stored at low temperatures.

## Conclusions

The inclusion of ethylene and oxygen absorbers in the fresh-cut cantaloupe packages have proven to be effective in maintaining some of the physico-chemical properties during 18 days of storage at 2°C indicating by no significant changes ($p<0.05$) to the colour and pH properties. The existence of ethylene absorber in the packages was proven to be able in preserving the firmness of the fruit better than the control and ethylene-oxygen absorbers packages. The total soluble solid (TSS) of the fruits in the ethylene and ethylene-oxygen absorbers packages were well preserved compare to the control package. The results showed potential application of the gas absorbers in fresh-cut fruit package to maintain its quality since they are capable in slowing down the metabolism rate of the fruits, hence increasing its shelf life.

## References


1. A. Watada, N. Ko and D. Minott, 1996, "Factors affecting quality for fresh-cut horticultural products", *Postharvest Biology and Technology*, vol. 9, pp. 115-125.
2. J.B. James and T. Ngarmsak, 2010, "*Processing of fresh-cut tropical fruits and vegetables: a technical guide*". Food and Agriculture Organization of the United Nations Regional Office for Asia and the Pacific Bangkok, Rap Publication. ISBN 978-92-5-106712
3. H.M. Lai, 2001, "Minimum-packaging technology for processed foods". Report of the APO Multi-Country Study Mission. SME-OS1-01.
4. O. Zaulia, M. Razali, H. Aminuddin, D. Che Omar, K.H. Ng and M. Habsah, 2006, "Effect of different packagings and storage temperatures on the quality of fresh-cut red chilli", *Journal Tropical Agricultural and Food Science*, vol. 34, no. 1, pp. 67-76.
5. R. Shewfelt, 1994, "Quality characteristics of fruits and vegetables". In: R.P. Singh and F.A.R. Oliveira (Eds.), *Minimal processing of foods and process optimization: an interfa*ce, pp. 171-189.
6. I. Luna-Guzman and D.M. Barrett, 2000, "Comparison of calcium chloride and calcium lactate effectiveness in maintaining shelf stability and quality of fresh-cut", *Postharvest Biology and Technology*, vol. 19, pp. 61–72.
7. M. Zainal Abidin, R. Shamsudin, Z. Othman, and R. Abdul Rahman, 2013, "Effect of postharvest storage of whole fruit on physico-chemical and microbial changes of fresh-cut cantaloupe (Cucumis melo L. reticulatus cv. Glamour)", *International Food Research Journal*, vol. 20, no. 1, pp. 501-508.
8. O. Lamikanra and M.A. Watson, 2007, "Mild heat and calcium treatment effects on fresh-cut cantaloupe melon during storage", *Food Chemistry*, vol. 102, pp. 1383-1388.
9. O. Lamikanra, B. Juaraez, M.A. Watson and O.A. Richard, 2003, "Effect of cutting and storage on sensory traits of cantaloupe melon cultivars with extended postharvest shelf life", *Journal of the Science of Food and Agriculture*, vol. 83, pp. 702-708.
10. E. Aguayo, V.H. Escalona and F. Arte´s, 2004, "Metabolic behavior and quality changes of whole and fresh processed melon", *Journal of Food Science*, vol. 69, pp. 148-155.

11. J. Moreno, R. Simpson, A. Baeza, J. Morales, C. Muñoz and S. Sastry, 2012, "Effect of ohmic heating and vacuum impregnation on the osmodehydration kinetics and microstructure of strawberries (cv. Camarosa)", *LWT Food Science and Technology*, vol. 45, no. 2, pp. 148-154.

12. J.C. Beaulieu and J.R. Gorny, 2001, "Fresh-cut fruits". In: K.C Gross, M.E. Saltveit and C.Y Wang, (Eds), *The commercial storage of fruits, vegetables, and florist and nursery stocks*, USDA Handbook, pp. 66- 149.

13. M.C. Arruda, A.P. Jacomino, C.I.G.L. and C.L Moretti, 2003, "Qualidade de melão minimamente processado armazenado em atmosfera modificada passive", *Horticultura Brasileira*, vol.21, pp.655-659.

14. V. Del-Valle, P. Hernandez-Munoz, A. Guarda and M.J. Galotto, 2005, "Development of a cactus-mucilage edible coating (Opuntia ficus indica) and its application to extend strawberry (Fragaria ananassa) shelf-life", *Food Chemistry*, vol. 91, no. 4, pp. 751-756.

15. M.S. Aday, C. Caner and F. Rahvalı, 2011, "Effect of oxygen and carbon dioxide absorbers on strawberry quality", *Postharvest Biology and Technology*, vol. 62, no. 2, pp. 179-187.

16. B.C. Benedetti, P. Gómez, M. Martins, A. Conesa and F. Artés, 2008, "Effect of pre-processing controlled atmosphere storage on the quality of fresh-cut galia melons", *Food Science and Technology International*, vol. 14, no. 5, pp. 13-19.

17. F.B. Abeles, P.W. Morgan and M.E. Saltveit Jr, 1992, "*Ethylene in Plant Biology*", 2nd ed., Acad. Press, San Diego CA.

18. N. Mir and R.M. Beaudry, 2000, "Modified Atmosphere Packaging" http://www.ba.ars.usda.gov/hb66/015map.pdf

19. M.R. Corbo, B. Speranza, D. Campaniello, D. D'Amato and M. Sinigaglia, 2010, "Fresh-cut fruits preservation: current status and emerging technologies", *Current research, technology and education topics in applied microbiology and microbial biotechnology. Formatex Research Center, Badajoz*, pp. 1143-1154.

20. T.L. Parnell, T. Suslow and Harris, 2003, "*Cantaloupe: Safe Method to Store, Preserve and Enjoy*". ANR Publication 8095. University of California, ISBN 978-1-60107-269-6

21. M. Martinez-Ferrer, C. Harper, F. Perez-Muroz and M. Chaparro, 2002, "Modified atmosphere packaging of minimally processed mango and pineapple fruits", *Journal of Food Science*, vol. 67, no. 9, pp. 3365-3371.

22. O. Lamikanra, J.C. Chen, D. Banks and P.A. Hunter, 2000, "Biochemical and microbial changes during the storage of minimally processed cantaloupe", *Journal of Agricultural and Food Chemistry*, vol. 48, pp. 5955-5961.

23. S.I. Portela and M.I. Cantwell, 1998, "Quality changes of minimally processed honeydew melons stored in air or controlled atmosphere", *Postharvest Biology and Technology*, vol. 14, pp. 351-357.

# Release of Oregano Essential Oil and Green Tea Extract from Ethylene Vinyl Alcohol Copolymer Films

**Virginia Muriel-Galet[1], Marlene J. Cran[2], Stephen W. Bigger[2], Pilar Hernández-Muñoz[1] and Rafael Gavara[1*]**

[1] *Packaging Lab, Instituto de Agroquímica y Tecnología de Alimentos, CSIC, Av. Agustín Escardino, 7, 46980, Paterna, (Valencia) Spain*
[2] *Institute for Sustainability and Innovation, Victoria University, Werribee Campus, PO Box 14428, Melbourne, 8001, Australia.*

[*] *Corresponding author. Email: rgavara@iata.csic.es*

**Abstract:** The aim of this work was the development of a new active film containing a combination of antimicrobial (AM) and antioxidants (AO) agents for food packaging applications. Oregano essential oil and green tea extract were incorporated into ethylene vinyl alcohol (EVOH) copolymer film with 29% molar ethylene content. Release studies were conducted at 23ºC in aqueous food simulants which were selected in accordance with the European Regulations. The major compounds of oregano essential oil and green tea extract were identified and quantified by GC and HPLC respectively. Once the migration reached equilibrium, the total antioxidant activity was measured in the food simulants using a standard antioxidant assay. In addition, the AM capacity of the film was tested *in vitro* against *Listeria monocytogenes* and *Escherichia coli* in a liquid media as well as in a vapor phase. The results suggested that the release kinetics of the active agent depend on the affinity between the active agents and the food simulants. In general, higher diffusion coefficients were obtained when films were exposed to 50% (v/v) ethanol and the antioxidant efficiency was observed to be greater. With regard to AM activity, the film showed growth inhibition in liquid media test and vapor inhibition assay.

Keywords: active packaging, antioxidant, antimicrobial, EVOH, release kinetics.

## 1 Introduction

Active packaging films containing antimicrobial (AM) and antioxidant (AO) compounds can offer additional protection and extend the shelf life of many perishable food products. The efficacy of any AM or AO additive depends on its ability to be released into the products over time. Green tea extract (GTE) and oregano essential oil (OEO) are recognised food additives that have shown promise in packaging applications. One of the more important properties of GTE is the antioxidant activity of the polyphenolic constituents. In addition, GTE shows AM activity against a range of microorganisms including *Bacillus cereus*, *E. coli* and *Candida albicans* [1]. Volatile agents such as OEO are well known for exhibiting strong AM properties [2] and recent studies have demonstrated concurrent antioxidant effects [3].

Ethylene-vinyl alcohol (EVOH) copolymer is a well-established packaging film material that can be incorporated with natural active agents such as GTE and OEO. When EVOH is exposed to a humid environment, it undergoes a plasticizing effect that can accelerate the migration of additives thus producing AM and AO effects on packaged food products [4]. The purpose of this study was to characterize the release of AM and AO compounds from EVOH films containing GTE and OEO. The antioxidant activity and the AM activity against *L. monocytogenes* and *E. coli* were also studied.

## 2 Materials and Methods

### 2.1 Film preparation

Films were prepared using EVOH containing 29% molar ethylene content. Films were made by casting film forming solutions containing 5% (w/w) OEO, 5% (w/w) GTE and a mixture of 5% (w/w) OEO and 5% (w/w) of GTE with respect to polymer content.

### 2.2 Migration of OEO and GTE from EVOH films

The migration of GTE and OEO from EVOH films into different aqueous food simulants was conducted at 23ºC. The food simulants included: (i) 10% (v/v) ethanol for aqueous foods; (ii) 3% (v/v) acetic acid for acidic foods (pH ≤ 4.5); and (iii) 50% (v/v) ethanol for lipophilic foods. Carvacrol, the major component of OEO, was quantified using gas chromatography (GC). Epicatechin (EC), the major AM and antioxidant component of GTE, was quantified using high performance liquid chromatography (HPLC) with a UV-visible absorbance detector.

### 2.3 Antioxidant activity of EVOH films

Once the migration reached equilibrium, the total antioxidant activity was measured in the three food simulants in terms of the radical scavenging ability of Trolox using a standard antioxidant assay by the DPPH method [5].

### 2.4 Antimicrobial activity of films in liquid medium

To evaluate their AM activity, a set of films was immersed in liquid medium and stored at 37 ºC for 24 h. After the corresponding storage time, the AM activity of the films was assayed against *L. monocytogenes* and *E. coli*.

### 2.5 Agar diffusion assay

Film disks of 2.5 cm Ø were adhered to the lid of a Petri dish inoculated with microorganism but without direct contact with the inoculum. Plates were then incubated at 37ºC for 24 h in the case of *L. monocytogenes* and *E. coli*. The diameter of the resulting inhibition zone was measured directly after the incubation period.

## 3 Results and Discussion

### 3.1 Migration of OEO and GTE components

The mechanism of action of the manufactured active EVOH films was the release of the incorporated agents into the food product or the surrounding headspace. Since the extent and kinetics of release of the diverse compounds present in the films would depend on the type of food product, a study on the release of carvacrol and epicatechin from the film into three food simulants was performed. The results presented in Figure 1 show the typical release profiles of these agents into various food simulants which show an exponential increase towards a maximum value. It is evident from these plots that neither of the two compounds showed a complete release into any of the three tested simulants. Carvacrol, a volatile essential oil extract, showed significantly higher overall release in all of the food simulants. With respect to the various simulants, the fatty food simulant yielded the highest extraction of both agents. The 3% (v/v) acetic acid and 10% (v/v) ethanol aqueous solutions provided very similar results.

To characterize the release of the substances from the films, the solution to Fick's equations considering the boundary conditions of the experiment was used. It was considered that films were isotropic and that the agents were homogenously distributed within the polymer matrix. The film is thin enough as to consider that no release takes place through the edges and that both surfaces are exposed to the migration simulant. The partition coefficient, *K*, and the diffusion coefficient, *D*, values were assumed to be constant throughout the experiment. Thus, the mass, $m(t)$, of agent released from a film of thickness, *l*, at a specific time, *t*, is given by:

$$\mathrm{m(t)} = \frac{c_p^0 \cdot V_s \cdot V_p}{V_s + K \cdot V_p} \cdot \left( 1 - \sum_{n=1}^{\infty} \frac{2\alpha(1+\alpha)}{1+\alpha+\alpha^2 q_n^2} \exp(-4Dq_n^2 t / \ell^2) \right) \qquad (1)$$

where $\alpha = V_S/(KV_P)$ which represents the ratio between the mass of compound in the liquid and that in the polymer at equilibrium, $V_S$ and $V_P$ are the volumes of simulant and polymer, $c_p^0$ initial concentration of the antimicrobial agent and $q_n$ is the positive solution to the equation: $\mathrm{tg}(q_n) = -\alpha q_n$.

Figure 1 includes the curves obtained from equation (1) using the *K* values and the *D* values which yielded the best fit to the experimental values. As can be seen in Figure 1 the theoretical values presented a good agreement with the experimental release data.

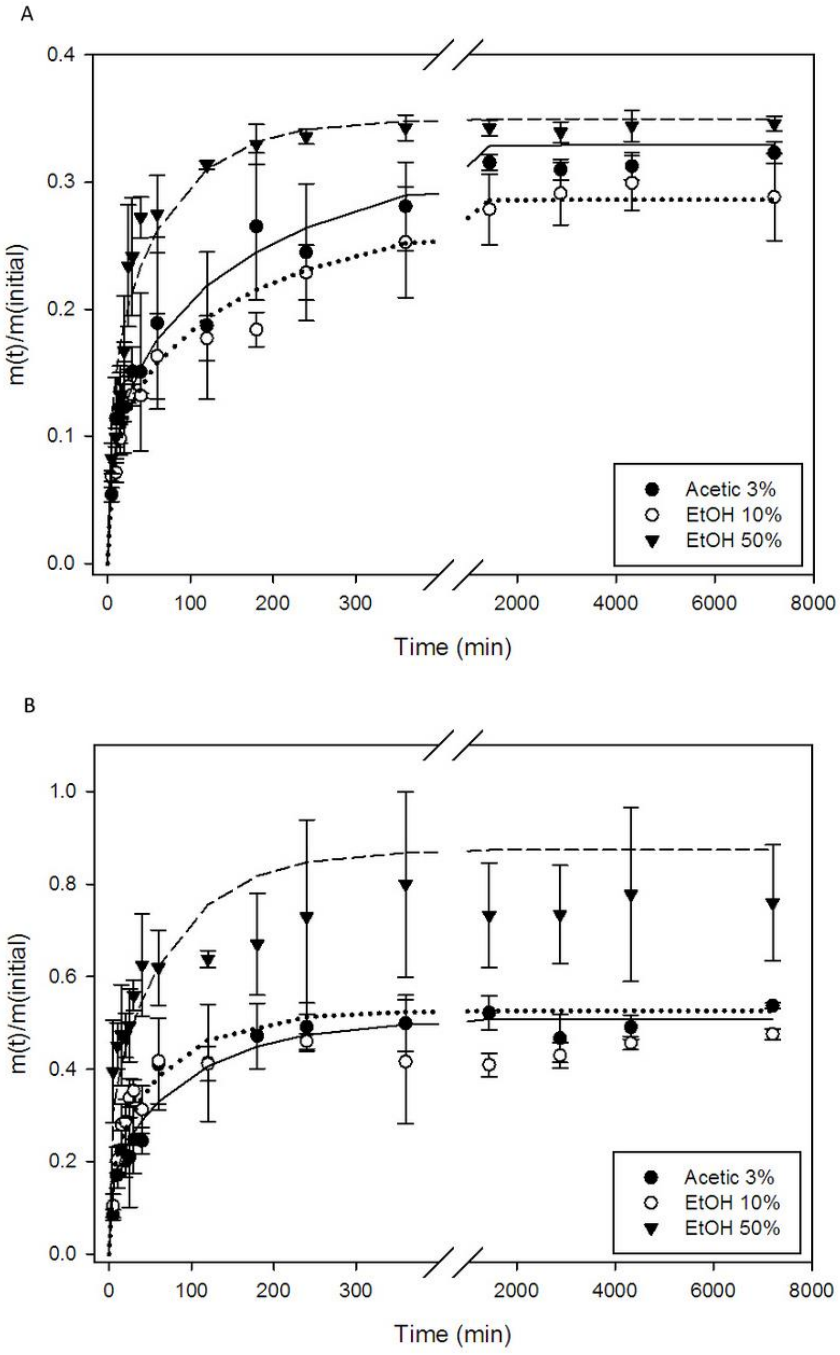



Figure 1. Release of the active agents (A) epichatechin and (B) carvacrol from EVOH-GTE+OEO films into: (●) 3% acetic acid, (○) 10% ethanol and (▼) 50% ethanol. Symbols represent the experimental data and lines correspond to the theoretical prediction obtained with equation (1).

It is evident that equation (1) adequately predicts the release profiles of the different film formulations. The values of *K* and *D* for the different samples and simulant systems are presented in Table 1. From these data, it can be determined that the simulant containing 50% (v/v) ethanol resulted in the highest and fastest release of all the systems with the lowest *K* and the highest *D* values. This mixture is a good solvent of the agents incorporated in the polymer that may explain this observation. In addition, the simulant produces the highest swelling of the polymer matrix resulting in a faster and more efficient diffusion of additive molecules through the polymer structure. As shown in Figure 1, carvacrol was

released faster than epicatechin in all simulants and this may be expected due to the smaller molecular size of the carvacrol molecule.

Table 1. Values of the partition coefficient, *K*, and diffusion coefficient, *D*, obtained by fitting equation (1) to the experimental release values.

| | Epicatechin | | Carvacrol | |
|---|---|---|---|---|
| Simulant | K | $D \times 10^{15}$/m $s^2$ | *K* | D $\times 10^{15}$/m $s^2$ |
| 3%(v/v/) acetic acid | 1860 ± 180 | 0.38 ± 0.07 | 800 ± 110 | 0.79 ± 0.16 |
| 10% (v/v/) ethanol | 2010 ± 230 | 0.29 ± 0.06 | 790 ± 260 | 1.34 ± 0.80 |
| 50% (v/v/) ethanol | 1610 ± 80 | 1.12 ± 0.10 | 150 ± 100 | 1.99 ± 1.00 |

## 3.2 Antioxidant activity of EVOH films

The antioxidant activity was determined in terms of mg of Trolox per g of film and the results are summarised in Table 2. The results show that there was no significant difference between the EVOH-GTE+OEO and EVOH-GTE systems in any of the food simulants. In agreement with the migration study, the higher affinity of the epicatechin with 50% (v/v) ethanol also increased the antioxidant activity. In the case of carvacrol, although an overall greater amount of this agent migrated from the films into 50% (v/v) ethanol, the antioxidant effect of OEO was lower than that of the GTE. This might be expected since the active agent of GTE is a well-known strong antioxidant and carvacrol is primarily an AM agent.

Table 2. Antioxidant activity of GTE and OEO after equilibrium release from EVOH film

| Film | **50% (v/v) Ethanol** | **10% (v/v) Ethanol** | **3% (v/v) Acetic Acid** |
|---|---|---|---|
| | mg Trolox/g film | mg Trolox/g film | mg Trolox/g film |
| EVOH-GTE+OEO | 62.42 ± 2.98[a] | 28.18 ± 2.47[a] | 13.17 ± 1.27[a] |
| EVOH-GTE | 65.82 ± 1.78[a] | 29.13 ± 7.29[a] | 16.72 ± 2.88[a] |
| EVOH-OEO | 27.85 ± 3.66[b] | 11.39 ± 4.59[b] | 9.66 ± 3.96[b] |

a, b indicate significant differences (Turkey's adjusted analysis of variance $P < 0.05$)

## 3.3 Antimicrobial test in liquid media

The antimicrobial activity of EVOH films with GTE+OEO, GTE and OEO was tested against *L. monocytogenes* and *E. coli* in liquid media and the results are presented in Table 3. A strong AM effect was observed with EVOH-GTE+OEO and EVOH-OEO that resulted in total inhibition against both microorganisms. In the case of EVOH-GTE a reduction of 1.25 log and 1.67 log was produced against *L. monocytogenes* and *E. coli* respectively compared to the control film suggesting GTE imparts a lesser degree of AM action.

Table 3. Antimicrobial effect of EVOH films against *L. monocytogenes* and *E. coli* in liquid media.

| | ***L. monocytogenes*** | ***E. coli*** |
|---|---|---|
| Film | Microbial count (log) | |
| Control | 8.79 ± 0.04 | 8.86 ± 0.09 |
| EVOH-GTE+OEO | Total inhibition | Total inhibition |
| EVOH-GTE | 7.54 ± 0.01 | 7.13 ± 0.14 |
| EVOH-OEO | Total inhibition | Total inhibition |

## 3.4 Agar diffusion assay

Table 4 shows the results of the agar diffusion assay obtained for the films against *L. monocytogenes* and *E. coli*. The films containing OEO show a greater inhibitory effect against *E. coli* (4.41 and 4.22 cm) than *L. monocytogenes*. As expected, no inhibition zone was formed against *L. monocytogenes* and *E. coli* with EVOH-GTE films.

Table 4. Antimicrobial effect of EVOH films against *L. monocytogenes* and *E. coli* in the vapor phase.

| | ***L. monocytogenes*** | ***E. coli*** |
|---|---|---|
| Film | Inhibition zone (cm) | |
| Control | None observed | None observed |
| EVOH-GTE+OEO | 3.31 ± 0.34 | 4.41 ± 0.30 |
| EVOH-GTE | None observed | None observed |
| EVOH-OEO | 3.19 ± 0.18 | 4.22 ± 0.22 |

## 3 Conclusions

Antioxidant and AM active films based on EVOH and natural agents were successfully developed using the method of casting. The release of the active agents is dependent on the affinity of the compound for the food simulants used and the ability of the food simulant to swell the polymer. In this study, the migration was greater in aqueous simulants of high ethanol content. As expected, the antioxidant activity of the films containing GTE was the most effective and the films containing OEO showed a strong AM effect against *L. monocytogenes* and *E. coli*. Overall, the results suggest that the EVOH films with AM and antioxidant agents show strong potential for further development as food packaging films.

## Acknowledgements

The authors acknowledge the financial support of the Spanish Ministry of Economy and Competitiveness, projects AGL2012-39920-C03-01, and fellowship funding for V. M-G.

## References

1. M. P. Almajano. R. Carbó. A. J. López Jiménez. M. H. Gordon, 2008, "Antioxidant and antimicrobial activities of tea infusions, *Food Chemistry*, vol. 108, pp. 55-63.

2. S. Burt, 2004, "Essential oils: their antibacterial properties and potential applications in foods - a review", *International Journal of Food Microbiology*, vol. 94, pp. 223-253.

3. T. Kulisic. A. Radonic. V. Katalinic. M. Milos, 2004, "Use of different methods for testing antioxidative activity of oregano essential oil", *Food Chemistry*, vol. 85, pp. 633-640.

4. V. Muriel-Galet. G. Lopez-Carballo. R. Gavara, R. P. Hernandez-Munoz, 2014, "Characterization of ethylene-vinyl alcohol copolymer containing lauril arginate (LAE) as material for active antimicrobial food packaging", *Food packaging and Shelf life*, vol. 1, pp. 10-18.

5. T. Kulisic. A. Radonic, A. V. Katalinic. M. Milos, 2004, "Use of different methods for testing antioxidative activity of oregano essential oil", *Food Chemistry* vol, 85, pp. 633-640.

# Methodology to Evaluate Performance of Active Ingredients as Oxygen Scavengers

**Ángela M. García[1*], Jorge A. Medina[1], Jacques Verdu[2] and Bruno Fayolle[2]**

[1] *Grupo de Materiales y Manufactura CIPP-CIPEM, Departamento de Ingeniería Mecánica, Universidad de los Andes, Bogotá, Colombia*
[2] *Ecole Nationale Supérieure d'Arts et Métiers, PIMM Paristech, Paris, France*

**Corresponding author. Email: am.garcia228@uniandes.edu.co*

**Abstract:** The development of oxygen scavengers for active packaging covers various sources of active components, e.g. inorganic elements, unsaturated compounds, acids, enzymes, clays, and polymers [1-6]. Despite the advances in active formulations, there is a lack of detailed information concerning the performance of oxygen scavengers. Data provided by manufactures may be limited and generalized [7, 8]. In addition, considerable differences between commercial data sheets and experimental studies have been reported [9]. Thus, there is an increasing need for tools to evaluate performance of polymeric and organic formulations.

Active ingredients used in this study were unsaturated esters and linseed oil. In this research, a new methodology is proposed with the aim to evaluate the performance of unsaturated-lipid compounds as oxygen scavengers. This methodology has an experimental section and other one of modelling. Experimentally, measurements of oxygen in headspace and thermogravimetric analyses (TGA) were performed at different temperatures and atmospheres (nitrogen, air, and oxygen) and served to determine the actual oxygen scavenging capacity of the active ingredients; and the model, is a serie of chain reactions based on the thermo-oxidation of unsaturated hydrocarbons.

Industries that already use active packaging, and those interested in this developing technology, can use the proposed methodology as a useful and simple tool to evaluate the oxygen scavenging performance in their specific applications and environments.

Keywords: oxygen scavengers, performance, temperature, modelling, unsaturated lipids, active packaging.

## 1 Introduction

Active packaging technologies are able to improve quality and shelf life of products, by means of components that would release or absorb substances into or from the packaged food, or the environment surrounding the food [10]. In 2011, gas scavengers accounted nearly 36% of the total market of active, intelligent and smart packaging, within these, oxygen scavengers are the most used because degradation of many products is related with oxidation [11].

In the present research, unsaturated fatty acids and esters are proposed as possible active ingredients for oxygen scavengers because they are susceptible to auto-oxidation initiated or activated by metals, UV radiations or temperature. Oxidation activated by temperature was evaluated by thermogravimetric tests and headspace measurements. In parallel thermo-oxidation has been modelled based on the oxidation of C-H bonds adjacent to double bonds as active sites.

## 2 Materials and methods

Analytical grade neat unsaturated esters: methyl oleate, methyl linoleate and methyl linolenate were used. Linseed oil used was grade double boiled and its composition was obtained by Gas-Liquid Chromatography (GLC) and is presented in table 1.

**Table 1:** Composition of Linseed oil double boiled

| Component | Weight concentration from GLC (%w/w) |
|---|---|
| Palmitic acid | 5,9 |
| Stearic acid | 3,4 |
| Oleic acid | 19,2 |
| Linoleic acid | 16,2 |
| Linolenic acid | 52,6 |
| Unknown | 2,7 |
| Total | 100 |

### 2.1 Thermal gravimetric analysis (TGA)

In the presence of oxygen, an increase in the mass of the oils caused by oxidative reactions is expected. Samples of the neat esters and linseed oil were analyzed using TGA 500 (TA Instruments) with isotherms of 60°C, 80°C and 110°C reached at a heating rate of 20°C/min. Themograms were obtained under nitrogen, air and pure oxygen atmospheres. In order to improve repeatability and reproducibility, and to avoid the effect of heat transmission by diffusion in TGA analysis, the mass in all the experiments was, in average, 4mg and duplicates were done in all cases.

### 2.2 Headspace measurements

Several samples of 1 ml. of active ingredient were placed into glass containers of 20 ml and after heated at 60°C, 80°C or 110°C to study thermo-oxidation; the oxygen in the headspace of the containers was measured at different times, using a portable spot check oxygen analyzer Model 901 (Quantek). Each sample was punctured once. Three replicates and two empty containers were measured each time to separate the effect of change of gas volume because increase of temperature.

## 3. Thermo- oxidation model

The following oxidation mechanism, of a hydrocarbon substrate with a single reactive site under oxygen excess at moderate temperature (<150°C), was proposed based on previous research [12].

Initiation

$$ROOH + ROOH \xrightarrow{k_{1b}} ROO^{\circ} + carbonyl + R^{\circ} + Scissions \quad (1)$$

Propagation

$$R^{\circ} + O_2 \xrightarrow{k_2} ROO^{\circ} \quad (2)$$

$$ROO^{\circ} + RH \xrightarrow{k_3} ROOH + R^{\circ} \quad (3)$$

Termination

$$R^{\circ} + R^{\circ} \xrightarrow{k_4} inactive\ products \quad (4)$$

$$R^{\circ} + ROO^{\circ} \xrightarrow{k_5} inactive\ products \quad (5)$$

$$ROO^{\circ} + ROO^{\circ} \xrightarrow{k_6} inactive\ products + carbonyls + O_2 \quad (6)$$

## 4 Results

### 4.1 Thermogravimetric tests

Thermogravimetric tests in nitrogen atmosphere showed evaporation phenomena caused by increase of temperature; a thermogram for methyl linolenate is given in Figure 1.

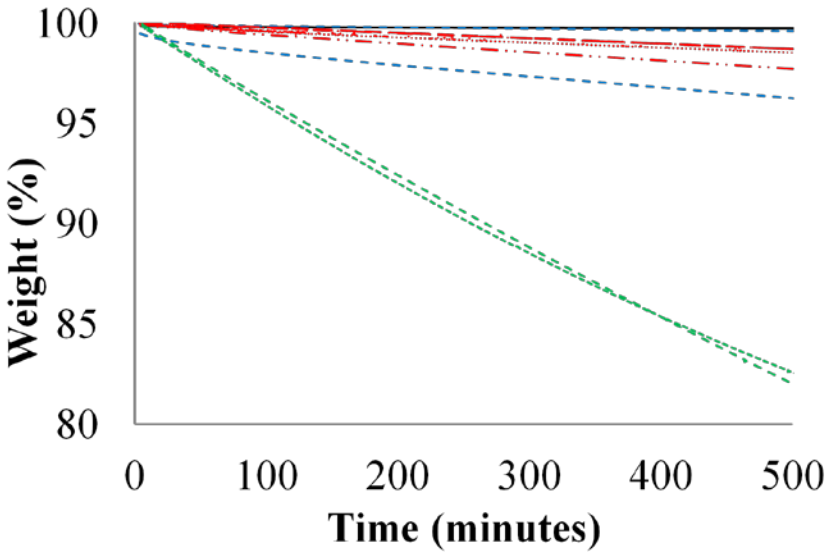



**Figure 1:** TGA of methyl linolenate at 40 ° C (—), 60°C (—), 80°C (—) and 110°C (—)., nitrogen atmosphere

Slopes of the plot in the thermogram under nitrogen atmosphere were calculated to include the effect of evaporation in subsequent analyses. Slope values for all active ingredients are plotted in Figure 2 below.

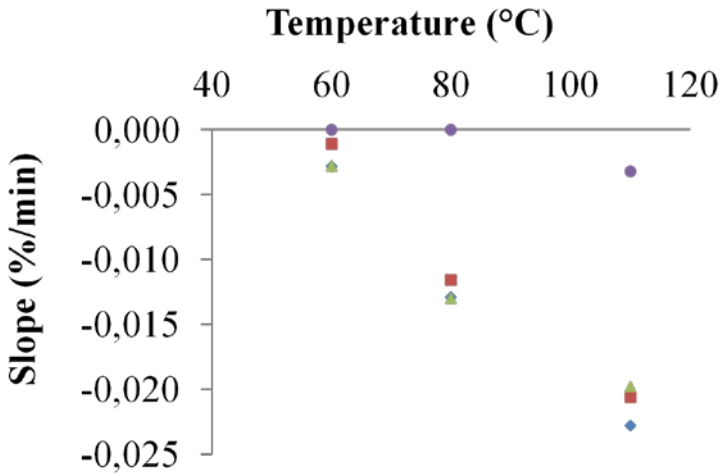



**Figure 2**: Values of slopes calculated from TGA under nitrogen atmosphere form methyl oleate (♦), methyl linoleate (■), methyl linolenate (▲) and linseed oil (●) at 60°C, 80°C and 110°C.

As expected, evaporation rate decreases at higher temperatures and the values for the slopes of neat esters are very close because they have similar molecular weights. Linseed oil slopes are less negative than slopes of neat esters in all the temperatures, which can be related with cross linking phenomena [13].

Although reactions of thermo–oxidation occur on air and pure oxygen atmospheres, slope values of thermograms obtained were negative at the highest temperatures because oxidation is combined with evaporation; at low temperatures the weight gained because oxidation can be better appreciated. Figure 3 shows results for methyl linolenate in air atmosphere.

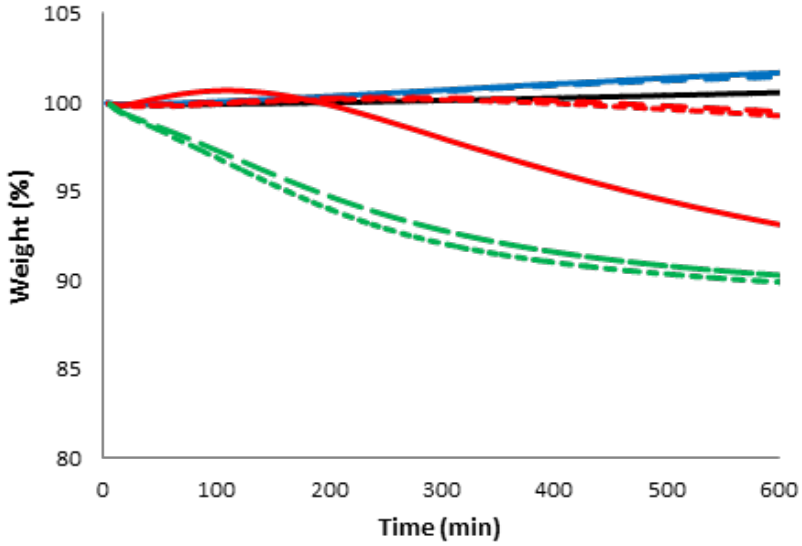



**Figure 3:** TGA of methyl linolenate on air atmosphere at 40°C (—), 60°C (—), 80°C (—) and 110°C (—).

In order to see oxidation phenomena solely, oxidation weight ($W_o$) was obtained as is shown in (7) and (8).

$$W_o(\%) = W_{air}(\%) - W_N(\%) \quad (7)$$

$$W_o(\%) = W_{Oxygen}(\%) - W_N(\%) \quad (8)$$

Where $W_o$ is the weight gained just by oxidation, $W_{air}$ is the weight obtained in TGA in air atmosphere, $W_N$ the weight obtained in TGA under nitrogen atmosphere and $W_{oxygen}$ the weight obtained in experiments under 100% oxygen atmosphere. Eliminating the effect of evaporation, the increase in oxidation rate with temperature can be appreciated (Figure 4)

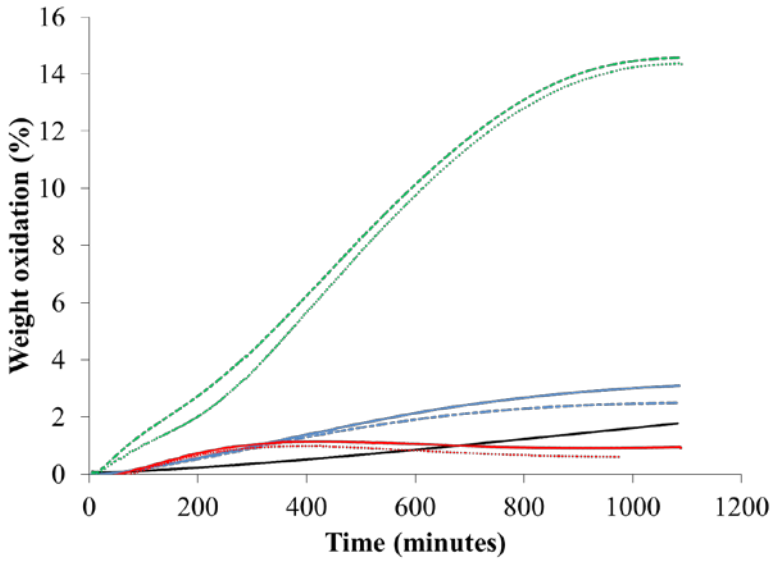



**Figure 4**: Results from TGA of methyl linolenate on air atmosphere at 40°C (—), 60°C (—), 80°C (—) and 110°C (—), expressed as $W_o$ (equation 7)

Mass gained expressed as mmol $O_2$/g ester was calculated with the data of TGA in atmosphere of air and pure oxygen. Figure 5 and Figure 6 show the results for methyl linolenate and linseed oil.

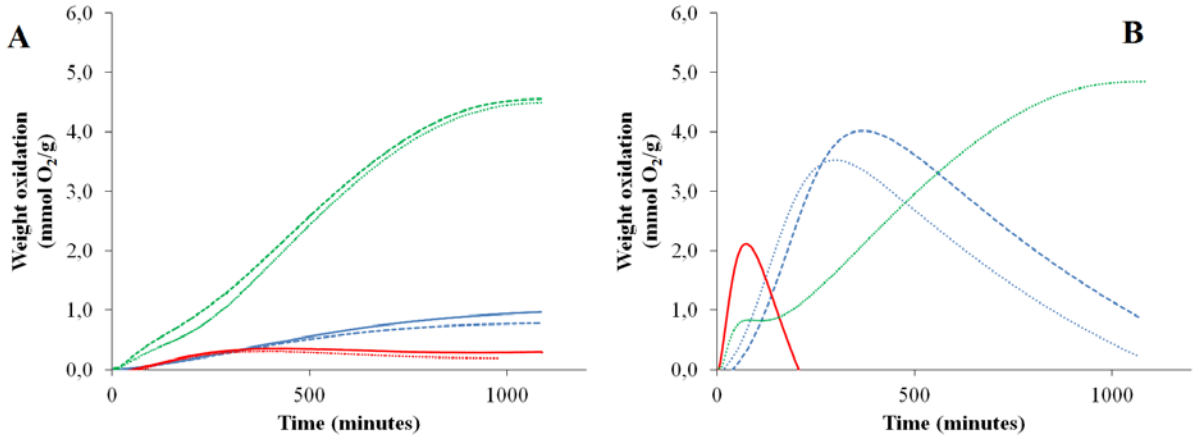



**Figure 5:** Weight gained vs. time for methyl linolenate at 60°C(—), 80°C(—) and 110°C (—)in atmosphere of **A**. air and **B.** oxygen.

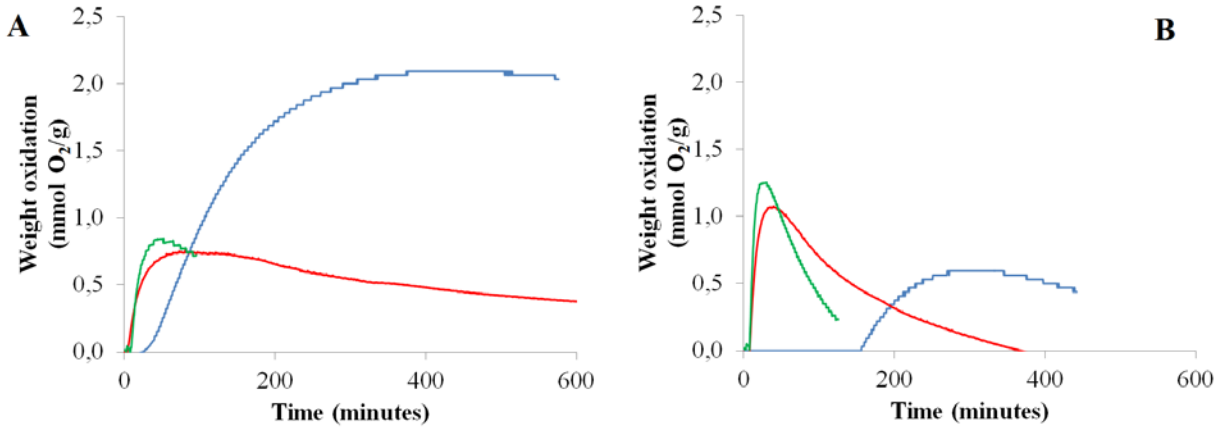



**Figure 6:** Weight gained vs. time for linseed oil at 60°C(—), 80°C(—) and 110°C (— ) in atmosphere of **A**. air and **B.** oxygen

Higher values of oxygen uptake were obtained for methyl linolenate, which have the highest number of unsaturations. The maximum conversion for methyl linolenate was 4 mmol $O_2$/g ester equivalents to 1.2 mmol $O_2$/mmol of methyl linolenate obtained at 110°C.

## 4.2 Headspace measurements

Similar calculations of oxygen consumed can be obtained by headspace measurements. Data collected can be plotted as the change of oxygen concentration in the headspace vs. time as shown in Figure 7 for linseed oil. In a confined headspace of 19 ml, 1 ml of linseed oil is capable to diminish the oxygen concentration of the headspace more rapidly at 110°C.

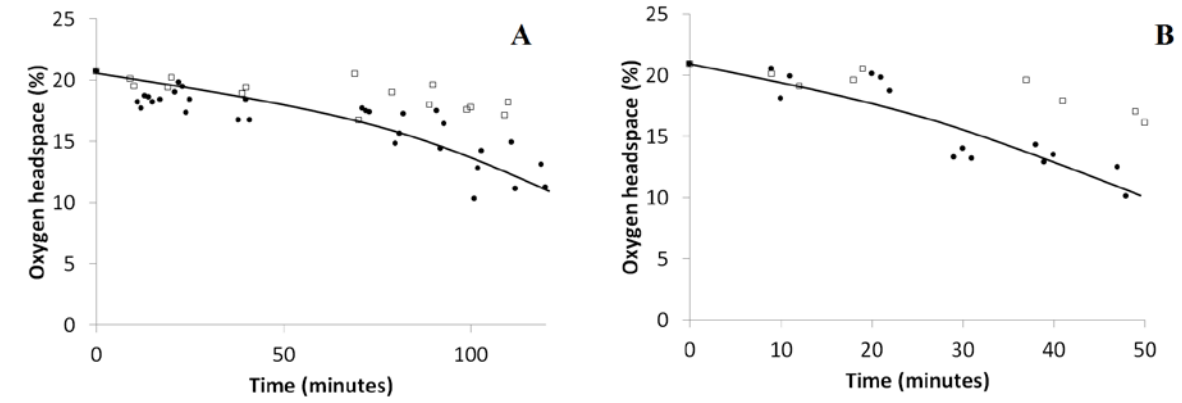



**Figure 7:** Oxygen concentration in the headspace vs. time for flasks with 1 ml of linseed oil at (A) 80°C (●) and (B) 110°C (●) in comparison with the change of oxygen concentration for empty flasks (□) at the same temperature conditions.

Based on data from headspace measurement, oxygen consumed can be calculated, Figure 8 shows a comparison between data calculated from TGA and from headspace experiments for linseed oil at 110°C in air atmosphere. Both plots show the same behaviour but differences in the values of oxygen scavenging capacity are observable. From headspace measurements maximum conversion was 0.1mmol $O_2$/g of linseed oil, while from TGA was 2.1 mmol $O_2$/g of linseed oil, this can be attributed to confined headspace volume in the case of headspace experiments. These results reveal the importance of a correct calculus and measurement of the oxygen scavenging capacity for active ingredients.

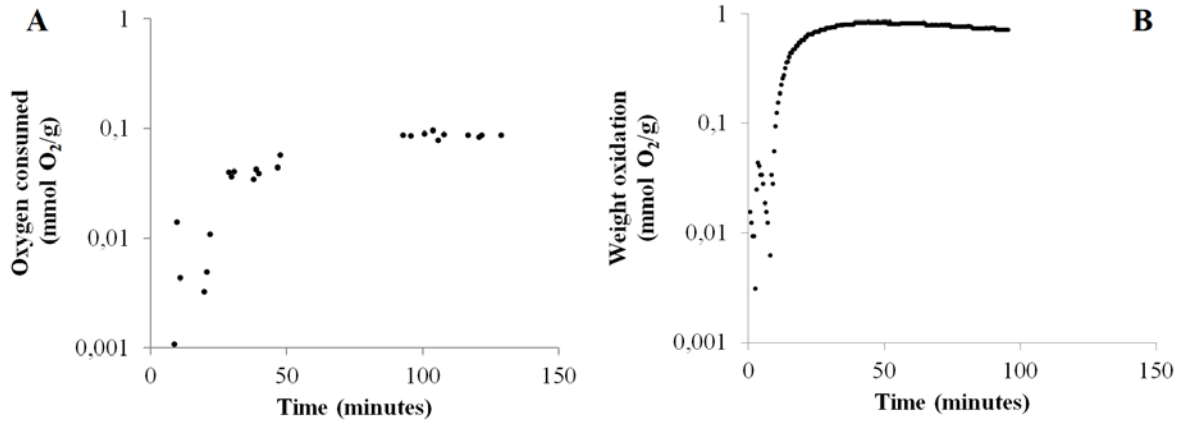



**Figure 8: A**. Change in headspace oxygen concentration expressed as mmol O2/g linseed oil, obtained from headspace measurements at 110°C. **B**. Weight change expressed as mmol O2/g linseed oil, obtained from TGA experiments 110°C in air atmosphere.

## 5 Conclusions

Quantitative equivalence between headspace measurements and thermogravimetric experiments had been demonstrate, showing the later as a novel, simple and rapid method to evaluate oxygen scavenging capacity for ingredients activated by temperature.

In the case of active ingredients studied, more promising results were for methyl linolenate at 110°C.

## References

1. Charles, F., J. Sanchez, and N. Gontard, , 2006, "Absorption kinetics of oxygen and carbon dioxide scavengers as part of active modified atmosphere packaging", *Journal of Food Engineering*. 72(1): pp. 1-7.

2. Garcia Mora, A.M., J.C. Salas Muñoz, and J.A. Medina Perilla, 2012, "Linseed oil as active ingredient in active packaging", in P*olymer Processing Society Americas Conference*. Niagara, Ontario.

3. 2013,"Active packaging film prevents lipid oxidation in oil-in-water emulsion systems". *Emerging Food R&D Report*, 23(10): pp. 5-5.

4. Vermeiren, L., et al., "Developments in the active packaging of foods", 1999, *Trends in Food Science & Technology*, 10(3): pp. 77-86.

5. Carranza, S., D.R. Paul, and R.T. Bonnecaze, , 2012, "Multilayer reactive barrier materials", *Journal of Membrane Science*, 399–400(0): pp. 73-85.

6. Cahill, P.J., et al., 2004,"Active oxygen Scavenging property- Imparted Copolymer".: Japón.

7. Solis, J.A. and B.D. Rodgers, 2001, "Factors affecting the performance of new oxygen scavenging polymer for packaging applications", *Journal of plastic film and sheeting,*. 17(4): pp. 339-349.

8. Merchán Sandoval, J.P., 2006, Implementación de un absorbedor de oxígeno en película para empaque activo, in Ingeniería Mecánica. Universidad de los Andes. pp. 87.

9. Miltz, J. and M. Perry, 2005, "Evaluation of the performance of iron based oxygen scavengers, with comments on their optimal applications", *Packaging Technology and Science*. 18(1): pp. 21-27.

10. Comisión Europea, 2009, Reglamento (CE) No 450/2009.: Diario Oficial de la Unión Europea.

11. Visiongain, 2010,The Active, Intelligent and Smart Food & Drink Packaging Market 2011-2021.

12. Richaud, E., et al., , 2012, "Rate constants of oxidation of unsaturated fatty esters studied by chemiluminescence", *Chemistry and Physics of Lipids*. 165(7): pp. 753-759.

13. Lazzari, M. and O. Chiantore, , 1999, "Drying and oxidative degradation of linseed oil", Polymer degradation and stability. 65(2): pp. 303-313.

# Developments in Antimicrobial Food Packaging Research

**Stephen W. Bigger[1*], Marlene J. Cran[2] and Intan S. M. A. Tawakkal[1]**

[1] *College of Engineering and Science, Victoria University, PO Box 14428, Melbourne, 8001, Australia*
[2] *Institute for Sustainability and Innovation, Victoria University, PO Box 14428, Melbourne, 8001, Australia*

[*]*Corresponding author. Email: stephen.bigger@vu.edu.au*

**Abstract:** The distribution of fresh and safe food products to consumers is becoming more reliant on the development of materials that can prevent or minimize food spoilage that occurs due to microorganisms. Antimicrobial (AM) food packaging encompasses a range of materials that incorporate AM agents into their formulations, either directly or in coatings. The preference for naturally derived AM agents, has resulted in considerable research with a strong focus on essential oils and extracts that are known to impart AM activity. However, these are typically volatile materials and considerable losses can occur during thermal processing of traditional packaging materials such as extruded polyethylene films. Recent advances to overcome these losses include the use of additives to retain the AM agents and the use of encapsulating technologies such as inclusion compounds that can protect the volatile agents during heat processing. Another important advance in AM packaging is the search for biodegradable materials that can be produced from renewable resources such as starch from wheat and corn. However, for some of these new and emerging materials, the production costs are often higher than those of typical synthetic packaging materials. There are some strategies that can reduce production costs such as the incorporation of natural fibres and fillers and this can offer other advantages including improved mechanical properties and an affinity for some AM agents. However, the biodegradability of many of these materials in certain environments is still under widespread investigation, particularly with the addition of AM agents that may retard biodegradation until the AM agents are dissipated or otherwise inactivated. This paper reports some recent progress in the development and characterization of a range of AM packaging materials at Victoria University.

**Keywords**: active packaging, antimicrobial agents, migration, encapsulation.

## 1 Introduction

Over the past few decades, the demand for high-quality food products from consumers has driven innovations in packaging and resulted in a novel class of packaging materials. Active packaging (AP) is based on the concept that the food, packaging and environment interact to enhance food safety and storage [1, 2]. Active packaging systems are therefore designed to change the environmental conditions of the packaged food in order to extend the shelf life or to improve safety or sensory properties whilst maintaining the quality of food products [3, 4]. There are several categories of AP systems including those incorporating oxygen scavengers, moisture scavengers, carbon dioxide scavengers or emitters, humidity absorbers or controllers, ethylene scavengers, and aroma emitters or absorbers [4, 5].

One class of AP involves the use of antimicrobial (AM) agents that are either incorporated in a coating layer or directly into the packaging material to prevent or minimize the growth of spoilage or pathogenic microorganisms [5-8]. Coating systems can be formulated from naturally derived or modified materials and can be sprayed, cast or otherwise deposited onto a polymeric substrate [8, 9]. Direct incorporation of AM agents can be achieved during material processing but in the case of elevated temperature processes such as film extrusion, this can often result in unacceptable losses of AM agents, particularly when volatile agents are used [10].

The range of AM agents that can be used in packaging include synthetic chemical compounds and naturally derived agents such as essential oils (EOs) and their extracts. The preference is for naturally derived materials as these are often perceived as a safer alternative to synthetically derived chemical agents [11]. An AM system can be generally categorized as either a migratory or immobilized system with a migratory system facilitating a slow or controlled release of a relatively volatile AM substance onto the food surface to prevent or delay microbial growth [12]. Antimicrobial films containing volatile EOs typically belong to the migratory system category. An immobilized or non-migratory system is essentially static and the AM agent must be in direct contact with the food to impart its AM activity.

The development of new AM packaging systems for a particular food product begins with the formulation of the AM materials with the first step to select an appropriate AM agent or agents. The target microorganisms that may spoil or otherwise contaminate the food product must be considered in making this choice and the AM agent(s) must be effective against these microorganisms. There are several techniques used to characterize the efficacy including *in vitro* tests and more importantly, tests on real food products [13]. Table 1 shows some common natural AM agents derived from the EO's of common herb varieties and the microorganisms against which they are effective. It is clear from this table that many of these naturally derived AM agents are effective against a wide spectrum of microorganisms and thymol, in particular, shows a significantly high level of AM activity.

**Table 1:** Relative AM effectiveness of thyme, oregano, thymol and carvacrol.

| Microorganism | Degree of inhibition[a] | Reference |
|---|---|---|
| Gram-negative bacteria | thymol, carvacrol > *p*-cymene | [14] |
| | thymol, carvacrol > linalool | [14] |
| | thymol, carvacrol > eugenol | [15] |
| | thymol, carvacrol > eugenol, geraniol, citral | [16] |
| Gram-positive bacteria | thymol, carvacrol > *p*-cymene, linalool | [14] |
| | thymol, carvacrol > cinnamaldehyde, eugenol > linalool, allyisothiosyanate | [17] |
| Yeast and moulds | thymol, carvacrol > eugenol | [18] |
| | thymol, carvacrol > *p*-cymene, linalool | [14] |

[a]Comparisons based on inhibition results from the same study.

Other important considerations in the development of effective AM packaging materials include a thorough characterization of the polymeric substrate with the physicomechanical properties among the more important aspects. The addition of an AM agent should not adversely affect these properties [19] and in the case of hydrophilic natural materials such as some starch-based films, it is also important that the environmental factors such as high relative humidity or water activity do not adversely affect material properties [20]. Another important consideration is the regulatory status of the AM agent as only substances that are "generally recognized as safe" (i.e. those that have "GRAS" status) can be used since AM agents that are incorporated into food packaging are considered in the USA to be food additives [21].

The migration or release of AM substances from the packaging matrix [22] should also be carefully considered, particularly in the case of migratory systems. A number of diffusion models can be applied to migrating AM systems [23] and the choice of model will depend on a number of factors including the distribution of AM agent in the packaging matrix, whether the diffusion is from one or both sides of the package, and the volume of solvent into which the migration occurs. It is evident that a comprehensive and strategic approach is needed to develop effective, mechanically sound, and safe AM films. This paper presents an overview of current and recent developments in the formulation and characterization of novel AM packaging materials at Victoria University.

## 2 Materials and Methods

### 2.1 Materials

The polymers used in the present study were low-density polyethylene (LDPE, XJF143/1700 Qenos, Australia) and polyethylene glycol (PEG) (A1683 PEG 4000 Ajax Finechem, Australia). A thermoplastic starch film blended with an aliphatic polyester (APTPS) was supplied by BioGrade®, Australia. Poly(lactic acid) (PLA, 7001D Ingeo™) was obtained from NatureWorks LLC, USA and kenaf fibre (bast) was purchased from Ecofibre Industries, Australia. The polymers used in the coating solutions were methylcellulose (MC) and hydroxypropyl methylcellulose (HPMC) purchased from Sigma-Aldrich, Australia.

The AM agents were linalool with a purity of 97% (L2602), carvacrol with a purity of 98% (W224502) and thymol with a purity of 99% (W306606) that were purchased from Sigma-Aldrich, Australia. Other chemicals include ethanol (95SG) supplied by CSR Distilleries Ltd., Australia, iso-octane (2,2,4–Trimethylpentane, OmniSolv®, TX 1389-1) supplied by EMD™ Chemicals Inc., USA, and glycerol purchased from AnalaR, Australia. Sodium hydroxide and acetic acid were purchased from Merck Chemicals, Australia. The encapsulation material β-cyclodextrin (β-CD) with purity ≥ 97% and water content 1.5% w/w was purchased

from Sigma-Aldrich, Australia. The media used in the studies was plate count agar (AM 144) purchased from Amyl, Australia. The microorganism *Escherichia coli* (UNSW 080300) was obtained from the culture collection of the University of New South Wales, Australia.

## 2.2 Activity of AM Agents Incorporated in LDPE Films

### 2.2.1 AM films prepared from LDPE and AM agent

Low-density polyethylene films of 45 - 50 µm thickness containing linalool or carvacrol were prepared from LDPE pellets. Additive-free LDPE pellets were ground and the powder was doped with linalool or carvacrol dissolved in isooctane. A pre-blended master batch powder containing approximately 15% w/w linalool or carvacrol was mixed with additive-free LDPE pellets and extruded into films using a single screw extruder with a diameter of 50 mm (Telford Smith, Australia). The films contained approximately 1.0% w/w linalool or carvacrol in their formulation. The temperature profile in the extruder was 195, 205, 210, 200, 210°C from the first barrel zone to the die [24].

### 2.2.2 Preparation of microorganisms

The stock cultures of *E. coli* were kept in nutrient broth (Amyl, AM 131) containing 30% v/v glycerol at -80°C. The working culture was obtained by growing cells on nutrient agar overnight at 37°C. The *E. coli* cells were then sub-cultured into nutrient broth twice before use whilst they were in the early stationary phase of growth. In order to harvest *E. coli* cells, nutrient broth that contained the twice-passaged *E. coli* was centrifuged (Sorvall®, Kendro Laboratory Products, USA) at 4000 × *g* for 10 min at 4°C. The supernatant was discarded and the precipitated cells were washed with a sterile 1% w/v peptone solution twice before being suspended in fresh nutrient broth and enumerated for the cell density. A certain density of *E. coli* was prepared by dilution with 1% w/v peptone solution.

### 2.2.3 Inhibition of microorganisms

Square pieces of film containing AM agents carvacrol or linalool were placed on the surface of individual nutrient agars that were inoculated with $10^5$ CFU $mL^{-1}$ of *E. coli* by the pour-plate method. The plates, prepared in quadruplicate, were then aerobically incubated for 24 h at 37°C. The AM activity of the tested agents was observed from the appearance of the inhibition zone around the square pieces of film.

## 2.3 Encapsulation of AM Additive

### 2.3.1 Preparation of β-CD/thymol complex

The β-CD complex preparation was achieved as follows: 3.835 g of β-CD was dissolved in 203 mL of water and heated to 55°C. Whilst the mixture was being vigorously stirred on a hot plate a 1 mL aliquot of ethanol was added followed by the addition of 0.5 g of thymol. The solution was covered and maintained at 55°C for 4 h with sufficient stirring after which the solution was cooled to room temperature and stirring was continued for 2 days at that temperature. The mixture of β-CD/thymol was then cooled to 4°C and maintained at this temperature for 24 h. The precipitated β-CD/thymol complex was recovered by vacuum filtration. The collected filtrate was allowed to dry in air for 5-9 days. A mass recovery of *ca*.71.3% was obtained from the reaction [25].

### 2.3.2 Preparation of LDPE films with thymol and β-CD/thymol complex

Low-density polyethylene films containing thymol or the β-CD/thymol complex were prepared using a laboratory hot press (IDM Instruments Pty. Ltd., Australia, Model No. L0003). For samples containing LDPE and thymol, the thymol was dissolved in ethanol and combined with LDPE pellets to ensure an even distribution of thymol before the ethanol was evaporated at room temperature. For samples containing the β-CD/thymol complex, a dry mixture of LDPE with the complex was formed. In both cases, the target concentration of thymol was *ca*. 10% w/w. To prepare the films, a sample of *ca.* 2 g of the resultant solid mixture was placed between Mylar™ films that were positioned between a set of aluminium plates. Film samples were created by pressing the solid mixture in the laboratory press that was preheated to 120°C. The temperature of the upper and lower platens of the press was maintained at 120°C for 2 min under a pressure of 30 kPa. The plates were quench-cooled with water to 80°C, then removed from the press and the samples removed from between the aluminium plates. The films were peeled off gently from the Mylar™ after they had cooled completely [25].

### 2.3.3 Quantification of thymol

The film samples were cut into small (*ca*. 1 g) pieces and each sample was extracted for 90 min under reflux extraction using 50 mL of ethanol. An aliquot of the extract was directly analyzed using gas chromatography (GC). A Varian Star 3400-CX GC equipped with a fused silica capillary column DB-5 (30 m × 0.25 mm i.d.,

film thickness 0.25 µm, J & W Scientific, USA) was used. The following conditions were applied: injected volume, 1.0 µL; initial column temperature, 80°C, heating rate: 5°C $min^{-1}$ up to 180°C, kept at this temperature for an additional 5 min; injector temperature, 250°C, split ratio, 1:100; FID detector temperature, 300°C; carrier gas, nitrogen. The AM agent content in each of the samples was calculated from prepared standard curves.

### 2.4 Preparation of Coated Starch-Based Films

The coating solution for APTPS films was prepared using MC and HPMC materials. The MC and HPMC were added slowly to absolute ethanol and heated, with stirring, on a magnetic hotplate. The heating was discontinued when the temperature reached 65°C. With continuous agitation, a mixture of PEG and distilled water (as plasticiser) was added slowly to the MC/HPMC dispersion whilst the dispersion cooled. This resulted in the formation of a uniformly clear coating solution or gel. The AM agent carvacrol was then added to the coating solution to form the final coating material with the AM agent at a target level of 3% w/w. The coating medium was applied to the starch-based material using a hand drawn glass roller and the film was then dried under ambient conditions (temperature 21°C, RH 38%) for 24 h. To control the thickness of the coating, the starch-based material was taped onto a 30 x 30 cm glass plate and the edges were framed using 3M™ masking tape.

### 2.5 Preparation of PLA/Kenaf Fibre Composites

#### 2.5.1 Preparation of kenaf fibres

Kenaf fibres were soaked in 5% w/v sodium hydroxide solution for 2 h at room temperature. The fibers were filtered and washed with distilled water before being neutralized by adding a few drops of acetic acid. The fibres were then filtered, washed and rinsed again with distilled water to remove excess acid and the latter confirmed using a pH meter. Finally, the fibres were dried overnight in an air oven at 105°C. Prior to mixing, the PLA resin and kenaf fibres were dried in an oven at 60°C overnight before blending with 5% and 10% w/w thymol.

#### 2.5.2 Processing PLA/kenaf and PLA/kenaf/thymol composites

A melt-blending process was used to prepare the composites using an internal mixer (Haake PolyLab OS, Germany) at a fixed screw speed of 50 rpm. The processing temperature and time were set at 155°C and 8 min respectively and a total mass of 50 g was required to fill the mixing chamber. The mixing torque curves together with stock temperature (actual temperature of the blend) were simultaneously obtained and monitored using Polysoft OS software during the mixing process.

### 2.6 AM Migration

The release of carvacrol from the MC-HPMC coatings on APTPS films into isooctane at 25°C was assessed in accordance with the double-sided, total immersion migration test (i.e. both sides of films immersed into the liquid stimulant). Film samples weighing *ca.* 0.5 g (4 pieces, 5 × 5 cm) were immersed in 100 mL of food simulant in a tightly sealed vessel that was mildly agitated (50 rpm) in an incubator shaker (Innova™ 4230, New Brunswick Scientific, U.S.A.). The migration test for each film in each simulant was performed at three temperatures: 10, 15 and 20°C. The amount of AM agent released was monitored until equilibrium was attained. An aliquot of the solution was analysed by GC analysis at different time intervals. The AM release into the food simulants was quantified under the GC conditions described previously.

## 3 Results and Discussion

### 3.1 Preparation and Characterization of AM Films and Composites

The critical steps required to prepare and characterize AM films and composites include material formulation, processing techniques, mechanical and physical testing as well as quantifying the efficacy of the AM agent against target microorganisms. In the case of volatile AM agents, techniques to reduce loss of natural AM agents during film processing should also be considered. Figure 1 shows the AM activity of the natural agents carvacrol and linalool incorporated in LDPE film against *E. coli* on nutrient agar. Although no microbial growth occurs under the film containing linalool in Figure 1(a), no zone of inhibition is observed. In the case of carvacrol (Figure 1(b)), stronger antimicrobial activity is evident with the presence of a significant inhibition zone.

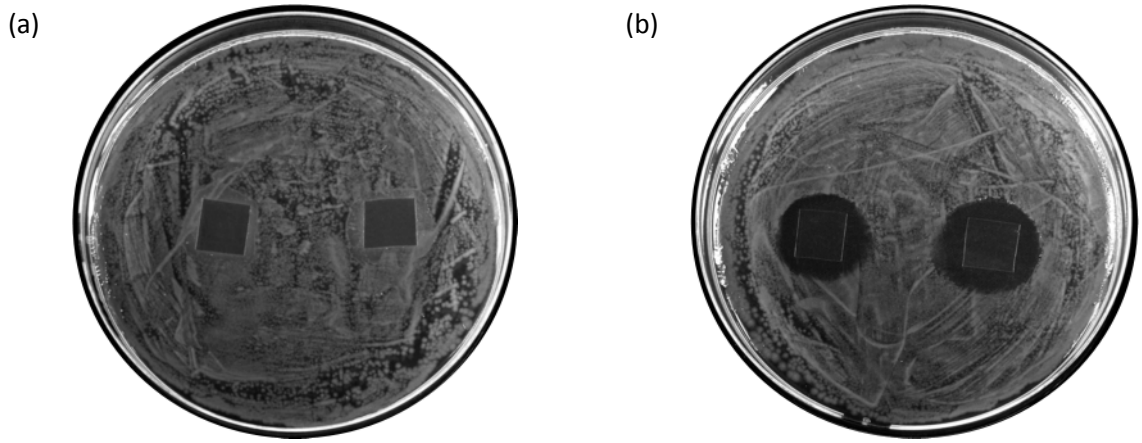



*Figure 1. Photographs showing the inhibitory effect of films containing: (a) linalool and (b) carvacrol against E. coli.*

### 3.2 Improving AM Agent Retention

Volatile agents are particularly susceptible to losses during processing at high temperature. Additives can be used to improve retention with some success but other techniques include the use of inclusion compounds such as β-CD to encapsulate the AM agents. Complexation of AM agents in the β-CD matrix can be achieved by a simple technique that can enable more than 90% of the AM agent thymol to be complexed and subsequently extracted into an ethanol solution [25]. Figure 2 shows that encapsulating thymol within the β-CD complex significantly retains the AM agent in LDPE film over the experimental time period whereas films that were processed with the free thymol lose most of this agent in less than 100 h. The release of thymol or any agent from the β-CD complex is critical in order to impart effective AM activity and this is currently under investigation.

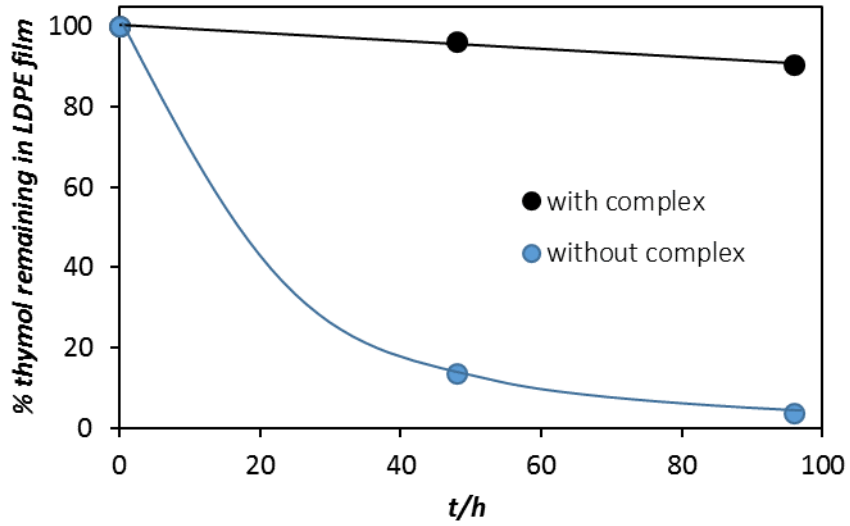



*Figure 2. Percentage of thymol remaining in LDPE film with and without β-CD complex.*

### 3.3 AM Packaging from Biopolymers and Biocomposites

In addition to polymers derived from crude oil, there are many new and improved biopolymers that have similar molecular structures and physicomechanical characteristics to the more conventional commodity polymers. An example is PLA, a polymer that is in the same class of polymers as polyethylene terephthalate (PET). Although it has similar properties, can be processed using conventional equipment, and is biodegradable, it is

unfortunately, relatively expensive to produce [26]. These costs can be reduced by introducing inexpensive fillers that can often impart improved mechanical properties to the biocomposite [27]. However, the addition of fillers can adversely affect the processability of biocomposites during extrusion but this can be improved with the use of processing aids. Figure 3 shows examples of the rheological profiles of 10% w/w kenaf filled PLA biocomposites in the presence of the AM agent thymol. In this case, the addition of thymol imparts a lubricating effect during processing resulting in a significant reduction in the processing torque. The peak in the melt torque shown in Figure 3 (curve (a)) observed at *ca.* 2 min corresponds to the time when the kenaf fibres are introduced into the mixer but this peak is absent in the case where kenaf fibres incorporated with thymol are introduced (see Figure 3, curve (b)). This may be due to the lubricating effect of the AM agent. This contention is also supported by the significantly lower equilibrium torque observed after *ca.* 6 min in the formulation containing thymol compared with the formulation without thymol.

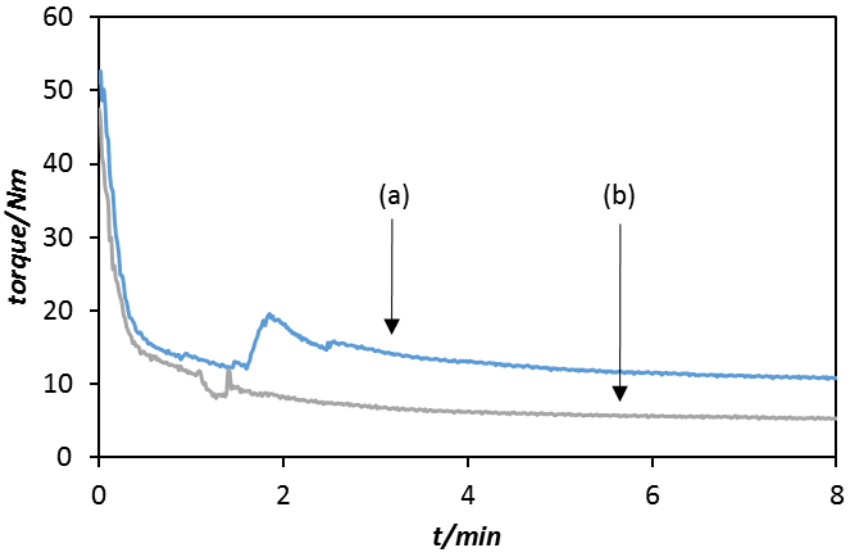



*Figure 3. Torque versus time for PLA kenaf fiber biocomposites containing: (a) no thymol and (b) 10% w/w thymol.*

### 3.4 Characterizing the Rate of AM Release

Several equations have been derived for the time dependent migration of the mass of an additive from a polymer film into a food simulant. The time over which migration occurs has been divided into "short" and "long" terms [23, 28]. The “short-term” migration of an additive is defined as the time for which $m_t/m_\infty < 0.6$ and is described by the following equation:

$$m_t/m_\infty = 4(Dt/\pi l)^{1/2} \quad (1)$$

where $m_t$ and $m_\infty$ are the amounts of additive released from the film up to time $t$ and equilibrium ($t = \infty$) respectively, $D$ is the diffusion coefficient and $l$ is the thickness of the film. A plot of $m_t/m_\infty$ versus $t^{1/2}$ will produce a straight line that passes through the origin and the diffusion coefficient can be obtained from the gradient of the line.

An approximation of the long-term migration is described by the following equation:

$$m_t/m_\infty = 1 - (8/\pi^2)\exp(-\pi^2 Dt/l^2) \quad (3)$$

The short-term/long-term boundary is traditionally where $m_t/m_\infty = 0.6$, however it has been suggested that this boundary can be varied in the event that the fit of these equations is not ideal. For example, it has been reported that the boundary may be shifted from 0.6 to 0.5 with little consequence in the theoretical analytical result [28, 29].

Figure 4 shows an analysis of the migration of the AM agent carvacrol from a biodegradable APTPS substrate coated with the agent dispersed in a mixture of MC, HPMC and PEG into the food simulant isooctane. The limited flexibility in determining the boundary as described above was invoked in the analysis in order to produce the best possible estimates of the diffusion coefficient and kinetic data associated with the release [22]. The linearity of these plots confirms the applicability of these models to describe the kinetic release of carvacrol from the coating system using the modified boundary conditions. The data also enables an estimate of the diffusion coefficient and kinetic data associated with the release [22]. These data are necessary in designing systems where the rate of dissipation of the AM agent during the lifetime of the film is such that it is effectively zero at the time when the material is to be disposed of either by composting or in landfill.

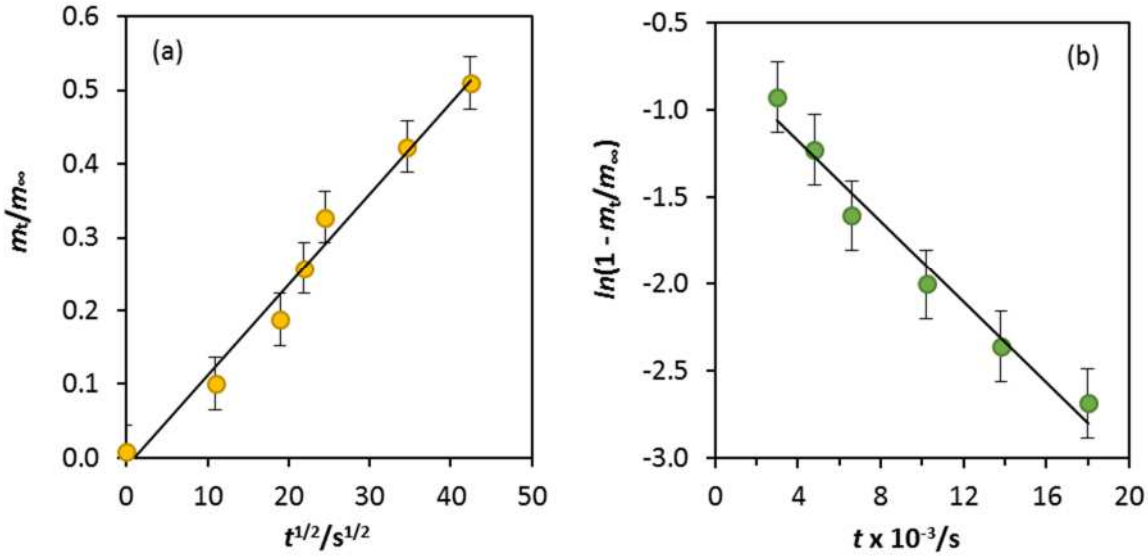



*Figure 4. Plots of: (a) $m_t/m_\infty$ versus $t^{½}$ and (b) $\ln(1 - m_t/m_\infty)$ versus t for the migration of carvacrol from MC-HPMC coatings on APTPS films into isooctane at 25 °C.*

## 4 Conclusions

Antimicrobial packaging materials can be developed by direct incorporation of AM agents or in coatings in order to control the proliferation of spoilage microorganisms. Natural AM agents derived from essential oils and their extracts are being used increasingly in active packaging systems. However, these are volatile materials that can suffer significant loss from the polymer matrix during thermal processing. Such unacceptable loss must be overcome for the development of commercially viable AM packaging materials. Some advances in this area include the use of additives that assist in retaining the AM additive or lubricants in the extrusion stage of film production, that decrease friction and that help disperse the additive within the polymer matrix whilst enhancing retention. The use of encapsulating technologies such as inclusion compounds may also overcome the problem of loss of volatile agents. In addition to developments in AM agent technologies, recent advances have been made in the search for packaging materials that can be produced from renewable resources. Certain types of these naturally derived materials are claimed to be more readily biodegradable than the traditional commodity packaging materials. The future challenges in this field of packaging science will be to produce materials that: (i) can be derived economically from natural and renewable sources; (ii) contain natural AM systems whose lifetimes in the active packaging are such that they will not affect the final biodegradation of the materials in the environment and (iii) will biodegrade in the environment in a way that produces useable products such as methane or compost that can be collected and reused.

## 5 References

[1] Rooney, M. L., Plastic in Active Packaging, in Materials and Development of Plastic Packaging, M.L. Rooney, Ed, 1995.

[2] Miltz, J., Passy, N., Mannhwim, C. H., Trends and applications of active packaging systems, in Food and Packaging Materials - Chemical Interaction, P. Ackerman, M. Jagerstad, and T. Ohlsson, Eds, The Royal Society of Chemistry. pp. 201-210, 1995.

[3] Ahvenainen, R., Active and intelligent packaging, in Novel Food Packaging Techniques, R. Ahvenainen, Ed, Woodhead publishing limited: Cambridge, England, 2003.
[4] Brody, A. L., Exploring MAP and active packaging, Food Technology vol.62 pp. 72-74, 2008.
[5] Han, J. H., ed. New technologies in food packaging: Overview, Elsevier Academic Press: Manitoba. 5-11 p, 2005.
[6] Suppakul, P., Sonneveld, K., Miltz, J., Bigger, S. W., Active packaging technologies with an emphasis on antimicrobial packaging and its applications, Journal of Food Science, vol.68 pp. 408-420, 2003.
[7] Kuorwel, K. K., Cran, M. J., Sonneveld, K., Miltz, J., Bigger, S. W., Evaluation of Antifungal Activity of Antimicrobial Agents on Cheddar Cheese, Packaging Technology and Science, vol.27 pp. 49-58, 2014.
[8] Kuorwel, K. K., Cran, M. J., Sonneveld, K., Miltz, J., Bigger, S. W., Antimicrobial Activity of Natural Agents Coated on Starch-Based Films against *Staphylococcus aureus*, Journal of Food Science, vol.76 pp. M531-M537, 2011.
[9] Rardniyom, C., Development of Multi-layer Films Containing Natural Antimicrobial Agents, PhD dissertation, Packaging and Polymer Research Unit, Victoria University, 2008.
[10] Suppakul, P., Sonneveld, K., Bigger, S. W., Miltz, J., Efficacy of polyethylene-based antimicrobial films containing principal constituents of basil, LWT - Food Science and Technology, vol.41 pp. 779-788, 2008.
[11] Han, J. H., Antimicrobial food packaging, Food Technology, vol.54 pp. 56-65, 2000.
[12] Appendini, P., Hotchkiss, J. H., Review of antimicrobial food packaging, Innovative Food Science and Emerging Technologies vol.3 pp. 113-126, 2002.
[13] Kuorwel, K. K., Cran, M. J., Sonneveld, K., Miltz, J., Bigger, S. W. Development of Starch-Based Antimicrobial Packaging Films, in Proceedings of 26th IAPRI Symposium on Packaging: Espoo, Finland, June 10-13, 2013.
[14] Cosentino, S., Tuberoso, C. I. G., Pisano, B., Satta, M., Mascia, V., Arzedi, E., Palmas, F., *In-vitro* antimicrobial activity and chemical composition of Sardinian *Thymus* essential oils, Letters in Applied Microbiology, vol.29 pp. 130-135, 1999.
[15] Olasupo, N. A., Fitzgerald, D. J., Gasson, M. J., Narbad, A., Activity of natural antimicrobial compounds against *Escherichia coli* and *Salmonella enterica*, Letters in Applied Microbiology, vol.37 pp. 448-451, 2003.
[16] Nazer, A. I., Kobilinsky, A., Tholozan, J. L., Dubois-Brissonnet, F., Combinations of food antimicrobials at low levels to inhibit the growth of *Salmonella* sv. Typhimurium: a synergistic effect?, Food Microbiology, vol.22 pp. 391-398, 2005.
[17] Yamazaki, K., Yamamoto, T., Kawai, Y., Inoue, N., Enhancement of antilisterial activity of essential oil constituents by nisin and diglycerol fatty acid ester, Food Microbiology, vol.21 pp. 283-289, 2004.
[18] Scora, K. M., Scora, R. W., Effect of volatile oils on mycelium growth of *Penicillium digitatum*, *P. italicum* and *P. ulaiense*, Journal of Basic Microbiology, vol.38 pp. 405-413, 1998.
[19] Kuorwel, K. K., Cran, M. J., Sonneveld, K., Miltz, J., Bigger, S. W., Physico-Mechanical Properties of Starch-Based Films Containing Naturally Derived Antimicrobial Agents, Packaging Technology and Science, vol.27 pp. 149-159, 2014.
[20] Kuorwel, K. K., Cran, M. J., Sonneveld, K., Miltz, J., Bigger, S. W., Water sorption and physicomechanical properties of corn starch-based films, Journal of Applied Polymer Science, vol.128 pp. 530-536, 2013.
[21] FDA. Antimicrobial food additives - Guidance. 1999 accessed: February 23, 2006; Available from: http://www.cfsan.fda.gov/~dms/opa-antg.html.
[22] Kuorwel, K. K., Cran, M. J., Sonneveld, K., Miltz, J., Bigger, S. W., Migration of antimicrobial agents from starch-based films into a food simulant, LWT - Food Science and Technology, vol.50 pp. 432-438, 2013.
[23] Crank, J., The Mathematics of Diffusion, Oxford University Press: Oxford, UK. 406 p, 1975.
[24] Suppakul, P., Study of antimicrobial polymeric packaging films containing basil extracts, PhD dissertation, School of Molecular Sciences, Melbourne, Australia, 2004.
[25] Al-Nasiri, G., Minimizing the Loss of Natural Antimicrobial Agents during the Thermal Processing of Food Packaging Films, BSc (Hons) dissertation, College of Engineering and Science, Victoria University, 2013.
[26] Achmad, F., Yamane, K., Quan, S., Kokugan, T., Synthesis of polylactic acid by direct polycondensation under vacuum without catalysts, solvents and initiators, Chemical Engineering Journal, vol.151 pp. 342-350, 2009.
[27] Faludi, G., Dora, G., Renner, K., Móczó, J., Pukánszky, B., Improving interfacial adhesion in PLA/wood biocomposites, Composites Science and Technology, vol.89 pp. 77-82, 2013.
[28] Miltz, J., Migration of low molecular weight species from packaging materials: theoretical and practical considerations, in Food Product-Package Compatibility, J.I. Gray, B.R. Harte, and J. Miltz, Eds, Technomic Publishing Co.: Lancaster, PA. pp. 30-43, 1987.
[29] Cran, M. J., Rupika, L. A. S., Sonneveld, K., Miltz, J., Bigger, S. W., Release of Naturally Derived Antimicrobial Agents from LDPE Films, Journal of Food Science, vol.75 pp. E126-E133, 2010.

# Biodegradable Cross-Linked Gliadin Films with Antifungal Activity for Active Packaging of Bread

**Mari Pau Balaguer[1], Pascale Chalier[2], Eva Almenar[3], Nathalie Gontard[2], Javier Zabaleta[4], Rafael Gavara[1], and Pilar Hernandez-Munoz[1*]**

[1] *Grupo de Envases, Instituto de Agroquímica y Tecnología de Alimentos (IATA-CSIC), Spain*
[2] *Ingénierie des Agropolymères et Technologies Emergentes, Université Montpellier 2, France*
[3] *School of Packaging, Michigan State University, United States*
[4] *Packaging, Transports, and Logistics Research Centre, Spain*

[*] *Corresponding author. Email: phernan@iata.csic.es*

**Abstract:** Protein-based bioplastics obtained directly from biomass are renewable and inherently biodegradable. However, some of their functional properties should be improved to be used satisfactorily in packaging applications, especially the mechanical and water resistance, what could lead to a reduction in their biodegradability. Moreover, these materials have a great potential to be used in the development of active films for food packaging applications. Their water sensitivity provides them with a mechanism for triggering the release of active volatile organic compounds that can be previously incorporated into the polymer matrix.

In this work wheat gliadin proteins were employed as raw material for the production of films. A chemical treatment which combines cinnamaldehyde with low pH in the reaction medium was used to cross-linking the proteins. Moreover, cinnamaldehyde is a well-characterized natural antimicrobial agent against a wide range of pathogen and food-decay microorganisms. Cinnamaldehyde was incorporated in different percentages. Glycerol was used as plasticizer, and films were produced by casting. Mechanical tensile tests and stability of films in water were evaluated. Biodegradation in compost was also checked. The kinetics release of cinnamaldehyde was evaluated at different relative humidities. Antifungal properties were tested in sliced bread.

The results showed that cinnamaldehyde treatment of gliadin films increased their cross-linking density, reducing their solubility in water and improving their mechanical resistance, without comprising their biodegradability. The release rate of cinnamaldehyde increased at high relative humidity conditions, what represents an excellent mechanism to retain the compound before its use, and to trigger and modulate its release rate according to the food product moisture. Gliadin films incorporated with cinnamaldehyde were highly effective against mold growth in bread, increasing the time lag from 4 days to 27.

Gliadin films incorporating cinnamaldehyde present improved functional properties, were biodegradable and effective against mold growth in bread, enabling their application in active food packaging.

Keywords: protein films, cinnamaldehyde, antimicrobial activity, active packaging, biodegradability, functional properties, bread.

## 1 Introduction

In the last decade, the use of renewable materials with biodegradable properties is gaining great interest (*1*). Proteins, from plant or animal origin, represent a suitable raw material for the production of novel bioplastics. Proteins possess moderate mechanical resistance, and have good barrier properties to oxygen and carbon dioxide at low and medium relative humidities (RH); however, their water stability and water vapor permeability should be improved to be employed satisfactorily in packaging applications (*2*). To this end, physical, chemical, and enzymatic treatments have been applied to proteins, enhancing the functionality of the resulting films (*3-5*). Among proteins, wheat gluten deserves special recognition due to its film-forming capacity, thermoplasticity, viscoelasticity, availability, low cost, etc. (*6*). It can be separated in its fractions, glutenins and gliadins, to maximize its range of uses (*7*).

Active packaging of foods can extend their shelf-life, and enhance their safety and quality by means of the interaction between the package, the product, and the environment (*8*). The use of naturally-occurring compounds extracted from plants is the last trend in active food packaging technologies (*9*). Essential oils and

their major constituents have shown great effectiveness against microbial growth (*10*). Cinnamaldehyde, an α,β-unsatured aldehyde from bark cinnamon essential oil, have demonstrated excellent antimicrobial properties, and due to its chemical structure could also be used as cross-linker of proteins.

The aim of this work was to employ cinnamaldehyde as cross-linker of wheat gliadins, and as antimicrobial for active packaging. The effect of cinnamaldehyde-treatment on the functional properties and inherent biodegradability of films together with the capacity of cinnamaldehyde to be released was evaluated. The applicability of the active films was tested in bread slices.

## 2 Materials and Methods

### 2.1 Materials

Crude wheat gluten, glycerol, ethanol, hydrochloric acid, cinnamaldehyde, and microcrystalline cellulose, all laboratory grade, were supplied by Sigma (Madrid, Spain). Compost was obtained from Tetma (Guadassuar, Spain)

### 2.2 Film formation and Conditioning

The gliadin-rich fraction was extracted from wheat gluten according to the method described by Hernandez-Munoz (*11*). Cinnamaldehyde was added as a cross-linker at different percentages, namely 1.5, 3, and 5% (g/100 g of protein), to the film-forming solution adjusted to pH 2. Glycerol was added as a plasticizer at 25% (g/100 g of protein). Gliadin control films without cinnamaldehyde were prepared at pH 6, the native pH of the film-forming solution. Films were prepared by casting and drying at 37 °C for 24 h.

### 2.3 Mechanical Properties

A universal machine Mecmesin model MultiTest 1-í (Landes Poli Ibérica, S.L., Barcelona, Spain) equipped with a 100 N static load cell was used to evaluate the maximum tensile strength ($\sigma_m$), percentage of elongation at break ($\varepsilon_b$) and Young's modulus (*E*) of the films according to ASTM standard method D882 (*12*). The films were conditioned at 50% RH for at least 1 week prior to testing. Film samples were cut into strips 2.54 cm wide and 10 cm long. The grip separation was set at 5 cm, and the cross-head speed at 25 mm·min$^{-1}$. At least 10 replicates from each sample were tested. The tensile properties were calculated from the plot of stress (tensile force/initial cross-section area) versus strain (elongation as a fraction of the original length).

The cross-link density (CLD) was assessed from the stress-strain curves by means of the following relationship (*13*) between Young's modulus (*E*) and CLD:

$$CLD = \frac{E}{3RT} \tag{1}$$

where R is the universal gas constant (8.314 J·mol$^{-1}$K$^{-1}$) and T the absolute temperature (K).

### 2.4 Stability in Water

Film specimens were cut into circles with a diameter of 2.5 cm (initial diameter, $\emptyset^i$), and dried for 10 days in a desiccator over silica gel (0% RH). They were weighed (initial dry weight, $W_d^i$). Then they were immersed in test tubes containing distilled water, and shaken occasionally. The films were removed from the solution at different time intervals over a 50-day period. The remaining water was removed from the film surface with absorbent paper before weighing (final wet weight, $W_w^f$). The films were replaced in the desiccator until they reached a constant weight (final dry weight, $W_d^f$). The percentage of water uptake, and weight loss were calculated as follows:

$$Water\ uptake\ (\%) = \frac{W_w^f - W_d^f}{W_d^f} \cdot 100 \tag{2}$$

$$Weight\ loss\ (\%) = \frac{W_d^i - W_d^f}{W_d^i} \cdot 100 \tag{3}$$

### 2.5 Biodegradation under Composting Conditions

The aerobic biodegradation of films was established by testing under controlled composting conditions at laboratory scale. The method was adapted from the ISO standard 14855-1 (*14*) which is based in the measure of

the $CO_2$ evolved. Film samples were ground to obtain particles around 1 to 2 mm. The respirometric unit consisted of a hermetic 2-L glass jar, which was modified for the air withdrawal with a rubber septum, and containing two polypropylene flasks of 60-mL capacity. One of the flasks contained 3 g of dry compost mixed with 50 mg of equivalent carbon of the ground dry samples (around 100 mg of sample). Vermiculite (1 g) was added to prevent the compost from becoming compacted, and to facilitate oxygen access. The water content of the compost was adjusted to reach 80% of the soil water retention capacity. The other flask contained distilled water in order to maintain the relative humidity at 100% inside the jar to avoid compost drying. The glass vessels were hermetically closed and incubated in the dark at 58 ± 2 °C. Biodegradation experiments included control (microcrystalline cellulose) and blank (compost alone) samples. All experiments were run in triplicate.

The $CO_2$ produced in each bioreactor was measured by withdrawal of 10 mL of the head-space air with a syringe, and posterior injection in an $O_2$ and $CO_2$ analyzer CheckMaster 2100 (Lippke, Neuwied, Germany). Oxygen concentration was also recorded and always maintained above 6% in order to maintain aerobic conditions.The theoretical amount of $CO_2$ that can be produced assuming that all the carbon of the test sample is transformed into $CO_2$ ($CO_2^{Th}{}_S$) was calculated from equation (3):

$$CO_2^{Th}{}_S = W_s \cdot C_s \cdot \frac{MW_{CO_2}}{MW_C} \quad (4)$$

where $W_s$ (g) is the dry weight of film sample introduced in the bioreactor, $C_s$ (g C/g dry sample) is the proportion of organic carbon in the dry film samples, $MW_{CO_2}$ is the molecular weight of carbon dioxide, and $MW_C$ is the molecular weight of carbon.

The percentage of biodegradation ($\%B$) was calculated from the cumulative amount of $CO_2$ produced, expressed as a percentage of the theoretically expected value for total conversion to $CO_2$ ($CO_2^{Th}{}_S$) by means of equation (5):

$$\%B = \frac{\sum CO_{2S} - \sum CO_{2B}}{CO_2^{Th}{}_S} \cdot 100 \quad (5)$$

where $\sum CO_{2_S}$ (g) is the cumulative amount of $CO_2$ produced in the sample bioreactors, and $\sum CO_{2_B}$ (g) is the cumulative amount of $CO_2$ produced in the blank bioreactors.

## 2.6 Kinetics Release of Cinnamaldehyde

Films were cut into small disks, each 2 cm in diameter, and they were weighed and placed in three different chambers maintained at 23 °C and at a constant RH of 30, 50, or 90% ± 5%. The RH was adjusted by using a humidified air flow through the chamber. Air was humidified by bubbling in a gas washing bottle containing water and placed in a cryostat at controlled temperature. The temperature differential imposed between the cryostat and the chambers allowed the air flux to reach the selected humidity. During each experiment, the chamber humidity was controlled using a hygrometer probe (Rotronic, Bassersdorf, Switzerland). Pieces of film were removed from the chambers at different time intervals for analysis; cinnamaldehyde content was immediately determined by solvent extraction and gas chromatography.

Cinnamaldehyde was extracted from films by immersing three pieces of film in 10 mL of n-pentane containing 100 µL of internal standard solution under continuous magnetic stirring for 24 h at 500 rpm and ambient temperature. The internal standard used was 2-nonanol (10 mg/mL in ethanol). The organic phase containing cinnamaldehyde and 2-nonanol was removed and dried over anhydrous sodium sulfate and analyzed by gas chromatography. Analyses were performed by a Varian 3800 GC (Les Ulis, France) equipped with a DB-WAX column (J&W Scientific) (30 m × 0.32 mm, film thickness 0.25 µm) and a flame ionization detector (FID). Hydrogen was used as carrier gas with a flow rate of 2 mL/min. The oven temperature was programmed to rise from 60 to 150 °C at 4 °C/min, then from 150 to 250 °C at 15 °C/min, and held at 250 °C for 10 min. Injector and detector temperatures were maintained at 250 °C. Injections were done in split mode with a 1:20 ratio. Quantification of cinnamaldehyde was performed using the internal standard and after determination of the response coefficient, which was equal to 0.990 ± 0.008. The extraction efficiency was estimated by depositing a known quantity of cinnamaldehyde on a gliadin control film (without the compound) and by applying the extraction procedure described above. The extraction yield was found to be 75% ± 1%. For each time and RH, the extraction was done in triplicate from two different films. Results were expressed in terms of remaining cinnamaldehyde at time *t* per gram of film.

## 2.7 Active Packaging of Bread

White bread was produced according to the traditional method using a bread-making machine. The ingredients employed were 500 g of white wheat flour from organic culture (Panadería Rincón del Segura S.L., Albacete, Spain), 10 g of dehydrated yeast (VITAM Hefe-Produkt GmbH, Hameln, Germany), 340 mL of water, 6 g of

salt and 12.5 g of sugar. After baking, the bread was cooled at ambient temperature for 30 min and sliced into portions of 1 cm thickness by means of a standard bread slicer (Model TP 60/2, E. Gabarró, Barcelona, Spain). The dimensions of the bread slices were approximately 12 cm × 7 cm and the weight was around 45 g.

Each bread slice was placed in a plastic bag (15 cm × 10 cm) of mono cast polypropylene of 30 µm thickness along with a piece (13 cm × 8 cm) of a gliadin film treated with 5% of cinnamaldehyde (G5C_pH2) (active packaging tests). Control packaging tests were performed in the same way without including the gliadin film. The plastic bags were closed using a manual sealing machine (Sealboy 420 SBM, Rovebloc S.A., Barcelona, Spain) and stored at 23 ± 2 °C and 50% RH. The antifungal effect was evaluated over time by visual inspection of the fungal growth. Antimicrobial packaging was considered effective only if there was a delay or no growth of molds in comparison with the control. Tests were performed in triplicate.

## 3 Results and Discussion

### 3.1 Mechanical Properties

The stress-strain (σ – ε) curves at 50% RH of the control and cinnamaldehyde-treated gliadin films are depicted in **Figure 1**. Chemical treatment with cinnamaldehyde at pH 2 modified the typical viscous behavior of the gliadin films (G_pH6), giving rise to a different mechanical profile. As the percentage of cinnamaldehyde increased, the stiffness of the films rose, and they presented greater tensile strength, indicating the formation of a cross-linked protein network.

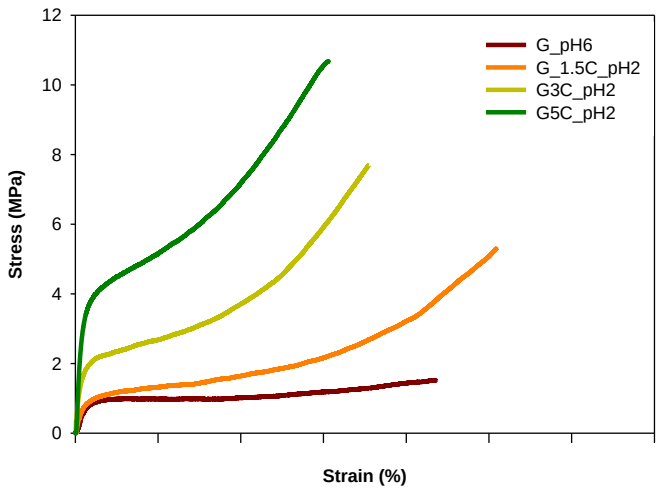



**Figure 1**: Stress-strain curves of gliadin films at 50% RH.

The mechanical parameters ($\sigma_m$, *E*, and $\varepsilon_b$) of the control and treated films conditioned at 50% RH are shown in Table 1. Cinnamaldehyde treatment gave rise to a considerable increase in the $\sigma_m$ and the *E*, and a decrease in the $\varepsilon_b$ of gliadin films. The $\sigma_m$ values for the cross-linked gliadin films with 3% and 5% cinnamaldehyde were higher than those obtained for cross-linked gliadin films with 40% epichlorohydrin (*15*), and 4% formaldehyde, glutaraldehyde or glyoxal (*16*). The cross-linking density was directly proportional to the amount of cinnamaldehyde added.

**Table 1:** Mechanical parameters of films tested at 50% RH.

| Sample | $\sigma_m$ (MPa) | $\varepsilon_b$ (%) | *E* (MPa) | CLD (mol/m$^3$) |
|---|---|---|---|---|
| **G_pH6** | 1.60 ± 0.24 | 226 ± 32 | 24.3 ± 4.9 | 3.20 ± 0.60 |
| **G1.5C_pH2** | 5.23 ± 0.83 | 248 ± 14 | 34.9 ± 6.5 | 4.72 ± 0.82 |
| **G3C_pH2** | 7.74 ± 0.83 | 180 ± 8 | 63.9 ± 21.7 | 9.75 ± 1.87 |
| **G5C_pH2** | 9.93 ± 1.21 | 146 ± 12 | 112 ± 11 | 15.19 ± 1.48 |

$\sigma_m$: Maximum tensile strength, $\varepsilon_b$: Elongation at break, E: Young's modulus. Reported values are means of 10 replicates ± standard deviation.

### 3.2 Stability of Films in Water

Figure 2 shows the water uptake (A), and weight loss (B) over time for the films containing 1.5%, 3%, and 5% of cinnamaldehyde. Control film could not be evaluated since it lost its integrity when immersed in water. The percentage of water uptake was inversely related to the amount of cinnamaldehyde added into the gliadin film-forming solution, and this trend was maintained over time. The weight loss after 24 h was similar for all the films, irrespective of the cross-linker concentration. This weight loss was around 22% and was mainly due to the migration of hydrophilic glycerol into the aqueous medium and, to a lesser extent, to the release of short polypeptide chains from the reticulated matrix. The loss of glycerol was confirmed by the lack of flexibility of the films after drying. The weight loss of all films increased progressively and the differences among them became more acute over time, reflecting changes in the structure of the protein matrix.

These findings draw attention to the improvement in the physical performance of cross-linked matrices, which enables the films with the greatest cross-linking to withstand water immersion conditions for longer periods of time.

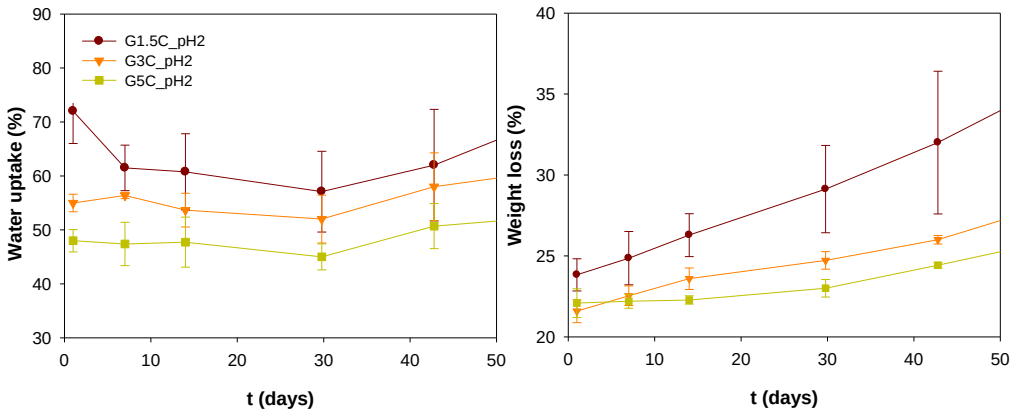



**Figure 2**: Physical changes in gliadin films kept in aqueous medium through 50 days of storage at ambient temperature: (A) water uptake (%), and (B) weight loss (%).

### 3.3 Biodegradation under Composting Conditions

Figure 3 shows the biodegradation kinetics of the control and cinnamaldehyde-treated gliadin films, and the cellulose employed as a positive reference.

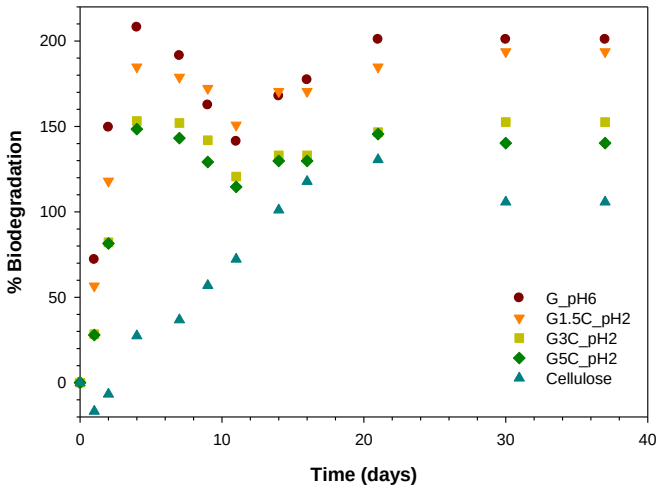



**Figure 3**: Biodegradation kinetics of control gliadin film, cinnamaldehyde-treated gliadin films, and positive reference.

Cellulose reached 100% biodegradation after 14 days; however, the maximum biodegradation was found after 21 days accounting for 130%. This behavior corresponding to a percentage of biodegradation greater than 100% was also observed for gliadin films more pronouncedly. This effect is known as priming and it occurs if the compost inoculum in the test reactor containing the samples is producing more $CO_2$ than the compost inoculum in the blank reactors (*17*). The negative beginning in the biodegradation curve of cellulose can be ascribed to the lag phase of biodegradation. Biodegradation profile of gliadin films reached a maximum after 1-2 days and then decreased during 4 days. This behavior was similar to that found for feather keratin films analyzed by Barone and Arikan (*18*). However, in the case of gliadin films after this minimum a recovery in the percentage of biodegradation was produced. It is believed that gliadin films were rapidly biodegraded by a growing microbial population achieving very rapid biodegradation rates. This fact could give rise to a sharp reduction of nutrients, and the feedstuff became insufficient for the living microorganisms which were also drastically reduced, diminishing the amount of carbon dioxide produced in comparison with the blank bioreactors. After a lag phase the microbial population was recovered, and continued the biodegradation in the same rate as the blank compost.

### 3.4 Kinetics Release of Cinnamaldehyde

Figure 4 shows the kinetics of cinnamaldehyde release from a gliadin film incorporating 5% of cinnamaldehyde at different relative humidities (30%, 50%, and 90% RH) and 20 °C. The release of cinnamaldehyde from the gliadin matrix was notably affected by the relative humidity of the environment. The higher the relative humidity, the faster the release kinetic of cinnamaldehyde was. Owing to the hydrophilic nature of gliadins, sorption of water promotes plasticization of the film and release of the volatile compound entrapped within the polymer network. This effect can be used to trigger release of the volatile compound, and to control the release rate. Therefore the films can be stored at low relative humidity conditions to avoid loss of cinnamaldehyde before their use. On the other hand, the high relative humidity conditions present inside packaged food, often associated with microorganism development, trigger release of the antimicrobial volatile compound when it is required.

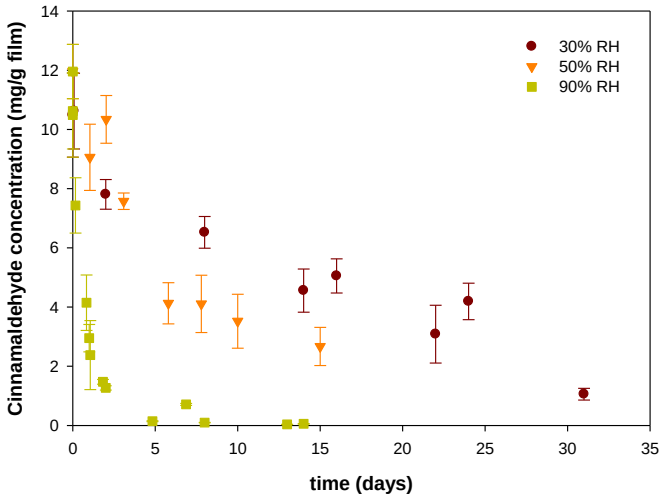



**Figure 4**: Kinetics of cinnamaldehyde release from G5C_pH2 film at different relative humidities and 20 °C.

### 3.5 Antifungal properties of Films in Bread

Mold growth appeared after only four days when bread was packaged with the control films. Active packaging of bread slices with cinnamaldehyde-treated gliadin films was highly effective in delaying fungal growth, and only one sample was slightly contaminated after 28 days of storage. Figure 5 shows the growth of naturally-present molds in bread in both the control and the active packaging samples after 1 month of storage.

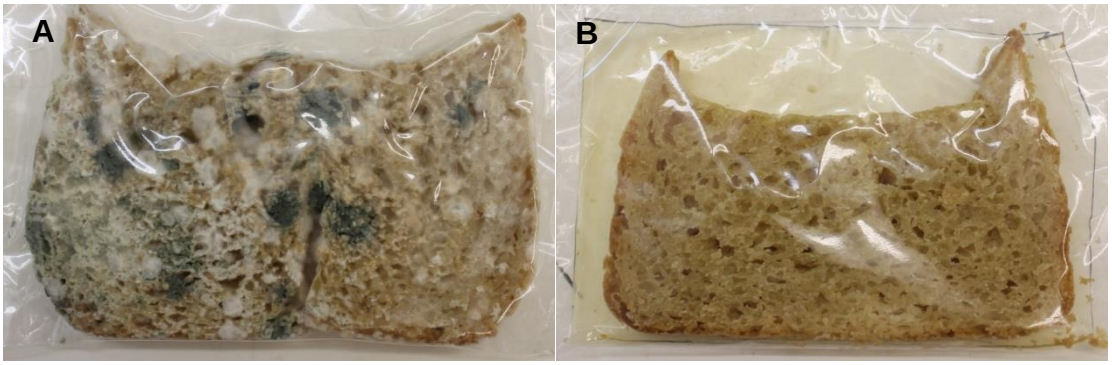



**Figure 5**: Growth of naturally-present molds in bread after 1 month in control packaging (A), and in active packaging (B).

The water activity of bread is around 0.95, therefore the humidity created in the internal atmosphere represents an excellent mechanism to trigger the release of the antimicrobial compound. According to the release kinetics it is expected that this release would start rapidly at high relative humidity. Once the partition equilibrium between the cinnamaldehyde in the film and the head-space is reached, the film acts as a reservoir.

Even though the microbiological shelf-life of sliced bread can be extended, it is also necessary to evaluate the sensory and physico-chemical properties to assess the potential of cinnamon essential oil or its constituents in the active packaging of bread.

## 4 Conclusions

Cinnamaldehyde-treated gliadin films presented improved mechanical resistance and water stability than control gliadin films. The addition of cinnamaldehyde did not hamper their inherent biodegradation, although films presented higher cross-linking degrees and antimicrobial activity. The release of residual cinnamaldehyde entrapped in the protein matrix can be modulated by the relative humidity of the environment. Their use in the active packaging of bread slices delayed mold growth. Therefore, these antimicrobial bioplastic films could be employed satisfactorily in active food packaging applications.

## Acknowledgements

The authors would like to thank the Spanish Ministry of Science and Innovation for financial support (project AGL2012-39920-C03-01 and M. P. Balaguer's FPI fellowship).

## References

1. Queiroz, A. U. B. and Collares-Queiroz, F. P., 2009, "Innovation and Industrial Trends in Bioplastics", *Polymer Reviews*, vol. 49, pp. 65-78.
2. Gennadios, A., McHugh, T. H., Weller, C. L. and Krochta, J. M., Edible coatings and films based on proteins. In *Edible coatings and films to improve food quality*, Krochta, J. M.; Baldwin, E. A.; Nisperos-Carriedo, M. O., Eds. 1994; pp 201-277.
3. Angellier-Coussy, H., Torres-Giner, S., Morel, M. H., Gontard, N. and Gastaldi, E., 2008, "Functional properties of thermoformed wheat gluten/montmorillonite materials with respect to formulation and processing conditions", *Journal of Applied Polymer Science*, vol. 107, pp. 487-496.
4. Pereda, M., Aranguren, M. I. and Marcovich, N. E., 2008, "Characterization of chitosan/caseinate films", *Journal of Applied Polymer Science*, vol. 107, pp. 1080-1090.
5. Rhim, J. W. and Ng, P. K. W., 2007, "Natural biopolymer-based nanocomposite films for packaging applications", *Critical Reviews in Food Science and Nutrition*, vol. 47, pp. 411-433.
6. Cornell, H. J. and Hoveling, A. W., *Wheat: Chemistry and Utilization*. Technomic publishing Company, Inc.: Lancaster, PA, 1998.
7. Hernandez-Munoz, P., Kanavouras, A., Ng, P. K. W. and Gavara, R., 2003, "Development and characterization of biodegradable films made from wheat gluten protein fractions", *Journal of Agricultural and Food Chemistry*, vol. 51, pp. 7647-7654.
8. Han, J. H., 2000, "Antimicrobial food packaging", *Food Technology*, vol. 54, pp.

9. Pereira de Abreu, D. A., Cruz, J. M. and Paseiro Losada, P., 2012, "Active and Intelligent Packaging for the Food Industry", *Food Reviews International,* vol. 28, pp. 146-187.

10. Burt, S., 2004, "Essential oils: their antibacterial properties and potential applications in foods - a review", *Int. J. Food Microbiol.*, vol. 94, pp. 223-253.

11. Hernandez-Munoz, P. and Hernandez, R. J. In *Glutenin and gliadin films from wheat gluten: preparation and properties*, IFT Annual Meeting, New Orleans, Louisiana, 2001.

12. ASTM, D882. Standard test method for tensile properties of thin plastic sheeting. In American Society for Testing Materials.: 2009.

13. Sekkar, V., Narayanaswamy, K., Scariah, K. J., Nair, P. R., Sastri, K. S. and Ang, H. G., 2007, "Evaluation by various experimental approaches of the crosslink density of urethane networks based on hydroxyl-terminated polybutadiene", *Journal of Applied Polymer Science,* vol. 103, pp. 3129-3133.

14. ISO, 14855-1. Determination of the ultimate aerobic biodegradability of plastic materials under controlled composting conditions - Method by analysis of evolved carbon dioxide - Part 1: General method. In 2005.

15. Song, Y. H., Li, L. F. and Zheng, Q., 2009, "Influence of Epichlorohydrin Modification on Structure and Properties of Wheat Gliadin Films", *Journal of Agricultural and Food Chemistry,* vol. 57, pp. 2295-2301.

16. Hernandez-Munoz, P., Kanavouras, A., Lagaron, J. M. and Gavara, R., 2005, "Development and characterization of films based on chemically cross-linked gliadins", *Journal of Agricultural and Food Chemistry,* vol. 53, pp. 8216-8223.

17. Kuzyakov, Y., Friedel, J. K. and Stahr, K., 2000, "Review of mechanisms and quantification of priming effects", *Soil Biol. Biochem.*, vol. 32, pp. 1485-1498.

18. Barone, J. R. and Arikan, O., 2007, "Composting and biodegradation of thermally processed feather keratin polymer", *Polym. Degrad. Stab.*, vol. 92, pp. 859-867.

# Effect of Nano-Semiconductors and Sacrificial Electron Donors on Color Transition of a Novel UV-Activated Bio-Oxygen Indicator

**Surachai Khankaew[1], Waraporn Boonsupthip[2,3], Chanassa Nandhivajrin[1], Chiravoot Pechyen[1,3*], Panuwat Suppakul[1,3*]**

[1] *Department of Packaging and Materials Technology, Faculty of Agro-Industry, Kasetsart University, Bangkok 10900, Thailand*
[2] *Department of Food Science and Technology, Faculty of Agro-Industry, Kasetsart University, Bangkok 10900, Thailand*
[3] *Center for Advanced Studies in Agriculture and Food, KU Institute for Advanced Studies, Kasetsart University, 10900, Thailand (CASAF, NRU-KU, Thailand)*

[*] *Corresponding author: chiravoot.p@ku.ac.th and panuwat.s@ku.ac.th*

**Abstract:** The usage of oxygen indicator is of increasing interest because oxygen is one of the major causes of food product deterioration. In order to monitor the quality and safety of shelf-stable food products related to either package leakage or gas permeability of packaging materials, oxygen indicator could be possibly employed. As a quality indicator being in a subclass of diagnostic packaging, oxygen indicator is one of the most important gas indicators. Due to the perceived lower risk to the consumer compared to synthetic redox dyes, a bio-redox dye could be used as a visual material in this indicator system. Anthraquinone derivative enables to apply as a colorimetric redox dye in a bio-colorimetric oxygen indicator that comprises nano-semiconductor (*n*SC), e.g. ZnO and $TiO_2$, and sacrificial electron donor (SED), e.g. glycerol and sorbitol, in cellulose-based solution. Effect of *n*SC and SED on color transition of UV-activated bio-oxygen indicator has been investigated. UV-activated bio-oxygen indicator label was prepared using a casting technique. After UV-activation, leuco-anthraquinone (colorless) changed to anthraquinone (orange-yellowish). It is ready to use as a bio-oxygen indicator label for monitoring the oxygen status. When this indicator label exposed to the air (20.9 %oxygen), the color gradually faded out to the original state of leuco-anthraquinone. The reflectance spectra, the total color differences (TCD), and the times of color changing are also reported.

Keywords: semiconductor, sacrificial electron donor, redox dye, oxygen indicator, UV-activated, intelligent packaging

## 1 Introduction

Detection of oxygen is important to many industrial processes, especially where an absence of oxygen, or the accurate control of its concentration, is essential. One area of particular interest is gas indicator (or leakage indicator) which in the monitoring of headspace gas within food packages [1], [2], since oxygen is responsible for a variety of food-spoiling processes, including promotion of microbial growth, lipid oxidation, protein decomposition and discoloration. Importantly, in order to extend shelf-life, many food packages utilize modified atmosphere packaging (MAP) or vacuum packaging [1-6]. In order to monitor the gas status, gas indicator has been used. Oxygen indicator is one of the most important gas indicators, which are in a subclass of diagnostic packaging being a member of intelligent packaging. It can react with a concentration of oxygen in a headspace of the package [2-5].

Many have studied and developed oxygen indicator for food products in different goals of usage. For example, Lawrie *et al.* [4] reported in a simple inkjet-printed, UV-activated oxygen indicator which colloidal $TiO_2$ particles in water-based inkjet-ink and Galagan *et al.* [7], [8] was developed the fadable ink for time-temperature indicator by function of diffusion of oxygen which used sodium antraquinone β-sulfonate as a redox dyes and used screen printing for applied to substrate, Marek *et al.* [9] researched in time-mornitoring sensor based on oxygen diffusion in an indicator with used mixed dye between redox dye, methylene blue and riboflavin, and the resulted of Mills and McGrady [9], Mill and Hazafy [10], Mill [11], and Zita *et al.* [13] were researched in a new photocatalyst used in $O_2$ indicator ink that can activated by UV-light.

Mills and Hazafy [10] has been developed a function of oxygen indicator to work under the light activation, It was consisted of nanoparticle mineral as a semiconductor photosensitizer (*n*SC), a sacrificial electron donor (SEC), and a redox dye in the form of an intelligent ink. In this system, the semiconductor, usually $TiO_2$, absorbs UV light in an activation step, creating electron-hole pairs. The photogenarated holes react rapidly with the sacrificial electron donor usually glycerol, leaving the photogenerated electrons to react with the redox dye (methylene blue (MB), polyviologens [14] or anthraquinone derivative [7], thereby generating a differently colored (usually bleached) reduced form of the dye, i.e. $D_{red}$, which is oxygen sensitive. The key ingredients, i.e. semiconductor power particles, redox dye and sacrificial electron donor are chosen so that they are readily dispersed/dissolved in water containing a polymer, such as hydroxyethyl cellulose (HEC) which acts as an encapsulation medium when this intelligent ink is printed and dries to form a UV-activated, $O_2$-sensitive indicator film.

Mills and Hazafy [10] reported the newest irreversible nanocrystalline $SnO_2$-based, $O_2$ indicator that consisting of a redox dyes - methylene blue (MB), a SED – glycerol, and *n*SC – $SnO_2$, that all were encapsulated within a polymer. Since the changes of color were depended upon the oxygen concentration**,** many research works reported that factors affecting this system included thickness of SC layer, bandgap energy of semiconductor, type of UV light sources, and type of redox dyes, as well as concentration of each component.

Obviously a vital feature of this type of indicator is the requirement for photons of energy ≥ the bandgap of the *n*SC, E bg, to drive the initial photoactivation step, usually $TiO_2$ because its bandgap is 3.2 eV, that is, photons of light of wavelength ≤388 nm are needed to activate an UV-activated indicator film. These photons lie in the UVA region of the electromagnetic spectrum of 320–400 nm [15].

The nano zinc oxide powder has a bandgap of 3.37 eV, which corresponds to emission in the UV region [16], it has the wurtzite hexagonal crystal structure. Commercial ZnO show this crystal structure under electron microscopic examination. The precise shape of the crystal depends on the method of formation. In regular zinc oxide these vary between acicular needles and plate shaped crystals. Zinc oxide can be induced to form a very large variety of crystalline shapes using specialized deposition methods. In recent years, many efforts have been devoted to ZnO-based photoelectrodes because ZnO possesses a wide energy band gap similar to that of $TiO_2$ and, at the same time higher electron mobility (7 orders of magnitude higher than that of $TiO_2$), easier fabrication of the various nanostructures and easier modification of the surface structure than $TiO_2$ [15], [16].

In contrast of this work, we focus on the development of a novel system of nanocrystalline based, UV-activated, bio-oxygen indicator label film, which used anthraquinone derivative as a bio-redox dye, and the effect of *n*SCs ($TiO_2$ and ZnO) and SEDs (glycerol and sorbitol) on the color changing of bio-oxygen indicator by using Taguchi method.

# 2 Experimental

## 2.1 Materials and chemicals

The redox dye, Sodium Anthraquinone-2-sulfonate ($C_{14}H_7NaO_5S$) and nano-semiconductor (*n*SC) which used in this research are titanium (IV) oxide, $TiO_2$ (anatase), and zinc oxide, ZnO, were purchased from Sigma-Aldrich (Gillingham, UK). Sacrificial electron donors (SED), glycerol ($C_3H_8O_3$) and sorbital were purchased from Ajax Finechem (NSW, Australia). Polyethylene-*b*-poly(ethylene glycol) (PE-b-PEG) which were S1=16:3 (*Mn* = 578), S2=16:11 (*Mn* = 920) and S3=25:16 (*Mn* = 1400), were used as a surfactant, methylcellulose (MC) (Methocel®, Dow Chemical, USA) was used as a bio-based polymer and distilled water and served as a solvent. Vacuum bag packaging (PA/PA/PE) was used to prepare the oxygen free condition.

## 2.2 Preparation of bio-oxygen indicator/polymer matrix and thin film

A novel UV-activated bio-oxygen indicator label film was integrated into a matrix of methylcellulose and water. For that purpose, an aqueous indicator solution was prepared which was consisted of various concentrations of a redox dye and type of *n*SCs, SEDs and surfactants as fallowing the **Table 2**. Then, they were mixed together with magnetic stirrer for 15 min, followed by 30 min of sonication from an ultrasonic bath. After that, it was added 5 g of 10 wt.% methyl cellulose aqueous solution and stirred for 10 min to ensure thoroughly mixing and dispersion of the various components. In order to make a bio-oxygen indicator label film, it was prepared by degassing and immediately poured onto the Petri dish. Later on, it was dried at room temperature and light-free for 24-36 h. After finished, it was peeled out of the dish and cut to a small circle (~1.2-1.5 cm diameter) and stored under cool, dark condition and used as required.

## 2.3 Design of experimental

Taguchi's method of experimental designs provides a simple, efficient, and systematic approach for the optimization of the experimental designs for quality and cost saving performance. To evaluate each independent factor or its interaction effects on the process characteristics, Taguchi used standard orthogonal arrays. [17]

The experiment was conducted with four controllable three-level factors of the process. The four evaluated factors evaluated were concentration of dye, type of *n*SC, type of SED and type of surfactant. The response was the total color difference (TCD) of indicator film.

Normally, the full factorial design would require $3^4 = 81$ experimental runs. However, the effort and experimental cost required for such a design could be prohibitive and unrealistic. In this study, 9 experimental run based on the orthogonal array $L_9$, as shown in **Table 1** and **2**, were conducted to study the four process factors. [18] ANOVA was performed to determine the effect of factors on the removal factors

**Table 1:** Taguchi design factors and theirs type or level.

| Factor | Level 1 | Level 2 | Level 3 |
|---|---|---|---|
| Concentration of dye (phr.) | 3 | 5 | 7 |
| type of *n*SC (5 phr.) | $TiO_2$ (T) | ZnO (Z) | $TiO_2$/ZnO (T:Z) |
| type of SED (50 phr.) | glycerol (G) | sorbitol (S) | glycerol/sorbitol (G:S) |
| type of surfactant (5 phr.) | S1 | S2 | S3 |

**Table 2:** Taguchi design $L_9$.

| formula | pattern | Dye concentration | *n*SC | SED | Surfactant |
|---|---|---|---|---|---|
| 1 | ++0- | 5 | Z | G:S | S1 |
| 2 | 00+- | 3 | T:Z | S | S1 |
| 3 | ---- | 1 | T | G | S1 |
| 4 | +0-+ | 5 | T:Z | G | S3 |
| 5 | -000 | 1 | T:Z | G:S | S2 |
| 6 | 0-0+ | 3 | T | G:S | S3 |
| 7 | 0+-0 | 3 | Z | G | S2 |
| 8 | -+++ | 1 | Z | S | S3 |
| 9 | +-+0 | 5 | T | S | S2 |

## 2.4 UV-activation, color recovery and confirmation step

Bio-coated paper and bio-oxygen indicator label film were packed and sealed with vacuum packaging (PA/PA/PE).

2.4.1 The UV-activation, the indicator label film were tested by place on coated paper. After that, it was exposed to UVA light with irradiance of 12.90 mW.h $cm^{-2}$. Experiments were conducted in triplicate and were recorded before photoactivation (original color) and after each time interval (5, 10, 15, 30, 60, 180, 300, 600, 900 and 1800 s) by a chroma meter spectrodensitometer (SpectroDens, Techkon®, Königstein, Germany) in L*, a*, b* color mode.

2.4.2 The color recovery step tested after UV-activated, opened the label film indicator to reacts with the ambient oxygen in air, the L*, a*, b* value were recorded before (colored) and after opened the vacuum package of indicator, which were measured at each time interval from 5, 10, 15, 30, 60, 120, 180, 240, 300 and 600 min.

2.4.3 The reactivation was prepared by using the effective factors from Taguchi's experiment design. The new bio oxygen-indicator thin film was selected and prepared following method 2.2. The UV-activation and color recovery step were tested by following method 2.4.1 and 2.4.2., the SEM image was used to observe the surface of the bio-oxygen indicator label film.

## 2.5 Color measurement

The main plot was then demonstrated, and the change in delta E ($\Delta E^*_{ab}$) or the total color difference (TCD) is expressed as follows:

Used ($L^*_1$, $a^*_1$, $b^*_1$) and ($L^*_2$, $a^*_2$, $b^*_2$), two colors in L*, a*, b* mode.

$$TCD = \sqrt{(L_1^* - L_2^*)^2 + (a_1^* - a_2^*)^2 + (b_1^* - b_2^*)^2} \quad (1)$$

Where ΔL* is the brightness difference between initiation ($L^*_1$) and each time interval ($L^*_2$), Δa* is the redness-greenness difference between initiation ($a^*_1$) and each time interval ($a^*_1$), and Δb* is the yellowness–blueness difference between initiation ($b^*_1$) and each time interval ($b^*_1$) [19].

## 3 Results and discussion

### 3.1 Function of the bio-oxygen indicator

The function of this bio-oxygen indicator was consisted of nanoparticle mineral as a semiconductor photosensitizer (*n*SC), a sacrificial electron donor (SEC), and a redox dye (anthraquinone). This system could be applied for a novel UV-activated, bio-oxygen indicator. Then, it was activated by pulse of the UV light, the initially color, leuco-anthraquinone (LAq) (due to $D_{ox}$) polymer indicator film is rendered a different color, yellowish (anthraquinone, Aq) (due to $D_{red}$), and oxygen sensitive. In the absence of oxygen, the UV-activated film remained original color indefinitely, but upon exposure to air it rapidly regains its original color as $D_{red}$ is reoxidised by oxygen to $D_{ox}$ in a dark reaction step, as shown in **Figure 1**.

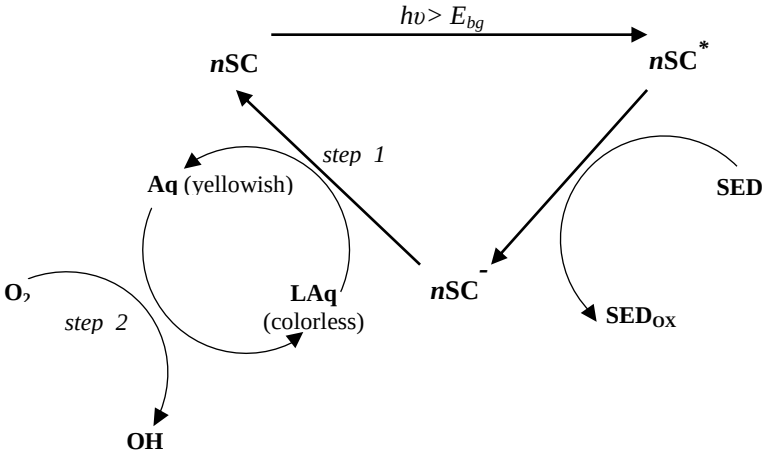
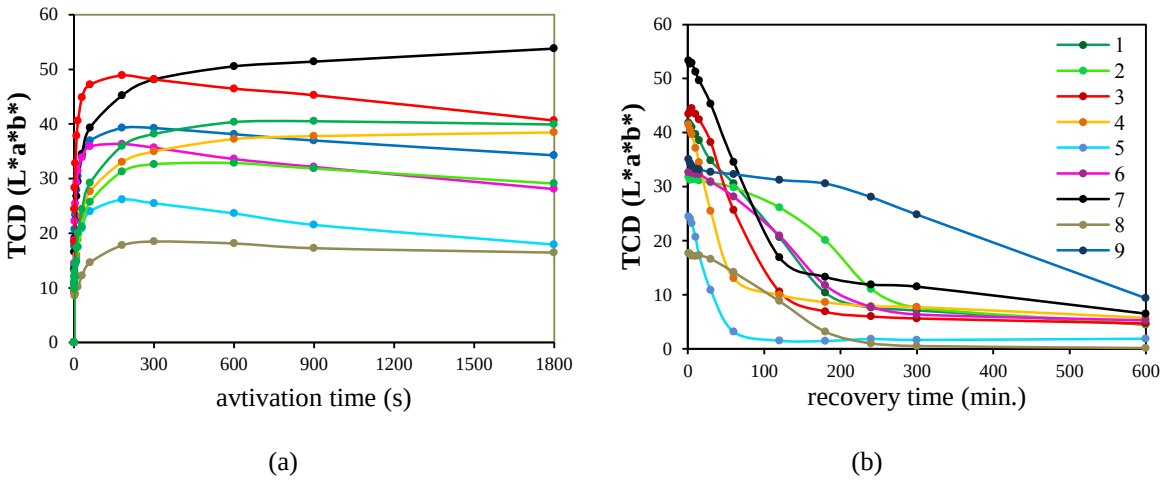



**Figure 1:** Mechanism of UV light driven reduction of leuco-anthraquinone (LAq) to anthraquinone (Aq) color (photoactivation, step 1) and its subsequent re-oxidation by oxygen (dark recovery, step 2).

### 3.2 Sensitivity of bio-oxygen indicator with UV-light and oxygen in air

3.2.1 The results showed that all samples yielded an increase in TCD value after these samples were exposed by UV-activation. This could be immediately distinct after five seconds and then the highest value of TCD was reached at a minimum of 180 s. The highest TCD values of sample no. 7, 3 and 1 were 53.79 at 1800 s, 48.92 at 180 s and 40.51 at 900 s, respectively. From **Figure 2** (a) it demonstrates that TCD values were attended to a decrease in their values after reaching the maximum, as shown in **Table 3**. **Table 4** represents color change of bio-oxygen indicators after exposure to UV light with various times.

3.2.2 The results of TCD of oxygen bio- indicator label when exposed to the air in dark condition at room temperature showed that TCD values were reduced corresponding to exposure time. Sample no.5 presented the fastest to fade from yellowish (Aq) to colorless (LAq). TCD value was closed to zero after 120 min of exposure. The TCD values of other samples were nearly at zero after approximately 600 min, as shown in **Table 5**, and **Figure 2** (b). After UV activation, the recovery of the color (i.e. TCD) of the indicator label is proportional to the concentration of oxygen in the ambient gas phase (**Table 6**).




(a) (b)

**Figure 2:** Changing of TCD, (a) UV-activation with times and (b) dark recovery in air.

**Table 3:** TCD of bio-oxygen indicator label after activation at different times.

| Activation time (s) | Response (TCD) | | | | | | | | |
|---|---|---|---|---|---|---|---|---|---|
| | (1) | (2) | (3) | (4) | (5) | (6) | (7) | (8) | (9) |
| 0 | - | - | - | - | - | - | - | - | - |
| 5 | 14.26 ± 0.63 | 11.82 ± 0.43 | 32.78 ±2.81 | 12.45 ± 0.48 | 11.99 ±0.92 | 25.47 ± 2.40 | 22.32 ± 1.12 | 8.93 ± 0.37 | 23.39 ± 1.90 |
| 10 | 17.37 ± 1.08 | 14.82 ± 0.63 | 37.83 ± 2.82 | 16.04 ± 0.20 | 15.56 ± 1.06 | 29.35 ± 3.38 | 26.77 ± 1.09 | 10.22 ± 0.29 | 27.94 ± 2.38 |
| 15 | 20.11 ± 0.96 | 17.43 ± 0.78 | 40.58 ± 2.57 | 18.83 ± 0.06 | 17.61 ± 0.44 | 31.45 ± 3.80 | 29.48 ± 1.44 | 10.21 ± 0.46 | 30.48 ± 2.88 |
| 30 | 24.41 ± 0.85 | 21.23 ± 0.77 | 44.86 ± 2.91 | 23.21 ± 0.44 | 20.88 ± 1.09 | 33.96 ± 4.57 | 34.50 ± 1.26 | 12.24 ± 0.59 | 34.07 ± 3.20 |
| 60 | 29.21 ± 0.88 | 25.72 ± 0.87 | 47.22 ± 3.15 | 27.67 ± 1.01 | 24.05 ±1.38 | 35.93 ± 4.69 | 39.31 ± 1.17 | 14.67 ± 0.82 | 36.99 ± 3.36 |
| 180 | 35.96 ± 0.92 | 31.28 ± 0.96 | **48.92 + 3.78** | 33.04 ± 1.85 | **26.23 + 1.67** | **36.38 + 4.44** | 45.22 ± 1.27 | 17.79 ± 1.25 | 39.30 ± 3.44 |
| 300 | 38.17 ± 0.95 | 32.64 ± 0.98 | 48.23 ± 4.20 | 35.01 ± 1.79 | 25.51 ± 1.67 | 35.70 ± 4.04 | 48.14 ± 1.07 | **18.49 + 1.41** | **39.32 + 3.56** |
| 600 | 40.35 ± 0.79 | **32.87 + 1.38** | 46.52 ± 4.36 | 37.29 ± 2.34 | 23.85 ± 1.25 | 33.73 ± 3.51 | 50.55 ± 1.06 | 18.15 ± 1.46 | 38.17 ± 3.35 |
| 900 | **40.51 + 0.98** | 31.89 ± 1.45 | 45.36 ± 4.61 | 37.81 ± 1.82 | 21.64 ± 1.55 | 32.43 ± 2.78 | 51.42 ± 0.85 | 17.27 ± 1.50 | 37.02 ± 3.10 |
| 1800 | 39.91 ± 2.26 | 29.11 ± 1.45 | 40.79 ± 5.20 | **38.50 + 1.74** | 18.05 ± 1.16 | 28.09 ± 3.42 | **53.79 + 0.98** | 16.47 ± 1.94 | 34.35 ± 2.86 |

## 3.3 Factors affecting TCD value

The ANOVA was carried out on these TCD values to identify the main factors. The ANOVA results were shown in **Table 7**, that the SED value was the most important variable of the system. It was also found that all of components have significant effects on the photoactivation process of bio-oxygen indicator.

The label films were conducted in photoactivation experiment step by using UV irradiation (12.90 mW.h $cm^{-2}$) and L* a* b* color measurement were operated through the experiment. Later on, total color differences (TCD) were calculated and the results were applied to predict trends of reaction of each factor (as shown in **Figure 3**). The results showed that the surfactant, S1 (*Mn* 578) was the greatest effect, followed by S2 (*Mn* 920) and S3 (*Mn* 1400), respectively. These have significantly shown an influence on color transition from LAq (colorless) to Aq (yellowish). These were more effectively when applied with $TiO_2$, ZnO and $TiO_2$/ZnO, respectively. Moreover, there were other factors (e.g. dye: 3 phr, and SED: glycerol (G)) affecting to these bio-oxygen indicators, as revealed in **Figure 3**.

**Table 4:** Color of bio-oxygen indicator film at difference times, photoactivation step.

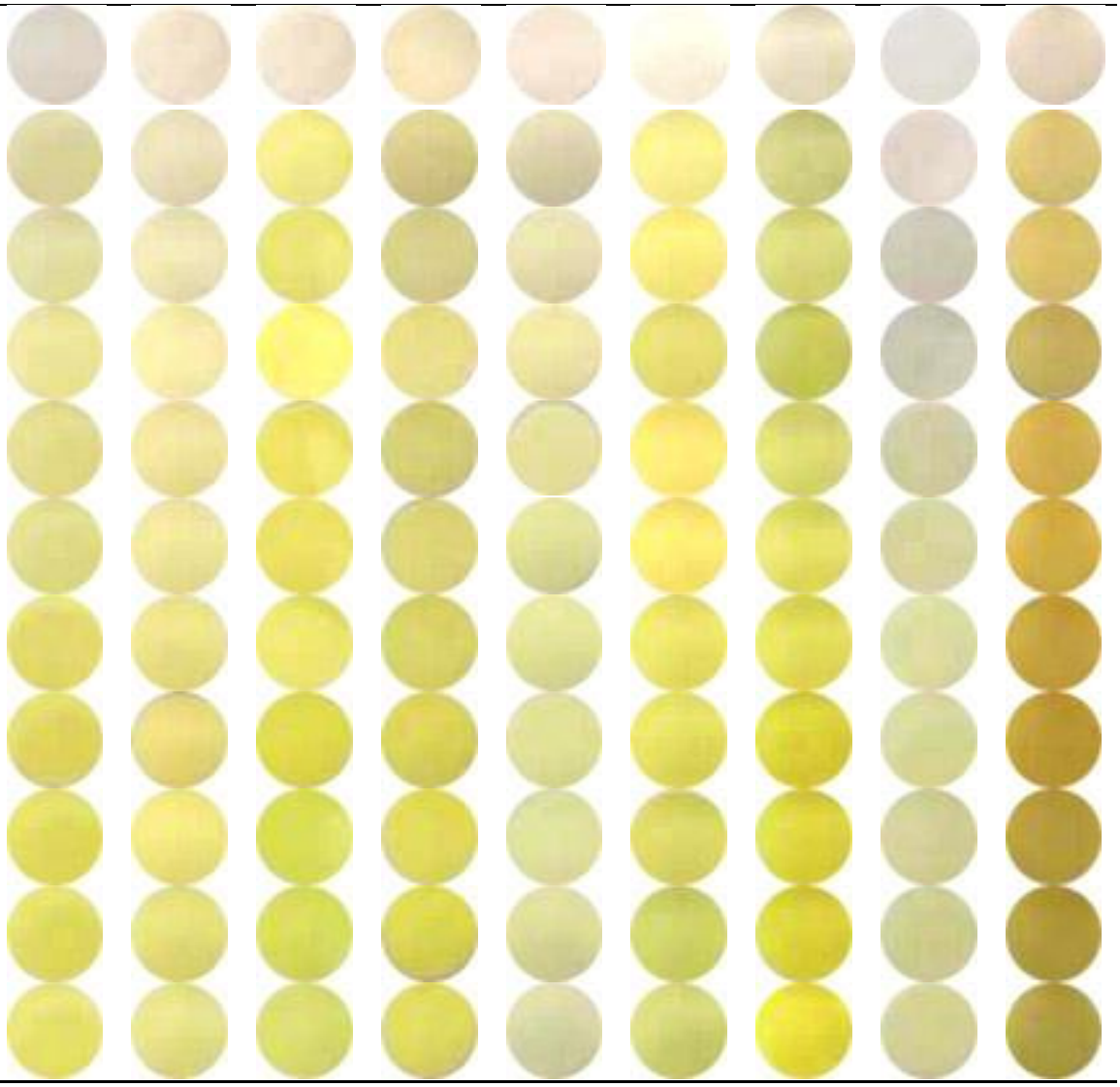
| Time (s) | TCD (photoactivation step) | | | | | | | | |
|---|---|---|---|---|---|---|---|---|---|
| | (1) A5/Z/G:S/S1 | (2) A3/T:Z/S/S1 | (3) A1/T/G/S1 | (4) A5/T:Z/G/S3 | (5) A1/TZ/G:S/S2 | (6) A3/T/G:S/S3 | (7) A3/Z/G/S2 | (8) A1/Z/S/S3 | (9) A5/T/S/S2 |
| Original |  | | | | | | | | |
| 5 | | | | | | | | | |
| 10 | | | | | | | | | |
| 15 | | | | | | | | | |
| 30 | | | | | | | | | |
| 60 | | | | | | | | | |
| 180 | | | | | | | | | |
| 300 | | | | | | | | | |
| 600 | | | | | | | | | |
| 900 | | | | | | | | | |
| 1800 | | | | | | | | | |

**Table 5:** TCD of bio-oxygen indicator label, dark recovery in ambient air (20.9 %oxygen).

| Recovery time (min) | Response (TCD) | | | | | | | | |
|---|---|---|---|---|---|---|---|---|---|
| | (1) | (2) | (3) | (4) | (5) | (6) | (7) | (8) | (9) |
| *Activated* | *39.40±0.80* | *31.70±0.17* | *45.20±0.34* | *40.54±0.21* | *25.10±0.68* | *33.13±1.03* | *50.13±0.12* | *20.31±0.07* | *31.29±1.04* |
| 5 | 36.98 ±0.92 | 27.20± 0.92 | 40.39± 1.56 | 33.98± 2.77 | 22.19± 0.96 | 27.29± 0.88 | 47.17± 0.95 | 17.31± 0.37 | 25.71± 0.88 |
| 10 | 35.70±1.40 | 27.15± 0.83 | 39.36± 0.49 | 31.44± 3.02 | 19.63± 1.05 | 27.10± 0.67 | 45.52± 1.53 | 17.27± 1.25 | 25.16± 0.84 |
| 15 | 34.57±133 | 26.93± 0.58 | 38.33± 0.59 | 28.74± 2.59 | 16.20± 2.33 | 27.05± 0.43 | 43.92± 1.67 | 17.41± 1.11 | 25.04± 1.16 |
| 30 | 30.82±2.29 | 26.57± 0.44 | 34.17± 0.69 | 19.77± 1.35 | 9.80± 2.05 | 25.70± 1.59 | 39.58± 1.41 | 16.76± 2.02 | 24.56± 0.99 |
| 60 | 26.55±2.38 | 25.64± 0.31 | 21.60± 1.27 | 7.29± 1.12 | 2.08± 0.74 | 22.88± 2.67 | 28.83± 1.41 | 14.31± 2.53 | 24.16± 0.63 |
| 120 | 16.62± 4.37 | 21.98± 1.05 | 6.47± 0.18 | 4.22± 1.39 | 0.43± 0.09 | 15.67± 2.75 | 11.18± 2.14 | 8.95± 2.64 | 23.09± 1.42 |
| 180 | 6.35±1.14 | 15.92± 1.94 | 2.79± 0.69 | 2.88± 1.31 | 0.37± 0.27 | 6.51± 5.04 | 7.58± 0.59 | 3.29± 2.51 | 22.42± 2.74 |
| 240 | 3.57±0.71 | 6.89± 2.42 | 1.90± 0.59 | 2.12± 1.44 | 0.76± 0.47 | 2.49± 2.62 | 6.13± 0.65 | 1.12± 0.70 | 19.92± 3.68 |
| 300 | 3.09±0.63 | 3.46± 0.35 | 1.53± 0.96 | 1.99± 1.37 | 0.58± 0.48 | 1.10± 1.14 | 5.77± 0.67 | 0.64± 0.33 | 16.69± 4.79 |
| 600 | 0.43±0.45 | 0.35± 0.49 | 0.60± 0.65 | 0.00± 0.73 | 0.80± 0.29 | 0.00± 0.52 | 0.77± 0.86 | 0.00± 0.25 | 1.21± 1.42 |

**Table 6:** TCD of bio-oxygen indicator film at difference time, dark recovery step.

| Time | TCD (dark recovery step) | | | | | | | | |
|---|---|---|---|---|---|---|---|---|---|
| | (1) A5/Z/G:S/S1 | (2) A3/T:Z/S/S1 | (3) A1/T/G/S1 | (4) A5/T:Z/G/S3 | (5) A1/TZ/GS/S2 | (6) A3/T/G:S/S3 | (7) A3/Z/G/S2 | (8) A1/Z/S/S3 | (9) A5/T/S/S2 |
| Original | | | | | | | | | |
| Activated | | | | | | | | | |
| 1m | | | | | | | | | |
| 3m | | | | | | | | | |
| 5m | | | | | | | | | |
| 10m | | | | | | | | | |
| 15m | | | | | | | | | |
| 30m | | | | | | | | | |
| 1h | | | | | | | | | |
| 2h | | | | | | | | | |
| 3h | | | | | | | | | |
| 4h | | | | | | | | | |
| 5h | | | | | | | | | |
| 10h | | | | | | | | | |

**Table 7:** Analysis of variance on TCD (UV-activation with time).

| Source | Degree of freedom (DOF) | Sum of Squares, SS | *F*-Ratio (F) | Prob > F |
|---|---|---|---|---|
| Dye (3 phr.) | 1 | 2009.29 | 96.10 | <.0001 |
| *n*SC ($TiO_2$) | 2 | 596.50 | 14.27 | <.0001 |
| SED (glycerol) | 2 | 9009.95 | 215.47 | <.0001 |
| Surfactant (S1) | 2 | 877.42 | 20.98 | <.0001 |
| Times | 1 | 58.45 | 2.79 | 0.0977 |

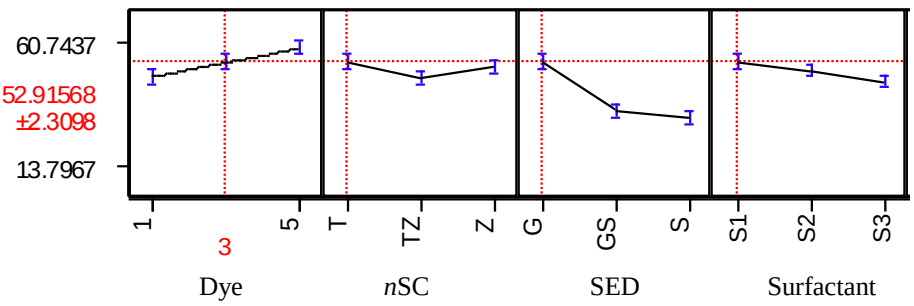



**Figure 3:** Mean of TCD values plotted against different factors

### 3.4 Confirmation of color transition of a selected bio-oxygen indicator

The work was also carried out to confirm the color transition of an bio-oxygen indicator with a selected formula of Aq/$TiO_2$/G/S1 = 3/5/100/10 phr and the activation time of 10 min. The results are shown in **Figure 4.** The demonstrate of a colorless LAq bio-oxygen indicator was gradually fading up to yellowish Aq after 5s of photoactivation and reaching the maximum intensity, in turn, the highest TCD value, after 10 min of photoactivation step. Afterwards, it was exposed to ambient air (~20.9 %oxygen) and was gradually fading down to its original color, LAq complete within *ca*. 10 h. This occurs because of properties of Aq that could be transformed to $Dye_{red}$ form at ~440-450 nm as shown in **Figure 5** which displayed the reflectance of bio-oxygen indicator label film, the time of dark recovery step of this indicator was about *ca.*12 h, which was slightly faster than methylene blue based, UV-activated oxygen indicator inkjet-printed (MB/$O_2$-IJ indicator) [4]. SEM images of bio-oxygen indicator film demonstrate that the surface has roughness surface due to the dispersion of *n*SC particle. Nanoparticles of $TiO_2$ were aggregate [15], [16] and displayed as large particle (*ca*. ~100 nm to 1 µm), see **Table 8**.

A bio-oxygen indicator was irreversible in response that the photoactivation step was repeated. Hence, once the original color was restored due to exposing to oxygen in ambient air, this color change could not be reversed, even if the ambient level of oxygen was then reduced to zero. Under such conditions the indicator will only convert and stay in its Aq form (yellowish) if it was activated by using UV light again. (step 1, **Figure 1**) It can be seen from **Figure 6** that an excess of SED within the indicator film allowed subsequent photoactivations at 600 and 1200 min to occur as quickly as the initial photoactivation. Although subsequent recoveries were similarly rapid, they were not as complete, indicating some degradation of anthraquinone dye with repeated use.

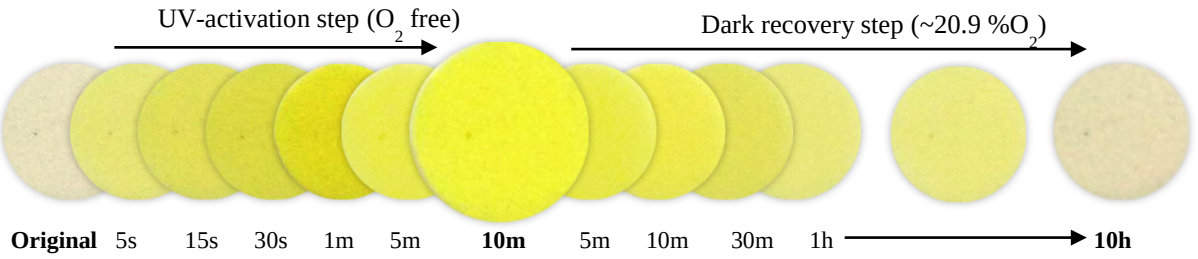



**Figure 4:** Color transition of an bio-oxygen indicator label

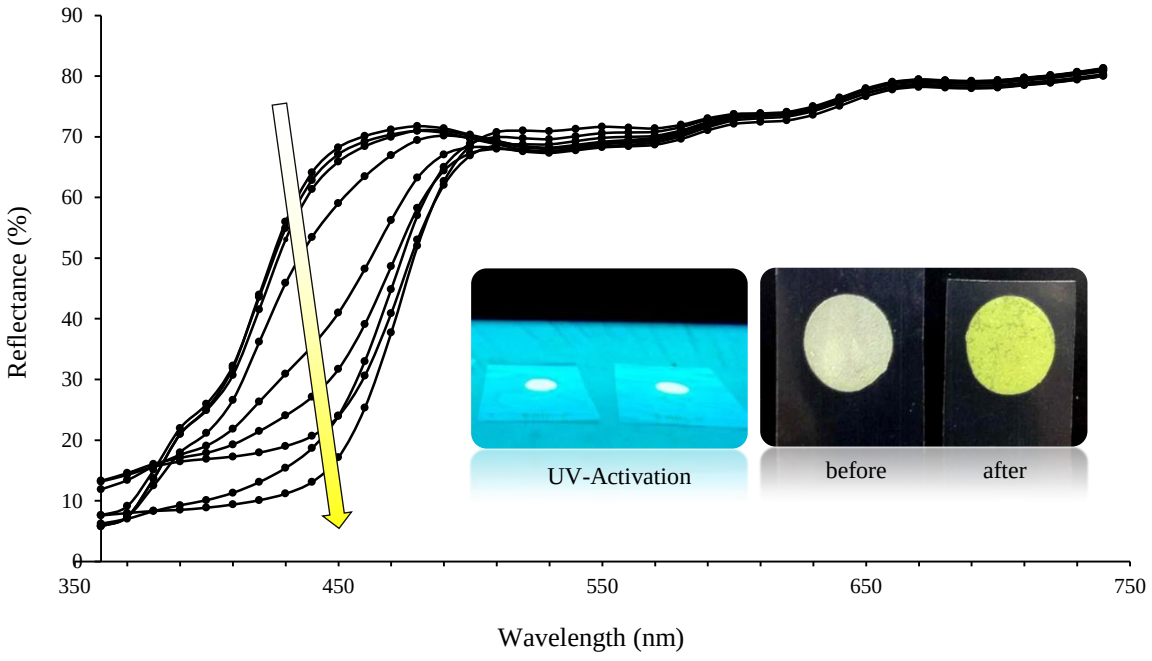
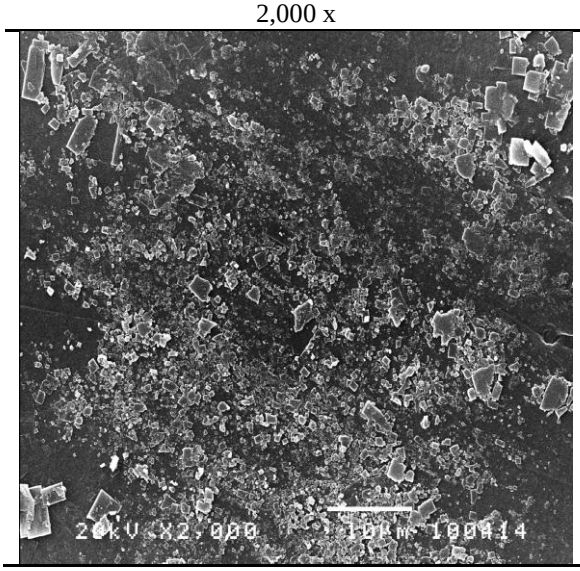
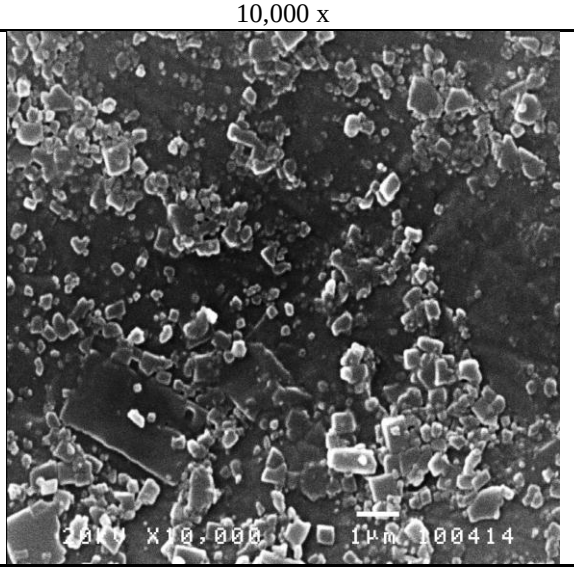



**Figure 5:** Reflectance of bio-oxygen indicator label.

**Table 8:** SEM image of bio-oxygen indicator film.

| 2,000 x | 10,000 x |
|---|---|
|  |  |

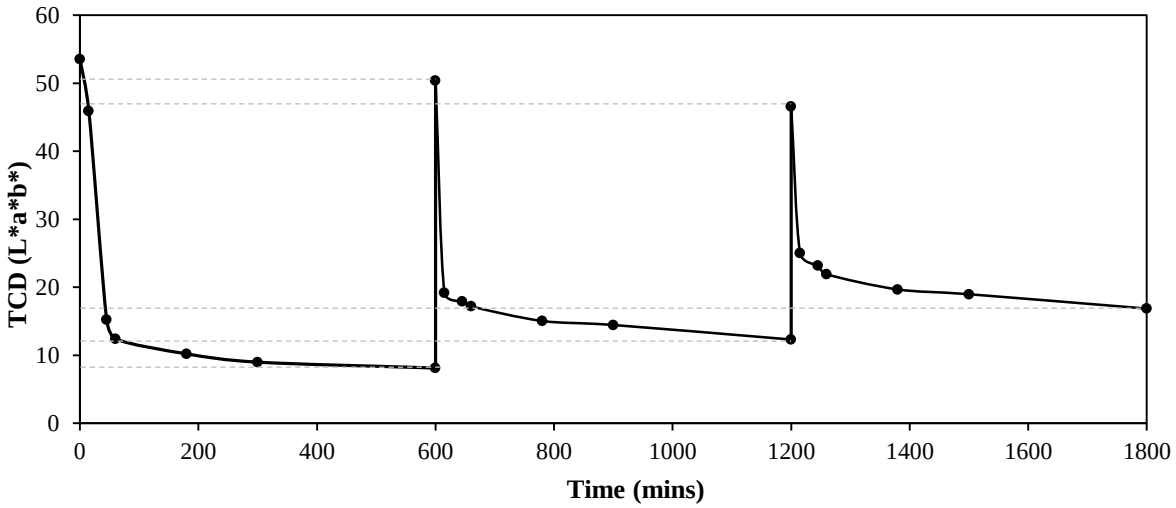



**Figure 6:** Change in TCD of Taguchi's sample, illustrating a series of 3 cycles of activation (each 10 min at 12.90 mW.h $cm^{-2}$) and dark recovery (each time monitored over 10 h) of an bio- oxygen indicator.

## 4 Conclusions

The system of a novel UV-activated bio-oxygen indicator was consisted of: polymer/dye/*n*SC/SED/surfactant, that the most effective factors of this indicator were SED, glycerol and the types of *n*SC, $TiO_2$ has effective more than ZnO and $TiO_2$:ZnO respectively, which were concluded by using Taguchi's method, $L_9$ experimental design. The bio-oxygen indicator white-color (leuco anthraquinone) label film is photoactivated to maximum TCD (anthraquinone, yellowish of TCD 53.52) in <180 s by UVA light (12.90 mW.h $cm^{-2}$) and recovers in ~10 h in dark conditions at room temperature (~27 ˚C, ~60 %RH, ~21 %oxygen). The reactivation of indicator by UV light is affected to the maximum TCD value of indicator and it has tended to decrease continuously. The use of bio-oxygen indicator in the food packaging is increasing. This bio-oxygen indicator can be applied as a coating by printing process such as screen printing or letterpress printing system. It has a potential for possible incorporation into packaging of oxygen scavenging materials and packed inside a package with oxygen sensitive products, such as fried food, meat or poultry products, pharmaceuticals and cosmetics.

## Acknowledgement

This work was financially supported by the Thailand research fund through the Royal Golden Jubilee (RGJ.) Ph.D. Program (grant no. PHD/2554/0054) is acknowledged.

## References

1. A. Mills, 2005, "Oxygen indicators and intelligent inks for packaging food", *Chemical Society eviews,* vol 34, pp. 1003-1011.

2. M. Samolander. E. Hurme. and R. Ahvenainen, 1997, "Leak indicators for modified atmosphere packages", *Trends in Food Science & Technology* , vol. 8, pp. 101-106.

3. P. Suppakul 2012, "Intelligent packaging", In: D.W. Sun (eds), *Hanbook of Frozen Food Processing and Packaging*, 2nd edition, CRC Press. Boca Raton, pp. 837-860.

4. K. Lawrie. A. Mills. and D. Hazafy, 2013, "Simple inkjet-printed, UV-activated oxygen indicator", *Sensors and Actuators B,* vol. 176, pp. 1154-1159.

5. K.L. Yam 2009, *The Wiley Encyclopedia of Packaging Technology: Intelligent Packaging*, 3rd Ed., A John Wiley & Sons, Inc., Publication, USA.

6. K.L. Yam. P.T. Takhistov. and J. Miltz, 2005, "Intelligent Packaging: Concepts a Applications", *Journal of Food Science*, vol. 70, pp. 1-100.

7. Y. Galagan. and W.–F. Su, 2008, "Fadable ink for time-temperature control of food freshness: Novel new time-temperature indicator", *Food Research International* , vol. 41, pp. 653-657.

8. Y. Galagan. S-.H. Hsu. and W.–F. Su, 2010, "Mornitoring time and temperature by methylene blue containing polyacrylate film", *Sensors and Actuators B*, vlo. 144, pp. 49-55.

9. P. Merek. J.J.V. Veléz. T. Haas. T. Doll. and G. Sadowski, 2013, "Time-monitoring sensor based on oxygen diffusion in an indicator/polymer matrix", *Sensors and Actuators B* 178, pp. 254-262.

10. A. Mills. and M. McGrady, 2008, "A study of new photocatalyst indicator inks", *Journal of Photo chemitry and Photobiology A Chemistry,* vol. 193, pp. 228-236.

11. A. Mills. and D. Hazafy, 2009, "Nanocrystalline $SnO_2$-based, UVB-activated, colorimetric oxygen indicator", *Sensors and Actuators B,* vol. 136, pp. 344-349.

12. Y. Galagan 2008, "Reversible photoreduction of methylene blue in acrylate media containing benzyl dimethyl ketal", *Journal of Photochemistry and Photobiology A: Chemistry*, vol. 195, pp. 378-383.

14. L. Roberts. R. Lines. S. Reddy. and J. Hay, 2011, "Investigation of polyviologens as oxygen indicators in food packaging", *Sensors and Actuators B,* vol. 152, pp. 63-67.

13. J. Zita. J. Krýsa. and A. Mills, 2009, "Correlation of oxidative and reductive dye bleaching on $TiO_2$ photocatalyst films", *Journal of Photochemistry and Photobiology A: Chemistry*, vol. 203, pp. 119-124.

15 H. Guo, X. He, C. Hu, Y. Tian, Y. Xi, J. Chen and L. Tian, 2014, "Effect of Particle Size in Aggregates of ZnO-Aggregate-Based Dye-Sensitized Solar Cells", *Electrochimica Acta*, vol 120, pp. 23-29.

16. O. Keleştemur, E. Arici, S. Yildiz and B. Gökçer, 2014, " Performance evaluation of cement mortars containing marble dust and glass fiber exposed to high temperature by using Taguchi method", *Construction and Building Materials,* vol. 60, pp. 17-24.

17. O. Keleştemur. E. Arici. S. Yildiz. and B. Gökçer, 2014, " Performance evaluation of cement mortars containing marble dust and glass fiber exposed to high temperature by using Taguchi method", *Construction and Building Materials,* vol. 60, pp. 17-24.

18. J. Zolgharnein. N. Asanjrani. M. Bagtash. and G. Azimi, 2014, "Multi-response optimization using Taguchi design and principle component analysis for removing binary mixture of alizarin red and alizarin yellow from aqueous solution by nano Y-alumina", *Spectrochimica Acta Part A: Molecular and Biomolecular Spectroscopy*, vol. 126, pp. 291-300.

19. F.J. Francis 1983, "Colorimetry of food", In: M. Peleg, and E.B. Baley, (eds.*), Physical Properties of Food*, AVI Publishing Westport, pp. 105-124.

# Effect of Photoinitiator and Binder Concentration on Color of Methylene Blue-based Oxygen Indicator

**Kanpicha Suwannawatanamatee[1], Withawat Mingvanish[2], Chana Yiangkamolsing[3], and Krittika Tanprasert[1*]**

*[1]Department of Printing and Packaging Technology, Faculty of Industrial Education and Technology*
*[2]Department of Chemistry, Faculty of Science*
*King Mongkut's University of Technology Thonburi, Bangkok , Thailand*
*[3]Department of Industrial Engineering, The University of the Thai Chamber of Commerce*

*[*]Corresponding author. Email: krittika.tan@kmutt.ac.th*

**Abstract:** Oxygen indicator is one of the mechanism to ensure that the low oxygen concentration in headspace is maintained. Oxygen indicator based-on methylene blue is effective and being used commercially in the tablet form. The oxygen indicator system consists of methylene blue, photoinitiator and binder. In this study, the objective was to evaluate the effect of methylene blue (redox dye) and 2,2-dimethoxy-2-phenyl acetophenone-benzyl dimethyl ketal (photoinitiator) on the color of the film formed using methylcellulose. Methylene blue concentration (with constant BDK concentration at 0.7%) affected the color of the film before and after UV irradiation as well as the color difference. The lower methylene blue concentration resulted in lighter film that reach its maximum color difference the fastest both for UV irradiation and oxygen exposure steps. MB concentration did not have effect on the magnitude of color difference in the range of 0.021 – 0.049% BDK concentration (with constant MB concentration at 0.021%) had less obvious effect on the color of the film before and after UV irradiation than MB concentration did. Film with 0.35% BDK required the least time to reach saturated color difference point but its magnitude of color difference were slightly (but significantly) less than that of film with 0.7 and 1.4% BDK. BDK concentration in the range of 0.35 – 1.4% had no effect on film color difference.

**Keywords:** oxygen indicator, methylene blue, BDK, methylcellulose, color

## 1 Introduction

Modified atmosphere packaging plays crucial roles in extending the shelf life of both perishable and shelf stable food products. In many cases, particularly for shelf stable, modified atmosphere packaging depends on the reduction of oxygen concentration in the package headspace and maintaining the low oxygen level throughout its shelf life. The reduction of headspace oxygen can be done through inert gas flushing, vacuum packaging, or oxygen absorbing/scavenging. Maintaining low oxygen level relies heavily on gas barrier properties of the packaging material and the integrity of the package to prevent re-entering of oxygen in to the package. This is very critical to the shelf life of many oxygen sensitive products, which their shelf life depends on headspace oxygen concentration. Oxygen indicator can be very useful as a leak indicator as well as an indicator of the shelf life of the packaged product.

One of commercial oxygen indicators is Ageless Eye, which is a tablet contained within the small plastic pouch and changes color from pink to blue when the oxygen concentration exceed certain limit. Ageless eye, developed by Mitsubishi Gas Chemical Co., Ltd., is based two dyes. One is methylene blue, which is a redox dye that is colorless in the absence of oxygen and turn to blue upon oxygen exposure. The other dye is Acid Red 52, a pink non-redox dye [1]. This gives Ageless eye a pink color in the absence of oxygen. Once the tablet react undergoes oxidation process, methylene blue is in transition from light blue to dark blue while Acid Red 52 remain pink. This gives the tablet the transition from pink to purple and blue, when the color of methylene blue obscure the color of Acid Red 52.

Methylene blue-based oxygen indicator consists of 3 main ingredients: dye (methylene blue), photoinitiator and binder. Dye will change color in relation with oxygen concentration and time of oxygen exposure. The Photoinitiator (2,2-dimethoxy-2-phenyl acetophenone-benzyl dimethyl ketal, BDK), under UV irradiation, is able to undergo a photocleavage reaction resulting in free radical, which reduces MB causing changes in its color [2]. This mechanism was proved to be applicable when the binder is acrylic resin although acrylic resin was somewhat reacted to free radicals [3].

There is a potential for other bio-based binder and methylcellulose was chosen to be study. The objectives is to evaluate the effect of methylene-blue (MB) and 2,2-dimethoxy-2-phenyl acetophenone-benzyl dimethyl ketal (BDK) on color of the oxygen indicator film based-on methylene blue principle with methylcellulose binder.

## 2 Experimental

### 2.1 Materials

Methylene blue (MB) (AR grade), obtained from Sigma-Aldrich® (USA), is used as a redox dye. 2,2-dimethoxy-2-phenyl acetophenone-benzyl dimethyl ketal (BDK), used as a photoinitiator, was obtained from Sigma-Aldrich® (USA), methyl cellulose (MC) solution (10% w/v), used as a binder, was prepared from dissolving metyl cellulose powder (Methocel®,Dow Chemical) in water. Ethanol, obtained Sigma-Aldrich®(USA), was used a solvent when forming methyl cellulosed film

### 2.2 Methylene blue-based oxygen indicator film forming

BDK and methylene blue were mixed with 7 mL ethanol using magnetic stirrer for 10 minutes prior to adding 3 mL of 10% (w/v) methyl cellulose solution. The mixture were then mixed again for 10 minutes. The solution was then formed into a film by solution casting technique. The mixture (10 mL) was poured on a petridish (diameter of 100 mm). The solution was let dried at ambient temperature of around 25-27°C for 24Hours. The film was then cut into 10 x 10 mm square and placed into high barrier plastic bag before vacuum sealed the packaged to ensure that the oxygen free atmosphere can be assumed. The film was then UV irradiated (774 mJ.min/cm$^2$) at a distance between the sample and the UV lamp of 10 cm.

### 2.3 Effect of Methylene-blue Concentration

Methylene blue-based oxygen indicator film was formed according to the method described in 2.2. BDK concentration was fixed at 0.7% (w/v) of the total solution while MB concentration was varied at 0.021, 0.035, 0.049 and 0.070% (w/v). The film sample was UV irradiated for 3600 seconds. During the irradiation, the sample was taken out briefly to measure the change in its color at 0, 15, 30, 60, 120, 240, 480, 960, 1920 and 3600 seconds. Upon removal from irradiation and the vacuum packaging, the film was exposed to oxygen in normal atmosphere (approximately 20.9%) for 1800 minutes. During the exposure to oxygen, the color of the sample was measured at 0, 0.25, 0.5, 1, 2, 4, 8, 16, 32, 60, 120, 180, 240, 300, 600, 1200 and 1800 minutes.

### 2.4 Effect of Photoinitiator Concentration

Methylene blue-based oxygen indicator film was formed according to the method described in 2.2. MB concentration was fixed at 0.021% (w/v) of the total solution while BDK concentrations were at 0.07, 0.35, 0.7 and 1.4 (w/v). The film sample was UV radiated and exposed to oxygen as described in 2.3.

### 2.5 Measurement of film color

Spectrodensitometer (SpectroDens, Techkon, Germany) was used for measuring L*, a* and b* of film, as an indicator of in CIE Lab during the irradiation and oxygen exposure period. The L*, a* and b* values obtained from the value were used for the calculation of color difference (ΔE) using the following equation

$$\Delta E = \sqrt{(L-L_0)^2 + (a-a_0)^2 + (b-b_0)^2} \quad (1)$$

where L, a and b represent L*, a* and b* of the sample of interest (in this case they are values measured at anytime greater than 0). $L_0$, $a_0$ and $b_0$ represent L*, a* and b* of the reference, which is the values at time = 0). Measurement for each treatment is done in triplicate and the values reported are an average and standard error of the data.

### 2.5 Statistical analysis

All values shown are average values of 3 replicates and error bars represent standard error. All data were compared using one-way analysis of variance. When the result of the analysis indicated significant difference Tukey was used for multiple comparison. The statistical analysis was done using SPSS version 17.

## 3 Results

### 3.1 Effect of methylene blue (MB) Concentration

The color of the film was monitor with CIE Lab color space, which consists of L*, a* and b* and the color difference (ΔE). L* value represent the lightness of the film. The lighter film is represented with the greater L*. a* and b* values indicate the color of the film and they have both negative and positive values. The positive a* indicates the redness while the negatives indicates greenness. For b*, the positive values is designated to yellowness while the negative value is for blueness. The greater absolute values of a* and b* implies the greater intensity of those colors. Color difference represents the difference in color calculated based on L*, a* and b* values.

When the film was formed, its color was blue but the shade of blue for each film was visually different. The difference of the film before UV irradiated was most pronounced for the film with 0.021% MB, which has the lighter shade of blue than other films. This agreed with the greater L* value. The a* and b* values of film with 0.021% MB was also significantly different from other films indicating that this film had less redness and more blueness.

When the film is exposed to UV irradiation the film changes to a transparent color. The color values of all films changed in similar manner. L* increased significantly showing that the color of the film is much lighter upon irradiation. The reduction of a* from positive to negative values indicates that the film shows more greenness. The increase of b* from negative to positive values shows the more yellowness (Figure 1a-1c). Color differences (ΔE) changed in a similar pattern as L* and b* (Figure 1d). The changes occurred because, upon irradiation, BDK reduced methylene blue to leuco methylene blue, which is colorless in nature [3]. However, our film still shows some color components. This maybe a contribution of methyl cellulose, which is used to form a film matrix, as well as some methylene blue that had not undergone the reaction. Film with 0.021% MB seemed to have the least unreacted MB as it had the greatest b* value, which indicates the least blueness.

Methylene blue concentration affected the change of L* and b* values more than it did on the a* value. L* and b* values of 0.021% MB had reached its saturated point, which is the point where color values did not significantly changed, 16 minutes faster than other film did (Figure 1 and 3). Upon 3600 seconds UV irradiation film with 0.07% MB was significantly darker (greater L*) and blueness (less b*) than other films which had no significant difference in L* and b* values.

Color difference (ΔE) increased with an increasing UV irradiation time (Figure 4). The value of color difference as well as the time required to reach the maximum value was affected by MB concentration. The magnitudes of color difference were about the same for film with 0.021, 0.035 and 0.049% MB upon 960 second irradiation and they were significantly greater than that of film containing 0.07% MB. The time required to reach saturation point or the maximum point of color difference had tendency to increase with an increasing MB content. It took 480 seconds for film with 0.021% MB and 1920 seconds for film with 0.035 and 0.049. Film containing 0.07% MB did not reach its saturation point after 3600 seconds of UV irradiation. The reason for the longer time required to reach the saturation can be a result of more reaction due to greater concentration of MB. However, the addition reaction for greater MB did not contribute much in term of color change.

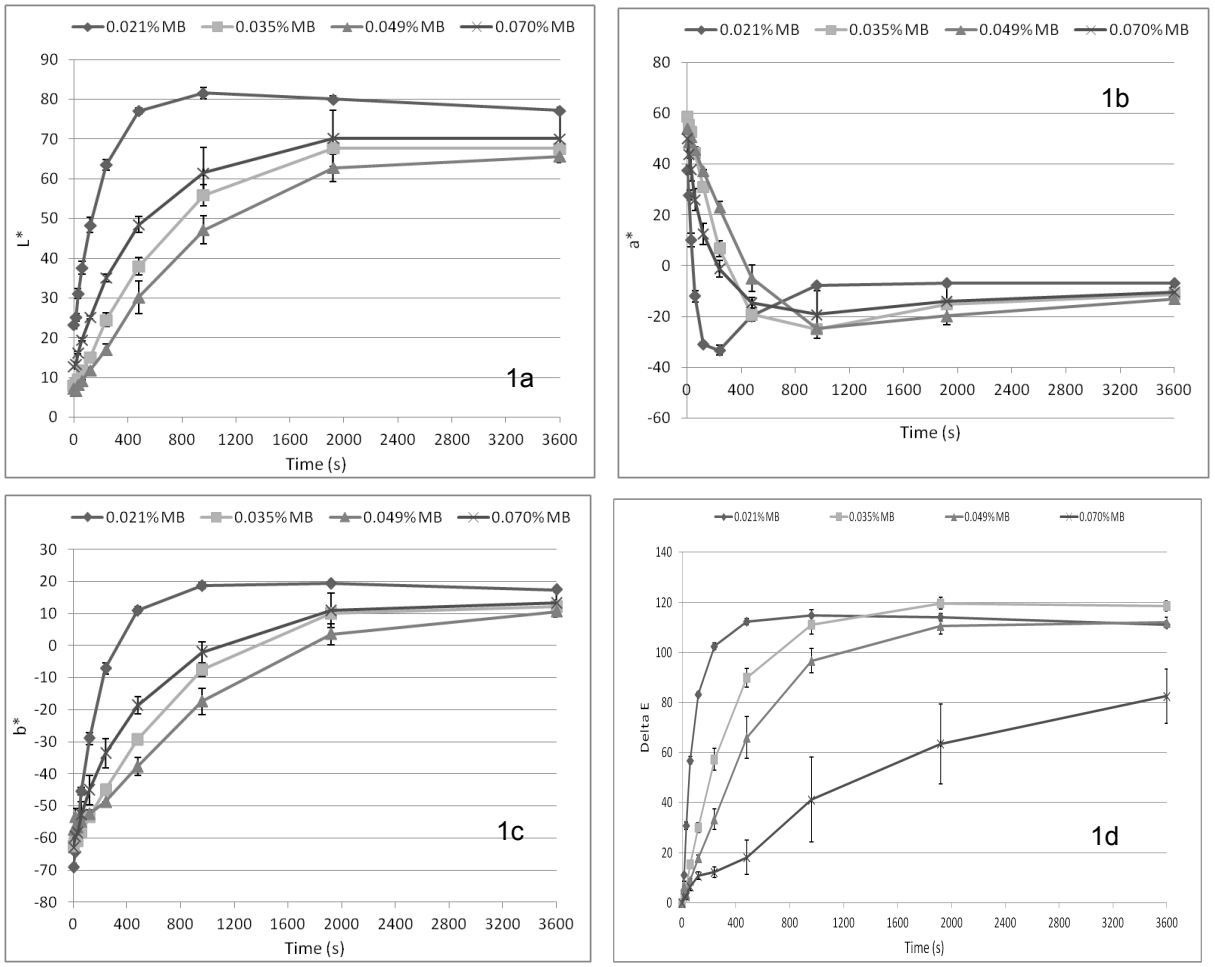



Figure 1: change in L* (1a), a* (1b), b* (1c) and color difference (1d) of film containing 0.7% BDK and 0.021% MB (diamond), 0.035% MB (square), 0.049% MB (triangle) and 0.07% MB (x) upon UV irradiation

After UV irradiated methylene-blue based film was exposed to oxygen the film regained its blue color as lecuo methylene blue was oxidized to methylene blue again [3]. The change can be observed with naked eyes as well as from the color measurement. L* and b* values reduced with an increasing exposure time indicating that the film was darker and had greater blue color (Figure 2a and c). The value of a* decreased at the beginning and increased afterward (Figure 2b). When compared at each oxygen exposure time the value of a* values only had minute difference regardless of the difference at the beginning of the exposure experiment. The difference between treatment (MB concentration) in L* and b* values remain similar throughout the experiment. Film with 0.07% MB was always darker than other films was. Film with 0.021% MB appeared to be significantly lighter than other film upon 3 hours of oxygen exposure. Similar to L* values, b* of 0.07% MB film were always less than other films but at the end of the 30 hours exposure all films had the same b* values.

Although the three color parameters were quite different at each exposure time, the magnitude of color difference (Figure 2d) of each film were not differ until the film was exposed to oxygen for 0.16 hours. At this point color difference of 0.07% MB were significantly less than that of other films and remain slightly less until 10 hours of oxygen exposure. After that ΔE values of all films were not significantly different. It implies that the differences in color parameters detected after exposure to oxygen were mainly the result of the initial difference of film before oxygen exposure. In term of time required to reach the saturation point of color difference, film containing 0.021% MB had the shortest time (2 hours) while film with other concentrations takes at least 10 hours. It was also noticed that the color difference after irradiation were greater than the color difference after oxygen exposure, which indicates that the films did not change the color back to their original color.

For BDK constant concentration at 0.7%, film with 0.021% MB, which is the lightest film, reached its color difference saturation point fastest both upon the UV irradiation and oxygen exposure. The magnitude of color difference for this film did not differ from film with 0.035 and 0.049% MB. Therefore the MB concentration of 0.021% was chosen for the next part of the study.

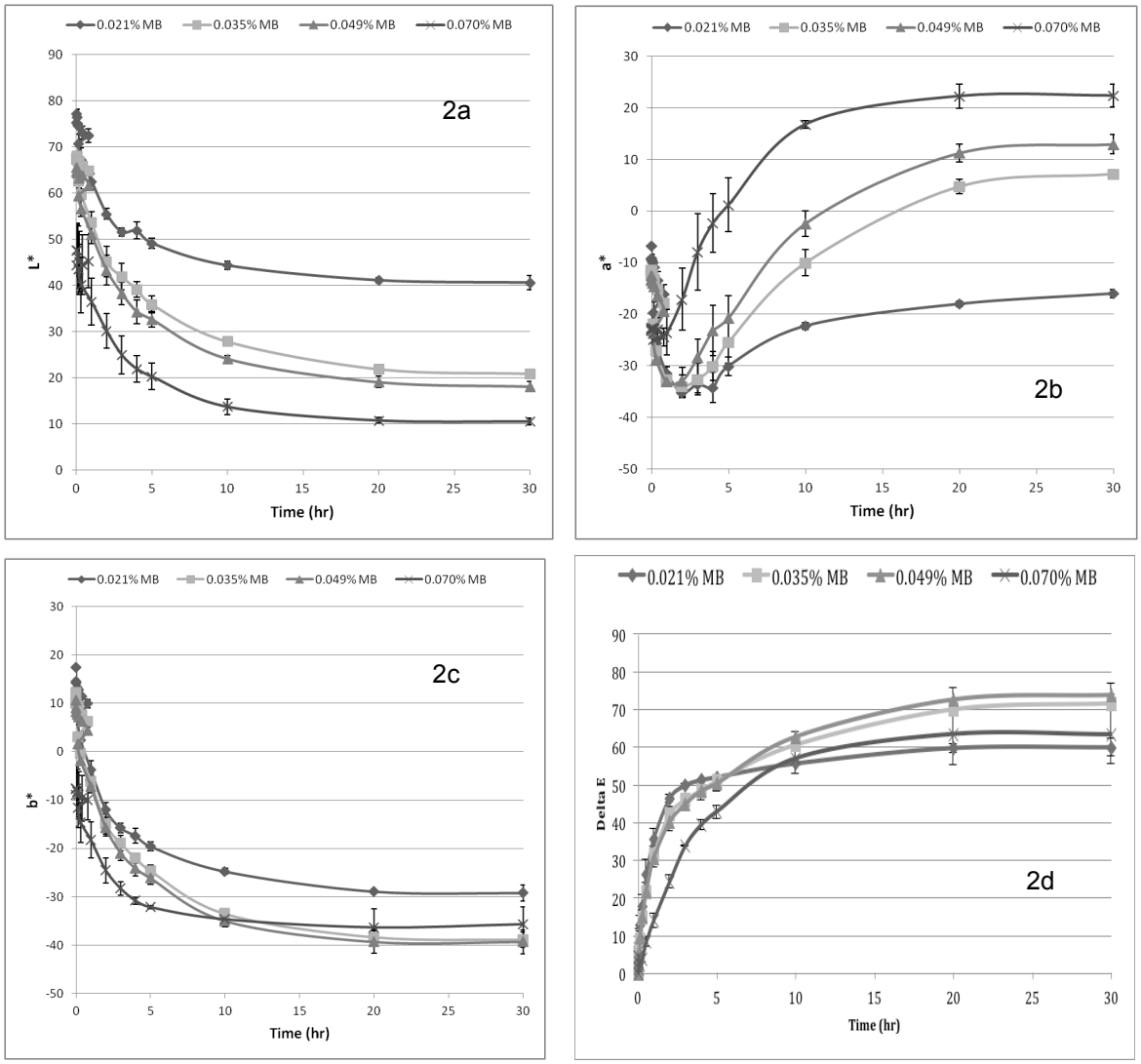



Figure 2: change in L* (2a), a* (2b), b* (2c) and color difference (2d) of film containing 0.7% BDK and 0.021% MB (diamond), 0.035% MB (square), 0.049% MB (triangle) and 0.07% MB (x) upon oxygen exposure

### 3.2 Effect of BDK Concentration

Films with various content of photoinitiator (BDK) was blue in color as a result of MB content. BDK concentration also played roles in the color variation of the film. The initial L* and a* values of all films were significantly different but the b* values were very similar. Film with the lowest BDK concentration (0.07%) had significantly less L* and higher a* values implying that this film was lighter and had more redness than films with higher BDK concentration. For other concentrations L* and b* of every film were significantly different but they were not in relation with the concentration of BDK.

Upon UV irradiation L*, a* and b* values change in the same pattern as the result previously stated in 3.1. After 3600 seconds of irradiation the film with 0.07% BDK had the lowest L* values (Figure 3a) while film with 0.35 and 0.7% BDK had the highest L* value. In term of a* values there were no significant difference between films except film with lowest BDK concentration (0.07%), which had significantly lower values (Figure 3b) indicating the more greenness the film had. BDK had significant impact on the value of b* after UV irradiation as b* values of all films were different and they increased with an increasing BDK concentration (Figure 3c). The film with higher BDK content was lighter and is more yellowish after irradiation. Color difference (ΔE) after UV irradiation of film containing 0.07% BDK was found to be the lowest indicating that it had the least change in color compared to the initial color. The highest change in color was observed in film containing 0.7 and 1.4% BDK. All BDK concentration had reached the color difference saturation point at the same time, which is about 3 hours (Figure 3d).

BDK concentration also affected the rate at which the color difference had reached its saturation point. For BDK concentration between 0.35 – 1.4%, the time required to reach maximum values of L*, b* and ΔE increased with an increasing BDK concentration. However, for the lowest concentration of BDK (0.07%), those values reached their maximum at the same time as film containing 0.7% BDK but at a magnitude of color change much lower.

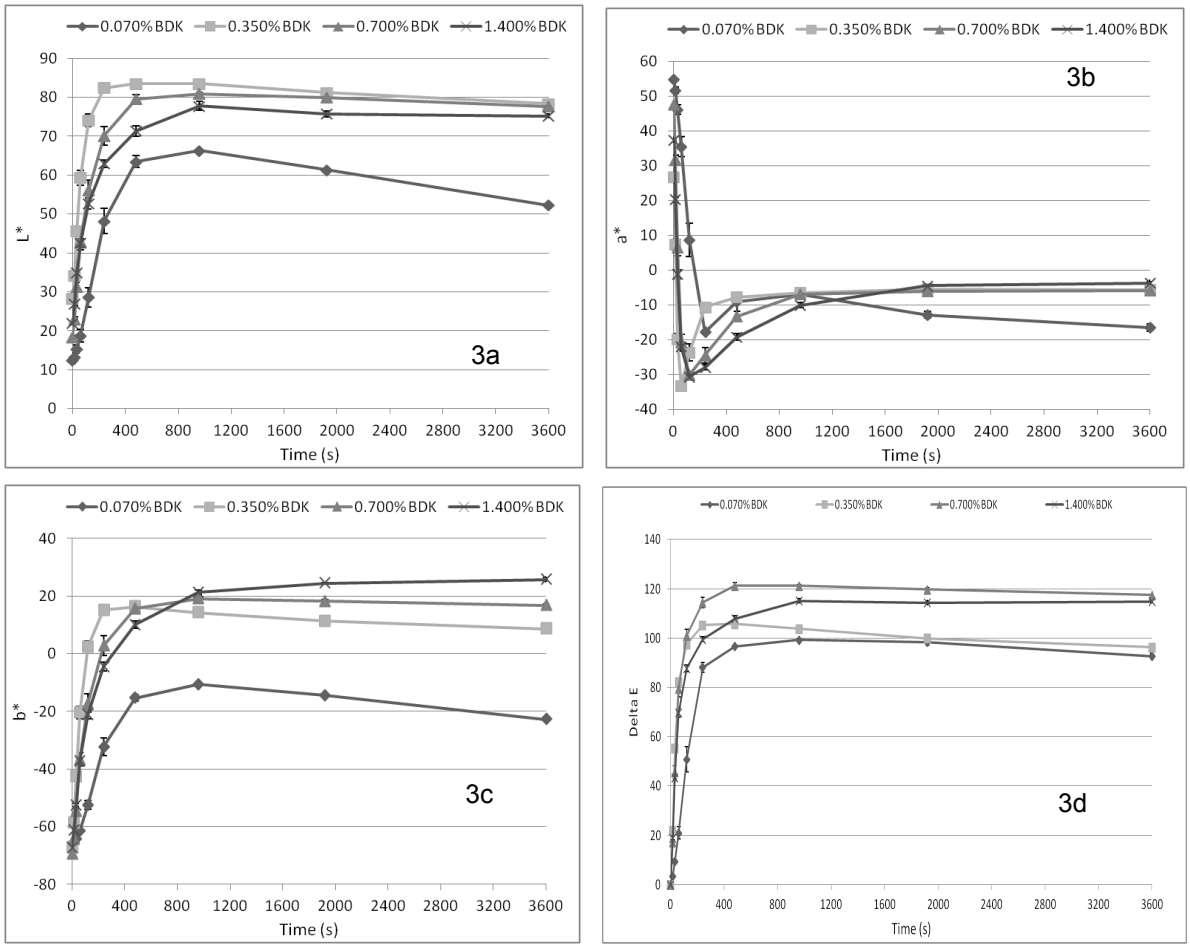



Figure 3: change in L* (3a), a* (3b), b* (3c) and color difference (3d) of film containing 0.21% MB and 0.07% BDK (diamond), 0.35% BDK (square), 0.70% BDK (triangle) and 1.40% BDK (x) upon UV irradiation

When films were exposed to oxygen in normal air their responses in term of L*, a*, b* and ΔE were similar to the pattern found in 3.1. However the difference in initial color before oxygen exposure had a great impact on the film after exposing to oxygen. This was obvious from Figure 4a-c,which shows graph with a very similar rise and fall but the beginning point of each graph (oxygen exposure time = 0) was different. The other support evidence were the change in color differences over time, which were statistically the same for films with BDK ranging from 0.35 – 1.4% (Figure 4d). The film containing 0.07% BDK had significantly less color difference. This agrees with the UV irradiation result (Figure 12), which shows the least color difference in the same film.

The result in the study of the effect of BDK shows that BDK centration of 0.07% was not enough to react with 0.021% MB. It also shows that the concentration of 0.35 and 0.7% were a better choice. The film with both concentrations had very similar properties except the film with 0.35% had less color difference upon irradiation but reached equilibrium faster. The latter reason made 0.35% BDKa better for detecting leak in packaging application.

## 4 Conclusions

Methylene blue concentration (with constant BDK concentration at 0.7%) affected the color of the film before and after UV irradiation as well as the color difference. The lower methylene blue concentration resulted in lighter film that reach its maximum color difference the fastest both for UV irradiation and oxygen exposure steps. MB concentration did not have effect on the magnitude of color difference in the range of 0.021 – 0.049%

BDK concentration (with constant MB concentration at 0.021%) had less obvious effect on the color of the film before and after UV irradiation than MB concentration did. Film with 0.35% BDK required the least time to reach saturated color difference point but its magnitude of color difference were slightly (but significantly) less than that of film with 0.7 and 1.4% BDK. BDK concentration in the range of 0.35 – 1.4% had no effect on film color difference.

## 5 References


1. Mitsubishi Gas Chemical Technical Information, 2007, “Agelees-Eye”.
2. Y. Galagan and W.F. Su, 2008, “Reversible photoreduction of methylene blue in acrylate media containing benzyl dimethyl ketal”, Journal of Photochemistry and Photobiology A: Chemistry 195, pp. 378-383.
3. Y. Galagan, S.H. Hsuand W.F. Su, 2010, “Monitoring time and temperature by methylene blue containing polyacrylate film”, Sensor and Actuators B 144, pp. 49-55.

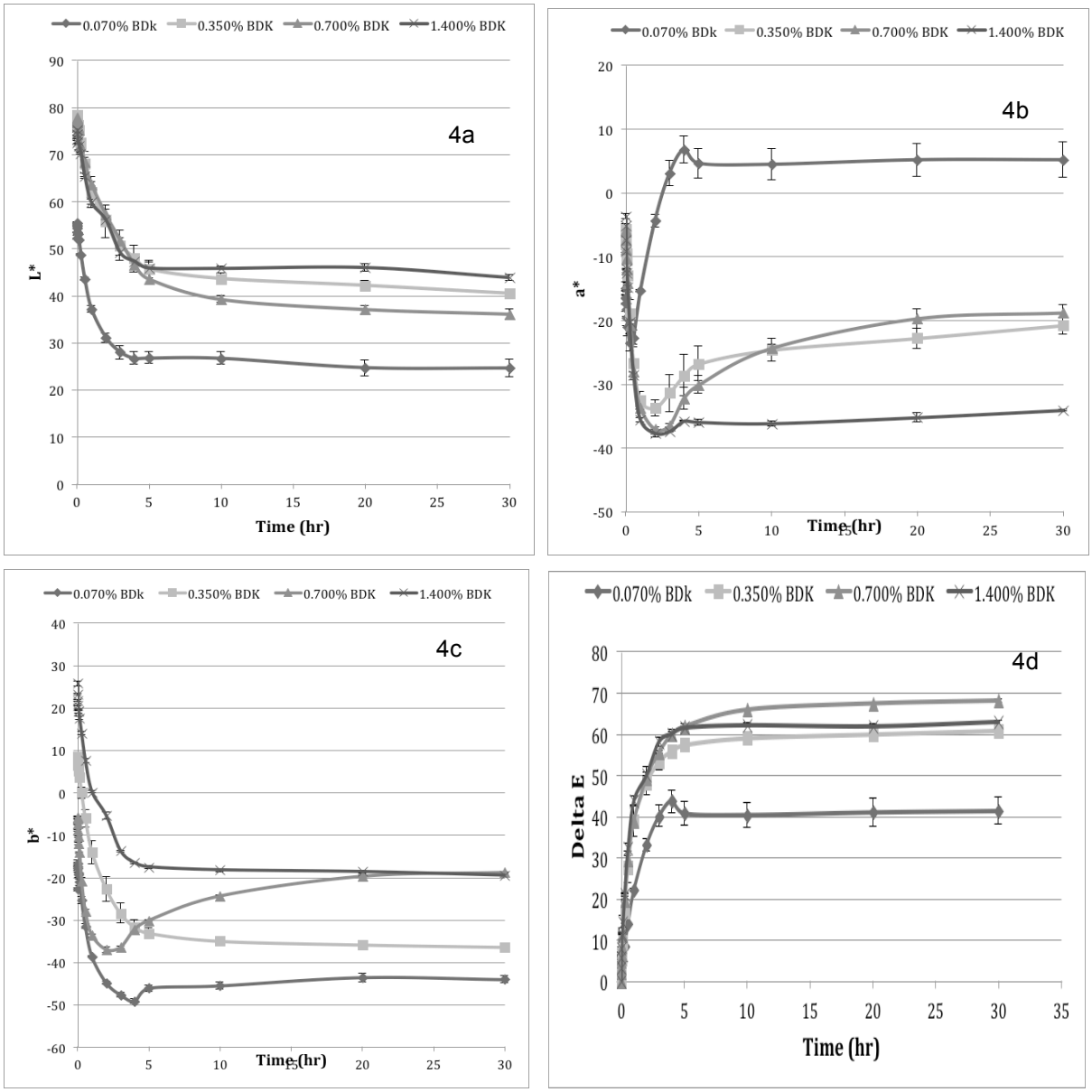



Figure 4: change in L* (4a), a* (4b), b* (4c) and color difference (4d) of film containing 0.21% MB and 0.07% BDK (diamond), 0.35% BDK (square), 0.70% BDK (triangle) and 1.40% BDK (x) upon oxygen exposure

# DISTRIBUTION PACKAGING

# Issues with Combining Road Elevation Spectral Models and Vehicle Vibration Response to Estimate Vehicle Dynamic Characteristics[#]

**Vincent Rouillard, Daniel Ainalis[*] and Michael Sek**

*College of Engineering and Science, Victoria University, Australia*

[*]*Corresponding author. Email: daniel.ainalis@live.vu.edu.au*

**Abstract:** The research presented in this paper focuses on the issues associated with the development of an experimental technique to estimate the dynamic characteristics of wheeled vehicles (namely the Frequency Response Function) using only in-service response data. In order to validate the approach and eliminate complexities associated with multi-wheel vehicles, a single-wheeled prototype vehicle was designed and commissioned. The vertical vibration acceleration of the prototype vehicle's sprung mass was measured during normal operation. The Power Spectral Density function was computed and used to estimate the Frequency Response Function of the vehicle. A number of experiments using various configurations of the single-wheeled prototype vehicle were undertaken, along with a series of vibration table experiments were also undertaken to provide a comparison with the estimated Frequency Response Functions.

The results show that the best estimate of the Frequency Response Function using the vehicle response data provides reasonable agreement with the measured laboratory experiments when the value of the slope of the spectral function is not set to the value recommended by the International Organisation for Standardisation. Another technique was further developed to estimate the value of the pavement spectral slope using only in-service response data; however this technique does not yield consistent and accurate estimates. Interestingly, the main resonance of the vehicle is in agreement between the vibration table and in-service response data around the sprung mass of all three vehicle configurations when inspected using linear scales (regardless of the variation in the spectral shape of the excitation), although the additional modes (including the unsprung mass) differs for all vehicles.

Keywords: vehicle dynamic characteristics; frequency response function; transmissibility; pavement spectral analysis; laboratory simulation; distribution vibration.

[#] This is the abstract of a peer-reviewed paper to appear in a Special Edition of Wiley's journal *Packaging Technology and Science* dedicated to the 19th IAPRI World Conference on Packaging 2014 hosted by Victoria University, Melbourne, Australia.

# Reduced-Order Modeling of the Linear Vibration Response of Expanded Polymer Cushion Material[#]

**Gregory Batt[1*], James Gibert[2] and Mohammed Daqaq[1]**

[1] *Clemson University, United States*
[2] *Clarkson University, United States*

[*]*Corresponding author. Email: gbatt@clemson.edu*

**Abstract:** The demand to lower costs and reduce the amount of packaging materials utilized in a packaged-product system has placed increased importance on the development of tools to model the behavior of packaging systems. This manuscript examines the accuracy and convergence of a reduced order model (ROM). The ROM is derived from an idealized packaging system consisting of a rod of polymer foam with an attached end mass. The work begins with an introduction to the complex cyclic softening and the viscoelastic and nonlinear stress-strain behavior exhibited by expanded polymer foam. The partial differential equations (PDE) and associated boundary conditions governing the motion of the system are obtained. The equations are reduced to a ROM using the assumed modes method. Approximate eigenvalues are compared to both exact and experimental eigenvalues reported in literature. Finally, the ROM is compared to the frequency response functions (FRF) of the exact solution and those obtained experimentally. Both results are used to determine the number of modal equations needed for the ROM to accurately capture the steady-state dynamic behavior of the packaging system.

Keywords: cushion modeling; viscoelastic; vibration; assumed mode; reduced-order.

[#] This is the abstract of a peer-reviewed paper to appear in a Special Edition of Wiley's journal *Packaging Technology and Science* dedicated to the 19th IAPRI World Conference on Packaging 2014 hosted by Victoria University, Melbourne, Australia.

# Estimation of the Dynamic Properties of Nonlinear Packaging Materials Using an Optimised Reverse Multiple Input/Single Output Based Approach[#]

**Matthew Lamb[*] and Anthony Parker[*]**

*College of Engineering and Science, Victoria University, Australia*

[*]*Corresponding authors. Email: matthew.lamb@vu.edu.au; anthony.parker@vu.edu.au*

**Abstract:** During the distribution phase, packaged consignments are exposed to a variety of environmental hazards (such as vibrations) which, if excessively severe, may cause damage to or even destroy the product. Structural deterioration can be tracked by monitoring variations in the packaging system's modal parameters, particularly its natural frequency (stiffness). Natural frequency estimates are often extracted using a least squares regression curve fit, applied to an estimate of the system's Frequency Response Function (FRF). FRF estimates are generally obtained using the Fourier transform with a single input and single output (SISO). This approach is suitable for many applications; however, as the nonlinearity of the system under analysis increases, the ability of this technique to accurately monitor changes in the system will decrease. In addition, when the excitation to the nonlinear system is varied (increased or decreased amplitude), a SISO based approach may indicate a shift in natural frequency (as a result of the varied input) even though no change in the condition of the system has occurred.

This paper discusses an approach which is designed to separate the linear component of the system's FRF using a reverse multiple input/single output (RMISO) algorithm. Such separation will allow traditional modal parameter extraction (curve fitting) techniques to be used to monitor the condition of nonlinear systems.

The paper presents the results of experiments in which expanded polystyrene samples were subjected to broad-band random base excitation with a free-moving load placed atop the cushion sample. Continuous acceleration measurements of the vibration table and the free moving load were used to compute the FRFs of the cushions and the differences between a conventional (SISO) approach and the proposed RMISO based parameter extraction technique were evaluated.

Keywords: RMISO; reverse path; modal parameter extraction.

[#] This is the abstract of a peer-reviewed paper to appear in a Special Edition of Wiley's journal *Packaging Technology and Science* dedicated to the 19th IAPRI World Conference on Packaging 2014 hosted by Victoria University, Melbourne, Australia.

# Future Demands in Distribution Dynamics Research

**Edward A. Church and Andrew J. Gruber**

*International Safe Transit Association, United States of America*

**Abstract:** There is risk of damage in every supply chain distribution environment. ISTA exists because hazards are predictable and damage can be prevented. Companies want assurance that they are designing and delivering the distribution packaging that meets the rigors of their supply chain at the lowest cost and smallest environmental footprint. They realize that a properly designed and tested package is a key element in an optimized supply chain. Proven creditability of test protocols and design standards provide confidence in managing supply chain risk and waste, but supply chains are constantly changing and expanding.

This presentation will outline the main research in distribution dynamic event levels and sequences in emerging market regions and finding any changes in existing channels already simulated in existing tests. ISTA believes this new research and the development of new testing techniques needs to be conducted to enable more rapid development of new or updated simulation test methods to reduce the risk of damage in distribution and reducing packaging waste.

Industry Best Practices need to be developed for the collection and analysis of distribution hazard data used to create laboratory testing standards. There is also a demand for expansion of distribution dynamic data such as for the E-commerce supply chain, intermodal shipments, and unique situations during the "last handlings" segment and other previously unstudied supply chain lanes, all including more temperature and humidity study. The presentation concludes with how others can be involved and contribute in the future.

Keywords: Package Testing, Supply Chain Simulation, Package Waste Reduction

## 1 Introduction

The hand writing has been on the wall for the past 20 years, but ISTA and the world is just getting around to doing something about it. We have known for some time there are that are gaps in our knowledge about distribution hazards in existing markets and now emerging markets around the world.

A lot of separate things have occurred to bring us to this point and we will go over some of them in this paper, but the key point is that we are here now and that it looks very promising. What was envisioned by several different thought leaders could be coming in the years ahead.

In the 1990's Dennis Young, then ISTA's Technical Director came up with the concept for ISTA's Test Series. The basis of which consisted of the existing ISTA tests that were called non-simulation integrity tests and newer tests that were classified as general simulation tests. General simulation tests are based upon the ability of test apparatus to do a better replication of real-world distribution hazards at performance levels derived from field measurement studies. The key factor here though is that Dennis recognized the potential of having packaged-product testing that are completely based upon actual field measurement or observed hazards and levels.

ISTA and ASTM (with their D-4169 tests) have refined and improved general simulation testing over the years since. ISTA established its 4AB web-based software application in 2006, but in reality ISTA's 4 Series: Enhanced Simulation Tests have not really been adopted because its use requires data capture, analysis and test development. Time and effort most, if not all, companies are unwilling to invest based upon the potential return in dollars and cents.

Things, however, have changed in the past few years and this change is driven by two key factors, cost reduction and environmental concern over waste from product damaged in shipment and product's being excessively packaged.

## 2 ISTA's Background

For over 65 years, ISTA has been the leading industry developer of testing protocols and design standards that define how packages should perform to ensure protection of their contents during the ever changing risks of the global distribution environment. Our non-profit, member-driven association sets the standards for optimizing

the resources in packages that are designed to be survivable, sustainable and successful. Worldwide, ISTA is the most trusted, knowledgeable and respected authority in predictive package-performance testing. We work quietly and effectively in the background helping our members develop more effective packaging.

ISTA's broad international membership base includes:

- companies (primarily brand owners) who manufacture and distribute products,
- carriers who provide the distribution means,
- organizations that supply packaging materials, testing equipment and services,
- testing laboratories that perform packaged-product performance tests
- universities that perform research
- packaging students preparing to enter the industry

## 2.1 Our Vision (How We Will Improve Our Industry)

We envision providing ISTA members with the confidence that they have the best package possible for their supply chain. We work to optimize the economic, social and environmental impact of the packaging systems used in countries throughout the world.

## 2.3 Our Mission (How We Promise To Do This)

ISTA's mandate is to enhance the effectiveness of package design and testing. We accomplish this by developing and delivering testing protocols, tools and educational programs designed and certified to ISTA performance and environmental standards.

## 2.4 What We Do And How We Do It

ISTA is the only international organization that certifies testing labs, packages and people providing industry recognized third-party credibility. Tested package-products, by certified professionals in certified labs provides confidence that the packaged-product will survive its supply chain challenges.

ISTA helps members control costs, reduce the risk of damage and minimize environmental impact during the distribution of packaged products.

ISTA enlists international input and follows a consensus approach to developing the intellectual property that is imbedded in our testing protocols and design standards.

# 3 Meeting the Challenge of the Future

## 3.1 The Future is Challenging Each of Us

ISTA has done an excellent job of staying ahead of the curve for the past 65 years. We have become THE trusted source for developing packaging design and test protocols that have become world standards. But the global shipping environment is changing rapidly. At ISTA we are committed to continuing this leadership, and therefore more value delivery to our members by assuring all of our protocols are appropriate for new operating environments as they emerge. Additionally, we are committed to enhancing the value of existing protocols through continuous monitoring and improvement. In surveying ISTA members we have found the following major concerns:

- Varying supply chain environments for which are difficult to package.
- Still some unknown distribution hazards in otherwise known environments
- Continued pressure to lower packaging costs
- Developing packaging with the smallest environmental footprint/waste
- Managing risk/Financial Loss
    - Product/Package Damage
    - Unsalables/Lost Sales/Lost Retail Distribution
    - Reputation/Brand Image

## 3.2 Resources Needed

ISTA has identified significant initiatives, based upon its long range plan to support the needs of its members, the packaging industry at large, and consumers. The cost of developing and delivering value through an agenda of this magnitude is significantly beyond ISTA's ability to incorporate additional major initiatives into our annual budget. To fund the research and development priority agenda, ISTA will enlist industry-led investments.

## 3.3 What We Are Trying To Do

ISTA has created an Advocacy Research & Value Delivery Program to encourage visionary industry members to financially support ISTA research. This will assure our long-term ability to develop knowledge that assists our members in their pursuit to improve the economic, social and environmental impact of their packaging systems.

## 3.4 Primary Research Activity

Commissioned research to enable more rapid development of information sources and "data driven" test methods to ensure ISTA processes are kept relevant both domestically and internationally to improve the "bottom line" of its members through waste reduction. The primary goals are:

**Damage Reduction** – Collect statistically significant distribution environment data from more regions and modes to develop tests for emerging markets and monitor existing regions to ensure test levels are current. These efforts will provide enhanced confidence in one's ability to reduce damage and unsaleables.

**Eliminate over packaging** – Develop and validate a new technique to quantify the level of packaging beyond the test threshold performance required to diagnose over-packaging resulting in packages with lower material cost and environmental footprint

To fund these vital initiatives, ISTA has created the ISTA Advocate Initiative to encourage visionary industry members to support ISTA's vision as we work to continually improve the economic, social and environmental impact of packaging systems. New resources from Advocate commitments will help ensure ISTA's long-term viability to serve its members and the broader packaging community with extraordinary, vital research and education.

ISTA will establish an Advocate Advisory Council reserved for those visionary industry members who are united in their commitment to ISTA's efforts to optimize the economic, social and environmental impact of packaging systems. Advocates recognize that their financial support will allow ISTA to increase the momentum of program and intellectual property development which, in turn, will improve their individual enterprises.

Each year, the Advocate Advisory Council will meet to provide major investors a significant voice in the direction, prioritization and implementation of the ISTA research agenda. Advocate Council-level investor's work in partnership with the Global Board, staff and elected leadership of ISTA to further the program initiatives and the strategic initiatives of the Association. They will weigh the value of projects – employing the advice, experience and recommendations of key members and partners of the industry. The Council will develop and work within operating guidelines that assure its efforts increase the value to the entire membership base as well as afford transparency in its accounting for expenditures and its method for awarding projects. An idea of the potential research, ISTA member benefit and how the funding will be used is shown in the table that follows:

**Table 1:** Potential Research Schedule

| Year | Project | Member benefit | Research $$ used for: |
|---|---|---|---|
| 2014-2015 | Accelerated Data Driven Test Development: New distribution simulation protocols need to be developed to better replicate the common hazards found in Asia Pacific distribution | Random vibration, drop height and orientations, other regional specific handling hazards protocols for SE Asia countries, resulting in 0.5% damage reduction and 5% material spend reduction | Contracted data study, staff technical analysis, and report writing |
| 2015-2017 | Eliminate Over Packaging: Develop a new testing Technique to be able to quantify the level of packaging beyond the test threshold performance required | Validating the performance of package designs that are not over-packaged resulting in packaging with a 2-5% reduction in material costs and lower environmental footprint (package waste and carbon footprint) | Working with Universities and research institutes to generate potential theories, research to determine most feasible approaches and then validation of final concept |
| 2015-2020 | Advocacy Council Research: Projects selected on an annual basis by majority vote of the Council | Varies with the project Goals established by the Council | Varies with the project Goals established by the Council |
| 2015-2020 | Advocacy Member Research: Specific research member funded | Specific to the Advocate member project | Funded by the advocate and varies with the project goals and objectives. Results shared with member base. |
| 2016 | Data Driven Test Development: India distribution protocols | Random vibration, drop height and orientations, other regional specific handling hazards protocols for India, resulting in 1.5% damage reduction and 5% material spend reduction | Contracted data study (extreme heat and humidity, harsh and extensive vibration, compression in the direction of the broadest packaging surface, mid-panel impacts and compression (i.e., stepping in the center of the large panels), and multiple impacts. |
| 2017-2018 | Data Driven Test Development: South America distribution protocols<br>Africa distribution protocols | Random vibration, drop height and orientations, other regional specific handling hazards, resulting in 1.5% damage reduction and 5% material spend reduction | Contracted data study, staff technical analysis, and report writing |

## 4 What Will Be the Benefits of This Research?

The results of this program would be new and revised ISTA test procedures with test sequences based upon more environmental measured data and observations with more accurate pass/fail threshold test levels to insure the proper test has been conducted. The industry would not be over packaging because the test was too severe or included test elements that do not exist in the distribution environment for that specific packaged-product.

The addition of new testing techniques to identify and quantify when a package system is over designed and has the potential to lead to packaging waste for each and every package shipped will be a major breakthrough and bring closure to a concept that has been talked about for years, but never seriously explored and resolved.

In the simplest form, all the players in the packaging industry will benefit because the program will ultimately lead to the “Just Right” Test that requires the “Just Right” level of performance and yields a “Just Right” package.

The following shows how each category of company will benefit directly to their operation.

**Table 2:** Benefits of New Testing Protocols and Processes

| Company Type | Direct Benefit |
|---|---|
| Shipper (Manufacturer) | Reduced Packaging Costs, Reduced Damage, Speed to Market, Obtaining Sustainability Goals |
| Packaging Supplier | Happy Customers, Reliable Designs |
| Carrier | Reduced Damage Claims |
| Third Party Testing Laboratory | More Companies Conducting Pre-shipment Testing |

Table 3 shows examples of potential direct and indirect costs associated with package damage in shipment for various packaging expenditures. Table 4 indicates the potential savings through a reduction in damage rate and a reduction in packaging spend based upon not over designing the protective capability of a package.

**Table 3:** Cost of Damage in Shipment

| Current Cost of Damage | | | | |
|---|---|---|---|---|
| | Direct Cost | | Indirect Cost | |
| Pack spend $ | Current Damage Rate | Damage (pack cost), $ | Cost Factor* | Indirect Cost of Damage, $ |
| 10,000,000 | 2.0% | 200,000 | 5 | 1,000,000 |
| 50,000,000 | | 1,000,000 | | 5,000,000 |
| 100,000,000 | | 2,000,000 | | 10,000,000 |
| 500,000,000 | | 10,000,000 | | 50,000,000 |

*Assuming a factor of 5 x direct cost including product cost, shipping cost, etc.

**Table 4:** Potential Saving from "Just Right" Packaging

| Potential Savings | | | | |
|---|---|---|---|---|
| Damage Cost Savings | | New Spend Savings | | |
| New Damage Rate** | Saving by reducing damage, $ | New Spend Rate | Reduction in Pack Spend, $*** | Potential Annual Saving, $ |
| 1.5% | 50,000 | 2% | 200,000 | 500,000 |
| | 250,000 | | 1,000,000 | 2,500,000 |
| | 500,000 | | 2,000,000 | 5,000,000 |
| | 2,500,000 | | 10,000,000 | 25,000,000 |
| | | | | |
| 2.0% | 100,000 | 2% | 200,000 | 800,000 |
| | 500,000 | | 1,000,000 | 4,000,000 |
| | 1,000,000 | | 2,000,000 | 8,000,000 |
| | 5,000,000 | | 10,000,000 | 40,000,000 |

**Potential Lower Damage Rate Due to New or Better ISTA Tests Procedures Developed from New Data Research

***Potential Reduction in Total Package Spend Due to Waste Reduction in Not Over Designing Packaging via New ISTA Process

## 5 Conclusions

ISTA's research program is anticipating the needs of tomorrow and will provide a unique venue and financial leverage for visionary leaders to address many of the major issues facing the ever evolving packaging and global distribution environments.

It will generate new knowledge to solve pressing distribution packaging issues and will allow packaging professionals and their companies to move into the future with increased confidence in their package performance. ISTA will incorporate this knowledge into its current and/or new testing procedures.

The packaging industry and its partners in the supply chain have an opportunity to profit through tools created to facilitate the development of the most effective packaging; that minimizes cost, product damage, eliminates packaging waste and lessens environmental impact.

## Acknowledgements

The author's want to acknowledging the support of Dwight Schmidt, an ISTA Global Board member for his strong support and involvement with the ISTA Advocacy Program.

## References

1. ISTA, January, 2014 "Advocacy Research & Value Delivery Program Prospectus

# The Application of Computational Methods to the Analysis of Unitized Load Performance

**Dale R. Knochenmuss**

*Senior Associate*
*Stress Engineering Services, Inc.*
*7030 Stress Engineering Way, Mason, Ohio, 45040, USA*
*Office: +1.513.336.6701*
*Mobile: +1.513.368.4659*
*Dale.Knochenmuss@stress.com*
*www.stress.com*

**Abstract:**

Computational methods based on finite element analysis (FEA) are widely used in the engineering and scientific communities. Applications in packaging have, to date, been mainly directed toward primary packaging with some limited extensions into secondary packaging. In primary packaging, computational methods utilizing solid modelling and FEA have had a transformative effect on package design, optimization and structural performance prediction – capabilities which can be realized prior to the first physical parts being manufactured.

Primary packaging represents only a portion of the larger world of packaging and the global supply chain systems which serve to protect, preserve and transport goods from manufacturer to end user. Opportunities exist to apply computational analysis methods to secondary (individual shipping unit) and tertiary (unitized load) packaging issues, but these applications have not been widely explored or presented in the literature. Technical challenges have contributed to the slower adoption of these tools as secondary and tertiary packaging systems are physically larger, incorporate more individual components (which can be geometrically complex), and often utilize multiple materials with anisotropic, nonlinear properties. All of these factors, and the interactions between them in the dynamic transportation environment, serve to increase the difficulty of performing meaningful analysis tasks with computational methods.

This paper discusses efforts to expand the use of computational tools to address transportation packaging problems involving full unitized loads consisting of shipping cases, pallets and unitizing films such as stretch wrap. Results of an FEA analysis of a full unit load are presented and examples are provided of the types of unique insights that can be generated from such analysis. Opportunities and challenges for further development are discussed.

Keywords: unit load, transportation packaging, finite element analysis (FEA), finite element model, stretch film.

## 1 Introduction

As packaging becomes more highly optimized, the changes implemented to achieve that optimization can have unintended consequences for the overall packaging systems into which the individual pieces are ultimately assembled. Changes to each component of the system have the potential to affect the strength and stability of the final shipping configuration, which is often a unitized load. The primary package, secondary package (or shipping case or bundle), pallet, and unitizing material (e.g. stretch film or shrink hood) all contribute to the successful performance of the overall unit load.

The advances that have been made in applying analytical tools to performance predictions for primary packages have so far had relatively less impact on secondary packaging and unit loads. While the problems to be solved for a unit load are conceptually similar to a single primary package, analyzing a unit load involves potentially modeling many packages, many cases, the pallet, and the film unitizing the entire load. This involves more separate components, additional materials, and the interactions between them at each point where they contact.

Assembling all of these details into a useful finite element model is challenging and can require significant computational resources to solve. This paper describes work that has been undertaken to expand the application of finite element analysis techniques to include stretch film-wrapped unit loads of boxes.

## 2 Background

Early tools for finite element analysis required a high level of specialized skill and were relatively expensive to use. This tended to drive their application toward high-value uses where the cost and effort could be justified. In rigid plastic packaging, for example, the development of new blow-molded bottle designs could be slow and expensive when it involved the fabrication of, and iterative modification of, expensive metal molds. The effort required to use computational tools to analyze bottle performance and molding processes were easier to justify because of the significant cost and development time savings that were possible with these tools.

With secondary packaging, primarily referring here to paperboard or corrugated fibreboard boxes, development cost and time have not been major issues. There are, after all, many empirical guidelines or "rules-of-thumb" to guide package designers and it is not difficult, expensive or time-consuming to fabricate and test sample boxes. The application of computational methods to secondary packaging was further discouraged by the complex geometry (particularly for corrugated fibreboard) and anisotropic, nonlinear material properties of fiber-based packaging materials. Such difficulties as these did not entirely dissuade the technical community, of course, as they almost never do. The published literature includes a significant body of work in which finite element analysis methods have been applied to paper [1, 2], board [3-14], and boxes or packages [12, 15-19].

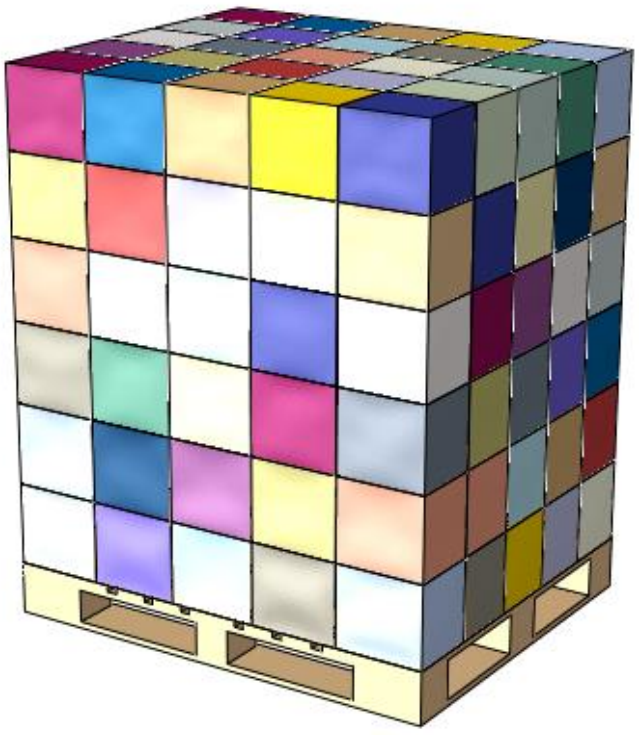


**Figure 1:** Unit Load Model

As analysis tools become more capable and easier to use, and improvements in the computer hardware to run them allow bigger models that execute faster, it becomes more practical to apply these tools to problems like the design of paperboard and corrugated boxes. There is a growing need for this capability as a result of the

accelerating trend toward reduction in packaging material use and the increasingly sophisticated demands being imposed on packaging. Being able, for example, to analyze the top load performance of a single box can be useful, but it represents only one of the many demands placed on packages during the overall product life cycle from manufacturing to the end user. A broader goal is to understand the behaviour of individual packages as well as the aggregation of multiple packages in unit loads and other tertiary packaging configurations (Figure 1) that are commonly used to transport and store goods for significant portions of their life through the distribution system.

Modeling a unit load such as that shown in Figure 1 has the obvious complication of requiring multiple packages to be analyzed instead of just one. In addition to there being more than one box, there are all of the contact interactions between boxes to consider. The boxes are obviously stacked on a pallet, which adds another structure to model, along with another set of material properties. Finally, the stack of boxes is wrapped with a unitizing stretch film to hold everything together. This adds still more contact and another material. The primary purpose of this paper is to describe efforts to build and execute finite element models which incorporate all of these component parts. The assembled unit load is then subjected to a dynamic motion event with the intent of discerning whether realistic performance characteristics can be predicted.

## 3 Finite Element Analysis Model Construction

Innovation in the packaging industry is developing ever more creative secondary packaging configurations, but the rectangular box made of paperboard or corrugated fiberboard is still very common. For the purposes of analyzing unit load performance, a model was constructed based on a box with exterior dimensions of 9.5” long x 7.9” wide x 8.75” high (241 mm x 201 mm x 222 mm). These boxes were arranged in unit load with layers having a 5 x 5 column stacked pattern, 6 layers high (Figure 1).

### 3.1 Pallet

The pallet was a conventional block-style wood design with a 40” x 48” (1016 mm x 1219 mm) footprint. It was modeled using 8998 nodes and 4772 solid brick elements (type C3D8R) with a modulus of 1.5E6 psi (10.34 GPa).

### 3.2 Boxes

A useful feature of finite element analysis is the ability to tailor the level of detail in the model based on the performance characteristics to be investigated and the output desired. With careful consideration of the assumptions and simplifications that are made, it is often possible to reduce the size and complexity of a model while retaining the essential features that are important to the final solution. In the case of the unit load model, the physical shape and stiffness of the contents of the boxes was identified as being a feature that could be safely eliminated. Depending on the fragility of the interior product, boxes are often designed to shield the contents from external loads so there is no expectation that there will be any load sharing contribution from the product.

In the analysis model, the boxes were constructed as hollow shells and given anisotropic properties representative of paperboard as reported in Beldie [15]. Paperboard is typically a multi-layer structure but the properties used for this model were those reported in [15] for a single overall laminate layer (Table 1). Each box consisted of 1870 nodes and 1868 elements (type S4R). The density of the box material was increased so the resulting total mass of each box would accurately simulate a filled box and the center of gravity would be at the center of each box.

**Table 1**: Paperboard Material Properties

| Imperial Units | | |
|---|---|---|
| Parameter | Units | Laminate |
| Density | (lb/in^3) | 1.89E-02 |
| Basis Weight | (lb/msf) | 62.7 |
| Thickness | (in) | 0.0246 |
| E1 | (psi) | 519018 |
| E2 | (psi) | 198383 |
| E3 | (psi) | 2596 |
| G12 | (psi) | 125139 |
| G13 | (psi) | 9442 |
| G23 | (psi) | 5671 |
| v12 | ~~~ | 0.38 |
| v13 | ~~~ | -2.2 |
| v23 | ~~~ | 0.54 |
| σ11y | (psi) | 1374 |
| σ22y | (psi) | 896 |
| σ33y | (psi) | 814 |
| σ12y | (psi) | 305 |
| σ13y | (psi) | 3.5 |
| σ23y | (psi) | 3.5 |
| σy0 | (psi) | 1373.5 |
| σpl | (psi) | 6526.7 |
| εpl | (in/in) | 0.05 |
| R11 | | 1.000 |
| R22 | | 0.653 |
| R33 | | 0.592 |
| R12 | | 0.384 |
| R13 | | 0.004 |
| R23 | | 0.004 |

| SI Units | | |
|---|---|---|
| Parameter | Units | Laminate |
| Density | (kg/m^3) | 522 |
| Basis Weight | (kg/m^2) | 0.306 |
| Thickness | (mm) | 0.624 |
| E1 | (MPa) | 3578.5 |
| E2 | (MPa) | 1367.8 |
| E3 | (MPa) | 17.9 |
| G12 | (MPa) | 862.8 |
| G13 | (MPa) | 65.1 |
| G23 | (MPa) | 39.1 |
| v12 | ~~~ | 0.38 |
| v13 | ~~~ | -2.2 |
| v23 | ~~~ | 0.54 |
| σ11y | (MPa) | 9.47 |
| σ22y | (MPa) | 6.18 |
| σ33y | (MPa) | 5.61 |
| σ12y | (MPa) | 2.1 |
| σ13y | (MPa) | 0.024 |
| σ23y | (MPa) | 0.024 |
| σy0 | (MPa) | 9.47 |
| σpl | (MPa) | 45 |
| εpl | (mm/mm) | 0.05 |
| R11 | | 1.000 |
| R22 | | 0.653 |
| R33 | | 0.592 |
| R12 | | 0.384 |
| R13 | | 0.004 |
| R23 | | 0.004 |

## 3.3 Stretch Film

Stretch film is applied to palletized product stacks to consolidate them into a unit load prior to transportation and/or storage. Stretch hooding is less often encountered but is preferable for some types of product and is more widely employed outside of North America. Stretch film is very versatile in that wrap settings, wrap patterns and film types can be relatively easily changed to accommodate the needs of a specific load.

The primary constituent of stretch film is commonly polyethylene. Modern films typically have multiple layers which may be highly engineered to achieve specific performance characteristics and may incorporate multiple materials in addition to the polyethylene. Film is supplied in rolls with 20" being a common roll width. Automated wrapping machines of the type found in most manufacturing facilities will apply film to a palletized load in a spiral pattern with significant overlap between each layer and extra wraps often applied at the top and bottom of the load. The goal is for the film to hold the product to the pallet and to generate a compressive force which holds the stacked product together.

Films are stretched well past yield during application and strains on the order of 100% to 300% are not unusual. Figure 2 shows a generalized stress strain curve for stretch wrap film. After initial yield, most films exhibit a plateau where further elongation occurs with relatively little increase in stress. If stretching continues, they enter a strain-hardening region where the stiffness of the film increases again and increasing amounts of force are required to create further stretching. It is generally preferable for films to be stretched into the strain hardening region for best performance in packaging applications as the increased film stiffness provides improved restraint against product motion. If stretching stops in the plateau region, movement of the product can cause additional stretching relatively easily and the compressive force which helps maintain the unitized load is more easily lost.

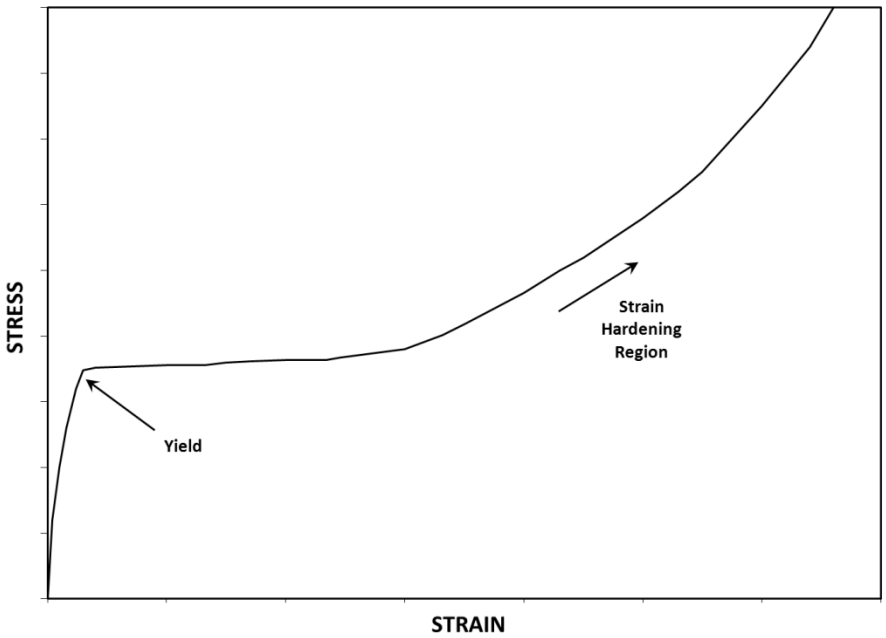



**Figure 2:** Generic Stretch Film Stress/Strain Curve

For the purposes of the unit load finite element analysis, the stretch film was modeled as a single sleeve with the thickness of one film layer which was mechanically stretched over the product stack and then released onto it. Modeling multiple wraps (often 15 to 20) of a narrower film roll is still a difficult computational problem. After application, the multiple wraps behave substantially as a single piece due to the intentional use of cling layers on the inner surface.

The film was considered as a membrane with a hyperelastic Marlow material model that also incorporated plasticity. No failure criteria were implemented in the material model. Given the importance of the amount of stretch on the performance of a unit load, film stretches of 150%, 200% and 250% were analyzed. Data extracted from the model and shown in Figure 3 illustrates the force required per inch of film width which was required to stretch the film.

The film had 69,084 nodes and 68,680 membrane elements of type M3D4R.

## 4 Analysis of Unit Load Model

The analysis was conducted using the ABAQUS explicit dynamic FEA code (Dassault Systèmes Simulia Corp., www.3ds.com). After stretching the film to the desired strain and releasing it onto the product stack and pallet, the load was given a constant straight line acceleration of 0.2G in the 48" direction of the pallet. Stress, strains, contact forces and other parameters of interest were calculated and stored during the analysis for later post-processing.

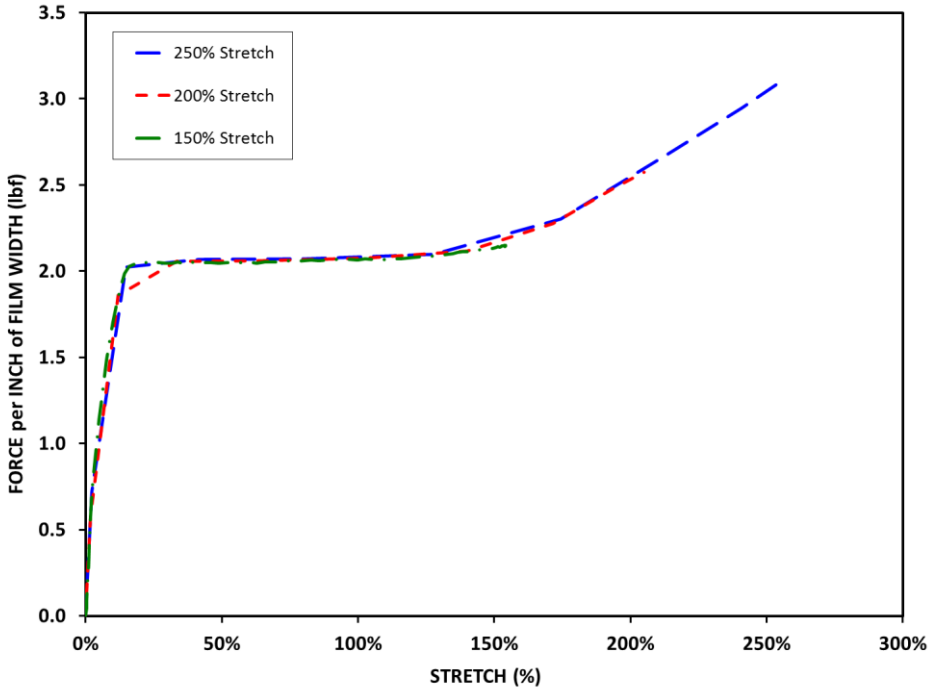



**Figure 3:** Force to Stretch Film per Inch of Film Width

## 5 Results

Figures 4, 5 and 6 show the unit load after applying the stretch film at 150% stretch, 200% stretch and 250% stretch, respectively. The left image in each figure shows just the deformed shape of the unit load and film. The right image has stresses superimposed on the deformed shape. Note that because of the different stretch ratios, the stress scales differ in each image.

Figure 3 illustrates the force required to stretch the film and shows that the force to reach 250% is approximately 50% greater than that required to stretch the film to 150%. This force difference manifested itself immediately after the film was released onto the boxes when it began to crush some of the box corners as seen in Figure 6.

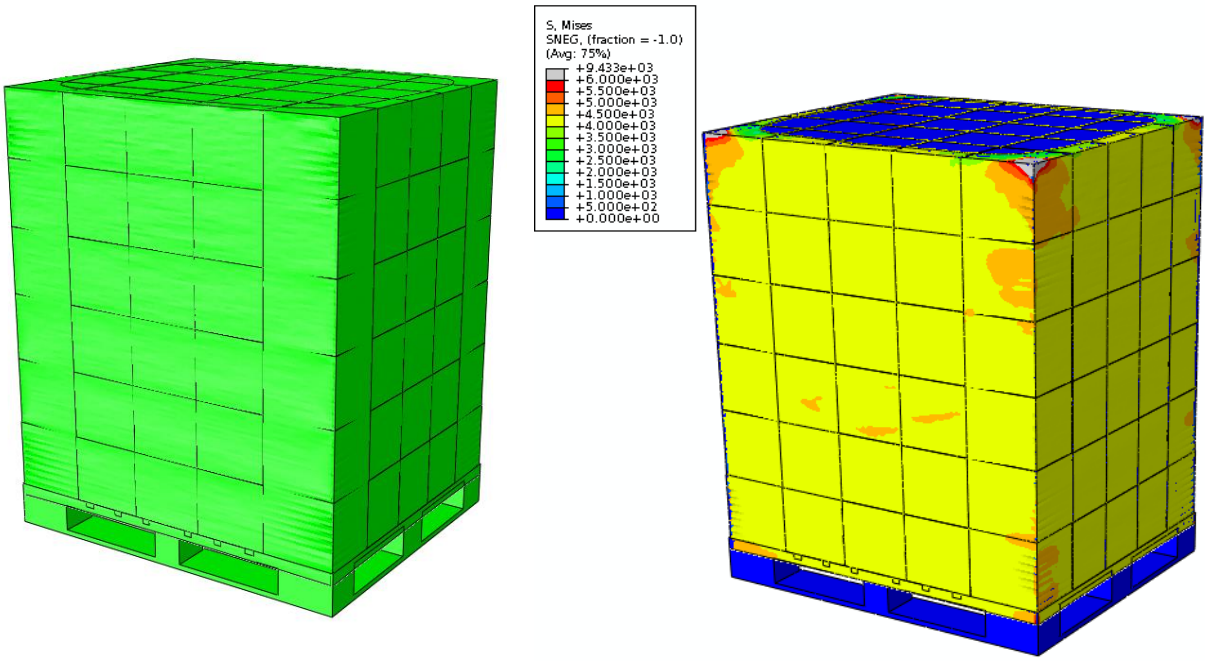



**Figure 4:** Unit Load with Film Applied at 150% Stretch, Right Image Shows Film Stress

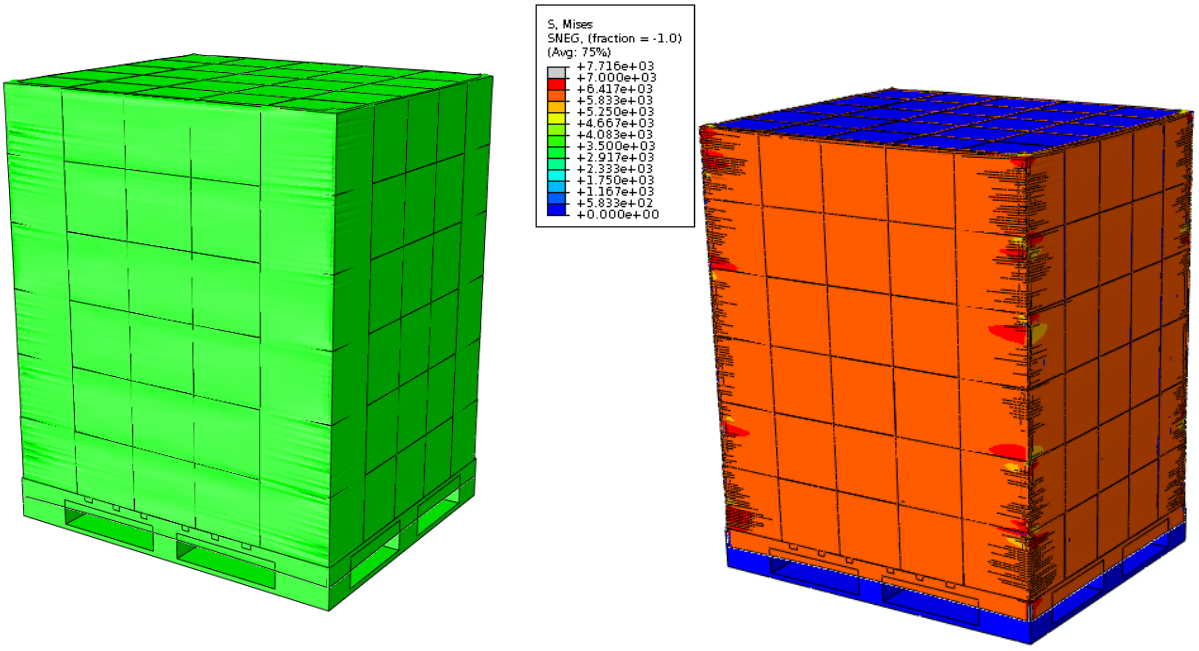



**Figure 5:** Unit Load with Film Applied at 200% Stretch, Right Image Shows Film Stress

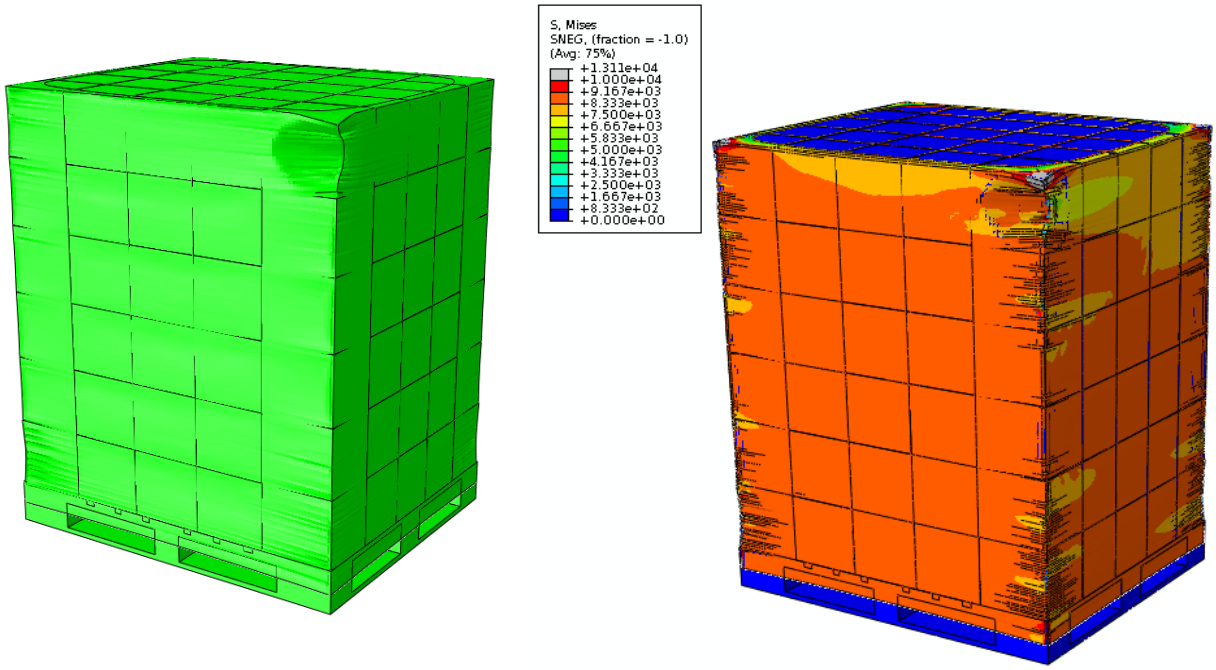



**Figure 6:** Unit Load with Film Applied at 250% Stretch, Right Image Shows Film Stress

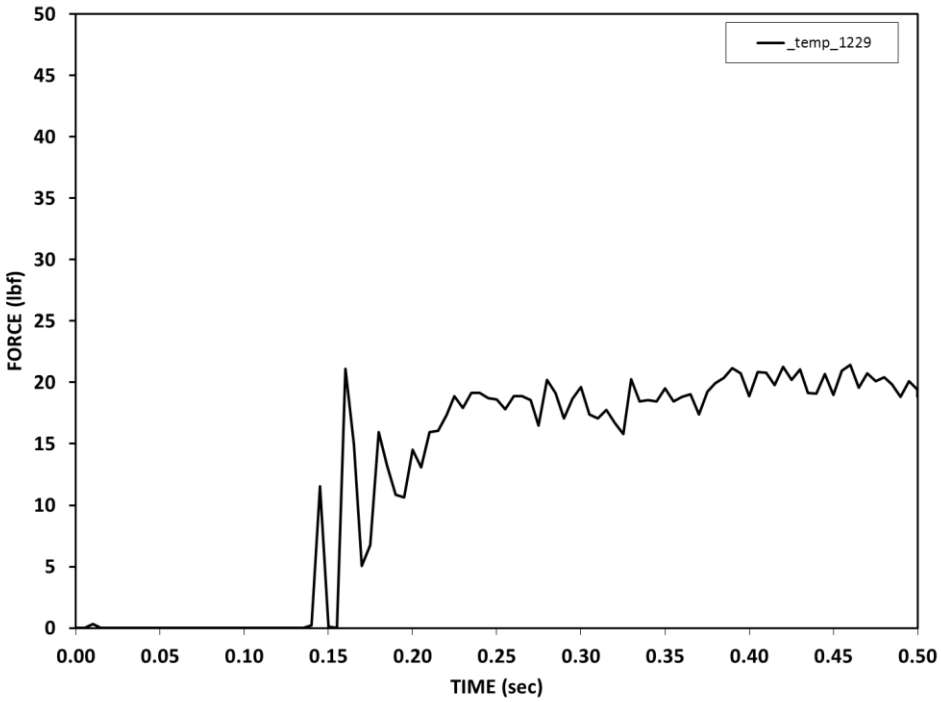



**Figure 7:** Horizontal Contact Force Between Boxes, 48” Direction, Top Layer, 150% Stretch

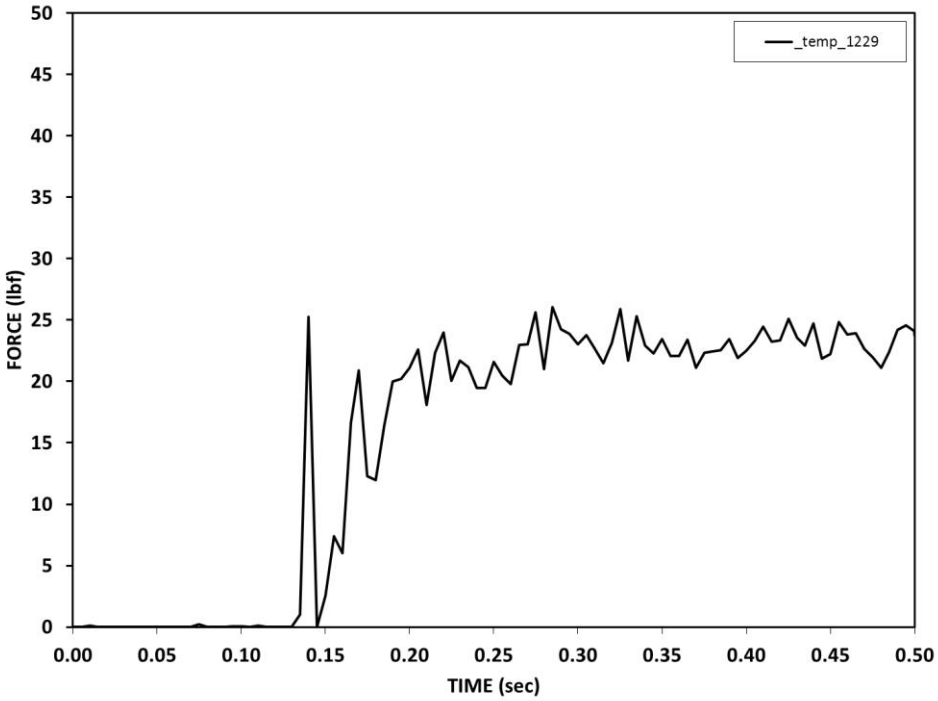



**Figure 8:** Horizontal Contact Force Between Boxes, 48" Direction, Top Layer, 200% Stretch

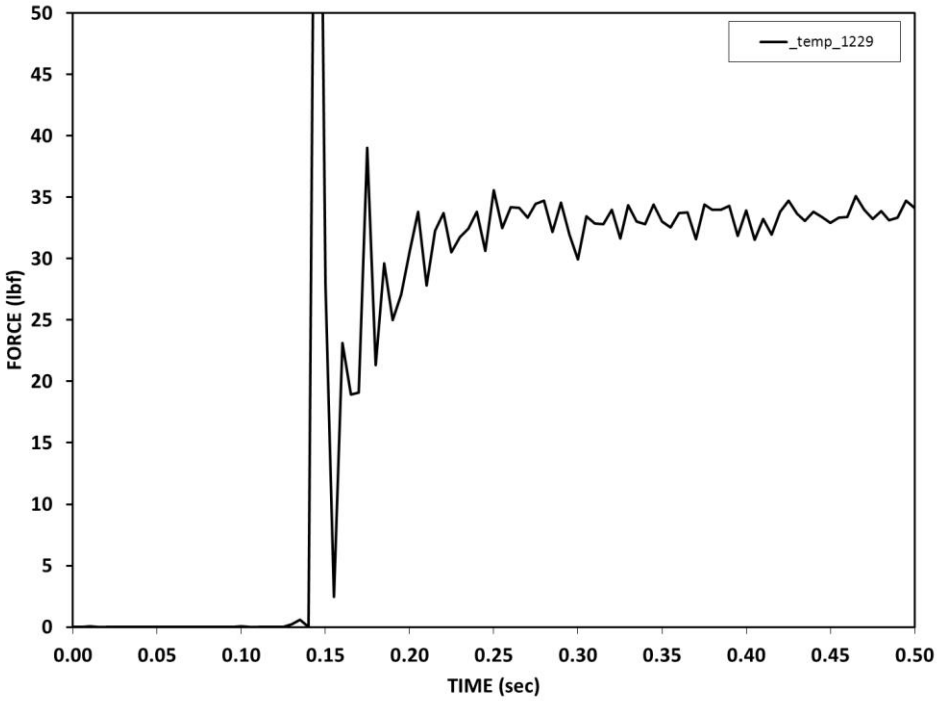



**Figure 9:** Horizontal Contact Force Between Boxes, 48" Direction, Top Layer, 250% Stretch

Contact forces transmitted between boxes were extracted for one of the corner box locations on the top layer to illustrate the effect of the film force. Figures 7 through 9 show the contact force generated in the 48" pallet direction between the corner and adjacent box as the film force is transferred to the boxes over a period of 0.5 second. Figure 7 shows the 150% film stretch analysis which develops a box contact force of about 18.5 lbf.

Figure 8 shows the 200% stretch analysis results and a final force of about 22.3 lbf. With 250% stretch a force of 33 lbf develops as shown in Figure 9.

These forces are also reflected in the stresses and contact pressures generated in the boxes as shown in Figures 10, 11 and 12. Consistent scales among the three sets of images aid in making comparisons between them.

After accelerating the unit load for 1 second, the box displacements that result are shown in Figures 13 through 15. Two views of each load are provided as the box motions were not always symmetrical. Although the load wrapped with film at 200% stretch did not experience box buckling at the time the film was applied (Figure 5), the addition of the acceleration dynamics overloaded some boxes as seen in Figure 14. The load with 250% stretch film developed more box damage during the acceleration which likely contributed to the large displacements of the boxes (Figure 15).

The 150% film in Figure 13 exhibited some layer sliding in the left image. The right image, showing the opposite side of the load, demonstrates more leaning or tilting. In general, the 150% film allowed more box motion than the 200% film. This is consistent with the expectation that producing higher film stretch and operating in the strain hardening region of the film should produce better load retention.

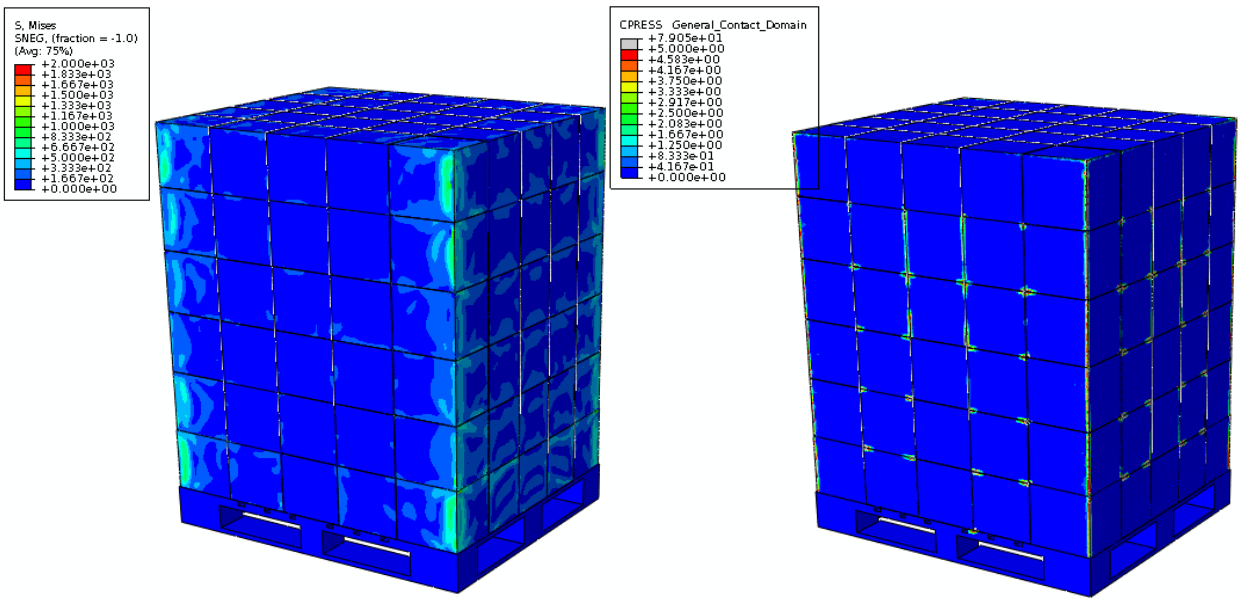



**Figure 10:** 150% Film Stretch Box Stresses (left) and Contact Pressure (right)

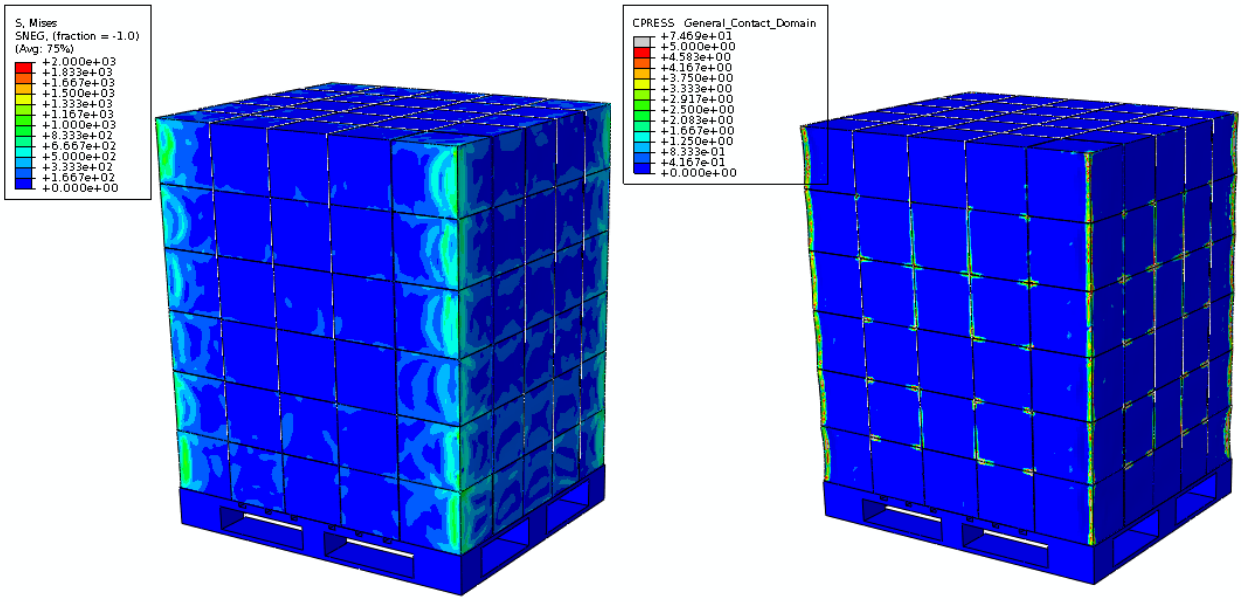



**Figure 11:** 200% Film Stretch Box Stresses (left) and Contact Pressure (right)

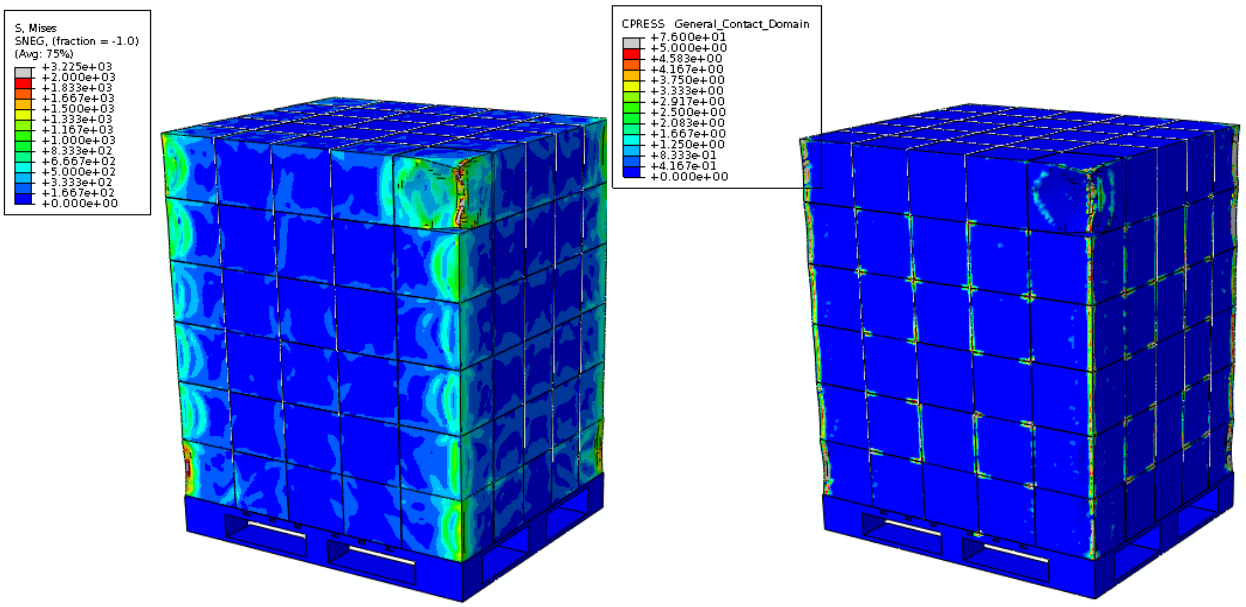



**Figure 12:** 250% Film Stretch Box Stresses (left) and Contact Pressure (right)

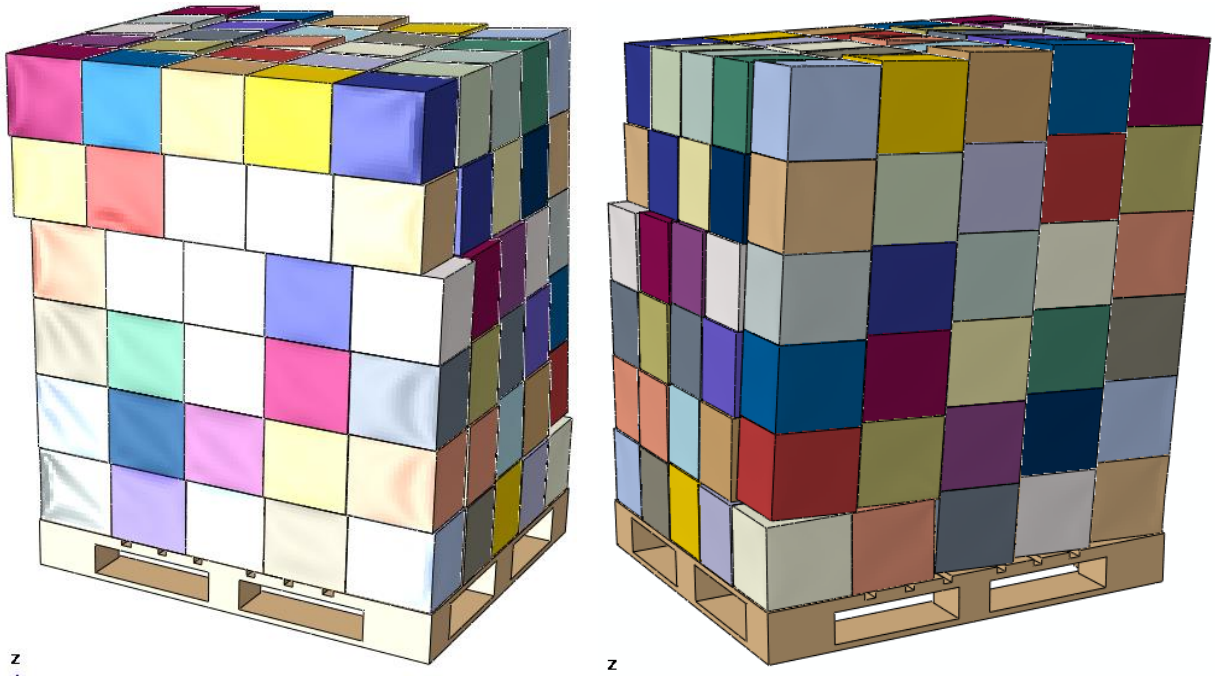


**Figure 13:** 150% Film Stretch, 2 Views of Box Displacement After 1 second of Acceleration at 0.2G

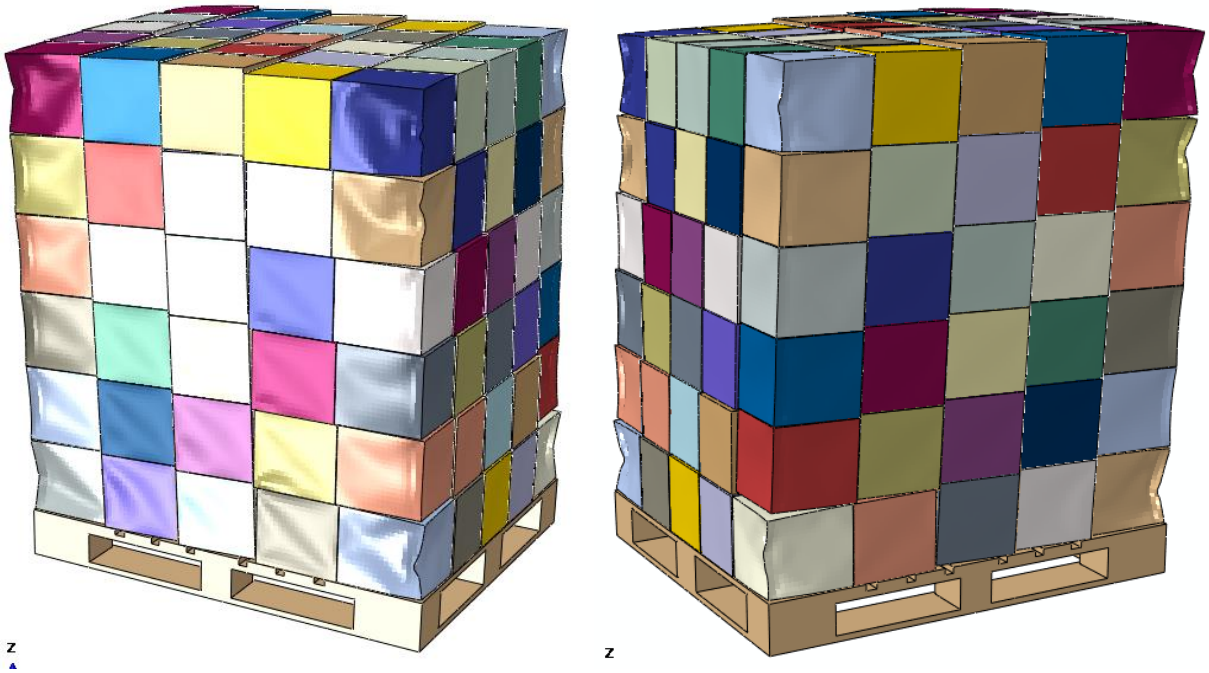


**Figure 14:**200% Film Stretch, 2 Views of Box Displacement After 1 second of Acceleration at 0.2G

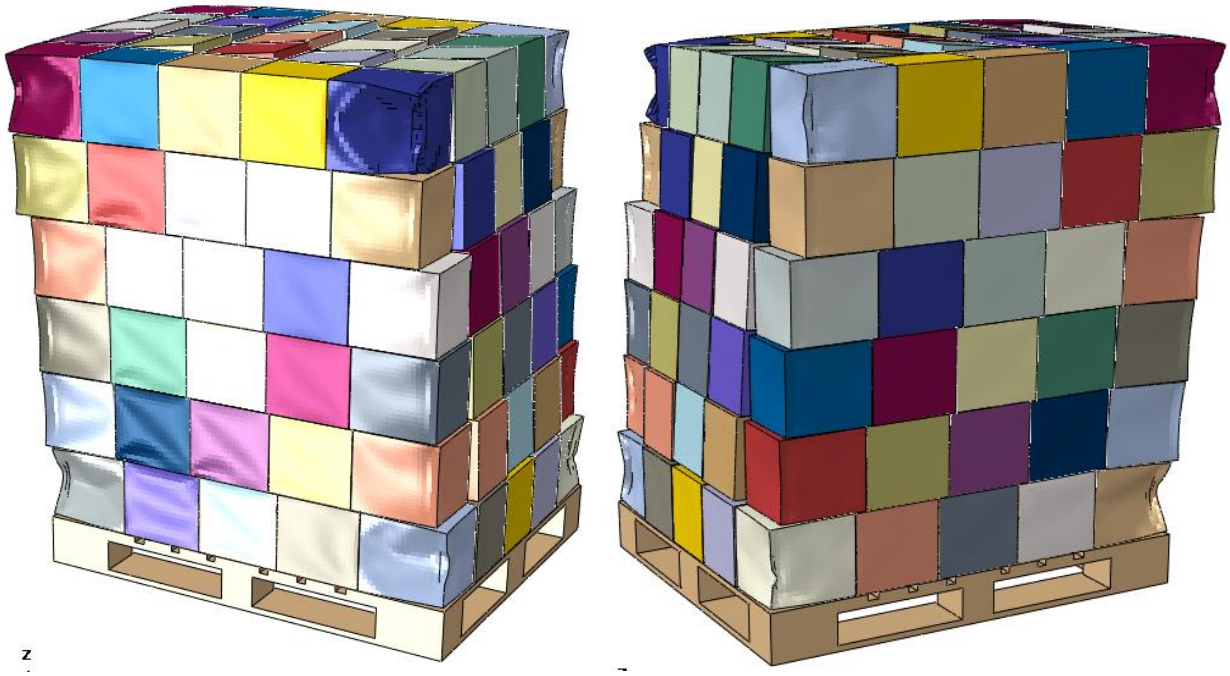


**Figure 15:** 250% Film Stretch, 2 Views of Box Displacement After 1 second of Acceleration at 0.2G

## 3 Conclusions

Computational methods have been used to perform meaningful analysis on full unitized loads and produce information which can be helpful in evaluating the static and dynamic performance of packages and unitizing methods. Realistic geometries, material properties and mechanical loads were implemented. The analysis produces far more detailed information than was presented here, but this paper attempted to provide a sampling to give some sense of what is possible.

Areas for further investigation include the incorporation of more detailed box geometries such as overlapping flaps, as well as the use of corrugated fiberboard material models. The fidelity of the stretch film model can be improved by varying the spatial thickness distribution to more closely approximate how the film is applied during actual wrapping operations. This would then expand the potential for evaluating performance differences that might result from changing wrap patterns.

It is also possible to apply vibratory motion inputs to the model to simulate vehicle transportation modes. Other industry researchers have pursued virtual synthesis of vehicle vibratory responses so the possibility of using that work to provide inputs to the computational analysis of packaging systems opens up intriguing new avenues for investigation.

## References


1. L. Carlsson, C Fellers and B. Westerlind, 1982, "Finite element analysis of the creasing and bending of paper", *Svensk Papperstidning*, vol 85, no. 15, pp. 121-126.
2. L. Wong, M.T. Kortschot and C.T.J Dodson, 1995, "Finite element analysis and experimental measurement of strain fields and failure in paper", *Proceedings of the International Paper Physics Conference*, Niagara-on-the-Lake, Ontario, Canada, Sep. 11-14, pp. 131-135.
3. J.C. Pommier and J. Poustis, 1990, "Bending stiffness of corrugated board prediction using the finite element method", in R.W. Perkins (ed), *Mechanics of Wood and Paper Materials*, ASME AMD, vol. 112, pp 67-70.

4. A.C. Gilchrist, J.C. Suhling, and T.J. Urbanik, 1999, "Nonlinear finite element modeling of corrugated board", ASME AMD, *Mechanics of Cellulosic Materials*, vol. 231, pp 101-106.

5. U. Nyman, 2004, "Continuum mechanics modelling of corrugated board", Doctoral thesis, Lund University, Division of Structural Mechanics, Lund, Sweden.

6. L.A.A. Beex and R.H.J. Peerlings, 2009, "An experimental and computational study of laminated paperboard creasing and folding", *International Journal of Solids and Structures*, vol. 46, pp 4192-4207.

7. M.E. Biancolini, 2005, "Evaluation of equivalent stiffness properties of corrugated board", *Composite Structures*, vol. 69, pp 322-328.

8. M.E. Biancoline, C. Brutti and S. Porziani, 2009, "Analysis of corrugated board panels under compression load", *Steel and Composite Structures*, vol. 9, no. 1, pp 1-17.

9. T. Daxner, T. Flatscher and F.G. Rammerstorfer, 2007, "Optimum design of corrugated board under buckling constraints", *7th World Congress on Structural and Multidisciplinary Optimization*, Seoul, Korea, May 21-25.

10. T. Flatscher, T. Daxner, D.H. Pahr and F.G. Rammerstorfer, 2011, "Optimization of corrugated paperboard under local and global buckling constraints", in R. de Borst and E. Ramm (eds), *Multiscale Methods in Computational Mechanics*, Springer Science, pp. 329-346.

11. R. Haj-Ali, J. Choi, B. Wei, R. Popil and M. Schaepe, 2009, "Refined nonlinear finite element models for corrugated fiberboards", *Composite Structures*, vol. 87, pp. 321-333.

12. T. Nordstrand, 2003, "Basic testing and strength design of corrugated board and containers", Doctoral thesis, Lund University, Division of Structural Mechanics, Lund, Sweden.

13. N. Navaranjan and B. Johnson, 2006, "Modelling and experimental study of creep behaviour of corrugated paperboard", *Appita Journal*, pp. 43-49.

14. M. Nygards, M. Just and J. Tryding, 2009, "Experimental and numerical studies of creasing of paperboard", *International Journal of Solids and Structures*, vol. 46, pp 2493-2505.

15. L. Beldie, 2001, "Mechanics of paperboard packages – Performance at short term static loading", Licentiate dissertation, Lund University, Division of Structural Mechanics, Lund, Sweden.

16. M.E. Biancolini and C. Brutti, 2003, "Numerical and experimental investigation of the strength of corrugated board packages", *Packaging Technology and Science*, vol. 16, pp47-60.

17. M.E. Biancolini, C. Brutti, and S. Porziani, 2010, "Corrugated board containers design methods", *International Journal of Computational Materials Science and Surface Engineering*, vol. 3, nos. 2/3, p 143-163.

18. T.J. Urbanik and E.P. Saliklis, 2002, "Comparison of postbuckling model and finite element model with compression strength of corrugated boxes", Proceedings of the 2002 Progress in Paper Physics Seminar, Rochester, New York, Sep. 8-13.

19. T.J. Urbanik and E.P. Saliklis, 2003, "Finite element corroboration of buckling phenomena observed in corrugated boxes", Wood and Fiber Science, vol.35, no. 3, pp. 322-333.

# Vibration Transmissibility of Packaging in Three-Substructures Coupled Product Transport System

**Yuan-Biao Zhang[1,2] and Zhi-Wei Wang[1,2*]**

[1] *Packaging Engineering Institute, Jinan University, China*
[2] *Key Laboratory of Product Packaging and Logistics of Guangdong Higher Education Institutes, Jinan University, China*

[*] *Corresponding author. Email: wangzw@jnu.edu.cn*

**Abstract:** Products are broken mostly because of vibration and shock in logistics, which has led to huge economic losses. A three-substructures multi-coordinate coupled critical component-product-transport system can be divided into three substructures: a critical component, a product and a vehicle, whose dynamic characteristics can be represented by Frequency Response Functions (FRFs). Vibration is passed among the three substructures through a fixed installation and a packaging which consists of numerous package units. The research of the cushioning effect of coupling points of packaging under vibration and shock is beneficial for the packaging design. Analysis of packaging vibration characteristic was obtained by using the substructure synthesis method of FRFs for the coupled system. The concepts of vibration contribution, vibration contribution ratio, overall vibration contribution and overall vibration contribution ratio to critical component response through each packaging unit are introduced to evaluate the vibration transmission ability of packaging units. The sensitivity analysis of vibration transmission parameter was obtained through the numerical simulation and physical prototype model experiment of packaging vibration transmission analysis.

Keywords: frequency response function, critical component-product-transport system, substructure method, vibration transmission ability.

## 1 Introduction

Products are broken mostly because of vibration and shock in logistics process which has led to huge economic losses. Three-substructures multi-coordinate coupled critical component-product-transport system is composed of a critical component substructure, a product substructure and a vehicle substructure, which are connected by a fixed installation and a packaging. Vibration and shock is passed among the three substructures through the fixed installation and the packaging which consists of numerous package units. The research of the cushioning effect of coupling points of packaging component under vibration and shock is beneficial for the packaging design.

A lot of research focused on the vibration transmission characteristics of product-packaging transport system. Sek et al.[1] used the R-MISO method based on FRFs to study vibration transmission characteristics of transport packaging system. Rouillard et al.[2] established the multi-layer stacked model of product-packaging transport system and studied the vibration characteristics of transport packaging system. Zhi-Wei Wang[3] and Jiu-Hong Jiang[4] analysed a two-degrees-of-freedom product-packaging transport system, focused on the dropping damage boundary curves and the dropping response based on the key component, and found that the dropping response of the key component was determined by the dimensionless dropping shock velocity, the frequency parameter ratio, the mass ratio and the damping parameters. Zhi-Wei Wang[5,6], Jun Wang[7] and Yuan-Biao Zhang[8] developed the inverse substructure method to analysize the two/three-substructures single/multi-coordinate coupled product-transport systems and carried out complete experimental verification on the physical prototype model of product-transport systems. Zhi-Wei Wang and Yuan-Biao Zhang[9] analysed the dynamic characteristics of refrigerator-truck transport system by using inverse substructure method.

Protection ability of packaging to product comes from the cushioning mechanism of product-packing transport system. In this paper, the FRFs of the critical component-product-transport coupled system were obtained by using the substructure synthesis method of three-substructures FRFs. The vibration contribution, vibration contribution ratio, overall vibration contribution and overall vibration contribution ratio to product response through each packaging unit are obtained by the FRFs of the coupled system. The sensitivity analysis of vibration transmission parameter was obtained through the lumped parameter model simulation and physical prototype model experiment of packaging vibration transmission.

## 2 Substructure synthesis method of three-substructures coupled system based on FRFs

A three-substructures multi-coordinate coupled critical component-product-transport system can be divided into three substructures: the critical component substructure (substructure *A*), the product substructure (substructure *B*) and the vehicle substructure (substructure *C*), whose dynamic characteristics can be represented by FRFs, as shown in Figure1. The vibration from logistic condition is passed among the three substructures through the fixed installation ( $c_1$ ) and packaging ( $c_2$ ) which consists of numerous package units.

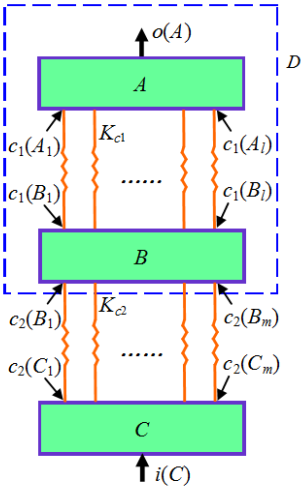



**Figure 1**: Three-substructures multi-coordinate coupled product-transport system.

The dynamical characteristics of the system and substructures are all represented by FRFs:

$$\{X_r\} = [H_r]\{F_r\} \tag{1}$$

$$[H_r] = \left(-\omega^2[M_r] + j\omega[C_r] + [k_r]\right)^{-1} \quad r = A, B, C, S \tag{2}$$

where, $\{X_r\}, (r = A, B, C, S)$ respectively represent the output response vectors of substructures $A, B, C$ and the coupled system $S$ . $\{F_r\}, (r = A, B, C, S)$ respectively represent the external input excitation vectors of $A, B, C$ and $S$ . $[H_r], (r = A, B, C, S)$ respectively represent the FRF matrices of $A, B, C$ and $S$ . $\omega = 2\pi f$ is the excitation frequency, and $[M_r]$, $[C_r]$ and $[k_r]$ ( $r = A, B, C, S$ ) are respectively the mass matrices, damping matrices and static stiffness matrices of *A*, *B*, *C* and *S*.

According to the substructure synthesis method, for the critical component-product-transport system shown in Figure 1, the system-level FRF can be achieved through the substructure-level FRFs and the coupling dynamic stiffness matrices. [8,9]

$$[H_S]_{o(A)i(C)} = [H_A]_{o(A)c_1(A)}[E_{c_1}][H_B]_{c_1(B)c_2(B)}[E_{c_2}][H_C]_{c_2(C)i(C)} \tag{3}$$

Where,

$$[E_{c_1}] = \left([H_A]_{c_1(A)c_1(A)} + [H_B]_{c_1(B)c_1(B)} + [K_{c_1}]^{-1}\right)^{-1} \tag{4}$$

$$[E_{c_2}] = \left([H_D]_{c_2(D)c_2(D)} + [H_C]_{c_2(C)c_2(C)} + [K_{c_2}]^{-1}\right)^{-1} \tag{5}$$

$$[K_{c_1}] = -\omega^2[M_{c_1}] + j\omega[C_{c_1}] + [k_{c_1}] \tag{6}$$

$$\left[K_{c_2}\right]=-\omega^2\left[M_{c_2}\right]+j\omega\left[C_{c_2}\right]+\left[k_{c_2}\right] \tag{7}$$

$$\begin{aligned}\left[H_D\right]_{c_2(D)c_2(D)}=&\left(\left[H_S\right]_{c_2(C)c_2(C)}\left[H_S\right]^{-1}_{c_2(\mathrm{B})c_2(C)}-\left[I\right]\right)^{-1}\\&\left(\left[H_S\right]_{c_2(B)c_2(B)}\left[H_S\right]^{-1}_{c_2(C)c_2(B)}\left[H_S\right]_{c_2(C)c_2(C)}-\left[H_S\right]_{c_2(B)c_2(C)}\right)\end{aligned} \tag{8}$$

Where, subscripts $o(A)$ is the response coordinate of substructure $A$; $i(C)$ is the excitation coordinate of substructure $C$; $c_1(A)$ and $c_1(B)$ are respectively the coupling coordinate of substructure $A$ and $B$ through $c_1$. $c_2(B)$ and $c_2(C)$ are respectively the coupling coordinate of substructure $B$ and $C$ through $c_2$. $\left[H_A\right]_{...}$, $\left[H_B\right]_{...}$, $\left[H_C\right]_{...}$ and $\left[H_S\right]_{...}$ are respectively the FRF matrix of substructure $A,B,C$ and coupled system $S$. For example, $\left[H_A\right]_{o(A)c_1(A)}$ is the FRF matrix of excitation from coupling coordinate $c_1(A)$ and response from response coordinate $o(A)$ in substructure $A$. $\left[K_{c_1}\right]$ and $\left[K_{c_2}\right]$ are respectively the coupling dynamic stiffness matrix about $c_1$ and $c_2$. $\left[M_{c_1}\right]$, $\left[C_{c_1}\right]$ and $\left[k_{c_1}\right]$ are respectively the mass matrix, damping matrix and static stiffness matrix of the coupling component $c_1$. $\left[M_{c_2}\right]$, $\left[C_{c_2}\right]$ and $\left[k_{c_2}\right]$ are respectively the mass matrix, damping matrix and static stiffness matrix of the coupling component $c_2$.

## 3 Analysis of vibration transmission of cushioning packaging units

The research of the cushioning effect of packaging component $c_2$'s coupling points under vibration and shock is beneficial for the packaging design. It is necessary to investigate the coupling points' vibration transmissibility, to analyse the cushioning effect of the coupling points in the three-substructures multi-coordinate coupled critical component-product-transport system. In the literature [8] introduced the concepts of the vibration contribution, vibration contribution ratio, overall vibration contribution and overall vibration contribution ratio to product response through each packaging unit base on two-substructures multi-coordinate coupled substructure synthesis method. In this paper, these concepts are introduced base on three-substructures multi-coordinate coupled substructure synthesis method.

According to equation (3) and the assumption that the three-substructures multi-coordinate coupled critical component-product-transport system is a linear system, the overall response of the critical component is the sum of the responses that the coupling points in $c_2$ pass to the critical component:

$$\begin{aligned}\left\{X_S\right\}_{o(A)}&=\sum_{p=1}^{m}\left\{X_S\right\}^{(p)}_{o(A)}\\&=\left[H_A\right]_{o(A)c_1(A)}\left[E_{c_1}\right]\left[H_B\right]_{c_1(B)c_2(B)}\left[E_{c_2}\right]\left[H_C\right]_{c_2(C)i(C)}\left\{F_S\right\}_{i(C)}\end{aligned} \tag{9}$$

where, $\left\{X_S\right\}_{o(A)}$ is the output response vector of the critical component coordinate $o(A)$, $\left\{X_S\right\}^{(p)}_{o(A)}$ $(p=1,2,\cdots,m)$ is the response transferred to the critical component through the $p$ th coupling point and $m$ is the number of coupling points, and $\left\{F_S\right\}_{i(C)}$ is the excitation vector of the vehicle coordinate $i(C)$.

In order to describe the ability of vibration transmission of $p$ th coupling point in the packaging component $c_2$ in the coupled critical component-product-transport system under road vibration excitation, we set

$$T(\omega)^{(p)}=\left[H_A\right]_{o(A)c_1(A)}\left[E_{c_1}\right]\left[H_B\right]^{(p)}_{c_1(B)c_2(B)}\left[E_{c_2}\right]^{(p)}\left[H_C\right]_{c_2(C)i(C)} \tag{10}$$

where, $T(\omega)^{(p)}$ denotes the vibration contribution that the critical component receives through $p$ th coupling point in $c_2$ under road excitation. And we define

$$b(\omega)^{(p)} = \frac{\left|T(\omega)^{(p)}\right|}{\sum_{p=1}^{m}\left|T(\omega)^{(p)}\right|} \tag{11}$$

where, $b(\omega)^{(p)}$ denotes the vibration contribution ratio that the critical component receives through $p$ th coupling point of $c_2$ in the total response of the product under road excitation.

It is a rather complicated course for the analysis of vibration contribution to the critical component under road excitation by the comparison of the spectrum values of $T(\omega)^{(p)}$ and $b(\omega)^{(p)}$ between different coupling points at each frequency. The radication of the quadratic sum of $T(\omega)^{(p)}$'s amplitudes is used in a excitation frequency domain to describe the overall vibration contribution of the critical component. We define,

$$\Gamma_{\omega_1:\omega_2}{}^{(p)} = \sqrt{\sum_{i=1}^{n}\left|T(\omega_i)^{(p)}\right|^2} \tag{12}$$

where, $\Gamma_{\omega_1:\omega_2}{}^{(p)}$ denotes the overall vibration contribution on the frequency range $\omega_1$ to $\omega_2$ that the critical component receives through the $p$ th coupling point, $n$ is the number of spectrum lines on the frequency range $\omega_1$ to $\omega_2$. Then,

$$\Phi_{\omega_1:\omega_2}{}^{(p)} = \frac{\Gamma_{\omega_1:\omega_2}{}^{(p)}}{\sum_{p=1}^{m}\Gamma_{\omega_1:\omega_2}{}^{(p)}} \tag{13}$$

where, $\Phi_{\omega_1:\omega_2}{}^{(p)}$ denotes the overall vibration contribution ratio on the frequency range $\omega_1$ to $\omega_2$ that the critical component receives through the $p$ th coupling point in the total response of the critical component.

Obviously, $T(\omega)^{(p)}$ and $b(\omega)^{(p)}$ are the function of road excitation frequency $\omega$. The greater $T(\omega)^{(p)}$ or $b(\omega)^{(p)}$, means the greater response transferred to the critical component through the $p$ th coupling point under road excitation, and the greater ability of vibration transmission or less cushioning effect at this $p$ th coupling point.

We determined the overall ability of vibration transmission of the $p$ th coupling point in $c_2$ on the frequency range $\omega_1$ to $\omega_2$ by $\Gamma_{\omega_1:\omega_2}{}^{(p)}$ and $\Phi_{\omega_1:\omega_2}{}^{(p)}$. This is a kind of macroscopic description, which can conveniently direct the design of cushioning packaging for the critical component.

## 3 Sensitivity analysis of vibration transmission

The sensitivity of vibration contribution $T(\omega)^{(p)}$ under the stiffness or damping of each packaging unit.

$$\begin{aligned}\frac{\partial T(\omega)^{(p)}}{\partial k_{c_2}{}^{(p)}} &= \left[H_A\right]_{o(A)c_1(A)}\left[E_{c_1}\right]\left[H_B\right]_{c_1(B)c_2(B)}{}^{(p)}\frac{\partial\left[E_{c_2}\right]^{(p)}}{\partial k_{c_2}{}^{(p)}}\left[H_C\right]_{c_2(C)i(C)} \\ &= \left[H_A\right]_{o(A)c_1(A)}\left[E_{c_1}\right]\left[H_B\right]_{c_1(B)c_2(B)}{}^{(p)} \\ &\quad \left(-\left[E_{c_2}\right]\left(\left[H_D\right]_{c_2(D)c_2(D)}+\left[H_C\right]_{c_2(C)c_2(C)}-d\right)\left[E_{c_2}\right]\right)\left[H_C\right]_{c_2(C)i(C)}\end{aligned} \tag{14}$$

Where，

$$d=\left[K_{c_2}\right]^{-1}\left(-\omega^2\left[M_{c_2}\right]+j\omega\left[C_{c_2}\right]+\frac{\partial\left[k_{c_2}\right]}{\partial k_{c_2}{}^{(p)}}\right)\left[K_{c_2}\right]^{-1} \tag{15}$$

$$\begin{aligned}\frac{\partial T(\omega)^{(p)}}{\partial c_{c_2}{}^{(p)}}&=\left[H_A\right]_{o(A)c_1(A)}\left[E_{c_1}\right]\left[H_B\right]_{c_1(B)c_2(B)}{}^{(p)}\\&\left(-\left[E_{c_2}\right]\left(\left[H_D\right]_{c_2(D)c_2(D)}+\left[H_C\right]_{c_2(C)c_2(C)}-e\right)\left[E_{c_2}\right]\right)\left[H_C\right]_{c_2(C)i(C)}\end{aligned} \tag{16}$$

Where，

$$e=\left[C_{c_2}\right]^{-1}\left(-\omega^2\left[M_{c_2}\right]+j\omega\frac{\partial\left[C_{c_2}\right]}{\partial c_{c_2}{}^{(p)}}+\left[k_{c_2}\right]\right)\left[C_{c_2}\right]^{-1} \tag{17}$$

According to equations (10)-(13), the sensitivity of vibration contribution ratio $b(\omega)^{(p)}$, overall vibration contribution $\Gamma_{\omega_1:\omega_2}{}^{(p)}$ and overall vibration contribution ratio $\Phi_{\omega_1:\omega_2}{}^{(p)}$ to critical component response through each packaging unit are obtained under the stiffness or damping of each packaging unit.

$$\frac{\partial b(\omega)^{(p)}}{\partial k_{c_2}{}^{(p)}}=\frac{\left|\partial T(\omega)^{(p)}/\partial k_{c_2}{}^{(p)}\right|}{\sum_{p=1}^{m}\left|\partial T(\omega)^{(p)}/\partial k_{c_2}{}^{(p)}\right|} \tag{18}$$

$$\frac{\partial \Gamma_{\omega_1:\omega_2}{}^{(p)}}{\partial k_{c_2}{}^{(p)}}=\sqrt{\sum_{i=1}^{n}\left|\partial T(\omega)^{(p)}/\partial k_{c_2}{}^{(p)}\right|^2} \tag{19}$$

$$\frac{\partial \Phi_{\omega_1:\omega_2}{}^{(p)}}{\partial k_{c_2}{}^{(p)}}=\frac{\partial \Gamma_{\omega_1:\omega_2}{}^{(p)}/\partial k_{c_2}{}^{(p)}}{\sum_{p=1}^{m}\partial \Gamma_{\omega_1:\omega_2}{}^{(p)}/\partial k_{c_2}{}^{(p)}} \tag{20}$$

$$\frac{\partial b(\omega)^{(p)}}{\partial c_{c_2}{}^{(p)}}=\frac{\left|\partial T(\omega)^{(p)}/\partial c_{c_2}{}^{(p)}\right|}{\sum_{p=1}^{m}\left|\partial T(\omega)^{(p)}/\partial c_{c_2}{}^{(p)}\right|} \tag{21}$$

$$\frac{\partial \Gamma_{\omega_1:\omega_2}{}^{(p)}}{\partial c_{c_2}{}^{(p)}}=\sqrt{\sum_{i=1}^{n}\left|\partial T(\omega)^{(p)}/\partial c_{c_2}{}^{(p)}\right|^2} \tag{22}$$

$$\frac{\partial \Phi_{\omega_1:\omega_2}{}^{(p)}}{\partial c_{c_2}{}^{(p)}}=\frac{\partial \Gamma_{\omega_1:\omega_2}{}^{(p)}/\partial c_{c_2}{}^{(p)}}{\sum_{p=1}^{m}\partial \Gamma_{\omega_1:\omega_2}{}^{(p)}/\partial c_{c_2}{}^{(p)}} \tag{23}$$

The lumped parameter model of the critical component-product-transport system was established, as shown in Figure 2. Six masses $m_1,\cdots,m_6$ form the critical component substructure $A$ by five connected components $k_1,\cdots,k_5$. Four masses $m_7,\cdots,m_{10}$ form the product substructure $B$ by three connected components $k_{10},\cdots,k_{12}$. Seven masses $m_{11},\cdots,m_{17}$ form the vehicle substructure $C$ by six connected components

$k_{17},\cdots,k_{22}$. Substructure $A$ and substructure $B$ coupled together by four connected components $k_6,\cdots,k_9$ of fixing installation. Substructure $B$ and substructure $C$ coupled together by four connected components $k_{13},\cdots,k_{16}$ of packaging. The parameters of the lumped parameter model of the critical component-product-transport system were in Table 1. According to the parameters of Table 1 and equation (2), the FRF matrices of the three-substructures multi-coordinate coupled system can be obtained.

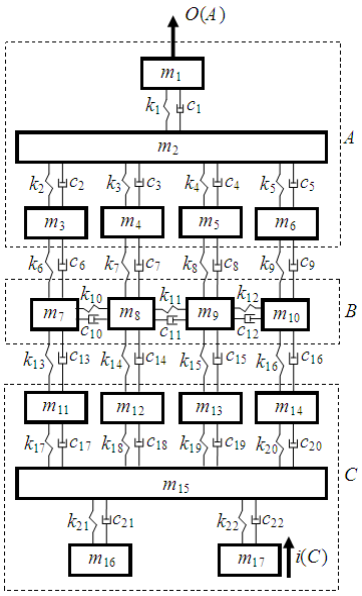



**Figure 2**: Lumped parameter model of critical component-product-transport system.

**Table 1:** Parameters of critical component-product-transport system model(international unit).

| | value | value | value | | value | value | value |
|---|---|---|---|---|---|---|---|
| $i=$ | $m_i$ | $k_i$ | $c_i$ | $i=$ | $m_i$ | $k_i$ | $c_i$ |
| 1 | 7 | 30000 | 5 | 12 | 48 | 28000 | 5 |
| 2 | 26 | 20000 | 5 | 13 | 40 | 4200 | 5 |
| 3 | 9 | 23000 | 5 | 14 | 66 | 4300 | 5 |
| 4 | 11 | 26000 | 5 | 15 | 1260 | 4100 | 5 |
| 5 | 5 | 28000 | 5 | 16 | 120 | 4600 | 5 |
| 6 | 8 | 3100 | 5 | 17 | 80 | 154000 | 5 |
| 7 | 11 | 3900 | 5 | 18 | | 172000 | 5 |
| 8 | 23 | 3700 | 5 | 19 | | 117000 | 5 |
| 9 | 10 | 4000 | 5 | 20 | | 163000 | 5 |
| 10 | 15 | 20000 | 5 | 21 | | 140000 | 5 |
| 11 | 37 | 25000 | 5 | 22 | | 182000 | 5 |

According to the equation (10), $T(\omega)^{(p)}$ was defined by FRF, but the FRF is depended on the physical parameters of structure. So research of influence of the physical parameters of each packaging coupling point on $T(\omega)^{(p)}$ and $b(\omega)^{(p)}$ can help to guide the design of packaging parameters.

For the three-substructures multi-coordinate coupled critical component-product-transport system model in Figure 2, when the stiffness of the first coupling point $k_{13}$ increase from 1000 N/m to 5000 N/m, the vibration contribution $T(\omega)^{(1)}$ and the vibration contribution ratio $b(\omega)^{(1)}$ of the first coupling point were respectively

shown in Figure 3(a) and Figure 3(b). The total vibration contribution $\Gamma_{10:80}^{(1)}$ and the total vibration contribution ratio $\Phi_{10:80}^{(1)}$ of four coupling point on the frequency range 10 Hz to 80Hz were shown in Figure 3(c) and Figure 3(d). The results show that the greater stiffness of the coupled point, the greater $T(\omega)^{(p)}$, $b(\omega)^{(p)}$, $\Gamma_{\omega_1:\omega_2}^{(p)}$ and $\Phi_{\omega_1:\omega_2}^{(p)}$.

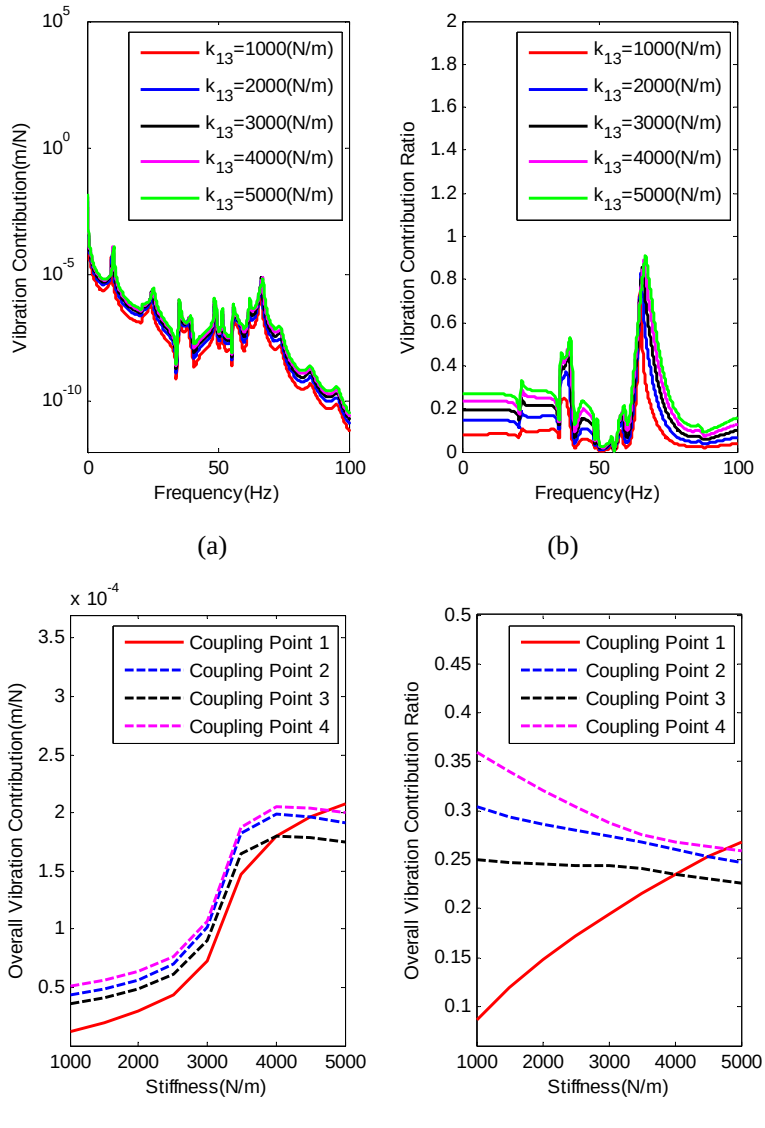



**Figure 3**: Influence of stiffness of the first coupled point on vibration transmission.

For the three-substructures multi-coordinate coupled critical component-product-transport system model in Figure 2, when the damping of the first coupling point $c_{13}$ increase from 1 Ns/m to 800 Ns/m, the vibration contribution $T(\omega)^{(1)}$ and the vibration contribution ratio $b(\omega)^{(1)}$ of the first coupling point were respectively shown in Figure 4(a) and Figure 4(b). The total vibration contribution $\Gamma_{10:80}^{(1)}$ and the total vibration contribution ratio $\Phi_{10:80}^{(1)}$ of four coupling point on the frequency range 10 Hz to 80Hz were shown in Figure 4(c) and Figure 4(d). The results show that the greater damping of the coupled point, the greater $T(\omega)^{(p)}$, $b(\omega)^{(p)}$, $\Gamma_{\omega_1:\omega_2}^{(p)}$ and $\Phi_{\omega_1:\omega_2}^{(p)}$.

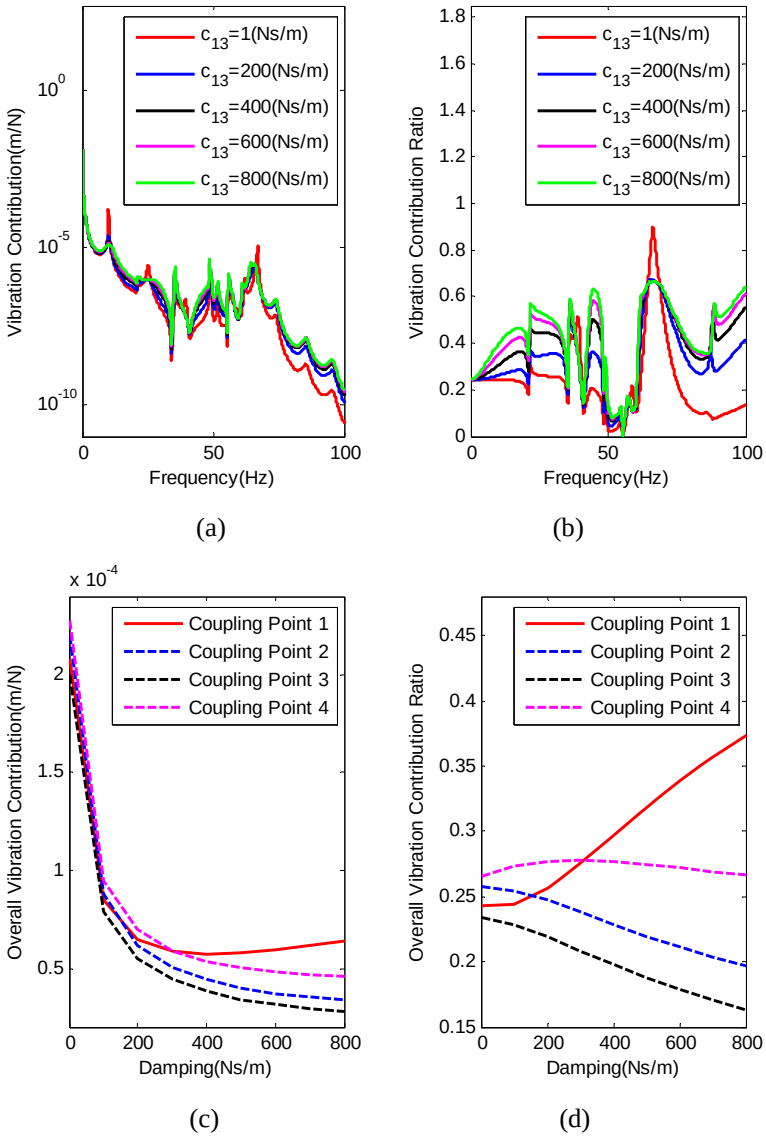



**Figure 4**: Influence of damping of the first coupled point on vibration transmission.

## 3 Experiment and analysis

For the physical prototype model of critical component-product-transport system shown in Figure 5, the experiments were used to verify the validity of the multi-coordinate coupled three-substructures synthesis method and the sensitivity analysis of vibration transmission.

In Figure 5, substructure $A$ simulated the critical component substructure, substructure $B$ simulated the product substructure, substructure $C$ simulated the vehicle substructure. The coupled part $c_1$ was made up of four EPS cushion pads (two of which can be seen in Figure 5). The four cushion pads in $c_1$ simulated the fixed installation, which were distinguished through numbers 1, 2, 3 and 4. For example, $c_1(b_p),(p=1,2,3,4)$ represented the four coupling points on substructure B. The coupled part $c_2$ consisted of four cushion pads (two of which can be seen in Figure 5). The four cushion pads in $c_2$ simulated the packing units, which were distinguished through numbers 1, 2, 3 and 4. For example, $c_2(c_p),(p=1,2,3,4)$ represented the four coupling points on substructure C. This physical prototype model simulated only the system structure of the three-substructures multi-coordinate coupled critical component-product-transport system.

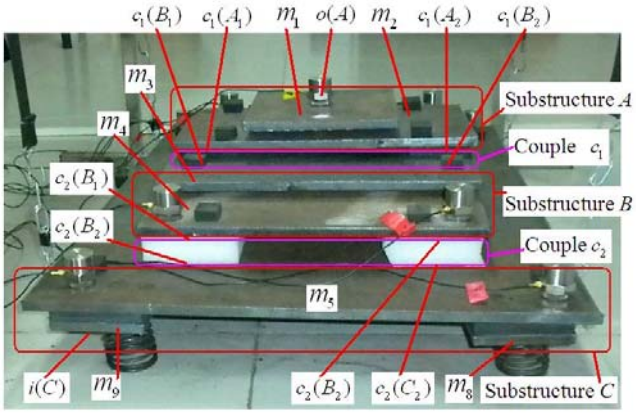



**Figure 5**: Physical prototype model of the three-substructures multi-coordinate coupled critical component-product-transport system.

For the physical prototype model in Figure 5, a testing system shown by Figure 6 was used, adopting the method of one-point excitation and four-point responses. For example, in order to get $\left[H_S\right]_{c_1(B_p)c_1(A_1)}$, $p=1,2,3,4$, the excitation at coupling point $c_1(A_1)$ was carried out with a hammer, and the four acceleration responses at coupling points $c_1(B_p),(p=1,2,3,4)$ were measured with four accelerometers. The acceleration FRFs was transformed into the displacement FRFs.

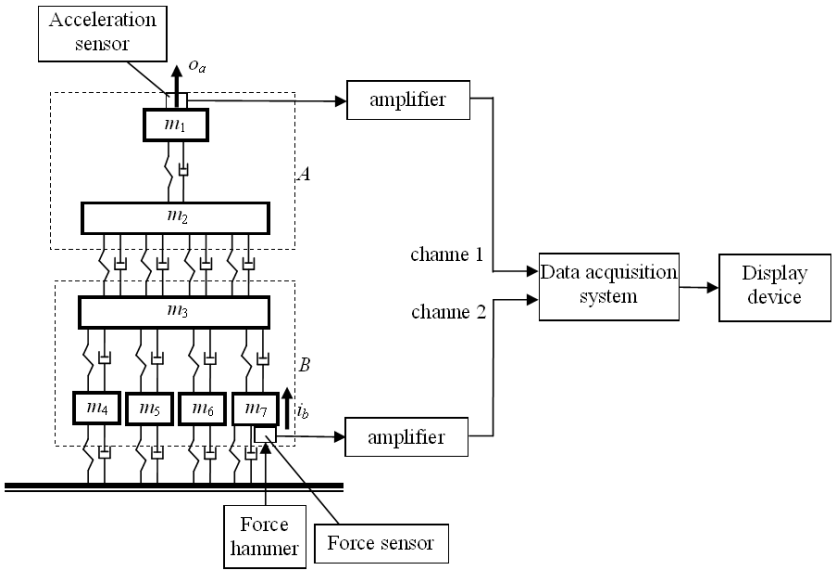
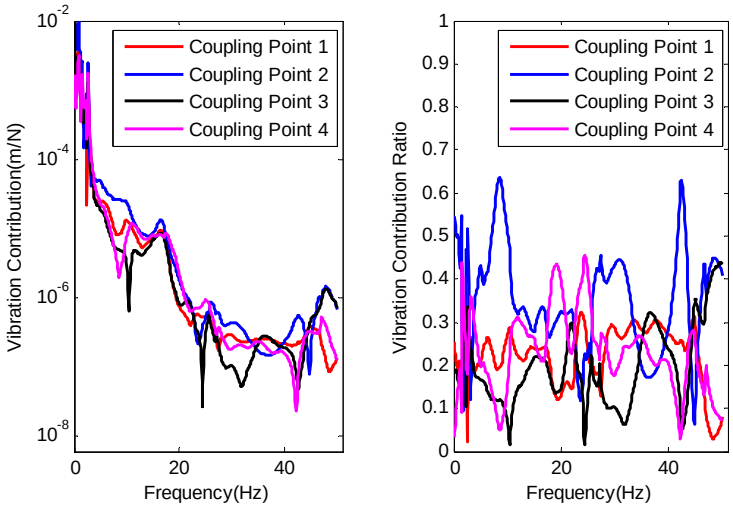



**Figure 6**: Testing system.

By using equation (10), the vibration contributions of four cushion pads were shown in Figure 7(a). By using equation (11), the vibration contribution ratios of four cushion pads were shown in Figure 7(b).




(a) (b)

**Figure 7**: Vibration contributions and vibration contribution ratios of four cushion pads.

The cushion pad 1 in Figure 5 was replaced by cushion pads of three different specifications (shown in Figure 8), and the experiment was repeated 3 times. The vibration contribution and the vibration contribution ratio of cushion pad 1 of three different specifications were respectively shown in Figure 9(a) and Figure 9(b). The overall vibration contributions and the overall vibration contribution ratios to the critical component on the frequency range 30 to 40 Hz through four cushion pads were respectively shown in Figure 9(c) and Figure 9(d). The results show that the stiffness of coupling points to vibration contribution parameters were positive correlation.

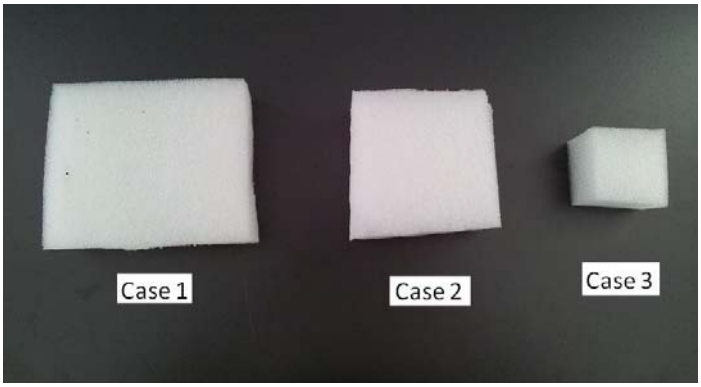
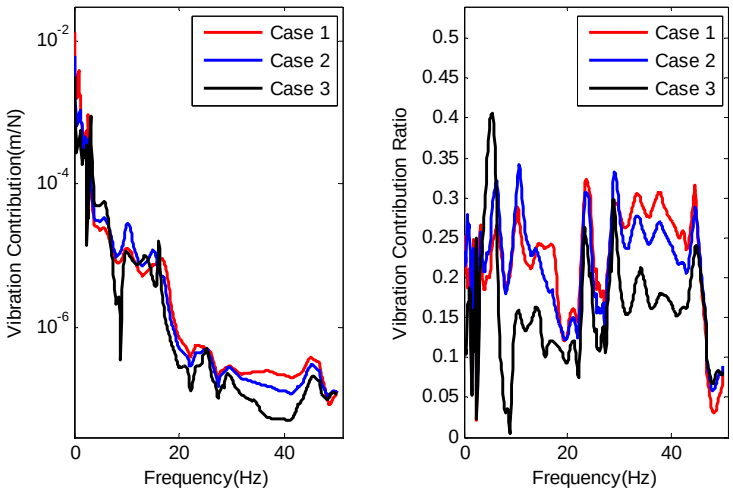
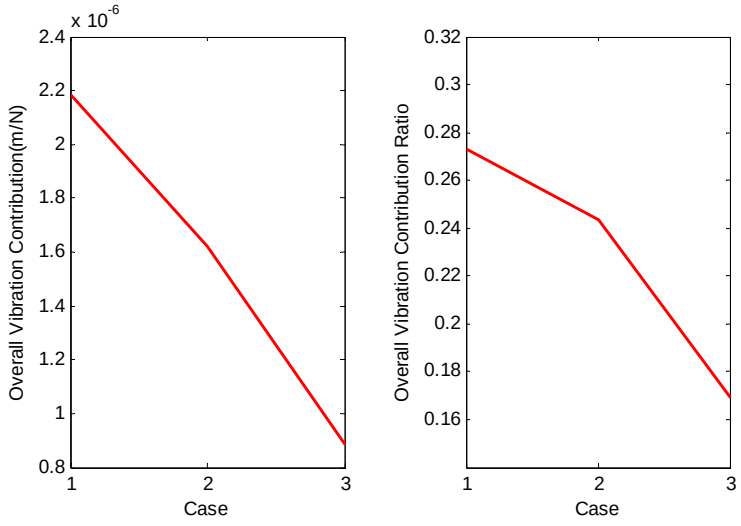



**Figure 8**: Cushion pads of three different specifications.




(a) (b)




(c) (d)

**Figure 9**: Vibration contribution parameters on vibration transmission.

## 3 Conclusions

Analysis of packaging vibration transmission characteristics were obtained by using the substructure synthesis method of FRFs for the three-substructures multi-coordinate coupled critical component-product-transport system. The concepts of the vibration contribution, vibration contribution ratio, overall vibration contribution and overall vibration contribution ratio to critical component response through each packaging unit were introduced to evaluate the vibration transmission ability of packaging units. The sensitivity analysis of vibration transfer parameter was obtained, through the numerical simulation and physical prototype model experiment of packaging vibration transmission analysis. The results show that the stiffness and damping of coupling points to vibration contribution parameters were positive correlation.

## Acknowledgements

The authors acknowledge the financial support of this research by the Key Laboratory of Product Packaging and Logistics of Guangdong Higher Education Institutes and the Fundamental Research Funds for the Central Universities, and Project 50775100 supported by National Natural Science Foundation of China.

## References

1. Sek MA, Rouillard V, Parker A J. A Study of Nonlinear Effects in a Cushion-product System on Its Vibration Transmissibility Estimates with the Reverse Multiple Input-Single Output Technique[J]. Packaging Technology and Science, 2013, 26(3): 125-135.
2. Rouillard V, Sek M A, Crawford S. The Dynamic Behaviour of Stacked Shipping Units During Transport. Part 1: Model Validation[J]. Packaging Technology and Science, 2004, 17(5): 237-247.
3. Zhi-Wei Wang, Jiu-Hong Jiang. Evaluation of Product Dropping Damage Based on Key Component[J]. Packaging Technology and Science, 2010, 23(4): 227-238.
4. Jiu-Hong Jiang, Zhi-Wei Wang. Dropping Damage Boundary Curves for Cubic and Hyperbolic Tangent Packaging Systems Based on Key Component[J]. Packaging Technology and Science, 2012, 25(7): 397-411.
5. Zhi-Wei Wang, Jun Wang, Yuan-Biao Zhang, et al. Application of the Inverse Substructure Method in the Investigation of Dynamic Characteristics of Product Transport System[J]. Packaging Technology and Science, 2012, 25(6): 351-362.
6. Zhi-Wei Wang, Jun Wang. Inverse Substructure Method of Three-substructures Coupled System and Its Application in Product-transport-system[J]. Journal of Vibration and Control, 2011, 17(6): 943-951.
7. Jun Wang, Zhi-Wei Wang, Li-Xin Lu. Step-by-step Decoupling Method for Inverse Substructuring Analysis of A Three-component Coupled Packaging System[J]. Journal of Vibration and Control, 2013: 1077546313490185.

8. Yuan-Biao Zhang, Zhi-Wei Wang. Investigation of Frequency Response Function of Product-transport System Based on Multi-coordinate Coupled Inverse Substructure Method[J]. Packaging Technology and Science, 2014,27(5):364-375

9. Zhi-Wei Wang, Yuan-Biao Zhang. Dynamic Characteristic Analysis of Refrigerator-Truck Transport System by Using Inverse Substructure Method[J]. Packaging Technology and Science, Article first published online: 1 APR 2014, DOI: 10.1002/pts.2072

# Measurement and Analysis of Vibration Levels in 2 and 3 Wheel Delivery Vehicles in South East Asia[#]

**Vanee Chonhenchob[1*], Muhammad Prasetya Kurniawan[1], Sher Paul Singh[2] and Sukasem Sittipod[1]**

[1] *Department of Packaging and Materials Technology, Kasetsart University, Thailand*
[2] *Packaging Forensic Associates Inc., United States*

[*]*Corresponding author. Email: vanee.c@ku.ac.th*

**Abstract:** Different types of small vehicles, such as three-wheel and two-wheel motorcycles are commonly used for domestic delivery in many countries in Asia, particularly in South East Asia. These types of vehicles exist mostly in the last leg of the supply chain. This study was initiated at the Technical Council meeting at International Safe Transit Association to understand the vibration levels that exist in delivering packages in SE Asia for the "last mile." The delivery process in these countries uses two- and three-wheel light vehicles to deliver printers and small packages. However this portion of data and testing has often been overlooked by test standards used in North America and Europe. It has generally been considered the fast, convenient and flexible way of product delivery. This paper presents the vibration measurement and analysis of different types of small vehicles, including three-wheel and two-wheel motorcycles typically being used in Thailand and Indonesia. Recorders were mounted on the vehicle floor to measure acceleration levels during movement in most common routes for the delivery. Measured data shows that lower vibration levels occurred in these vehicles as compared to the other types of vehicle previously studied. Vibration levels in the two-wheel vehicles with trunk containers were higher than those in the three-wheel vehicles. Plastic trunk containers in the two-wheel motorcycles produced lower vibration levels than aluminium containers due to damping structural effects of the plastic materials.

Keywords: vibration; power spectral density; small vehicle; delivery.

[#] This is the abstract of a peer-reviewed paper to appear in a Special Edition of Wiley's journal *Packaging Technology and Science* dedicated to the 19th IAPRI World Conference on Packaging 2014 hosted by Victoria University, Melbourne, Australia.

# New Standardized Package System for Imported Fresh Mangos to the United States from Mexico and Guatemala

**Sher Paul Singh,[1*] Koushik Saha,[2] Vanee Chonhenchob,[3] Jay Singh[4]**

[1] *Professor Emeritus, Michigan State University, East Lansing, MI 48824, USA*
[2] *Asst. Prof., Packaging Program, Cal Poly State University, San Luis Obispo, CA 93407 USA*
[3] *Assoc. Prof., Department of Packaging and Materials Technology, Kasetsart University, Bangkok 10900, Thailand*
[4] *Professor, Packaging Program, Cal Poly State University, San Luis Obispo, CA 93407, USA*

[*] *Corresponding author. Email: singh@msu.edu*

**Abstract:** This study conducted a review of current packaging systems for mangos that are imported into the US from Mexico and Guatemala. Over 1500 growers use over hundred different styles of shipping containers to ship fresh mangos into the United States retail stores. The study reviewed post-harvest, processing, packaging, and shipping conditions for fresh mangos to develop a new standardized packaging system that meets the physical, climatic and sustainable challenges. Various packing houses, corrugated tray manufacturers, importers and retailers were visited in Mexico, Guatemala, and United States. The paper presents findings based on strength of boxes and requirements for temperature control.

## 1 Introduction

Mangos of different varieties, sizes and shapes are imported into the United States from different countries using various forms of packaging. Quality requirements for mangos have been described in the standards.[1,2] The most common shipping method is the use of paper corrugated trays, which are column-stacked on wood pallets, and where each tray can hold approximately 4 kg of fruit. The range of corrugated board, style of tray, size (length, width, and height), number of vent holes, interlocking tabs, quality of printing and graphics, method of erecting, vary significantly even from the same region or country. This study funded by the National Mango Board, reviewed the post-harvest treatment of mangos, packaging, transportation and handling to develop a new standardized packaging system that meets the physical and climatic challenges, and is sustainable.

Mangos are harvested and received in packing houses where they are washed and graded by size and subjected to varying types of pre-cooling (water immersion, forced air cooling, directly packaging in trays and loading in refrigerated trailers, etc.). The packaged trays are stacked on wood pallets, subjected to pre-cooling in most cases, and shipped in temperature controlled ISO containers or trucks to the United States as seen in Figure 1. This study compared both the structural performance of existing corrugated trays based on design and material performance for "physical" challenges, and pre- and post-cooling performance for "climatic" challenges. Mangos are imported with a complex interaction between growers, packers, importers, wholesalers, and retailers whose needs vary based on customer needs and price points. Various packing houses, corrugated tray manufacturers, importers and retailers were visited in Mexico, Guatemala, and United States.

Data was reviewed for almost all different kinds of mango boxes being imported into the US today, and inspecting six mango packing houses in Mexico and three mango packing houses in Guatemala, to ascertain the needs for different types of boxes that are currently being used. It was observed that a given box (tray) contained between five to twenty mangos, depending on the size, shape and height of the fruit, leading to different box sizes, resulting in a challenge to establish a standardized box. Also, various corrugated board combinations are used to manufacture mango boxes depending on the availability of paper for the liners and medium, and the capability of a given packaging supplier. Similarly, there was no uniformity in the number of vents or side cut-outs in the box to facilitate cooling. Boxes (trays) are both manually and automatically erected based on the size of a given grower or packer. A "good" tray needs high strength (to prevent box collapse or stack leans as seen Figures 2 and 3 and a large amount of openings for pre-cooling (as well as maintaining temperature during shipping, storage and retail).



Washing



Grading



RPC filling for water immersion cooling



Carton erecting



Carton filling



Carton handling for palletizing




Palletizing and Strapping



Forced air cooling



Loading into Reefer truck

**Figure 1**: Post-harvest treatments, packaging and shipping conditions for mangos imported to the United States.



**Figure 2**: Box collapse due to unstable stacking.



**Figure 3**: Stack Leaning.

## 2 Materials and Methods

Over 30 different paper corrugated trays were reviewed from various countries including Mexico, Guatemala, Brazil, Ecuador, India and Puerto Rico. After reviewing over thirty different designs, thirteen different types of boxes were selected for structural performance (compression strength and stacked vibration) study (Figure 4). This consisted of nine commercially available and currently being used boxes from Mexico and Guatemala and four designed and fabricated at Michigan State University. The compression strength test compares stacking performance, whereas the vibration test done with mango in boxes evaluates dynamic performance and bruising to the fruit during transportation. Mangos were randomly selected to ascertain weight loss, firmness, color, total soluble solids to develop bruising index.


Mango Box Design 1


Mango Box Design 2


Mango Box Design 3


Mango Box Design 4


Mango Box Design 5


Mango Box Design 6


Mango Box Design 7


Mango Box Design ‘MSU’


Mango Box ‘Shipped’


Mango Box Design ‘Smurfit MSU’


Mango Box Design ‘Inland MSU’


Mango Box Design ‘MSU Double wall’


Mango Box Design ‘Ataulfo’

**Figure 4**: Different types of boxes selected for structural performance.

### 2.1 Stack Performance Testing

The compression strength of a stack of three boxes was determined for each type of box in accordance with ASTM D642 on a compression tester (Model 152-30K, Lansmont, Inc., Monterey, USA). The data was collected for comparing the design and board combination effects on the stack strength. The 12 different types of mango boxes were selected for this study. Each type of box was column stacked 3 high prior to compression testing.

### 2.2 Dynamic Performance Testing

The sample boxes were filled with 9–10 pre-cooled mangos (4°C/80%RH). The boxes were single column stacked 16 layers high on a customized pallet. This pallet was prepared to recreate the effects of deck board spacing on a pallet during shipping. A random vibration test was performed in accordance with ASTM D 4728. The random vibration spectrum used had an overall Grms of 0.52 G, in accordance with ASTM D 4169. They were subjected to random vibration for 60 minutes to represent a 500 mile trip during distribution, on a vibration table (Model 10000-10, Lansmont, Inc, Monterey, CA, USA). After the vibration test these mango filled boxes were placed in room at 23°C/50% RH. After 24 and 48 hours mangos were inspected for permanent deformation, scuffing and bruising. These results were compared to determine quality of mango after shipping in different type of boxes.

## 3 Results and Discussion

### 3.1 Stack Performance Testing

Comparing the results for the 12 boxes as seen in Table 1, it was determined that the '*MSU 250*' design (1858.1 lb) was the strongest, whereas, the weakest box was determined to be a '*Shipped*' box with a residual strength of 502.7 lb. These boxes were retrieved from a pallet load of mangos sent by the grower to Michigan State University via 'Less than truckload' shipment. It was interesting to note that the '*Inland MSU*' and '*Smurfit MSU*' design was among the most structurally sound boxes compared to the seven commercially available mango box designs.

**Table 1:** Compression Strength of Commercial and Prototype Mango Boxes.

| Design | Peak Force | Deflection @ Peak |
|---|---|---|
| **1** | 971.4 (σ = 66.4) | 1.9 (σ = 0.40) |
| **2** | 846.6 (σ = 43.3) | 1.6 (σ = 0.10) |
| **3** | 884.7 (σ = 884.7) | 1.7 (σ = 0.50) |
| **4** | 660.4 (σ = 660.4) | 2.0 (σ = 0.60) |
| **5** | 1303.3 (σ = 1303.3) | 2.0 (σ = 0.20) |
| **6** | 1065.7 (σ = 77.1) | 1.25 (σ = 0.09) |
| **7** | 747.8 (σ = 70.9) | 0.90 (σ = 0.49) |
| **MSU** | 836.4 (σ = 97.7) | 0.8 (σ = 0.10) |
| **MSU 250** | 1858.1 (σ = 68.2) | 0.75 (σ = 0.10) |
| **Shipped** | 502.7 (σ = 38.2) | 1.3 (σ = 1.2) |
| **Smurfit MSU** | 1139.9 (σ = 96.2) | 0.92 (σ = 0.08) |
| **Inland MSU** | 1559.8 (σ = 150.7) | 0.80 (σ = 0.07) |

## 3.2 Dynamic Performance Testing

After subjecting each box type to a random vibration test for 60 minutes, they were stored for a period of 24 hours at 23°C/50% RH prior to making observations for permanent deformation, scuffing and bruising. It was determined that after 24 and 48 hours observation '*Inland MSU*' design had the least bruising and '*MSU Double Wall*' had the maximum bruising (Table 2). Bruising in mangos is a direct result of the amount of physical abuse a mango experiences in a box during transportation. Bruising during transportation accelerates rotting when mangos are stored at room temperature and condition. In order to minimize this effect the box design should hold the mangos in a tight array preventing it from bouncing in the tray during transportation. Therefore comparing the bruising data for all the 12 designs it can be said with certainty that the '*Inland MSU*' design is the best option to minimize bruising during transportation.

**Table 2:** Mechanical Damage on Mangos after Vibration Testing.

| Design | Permanent Deformation | | Scuffing | Bruising | |
|---|---|---|---|---|---|
| | 24 hrs | 48 hrs | | 24 hrs | 48 hrs |
| **1** | 105 | 105 | 0 | 35 | 74 |
| **2** | 56 | 56 | 0 | 23 | 65 |
| **3** | 66 | 66 | 0 | 15 | 52 |
| **4** | 5 | 5 | 0 | 8 | 17 |
| **5** | 5 | 5 | 0 | 15 | 16 |
| **6** | 18 | 18 | 0 | 7 | 9 |
| **7** | 9 | 9 | 0 | 6 | 13 |
| **MSU** | 5 | 5 | 0 | 7 | 21 |
| **MSU Double Wall** | 154 | 154 | 0 | 25 | 116 |
| **Ataulfo** | 123 | 123 | 0 | 30 | 40 |
| **Smurfit MSU** | 9 | 9 | 0 | 6 | 10 |
| **Inland MSU** | 18 | 18 | 0 | 7 | 6 |

## 4 Discussion

Comparing the results, it was found that MSU designed boxes outperformed the commercially available boxes. It showed better resiliency than commercially available boxes subjected to compression. Similarly, after analyzing mangos for permanent deformation, scuffing and bruising after the vibration test, it was observed that MSU designed boxes maintained better overall quality of mangos compared to mangos packed in commercially available boxes.

Figure 5 shows the new box (tray) design developed at Michigan State University that has maximized the opening area in both vertical and horizontal orientation, while having the highest compression strength. MSU Design in Figure 6 shows the stacked configuration on a pallet.

This study has developed a methodology and design that forms a standardized box that ships mangos from exporting countries to the United States of America. This study developed a box which would easily adapt to corrugated systems currently being used. The research needs to be further expanded to adapt to the common footprint. Common foot containers are those containers whose outer dimensions make them fit in a 5 per layer or 10 per layer on a standard (USA) GMA 40 inch × 48 inch standard pallet. It must be noted that shifting to a common foot print container will require more strength and will contain more fruit. We propose a new study that allows us to visit growers and packers to insure our new design can be adapted to various equipment used by corrugated and packing houses.




**Figure 5**: New Standardized Tray for Imported Mangos with Vent Holes for Air Circulation.

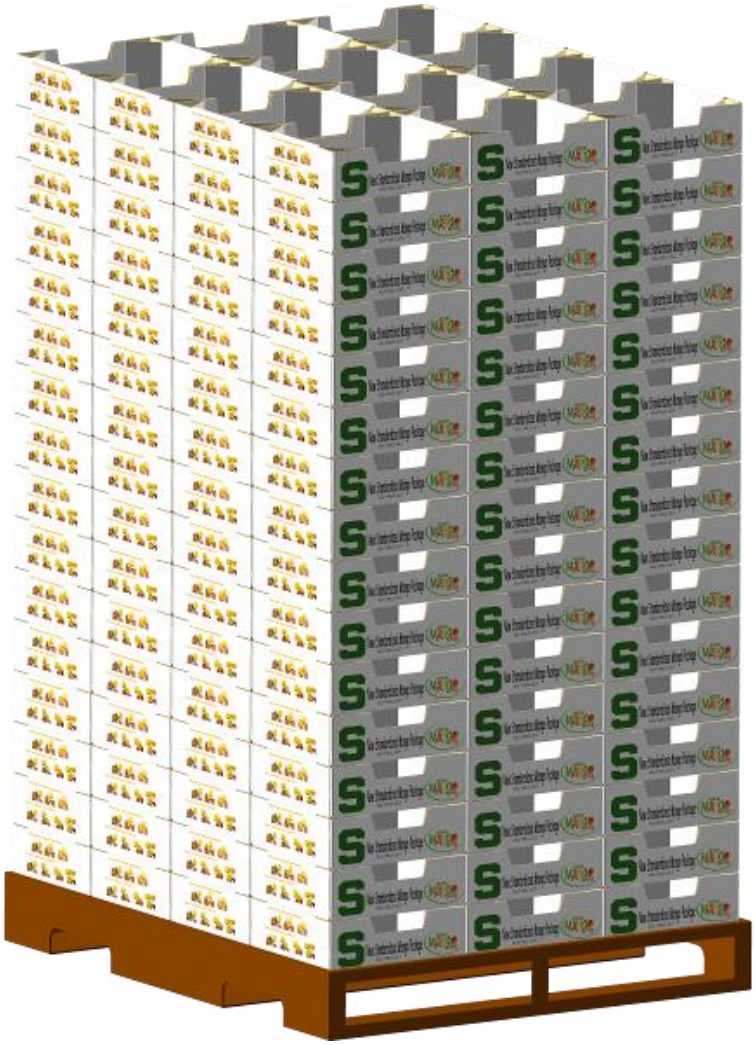


**Figure 6**: Foot pint for Palletizing New Standardized Tray for Imported Mangos.

## 5 Conclusions

The results from this study can be concluded as follows:

1) The new tray is stronger than all others evaluated from various mango producing countries. This is because of its DESIGN.
2) The new tray uses less material, and the strength is due to its design features. Therefore it should not COST more than existing designs. There may be initial set up costs for die cutting, but these will be quickly amortized over a few months.
3) Most carton erecting machines like the ones we visited can make the recommended box design.
4) The blanks can also be hand glued for smaller manufacturers.
5) Since it uses less paper/corrugated it is a sustainable design.
6) It offers more or similar venting than all designs we have reviewed and therefore should give better shelf life to mangos at retail level.
7) The tray is standardized to fit a GMA 40 x 48 inch pallet.
8) This tray permits 12 trays (boxes) per layer and can be stacked 16 high for a total of 192 trays or boxes per pallet.
9) Recommend developing a common foot print container that is adaptable to the US grocery warehouse and retailers.
10) Based on our review and expected Produce Marketing Association (PMA) and Grocery Manufacturers Association (GMA) footprints for retail sales, we recommend using a 10-down tray. This means that 10 trays will fit one layer of standard GMA pallet (40 x 48 inches or 1000 x 1200 mm). This would be an easier transition in the coming 2-4 years from the existing sizes and market expectations.
11) In the long run a 10 down tray will be ideal as it will use the least material, but needs a different design to allow for additional strength in the large bottom face.

## Acknowledgements

The authors would like to thank Mr. William Watson and Dr. Leo Ortega of the National Mango Board for funding this research and providing valuable insight during the entire project. The National Mango Board can be reached at www.nmb.org.

## References

1. USDA. 2007. United States Standards for Grades of Mangos. United States Department of Agriculture
2. CODEX. 2005. CODEX Standard for Mangoes. CODEX STAN 184-1993, AMD 1-2005 (http://www.codexalimentarius.org/codex-home/en/).

# An introduction to next-generation loggers for measuring distribution hazards on the product and package

**Changfeng Ge[1*], Saravana Kumar Nadar[2], Andrew S. Grimaldi[3], Robert Brockhurst[3] and Michael Brockhurst[3]**

[1]Department of Packaging Science, Rochester Institute of Technology, United States.

[2] Department of Computer Science, Rochester Institute of Technology, United States.

[3] Department of Electrical Engineering Technology, Rochester Institute of Technology, United States

*Changfeng Ge. Email: cfgmet@rit.edu

Keywords: Data logger, distribution, real time, wireless, product.

**Abstract:** This paper introduces two working data logger prototypes and the cloud based data analysis system that were trademarked and patented as Pak-Track™-I and Pak-Track™-II. The Pak-Track™-I is designed to wirelessly record and report information in real time about individually packaged products during transit. The system allows the user to immediately view the data with a Global Positioning System (GPS) location via a secured website or Android tablet. The Pak-Track™-II is a standalone device that stores all measurements on internal memory without communicating over a network. The cloud based server and website analyzes and displays the data collected to further study the effects that transportation and handling had on the product and package. The lab obtained vibration and drop data are within expected limits for the purpose of validation. Two field tests were conducted, testing the configuration and setup of the sensors, real time monitoring, display, and analysis. Finally, the collected vibration data was sent to Matlab to generate the PSD chart for validating the FFT algorithm used in the system.

**Key words**: Data loggers, real time, packaging, transportation.

## 1. Introduction

The packaging and distribution of goods is a multi-billion dollar business worldwide. During package handling and transportation, a significant number of goods are damaged by distribution hazards such as temperature, humidity, shock, and vibration. A good understanding of the environment in which the goods were shipped is an essential part of the packaging evaluation process. One way of achieving this aim is to composite the data collected in the distribution environment for simulation in a package testing laboratory. In the past 20 years or more, a great deal of effort by packaging engineers was made to measure the distribution hazards using environment data loggers, which are used as a reference for pre-shipment laboratory testing. Electronic circuit and battery based loggers such as Saver were developed and have been widely used in the industry [1]. These self-contained devices provided the packaging engineer with a broad range of time based measurements that include temperature, humidity and 3-axis impact and vibration data. The collected data in the time domain can be further processed for the use of the packaging design. The impact data G- value can be converted to drop heights so that the engineer can design proper cushioning. Vibration data is useful in power spectral density (PSD) format which can be used in creating random vibration testing spectrums for random vibration tests in the laboratory.

While these units are useful to mount on the truck to record the actual vibration level and the temperature, it is statistically not confident to record the impact/shock of the package during the handling and transition. The drop events are randomly occurring and uncontrollable compared to vibration. It is impossible to install loggers for every package in order to catch the drop events due to the cost of the loggers. Most loggers record the time when the events happened, but not the location. In most cases, data collected about the transport means and handling hazards on the specially designed dummy package system ( for data loggers) are not enough. Instead, it is most important to understand the impact of the product itself or the product's primary packaging. A large and heavy logger does not serve this purpose because the shock event acting upon an actual product and the loggers are different in terms of damping.

In the pharmaceutical and medical industries, goods such as vaccines require an immediate and real time alert when the temperature to be controlled is at a range of 2-8 $^{0}$C [2]. In response to the requirements of monitoring the individual unit packaging, handling, and transportation, sensor based RFID tags are developed and used very recently by pharmaceutical and perishable product producers to monitor the temperature and humidity of their products [3]. The size of the sensor based RFID tag is small, and the cost is much lower compared to the environmental data loggers, the integration of the sensors into RFID environment enable the user to track the information of single unit packages with relatively lower cost. However, two major limitations limit the application of RFID to replace the conventional data loggers. A RFID tag needs a RFID gate to retrieve the collected data, and the vibration acceleration recorded by RFID tag cannot provide the actual impact value as it only tells the trigged vibration level.

Rouillard [4] discussed how compression of the vehicle vibration data could be used to allow small packets of data to be easily transmitted over a network at regular intervals or when requested. Rouillard's effort could have been modified to incorporate a real-time GIS operation and be commercialized. Chen et al.[5] developed a real time sensor monitoring system called ARG-US TransPort, which tracks nuclear and radioactive Material Packages in Transport. The ARG-US TransPort project integrated an off-the –shelf RFID sensor/reader into a vehicle tracking system incorporating global positioning system (GPS) and satellite communication modules. This project records and transmits only temperature and messages data in real time.

Rochester Institute of Technology (RIT) has developed two type of data loggers that have been trademarked and patented as Pak-Track$^{TM}$. The first logger is the Real-Time Monitoring System Pak-Track$^{TM}$-I. This device functions through the use of a Wireless Sensing Network (WSN), Global Positioning System (GPS), Cellular Wireless Network, and a Cloud Server to track and monitor a product during transit. The second logger developed at RIT is the Pak-Track$^{TM}$-II. The function of this device is like most of the data loggers in the market but it is developed in a way that is in-expensive, light and small. Both devices can be rigidly attached to the goods, packaging, or transport vehicles so that they can record the temperatures, humidity, shocks and vibrations acting upon them. Both devices also share the same platform on the cloud for data analysis and display.

## 2. Materials and Method

### 2.1 Description of the System

The Real-Time Package Tracking and Monitoring System Pak-Track$^{TM}$-I was designed to wirelessly record and report distribution hazards about individual packages during transit, and for the user to immediately view the data(figure 1). Data is acquired through the use of three types of devices; an endpoint, a router, and a coordinator. The endpoint device is designed to be as small as possible so that it can be attached to each individual package. The endpoint device is equipped with multiple sensors allowing it record temperature, humidity, shock, and vibration. The router device's purpose is to route the wirelessly transmitted data from the endpoint devices to the coordinator in the event an endpoint device is too far away, or can otherwise not communicate directly with the coordinator. The coordinator collects the transmissions from all of the other devices, and sends the accumulated data to a tablet to be stored or uploaded to the server. The coordinator is also responsible for issuing user commands to the other devices

such as setting a critical temperature threshold or how often data from each sensor is sampled. The server also has an email notification system built into it. It is able to notify users via email using Amazon Simple Email Services if a package exceeds a particular threshold. The coordinator also has a security digital (SD) card that acts as temporary storage to store the data to be transmitted.

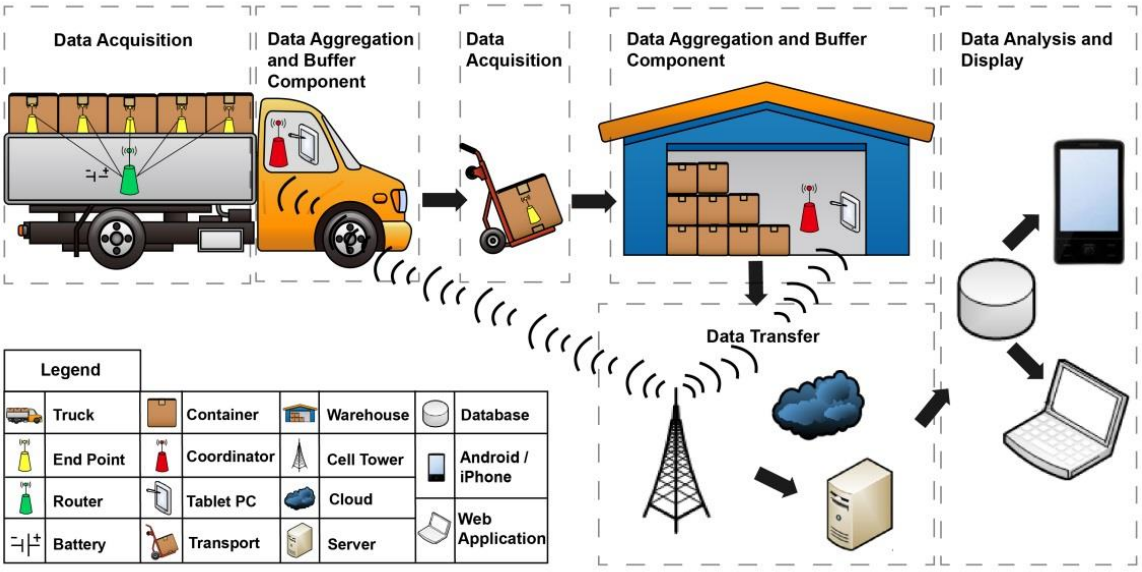



Figure 1: Pak-Track™-I Multi-tier High Level Architecture Framework

The Pak-Track™-II device is designed to be a standalone cost effective device that does not communicate over a network but rather stores all sensor information on internal memory. The Pak-Track™-II is able to record temperature, humidity, vibration, and shock information, storing the data to be recovered upon arrival.

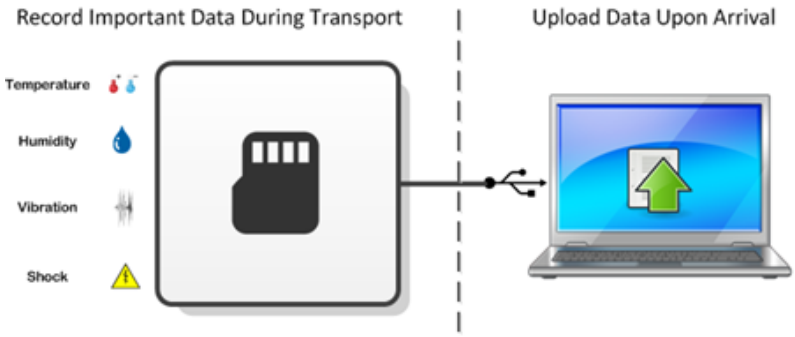
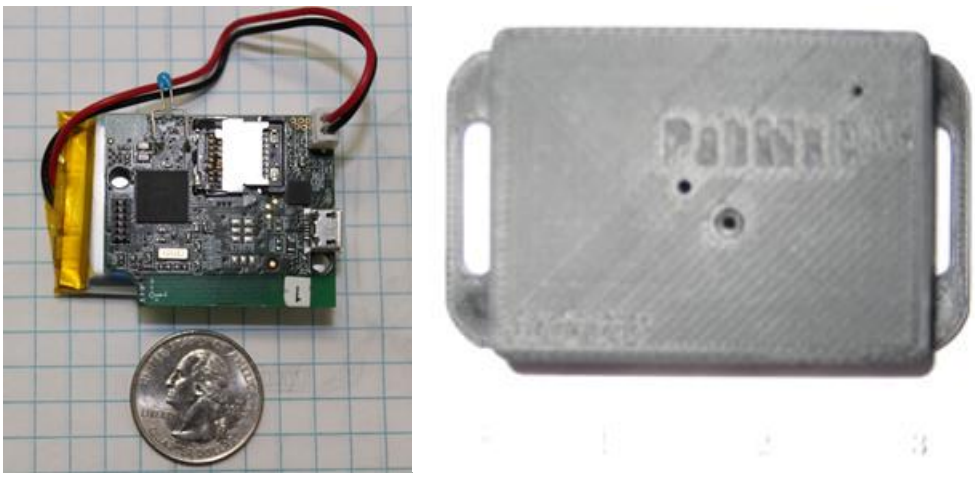



Figure 2: Pak-Track™-II Architecture

The data can be accessed by connecting a standard USB cable and using a simple application that will extract and upload the saved data. Once uploaded, the data can be viewed and analyzed in the same fashion as the data captured in the Real-Time Tracking System. The client software collects the data from the Pak-Track™-II and sends the data to the server for further processing and permanent storage. This way, the Pak-Track™-II can be reused with other packages.

Both devices share the same state-of-the-art technologies. A photograph of the PCB is illustrated in the Figure 3. The difference between the two devices is that the Pak-Track™-I is equipped with a radio on the board and does not have large data storage, whereas the Pak-Track™-II has large data storage, but no radio. The PCB board is only

slightly larger than a quarter dollar and it is powered with a rechargeable battery that is underneath the PCB board in the picture. Both Pak-Track™-I and Pak-Track™-II have a Micro USB connector that is used for charging the battery, configuring the sensor, and uploading collected data in the case of the Pak-Track™-II.



(a) (b)

Figure 3: The PCB Board and the Rechargeable Battery(a); the Enclosed Pak-Track-I Device(b)

## 2.2 Validation and Field Test

The first step of the setup process is to configure the devices. A PC, Mac, or Android Tablet application can be used to configure the Pak-Track™-I and Pak-Track™-II. For the validation and field tests, the specifications were set using the PC and Mac application. Threshold levels were set for temperature, humidity, vibration, and shock, so that when breached, the event would be recorded, allowing the user to easily modify exactly what type of information they wish to receive. The devices can also be programed for how often data is sampled, so even when there is no important event, they can monitor the status of the package for its entire journey.

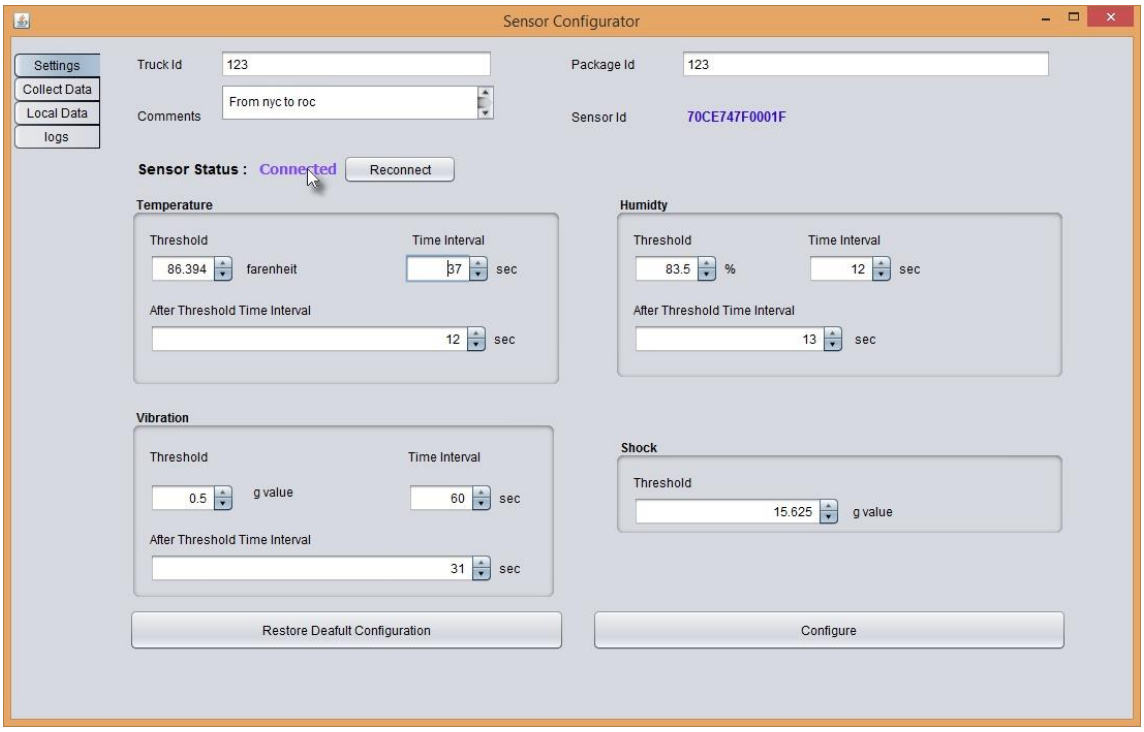



Figure 4: Pak-Track$^{TM}$ PC and Mac Configurator Application

With the specifications set up, vibration and impact tests were carried out in the lab for validation purposes. The impact test was carried out using a drop tester (Lansmont, IL). A Pak-Track$^{TM}$-I and a test accelerometer were placed next to each other on a wooden box enclosed in a corrugated box. The data collected by the test accelerometer was channeled into TestPartner software (Lansmont, IL) for obtaining the peak acceleration G and the shock duration as well as velocity change during impact, which were then compared to the G-values collected by the data acquired by the Pak-Track$^{TM}$-I. The random vibration test was based on the ISTA steel spring truck spectrum. The Pak-Track$^{TM}$-I was fastened on the vibration table and the collected data was channeled wirelessly to the system's server so that the recorded RMS value of the vibration table's RMS value could be compared.

Two field tests were conducted. The Pak-Track$^{TM}$-I device was placed on a moving truck that traveled from Rochester, NY to Western Massachusetts for testing the real time monitoring. In addition, the trip also served the purpose of testing the penetration level of the endpoint devices in an enclosed truck container, as well as the transmissibility over a network and whether the location of the moving truck can be displayed simultaneously. As designed, the user should be able to view a Google map showing all of the locations where sensor data was recorded. Another field test was to test the function of Pak-Track$^{TM}$-II. The trip went from Rochester, NY to East Lansing, Michigan via FedEx services as small parcel package.

## 2.3 Data analysis and display

Using a secure website or Android tablet, the user can view all of the data recorded by the devices. The service provides the user with logs of all of the data, various graphs, and analysis tools to further study the effects transportation had on the package. The data collected by Pak-Track$^{TM}$-I and II can be analyzed and displayed on the website in the cloud (table 1).

Table 1: Data Types Displayed on the Website

| Data | Display format | Data sampled | Display time |
|---|---|---|---|
| Temperature | Temperature in time domain | Intermittent | Real time * |
| Humidity ( %RH) | Humidity in time domain | Intermittent | Real time |
| Location | Google map and Latitude and longitude* | Continuously | Real time |
| Vibration in time domain | G-value versus time | Threshold or intermittent | Real time |
| Shock value | G- value versus time | Threshold | Real time |
| Vibration PSD frequency | PSD versus frequency | Selected period | Real time |
| Drop height /Instantaneous shock | Drop height//Instantaneous versus impact direction-bar chart | Entire journey | Real time |
| Drop frequency (times) | Drop times versus drop direction-bar chart | Entire journey | Real time |
| Shock value | G- values versus drop height | Entire journey | Real time |

* Pak-Track™-I only

For Pak-Track™-II, the user can upload the collected data to the cloud based server or download the data locally. While the Pak-Track™-II does not record GPS location, all data is date and time stamped so the user will always know when an event occurs.

## 3. Results

### 3.1 Validation Test

The vibration test profile used for the validation test was the ISTA steel spring truck spectrum with an average RMS value of 0.542G. A total of 110 sampling were collected by Pak-Track™-I during the vibration test, each sampling consists of 1024 data points. The data was transmitted wirelessly to the server in the cloud. The average RMS value of the110 sampling recorded by the Pak-Track™-I was 0.587G, which is close to the vibration table value when considering the effect of the PCB structure. Table 2 shows the compared results between the G-values collected by a test accelerometer and the Pak-Track™-I using the Lansmont drop tester with a 24 inch drop height. The C1,2,3,4,5 in Table 2 represent accelerometers connected to Lansmont test partner. S1,2,3,4,5 represent five different Pak-Track™-I devices. These two-group sensors return different results well within the range of interest for validation purposes.

Table 2: G-Value Comparison between a Test Accelerometer and the Pak-Track™ Device

| Drop direction | Axis | Sensor 1 | | Sensor 2 | | Sensor 3 | | Sensor 4 | | Sensor 5 | |
|---|---|---|---|---|---|---|---|---|---|---|---|
| | | C1 | S1 | C2 | S2 | C3 | S3 | C4 | S4 | C5 | S5 |
| Z-face | X | 45.48 | 17.19 | 31.89 | 9.38 | 33.58 | 12.50 | 35.64 | 10.94 | 36.01 | 10.94 |
| | Y | 26.71 | 54.69 | 28.03 | 35.94 | 20.20 | 34.38 | 24.81 | 40.63 | 20.91 | 37.50 |

| | | | | | | | | | | | |
|---|---|---|---|---|---|---|---|---|---|---|---|
| | Z | 58.14 | 65.63 | 57.78 | 54.69 | 56.18 | 42.19 | 57.65 | 46.88 | 55.43 | 46.88 |
| | RMS | 78.50 | 87.14 | 71.70 | 66.11 | 68.50 | 55.84 | 72.18 | 62.99 | 69.33 | 61.02 |
| Y/Z – edge | X | 31.31 | 26.56 | 43.67 | 35.94 | 49.52 | 39.06 | 50.21 | 46.88 | 54.30 | 46.88 |
| | Y | 26.32 | 28.13 | 37.40 | 42.19 | 40.51 | 42.19 | 40.66 | 40.63 | 40.26 | 46.88 |
| | Z | 7.84 | 7.81 | 8.65 | 10.94 | 7.77 | 6.25 | 8.32 | 7.81 | 14.61 | 7.81 |
| | RMS | 41.65 | 39.47 | 58.14 | 56.49 | 64.45 | 57.83 | 65.14 | 62.52 | 69.16 | 66.75 |
| X/Y/Z-Corner | X | 42.15 | 40.63 | 69.41 | 67.19 | 74.70 | 71.88 | 79.29 | 76.56 | 80.12 | 79.69 |
| | Y | 34.70 | 43.75 | 51.14 | 59.38 | 48.35 | 62.50 | 50.94 | 65.63 | 52.70 | 65.63 |
| | Z | 29.67 | 31.25 | 48.55 | 43.75 | 51.03 | 46.88 | 55.69 | 53.13 | 56.74 | 56.25 |
| | RMS | 62.14 | 67.39 | 98.95 | 99.77 | 102.58 | 106.16 | 109.47 | 113.98 | 111.43 | 117.57 |

### 3.2 Field Test Results

There are many logs and graphics collected from the two field tests. The display on the website for both trips are similar with the only difference between the two being that Pak-Track$^{TM}$-I has real time data and the data for Pak-Track$^{TM}$-II was pushed to the server when the trip was completed. The screenshots displayed in this paper are a combined selection.

1) Temperature graph of the Pak-Track$^{TM}$-II
2) Humidity graph of the Pak-Track$^{TM}$-II
3) The shock events collected by the Pak-Track$^{TM}$-II
4) The drop height versus Instantaneous shock-II
5) The vibration logs in real time by Pak-Track$^{TM}$-I
6) The vibration graph in real time by Pak-Track$^{TM}$-I
7) Vibration display in google map by Pak-Track$^{TM}$-I
8) PSD chart for the collected vibration data by Pak-TrackTM-I

Figures 5 through 7 display sample data collected by the Pak-Track$^{TM}$-II during the FedEx shipment. Figures 5 through 6 show the temperature and humidity graphs. In Figure 7, a significant impact was recorded during transit.

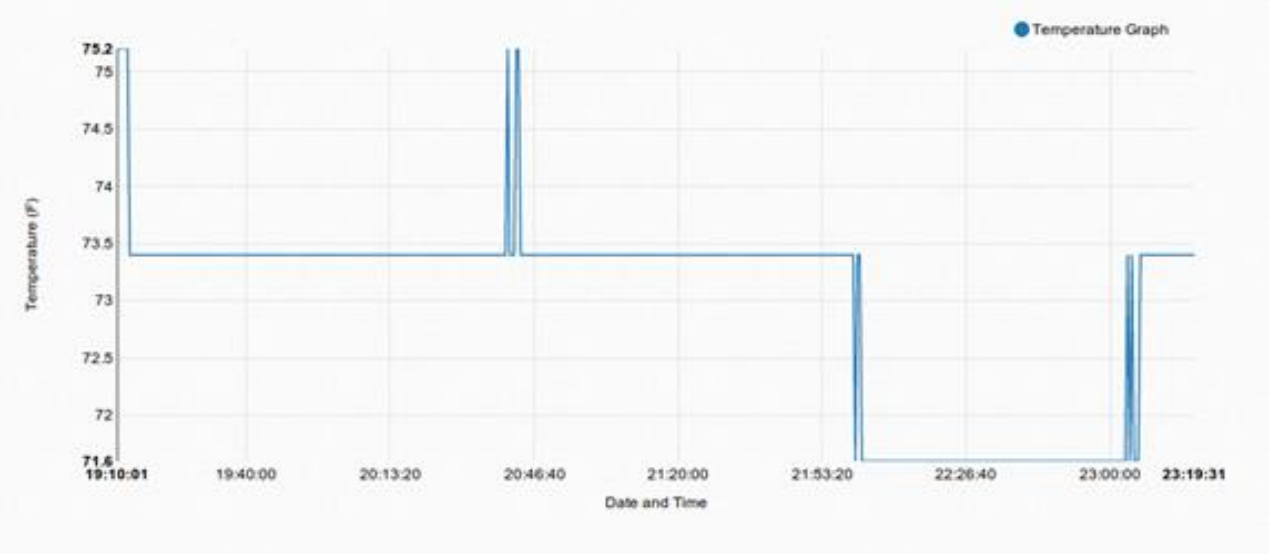



Figure 5: Screenshot of Temperature Graph Recorded in FedEx Carrier Shipment

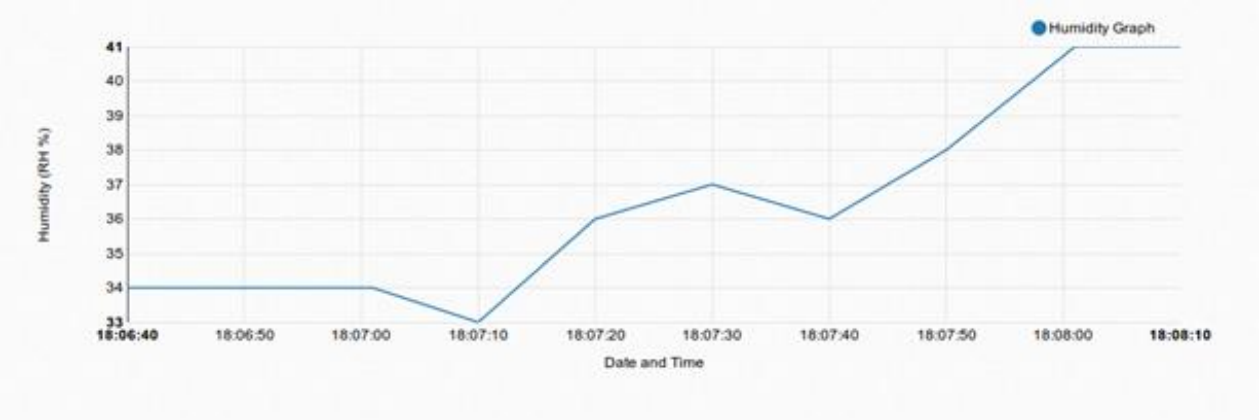



Figure 6: Screenshot of Humidity Graph Recorded in FedEx Carrier Shipment

Shock Table (Showing 14 results) Top 100 % Refresh

| Location | Shock (Max-G) | Drop-Height (m) | Orientation | Analysis |
|---|---|---|---|---|
| Show on map | X 42.1875 g<br>Y -23.4375 g<br>Z 96.875 g | 0.36 m | [3] | View Graph |
| Show on map | X 171.875 g<br>Y 31.25 g<br>Z -139.0625 g | 0.11 m | [3] | View Graph |
| Show on map | X 182.8125 g<br>Y 26.5625 g<br>Z -39.0625 g | 0.37 m | [5] | View Graph |
| Show on map | X -168.75 g<br>Y -179.6875 g<br>Z 154.6875 g | 0.44 m | [5,2,3] | View Graph |
| Show on map | X 23.4375 g<br>Y 28.125 g<br>Z -25.0 g | Instantaneous Shock | [2,1] | View Graph |
| Show on map | X -156.25 g<br>Y -146.875 g<br>Z 117.1875 g | 0.32 m | [6,4] | View Graph |
| Show on map | X -12.5 g<br>Y -15.625 g<br>Z -100.0 g | Instantaneous Shock | [1] | View Graph |

Figure 7: Screenshot of Shock Data Recorded in FedEx Carrier Shipment

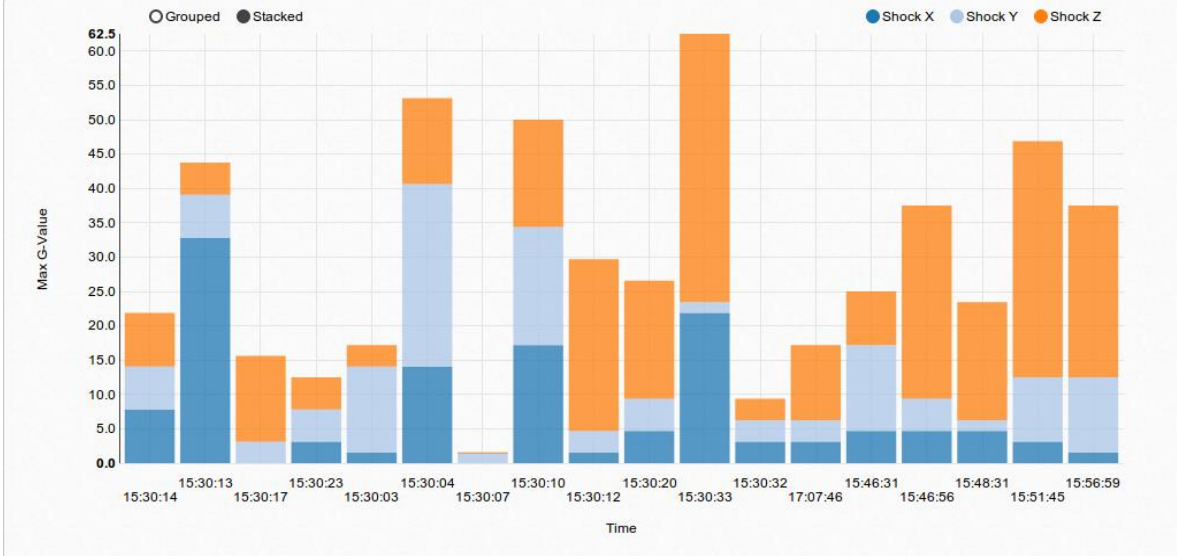



Figure 8: Drop heights versus Instantaneous Shock

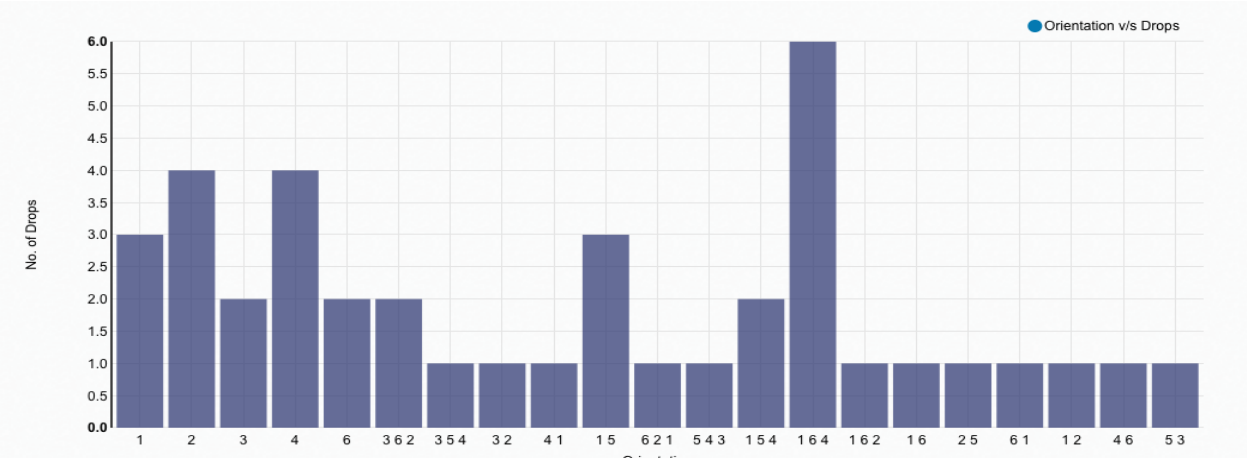
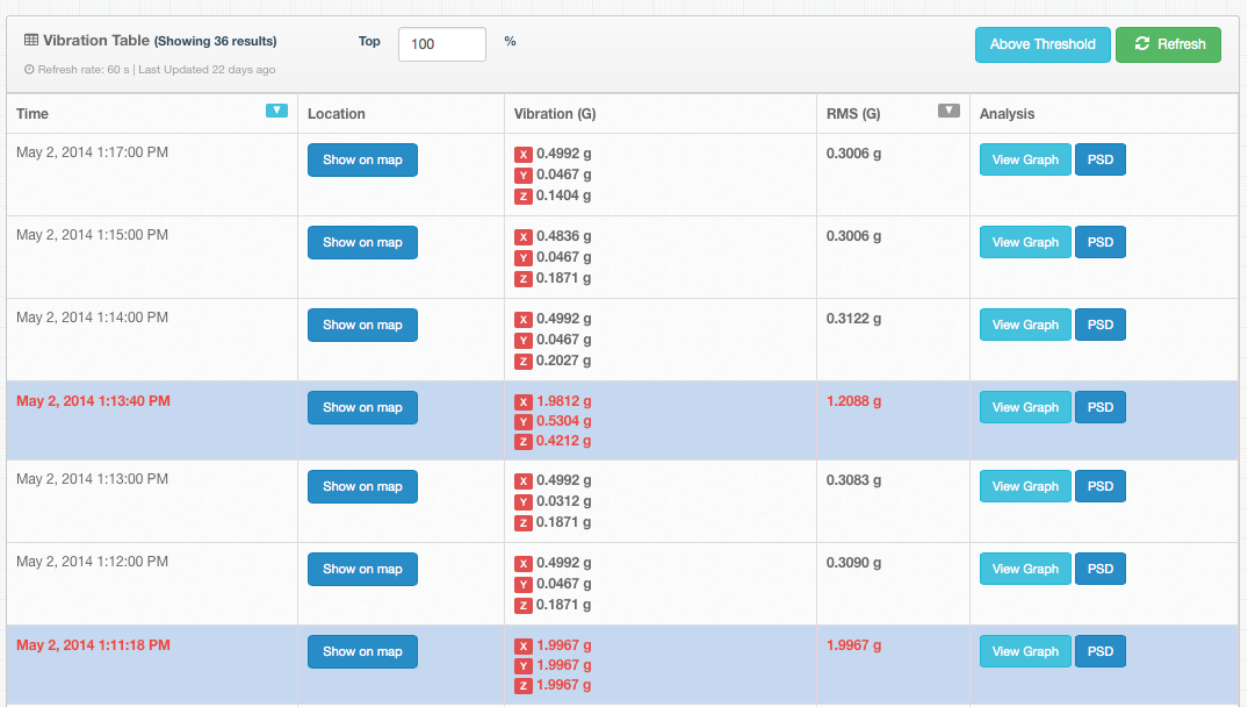



Figure 9: Drop Orientation versus Number of Drops

Figures 10 through 12 illustrate the real time tracking of the moving truck. Figure 10 displays the real time vibration data where the first column states the date and time of when the events occurred. The sampling rate was set for every 30 seconds. The second column in the screenshot indicates the location of the moving truck, showing the latitude and longitude values. The third column shows the maximum 3-axis G-value recorded by the vibration sensor for that sampling event. The Z-direction represents the vertical vibration. The fourth column consists of two buttons for user to choose the time domain graph or PSD function. Figure 11 shows the graphs featuring same data as the Figure 10. Figure 13 is a comparison in PSD between a Matlab FFT and PSD calculated based on the algorithm in the server. The two curves are identical.



Vibration Table (Showing 36 results) Top 100 % Above Threshold Refresh

Refresh rate: 60 s | Last Updated 22 days ago

| Time | Location | Vibration (G) | RMS (G) | Analysis |
|---|---|---|---|---|
| May 2, 2014 1:17:00 PM | Show on map | X 0.4992 g<br>Y 0.0467 g<br>Z 0.1404 g | 0.3006 g | View Graph PSD |
| May 2, 2014 1:15:00 PM | Show on map | X 0.4836 g<br>Y 0.0467 g<br>Z 0.1871 g | 0.3006 g | View Graph PSD |
| May 2, 2014 1:14:00 PM | Show on map | X 0.4992 g<br>Y 0.0467 g<br>Z 0.2027 g | 0.3122 g | View Graph PSD |
| May 2, 2014 1:13:40 PM | Show on map | X 1.9812 g<br>Y 0.5304 g<br>Z 0.4212 g | 1.2088 g | View Graph PSD |
| May 2, 2014 1:13:00 PM | Show on map | X 0.4992 g<br>Y 0.0312 g<br>Z 0.1871 g | 0.3083 g | View Graph PSD |
| May 2, 2014 1:12:00 PM | Show on map | X 0.4992 g<br>Y 0.0467 g<br>Z 0.1871 g | 0.3090 g | View Graph PSD |
| May 2, 2014 1:11:18 PM | Show on map | X 1.9967 g<br>Y 1.9967 g<br>Z 1.9967 g | 1.9967 g | View Graph PSD |

Figure 10. Vibration Data Recorded in a Moving Truck.

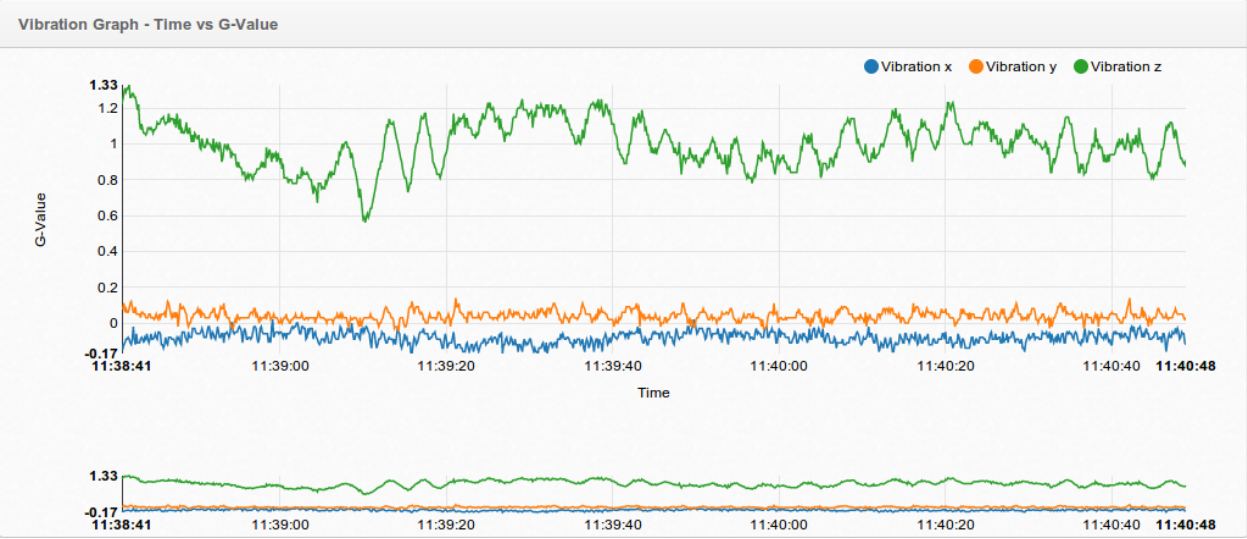



Figure 11: Screenshot of 3-Axis Vibration Data

Figure 12 illustrates what a Google Map, based on the latitude and longitude of where the vibration events happened, looks like.

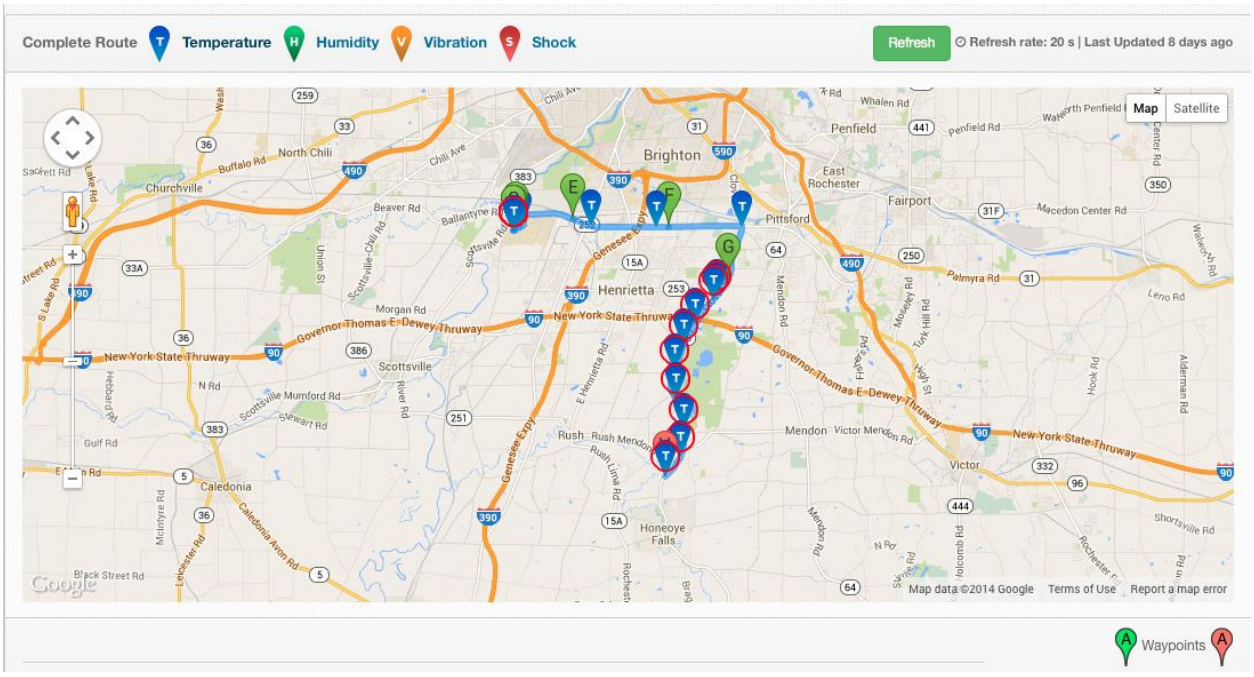



Figure 12: Screenshot of the Moving Truck on Google Maps

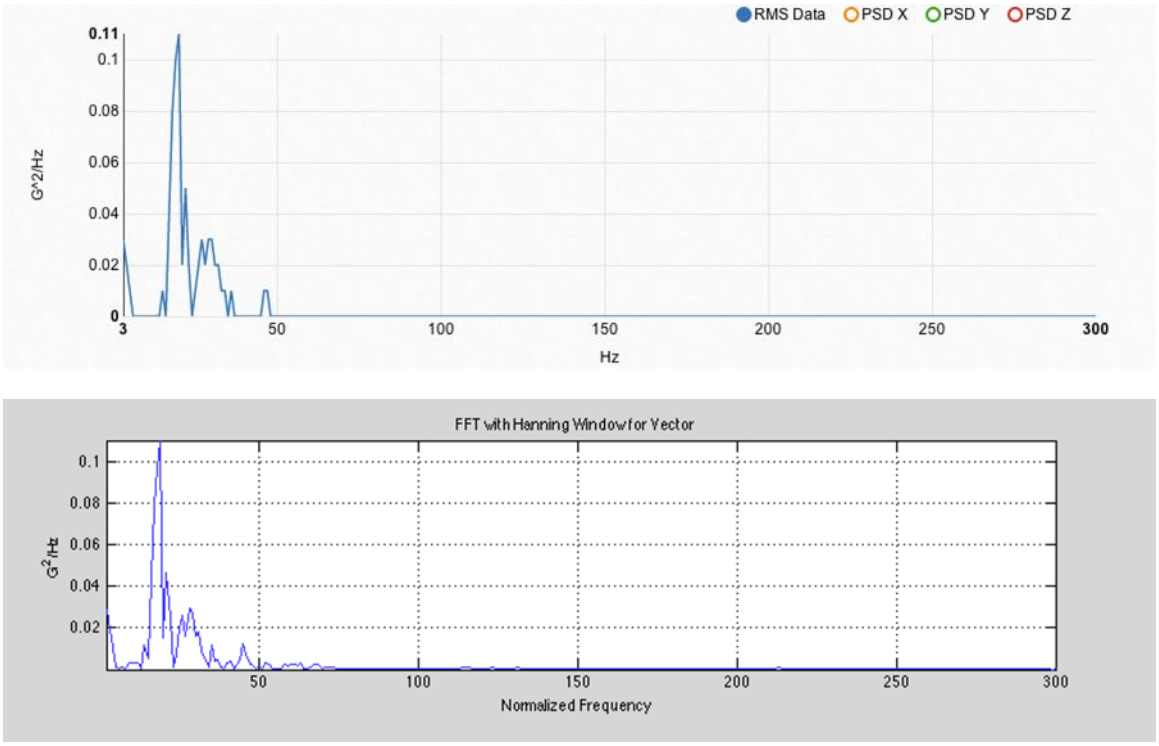



Figure 13: Screenshot of PSD for the Data in Figure 8 and the PSD Chart from Matlab

## 4. Conclusion

This study introduced two data loggers and their data analysis system based on state-of-the art technologies. The high level architecture and system structure were explained. The validation and field tests showed reasonable,

reliable results and both devices have performed well as originally designed. Pak-Track™-I is suitable for the application of dangerous goods, cold chain and other areas where GPS location and real time alerts are necessary. The Pak-Track™-II can be attached to individual products to record important information when the product is in distribution and transit.

The Pak-Track™–I and II demonstrated the potential to be alternative and cost effective solutions to the loggers on the market. Future works will involve developing a variety of Pak-Track™ devices that have different applications (sensors) for different industry sectors. While the current production cost for enclosing the board is more expensive than the board itself due to the use of 3D printing technologies, the cost of both devices should be reduced in the near future so that a wide range of industry sectors can use them.

## References

1. W.I. Kipp, 1998, "Understanding Today's Transport Environment Measuring recorders". *ISA International Instrumentation symposium.* pp.1-13.
2. S.E. Zweig, 2006, "Advances in vaccine stability monitoring technology". *Vaccine*, vol.25, pp.5977-5985.
3. E. Abad. F. Palacio. M. Nuin. de Zárate G.A. J.M. Gómez. and S. Marco, 2009, "RFID smart tag for traceability and cold chain monitoring of foods: Demonstration in an intercontinental fresh fish logistic chain". *Journal of food engineering*, vol. 93, issue4, pp.394-399.
4. V. Rouillard, 2002, "Remote Monitoring of Vehicle Shock and Vibrations". *Packaging Technology and Science*, vol.15, pp.83-92.
5. K. Chen. B. Craig. M. Jusko. H.C. Tsai. and Y. Liu. J. Shuler ,"Real-Time Tracking of Nuclear and Radioactive Material Packages in Transport". Available at:http://www.dis.anl.gov/pubs/67880.pdf

# Indirect Inverse Sub-Structuring Theory for Coupling Dynamic Stiffness Identification of Complex Interface between Packaged Product and Vehicle Transport System[#]

**Jun Wang[1*], Guo-Hua Sun[2*], Li-Xin Lu[1*] and Teik C Lim[2*]**

[1] *Jiangnan University, China*
[2] *University of Cincinnati, United States*

[*] *Corresponding authors. Email: packei@yahoo.com.cn; sungh@ucmail.uc.edu; lulx@jiangnan.edu.cn; teik.lim@uc.edu*

**Abstract:** Inverse sub-structuring method has been recently proposed and applied for inverse analysis of the dynamical response of product transport system. The component-level frequency response functions (FRFs) and the coupling dynamic stiffness for facilitating the cushioning packaging design are all predicted from only the system-level FRFs. However, the system-level FRFs from coupling degree of freedoms (DOFs) may not be measured accurately due to the difficulties of vibration excitation and response measurement for the coupled interface between packaged product and vehicle within the limited accessible space. The aim of this paper is to develop a new FRF-based indirect inverse sub-structuring method for the analysis of the dynamic characteristics of a three-substructure coupled product transport system without measuring system-level FRFs in the coupling DOFs. A closed-form analytical solution to inverse sub-structuring analysis of multi-substructure coupled product transport system is derived. The proposed method is validated by a lumped mass-spring-damper model, and the predicted coupling dynamic stiffness is compared with the direct computation, showing exact agreement. Then, the FRF tests of a physical prototype of multi-substructure coupled product transport system are performed to further check the accuracy of the suggested method. The method developed offers an approach to predict the unknown coupling dynamic stiffness from measured FRFs purely. The proposed method may help to obtain the main controlling factors and contributions from the various structure-borne paths for product transport system.

Keywords: multi-component coupled product transport system; frequency response function; indirect inverse sub-structuring theory.

[#] This is the abstract of a peer-reviewed paper to appear in a Special Edition of Wiley's journal *Packaging Technology and Science* dedicated to the 19th IAPRI World Conference on Packaging 2014 hosted by Victoria University, Melbourne, Australia.

# Carton Clamp Test Methodologies and the Effects on Load Containment and Retention[#]

**Jay Singh[*], Koushik Saha**

*Cal Poly State University, United States*

[*]*Corresponding author. Email: jasingh@calpoly.edu*

**Abstract:** A carton clamp is an alternative material handling device for moving packages and material. The need for changing the clamping force for variations in size, shape, and weight of the load creates the potential for under-clamping (slippage) and over-clamping (compressive damage). Currently there are two test standards that provide lab based forklift/clamp testing guidance - ISTA 3B and ASTM 6055. While ISTA provides a stationary simulation of carton clamp handling, ASTM offers a more mobile approach. The ISTA recommended testing equipment tends to be fairly expensive and is not easily accessible in North American test facilities. The ASTM standard proposes the use a carton clamp truck as used in industry, but does not specify any specific parameters making repeatability between laboratories and practitioners ambiguous. This study examined the implementation a carton clamp lift truck as found in industry allowing for mobile (hazard course) testing. A modified version of ISTA 3B was paired off against ASTM 6055 for evaluating both column and cross stack pallet patterns with a variety of treatments. This study attempted to determine if carton clamps as found in industry are capable and repeatable enough to provide consistent data. This study also examined the test methodologies' effect on load containment via stretch film force, load retention via unitized load slippage, and the effects of ride height and driver interaction. The study sought to understand if these effects are uniform across the unitized load, or if particular layers of the load more affected than others.

Keywords: carton clamp; clamp force; unit load; load containment; load retention.

[#] This is the abstract of a peer-reviewed paper to appear in a Special Edition of Wiley's journal *Packaging Technology and Science* dedicated to the 19th IAPRI World Conference on Packaging 2014 hosted by Victoria University, Melbourne, Australia.

# Combination Cushioning Pad Design and Drop Simulation

**Hua Guangjun*, Xie Yong**

*Packaging and Material Engineering College, Hunan University of Technology, 412007, Zhuzhou, P.R.China*

*Corresponding author. E-mail: 846620681@qq.com

**Abstract:** The combination cushioning packaging has been widely used in large household appliances and instruments in recent years. The combination cushion can not only play the advantages of different materials, but also promote the application of biodegradable material and other traditional plastic cushioning materials. Based on energy equivalent and traditional cushioning design theory, the equivalent cushioning coefficient formula of overlay combination cushion is derived. The formula proposed is very simple in form, and has not made any linear assumption in the derivation process. So it is very universal and can be used for the overlay cushion structure design of linear materials and non-linear materials.In order to verify the validity of the formula and improve the analysis efficiency, simulation and experiment method was both adopted. Firstly, based on static cushioning coefficient - maximum stress curve and the combination cushioning design method, two typical cushioning materials was chosen and the combination cushioning pad was designed. Then, the finite element models of combination cushioning pad structure were established based on ANSYS/LS-DYNA and the cushioning properties were analyzed. Lastly the experiment was carried on with vertical impact machine. Both the simulation and experiment result was close to the theoretical value. The studies show that the equivalent cushioning coefficient foumula is validity. The formula can be used to design the combination cushioning.

Keywords: Cushioning Design; Simulation Analysis; ANSYS / LS-DYNA; Combination Cushioning

## 1 Introduction

Both the plastic cushioning materials and the paper-based cushioning materials were widely used in transport packaging. Generally, the plastic cushioning materials has the advantages of lightweight, soft and excellent cushioning properties. But some of which had been limited to use as the property of not easy natural degradation. The paper cushioning materials is biodegradable, but their buffer performance is not so good. Currently, the overlay combination cushion has been used in household appliances and instruments. The combination cushion is usually consists of two layers. The inner layer is made by soft material used to protect the surface of the product and absorb some impact energy. The outer layer is commonly made by honeycomb or corrugated cardboard used to fix product and absorb part of the impact energy. As lacking the guidance of combination cushion design method, the design of overlay combination cushion were mainly depend on the experience of engineers and experiments[1].

Some scholars has investigated the performance of combination cushion by experimental means[2]. The research on method of combination cushion design is not sufficient[3]. Based on energy equivalent and traditional cushioning design theory, the equivalent cushioning coefficient formula of overlay combination cushion is derived in the following content. And the validity of the formula was verified by imulation and experiment method.

## 2 Equivalent Cushioning Coefficient of Overlay Combination Cushion

Generally, the cushion structure design is based on the cushioning coefficient - maximum stress curve or maximum acceleration - static stress curve[4][5]. The overlay combination showing in Figure 1(a) is the main form of combination cushion with different materials. So the study is focused on the equivalent cushioning coefficient of overlay combination.

### 2.1 Cushioning Coefficient

Cushioning coefficient of cushioning material is defined as the reciprocal of cushioning efficiency, which is usually expressed by (1):

$$C = \frac{\sigma_m}{e} \tag{1}$$

Where, $C$ is the cushioning coefficient; $e$ is the energy absorption unit volume, $e = \int_0^{\varepsilon} \sigma d\varepsilon$ ; $\sigma_{\mathrm{m}}$ is the maximum stress.

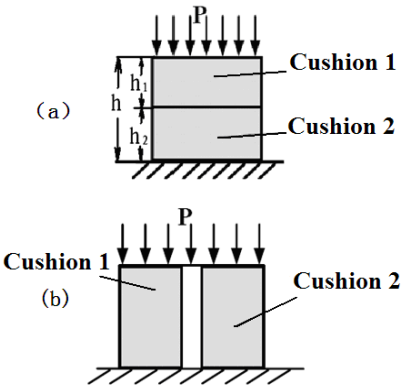



**Figure 1** Sketch of combination cushion

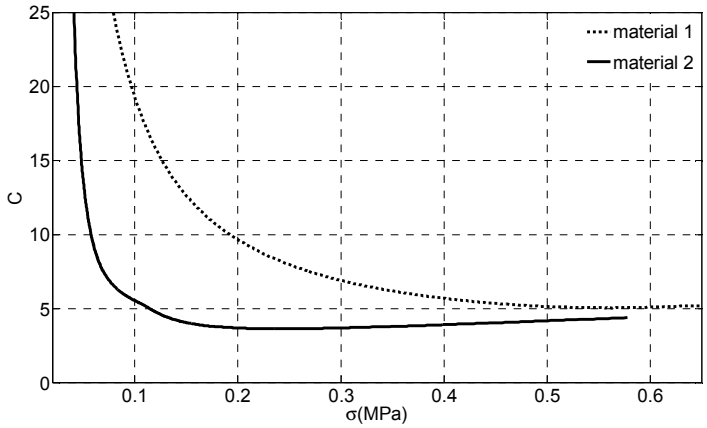



**Figure 2** $C$-$\sigma_m$ curves of two materials

## 2.2 Equivalent Cushioning Coefficient of Overlay Combination Cushion

For the overlay combination cushion shown in Figure 1 (a), suppose the energy absorption unit volume of cushion 1 and cushion 2 is $\boldsymbol{e_1}$ and $\boldsymbol{e_2}$ respectively. The equivalent energy absorption unit volume of the overlay combination cushion is:

$$e = \frac{Ah_1e_1 + Ah_2e_2}{A(h_1 + h_2)} = \frac{h_1e_1 + h_2e_2}{h_1 + h_2} = \frac{h_1e_1 + h_2e_2}{h} \tag{2}$$

Where, $A$ is the area of cushion; $h_1$ and $h_2$ is the thickness of cushion 1 and cushion 2. Let $\alpha = h_1/h$, $\beta = h_2/h$, $\alpha + \beta = 1$ and substitute them into (2). The simplified formula is:

$$e = \alpha e_1 + \beta e_2 \tag{3}$$

Relating (3) and (1):

$$C_e = \frac{\sigma}{\alpha e_1 + \beta e_2} \tag{4}$$

Where, $C_e$ is the equivalent coefficient of overlay combination cushion; $\sigma_1$ and $\sigma_2$ is the stress of cushion 1 and cushion 2. On condition of overlay combination, the relationship of $\sigma_1 = \sigma_2 = \sigma$ is existing. Then the cushioning coefficients of cushion 1 and cushion 2 are:

$$C_1 = \frac{\sigma_1}{e_1} = \frac{\sigma}{e_1} \Leftrightarrow e_1 = \frac{\sigma}{C_1} \tag{5}$$

$$C_2 = \frac{\sigma_2}{e_2} = \frac{\sigma}{e_2} \Leftrightarrow e_2 = \frac{\sigma}{C_2} \tag{6}$$

Where, $C_1$ and $C_2$ is the cushioning coefficient of material 1 and material 2 respectively. Institute $e_1$ and $e_2$ into (4) can get (7)

$$C_e = \frac{C_1C_2}{\alpha C_1 + \beta C_2} \tag{7}$$

In (7), if $C_1$<$C_2$, then $C_1$<$C_e$<$C_2$. The formula (7) indicates the equivalent cushioning coefficient can be adjusted between $C_1$ and $C_2$ show as Figure 2. It also shows that the cushioning performance of overlay combination cushion is not only determined by the cushioning properties of the two overlay materials, but also determined by the proportion of the materials. The equation is applicable to the overlay combination of linear materials and non-linear materials as there is not any linearity assumption in the derivation process. The formula is available on condition the areas of the two overlay pads is not equal, as the deformation and buffer effect are mainly occurred in the overlap region. For the parallel combination shown in figure 1 (b), the equivalent coefficient formula can also be derived by similar process.

## 3 Design and verify

### 2.1 Proprety of the combination materials

Expanded polyethylene(EPE) and honeycomb was selected to design combination cushion. The dencity of the selected EPE is 29.72Kg/m$^3$, and the thickness is 50mm. The stress-strain curve of EPE is shown in Figure 3. The cellular side length of honeycomb is 6mm, and the thickness is 20mm. Properties of corrugating medium and liner board of honeycomb is shown in table 1. The stress-strain curve of honeycomb is shown in Figure 4. In Figure 4, the stage before the maximum stress is mainly elastic deformation. After the maximum stress, the honeycomb is crushed into dense phase. In the dense phase,the honeycomb has lost its excellent mechanical properties and no longer reliable. Therefore it is recommended that the using of honeycomb is limited to the region before buckling. The $C-\sigma_m$ curve of honeycomb before buckling is shown in Figure 5.

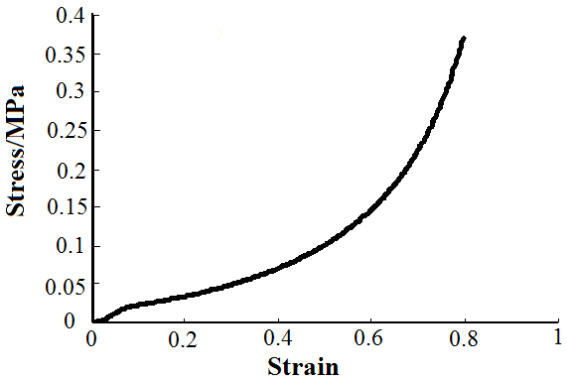



**Figure 3** Stress-strain curves diagram of EPE

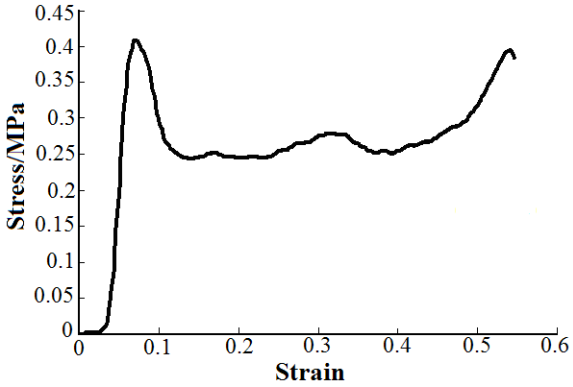



**Figure 4** Stress-strain curves diagram of honeycomb

**Table 1: Properties of corrugating medium and liner board**

| sample type | corrugating medium | | liner board | |
|---|---|---|---|---|
| testing data | cross direction | machine direction | cross direction | machine direction |
| grammage[g/m$^2$] | 123.89 | 123.89 | 299.84 | 299.84 |
| thickness[mm] | 0.202 | 0.202 | 0.39 | 0.39 |
| apparent density[Kg/m$^3$] | 613.3 | 613.3 | 768.8 | 768.8 |
| tensile strength[KN/m] | 3.129 | 6.656 | 7.68 | 18.506 |
| stretch at break[%] | 3.1 | 2.14 | 3.98 | 4.12 |
| folding endurance | 31 | 153 | 39 | 92 |
| tearing resistance[mN] | 109.2 | 74.8 | 251.2 | 211.2 |
| compressive strength -ring cursh[KN/m] | 0.487 | 0.719 | 2.08 | 2.64 |
| stiffness[mN·mm] | 1890 | 750 | 21637.5 | 6590 |
| bursting strength [Kpa·m$^2$/g] | 3.19(top side) | 3.55(verso) | 2.80(top side) | 3.13(verso) |

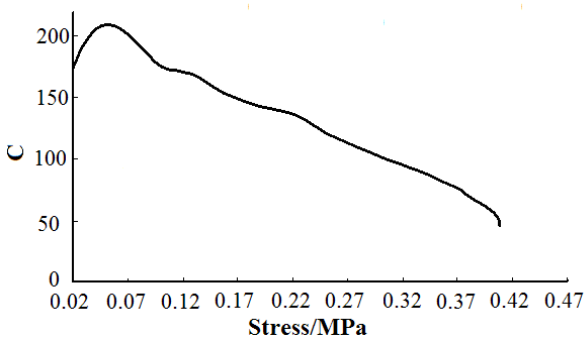



**Figure 5** $C-\sigma_m$ curves diagram of honeycomb

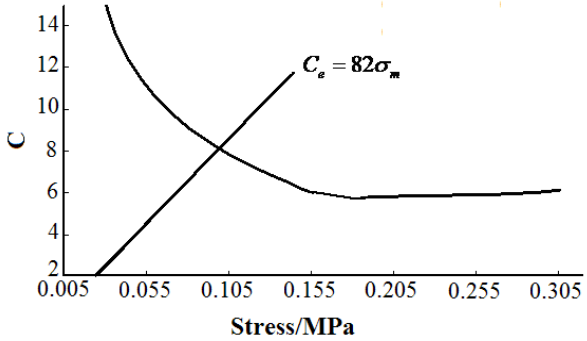



**Figure 6** Combination $C-\sigma_m$ curves diagram

## 2.2 Combination cushion design

Suppose a product weighs 5.8kg, and it's length,breadth and height are 200mm. The drop height is 600mm. Select the honeycomb and EPE in section 2.1 to design combination cushion， the total thickness of the cushion is 70mm. According to (7), the equivalent cushioning coefficient-maximum stress curve of the honeycomb and EPE is shown in Figure 6. The area and thickness of the cushion structure is calculated as equration (8) and (9).

$$h = C_e H / G_m \tag{8}$$

$$A = WG_m / \sigma_m \tag{9}$$

Institute the parameters h,A,W and H into (8) and (9) can get line $C_e = 82\sigma_m$. The intersection piont of the line with the $C-\sigma_m$ Curve shown in Figure 6 is ($\sigma_m = 0.1MPa$, $C_e = 8$). Institute the intersection point value into (8) or (9) can get $G_m = 69g$. It is the theoretical acceleration of the combination cushion.

## 2.3 Simulation based on ANSYS/LS-DYNA

In order to verify the combination cushion design based on the equivalent coefficient, simulation and experiment analysis method was adopted respectively. The combination cushion's finite element model was built and analysied with the DTM module of ANSYS / LS-DYNA[6]-[9]. The drop testing model is shown is Figure 7. The simulation gravity acceleration of drop testing tests is shown in Figure 8. Figure 8 shows that the maximum impact acceleration is 64g, which is very close to the theoretical values. It is believed that the error between the calculation and simulation is caused by the errors of material propreties describtion in finite element software.

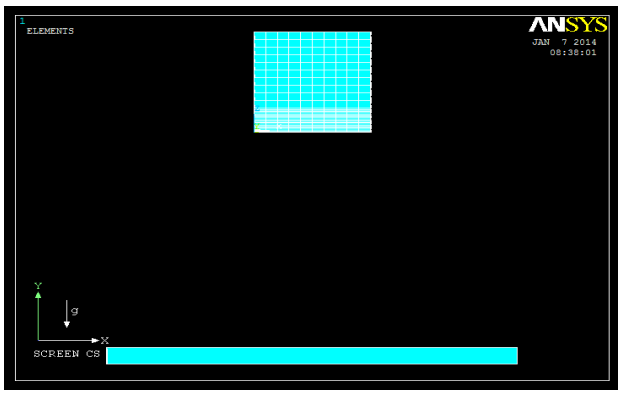



**Figure 7** Simulation drop testing model

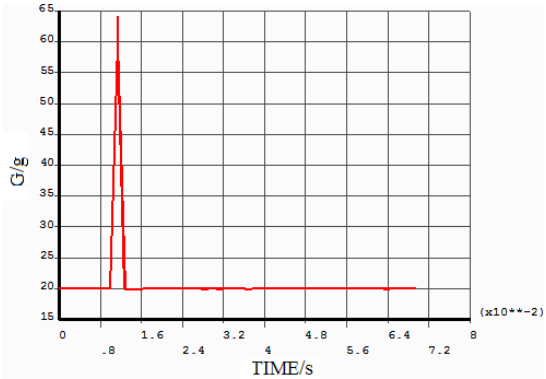



**Figure 8** Accelration curve of simulation

## 2.4 Experimental Analysis

The experiment was carried on by vertical impact machine shown in Figure 9. The combination cushion is made by EPE and honeycomb in section 2.1. The Weight of hammer is 5.8kg, and the drop height is 600mm. The impact value as shown in Figure 10 is about 63g, which is also slightly less than the theoretical acceleration. The results show that the combination cushion design based on equivalent cushioning coefficient is conservative and feasible.

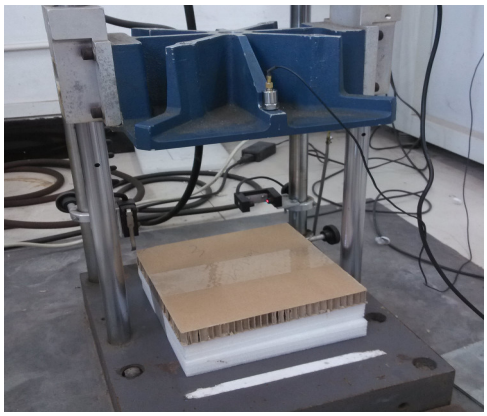


**Figure. 9** Drop testing

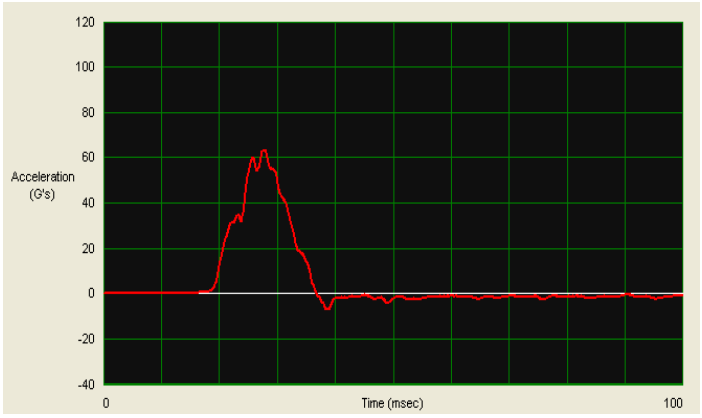



**Figure. 10** Drop testing accleration curves

## 3. Conclusion

1）Based on the buffer mechanism, the equivalent coefficient formula of overlay combination buffer was derived. The equivalent coefficient formula proposed in this paper can be used for the overlay cushion structure design of linear materials and non-linear materials.

2）Both the simulation and experiment results was close to the theoretical peak acceleration $G_m$. It shows that combination cushion design based on equivelant cushioning coefficient is feasible.

3) The combination cushion design, simulation and experiments work in this paper are relatively junior. The depth and meticulous work needs to be further expanded.

## Acknowledgements

The work is supported by National Natural Science Foundation of China (Grant No: 61170101).

## References

[1] Tian Peng, Hua Guangjun, 2013, “Impact of Scale Effect on Cushioning Properties of Expanded Polyethylene”,Packaging Journal,Vol.5,No.4,pp.30-33.

[2] Yan Lirong, Xie Yong,2010, “Dynamic Cushioning Properties of Combination of Honeycomb Paperboard and EPE” ,Packaging Engineering, Vol.31,No.19,pp.13-16.

[3] Hua Guangjun , Xie Yong,Tian Peng, et al. 2012, “Research on equivalent cushioning property and design idea of overlay combination cushion”,Applied Mechanics and Materials, Vol.200,pp.22-26.

[4] Wei Zhuan, Hua Guangjun.,2012, “Research on Cushioning Package Design Methods Based on Infinitive Equations”,Applied Mechanics and Materials, Vol.200,pp.126-130.

[5] Hua Guangjun,Zhao Dejian, Xie Yong， et al. 2013, “Discussion and Analysis on Mathematical Connotation of Cushioning Packaging Design Method”， Packaging Engineering, Vol.33,No.23,pp.13-16.

[6] Yang Shuyi，Liu Deshun，Zhao Jiyun, 2012, “Drop impact crashworthiness analysis of mobile hard disk based on LS-DYNA”,Journal of Viberation and Shock,Vol.31,No.9,pp.13-18.

[7] Shi B J, Shu D W, Wang S, et al. 2007, “Drop test simulation and power spectrum analysis of a head actuator assembly in a hard disk drive” ,International Journal of Impact Engineering, Vol.34,pp.120-133.

[8] Xiang Hong, Wan Chen, Wang Jun, 2012, “A Method to Determine the Critical Damage Dropping Height of Potato”, Packaging Journal,Vol.4,No.3,pp.30-33.

[9] Lu Lixin, Wang Zhiwei, 2007, “Dropping Impact MechanicaCharacteristics of Apple”. Transactions of the Chinese Society of Agricultural Engineering, Vol.23,No.2.254-258.

# Damage to Carton Board Packages Subjected to Concentrated Loads

**Daniel Eriksson[1*], Christer Korin[1] and Fredrik Thuvander[2]**

[1] *School of Science and Technology, Örebro University, Sweden*
[2] *Department of Engineering and Physics, Karlstad University, Sweden*

[*] *Corresponding author. Email: daniel.eriksson@oru.se*

**Abstract:** Carton board packages subjected to concentrated loads near the edges are damaged in a characteristic way. This paper reports an attempt to simulate the damage process in the lab and Package Collapse Loads measured for this load case.

Packages were compressed by a concentrated load. The position of load application was varied along a line parallel to a crease and the package was rotated in order to test the influence of the height of the load carrying panel. Force and displacement were recorded and the damage evolution during the test was studied. The damage produced was examined using x-ray tomography. The nature of damage at different stages of damage evolution was studied.

Both the visual appearance of the damage and the force-displacement curve were similar in all tests. The Package Collapse Load has little dependence on where along a line parallel to a crease of the package the point load is applied. Damage started developing at the crease and a yield line perpendicular to the crease and parallel to the direction of the load developed. When the displacement increased further, a parabolic yield line, symmetric around the previous one, developed. The start of the damage development was associated with at peak in the force-displacement curve. Stiffness was more geometry dependent than strength. On macro scale, the visual appearance of the damage due to concentrated loads shows no significant dependence on geometry.

Keywords: package collapse load, carton board, packaging, strength, concentrated load, x-ray tomography.

## 1 Introduction

Carton board is an important packaging material used mainly for primary packaging and it is the interface towards the consumer. One of the requirements on packaging is to protect the product from various physical hazards it may encounter on its way from the manufacturer of the product to the user of the product and potentially also during use, depending on the type of product. Primary packaging can be viewed as an integral part of the product [1] and its performance will likely influence the users' attitudes towards the product and the brand. Thus, it is important to understand how to evaluate packaging performance in various situations throughout the value chain. For example, a product whose package appears damaged is likely to be less desirable for a consumer, even though the goods inside the package are unaffected.

Box compression, e.g. Box Compression Resistance (BCR), is the traditional measure for mechanical strength of packaging and has been the subject of a few studies [2]–[6]. A comprehensive review was published recently by Frank [7]. Box compression gives a measure of the maximum momentary load a box can carry. When boxes are used, the load may be extended over a longer period of time for example when boxes are stacked in a warehouse. In that case the maximum load that the box can support is less due to creep. The strength in such a situation is to a large extent dependent on BCR and time, but there are other factors such as climate and vibrational loading during transport that also have an influence [7]. The work by Ristinmaa *et al.* [6] gives a good description of the characteristics of box compression damage.

For load distributions other than perfect stacking the available data is limited. Frank [7] cites a few sources on the influence of interlocking stacking patterns. Panyarjun and Burgess [8] tried to study three-point bending of long packages made from corrugated board. They reported local failure at the point of load application rather than an actual bending failure. They suggested that the failure load depends mainly on the width of the area that the load is applied over and the Edge Crush Test, ECT, value of the corrugated board. There is also a study that reports some data from simulations and experiments on concentrated loading of two types of packages [9].

The present work was done in order to study the damage that carton board packages develop under concentrated loads in detail. An inspection of packages on the shelves of a local retailer revealed packages damaged in a way

that looked like what would be expected from even compression, but also another type of damage shown in Figure 1. These packages seem to have been damaged by a concentrated load.

A packaging designer that wants to prevent damage from concentrated loads needs to understand the mechanisms behind it. Perhaps the mechanism is similar to that in box compression and an expression similar to the empirical formulae published for Box Compression Resistance [3], [5], [6] could be devised for the case of a concentrated load.




**Figure 1**: Damage on packages found on the shelves of a local retailer that looks like it has been caused by a concentrated load.

Ristinmaa *et al.* [6] studied how damage evolved during the Box Compression Test in order to establish an empirical framework for predicting the Package Collapse Load, PCL, for that load case, defined by the peak load in the load-displacement curve. Thus, if one wants to find PCL for a concentrated load it seems reasonable to study the damage mechanism in greater detail also for the case of concentrated load. For that, it is necessary to develop a displacement controlled setup where packages can be subjected to concentrated loads and the load-compression response can be recorded.

The aim of this paper is to

1. Demonstrate a method that can replicate the damage that carton board packages sustain when subjected to concentrated loads.
2. Use that method to find the influence of some parameters on the Package Collapse Load, PCL.
3. Provide data for a discussion of the damage mechanisms involved.

## 2 Method

The experimental setup is explained in Figure 2. A tensile testing machine, Lloyd Instruments LX5K, was equipped with a fixed plate and an indenter. The package rested on the fixed plate while the indenter compressed the package from the opposite face. The indenter touched the face 5 mm from the edge, thus most of the load would be carried by one of the package's side panels. The distance, *x*, denotes the position of the indenters centre measured from the left face of the package. Compression was set to progress at a rate of 100 mm/s until a prescribed displacement was reached. The displacement is measured from the point where a threshold load of 5 N was reached. This threshold was implemented to compensate for manufacturing tolerances. After the prescribed displacement was reached the indenter returned at the same speed. During the whole loading and unloading, displacement and force were measured continuously and logged.

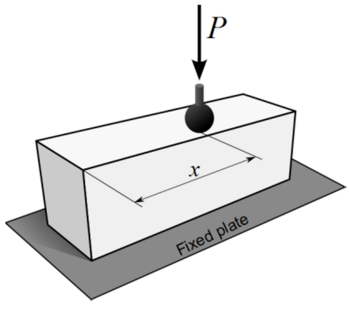



**Figure 2**: Sketch of the experimental setup.

In order to establish that the behaviour observed was not merely an artefact of the particular design and material, two package designs manufactured from two different materials were tested. Package A was of type A20.20.03.01 [10] manufactured in an industrial converting facility. Package B was of type A55.20.01.03 [10] manufactured using rapid prototyping equipment. Material data for the packages is summarized in Table 2 and cut-out sketches along with measurements of the packages are shown in Figure 3. A photo showing the two packages side by side is found in Figure 4. The choice of package sizes and materials was made with the intention of securing a large difference between the packages.

Package A was tested in three orientations as indicated in Figure 5. This was done in order to study the influence of the height of the load carrying panel. This parameter is very important for the PCL in box compression and it could be expected to have at least some influence also in the case of concentrated loads.

**Table 1**: Summary of the parameter combinations tested. X denotes tested combination of parameters.

| Indenter type | | Cylinder | | | Sphere | | |
|---|---|---|---|---|---|---|---|
| Point of load application, *x*/*H* | | 2/11 | 1/2 | 8/11 | 2/11 | 1/2 | 8/11 |
| A | I | X | X | X | X | X | X |
| | II | | | | X | X | X |
| | III | | | | X | X | X |
| B | N/A | | | | | X | |
| Package | Orientation | | | | | | |

**Table 2**: Material specifications for the materials used in packages A and B.

| | Package A | Package B |
|---|---|---|
| Trademark | Korsnäs White 290 | Korsnäs Carry 350 |
| Bending Resistance MD 15° (mN) | 430 | 805 |
| Bending Resistance CD 15° (mN) | 230 | 390 |
| SCT MD (kN/m) | 6.9 | 10.0 |
| SCT CD (kN/m) | 5.5 | 7.3 |
| thickness (µm) | 425 | 500 |
| Grammage (g/m$^2$) | 290 | 350 |

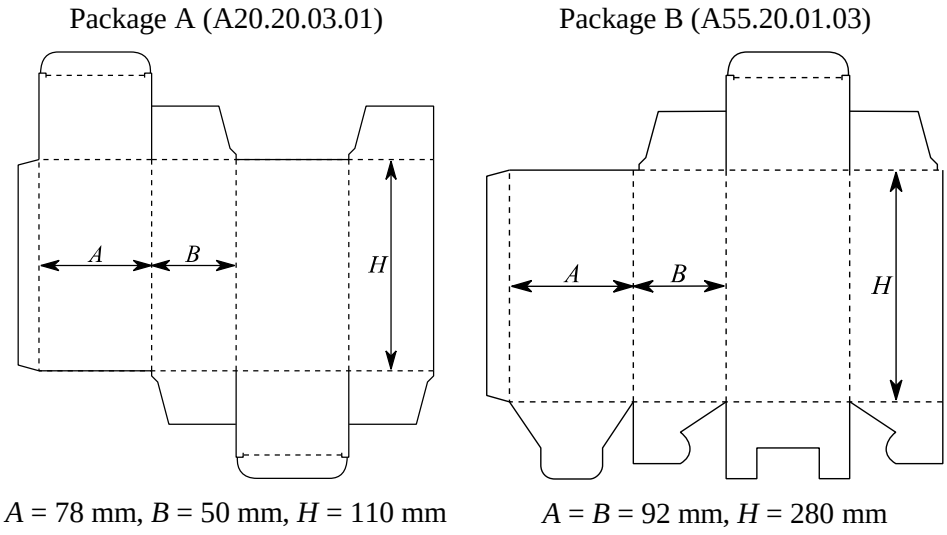



**Figure 3**: Cutout sketches of the packages tested. Dashed lines show creases.




**Figure 4**: Photograph of package A (lower left) and package B (upper right).

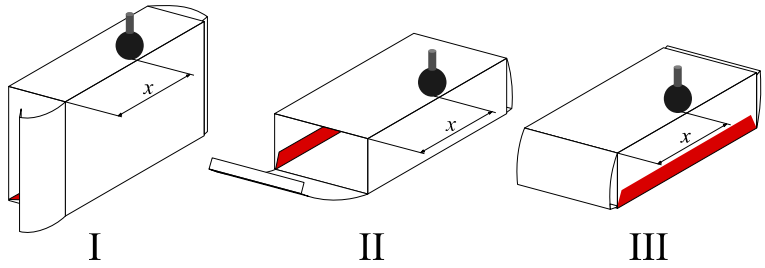



**Figure 5**: Definition of the three orientations of package A. Flaps are shown open or not at all in order to reveal the location of the glue flap (shaded).

The size and shape of the indenter could also influence the PCL. In order to estimate this influence, two different indenters were used. One was spherical with a diameter of 28 mm. The other one was cylindrical with a diameter of 6 mm.

The last parameter that was varied was the position of load application. This was only done on package A. The distance from the bottom of the package to the point of load application was 30 mm, 55 mm, and 80 mm, respectively. This was done in order to quantify the influence of proximity to a stiff corner of the package. Note that the package design of package A is such that 30 mm and 80 mm are not equivalent. One is supported by a fold and the other by a short tuck-in flap.

All tests were performed in the indoor climate that was measured but not controlled to standard. During the tests on package A, and for a period of one week prior, the climate was recorded once per minute. The data is summed up in Figure 6. The climate for the tests on the package B was not recorded to the same detail. The results for package B are included anyway since they, despite lacking climate data, give information and insight on the generalizability of the results in this study.

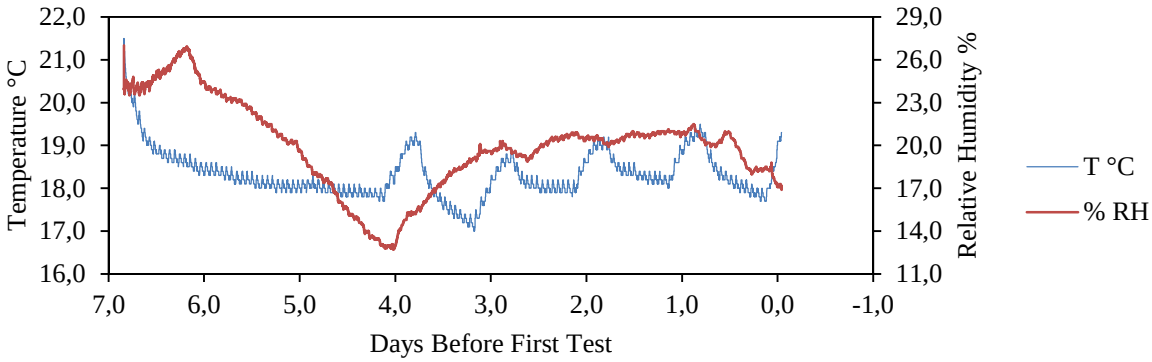



**Figure 6**: Climate data recorded prior to and during the test on package A where samples were stored and experiments conducted. Accuracy stated by manufacturer of climate logger: %RH ±5, temperature ±1°C.

In addition to the parameter study, two more packages of type B were tested. These samples were examined using x-ray tomography, this in order to study the initiation and progression of damage in close detail. One package was compressed to the point where damage was initiated, 6 mm, and for comparison another package was compressed 4 mm further, 10 mm in total. X-ray tomography is a non-destructive method that enabled studies of the interior of a material. It provides micrographs of any cross-section through the studied object. The tomograph was a Nikon HT 225. The cathode voltage was 59 kV.

## 3 Results

The load-displacement curve appears similar in all the tests performed in this study. Therefore, it is useful to present a schematic description of the curve introducing some characteristics that are referenced later in this section. Figure 7 shows an example of what the load-displacement curve looked like. Only the compression part is shown because the unloading parts of the curves show no differences. All curves had a primary peak, $PCL_I$, some had a secondary peak, $PCL_{II}$, and most showed an increasing load the last millimetres before the indenter returned. $PCL_{II}$ was larger than $PCL_I$ in some cases and smaller in others. Stiffness was defined as the greatest slope of the load-displacement curve before $PCL_I$.

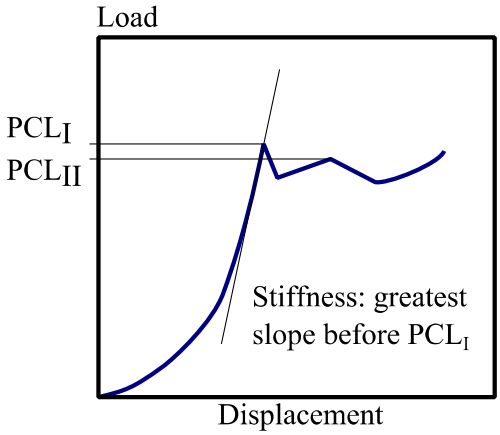



**Figure 7**: Schematic representation of a typical load-displacement curve recorded in the study introducing PCL and stiffness as characteristics of the test. The part of the curve associated with the return has been omitted.

The two packages A and B showed very similar damage behaviour under the test conditions. Figure 8 shows the load-displacement curve recorded for package A with orientation I, spherical indenter, and $x / H = 1/2$ side by side with the load-displacement curve recorded for package B with corresponding parameter values. The first visible damage in both cases is a yield line parallel to the direction of load application. After some further displacement a second yield line appears with a concave shape roughly symmetric around the first one. The measured values of $PCL_I$ are not comparable because of the uncertainty about the climate when package B was tested.

Variation of the orientation of the package had a strong influence on the slope of the load-displacement curve, but the influence on $PCL_I$ was small. In Figure 9 the graphs from the three different package orientations for $x = 55$ mm have been superimposed and three snapshots from each test are shown. As one would expect, the case where the short panel with glue flap shows the steepest rise, i.e. it has the highest stiffness. After that comes the low panel without glue flap and the most compliant is the high panel.

It is notable that the two-peak shape of the load-extension curve observed for the high panel does not reproduce for the low panel. The final damage looks similar for both high and low panel, but it seems as though the low panel has been going through multiple cycles of extending the parallel crease and creating a parabolic crease. The low panel hence appears more “crushed” than the high panel.

In Figure 10 the load-displacement curves from the test with the cylindrical indenter are shown superimposed with the ones with a spherical indenter. The indenter change does not seem to change $PCL_I$ drastically and the data is inconclusive on this matter. The curves are virtually inseparable until a point at about 50–70% of maximum load, where the curve for the spherical indenter starts to deviate on a steeper path. For all tests with cylindrical indenter the curve shows a more distinct first peak than was the case when a spherical indenter was used. In two of the curves a flat second peak can be distinguished.

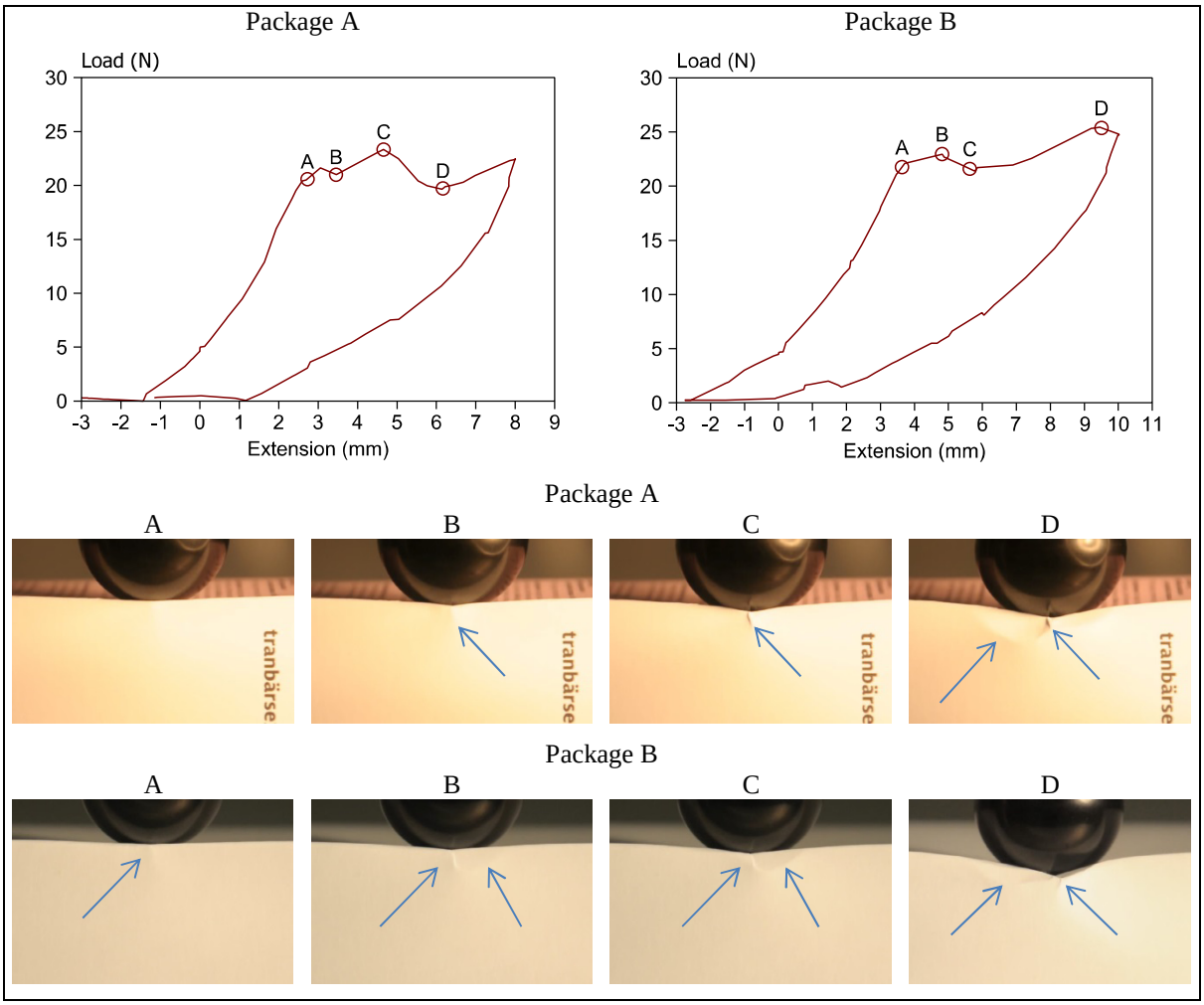



**Figure 8**: Load-displacement curves for packages A and B loaded in the middle of the panel. Snapshots below show how damage progresses. In both cases, damage starts as a yield line parallel to the direction of the load.

An examination of the video from the tests shows that the peaks are connected with distinct failure progression. Snapshots from the video for $x$ = 55 mm are shown in Figure 11. They show that the steep decline of the curve after the first peak corresponds to a rapid development of a crease parallel to the direction of load application. This crease is then taking some compressive displacement until the second peak (if it can be distinguished) after which the parabolic crease develops. For all three positions of the indenter the resulting damage had the same visual appearance as exemplified in Figure 11.

Figure 12 shows force-displacement curves recorded at different positions $x$ on three different orientations. Orientation I shows a variation of stiffness between the positions that is hard to distinguish for the other orientations. The data shows no obvious trend for $PCL_I$; it seems to be rather independent of position. The sudden drop in the middle of the elastic part of orientation III with $x$ = 30 mm is due to a slip between a flap and the rest of the package. This was established when examining the video from the test.

Force-displacement curves for the packages that were investigated in x-ray tomography are presented in Figure 13. The two curves show approximately the same maximum load. Visual inspection of the packages revealed barely visible damage on the package deformed to 6 mm and fully developed damage on the package deformed to 10 mm. X-ray tomography confirmed this. The 3D regenerations in Figure 14 show voids in a brighter shade. Thus it is possible to see where the board has delaminated. Figure 14 (a) shows the initiation of damage whereas Figure 14 (b) shows the final stage.

Magnified cross-sections of the damaged regions are presented in Figure 15 and Figure 16. It seems as though the delaminated area is wider close to the crease (Figure 15 (a) and Figure 16 (a)) and narrows as the failure progresses (Figure 15 (b) and Figure 16 (b)).

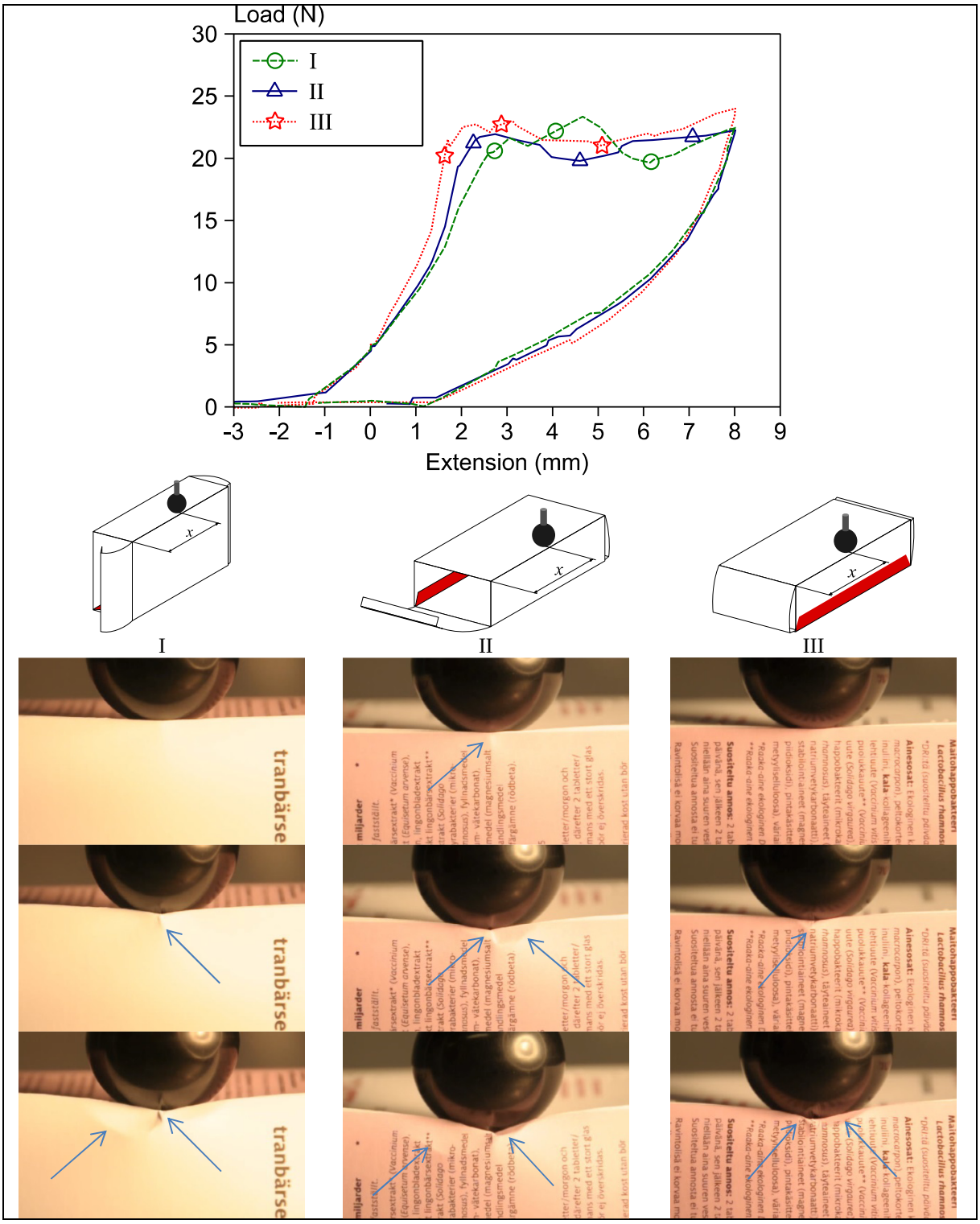



**Figure 9**: Load displacement curves and snapshots for different orientations of package A. $x$ = 55 mm.

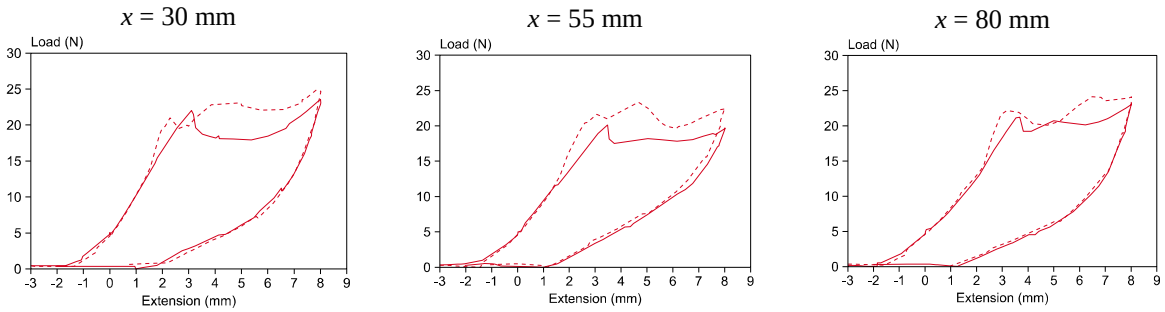



**Figure 10**: Load-displacement curves recorded using cylindrical indenter (——) and spherical indenter (– –).

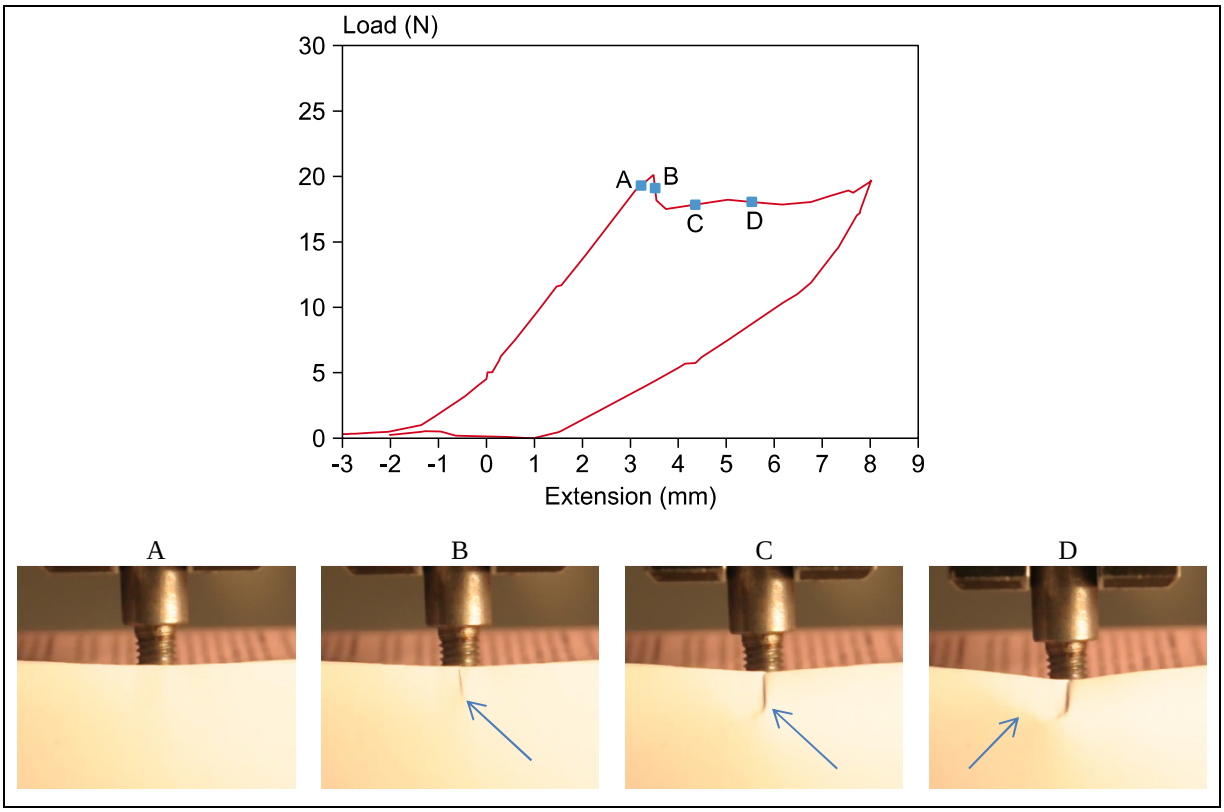



**Figure 11**: Example ($x$ = 55 mm) of load-displacement curve and snapshots recorded when using the cylindrical indenter.

## 4 Discussion

The results presented in this paper suggest that the strength of boxes subjected to concentrated loads is to a large extent dependent on material properties. Changes of box orientation that would cause large difference in Package Collapse Load in box compression [6] make almost no difference to the Package Collapse Load under a concentrated force.

The shape of the indenter had a strong impact on the nature of failure progression. As can be seen from Figure 11, the smaller cylindrical indenter led to failure progressing rapidly in an unstable manner. With the spherical indenter on the other hand, no sudden drops in load were registered indicating that failure progressed in a stable manner at all times. Stable failure progression occurs when the elastic energy that would be released by failure progression is lower than the energy required to progress failure. If the elastic energy available is large enough to progress failure the damage will develop rapidly until the elastic energy has been consumed or the specimen has failed completely, cf. [11].

Comparing the four examples of damaged packages from a retailer in Figure 1 with the damage observed in this study the similarities are obvious. Since the only data available at this point is macroscopic, no certain conclusions can be drawn. More investigations are needed in order to find a suitable method simulating concentrated loads.

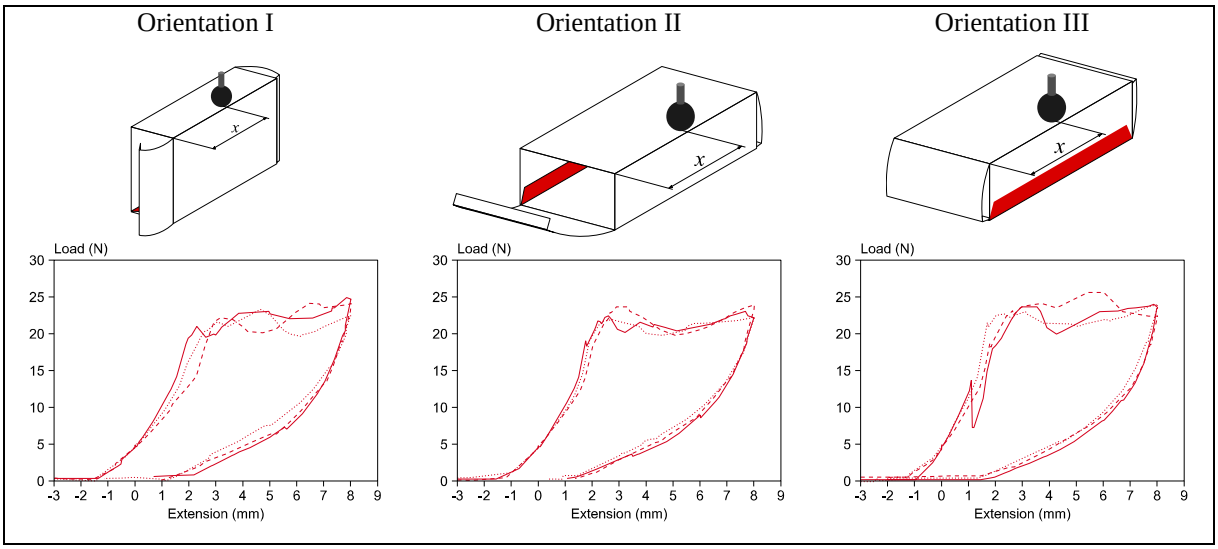



**Figure 12**: Force-displacement curves measured at positions $x$ = 30 mm (—), $x$ = 55 mm (····), and $x$ = 80 mm (– –) on the three tested orientations.

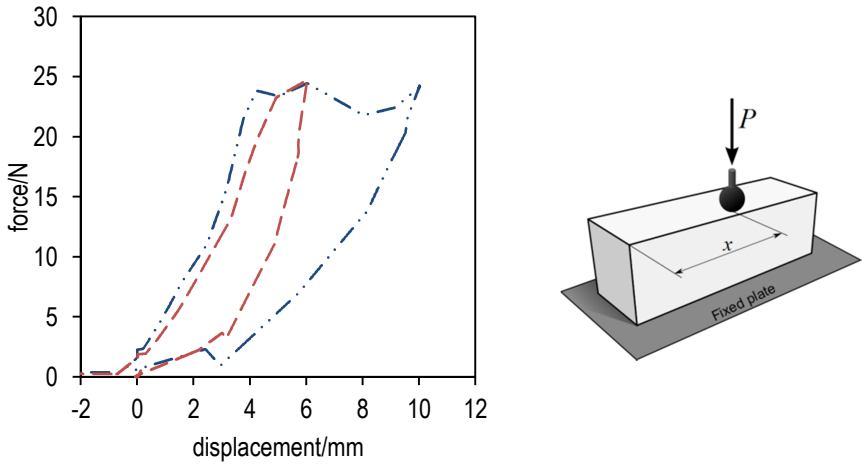
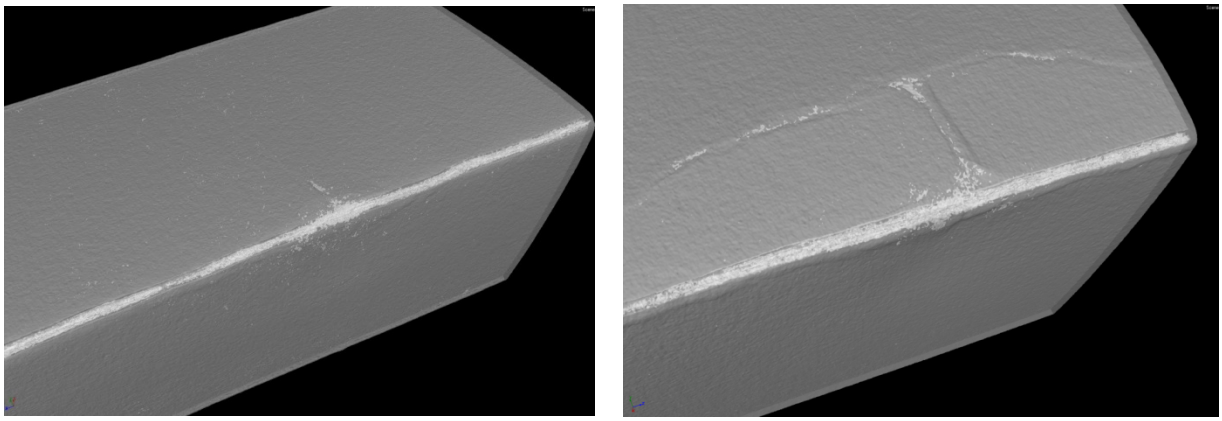



**Figure 13**: Force-displacement curves obtained when samples package B where prepared for x-ray tomography. These were done at $x$ = 140 mm, i.e. at half $H$. Samples were compressed to 10 mm (–···–) and 6 mm (– –), respectively.

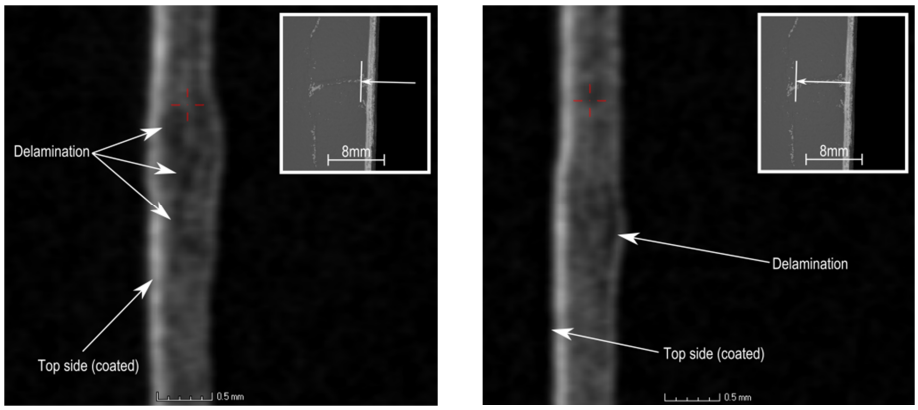
Closer studies are needed in order to understand exactly what drives failure progression. A tentative hypothesis is given below, with references to the observations in the experiments.

1. As the load increases, shear stresses are acting to progress the delamination introduced during creasing. In the x-ray tomograms it can be seen that the delamination has a wider front close to the crease. The tomogram of the package deformed to 6 mm, Figure 14 (a), shows that damage is initiated at the crease.
2. When a certain load is reached, a compressive yield line develops. The development can be either unstable or stable depending on the amount of elastic energy available as discussed above.
3. When the yield line has progressed to a certain point, stable conditions are restored (if progression was unstable).
4. The yield line deforms in compression. Eventually the bending stress in the surrounding board leads to the development of a parabolic yield line.



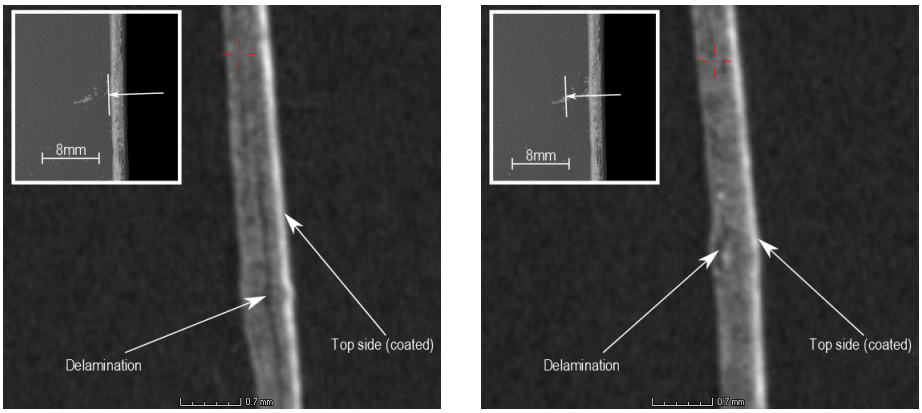
(a) (b)

**Figure 14**: X-ray tomograms showing damage on packages compressed to 6 mm (a) and 10 mm (b). Images show 3D volumes generated from tomography data. The volumes have been rendered slightly transparent in order to visualize delamination.




(a) (b)

**Figure 15**: X-ray tomograms of the package deformed to 10 mm. The figures are cross-sections of the board through the primary damage line. Inserts shows where the cross-sections were taken. Delaminated areas in the main image are darker than the surrounding board since the density is lower in those areas. One surface of the board is brighter than the other. This is the coated top side, which is denser than the base material.




(a) (b)

**Figure 16**: X-ray tomograms of the package deformed to 6 mm. The figures are cross-sections of the board through the primary damage line. Inserts shows where the cross-sections were taken. Delaminated areas in the main image are darker than the surrounding board since the density is lower in those areas. One surface of the board is brighter than the other. This is the coated top side, which is denser than the base material.

## 5 Conclusions

- Package Collapse Load has little dependence on where along a line parallel to a crease of the package the point load is applied.
- Stiffness is more geometry dependent than strength.
- On macro scale, the visual appearance of the damage due to concentrated loads shows no significant dependence on geometry.

## Acknowledgements

The authors would like to thank the following parties for their contributions to this research: BillerudKorsnäs for access to equipment and material and for valuable discussions, Tetra Pak for valuable discussions, SchurPack Sweden for supplying material, and Bofors Testcenter for performing x-ray tomography.

## References

1. M.Löfgren, 2005, "Winning at the first and second moments of truth: an exploratory study", *Managing Service Quality*, vol. 15, no. 1, pp. 102-115.
2. L. Beldie, G. Sandberg and L. Sandberg, 2001, "Paperboard packages exposed to static loads – finite element modelling and experiments", *Packaging Technology and Science*, vol.14, no. 4, pp. 171-178.
3. R.C.C. McKee, J.W.W. Gander and J.R.R. Wachuta, 1963, "Compression Strength Formula for Corrugated Boxes", *Paperboard Packaging*, vol. 48, no. 8, pp. 149-159.
4. H. Grangård and J. Kubát, 1969, "Some aspects of the compressive strength of cartons", *Svensk Pappers-tidning*, vol. 72, no. 15, pp. 466-473.
5. H. Grangård, 1970, "Compression of board cartons, part 1: correlation between actual tests and empirical equations", *Svensk Papperstidning*, vol. 73, no. 15, pp. 462-465.
6. M. Ristinmaa, N. S. Ottosen, and C. Korin, 2012, "Analytical prediction of package collapse loads – basic considerations", *Nordic Pulp and Paper Research Journal*, vol. 27, no. 4, pp. 806-813.
7. B. Frank, 2014, "Corrugated box compression – a literature survey", *Packaging Technology and Science*, vol. 27, no. 2, pp. 105-128.
8. O. Panyarjun and G. Burgess, 2001, "Prediction of bending strength of long corrugated boxes", *Packaging Technology and Science*, vol. 14, no. 2, pp. 49-53.
9. C. Everitt, G. Marin, P. Ekfeldt, H. Huang, and M. Nygårds, 2013, "Package performance BCT and point loading of paperboard packages", *Innventia Report No. 441*, Innventia, Stockholm.
10. European Carton Makers Association, 2009, *The ECMA code of folding carton design styles*, The Hague.
11. J. Tryding and P. J. Gustafsson, 2001, "Analysis of Notched Newsprint Sheet in Mode I Fracture", *Jounal Pulp and Paper Science*, vol. 27, no. 3, pp. 103-109.

# Evaluation Method of Abrasion Damage on Corrugated Board

**Meishu PIAO[1], Akinari TAKAHASHI[2], Katsuhiko SAITO[3*] and Akira HIGASHIYAMA[4]**

[1] *Graduate Student, Kobe University, Japan*

[2] *Post-Graduate Student, Kobe University, Japan*

[3] *Transport Packaging Laboratory, Kobe University, Japan*

[4] *Rengo CO.,LTD, Japan*

[*] *Corresponding author. Email: ksaito@maritime.kobe-u.ac.jp*

## Abstract

The purpose of packaging research is to improve the protection, functionality, convenience and design and to promote economic and environmental initiatives. Most importantly, proper packaging protects goods from external forces such as vibration, shock and compression. However, products are increasingly being shipped in aesthetically pleasing boxes that advertise the product through images and product information which will be displayed in shops. Appearance plays a greater role than ever before, and when a corrugated box is even slightly abrasion damaged as a result of vibration during transportation, unspoiled goods may be returned as damaged. Because abrasion damage is visually evaluated by humans, its definition and degree are subjective and differ among the evaluators.

This study proposes an objective and a quantitative evaluation method and compares the results with those determined through visual evaluation.

We reproduce abrasion damage by using a friction tester. The abrasion area is filmed as an image of abrasion damage. When analysing this image, we establish a new standard for evaluating the degree of abrasion damage. In addition, we construct and distribute a questionnaire and use the results to confirm the extent to which our method agrees with visual evaluation.

The proposed method is determined to provide an objective evaluation of abrasion damage that is compatible with the results of visual evaluation.

Keywords: Corrugated board, abrasion damage, friction test, image analysis, visual evaluation

## 1 Introduction

The most important function of packaging is to protect goods from external forces. However, more and more products are now being shipped in aesthetically pleasing boxes which advertise the product through images and product information and which will be displayed in shops. Appearance plays a greater role than ever before, and when a corrugated box is even slightly abrasion damaged by vibration during transportation, unspoiled goods may be returned as damaged. Trost, Rättö & Blohm (2013) [1] reported that during transport and handling, the package is subjected to various potential causes of damage, both as scratches on the printed surface but also as physical damage on the packaging itself. Figure 1 shows an example of abrasion damage to a corrugated cardboard box. If this damage occurs such that part of the barcode is obscured, the package cannot be scanned and will require repackaging. However, very few studies focus on abrasion damage to packages. Moreover, because abrasion damage is visually evaluated by humans, its definition and degree are subjective and differ among evaluators.



**Figure 1**: Example of abrasion damage to a corrugated cardboard box.

In this study, therefore, we propose an objective and a quantitative evaluation method and compare the results with those determined by visual evaluation.

## 2 Friction Test of Corrugated Sheet

First, we reproduced abrasion damage to large and small corrugated boards by using a friction tester (Sutherland Ink Rub Tester, Toyo Seiki Co., LTD, Japan), as shown in Figure 2. The corrugated sheet material was LB210/MC120/LB210, A flute. The size of the large board was 100 mm × 220 mm and that of the small board was 50 mm ×100 mm.

The large specimen was affixed to the bottom plate of the machine, and the small specimen was placed under the spindle. The spindle was then loaded onto the large specimen, and the corrugated sheet was rubbed by the reciprocating motion of the spindle following the arrows as shown in Figure 3. The weight of spindle was 3.131 kg, and the period of spindle motion was approximately 1.3 s per reciprocating motion.

The specimen was kept under conditions of 23 °C and 50% humidity for more than 24 h to prevent the effects of moisture as much as possible.

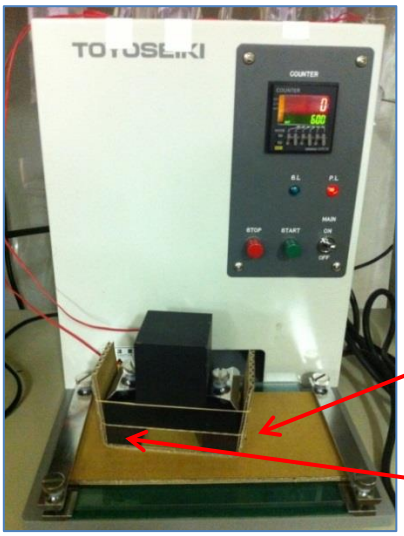


**Figure 2**: Friction tester.

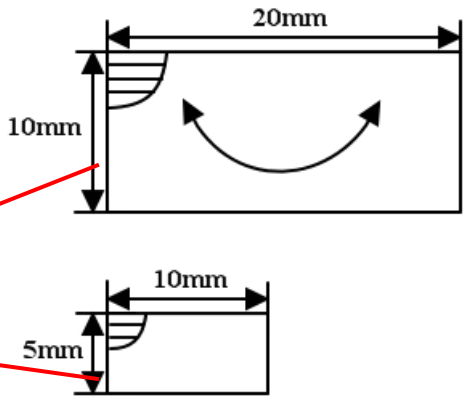



**Figure 3**: Specimens.

Figure 4 shows abrasion damage produced by the friction tester. When the corrugated sheets rubbed against each other, parts of the surface of the sheet were removed through friction.



**Figure 4**: Abrasion damage produced by the friction tester.

# 3 Image Analysis

## 3.1 Process of Image Analysis

Packaging damage is usually caused by vibration during transportation or shock during handling. Because appearance is considered a critical factor, even slight abrasion is regarded as damage.

Our proposed objective and quantitative evaluation method for determining the extent of damage to packaging is based on image analysis, which is used to detect scratches on metal and glass.

The image analysis process consists of the following steps:

1. Film the abrasion area with a *charge coupled device (*CCD) camera.

2. Correct the brightness bias caused by LED light.

3. Extract the region damaged by abrasion.

## 3.2 Photography

### 3.2.1 CCD Camera

In this study, we used a CCD camera (GE60, Library Co., Ltd. Japan; Figure 5) to photograph abrasion damage. This camera had the ability to record 8 bits of brightness information for each image pixel. The brightness is shown as an integer value from 0 to 255, in which brightness strength relates to larger values. To compensate for the effect of light during the photography, we covered the CCD camera, light source (LED light) and specimen with a box and black-out curtain to block the outside light (Figure 5).

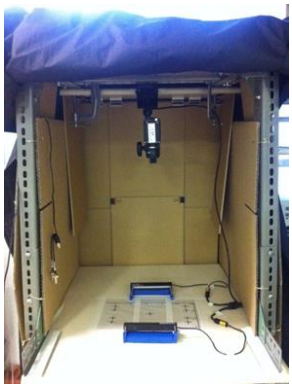


**Figure 5**: CCD camera covered with black-out curtain.

### 3.2.2 LED Light

When filming the subject with a monochrome camera, light of the subject's complementary colour was used to clearly reveal contrast. The colour of the corrugated sheet used in this study is close to orange. As shown in Figure 6, the complementary colour of orange is blue. Therefore, we used a blue LED light (MBRL-CB13015,

Schott Moritex Co., Ltd. Japan; Figure 7).

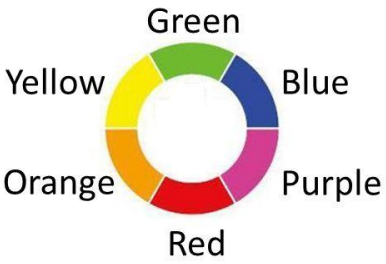



**Figure 6**: Complementary colours appear opposite each other on the colour wheel.

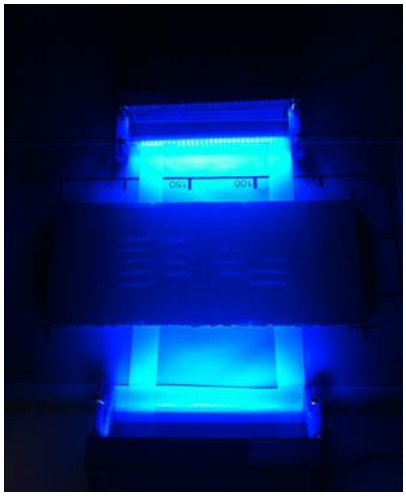


**Figure 7**: Blue LED light used in this study.

### 3.2.3 Image Analysis Software

The image analysis software used in this study was Cosmos32 ver.6.5 (Library Co., Ltd. Japan; Figure 8). Cosmos32 supports various images such as static, moving, high-resolution, monochrome and colour images and can be used for extraction, measurement and analysis of particle image, density and colour. In addition, we used this software to convert data to *comma separated values* (CSV) so it could be processed by Microsoft Excel software.

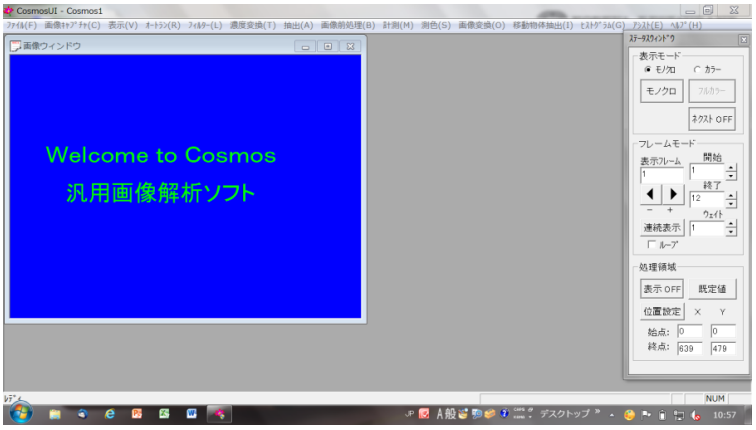



**Figure 8**: Initial screen of Cosmos32 software.

### 3.3 Brightness Correction

Because LED light is inadequate for illuminating a subject in uniform brightness, brightness bias occurs in the image. Therefore it is necessary to perform image calculation to correct this bias by removing background noise. The brightness of our specimen prior to testing was not uniform, as shown in Image A of Figure 9. We assumed the brightness of any pixel as $x_{ai}$, and we created an image with brightness $x_{bi}$ of $x_{bi} = 255 - x_{ai}$ in order to correct the brightness bias (Image B of Figure 9). We then superimposed the image obtained after testing (Image C) onto Image B in order to create Image D, which is without brightness bias, for analysis use. Figure 10 shows the process of image correction, and Figure 11 shows a simplified illustration of correction.

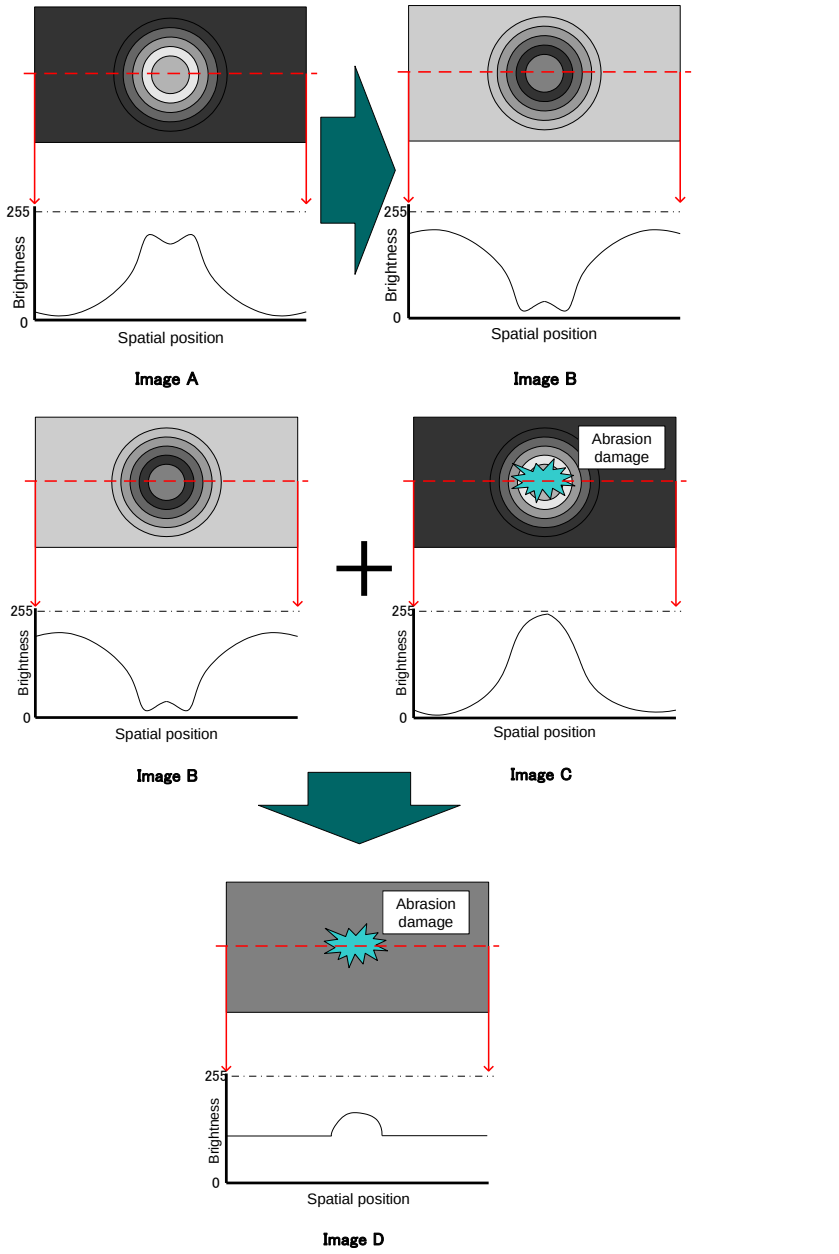



**Figure 9**: Conceptual diagram of image correction for brightness bias.

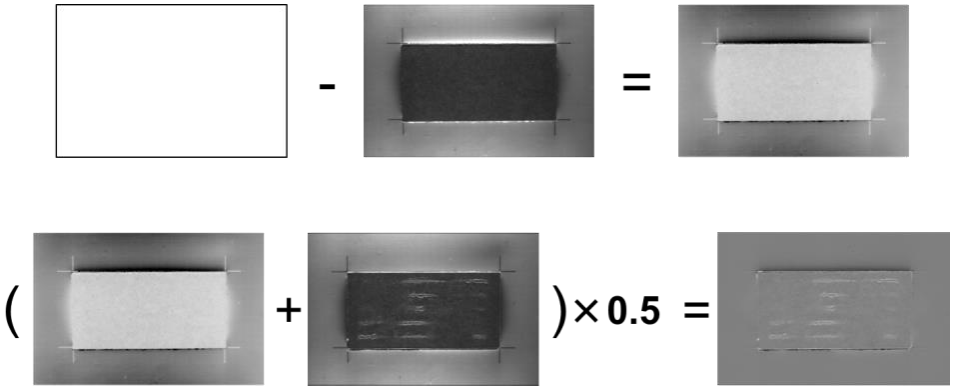



**Figure 10**: Process of image correction.

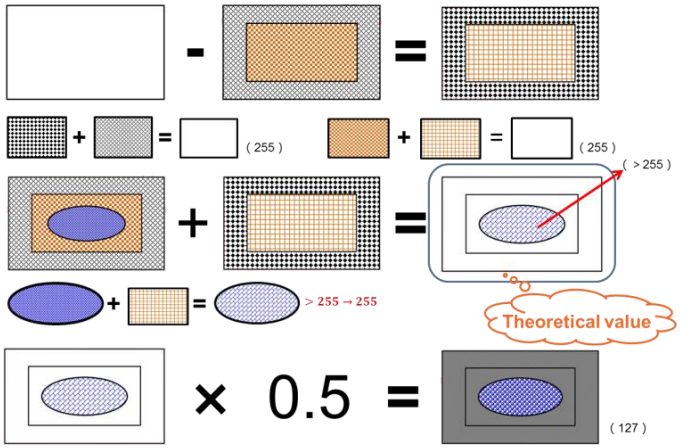



**Figure 11**: Simplified illustration of image correction.

### 3.4 Extraction

When extracting the area damaged by abrasion, the most important point is determining the threshold of brightness. The area of the abrasion damage is the product of the number of pixels whose brightness is higher than the threshold of brightness and the area of damage per pixel. The brightness distribution of the abrasion damaged area is expressed by the histogram of brightness whose brightness is higher than the brightness threshold in the analytical image.

We defined the threshold of brightness as that when the extraction area is the same as the visual abrasion damage. Because the specimens used in this study originated from the same lot of corrugated sheets, the brightness threshold should be the same. We determined that the brightness threshold of our samples was 140. Figure 12 shows the extraction image of one of the samples.

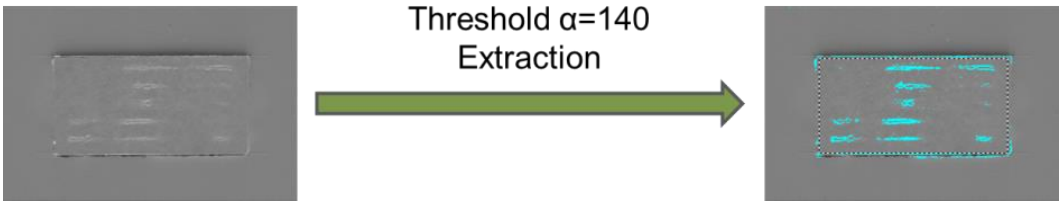



**Figure 12**: Extraction image.

## 4 Evaluation Method of Abrasion Damage

As shown in Figure 13, abrasion damage has three patterns: different area, different brightness and different area and brightness. Thus, when evaluating abrasion damage, both abrasion area and brightness should be considered.

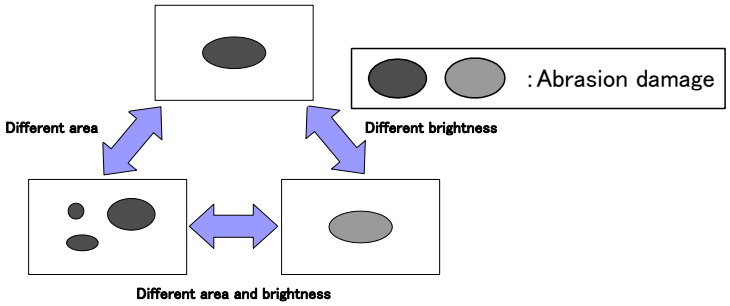



**Figure 13**: Relationship of abrasion damage.

Accordingly, to evaluate the degree of abrasion damage, we established a standard known as the Comprehensive Abrasion Damage Index (CADI), which can be used to evaluate the composite area and brightness.

$$\boldsymbol{CADI} = \sum_{i=\alpha+1}^{\beta} \frac{i-\alpha}{\beta-\alpha} \times \boldsymbol{S_i} + \sum_{i=\beta+1}^{\gamma} \boldsymbol{S_i}, \quad (1)$$

where $\alpha$ is the brightness threshold, $\beta$ is the brightness of being judged "annihilation". Since corrugated board is made of several layers of papers whose brightness are different. When the first layer is rubbed and the second layer appears, the trend of average brightness will change. $\beta$ is the brightness when the average brightness trend changes. γ is the maximum brightness of appearance. $s_i$ is the area ratio of brightness $i$.

$$\boldsymbol{S_i} = \boldsymbol{S_a} \times \frac{\boldsymbol{K_i}}{\boldsymbol{100}} = \frac{\boldsymbol{S}}{\boldsymbol{S_b}} \times \frac{\boldsymbol{A_i}}{\boldsymbol{S}} = \frac{\boldsymbol{A_i}}{\boldsymbol{S_b}}, \quad (2)$$

where $S_a$ is the area ratio of abrasion region, $K_i$ is the appearance probability of brightness $i$, $S$ is the area of abrasion damage, $S_b$ is the friction area and $A_i$ is the area of brightness $i$.

And abrasion damage area ratio (ADAR) can be calculated by following formula.

$$\boldsymbol{ADAR} = \sum_{i=\alpha+1}^{\gamma} \boldsymbol{s_i} \quad (3)$$

Figure 14 shows the entire process of the abrasion damage evaluation.

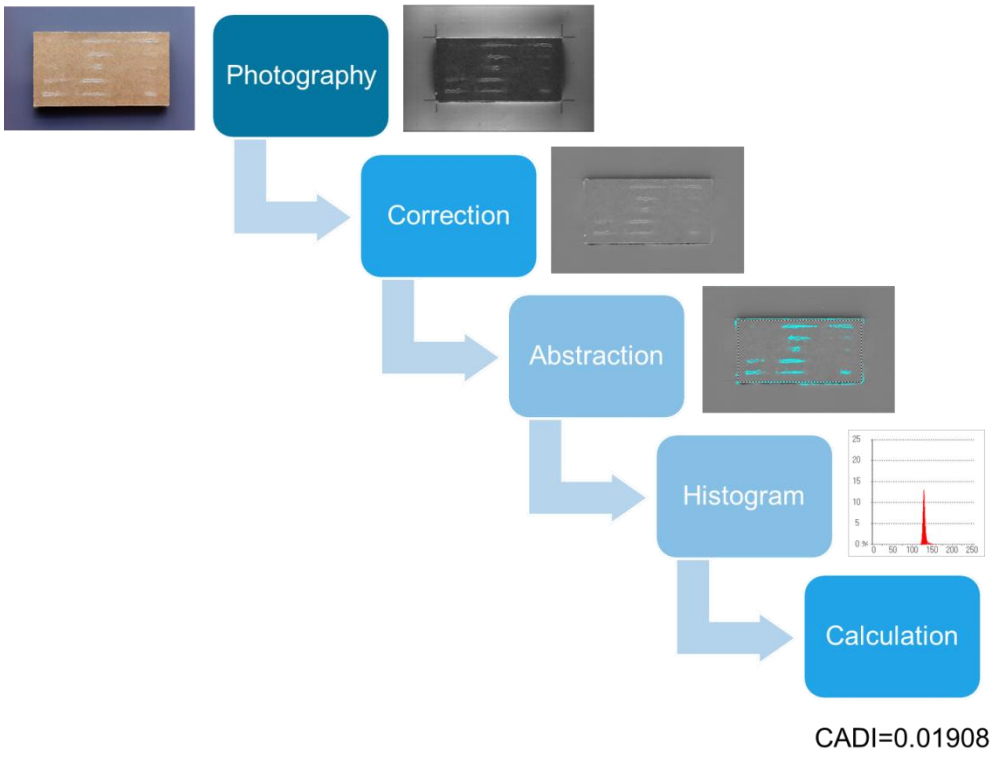



**Figure 14**: Process of abrasion damage evaluation.

## 5 Questionnaire

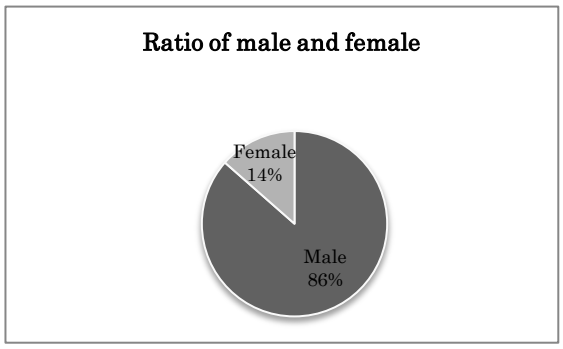
After conducting our evaluation, the following questions remained:

- Threshold α (140 in this study) is the brightness when the extraction image is the same as the visual abrasion. Is this value objective, and what is the basis?
- To what degree is the abrasion of CADI = 0.01908?
- What effect does the abrasion of CADI = 0.01908 have on consumer behaviour?

Thus, we conducted a survey of consumer attitude regarding abrasion damage to a corrugated sheet (LB210/MC120/LB210, A flute).

We developed and distributed a questionnaire at the Tokyo Metropolitan Industry and Trade Center on 1–3 October 2013 to 185 participants of Pack Show 2013, and the effective number among them was 170 people.

Figure 15 shows the ratio of male and female participants, and Figure 16 shows the ratio of age.



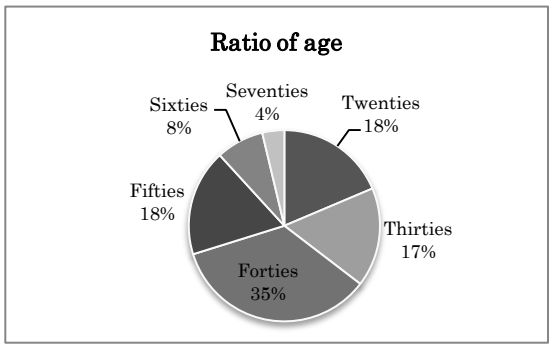
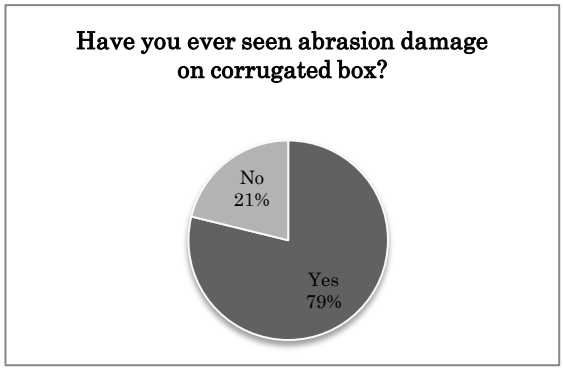




**Figure 15**: Ratio of male and female.

**Figure 16**: Ratio of age.

First, we asked some questions to reveal consumers' attitudes regarding abrasion on corrugated cardboard boxes of goods. Figures 17–20 shows the questions and the ratios of answers.



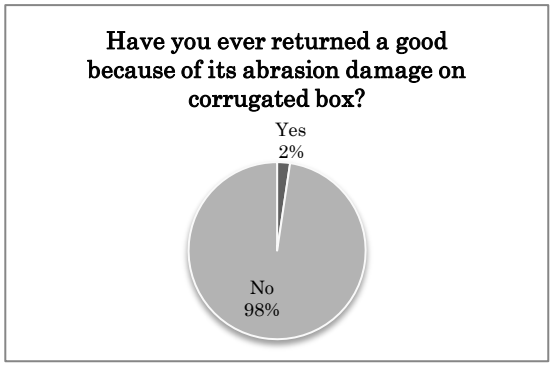
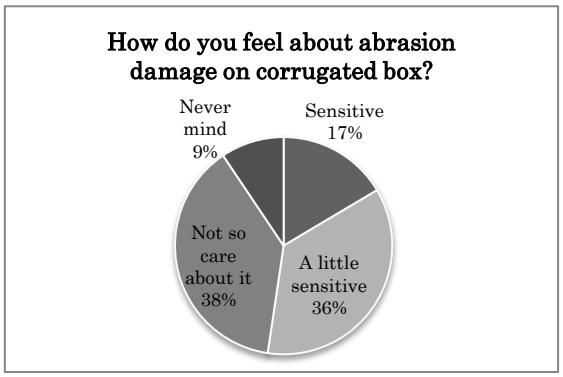




**Figure 17**: Question 1 and the ratio of the answer.

**Figure 18**: Question 2 and the ratio of the answer.



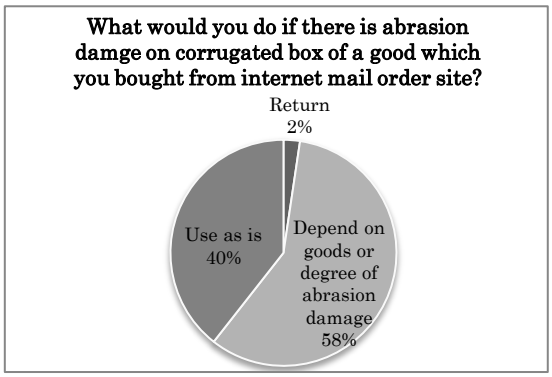




**Figure 19**: Question 3 and the ratio of the answer.

**Figure 20**: Question 4 and the ratio of the answer.

Next, we created a sample with seven specimens that have different degrees of abrasion damage. Figure 21 shows the sample, with No.① as an undamaged corrugated sheet and No.⑦as the sheet with the most severe abrasion damage.

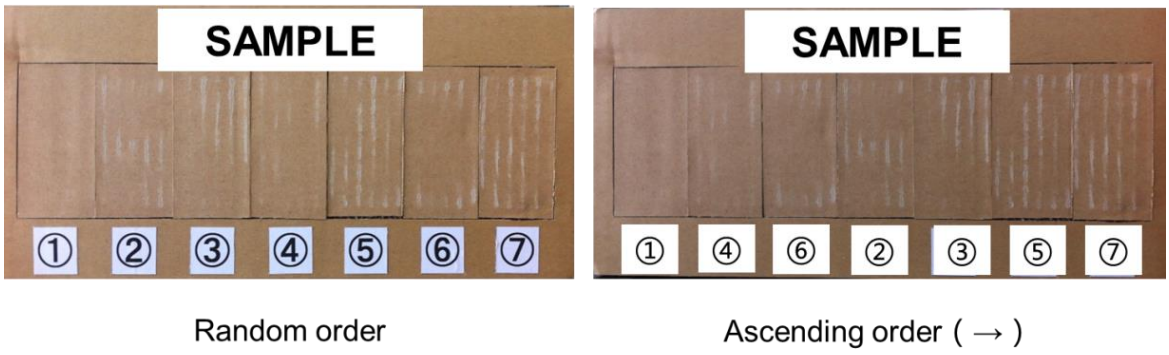



**Figure 21**: Sample used in the questionnaire.

We randomly arranged the other specimens and asked the following two questions:

1. If there has been abrasion such as No. ①– No. ⑦on a corrugated box of items, would you buy it?

The results appear in Figure 22. The numbers of the specimens in Figure 22 are in an ascending order of abrasion damage degree. As expected, the degree of abrasion damage becomes more severe, the acceptable ratio falls. From Figure 22, we can also see nearly 60% of answerers said "It's OK." to the No.⑦ abrasion damage when it appeals on the corrugated boxes of can beers. However, about half of the answerers said they would not buy a PC in corrugated box whose abrasion damage as No.② specimen in Figure 21.

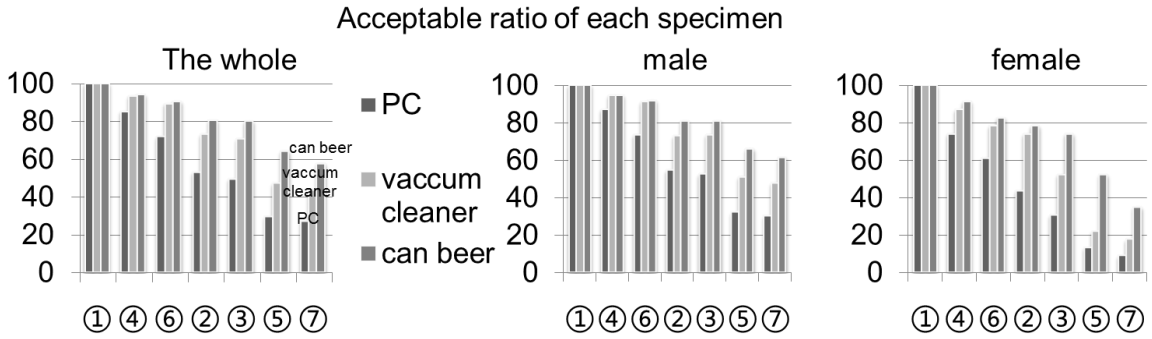
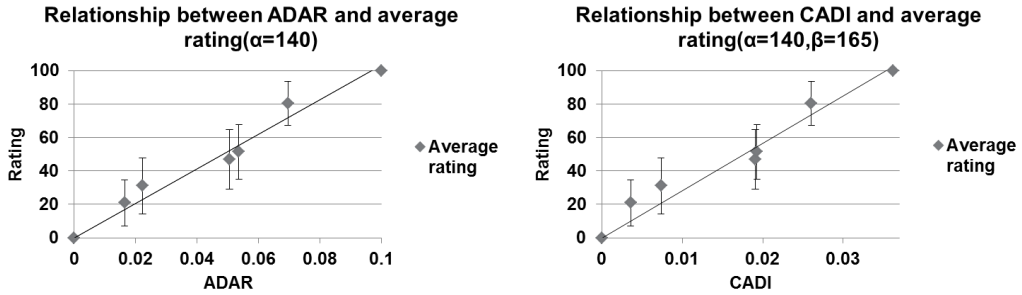



**Figure 22**: Acceptable ratio of each specimen.

2. Assuming that the abrasion damage degree of specimen No. ① is 0 and that of No. ⑦ is 100, then please rate the specimens from No. ② through No. ⑥.

Graph A in Figure 23 shows the relationship between ADAR and average ratings of the specimens. Graph B shows the relationship between CADI results and the average ratings of the specimens.




A B

**Figure 23**: Relationship between the evaluation value and average rating.

**Sum of squared deviation**

To determine the approximate degree between the evaluation value and the ratings, we used the theory of the

sum of squared deviations, which is an index of sample dispersion and can be calculated as

$$S=\sum_{i=1}^{170}(x_i-\bar{x})^2, \tag{3}$$

where $x_i$ is the sample data and $\bar{x}$ is the average rating of the samples.

Because the ratings of No. ①and No. ⑦were determined, we substituted the values on the line that linked No. ① to No. ⑦($\tilde{x}_j$ in Figure 23) into Eq. (4) rather than $\bar{x}$ in Eq. (3). We then calculated the sum of the squared deviations as

$$S=\sum_{i=1}^{170}\sum_{j=1}^{7}(x_{ij}-\tilde{x}_j)^2, \tag{4}$$

where $S$ is the sum of the squared deviations, $i$ is the number of survey participants (1–170) and $j$ is the number of specimens (①–⑦). For example, $x_{14}$ represents the No. ④ specimen rating from survey participant No. 1.

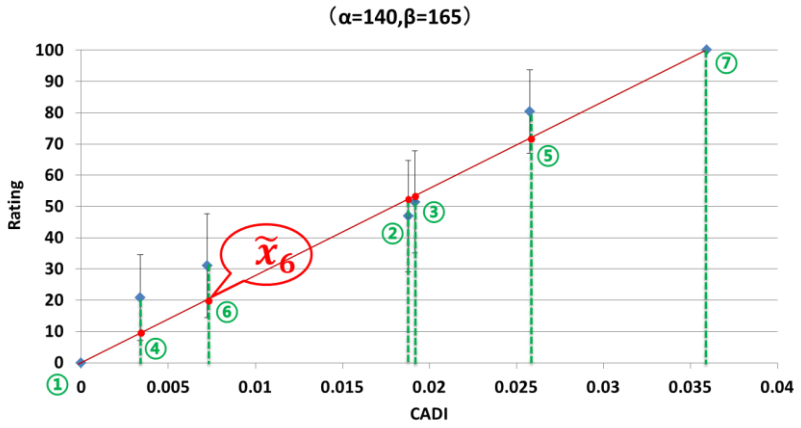



**Figure 24**: Relationship between CADI and average rating.

Then we changed the value of $\alpha$ and $\beta$ and calculated the sum of squared deviation. From the results shown in Figure 25, we can see that the minimum value of sum of squared deviation is 238080.1 when the threshold brightness $\alpha$ is 136 and the brightness of being judged as 'annihilation' $\beta$ is 141. We can also know from the Figure 25 that the minimum of sum of squared deviation when evaluate with the ADAR ($\alpha$=138) is 238251.1 and it is bigger than the value when evaluate with CADI.

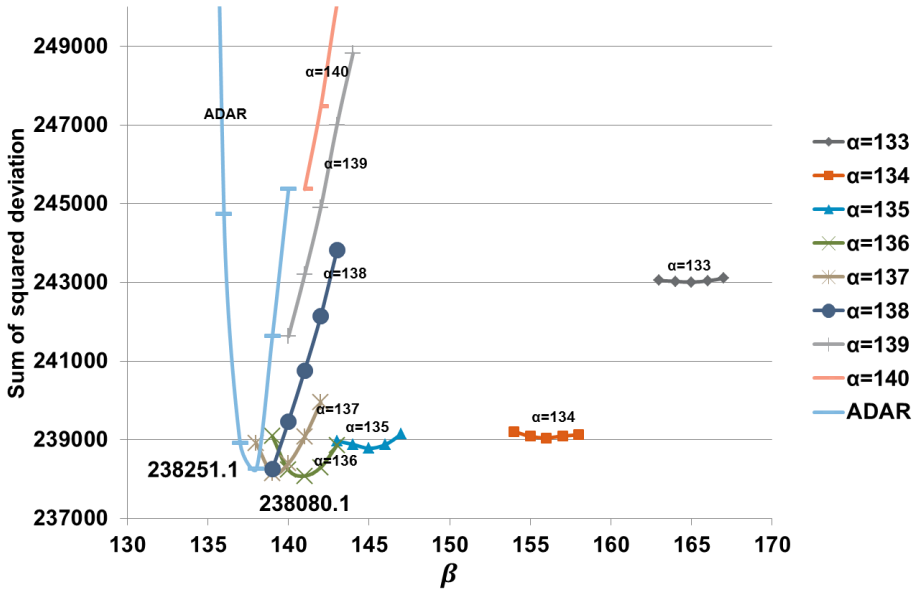



**Figure 25**: Relationship between $\alpha, \beta$ and the sum of the squared deviations.

Figure 26 shows the relationship between the various evaluation values and the average ratings.

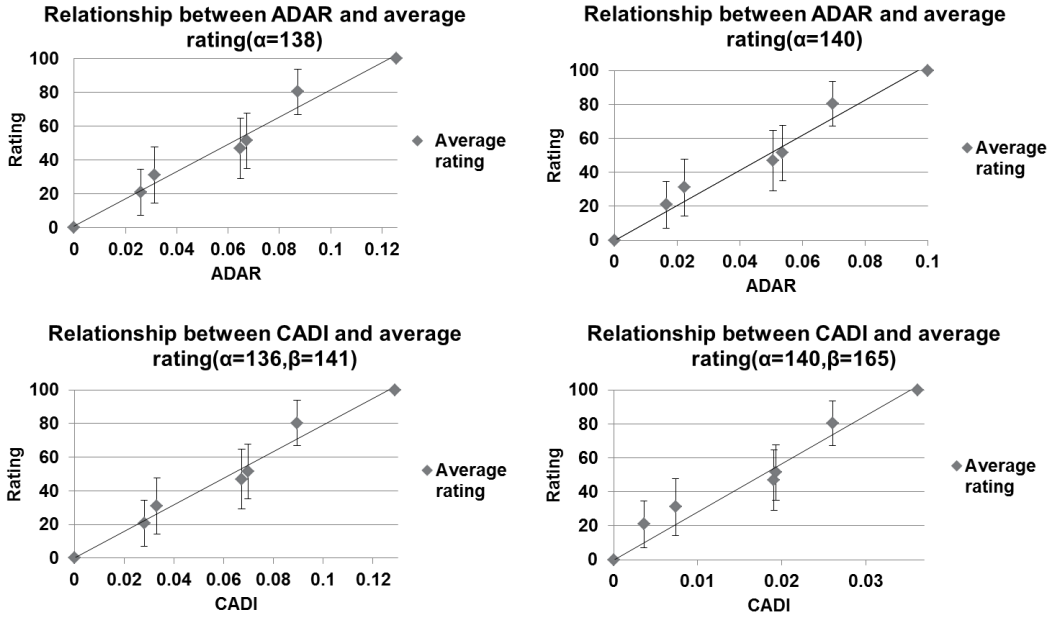



**Figure 26**: Relationship between various evaluation values and average ratings.

Figure 27 shows the extraction images of $\alpha$ = 138 and $\alpha$ = 136.

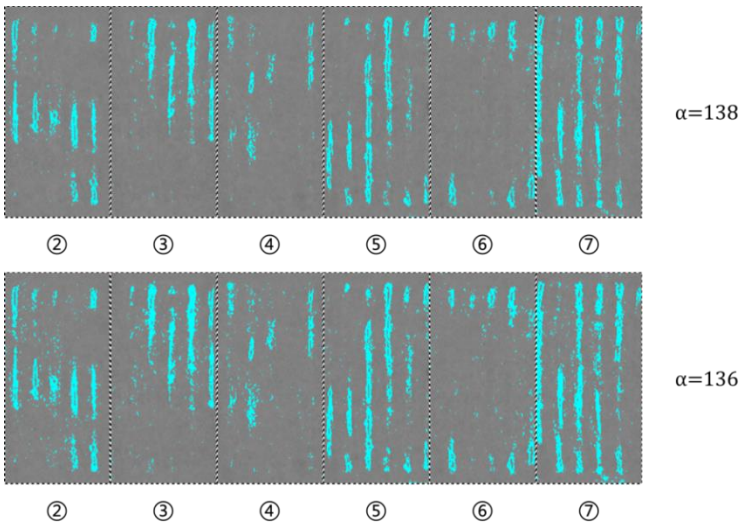



**Figure 27**: Extraction images of $\alpha$ = 138 and $\alpha$ = 136.

Assuming that the sum of the squared deviations evaluated with CADI as $s_1$, and that evaluated by ADAR as $s_2$, then $s_{1min} < s_{2min}$. In other words, the results of evaluation by CADI are closer to those by visual evaluation than those by ADAR.

## 6 Conclusions

In this study, the results of CADI and ADAR were both similar to the results of visual evaluation. That means both CADI and ADAR can be used to evaluate the damage. However, while it is only slight, the results of evaluation by CADI are closer to those evaluations by visual than those by ADAR. From this we can also get a result that abrasion damage is related to not only abrasion damage area but also brightness.

## 7 References


1. T. Trost, P. Rättö & E. Blohm, 2013, "Packaging Wear during Transport Simulation-Comparison between Laboratory Coated Samples and Commercial Samples," *poster 26 of 26th IAPRI Symposium on Packaging 2013*, Espoo, Finland, June 10-13, pp. 626-635.
2. J. Li, K. Saito, 2008, "Damage Evaluation of Abrasion on Corrugated Board", *Journal of Packaging Science & Technology, Japan*, vol. 17, no. 3, pp.185-189(in Japanese).
3. K. Matsuura, K. Saito and A. Higashiyama, 2010, "Abrasion Damage Evaluation of Stacked Corrugated Board by Rocking Motion," *Journal of Packaging Science & Technology, Japan*, vol. 19, no. 4, pp. 289-296(in Japanese).
4. F. Ando, K. Saito and A. Higashiyama, 2012, "Simplified Vibration Test for Corrugated Box Abrasion," *Journal of Packaging Science & Technology, Japan*, vol. 21, no. 3, pp. 213-2218(in Japanese).

# Shock Analysis during Fruits Export from Japan to Neighbouring Regions

**Hiroaki Kitazawa[1,2*], Yutaka Ishikawa[1] and Katsuhiko Saito[3]**

[1] *Ph. D. Candidate, Graduate School of Maritime Sciences, Kobe University, Japan*
[2] *Food Engineering Division, National Food Research Institute, Japan*
[3] *Transport Packaging Laboratory, Kobe University, Japan*

[*] *Corresponding author. Email: ktz@affrc.go.jp*

**Abstract:** In order to determine measures to prevent damage to fruit from shock during export from Japan to neighbouring regions, we measured the shock frequency and level during the transport of strawberries, cherries, apples, pears, and peaches to Taiwan, Hong Kong, and Thailand by using an acceleration recorder. In addition, we determined the effects of the shock frequency and level on the commercial quality of cherries using two kinds of packaging in order to develop effective cushioning packaging. We compared the shocks to fruit during air and marine transport and found that the former produced higher shock severity and frequency because of the severe shock generated upon loading and unloading at airports. Because the landing shock was very low, we guessed that such severe shock occurred when the samples were handled or loaded on a container dolly. For the cherries, we found that the shock during transport was reduced when several corrugated fibreboard containers were loaded into a larger corrugated fibreboard box (improved packaging) rather than the conventional packaging style of fastening two or three corrugated fibreboard boxes together by plastic bands. This suggests that not only was shock absorbed by the larger box but also that the handling changed. The quality of fruit after transport was better with the improved packaging than with conventional packaging. Based on these findings, cushioning packaging can be designed to reduce the damage to fruit caused by shock during transport.

**Keywords:** acceleration, cushioning packaging, export, fresh produce, shock.

## Introduction

The Japanese government wants to expand the export of fresh produce such as strawberries, cherries, and peaches [1]; the main target areas are neighbouring regions such as Taiwan, Hong Kong, and Thailand.

Stresses like shock and vibration that afflict fresh produce during transportation have been alleviated by improvements in transportation, including the quality of trucks [2] and roads [3]. Despite these improvements, shock during transport remains a major cause of damage to fresh produce such as soft fruits [4]. Especially, our previous research suggested that the shock conditions in neighbouring regions are more severe than in Japan [4]. Therefore, fruit export from Japan to neighbouring regions may require robust cushioning packaging. However, there is no information on suitable packaging for export from Japan to neighbouring regions.

In this study, we measured the shock frequency and level during the transport of strawberries, cherries, apples, pears, and peaches by using an acceleration recorder in order to determine measures to prevent damage to the fruits from shock during export. We also considered the difference in shock conditions during marine and air transport because there have been few reports about the shock frequency and level to fresh produce during marine transport.

Strawberries and cherries have short shelf lives compared with apples, pears, and peaches. Therefore, using marine transportation to export these fruits is difficult. Thus, the shock conditions during air transport need to be considered for the design of suitable packaging for strawberry and cherry export. Based on this point, we determined the effects of different packaging styles on the shock frequency and level and the cherry quality after export via air.

## Materials and Methods

### Routes for Shock Analysis during Export

Figure 1 is a map showing the regions considered in this research.

Strawberries were transported from Fukuoka, Japan to a department store in Bangkok, Thailand. Transportation from Fukuoka to Narita was by truck, mostly on highways. Transportation from Narita International Airport (NIA) to New Bangkok International Airport (NBIA) was by airplane. Transportation from NBIA to the department store was by truck.

Apples and cherries were transported from Yamagata, Japan to a department store in Taipei, Taiwan. Transportation from Yamagata to NIA was by truck. Apples were transported from Kawasaki Port, Kanagawa to Taipei Port by ship. Cherries were transported from NIA to Taiwan Taoyuan International Airport (TTIA) by airplane. In Taipei, both fruits were transported by truck.

Pears were transported from Imari, Japan to a department store in Taipei, Taiwan. Transportation from Imari to Tokyo Port was by truck. Then, these were transported from Tokyo Port to Taipei Port by ship. In Taipei, these were transported by truck.

Peaches were transported from Yamagata, Japan to a department store in Hong Kong, China. We compared the difference in shock frequency and level during export via air and marine transport. One group of peaches was transported from Yamagata to NIA or Tokyo Port by truck. Then, the fruit transported to NIA were transported to a department store in Hong Kong via Hong Kong International Airport (HKIA). The other group of peaches was transported to Tokyo Port and then transported to Hong Kong Port. In Hong Kong, both fruits were transported by truck.

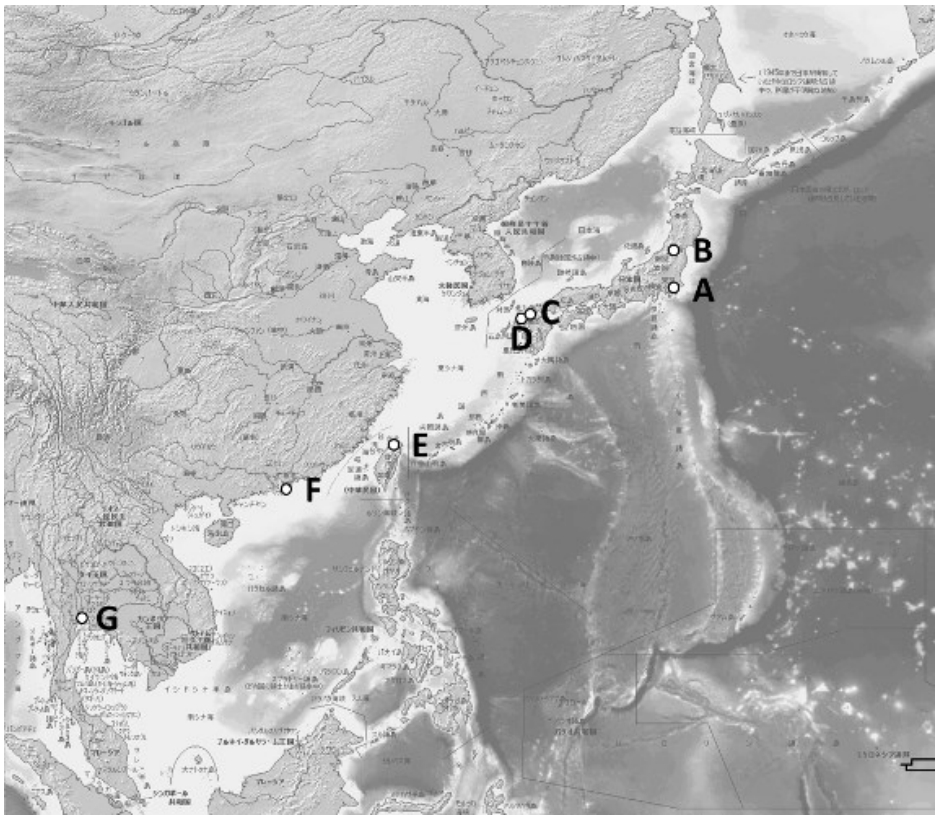



Figure 1. Regions considered in this research: (A) Narita, (B) Yamagata, (C) Fukuoka, (D) Imari, (E) Taipei, (F) Hong Kong, and (G) Bangkok.

### Shock analysis conditions

Shock was measured by a 3-D accelerometer (DER-mini, Shin-ei Technology) that weighed about 800 g including batteries. The recorder was attached to the bottom of boxes by double-sided tape (Figure 2). The measurement conditions were as follows: sampling of 1.0 ms and data trigger level of 5%. To compare the shocks to the peaches during air and marine transport, we also used another type of accelerometer (G-Men, NR50α, SRIC; Figure 3). For peach export, four boxes containing the fruit were fastened together by plastic bands. The box containing the accelerometer was set at the bottom of the boxes.




Figure 2. Accelerometer in box (for strawberry [5] and peach export [6]).



Figure 3. Accelerometer to compare shocks to peaches during air and marine transport [6].

The accelerometer was attached to the bottom of the box or embedded in polystyrene foam.

**Effect of difference in packaging styles on damage to cherries**

We used two kinds of packaging for exporting fruit from Yamagata, Japan to Taipei, Taiwan. The tested packaged styles are shown in Figure 4, and the details are as follows:

**Conventional packaging (Control):** The test sample was a corrugated fibreboard box containing two PET resin-made trays packed with 500 g of cherries. This is the most common packaging style for cherries in Japan. Three boxes were fastened together by plastic bands.

**Improved packaging:** Individual boxes were the same as those used for the control. Five boxes were then fastened together by plastic bands, and two fastened boxes were loaded into a larger corrugated fibreboard box.




Figure 4. Packaging styles for cherry export [7]. Left: conventional packaging (control). Right: improved packaging.

The export routes and shock analysis conditions are given above. After the fruit arrived in Taipei, we investigated the rate of damaged fruit and the degree of damage. The degree of damage was calculated by using the following formula:

$$\Sigma\,(S \times n) / N$$

where $S$ stands for the damage scores (1: slight, 2: severe), $n$ is the number of damaged fruits, and $N$ is the total number of fruits.

## Results

### Shock analysis

**Strawberry (via air):** Figure 5 shows typical shock data for strawberry transported via air from (a) Fukuoka to NIA, (b) NIA to NBIA, and (c) NBIA to the department store in Bangkok. The most shock was recorded when strawberries were loaded to the airplane. The maximum shock acceleration of 50 G during overall transportation occurred during loading at NIA. No shock was detected during airplane transportation.

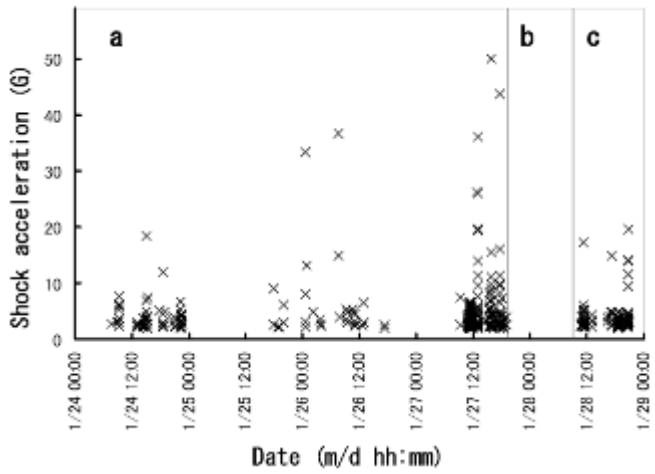



Figure 5. Shock during air transport of strawberries from Fukuoka to Bangkok [5]: (a) Fukuoka → NIA (truck),

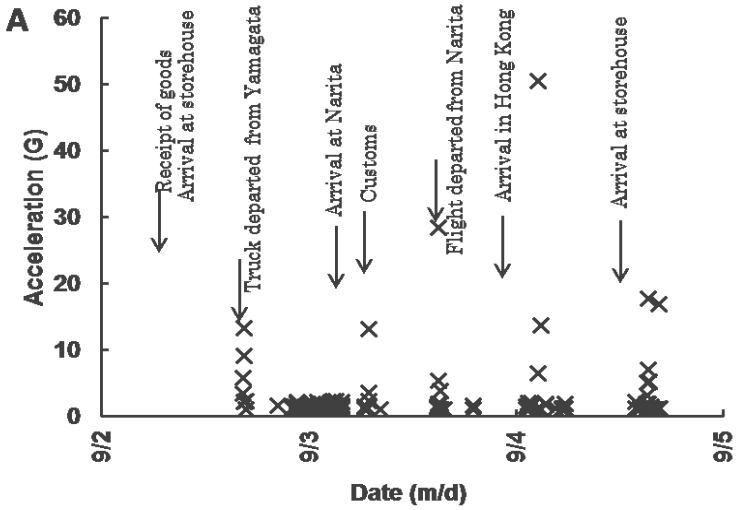
(b) NIA → NBIA (air), and (c) NBIA → department store in Bangkok (truck). Dots indicate shock occurrence and acceleration.

**Apples and pears (marine transport):** Table 1 presents the shock frequency during marine transport of apples and pears. Most of the shock to the apples occurred during land transport in Japan and Taipei. The shock level and frequency were greater in Taipei than in Japan. Only one shock was observed during marine transport. For the pears, several shocks were observed during marine transport. The shock frequency was greater in Taipei than in Japan, while the maximum shock acceleration of over 20 G occurred in Japan.

Table 1 Acceleration during marine transport of apples and pears [6].

| **Apple** | Acceleration | | | | | |
|---|---|---|---|---|---|---|
| Route (Method) | 2.5-5G | 5-10G | 10-20G | 20G- | Total | Maximum acceleration (G) |
| Yamagata→Kawasaki (Truck) | 18 | 7 | 2 | 0 | 27 | 19.5 |
| Kawasaki→Taipei (Ship) | 1 | 0 | 0 | 0 | 1 | 3.0 |
| Transportation in Taipei (Truck) | 34 | 11 | 5 | 4 | 54 | 33.9 |
| Total | 53 | 18 | 7 | 4 | 82 | |
| **Pear** | Acceleration | | | | | |
| Route (Method) | 2.5-5G | 5-10G | 10-20G | 20G- | Total | Maximum acceleration (G) |
| Imari→Tokyo (Truck) | 17 | 5 | 2 | 1 | 25 | 20.6 |
| Tokyo→Taipei（Ship） | 21 | 6 | 2 | 0 | 29 | 15.4 |
| Transportation in Taipei (Truck) | 28 | 5 | 4 | 0 | 37 | 13.9 |
| Total | 66 | 16 | 8 | 1 | 91 | |

**Peaches (air transport versus marine transport):** Figure 6 shows the **s**hock level and frequency data of peaches transported from Yamagata to Hong Kong. The air transport showed a similar tendency to the strawberry export; that is, large shocks frequently occurred at the airport. On the other hand, few shocks were observed during marine transport except when the samples were being transported over land. Both the shock level and frequency were less than during air transport.



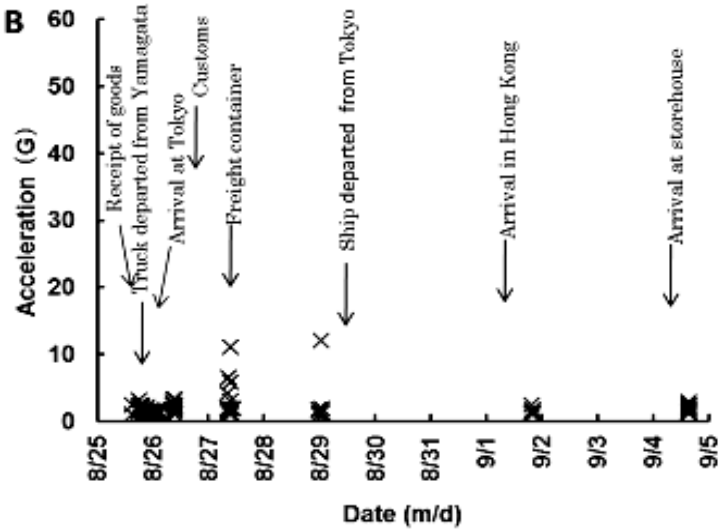
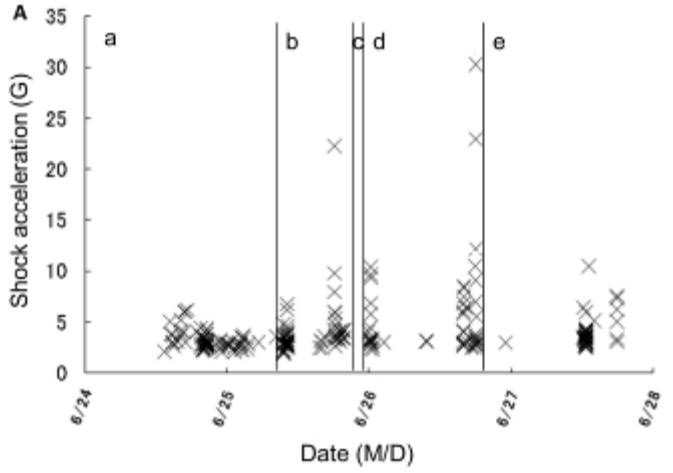



Figure 6. Shocks to peaches during transport from Yamagata to Hong Kong [6]: (A) air and (B) marine.

**Effect of difference in packaging style on damage to cherries**

**Shock analysis:** Figure 7 shows typical shock data for the cherries during air transport. The timing of the shock occurrences was similar for both packaging styles. The analysis results showed that large and high levels of shock occurred at the airport, which supported the air transport results for strawberries and peaches. Both the shock level and frequency were less with the improved packaging than with the control.



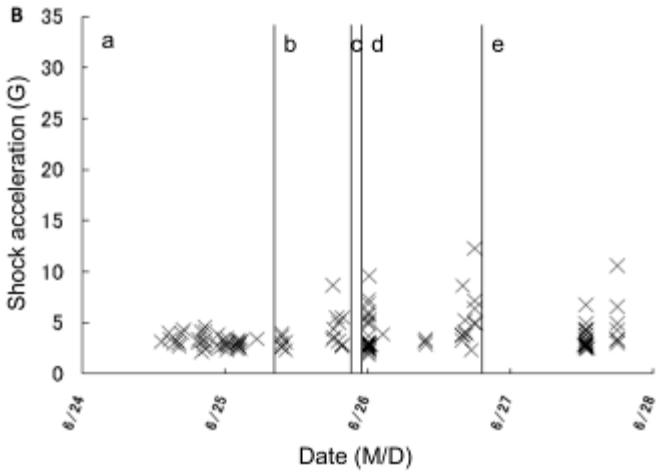



Figure 7. Shock during air transport of cherries from Yamagata to Taipei [7]: (A) conventional packaging (control) and (B) improved packaging. (a) Yamagata → NIA (truck), (b) in NIA, (c) NIA → TTIA (air), (d) TTIA, and (e) TTIA → department store in Taipei (truck). Dots indicate shock occurrence and acceleration.

**Cherry quality:** Table 2 presents the fruit quality after arrival in Taipei. Both the rate and degree of damage were less with the improved packaging than with the control.

Table 2 Effect of difference in packaging style on damage to cherries during transport [7].

| Packaging style | Rate of damage fruit (%) | Degree of damage |
|---|---|---|
| Conventional (Control) | 34.3 | 1.4 |
| Improved | 23.3 | 1.0 |

## Discussion

Our results suggest that large shocks frequently occurred at airports, although there was no shock during air transport (Figures 5–7). Takagi et al. [8] reported that loading goods on a container dolly caused severe shocks at an airport. In our study, such a process may also induce severe shock. Thus, severe shock conditions at airports should be assumed when designing cushioning packaging for export via air.

We found that the shock severity and frequency via marine transport were lower than via air transport (Table 1 and Figure 6). Therefore, we concluded that marine transport is more advantageous than air transport for fruit export to neighbouring regions.

However, the quality of strawberries and cherries rapidly deteriorates during storage [9][10]. Because of this drawback, marine export of strawberries and cherries to neighbouring regions will be difficult, although marine transport will be useful for apples, pears, and peaches because these fruits have longer shelf lives. To design suitable packaging for the air transport of cherries, we investigated the effect of different packaging styles on the fruit quality. Both the rate and degree of damage to the cherries were less with the improved packaging than with the control after arrival in Taipei (Table 2). The shock analysis results suggest that both the shock level and frequency were reduced by the improved packaging style (Figure 7). Therefore, we believe that the shock was absorbed by the large box (Figure 4). In addition, the handling might have been changed because the improved packaging style was larger and heavier than the control.

## Conclusions

Our results suggest that the frequency of shock occurrence during land transport in neighbouring regions was higher than during in Japan. They also suggest that we should change the packaging style from that used

domestically for exporting fruit to neighbouring regions. The results for the cherries suggest that loading several corrugated fibreboard boxes into a larger corrugated fibreboard box allowed shock to be absorbed by the large container, and handling became more careful. Therefore, such a packaging style would be useful for the export of fruits from Japan to neighbouring regions. Based on these findings, we intend to propose a more effective packaging style.

## Acknowledgements

This work was supported by the Research Projects for Utilizing Advanced Technologies in Agriculture, Forestry and Fisheries (Nos. 1913 & 22067) for the Ministry of Agriculture, Forestry and Fisheries of Japan.

## References

1. MAFF (Ministry of Agriculture, Forestry and Fisheries of Japan), 2007, "General export strategy for agricultural, forest and fishery products", Online, Available: http://www.maff.go.jp/j/shokusan/export/e_senryaku/pdf/01honbun.pdf, [10 Apr. 2014].
2. T. Tamakoshi. K. Nakasu. M. Ishio and S. Nakatani, 2004, "Study on dynamic effects on bridges of large-sized vehicles (I)", *Technical Note of NILIM*, no. 179.
3. N. Nakamura. T, Umehara. H, Okadome. K. Nakano. S. Maezawa and T. Shiina, 2007, "Effcts of vibration frequency and direction on damage of strawberries", *Journal of the Society of Agricultural Structures, Japan*, vol. 38, no. 2, pp. 101-108.
4. Y. Ishikawa. H. Kitazawa and T. Shiina, 2009, "Vibration and shock analysis of fruit and vegetables transport -Cherry transport from Yamagata to Taipei-", *Japan Agricultural Research Quarterly*, vol. 43, no. 2, pp. 129-135.
5. H. Kitazawa. Y. Ishikawa. F. Lu. Y. Hu. N. Nakamura and T. Shiina, 2010, "Analysis of shock during strawberry transport and damage estimation", *Horticultural Research (Japan)*, vol. 9, no. 2, pp. 221-227.
6. Y. Ishikawa. H. Kitazawa and T. Konno, 2013, "Comparison of shock during fruit export via air and marine transportation", *Food Preservation Science*, vol. 39, no. 1, pp. 25-30.
7. Y. Ishikawa. H. Kitazawa and K. Takahashi, 2012, "Reducing shock to cherry cargoes during export", *Food Preservation Science*, vol. 38, no. 3, pp. 135-140.
8. M. Takagi. K. Imakita. N. Kamba and H. Wada, 2010, "Action to safety transportation for cultural assets", *Abstracts of Meeting of the Society of Packaging Science and Technology*, Tokyo, Japan, Jul. 8-9, no. 19, pp. 136-137.
9. H. Kitazawa. T. Sato. N. Nakamura and S. Motoki, 2013, "Effects of post-harvest cooling delay on weight loss, soluble solid and ascorbic acid contents of strawberry fruit", *Journal of Food, Agriculture and Environment*, vol. 11, no. 3-4, pp. 372-376.
10. Y. Ishikawa. H. Kitazawa. Y. Kuwana and K. Takasago, 2008, "Modified atmosphere packaging for maintaining freshness of sweet cherry fruit", *Food Preservation Science*, vol. 34, no. 6, pp. 311-316.

# Comparison of two vibration recording methods depending on the data-recorder position

**Victor HUART [b,c], Jean-Charles CANDORE [b], Jean-Baptiste NOLOT [a], Jérôme PELLOT [c],Nicolas KRAJKA[c], Serge ODOF [a, b] and Damien ERRE [a,b]**

[a] ESIReims-ESIEC : Ecole Supérieure d'Ingénieur de Reims, Reims, France

[b] GRESPI / Université de Reims Champagne-Ardenne, Reims, France

*Esplanade Roland Garros, BP 1029, 51686 Reims Cedex 2, France*

[c] METROPACK

*30-32, rue du Capitaine Georges Madon, ZAC Croix Blandin, 51100 Reims, France*

**Abstract**: Transport measurement is the basis of transport analysis. Its study permits us to detect problems and ensure of the goods safety regarding their packaging. It requires sensors able to record every environmental stress. We generally use a data recorder fixed on the exciter system and then we reproduce the signal on a vibration table in a laboratory. But, can we record stresses by placing the sensor directly on the studied system instead of fixing it on the truck, plane, train… or any exciter system?

Indeed, we are not always able to record this way for each case and during the whole transport duration. Transport conditions (changes of means of transport during the journey…) and transporters' notifications (vehicle measurement prohibited directly on the structure, or driver efficiency study…) impose, in some cases, to measure stresses directly on the package.

Usually, vibrations tests protocols are based on the exciter system recording and the regulation of the vibration table.

But if the record is done directly on the packaging system, how can we realize the simulation on a vibration table? Do these two different ways generate many results differences? And what is the best method to use?

In this work, signal of packaging system will be compared to a truck one during the same transportation. PSD signals collected from packaging systems will be compared to PSD collected from the truck. For each measurement point, probability densities of accelerations will also be compared. Overall, this study will allow us to determine if a difference of severity exists between the two recording methods by using an appropriate simulation protocol in laboratory.

# 1 Introduction

The transportation of goods across the world rises up each year. These transportations generate various kinds of constraints.

Last year, more than 300 million bottles of Champagne were sold over the world. Obviously the region Champagne in France generates a wide distribution network.

However, due to the proximity of the producers, links between Houses of Champagne and sale points are organized on relatively short distances. The main roads used are national roads and motorways to link the differents cities. Pallets of Champagne are dispatched across all outlets of cities.



In the present case, as in many others, many transhipments and vehicle changes occur (notably during pallets dispatching). These logistical changes do not allow us to follow easily data recorder on various truck beds. The only way to record correctly the constraints suffered by goods is by fixing the sensors on the pallets.

In this work, we have recorded a small Champagne pallet shipping on a typical logistic path (Fig 5-a and 5-b). The recording has been done simultaneously on the truck-bed and the base of pallet (Fig 1 and Fig 2).

Random vibration tables are able to reproduce recorded signals of shipping. Acceleration sensors permit to regulate and control the table. Depending on the recording zone, we have realised the table regulation on the table tray (which is usually used) or on the packaging system at the same place as the recording was done.

Those two simulations are in the same time recorded on the vibrations table by data recorders with the same configuration of real tests. Then those two regulation zones recordings have been compared to the real ones.

**Method 1: Saver on truck bed: regulation of the vibration table tray**

This method is the usual one, mostly employed in transport studies [1][2][3]. It permits to have the different constraints emitted by various transportation gears.

**Method 2**: Saver on pallet bottom: regulation on the bottom of the pallet.

This method is the alternative one which permits to alleviate transportation change problems. This method consists in recording directly constraints felt by goods [4].

## 2 Experimentations

### 2.1 Packaging measurement set-up

The packaging system studied is a Pallet of Champagne on an half-European pallet of 500 = Kg. (Figure 1). Recording systems used are Lansmont Saver 3X90, a tri-axial piezoelectric accelerometer. One of these sensors is placed at the bottom of the pallet. This data recorder is mounted on a steel plate and fixed on the box with 4 screws (Figure 2). Experiments were carried out on three types of road: motorway, national road and city road.




**Figure 1** : Pallet of Champagne studied

## 2.2 Truck set-up

The second Saver destined to measure excitatory signal is mounted on a steel plate and fixed on the truck bed with 4 screws just next to the pallet (Figure 2)




**Figure 2** : Set-up of the truck

## 2.3 Saver 3X90 set-up

The signal is recorded continuously during all transportation phases with a:

- $^{+}/_{-}$ 100 g scale
- Sample rate : 500 Hz
- Signal filtration : 250 Hz

The signal is a continuous recording. It is composed of a **32.768 sec**-events sequence. The following work consists in comparing the recording on the pallet and the usual recording on the bed truck.

## 2.4 Simulation set up.

In the two cases presented below, the simulation is recorded simultaneously with two identical savers (SAVER 3X90) in the same configurations as during the real transport.

## 3 Regulation on the pallet

The regulation captor is fixed on the saver which was used to record the constraints suffered by the pallet. This is the second simulation method. The aim of this simulation is to be able to reproduce the stresses suffered by and recorded on the pallet.

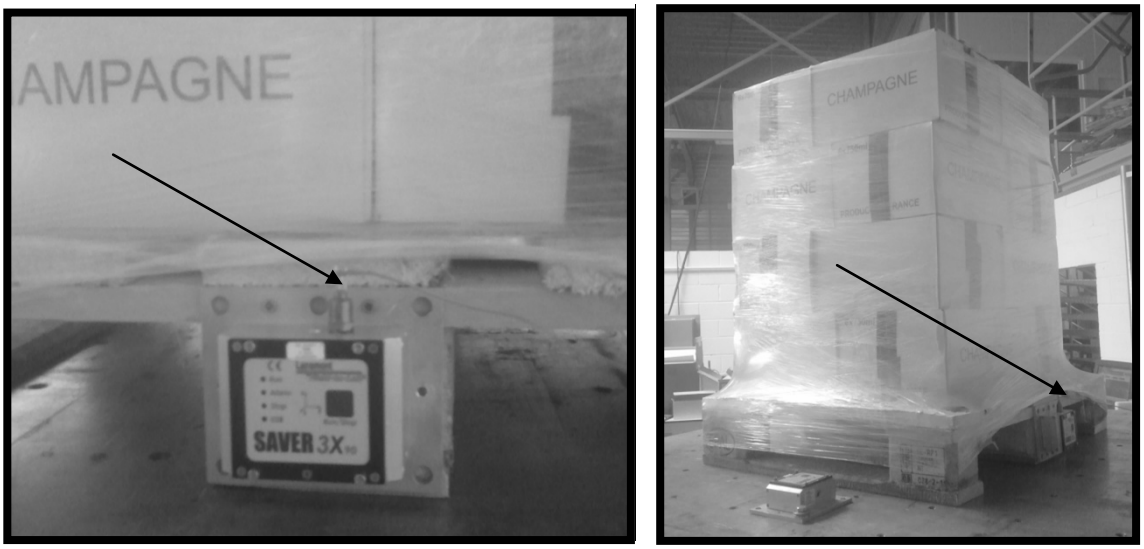



**Figure 3:** Simulation of the pallet transport.

## 4 Regulation on the table tray

In the first simulation method, the table is regulated as usual, on the vibration table tray. The truck recording is reproduced.

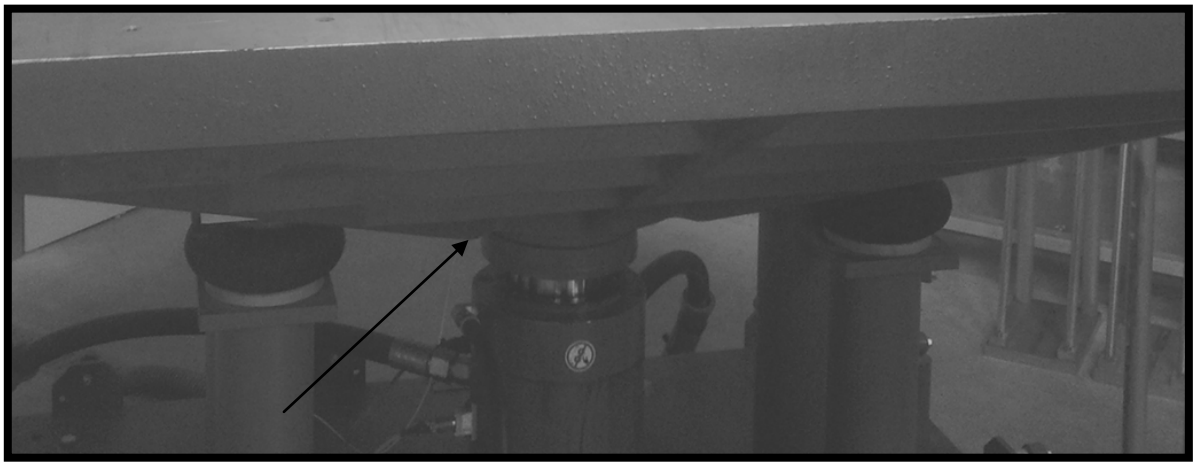


**Figure 4 :** Simulation of the truck.

## 5 Detail of the journey

Chapagne pallet was shipped between two cities : Reims (Marne, France) and Châlon-en-Champagne (Marne, France) (Fig 5-a and 5-b). This journey has three distinct phases: National road, motorway and city road.

**_The first phase**: **National** road form ***Reims*** to ***Châlon-en-Champagne*** (45 km) (grey).

**_The second phase**: **Motorway** from ***Châlon-en-Champagne*** to ***Reims*** (50 Km) (white).

**_The third phase**: **City road**: ***Reims*** (15km) (black).




**Figure 5-a :** Global itinerary of the truck




**Figure 5-b :** Global itinerary of the truck focused on the city part

# 6 Result of differences phases.

## 6.1 National road comparison.

The different statistical parameters are grouped on Figure 6 so as to realise a scheme of both signals. Concerning the level distributions parameters, the second method presents a slight advantage for both the recording and the regulation on the pallet (method 2). We can also notice that the maximal acceleration recorded during the transport is much better represented by both the recording and the regulation on the pallet. Only the mean $G_{rms}$ is more coherent with the truck recording (method 1). The PSD reproductions are equivalent for both methods.

## 6.2 Motorway phase.

The motorway phase delivers less powerful low frequencies than the national road and higher PSD for frequencies over 10Hz. Apparition probabilities densities stand equal to those from the national road.

On Figure 7 we grouped the different statistic parameters as to realise a scheme of the two signals. Concerning the level distributions parameters there is a slight advantage for method 1. Nevertheless we notice that the

maximal acceleration measured during the transport is much better represented by method 2. The recording and regulation on the pallet provides better results too.

### 6.3 City road phase.

We can see on Figure 8 that the city phase is different from the other ones. The low speed, the numerous stops and turns increase the low-level accelerations probabilities a lot.

On Figure 8, concerning the distribution parameters levels, both methods stay quite far from reality but gaps are identical. This difference can be due to the Gaussian-like nature of the signal emitted by the table though the real signal corresponds to a modified Gaussian [5][6]. Nevertheless we notice that both the maximal acceleration recorded during the transport and the PSD levels are much better represented by both the recording and the regulation on the pallet (method 2). Moreover PSDs are equivalently more respected in both cases.

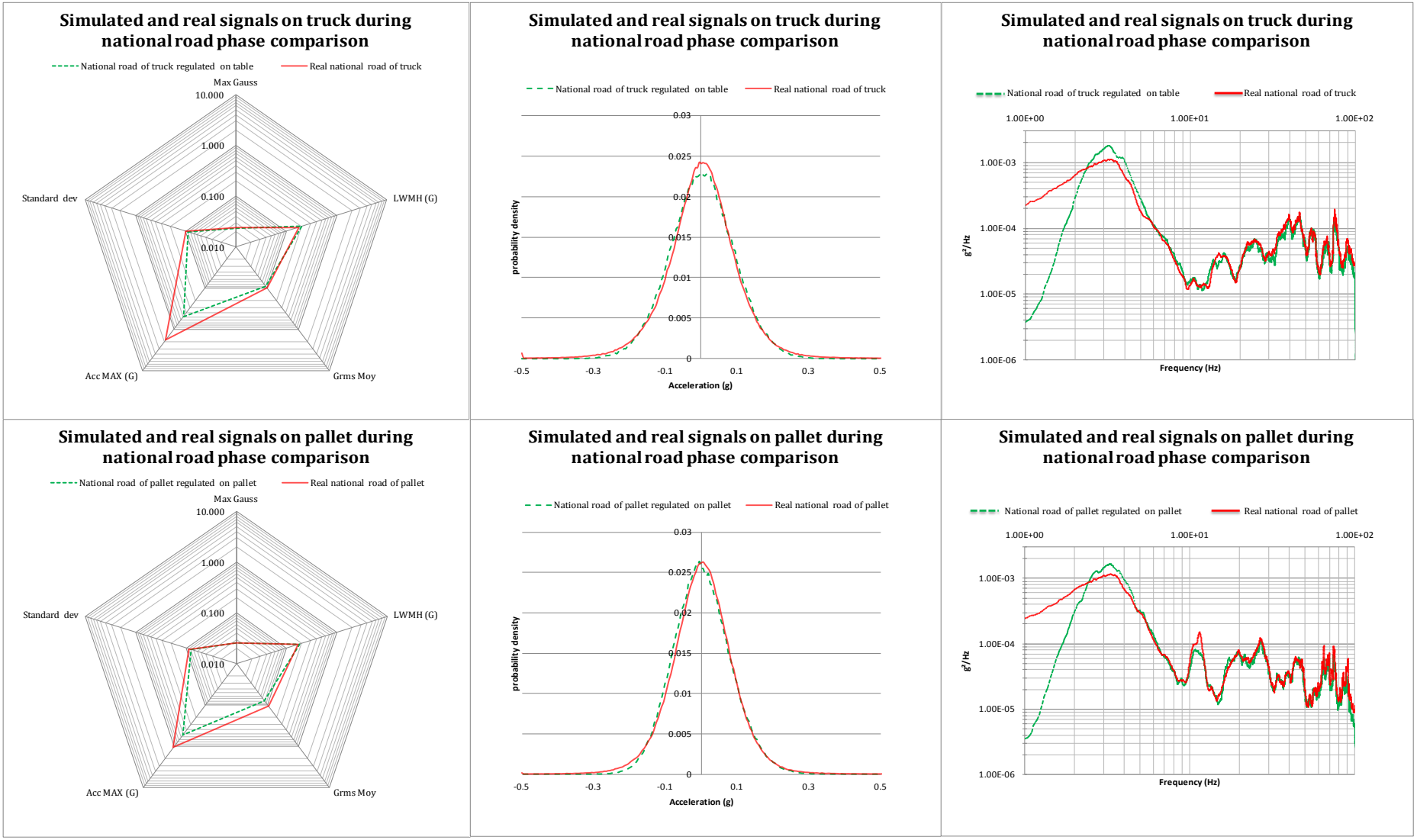



**Figure 6** : Comparison between method 1 (top) and method 2 (bottom) on national road.

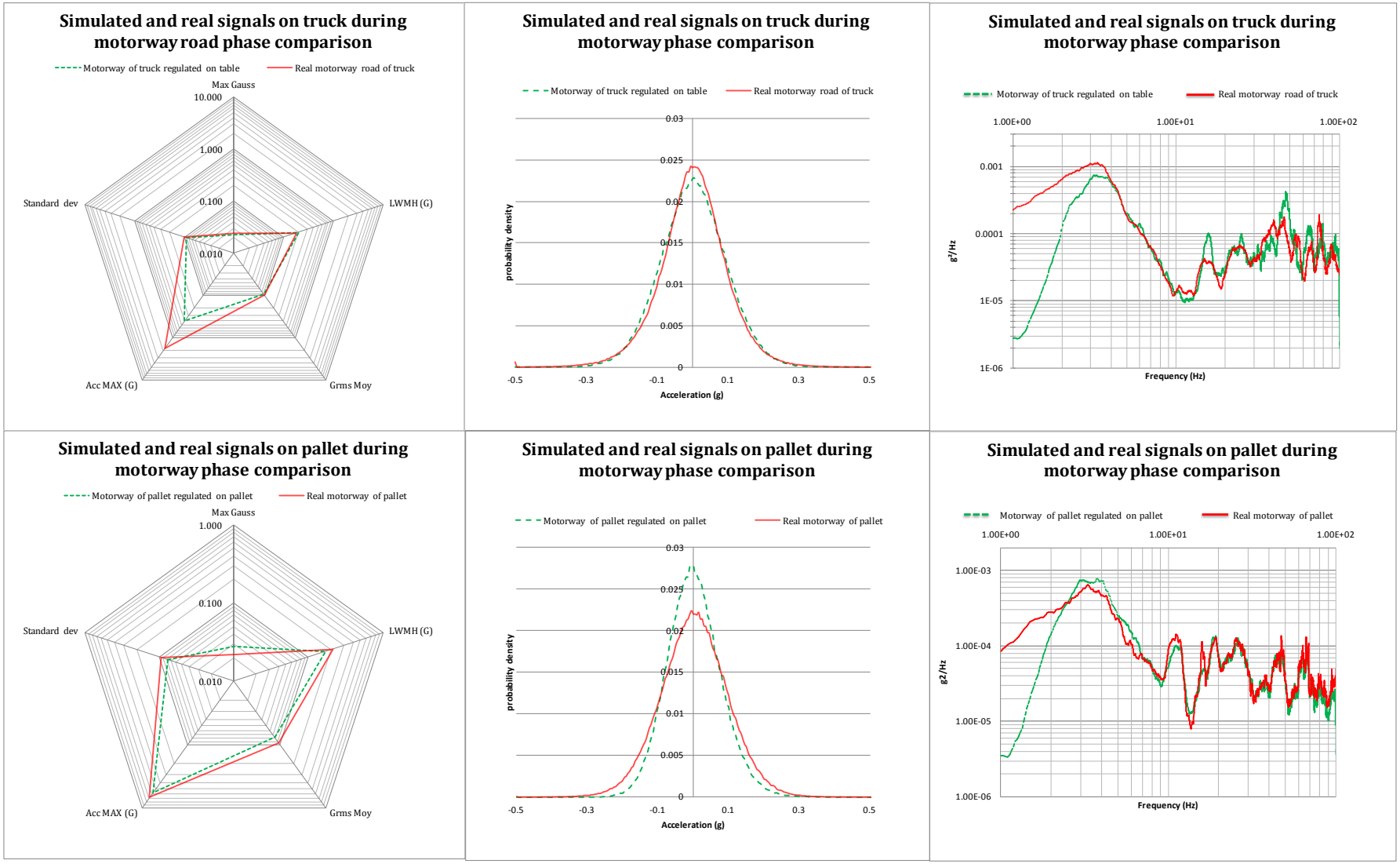



**Figure 7 :** Comparison between method 1 (top) and method 2 (bottom) on motorway

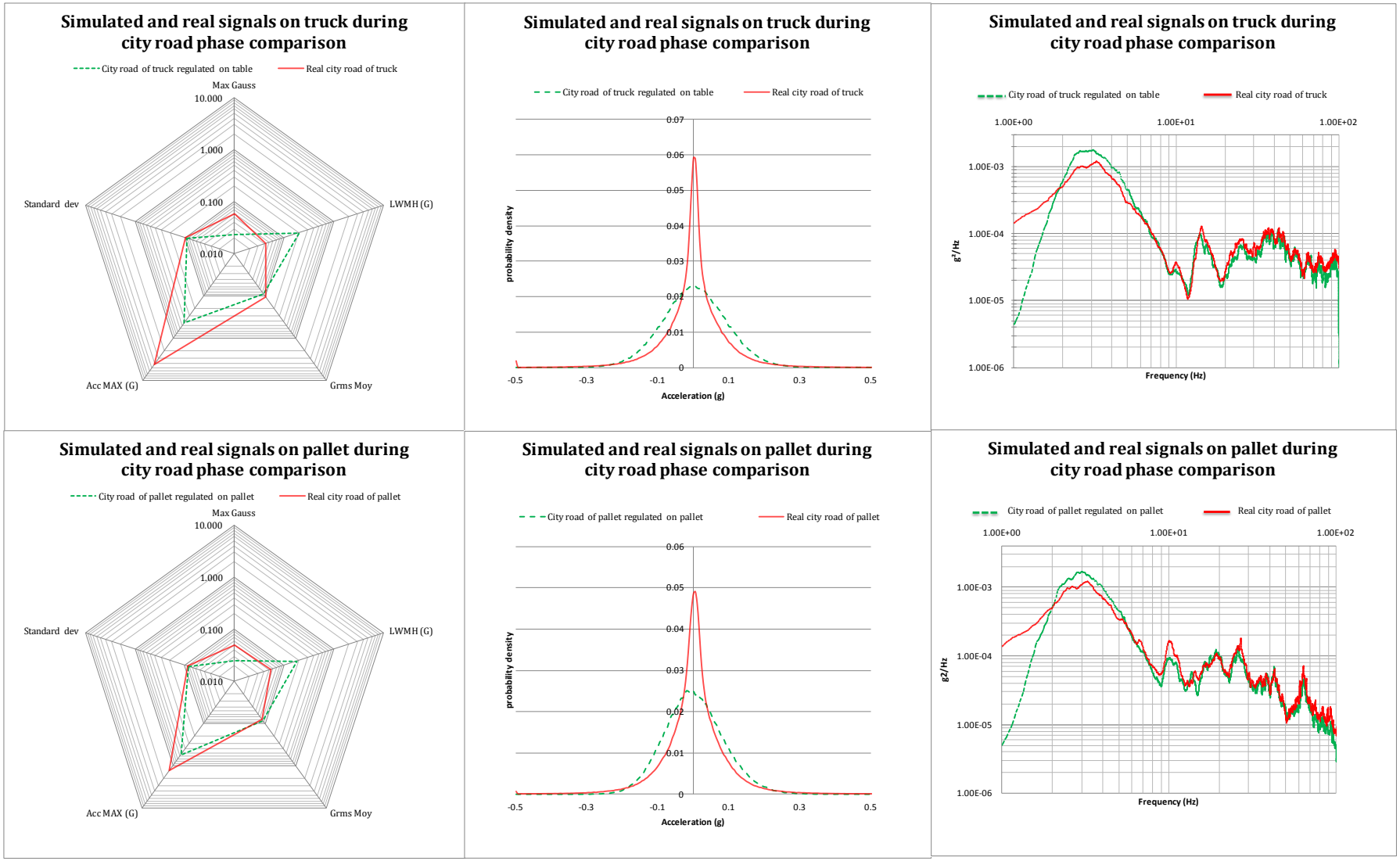



**Figure 8 :** Comparison between method 1 (top) and method 2 (bottom) on city road

## 7) Conclusion.

Given the different results for the different phases we cannot conclude on the viability of one method compared to the other one. The usual recording method consisting in fixing the sensor on the excitatory system (truck, train, boat...) provides satisfying results as long as the regulation is done on the vibration table tray. The method consisting in fixing the sensor on the studied system is as pertinent providing that the vibration table regulation is made directly on the packaging system close to the recording zone.

Given these results, it is possible during an international transportation study comprising many transportation changes and many handling to make the recording on the packaging system. Then the regulation of the vibration table must be done on the packaging system.

## References


[1] Singh SP, Marcondes J. Vibration levels in truck shipments as a function of suspension and payload. *Journal of Testing and Evaluation,* 1992; 20(6): 466–469.

[2] Rouillard, V., Sek, M., and Perry, T. (1996). Analysis and Simulation of Road Profiles. *J. Transp. Eng.*, 122(3), 241–245.

[3] Jarimopas. B, Singh. SP , Saengnil, W ;Measurement and analysis of truck transport vibration levels and damage to packaged tangerines during transit, *Packaging Technology and Science*, 2005;18(4):pp 179-188.

[4] Jean-Charles Candore , Victor HUART, J.B. Nolot , N. Krajka , Serge ODOF , Damien ERRE Severity of road - railroad transport and time compression of vibration test, *26th IAPRI Symposium on Packaging*, Espoo, Finland, June 10 - 13, 2013.

[5] Hosoyama. A,Saito.K, Nakajima. T ; Non-Gaussian random vibrations using kurtosis, *Proceedings of 18th IAPRI World Packaging Conference*, San Louis Obispo (CA), USA, 2012, pp 35-40.

[6] S. Otari, S. Odof, J. B. Nolot, P. Vasseur, J. Pellot, N. Krajka and D. Erre ; Statistical Characterization of Acceleration Levels of Random Vibrations During Transport, *Packaging Technology and Science,* 2011; 24(3), pp 177-188.

# Transport simulation testing for stretch wrap film optimisation and palletised load safety (DUOPLAST Business Case)

**Manuel-Alfredo Garcia-Romeu-Martinez[1*], Juan Alcaraz-Llorca[2] and Christoph Graefe[3]**

[1] *ITENE (Technological Institute of Packaging, Transportation and Logistic), Valencia, Spain*
[2] *ITENE (Technological Institute of Packaging, Transportation and Logistic), Valencia, Spain*
[3] *DUOPLAST AG, Sünna, Germany*

[*] *Corresponding author. Email: mgarciaromeu@itene.com*

**Abstract:** Nowadays competitiveness is a must for the subsistence of any company, but it is even more important for European manufacturing companies that have to compete in the global markets with lower cost competitors. Differentiation is a key strategy to achieve that differentiation and that is the strategy that DUOPLAST AG, a German manufacturer of stretch wrap film, has chosen to increase its competitiveness.

Palletised loads stability is an issue that is achieving nowadays a high degree of importance. Weight reduction of primary and transport packaging is making tertiary packaging as stretch wrap more and more strategic. Also cost reduction trends put pressure on stretch wrap film optimisation. Besides being a commodity product, stretch wrap film proper application is governed by many parameters that makes it complex.

Taking this into account, DUOPLAST AG has converted a commodity product like stretch wrap film in a high value added product by incorporating in-house transport simulation testing to its daily operation. This allows them not just to sell kilograms of film, but film and the most optimised way to apply it to the different product references of its customers. This service improves customer satisfaction by both reducing process complexity and improving performance reliability.

The presentation will show how transport simulation testing can be used for stretch wrap film optimisation for safety, stability and cost optimisation. It will show which the minimum equipment is required for that optimisation and how DUOPLAST AG got its own in-house transport simulation centre. It will finally show real cases of stretch wrap film optimisation.

Keywords: stretch film, tertiary optimization, stability testing, transport simulation testing, improving performance, blown film

## 1 Introduction

In the majority of applications, Stretch wrap film is the most economical solution for achieving proper pallet load stability.

As more fully automatic pallet stretch wrap equipment used, more level of reducing costs can be achieved. For instance:

Manual stretch wrap film

- Hand wrap is not able to wrap every load exactly the same way.
- Pallet wrapping with hand wrap leaves a rather erratic and uneven look.
- There is a right way and a wrong way to wrap a pallet with hand wrap. You must continually train employees.
- No one likes hand wrapping. Potential complaints or damage due to poorly wrapped product.
- Unnecessary extra revolutions of film being applied.
- Hand wrapping a pallet manually prevents you from obtaining any type of repeatability.

Semi or Fully automatic stretch wrap film

- Consistent and uniform application.
- Clean professional finished product.
- Non-employee errors.
- Load integrity and damage control.
- Film savings.
- Quality control.

### 1.1 Aspects that are driving the optimization on tertiary packaging

The first aspect is the multinationals are ever more driven to reduce the carbon foot-print of their products. Until recently saving packaging costs was focused on reducing weight of the primary and the reduction or elimination of the secondary packaging. Now tertiary film is being a new focus of reducing packaging costs.

Other aspect is that chemical companies are developing new catalyst structures that allow to achieve thinner films and stronger than existing solutions (metallocene and chrome catalyst, bimodal polyethylene,…). Actually many of chemical companies are racing to develop an ever-increasing performance and number of polymerization catalyst.

Also Europe and worldwide legislation is strongly focusing on the security aspect of transportation and logistics. IMO (International Maritime Organization), ILO (International labour Organization) and UNECE (United Nations Economic Comission for Europe).

According to EU and IMO directives [1], the consignor (who prepares a consignment for transport) is responsible that packages (primary and secondary) and unit loads (complete transport packaging, primary, secondary and tertiary) are suitable to withstand the stresses expected under normal transport conditions, be it road, train or ship.

Based on the Directive of the European parliament and of the Council on the technical roadside inspection of the roadworthiness of commercial vehicles circulating in the Union [2] and from a legal standpoint, the securing system should prevent all movements of all parts of the cargo. This means that all load units should behave as a rigid block.

This being said, a pallet transported on the road must withstands a determined level of g acceleration, for example when the vehicle brakes, while the pallet remaining completely rigid.

### 1.1 Potential for improvement reducing tertiary packaging film

Control over stretch wrap processes at the end of packing line is an important task that can save costs, not only on tertiary packaging, if not also reducing costs for damages and returned goods due to lack of stability. Many companies, although they have automatic wrapping machines, they are not taking full advantage of it. For example, they use the same wrapping program for a variety of products and configurations, either for convenience, or lack of control over the operators of the wrapping machines or lack of knowledge of the potential savings of applying the correct wrapping program.

In our experience in last years about optimization and validation of unit loads, we obtained that 60% of the pallets we were dealing with were not rigid (under-packaged), 25% of the pallets were rigid but too expensive (over-packaged), and only 15% of the pallets were optimized (right-packaged). Therefore there is a clearly huge potential for improvement, because 85% of the pallets that companies are introducing in theirs distribution cycles, could be not optimized.

## 2 How to fulfil successfully tertiary film optimization without compromising the stability of the unit load

For proper setting up of stable unit loads and tertiary film optimization it is necessary to have a deep know how in wrapping film behaviour, machinery wrapping processes and evaluation testing focus on tertiary film optimization.

There are several factors that influence the goal of obtaining a stable unit load with the right amount of tertiary stretch film used:

Type and shape of primary and secondary packaging

The first important factor is about what type of product or packaging is present in the unit load to stretch (bottles of plastic or crystal, cans, plastic boxes, corrugated cardboard boxes, shelf ready packaging systems (SRPs), trays). Mainly if the product or grouping packaging are rigid or not, light or heavy, and the product is in boxes or not.

Friction coefficient of secondary packaging units

The second factor is about the friction coefficient between the surfaces of product or packaging in contact. "Surface resistance to relative motion" is its simple definition

According to the tribology theory for dry contact friction of Bhushan [3], friction resistance is contributed by:

- Adhesion of the sliding surface.
- Deformation of surface asperities in contact,
- Plowing by wear particles and hard asperities, and
- So called, ratchet mechanism, which is due to a lateral force required for the contact asperities to climb against each other.

Coulomb friction is an approximate model used to calculate the force of dry friction. This force is equal to the product of the normal force (directed perpendicular to the surface) exerted by each surface on the other, multiplied by the friction coefficient between the surfaces.

As greater is the coefficient friction and greater is the normal force, less force will need to exert the film to keep the unit load stable. But this is only true if both surfaces are in permanent contact. In the moment that a stack is bumped in the distribution cycle or the layers start to resonate the force of friction reduces and could be insignificant in some situations. If this occurs for a unit load with some specific product, packaging or distribution cycle, the coefficient of friction becomes a factor that it is not going to help to keep stable this unit load.

Stacking pattern of the pallet

The pattern for stack depends upon the shape of the cartons to be stacked. Usually they are stacked in column, inter-lock or with empty spaces.

Square items are usually stacked as columns and rectangular cartons can be stacked in a row, brick or pinwheel pattern.

The use of interlocking patterns should only be used when the weight of the loads will not exceed the load bearing strength of the cartons when stacked in this way.

If the edges are not aligned the strength of the stack is reduced.

Stacking cartons by column and using the interlocking method can provide stability with only loss of load bearing strength of the stack.

When the second top layer is interlocked to provide stability, the lower layers are all column stacked to increase load bearing strength.

Application of tie sheets

Usually tie sheets are made of corrugated board sheets single or double with some non-slippery surface treatment.

Layers of cardboard or rubber can be placed between layers of cartons or goods. This sheet provides interlock between the columns and prevents the columns from falling over. Sometimes they have some non-slippery surface treatment in order to increase the friction coefficient.

This is a simple and cheap way of providing stability. A disadvantage however is the cartons or goods are still separate from each other and may move if the stack is bumped.

Bottom roping for a good connection between pallet and load

Millions of loads slide off their pallets during shipment each year, causing billions of dollars of damage and waste. A film cable placed just below the top deck board of a pallet fixes the problem. It prevents the load from sliding off its pallet and getting damaged during shipment.

Roping bunches the bottom of the film into an accordion-like a rope. Rolling the bottom 8 to 15 cm of the film into a tight cable during the last part of the stretch wrapper's wrap cycle and driving it down onto the pallet -- about 3 cm below its deck board -- is the most effective way to lock the load to the pallet.

This method works better than regular roping because it's hard to position the regular rope just where you want it on the pallet -- high enough to keep from being punctured by pallet jack or forklift forks and low enough to secure the load to the pallet. Regular roping also tends to unbunch during the stress of shipment, which reduces its effectiveness.

Selection of stretch film

Stretch film is a high elongation, polyethylene based film that is commonly used to wrap products on pallets (unitizing), to protect products during storage and shipment (protection) and to secure them to each other and the pallet (load stability). This often helps to reduce products loss, to discourage load tampering and to reduce people injury in handling manipulation and vehicle transportation.

There are a variety of widths (2"-5" Banding, 12"-20" Hand Grade, 20" Machine Grade), thicknesses gauge (30, 40, 50, 60, 70, 80, 90, 100 … 200) and types of stretch film (most commonly used extrusion processes – blown stretch film and cast stretch film)

For these materials, a stress-strain curve, see Figure 1, is the most common way to graphically display and compare material properties data. The ability of a film to elongate when a pulling force is applied and then relax (retract) once the pulling force is removed is known as a films Elasticity. Tensile Strength is the amount of force required to hold the film at a certain percent elongation, Soroka [4]). The slope of the line before the proportional limit is known as the Elastic Modulus, after which the slope is no longer linear but the film is still in an elastic state, Hernandez, et al. [5]. After the Yield Stress occurs the material will continue to strain (elongate) without additional stress (increase in force requirement). Once the yield stress is reached, the film will experience permanent deformation with the continuous application of strain. This deformation is non recoverable, German [6] and is the general region in which stretch wrap is designed to perform. The force required to pull beyond the yield stress actually causes the film to start to change on the microscopic level. Strain hardening and necking coincide after the yield point and before the Breaking Point in the inelastic region, Peacock [7].

The strain hardening function is generally considered a positive attribute for stretch film. This is where the percentage of crystallinity within the stretch film continues to grow as the film is elongated (attributes of crystallinity will be discussed later). A desired percent crystallinity is determined by different film manufacturers. This aligning and eventual break down (after the ultimate stress) of the molecules causes the film to decrease in width called necking, Hernandez, et al. [5]; ITW [8].

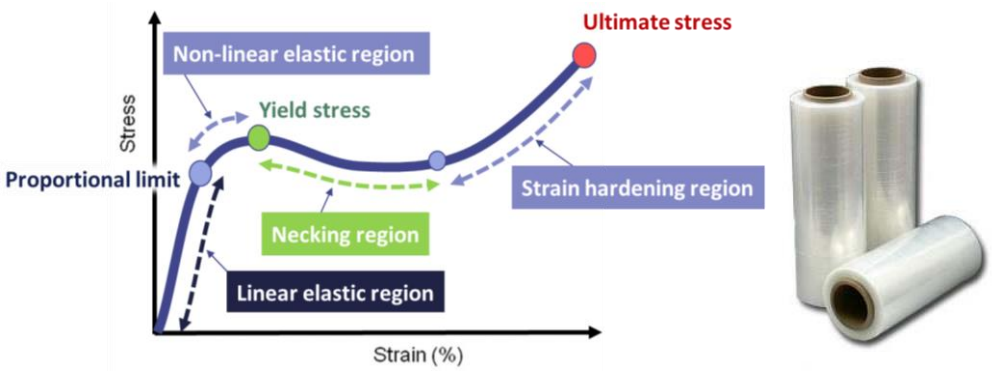



**Figure 1**: Typical stress-strain curve of a film

Why Pre-stretch?. Pre-strech is the process that allows stretch film to be stretched before (pre) being applied to a load. Film is prestretched when it is elongated mechanically between the two film carriage rollers due to the gearing ratio and diameter of the rollers. As the surface of the secondary roller is rotating faster than the Primary the film gets pulled between them and stretches.

- Film Strength: As you stretch the film, the tensile strength of the film increases so it is significantly (for example 2X) stronger once you pass the point of permanent deformation.
- Film Memory: The elastic characteristic of pallet stretch wrap that makes it want to return to its pre-stretched length. Stretch film memory exerts holding force on a wrapped load, keeping items packaged tightly together for secure shipment. The memory of the film wants to return it to its initial form. However the more you pre-stretch the lower the memory. If the film is applied to a load with no film force, minutes later you can observe that the film has tightened due to the film elastic memory as it tries to return to its original size. It is this film memory (like an elastic band on your hand) that differentiates stretch film from other means of unitizing. Settling that occurs during shipment can loosen other methods of unitizing where stretch film memory takes up the slack and continues to secure the load. Film Memory is the single most important reason for prestretching film.
- Film Economies: The cost of consumables (film) is reduced drastically compared to wrapping a load with film that has not been pre-stretched ie. Handwrap film. Payback of capital expenditure of less than 12 months is easily obtainable.
- Film Force or Tension: Film force is the tension created in the film due to the films attempt to return to its original state after having been stretched. A low film force inhibits the film from returning back towards its original state. Increasing this force will cause the film to stretch (post stretch).
- Post-stretch: Post stretch is the stretch in the film created by the film tension between the film carriage and the load being wrapped. It is also known as Force to Load. Although maximizes de load retention capabilities of the film, as this "Tension" stretch is usually concentrated on the corners of a load, it can crush and damage if set too high. As you use the load to create the tension, also there is a danger of pulling the layers apart. Depending on the product to be wrapped this form of stretch may not be desirable. (Empty P.E.T bottles for instance)
- Stretch consistencies: Stretching using tension or a brake (post stretching) does not provide uniform stretch and thus is not able to repeat its performance day after day. This can lead to intermittent load failures. As pre-stretch is more controllable than post-stretch it is typically more desirable to maximize pre-stretch and minimize post stretch.

Wrapping program settings

Proper stretch wrapping of unit loads is an important part of the overall quality of the product delivered to both internal and external customers.

In wrapping machines, there are several parameters that are important to know and apply when it is wrapping a unit load:

- Layers: Each layer must be wrapped with an acceptable amount of stretch film such that the layer is well contained. No layer of product should be shipped without acceptable stretch wrap.
- Top wraps: Top wraps are the extra revolutions of stretch film applied to the top portion of the load to be wrapped. As the top layers are susceptible to shifting in transit extra layers of stretch film (top wraps) is applied.
- Coverage: The wrap must extend above the top of the unit load approximately 5-10 cm pending equipment capability. Additionally, a minimum of two full wraps must be placed on the top of the load before the down traverse begins.
- Roping: If your machine is capable to bunch the bottom of the film into an accordion-like a rope, you could apply this to rigid products during all the wrapping cycle or in specific strategic places.
- Bottom Roping: Also during the last part of the stretch wrapper's wrap cycle you can drive the rope down onto the pallet to lock the load to the pallet.

- Wrap to Pallet: When feasible, all palletized loads should be wrapped to the pallet, with the stretch wrap flowing around the pallet below the top deck boards
- Bottom wraps: Bottom wraps are the extra revolutions of stretch film applied to the bottom portion of the load to be wrapped. This helps to maintain the unit load attached to the pallet.
- Overlap: As stretch film is applied to a load the stretch film is typically applied so that the next layer of stretch film is applied over the previous layer. This overlapping of film layers increases load retention. By slowing the vertical movement of the stretch film carriage the larger the overlap created. Minimum overlap of 5 cm is required during film traverse up or down. This eliminates gaps in the film, which is unacceptable.
- Pre-stretch: Depending on the machine and the film you could use an higher % of pre-stretch that are going to reduce the cost of the tertiary packaging applied to hold the unit load.
- Force-to-Load or Tension Stretch: It is measured with a simple weight gauge-dynamometer and plate. Once established, provide a means to maintain a consistent force to load setting through periodic measurements.

Selection of the testing protocol

Several options exist to choose as testing protocols. This can be applied to simulate the hazards of the distribution cycle into the unit load. These testing protocols are based on standards or in tailored or monitored distribution cycles:

- Pure based on standards: ISTA / ASTM / ISO
- Tailored based on new monitored distribution cycle or particular routes, well adapting the standards or with including new tests.

In order to be more accurate for a particular route and to get more saving costs and packaging optimization, it is necessary to adapt the standards. This could be used in two ways:

- Tailored schedules (the traditional testing): Only base on the tests described on standards but changing the sequences, the PSD plots, the RMS levels, the horizontal impact speed, the drop height from rotational or edge drops, …
- Tailored schedules (the upcoming testing): Including in the schedule new tests (more realistic simulation – multi-axial testing, vehicle accelerating or braking)

## 2.1 How to measure stretch wrap parameters

One important key, in order to try to be consistent in the parameters that you are applying during wrapping process day after day to the same unit load that you have previously defined and optimized, is how to assure that you and consequently your wrapping machines are applying the same quantity of film to get the same retention force needed to keep stable the load, as first day.

The quantity of film used is easily to obtain and measure, you only need to have a weighing scale to measure the total film used to wrap the pallet once film is applied and removed.

The parameter that most affect the quantity of film used to wrap the unit load is the pre-stretch level applied, called “film wrap stretch” and the parameter that give us an idea of the contention force applied to keep stable the load is called “load retention force”.

### 2.1.1 Film wrap stretch

There are two methods in order to measure the % of Film Stretch once the film is applied to the load. The first method consist in use some test kit provided by some manufacturer of film testing equipment where you need to spend some money in extra equipment, or the second method that consists in use a pen, a measurement tape and some skill using the film, cheaper than first method. The steps to carry out this measurement using this method are the following ones, Figure 2:

1. Starting from 2 meters we mark with a black marker pen four marks of 5 mm wide by 30 mm high, spaced 10 cm between them.

2. We'll have to roll the 3 meters film, as it was before you made the marks.
3. After the film wrap is applied to the load, measure the distance between two consecutive marks.
4. Any increase in the length between the original marks applied every 10 cm is the film wrap stretch. For example, if the measurement is 30 cm stretch equals 200%

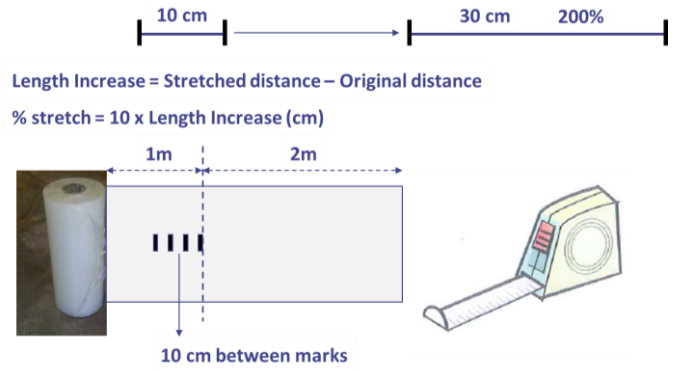



**Figure 2**: Method to measure film wrap stretch

### 2.1.2 Load retention force

The load retention force is also called force-to-load-test, tension or containment force. There are several methods in order to measure the containment force once the material has been applied to a unit load. There are methods based on ASTM D 4649-03 and methods not based on standard but widely used.

Methods based on ASTM D 4649-03

The steps to carry out this measurement using the method stated in the ASTM D 4649-03are the following ones, Figure 3:

1. Place a bathroom scale or strain gauge under the wrap before the film is applied to the unit load.
2. Apply the desired film in the desired wrap pattern.
3. The center of the scale or gauge should be 25.4cm (10”) from the top and 45.7cm (18”) in from the side.
4. The device should record more than just the max data as the amount of force a given film can exert changes over time.
5. The data should be recorded in pounds (ASTM, 2003a).

ASTM D 4649 (ASTM, 2003b) states that the containment force should be evaluated 45.7cm (18”) down and 25.4cm (10”) over from the top corner of the side of a unit load that is 121.9cm (48”) across. However, the location for containment force evaluation changes depending on the sales person or company. Some follow the ASTM specification but others have moved the evaluation location point to 25.4cm (10”) down and 25.4cm (10”) over or to the middle of the unit load. The distance pulled is also changed per user; some companies pull the film out between 2.54cm (1”) to 7.62cm (3”).

Snap back measurement method

Is an informal film evaluation method that is used to measure the amount of pressure a stretch film applies to a unit load. The steps to carry out this measurement using this method are the following ones, Figure 3:

1. Apply the film to the unit load.
2. The film is cut off the unit load in one vertical swipe.
3. The film is pulled off the unit load by the evaluators.
4. The film is reapplied to the unit load.
5. The distance between the edges of the film is measured and recorded.

The tension in this method, expressed in percentage, is obtained dividing the snap back gap measured by the perimeter of the unit load. If one film has a larger snap back gap than the other, then that film was applying more inward force to the unit load. For example, for an euro-pallet if the gap measured is 60 cm, the tension is 15%.

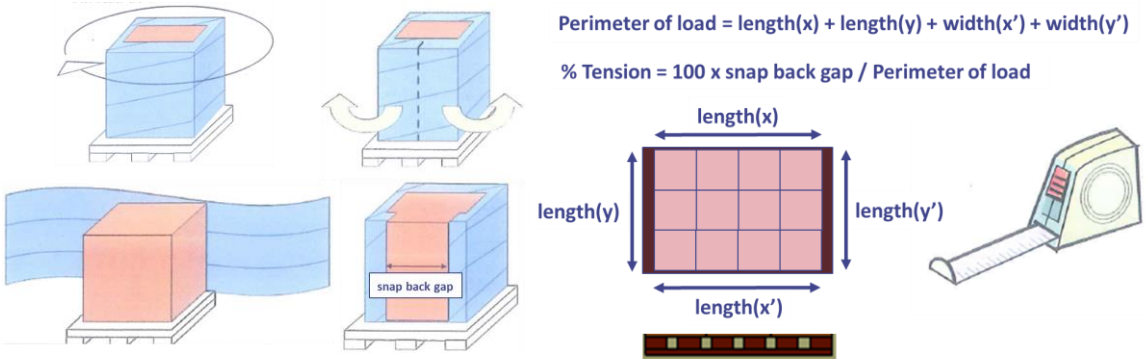



**Figure 3**: Method to measure load retention force based on snap back measurement

## 2.2 Evaluation testing focus on tertiary film optimization

Based on our experience obtained in the last years, we have developed the right methodological steps, testing protocols and proper equipment for tertiary film optimization and validation, in an effective way to assure the stability of the load and film optimization in a particular distribution cycle. Following are described the proper steps:

1. To develop a tailored protocol for testing simulation and validation adapted to the real distribution cycle for a product and for a particular company.
    a) Monitoring the distribution cycle of the company.
    b) Developing the tailored protocol based on
        - Tests described on standards but changing the sequences, the PSD plots, the RMS levels, the horizontal impact speed, the drop height from drops,…
        - Including in the schedule new tests (more realistic simulation – multi-axial testing, vehicle accelerating or braking)
2. To optimize the tertiary film using internal procedure with simple stability tests.
    a) Defining the right machinery wrapping parameters according to the capability of stretch wrapping machines of the company.
    b) Observing film and load stability behavior using internal tests procedure focus on tertiary film optimization (simple stability tests).
3. To undertake complete testing simulation for the validation of the film optimization previously defined by the internal procedure.

### 2.2.1 Developing a tailored protocol for testing simulation and validation

Nowadays the testing protocols that companies and testing laboratories are using are based on the traditional standards, for instance ISTA, ASTM or ISO. The testing protocols that are described on them usually when they are applied to unit loads tends to over pack and use more packaging that really it is needed. This is why tailored protocol should be used to optimize accurately the packaging of the unit load. In order to get this tailored protocol, the distribution cycle of the product that is going to be packed forming the unit load, should be monitored for obtaining the right level of the hazards that need to survive during real handling, storage and transportation operations.

To obtain good data from a real monitoring, first of all we usually build a “dummy pallet” with all the data recorders and electronics on it, see Figure 4. Then the exterior face of the unit load it is finished with the same product that is going to be transported. This is done because we want to hide all the equipment avoiding that handling workers or vehicle drivers knows what is going on and disturb his real behavior during their work. For

the specific route we usually considered adequate to undertake two replicates at least. If, after analyzing the data from these two monitoring, the dispersion of them is high and unusual it will be necessary to undertake additional monitoring. If it is possible track monitoring by us will take place during the journey. In this way it is possible to identify possible non-representative events (accidental) or unusual driving behavior, that allow us to obtain an appropriate results in the later data analysis.



**Figure 4**: "dummy pallet" with all the data recorders and electronics on it

The electronics used are based on inertial units and data recorders. These units record tri-axial acceleration (vertical-longitudinal-lateral), rotational rates (pitch, roll and yaw), temperature and humidity. Entire acceleration-vs.-time waveforms of the shocks and vibrations which occur during handling and transportation are measured and stored. These instruments represent the most powerful and sophisticated for the purpose. Data can be analyzed in both the time and frequency domains, or compiled statistically.

Either alone or combined with an environmental chamber, vibration testing is a critical step in the successful development of new products and packaging. During the last 30 years, Vertical Random Vibration has been employed in package testing laboratories.

About the technique used for random vibrations

In the 80s until 1998 few PSD profiles were available (rail, truck, air). These three PSD were used with little questioning or exploration of alternatives.

As field data recorder came into common usage about 14 years ago, researchers began to report many different PSD shapes and intensities, and to try out these new PDSs in laboratory tests. It became increasingly recognized that used of the standard three PSD profiles not always produce results that correlated well with actual field performance. Also there was great interest in obtaining and using test profiles that "matched" the transport situations to be simulated. Many successes (improved correlations) were reported.

The current typical approach for random vibration testing of package is to simulate transport with a single PSD spectrum applied for a given time duration. The original three PSDs are still in use, but other spectra are also common. This rather simple (by today's standards) methodology still serves quite well to solve and avoid problems, control costs, and optimize designs. But recently research into random vibration for package testing has risen to a new level, driven by the need and desire for ever more accurate simulations. Now, in addition to the realization that PSD shapes and intensities are important, the fundamental "character" of transport vibration is being investigated. Is it non-Gaussian?, Is it non-stationary?. Are there superimposed shocks?. Is needed to test with multi-axis shakers (horizontal, longitudinal, pitch and roll vibrations)?

Stationary random vibration is defined by statistical properties which do not change with time. In the transportation environment, such a condition might be approximated by a truck traveling long distances over the same type of road at the same speed, or an airplane flying for hours through relatively smooth air. But if the road surface or vehicle speed changes, or if there is air turbulence or other differences, the statistical characteristics are altered and we have significally non-stationary and non-gaussian vibration (Rouillard et al., [9,10], see Figure 5.

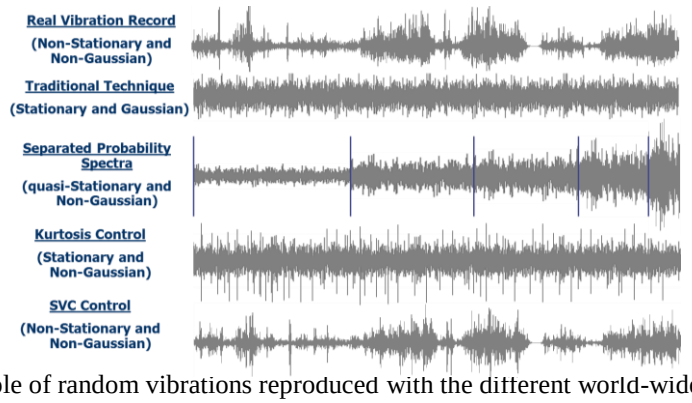



**Figure 5**: Example of random vibrations reproduced with the different world-wide-used methods

ITENE in the last six years has been involved developing technology to simulate more accurately the vibrations founded out in the distribution cycle. ITENE supported the computer controlled hardware developed by Dr. Vincet Rouillard and Dr. Michael Sek for the generation of non-stationary (varying RMS) and non-Gaussian (high kurtosis) random vibrations, see Figure 6.

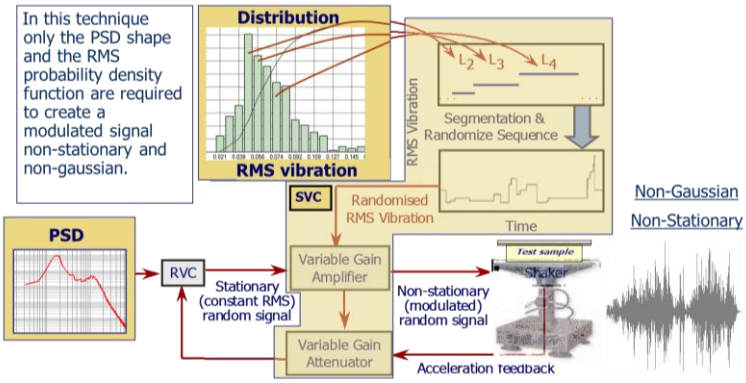



**Figure 6**: Non-stationary and non-Gaussian method for synthetizing random vibrations

About the needed to test with multi-axis shakers (horizontal, longitudinal, pitch and roll vibrations)

Historically, single-axis, single-shaker testing is the method of choice. However, complex, multi-axis motions are characteristic of field environments. The more a vibration test can replicate the field environment, the more realistically it can induce a vibration stress loading equivalent to that experienced by the product or packaging in the field. Realism is important for several reasons (Clyde Harman and Michael Pickel, [11]):

- First, multi-axis testing excites all modes simultaneously with a more realistic stress loading. However, sequential single-axial excitation may not excite all the critical modes of the test object concurrently and, as a result, may fail to detect defective design.
- Second, tested products and packaging may pass uniaxial testing but fail under actual operating conditions.
- Third, fatigue damage is increased by a factor of two with three-axis excitation.

About 6 degrees of freedom measurements, Carlos Bernad [12], obtained that:

- Real movements of the truck load bed during transport cannot be properly described with vertical acceleration alone.
- As was expected, the vertical acceleration showed higher vibration energy than lateral and longitudinal accelerations.
- Regarding the rotational movements, the yaw clearly showed the least vibration amplitude, while the pitch and roll were comparable. The yaw can be neglected without significant effects.

- Shipping units, because of their shape, present resonances associated to bending modes, and obviously, these resonances cannot be excited with pure vertical acceleration. Even the consideration of lateral and longitudinal vibration is not able to resolve this situation.

Batt [13], has argued in a presentation at the 2010 International Transport Packaging Forum that X and Y accelerations might be relevant at certain frequencies, but although they allow bending-like modes to appear with horizontal movements, the response provoked is small compared with that caused by rotational accelerations (pitch and roll).

ITENE, several year ago, developed and patented a machine that can be installed on top actual vertical vibration machines, that reproduces controlled pitch and roll vibrations at the same time than vertical vibrations are produced by the actual world-wide-used methods, Figure 7.



**Figure 7**: Non-stationary and non-Gaussian method for synthetizing random vibrations

### 2.2.2 Optimizing the tertiary film using internal procedure with simple stability tests

Proper stretch wrapping of unit loads is an important part of the overall quality of the product delivered to both internal and external customers.

First of all, the product is palletized at laboratory following the customer's defined pattern, using the same materials and stretching parameters currently used. Then a simple schedule of testing based on stability issues are undertaken. During this tests we observe the behavior of the palletized loads and its packaging (corrugated board, film, …) in order to identify the possible optimizations. An iterating simple stability tests process is carried on. New wrapping parameters are defined according to the capability of stretch wrapping machines of the company and based on the observed behavior of the load.

The simple stability test schedule used in this optimization stage are the following ones:

- Rotational flat drop (Figure 8)
- Horizontal impact (with hazard block) (Figure 8)

If these tests are passed successfully, before going to the complete validation stage, additional tests could be included to reveal possible non-stabilities or undesirable behavior of packaging or the unit load:

- Horizontal acceleration (Figure 8)
- Loop forklift circuit (Figure 8)

The wrapping program settings that are analyzed and defined during the iterating process are mainly which number of layers we are going to use and where they are located (top, bottom, coinciding with the bottom or top of the products), the film overlap, pre-stretch and force-to-load level. If the customer machine is able to use ropes during wrapping process also this is taken into account, because depending of the product, could be the only way to keep stable the unit load. Other parameter as "coverage" and "wrap to pallet" also are taken into account.

### 2.2.3 Undertaking complete testing simulation for validation of the film optimization obtained

A tailored testing protocol completely defined, that reproduce those physical and mechanical hazards associated to a particular company transport process, could be used to design the most suitable packaging system to guarantee the product arrives in perfect condition to its destination (packaging optimization and cost saving).

A tailored protocol (Figure 8) for complete testing simulation and validation could include, for example, the following test schedule:

- Handling

1. Loop forklift circuit
    - ✓ Based on ISTA 3B "Packaged Products for less-than truckload (LTL) shipment".
    - ✓ Circuit on two consecutive faces.
2. Rotational flat drop
    - ✓ Based on En ISO 14149 "Packaging – Complete, filled transport packages and unit loads – Impact test by rotational drop"
    - ✓ Drop edge in two consecutive edges.
    - ✓ Drop height of 7 cm.
3. Horizontal impact
    - ✓ Based on En ISO 2244 "Packaging – Complete, filled transport packages and unit loads – Horizontal impact tests" and ISO 10531 "Packaging – Complete, filled transport packages – Stability testing of unit loads"
    - ✓ Impact face in two consecutive faces.
    - ✓ Impact velocity of 0.80 m/s.
4. Horizontal acceleration
    - ✓ Based on EUMOS 40509 (EUROPE MOVE IT SAFE)
    - ✓ Acceleration direction in two consecutive faces.
    - ✓ Jerk acceleration of 0.4 g's and 300 ms duration jerk constant acceleration.

- Multi-axial Vibration (vertical+pitch+roll)
    - ✓ Vertical vibrations combined simultaneously with pitch & roll vibrations.
    - ✓ Based on ASTM D4169 "Standard Practice for Performance Testing of Shipping Containers and systems", ASTM D4728 2Test Method for Random Vibration Testing of Shipping Containers" and method of synthesizing non-Gaussian random vibrations.

5. Random vibration (Semi-trailer in road) (Figure 9)
    - ✓ 60 min duration with vertical vibration (0.12 g's RMS), pitch vibration (0.75 º/s RMS), roll vibration (0.90 º/s RMS).
6. Random vibration (Train) (Figure 9)
    - ✓ 210 min duration with vertical vibration (0.13 g's RMS), pitch vibration (0.30 º/s RMS), roll vibration (0.68 º/s RMS).
7. Random vibration (Automatic Storage)
    - ✓ 12 min duration with vertical vibration (0.12 g's RMS), pitch vibration (0.35 º/s RMS), roll vibration (1.14 º/s RMS).
8. Random vibration (Van last mile in road)
    - ✓ 25 min duration with vertical vibration (0.12 g's RMS), pitch vibration (0.89 º/s RMS), roll vibration (0.78 º/s RMS).

- Handling

9. Loop forklift circuit
10. Rotational flat drop
11. Horizontal impact
12. Horizontal acceleration

Tests could be based on standards but changing the sequences, the PSD plots, the RMS levels, the horizontal impact speed, the drop height from drops,… This levels are established from the analysis of the data obtained in the real monitoring previously carried on. In this way you are applying the right level of the hazards that need to survive the product, packaging and unit load, during real handling, storage and transportation operations.

Also could include in the schedule new tests (more realistic simulation – multi-axial testing, vehicle accelerating or braking)



**Figure 8**: Tailored protocol (Handling- Multi-axial Vibration (vertical+pitch+roll)-Handling)

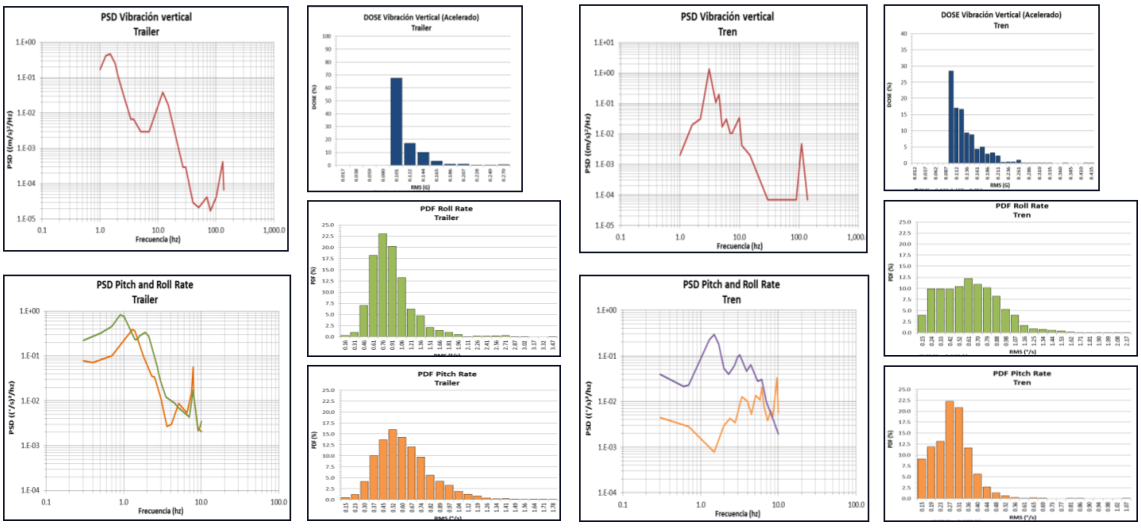



**Figure 9**: Random vibration (Left, Semi-trailer in road), (Right, Train)

## 3 In-house transport simulation centre for transport simulation and stretch wrap film optimisation (DUOPLAST Business Case)

DUO PLAST® is a leading, innovative manufacturer in the packaging film market / stretch film market. They offer innovative and modern packaging solutions for different fields of application. Stretch films made by DUO PLAST® are used in the industrial and agricultural sector and for the packaging of food products.

The business unit DUO LAB, Figure 10, is the result of the consistent ongoing development of expertise in the field of cargo security and the investigation of flexible packaging materials. With the particular developed Technology Centre for Load Unit and Cargo Security two years ago, they have included in his know-how deep knowledge and advance equipment. This added to the deep know how in film behaviour and machinery wrapping processes that they have been developing during 31 years, are able to undertake proper consulting and testing focus on tertiary film optimization and cargo load security.




**Figure 10**: DUO PLAST transport simulation center

The in-house transport simulation centre was equipped with the last technology produced by ITENE for packaging and unit-load evaluation and optimization. Base on ITENE´s know-how and expertise during over 15 years working in the field of packaging engineering, physical and mechanical hazards associated to the transport process, as well as designing and implementing tailor-made transport simulation centre for ITENE´s facilities and for different customers, ITENE installed at DUOPLAST LAB the following equipment:

- Multi-axial transport simulation table inside a climatic chamber, consisting of a vertical vibration table and pitch&roll module, in order to simulate the most important vibrations (vertical and rotational pitch and roll) produced by various means of handling and transportation under real climatic conditions, see Figure 11.
- Horizontal Stability & Impact Machine, in order to simulate the most important shocks, impacts and accelerations, that affect the safety and stability of the load, produced by various means of handling and transportation, see Figure 12.
- Shock & vibration data recorder and inertial unit, in order to register the temperature, humidity, shocks and vibrations that occurs during the distribution cycle. This equipment could be used to define the levels of testing protocols.



**Figure 11**: DUO PLAST (left), ITENE (right), multi-axial transport simulation table



**Figure 12**: DUO PLAST (left), ITENE (right), horizontal stability & impact machine

The vertical vibrations that simulate this technology are those produced by:

- The suspensions of the vehicles on the road transport.
- Air turbulence in air transport.
- Automated and manual means of handling used in warehouses, hubs at airports and seaports.
- Engines, imbalanced masses and structural vibrations of vehicles and containers.

The pitch & roll vibrations (rotations) that simulate this technology are those produced by:

- The pilot of the aircraft doing the maneuvers or trimming the aircraft (ailerons produce rolling movement and elevators produce pitching movement)
- Pitch in road vehicle transport, is due mainly to changes in the slope of the road; accelerating and decelerating (speeding and breaking) the vehicle; road imperfections like potholes and speed bumps.
- Roll in road vehicle transport, is due mainly to changes in direction, road curves, longitudinal imperfections in the road affecting one side of the vehicle; transversal wind gusts.
- Pitch in sea transport, is due mainly to waves in the longitudinal direction of the vessel.
- Roll in sea transport, is due mainly to waves in the transversal direction of the vessel; transversal wind gusts acting on the boat's structure; changes in the course of the vessel.
- Automated and manual means of handling used in warehouses, hubs at airports and seaports.

The shocks, impacts and horizontal acceleration that simulates this equipment are those produced by:

- Loads by hitting the walls of the container, the walls of the vehicle or hitting on other loads, produced by a sudden speeding or sudden breaking.
- Rail car switching operations depending on the type of draft gear of the rail, standard type or long travel draft gear type.
- Automated and manual means of handling used in warehouses, hubs at airports and seaports (Marshalling or loading operations). Unit loads may be subjected to impacts when handled with mechanical equipment such as powered pallet trucks (pallet jacks), forklift trucks, straddle carriers, or other heavy materials handling equipment.

With the installation of this equipment and the transference of know-how and methodologies developed and used by ITENE, the technicians and engineers responsible for taking profit the transport simulation centre, are able:

- To evaluate the behavior of the developed packaging prototypes in the laboratory against horizontal dynamic forces produced by impacts and shocks and the variations of vertical and rotational compression forces produced by vibrations and dead weight when they are shipped or transported (single unit and palletized loads).
- To evaluate how well is working a tertiary film used to keep stable and compacted the packaging and products, when is shipped or transported.
- To simulate the vertical and rotational forces produced to a packaging or to the whole palletized load, during transportation according to one of the steps of a testing schedule or procedure.
- To simulate the most important shocks and impacts that affect the safety and stability of the load, produced by various means of handling and transportation.
- To simulate the most important horizontal accelerations (speeding, slowing down and breaking) that affect the safety and stability of the load, produced by various means of handling and transportation.

## 4 Real case of stretch wrap film optimisation

In the following example a big producer of soft-drinks had as main objective to assure the stability of the load trying at the same time to optimize tertiary film in a particular distribution cycle. The unit load was made of Glass bottles in 6 pack (carton) in ½ pallet. Its particular distribution cycle included mechanical handling, automatic storage & handling, road vehicle (semi-trailer), train and road vehicle (van last mile).

The acceptance criteria provided by the customer was the following one:

- Maintains stability (not falling apart).
- Maintains corners aligned.
- Pallet over-flight or inclination less than 3 cm.
- Packaging suitable for “normal sales”.

In order to obtain the main objective and solve the problem of stability that the unit load actually was presenting (Figure 13), the methodology described in this paper was applied.

1. Firstly a tailored protocol for testing simulation and validation adapted to the real distribution cycle for the product and for the particular company. It was monitored the complete distribution cycle, and a tailored protocol was developed based on tests described on standards but changing the sequences, the PSD plots, the RMS levels, the horizontal impact speed, the drop height from drops and including in the schedule more realistic tests like multi-axial testing and vehicle accelerating or braking.
2. Secondly wrapping parameters, according to the capability of stretch wrapping machines of the company, were established and obtained in an iterative optimization process using the internal procedure and simple stability tests described before.
3. Then when the film optimization previously defined by the internal procedure was obtained, the unit load was subjected to the complete testing simulation described in the tailored protocol (Figure 8-9), for the proper validation.



**Figure 13**: Left - Instability that the unit load was presenting, Right – Instability solved afterwards

The results obtained after applying this methodology are following presented:

- About the stability of the unit load.
  - ✓ Before - Pallet over-flight or inclination more than 15 cm
  - ✓ After - Pallet over-flight or inclination less than 3 cm (see Figure 30)
- About the film optimization.
  - ✓ Before - 20 film wraps at 200% pre-stretch → Total film weight per pallet of 283 gr
  - ✓ After - 18 film wraps at 250% pre-stretch → Total film weight per pallet of 218 gr

Finally the acceptance criteria was passed successfully and it was obtained approximately a 23% savings on tertiary film. With a 10% less film wraps we obtained the 23% savings on tertiary film mainly due to the increasing of 1.25 times the pre-stretch parameter. The stability of the load was obtained with the right setting of the parameters of the film wrapping machine.

The manufacturing units per hour of this product was 80 pallet per hour, 12 hours per day during 360 days per year. In total a film consumption of 75340 ton, with the new film optimization obtained. Resulting 22464 kg per year of savings.

## Conclusions

Control over stretch wrap processes at the end of packing line is an important task that can save costs, not only on tertiary packaging, if not also reducing costs for damages and returned goods due to lack of stability. Based on our experience in the last years, only 15% of the pallets are optimized (right-packaged), then ¡¡85% of your pallets could be not optimized¡¡. There is a clearly huge potential for improvement.

As more fully automatic pallet stretch wrap equipment used, more level of reducing costs can be achieved. You need to assure that you and consequently your wrapping machines are applying the same quantity of film to get the same retention force needed to keep stable the load, as first day. The constancy in the parameters that you are applying during wrapping process day after day to the same unit load that you have previously defined and optimized, is a quality control check that should be done in the companies periodically.

To fulfill successfully tertiary film optimization you should to incorporate deep know how on film behavior, machinery wrapping process and evaluation testing focus on tertiary film optimization.

The selection of the testing protocol is very important. For optimization better to use tailored protocols adjusted to the particular distribution cycle of the product, including in the schedule more realistic simulation tests (multi-axial testing, vehicle accelerating or braking). As real transport environment is non-stationary and non-gaussian there is a need to use new methods to improve the vertical random vibration testing being utilized in industry

protocols today. As packaging response and bending modes can only be properly excited when the pitch and roll accelerations are taken into account there is a need to test with multi-axis shakers (better 6 DOF but Vertical, Pitch and Roll at least). Adding the pitch and roll module to actual vertical vibration tables, could be a good approach to better simulate the real movements and modes of the unit load. Adding the signal modulation control module to actual random vibration controllers for the generation of non-stationary (varying RMS) and non-Gaussian (high kurtosis) random vibrations, could be a good approach to improve random vibration testing. This technology developed recently could upgrade easily the actual testing laboratories and companies that have a vertical vibration machine.

In order to obtain an high degree of film optimization and saving time and costs it is necessary to include, before going to the complete validation stage, the simple stability test schedule compound by rotational flat drop and horizontal impact (with hazard block). If these tests are passed successfully, before going to the complete validation stage, additional tests like horizontal acceleration and loop forklift circuit could be included to reveal possible non-stabilities or undesirable behavior of packaging or the unit load.

Although pre-stretch is one of the most important parameter to obtain high percentage of saving costs, the wrapping program settings that should also analyzed and defined during the iterating optimization process are mainly which number of layers we are going to use and where they are located, the film overlap and force-to-load level, coverage and wrap to pallet. If the customer machine is able to use ropes during wrapping process also this is taken into account, because depending of the product, could be the only way to keep stable the unit load.

## References


1. Code of Practice for Packing of CTU's - °2014, http://www.unece.org/fileadmin/DAM/trans/doc/2011/wp24/IMO_ILO_UNECE_Guidelines_packing_cargo_1997_01.pdf
2. http://ec.europa.eu/transport/road_safety/events-archive/2012_07_13_press_release_en.htm, http://ec.europa.eu/transport/road_safety/vehicles/doc/cargo_securing_guidelines_en.pdf
3. Bhushan, B., 2013, "Principles and Applications of Tribology (Second ed)", Online ISBN: 9781118403020
4. Soroka, W., 1999, "Fundamentals of Packaging Technology (Second ed.)"
5. Hernandez, R. J., Selke, S. E. M., & Culter, J. D., 2000, "Plastics Packaging: Properties, Processing, Applications and Regulations", Cincinnati, OH: Hanser Gardner Publishers.
6. German, P. M., 1998, "Stretch Films: Background and Basics. Paper presented at the TAPPI Polymers Lamination and Coatings Conference", San Francisco, CA.
7. Peacock, A. J., 2000, "Handbook of Polyethylene (10 ed.)", New York, NY: Marcel Dekker, Inc.
8. ITW Mima Packaging Systems, 2009, "Stretch Wrapping Glossary from http://www.stretch-wrap-machines.co.uk/?page=StretchWrapGlossary"
9. Rouillard, Vincent and Sek, Michael A and Perry, T, 1996, "Analysis and Simulation of Road Profiles. Journal of transportation engineering", 122 (3). ISSN 0733-947X (print) 1943-5436 (online)
10. Rouillard, Vincent and Sek, Michael A., 2000, "Monitoring and Simulating Non-stationary Vibrations for Package Optimization", Packaging Technology and Science, 13 (4). pp. 149-156. ISSN 0894-3214 (print) 1099-1522 (online)
11. Harman, C., Pickel, B., 2066, "http://www.evaluationengineering.com/articles/200606/multi-axis-vibration-reduces-test-time.php", Spectrum, June
12. Bernard, C., Laspalas, A., Gonzalez, D, Liarte, E., Jiménez, M., 2010, "Dynamic study of stacked packaging units by operational modal analysis", Packaging Technology and Science, DOI: 10.1002/pts.883, Feb (online)
13. Batt, G. presentation at the 2010 International Transport Packaging Forum

# Vibration Performance for Biocushion Materials

**Daniel Goodwin[1]*, Changfeng Ge[1], Thomas Kausch[1], Carlos Diaz[1] and Amanda Gordon[1]**

[1] *Department of Packaging Science, Rochester Institute of Technology, USA*

[*] *Corresponding author. dlgipk@rit.edu*

**Abstract:** In recent years, protective package design considerations have added sustainability criteria to the performance aspects for cushioning material selection. Various biodegradable and renewable materials have been investigated in an effort to design environmentally effective package protective systems. Everything from popcorn to mushrooms has received attention in this process. A preliminary study at Rochester Institute of Technology determined the shock and vibration performance characteristics of mushroom-based cushioning. The root-like structure of mushrooms, called mycelium, is used as a binding material for agricultural waste to create an all-natural composite cushioning system. The cushioning material is promoted as 100% renewable and compostable by the supplier. The RIT study focused on material performance in reducing transmitted shock levels under ASTM D-1596 Standard Test Method for Dynamic Shock Cushioning Characteristics of Packaging Material. A Lansmont M23 cushion tester was used to compile results. Testing also included the evaluation of the amplification/attenuation characteristics of the materials, using resonance search techniques as a means of assessing performance under load with respect to vibration input. Vibration testing required use of a Lansmont 7000-10 electrohydraulic vibration tester and generated the input through a sinusoidal signal with a spectrum of 3 – 100 Hz. The preliminary study was limited to cushion thicknesses of 1 and 2 inches (2.54 and 5.08 cm) and was performed under standard laboratory conditions of temperature and humidity. Vibration performance testing resulted in inconsistent resonance levels. The current study addressed the inconsistent levels found in the preliminary research. The testing protocol for cushion evaluation was modified to include a random vibration signal input. It was found to produce improved results, but the levels were still not within the range expected mathematically. The testing protocol also identified the importance of the fixture for mounting the load.

Keywords: biocushions, mushroom cushions, biodegradable packaging, performance curves.

## 1 Introduction

Plant-based feedstocks are used in the production of biocushion materials. These packaging system components are promoted by their suppliers as renewable and sustainable products. However, a central question has emerged regarding the methods by which performance of these biomaterials can be quantified. Performance data on some of the biomaterials, Green Cell Foam® for example, has been published. This is not the case for all such materials. Traditional methods of determining shock and vibration performance characteristics may not be applicable to all forms of these new package components and modified testing procedures may be needed.

A study completed by the Department of Packaging Science at Rochester Institute of Technology (RIT) [1] determined that standard methods of determining shock performance of a mushroom-based cushioning material can be developed using ASTM D-1596 Standard Test Method for Determining Dynamic Shock Cushioning Characteristics of Packaging Materials [2]. However, a common industry practice for determining vibration cushioning characteristics of the same material failed to provide suitable data for cushion design applications. The current study investigated a modified protocol for the industry practice and obtained varied and inconclusive results.

## 2 Research methodology

Testing replicated the previous study but modified the test protocol to assess the viability of a random vibration signal to generate performance characteristics that would yield information allowing for cushion design applications.

## 2.1 Mushroom cushion specimens

The mushroom-based cushion specimens were produced by inoculating cleaned agricultural waste materials with mushroom filament roots. The roots, or mycelium, grow after the mixture is placed in a mold and bind with the waste. After the appropriate length of growing time, approximately 10 days, the mixture is heated and dried. This stops the growth process and the molded cushion is ready for use [3]. Specimens used in the current study were classified as Low Density by the supplier.

One performance benefit of the mushroom cushions is that the surface of the material is non-abrasive and the cushions also act as a desiccant. In addition, this material category is exempt from tariffs that are levied by some countries on petrochemical materials [4].

## 2.2 Test protocol

The test protocol for determining vibration characteristics requires cushion specimens to be placed on an electrohydraulic vibration table and subjected to input signals while under a top load configuration. After each exposure, the natural frequencies, as well as the high and low amplification frequency limits, are recorded. As data is collected over the appropriate loading range, the frequency response levels should decrease in accordance with the expected values predicted by Equation (1) below.

$$f_n = \frac{1}{2\pi}\sqrt{\frac{kg}{w}} \qquad (1)$$

$f_n$ = natural or resonant frequency (Hz)

k = spring constant (lb/inch)

g = gravitational constant (in/sec$^2$)

w = weight (lbs)

Observing the decrease in natural frequency will determine the amplification range of the cushion as the load increases. The various phases of attenuation, amplification and direct coupling can be plotted to make this determination. The packaging professional can then select the appropriate cushion to use for a given product and available load-bearing area, as described in Goodwin and Young and the Lansmont Six-step Method [5][6].

## 2.3 Test protocol modification

The previous research on the mushroom-based cushions utilized a Lansmont 7000-10 electrohydraulic vibration system to input a sinusoidal signal for each loading. The signal input was set to a constant acceleration of 0.5 g and the spectrum width was 3 – 100 Hz. Responses were plotted in the format shown in Figure 1.

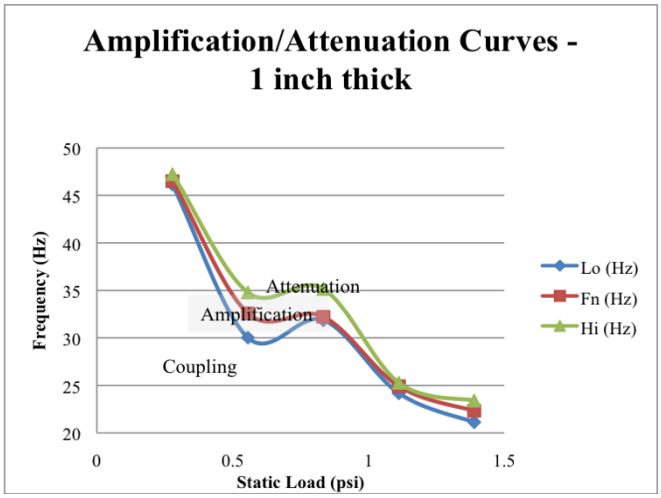



Figure 1: Medium density cushion – 1 inch.

It is noted that the performance curve has an inconsistent response area in the mid-loading range, approximately 0.5 – 0.75 psi (3.45 – 5.18 kPa). For the current study, it was determined that the input signal be modified from sinusoidal to random vibration. A random signal with a 0.54 $g_{rms}$ and a spectrum of 1 – 200 Hz was used to excite the cushion at increased increments from 0.3 to 1.4 psi (2.07 to 9.7 kPa). The random profile is shown in Figure 2 and represents a leaf-spring truck, as presented in ASTM D-4169 Standard Practice for Performance Testing of Shipping Containers and Systems [7].

Five specimens of both 1- and 2-inch (2.54 and 5.08 cm) thicknesses were subjected to the random input signal while under increasing loads. Cushion samples were 6 by 6 inches (15.24 by 15.24 cm). Results are given in the next section.

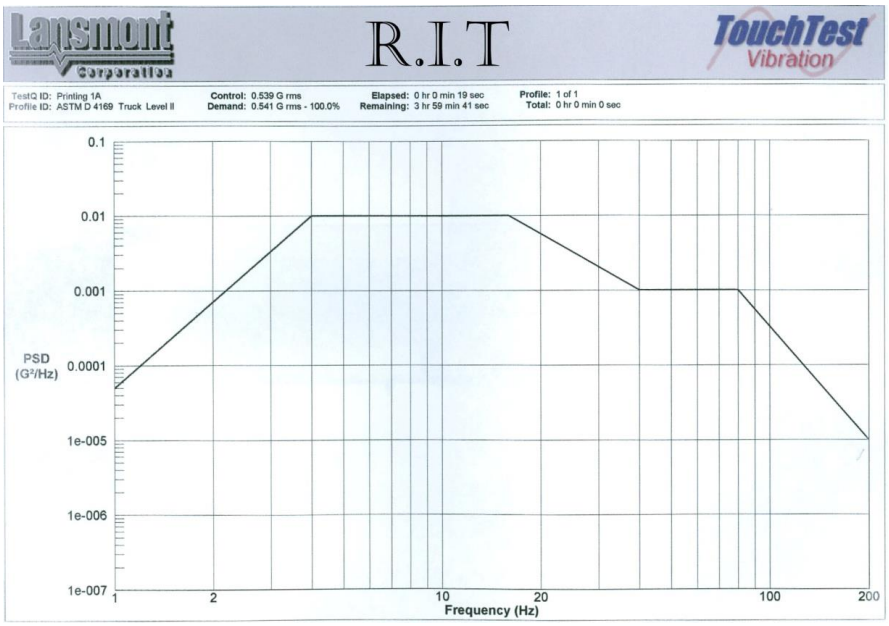



Figure 2: Random vibration input signal.

## 3 Results

Figures 3 and 4 represent the performance curve configurations using the random vibration signal input.

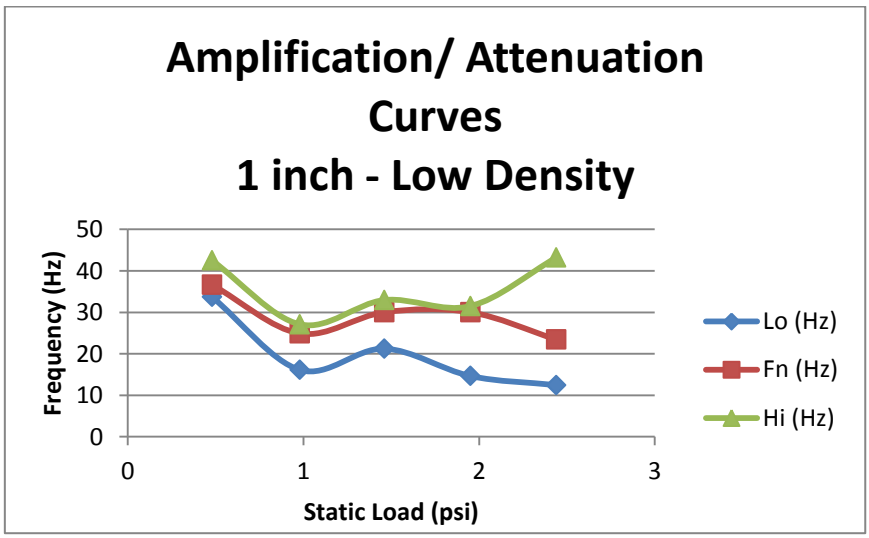



Figure 3: Low density cushion – 1 inch.

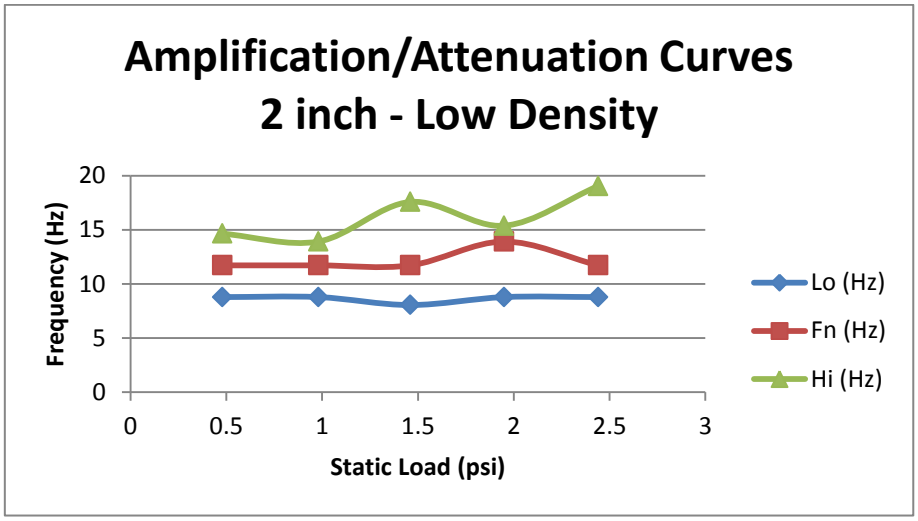



Figure 4: Low density cushion – 2 inch.

Protective cushion design requires the product critical component resonant frequency fall into the area above the Hi frequency at the anticipated static loading level. The erratic nature of the curve will make this difficult to predict.

## 4 Conclusions and discussion

It is noted that the performance curves shown in Figures 3 and 4 do not represent the frequency responses predicted in Equation (1). Figure 3 indicates a slight increase in resonance in the mid-range of the loading scale. Figure 4 represents a nearly constant resonance over the entire loading range. Both the 1-inch and 2-inch cushions should indicate decreasing resonant frequencies with increased static load.

This deviation from the theoretical performance characteristics is due to the lack of uniform density in the cushion material. Observation of the specimen structures revealed a disparity in cavity diameter throughout the cross-sectional area of the material. Given the production process described above, this phenomenon is the result of the natural growth process of the mycelium as it binds the agricultural waste in the mold. This process relies on biological factors and is difficult to control. Equation (1) indicates the resonance frequency of the cushion under load will decrease as the load is increased, provided the spring constant, k, remain unchanged. Given the variation in the size of the inner cavities of the cushion specimens, the effective spring constant varies and creates the subsequent variations in the resultant resonance frequencies.

Figures 5 and 6 present a comparison between the mushroom cushion and polystyrene, a traditional package cushioning material. In Figure 5, the cross-sectional view of the mushroom cushion shows the components are randomly distributed and tend to be more solidly bonded around the outer portion of the material. It is more fibrous in nature and does not have much resilience. The enlarged cross-sectional view of polystyrene in Figure 6 shows the cellular structure that allows the material to behave like an elastic solid that will generate an elastic modulus and produce resilience under the repeated cycles of vibration input [8]. Due to this variation, the mushroom cushion will not maintain a constant k-value over the loading range.

The conventional industry practice of plotting the resonant frequencies of cushioning materials, under increasing loads, will not yield appropriate performance curves for this material. Proper cushion design will require a case by case approach, where the needs of specific products must be assessed and the protective material produced in accordance with those needs.



Figure 5: Cross-section of mushroom cushion.

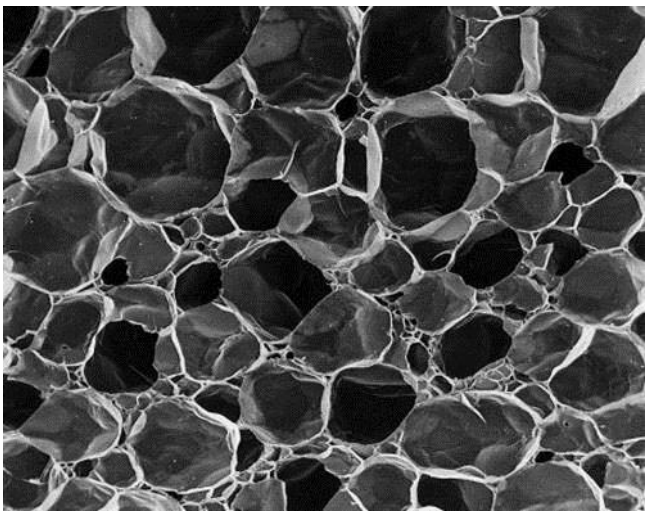


Figure 6: Enlarged cross-section of polystyrene cushion.

## Acknowledgements

The Department of Packaging Science at RIT would like to thank Ecovative, of Green Island, NY, for supplying test samples for this study.

## References

1. D. Goodwin, et. al., 2013, "Shock and Vibration Protection Based on Biocushion Performance Curves", *Proceedings of the IAPRI 26th Symposium on Packaging*, Helsinki, Finland, June 10-13.
2. ASTM D-1596 Standard Method for Determining Characteristics of Cushioning for Packaging Materials. *ASTM International*, West Conshohocken, PA, June 2012.
3. http://www.greenerpackage.com/print/4795. Accessed 28 November 2012.
4. http://www.greenerpackage.com/print/4944. Accessed 28 November 2012.
5. D. Goodwin and D. Young, *Protective Packaging for Distribution*, DEStech Publications Inc., Lancaster, PA, 2011.

6. http://www.lansmont.com. Accessed 25 October 2012.

7. ASTM D-4169 Standard Practice for Performance Testing of Shipping Containers and Systems, *ASTM International*, West Conshohocken, PA, 2012.

8. http://hanalon.en.ec21.com/PE_Foam--5753969.html. Accessed 16 April 2014.

# *How to choose the resistance to vertical crushing of stacked cardboard box suitable for your trip*

**Jean-Baptiste Nolot [1*], Philippe Delloque [1], Jean-Charles Candore [1], Victor Huart [2], Jérôme Pellot [2], Alain Copinet [1], Serge Odof [1] and Damien Erre [1]**

[1] *ESIReims, University of Reims Champagne Ardenne, FRANCE*
[2] *METROPACK, FRANCE*

[*] *Corresponding author. Email: jb.nolot@univ-reims.fr*

**Abstract**: In the packaging field, the most widely used material is cellulose: boxboard and corrugated. This material is present in the primary packaging (in a cardboard case) and in grouping case or in pallet boxes. The most common form is the parallelepiped box with contiguous flaps.

The main feature of this case is the resistance to vertical crushing (RVC). Usually, this system is studied with static method. (Constant application speed of stress about 10mm/min). However, during transport, systems are subjected to dynamic loads such as shock or vibration.

The usual procedure consists on the determination of a static RVC where an empirical coefficient is applied to estimate a dynamic RVC linked to the true transport constraints.

This work suggest an alternative approach:

## 1 Introduction

Usually transport uses corrugated cardboard cases. The boxes are placed on a pallet stacked and wrapped with a stretching film. The load is then cohesive.

Double corrugated EB cardboard cases are used (Basis weight = 654 g/m²). Dimensions are the following: Length = 230 mm, width = 180 mm, Height = 300 mm. Properties of the material samples are in Table 1.

**Table 1:** Properties of the material samples.

| Sample type | Thickness [mm] | Resistance to vertical crushing [N] | Resistance to bending [N] | Edge crush test [N] |
|---|---|---|---|---|
| Double corrugated EB cardboard Cases | 4.3 | 2344 | 30.2 | 829 |

Resistance to Vertical Compression according to standard NFH 13-001
Edge Crush Test according to standard ISO 3037
All experimentations have been realized in the following conditions: 23°C ï 50% Relative Humidity.
Paper used: type and weight data following manufacturer, Smurfit Kappa, plant of Brignoles (Var, France):

Ref = EB30 K135/C090/C090/HP125/TL120
K = kraft paper
C = recycled paper
HP = High performance paper
TL = test liner paper
Numbers: weight in g/m2

Data collected concern two transports by truck between two plants and a carriage transport inside a plant. Loading and unloading of truck are also recorded. Features of transport are given in the table 2.

**Table 2:** Trip & Pallet characteristics.

| Trip type | Transportation | Distance [km] | Pallet weight [kg] | Road |
|---|---|---|---|---|
| 1- Reims / Epernay | Truck (19 tonnes) | 31 | 245 | Secondary road |
| 2- Reims / Recy | Truck (19 tonnes) | 43 | 263 | Highway |
| 3- Factory | Forklift (2.5 tonnes) | 1.1 | 236 | Internal Factory |

3 EURO pallets (800 x 1200 mm) are used.

They are homogeneous. Loading is perfectly cohesive. The masses of pallets are given in table 2.

Two SAVER 3X90 recorders (Lansmont) are screwed to each pallet diagonally at opposite position.

Instruments set-up permits to record shocks after exceeding a trigger of 3G with an acquisition rate of 2500 samples / second. Recordings were filtered at 500 Hz.

Real vertical constraints of shock on current packaging during transportation and manipulations are recorded

## 2 Constraints recorded on the field

Only vertical shocks are concerned.

10 strongest shocks of each transport are stored and analyzed.

Maximum values of acceleration (Amax, G), shock Time (T, sec) and speed variation (ϕV, m/s) are measured.

Data are shown in **Figure 1**:

Each point (ϕV, Am) represents a vertical shock. 3 transports are represented.

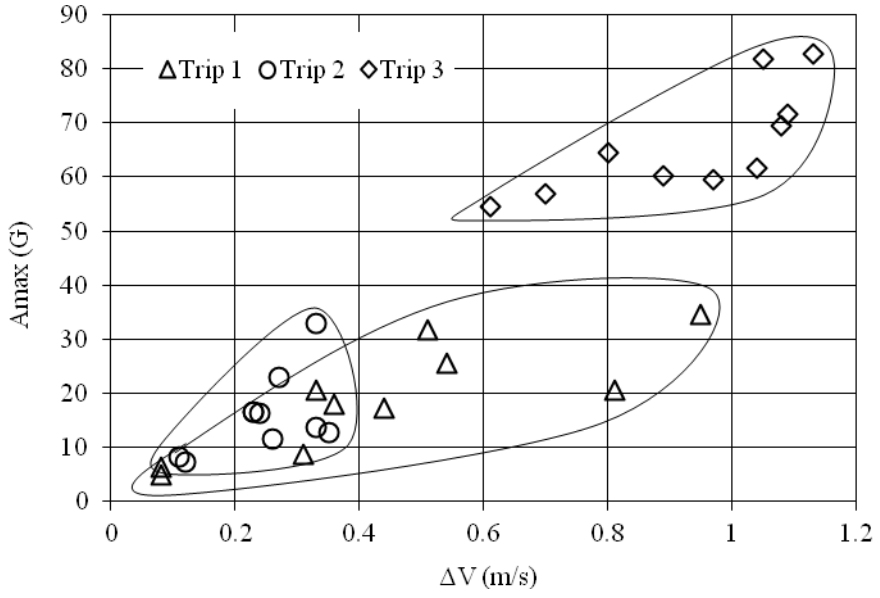



**Figure 1**: Verticals Shocks on pallets from 3 different trips

## 3 Fragility Tests of cases

The limit strength of the cardboard case (define Table 1) is define experimentally. ASTM D3332
Different masses (M) are placed on the top of the case. The mass is stuck on the top of box. This is the specimen.
The box (and the masse above) is placed and stuck on the Shock Tester (Lansmont)
TP3 software (Lansmont)
The recording system TP3 (Lansmont) saves shocks generated by the Shock Tester.
The shock is measured on the bottom of specimen. (On the table of the Shock Tester)
Different kinds of shocks are injected.

**1/ Short impact:** The lab generates a half-sine wave with low impact velocity by the mechanical impact machine, accompanied by a short impulse time, upon the specimen.

On completion of the first impact, a thorough inspection takes place on the appearance and functionality of the product. No deformation and no flexion must be seen on the box. If no anomaly is found, a second impact is performed with a slightly increased impact velocity. The test goes on in this manner with gradually increased impact velocities until the product is damaged (which gives the critical design velocity φVc of the specimen).

**2/ Long impact:** The specimen is given a low acceleration trapezoid. After one shock, the product is visually inspected and checked for any malfunctions carefully. If there are no defects or malfunctions, then the product is given a slightly higher acceleration shock. This is conducted repeatedly until the product fails to find the product's critical acceleration (Ac). This data will be given to package designers to improve the packaging design for its best protection and will be used for reference during packaged drop test.

Two data are notified:
The specimen's critical velocity (φVc)
The specimen's critical acceleration (Ac)

The damage boundary curves (Figure 2) of cardboard box with mass (M) on the top are established.

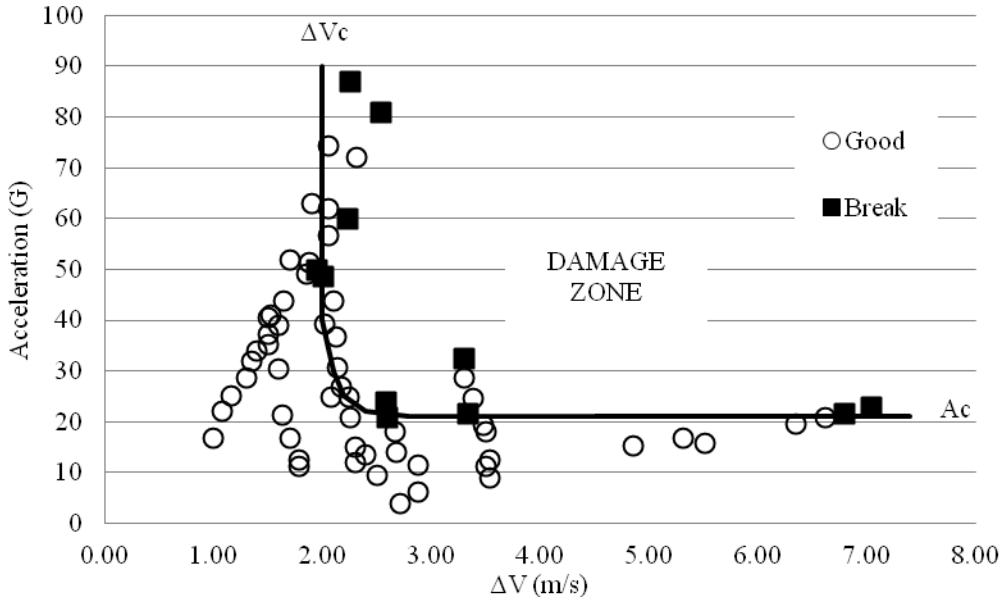



**Figure 2**: Damage Boundary Curve ï Double corrugated EB cardboard box With Preload M=6.9 kg

For example: With M = 6.9 kg ï Ac = 21.2 G - φVc = 1.98 m/s

## 3 Fragility versus masse (M) on the top

Several experiments are performed by varying the mass M.

The table 3 below presents the results:

**Table 3:** Properties of the material samples.

| Masse M [kg] | Critical Acceleration Ac [G] | Critical Velocity φVc [m/s] |
|---|---|---|
| 2.4 | 110.1 | 3.62 |
| 3.9 | 58.7 | 3.04 |
| 6.9 | 21.2 | 1.98 |
| 11.9 | 15.0 | 1.4 |
| 16.9 | 10.2 | 0.92 |
| 21.9 | 7.4 | 0.80 |

The different damage boundary curves (Figure 3) of cardboard box with different mass (M) on the top are established.

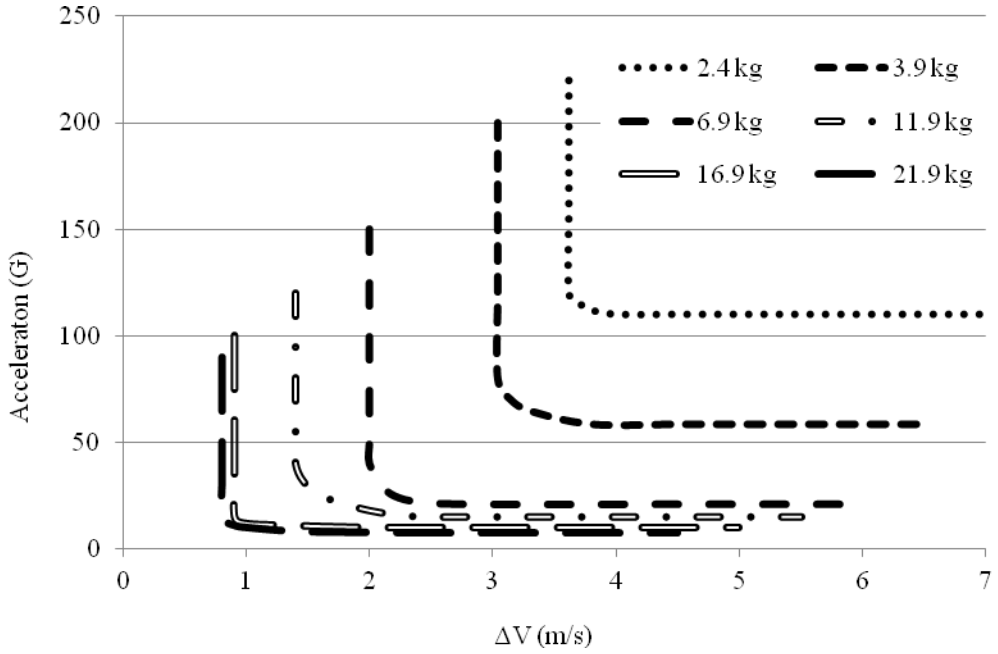



**Figure 3**: different damage boundary curves versus masse M

These measures permit to determine the position of critical points (φVc ï Ac) depending on the mass M.

The following equation defined the critical acceleration depending on the mass M:

$$Ac = 286.85\ M^{-1.202} \quad \text{with } R^2 = 0.982$$

The equation of the variation of speed depending on the mass M is the following:

$$\varphi Vc = 7.4444\ M^{-0.711} \quad \text{with } R^2 = 0.982$$

Position of critical points is shown on Figure 4:

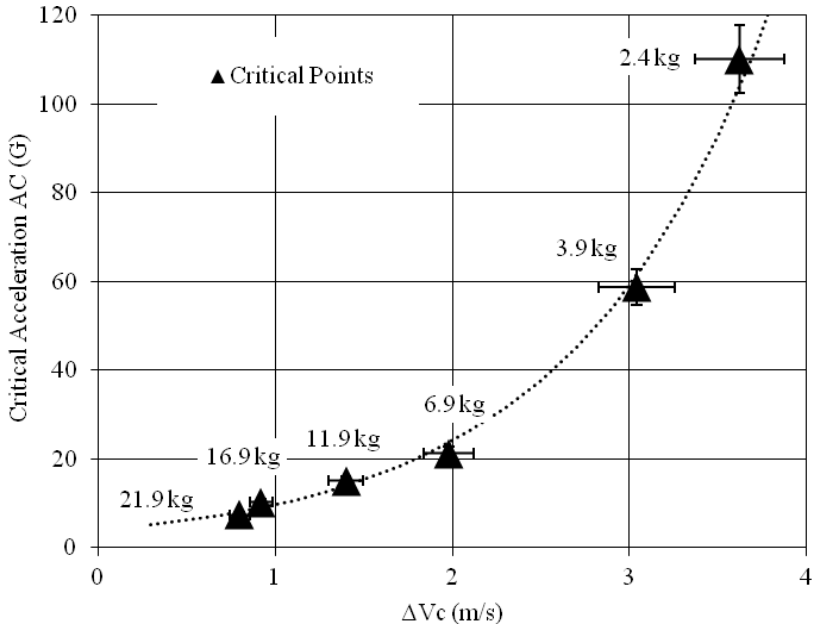



**Figure 4**: Position of critical points versus masse M

## 4 Comparison between damage and trip

Following these results, it can be possible to choose the maximum acceptable mass of stacking for this Double corrugated EB cardboard box and its transport.

Shocks encountered in transport are critical values that it will be not exceeded.

By projecting extreme points of each transport on the curve of critical points, the maximum acceptable weight (M) is calculated.

Figure 5 below shows the reading.

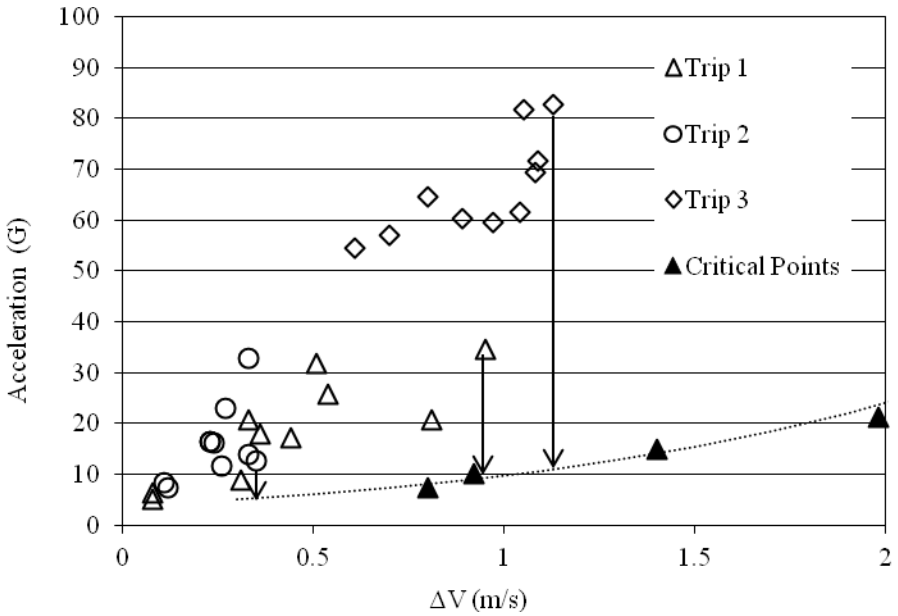



**Figure 5**: Comparison between damage and trip

Maximal acceptable masses (M) on the top of Double corrugated EB cardboard box are the following:

**Table 4:** Mass supported by trip

| Trip type | Acceleration Maxi Amax [G] | Velocity Variation ϕV [m/s] | Masse Maximum [kg] |
|---|---|---|---|
| Trip 1 | 37.4 | 0.95 | 18.1 +/- 0.5 |
| Trip 2 | 32.9 | 0.35 | 73.7 +/- 0.5 |
| Trip 3 | 82.8 | 1.13 | 14.2 +/- 0.5 |

## 5 Conclusion

This method allows-us to choose the acceptable mass which can be stacked during transport.

The physical factor limiting the compressive strength of a cardboard box in the dynamic phenomena such as shock is the variation in maximum critical speed (ϕVc) that preloaded box can accept. This study shows that the acceleration measurement is not sufficient to develop a protective packaging.

Therefore, it is necessary to bring greater attention to the measurement of speed variation of shocks.

This method requires the position sensor on the pallet.

# Influence of corrugated cardboard corners in shock damping: Case of a 100% cardboard packaging.

**Philippe Delloque [1*], Jean-Baptiste Nolot [1], Jean-Charles Candore [1], Victor Huart [2], , Alain Copinet [1], Serge Odof [1],Nicolas Krajka [2]and Damien Erre [1]**

[1] *ESIReims, University of Reims Champagne Ardenne, FRANCE*
[2] *METROPACK, FRANCE*

[*]*Corresponding author. Email: philippe.delloque@univ-reims.fr*

## 1 / Introduction :

Goods shipped in corrugated box have generally cushioning foams issued from petroleum industry (polystyrene, polyurethane, polypropylene,é ).

This study tried to characterize the damping capacity of a cardboard corner.

Two specific tests were realized to determine the corner capacity of a box to dump shocks without cushioning foam adding in this part.

## 2 / description of experiences :

### a / Falls of entire boxes on corners :

We made a wooden box 150x200x300 mm. We cut both corners of 7 cm edge length. The box weight was 1100 g. For the purposes of the experiment, we add wooden boards to increase the mass as following: 1560 g, 1970 g, 2360 g, 2930 g, and 3500 g. Using a rapid prototyping machine (Zund M- 1600 and its associated software ArtiosCAD and Impact), we manufactured corrugated cardboard box, an American box type, in EB type, with internal dimensions 150x200x300 mm. The box was glued with hot melt glue. The wooden box without two corners has been installed inside the cardboard box, a three axis acceleration sensor screwed inside.Boxes were closed for the tests by a standard adhesive of 50 mm width. The falls were realized by using a Lansmont drop tester. To records accelerations, the Lansmont software TP3 was used. Boxes fall at four different heights: 30 cm, 40 cm, 50 cm, and 60 cm. We used for our results the records of the resultant of the three axis of the shock.

**b / falls of corners only :**

We manufactured corrugated cardboard corners, EB type, with the rapid prototyping machine. We simulated falls using the machine Lansmont cushion tester. We used different masses as following: 950 g, 1422 g, 1927 g, 2363 g, 2835 g, and 3340 g. These different masses were fall at four different heights: 30 cm, 40 cm, 50 cm, and 60 cm.The drop height of the cushion tester is adjusted according to the amount equivalent to a free fall impact velocity.An acceleration sensor was positioned on the plate supporting the masses, the acquisition is performed by the Lansmont software TP3.We performed two series of measurements with two different techniques to keep the cardboard corner in place: one with a wooden frame and one with a standard adhesive, 50 mm width.

**c / Corrugated cardboard EB characteristics :**

Resistance to Vertical Compression according to standard NFH 13-001 = 2350 N

Edge Crush Test according to standard ISO 3037 = 829, 3 N

Paper used: type and weight data following manufacturer, Smurfit Kappa, plant of Brignoles (Var, France):

Ref = EB30 K135/C090/C090/HP125/TL120

K = kraft paper

C = recycled paper

HP = High performance paper

TL = test liner paper

Numbers: weight in g/m2

## 3 / Results obtained :

### a / Falls of entire boxes on corners cases :

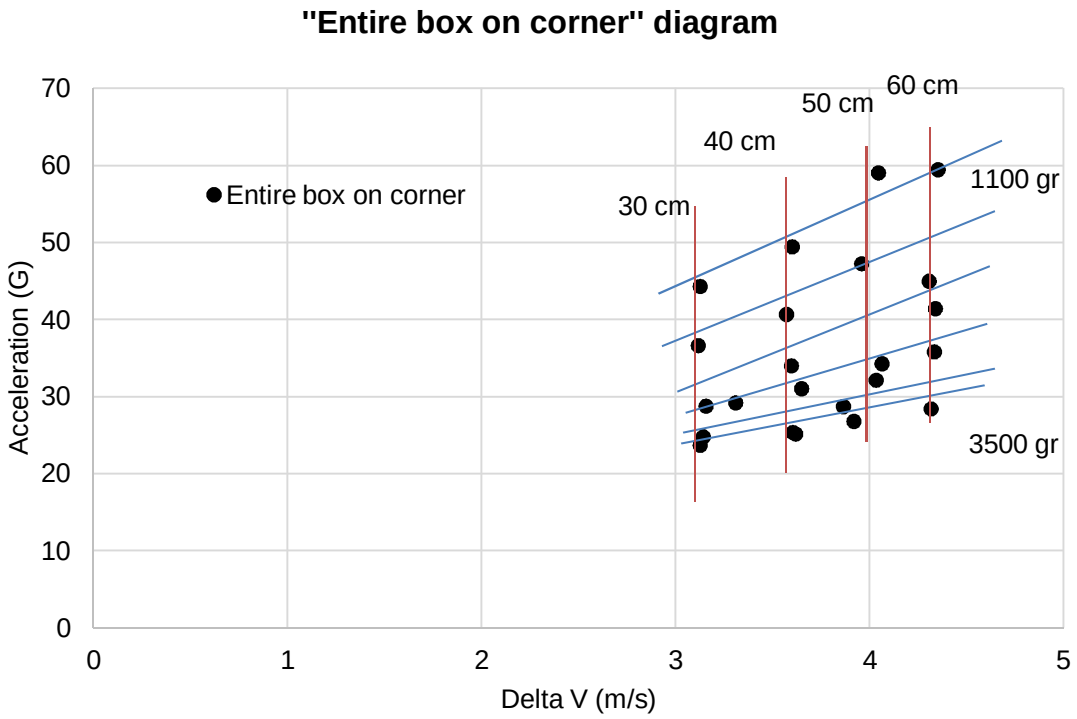



Fig 1: Free drop of ôôEntire box on cornerôô

The diagram (Fig 1) has allowed us to do these four findings :

ÅFor each fall heights, the Delta V is constant.

ÅThe variation of intensity of the acceleration during the impact is inversely proportional to the mass.

ÅFor one mass, the shock increases with increasing height.

ÅThe absorption of the impact energy by the corner is higher if the mass increases, in the limit of deformation of the corner.

**b / Falls on corner only cases, maintained by a wooden frame :**

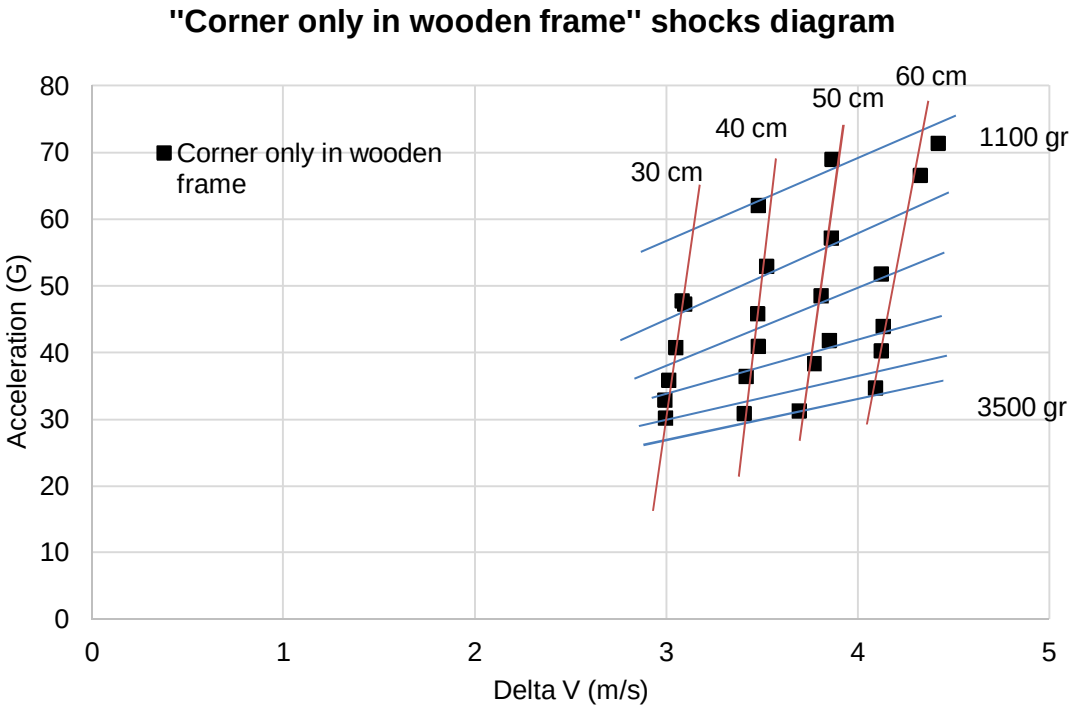



Fig 2: Free drop of mass on ôCorner only in wooden frameô

The diagram (Fig 2) has allowed us to do these four findings :

- For each fall heights, the Delta V is slightly increasing.
- The variation of intensity of the acceleration during the impact is inversely proportional to the mass.
- For one mass, the shock increases with increasing height.
- The absorption of the impact energy by the corner is higher if the mass increases, in the limit of deformation of the corner.

The last three findings are equivalent to the results of the falls of entire boxes on corners cases. However, the general level of energy is higher, which means the impact is overestimated in comparison to the entire box.

The following diagram (Fig 3) highlights this phenomenon:

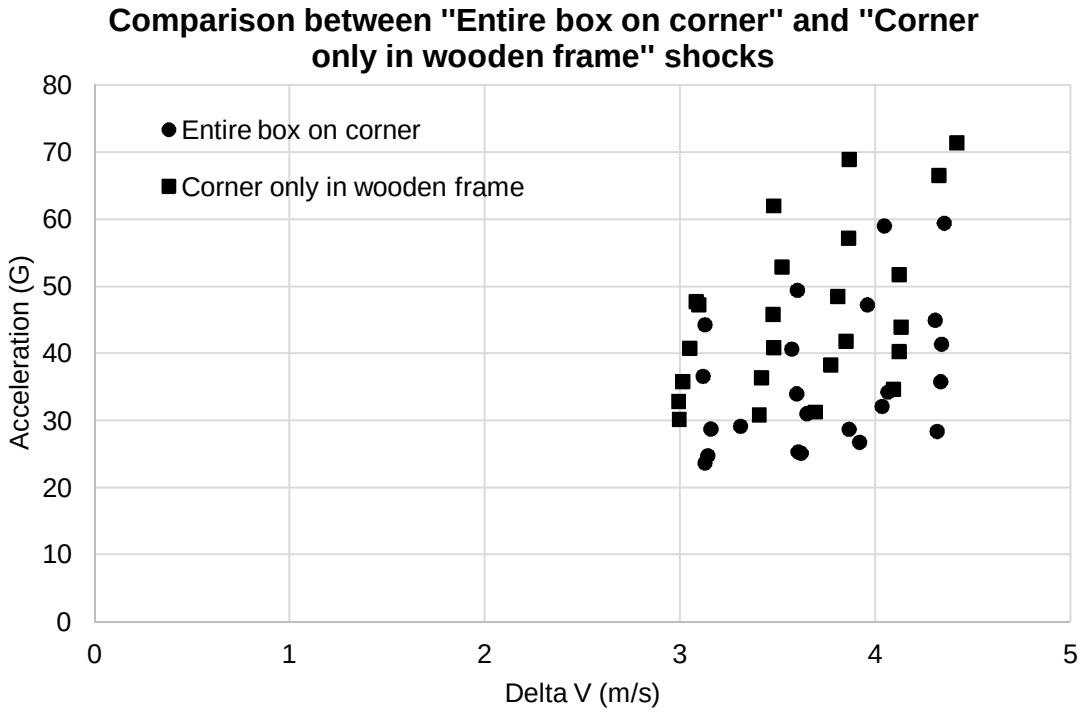



Fig 3: Comparison between ôEntire box on cornerö and ôCorner in wooden frameö

**c / Falls on corner only cases, maintained by standard adhesive :**

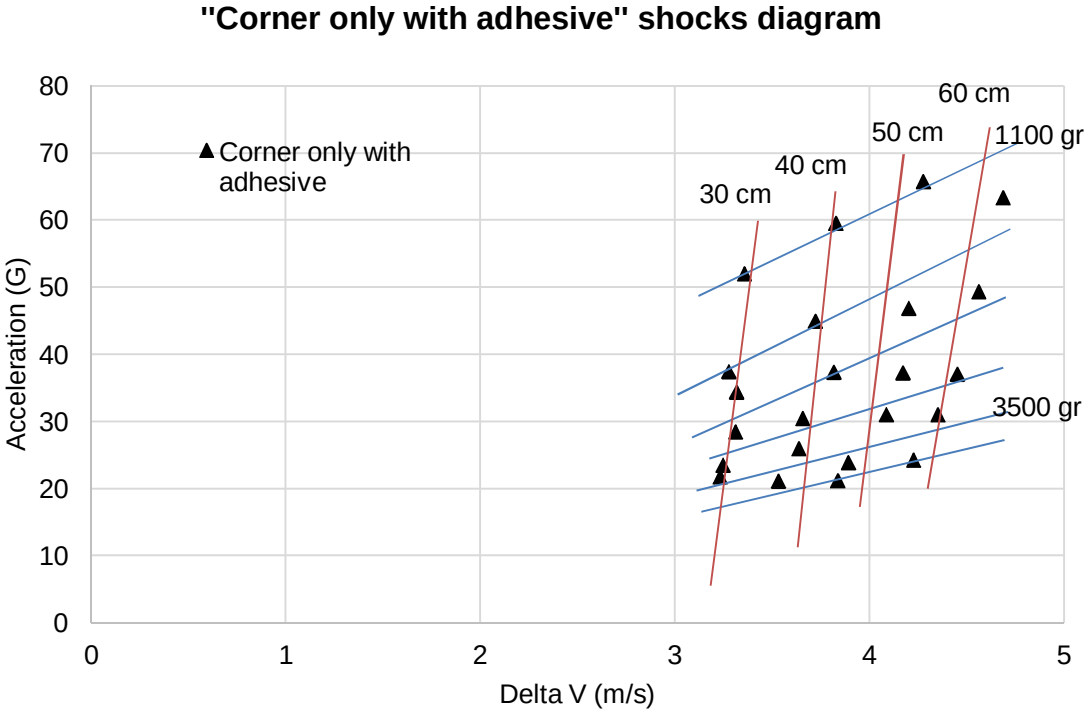



Fig 4: Free drop of mass on ôCorner only with adhesiveö

We findings the same that we had on the corner only in wooden frame, with a variation of the impact level energy. This case is closer than the result of entire boxes. There is a small underestimation of impact in the high masses.

The following diagram (Fig 5) shows it is almost equal :

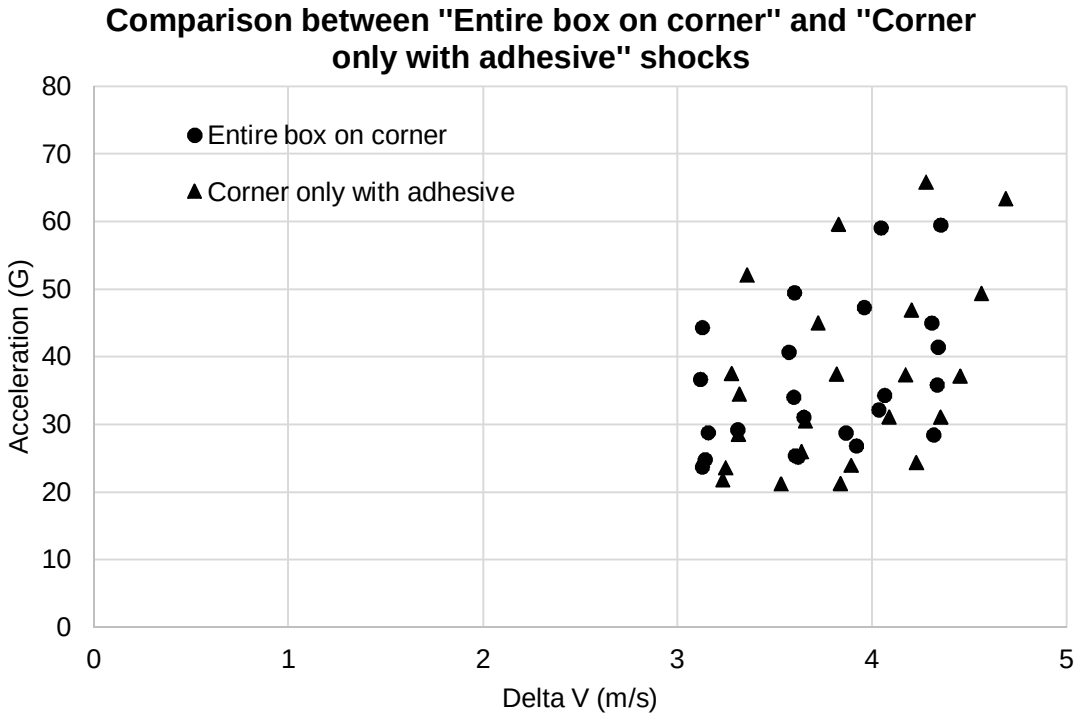



Fig 5: Comparison between õEntire box on cornerö and õCorner only with adhesiveõ

## 4 / Conclusion :

It is pertinent to use both cushion tester and cardboard corner shaped, provided the corner is maintained with adhesive, to get closer to an entire box corner shock. The corrugated cardboard, flute EB, is concerned by this approach. Studies are in progress to confirm or not if the behavior of other types of cardboard or flute is equivalent as ñentire boxò or ñcorner onlyò.

Finally, this study shows that cardboard box corner is an excellent cushion and an efficient shock absorber insofar as the deformation is dimensionally smaller than the value to reach the object to be protected in the box. Furthermore, depending on the rigidity of the cardboard, the mass of the object to be protected is different : on our flute EB cardboard study, a rigid cardboard, the best protection is clearly on the higher masses, that means a lower energy shock.

Future studies will be realized to show if the rigidity of cardboard varies its shock absorbing efficiency depending of masses of objects to be protected.

# Impact of Liquid Nitrogen Dosing on Application and Removal Torque of Wine Bottle Closures

**Colton Baptista[1], Koushik Saha[1*], and Jay Singh[1]**

[1] *Packaging Program, Cal Poly State University, USA*

[*] *Corresponding author. Email: ksaha@calpoly.edu*

**Abstract:** Several studies have been performed that test the finish performance of different types of wine bottles with specific closures systems. However there is a lack of research for closure performance with regard to liquid nitrogen dosing, and its performance within a distribution environment. This study evaluated closure performance of two different types of wine bottles. A standard 750ml glass bottle, produced by 'Verallia Glass Company' and standard 750ml plastic wine bottle produced by 'EnVino Bottles'. Bottles were manually filled to approximate standard fill levels, before they were properly dosed with Liquid Nitrogen as needed and the proper application torque was applied to properly secure the container. The dosing amounts were calculated by measuring the approximate amount of headspace in each type of bottle and then using a Cryotech Calculation chart determining the amount of liquid nitrogen needed to fill that headspace. Glass and plastic bottles were injected with 0.043g and 0.037g of liquid nitrogen respectively. Subsequently, these bottles were subjected to ambient and tropical temperature conditioning prior to simulating a distribution environment as per ISTA 2A test procedure. A Chart Cryotech introdoser was utilized for the liquid nitrogen dosing and an Imada DTX-80 table top torque tester was utilized to record the proper application and removal torque of all bottles in the study. The findings of this study can be beneficial to those in in the wine industry, to determine how liquid nitrogen dosing, distribution environments and different environmental conditions could affect the performance of screw top closures.

Keywords: Finish Performance, Liquid Nitrogen dosing, Application/Removal torque, Wine bottle, Plastic Wine bottle, Distribution testing

## 1 Introduction

There is limited research in this area other than a prior study done by Nakamura et al [1] where closure performances were evaluated under liquid nitrogen dosing and various environmental conditions during distribution. Nakamura et al [1] studied the impact on closure performance of PET bottles as an effect of liquid nitrogen dosing. As a continuation of this previous research, this current study expands on the evaluation of closure performance as an effect of liquid nitrogen dosing to wine bottles made from glass and plastic material as currently used in the wine industry. This study examines the benefits of using screw top closures for wine bottles over the traditional cork closures. While screw top closures eliminate the risk of wine products becoming spoiled by cork residue or oxidation, it also allows the implementation of other beneficial technology such as liquid nitrogen dosing, which has shown to enhance wine preservation [2]. Dosing sealed products with liquid nitrogen has been proven to increase shelf life of beverages and food products alike, while in some cases supplementing in strength for certain types of packaging such as plastic packaging [2].

The purpose of this study was to test the closure finish performance of screw caps on wine bottles under liquid nitrogen dosing, varied temperature conditions and a distribution environment. In this study two types of standard size wine bottles made from glass and plastic material were used with Roll-on Pilfer Proof (ROPP) finishes. 30mm aluminium screw cap closures were used to secure both bottle types. The bottles were filled with water as a simulant to proper filling levels and then dosed with liquid nitrogen at the recommended levels. After dosing the bottles were sealed with the screw caps to a recommended torque level based on ISTA standards. To find the proper torque level, the finish diameter of the bottle in millimetres is divided by two [3]. This gives you the amount of force needed in inch-pounds to create a proper seal. Then the bottles were exposed to either ambient or tropical environmental conditions for 24 hours. The distribution testing used for the bottles followed ISTA procedure 2A [4] which is designed for packaged products that weigh 150 pounds (68 kilograms) or less. Following which the removal torque for each bottle was recorded and the data was used to determine the closure performance for the bottles.

## 2 Materials and Methods

In this study two types of standard size wine bottles made from glass and plastic material were used with ROPP finishes (Figure 1). A 30 millimetre diameter aluminium screw top closures was used to seal the bottles (Figure 1). Table 1 lists the bottle specifications used in this study. A Regular Slotted Container made from a C-flute corrugated fibreboard with a board combination of 44/34/44 lb. was created to serve as a shipper to hold 6 bottles. The dimensions for the glass and plastic bottle shippers were 246 X 79 X 319 mm and 225 X 148 X 301 mm respectively.



A B C

**Figure 1**: **A**: Screw Cap, **B**: Glass Bottle, **C**: Plastic Bottle

**Table 1:** Bottle Specifications

| | Glass Bottle | Plastic Bottle |
|---|---|---|
| Bottle Weight | 419.57 grams | 34.02 grams |
| Finish | 30 mm ROPP | 30 mm ROPP |
| Maximum Diameter | 79.3 mm | 72.3 inches |
| Height | 303 mm | 284 mm |

A Cryotech International "Introdoser Injector System" was used to dose the bottles with liquid nitrogen (Figure 2). An "Imada DTX-85B" Table top torque tester was used to measure the application and removal torque of the bottles (Figure 2). Liquid Nitrogen was dosed into the necessary bottles manually subsequently the bottles were manually sealed to the recommended application torque. Since both bottles had the same finish diameter of 30mm, the application torque recommended for both bottles was 15 in-lb [3].




A B

**Figure 2**: **A**: Liquid Nitrogen Doser Injector System, **B**: Table Top Torque Tester Imada DTX-85B,

Following was the stepwise procedure to dose glass or plastic wine bottles with liquid nitrogen:

1. The bottles were first filled with 750 ml of water to serve as a product simulant.
2. The bottles were then secured onto the Imada torque tester by using peg grips (Figure 2).
3. The torque tester was then lined up with the Cryotech doser so that the openings of the bottles were directly the dosing head of the doser. The dosing head was within 51 mm above the openings of the bottles.
4. The doser dispensed liquid nitrogen in exact amounts by a measure in milliseconds. Before dosing, the doser is set to apply the correct amount of liquid nitrogen and that the bottle is in place.
5. The torque tester was set to peak mode to measure the greatest amount of torque applied accurately to reach the recommended application torque.
6. In one hand the researcher held the doser button to begin the process of dosing while with the other hand held a screw cap to secure the bottles.
7. Upon pressing the doser button, the pre-set liquid nitrogen was injected into the bottle. Subsequently the screw cap was immediately applied on to the bottle. If the torque tester showed the cap has not achieved enough torque to reach the recommended level, addition torque was applied to the cap until the tester read the recommended torque level.
8. Once properly sealed, the torque was recorded and the bottles were labelled and put into their appropriate shippers to undergo proper environmental and distribution testing.

The dosing amounts were calculated by measuring the approximate amount of headspace in each type of bottle and then using a Cryotech Calculation chart determining the amount of liquid nitrogen needed to fill that headspace [5]. For the glass bottles the dose duration was 39.75 milliseconds equalling to an amount of 0.043 grams of liquid nitrogen injected into the bottles. Whereas for the plastic bottles the duration was 33 milliseconds which would be 0.0357 grams of liquid nitrogen injected. The experimental plan for this study needed 40 bottles for each type (plastic and glass) (Table 2). Table 2 shows the combination of treatments both type of bottles endured before determining the removal torque.

**Table 2:** Experimental Plan.

| Bottle Treatment | LN2 Dosing | Environmental conditioning | Distribution Testing | No. of Bottles |
|---|---|---|---|---|
| 1 | Yes | Ambient | Yes | 5 |
| 2 | Yes | Ambient | No | 5 |
| 3 | Yes | Tropical | Yes | 5 |
| 4 | Yes | Tropical | No | 5 |
| 5 | No | Ambient | Yes | 5 |
| 6 | No | Ambient | No | 5 |
| 7 | No | Tropical | Yes | 5 |
| 8 | No | Tropical | No | 5 |

## 3 Results and Discussions

The percent differential in torque was calculated according to equation 1. A higher percent differential indicates a lower removal torque was required to disengage a closure. Treatment 6 as shown in Table 2 was considered as the control group for both plastic and glass bottles for comparison with the other seven treatments. The control group did not have any liquid nitrogen in the head space and was stored in ambient conditions without exposing it to the elements of distribution testing. The data presented in Table 3 & 4 shows the percent differential between the application and removal torques of the glass and plastic bottle closures respectively.

$$Percent\ Differential = \frac{Application\ Torque - Removal\ Torque}{Application\ Torque} \times 100 \quad (1)$$

### 3.1 Glass Bottle Closure Performance

Comparing glass bottle closure treatments with the control group, it was observed that the mean percent differentials for treatment 1, 5, and 7 were higher by 13.96%, 14.13%, and 7.86% respectively. This indicates that the amount of torque needed to disengage caps in comparison to the application torques was less than the torque required to disengage caps from bottles of the control group. The bottle closure treatments 1,5, and 7 all experienced distribution testing, indicating that closure performance was affected by the distribution elements compared to the bottle closures which did not experience any distribution related abuse.

Bottle closure treatments 2,3, and 4 had percent differentials which were similar to the control group. Bottle closure treatment 2's percent differential was 0.26% higher than the control group. Bottle closure treatment 3's percent differential was 1.74% lower than the control group and treatment 4's percent differential was 2.18% higher than the control group. These groups all underwent liquid nitrogen dosing with different combinations of environmental and distribution testing.

Only treatment 8 had a percent differential that was noticeably lower than the control group by 11.49%.This indicates that treatment 8 bottle closure required lesser amount of removal torque compared to its application torque which was higher than the control group's removal torque compared to its application torque.

**Table 3:** Percent Differential between Application and Removal Torque for Glass Bottles

| Bottle Treatment | Mean Percent Differential | Range of Percent Differential |
|---|---|---|
| 1 | 36.64% | 21.57% to 44.74% |
| 2 | 22.94% | 10.74% to 31.58% |
| 3 | 20.94% | 10.53% to 28.29% |
| 4 | 24.86% | 11.61% to 37.58% |
| 5 | 36.81% | 19.74% to 56.67% |
| 6 | 22.68% | 13.91% to 35.06% |
| 7 | 30.54% | 21.19% to 37.75% |
| 8 | 11.19% | 0.01% to 18.67% |

### 3.2 Plastic Bottle Closure Performance

Comparing plastic bottle closure treatments with the control group was observed to have noticeably higher percent differentials. This indicated that all the treatments resulted in affecting bottle closure performance as they needed less torque to open the bottles compared to the control group.

The percent differentials for treatments 2 and 8 were slightly higher than the control group by 8.7% and 14.32% respectively. These condition combinations did not undergo any distribution testing while they differed in environmental testing and nitrogen dosing.

Treatments 1, 3, and 5 had percent differentials that were moderately higher, than the control group by 21.54%, 28.54%, and 31.37% respectively. These treatments underwent distribution testing while differed in combinations of environmental conditioning and nitrogen dosing.

Treatrmentss 4 and 7 showed the greatest increase in percent differential compared to the control group by 44.8% and 54.37% respectively. Both underwent tropical conditioning, while treatment 4 was nitrogen dosed without a distribution test and treatment 7 underwent a distribution test without nitrogen dosing.

**Table 4:** Percent Differential between Application and Removal Torque for Plastic Bottles

| Bottle Treatment | Mean Percent Differential | Range of Percent Differential |
|---|---|---|
| 1 | 39.18% | 25% to 48.37% |
| 2 | 26.34% | 20.13% to 31.33% |
| 3 | 46.18% | 35.1% to 56.38% |
| 4 | 62.44% | 54.3% to 84.11% |
| 5 | 49.01% | 42.11% to 57.05% |
| 6 | 17.64% | 7.95% to 24% |
| 7 | 72.01% | 70.86% to 73.15% |
| 8 | 31.96% | 16% to 42.21% |

## 4 Conclusions

This experiment examined the closure performance of screw caps undergoing various treatments. The performance was measured by using percent differentials between application and removal torque after the closures experienced different treatments which included liquid nitrogen dosing, environmental conditioning, and distribution simulation.

For the glass bottles, distribution testing seemed to have the greatest impact in reducing the amount of torque needed to remove the closures. Bottles that received distribution testing typically had higher percent differentials, signifying lower torque removal values, than bottles that did not receive distribution testing. The data suggests tropical environments require greater torque to remove the closures compared to the group's ambient counterparts. Liquid Nitrogen dosing at recommended levels, seems to have relatively small impact in closure performance. Most treatments with liquid nitrogen dosing had percent differentials similar to the control group. None of the data expressed significant correlations between bottles that were liquid nitrogen dosed and bottles that were not.

For the plastic bottles, all the treatments showed an increase in percent differentials compared to control group, which means less removal torque was needed to remove bottle closures. However, there was variation on how the conditions affected the removal torques. Distribution testing delivered the most consistent results related to removal torque value. Both environmental conditioning and liquid nitrogen dosing exhibited significant variation in their effect on lowering removal torque. In individually testing these conditions, liquid nitrogen dosing in ambient conditions and tropical conditions without liquid nitrogen dosing or distribution, proved to yield the smallest impact in lowering torque levels. Collectively all the conditions (liquid nitrogen dosing, environment, and distribution testing) tended to yield greater reductions in removal torque values, however, distribution testing, specifically, seemed to play the most significant role in reducing torque value.

The findings in this study can be beneficial to those in the beverage industry, particularly the wine industry, to determine how liquid nitrogen dosing, distribution environments and different environmental conditions could affect the performance of screw top closures.

## Acknowledgements

The researchers will like to thank Cryotech Chart Inc. for providing the liquid nitrogen dosing system and Verallia Glass Company and EnVino Bottles for providing glass and plastic wine bottles for this research project.

## References

1. C. Nakamura, K. Saha and J. Singh. “Impact of Liquid Nitrogen Injection and Application Torque on the Finish Performance and Removal Torque of Closures for PET Beverage Bottles” 18th IAPRI World Packaging Conference, Proceeding June 17-21, 2012, San Luis Obispo, CA

2. R., C. Ghidossi, C. Poupot, A. Thibon, P. Pons, L. Darriet, G.D.R. Riquier and M. Mietton Peuchot. 2012 "The Influence of Packaging on Wine Conservation." Food Control no.23, pp: 302-11.

3. S.P. Singh, G. Burgess, and J. Singh. 2003, “Package performance testing of dangerous goods in high-altitude shipments” Packaging Technology and Science, no.16, pp: 119–130.
4. International Safe Transit Association. “ISTA Testing Procedure 2A” East Lansing, Michigan, 2011.
5. Chart Cryotech International “Introdoser Information” San Jose, CA.

# LOGISTICS & SUPPLY CHAIN

# The Sacks of Rome?[#]

**Diana Twede**

*Michigan State University*

*Email: twede@anr.msu.edu*

**Abstract:** While they have long been ubiquitous for shipping granular products, no one actually knows when textile sacks were first used for large shipments of grain, nor is it known when textiles were first used to make shipping sacks. This research is a first attempt to question when the "packaging technology" of shipping sacks was first used on a large scale.

Hypothesis: the ancient Egypt-Rome grain trade (after Egypt's annexation in 30 BC) had adequate scale, organization, natural resources, and technological resourcefulness to ship in sacks.

Grain and linen textiles were both major exports from Egypt, and most archaeologists and historians assume that sacks were used to ship grain from ancient Egypt to Imperial Rome. Some scholars compare the packaging of wine and olive oil in amphorae, assuming that grain was carried in sacks, even though no actual examples have ever been found (one disadvantage of package biodegradability). The Roman Empire's control of the supply chain also argues for a technical, systemic approach like shipping in sacks. Other archaeologists question the assumption because the evidence produced to support the use of sacks is inconclusive.

This research uses a packaging logistics approach to examine artifacts and research into Egyptian textiles and the Nile-to-Rome grain supply chain. The physical infrastructure ruins at the Ports of Ostia and Trajan's Portus are explored, and artifacts relating to the ancient saccari (porters) are investigated. Evidence is presented to support the (null) hypothesis that the grain was most likely not shipped in sacks, but was stowed and stored in a breakbulk manner.

Reasons for the lack of packaging are speculated to include factors relating to the economics of package production, product inspection and distribution. This research sheds light on the history of packaging technology, and deepens our understanding of the relationship between packaging, economics and supply chain management.

Keywords: sacks; distribution; grain; distribution packaging; ancient packaging; Roman ports.

[#] This is the abstract of a keynote address presented at the 19th IAPRI World Conference on Packaging 2014 hosted by Victoria University, Melbourne, Australia.

# RFID Tag Characterization by Studying their Backscattering Response

**S. Vikram Singh*, Morten Pedersen, Alexander Bardenstein and Søren R Ostergaard**

*Packaging and Logistics, Danish Technological Institute, Denmark*

*Corresponding author. Email: shas@teknologisk.dk*

**Abstract:** There are numerous techniques for measuring radar cross-section of loaded antenna, similar to radiofrequency identification (RFID) tag. These techniques typically involve separate transmitter antenna and receiver antennas and complex RF hardware, especially decoupling (components of transmitter and receiver) equipment. We have been able measure radar cross-section "backscattering" of an RFID tag simply by using two-port Network Analyzer (NA). Here we used one port of the NA as a transmitter antenna, whereas the other port as receiver antenna and the $S_{21}$ parameters as "backscattering signal" were measured. These measurements are aimed to study ageing of the high-frequency RFID tags and to characterize tags functionality attached to the metallic containers.

The measurements were performed on new and used RFID tags from Container Centralen A/S. The transmitter and receiver antenna were placed 1m away from the RFID tag-container (where container is also a part of antenna). By a statistical estimation we decided to perform tests on 120 randomly chosen used container-RFID tag samples and were cross-checked with 23 new sample tags. The measurements showed only a slight ageing effect, however we observed the huge influence of the containers on the measurements. In this connection, the weight, conditions of front frame face (due to paints, stickers, etc.) and even the positioning of the logo of the producers had substantial influence on the backscattered signal. The measurements were performed in 860-875 MHz frequency band. All the measurements were performed within the temperature range of 20-25 $^0$C, keeping in with the optimum operation temperature for the NA. An empty hall with wooden floor was chosen for the measurements. This area was less affected from interferences such as reflection from the wall or nearby metal objects. All the adjacent glass windows were covered with wooden plates, it lowered the disturbance. The chosen area provides consistent results.

Keywords: radiofrequency identification (RFID) tag, backscattering of an RFID tag, S-parameters measured by network analyser.

## 1 Introduction

Radio Frequency Identification, or "RFID", technology has become a tremendously important element in supply chain management [1-5]. It uses radio waves to automatically identify RFID tagged objects – such as crates, pallets, commodities, etc. Each RFID tag contains a unique Electronic Product Code (EPC), which is a kind of "license plate" of the tagged item [2]. The EPC holds very detailed information, as it combines information on the manufacturer and the type of object along with a specific serial number that relates to the particular item being monitored.

An RFID tag (sometimes called an RFID transponder) consists of a chip, some memory and an antenna [3]. RFID tags that contain their own power source are known as active tags. Those without a power source are known as passive tags. A passive tag is briefly activated by the radio frequency (RF) scan of the reader. The electrical current is small -- generally just enough for transmission of an ID number, whereas, active tags have more memory and can be read at greater ranges. In this work backscattering on a passive RFID tag was performed.

An interrogator receives from a Tag by transmitting an unmodulated RF carrier and listening for a backscattered reply [5-8]. Tags communicate information by backscatter modulating the amplitude and/or phase of the RF carrier. There are several techniques for measuring radar cross-section of loaded antenna, similar to RFID tag [6-8]. Such measurments typically involve separate transmitter and receiver antennas and complex RF hardware, especially decoupling (rf components of transmitter and receiver) equipment. We propose to measure radar cross-section "backscattering" of an RFID tag using a simple setup mainly be performed by using two-port Network Analyzer [6, 9]. We propose to use one port of the Network Analyzer as a transmitter, whereas the other port as receiver.

## 2 Experimental and Results

### 2.1 Experimental setup and technique

ENA Series Agilent network analyzer (E5071C, 9 kHz – 8.5 GHz) was utilized for the backscattering measurements. The transmit antenna ($T_x$) was connected to port 1 of the ENA and the receive antenna ($R_x$) to port 2 of the ENA (see figure 1). For all the cases $T_x$ power was fixed at 10 dBm. However, the tags were also

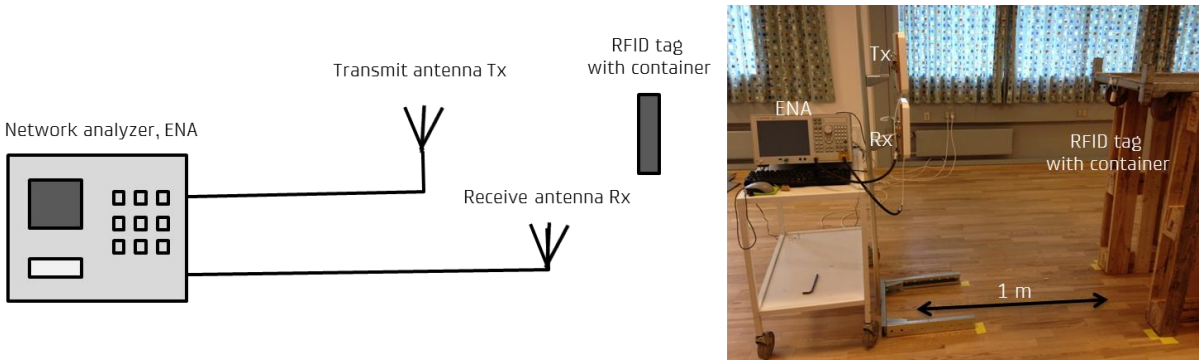



**Figure 1**: The experimental plan sketc with transmitter antenna, receiver antenna, ENA and RFID tag is shown on left; The picture shows the real arrangement of the devices on right.

interrogated with as large as 17 dBm signal, as confirmation on its influence on the measurements. It did not influence our final conclusions; hence no such data is included or discussed here. The tags with container were placed 1 meter away from the antenna assembly. The $S_{21}$ parameters "the Tag Backscattering signal" were measured. For these ultra-high frequencies (UHF) RFID tags it was required to interrogate in the range 860-875 MHz band. These measurements were performed in steps of 0.1 MHz. The two Motorola AN480, LHCP, 860-956 MHz, 6dBil antenna were used, note that such antenna can be used as transmitter and receiver antenna. Very short cables were used 0.62 m. Note that excellent quality 3 m cable can take away as large as -4 dBm. The RFID tagged containers were placed on wooden rack to avoid reflections from any metals in the circuitry. The wheels (also contains metal) of the containers were adjusted so that they were facing with the thinner side towards the antenna during the measurements. The measurements were performed in a big hall with wooden floor. This area was less affected from interferences such as reflection from the wall or nearby metal objects. All the adjacent glass windows were covered with wooden plates; it lowered the disturbance due to reflections. Over and above the chosen area provides consistent results.

### 2.2 Sample size

The purpose of this work was to evaluate aging of these commercial tags which were attached to the transportation and logistics containers. The containers were exposed to severe conditions al around the world. It is indeed not possible to measure all the tags, hence simple statistical calculation was utilized to decide the number of samples to be chosen.

We assumed that if the error in RFID backscattered signal amplitude ($\Delta A$) measurements of such kind will include two parameters; $F(\Delta A) = f(\Delta A_i, \Delta A_s)$. The first one is attributed due to instrumental error ($\Delta A_i$), whereas the second one is the so-called statistical distribution of such measurements ($\Delta A_s$) involving all kind of errors [10].

The instrumental error is dependent on the used devices which will mainly include the antenna, Network Analyzer and the position and shielding of the RFID tags. This is inherited in the instrument and can be minimized by proper and rigorous calibrations. It is the statistical part $\Delta A_s$ which would be the defining factor in selecting the optimum number of samples (measurements). It is very tricky to pick the right statistical test for such measurement. Moreover, it can be assumed that $\Delta A_s$ will follow a normal distribution, and based on that the estimation of the minimum number of measurement samples ($N_L$) can be performed to generalize the result (for infinite number of samples $N\infty$). Statistically the problem can be described as: We require a continuous probability distribution for estimating the mean of a normally distributed population in situations where the sample size is small ($N_L$ in our case) and population standard deviation is unknown. Under such conditions Student's t- distribution is recommended.

$$t \equiv (x-\mu)/(s/N^{1/2}) \qquad (1)$$

Here t (→ΔA) is the distribution, where x is sample mean, μ is population mean, s is estimator for the population standard deviation (as it is unknown) and N is the number of independent measurements. As N increases the distribution becomes normal distribution and is best for N as large as infinite. However, it is well established that for the confidence interval of 90% to 99.5% already at N = 120 samples can describe the proper trend of measurement error involved.

Precisely, for this study 120 tagged old containers were chosen randomly and their change in performance was compared to 23 new RFID tags attached on one used container. Three of the new tags were so-called special tags.

## 2.3 Results and discussions

The containers itself had a huge influence on the measurements as the containers are a part of the RFID antenna. These old containers contained distinct marks, dents, stickers and in some cases two (active and inactive) tags were attached. The backscattered signals were also largely affected by the dimensions of the tag hook of the container, position of the metal logo plate and paint in the front bar or even on the hook. These parameters gave in general below average signal. Especially the one with displaced metal logo plate gave the signal with larger absorption close to 871 MHz. The weight of the container (we measured variations as large as 17 kg to 21 kg) also influenced the response. In general heavier container gave above average values.

The measurements were performed in 860-875 MHz band in steps of 0.1 MHz for a reading distance of 1 meter, moreover, the analysis and conclusions are presented for the 865.0 to 869.9 MHz band. Before every set of measurement a standard procedure was followed to check the reproducibility of the measurement. For this we standardized one tag and container setup. This was done before starting a new batch, generally after 20 tag containers. This standard test was also performed to cross check measurement reliability, if a far below average backscattered tag was measured. The backscattered signal strength measured in this study is larger than the previous provided reference report "Confidential". This is attributed to fine and highly sensitive ENA and very short high quality cables utilized due to low losses in the cable.

The backscatter data of the new special tags are shown in Fig.2. The variation (Δ) in the backscattering data

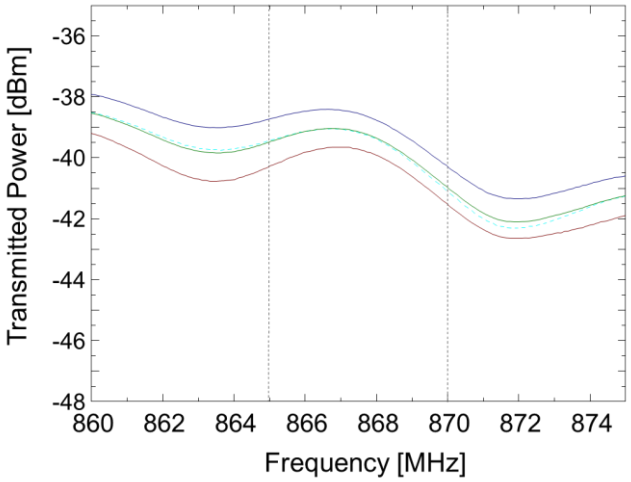



**Figure 2**: The backscattering measurement on 3 new so-called special tags. Here the blue curve is maximum, brown is minimum and green is average.

for the special tags is Δ ≈ 1.15 dBm. This Δ was measured at 867.5 MHz. The rest of the data obtained from the other tags were compared to these special tags, and based on this comparison the degree of deterioration/ageing was decided. These measurements were performed on one container by replacing the three tags one after the other measurement.

Moreover, the old tags were measured with original container, and the backscattering data of the old tags are summarised in Fig. 3. The variation in the backscattering data for old tags was Δ ≈ 4.7 dBm, which was larger

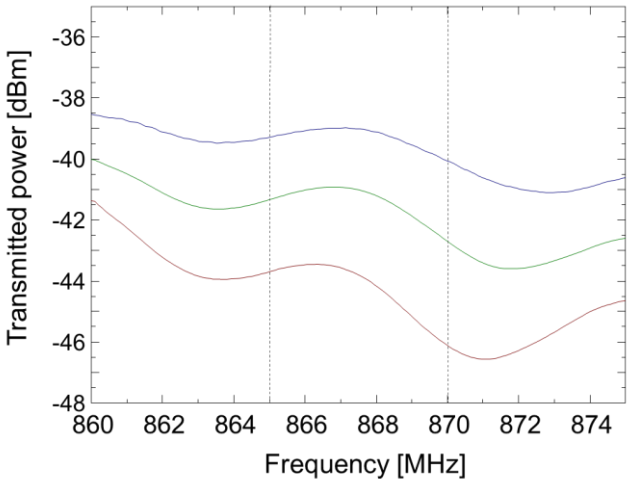



**Figure 3**: The backscattering measurement on 120 old tags. Here the blue curve is maximum, brown is minimum and green is average.

than the special tags. However, taking into account the influence of the differences in container this comparatively large scatter is not that dramatic. The backscattering was highly dependent on differences in the containers, data not shown here.

To study the influence of the containers, the measurements on the new tags were performed by attaching them on different containers. This was also to keep the measurements as close to the realistic situation as possible. We expected this will result into comparatively large variation in average at 867.5 MHz compared to that of the special tags. The backscattering data on the new tags is summarized in Fig. 4. The variation in the backscattering

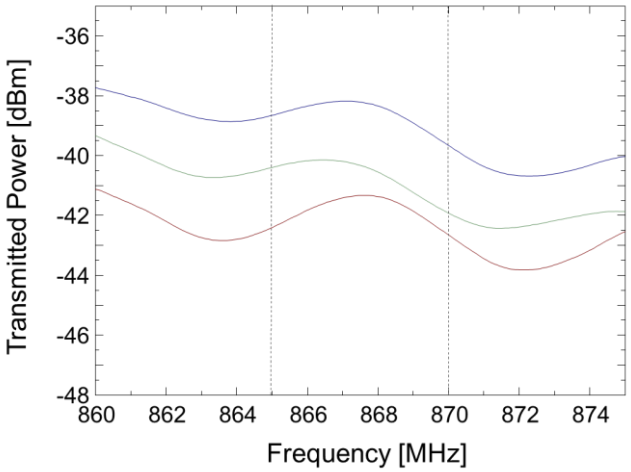



**Figure 4**: The backscattering measurement on 20 new tags. Here the blue curve is maximum, brown is minimum and green is average.

data for new tags was $\Delta \approx 3.15$ dBm. The average is towards the low signal side as we chose a huge variation in the look and weight of the containers.

The averages of all the three kinds of tags are summarized in Fig. 5, as expected the special tags generated the backscattered signals of highest strength. Only slight aging effect could be seen by comparing the averages of the used and the new tags backscattering.

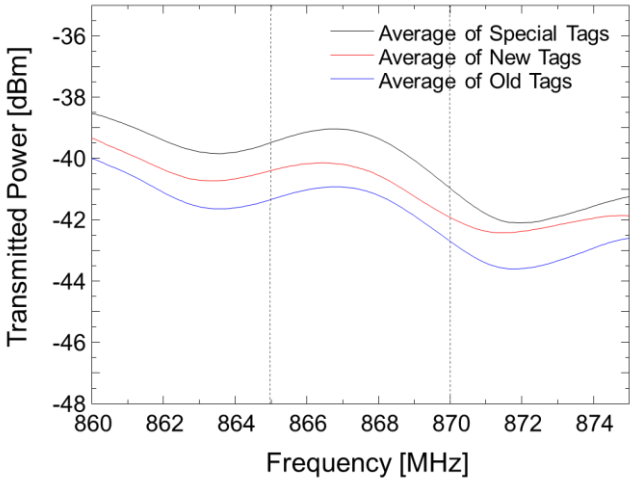



**Figure 5**: Comparison between the special, new and old tags.

## 3 Conclusions

We were able to measure the backscattering by using NA. The variation (Δ) in the backscattering data for special tags is $\Delta \approx 1.15$ dBm. The variation in the backscattering data for new tags is $\Delta \approx 3.15$ dBm. The variation in the backscattering data for old tags is $\Delta \approx 4.70$ dBm. The comparison between the average of the special tags, new tags and the used tags indicate reduced performance of the used tags. The difference between the average of 20 new tags to that of 120 old tags was highest 0.93 dBm (at 865 MHz) and lowest 0.62 dBm (at 868.8 MHz). To avoid the huge influence of the container a "single golden" container could have been adapted; however, we can also conclude that this is far from the real situation. Containers have huge impact on the response signal, and the tag and container assembly are inseparable if any practical conclusions are to be made.

## Acknowledgements

We acknowledge Container Centralen A/S for the funding through a commercial task.

## References

1. D.M. Dobkin, 2008, "The RF in RFID: Passive UHF RFID in practice", Burlington, MA: Newnes.
2. EPC™ Radio-Frequency Identity Protocols Class-1 Generation-2 UHF RFID Protocol for Communications at 860 MHz – 960 MHz, version 1.2.0, 23 Oct. 2008, [Available:] http://www.gs1.org/gsmp/kc/epcglobal/uhfc1g2/uhfc1g2_1_2_0-standard-20080511.pdf
3. J.D. Griffin and G.D. Durgin, 2009, "Complete link budgets for backscatter-radio and RFID systems", *IEEE Antennas and Propagation Magazine*, vol. 51, no. 2, pp. 11-25.
4. Container Centralen UHF tag details, http://www.container-centralen.dk/faq/cc%20container.aspx
5. J.D. Griffin and G.D. Durgin, 2008, "Gains for RF tags using multiple antennas", *IEEE Antennas and Propagation*, vol. 56, no. 2, pp. 563-570.
6. P.V. Nikitin and K.V.S. Rao, 2005, "Measurements of backscattering from RFID tags", *Proceedings of antenna measurement techniques association symposium*, Newport, RI, pp. 1-4.
7. P.V. Nikitin and K.V.S. Rao, 2006, "Theory and measurement of backscattering from RFID tags", *IEEE Antennas and Propagation Magazine*, vol. 48, no. 6, pp. 212-218.
8. K.V.S. Rao, S.F. Lam, and P.V. Nikitin, 2010, "UHF RFID tag for metal Containers", *Proceedings of Asia-Pacific Microwave Conference*, Yokohama, Japan, pp.179-182.
9. ENA Series Agilent network analyser (E5071C, 9 kHz – 8.5 GHz) [details available] http://www.home.agilent.com/en/pd-832695-pn-E5071C/2-port-test-set-9-khz-to-85-ghz-without-bias-tees?&cc=DK&lc=dan
10. W.N. Venables and B.D. Ripley, 2002, "*Modern Applied Statistics with S"*, Fourth Edition, Springer.

# Elastic Modulus Prediction of Corrugating Medium under Different Temperature and Relative Humidity

**Dong Mei Wang[*1], Qianghua Liao[2],Hongge Guo[3]**

1.*Media and Communication school, Shenzhen Polytechnic, Shenzhen 518055, P. R. China*
*2. School of Mechanical and Electrical Engineering, Shenzhen Polytechnic, Shenzhen 518055, P. R. China*
*3. Key laboratory of Rubber-plastics, Ministry of Education, Polymer Science and Engineering Institute, Qingdao University of Science and Technology, China*
*[*]Corresponding author. E-mail:sxxawdm@sina.com*

**Abstract:** The influence of the temperature and relative humidity on the moisture content of corrugating medium was studied by experiments. The ideal three-dimensional diagram between the moisture content and the temperature and relative humidity was constructed by the GAB model. The prediction equation of the moisture content and the relative elastic modulus was fitted after analyzing the test results by Matlab software. The results show GAB model can predict the moisture content of corrugating medium in different temperature and humidity conditions, and the fitting equation can describe the relation between the elastic modulus of corrugating medium and the moisture content. The predicted elastic modulus can be used to evaluate the cushioning properties of corrugated sandwich paperboard.

Keywords: corrugating medium, moisture content, elastic modulus.

## 1 Introduction

More and more corrugated sandwich, hexagonal honeycomb core products, which are made from corrugating medium, were applied to prevent the products from damage in real-life logistics environment [1], people start to pay attention to the mechanical properties of corrugating medium, such as grammage, ring crush, bursting strength and so on. However, the elastic property of corrugating medium was neglected. Elastic modulus is commonly used to characterize the elastic property of materials.

The corrugating medium, mainly composed of plant fibers, is porous and can absorb moisture from the external environment at any time [2]. Environmental conditions greatly affect the moisture content of corrugating medium [3], and then affect the mechanical performance [4]. The mechanical properties of paper structural materials can be predicted and the packaging can be optimized by evaluating the elastic modulus of corrugating medium under different temperatures and relative humidities. Therefore, it is significant to study the influence of temperature and relative humidity on the elastic modulus of corrugating medium.

At present, there are some literatures on the moisture content and the elastic modulus of corrugating medium. Nissan [5] took the paper as porous structural material made of hydrogen bond, and proposed an exponential relationship between elastic modulus and moisture content, described by $E_m=E_0/e^m$,where $E_m$ is the elastic modulus at any moisture content, $E_0$ is the elastic modulus at m=0, m is moisture content. However he did not study the relationship between moisture content and temperature and relative humidity, neither did heset up the equation of elastic modulus corresponding to temperature and relative humidity. Petch [6] considered the effect of temperature on the elastic modulus and put the parameter of temperature into the exponential equation mentioned above, but he did not consider the influence of relative humidity on the elastic modulus. Allaoui [7] studied the relationship between the elastic modulus of corrugating medium and relative humidity, and found

that the elastic modulus decreases as the relative humidity increases, especially in high humidity conditions(*RH*>70%), the elastic modulus decreases dramatically. But he did not induce the equation of the relationship between the elastic modulus of corrugating medium and relative humidity. On the basis of J/BT 6544-93, Wang [8] designed the method of measuring the elastic modulus of corrugating medium. The method can be a reference for studying the influence of environmental conditions on the elastic modulus of corrugating medium.

The primary aim of this study is to valuate the relationship between the moisture content of corrugating medium and environmental temperature and relative humidity. The second aim of this study is to explore the relationship between the elastic modulus and the moisture content of corrugating medium, and then to seek an equation of the relationship between the elastic modulus of corrugating medium and environmental temperature and relative humidity to predict the mechanical properties of paper structural materials in different environmental conditions.

## 2 Experiment

### 2.1 Materials

The corrugating medium is supplied by the HONICEL Paper Honeycomb Products Company (Guangzhou, China). It was made from recycled fiber. The parameters of materials are shown in Table 1.

**Table 1:** Parameters of corrugating medium.

| Size(mm×mm) | Grammage(g/m$^2$) | Poisson ratio | Direction | Thickness(mm) |
|---|---|---|---|---|
| 150×12.5 | 120 | 0.28 | cross-direction | 0.25 |

### 2.2 Experimental methods

#### 2.2.1 Pre-condition of temperature and relative humidity

All specimens were pre-conditioned in accordance with GB/T 4857.2-2005 [9], the experimental conditions are shown in Table 2. The experiment equipment is a temperature and humidity programmable controller (CS/CP-KMH-1000R, Komeg Technology Co.Ltd., Dongguan, China). The specimen is placed within the working space of the experiment, and is exposed in the specified conditions for 48h. During the test, the conditioning atmosphere has free access to the top, sides and at least 75% of the base.

**Table 2:** Experimental conditions.

| | | | | | |
|---|---|---|---|---|---|
| Temperature *T*(°C) | 5 | 20 | 30 | 40 | 50 |
| Relative Humidity *RH*(%) | 30 | 50 | 70 | 80 | 90 |

P.S. As the temperature is below zero, the relative humidity can not be determined. Therefore the temperature which is below zero is not considered.

#### 2.2.2 The experiment of moisture content

The experimental equipment is a moisture test apparatus (SFY20A, Houwang Technology Co.Ltd., Shenzhen, China). The specimen which was pre-conditioned is placed into the equipment. The time is set for five minutes; the temperature is 100°C. After the adjustment, the equipment is started. Five minutes later, the moisture content of specimens is recorded.

#### 2.2.3 The experiment of elastic modulus

Since there is no clearly defined experimental method for elastic modulus of paper, the experimental method is referenced to GB/T 1447-2005 [10].The experiment equipment is computer-controlled electronic universal testing machine (M-3050, Shenzhen Reger Instrument Co, Ltd, Shenzhen, China). During the test, the gauged distance is set into 100mm; the stretching speed is 1mm/min. At the end of the experiment, the load value corresponding to the stain was 0.07% and 0.08% is recorded, and the elastic modulus of corrugating medium is calculated in accordance with GB/T 1447-2005[10], Fiber-reinforced plastics composites – Determination of tensile properties.

## 3 Results and discussion

### 3.1 GAB model

On the basis of unimolecular layer adsorption theory and the BET multi-molecular adsorption theory, Guggenherm, Anderson and De Boe propose the GAB model. After constantly modified and the parameter of temperature increases, GAB model becomes a three-parameter model. Below is the mainly composed of plant fibers,

$$GAB(T, RH) = m = \frac{a \cdot b \cdot (\frac{c}{T}) \cdot RH}{(1 - b \cdot RH)[1 - b \cdot RH + b \cdot (\frac{c}{T}) \cdot RH]} \quad (1)$$

Where $m$ is the equilibrium moisture content; $T$ is temperature; $RH$ is relative humidity; $a$, $b$ and $c$ are the model parameters.

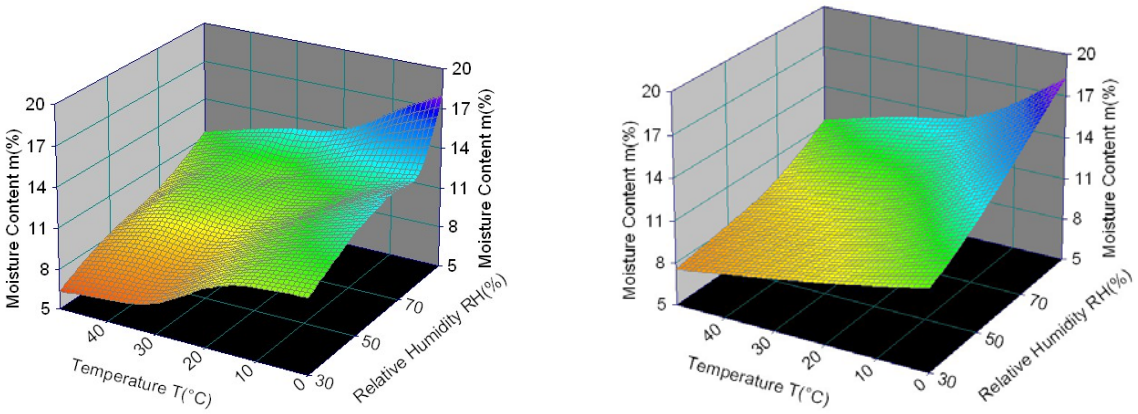
The GAB model is one of the best models which include theoretical significance of thermodynamics. It is suitable for a variety of items. This paper fits the moisture content of corrugating medium with the GAB model.

### 3.2 The relationship between the moisture content of corrugating medium and temperature and humidity

**Table 3:** Experimental results of the moisture content of corrugating medium in different temperature and relative humidity.

| | Temperature $T$(°C) | | | | |
|---|---|---|---|---|---|
| Relative Humidity $RH$(%) | 5 | 20 | 30 | 40 | 50 |
| 30 | 10.41 | 9.32 | 7.31 | 6.67 | 6.33 |
| 50 | 12.03 | 10.15 | 8.88 | 9.09 | 8.24 |
| 70 | 12.59 | 10.99 | 10.88 | 10.87 | 9.24 |
| 80 | 13.16 | 12.03 | 11.06 | 11.38 | 10.22 |
| 90 | 17 | 13.89 | 13.19 | 12.39 | 11.42 |

The experimental data of the moisture content tests is shown in Table 3. In order to perfectly characterize the relationship between the moisture content of corrugating medium and environmental temperature and humidity, the three-dimensional diagram of the relationship between the moisture content of corrugating medium and environmental temperature and humidity is drawn in light of the experimental data. The experimental diagram is shown in Figure 1a.




a b

a. The experimental diagram of the moisture content of corrugating medium under different temperature and relative humidity;

b. The ideal diagram of the moisture content of corrugating medium under different temperature and relative humidity.

**Figure 1:** Comparison of experimental and theoretical diagram of the moisture content of corrugating medium

Making use of matlab to fit a curve, estimate parameter and describe the diagram. Error estimates were calculated by Levenberg-Marquardt's algorithm, the value of convergence of variance and model parameters is $10^{-20}$, and there is no limit in iteration times. The fitting results are listed as follows:

$a$=10.1157，$b$=0.00366，$c$=421.1393，$R^2$=0.9916. Combining the results with equation (1), the GAB model of the moisture content of corrugating medium is obtained,

$$m = \frac{15.6RH}{(1-0.00366RH)[1-0.00366RH+1.54*\frac{RH}{T}]T} \quad (2)$$

The ideal three-dimensional diagram of the moisture content of corrugating medium is described in accordance with equation (2).The ideal diagram is shown in Figure 1b.

According to equation (2) or figure 1b, the ideal moisture content of corrugating medium in a specific environment temperature and humidity can be identified. The three-dimensional diagram of the moisture content is simple and intuitive. It is easier to obtain information from the diagram, which is important for studying the relationship between mechanical property of corrugating medium and environmental temperature and relative humidity.

### 3.3 The relationship between the elastic modulus and moisture content of corrugating medium

The corrugating medium's tensile stress-strain curves are similar under different environmental conditions. They all show three stages, that is, linear elastic stage, tensile yield stage and fracture stage. A typical tensile stress-strain curve of corrugating medium is shown in Figure 2.

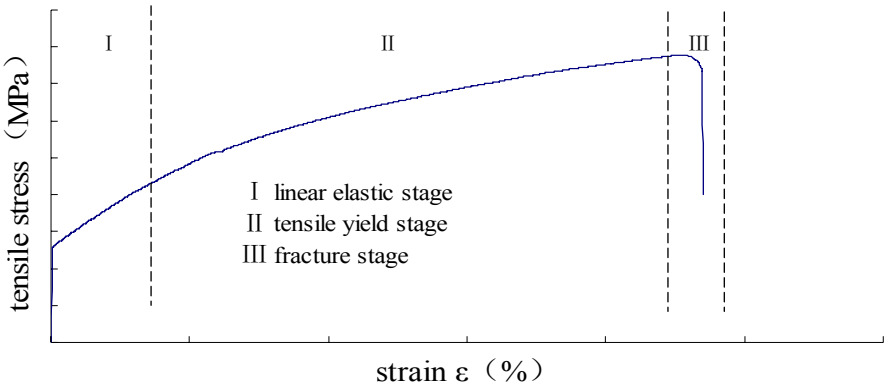



**Figure 2:** Typical tensile stress-strain curve of corrugating medium

The variety of environmental temperature and relative humidity affects the moisture content of corrugating medium, and then affects the mechanical properties of corrugating medium. For this purpose, the relationship between elastic modulus and moisture content of corrugating medium was studied.

The elastic modulus of corrugating medium is to a great extent influenced by the material parameters, such as thickness, grammage and so on. Therefore, the results of this study would not apply to any other corrugating medium. In order to characterize the influence of moisture content on elastic modulus perfectly and compare the mechanical properties of paper made from different materials conveniently, a relative elastic modulus measure can be utilized（*%E*）[11], in which the experimental elastic modulus is divided by a standard elastic modulus corresponding to a given equilibrium moisture content found at standard conditions(23°C and 50%*RH*). Therefore, all experimental elastic modulus are related to the elastic modulus determined for an identical corrugating medium conditioned at 23°C and 50% *RH*.

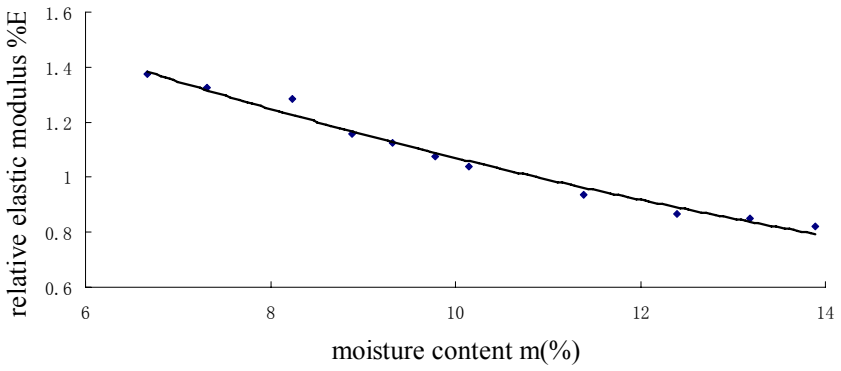



**Figure 3:** The relationship between the relative elastic modulus and the moisture content of corrugating medium

The relationship between the relative elastic modulus and moisture content of corrugating medium obtained from the experiment is shown in Figure 3.The figure 3 indicate that the relative elastic modulus declines with the increase of moisture content. Base on the theory of hydrogen bonding, Nissan studied the elastic modulus of porous structural material and found that there is an exponential relationship between the elastic modulus and the moisture content of porous structural material [5]. Since the paper is a porous solid, the matlab was utilized to fit the relationship between relative elastic modulus and moisture content of corrugating medium exponentially and the predictive model for the relative elastic modulus was assessed. The predictive model is

given as follows:

$$\%E=2.3084e^{-0.0769m} \quad (3)$$

Where *%E* is relative elastic modulus; m is moisture content of corrugating medium.

The predictive model was F-tested by software SPSS 17.0.The results are $R^2$ =0.9726 (coefficient of determination), *MRD*=3.752% (mean residual deviation). Therefore, the predictive model fit suitably. The model was utilized to predict the elastic modulus and the predicted and experimental values are in good agreement. This shows that the model can be used to describe the relationship between the elastic modulus and the moisture content of corrugating medium.

Substituting Eq. (2) into Eq. (3), and the equation which describes the relationship between relative elastic modulus and moisture content was obtained, as follows:

$$\%E = 2.3084e^{\frac{-1.1996RH}{(1-0.00366RH)(1-0.00366RH+1.54*\frac{RH}{T})T}} \quad (4)$$

The three-dimensional diagram was drawn in accordance with equation (4) and shown in Figure 4.The comparison of experimental *% E* and predictive *% E* is listed in Table 4. The comparison diagram of experimental value and predictive value is shown in figure 5, the coefficient of determination $R^2$=0.9613.This proves that the model fits well. It is easy to find that both relative humidity and temperature affect relative elastic modulus from the Figure 4. As the relative humidity increases, the relative elastic modulus decreases. Conversely, increase of the temperature will strengthen the relative elastic modulus，as the higher temperature will cause evaporation of moisture from corrugating medium, thereby lowering the moisture content, the relative elastic modulus will be higher.

**Table 4:** The comparison of experimental *% E* and predictive *% E*.

| | Temperature *T*(°C) | | | | |
|---|---|---|---|---|---|
| Relative Humidity *RH*(%) | 5 | 20 | 30 | 40 | 50 |
| 30 | 1.103/1.039 | 1.123/1.227 | 1.326/1.325 | 1.375/1.408 | 1.447/1.478 |
| 50 | 0.924/0.933 | 1.039/1.051 | 1.157/1.120 | 1.154/1.181 | 1.283/1.238 |
| 70 | 0.821/0.838 | 0.904/0.919 | 0.958/0.969 | 1.112/1.015 | 1.113/1.060 |
| 80 | 0.786/0.791 | 0.874/0.859 | 0.931/0.902 | 0.938/0.942 | 1.003/0.981 |
| 90 | 0.704/0.742 | 0.819/0.801 | 0.849/0.837 | 0.868/0.872 | 0.891/0.905 |

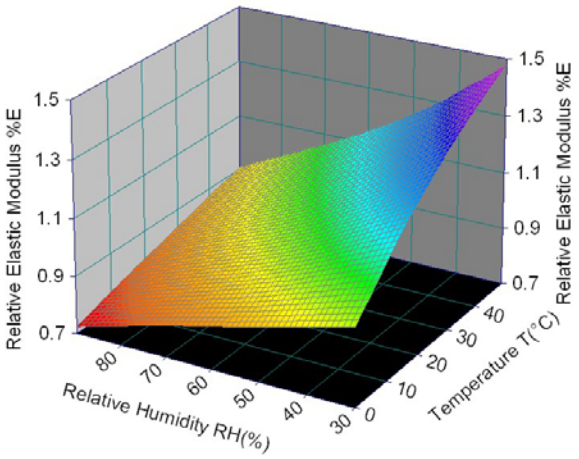



**Figure 4:** The three-dimensional diagram of relative elastic modulus predicted from different humidities and temperatures by the model given in equation 4.

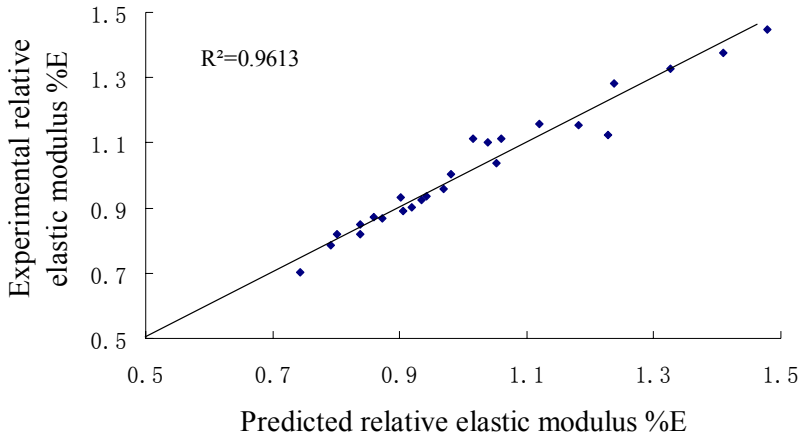



**Figure 5:** The linear relationship between experimental *% E* and predicted *% E*.

The three-dimensional diagram is simple and easy to understand for packaging designers, and provides a quick and convenient method for estimating the elastic modulus of corrugating medium in different environmental conditions. In real-life logistics environment, varying environmental conditions, with both short and long-lasting changes in temperature and relative humidity, are more likely, and it is well known that to a greater extent the varying conditions affect mechanical properties than constant conditions. Hence, it is important to validate the relative elastic modulus in response to cyclic environmental conditions as well, to obtain a full understanding of the mechanical functionality of corrugating medium used for packaging.

## 4. Conclusions

(1) Based on the test analysis, the moisture content of corrugating medium alters as the environmental conditions change. When the relative humidity is constant, as the temperature rises, the moisture content decreases; when the temperature is constant, as the relative humidity rises, the moisture content increases.

(2) The relationship between the elastic modulus and the moisture content of corrugating medium is exponential, that is to say, as the moisture content rises ,the elastic modulus of corrugating medium decreases exponentially. The predictive model which was fitted is given as follows:

$$\%E = 2.3084e^{\frac{-1.1996RH}{(1-0.00366RH)(1-0.00366RH+1.54*\frac{RH}{T})T}} \quad (5)$$

After verification, the model can predict the elastic modulus of corrugating medium under different temperatures and humidity conditions.

(3) The three-dimensional diagram drawn in accordance with the model is more direct. It can predict the mechanical properties of corrugating medium under different environmental conditions by combining model and three-dimensional diagram.

## Acknowledgements

The authors are grateful to HONICEL Paper Honeycomb Products Company for its help in experiments. Contract/grant sponsor: National natural science foundation of china project (50905120), natural science foundation of Guangdong project (S2011010001073) and science and technology grant project of Shenzhen (JCYJ20120823171953279).

## References

1. A.L. Nevins, J.E. Bronlund, A.J. Mawson, I. Chalmers and A. McKenzie, 2004, "The effect of moisture on the strength of corrugated cardboard packaging", *Proceedings of ICEF9*, Montpellier, France.
2. ISO 187:1990(E): Paper, board and pulps – standard conditioning and testing and procedure for monitoring the atmosphere and conditioning of samples. In ISO Standards Handbook for Paper, Board and Pulps, 1998. ISO: Geneva, 1998.
3. M.E. Parker, J.E. Bronlund and A.J. Mawson, 2006, "Moisture sorption isotherms for paper and paperboard in food chain conditions", *Packaging Technology and Science*, vol. 19, pp. 193-209.
4. W.A. Wink, 1961, "The effect of relative humidity and temperature on paper properties", *TAPPI*, vol. 6, pp. 171.
5. A.H. Nissan, 1967, "The significance of hydrogen bonding at the surfaces of cellulose network structures", *Surface and coatings related to paper and wood*, Syacuse University Press, New York, pp. 221-268.
6. M.G. Pecht and M. Johnson, 1985, "The strain response of paper under various constant regain states", *TAPPI*, vol. 68, no. 1, pp. 90-93.
7. S. Allaoui, Z. Aboura and M.L. Benzeggagh, 2009, "Effects of the environmental conditions on the mechanical behaviour of the corrugated cardboard", *Composites Science and Technology*, vol. 69, no. 1, pp. 104-110.
8. D.M. Wang, 2008, "Method to Measure Elastic Modulus of Raw Paper", *Paper and Paper making*, vol. 2, pp. 82-84.
9. GB/T 4857.2-2005.Packaging-Basic tests for transport packages-Part2 : Temperature and humidity conditioning, National Standard.
10. GB/T 1447-2005. Fiber-reinforced plastics composites – Determination of tensile properties, National Standard.
11. G. Sorensen and J. Hoffmann, 2003, "Moisture sorption in moulded fibre trays and effect on static compression strength", *Packaging Technology and Science*, vol. 16, pp. 159-169.

# A Method Review and a Case Study of Packaging Design Difference of Automobile KD Parts and After-sale Parts with an Application on Transport

**XU Weifeng [1] , Zhao Yu [2] and LU Binglin[3*]**

[1] *General Manager, China Packaging Tianjin Technology Development Co. Ltd, Tianjin, China*
[2] *Senior Engineer, China Packaging Research and Test Center, Tianjin, China*
[3] *Marketing Director, China Packaging Research and Test Center, Tianjin, China*

[*] *Corresponding author. Email: louis@packagetest.net*

**Abstract:** A knock-down package is a packaged kit containing the parts needed to assemble a product. The parts are typically manufactured in one country or region, and then exported to another country or region for final assembly. A common form of knock-down is a completely knock-down (CKD), which is a complete kit needed to assemble a product. An incompletely disassembled kit is known as SKD for semi-knocked-down. Both types of KDs, complete and incomplete, are collectively referred to within the auto industry as knocked-down export. Implementation of an integrated solution to packaging of automobile KD parts is an important issue to automobile exporters in China. Generally, automobile after-sale packaging is used in the domestic auto sale service. The paper compares transport packaging solutions used in the Chinese domestic after-sale service with those adopted for export and investigates their effect on the growth of business. Unitized loads of packaged-parts applied to export which is required to consider with climate environment and available facility of transport system. Both of CKD/SKD packaging process and materials selection play a key role in supply chain management as well as provide cost reduction and damage decline. Packaged after-sale parts are required to match diversity of product and instant customer response management from each manufacturer. A case study will be presented with KD packaging of a China's own-brand vehicle and after-sale parts packaging of an international brand cars.
**Key words:** KD packaging, Packaging integrated solution, Transport, Supply chain, Automobile export, After-sale part.

## Introduction

Chinese automobile industry was built in 1953.The size of it broke through the scale of 1 million in 1992. It rapidly developed from 2001 to 2008, on average rise of one million each year. With the mushrooming development of automobile industry, the competition is increasingly fierce. How to improve the core competitiveness and price advantages has become the focus of every automobile manufacture enterprise. In recent years, enterprise pay more and more attention on the logistics costs, most automobile companies have started to focus on the improvement of its own logistics system optimization and continuous.

### (1) The significance of transportation package design in terms of the KD parts exports

According to 2013 statistics, Chinese auto export has reached to 1 million each year, in which exports by way of Knocked-Down(KD) accounted to 400 thousand. As an important economic growth point, Auto export has been concerned by automobile manufacture enterprises. The package design of KD export plays an indispensable role in auto export supply chain. It is reflected by the market demand for exports in KD export project, the requirements of export partners, the certification of product, the preparation of production, and in the initial stage of trial production as well as mass production. The pattern of Knocked-Down (KD) auto export can be specific subdivision for CKD (Complete Knocked-Down) and SKD (Semi Knocked-Down), respectively meaning completely break up and incompletely break up. Automobile KD parts are many varieties, irregularly shaped and requiring high package technology; and these parts experience warehousing, forwarding, loading and uploading in logistics process; there may be the mechanical load in the process which may damage the product; therefore, the auto KD package is significant and indispensable. At the same time, the abnormal climate change greatly influences the packaged products in entire logistics process. The outer package has to prevent functional deformation, rust and eclipse.

### (2) The significance of transport packaging design for auto aftermarket spare parts

Automotive aftermarket spare parts are needed in maintenance as well as overhaul in use process and the repairing needs after traffic accidents. It shown by statistics, the market scale of only Chinese auto aftermarket accessories reached 300 billion in 2010. The logistics of vehicle and auto parts has been becoming mature, while auto after-sale service spare parts logistics is in its infancy stage. Because the automobile after-sale spare parts need to be characterized with low damage rate, reduction of cost and stability supply, the packaging requirements of automotive aftermarket spare parts logistics is very high. In meet not only transport packaging requirements of the roads, railways, waterways transportation, and the multimodal transport, the auto after-sale spare parts logistics but also need to achieve the turnover operability of the consolidation and a single goods in process of the delivery of goods, storage, transportation and consignment. Automobile manufacturing enterprises are in the core position in the automobile manufacturing supply chain, controlling various spare parts manufacturing, logistics, and the material supply of packaging and technical service suppliers. [1] Automotive aftermarket spare parts transport packaging design using the packaging requirement plan generated by auto production plan, and the packaging requirements produced by Visible record management, both of it forecast the requirements of packaging technological design as well as packaging materials, for guiding the procurement scale of packing materials and the quantity of packaging technological design plan. The push-pull hybrid model can make the spare parts packing material supply more stability, lower cost of spare parts packaging design, and higher transportation safety guarantee.

## The application of transport packaging design in automobile manufacturing industry

### (1) The role of packaging in the automobile manufacturing industry

With the globalization of automobile manufacture as well as parts purchasing, and the higher requirements of flexible, linear productive processing, this correspondingly requires the punctuality, accuracy rate and quality rate of logistics material flow. More and more automobile manufacturing enterprises use electronic information in order to promote supply chain model for automobile manufacturing activity, applying Just-In-Time (JIT) as a core of lean production management and logistics packaging management. With rapid development of logistics industry in China, and the increasing market demands of greater auto manufacturing industrial scale, it puts higher requirements forward to the package which is applied on the auto trade exports and domestic after-sales parts. Both appropriate packaging design and reasonable choice of packaging materials play an important role in improving internal and external logistics efficiency of factory, reducing manufacture costs, ensure the quality of components, fitting with the packaging on-site operation in order to guarantee the manufacturing efficiency.

### (2) The category of automobile product packaging

Achieving standardization of packaging design, serialization of packaging materials, procedures of packaging technology, standardization of package size and information of integrated package, is to do the best to track and improve packaging program and optimize the logistics supply chain efficiency, and ultimately to increase profits and improve core competitiveness for the car manufacturing companies. Whether it is KD exports kit or aftermarket spare parts package of automobile, it must follow the several requirements below: safety, quality,

cost, ergonomics and customer satisfaction. It is necessary to ensure the security of packages in use, transportation, handling and other aspects; to guarantee the quality of the packages in the transport conditions, geographical and climatic conditions, handling and other processes; to guarantee the superior of packages for lower manufacturing costs; to care for staffs and ensure rationality of the package in the handling, unpacking process; and to meet the requirements of customers, including packaging appearance, size, and other aspects of the proposed functionality.[2]

### (3) The features of automobile KD kit and aftermarket spare parts package

A knock-down kit is a kit containing the parts needed to assemble a product. The parts are typically manufactured in one country or region, and then exported to another country or region for final assembly. CKD package needs to set the car assembled products, parts and components in according to the type of packaging; SKD packaging is to package in accordance to the vehicle engine, chassis, body and other assembly parts for packaging. These two types of automobile products by KD shipping packaging are engineering techniques that exported to foreign markets, resources and support that counts shipping and receiving of product and pricing information, it is commonly use for the automobile industry, heavy truck industry and rail vehicle industry, and electronic products, furniture and other products. With the packaging technique using CKD and SKD, the imported tariff could be avoided in order to benefit from tariff regulation. KD packaging design focuses on the size of spare items, the protection, and the size of transportation package as well as the cost of logistics.

After-sales spare parts packaging is the logistics packaging object, and the service extension of car manufacturer, both of which are the carrier of disseminating the brand of the cars. After-sales spare parts package design can further reduce the cost of parts and achieve the unity with both minimal packaging rationalization and the minimum sales unit, as well as reduce the damage caused by repeated disassemble on the spare parts and the outer packaging. Such packaging is designed to focus on the protection of the individual- part packaging and the operability of packaging technology; besides, it also focuses on the design of cushion packaging design and the packaging costs.

## Case studies

### (1) Cases of automobile KD kit

The total number of a car parts are around 1000, the spare parts could be divided into 5 classes based on the shape and fragility of the part, and the same part of the spare gadgets can be assigned to the same package format, shown in Table 1.

The determination of transportation packaging design is based on the packaging sizes of various parts, the product features, as well as the choice of packaging materials.

**Table 1:** Category automotive key parts.

| Category | Name of key parts | | | |
|---|---|---|---|---|
| Large parts of car body | Side panels | FDTC | fender | Roof |
| Large/medium parts of car body | Front and rear floor | Floor connection channel | Body interpolate | Lower dashboard |
| | Wheel plate | Connecting beam | Reinforcement | Sill plate |
| Total garnish | Bumper skin | Dashboard | Door trim | Crest |
| | Pillar trim | Wheel trim | Trim | Front and back interior |
| Small parts of car body | Assembling small pieces | Fastener | | |
| Precious piece/hazardable & vulnerable parts | Engine | Gearbox | Air box | Condenser |
| | Airbag | Front and rear lights | Electronic Modules | Compressor |

Taking the large parts of the car body for instance, the sides of the car, the four doors, the bonet and the boot, the wing board and the car's top are all belong to the big parts and the car's out- scene part, which set a strict requirement to the car's outline and the car's facet painting effect. These gadgets can not be damaged, deformed and scrached during tranportation. The packging format is chosen mostly based on the steel boxes and wooden boxes, the former ones have strong structural intensity, big usage space, accurate position, easily equiped feature, good operational function, all of which are commonly accommodated by foreign CKD packaing companies. The domestic CKD mostly accommodates the wooden packages that could skip the process of exported quarantine steming, and also could be degraded, therefore it is widely employed. Compared with the former two methods, the paper package has the advantages of cheaper cost, abundent rescources, and envirment-friendly degradle process, therefore it is also wildly used in the car packing industry. Japan is a country that prefers paper packaing, it has the cases using paper package when it comes to big car CDK packaging. But using paper package for big cars gadgets is not quite common overral. The five or more than five positioning as the principle of transport packaging design, it limits parts within the space of six degree of freedom (DOF), for making ensure the parts without displacement, as shown in Figure 1. Alien groove space positioning accurate card slot position, notches and exterior contacted by surface of each, the minimum distance of each part not less than 10mm; Cushion material choosing EVA or EPE foam material, poor sitffness of components (such as: lateral confining and fender), choosing the low hardness cushion material; the roof can be stacked, cushion used between layer and layer as protection, as shown in Figure 2; the four-doors, two-cover of the assembly form export, adopts the outside plate space positioning, the overall positioning of inside plate, unseparated situation as shown Figure 3; other fittings of large components of car body can regard as small knock-down pieces.



**Figure 1:** Large components of car body positioning.

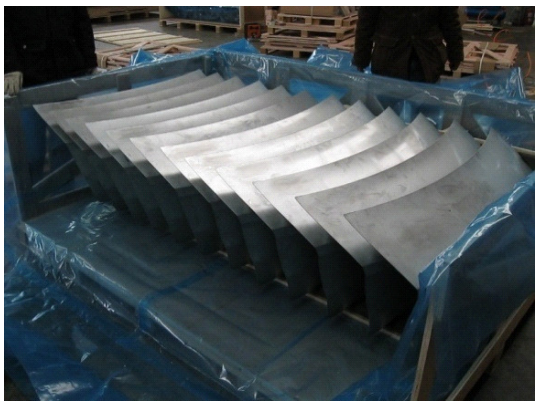


**Figure 2:** Superimposed stacked roof parts.

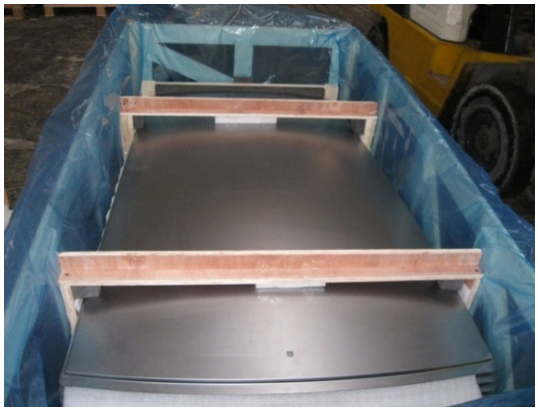


**Figure 3:** Four-door two-cover separate positioning.

Taking precious piece and vulnerable parts for instance, these parts content: Engine, gearbox, air box, condensor, compressor, airbag, front and rear lights, Electronic Modules and etc. The cost of gadgets is high, the fragility of gadgets or hazardable parts is low, due to which precious piece/hazardable & vulnerable parts are easy affected by the vibration, shock, temperature and humidity changes. Regarding this, the cushion and protection design is needed to avoid damage of parts. The packaging employs individual part packaging, using polymer plastic bags, shown in Figure 4; Wrapping of cushion material is regarding to the parts shape, shown in Figure 5. Cardboard insertion or EPE separate protection is applied to small size or regular shape parts, shown in Figure 6 and Figure 7.



**Figure 4:** Polymer plastic bagging individual component packaging.



**Figure 5:** Cushion materials wrapping individual component packaging.



**Figure 6:** Cardboard insertion positioning packaging.



**Figure 7:** EPE separate protection packaging.

Another important mission of automobile KD kit is to design the size of transporting package and reduce costs on logistics. SKD can realize reducing costs mainly relying on improving package box loading rate. The requirement of package size is 85% or higher of package box loading rate. Taking the inner size of container with 12m×2.35m×2.68m for instance, in order to meet the requirements of loading rate and operation, the length of container is 11.9m, width is 2.28m, height is 2.5m. The outer shape size of package box can be designed as the specification provided in Table 2, and can be used crossly.

**Table 2:** Specification of outer shape size of package box.

| Package box | mm | | | | | | |
|---|---|---|---|---|---|---|---|
| Length | 2280 | 1960 | 1700 | 1480 | 1300 | 1140 | 980 |
| Width | 2280 | 1140 | | | | | |
| Height | 1250 | 830 | 625 | 500 | 1000 | 1500 | 1660 |

### (2) Case of automobile after-sales spare parts package

There is a close contact between automobile after-sales spare package logistics package and the industry chain, which involves automobile manufactures, auto parts manufacturers, auto parts dealers and auto repair service providers. Normally, automobile enterprise chooses third-party logistics to provide the service of aftermarket spare parts distribution, which includes: transportation, warehousing and the management among parts warehouses. The production and marketing characteristics of automobile after-sales spare parts are evident, which benefits from the combination of transportation package and marketing package of after-sale spare parts. To guarantee the distribution of after-sales spare parts, the cooperation between the package design & manufacture and spare parts demanding planning as well as the inventory planning is needed. The design of transportation package plays a critical role in spare parts protection during warehousing, transportation, turnover, distribution and etc.

Taking headlights, door, car mirrors and front windshield as example, shown in Figure 8. Normally, the package of automobile after-sales spare parts is in the form of individual component, most of which are design of paper package, cushioning material and lining support, shown in Figure 9. Also packaging process operability, time costs, material costs and the strength of the package need to be taken into consideration, seen in Table 3.

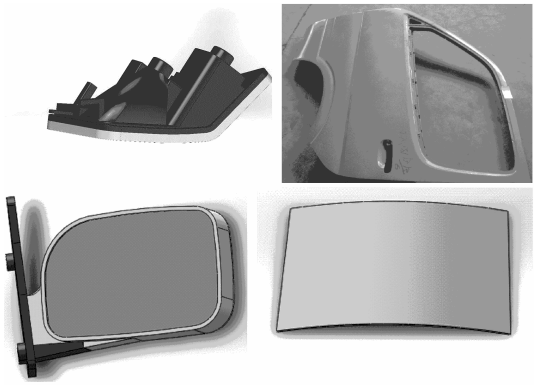


**Figure 8:** Models of after-sales parts.

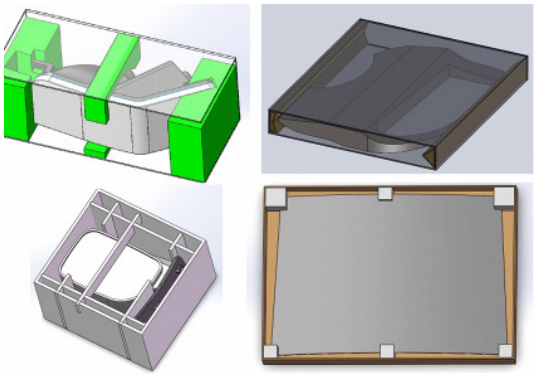


**Figure 9:** Models of transportation package of after-sales parts.

**Table 3:** Common packaging materials and specifications.

| Package material | Specification and type | |
|---|---|---|
| Paper package | AB flute Double corrugated boxes | |
| Cushioning material | EPE 28kg/m³ | Bubble bag |
| Lining support | AB flute Double corrugated | |

## 4 Automobile KD kit and after-sales spare parts transporting package design steps

### (1) Automobile fender KD transporting package design

Fender is the exterior body panels to cover wheels. It is named from its birdlike wings shape of the old body shape, and is categorized as the upper and lower fender. It is assembled above the wheels of the vehicle, as the vehicle side outer panel. It is made of resin, and is formed integrally with the resin by the outer plate portion and the reinforcement portion. Outer plate portion is exposed on the side of the vehicle, while the reinforcement portion is assembled at the extending plate of the outer edge portion, which is inside the adjacent portion of the outer plate component. Meanwhile, Coordinating portion is formed alongside of the outer plate portion and the reinforcement portion. Hence, fender is a component of irregular shape with multiple contact points, face, and difficult to locate gravity point.

Automobile fender KD package design plan is based on the research on the characteristic of fender itself and LOT, which is determining the package box size, material type, and position structure. LOT is the export parts order regarding to corresponding order quantity of single vehicle usage. Normally, the LOT24 mode is preferred, and in which mode there are 24 parts in one package box. Assuming the export mode is PBP①, no special requirements of packaging modulus, in order to reduce the costs on logistics.

Taking the package box of fender LOT24 for instance, it is shown in Figure 10.

The wooden package box of fender is made up of outer package box, the bottom limiting, the lateral limiting, compression bar and etc., shown in Figure 11. In order to ensure no parts displace, the DOF of the parts needs to be limited with 3 axial directions. The positioning of lower fender applies 6 points positioning principle, while the positioning principle of upper fender should be 5 positioning at least.

The outer package box of fender is wooden box. It makes up of bottom bracket, two side panels, top panel and joint using pining between plywood. The joint condition is shown in Figure 12.[3]

The positioning of the fender in Package design composes of four bottom limiting, three side limiting and setting up three compression bars. According to the shape of parts, bottom limiting and can choose u-shaped slot and triangular slotting. The connection between the parts and the slotting should be as near as possible for easier movement of parts. Compression bar consists of EVA or EPE, and plywood, the connection between the parts and the slotting should be as near as possible for easier movement of parts. According to the shape of parts, it chooses the U-shaped slot. The positioning on parts of compression bar should choose a place where the arc is low.

The design of outer packaging wooden box is based on available space and specifications of the container. If the design is based on the size shown in Table 4, the usage of package box can reach 89.3%.[4]

**Table 4:** The outer size of wooden package box for fender

| Size | | | mm |
|---|---|---|---|
| | Length | Width | Height |
| Preferred size | 2280 | 1480 | 1250 |

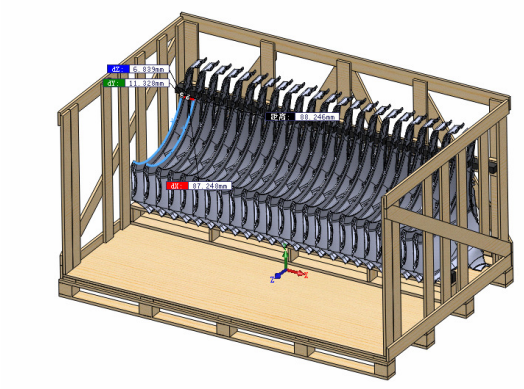


**Figure 10:** Wooden packaged automobile fender LOT24.

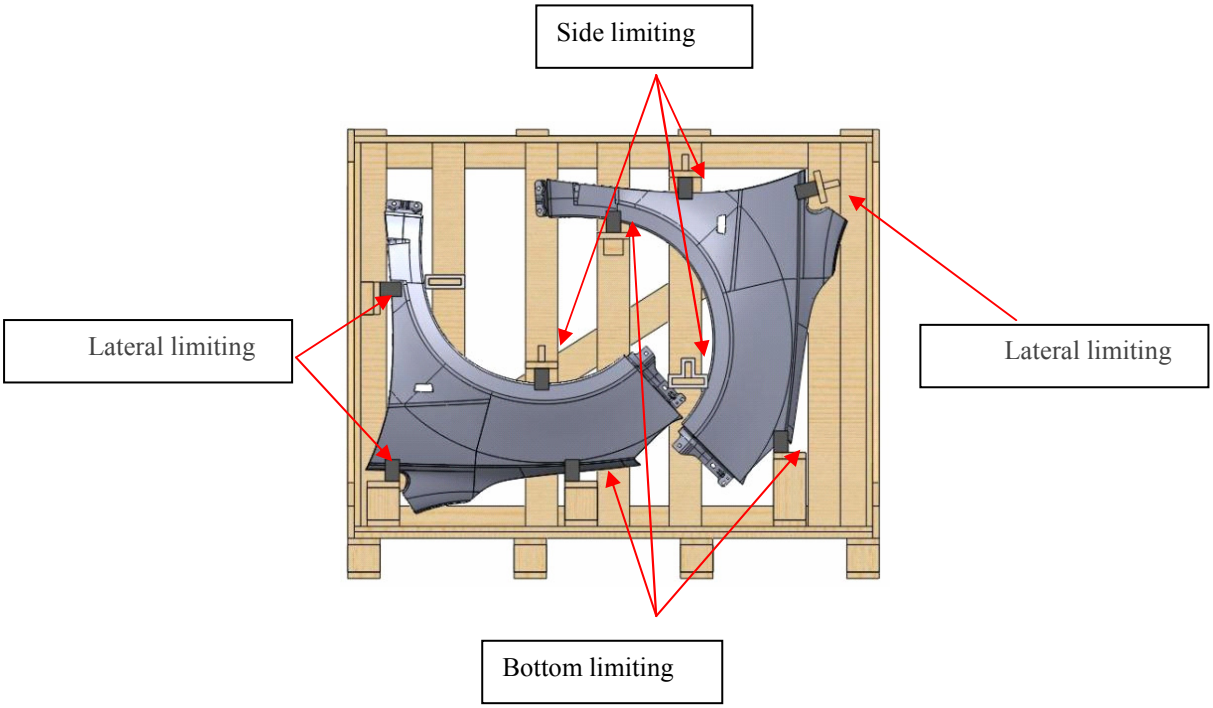



**Figure 11:** Construction components of fender wooden package box.

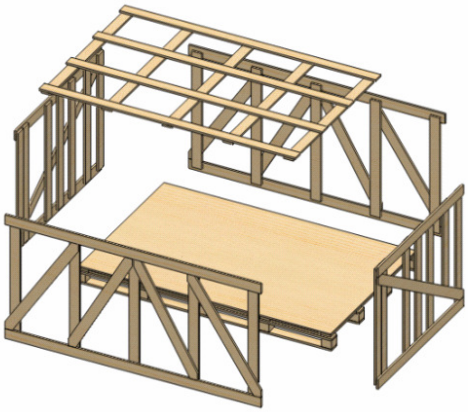


**Figure 12:** Construction components of wooden box frame.

## (2) Automobile after-sales spare fender transportation packaging design

The decision on package design is based on the method of packaging design six-step, which determines the product flow environment, the product characteristics, product design improvements, packaging materials choosing, packaging design improvements, and packaged-product validation.

The key factors of product distribution environment are determined by analyzing product breakage, shown in Figure 13. The evident product defects, product angular parts of the deformation, surface scratches of fender packages are shown in the figure.



**Figure 13:** Damaged fender through physical distribution.

The specialty of automobile spare fender is its irregular shape, and its difficulty in locating center of gravity because of the inner packaging container with a plurality of contact points, the surface.

The automobile spare fender is designed to fit the automobile whole scale design, the product design itself is not supposed to change.

As after-sales spare parts, it is individual package in the packaging. The package material is using corrugated cardboard, EPE cushioning material and tape. According to the packaging material supplier specifications, corrugated board selects AB flute, the density of EPE is 28kg/m$^3$.

According to quality estimating, the fragility of fender is 53g, fender weighs is known as 5kg.
Equation $Gs=102.22 \times W^{-0.4}$ (1)
Gs- Fragility, g
W- Weighs, kg
Based on EPE dynamic cushioning material impact cushioning curve, the minimum cushion factor C of cushioning material is known as 2.3, the corresponding maximum static stress is 0.25kg/cm$^2$, and so the design of thickness and area of the cushioning material can be de decided, shown in Figure 14.

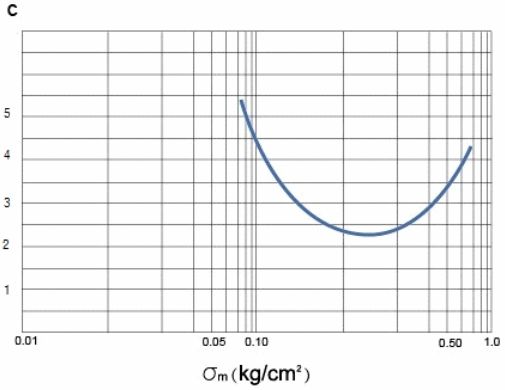



**Figure 14:** Density is 28 kg/m$^3$ EPE maximum static stress-cushion factor curve.

Calculated by the formula, refer the drop height of ISTA 3A is 600mm. EPE minimum cushion thickness T and area A are 26mm and 0.106m$^2$ respectively.

$A = W G / \sigma m$ (2)[5]

A- Minimum cushion area, m$^2$
W- Weighs, kg
G- Fragility, g
σm- Maximum static stress, kg/cm$^2$

$T = C H / G$ (3) [5]

T- Minimum cushion thickness, mm
C- Minimum cushion factor
H-Drop height, mm
G- Fragility, g

EPE cushion design is EPE cushion pad mounted to fender, to realize the function of corner protection and positioning. The size of cushion pad is 250mm × 200mm × 100mm; the minimum cushion thickness design is 50mm. It is shown in Figure 15. The smallest surface of corrugated boxes is selected as sealing surface, to ensure stacking strength of the package, shown in Figure 16.

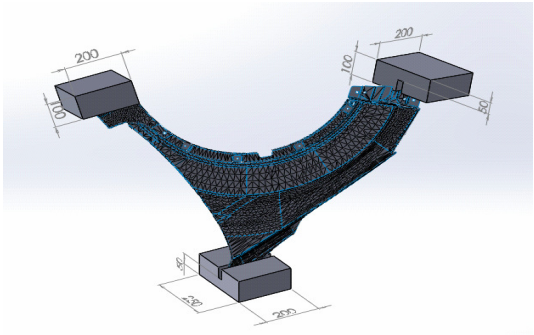



**Figure 15**: Fender cushion package EPE pad design.

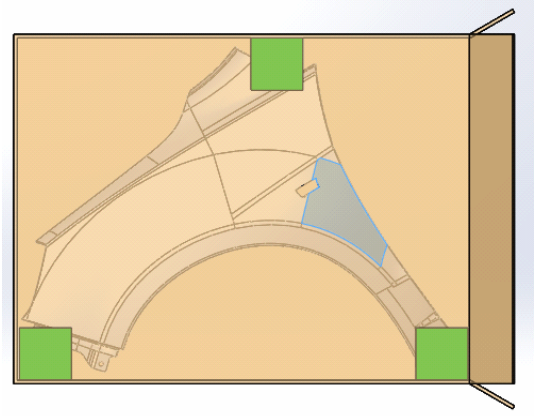


**Figure 16:** Packaged-fender.

## 5 Conclusion and Prospect

In summary, the automotive KD kit and transport packaging design features of aftermarket spare parts packaging need to integrate the features of automotive products, the conditions of logistical environmental, as well as the cost control requirements. They supply pulling power for automobile manufacturing chain using packaged integration services, and provide important technical support to logistics services.

Logistics services is a transportation service based on demand-driven of orders in the application of automotive production, thereby reducing the total cost of the entire automobile manufacturing supply chain. Packaged integration services provide the solutions based on product-based logistics packaging for the LLP ②mode of

automotive parts into the factory. The combination of Integrated Packaging and Logistics LLP model is an effective way to improve operating margins of car manufacturers and enhance brand competitiveness.

It is particularly important to the efficiency of the supply chain that cooperation between different subjects integrated automotive products in the packaging supply chain. The world's leading automobile manufacturers has been a great success in the automotive export logistics packaging, sale and spare parts logistics packaging. The core technology and experience requires development and innovative use for further analysis based on a combination of China's stage of economic.

Note:
①Customers place parts order according to the needs, minimum order number is a standard package unit normally.
②Lead Logistics Partner in the lead place is supplemented in the next page.

## References


1. He Mingke. Zhang Yiran, 2011(7), "Automobile parts entrance logistic research", *China process economic,* pp. 31-36.
2. *SGM Automobile parts lean packaging rules*, 2010, China.
3. GB/T 7284 Wooden Framed Case, 1998.
4. Ding Yi. Chen Limin, 2012(5), "Automobile SKD Car Body and Kit Packaging Solution". *Packaging Engineering,* Vol 33.
5. Peng Guoxun. Pan Songnian, 1999,*Transport Packaging,* Print industry Pulisher, Beijing, China.

# The Status of Wood Pallet Repair Operations in the United States: A Survey Study

**Laszlo Horvath[1*], Jonghun Park[1], and Robert J. Bush[1]**

[1] *Department of Sustainable Biomaterials, Virginia Tech, USA*

[*] *Corresponding author. Email: lhorvat@vt.edu*

**Abstract:**
There are approximately 1.84 billion pallets in circulation within the United States. Every year, 321 million of these wooden pallets needs to be repaired, typically by designated pallet repair facilities. Due to increasing tipping fees by landfills and increasing environmental cautiousness by companies, the number of pallets repaired has significantly increased over the last 15 years. The processes used to repair pallets are important to the quality of repaired pallets. Meanwhile, increasing environmental awareness and concerns regarding sustainability have resulted in increasing use of quantitative techniques such as life cycle analysis to evaluate the environmental impacts of wood pallets used in the United States supply chain. The reliability of a life cycle analysis depends on the data provided by the life cycle inventory (LCI) database and the construction of an accurate LCI database requires detailed understanding of the types of repair operations used within the wood pallet repair operation.

Therefore, the main goal of this study was to identify the common repair practices used by the U.S. wood pallet repair industry to support accurate and comprehensive LCI for the wood pallet repair industry.

Data for the study were collected using an online survey of the United States wood pallet repair industry. The study examined the characteristics of wood pallets purchased, received, or repaired by industry participants; the processes used by the industry; and the characteristics of wood pallets repair businesses in general.

The results revealed that vast majority of the respondents repaired 48 in x 40 in. stringer class pallets and the main mode of repair was c-block type repair. Results showed that the majority of respondents are using extensive manual labor in their repair processes; however, a higher level of automation has found in notching, trimming, and sorting/stacking processes. Sixty-six percent of the respondents reported grinding unusable wood into chips or mulch and 16 percent of the respondents had a furnace or boiler to utilize wood scrap.

Keywords: pallet repair, wooden pallet, automation, unit processes.

## 1 Introduction

Internationally, the world container trade industry moved 151 million TEUs (20-foot equivalent unit), equivalent to around 1.2 billion tons of dry goods in 2011 [1]. The majority of the goods were transported in a unit load form that can be defined as "a single item, a number of items, or a bulk material, that is arranged and restrained so that the load can be stored, picked up, and moved between two locations as a single mass" [2]. Pallets are the backbone of the unit load because they serve as an interface between material handling equipment and the packages while providing a high level of standardization and protection from the hazards of material handling [3]. Currently, there are approximately 2 billion pallets in circulation within the United States [4]. Although, pallets can be made using many different materials, the majority of pallets (92%) used within the U.S. are made of solid wood [5]. Wooden pallets can be classified into two categories based on their durability: limited-use or multiple-use [6]. ANSI MH1 [6] standard states that limited-use pallets are "designed for an average of up to nine trips, with an average of five handlings per trip and an average handling environment as defined in the Pallet Design System." while multiple-use pallets "designed for repeated use for more than one unit load with an average minimum "life-to-first-repair" of ten trips, or more, assuming an average of five handlings per trip and an average handling environment as defined in the Pallet Design System". Once pallets are damaged or declared unusable based on the requirements is ISO 18613 [7], they often are sent to pallet repair companies. Pallet repair is one of the most common end-of-life scenario for a wooden pallet (Bush and Araman 2009) and the production of repaired pallets doubled between 1995 and 2006 [8]. In 2006, 321 million wooden pallets were repaired in the U.S. [9]. Financial issues such as increasingly high tipping fees and increasingly strict environmental regulations such as the ban of wooden pallets from landfills in North Carolina are the major reasons for the steep increase of the amount of pallets repaired in the U.S. Meanwhile, studies showing that the durability of repaired pallets could be comparable to the durability of a new pallet in some supply chains [10] and the low purchase price of repaired pallets [11] also contribute to their increasingly wide utilization.

Fueled by initiatives such as the Walmart score card, sustainability has become important in corporate decision making. Quantitative techniques such as Life Cycle Analysis (LCA) increasingly are used to support the decision making, however, the accuracy of LCA greatly depends on the data provided by a life cycle inventory (LCI). The lack of information on the types of operations commonly used by pallet repair companies inhibits the development of an industry wide LCI for the pallet repair process.

The objective of this study was to develop information about repair practices used by the U.S. wood pallet repair industry to support accurate and comprehensive LCI for the wood pallet repair industry.

## 2 Methods

An electronic survey of the wooden pallet recycling industry was conducted to obtain information including the level of automation used for the wooden pallet repair operation.

*Survey Design*

An electronic questionnaire consisting 22 questions was developed using the survey software Qualtrics. The survey was divided into two parts; 10 questions focused on specific process in the pallet repair facility and the remaining 12 questions focused on the general facility information such as materials used for the repair, end-of-life for wood scrap, and typical distances travelled to procure pallet cores. The questions were designed using industry input, existing literature, and previous research studies. The questions included close-ended inquiries, partial open-ended inquiries with and *othe*r option, and open-ended inquiries with short answers. The questions solicited answers for the 2012 calendar year.

*Survey Data Collection*

The sample frame for the study was developed using the member list of the National Wood Pallet and Container Association (NWPCA) posted at www.palletcentral.com. A total of 343 facilities were included.

The survey was pretested using ten randomly selected facilities in order to check overall quality, clarity and comprehension [12]. Minor changes were made based on the comments submitted by the pretest respondents and the revised questionnaire was administered to the sample frame. Two weeks after the initial mailing a reminder email was sent to all non-respondents. The reminder email was repeated two additional times, at two week intervals, and closed eight weeks after the initial distribution.

*Data Analysis*

Descriptive statistics, including means and standard deviations were used to analyze the data.

*Limitations of the Study*

The results of the study possessed the general limitations of all mail in surveys as outlined in [13]. First, only one person per organization was contacted and this may have resulted in a single respondent bias [14]. Secondly, using the NWPCA membership list as a proxy for the pallet repair industry in the United States of America, may have create a bias in the results of the study if NWPCA members differ systematically for the population of interest. Lastly, the relative low response rate (11 percent) reduces the reliability of generalizations from sample to the entire wood pallet repair industry.

## 3 Results and Discussion

*Response rate*

Among 343 facilities surveyed in the study, responses were provided by 53 facilities (15%, N=343) among which 14 facilities (26% of the total respondents) did not operate the pallet repair business in 2012; therefore, were excluded from the study. Overall 39 valid responses were received resulting an 11 percent response rate.

*Company characteristics*

Majority of survey respondents were owners, presidents, partners or vice-presidents (46%). An additional 28% of respondents held titles of operation manager, general manager, plant manager, or director. A small number of respondents were sales mangers (8%) or did not provide their position (18%). Most responses were received from the North Central States (32%), followed by the South Atlantic States (29%), the South Central States (18%), the Mid-Atlantic States (8%), the Pacific States (5%), the Mountain States (5%), and the New England States (3%).

One-third of the respondents (33%) reported annual gross sales from 5 to 10 million dollars, 31 percent from 1 to 5 million dollars, 22 percent from 10 to 20 million dollars, eight percent had more than 30 million dollars, and

six percent had less than 1 million dollars. Concerning the number of recovered pallets, 28 percent of respondents recovered over 1 million pallets, 27 percent recovered from 500,000 to 999,999 pallets, 21 percent recovered from 100,000 to 499,999 pallets, 10 percent recovered from 10,000 to 99,999 pallets, and 3 percent recovered less than 9,999 pallets.

The mean number of employees (full-time and part-time) per facility was 61. Twenty-five percent of the facilities had 1 to 20 employees, 58 percent had 20 to 100 employees, and 17 percent had more than 100. These results correlates well to the findings of Quesada Pinada et al. [15]. The majority of the employees (82%) were full time production, 15 percent was full time non-production, and 3% were part time production. Most of the facilities (88%) had only full time production employees.

The majority of the respondents (82%) operated both a new pallet manufacturing and pallet repair businesses while only 12 percent operated only a pallet repair business. Thirty percent of the respondents received only stringer class pallet cores while 60 percent received both block and stringer class pallet cores. No responding facility reported receiving only block class pallet cores. Among the facilities that received both block and stringer class pallets, the average proportion of stringer class pallets was 93 percent.

The most common pallet size that was purchased, received, or repaired by the respondents was 48 in. x 40 in. The most common pallet sizes are listed in Figure 1. The trend observed for the most commonly received pallet sizes align well with the findings on Bush and Araman [8] who found that only 26.9 percent of all pallets used in the US are 48 in. x 40 in. while about 50 percent is a custom size. In the current study, 86 percent of the cores received by the pallet repair facility was 48 in. x 40 in. The difference might be resulted by that custom pallet sizes are mainly designed for single use applications; therefore, they are not processed by pallet repair facilities.

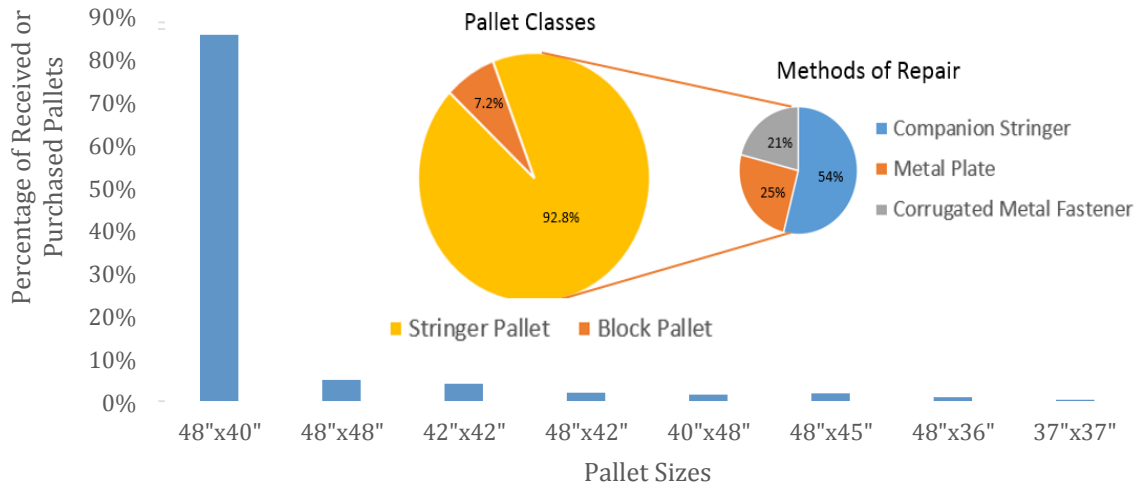



**Figure 1:** Percentage of pallet sizes and styles received or purchased by the respondents and repair methods used for stringer pallet repair process.

The most common distance travelled to collect cores were 11-50 miles (62% of respondents) while 21 percent and 5 percent of the respondents willing to travel between 51-100 miles or between 100-200 miles, respectively. Only 2% of the facilities sourced their cores locally (0.1-10 miles). Although, the typical distance travelled is mainly determined by the transportation cost [16], the competition over a limited number of cores might be a major determining factor.

Effective utilization of waste materials could greatly contribute to the financial feasibility of the pallet repair facility. Sixty-three percent of the facilities indicated that they have a grinder to convert wood waste into mulch and 11 percent of respondents had a furnace/boiler on site to use wood waste for bioenergy. LeBlanc [17] reported that the feasibility of having a grinder or furnace on site greatly depends on the geographical location, market variations, financial means, and availability of space. However, this study failed to show a statistically significant correlation between gross sales, employee numbers, number of pallets recovered and the presence of an on-site grinder or furnace.

*Unit process types*

The results of the 10 questions focused on specific process in the pallet repair facility are presented in Figures 2 and 3. All respondents of the survey reported to use forklifts to unload incoming pallets and to load outgoing

trailers. Following the unloading process the pallets are inspected to determine overall grade. The majority of the respondents (87%) inspect incoming pallets visually without any scanning equipment while 12 percent utilized scanning machines but without the operator making the final decision regarding grades. Thirty-eight percent of the respondents reported that they sort and stack pallets with machine-controlled infeed and outfeed stackers, 36 percent stacked and sort pallets manually, and 26 percent used forklifts.

Typically, when the incoming cores are severely damaged, the core is sent to the dismantling station. The most common dismantling method used by companies is a horizontal band saw (87% of respondents used this type of equipment of dismanteling pallets), while dismantling bars and hammers (5%), machine controlled infeed/outfeed dismantling systems (5%), and disc or shear type dismantling systems (3%) were only used by far fewer respondents.

Often, dismantled boards need to be cut to a different size to be used during the repair process. The majority of the responding firms used machine controlled infeed/outfeed trim saws (62%) while 20 percent used single head or dual-head table saws. Approximately 18 percent of responding firms used radial-arm saws with manual feed for cut to size operations. Dismantled and trimmed stringers were notched by 74 percent of the respondents and the majority of the companies (69%) who have notching process uses single-head or double-head notching machines with manual feed. Thirty-one percent of the responding firms used machine controlled infeed/outfeed notching machines.

Transport of pallets within the warehouse was accomplished by forklifts (85% of respondents) and powered conveyors (15%).

When it comes to the repair of the incoming cores, seventy-seven percent of the respondents repaired the damaged cores using hand held nail guns on a repair table. Thirteen percent of firms used machine controlled infeed/outfeed nailing systems and only 10 percent used hammers on a repair table. The majority of the companies (80%) reported that they were using companion stringers for pallet repair. Half companion stringers were utilized by 89 percent of the companies, C-blocks were utilized by 36% and only 11 percent used full companion stringers for pallet repair. Although the strength and stiffness of repaired wooden pallets are the greatest with full companion stringers [18].

Pallet repair facilities were using paint primarily for the removal of the heat treatment mark to ensure compliance with ISPM 15 and for custom coloring of pallets. When asked about their paint usage, 15 percent of the respondents indicated that they do not use paint in their operation. Eighty-five percent of the respondents who painted or marked their repaired pallets used spray paints or paint buckets and rollers by hand while high-pressure systems and machine controlled spray systems were used by only 9 percent and 6 percent of the respondents, respectively.




**Figure 2:** Summary results of the percentages of the currently used unit processes in the wooden pallet repair industry.




**Figure 3:** Summary results of the percentages of the currently used unit processes in the wooden pallet repair industry. Continued

The responses related to the unit processes indicate that the majority of the unit processes during the wood pallet repair operation involve a significant amount of human labor. Although, some processes such as notching, board trimming and sorting / stacking uses a higher level of automation than do others. The overall lower level of automation, might be the result of the limited availability and high market price of the fully automated pallet repair / manufacturing systems and labor regulations in the U.S. Due to the greater level of standardization and higher labor cost, higher level of automation can be found within the European Union [19,20,21]. It is predicted that due to increasing competition within the wooden pallet industry [22] and more strict labor regulations such as The Patient Protection and Affordable Care Act [23] more U.S. companies will invest in automated systems to achieve better productivity, increased quality, and reduce the labor costs.

## 4 Conclusion

The most common pallet class repaired by wooden pallet repair companies was the stringer class pallet and the most common size (86 percent of the received cores) was 48 x 40 inch. The most commonly use method of repair was the use of companion stringer (54%) while metal plate and corrugated metal fasteners were used by 25 percent and 21 percent of the respondents, respectively. Eighty-nine percent of the respondents who used companion stringers for repair reported that they are using half companion stringer, 36 percent utilizes C-blocks, and only 11 percent uses full companion stringer, even though the strength and stiffness of repaired wooden pallets are best maintained by using companion stringer repairs. The majority of the material handling within the pallet repair factory was done by forklifts and powered conveyors. Based on the responses, the majority of the repair operations used a high level of manual labor; only board trimming, sorting/stacking, and notching operations utilized higher levels of automation. Automation levels may change in the future due to increased competition and more strict labor regulations such as The Patient Protection and Affordable Care Act. The high level of manual labor utilized during the pallet repair process also provides an opportunity to adopt the principles of lean manufacturing to optimize processes.

The results of this study are a first step toward understanding the processes most commonly used in the U.S pallet repair industry and a necessary step toward the construction of a detailed and representative LCI database for the wood pallet repair industry.

## 5 Acknowledgement

The study was supported financially by the members of the Center for Packaging and Unit Load Design at Virginia Tech. The authors also would like to recognize the support of all participating companies and the National Wood Pallet Association (NWPCA) and the Pallet Enterprise Magazine for their help promoting the study.

## 6 References

1. UNCTAD, 2012, “Review of Maritime Transport. Geneva, Switzerland: United Nations conference on trade and development (UNCTAD)”, United Nations Publication.
2. M.S White and P. Hamner, 2005, “Pallets Move The World - The Case for Developing System-Based Designs for Unit Loads.”, Forest Product Journal, Vol. 55, No. 3, pp. 8-16.
3. M.S. White, 1995, “The Impact of Pallet Design on the Performance of Unit-Loads. Distribution Packaging Technology”, International Association of Packaging Professionals (IoPP), Ed: M.R. Fiedler, pp. 263-272.
4. U. Buehlmann, M. Bumgardner and T. Fluharty, 2009, “Ban on landfilling of wooden pallets in North Carolina: an assessment of recycling and industry capacity”, *Journal of cleaner production*, Vol. 17, No. 2, pp. 271-275.
5. B.Trebilcock, 2013, “Reader Survey: Talking pallets with Modern’s readers”, *Modern Material Handling*, Spetember 2010, pp. 24-29.
6. ANSI, 2005, “Pallets, Slip Sheets, and Other Bases for Unit Loads”, Material Handling Industry, Charlotte, NC, USA, pp. 208.
7. ISO, 2003, “Repair of flat wooden pallets”, International Standard Organization, Geneva, CH, pp 14.
8. R.J. Bush, P.A. Araman, 2009, “Pallet Recovery, Repair and Remanufacturing in a Changing Industry: 1999 to 2006”, Pallet Enterprise, Vol. 29, No. 8, pp. 24-27.
9. R.J. Bush, P.A. Araman, 2008, “Final Report - Updated Pallet and Container Industry Production and Recycling Research”, Blacksburg, VA, USA.
10. J.W. Clarke, M.S. White and P.A. Araman, 2005, “Comparative performance of new, repaired, and remanufactured 48-by 40-inch GMA-style wood pallets”, *Forest products journal, Vol. 55, No.* 12, pp.
11. Ray, C. D., Michael, J. H., & Scholnick, B. N. (2006). Supply-chain system costs of alternative grocery industry pallet systems. *Forest products journal, 56*(10).
12. L.M. Rea and R.A. Parker, 1997, *Designing and conducting survey research: a comprehensive guide,* 2nd Ed., Jossey-Bass Inc., San Francisco, CA., pp. 254.
13. P.L. Alreck and R.B. Settle, 2003, *The survey research handbook,* 3rd Ed., McGraw-Hill/Irwin, New

York, New York. pp. 463.

14. E. Blair and S. Burton, 1987, “Cognitive Processes Used by Survey Respondents to Answer Behavioral Frequency Questions”, *Journal of Consumer Research*, vol. 14, no. 2, pp. 280-288.
15. H. Quesada-Pineda, S. Sanchez-Gomez and P. A. Araman, 2012, “A quantitative study of the US wood pallet industry based on supply chain management practices”, Journal of Applied Packaging Resoure, vol. 6, no. 1 pp. 1-26.
16. C.G. Bouffier, C.C. Downing and B.W. Riall, 1995, “Pallet Disposal: Current Situation and Opportunities for Change”, Georgia Tech Research Corporation, Atlanta, GA, pp.59.
17. R. LeBlanc, 2003, “Companies Taking Closer Look At Managing Residuals”, Pallet Enterprise, May 2003.
18. J. Clark, M.S. White, P. Araman, 2005, “Effect of Stringer Repair Methods and Repair Frequency on GMA Performance.”, Pallet Enterprise, February, 2005.
19. R. LeBlanc, 2005, “Dutch Pallet Manufacturer Combines Veteran Expertise, New Technology: Phoenix-Pallets Adds Swedish Robotic Equipment to Increase Production”, Pallet Enterprise. November 2005.
20. C. Brindley, 2013, “The Future of Pallet Production…Today – Robots Effectively Used in Auropean Pallet Companies”, Pallet Enterprise, November, 2013. p. 30-35.
21. C. Brindley, 2014, “Asljunga Pallan Relies on Robots and High Level of Automation to Compete in Trough Eurpoen Market”, Pallet Enterprise, March, 2014. p. 24-31.
22. Neville, 2013, “Skidding along: Renewed manufacturing activity will boost revenue despite increased competition” In: IBISWorld Industry Report 32192: Wood Pallets & Skids, IBISWorld, lnc. pp. 36.
23. PPACA, 2010, “The Patient Protection and Affordable Care Act.”, source: http://www.gpo.gov/fdsys/pkg/BILLS-111hr3590enr/pdf/BILLS-111hr3590enr.pdf, Accessed: April 17, 2014.

# MEDICAL, COSMETICS & PHARMACEUTICAL PACKAGING

# Microbiological stability of shampoo stored in polymeric packaging modified with nanosilver

**Zenon Foltynowicz*, Dorota Rodewald and Daniela Gwiazdowska**

*Faculty of Commodity Science, Department of Product Quality and Ecology, Poznan University of Economics, Poland*

**Corresponding author. Email: zenon.foltynowicz@ue.poznan.pl*

**Abstract:** Microbial stability of cosmetics, provided by preservatives, determines their safe use. However, despite the positive impact of preservatives, they also demonstrate side effects in the form of an allergic reaction to the users. Therefore, alternative methods of preserving cosmetic products are currently investigated. The aim of the study was to replace the preservatives, mainly parabens, contained in cosmetic formulations, through the use of nanosilver, but not entering them into cosmetics, but into its packaging. It is expected therefore to reduce the exposure of users and the aquatic environment on silver nanoparticles, which impact is yet not fully discovered. A shampoo without parabens was stored in nanosilver modified PP and PE containers, as well as in non-modified packaging and glass flasks, as a comparison. Additional reference samples were shampoos with preservatives stored in both non-modified PP and PE containers and in glass flasks. Evaluation of the microbiological stability of the shampoo (with and without parabens) were performed against *Staphylococcus aureus* (Gram-positive bacteria), *Pseudomonas aeruginosa* (Gram-negative bacteria) and *Candida albicans* (fungi). Testing the migration of silver from the packaging into the product as well as the effect of nanosilver particle size and concentration were also done. The results of the investigation confirm that the use of nanosilver in polymer packaging of selected cosmetic formulation (such as shampoo) can be, in certain circumstances, an effective method of the product preservation.

Keywords: nanosilver modified PP and PE containers, parabens, microbial stability.

## 1 Introduction

Cosmetics and personal care products are products of everyday use and they come into direct interaction with the human skin. In spite of cleaning or nourishing properties they should be safe for the user and for the environment. Safety of these products is ensured by their microbiological stability. Microorganisms may cause undesirable effects in the cosmetic preparation, that may occur by change in odor or consistency. More importantly, changes in cosmetic products caused by microorganisms can lead to adverse reactions in contact with the human skin. To prevent microbiological changes in the products, preservative substances are used. Preservatives are compounds demonstrating antimicrobial activity. This is especially important in the case of cosmetics with a high water content, because the risk of contamination by microorganisms is then higher. This kind of environment promotes the growth of pathogenic bacteria e.g. *Staphylococcus aureus* and *Pseudomonas aeruginosa*. The use of preservatives in cosmetic products can extend their stability, what extends the safe use of the product. The presence of a preservative prevent also the formation of products of metabolism of microorganisms, which can cause skin and mucous membranes irritations [1-4].

It appears, however, that the synthetic preservatives may cause allergic reactions to the users and pose a potential threat to the environment (particularly water) [5]. One of the most commonly used preservatives in cosmetics are esters of p-hydroxybenzoic acid, called parabens, such as methylparaben, ethylparaben, propylparaben, butylparaben [6]. It is said that parabens are not strong allergens, but the prevalence of their use makes them frequent sensitizers. Excessive cosmetic preservation can lead to allergic symptoms of consumers, since these symptoms are also dependent on the dose, on which skin is exposed to [1-4].

Current trend is to minimize the use of preservatives in cosmetic products. It is the result of attempts to reduce the adverse effects of cosmetics. This issue, however, requires special attention, because a smaller amount of preservatives in the product reduces its stability, and therefore shortens the period of safe use of cosmetics. Therefore, an attempt was made to create a new way of cosmetic products preservation without using conventional substances.

The development of the cosmetics market in terms of improving the efficiency of the active ingredients can proceed in two ways [7]:

- in the development of advanced technologies such as the use of nanomaterials, or
- on the way to improve well-known natural, organic ingredients, and finding for them new and revolutionary applications.

Cosmetic packaging (which is inherent with the cosmetic) has an increasingly important role in ensuring safety of the product and its users. What matters is the size and the closing of the packaging, but the packaging material is also important. As a result of technological advances in the packaging industry, new types of polymeric materials are emerging. There is a desire for better protection of the products quality in the prolonged period of their validility [8-9].

One of the latest trends in packaging industry are nanocomposites. Composites, because of the addition of nanomaterials, are gaining a better, enhanced or entirely new properties. Polymer nanocomposite is a two-phase polymer, in which particles of the filler are well dispersed in a polymer matrix and at least one of the dimensions of these particles does not exceed a few nanometers. In a wide range which nanotechnology covers, polymer nanocomposites have become a promising area of research and development [10-12].

Cosmetics are one of the largest group of consumer products where the application of nanotechnology and nanomaterials is present. The most commonly used nano-ingredient in consumer products is nanosilver, due to its antimicrobial properties. Reducing silver to nanometric size increases the active surface of the particles, so that biological and chemical activity of the silver is increased. This indicates a potential increase of silver nanoparticles' effectiveness against microorganisms. It is suggested then that the nanosilver can be a good preservative [13-14].

Nanomaterials are one of the most dynamically developing issues relating materials science in recent years [15]. In the research study "Nanotechnology Market Outlook 2017", RNCOS' analysts have identified that the global nanotechnology industry has been growing at a rapid pace with rising applications in different sectors. According to their assessmnet the global nanotechnology market is anticipated to grow at a CAGR (Compounded Annual Growth Rate) of around 19% during 2013-2017 [16].

In this work it is proposed to replace the preservatives contained in cosmetic formulations, through the use of nanosilver, but not entering them into cosmetics, but into its packaging. It is expected therefore to reduce the exposure of users and the aquatic environment on silver nanoparticles, which impact is yet not fully discovered. Achieving a satisfactory level of cosmetic stability, using discussed solving, would allow to increase product quality and consumer satisfaction.

## 2 Materials and methods

Shampoo was selected as a cosmetic preparation to study. Shampoos have the largest market share of cosmetic products, both Polish and European level. As washable products, shampoos can create the risk to aquatic organisms. Whereas as products with a high water content (70 - 80%), shampoos are favourable environment for the growth of pathogenic microorganisms. That is why ensuring their microbiological stability is especially important. The most commonly used type of shampoo package is bottle made of plastic, usually polyethylene (PE) or polypropylene (PP). Therefore, PE and PP were selected as tested packaging materials.

Cosmetic formulations of hair shampoo were prepared in two groups. One was prepared according to conventional recipe, using mixture of parabens which are the most widely used preservatives in cosmetics. Another one was prepared according to the recipe modified by elimination of preservatives.

Cosmetic preparations were stored in two types of packaging containing nanosilver: boxes made of polypropylene (PP-nAg) and bags made of polyethylene foil (PE-nAg).

Components of the polyethylene film were extruded at the Institute of Polymer Materials and Dyes (IMPiB) in the form of granules on the twin-screw extruder with co-rotating screws at a temperature of 180 - 200 ° C. The resulting granulation was then dried. Final PE-nAg foil (thickness 20 μm ± 2 μm) was produced by extrusion blow molding on the line for the production of single-layer film. There were five different foils obtained. Then bags (5 cm x 5 cm) from obtained foil were made using foil welding machine. The other type of packaging - PP-nAg boxes were derived from the market. The study was conducted on four different boxes containing nanosilver, from different manufacturers. Packaging differed in concentration and size of the silver particles, both for PE foils and for PP boxes. Generally in foils silver concentration was higher and silver particles were bigger.

Packaging made of PP and PE without nanosilver were used as a control samples. Additional reference samples were shampoos stored in glass flasks.

Variants of the tested samples were as follows:

- Shampoo without preservatives stored in PE/PP packaging with nanosilver,
- Shampoo without preservatives stored in PE/PP packaging without nanosilver,
- Shampoo with parabens stored in PE/PP packaging without nanosilver,
- Shampoo without preservatives stored in glass flasks,
- Shampoo with parabens stored in glass flasks.

Preservation test was made according to Pharmacopoeia, in order to verify preservative activity of nanosilver (in packaging) to cosmetics. As recommended by the Pharmacopoeia, the test was performed on the most common human pathogen *Pseudomonas aeruginosa* (gram negative bacteria), *Staphylococcus aureus* (gram positive bacteria), *Candida albicans* (fungus).

Microorganisms selected for testing were replicated before each test on fresh medium slants, appropriate for the organism, as follows:

- CASO agar for bacteria *Staphylococcus aureus* and *Pseudomonas aeruginosa*,
- Sabouraud chloramphenicol for yeast *Candida albicans.*

In order to replicate microorganisms were incubated for 24 hours at:

- 37 °C for *Staphylococcus aureus* and *Pseudomonas aeruginosa*,
- 30 °C for *Candida albicans.*

After 24 hours of incubation, obtained cultures of microorganisms were taken from the slants and then suspended in saline with a density of $10^8$ cfu/ml (cfu - colony forming units). The specified density was determined by measuring the transmittance at a wavelength of 600 nm using a UV-VIS spectrophotometer. The relationship between the transmittance and the number of cfu/ml determined by plating method for tested microorganisms strains was previously set.

The transmittance was:

- 90% for *Pseudomonas aeruginosa*,
- 60% for *Staphylococcus aureus,*
- 40% for *Candida albicans.*

Preservation test according to Pharmacopoeia is based on a single introduction of test strains to the samples of the product. It is made to simulate a secondary infection that may occur during use of the product by the consumer. The appropriate suspension (1%) of each strain was introduced to the preserved samples. Samples were tested after 2, 7, 14 and 28 days. Cells number was determined by the plating method using CASO agar for bacteria and Sabourad agar with chloramphenicol for fungus.

## 3 Results

Table 1. shows results from the test conducted on polypropylene boxes. In the containers containing nanosilver, marked with numbers from 1 to 4, shampoo without preservatives was stored. Containers without nanosilver were control samples and have been divided into two parts. In some of them shampoo without preservatives was stored (sample 5 (bK)), while in the remaining shampoo with parabens was stored (sample 6 (K)).

Test maintained in accordance with the European Pharmacopoeia 6.0 meets the acceptance criteria in relation to the bacteria, if within two days there is the reduction of the number of bacteria by 2 logarithms, within 7 days of 3 logarithms and up to 28 days there will be no further increase in the number of bacteria and it will stabilize at the lower level than the starting level. In the case of fungi acceptance criterion is met if within 14 days there is the reduction of the number of fungi by 2 logarithms and, like bacteria, up to 28 days there will be no increase in the number of fungi and it will stabilize at a level lower than the start. The number of microorganisms after 28 days is especially important during the test assessment [17].

**Table 1:** Preservation test results as a number of microorganisms [cfu/ml].

| | **Starting number of microorganisms** | **After 2 days** | **After 7 days** | **After 14 days** | **After 28 days** |
|---|---|---|---|---|---|
| ***Pseudomonas aeruginosa*** | | | | | |
| 1 | $5{,}9\cdot10^{7}$ | $1\cdot10^{5}$ | $5{,}5\cdot10^{0}$ | $4{,}8\cdot10^{5}$ | $5{,}6\cdot10^{4}$ |
| 2 | $5{,}9\cdot10^{7}$ | $5\cdot10^{4}$ | $8{,}3\cdot10^{1}$ | $5{,}4\cdot10^{5}$ | $6{,}2\cdot10^{4}$ |
| 3 | $5{,}9\cdot10^{7}$ | $5\cdot10^{3}$ | $1{,}7\cdot10^{6}$ | $5{,}6\cdot10^{6}$ | $4{,}4\cdot10^{6}$ |
| 4 | $5{,}9\cdot10^{7}$ | $1{,}8\cdot10^{2}$ | $1{,}6\cdot10^{6}$ | $6{,}4\cdot10^{6}$ | $4{,}2\cdot10^{6}$ |
| 5 (bK) | $5{,}9\cdot10^{7}$ | $2\cdot10^{1}$ | $7{,}8\cdot10^{5}$ | $6{,}2\cdot10^{6}$ | $5{,}4\cdot10^{6}$ |
| 6 (K) | $5{,}9\cdot10^{7}$ | $5\cdot10^{0}$ | 0 | 0 | 0 |
| ***Staphylococcus aureus*** | | | | | |
| 1 | $2{,}4\cdot10^{7}$ | $5\cdot10^{0}$ | 0 | 0 | 0 |
| 2 | $2{,}4\cdot10^{7}$ | $3\cdot10^{3}$ | 0 | 0 | 0 |
| 3 | $2{,}4\cdot10^{7}$ | $1{,}5\cdot10^{5}$ | 0 | 0 | 0 |
| 4 | $2{,}4\cdot10^{7}$ | $1\cdot10^{5}$ | 0 | 0 | 0 |
| 5 (bK) | $2{,}4\cdot10^{7}$ | $3{,}5\cdot10^{5}$ | 0 | 0 | 0 |
| 6 (K) | $2{,}4\cdot10^{7}$ | $3\cdot10^{3}$ | 0 | 0 | 0 |
| ***Candida albicans*** | | | | | |
| 1 | $7{,}4\cdot10^{4}$ | $2{,}9\cdot10^{2}$ | $8\cdot10^{1}$ | 0 | 0 |
| 2 | $7{,}4\cdot10^{4}$ | $7\cdot10^{1}$ | $1{,}6\cdot10^{2}$ | $8\cdot10^{2}$ | $3{,}4\cdot10^{2}$ |
| 3 | $7{,}4\cdot10^{4}$ | $1{,}6\cdot10^{4}$ | $6{,}3\cdot10^{4}$ | $6{,}3\cdot10^{5}$ | $2\cdot10^{5}$ |
| 4 | $7{,}4\cdot10^{4}$ | $1{,}6\cdot10^{4}$ | $4{,}8\cdot10^{5}$ | $1{,}1\cdot10^{5}$ | $1{,}4\cdot10^{5}$ |
| 5 (bK) | $7{,}4\cdot10^{4}$ | $1{,}1\cdot10^{5}$ | $2{,}7\cdot10^{6}$ | $6{,}3\cdot10^{6}$ | $3{,}9\cdot10^{6}$ |
| 6 (K) | $7{,}4\cdot10^{4}$ | $1{,}7\cdot10^{4}$ | $5{,}9\cdot10^{4}$ | $2\cdot10^{5}$ | $2{,}6\cdot10^{5}$ |

Table 1 shows results of the preservation test for each microorganism strain separately. For each sample the number of microorganisms are given after 2, 7, 14 and 28 days. Table 1 presents the average values. Based on these results it can be concluded that in the case of *Pseudomonas aeruginosa*, the largest decrease in population were found in containers 1 and 2, two different polypropylene boxes containing nanosilver, in which a cosmetic preparation without preservatives was stored.

Growth of *Staphylococcus aureus* was inhibited in virtually all containers. It was found that in containers 1 and 2 (containing nanosilver), decrease in the number of bacteria was much greater than in a container without nanosilver. The highest effectiveness in the first period of the test showed sample 1 (box with nanosilver), then samples 2 (box with nanosilver) and 6 (shampoo with parabens in box without nanosilver – control sample). The least effective in first days of the test were samples 3 (box with nanosilver), 4 (box with nanosilver) and 5 (shampoo without preservatives in a box without nanosilver – control sample).

From the obtained results it was also observed that the greatest degree of fungal growth inhibition of *Candida albicans* was reported in boxes 1 and 2, the same as in the case of bacteria.

It was noted that the shampoo stored in boxes 1 and 2 satisfy the criterion of preservation test according to European Pharmacopoeia 6.0, with respect to *S. aureus* and *C. albicans*. In case of *P. aeruginosa* the test criterion was not fully satisfied, that is why more research are needed in this situation.

In order to verify results and for comparison purposes, a preservation test was carried out using references samples, which were shampoos stored in glass flasks. Glass was selected as an inert and possible to sterilize material. A comparative test using glass flasks was carried out in order to avoid possible impact of packaging without the addition of nanosilver on the development of microorganisms and to confirm the differences in the growth of the tested bacteria and yeasts in the samples preserved and those without preservatives. It was concluded that in the cosmetic formulations without preservatives growth of bacteria *P. aeruginosa* and *C. albicans* was not inhibited. As in previous tests, *S. aureus* has proved to be the most sensitive microorganism.

Higher growth of microorganisms in the shampoos stored in glass flasks comparing to those stored in PP boxes confirms the antimicrobial effectiveness of the plastic containers with nanosilver.

The evaluation of microbiological stability of shampoo stored in PE packaging were performed on a specially prepared bags made of the PE foil. The same as for PP-nAg boxes, also in the case of PE-nAg foils, most of the samples exhibits the best preservative results against *S. aureus*. At the same time PE-nAg foils showed much lower preservative effectiveness comparing to PP-nAg boxes 1 and 2.

## 4 Conclusions

It was concluded that the use of nanosilver in polymer packaging of shampoo can be, in certain circumstances, an effective method of the product preservation.

It was noted that two of the four tested boxes with nanosilver show good preservation effect against all three tested strains. These two boxes were tested again and the preliminary results for them has been confirmed. It was concluded then, that PP-nAg boxes with nanosilver concentration more than 6 ppm, and less than 10 ppm and with the particles size from 3 to 28 nm, present good antimicrobial properties against gram-positive bacteria *S. aureus* and fungi *C. albicans*. At the same time they have met the test criteria according to European Pharmacopoeia. When it comes to *P. aeruginosa* more research are needed, because at this moment the test criteria were not fully satisfied. It was found that the strongest antimicrobial effect is observed against *Staphylococcus aureus*, both for PP boxes and PE bags. According to the preservation test, PP-nAg boxes showed better preservative properties than PE-nAg bags, which were not effective enough. The growth of microorganisms was higher in the glass flasks samples. It also confirms the antimicrobial effectiveness of tested plastic containers with nanosilver.

## References


1. M.D. Lundov. L. Moesby. C. Zacharie. J.D. Johansen, 2009, "Contamination versus preservation of cosmetics: a review on legislation, usage, infections, and contact allergy", *Contact Dermatitis*, no. 60, pp. 70-78.
2. S. Kokura. O. Handa. T. Takagi. T. Ishikawa. Y.Naito. T. Yoshikawa, 2010, „Silver nanoparticles as a safe preservative for use in cosmetics", *Nanomedicine: Nanotechnology, Biology, and Medicine*, no. 6, pp. 570-574.
3. D. Sasseville, 2004, "Hypersensitivity to preservatives", *Dermatologic Therapy*, vol. 17, pp. 251-263.
4. R.F. Davies and G.A. Johnston, 2011, "New and emerging cosmetic allergens", *Clinics in Dermatology*, no. 29, pp. 311-315.
5. L.L. Dobbins. S. Usenko. R.A. Brain and B.W. Brooks, 2008, "Probabilistic ecological hazard assessment of parabens using *Daphnia Magna* and *Pimephales Promelas*", *Environmental Toxicology and Chemistry*, vol. 28, no. 12, pp. 2744-2753.
6. E. Lee. S. An. D. Choi. S. Moon and I. Chang, 2007, "Comparison of objective and sensory skin irritations of several cosmetic preservatives", *Contact Dermatitis*, no. 56, pp. 131-136.
7. A. Mihranyan. N. Ferraz. M. Strømme, 2012, "Current status and future prospects of nanotechnology in cosmetics", *Progress in Material Science*, no. 57, pp. 875-910.
8. A. Muñoz-Bonilla. M. Fernández-García, 2012, "Polymeric materials with antimicrobial activity", *Progress in Polymer Science*, no. 37, pp. 281-339.
9. Z. Foltynowicz and D. Rodewald, 2011, „Opakowania polimerowe zawierające nanosrebro", (in Polish: Polymeric Packaging Containing Nanosilver), *Tworzywa Sztuczne w Przemyśle (Polymers In Industry)*, no. 4, pp. 13-14.
10. F. Kampers and T. Hoermann, 2009, "Nanotechnology in Food and Packaging: Where are we now and where will we go?", *Nano The Magazine for Small Science*, no. 13, pp. 028-030.
11. D.R. Paul and L.M. Robeson, 2008, "Polymer nanotechnology: Nanocomposites", *Polymer*, no. 49, pp. 3187-3204.
12. J.H. Koo, 2006, "*Polymer Nanocomposites: Processing, Characterization, Application*", The McGrow Hill Inc.

13. J.S. Kim. E. Kuk. K.N. Yu. J-H. Kim. S.J. Park. H.J. Lee. S.H. Kim. Y.K. Park. Y.H. Park. C-Y. Hwang. Y-K. Kim. Y-S. Lee. D.H. Jeong. and M-H. Cho, 2007, "Antimicrobial effects of silver nanoparticles", *Nanomedicine: Nanotechnology, Biology, and Medicine,* no. 3, pp. 95-101.

14. Z. Foltynowicz. V. Kočí. D. Rodewald, 2010, "Impact of chosen consumer products containing nanosilver on microorganisms", in: Wybieralska K. (ed.), *Current Trends in Commodity Science. Selected Quality Problems*, Poznan University of Economics, no. 160, pp. 29-36.

15. B. Leoci. S. Massari, 2003, "Nano-Scale Sciences and Nano-Technology: a New Role for Commodity Sciences?", *Journal of Commodity Science*, no. 42 (4), pp. 205-216.

16. RNCOS, 2013, *Nanotechnology Market Outlook 2014*, Report, RNCOS Industry Research Solutions, May 2013.

17. *European Pharmacopoeia 6.0*, Council of Europe, European Pharmacopoeia Commission, 2007.

# Evaluation of Opening Status of PTPs with Three Elements from Push to Go Out from Package

**Kiyoshi Kubota[1*], Masaki Takeda[2], Mikio Murata[3], Kiyomi Sadamoto[3]**

[1] *Daiichi-Sankyo Co., Ltd., Japan*
[2] *Sumitomo Bakelite Co., Ltd., Japan*
[3] *Yokohama College of Pharmacy, Japan*

[*] *Corresponding author. Email: kubota.kiyoshi.f7@daiichisankyo.co.jp*

**Abstract:** In the pharmaceutical packaging, we think the opening characteristics to be extremely important to greatly influence the taking medicine compliance of the patient.We showed that the difference of opening status depend on various PTPs, and the factors which affect the opening status. So we analyze the mechanism of these results with several factors such as material, structure, and balance of fractional void. To analyze the difficulty of opening PTPs, considering all procedure of opening PTPs, and set the three step factors such as push, break aluminum, and go out pill from packages.These steps have following relations for PTP characteristics.

Step1. Until transforming a pocket and beginning to push the pill :
Dimension of pocket, rigidity of pocket's material, difference between pocket's height and thickness of pill, thickness of the top of pocket
Step2. Until breaking aluminum film:
Thickness and tenacity of aluminum film, thickness at the corner of pocket
Step3. Until going out pill :
Having stress-relaxation or not after breaking aluminum, smoothly discharging or not

We should pay attention to these different factors to establish most suitable PTP opening characteristics in the situation that materials or the shape of the PTP pockets were limited. And we devised the method which calculating the area of the radar chart comprised of the sensuality evaluation score of 3 steps as a method to express these elements in one substitute property value. We named this method "The PTP Opening Texture".
After evaluating the sample which slightly varied in the molding condition by "The PTP Opening Texture", we knew that we could detect the standards of the parameter functionally.

Keywords: PTP, opening status; NRS(Numeric Rating Scale), raider chart, Opening Texture.

## 1 Introduction

To design the PTP in response to the cause of the phenomenon such as patient (RA with the finger handicap, single paralysis) , cannot open PTP[1),2)], It is necessary for us to pay much attention. We studied opening characteristics of the PTP[3)] so far, but there were the following problems.

1. It is hard to predict the use characteristics of the patient with the handicap from the sensuality test result by the physically unimpaired person.
2. When the patients themself with the handicap perform a sensuality examination, the detectability of problem product rises, but the reliability of the rating falls.
3. Therefore correlation analysis with the elements of the rating-based PTP (extraction of problematic factors in PTP) becomes difficult.
4. The difficulty of taking of the tablet is not same with every product. For example, difficulty in transformation of pocket, in breaking aluminum foil, in pushing out.

We divided a process to pick up a tablet from PTP and thought about evaluating sensuality by each step. As a method to express the totally opening status, we made a radar chart with each rating and thought about calculating the area.

## 2 Objective and methods

### 2.1 Calculation method of the rating using the radar chart

We divide the step before a tablet being taken out from PTP into following three steps. Panelist acquires a score by sensuality evaluation by each step in reference to table 1. We write three angles radar chart (Fig.1) with three provided score, and calculate the inside area by equation (1). Figure 2 is obtained by every case, and by maximum area (32.5; a, b, c=5,5,5) convert them into ten phases of score to obtain Figure 3.
The means of ten phases of score as totally opening status is shown in Figure 4.

Step1. Until transforming a pocket and beginning to push the pill : A-axis, NRS score is “a”
Step2. Until breaking aluminum film: B-axis, NRS score is “b”
Step3. Until going out pill : C-axis, NRS score is “c”

**Table 1:** NRS (Numeric Rating Scale) of each step

| | Cannot | Very difficult to | Slightly difficult to | Not to be (difficult, easy ) | Slightly easy to | Very easy to |
|---|---|---|---|---|---|---|
| Step.1 transform a pocket and start to push the pill | 0 | 1 | 2 | 3 | 4 | 5 |
| Step.2 transform a pocket till breaking aluminum foil | 0 | 1 | 2 | 3 | 4 | 5 |
| Step.3 pick out a tablet from PTP’s pocket | 0 | 1 | 2 | 3 | 4 | 5 |

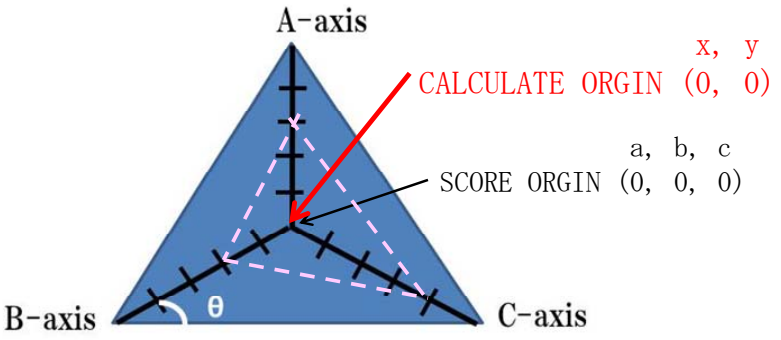



**Figure1**: Three angle radar chart

Calculating formula of the triangle area= ½×ABS[(-0.866b×(-a-0.5c))-(-a-0.500b)×0.866c)] (1)

NRS A-axis=a, NRS B-axis=b, NRS C-axis=c
Coordinate of A=(0, a), B=(-0.886b, -0.5b), C=(0.866c, -0.5C)

| a= | 5 | | | | | | 4 | | | | | |
|---|---|---|---|---|---|---|---|---|---|---|---|---|
| b＼c | 5 | 4 | 3 | 2 | 1 | 0 | 5 | 4 | 3 | 2 | 1 | 0 |
| 5 | 32.5 | 28.5 | 24.1 | 19.8 | 15.4 | 11.1 | 28.5 | 24.5 | 20.6 | 16.7 | 12.8 | 8.9 |
| 4 | 28.4 | 24.5 | 20.6 | 16.7 | 12.8 | 8.9 | 24.5 | 21.0 | 17.5 | 14.1 | 10.6 | 7.1 |
| 3 | 24.0 | 20.6 | 17.1 | 13.6 | 10.1 | 6.6 | 20.5 | 17.5 | 14.5 | 11.4 | 8.4 | 5.3 |
| 2 | 19.6 | 16.6 | 13.6 | 10.5 | 7.5 | 4.4 | 16.6 | 14.0 | 11.4 | 8.8 | 6.2 | 3.5 |
| 1 | 15.2 | 12.6 | 10.0 | 7.4 | 4.8 | 2.2 | 12.6 | 10.5 | 8.3 | 6.1 | 3.9 | 1.8 |
| 0 | 10.8 | 8.7 | 6.5 | 4.3 | 2.2 | 0.0 | 8.7 | 6.9 | 5.2 | 3.5 | 1.7 | 0.0 |

| a= | 3 | | | | | | 2 | | | | | |
|---|---|---|---|---|---|---|---|---|---|---|---|---|
| b＼c | 5 | 4 | 3 | 2 | 1 | 0 | 5 | 4 | 3 | 2 | 1 | 0 |
| 5 | 24.1 | 20.6 | 17.1 | 13.6 | 10.1 | 6.6 | 19.7 | 13.2 | 13.6 | 10.5 | 7.5 | 4.4 |
| 4 | 20.6 | 17.5 | 14.5 | 11.4 | 8.4 | 5.3 | 16.6 | 14.0 | 11.4 | 8.8 | 6.2 | 3.5 |
| 3 | 17.1 | 14.4 | 11.8 | 9.2 | 6.6 | 4.0 | 13.6 | 11.4 | 9.2 | 7.0 | 4.8 | 2.7 |
| 2 | 13.5 | 11.4 | 9.2 | 7.0 | 4.8 | 2.7 | 10.5 | 8.7 | 7.0 | 5.3 | 3.5 | 1.8 |
| 1 | 10.0 | 8.3 | 6.5 | 4.8 | 3.1 | 0.0 | 7.4 | 6.1 | 4.8 | 3.5 | 2.2 | 0.9 |
| 0 | 6.5 | 5.2 | 3.9 | 2.6 | 1.3 | 0.0 | 4.3 | 3.5 | 2.6 | 1.7 | 0.9 | 0.0 |

| a= | 1 | | | | | | 0 | | | | | |
|---|---|---|---|---|---|---|---|---|---|---|---|---|
| b＼c | 5 | 4 | 3 | 2 | 1 | 0 | 5 | 4 | 3 | 2 | 1 | 0 |
| 5 | 15.3 | 12.7 | 10.1 | 7.5 | 4.8 | 2.2 | 11.0 | 8.8 | 6.6 | 4.4 | 2.2 | 0.0 |
| 4 | 12.7 | 10.5 | 8.3 | 6.1 | 4.0 | 1.8 | 8.8 | 7.0 | 5.3 | 3.5 | 1.8 | 0.0 |
| 3 | 10.1 | 8.3 | 6.6 | 4.8 | 3.1 | 1.3 | 6.6 | 5.3 | 3.9 | 2.6 | 1.3 | 0.0 |
| 2 | 7.4 | 6.1 | 4.8 | 3.5 | 2.2 | 0.9 | 4.4 | 3.5 | 2.6 | 1.8 | 0.9 | 0.0 |
| 1 | 4.8 | 3.9 | 3.1 | 2.2 | 1.3 | 0.4 | 2.2 | 1.8 | 1.3 | 0.9 | 0.4 | 0.0 |
| 0 | 2.2 | 1.7 | 1.3 | 0.9 | 0.4 | 0.0 | 0.0 | 0.0 | 0.0 | 0.0 | 0.0 | 0.0 |

**Figure 2**: Inside area calculated by NRS of each step

| a= | 5 | | | | | | 4 | | | | | | 3 | | | | | |
|---|---|---|---|---|---|---|---|---|---|---|---|---|---|---|---|---|---|---|
| b＼c | 5 | 4 | 3 | 2 | 1 | 0 | 5 | 4 | 3 | 2 | 1 | 0 | 5 | 4 | 3 | 2 | 1 | 0 |
| 5 | 10 | 9 | 7 | 6 | 5 | 3 | 9 | 7 | 6 | 5 | 4 | 3 | 7 | 6 | 5 | 4 | 3 | 2 |
| 4 | 9 | 7 | 6 | 5 | 4 | 3 | 7 | 6 | 5 | 4 | 3 | 2 | 6 | 5 | 4 | 3 | 3 | 2 |
| 3 | 7 | 6 | 5 | 4 | 3 | 2 | 6 | 5 | 4 | 3 | 3 | 2 | 5 | 4 | 4 | 3 | 2 | 1 |
| 2 | 6 | 5 | 4 | 3 | 2 | 1 | 5 | 4 | 3 | 3 | 2 | 1 | 4 | 3 | 3 | 2 | 1 | 1 |
| 1 | 5 | 4 | 3 | 2 | 1 | 1 | 4 | 3 | 3 | 2 | 1 | 1 | 3 | 3 | 2 | 1 | 1 | 0 |
| 0 | 3 | 3 | 2 | 1 | 1 | 0 | 3 | 2 | 2 | 1 | 1 | 0 | 2 | 2 | 1 | 1 | 0 | 0 |
| a= | 2 | | | | | | 1 | | | | | | 0 | | | | | |
| b＼c | 5 | 4 | 3 | 2 | 1 | 0 | 5 | 4 | 3 | 2 | 1 | 0 | 5 | 4 | 3 | 2 | 1 | 0 |
| 5 | 6 | 4 | 4 | 3 | 2 | 1 | 5 | 4 | 3 | 2 | 1 | 1 | 3 | 3 | 2 | 1 | 1 | 0 |
| 4 | 5 | 4 | 3 | 3 | 2 | 1 | 4 | 3 | 3 | 2 | 1 | 1 | 3 | 2 | 2 | 1 | 0 | 0 |
| 3 | 4 | 3 | 3 | 2 | 1 | 1 | 3 | 3 | 2 | 1 | 1 | 0 | 2 | 2 | 1 | 1 | 0 | 0 |
| 2 | 3 | 3 | 2 | 2 | 1 | 1 | 2 | 2 | 1 | 1 | 1 | 0 | 1 | 1 | 1 | 1 | 0 | 0 |
| 1 | 2 | 2 | 1 | 1 | 1 | 0 | 1 | 1 | 1 | 1 | 0 | 0 | 1 | 1 | 0 | 0 | 0 | 0 |
| 0 | 1 | 1 | 1 | 1 | 0 | 0 | 1 | 1 | 0 | 0 | 0 | 0 | 0 | 0 | 0 | 0 | 0 | 0 |

**Figure 3**: Ten phases of score as totally opening status

| Score | | level of opening status |
|---|---|---|
| 0 | : | cannot open |
| 1, 2 | : | very difficult to open |
| 3, 4 | : | slightly difficult to open |
| 5, 6 | : | not to be difficult, not to be easy to open |
| 7, 8 | : | slightly easy to open |
| 9, 10 | : | very easy to open |

**Figure 4**: Level of opening status

### 2.2 Relation with each step's score (a, b, c) and PTP properties

The score of each step is connected directly with PTP properties. Therefore the faults of the product (the points that must be improved) become clear from these scores.

**A-axis: Until transform a pocket and begin to push the drug**

(1)A pocket shape influences to "a", if diameter is small generate a big point pressure.
(2)The thickness of top & corner of pocket and hardness of film are influence a value of "a" .
: The stress to a finger is decided by the rigidity of pocket and concentration of the pressure points.
(3)Height porosity [difference of the pocket's height between the tablet's thickness] influences the degree of transformation of pocket. If a height Porosity is big, big transformation of pocket is necessary.

**B-axis: Until finish to break aluminum foil**

(1)In this step we need the force to transform the pocket and break the aluminum foil .
So, in addition to the factors same as A-axis, easiness of tear of the aluminum is important.
(2)It depend on the thickness and tenacity of the aluminum foil.
: If there is relaxation of the stress just after aluminum was broken , the burden to panelist's finger lightens and becomes easy to push. It is very important functionally.

**C-axis: Until pick out a tablet (capsule)**

(1) In this step the transformed pocket puts a drug , broken aluminum foil obstructs smooth discharge.
(2) Porosity and hardness of film (pocket, aluminum) are influence a value of "c" .
: The characteristic that tablet is exhausted smoothly is the most important to the panelist who has small pinch power (like RA patients) .

### 2.3 The experiment using PTP Opening Texture

We evaluated the samples which were manufactured experimentally under the limited condition.
Figure 5 shows PTP parameters in this experiment, and Figure 6 shows the pushing out characteristics of the tablet which were measured by load sell. These samples were manufactured from the same material, same mould and same tablet. However, we change only the moulding conditions of the Brister machine and changed the height and the wall thickness of the pockets to 3 levels.
The result that performed the sensuality examination about these samples is Figure 7. The properties of PTP were reflected to the each step's score and the difference about the totally opening status was recognized.

| | Height of Pocket | Thickness the corner of Pocket | [Common] Condition |
|---|---|---|---|
| TA | 3.4 mm | 0.19 mm | ▪Shape of tablet [Same Products]<br>▪Diameter of Pocket [Same Mold]<br>▪Same Material PVDC/PVC 330μm |
| TB | 4.6 mm | 0.15 mm | |
| TC | 5.2 mm | 0.10 mm | |

**Figure 5**: Samples' properties for the Sensory Evaluation by the "PTP Opening Texture"

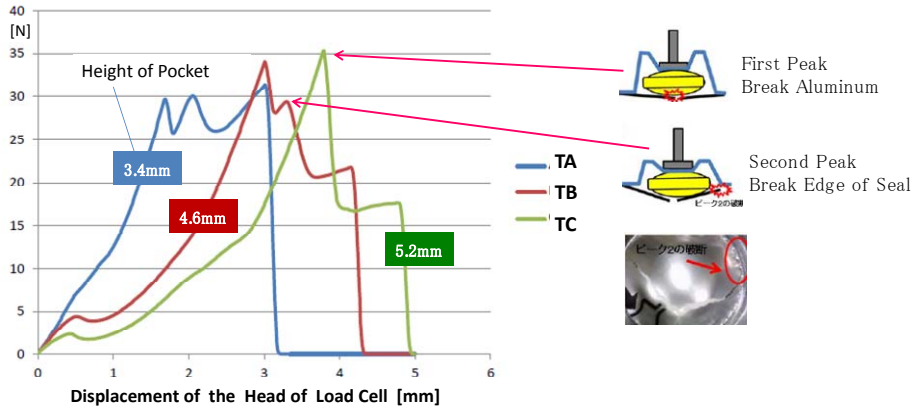



**Figure 6**: Profile of force measured with the load cell during pushing out the tablet

| | a ; A-axis | b : B-axis | c : C-axis | Texture NRS |
|---|---|---|---|---|
| TA | 2 | 4 | 4 | 4 |
| TB | 3 | 5 | 2 | 4 |
| TC | 4 | 5 | 3 | 6 |

**Figure 7**: NRS of each step and totally opening status

## 3 Conclusions

- We can evaluate easiness (or difficulty) of pick off of the tablet from pocket by using Texture NRS, and three elements [a, b, c Score] shows the improvement points of the PTP.
- When we must use hard film to secure the quality of pharmaceutical products, by the molding condition of the pocket, opening characteristics of the tablet can be improved.
- When a PTP characteristics is decided in plural limitations, the method to calculate the area of the radar chart is useful to find the level of opening status.

## References


1. 1. Kiyomi Sadamoto, et al “The effect of pinch strength to the ability of opening medical package in patient with Rheumatoid Arthritis” Human Engineering Vol. 48, No4 204-206 (2012)
2. Masaru Mizoguchi, Takaharu Sadamoto, Kiyoshi Kubota, Takahiro Yamanouchi, Kiyomi Sadamoto
3. “Useful evidence of pinch power for evaluation of opening PTP in patients with Rheumatoid Arthritis” IAPRI abstract 8-9 2012
4. Kiyomi Sadamoto, Kiyoshi Kubota, Masaru Mizoguchi “Study the opening status of PTP ; Considering
5. differences in various PTP” IAPRI 268-274 2013

# PACKAGING DESIGN, ERGONOMICS & HUMAN FACTORS

# The study of uncertainty elements related to heat seal strength by comparison of standard testing methods

Chana Yiangkamolsing[1*] and Kazuo Hishinuma[2]

[1]*Department of Industrial Engineering, The University of The Thai Chamber of Commerce, Thailand*

[2] *HISHINUMA CONSULTING ENGINEER OFFICE, Japan*

**Corresponding author. Email: chana99@hotmail.com*

**Abstract:** The heat seal technique has been widely used in packaging applications as a plastic packaging material for several decades. The expected functions of heat sealing are package integrity/sealing and opening. Heat seal strength has to balance these two opposing factors; namely, opening and package integrity/sealing. ASTM F88-** attempts this by using the heat seal control.[1] Heat seal strength testing is made from specimens of a certain size, and then heat seal strength is measured by the tension tester. There is “inconsistent expression” (transversely) in the heat seal strength measurement as follows.

1) There is an approximation of heat seal strength value.
2) Results of heat seal strength value and temperature value are inconsistent in all testing at any temperature values.

The cause of inconsistent heat seal strength can be explained by applying the definitions of “heating temperature” and “heating time”. The original definitions of testing methodology were defined by ASTM and JIS standard [1,2], but the new definitions differ from the ASTM and JIS standards. These definitions changed to “Heating speed” which greatly influenced the measurement of heat sealing strength and was discovered two years ago. (“Hishinuma Effect”) [3,4] It is understood that the “Hishinuma Effect” makes a great difference to the heat seal information. We are deriving 17 categories and 65 items which are the cause of "Uncertainty element" which obfuscates the crossing of the heat seal characteristic.[5] They are reported in this paper based on the examination and the action plan of the influence of “Hishinuma Effect" on "Uncertainty".

Keywords: heat sealing, MTMS, “Hishinuma Effect”, sealing, opening, closing, heating temperature, heating time.

## 1 Introduction

Heat seal technology is one method for developing polymer material. Two plastic sheets are bonded by heating them up and cooling them down in the heat sealing process. The Heat seal technique is very important for food and drug packaging manufacture. Originally, the expected function of heat sealing was sealing or package integrity. Today, many consumers are concerned about easy opening and food safety from packaging. They face difficulty in opening packages and improvements from the manufacturers. Hence, heat sealing needs to deliver both package integrity/sealing and ease of opening. Heat sealing needs to balance both an opening and sealing performance.[ 6,7]

Currently there are many conventional testing methods widely used for testing seal strength such as JIS Z 0238 and ASTM F88-** and their references. Mentioned standards are destructive tests for tensile strength of completed products and specimens.[1,2] The contents of JIS Z 0238 specific on not only the standard test for seal strength, bursting, falling, pressure resistance, and leakage but also recommendation for reference value of heat seal strength in many applications. Heat sealing is important not only to plastic bags but also to other thermoplastic packaging. The relationship between LDPE-coated paper and heat seal strength was studied. The

variation of seal strength is explained by surface oxidation which is also the cause of heat seal strength deterioration and enhancement.[9] Heat seal strength is also applied with an ultrasonic sealing machine. Scanning Electron Microscope (SEM) was used to detect pinpoint and seal defect.[10] C-scan of ultrasonic SEM and optical microscopic images provide ultrasonic heal sealing. Non-uniform heat seal temperature, pressure, time, misalignment of heat jaws or non-parallel sealing were parameters for unstable ultrasonic sealing. Finite Element Analysis was used to predict interfacial temperature corresponding with heating time during sealing.[11] If we can take precise information of seal strength phenomena, the model will be more high accurate. However, it has not revealed the heat seal phenomenon, it is very important for more accurate model

The main contents of ASTM F88 standard are describe on apparatus for measuring, holding methods, sampling methods, aging, and procedures for seal strength measurement, and an average seal strength calculation. Many failure modes are described in this standard. ASTM F88 and other standards are not designed to control seal, nor package opening. They are simply a method to seal and measure peeling force for packages. The virtue of a norm is its repeatability and data comparison among their users. Although F88 does not specify a temperature measurement location, this is part of method's uncertainty. Both standards cannot guarantee the reliability of functions of heat sealing, because they do not cover a lot of validation methodologies expected of the heat sealing. However, both standards cannot guarantee the reliability of functions of heat sealing. The function design of heat sealing can be designed by analyzing a precise heat sealing strength. Crystalline structure is also a factor that affects seal strength. It is known that the distribution of molecular weight of a finished film and the seat changes easily on the condition in the manufacturing process.[8]

**M**easuring **T**emperature of **M**elting **S**urface (MTMS) is used for predicting the strongest peelable seal, also for analyzing an advanced heat seal testing. Temperature at the Interfacial surfaces is measured by using the small temperature sensor. Temperature response is plotted by computer software. The inflection point or fusion point is identified. The inflection point is the changing state from the solid to melting state of material surface.[12] the boundary temperature between peeling seal and tearing seal can be identified by using MTMS. Tensile strength profile making begins with testing a method for heating temperature corresponded with seal strength as following steps. This first step is used to explain and analyze a defection point or a fusion point of thermoplastic material and its seal strength. Special materials with special design of melting point were used by the authors. Secondly, prepare samples in a proper dimension and test heat seal strength measurement. Thirdly, use the method for testing elements related to heating seal analysis. Fourthly, set guide- lines for manufacturers by considering results from the analysis of their functions. Finally, present a feasible solution for manufacturers to apply it.

The cause of inconsistent heat seal strength can be explained by definition of inconsistent "heating temperature" and "heating time". As for "Heating temperature" in the heat sealing and "Time" definition, ASTM F2029 is enacted only after it becomes in 2000. These original definitions of testing methodology were defined by ASTM and JIS standard, but the new definitions "Heating speed" greatly influence the appearance of heat sealing strength profile was discovered two years ago. ("Hishinuma Effect") It has been understood that "Hishinuma Effect" greatly takes part in the difference of the heat seal information.

In this paper, we are deriving 17 categories including 65 items of "Uncertainty element" leads to obstruct the inconsistency of the heat seal characteristic. This report is based on the examination and the action plan of the influence of "Hishinuma Effect" on "Uncertainty" in this paper. Details of "Hishinuma Effect" will be reported in another reference paper. This paper begins with state of the art heat sealing technology, the current state of heat sealing technique, and the definition of temperature control. It also discusses the novelty of "uncertainty elements" which affects the accuracy and reliability of heat seal strength, the outline of "Hishinuma Effect", the MTMS technique, and a conclusion with application.

## 2 State of the art heat sealing technology

### 2.1 The current state of heat seal technique

"Temperature", "Time", and "Pressure" have been handled as the main control elements of heat sealing strength so far. However, these definitions of these three elements were vague resulting from the regulations among different standards. Therefore, the same result of a measurement was difficult to achieve, and there were a lot of problems in the crossing of heat sealing strength for the same specimen. As a result, it will overemphasize it to the use of the tear seal region of heat sealing strength that does not consider the peel seal region. Coexisting of "Openability" and "Closability" that ASTM F88-** (1968 enactments), a worldwide standard of the examination method of the heat sealing expects of the heat seal technique, has not been achieved today.

Heat seal strength testing is made from a specimen of certain size, and then heat seal strength is measured by tension tester as mentioned in the standards. Preparing specimens are similar in every standard but results may different. Dimension, thickness, and material of a specimen effect to elongation of heat seal. If we consider during pulling specimen, it is purposely ensure that tearing does not occur randomly on the leg of specimen, and pulling forces of tensile testing is only applied at the sealed area. On the other hands, there are major problems with the inconsistence of the heat seal strength measurement as follow.

1) There is an approximation of heat seal strength value during testing.
2) The result of heat seal strength value and temperature value and does not correspond in each temperature value. Heat seal strength should not be much different in every testing.

### 2.2 Removal of "Uncertainty element" that rules heat sealing

The maximum expectation of the heat seal technique is the development of coexisting about "Openability" and "Closability". The conflicting result of the component related to this problem was shown in **Figure 1.** [7]

Using proper heating in the sealing process can guarantee both Openability and Closability of a package. It can succeed by only managing melting surface temperature or interfacial temperature control. Proper heating control can reduce a pinhole, “polyball “, and tuck in the heat sealing process. To achieve proper heating, it needs to add the mechanism analysis result of the cross-relationship of each component. It is possible to confirm that the thread guide position of specimens is also important. It is discuss later.

To these certain achievement, we need to understanding following requirements.

①The adhesive quality of the plastics material (heat seal characteristic) is individually understood.

②It is necessary to confirm whether the function that the selected material expects it for commercialization can be demonstrated.

③The effective utilization of peel sealing can guarantee heat seal problem such as tuck, “polyball”, tearing.

④" Hishinuma Effect " has exerted a big influence within the range of the heating temperature of the peeling seal. Therefore, it is necessary to understand the heating way of the object in the process exactly.

### 2.3 Uncertainty elements effect to heat sealing and related elements of “Hishinuma Effect”

Each analysis should also competently understand the appearance characteristic of Heat sealing strength.

"Uncertainty element" - related to the heat seal characteristic was enumerated, and the result (outline) of the impact statement to the difference of heat sealing strength was shown in **Table 1.** (The display of research results of the correspondence of each item of JIS, ASTM, each maker, and “MTMS" was omitted.)

### 2.4 Difference of heat seal strength appearance by how to put material

To make heat seal strength highly reliable, the position of specimen on a heating jaw during the heat sealing process needs to be controlled. The position of specimen on the heat jaw can be of two types. It is called the A mode heating and the B mode heating as shown in **Figure 2.**

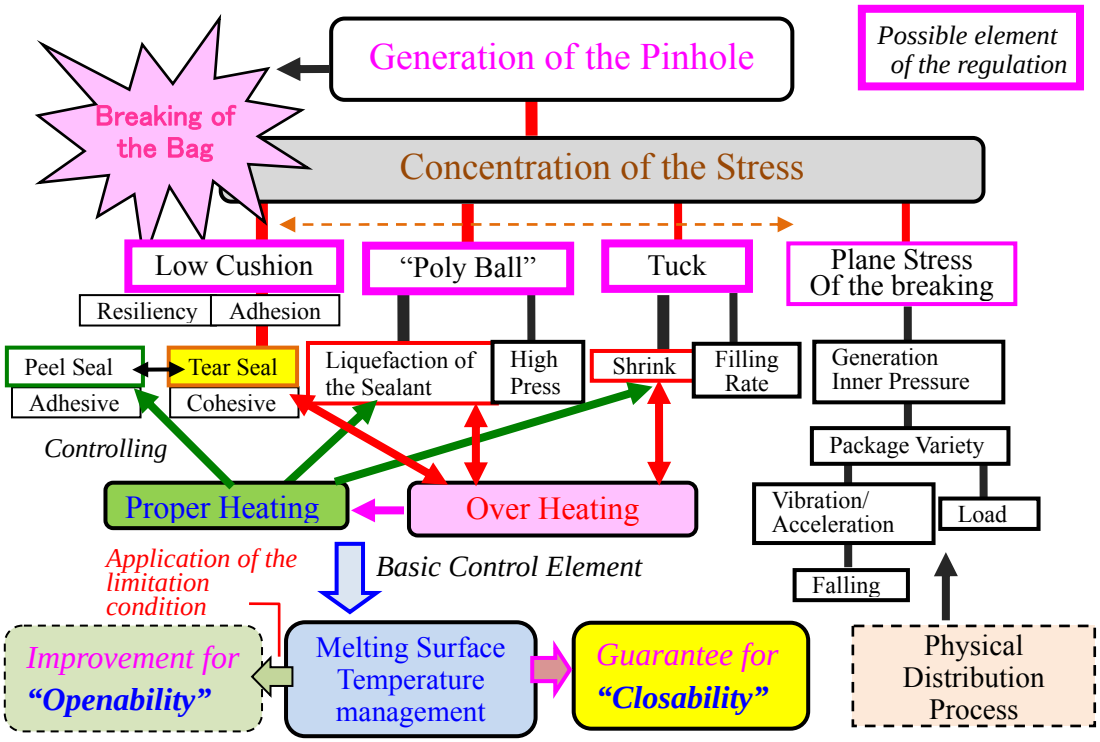



**Figure 1:** The control of Closability and generation analysis of mechanism of breaking the bag by "The Multi Complex Analysis"

The heat flow rate from a high temperature area passes through a low temperature area. In mode A, heat transfers to both sides of a non-heating surface whereas in mode B, heat transfers to only one side of non-heating surface. The interfacial temperature of mode B is slightly higher than the interfacial of mode A because heat transfer only one side from seal area to circumstances along material direction, and the another edge of seal area, temperature is building up. When we consider a peel seal zone, higher temperature leads to higher heat seal strength. It is recommended to use the B mode heating to make heat seal strongest and more reliable. If the specimen of mode A heating slightly moves either left or right, the heat seal strength is also changed slightly.

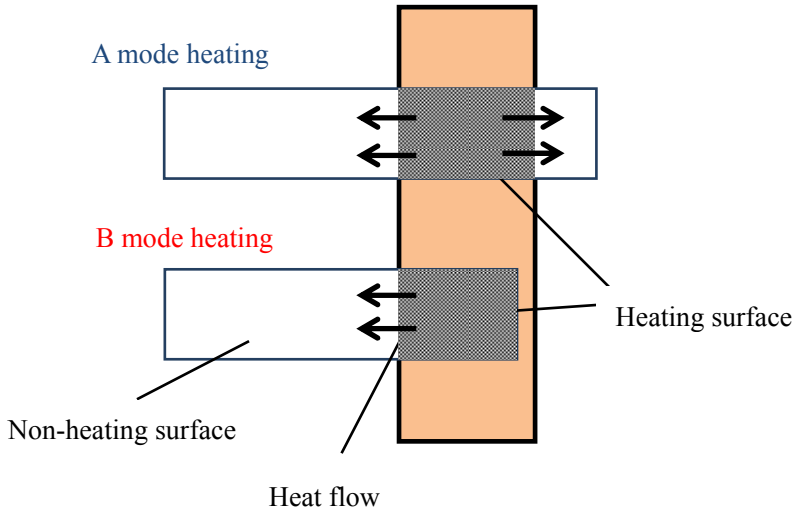



**Figure 2:** Specimen with position control during heat sealing process

**Table 1:** The uncertainty elements related to the appearance of heat seal strength
(The addition of " Hishinuma Effect " )
●; Big Influence Items, [H-e];"Hishinuma Effect" Influence Level : ★ ; Negative, ☆ ; Positive

| Object Items | Influence level | Influence level of H-e |
|---|---|---|
| 1. ≪Temperature≫ | ● | |
| (1) Selection of temperature adjustment point | ★★★ | |
| (2)Surface temperature of heated block | ☆☆ | |
| (3)Melting surface temperature | ☆☆☆ | ※ |
| (4)Equilibrium temperature | ☆ | ※ |
| (5)CUT | ☆ | ※ |
| (6) Transition temperature | ☆☆ | ※ |
| (7)Heating spots | ★ | |
| 1)Abiogenesis | ☆☆ | ※ |
| 2)Device originating | ★★ | ※ |
| 2. ≪Time≫ | ● | |
| (1)Arrival time to equilibrium temp | ★ | ※ |
| (2)CUT | ☆ | ※ |
| (3)Intermittent operation time | ★ | ※ |
| (4)Transition time | ☆ | ※※ |
| **(5)"Heating speed"** | ☆☆☆ | ※※ |
| 3. ≪Pressure≫ | ● | |
| (1)Non-management | ★ | ※※ |
| (2) 0.1－0.3 MPa | ☆ | |
| (3) ＜0.08 | ★★★ | ※ |
| (4) ＞0.4 | ★★ | |
| (5)Abiogenesis | | |
| 1) No uniformity of gap(horizontal) | ★★ | ※ |
| 2) No uniformity of gap(Depth) | ★★ | ※ |
| 4. ≪Heating way≫ | | |
| (1) Outside heating | ● | |
| 1)Two sided same temperature heating | ☆☆ | ※※ |
| 2)One sided heating | ★★ | ※※※ |
| (2) Internal heat generation | ● | |
| 1) two side | ☆ | ※※ |
| 2) One side | ★★ | ※※※ |
| 5. ≪Heating ability≫ | | |
| (1) Output of heat source | ★★ | ※ |
| (2) Thermal capacity of heated block | ★★ | ※ |
| (3) Thermal conduction of heated block | ★ | ※ |
| 6. ≪Size of heating Specimen≫ | ● | |
| (1) 15 ㎜ | ★ | |
| (2) 20 ㎜ | ☆ | |
| (3) 40 ㎜ | ☆☆ | ※ |
| (4) ＜15 ㎜ | ☆ | ※ |
| 7.≪Size adj. of specimen≫ | ● | |
| (1)15 ㎜ | ☆ | |
| (2) Measurement in the vicinity of 15 ㎜ | ☆☆ | |
| (3) 25.4 ㎜ | ★ | |
| (4) 5－10 ㎜ | ☆ | |

| Object Items | Influence level | Influence level of H-e |
|---|---|---|
| 8.≪Distance of tensile test≫ | ● | |
| (1) Over 100 ㎜ | ★★ | |
| (2) 20－40 ㎜ | ☆☆ | |
| 9.≪Reinforcement for tensile test ≫ | ● | |
| (1) non | ★★ | |
| (2)Reinforcement | ☆☆ | |
| 10. ≪Selection of speed of tensile test≫ | ● | |
| (1)100 ㎜／min. | ☆ | |
| (2)300 ㎜／min. | ★ | |
| 11.≪Extraction method of tensile test≫ | ● | |
| (1) maximum value | ★★ | |
| (2)Mean value | ★★ | |
| (3)Each mode | ☆☆ | |
| 12.≪Cover material≫ | ● | |
| (1) Non | ☆☆ | |
| (2) Flat Teflon | ☆☆ | |
| (3) Soaking of Teflon in the glass Wool | ★★ | |
| 13.≪Thickness of material≫ | ● | |
| (1)Thin | ★★ | |
| (2)Thick | ★ | |
| 14.≪Growth rate of material≫ | | |
| (1)Big | ★★★ | |
| (2)Small | ★ | |
| 15.≪Lamination≫ | | |
| (1)Lamination strength | ★★★ | |
| (2)Difference of the expansion between lamination materials | ★★ | |
| 16.≪Consideration of peeling & tearing seal≫ | | |
| (1) Range of peeling seal | ☆☆ | ※ |
| (2) Boundary temperature | ☆☆ | ※※ |
| (3) Peeling energy | ☆☆ | ※ |
| 17. ≪ Sealing≫ | | |
| **(1) Closing** | ★★★ | |
| 1) Heat sealing strength | ★★ | ※※ |
| 2) Pinhole | ★★★ | |
| 3) Edge break | ★ | ※ |
| **(2) Opening** | ★ | |
| 1) Width of heat seal | ● | |
| 2) Heat sealing strength | ★★ | ※ |
| 3) Selection of peel sealing | ☆☆ | ※ |

●; It put on the change in each item, and this mark was put to the item with a large participation.
There are a lot of numbers of marks of items with a large influence.
☆; The difference of heat sealing strength is essentially ameliorable in the correspondence of this item.
★; This relates to both the influence and the improvement, and careful handling is required.
The phenomenon “Hishinuma Effect” of appearance of heat sealing strength greatly changing by "The heating speed" has been discovered.
＊; The sign was fixed to items that "Hishinuma effect" relates in Table 1.
Many differences of past heat seal strength can understand the situation that “Hishinuma Effect" rules.

## 2.5 Analysis of definition of temperature applied to heat sealing and the “Dwell Time”

Heating temperature and pressurizing in the heat sealing process are often executed by packaging machinery and their intermittent operation. **Figure 3** showed the typical intermittent heating method.

“Dwell time” that [ASTM F2029] defines is Action period of heating bar. Three examples (A, B& C) of the melting surface temperature response (First delay) given to action period of the representative were shown in the figure 3. Operating rate has been decided usually by user’s testing and intuition on site. Therefore, the selection of “Dwell time” is not necessarily reasonable. If the melting surface temperature response of dwell action is measured, it is reasonable and desirable. In many cases, the heating temperature is changed slightly, the heat sealing strength of a completed specimens are measured, and the heating temperature that corresponds to dwell time has been selected. In such a situation, the confirmation and the setting of "Heating speed" are difficult.

In manufacture process, normally operators adjust temperature based on temperature controller. If we consider different heat sealing machinery, it is clear that different in location of temperature sensor. This is a cause of

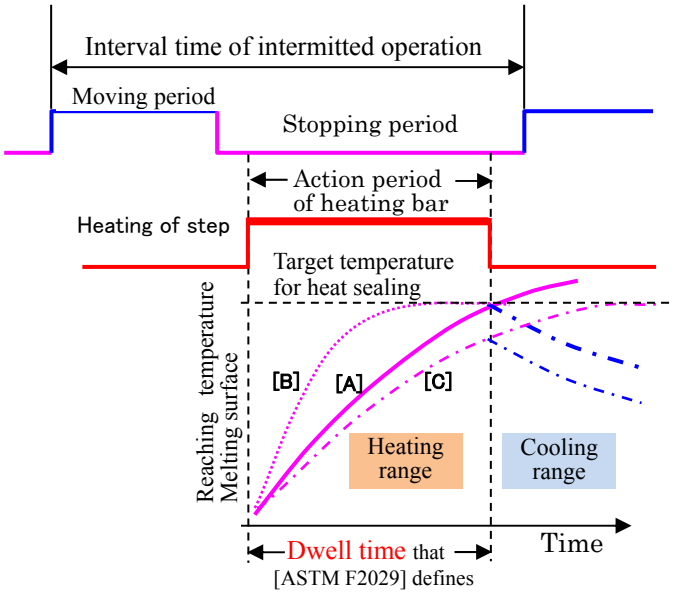



**Figure 3**: Explanation of relation between [Dwell time] and response of heating in intermittent operation.

imprecise heating temperate and it affect to heat seal strength.

There are many points of temperature measurement. The definition point of the heating temperature in two sided heating of the Jaws method includes three points.

(1) Temperature adjustment value of heated bar
(2) Surface temperature of heated bar that comes in contact with material
(3) Interfacial bonding layer temperature of material (Melting Surface Temperature)

**Figure 4** showed the definition location of temperature measurement. Point A is temperature sensor position.

Different heat sealing machines have different sensor positions. A temperature controller can control temperature around a sensor position not interfacial of thermoplastic material. Point B can be used to control interfacial temperature; we call surface temperature of heating block. If we know the characteristic of temperature response, we can control interfacial temperature by surface temperature of heat jaw. The interfacial temperature of two films can be measured by using a small sensor put between the center of material and center of heat jaws. The small sensor use only for measurement for identify interfacial temperature, but cannot use in production but in the production we use only sensor at point A and B.

The comparison of definitions of the heating temperature of the heat sealing in each standard was summarized in **Table 2.** It can be seen that different standards lead to different temperature values. The definition of heating temperature is static. However, the actual heating process is considered with time. Therefore, the dynamic transition temperature control is demanded for the temperature management at work site. Two kinds of temperature can be defined in the transition temperature roughly and separately.

(1) Equilibrium temperature of can adjustment. Normally it is temperature setting of a temperature controller.

(2) Selection of transition temperature. Transition temperature is boundary between peel seal and tear seal of two plastic sheets.

Definition of "Come up time" (CUT) is 95% of maximum temperature. **Figure 4** showed this definition. When a dynamic temperature is selected, the application of the melting surface is used for heat sealing process.

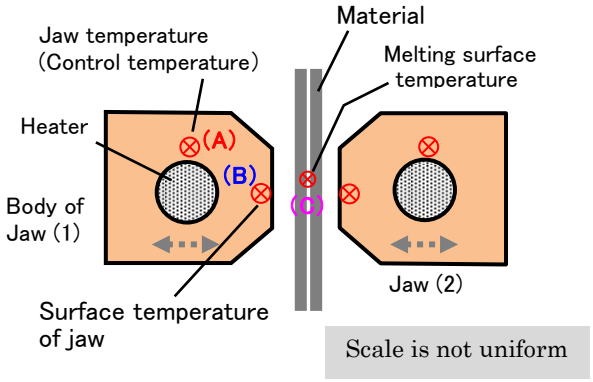



**Figure 4:** The definition with three kinds of heating temperatures

**Figure 5** illustrates heat seal strength transition due to various heating speed from arrival time 0.13 to 3.09 sec. The blue heat seal strength pattern is high heating speed (arrival time 0.13 sec) and the dark green heat seal strength pattern is low heating speed (arrival 3.09 sec). The dash line of heat seal strength means heat seal strength increase due to reinforcement by using transparent tape. If not used for reinforcement, material is elongation leading to the heat seal strength in a normal line. If used for reinforcement, material is difficult to elongation, tension force concentrates on maximum heat seal strength. The level of maximum heat seal strength increases from 17 N to 22 N (increase 5 N) because of the reinforcement. Heat seal strength above 10 N can guarantee Openability and Closability of the package.

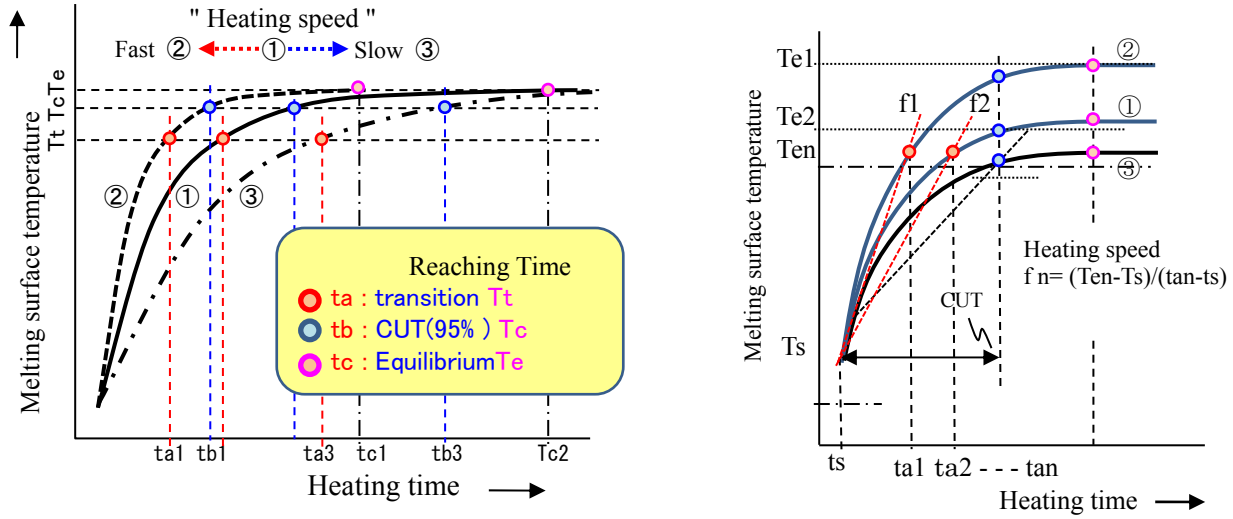
In this test, temperature control in high accuracy based on **Table 1** becomes indispensable. The melting surface temperature method is actually controlled in the experiment and laboratory. The service condition of a real machine is set from a simultaneous result of a measurement of the melting surface temperature and the surface temperature of the heated body of an actual material. [12][13][14]

## 2.6 Definition of "Come up time" (CUT) and introducing "Hishinuma Effect"

Definition of "Come up time" (CUT) is 95% of maximum temperature. **Figure 5** showed their definition.

**Table 2:** Measuring method of Heat Sealing strength of the standards

| | Candidate part Temperature accuracy(℃) | Interval (℃) | Heating Time for Testing (s) | Adaptation pressure (MPa) | Measurement-Points with heat seal Strength |
|---|---|---|---|---|---|
| **ASTM F2029** | [A]Point of Fig.3 Control temperature of the heating bar Accuracy :±1℃ | 5～10 | (1)Equilibrium: 1-10<br>(2)Transient:<br>～25μm; 0.5<br>25～64μm; 1.0 | 0.138～0.413 (20－60psi) | Non- regulation |
| **F88-**** | Non- regulation | Non-regulation | Non- regulation | Non-regulation | Average of 10～80% |
| **ISO 17557** | [A] Control temperature of the heating bar Non- regulation | 5 Inter-polates. | (Equilibrium) : 1.0 | 0.2 | (Unclear) |
| **JIS Z 0238** | Non- regulation | Non-regulation | Non- regulation | Non-regulation | Max. Value |
| **Catalog data of maker** | [A] Control temperature of the heating bar (Unclear) | 5 | Equilibrium: 0.5,1.0,3.0s ･･･ | 0.1～0.4 | (Unclear) |
| "MTMS" (Proposal of Author) | [B] Point of Fig.3 Surface Temperature [C] Point of Fig.3 Melting surface Temp. Accuracy :±0.1℃ | 0.2～2 | (1)Reaching Time to (- 0.1℃)<br>(2) direct Instrument of transient | 0.1～0.25 | Center of Sealing Plane or Max. heating point |




(a) Definition with three kinds of heating time when changed heating speed

(b) Definition with three kinds of heating time when changed heating temperature

**Figure 5:** Definition with three kinds of heating temperature and time

**Figure 4(a)** showed the change of the speed of the melting surface temperature response corresponding to thickness of material. **Figure 4 (b)** is a melting surface temperature response corresponding to the surface of heating bar temperature. "The heating speed" has the changing feature though CUT is almost the same even if the

heating temperature is changed by the same material. The treatment to which the same heat sealing strength appears has been done in the heating of the same temperature so far. For instance, it was believed that heat sealing strength that corresponded to every heating temperature appeared in the heating of [Tt, Tc and Te] of (a). It was assumed the one that the same heat sealing strength appears similarly for (b) in the heating of [Ten].

When a dynamic temperature is selected, the application of the melting surface is used for heat sealing process.

Then, we can obtain the new phenomenon (Hishinuma Effect) that "Heating speed" rules. “Hishinuma Effect" confirms a similar phenomenon with HDPE, LDPE, LLEPE, and CPP. It explains here as an example of the measurement result of CPP(50 $\mu$ m). **Figure 6** is a measurement example with “Hishinuma Effect" of [50 $\mu$ m ].

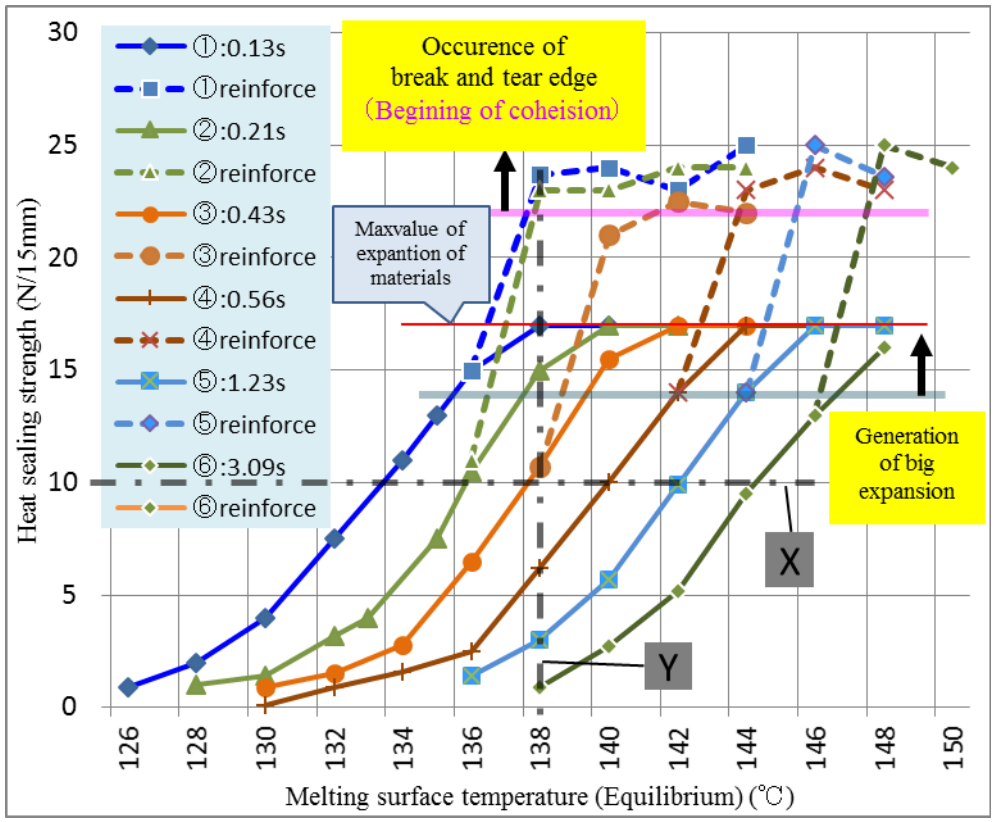



**Figure 6**: [Example of “Hishinuma Effect”];
Determination case example of the transition of the expression of heat sealing strength by "Heating Speed"( CPP; 50 μm)

These illustrates heat seal strength transition due to various heating speed from arrival time ① 0.13 to ⑥3.09 sec. The blue heat seal strength pattern is high heating speed (arrival time 0.13 sec) and the dark green heat seal strength. pattern is low heating speed(arrival 3.09 sec).The dash line of heat seal strength means heat seal strength increase due to reinforcement by using transparent tape. If not used for reinforcement, material is elongation leading to the heat seal strength in a normal line. If used for reinforcement, material is difficult to elongation, tension force concentrates on maximum heat seal strength. The level of maximum heat seal strength increases from 17N to 22N (increase 5N) because of the reinforcement. Heat seal strength above10N can quarantine Openability and Closability of the package. In this test, temperature control in high accuracy based on **Table 1** becomes indispensable. The melting surface temperature method is actually controlled in the experiment and laboratory. The service condition of a real machine is set from a simultaneous result of a measurement of the melting surface temperature and the surface temperature of the heated body of an actual material. [12][13][14]

If the influence of "Heating speed" is taken in this sample, the temperature span becomes it from 126 to 150℃. And, the heat sealing strength becomes it from 15 to about 25N/15mm. The heat sealing strength obtains a

wide-ranging result by the difference of the setting of the measurement condition. Which respect is shown and the value will show the heat sealing strength of this material very much. The cause of a poor crossing of the heat seal data is here. Data that "The heating speed" does not influence small becomes 148℃ that bonds cohesion for this material. This heat condition deviates far from the heat condition of the peeling seal.

## 2.7 Concrete analysis of "Hishinuma Effect"

Heat seal strength pattern in **Figure 6** can be assumed that it is repetitive same result when the same temperature is selected. The result shown is the same heating temperature but different arrival time; hence, heating speed has been changed. "Hishinuma Effect" was discovered as a result of controlling heating Speed accurately, and measuring appearing heat sealing strength. "Heating Speed" is easily transmutable by the cover and the heating of the Teflon seat where thickness is different from the same material. The authors confirmed "Hishinuma Effect" appearing on the heat sealing process of any thermoplastic material. **Figure 6** showed the measurement case with cast polypropylene (CPP) 50μm. The displacement of the appearance of heat sealing strength by "Heating Speed" can be understood. Melting surface temperature to constant heat sealing strength can be seen from the intersection of line X and each data inserted in **Figure 6**. "Hishinuma Effect" where the displacement of heat sealing strength to line Y and constant melting surface temperature from the intersection of each set of data is generated can be seen.

During heat jaws closing then opening, after stop heating in heat sealing process, temperature at interfacial surface is not reach to equilibrium temperature but the temperature rise is used regularly in production sites. Therefore, "Hishinuma Effect" is a major influence on the site.

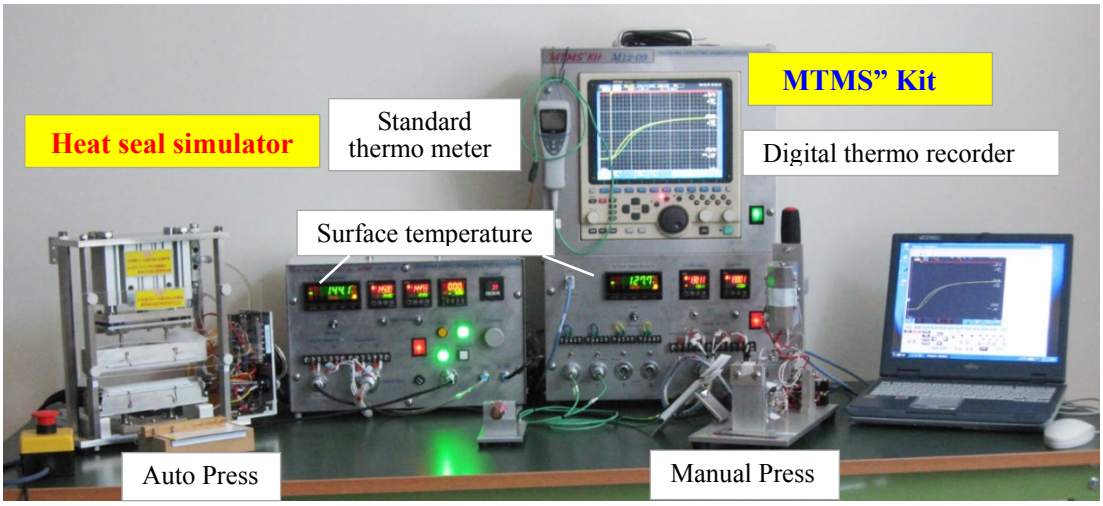



**Figure 7:** "MTMS Kit" latest Model for measurement of heat seal characteristic of High accuracy (Open to the Public)

## 2.8 Use of "MTMS" for improvement of heat sealing technique

Measurement **M**ethod for **T**emperature of **M**elting **S**urface: "MTMS" has two big features.[13][14][15]

(1)The temperature response on the bonding surface can be measured directly at high sensitivity/high speed.

(2)It is possible to apply it to the analysis of all the heat seal characteristics based on melting surface temperature data.

The mentioned experiments were conducted by using "MTMS kit" which is an indispensable tool to the definition and the measurement of heating speed. As for the latest "MTMS" kit, the "simulation unit" of the heat sealing is added to the melting surface temperature measurement unit. When various attachments are installed, the operation simulation of the production device can be done by the "MTMS" kit. **Figure 7** showed photos of the latest

“MTMS" kit. “MTMS" kit is open to the public. Thy used with five universities and numerical enterprise in several countries already.

## 3 Conclusions

### 3.1 Confirmation and measures of "Uncertainty element" that “Hishinuma Effect" rules

The heat sealing has been treated as a “Two Dimension phenomenon” with the heating temperature so far.

Because "Heating Speed" was defined by "Attainment temperature" and "Arrival time", the heat sealing was a “Three Dimension” phenomenon of "Attainment temperature" and "Arrival time".

“Arrival time” changes by the thermal capacity of the thickness and heat conduction characteristic of the material though the target heating temperature for the direct regulation.

Heat sealing strength that appears by using different thickness of material, different cover material and Heat jaw's parallel, etc. changes into the same material. “Hishinuma Effect" influences most of the appearance of the item of heat sealing strength as shown in **Table 1**. Therefore, it is necessary to change past common sense basically.

### 3.2 Application of reasonable temperature

It persists in the following matter to competent heat seal strength acquisition.

(1)The application temperature is adopted surface of the heated body temperature and melting surface temperature is adopted. [16]

(2)It provides for "Heating Speed" when measuring it.

(3)The lab data is applied to the equipment of the site referring to the melting surface temperature response.

### 3.3 Review of tension test

ASTM F88 - and JIS Z 0238, the distance is provided for 100 ㎜ or more between the tension test gripping. The tension test is precisely observed. Tensile strength will measure expansion strength of material when bonding strength exceeds expansion strength of material. The distance amplifies the influence of the expansion between long specimens gripping. [17] The current standard is not competent in the measurement of reasonable bonding strength. The authors adjusted the distance to 30 ㎜ or less between gripping, and measured if it reinforced the specimen.[18]

It resulted in a competent measurement of heat sealing strength by these measures.

### 3.4 Aggressive development of “Hishinuma Effect"

This study is used for high precise heat seal testing method which is considered with parameter of "Heating speed". “Hishinuma Effect" had exerted a big influence on past heat seal technology. When past technology is reviewed referring to the phenomenon of the new discovery, a lot of new measures can be found.

Finite Element Analysis was used to predict interfacial temperature corresponding with heating time during sealing. However, if we more understand phenomenon of heat sealing, the model can predict more accurate.

The development of the device that can be set independently within the range of Dwell time is hoped for as present measures at the heating time.

## Acknowledgements

We would like to thank every manufacturing company of packaging commodity, packaging material and packaging machinery that inform us of various problems that relate to heat sealing.

## References

1. ASTM F88-**, Standard Test Method for Seal Strength of Flexible Barrier Materials, ASTM: West Conshohoken, PA
2. JIS Z 0238, Testing Method for Heat Sealed Flexible Packaging, Japanese Standard Association, 1998

3. Hishinuma K., The discovery of the expression conversion with heat seal strength by the heating speed *Proceeding of annual meeting of the Society of packaging science & technology, Japan*, Kyoto, 2011 July7-8, pp.134-135 (Japanese)
4. Hishinuma K., "Discover of transition of appearance on the heat seal characteristic by heating velocity for plastics packaging materials -Heat sealing strength was three dimension phenomenon" *The canners journal* , 2012, vol.91,No.11, pp.21-34
5. Hishinuma K., 2013, "Examination of disagreement (non-crossing) factor of measurement value of heat sealing strength", *Proceeding of annual meeting of the Society of packaging science & technology,* Japan, Tokyo, Japan, July9-10, pp.26-27
6. Yiangkamolsing C., & Hishinuma K., Failure analysis and improvement of heat sealing testing method, *Proceeding of IAPRI world Conference*, Tianjin, China, 2010,October 13-150, pp.104
7. Hishinuma K., Analysis and simulation of opened stress mechanism on heat sealing surface, *Proceeding of IAPRI world Conference*, Tianjin, China, 2010,October 13-150, pp.201-202
8.Tsujii Tetsuya, U.S. Ishiaku, Machiko Mizoguchi, Hiroyuki Hamada, 2003, The Effect of Heat Sealing Temperature on the Properties of OPP/CPP Heat Seal Part II Mechanical Properties, *Journal of Applied Polymer Science*, Vol.99, pp. 513-519
9. Mikko Tuominen, M.Ek, P.Solaranta, M. Toivakka, J.Kuusipalo, The Effect of Frame Treatment on Surface Properties and Heat Salability of Low-Density Polyethylene Coating. *Packaging Technology and Science*, 2013;26:201-214
10. Zehra Ayhan, Seal Bond Characterization of Laminated Plastic Food Cups by Scanning electron and Optic Mictosccopes, *Packaging Technology and Science*, 2004;17:205-211
11. Prasadarao Meka,& Ferdinand C.Stehling, Heat Sealing of Semicrystalline Polymer Film. 1. Calculation and Measurement of Interfacial Temperature: Effect of Process Variables on Seal Properties. *Journal of Applied Polymer Science*, 1994, 51:89-103
12. Dinesh Aithani*, Hugh Lockhart, Rafael Auras, Krittika Tanprasert, Heat Sealing measurement by an innovative technique, *Packaging Technology and Science,* 2006, September/October, Volume 19, Issue 5, pages 245–257,
13. Hishinuma K., "Newly Technical Development for Reform of Heat Seal management", *Proceeding of IAPRI world Conference*, Michigan, USA, 2002, June23-28, pp.962-971
14. Hishinuma K., *HEAT SEALING TECHNOLOGY and ENGINEERING for PACKAGING*, DEStech Publications, USA, 2009, pp.49-70
15.Hishinum K., US Patent;6,197,136 B1,2001
16. Hishinuma K., *HEAT SEALING TECHNOLOGY and ENGINEERING for PACKAGING*, DEStech Publications, USA, 2009, pp.170-173
17. Hishinuma K., *HEAT SEALING TECHNOLOGY and ENGINEERING for PACKAGING*, DEStech Publications, USA, 2009, pp.230-231
18. Hishinuma K., *HEAT SEALING TECHNOLOGY and ENGINEERING for PACKAGING*, DEStech Publications, USA, 2009, pp.126-128

# An Empirical Study for Exploring Reusable Packaging Attributes[#]

**Ahmed Babader*, Jun Ren and Karl Kones**

*School of Engineering, Technology and Maritime Operations*
*Liverpool John Moores University, United Kingdom*

[*]*Corresponding author. Email: a.b.babader@2011.ljmu.ac.uk*

**Abstract:** Packaging systems are influenced by many elements throughout their life cycle. The environmental impact of packaging has become an issue in many counties. Much effort has been made to reduce amount of packaging going into landfill. Refillable packaging was discovered as a possible solution in term of reuse packaging; however, packaging used for secondary uses is another reuse technique to deal with packaging which needs investigation. Reusable packaging attributes are the functional characteristics of packaging to be reused as being key benefiting consumers, industries and environment. The paper seeks to address reuse as a sustainable waste route option for open loop system in packaging lifecycle. It specifically proposes to determine reusable packaging attributes in relation to consumers' orientation, to discover the packaging designers' drivers and opportunities related to the design of reusable packaging. An integrated approach is used to identify packaging attributes in literature. An empirical study was conducted to develop and test the design packaging attributes relationship with reusable packaging which identified in extant literature. Qualitative research was conducted to identify the packaging attributes from packaging used for secondary uses using questionnaire. The reusable design packaging attributes model was proposed. The model can be used to help improve the packaging sustainability performance. The model interprets 'BS En 13429:2004 reuse of packaging' standard and helps designers/manufactures in early phases of design packaging to understand the reuse of packaging requirements and procedures.

Keywords: reusable packaging; empirical study; waste packaging; reusable packaging attributes.

[#] This is the abstract of a peer-reviewed paper to appear in a Special Edition of Wiley's journal *Packaging Technology and Science* dedicated to the 19th IAPRI World Conference on Packaging 2014 hosted by Victoria University, Melbourne, Australia.

# Relationship between Peel Angle and Peel Force in Peelable Semi-Rigid Packaging Comprising Tyvek® and PETG[#]

**Javier de la Fuente[1*], Gary Burgess[2], Laura Bix[2] and Tamara Bush[2]**

[1] *Cal Poly State University, United States*
[2] *School of Packaging, Michigan State University, United States*

[*]*Corresponding author. Email: jdelafue@calpoly.edu*

**Abstract:** Testing standards such as ASTM F88 and ASTM F2824 acknowledge the effect of peel angle on peel force during package opening. Understanding the relationship between peel angle and peel force is critical to minimize people's physical effort while opening both semi-rigid and flexible packaging. However, the literature does not provide any mathematical relationship in this regard.

In order to start filling this gap, peel force measurements were collected for two test conditions (A and B) of PETG trays and Tyvek® lids at peel angles varying every 15° intervals. Test conditions had different seal geometries and peel directions. In condition A, trays were completely sealed. In condition B, trays were partially lidded and the sealed areas were comprised of two parallel rectangular areas.

Experimental data for force vs. angle for both conditions followed a U-shaped pattern with minimum values at peel angle 45°. Beyond 90° peel forces increased rapidly. Statistical analysis of the 0-90° range suggested four homogenous subsets that resulted in statistically differing forces. Classical mechanics was used to derive an equation in which peel force is a function of peel angle. Two approaches were taken to fit the data to this equation: linearization and nonlinear regression. The final equations show good agreement with experimental data.

Findings have implications for package design, usability, and peeling simulations. If materials combination and manufacturing process conditions are kept constant, the experimental data suggest that the force needed to peel off a semi-rigid package depends on two factors: peel angle and peel line width.

Keywords: peel angle; peel force; usability; peelable seal; semi-rigid packaging; package design.

Paper ID = 18

[#] This is the abstract of a peer-reviewed paper to appear in a Special Edition of Wiley's journal *Packaging Technology and Science* dedicated to the 19th IAPRI World Conference on Packaging 2014 hosted by Victoria University, Melbourne, Australia.

# A review of thermoplastic composites vapour permeability models: Applicability for barrier dispersion coatings

**Gonzalo A. Martinez-Hermosilla[1*], Behudin (Beko) Mesic[2], John E. Bronlund[1]**
[1]*School of Engineering and Advanced Technology, Massey University, New Zealand*
[2]Scion Research, New Zealand
[*]*Corresponding author. Email: G.Martinez@massey.ac.nz*

**Abstract:** One of the purposes of thermoplastic composites films and barrier dispersion coatings is to minimise the permeation of gases. In both cases, fillers and other additives are added during the film preparation to improve barrier properties. A high level of understanding has resulted from the study of the interaction between filler and polymer phases of thermoplastic composites and a number of models have been developed to predict the relative permeability of these materials. However, barrier dispersion coatings have not been modelled in this way. The aim of this review was to discuss similarities and differences of thermoplastic composites and barrier dispersion coatings that may influence the applicability of the models for barrier dispersion coatings applied to paper based materials. The models were developed as a function of the amount of fillers added in thermoplastic composites films and geometrical characteristics of the fillers such as size, thickness, shape, and the distribution of fillers in the film. Two and three dimensional models with oriented and random arrangement of fillers were presented. Due to the parallel orientation and the similar length and width of fillers used in barrier dispersion coatings, three dimensional models were more suitable to predict relative permeability. These models assumed plate or circular shaped fillers with parallel orientation. In order to prove the models, experimental information was required. Very limited data for barrier dispersion coatings with varying the amount of fillers has been reported in the literature. For this reason, further experiments are required under varied combinations of aspect ratio and the volume fraction of fillers.

Keywords: Barrier dispersion coating, thermoplastic composites, relative permeability, modelling.

## 1 Introduction

Paper based materials have limited vapour barrier properties. Several techniques have been developed to overcome this limitation, such as the inclusion of coatings/waxes or the use of secondary materials such as polymer layers. Barrier dispersion coating is one such technology, where a coating is applied on the substrate surface forming a solid barrier layer [1] to reduce the transfer rates of water vapour, water, grease and oil, various gases, and impurities [2].

Barrier dispersion coatings normally consist of mineral fillers, such as clay and talc, contained in a polymer phase applied on a substrate [3]. Both major components have an important role to play in barrier functionality; the polymer phase forms a film and the fillers improve barrier properties and assist with printability, gluability and help prevent blocking. In addition, other additives such as thickeners, dispersants or waxes can also be included [4-6]. The function of fillers is to stop or minimise gas transport through the coatings. The choice of filler is often governed by specific coating properties and its runnability on coating equipment.

Mineral fillers are used in a similar way in thermoplastic composites [7] where their functions of effectiveness have been studied for decades. A number of models to predict permeability as a function of filler shape and volume fraction have been developed [8] and to the best of our knowledge, to date no models have been developed for prediction of barrier dispersion coating performance. For this reason, the objective of this paper is to discuss similarities and differences of thermoplastic composites and barrier dispersion coatings that may influence the applicability of the models for barrier dispersion coatings applied to paper based materials.

## 2 Barrier dispersion coatings

Barrier dispersion coatings consist mainly of fillers contained with a continuous polymer phase such as a co-polymer latex dispersion [1, 3]. The most commonly used polymer phases are latexes such as styrene-butadiene, styrene-n-butyl acrylate and linear vinyl acetate [3]. The latex provides important barrier properties; however, the demand of better performance has resulted in further improvement by addition of mineral fillers and other

additives in coating formulations (Table 1). The addition of mineral fillers in dispersion coatings significantly improves the barrier properties by increasing the length of the diffusion pathway for permeants [5] as shown in Figure 1. The tortuosity is mostly governed by the characteristics of the fillers such as elongation, aspect ratio, surface area, shape, the filler volume fraction and their spatial distribution in the polymer phase [8]. The term aspect ratio is generally used to describe the length (longest dimension) to thickness (shortest dimension) ratio. In this work, elongation is defined as the length (largest dimension) of fillers divided by width (second largest dimension). Because the assumptions used in the model development, the aspect ratio is defined as the width (second largest dimension) of fillers divided by thickness.

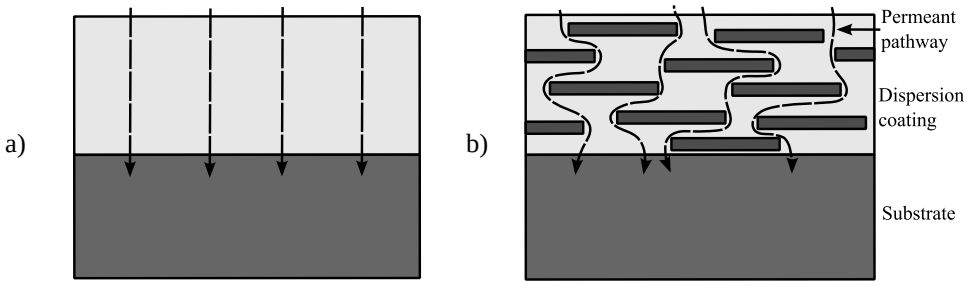



**Figure 1:** Diffusion of permeant through barrier dispersion coatings a) without fillers b) with fillers.

**Table 1:** Water vapour permeability of unfilled and filled polymer phases on different subtracts.

| Polymer phase/Substrate | Coat weight ($g\ m^{-2}$) | Water vapour permeability ($g\ m\ m^{-2}\ d^{-1}\ Pa^{-1}) \times 10^{-7}$ | Measuring Standard | Ref |
|---|---|---|---|---|
| Styrene-acrylate | | | | |
| Coating based on pure polymer phase/ Kraft paper, 90 $g\ m^{-2}$ | 4.8 | 4.41 | ASTM E96-90 | [9] |
| Coating based on polymer phaseand 25 wt% kaolin clay / hard-sized board, 200 $g\ m^{-2}$ | 6.5 | 3.63 | TAPPI T4448 OM-89 | [5] |
| Styrene-butadiene | | | | |
| Coating based on pure polymer phase/White top Kraftliner, calendered, 160 $g\ m^{-2}$ | 3.1 | 1.99* | TAPPI T4448 OM-87 | [4] |
| Coating based on polymer phaseand 60 wt% kaolin clay / white top Kraftliner, calendered, 160 $g\ m^{-2}$ | 12.6 | 1.07* | TAPPI T4448 OM-87 | [4] |

*: Calculated from reported water vapour transmission rate and coating thickness

The filler size distribution, fillers shape and hydrophilic/hydrophobic properties are the main characteristics of the fillers that effect the reduction of permeability [4]. Narrow filler size distribution and plate shaped fillers with a high aspect ratio, such as kaolin clay and talc, improve the barrier properties of coatings because these maximise the permeant diffusion pathway length [4, 10]. The chemical composition affects the hydrophilic/hydrophobic character of the fillers. Hydrophobicity in talc or hydrophobic clays usually contributes to the reduction of moisture permeability in barrier coatings for paper [3, 4]. However, their hydrophobic nature and the difficulty of dispersing them in water are often linked with use of dispersants [11]. Beside dispersants, several others additives are normally used to facilitate the coating processing (e.g. thickeners, antifaomers, surfactants, alkalis, waxes, co-binders such starches and water retention agents) [1, 3, 11].

The quantity of the fillers used for coating formulation must be lower than the critical pigment (filler) volume concentration (CPVC). This parameter represents the concentration of binder (polymer) that is just enough to coat all the filler particles and fill the intervening spaces [12]. For good flexibility, low blocking tendency and good barrier properties, the quantity of fillers normally used is from 40% to 50% vol [5, 13].

Better barrier properties can be achieved when the fillers are oriented parallel to the base substrate surface. Variations in the angle of orientation could affect the pathway length for the permeant, reducing the capability of the fillers to improve the barrier properties [4]. Uneven topography of the substrate gives less pronounced orientation of the fillers to the coated specimen [4]. However, high filler content and thin thickness of the barrier

dispersion impose, in part, parallel orientation of the fillers [6, 14]. The orientation of the fillers improves when calendering is applied to coatings [15].

The final aspect that affects the performance of dispersion coatings as barriers is the coating layer structure. During the coating consolidation, the water of the coating is removed forming an immobilised three-dimensional structure [3, 16]. This process affects the distribution of the polymer phase, filler orientation, air space around fillers and the polymer phase or final thickness of the coating and therefore influences many properties of the coating such as porosity and gloss [16, 17]. The thickness of a normal and single wet coating layer, including polymer phase, fillers and additives, is between 5 and 20 μm, roughly equivalent to a wet coat weight from 5 to 20 g $m^{-2}$. After the dewatering and drying processes the thickness and dry coat weight is reduced and, depending to the solid content of the coating, the reduction could be relatively high. About a half or less of the original thickness can be reached after drying.

It is important to note that the uniformity of the coating thickness is affected by the surface of the substrate [18]. Uneven substrates require filling of all irregularities to reduce the occurrence of uncovered areas [1, 18]. It is common to treat the substrate surface with a pre coating to smooth the surface and as a result homogenise the thickness of the coating to avoid uncoated areas [19]. Additionally, new application techniques such as curtain coating and spray coating follow the irregularities of the substrate, resulting in coatings with even thickness [13].

## 3 Thermoplastic composite films

Thermoplastic polymer films such as those formed from polyethylene, polypropylene, or polystyrene are widely used particularly for plastic packaging due to relatively low cost, the light weight, shatter resistance, and good mechanical properties [7, 20, 21]. The process to convert polymers to thermoplastic films normally begins with plastic pellets which are melted by extrusion at temperatures higher enough to cause melting [21, 22]. During the extrusion, additives could be used to achieve efficient and uniform composition of the melting [22]. To complete the process, the melt is filtered to remove any impurities and then formed into plastic sheets, films [22, 23] or applied as extrusion coatings on different substrates thus forming the thermoplastic layer. The plastic sheets/films can be moulded, laminated or thermoformed [21-23]. The plastic sheets are commonly thinner than 100 μm; however, the final thickness depends on each process and the use of the barrier. In this way, thermoplastic polymer films/coatings could be 6 μm thick for a single web of plastic layer, up to 250 μm thick in the case of thermoforming sheets [23].

Regardless the barrier properties of barrier films, the conditions of exposure affect the permeation of vapour thought barrier films. The main conditions effecting barrier properties are the relative humidity, temperature, exposure time, and barometric pressure [24]. For example, the diffusivity, or the speed that the vapour diffuses through the barrier film, increases if the temperature becomes higher [23]. Thus, important differences can be observed if the measurement conditions change [1]. To make comparable experiments, the evaluation of barrier film performance has to be carried out under standard conditions [24]. Several standard methods have been developed based on conditions of exposure and measuring methods. The standards normally estimate barrier properties based on measurement of water vapour transmission rate by exposing barrier film samples at different levels of vapour concentrations in the sample sides creating a driving force for diffusion. The diffused vapour is measured by mass changes that could be estimated by precision scales or sensitive detectors such as thermal conductivity detectors, infrared detectors, and others [21, 24]. The water vapour permeability of several thermoplastic polymer films is shown in Table 2.

**Table 2:** Water vapour permeability of thermoplastics polymer used in packaging [25].

| Thermoplastic polymer | Water vapour permeability ($g\ m\ m^{-2}\ d^{-1}\ Pa^{-1}$) × $10^{-7}$ | Measuring standard |
|---|---|---|
| Poly(ethylene terephthalate) (PET) | 2.09-8.37 | ASTM E96 |
| Polypropylene (PP) | 0.84-1.67 | ASTM E96 |
| Polyethylene (PE) | 2.09-8.37 | ASTM E96 |
| Polystyrene (PS) | 4.19-16.7 | ASTM F1249 |
| Poly(vinyl chloride) (PVC) | 4.19-8.37 | ASTM F1249 |
| Poly(vinyl alcohol) PVAL | 126 | JIS Z0208 |
| Ethylene vinyl alcohol (EVOH) | 4.19-12.6 | JIS Z0208 |
| Poly(vinylidene chloride) PVDC | 0.42 | ASTM E96 |

As shown in Table 2, the thermoplastics polymers are to some degree permeable to water vapour and also to other low molecular weight compounds such as gases [23]. By incorporation of inorganic or organic fillers with

certain geometries such fibres, flakes, spheres or particulates, the barrier performance of thermoplastic polymer can be improved as in barrier dispersion coatings [7, 26]. The combination of thermoplastic polymers and fillers are referred to as thermoplastic composites.

Numerous types of fillers are available for the thermoplastic composite formulation such silicates, graphite nanoplateles, and carbon nanotubes; however, the availability, platelet morphology (high aspect ratio and large specific surface area) and high cation exchange capacities of the clay fillers have attracted the majority of the composite development and investigation to provide barrier properties [7, 27-29] (Table 3). These characteristics make thermoplastic composite fillers particularly effective to improve barrier properties. For this reason, low concentrations of fillers (0.5 to 5 wt %) are normally required to significantly reduce the permeability of thermoplastic composites by up to four orders of magnitude [13, 30, 31]. It is important to note that larger quantity of fillers in thermoplastic composites increases the chances of agglomeration of the fillers [7, 32], blocking tendency of the fillers, and viscosity of the composites [13] affecting the dispersion of the fillers in the matrix and as a consequence their effectiveness in the reduction of permeability.

**Table 3:** Characteristics of fillers used in barrier dispersion coatings (BDC) and thermoplastic composites (TPC) (based on [3, 4, 27, 32-36]).

| Fillers | Equivalent diameter (μm) | Shape | Aspect ratio | Surface area ($m^2$ $g^{-1}$) | Typical quantity | Used for |
|---|---|---|---|---|---|---|
| Kaolin clay | 0.3-5 | Hexagonal plate | 10-80 | 67-72 | ≤ 43-50% * | BDC |
| Talc | 0.3-5 | Plate | 30 | 67-70 | -- | BDC |
| Plastic fillers | | | | | | |
| Solid | 0.1-0.5 | Spherical | 1 | -- | -- | BDC |
| Hollow | 0.4-1.0 | Spherical | 1 | -- | -- | BDC |
| Calcined kaolin | 0.7 (median) | Aggregate plate | 4.8- 7.4 | 14-22 | -- | BDC |
| Alumina trihydrate | 0.2-2 | Plate | -- | 5-90 | -- | BDC |
| Silicates | | | | | | |
| Montmorillonite clay | 0.1-0.15 | Plate | 10-1,000 | 750-760 | ≤ 5 wt% | TPC |
| Saponite clay | 0.2-0.3 | Plate | 165 | ~750 | ≤ 10 wt% | TPC |
| Hectolite clay | 0.05-0.06 | Plate | 46 | ~750 | ≤ 5 wt% | TPC |
| Ground calcium carbonate | 0.7-2 | Cubic, prismatic, plate | -- | 74-78 | -- | TPC |
| Graphite nanoplatelet | 2-20,000 | Flake | 200-1,500 | 2,630 | -- | TPC |
| Carbon nanotubes | -- | Fibre | -- | 10-20 | -- | TPC |

*: Based on Critical Pigment Volume Concentration (CPVC)

A homogeneous dispersion of the fillers in the polymer matrix is required to generate structure with a long tortuous pathway for diffusion [8, 29, 30, 37]. Because of the aggregated nature of some fillers such as montmorillonite, solvents soluble in the applied thermoplastic are used to improve the interaction between fillers and binder, increasing the exfoliation of the fillers in the matrix [38].

The dispersion of the fillers into the thermoplastic composite could also generate disorientation of the fillers resulting in a decrease of the barrier properties because the pathway length for permeant diffusion is shortened [27, 32, 39]. In addition, the low quantity of fillers normally required in thermoplastic composites gives extra space available for filler arrangement and as a consequence, the filler orientation may vary considerably. This is unlike the case of barrier dispersion coating, where the angle of filler orientation is reduced and most are oriented parallel with the substrate surface [15].

The study of the interaction between fillers and polymer of thermoplastic composites has resulted in a high level of understanding and models to predict mechanical and barrier properties have been developed [7, 8]. Below is a summary of the most extensively cited models to predict permeability of thermoplastic composites.

## 4 Models for prediction of permeability for thermoplastic composites

Numerous authors have developed models to predict relative permeability for thermoplastic composites. All models represent the effect of hypothetically impermeable and uniformly sized fillers in the polymer matrix on the relative permeability $(P_f/P_u)$. In general, the relative permeability of filled barriers is governed by the concentration of fillers or volume fraction ($\emptyset_F$) and the tortuosity ($\tau$) which accounts for the extra distance that

the permeant must diffuse around the fillers (Equation 1). The different types of fillers are represented by combination aspect ratio and shape of the fillers.

$$\frac{P_f}{P_u} = \frac{1 - \emptyset_F}{\tau} \quad (1)$$

where $P_f$ and $P_u$ are the filled and unfilled permeability of the thermoplastic composite.

The initial modelling approaches were based on oriented arrangement of the fillers which were equally distanced to each other, forming parallel layers. Normally the fillers were assumed to be rectangular shaped fillers with infinite depth and known height and length forming a two-dimensional geometry (Figure 2).

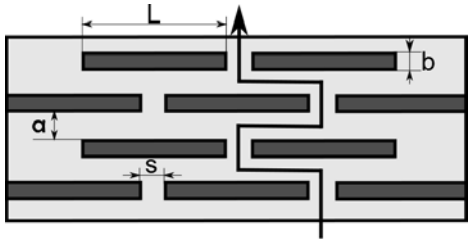



**Figure 2:** Geometry of the dispersion assuming oriented arrangement of the fillers. Where L is the second largest dimension of the filler particles, b is the filler particle thickness, $a$ and $s$ are the distance between filler particles in the thickness and width directions respectively.

One of the first models to predict relative permeability in polymers filled to dilute composites ($\alpha \cdot \emptyset_F \ll 1$, where $\alpha$ is the aspect ratio of the fillers) with oriented fillers was developed by Nielsen [40]. The author indicated that the relative permeability of filled thermoplastic composite is inversely proportional to the tortuosity which is affected by the distance of the permeant pathway. Nielsen assumed that the pathway of the permeant is exactly through the middle of the gaps between fillers (Figure 2). Under this assumption, the model predicts the maximum possible tortuosity and consequently is the best scenario for barrier films with this assumed geometry.

Similarly Cussler et al. [41] studied the effect of the oriented arrangement of the fillers for semi dilute regimes ($\alpha \cdot \emptyset_F \gg 1$), including not only the effect of the resistance generated by fillers; but also the resistance of the space between fillers in the coating width direction ($s$) against the flux of permeant (Figure 2). Comparisons between experimental data and predictions indicate that the Nielsen and Cussler et al. models are more appropriate for films with $\emptyset_F$ lower than 10% when applied to different type of coating materials and fillers evaluated for several gases [8, 42-44].

The Cussler et al. model was developed as a simplification of an earlier model created by Wakeham and Mason [45]. Assuming a single and perforated layer, the diffusion was further extended to the constriction of $s$ and the resistance related to the length of the pores in the width direction [8, 46]. Analogous to the Wakeham-Mason model, Aris [47] developed a model by defining the same factors described above; however, in the case of Wakeham-Mason, the definition of the constriction resistance is independent of $\alpha$ and the Aris definition is not [7, 8].

The oriented arrangement of the fillers represents the best scenario that filled films could reach for a given volume fraction. In many cases this assumption over simplifies the structure of real coatings because the fillers tend to be randomly located. For this reason, other authors have included the random arrangement of the fillers as a factor to consider during model development (Figure 3).

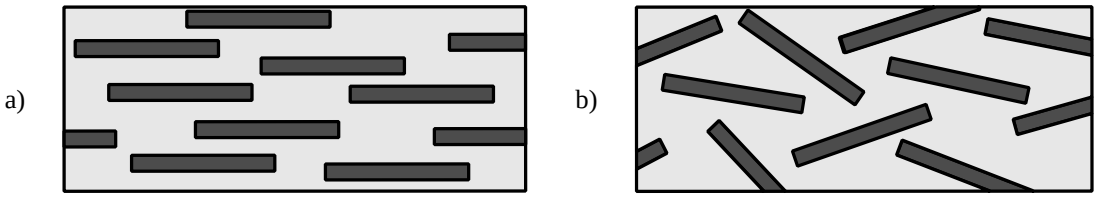



**Figure 3:** Random arrangement of the fillers into the coating with a) parallel orientation and b) non parallel orientation.

Lape et al. [48] developed a model for composites filled with monodispersed flakes with random orientation as shown Figure 3a. The permeant pathway is determined by using the probability of the permeant to pass through the shortest and the longest pathway around fillers. This compensation reduces the pathway distance to 2/3 of the length that the fillers cause in the case of the oriented arrangement.

Sun et al. [37] indicated that the fillers tend to be parallel oriented when $\emptyset_F$ is high (Figure 3a), supporting the assumption presented by Lape et al. [48]; however, at low $\emptyset_F$ it is possible to observe fillers with different angle of orientation (Figure 3b). The random arrangement of the fillers with non-parallel angles of orientation into the films was analysed by Bharadwaj [32] based on a modification of the Nielsen model. Completely dispersed fillers reduce the distance of the permeant pathway, deteriorating the barrier properties of the films. This reduction is directly associated to the angle of the fillers compared to the direction of the permeant flux. Based on the above observation, Bharadwaj counteracted the reduction of tortuosity by adding a parameter of order ($S$) defined by Tsvetkov [49].

Other authors have developed models assuming flakes or disk shaped fillers. This assumption changes the perspective of the model to three-dimensional geometries. Fredrickson and Bicereno [50] and Gusev and Lusti [51] considered randomly located disk shaped fillers. The model of Fredrickson-Bicereno is based on multiple scattering theory for semi dilute regimes ($\alpha \cdot \emptyset_F \gg 1$). In the case of Gusev-Lusti, a finite element method simulation was used to solve the Laplace's equation for the local chemical potential. Despite the same assumptions used in both models, the Fredrickson-Bicenaro model predicted a higher relative permeability than the Gusev-Lusti model particularly at relatively high $\emptyset_F$ and $\alpha$ [8, 51]. These differences could be more than one order of magnitude in cases of $\emptyset_F$ > 5% and $\alpha$ > 1,000 [51].

Assuming an oriented arrangement of hexagons, Moggridge et al. [52] developed a model based on the previous work carried out by Cussler et al. [41]. The structure supposes three layers of hexagonal fillers to avoid direct diffusion through the film. As used in the Fredrickson and Bicenaro model, a shape factor of 2/27 was used to correct the prediction under this scenario.

A summary of the models described above and their performance are presented in Table 4 and Figure 4 respectively.

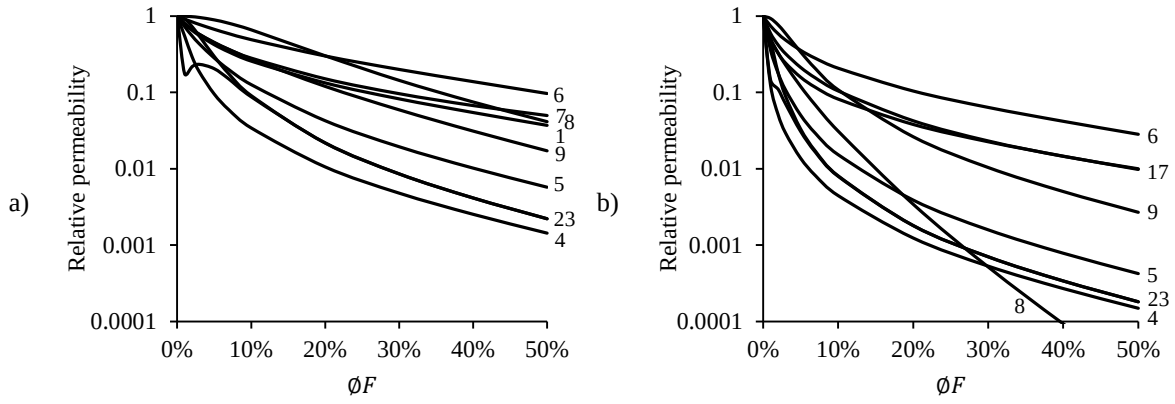



**Figure 4:** Relative permeability of filled films (aspect ratio of the fillers equal to a) 50 and b) 200) as a function of the volume fraction of the fillers $\emptyset_F$. The models are 1: Nielsen, 2: Cusller et al., 3: Wakeham-Mason, 4: Aris, 5: Lape et al., 6: Bharadwaj, 7: Fredrickson-Bicerano, 8: Gusev-Lusti, 9: Moggridge et al.

As shown Figure 4, all models are very sensitive to changes in the volume fraction of fillers. It is possible to achieve reduction up to three orders of magnitude in the relative permeability for barriers with 50% volume fraction of fillers, and even higher if the aspect ratio of fillers increases; however, similar models predict different relative permeabilities. As expected, the Nielsen model predicts higher relative permeability of the barrier compared with the Cussler et al., the Wakeham-Mason and the Aris models due to the effect of slit constriction that these three models assumed.

Compared with models with oriented arrangement, the Lape et al. and the Bharadwaj models predict higher relative permeability due to the shorter diffusion pathway produced by the random arrangement of the fillers. Also, the Bharadwaj model predicted higher relative permeability than the Lape et al. model because of the reduction of barrier properties caused by the angle of orientation.

At low aspect ratio, the Fredrickson-Bicerano and the Gusev-Lusti models predict similar performance for the barriers; however, the Moggridge et al. model estimated better barrier properties because the regular arrangement of the fillers creates an overlapping structure reducing the spaces among fillers. Interestingly the Gusev-Lusti model is more sensitive to changes of the aspect ratio of the fillers than the other models. The reduction in the predicted relative permeability reached several orders of magnitude at high aspect ratio (Figure 4b).

**Table 4:** Summary of the presented model where C, R, and H mean circular, rectangular, or hexagonal filler shape and D means geometrical dimension

| Model | Equation | Aspect ratio (slit aspect ratio $\sigma$) | | Shape | D |
|---|---|---|---|---|---|
| Nielsen [40] | $\frac{P_f}{P_u} = \frac{1-\emptyset_F}{1+\alpha\emptyset_F}$ | $\alpha = \frac{L}{2b}$ | (2) | C/R | 2 |
| Cussler et al. [41] | $\frac{P_f}{P_u} = \left(1+\frac{\alpha^2{\emptyset_F}^2}{1-\emptyset_F}\right)^{-1}$ | $\alpha = \frac{L+s}{2b}\ s \ll L$ | (3) | R | 2 |
| Wakeham-Mason [45] | $\frac{P_f}{P_u} = \left(1+\frac{\alpha^2{\emptyset_F}^2}{1-\emptyset_F}+\frac{\alpha\emptyset_F}{\sigma}+2(1-\emptyset_F)ln\left(\frac{1-\emptyset_F}{2\sigma\emptyset_F}\right)\right)^{-1}$ | $\alpha = \frac{L+s}{2b}\ \sigma = \frac{s}{2b}$ | (4) | R | 2 |
| Aris [47] | $\frac{P_f}{P_u} = \left[1+\frac{\alpha^2{\emptyset_F}^2}{1-\emptyset_F}+\frac{\alpha\emptyset_F}{\sigma}+\frac{4}{\pi}\frac{\alpha\emptyset_F}{1-\emptyset_F}ln\left(\frac{\pi\alpha^2\emptyset_F}{\sigma(1-\emptyset_F)}\right)\right]^{-1}$ | $\alpha = \frac{L+s}{2b}\ \sigma = \frac{s}{2b}$ | (5) | R | 2 |
| Lape et al. [48] | $\frac{P_f}{P_u} = \frac{1-\emptyset_F}{\left(1+\frac{2}{3}\alpha\emptyset_F\right)^2}$ | $\alpha = \frac{L}{2b}$ | (6) | R | 2 |
| Bharadwaj [32] | $\frac{P_f}{P_u} = \frac{1-\emptyset_F}{1+\alpha\cdot\emptyset_F\cdot\frac{2}{3}\cdot\left(S+\frac{1}{2}\right)}\quad S=0$ | $\alpha = \frac{L}{2b}$ | (7) | R | 2 |
| Fredickson-Bicerano [50] | $\frac{P_f}{P_u} \approx F_m\left(\frac{\pi}{ln\alpha}\alpha\emptyset_F\right)\quad F_m(x) = \left(\frac{1}{m}\sum_{j=1}^{m}\frac{1}{1+a_j x}\right)^2$ | $\alpha = \frac{L}{2b}$ | (8) | C | 3 |
| Gusev-Lusti [51] | $\frac{P_f}{P_u} = exp\left[-\left(\alpha\frac{\emptyset_F}{x_0}\right)^{\beta}\right]\ \beta = 0.71\quad x_0 = 3.47$ | $\alpha = \frac{L}{b}$ | (9) | C | 3 |
| Moggridge et al. [52] | $\frac{P_f}{P_u} = \left(1+\frac{2}{27}\frac{\alpha^2{\emptyset_F}^2}{1-\emptyset_F}\right)^{-1}$ | $\alpha = \frac{L}{2b}$ | (10) | H | 3 |

## 5 The applicability of models to barrier dispersion coatings

As the literature has shown, upon increasing the quantity of the fillers, the barrier properties of both barrier dispersion coatings and thermoplastic composites improve. In Table 4, there are a number of models that could potentially be applied to dispersion coatings. These differ with respect to orientation and filler particle elongation. These factors must be considered in selecting which models are most appropriate for barrier dispersion coatings.

In the barrier dispersion coatings, the fillers are spatially arranged randomly and depending on the coating conditions can have non-parallel orientation. Thermoplastic composites are more susceptible to distribution of the filler with non-parallel orientation due to the low volume fraction of the fillers and the relative high film thickness compared to barrier dispersion coatings. The opposite case is present in barrier dispersion coatings where the freedom of rotation of fillers is limited by the large amount of fillers and reduced coating thickness. In assuming oriented arrangement of the fillers with parallel orientation (Figure 2), the possibility for rotation of the fillers is limited by the length of the fillers and the spaces between the layers of fillers (Figure 5). In this way, the maximum angle of orientation for fillers can be calculated by the following geometric considerations:

$$\gamma_F = \gamma_1 - \gamma_2 \tag{11}$$

$$\gamma_1 = \sin^{-1}\left[\frac{1}{r}\cdot\left(a+\frac{b}{2}\right)\right] \tag{12}$$

$$\gamma_2 = \sin^{-1}\left(\frac{b}{2\cdot r}\right) \tag{13}$$

$$r = \frac{1}{2}\sqrt{L^2+b^2} \tag{14}$$

$$\emptyset_F = \frac{L\cdot b}{(L+s)\cdot(a+b)} \tag{15}$$

where $\gamma_F$ is the maximum angle of filler orientation, $\gamma_1$ is the angle formed for the diagonal between the centre of the filler and a corner with reference the original position of the filler, $\gamma_2$ is the angle formed for the diagonal between the centre of the filler and a corner with reference the rotated position of the filler, $L$ and $b$ are the length and thickness of the fillers, $r$ is the diagonal length (hypotenuse) formed between a corner and the centre of a filler, and $a$ and $s$ are the space between two parallel filler layers and the slit between two filler particles.

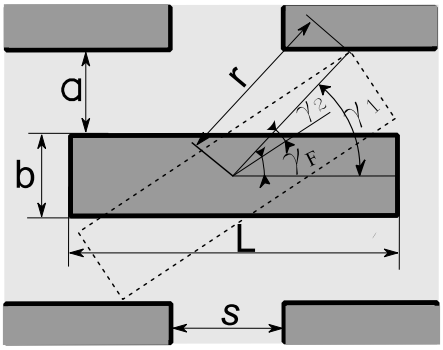



**Figure 5**: Maximum angle of orientation for fillers with oriented arrangement.

As shown in Figure 6, the possible angle of orientation decreases if the volume fraction and the aspect ratio of the fillers increase. In the case of barrier dispersion coatings, the angle of filler orientation is much reduced due to the large $\emptyset_F$ and the thin coating thickness. Even for low volume fraction, the angle of orientation is not considerably high to justify the need for models that include the random orientation of the fillers. It is important to note that the above results are valid for areas where the substrate surface does not affect the orientation of the filler such as pre coated substrates.

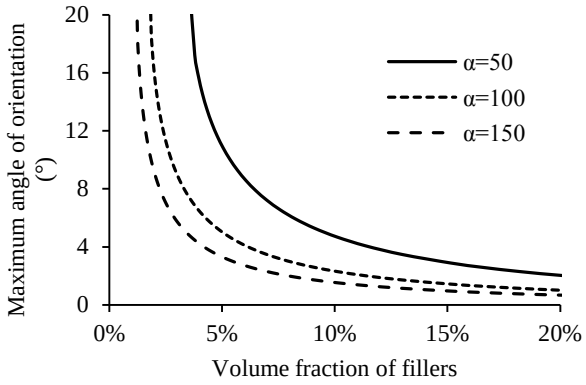



**Figure 6:** Theoretical maximum angle of filler orientation for three fillers aspect ratio (α) estimated from the centre of the fillers.

The majority of the presented models assume the elongation ratio (E) is infinite (i.e. The Nielsen, Cussler et al, Wakeham-Mason, etc.). This makes them more applicable for fillers with large E. Based on Equation 2, the error of assuming two dimensions can be estimated from Equation 16, where the relative permeability uses for the third dimensional aspect ratio (αE) is compared to the relative permeability ignoring the third dimensional effect.

$$R = \frac{\left({}^{Pf}/_{Pu}\right)_{predicted\ using\ \alpha E}}{\left({}^{Pf}/_{Pu}\right)_{predicted\ using\ \alpha}} = \frac{1 + \frac{C}{2 \cdot b} \cdot \emptyset_F}{1 + \frac{L}{2 \cdot b} \cdot \emptyset_F} \quad (16)$$

where $C$ is the length in the width direction. According to Figure 7, if the elongation is very large, the ratio R tends to zero and the two dimensional models is valid. It can be seen that an elongation of 10 would result in approximately a 10% error in the prediction of relative permeability for several amount of fillers. For elongation ratios higher than 10, the two dimensional models are likely to be suitable. The fillers used for both thermoplastic composites and barrier dispersion coatings normally are plate or flake shaped where the length and width are relatively similar (E≈ 1) [3, 33, 53]. Because these particle shape factors, the most appropriate models to predict relative permeability of barrier dispersion coatings are those that assume three-dimensional geometries and parallel orientation of the fillers.

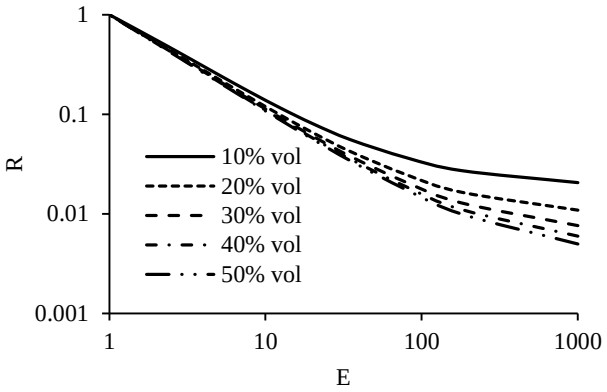



**Figure 7:** Relative permeability of length coating direction and width coating direction R using the Nielson model [40] as a function of the elongation (E) of the fillers for five volume fractions.

As a result of above discussion, the Fredickson-Bicenaro model, the Gusev-Lusti models and the Moggridge et al are the most appropriated for barrier dispersion coatings. The models all assume good dispersion of filler particles. In thermoplastic composites, this is generally true because the low volume fraction and for this reason they are applied for volume fractions lower than 20% [7, 32]. The quantity of fillers required for barrier dispersion coatings is several times higher than that used for thermoplastic composites due to the relative small aspect ratio and surface area of the fillers. This indicates that the preparation of barrier dispersion coatings may be sensitive to agglomeration, particularly around the critical pigment volume concentration (CPVC), which further reduces the already relative low aspect ratio of the fillers (Table 3). The CPVC varies depending on the filler properties but ranges from 50% vol to 55%vol [3]. When agglomeration occurs, higher permeability will occur. Although industrial coating applications would avoid agglomeration. The models can be used to demonstrate this increase in permeability by decreasing in aspect ratio ($\alpha$).

Figure 8 shows the effect of the decreasing aspect ratio on relative permeability at volume fraction in the expected CPVC range using the Moggridge et.al. model [52]. The relative permeability can importantly increase if the aspect ratio of filler is reduced particularly in cases where the original aspect ratio of lower than 15. This effect is stronger if the volume fraction of filler increases.

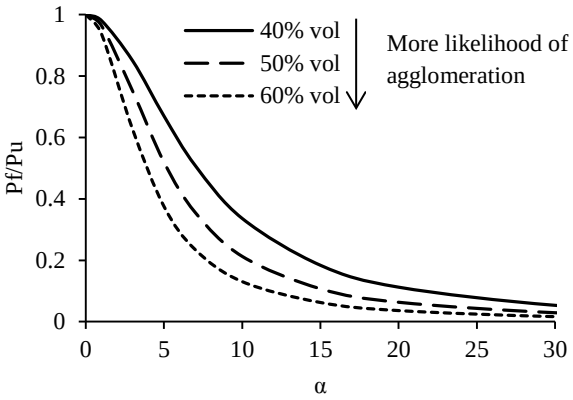



**Figure 8:** Effect of aspect ratio (α) on the reduction of relative permeability for a filled coating using the Moggridge et al model [52] for three volume fractions of fillers.

As the models were proposed, the characteristics of the continuous polymer phase are not included and the models just predict the changes of the final diffusivity of filled barriers with respect to the diffusivity of unfilled barriers. Likewise, the conditions that the barriers are exposed do not play any role in the relative permeability. Under this scenario, for probing that the models work properly for barrier dispersion coatings, characteristics of unfilled and filled coatings such as known coating thickness or polymer diffusivity are required. Unfortunately, this is a very challenging task, difficult even under laboratory scale conditions. There is a little experimental data for dispersion coating with varying fillers volume fraction and /or aspect ratio which is suitable to validate the use of the models. Schuman et al [4] is the only report that attempts to predict barrier coating performance in this way. Their experimental data were for a kaolin clay/latex system including only two different volume fractions and one filler particle aspect ratio. They found that the Moggridge et al model fitted the trend although they had to dramatically reduce the aspect ratio of the fillers from 45 in the experiment to 12 for the model input. These data are not sufficient to evaluate the effectiveness of the models for prediction of permeability through barrier dispersion coatings. For this reason, further experiments are required for model validation including a large range of aspect ratio and volume fraction of fillers.

## 6 Conclusions

A number of models have been developed to predict the permeability of thermoplastic composites. The models are normally based on idealised geometries, where the fillers are arranged in an oriented or random way. Also, specific filler shapes are assumed that create, in most cases, a two dimensional geometry of the barrier films. The heterogeneous characteristics of the barrier dispersion coatings such as uneven coating thickness, particles size and lower elongation of the fillers limit the use of the presented models in prediction of barrier dispersion coating performance. For thermoplastic composite, the models are valid for only low volume fraction of the fillers ($\emptyset_F$ < 10%) as above this value filler agglomeration occurs. The amount of fillers used for barrier dispersion coatings is much higher (40-50%) before agglomeration occurs ($\emptyset_F$ > CPVC) and therefore the models are potentially applicable to up to this range.

Those models that assumed plate shaped fillers are the most suitable to predict relative permeability of barrier dispersion coatings (the Fredickson-Bicenaro [50], the Gusev-Lusti [51] and the Moggridge et al. [52] models). These models assumed parallel three-dimensional fillers with circular or hexagonal shaped filler particles. The conditions agree with the characteristics of barrier dispersion coatings. Normally, the fillers used in barrier dispersion coatings such as clay or talc are defined as plate shaped fillers and they tend to be parallel to the substrate due to the high volume fraction and low thickness of the coatings. Very little data for dispersion coatings with variable α and $\emptyset_F$ have been reported in the literature. Based on this, further experimental investigations are required to validate the models over a wider range of aspect ratio and filler volume fraction.

**Acknowledgement**

The authors are grateful to Scion Research to support this investigation.

## References

1. T. Kimpimäki, A.V. Savolainen 1997, “Barrier dispersion coating of paper and board”, In: J. Brander and I. Thorn (eds.). *Surface Application of Paper Chemicals*, Chapman & Hall, Victoria, Australia, pp. 208-228.

2. M. Vähä-Nissi, K. Kervinen, A. Savolainen, S. Egolf, W. Lau, 2006, "Hydrophobic polymers as barrier dispersion coatings", *Journal of Applied Polymer Science*, vol 101, pp. 1958-1962.
3. E. Lehtinen. *Pigment coating and surface sizing of paper*. Gummerus Printing: Finland, 2000.
4. T. Schuman, A. Karlsson, J. Larsson, M. Wikström, M. R., 2005, "Characteristics of pigment-filled polymer coatings on paperboard", *Progress in Organic Coatings*, vol. 54, pp. 360-371.
5. C. Andersson, M. Ernstsson, L. Järnström, 2002, "Barrier properties and heat sealability/failure mechanisms of dispersion-coated paperboard", *Packaging Technology and Science* , vol. 15, pp. 209-224.
6. K. Rissa, T. Lepistö, K. Yrjölä, 2006, "Effect of kaolin content on structure and functional properties of water-based coatings", *Progress in Organic Coatings*, vol. 55, pp. 137-141.
7. S. Solovyov, A. Goldman, 2008, *Mass Transport and Reactive Barriers in Packaging: Theory, applications and design*. DEStech Publications: Pennsylvania.
8. G. Choudalakis, A.D. Gotsis, 2009, "Permeability of polymer/clay nanocomposites: A review", *European Polymer Journal*, vol. 45, pp. 967-084.
9. C. Andersson, L. Järnström, 2002, " Heat sealability and water vapour permeability of barrier dispersion coatings", *Tappi Coating and Graphic Arts Conference and Trade Fair*, Florida, USA, May 5-8, pp.415-423.
10. C. Kugge, B. Johnson, 2008, "Improved barrier properties of double dispersion coated liner", *Progress in Organic Coatings*, vol. 62, pp. 430-435.
11. B. Mesic, C. Kugge, L. Järnström, 2010, "Superhydrophobic paper coating containing nonconventional clay", *Tappi Journal*, vol. 9, no. 11, pp. 33-40.
12. R.H. Braunshausen, R.A. Baltrus, L. De Bolt, 1992, "A review of methods of CPVC determination (critical pigment volume concentration)", *Journal of Coatings Technology*, vol. 64, pp. 51-55.
13. C. Andersson, 2008, "New ways to enhance the functionality of paperboard by surface treatment: A review", *Packaging Technology and Science*, vol. 21, no. 6, pp. 339-73.
14. G. Chinga, T.Helle, P.O. Johnse, 2000, "Characterization of pigment coating layer structure using SEM and digital image", *Tappi Conference and Trade Fair*, Washington, USA, May 1-4, pp. 309-319.
15. K. Rissa, T. Lepisto, M. Vaha-Nissi, A. Savolainen, 2000, "Orientation of talc fillers in dispersion coatings", *Nordic Pulp and Paper Journal*, vol. 15, pp. 357-361.
16. G. Eksi, D.W. Bousfield, 1997, Modeling of coating structure development, *Tappi Journal*, vol. 80, no. 2, pp. 125-135.
17. P. Lepoutre, 1989, "The structure of paper coating: An update", *Progress in Organic Coatings*, vol. 17, no 2, pp. 89-106.
18. R. Allem, 1998, "Characterization of paper coatings by scanning electron microscopy and image analysis", *Journal of Pulp and Paper Science*, vol. 24, no. 10, pp. 329-336.
19. T. Schuman, M. Wikström, M. Rigdahl, 2004, "Dispersion coating with carboxylated and cross-linked styrene-butadiene latices 2: Effects of substrate and polymer characteristics on the properties of coated paperboard", *Progress in Organic Coatings*, vol. 51, pp. 2228-2237.
20. J. Brandsch, O.G. Piringer. "Characteristics of plastic materials". In: O.G. Piringer and A.L. Baner (eds.), *Plastic packaging materials for food: Barrier function, mass transport, quality assurance, and legislation*, Wiley-Vch, Germany, 2000, pp. 9-45.
21. D.S. Lee, K.L. Yam, L. Piergiovanni, 2008, *Food packaging science and technology*. CRC Press: Florida.
22. K.R. Osborn, W.R. Jenkins, 1992, *Plastic films: Technology and packaging applications*. Technomic Publishing Company: Pennsylvania.
23. G.L. Robertson, 2006, *Food packaging: Principles and practice* (2nd ed). CRC Press: Florida.
24. Johnson, B. and R. Demorest 2009, "Testing, permeation and leakage", In: K. L. Yam (eds), *The Wiley Encyclopedia of Packaging Technology*, John Wiley & Sons, New York, pp. 1207-1213.
25. Plastic Design Library, 1995, *Permeability and other properties of plastics and elastomers*. William Andrew Publishing, New York.
26. H.M.C. de Azeredo, 2009, "Nanocomposites for food packaging applications", *Food research international*, vol 42, pp. 1240-53.
27. S. Sinha Ray, M. Okamoto, 2003, "Polymer/layered silicate nanocomposites: A review from preparation to processing", *Progress in Polymer Science*, vol. 28, pp. 1539-1641.
28. H.M. Park, W.K. Lee, C.Y. Park, W.J. Cho, C.S. Ha, 2003, "Environmentally friendly polymer hybrids: Part I Mechanical, thermal, and barrier properties of thermoplastic starch/clay nanocomposites", *Journal of Materials Science*, vol. 38, pp. 909-915.
29. A. Arora, G.D. Padua, 2010, "Review: Nanocomposites in Food Packaging. Journal of Food Science", *Journal of Food Science*, vol. 75, no. 1, pp. 43-49.
30. P.C. LeBaron, Z. Wang, T.J. Pinnivaia, 1999, "Polymer-layered silicate nanocomposites: An overview", *Applied Clay Science*, vol. 15, pp 11-29.

31. J. Lange, Y. Wyser, 2003, “Recent innovations in barrier technologies for plastic packaging: A review”, *Packaging Technology and Science*, vol. 16, no. 4, pp. 146-157.
32. R.K. Bharadwaj, 2001, “Notes: Modeling the barrier properties of polymer-layered silicate nanocomposites”, *Macromolecules*, vol. 34, pp. 9138-9192.
33. H. Holik (Ed.). Handbook of paper and paperboard . Wiley-VCH: Germany, 2006.
34. W.M. Bundy, J.N. Ishley, 1991, “Kaolin in paper filling and coating”, *Applied Clay Science*, vol. 5, pp. 397-420.
35. A.L. Andrady, 2008, *Science and technology of polymer nanofibres*. John Wiley & Sons, New Jersey.
36. F. Hussain, H. Mehdi, 2006, “Review article: Polymer-matrix nanocomposites, processing, manufacturing, and application: An overview”, *Journal of Composite Materials*, vol. 40, pp. 1511-1575.
37. L. Sun, W.J. Boo, A. Clearfield, H.J. Sue, H.Q. Pham, 2008, “Barrier properties of model epoxy nanocomposites”, *Journal of Membrane Science*, vol. 318, pp. 129-136.
38. M. Alexandre, P. Dubois, 2000, “Polymer-layared silicate nancomposites: Preparation, properties and uses of a new class of materials”, *Materials Science and Engineering*, vol. 28, pp. 1-63.
39. R.D. Maksimov, S. Gaidukov, J. Zicans, J. J., 2008, “Moisture permeability of a polymer nanocomposite containing unmodified clay”, *Mechanics of Composite Materials*, vol. 44, no. 5, pp. 505-514.
40. L.E. Nielsen, 1967, “Models for the permeability of filled polymer systems”, *Journal of Macromolecular Science, Chemistry*, vol. 1, pp. 929-942.
41. E.L. Cussler, S.E. Hughes, W.J. Ward, III, R. Aris, 1988, “Barrier membranes”, *Journal of Membrane Science*, vol. 38, pp. 161-174.
42. C. Lu, Y.W. Mai, 2007, “Permeability modelling of polymer-layered silicate nanocomposites”, *Composites Science and Technology*, vol. 67, pp. 2895-2902.
43. S. Nazarenko, P. Meneghetti, P. Julmon, B.G. Olson, S. Qutubuddin, 2007, “Gas barrier of polystyrene montmorillonite clay nanocomposites: Effect of mineral layer aggregation”, *Journal of Polymer Science: Part B: Polymer Physics*, vol. 45, pp. 1733-1753.
44. Z.F. Wang, B. Wang, N. Qi, H.F. Zhang, L.Q. Zhang, 2005, “Influence of filler on free volume and gas barrier properties in styrene-butadiene rubber studied by positrons”, *Polymer*, vol. 46, pp. 719-724.
45. W.A. Wakeham, E.A. Mason, 1979, “Diffusion through multiperforate laminae”, *Industrial and Engineering Chemistry Fundamentals*, vol. 18, no. 4, pp, 301-305.
46. W.R. Falla, M. Mulski, E.L. Cussler, 1996, “Estimating diffusion through flake-filled membranes”, *Journal of Membrane Science*, vol. 119. pp. 129-138.
47. R Aris,1986, “On a problem in hindered diffusion”, *Archive for Rational Mechanics and Analysis*, vol. 12, pp. 83-91.
48. N.K. Lape, E.E. Nuxoll, E.L. Cussler, 2004, “Polydisperse flakes in barrier films”, *Journal of Membrane Science*, vol. 234, pp. 29-37.
49. V.N. Tsvetkov,1942, “Molecular ordering in the anisotropic liquid”, *Acta Physicochimica URSS*, vol. 16, pp. 132-47.
50. G.H. Fredickson, J. Bicerano, 1999, “Barrier properties of oriented disk composites”, *Journal of Chemical Physics*, vol. 110, no. 4, pp. 2181-2188.
51. A.A. Gusev, H.R. Lusti, 2001, “Rational design of nanocomposites for barrier applications”, *Advanced Materials*, vol. 13, no. 21, pp. 1641-1643.
52. G.D. Moggridge, N.K. Lape, C. Yang, E.L. Cussler, 2003, “Barrier films using flakes and reactive additives”, *Process in Organic Coatings*, vol. 46, pp. 231-240.
53. D. Gelinas, D. Vidal, 2010, “Determination of particle shape distribution of clay using an automated AFM image analysis method”, *Powder Technology*, vol. 203, no. 2, pp. 254-64.

# The Functional Analysis Methodology for Environmentally Conscious Packaging Design

**Jeeranuch Buddeejeen [1*] and Athakorn Kengpol[2]**

[1] *Department of Printing and Packaging Technology, School of Science and Technology, Sukhothai Thammathirat Open University, Thailand*
[2] *Advanced Industrial Engineering Management Systems Research Center, Department of Industrial Engineering, King Mongkut's University of Technology North Bangkok, Thailand*

[*] *Corresponding author. Email: jeeranuch_pk13@hotmail.com*

**Abstract:** The roles of packaging design are to preserve the product, protect its damage throughout transportation, and fulfil stakeholder's complicated needs. Moreover, the customers become more environmental conscious to consider in eco packaging before buying. The varieties of tools assist design teams to develop the eco packaging design concepts by integrating environmental aspects into design and development phase. However, the eco packaging design methodology is an inconceivable support for functional analysis into life cycle packaging. The objective of this research is to develop a functional analysis methodology for supporting environmentally consciousness design of packaging. The methodology is obtained in three tools: Eco Packaging Design Checklist (EPDC), Function Analysis System Technique (FAST), and Functional Benchmarking (FB). The proposed methodology is tested through application to the secondary packaging for containment of electronic components. The proposed methodology is crucial to consider not only environmental aspects but also functional aspects. This can assist effectively for design teams to identify the functional packaging in conceptual design phases. The advantages of this methodology are to define the environmental impact in the early design phase by using EPDC tool. This step can be assessed the environmental problems with its easiness and fastness and pointed to the critical requirements and notified for environmental impact situation of current packaging. The FAST tool can help to define the function of current packaging and organized the logical relationships between functions. The design team can clarify to the primary and secondary functions of current packaging and determined the mission statement. The FB is applied to clarify in functional requirements based upon customer's need and compare the functional improvement level with competitors in the current market. This step can help the design team to prioritize the functional requirements to improvement. The methodology has a majoring benefit than applying those three tools independently. The recommendations, limitations and further researches are also presented in this research.

Keywords: eco packaging design, functional analysis, eco packaging design checklist, function analysis system technique, functional benchmarking.

## 1 Introduction

Packaging most often prevents goods damage during transportation. Especially, the sensitive and fragile goods such as electronic products can break easily in transit. These products require the secondary packaging with complicated structure to protect the product quality. Customers often discard secondary packaging quickly after purchasing and then become to packaging waste after buying goods. It is importantly required the systematic waste management and completely reduced in the air, water and land pollutions. This quick discarding and disregarding packaging causes the environmental impact of packaging very exactly to the end users, therefore the packaging gives a negative environmental image. Moreover, packaging may be attributed to factor other than the packaging material itself approximately 90 percent that hidden costs of manufacturing and supply chain activities as quality inspection, inventory footprint area, transport and logistics load, disposal elimination [1]. The most of decreasing environmental impacts is to design properly packaging for reusability and recycling, which is very good for environment friendly.

Many countries including some US States, Canada, Western and Eastern Europe, South Africa, Australia, Brazil, China, Japan, Taiwan, Tunisia, and South Korea have implemented environmental packaging requirements to allocate and distribute waste management costs, shift responsibility onto the Extended Producer Responsibility (EPR), and to decrease the environmental impact of packaging. This trend reinforces the consciousness of environmental responsibility of competitive companies, industries, and global business. The Packaging and Packaging Waste Directive (94/62/EC) is a measure with environmental goals of packaging. The Directive applies to all packaging placed on the EU market, and all packaging waste of at industrial, commercial sites and

from private homes. It is required the minimized packaging, design for recovery, reuse packaging and non-toxic or heavy metals should be restricted in the packaging material and production. The packaging wastes are involved to environmental issue and required with stakeholder responsibility. The companies can apply the eco packaging design as the means of considering to environmental conscious and ensuring the safe delivery of a product to end user in complete condition at the minimum overall environmental impact [1]. It is difficult to combine and balance between decreasingly environmental impact and maintainable quality function. Whatever the reason, it is considered to develop the methodology for functional analysis for environmental conscious in packaging design at the conceptual design phase. The objective of this research is to develop a methodology for effective support of the packaging in conceptual design for packaging eco design activities. This methodology is verified through application in secondary packaging of electronic components. Especially, the proposed methodology whose core is the expanding into the analysis of environmental and functional requirements by applying three tools as Eco Packaging Design Checklist (EPDC), Function Analysis System Technique (FAST), and Function Benchmarking (FB). In addition, connecting three consecutive tools is formalized by correlating the outputs of the preceding tool and the inputs of the following one. The framework of this research consists of an overview of the current eco design tools with defining functional packaging, a description of the proposed packaging design methodology, and application of the method to the electronic components industry. Then, discussion and conclusion are presented in this research.

## 2 Eco Design tools

According to the previous studies about the eco design tool for functional analysis, many tools have been developed for eco design to support design team at conceptual design phase. The following literature relates to the model above.

### 2.1 Eco Packaging Design Checklist method (EPDC)

EPDC means a set of items used for assessing a packaging from environmental viewpoints through life cycle. This is used for packaging assessment which aims at improving the packaging on environmental aspects considering the possible environmental impacts [2]. For instance, Wimmer [3] apply EPDC to evaluate an existing product and come up with target oriented eco design improvements by specific requirements its life cycle. This method, with its easiness and fastness, is one of those general most for applying in industries. This is effective especially for systematizing environmental review in a manufacturing. Nevertheless, this is not significant purpose for environmental assessment and unclear result for design direction.

### 2.2 Function Benchmarking (FB)

This tool is the measurement of properties of a packaging. The measurements can be compared to a baseline of current packaging or competitors in the market, both with similar functionality [4]. It may be beneficial to validate periodically the choice of properties against the results of a more detailed analysis. For supporting in this advantage, Svanes et al. [5] use FB tool for studying in the sustainable packaging design in case study of food industry. This model is applied in decision support of sustainable packaging by following five quantitative indicators for comparison between different packaging solutions. However, FB does not show how to solve the problem for design improvement.

### 2.3 Function Analysis System Technique (FAST)

FAST assists to define the problem objectively and organize the logical relationships between functions. The FAST diagram can be used to verify and show how a proposed design achieves the functional requirements of packaging. This tool can be identified the unnecessary and duplicated functions [6]. The design team can use the FAST diagram to communicate functional mapping between design team and find the way to design improvement in general, not only eco packaging design.

### 2.4 Life Cycle Assessment (LCA)

LCA is a method to assess environmental impacts of a product or packaging [7]. It requires comprehensively the quantitative information of the life cycle on the environment. Many researchers apply LCA for assessing packaging and product in the design and development phase such as Madival et al. [8], Nielsen and Wenzel [9], and Verghese et al. [10]. The results can be identified the life cycle impacts and evaluated the environmental performances. Although it discloses the quantitative environmental profile relatively based upon the structural design of packaging. It has some disadvantages to collect complicatedly and significantly with the life cycle inventory with starting from material requisition phase and finishing onto the end of life phase. Therefore, it cannot be achieved in the early design stage at the conceptual design phase.

### 2.5 Quality Function Deployment for Environment (QFDE)

This tool is used to analyse customer and environmental requirements throughout the packaging design development process [11]. Gathering and analysing the voice of the customer for environment is critically important to provide the oriented customer's needs for developing requirement of packaging. Later, customer needs should be translated into technical attributes. QFDE clarifies the relationship between customer requirements and functional quality characteristics. Then, it can be correlated, while functional quality characteristics and packaging components. QFDE method, with its easiness is one of common most in industries same as EPDC tool. For example, Masui et al. [11] develop QFDE to assist design team in considering environmental concerns in the early design stage of product development. This research is corresponding with Bergquist and Abeysekara [12]. They develop the systematically to match between human needs and the product characteristics in the area of ergonomic design. However, this is neither productive for tangibility the problem solving and nor helpful idea generation.

Although, many tools have been developed for eco design, no method or tool available independently supports effectively in functional packaging design at conceptual design phase. So, some researchers apply by integrating tools to support systematically in eco design. For example, Sakao [13] and Kobashachi [14] uses the various eco design techniques for developing eco products and support the decision making process at the conceptual design phase. These researchers suggest that the integrated methodology has a benefit than is obtained from utilizing those tools independently. So, as a result, the current method cannot support in the functional analysis extremely enough in industries. EPDC, FAST, and, FB each of which has potential for providing the packaging function and concept design. The proposed methodology is connected with the following disadvantages when applied independently.

## 3 The proposed methodology

The objective of this research is to develop the functional analysis methodology for eco packaging design. First, the analysis of a design packaging in eco design requires defining in the environmental impacts. Among others, it is crucial, by definition of eco design, to consider the whole life cycle of a packaging from various environmental aspects. It is EPDC that can fulfil these requirements. Second, after understanding in critical impact its life cycle packaging is identified from previous step. The output can be focused in critical phase and define objectively the environmental requirements**.** The Identifications of environmental aspects are systematically translated into the design teams' language. The FAST tool can be used to communicate functional mapping between design team. This tool is analysed the function of packaging and organize the logical relationships between functions. FAST can be accomplished to clarify to the primary and secondary functions of current packaging and determined the mission statement to design improvement. After Second, the functional problem definition needs to consolidate the two major aspects of environmental impact and functional analysis. Third, The FB is applied to identify in functional requirements based upon customer's needs. This section compares with competitors in the current market and analyses the functional improvement level of current packaging. The methodology adopts FB because not only function but also qualities can be addressed. The improvement ratio can be evaluated. The procedure of the proposed methodology is illustrated in Figure 1.

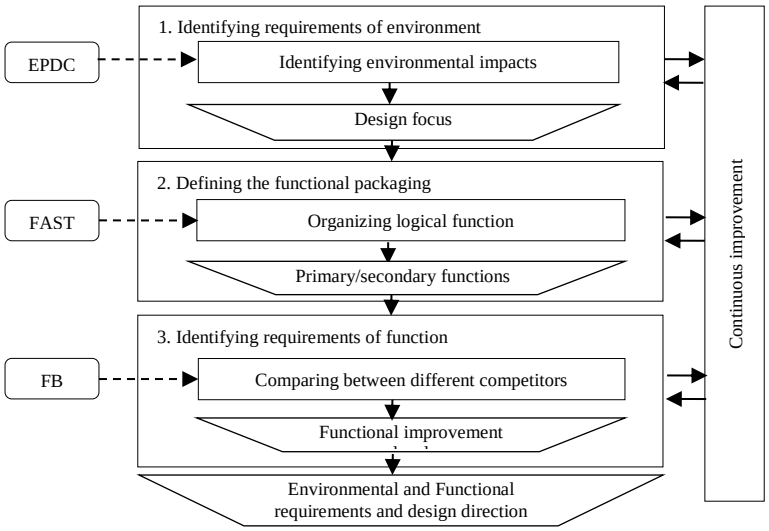



**Figure 1**: The proposed functional analysis methodology for eco packaging design

Figure 1 shows the overview of the functional analysis methodology for environmentally consciousness in packaging design. The steps of object analysis, problem definition, and solution identification with the use of the three tools explained in the previous section are embedded in the upper stream from step 1 to 3. The outputs of those steps are explained in more detail in table 1 with the inputs needed by the tools. For example, the first output of EPDC is used as the second input of FAST. Each step of figure 1 is explained in Table 1.

**Table 1:** Input and output of the three tools and the interrelation among item

| Tools | Inputs (I) | Outputs (O) |
|---|---|---|
| EPDC | 1.Quantitative environmental criteria of the life cycle packaging | 1.Quantitative environmental impacts of critical phase (O1→) |
| FAST | 2. (O1→I2) Translated to engineers' language | 2. organization in the logical relationships between functions (O2→)<br>3. Determined primary and secondary function (O3→) |
| FB | 3. (O2,O3→I3) Functional requirements<br>4. (O4→I4) Function to be improved | 4. Improvement ratio (O4→)<br>5. Identified functional requirements and determined design improvement |

According to Table 1 Input and output of the three tools, the detail is shown as following details.

**Step 1:** Identifying requirements of environment

The requirements of the environment are identified. For the latter, a standardized set of stakeholders ( $n$ ) in life cycle is adopted. The requirements from various stakeholders within the packaging life cycle have been integrated from Material requisition, Manufacturing, Distribution, End used, and disposal. The output can be focused in critical phase and define the environmental requirements objectively**.**From this step is known the environmental requirement priority by calculated the environmental difference level ( $D_i$ ) from comparison between environmental importance ( $A_i$ ) with current packaging ( $B_i$ ). The parameter $D_i$ can be modified value in the normal score by presenting with the normal environmental priority ( $N_i$ ). The Quantitative environmental impacts on the life cycle stage are calculated as the equation (1) - (3).

$$A_i = \frac{\sum_{t=1}^{5}\left[t(X_t)\right]}{n}, B_i = \frac{\sum_{t=1}^{5}\left[t(X_t)\right]}{n} \quad (1)$$

$$D_i = \left(\frac{A_i - B_i}{A_i}\right)\times 100 \quad (2)$$

$$E_i = D_i \Big/ \sum_{i=1}^{I} D_i \quad (3)$$

Where, $X_i$ = environmental impact weighting score at $i$ (1,…,5) by 1 score means low environmental impact and 5 score means high environmental impact

**Step 2:** Defining and organizing the primary and secondary functions

After understanding in critical impact its life cycle packaging is identified from previous step. The design teams can define function systematically to translate into the engineering language by focusing directly onto the critical phase. FAST diagram is applied to organize thoroughly the logical relationships between functions. The design team can define the unnecessary and duplicated functions. This tool can be accomplished to clarify to the primary and secondary functions of current packaging and determined the mission statement to design improvement. The result form FAST diagram is applied to the next step for understanding functional requirements and improvement level of current packaging in market situation.

**Step 3:** Identifying requirements of function and determining the design improvement

As the result from previous step, the primary and secondary functions are identification. Next, it is expanding to functional requirements and translating to engineering characteristics. FB tool is applied to clarify in functional requirements based upon the real customer's needs. This section compares with competitors in the current market. The primary and secondary functions from the previous step are incorporated as the requirements with their weighting in FB. Moreover, it can be determined find out the functional improvement level of current packaging. It is more efficient for design teams to focus on more influential packaging to improve the functional requirements. Thus, the important requirements are investigated by improvement ratio ( $E_i$ ). The importance score of functional requirements which each of competitors ( $C_i^k$ ) are prioritized with score levels (1 is the lower

importance, 5 is the highest importance). The improvement ratio of functional requirements ( $F_i$ ) and Priority Improvement Number ( $PI_i$ ) are calculated as the equation (4) - (7).

$$I_i = \frac{\sum_{t=1}^{5}[t(X_t)]}{n}, C_i^k = \frac{\sum_{t=1}^{5}[t(X_t)]}{n} \quad (4)$$

$$F_i = \underset{i}{Max}\, C_i^k(k_1, k_m) \big/ B_i \quad (5)$$

$$PI_i = \sum_{i}^{I} F_i I_i \quad (6)$$

$$N_i = F_i I_i \Big/ \sum_{i=1}^{I} F_i I_i \quad (7)$$

Where, $\underset{i}{Max}\, C_i^k(k_1, k_m)$ is the chief competitor or the highest importance score in groups ( $k$ ) with $k$ (1,….,$m$ ). The $PI_i$ parameter can be modified value in the normal score by presenting with the Normal Priority Improvement Number ( $N_i$ ). The design teams demonstrate the functional analysis by applying the Pareto's rule 80: 20. This step can be pointed to improve design direction. The MUST and WANT interpretations are described as following.

**MUST** is the critical requirements (20%) of packaging requirements that are high Normal Improvement Priority (% $N_i$ ), high Importance level ( $I_i$ ), and high Improvement Raito ( $F_i$ ).

**WANT** is the uncritical requirements (80%) of packaging requirements that are high Importance level ( $I_i$ ), and low Improvement Raito ( $F_i$ )

## 4 The empirical study in electronic components company

The electronic component is one of the most sensitive products to handling and transportation. It also requires good protective packaging to keep its quality during the manufacturing process and transportation. Moreover, the trend of the new technology also requires smaller and lower weight electronic products whilst with high capacity. From development trend, the electronic components become more fragile and sensitive. So, it is required the material supports such as secondary packaging to preserve the sensitive components during transportation. If packaging is better than necessary or it is an over packaging, the company could lose much money. This task is important directly to design teams who design the appropriate packaging by balancing cost and quality. The design teams should understand in the necessary requirements from stakeholders. That is why this research proposes a way to develop a systematic methodology for functional analysis in packaging design which focuses on the conceptual design phase.

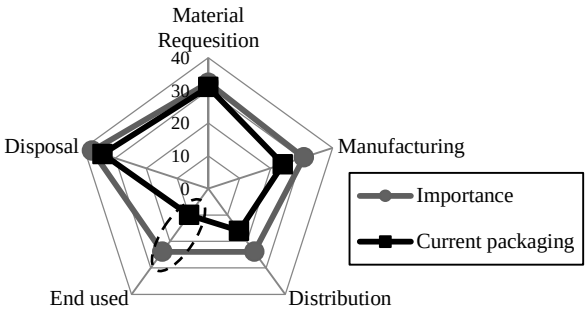
**Step 1:** Identifying requirements of environment

First, EPDC is carried out to determine environmental requirements of life cycle and their weighing in Table 2. The checklist starts with a needs analysis which consists of a series of criteria concerning the environmental function. The main criteria in a need analysis are to define the packaging fulfil its life cycle. Those life cycle stages are following as Material requisition, Manufacturing, Distribution, End used, and disposal. The result of EPDC is illustrated in Table 2.

Second, the set is adjusted the importance score according to the design target of packaging. Third, the quantitative weighting is preferably in equation (1) with five levels for each importance of environmental requirements ( $A_i$ ) and current packaging ( $B_i$ ). EPDC is achieved to show impacts on the environment of life cycle. The EPDC analysis is illustrated in Figure 2.

**Table 2:** Eco Packaging design checklist

| Requiremnets | Checklists | Score | | | |
|---|---|---|---|---|---|
| | | Importance | Current packaging | %Difference | % Normal Priority |
| Material | -Non toxicity | 4.75 | 5 | -5.3 | -1% |
| Requesition | -Recyclable materials | 4.87 | 5 | -2.7 | 0% |
| | -Reduced emission | 4.32 | 3 | 30.6 | 5% |
| | -Cleaner material | 3 | 4 | -33.3 | -5% |
| | -Renewable materials | 3.2 | 2 | 37.5 | 6% |
| | -Lower direct material | 4.98 | 4 | 19.7 | 3% |
| | -Lower indirect material | 3.5 | 4 | -14.3 | -2% |
| | -Lower energy | 3.7 | 4 | -8.1 | -1% |
| | **Sum** | **32.32** | **31** | **4.08** | |
| Manufacturing | - Production Machinability | 4.97 | 3 | 39.6 | 6% |
| | -Common equipments | 4.97 | 3 | 39.6 | 6% |
| | -Cleaner production | 3.4 | 4 | -17.6 | -3% |
| | -Lower energy | 4.2 | 4 | 4.8 | 1% |
| | -Lower emission | 4.1 | 4 | 2.4 | 0% |
| | -Tear down in process | 4.5 | 4 | 11.1 | 2% |
| | -Ease of assembly | 4.6 | 2 | 56.5 | 8% |
| | **Sum** | **30.74** | **24** | **21.93** | |
| Distribution | -Storage area efficient | 4.98 | 4 | 19.7 | 3% |
| | -Container load efficient | 4.78 | 4 | 16.3 | 2% |
| | -Backhaul efficient | 4.91 | 1 | 79.6 | 12% |
| | -Common material handling | 4.3 | 5 | -16.3 | -2% |
| | -Energy used efficiency | 4.95 | 2 | 59.6 | 9% |
| | **Sum** | **23.92** | **16** | **33.11** | |
| End used | -Ease of use | 4.98 | 1 | 79.9 | 12% |
| | -Safety use | 5 | 2 | 60.0 | 9% |
| | -Useful lifetime | 4.86 | 2 | 58.8 | 9% |
| | -Adjustable size in storage | 4.5 | 1 | 77.8 | 12% |
| | -Reuseability | 4.6 | 4 | 13.0 | 2% |
| | **Sum** | **23.94** | **10** | **58.23** | |
| Disposal | -Lower energy consumption | 3 | 4 | -33.3 | -5% |
| | -Modular disassembly | 4.95 | 4 | 19.2 | 3% |
| | -Lower waste emission | 3.4 | 4 | -17.6 | -3% |
| | -Waste reusability | 4.89 | 4 | 18.2 | 3% |
| | -Waste recyclability | 4.35 | 4 | 8.0 | 1% |
| | -Lower disassembly time | 4.7 | 3 | 36.2 | 5% |
| | -Identifiable waste materials sorting | 3.78 | 4 | -5.8 | -1% |
| | -Transformative function | 4.15 | 2 | 51.8 | 8% |
| | -Non toxic treatment | 4.15 | 5 | -20.5 | -3% |
| | **Sum** | **37.37** | **34** | **9.02** | |




| Life cycle phase | Importance | Current packaging | %Difference |
|---|---|---|---|
| Material Requesition | 32.32 | 31 | 4.08 |
| Manufacturing | 30.74 | 24 | 21.93 |
| Distribution | 23.92 | 16 | 33.11 |
| End used | 23.94 | 10 | 58.23 |
| Disposal | 37.37 | 34 | 9.02 |
| Total | 148.29 | 115 | 22.45 |

**Figure 2:** Eco Packaging Design Checklist in the current packaging

According to Figure 2 illustrates that the end used stage (%Difference = 58.23) is the most highly weighted among the serious environmental requirements in the problem situation of current packaging. The total score of life cycle impact is shown in the Figure 3.

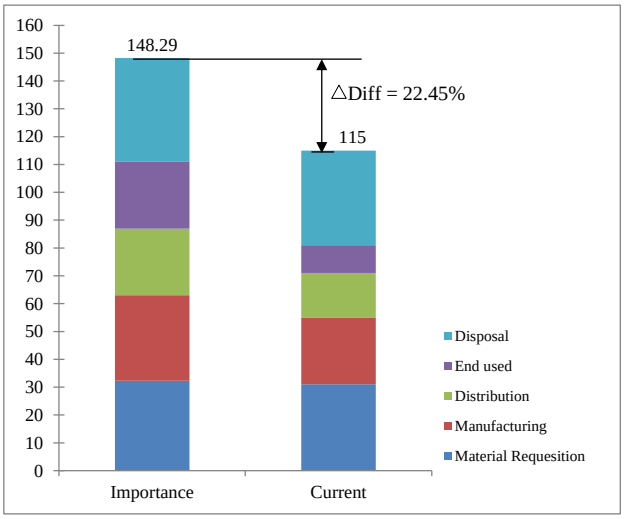



**Figure 3**: Total score of the environmental requirements

According to the Figure 3 shows that the total environmental requirements score of current packaging is larger difference with the importance weighting score (%difference = 22.45). It should be pointed out that the some environmental requirements in current packaging can be improved specially at the end used stage referring form the previous result in Figure 2. The critical environmental requirements are defined by using Pareto's rule 80:20 is shown in Figure 4.

| No. | Checklists | % Normal Priority | Cumulative Frequency |
|---|---|---|---|
| 1 | -Ease of use | 12% | 12.01% |
| 2 | -Backhaul efficient | 12% | 23.99% |
| 3 | -Adjustable size in storage | 12% | 35.68% |
| 4 | -Safety use | 9% | 44.70% |
| 5 | -Energy used efficiency | 9% | 53.66% |
| 6 | -Useful lifetime | 9% | 62.50% |
| 7 | -Ease of assembly | 8% | 71.00% |
| 8 | -Transformative function | 8% | 78.79% |
| 9 | - Production Machinability | 6% | 84.75% |
| 10 | -Common equipments | 6% | 90.71% |
| 11 | -Renewable materials | 6% | 96.34% |
| 12 | -Lower disassembly time | 5% | 101.78% |
| 13 | -Reduced emission | 5% | 106.37% |
| 14 | -Lower direct material | 3% | 109.33% |
| 15 | -Storage area efficient | 3% | 112.29% |
| 16 | -Modular disassembly | 3% | 115.18% |
| 17 | -Waste reusability | 3% | 117.91% |
| 18 | -Container load efficient | 2% | 120.36% |
| 19 | -Reuseability | 2% | 122.33% |
| 20 | -Tear down in process | 2% | 124.00% |
| 21 | -Waste recyclability | 1% | 125.21% |
| 22 | -Lower energy | 1% | 125.92% |
| 23 | -Lower emission | 0% | 126.29% |
| 24 | -Recyclable materials | 0% | 125.89% |
| 25 | -Non toxicity | -1% | 125.10% |
| 26 | -Identifiable waste materials sorting | -1% | 124.22% |
| 27 | -Lower energy | -1% | 123.00% |
| 28 | -Lower indirect material | -2% | 120.85% |
| 29 | -Common material handling | -2% | 118.41% |
| 30 | -Cleaner production | -3% | 115.75% |
| 31 | -Lower waste emission | -3% | 113.10% |
| 32 | -Non toxic treatment | -3% | 110.02% |
| 33 | -Cleaner material | -5% | 105.01% |
| 34 | -Lower energy consumption | -5% | 100.00% |

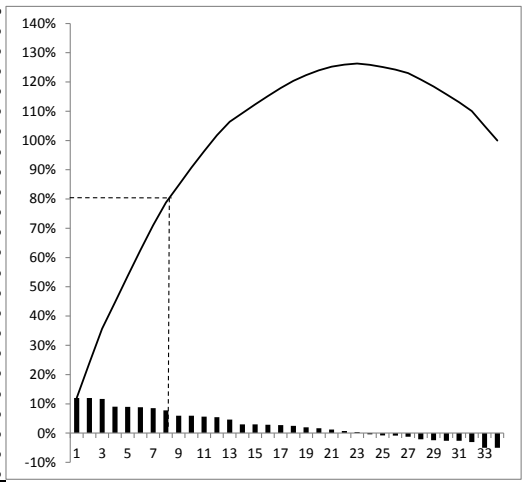



**Figure 4**: Total score of the environmental requirements

According to the Figure 4 is shown in the environmental requirements of current packaging by using Pareto's rule 80:20. The design teams can define the critical environmental requirements for focusing on packaging conceptual design. These are following of the eight environmental requirements; ease of use, backhaul efficient,

adjustable size in storage, safety use, energy used efficiency, useful lifetime, ease of assembly, and transformative function.

**Step 2:** Identifying packaging functions

First, FAST diagram can define the packaging specifications to address the requirements especially in end used stage following the result from the EPDC previous step. Second, the packaging designers should be set the mission statement of packaging to focus on design in end used stage. This step can be obtained the common function, high order function, and right customers who are highlighted affect directly from packaging design. The mission statements are following as details.

| | |
|---|---|
| Mission statement | Secondary packaging for electronic components inside factory |
| Common Function: | Containment the electronic components are typically grouped together in one packaging |
| Higher Order Function: | -High productivity |
| | -Eco friendly |
| Right Customers: | End user (Distributor and operators inside electronic components ) |

Third, FAST diagram analyses the primary and secondary function at the end used stage. This is illustrated in Figure 5.

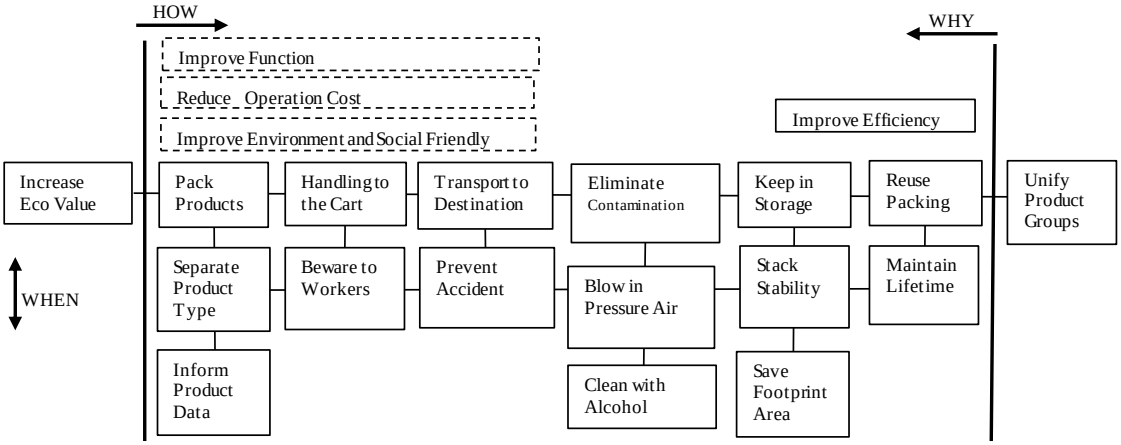



**Figure 5:** FAST diagram for secondary packaging of electronic components

According to Figure 5, the FAST diagram for secondary packaging of electronic components at the end used stage is presented. The common function of current packaging is to unify product groups. Then, target of proposed packaging design or the high order function is increasing eco value. The design team defines the primary and secondary functions at the end used stage and identify by each of process activities. The primary functions are following as pack products, handling to the cart, transport to destination, eliminate contamination, keep in storage, and reuse packing. In addition, the secondary functions are following as separate product type, inform product data, beware to workers, prevent accident, blow in pressure air, clean with alcohol, stack stability, save footprint area, and, maintain lifetime. This step can assist design teams to define and organize the logical relationships between functions. FAST diagram can be used to verify and show how a proposed design achieves the requirements of the functional packaging. The results from FAST have been added to FB in the next step for understanding in the current situation and identifying the improvement level.

**Step 3:** Identifying requirements of function and determining the design improvement

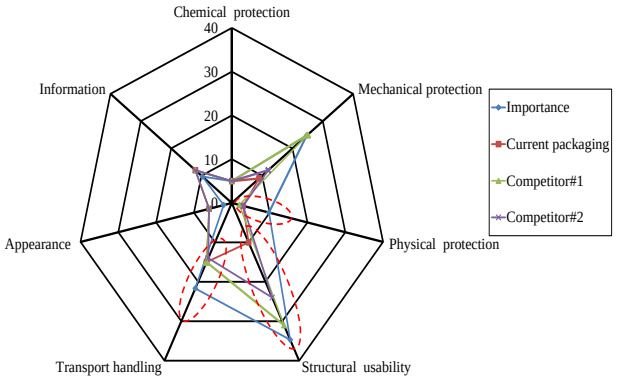
The design focus is represented in functional requirements, as well as comparing with the competitors in the market. It is very important to consider not only environmental requirements bus also functional requirements. The outputs from FAST are helpful to understand the design focus on functional packaging design. In the conceptual design, the design teams require the functional requirements from customers to set the input for driving in design concept. First, FB is fulfilled to define functional requirements from stakeholders weighing. The result of case study is shown in Table 3.

The requirement starts with a functional analysis, which consists of a series of criteria concerning the function based upon the result from FAST in previous step. Second, the set is adjusted the importance score ($I_i$) according to the target of packaging (baseline). Third, the quantitative weighting of competitors ($C_i^k$) is preferably in equation (4) with five levels for each functional requirements. This step can define the chief

competitor ( $\underset{i}{Max}\, C_i^k(k_1, k_m)$ ) or the highest importance score in groups. Fourth, the improvement ratio ( $F_i$ ) can be calculated preferring in equation (5). The both of $F_i$ and $I_i$ parameters are related with $PI_i$ as equation (6). The $PI_i$ results can be modified value in the normal score by presenting with the normal environmental priority ( $N_i$ ) in equation (7). Each requirement is higher $N_i$ score, that meaning is effected largely influencing the functional impacts and improved seriously functionality of current packaging. The FB result is illustrated in Figure 6.

**Table 3:** The functional requirements of secondary packaging for containment of electronic components

| | | | Score | | | | | | | Evalution | | | | | | |
|---|---|---|---|---|---|---|---|---|---|---|---|---|---|---|---|---|
| | | | Importance | Current packaging | Competitor#1 | Competitor#2 | Improvement raito | Priority improvement number | % Normal Priority | 1 low | 2 | Surverying company (▶) 3 | Chief competitor ( ⊗) 4 | 5 hight | | Interpretation |
| Criteria | Sub criteria | Checklists | | | | | | | | | | | | | | |
| Lifetime preservation | Chemical protection | -Compatable material type | 5.00 | 5.00 | 5.00 | 5.00 | 1.00 | 5.00 | 1.69 | | | | | ⊗ | | |
| | | -Chemical migration | 0.00 | 0.00 | 0.00 | 0.00 | 0.00 | 0.00 | 0.00 | | | | | | | |
| | | -$CO_2$,$O_2$ gas vapors | 0.00 | 0.00 | 0.00 | 0.00 | 0.00 | 0.00 | 0.00 | | | | | | | |
| | | -Micro organisms | 0.00 | 0.00 | 0.00 | 0.00 | 0.00 | 0.00 | 0.00 | | | | | | | |
| | | -Anti contamination | 0.00 | 0.00 | 0.00 | 0.00 | 0.00 | 0.00 | 0.00 | | | | | | | |
| | | -Odor protection | 0.00 | 0.00 | 0.00 | 0.00 | 0.00 | 0.00 | 0.00 | | | | | | | |
| | Mechanical protection | -Shock | 4.98 | 1.00 | 5.00 | 1.00 | 5.00 | 24.90 | 8.40 | | | | ⊗ | | | MUST |
| | | -Compression | 4.95 | 5.00 | 5.00 | 4.00 | 1.00 | 4.95 | 1.67 | | | | | ⊗ | | |
| | | -Vibration | 4.89 | 1.00 | 5.00 | 1.00 | 5.00 | 24.45 | 8.25 | | | | ⊗ | | | MUST |
| | | -Puncturing | 4.93 | 1.00 | 5.00 | 2.00 | 5.00 | 24.65 | 8.32 | | | | ⊗ | | | MUST |
| | | -Abrasion | 4.88 | 1.00 | 5.00 | 4.00 | 5.00 | 24.40 | 8.24 | | | | ⊗ | | | MUST |
| | Physical protection | -Temperature control | 0.00 | 0.00 | 0.00 | 0.00 | 0.00 | 0.00 | 0.00 | | | | | | | |
| | | -Light protection | 0.00 | 0.00 | 0.00 | 0.00 | 0.00 | 0.00 | 0.00 | | | | | | | |
| | | -Humid resistant | 0.00 | 0.00 | 0.00 | 0.00 | 0.00 | 0.00 | 0.00 | | | | | | | |
| | | -Contamination | 4.90 | 1.00 | 1.00 | 1.00 | 1.00 | 4.90 | 1.65 | ⊗ | | | | | | WANT |
| | | -Rusting | 0.00 | 0.00 | 0.00 | 0.00 | 0.00 | 0.00 | 0.00 | | | | | | | |
| | | -Sterility loss | 0.00 | 0.00 | 0.00 | 0.00 | 0.00 | 0.00 | 0.00 | | | | | | | |
| | | -Child resistant | 0.00 | 0.00 | 0.00 | 0.00 | 0.00 | 0.00 | 0.00 | | | | | | | |
| | | -Tamper evidence | 0.00 | 0.00 | 0.00 | 0.00 | 0.00 | 0.00 | 0.00 | | | | | | | |
| | | -Maintainability | 4.92 | 2.00 | 1.00 | 2.00 | 1.00 | 4.92 | 1.66 | | ⊗ | | | | | WANT |
| Convenience | Structural usability | -Uncomplicated structure | 5.00 | 1.00 | 4.00 | 3.00 | 4.00 | 20.00 | 6.75 | | | | ⊗ | | | MUST |
| | | -Reusability | 0.00 | 0.00 | 0.00 | 0.00 | 0.00 | 0.00 | 0.00 | | | | | | | |
| | | -Comfortable opening | 0.00 | 0.00 | 0.00 | 0.00 | 0.00 | 0.00 | 0.00 | | | | | | | |
| | | -Quantity measuring aids | 0.00 | 0.00 | 0.00 | 0.00 | 0.00 | 0.00 | 0.00 | | | | | | | |
| | | -Comfortable grip | 4.98 | 1.00 | 5.00 | 5.00 | 5.00 | 24.90 | 8.40 | | | | ⊗ | | | MUST |
| | | -Comfortable pouring | 4.95 | 1.00 | 5.00 | 2.00 | 5.00 | 24.75 | 8.35 | | | | ⊗ | | | MUST |
| | | -Dispensing devices | 0.00 | 0.00 | 0.00 | 0.00 | 0.00 | 0.00 | 0.00 | | | | | | | |
| | | -Controlled dosing | 0.00 | 0.00 | 0.00 | 0.00 | 0.00 | 0.00 | 0.00 | | | | | | | |
| | | -Durability | 4.94 | 1.00 | 5.00 | 3.00 | 5.00 | 24.70 | 8.34 | | | | ⊗ | | | MUST |
| | | -Component optimisation | 4.97 | 1.00 | 5.00 | 1.00 | 5.00 | 24.85 | 8.39 | | | | ⊗ | | | MUST |
| | | -Weight optimisation | 4.88 | 2.00 | 3.00 | 5.00 | 2.50 | 12.20 | 4.12 | | | | ⊗ | | | MUST |
| | | -Volume optimisation | 4.97 | 3.00 | 4.00 | 5.00 | 1.67 | 8.28 | 2.80 | | | | ⊗ | | | |
| | Transport handling | -Packed size capacity | 4.88 | 1.00 | 2.00 | 1.00 | 2.00 | 9.76 | 3.29 | | ⊗ | | | | | MUST |
| | | - Material handling ability | 3.50 | 4.00 | 4.00 | 4.00 | 1.00 | 3.50 | 1.18 | | | | | ⊗ | | |
| | | -Standard size | 3.60 | 4.00 | 4.00 | 4.00 | 1.00 | 3.60 | 1.22 | | | | | ⊗ | | |
| | | -Returnability | 4.75 | 2.00 | 1.00 | 2.00 | 1.00 | 4.75 | 1.60 | | ⊗ | | | | | WANT |
| | | -Stable stacking | 4.95 | 4.00 | 4.00 | 3.00 | 1.00 | 4.95 | 1.67 | | | | | ⊗ | | |
| Communication | Appearance | -Selling capability | 1.03 | 3.00 | 3.00 | 3.00 | 1.00 | 1.03 | 0.35 | | | | ⊗ | | | |
| | | -Promotional branding | 0.00 | 0.00 | 0.00 | 0.00 | 0.00 | 0.00 | 0.00 | | | | | | | |
| | | -Display attractiveness | 1.12 | 3.00 | 3.00 | 3.00 | 1.00 | 1.12 | 0.38 | | | | ⊗ | | | |
| | Information | -Manual instructions | 1.11 | 2.00 | 2.00 | 2.00 | 1.00 | 1.11 | 0.37 | | | ⊗ | | | | |
| | | -Legal information | 3.00 | 3.00 | 3.00 | 3.00 | 1.00 | 3.00 | 1.01 | | | | ⊗ | | | |
| | | -Product identification | 1.50 | 4.00 | 4.00 | 4.00 | 1.00 | 1.50 | 0.51 | | | | | ⊗ | | |
| | | -Traceability | 4.09 | 3.00 | 3.00 | 3.00 | 1.00 | 4.09 | 1.38 | | | | ⊗ | | | |
| | | Total | 107.67 | 60.00 | 96.00 | 76.00 | 1.60 | 296.26 | 100.00 | | | | | | | |




| Criteria | Importance | Current packaging | Competitor#1 | Competitor#2 |
|---|---|---|---|---|
| Chemical protection | 5.00 | 5.00 | 5.00 | 5.00 |
| Mechanical protection | 24.63 | 9.00 | 25.00 | 12.00 |
| Physical protection | 9.82 | 3.00 | 2.00 | 3.00 |
| Structural usability | 34.69 | 10.00 | 31.00 | 24.00 |
| Transport handling | 21.68 | 15.00 | 15.00 | 14.00 |
| Appearance | 2.15 | 6.00 | 6.00 | 6.00 |
| Information | 9.70 | 12.00 | 12.00 | 12.00 |
| Overall | 107.67 | 60.00 | 96.00 | 76.00 |
| %Difference | Baseline | 44.3 | 10.8 | 29.4 |

**Figure 6:** Radars chart of packaging functionality

According to Figure 6 shows the critical point of function by comparison with competitors in the secondary packaging for electronic components in the current market. The weak points of current packaging are defined with three functionalities following as physical protection, structural usability, and transport handling. The overall functionality of packaging requirements at the current market is illustrated in Figure 7.

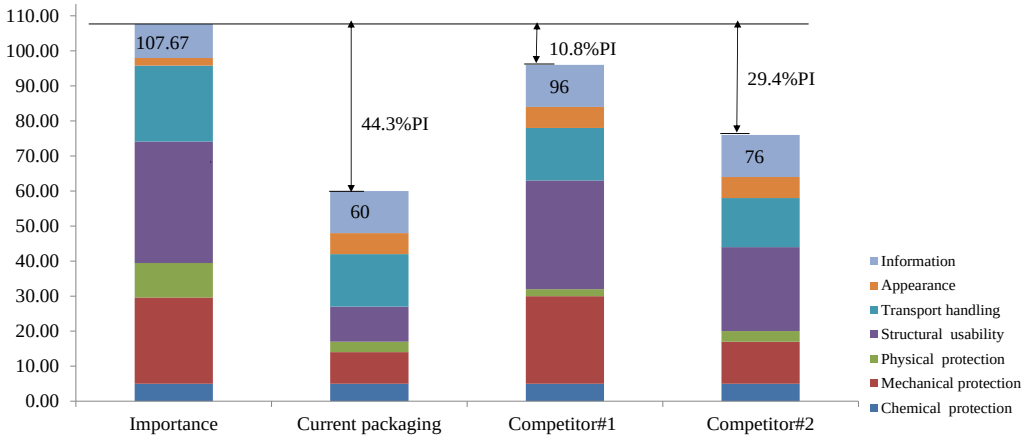



**Figure 7:** The overall functionality of packaging requirements

| No. | Product/Packaging Requirements | % Normal Priority | Freqeuncy |
|---|---|---|---|
| 1 | -Shock | 8.40 | 8.40 |
| 2 | -Comfortable grip | 8.40 | 16.81 |
| 3 | -Component optimisation | 8.39 | 25.20 |
| 4 | -Comfortable pouring | 8.35 | 33.55 |
| 5 | -Durability | 8.34 | 41.89 |
| 6 | -Puncturing | 8.32 | 50.21 |
| 7 | -Vibration | 8.25 | 58.46 |
| 8 | -Abrasion | 8.24 | 66.70 |
| 9 | -Harmless structure | 6.75 | 73.45 |
| 10 | -Weight optimisation | 4.12 | 77.57 |
| 11 | -Packed size capacity | 3.29 | 80.86 |
| 12 | -Volume optimisation | 2.80 | 83.66 |
| 13 | -Compatable material type | 1.69 | 85.34 |
| 14 | -Compression | 1.67 | 87.01 |
| 15 | -Stable stacking | 1.67 | 88.69 |
| 16 | -Maintainability | 1.66 | 90.35 |
| 17 | -Contamination | 1.65 | 92.00 |
| 18 | -Returnability | 1.60 | 93.60 |
| 19 | -Traceability | 1.38 | 94.98 |
| 20 | -Standard size | 1.22 | 96.20 |
| 21 | - Material handling ability | 1.18 | 97.38 |
| 22 | -Legal information | 1.01 | 98.39 |
| 23 | -Product identification | 0.51 | 98.90 |
| 24 | -Display attractiveness | 0.38 | 99.28 |
| 25 | -Manual instructions | 0.37 | 99.65 |
| 26 | -Selling capability | 0.35 | 100.00 |

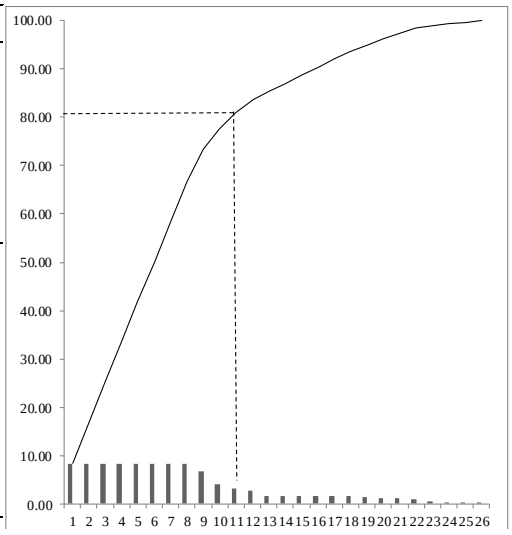



**Figure 8:** MUST/WANT functional requirements

According to the Figure 7 illustrates that the packaging competitor#1 is highest functional requirement score (96 points) and lowest percent improvement (10.8% *PI* ). The current packaging is lowest functional requirement score (60 points) and highest percent improvement (44.3% *PI* ). This stage is to clarify the situation and compares with competitors in market. The results show the strong points and weak points of current packaging.

The design teams can fine the direction to develop the concept packaging by analyzing MUST/WANT functional requirements from applying Pareto's rule 80: 20. The results are presented in Figure 8. The critical functionality is MUST requirements that are high Normal Improvement Priority (% $N_i$ ), high Importance level ( $I_i$ ), and high Improvement Raito ( $F_i$ ). These requirements have the lists of packaging requirements as follows; shock, comfortable grip component optimization, durability, puncturing, vibration, abrasion, harmless structure, weight optimization, and packed size capacity. These are very important with customer requirement and needs to improvement seriously. Continuously, the uncritical functionality (80%) is WANT requirements that are high Importance level ( $I_i$ ), and low Improvement Raito ( $F_i$ ).These requirements have the lists of packaging requirements following as contamination, maintainability, and return ability. These are very important with customer satisfactions and require to progressive development. The objective of the empirical case study in secondary packaging of electronic components company is to develop the methodology of functional analysis for eco packaging design. This methodology is crucial to consider not only environmental requirements but also functional requirements. As the results of case study is to start from identified the critical environmental impact its life cycle packaging by applying EPDC. This step is known the critical environmental impacts of current packaging for setting the scope of design. Then, Functions of packaging focus especially in critical phase and organized the primary and secondary function by using FAST. Finally, Functions of packaging are translated to engineering characteristics and identified the functional improvement level for design direction.

## 5 Conclusions

The functional analysis methodology for environmentally conscious packaging design is presented in this paper. The objective of this research is to develop a functional analysis methodology for supporting environmentally consciousness in packaging design at conceptual design phases. The methodology is obtained from using three tools: EPDC, FAST, and FB. The presented methodology is tested through application to the secondary packaging for containment electronic components. This method, in addition, can determine the environmental and functional requirements. The methodology has majoring advantages than applying those three tools independently. The advantages of this research are supporting with the result of Sakao [13] in eco design methodology. He develops the methodology for environmentally conscious by integrating three tools as LCA, QFD, and TRIZ (theory of inventive problem solving) into product design at conceptual design phase. However, his research has some gap in the early design phase is very difficult to collect complicatedly and significantly with the life cycle inventory of quantitative environmental profiles.

According to this research can fulfil in gap of the research problem by applying three tools with its easiness, fastness, and idea generation for design team in industry. The methodology uses EPDC tool to assess the environmental impacts. The results can be pointed to the critical requirements and notified for environmental impact situation of current packaging. After design team understanding in environmental impacts and current situation of packaging, the functional packaging is identified by using the results from previous step. As an output, the focus design in the packaging usage phase. The FAST tool can be helped to define the functional problem objectively and organized the logical relationships between functions. The design team can be clarified to the primary and secondary functions of current packaging and determined the mission statement to design improvement. In addition, this methodology is crucial to consider not only environmental aspects but also functional aspects. The FB is applied to clarify in functional requirements based upon customer's needs. This section compares with competitors in the current market and analyses the functional improvement level of current packaging. FB can help the design teams to prioritize the functional requirements to design improvement. However, the section of defining functional analysis by applying FB tool is rather sensitive in chief competitor selection. Because the current secondary packaging for electronic components in the current market have been increasing competitors of various options for containment electronic components.

The design team should be classified the competitor's categories before deciding which baseline reference by using the recommended tool as Kano's Model [4] for prioritizing the competitors of packaging. The limitation of this methodology is suitably applied in the secondary packaging for containment electronic components inside factory. The general requirement in this packaging type is not serious to consider into graphic design for good appearance and attractiveness than primary packaging type. Therefore, this methodology will be applied into other types such as primary packaging, it should be crucial to consider not only functional and environmental aspects bust also satisfactory aspects from customers. The further studies, this research could also include further in idea generation for the eco packaging design after identifying in environmental and functional requirements. The researcher will develop the methodology to support the idea creativity and how to select the appropriated idea by integrating the values of the functional and environmental perspectives.

## Acknowledgements

The authors would like to gratefully acknowledge the substantial support provided by Department of International Affairs and Department of Printing and Packaging Technology, School of Science and Technology, Sukhothai Thammathirat Open University (STOU).

## References

[1] J.H. Briston and T.J. Neill, 1972, Packaging Management, Gower Press, London pp. 1-4.

[2] International Standard Organisation, 2002, ISO/TR 14062: Environmental Management-Integrating Environmental Aspects into Product Design and Development.

[3] W. Wimmer, 2001, Eco Design Pilot, Kluwer Academics Publishers, Vienna.

[4] R.G. Day, 1993, Quality Function Deployment linking a Company with Its Customers, ASQC Quality Press, United State of America.

[5] E. Svanes, et al., 2010, "Sustainable packaging design: a holistic methodology for packaging design", Packaging Technology and Science, vol. 23, pp.161-175.

[6] D.L. Miles, 1972, Techniques of Value Analysis and Engineering, McGraw-Hill, New York.

[7] International Standard Organisation, 2006, ISO14040: Environmental management: Life Cycle Assessment: Principles and framework.

[8] S. Madival, R. Auras, S.P. Singh, and R, Narayan, 2009, "Assessment of the environmental profile of PLA, PET and PS clamshell containers using LCA methodology", Journal of Cleaner Production, vol.17, pp. 1183-1194.

[9] P.H. Nielsen and H. Wenzel, 2002, "Integration of environmental aspects in product development: a stepwise procedure base on quantitative life cycle assessment", Journal of Cleaner Production, vol. 10, pp. 247-257.

[10] K.L. Verghese, R. Horne, and A. Carre, 2010, "PIQET: the design and development of an online 'streamline' LCA tool for sustainable packaging design decision support", International Journal of Life Cycle Assess, vol. 15, pp. 608-620.

[11] K. Masui, T. Sakao, and A. Inaba, 2001, "Quality function deployment for environment: QFDE (1st Report): A methodology in early stage of DfE", IEEE, pp. 852-857.

[12] K. Bergquist and J. Abeysekara, 1996, "Quality Function Deployment (QFD) – A means for developing usable products", International Journal of Industrial Ergonomics, vol.18, pp. 269-275.

[13] T. Sakao, 2007, "A QFD-centred design methodology for environmental conscious product design", International Journal of Production Research, Vol.45, No.18, pp. 4143–4162.

[14] H. Kobayashi, 2006, "A systematic approach to eco- innovative product design based on life cycle planning", Advanced Engineering Informatics, Vol.20, pp.113-125.

# Easy Opening or a Lost 16% Sale

**Søren R Østergaard[1] and Helle Antvorskov[1*]**

[1] *Packaging, Danish Technological Institute, Denmark*

[*]*Corresponding author. Email: hean@dti.com*

**Abstract:** The consumers expect the packaging to be functional and to fulfil their specific needs in every way. A national Danish project has documented that 40 per cent experience difficulties, when handling and opening packaging at least once a month, and as a consequence, 16 per cent of the consumers refuse to buy the product next time they go shopping. The issues are worsening due to the expansion of the elderly population in the upcoming decades all over the world. In Denmark the amount of people in the age more than 65 years old will rise to index 170 in 2050 compared to 2010. It is also noticeable that 700,000 people in Denmark have a rheumatic associated condition, which account for 13 per cent of the population. Therefore, the chance of excluding a part of an enterprise´s target group is every likely, making easy-to-open packaging more relevant than ever. From our experience, the enterprises' most common attitude toward changing the packaging design is associated with economic frustration. Most enterprises have very expensive and effective packaging lines and often the enterprises do not recognize the economic potential of a new packaging design. The trade-off of consumers is simply not common knowledge of many small and medium sized enterprises. The culture among the consumers in Denmark means, that the consumers do not communicate problems directly to the enterprises. They tell their neighbours and friends if they experience difficulties with a product. This attitude makes is almost impossible to rely on complains as an indicator of the consumer satisfaction with a product. The enterprise needs to collect the information directly from the consumer in order to evaluate the performance of their products. The project "User friendly packaging – Guideline for the industry" seeks to address these issues. The main deliverable is a web-based guideline. The guideline contain collected knowledge regarding the attitudes of the consumers and issues to address about packaging design, also, the guideline contain a step by step process to develop easy-to-open packaging. The guideline is constructed in a way that allows the enterprise to pick and choose in respect to the enterprise´s needs and competences. The main focus in the development of the guidelines has been to produce a tool that function in a practical manner instead of communicating the absolute scientific truth.

Keywords: Easy opening, lost sale, guideline, usability, packaging performance, consumer.

## 1. Easy opening and packaging

### 1.1 The validity of the study and grouping of data

The test group consists of 285 persons, and is therefore too small a number to be statically valid.

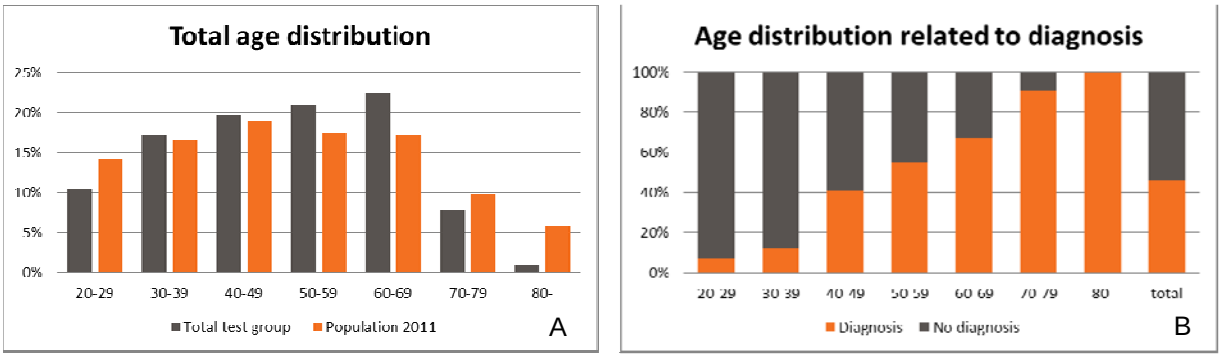



**Figure 1:** see the caption on the following page

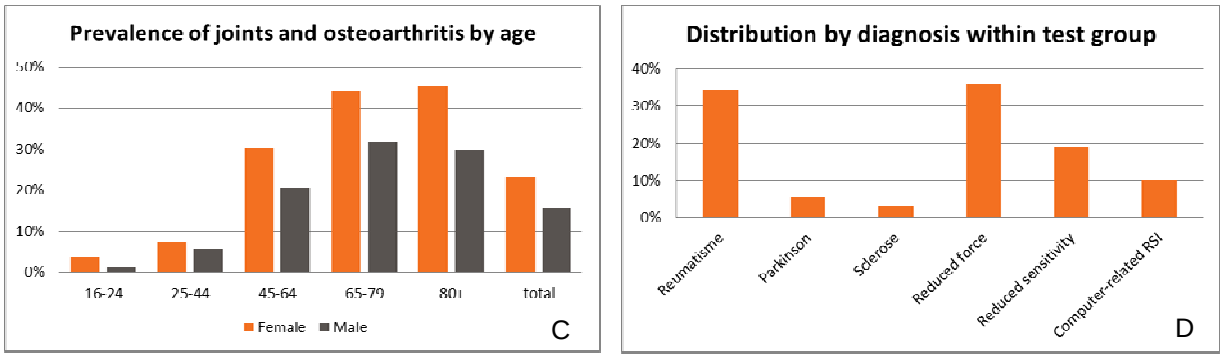



**Figure 1**: Group composition classified on age and occurrence of "diagnosis" according to image D. image A shows the total test group compared to the age distribution of the population in Denmark (Source: Statistics Denmark, 2011). Image B shows the age distribution of the test group classified as "diagnosis" and "no diagnosis", where the group with a diagnosis make up 46 % of the test group. Image C shows the spreading of osteoarthritis or rheumatoid arthritis in the population divided on gender (Source: public health group survey report, National Institute of Public Health, Copenhagen 2007.) Image D shows the classification for the whole test group of diseases and decreased functionality, which overall is classified as "diagnosis".

Problems with the packaging are evaluated subjectively by the consumer:

Subsequently the data material is grouped according to how often the test group experiences problems with packaging. It is completely subjectively for each respondent to determine when an experience with a packaging becomes a problem. Experiences with user studies, from the project User friendly Packaging, shows that there is a significant difference to how difficult a packaging must be before it is seen as a problem. It solely depends on the general philosophy of life and frame of reference of the respondent. The classification of the group with and without diagnosis is shown in Figure 2. It can be seen from Figure 2A, that the test group without diagnosis relatively often experiences problems with packaging, as approx. 20 % experiences problems on a weekly basis and over half of the group experiences problems at least once a month. Only approx. 20 % almost never experiences problems. The conclusion is that regardless if it is real problems with the packaging, it can be established that the problems with packaging take up a lot in the conscience of the reference group. The point is therefore, that the subject is of great importance to the everyday life of the ordinary population.

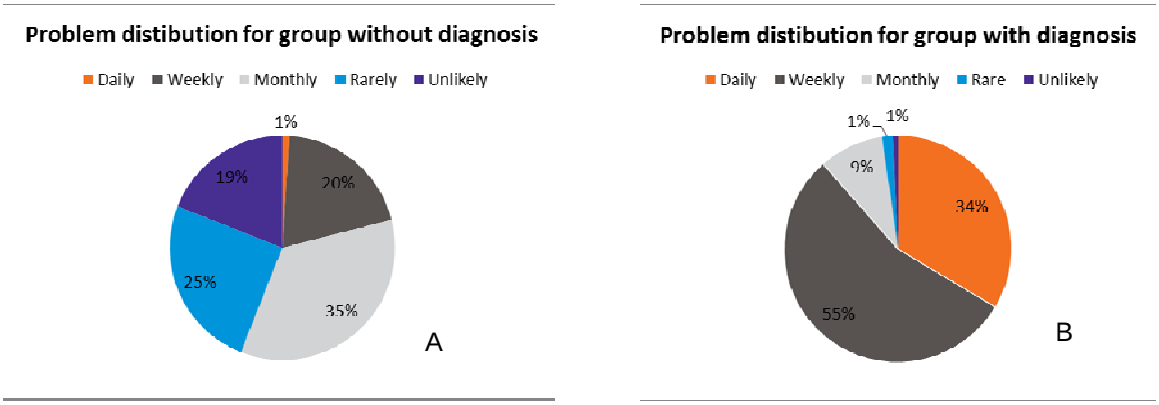



**Figure 2:** Distribution of how many per cent and how often each group experiences problems with packaging, where group A) is persons without a diagnosis and group B) persons with a diagnosis, which affects the function of arms and hands (see Figure 1D for definition of diagnosis).

As it was expected, it can be seen from Figure 2B, that the group with a diagnosis often experiences problems with packaging. 34 % experiences problems daily, while almost 90 % of the group experiences problems at least once a week.

If these figures are compared to the population survey from 2006[1] it can be determined, that the group with daily problems with packaging add up to 100.000-200.000 persons depending on packaging type, corresponding to group 1 in Figure 2A.

[1] http://www.gigtforeningen.dk/files/presse/gigtforeningen_noegletal.pdf

## At least 200.000 persons in Denmark have daily problems with packaging

The Danish rheumatoid arthritis society states that approximately 700.000 persons have osteoarthritis or rheumatoid arthritis, of these 210.000 persons have been diagnosed by a physician. The age composition can be seen in Figure 1C.

Internationally it is estimated that 10 % of men and 18 % of women at the age of 60 or more have symptomatic osteoarthritis. The occurrence culminates in the age group 65-74 years among women and in the age group 75 years or more among men[2].

### 1.2 Consumers attitude to user friendly packaging

## Classification according to experienced problems

In the following classification of data there has not been distinguished between consumers with diagnosis and consumers with average strength according to Figure 2, but only on the frequency of the consumers experienced problems. It makes sense, as it is the consumer's experience with packaging which is essential for the consumer's behaviour and motivation for choosing user friendly packaging in future purchases. The test group is divided into 5 groups and the classification can be seen in Figure 3A:

- Group 1 – Daily problems
- Group 2 – Weekly problems
- Group 3 – Monthly problems
- Group 4 – Rarely problems
- Group 5 – Almost never problems

In Figure 3B it can be seen, that the majority of persons with decreased functionality is found in group 1 and group 2, as was expected. It can be seen, that there is an exact identity between the occurrence of arthritis and reduced strength, which make probable the influence of arthritis in the everyday life of consumers.

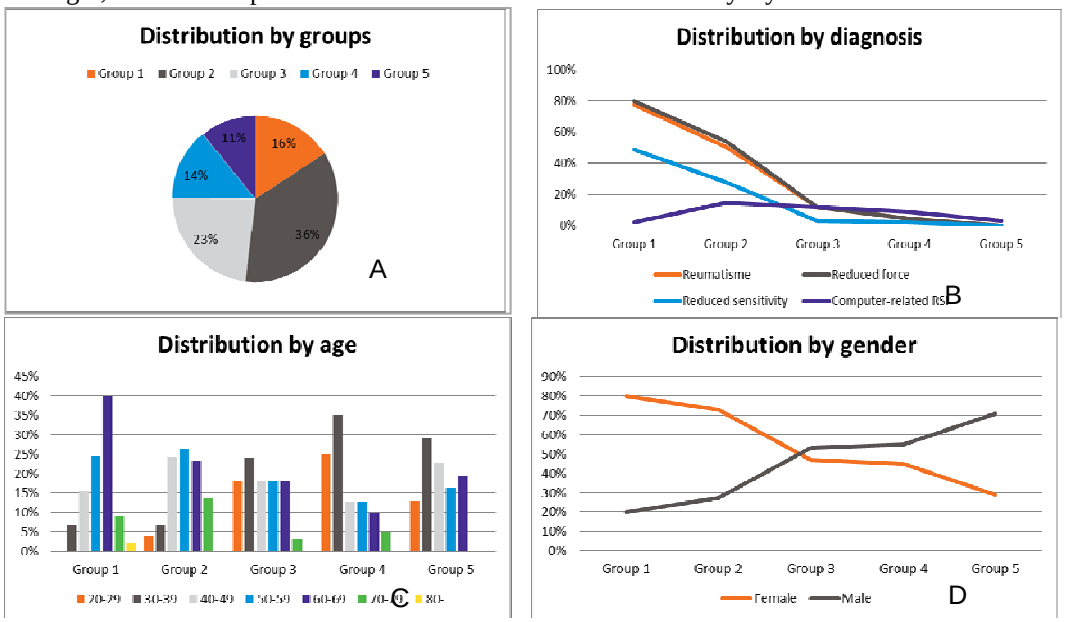



**Figure 3:** A) Classification of the test group of 285 persons into the 5 groups: Group 1 – Daily problems, Group 2 – Weekly problems, Group 3 – Monthly problems, Group 4 – Rarely problems, Group 5 – Almost never problems. B) Percentage division of characteristics of the groups, where characteristics are summed up to 100 % for each group separately, as there is a difference in total number between the groups. The contribution from Sclerosis and Parkinson is not included for the sake of clarity. C) Classification of age in intervals of 10 years for the groups. D) Percentage gender ratio of the groups, where it has been summed up to 100 % for each group separately.

[2] Woolf AD, Pfleger B. Burden of major musculoskeletal conditions. Bull World Health Organ 2003; 81(9):646-56.

## Reasons to why the consumers have problems with packaging

A condition for solving the consumer's problems with packaging is to understand why the consumers experiences problems. It is also interesting to gain knowledge of how the consumer act upon the problems they experience. This will be illustrated in the following.

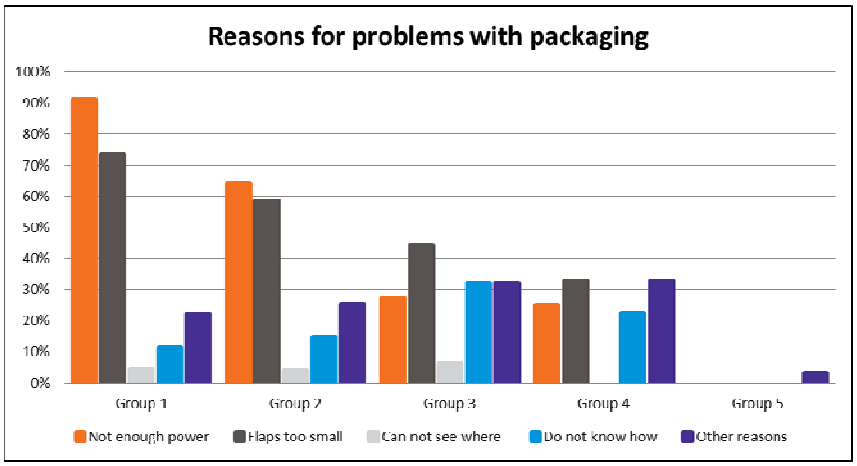



**Figure 4:** Percentage classification of causes to problems with packaging for the 5 groups (Note: A respondent can indicate more reasons for problems in the same answer) See group characterises in Figure 3 (Part 1.2).

## 16 % deselect poor packaging

Repetitive frustration and now and then injuries caused by difficult packaging result in some consumers deselecting products. The study shows (see Figure 5), as it was expected, that the motivation for deselecting poor packaging is proportional to the frequency of experienced problems with the packaging. Group 1 indicates that 80 % deselects products, and compared with prior estimations for the group it means that 160,000 persons deselect products solely because of the packaging. The packaging which poses the largest problems are according to the Rambøll report made for The Danish rheumatoid arthritis society, 2006[3] glasses with screw lid, sliced cold meat packages with corners and medicine glasses.

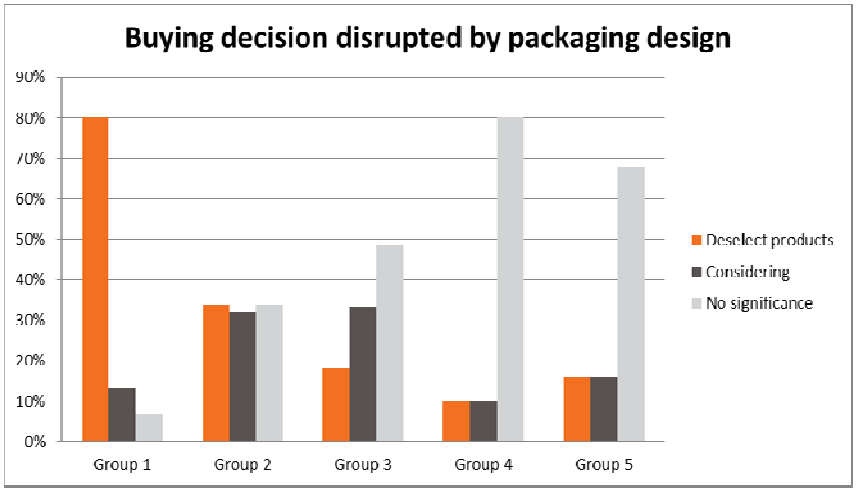



**Figure 5:** Classification in percentage for persons in the 5 groups, who deselect products due to poor packaging, where the user friendliness of the packaging form a selection criteria equally to price and brand, and finally where user friendliness is not of significance for the choice of products.

[3] http://www.gigtforeningen.dk/files/presse/gigtforeningen_noegletal.pdf

## 1.3 Consumers attitude to and use of tools for packaging

Tools are by many seen as the solution to many of the problems, which the consumer experiences with packaging. In this section we will focus on the consumers view on the use of tools.

### The consumers want to open the packaging with their hands

In the study we asked the consumers, what their general views on tools were. It can be seen from Figure 6, that 30-40 % of all consumers think that it is OK to use tools, if it clearly appears that the packaging should be opened using tools, but that a slightly larger part would prefer that all packaging could be opened without. The main thing is though, that the consumer finds it completely unacceptable that use of tools is necessary if it appears from the packaging that it can be opened by hand.
In Figure 7 is shown the consumer's general experience with opening with tools vs. opening with the hands. The Figure shows, that the most exposed consumers in general think that it is easier to open with tools rather than with the hands, whereas the more fit part of the groups thinks that opening with the hands is the easiest. If the result in Figure 11 is compared with Figure 6 it is interesting, that the consumers who prefer to open packaging without use of tools, at the same time think that it is easier to use tools. This paradox will be illustrated later.

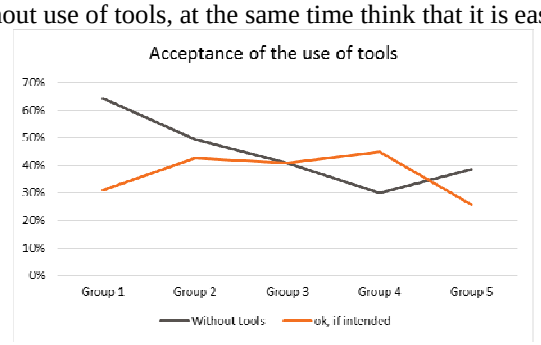



**Figure 6:** Acceptance of use of tools for opening of packaging for the 5 groups. See group characteristics in Figure 3 (Part 1.2).

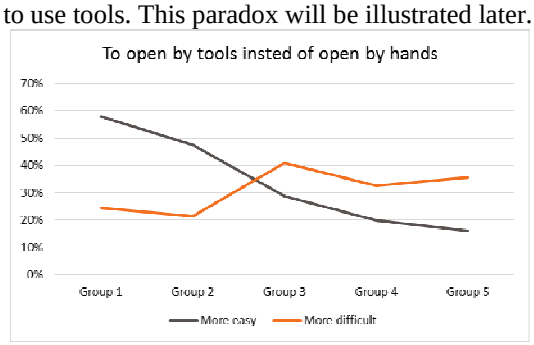



**Figure 7:** The 5 group's opinion on tools being easier to use than opening with the hands. See group characteristics in Figure 3 (Part 1.2).

There is a difference between how acceptable the use of tools is in different situations. This means, that 5-10 % of all consumers accept the use of tools for opening on-the-go products. If the packaging is to be opened at the office the acceptance rises to 15-35 %, whereas 50-70 % of the consumers accept the use of tools in a kitchen.

### Less than half of the consumers accept the use of a knife

The consumer can as starting point use a tool, yet not think that it is okay to use it. In this study it appeared that the use of scissors and can opener is accepted of about 70 % in all groups, whereas for instance the use of a knife is only accepted by 10-50 %. Group 1 regards the knife as least acceptable (10 %). It can perhaps be a consequence of the fact, that this group as starting point is more exposed to getting injured than others.
A logical thought of the lacking acceptance of a tool, is that the consumer estimates the tool as being difficult to use. In Figure 8 can be seen how big a part of each group, who finds different tools difficult to use.

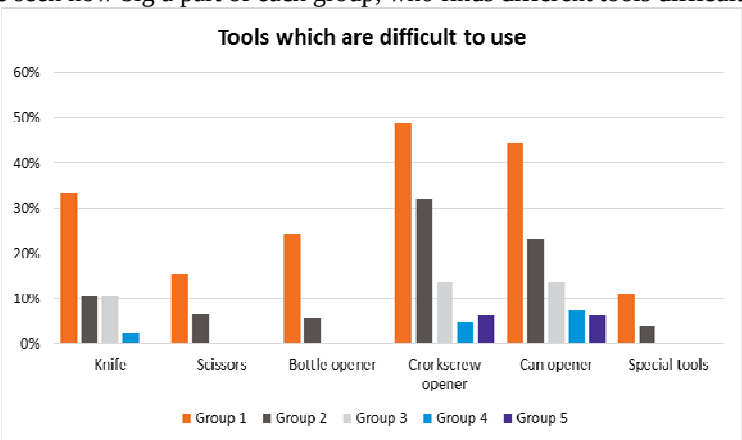



**Figure 8:** Classification in the five groups, whether they think the different types of tools are difficult to use.

If the group's positive acceptance is plotted with how difficult the group estimates the tool a moderate coherence (R-values between 0.4-0.8) appears for all tools, though not for the can, where there is no coherence. This indicates, that acceptance of the can opener cannot be linked to whether it is difficult or easy to use. Perhaps because most consumers today often prefer a pull-ring opening for cans and therefore does not need can openers. In that way it shows how packaging development can move the consumer's level of expectation regarding use of tools. Similarly is plotted the group's "acceptance" and "no acceptance" against "difficult to use" and "easy to use". Group 5 differs from the other groups by having few problems with handling tools, but at the same time having low acceptance for the use of tools. Specialized tools differ from the other tools (knife, scissors, can opener and corkscrew) by having reversed correlation, where the acceptance is smallest for those who think the tools are the easiest to use. The acceptance of specialized tools is largest for Group 1 (38 %) and falls proportionally to the less the groups use tools on an everyday basis. 26 % of Group 5 accepts specialized tools. This trend can partly be due to Group 5 sympathizing with Group 1 consumers and partly because they consider it completely unlikely that they should be in need of specialized tools, and therefore it is unacceptable.

### What does it mean to the consumer to use specialized tools?

It is interesting, that the consumers who prefer to open packaging without tools, at the same time think, that it is easier to use tools. In the previous section it was also illustrated, that in spite of the tools being easy to use, this does not mean that it is also accepted.

In Figure 17 is shown the spread of different feelings for Group 1-3, when they use specialized tools. From the figure it can be seen, that between 75-100 % of the consumers in the groups think about the fact that they use specialized tools. Even though the use of specialized tools give a negative feeling in the way that they feel dependent of tools, sick/old and different, specialized tools also contribute to a feeling of independence and pride in being able to make it on one's own. Specialized tools are thus not only a bad thing, but it is also important to focus on the packaging becoming easier to handle for all groups of consumers and the development of more tools is not the solution.

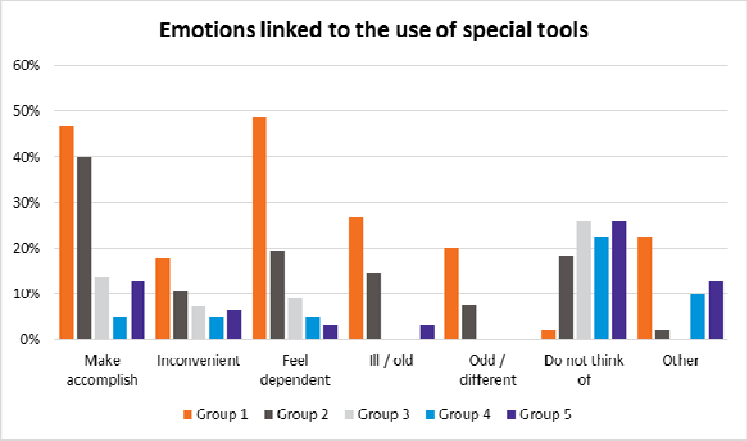



**Figure 9:** Spread of feelings concerning use of specialized tools for grope 1-3.

## 2. Guideline

### 2.1 Stakeholders

| | |
|---|---|
| Consumers | • Packaging is poor<br>• The problem is the industry |
| Supermarkets | • Packaging shall protect and promote the products<br>• The problems is the suppliers |
| FMCG producers | • Packaging shall protect and promote the products<br>• The problems is the price of the packaging |
| Packaging producers | • Packaging can be better<br>• Payment for the extra service |

**Figure 10:** Conflicting stakeholders

As the stakeholders only have done a little DTI has made a Danish guideline in order to focus the producers on the 16 % last sale and in the same time demonstrate that it is not difficult to have easy access to you product. Fundamental you have no reason to seal your consumer out from you products.

The Danish guideline www.brugervenligemballage.dk translated to English in www.userfriendlypackaging.com.

## 2.2 User-friendly packaging – a practical guide to companies and packaging designers

The scope is to give companies and packaging designers an idea of the end users' needs and approach, get inspiration from actual cases and get help to make your packaging more user-friendly – from the first idea to the finished packaging.

*Useful advice*

Some useful advice when your company engages in developing more user-friendly packaging.

| | |
|---|---|
| Graphics and colour | • Use contrasts to bring out the opening.<br>• Use a simple and easy to read opening instruction (text/illustration).<br>• Large amounts of information can be confusing – consider what will be important. |
| Design | • Use a design which brings out the opening.<br>• Use big size flaps, pull rings and screw caps.<br>• A square shape is easier to hold than a round shape |
| Material | • Use material which doesn't easily break when the packaging is opened.<br>• Use furrows/structure and different materials in order to secure a good grip in the packaging. |
| End user's physical strength | • Use packaging that doesn't require a lot of strength or fine motor skills.<br>• Avoid double packaging.<br>• Use packaging which can be opened in more than one way. |
| Re-seal | • Only use re-seal which actually works and makes sense.<br>• Test re-seal functions on end users. |
| Tests | • Test the packaging on end users (e.g. via end user observations and mechanical tests) throughout the entire development process.<br>• Test packaging on kids and elderly then all can use your package |
| End users | • Be aware that end users are used to opening packaging in a certain way.<br>• Be aware that your end users have different preconditions – culturally and physically. |

*Process from start to end*




Phase 1 Insight
Purpose: Starting a process resulting in a more user-friendly packaging.

Phase 2 Research
Purpose: To gather knowledge to be used when choosing types of packaging and designing questions for end user studies.

Phase 3 End user observations
Purpose: To use interviews/video observations to identify the end user's actual use of the company's products and inspire to further innovation.

Phase 4 Workshop
Purpose: Initiating the first idea generation concerning more user-friendly packaging and obtain a shared insight in and understanding for user-friendly packaging throughout the company.

Phase 5 Concept analysis
Purpose: To gather knowledge and work on with the ideas from phase 4 as well as determining which ideas can be realised.

Phase 6 Prototype
Purpose: To produce a prototype which can be used in end user tests and tests on internal company representatives.

Phase 7 Evaluation
Purpose: To evaluate the user-friendliness of the final solution as well as initiate any adjustments needing to be made before the solution is put into production.

*Packaging design*

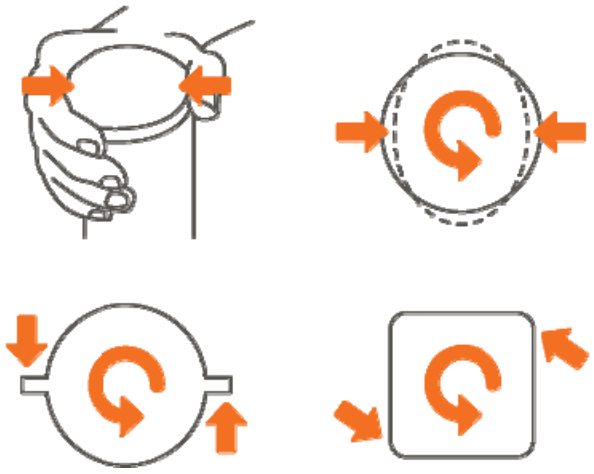


**Figure 11:** Screw led design can reduce opening torque

*Graphics and choice of colour*

Graphics and choice of colour are extremely important for the perception of a packaging. End user tests show that people often don't use the opening mechanisms integrated in the packaging. Therefore it is important that the opening mechanism is made clear by marking or contrasts on the packaging.

Often design, colour or text intended to instruct the end users is hidden in order to get a nice overall impression of the packaging. It is important to mark where the opening mechanism is situated and on some packaging types it can furthermore be made clearer what way to hold the packaging when opening it. At the same time it is important that the graphics on the packaging supports the design so that the packaging is opened as intended without excessive use of force.

Below you will see some examples of good and bad use of graphics and choice of colour in some types of packaging making it clear where and how to open the packaging.

Useful advice on better graphics and choice of colour for the packaging

- Easy-to-read instructions – make it easy to open the packaging.
- Simple and clear graphics on the opening mechanism – make contrasts on the lid/the flap.
- Clear graphics – the graphics pointing out the opening mechanism should be contrasted to the rest of the packaging.
- Clear writing – use contrasts. Writing works best dark on a light background or vice versa.

- Avoid or minimise unnecessary information on the packaging in order to make the opening instructions are clearly legible.
- Large letters – make sure that the letters are easy to read.




**Figure 12:** Illustrated instruction

## 2.3 Testing your own packaging

Danish Technological Institute has developed a tool for companies in order to evaluate the performance of specific packaging designs. This tool is based on data from Department of Trade and Industry, UK and Packforsk, Sweden. These data is used to estimate performance of 5 different opening situations for packaging.

Use the calculation model in User-friendly Packaging to get an estimate of how many people are able to open different packaging types based on packaging dimensions and the target group's critical strength. The critical strength is the maximum strength possessed by the target group.

Right you will find calculation models for screw caps, flaps and bags, can with lift ring, can with pull ring and pull of cork. The models have been adjusted in a way that makes it possible to simulate the effect of the end user's ability to transfer force to packaging types of different dimensions.

Choose calculation model based on type of grip. Not all types of packaging are included in the calculation models. Each company must decide which model will be the best suited for each case. The essential question is what grip is being used in the opening procedure.

The calculation for flaps and bags is included in one model as the same grib is used for both. In order to use this type of calculation model the grip used in the opening procedure has to be a pincer grip. No calculator model has yet been developed for calculating "bag grips".

From these cases you will see that it is not appropriate blindly to trust the model's results as it will often be a combination of the end user's physical strength and their cognitive analysis of the packaging – that is their understanding of how the packaging should be opened – which decides how the end user perceives the packaging regarding accessibility.

Calculation models:

- Calculation model for screw caps
- Calculation model for flaps and bags
- Calculation model for cans with lift of ring
- Calculation model for pull of ring
- Calculation model for arm pull of cork

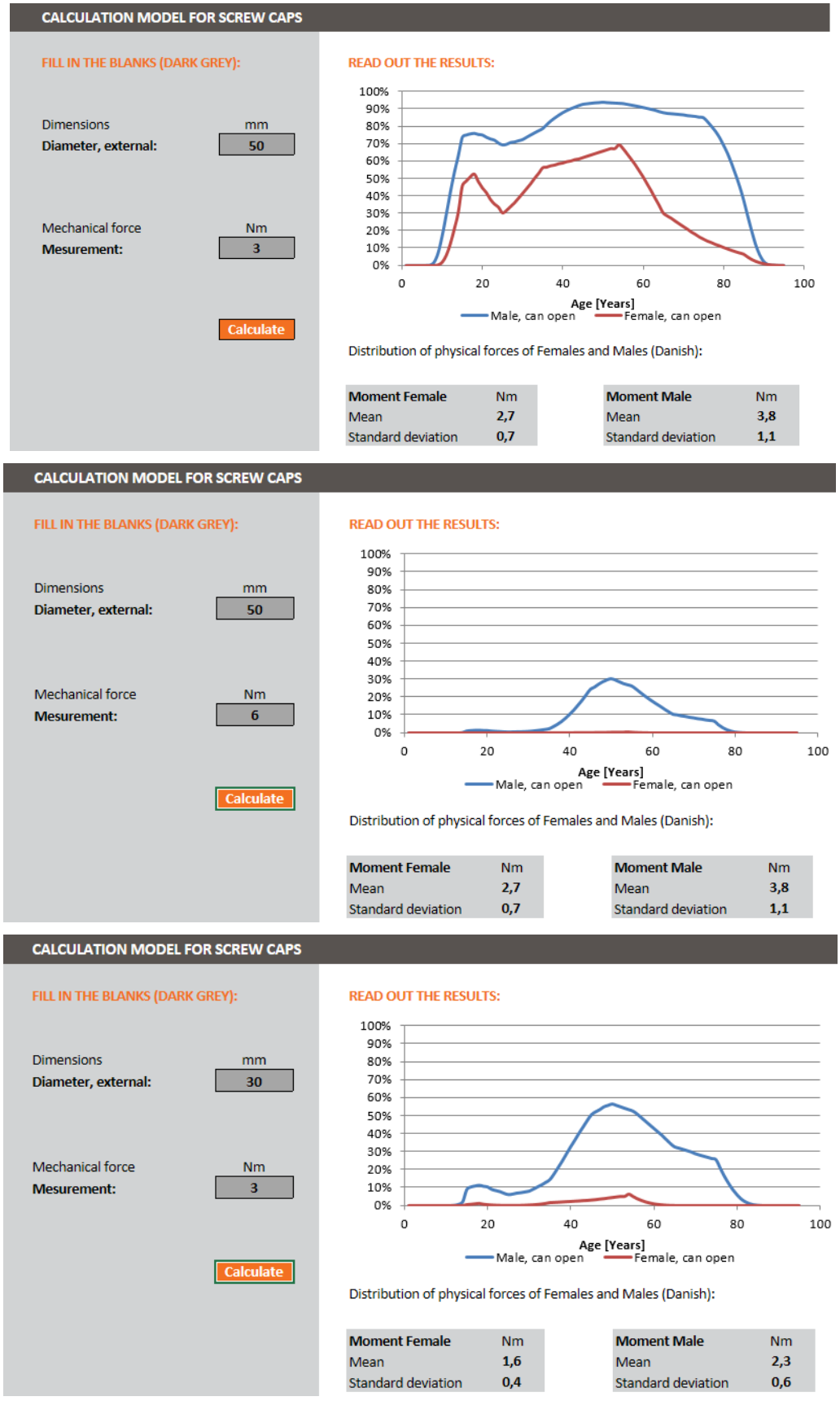



**Figure 13:** Calculation model for screw cabs with different data

The needed measurement equipment can be purchased for less than €100. For this reason the calculation tool can be a great help for evaluation of a packaging design.

Many have asked us about the lost forces in the age group 18-35 years – especially for females. We have no answer. It can be a little statistical deviation projected up. It can also be the real situation describing the life style today. It was decided to use the data as they are with a remark that this is not scientific documented data but the best business approach on the information we had.

## 3 Conclusions

Danish Technological Institute has developed a practical tool for companies and designers. The guideline is for all. But the data in the calculation model is based on a few measurements in UK, Sweden and Denmark. For this reason the calculation is not based on science – still it is a practical tool.

## Acknowledgements

DTI would like to acknowledge the Danish Ministry of Industry for the big financial support in this project.

## References

1. Woolf AD, Pfleger B. Burden of major musculoskeletal conditions. Bull World Health Organ 2003; 81(9):646-56.
2. Gigtforeningens nøgletal, 2006 (www.gigtforeningen.dk/files/presse/gigtforeningen_noegletal.pdf)
3. Sundhed og sygelighed i Danmark, Statens Institut for Folkesundhed, 2005
4. Rambøll´s befolkningsundersøgelse for Gigtforeningen 2006 (Confidential)
5. How to improve safe packaging disposal instructions, Government consumer safely research. Department of Trade and Industry, 1994.Strength data for design safety- Phase 2, Government consumer safety research, Department of Trade and Industry, 2002. (http://webarchive.nationalarchives.gov.uk/+/http://www.berr.gov.uk/files/file21827.pdf)
6. Danmarks statistik, 2011 (www.statistikbanken.dk)
7. Antvorskov H. & Geert B. R. (2011) Project report: “User-driven Guideline for the Industry: Accessible Packaging for Elderly and Disabled” http://www.userfriendlypackaging.com
8. Statistics of Denmark. Forecast of Danish population 2010-2050. Date: 2010.10 - http://www.statistikbanken.dk
9. Government Consumer Safety Research, Department of Trade and Industry, How to improve safe packaging disposal instructions, 1994
10. Antvorskov H. (2007), “Retail and consumer attitude towards communicative packaging”, IAPRI Packaging Symposium, London, UK
11. Agelab http://www.agelab.dk (2006) Date: 2012.03
12. Orth, U. & Malkewitz, K (2008) Holistic Packaging and Consumer Brand Impressions. Journal of Marketing, vol 72, no 3, 64-81
13. Hestad, M. (2006). "Pure shape - To realise intended meaning in practise". Design and semantics of form and movement (DeSForm), Northumbria University.
14. Meyers,H. & Gerstman, R. (2005) the visionary Package – using packaging to build effective brands. Palgrave Macmillan: New York
15. Young, S. (2004) Breaking down the barriers to packaging innovation. Design Management Review, vol. 15, no 1, 68-73
16. Gough, K. (2006) On a Plate: making food packaging easier to use. I-design programme publication. Helen Hamlyn Research Center
17. Yoxall, A., Luxmoore, J., Austin, M., Canty, L., Margrave, K. J., Richardson, C. J. , Wearn, J., Howard, I. C. & Lewis, R. (2007): Getting to Grips with Packaging: Using Ethnography and Computer Simulation to Understand Hand-Pack Interaction. Packaging Technology and Science, volume 20, p. 217-229.
18. Consumer Affairs, Department of Trade and Industry, (2002) Strength data for design safety phase 1-2
19. Heinö, R. & Åström, A. & Antvorskov, H. & Mattsson, M. & Østergaard, S. (2008) Easy Open Pack – Scientific background for the basis of an international standard for easy-to-open packages. Nordic cooperation project (NICe).

# Packaging for Personalized Food for Nutrition of Elderly Consumers Made Using Rapid Manufacturing

**Alexander Bardenstein[1*], George Dunwoody[2], Patrizia Cinelli[3], Joost Valeton[4], Giuseppe Amato[5], Søren Østergaard[1], Dietmar Langer[6], Marc Langer[6], Stanislav Landa[1], Helene Wagtberg[1], Stephen Webb[2], Matthias Kück[7] and Sandra Forstner[7]**

*[1] Packaging Section, Danish Technological Institute, Denmark*

*[2] RTD Services, Austria*

*[3] University of Pisa, Department of Civil and Industrial Engineering, Italy*

*[4] Roth & Rau B.V., the Netherlands*

*[5] FEMTO Engineering S.R.L., Italy*

*[6] SANALOGIC GmbH, Germany*

*[7] BIOZOON Food Innovations GmbH, Germany*

*[*]Corresponding author. Email: alb@dti.dk*

**Abstract:** Development of packaging concept allowing manufacture, distribution, graduated microwave heating and consumption of multicomponent personalized meals is one of the most complex tasks in the project "Development of PERsonalized FOod using Rapid MAnufacturing for the Nutrition of elderly ConsumErs" (project acronym PERFORMANCE) funded by the FP7 European R&D Programme. In the project, a personalized holistic food supply chain for elderly people suffering from dysphagia, decreased organoleptic perception, mastication and swallowing problems will be developed and validated. Thus, the project deals with the delicate gelled rapidly manufactured (3D printed) personalized food that must be homogeneously heated in domestic microwave appliances up to temperatures required for safe consumption. Other imprescriptible requirements are convenience, aesthetical acceptability, and durability. The packaging concept and physical design allowing graduated simultaneous heating of the food varieties is suggested in response to these challenges. The physical design is based on utilization of packaging elements with variable microwave transmission capabilities. The transmission is controlled by perforated electro conductive patterns that are deposited using ink-jet metal printing. Geometry and dimensions of perforations are optimized by means of finite-element method computer simulations. The paper gives a feature-based description and an elementwise analysis of the packaging concept, though with a strong bias to the provision of homogeneous microwave heating.

Keywords: elderly consumers, personalized food, active packaging for controlling microwave heating

## 1 Introduction

Due to the demographic changes caused by the increased life expectancy and reduced fertility rates, a number of elderly people (over 65 years) worldwide is constantly increasing. While they currently represent 17.6% of the total European (EU 27) population, it is predicted that this percentage will be increased to 29.6% by 2050 resulting in 150.000.000 European citizens being over 65 years of age [1]. Quality of life, independency in daily activities and prevention of chronic diseases is highly influenced by a balanced diet and a health-promoting lifestyle. However, together with a higher degree of chronic diseases, this age group experiences a serious decline in their physical and physiological capabilities such as mastication and swallowing, anorexia and reduced sensorial capabilities etc. This results in up to 50% of residents in nursing homes being malnourished [2]. Due to their limited eating and sensorial capabilities, their meal has to have a special texture (pureed, thickened or gelled) and an intensified aroma.

This is why the PERFORMANCE project pursues the goal to develop, implement and validate a holistic personalized food supply chain for frail elderly persons living either in nursing homes, ambient assisted living facilities or simply at home (visited by nursing services) and facing swallowing and/or masticating problems [3, 4]. The personalised meal goes beyond composition and portion size to include individual nutrient requirements and modified textures, which have the appearance and natural taste of traditional meals. Figure 1 shows an example of the appearance of such a personalized meal.

Therefore, the project deals with the delicate gellified rapidly-manufactured (printed by means of specially designed and built 3D food printers) personalized meals, which have to be heated up to +75°C within a few minutes. Obviously, this is only microwaving that enables such kind of heating because it delivers the energy

directly into the food volume, without losing energy, i.e. without losing time and/or power, for preheating of dishes, surrounding air, water, or oil. Thus, the PERFROMANCE concept assumes an active microwavable packaging solution for the personalized foods. Specifically, this is the packaging that alongside with conventional packaging tasks, such as to preserve, contain and protect the contents of the product it surrounds and to provide information to the service personnel and consumer, also changes the electromagnetic field configuration and thus the heating pattern of the product contained within [5].




**Figure 1**: Example of the PERFORMANCE personalized meal.

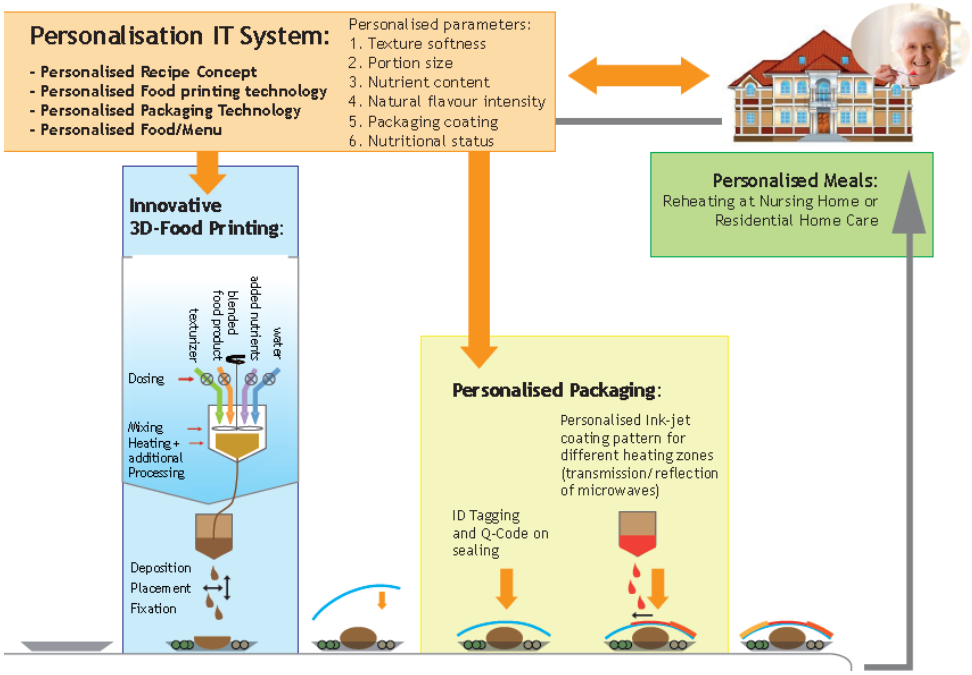



**Figure 2**: Schematic process diagram of the PERFORMANCE holistic supply chain of the personalized food for nutrition of elderly consumers made using rapid manufacturing.

The schematics of the PERFORMANCE supply chain developed in the project is shown in Figure 2. It comprises four functional interacting subunits: Personalization IT System, 3D-Food Printing, Personalized Packaging and Personalized Meals' Heating and Serving. This paper focuses on the Personalized Packaging Concept and peculiarities of the microwave re-heating of Personalized Meals.

## 2 Microwave-active packaging design

It is noteworthy that in the last years, due to the high degree of convenience and the easy and safe preparation especially important for elderly consumers or consumers with disabilities, microwaving had gained increasing importance [6]. Several studies have shown that microwave cooking, if properly used, does not change the nutrient content of foods largely than conventional heating [5-7]. In fact, it has been observed that there is a tendency towards greater retention of many micronutrients with microwaving [7], probably due to the shortening of the preparation time discussed above. The main problem with microwaving is the uneven heating caused both by the diversity of thermal and dielectric properties and shapes of the foods, and by uneven distribution of the electromagnetic field in the cavity of the oven [6, 7]. However, the heating inhomogeneity is inadmissible for the PERFORMANCE supply chain concept due to feeding practices of frail and disabled elderly persons and reduced thermal stability of the personalized gelled food. Therefore, the microwave-active packaging concept shown schematically in Figure 3 has been implemented in the project.

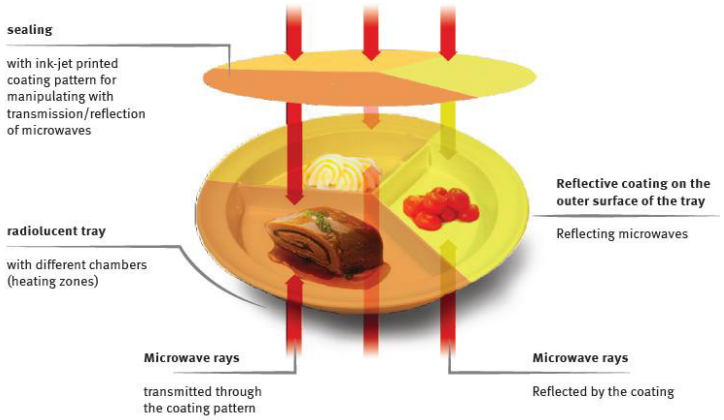



**Figure 3**: Conceptual drawing of the PERFORMANCE microwave-active packaging.

Figure 3 illustrates the innovative approach devised for PERFORMANCE: the microwave-active packaging elements are ink-jet printed partially reflective patterns that control electromagnetic power losses in each component of the personalized meal. The term 'partially reflective pattern' means a pattern of perforations in the electrically conductive sheet (coating) whose thickness is significantly larger than the microwaves' penetration depth (the so-called skin layer thickness) [5]. For instance, a layer of aluminium that is thicker than ca. 2.6 μm totally reflects 2.45-GHz microwaves in domestic microwave appliances [8]. Thus, the central idea of this concept is that the microwave heating rates in the meal components are controlled by geometries and ratios of surface areas of totally reflective, partially reflective (patterns of perforations) and transparent packaging elements. The implementation of the ink-jet printing of the microwave-transmitting patterns enables flexible personalization of the concept in the sense that each personalized meal composition can be re-heated homogeneously and with the same rate regardless of the mass and type. Ideally, a start button of the microwave oven should control this heating system.

Toward this aim, following studies of microwave heating of gellified, personalized foods were carried out in the frame of the PERFORMANCE projects and partly reported in Ref. [9]:

1. The complex dielectric constants of eight different gellified food materials were measured at the frequency of 2.45 GHz that is used in domestic microwave appliances. The dielectric permittivity ($\varepsilon'$) and the dielectric loss factor ($\varepsilon''$) were characterized. This enabled calculation of the 2.45-GHz microwave electromagnetic field penetration depth ($d_p$) in these foods [5]. The measurements and calculations have revealed that the penetration depths and hence the microwave absorption values are weakly dependent on the temperature and kind of gellified food material in the temperature range from 0ºC to +60ºC. They are significantly the same for all characterized food materials. The 2.45-GHz microwave penetration depth smoothly increases from

approximately 10 mm at 0ºC to 10…20 mm at 55ºC. This is in good agreement with the commonly used reference value of 16 mm in the water at 20ºC [5].

2. The specific heat capacity ($C_p$) for the same foods was measured and estimated using polynomial approximations of the temperature and composition dependencies recommended by the handbook [10] for foods presented as aggregations of moisture, proteins, carbohydrates, fibers, fats, and ashes. The same kind of approximations, also given by [10], were used for estimations of the thermal conductivity coefficient ($\kappa$) and the mass density ($\rho$). This enabled calculations of the thermal diffusivity ($\chi = \kappa/(\rho \cdot C_P)$) that characterizes the heat diffusion rate in materials (the higher the thermal diffusivity is, the faster the thermal equilibrium is reached, or in other words, the faster the hot/cold spots caused by microwaving disappear). The measurements and calculations revealed that all kinds of personalized foods have their specific heat capacities and thermal diffusivities in the thawed state within narrow ranges of values of $3590 \pm 240$ J·kg$^{-1}$·K$^{-1}$ and $(0.75 \pm 0.10) \times 10^{-7}$ m$^2$·s$^{-1}$, respectively. It should be noted here that virtually all food materials have thermal diffusivities of approximately $1 \times 10^{-7}$ m$^2$/s, if they are in the thawed state [3]. This value of the diffusivity is 2-3 orders of magnitude lower than that for typical solids and therefore reflects extremely slow temperature equalization. It can be therefrom concluded that the gellification makes this process yet slower.
3. Comprehensive FEM computer simulations of microwave re-heating of personalized food in the PERFORMANCE standard microwave oven, model CLATRONIC™ MW781, and their experimental validation were carried out [9]. COMSOL Multiphysics software with Radio Frequency Electromagnetics and Heat Transfer simulation modules was used to simulate distributions of electromagnetic power losses and temperature. The following averaged parameters have been attributed to the food: the specific heat capacity $C_P = 3590$ J·kg$^{-1}$·K$^{-1}$, the thermal diffusivity $\chi = 7.5 \times 10^{-8}$ m$^2$·s$^{-1}$, the dielectric permittivity $\varepsilon' = 67.5$ and the dielectric loss factor $\varepsilon'' = 13.5$, which resulted in the 2.45-GHz microwave electromagnetic field penetration depth $d_p = 12$ mm. The simulation models were built both for the microwave-passively and actively packaged food. However, the models did not include microwave-transparent packaging elements. This means that the models for the case of passive packaging comprised only the microwave oven cavity, its waveguide and food items. On the contrary, the models corresponding to microwave-active packaging included reflective elements and were set-up for the purpose of optimization of topology and dimensions of the perforated patterns. As described in Ref. [9], the packaging model was a thin-wall cylindrical cage. The side surface of the cage has been set as a continuous reflective wall. The top and bottom surfaces included the investigated patterns of perforations thereby implementing the concept shown in Figure 3. Comparison of the simulation results for different patterns, which also included parametric sweep of their characteristic dimensions, allowed selection of the patterns that ensured the most homogeneous heating. These are proved to be patterns of square perforations of the side length of 0.7…1.5 cm whose geometrical openness value [9] exceeds approximately 15%.

Based on these results, the microwave-active packaging concept that is shown in exploded view in Figure 4 has been suggested.

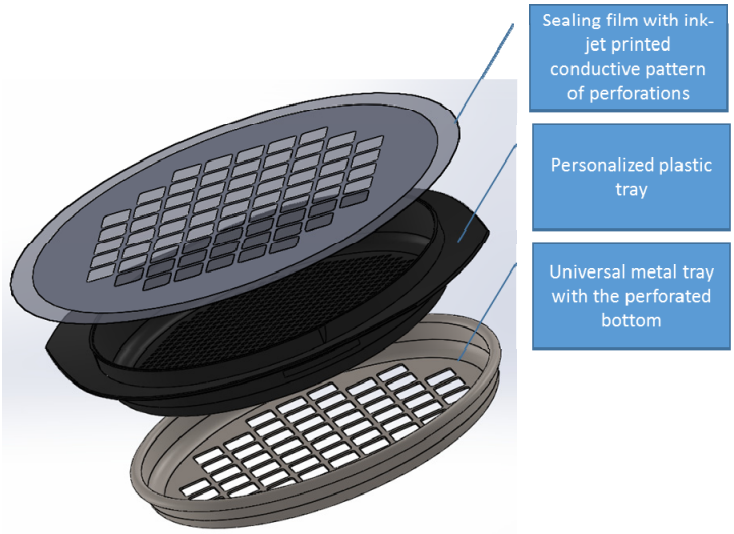



**Figure 4:** Microwave-active packaging concept comprising a plastic tray, a metallized top sealing film and a universal bottom metallic tray with patterns of square perforations.

The bottom part of this microwave-active packaging is not personalized since the pattern of perforations should be optimized and fixed thereafter; otherwise, this perforated metal tray should be manufactured for many personalized food compositions. Thus, the main personalization tool is the top perforated pattern printed on the sealing film. It enables homogeneous re-heating of different food compositions. The bottom metal tray's functions are therefore total lateral shielding and partial bottom shielding. Thereby this packaging element contributes into equalization of the distribution of microwave power losses in the food as it is described in Ref. [9]. Functionally, this perforated metal tray works as a universal reusable microwave kitchen utensil. It will be manufactured in as many numbers, as many standard PERFORMANCE microwave ovens will be used for the concept demonstration and validation.

The third packaging component is the plastic tray that carries the food. Its design and functions are discussed below.

Figures 5 and 6 illustrate the impact of the proposed packaging on the heating homogeneity. They show results of 3D FEM simulations carried out for two models built for the microwave-passive packaging (see Figure 5) and for the active packaging shown in Figure 4 (see Figure 6). The following meal composition and geometry were used: two 71.68-cm³ flat round cakes of gelled potato and carrot, and two 25.61-cm³ gelled beef sausages. The total weight of the meal was therefore about 200 g. The FEM model is quasi-stationary and rotation of the turntable in the oven is not taken into account [9]. The electromagnetic power losses in the food samples, i.e. averaged power absorbed per unit volume, have been calculated as $P = 2\pi f \varepsilon_0 \varepsilon'' |E|^2$ [3], where $E$ is the electric field strength, $\varepsilon_0 = 8.85\times 10^{-12}$ F·m$^{-1}$ is the permittivity of free space, and $f = 2.45$ GHz. In order to be able to characterize the performance of the microwave-active packaging, the relative inhomogeneity $\boldsymbol{i}$ of the microwave power losses in the food was derived from the simulation results as $i = (P_{max} - \langle P \rangle)/\langle P \rangle$, where $P_{max}$ is the maximum electromagnetic power losses in the food object, and $\langle P \rangle$ is the average power losses in the same object. Then the average inhomogeneity of the power losses in the whole meal $\langle i \rangle$ was calculated by the averaging of the inhomogeneity in all food items.

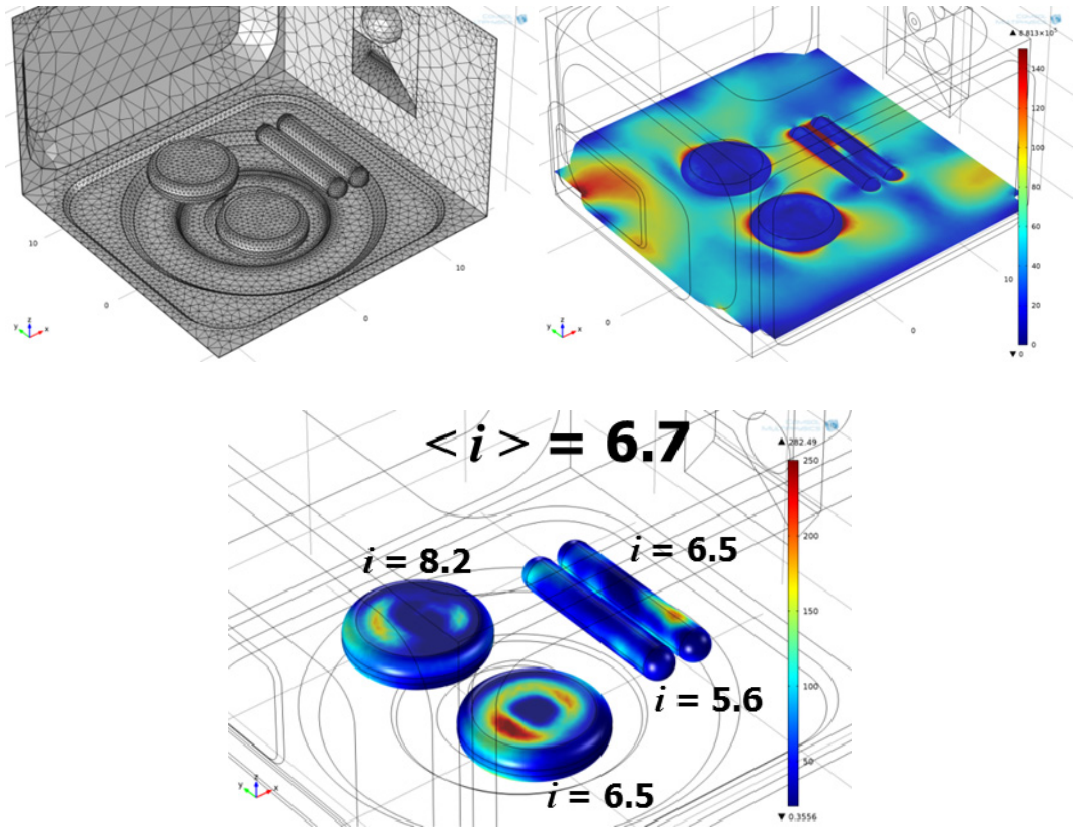



**Figure 5:** Meshed 3D CAD model drawing of the modeling meal in the PERFORMANCE standard microwave oven without shielding packaging, electric field strength (in V/m) distribution, and electromagnetic power losses (in W/cm$^3$) in the meal components.

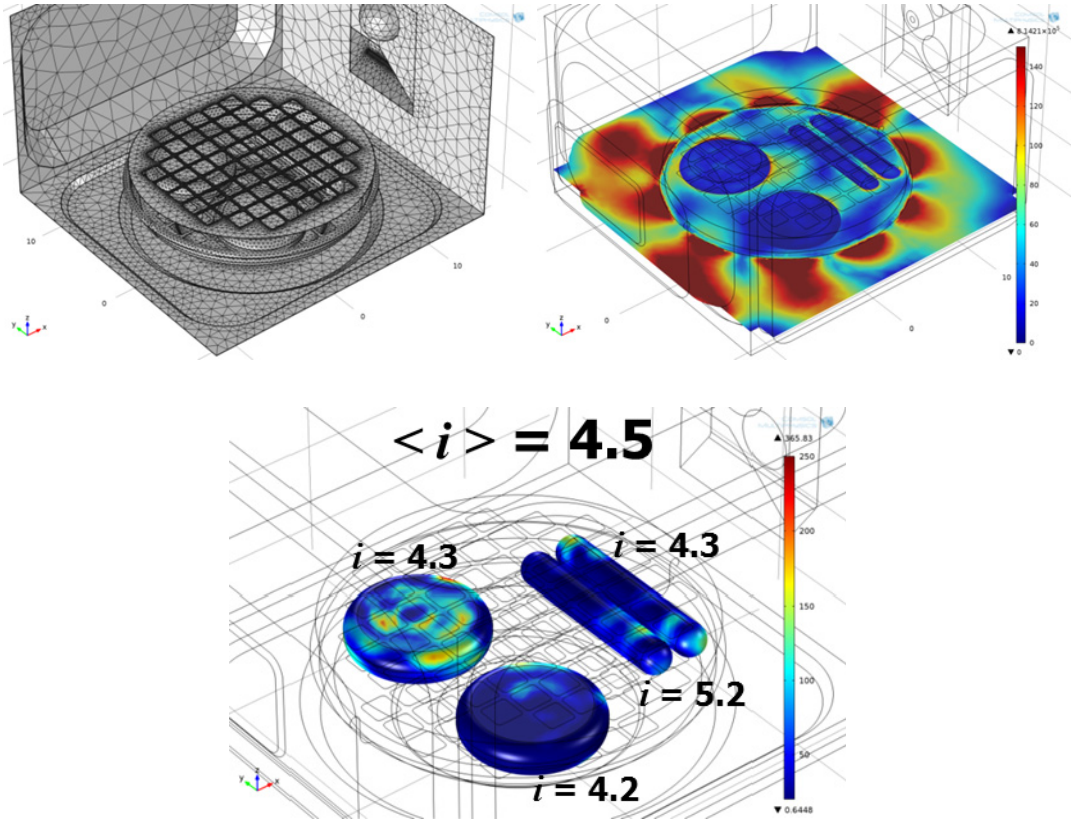



**Figure 6:** The same type of results as in Figure 5, but for the active packaging shown in Figure 4.

By comparing the results presented in Figures 5 and 6, it can be ascertain that the implementation of microwave-active packaging shown in Figure 4 can reduce heating inhomogeneity by up to 48%, and does not result in higher inhomogeneity at the worst. The average reduction of inhomogeneity achieved in the whole meal by means of implementation of the active packaging shown in Figures 4 and 6 is about 33%.

Thus, further development of microwave packaging aims in generation of such multizone patterns of perforations in the metallized sealing film that would ensure approximately the same microwave energy absorption rate in all components of all possible compositions of the PERFORMANCE personalized meals.

This work requires implementation of the 3D CAD models of the personalized food objects in COMSOL Multiphysics environment, and not all the models have as yet been developed. Nevertheless, some of them are already available for rapid manufacturing by means of 3D printing and presented in Figure 7. Our forthcoming plan is to start simulations and pattern optimization for the personalized meal composition and geometry shown in Figure 8. The surface of the sealing film coated by pattern of perforations will be divided to three functional zones located above proteins-reach and carbohydrates-reach foods and vegetables. The geometrical openness of the pattern in the zones will be optimized to enable the same heating rate and time in order for all foods to achieve the required temperature.

## 3 Implementation of sealing film with ink-jet printed metal pattern

In the studies of geometry and dimensions of conductive patterns deposited on the sealing film reported above, we simply assumed that the coating totally reflects 2.45-GHz microwaves. We did not take into account its real electrical conduction and thickness, or by other words, the coating material. Since the diversity of composition and size of the personalized meals require fast restructuring of the pattern, the coating is deposited on the sealing film by means of ink-jet printing of metallic inks. And the only metallic inks that are currently available commercially and allow processing under conditions, which are compatible with polymer films on which the metal has to be printed, are silver inks.

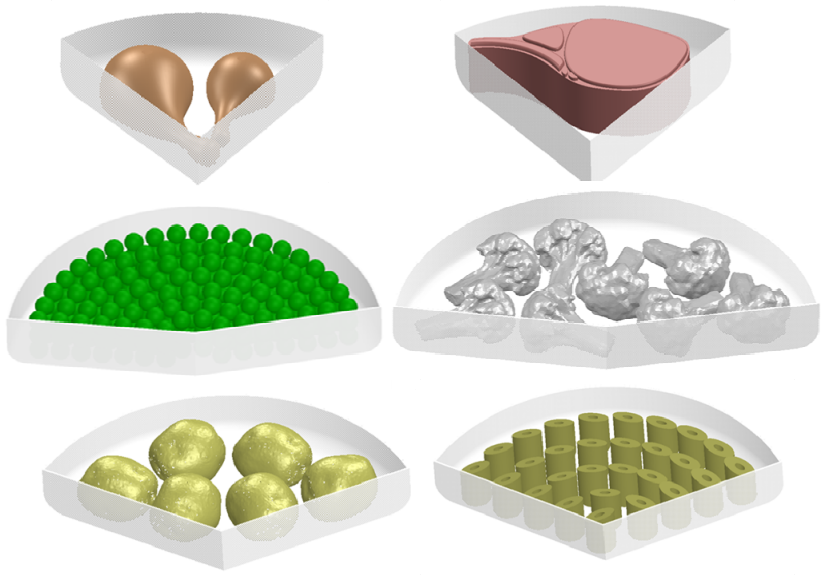


**Figure 7:** Examples of 3D CAD personalized food models developed by the PERFORMANCE team at the Netherlands Organization for Applied Scientific Research (TNO): chicken legs, pork chop, green pea, cauliflower, potatoes and pasta.

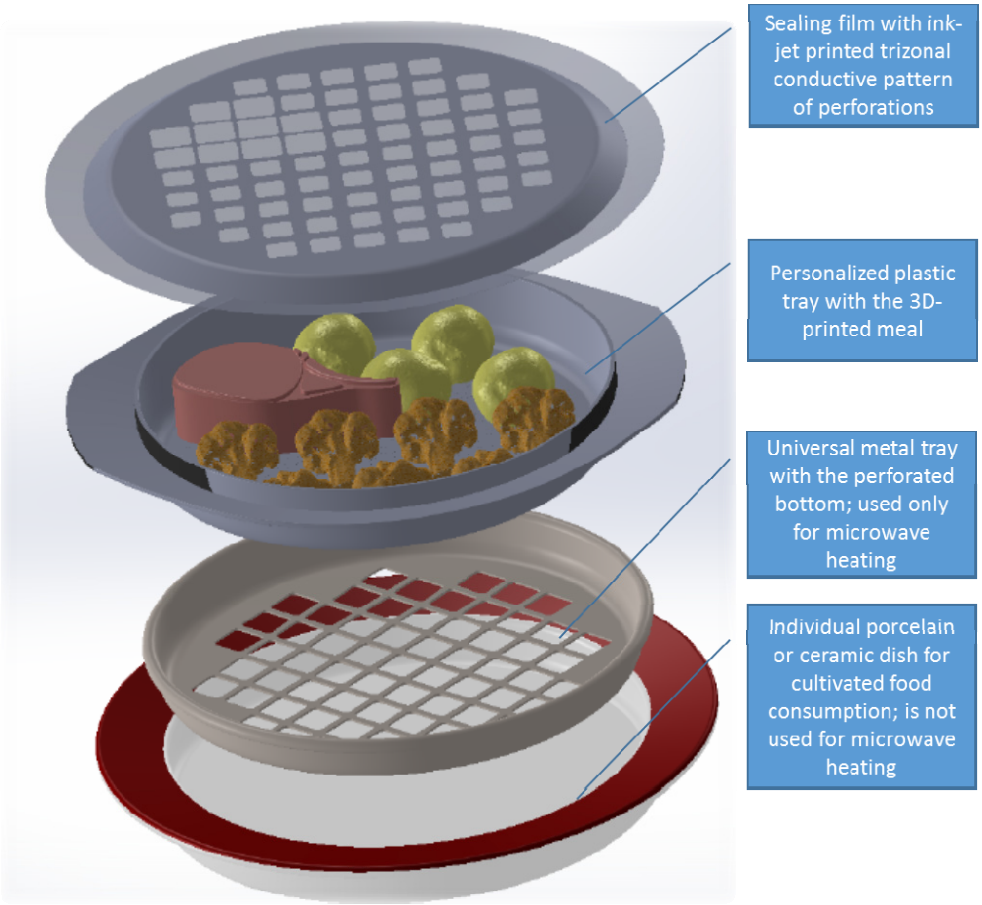



**Figure 8:** CAD drawings of the PERFORMANCE personalized meal packed in all microwave-active and passive components, including a porcelain or ceramic dish for cultivated and safe consumption.

Thus, the coating material is a porous silver film formed on the sealing film after sintering of the inks. Its electrical conductivity is significantly different from the conductivity of the bulk silver and depends on many factors, which are difficult to control, for example, temperature and roughness of the sealing film. Therefore, the conductivity of the printed and sintered coating should be measured in order to control its capability to reflect 2.45-GHz microwaves. According to our estimations, the sheet electrical resistance of the totally reflective metal film should be of the order of 0.1…0.2 Ω/□ (Ohms per square). This is also confirmed by experiments. For example, a typical sheet resistance value of 0.18 Ω/□ is reported in Ref. [11] for the totally reflective metal structure. The ink-jet printed silver coating with such resistance has a characteristic thickness of 3.5-5.0 μm. For comparison, the 1-2 μm thick foil of bulk silver is already a total reflector.

The depositions made for proof-of-concept studies of the PERFORMANCE packaging concept were carried out on polyethylene-terephthalate (PET) films of different thickness ranging from 40 to 150 μm. The inkjet printer PiXDROs LP50 was used in the experiments. The LP50 desktop printer system is an advanced inkjet printer tool. It has been specially designed for research and development of inkjet processes and applications as well as for evaluation and development of inkjet materials. The sealing film with the ink-jet printed metal pattern is shown in Figure 9.

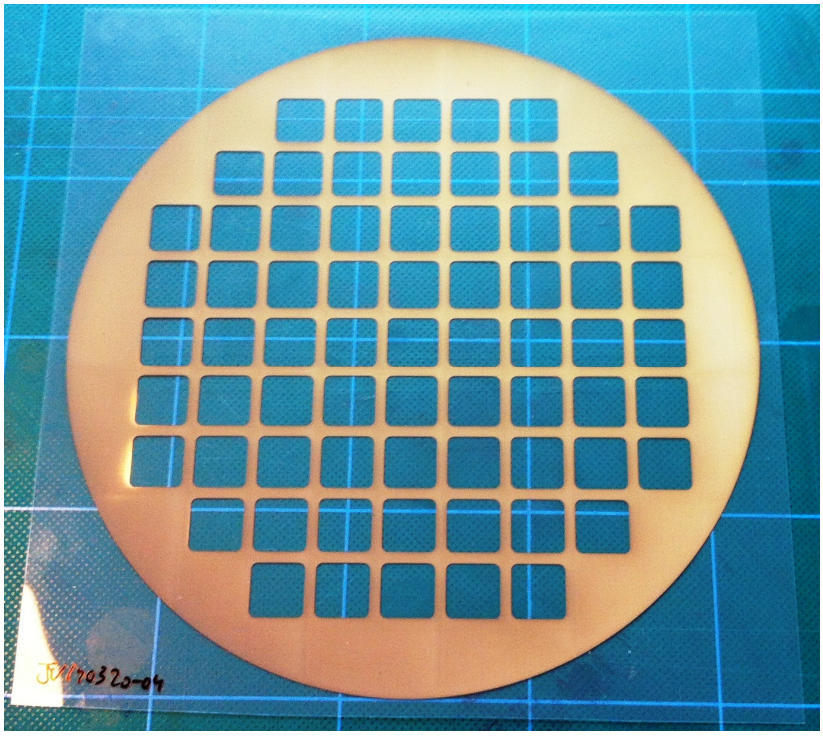


**Figure 9:** Ink-jet printed microwave-transmitting silver pattern on PET film.

After the printing and sintering of the metallic inks, the sealing film was laminated with another PET film that covered the printed pattern. This resulted in high electric and mechanical strength and flexibility of the printed metal coating.

After sealing film preparation, the entire packaging system shown in Figure 4 was put in the microwave oven for physical validation. No microwave discharges were observed in the experiments that confirms the high electric strength of the metalized laminated sealing film.

The PERFORMANCE supply chain will require implementation of a continuously operating industrial ink-jet printing unit combined with the laminating and sealing units. The functional diagram of such a system is shown in Figure 10.

Since the most likely material for the plastic tray manufacturing is polypropylene (PP), the sealing film material will be of the type of Mylar™ RL family PET film or similar. The main advantages of this type of sealing film laminate are as follows: adhesion to many polymer plastics, including PP and PET, and even to aluminium foil; enables peelable seal; is microwaveable and thermally stable; has good barrier properties.

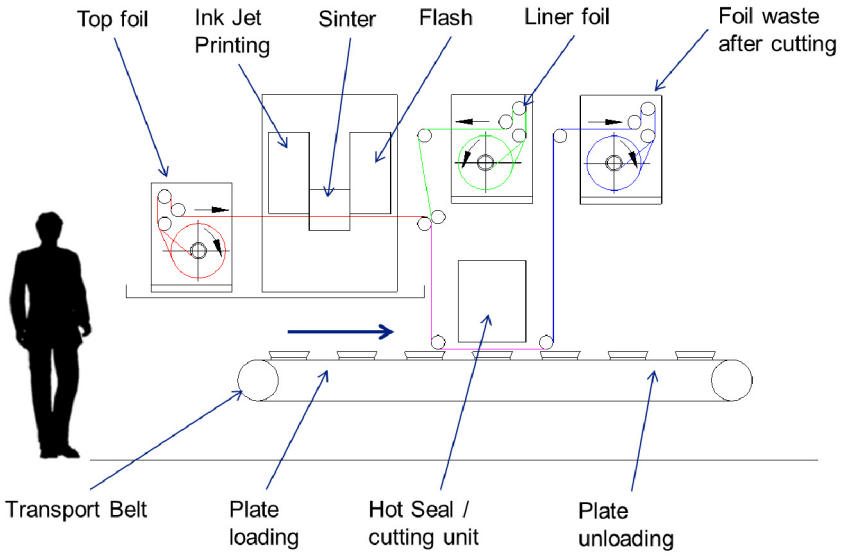



**Figure 10:** The functional diagram of a feasible continuously operating unit for preparation of the sealing film and its application on the tray.

## 4 The Split-Plate packaging concept

The developed packaging concept has an important contradiction: It is technically easier to print personalized food, transport and re-heat it in the light and shallow, colourless thin-wall disposable plastic tray. However, this tray is too unstable and therefore unsafe for the hot food consumption by old and frail people. Moreover, many of these people have weak sight and cannot see the edge of the colourless tray. This is why the special deep porcelain or ceramic dishes for elderly persons, which have the red-colour rim, are commercially available. Moreover, eating from porcelain or ceramic dish is undoubtedly more pleasant and cultivated. In order to overcome this contradiction, the so-called Split-Plate concept was suggested.

This concept is called so because the plastic tray will be designed to be inserted into the dish. Thus, the packaging is 'splited' with regard to the use of different components at different stages of the PERFORMANCE supply chain:

1. Personalized food printing on the plastic tray
2. Deposition of QR-coding labels with the parameters and IDs of the consumer, meal composition, its weight etc. on the plastic tray
3. Sealing of the plastic tray
4. Deliver of the meal in the plastic tray
5. Microwave reheating in the sealed plastic tray inserted into the perforated metal tray
6. Splitting of the plastic and metal trays and peeling of the sealing film
7. Consumption of the food from the plastic tray inserted into the individual porcelain or ceramic dish.

## 5 Conclusions

The PERFORMANCE project will develop specialised food products ('personalised nutrition') focusing on the needs of a growing particular consumer group – the elderly. The project's key objectives are:

- Production of a variety of personalised meals and food products, which consider the preferences of each individual person.
- Personalised meal composition, portion size, nutrient content (e.g. carbohydrates, proteins, lipids, minerals) and texture (softness/hardness) and vitamins.
- Personalised packaging concept with an integrated and unique identification code, special disposable trays and a sealing comprising ink-jet printed pattern controlling individualised heating of a meal.

The most important result is that PERFORMANCE will enable frail and elderly persons to become more independent while managing swallowing and masticating difficulties. The project represents advances in manufacturing and supplying personalised food. New food texturizing systems combined with 3D-printing technology, flexible microwave-active packaging and preparation solutions will enhance the functionality, nutritional and organoleptic value of food.

## Acknowledgements

Authors would like to acknowledge the EU Seventh Framework Programme (FP7-KBBE) for providing financial support for this research and thank all participants of the PERFORMANCE project for fruitful and encouraging collaboration.

## References

1. DG SANCO: HEIDI® tool on European Health information, 2011.
2. Tackling Malnutrition: Oral nutritional supplements as an integrated part of patient and disease management, report published MNI Report, published July 2010.
3. http://cordis.europa.eu/search/index.cfm?fuseaction=proj.document&PJ_RCN=13217378
4. http://www.dailymail.co.uk/sciencetech/article-2611143/Scientists-develop-3D-jellifed-smoothfood-looks-just-like-everyday-meals.html
5. C.R. Buffler, 1993, *Microwave Cooking and Processing. Engineering Fundamentals for the Food Scientist*, AVI Book, NY, pp. 84-97.
6. H. McGee, 2004, *On Food and Cooking: The Science and Lore of the Kitchen*, 2nd Ed., Scribner, NY.
7. A. Lassen and L. Ovesen, 1995, "Nutritional effects of microwave cooking", *Nutrition & Food Science*, vol. 95, no. 4, pp. 8-10.
8. J.R. Wagner, 2010, *Multilayer Flexible Packaging: Technology and Applications for the Food, Personal Care, and Over-the-Counter Pharmaceutical Industries (Plastics Design Library)*, 1st Ed., Elsevier, Oxford-Burlington.
9. E. Tsakadze and A. Bardenstein, 2013, "Packaging for graduated microwave heating of food for personalized nourishment", *Proceedings of 26th IAPRI Symposium on Packaging*, Espoo, Finland, June 10-13, pp. 439-447.
10. ASHRAE, 2010, Handbook on Refrigeration.
11. S. Agneessens, P. Van Torre, E. Tanghe and G. Vermeeren, 2012, "On-body wearable repeater as a data link relay for in-body wireless implants", *IEEE Antennas and Wireless Propagation Letters*, vol. 11, pp. 1714-1717.

# Attention Grabbing Power of Branded vs. Unbranded Packaging

**Mikyeung Bae[1*], Bridget K. Behe[2], Patricia T. Huddleston[1], Lynne Sag[2]**

*[1]Department of Advertising and Public Relations, Michigan State University, USA*
*[2]Department of Horticulture, Michigan State University, USA*

*[*]Corresponding author. Email: baemikye@msu.edu*

This study, guided by Elaboration Likelihood Model (ELM) and the Selectivity Model (SM), examined the effect of brand, involvement, expertise and demographic characteristics (e.g., age, gender) on visual attention to product and its packaging. We also investigated whether visual attention influenced perceived product attractiveness. Using a Tobii X1 light eye-tracking device, we collected data from 108 subjects who were randomly assigned to brand/no brand packaged garden plant condition. Visual attention was measured by total visit duration (TVD) to the product. The results of a multivariate analysis of variance (MANOVA) revealed that visual attention to branded packaging was significantly higher than the unbranded plant. Consumers with moderate expertise with the product first attended to the branded packaging and paid the greatest attention to the branded one. Gender and age influenced information search patterns. Females showed longer total visit duration (TVD) both on the branded pot and plant than men. This finding indicates that females engage in comprehensive information processing, whereas males employ heuristics processing. The mature group not only showed the shortest time to first fixation (TFF) on the branded pot and plant but also gazed both at branded plant and branded pot for the longest time among age groups Brand, involvement, and gender significantly influenced perceived product attractiveness.

We found no relationship between perceived product attractiveness and visual attention but brand significantly influenced perceived product attractiveness. It is worth noting that highly involved consumers perceived the product as less attractive compared to less involved consumers in this study. Perceived product attractiveness was higher for women. Our findings imply that branded packaging has greater attention grabbing power than non-branded packaging and that consumers perceived branded products as more attractive.

*Keywords: brands, eye-tracking, visual attention, involvement, expertise, attractiveness*

## 1 Introduction

A recent study found that 76 % of all purchase decisions were made in-store and product packaging and displays were crucial visual cues in decision making at the point of purchase (POP) [1]. Accordingly, an increasing amount of marketers' advertising budgets has been diverted into the promotion of in-store marketing in order to grab consumers' attention at the point of purchase (POP). The availability of inexpensive eye-tracking technology has facilitated the study of consumer attention. However, until lately less attention has been given to actual product display or the retail setting in which they are situated [2].

The aim of our study is to investigate the role played by brand name as an external cue on packaging in consumer decision-making. The study also examined whether in-store marketing influences product attractiveness, assessed by using an eye-tracking device. In particular, we looked at consumer characteristics

such as product involvement and expertise and their effects on influencing in-store attractiveness. Understanding visual attention given to branded or unbranded product, displays, and packaging will help in

improving marketers' or retailers' visual marketing efforts. In addition, given that visual attention is often a precondition to subsequent processes which lead consumers to product choice, directly gauging precisely what captures visual attention in retail setting should shed light on designing product packaging that will facilitate consumer decision-making.

## 2 Literature review and hypotheses

### 2.1Brand

Branding has been considered as one of the most effective ways to compete in a market because properly created and managed brands can be an invaluable advantage for a company [3]. Regarding package content, Miller [4] and Simon [5] indicated that particular elements of product information can be recoded and integrated into higher order-units that typically convey more meaning and are easier to store in and retrieved from long-term memory. Brand name probably represents higher-order information units in consumer decision-making [6] [7]. Accordingly, we expected that brand name would be among the first information dimensions visually selected by consumers in decision making, and hypothesized that participants would first fixate on the brand name and then they attend to the product with brand name as follows:

H1a: *The time to first fixation (TFF) on branded package will be shorter than unbranded package.*
H1b: *The time to first fixation (TFF) on the merchandise itself with branded package will be longer than one with unbranded plant*

A brand can be considered as a primary factor to not only draw consumers' first attention but also to pay higher level of attention in decision making process [8][9][10][11]. The following hypotheses, thus, was proposed:
H1c: *The total visit duration (TVD) on branded merchandise will be longer than the unbranded.*

### 2.2 Involvement

*Involvement and the Elaboration Likelihood Model (ELM)*

The Elaboration Likelihood Model (ELM) suggests that involvement influences the amount of mental and physical effort a consumer puts into the purchasing processing [12] [13]. Highly involved consumers will search for more information in greater detail and use more criteria in their buying decision than others [14]. Park [15] demonstrated that consumers with high product involvement with the product formed more effortful assessments of brand's ad information, such that their response time for generation brand evaluation was longer than less involved consumers. Based on the literature review, the following hypotheses were proposed:

H2a: *Consumers with higher product involvement will have a shorter TFF on the merchandise compared to consumers with lower involvement.*
H2b*: Consumers with higher product involvement will have longer TVD on the merchandise and branded packaging compared to consumers with lower involvement.*

### 2.3 Expertise

Bettman and Park [16] suggested that the low expertise group did not have the requisite ability to process information, which might lead to a lack of motivation to process. On the other hand, the high group had enough ability but not necessarily enough motivation to process much of current information since they could rely on information stored in memory based on prior experiences. The moderate group, however, might be motivated enough to devote a substantial processing effort to choose the product. Based on Bettman and Park's [16] study, the current study proposed the following hypothesis:

H3a*: For moderate product expertise, the shorter their time to TFF on the packaging information compared to higher or lower expertise.*
H3b*: For moderate product expertise, the longer their TVD on branded packaging than higher or lower expertise.*
H3c*: For higher product expertise, the shorter their TVD on the branded merchandise than moderate or lower expertise.*

Some scholars argued that separating the effects of involvement and domain knowledge were

problematic [17] reporting that involvement was positively related to domain knowledge. Along these lines, a research question is proposed as to whether involvement and expertise could interdependently affect consumer information:

RQ1: *Is there any interaction effect between involvement and expertise on visual attention?*

## 2.4 Gender and the selectivity model (SM)

Meyers-Levy [18] proposed a selectivity model (SM), which posited that males often do not process all available information cues but instead are highly selective in information processing and use heuristic strategy. By contrast, females engage in comprehensive and more detailed analysis of specific message content [19].

We hypothesized that males would use the brand name as a heuristic device to maximize the search efficiency. Males, therefore, would first gaze at the branded pot and make less conscious efforts to process information. On the contrary, females would exhibit greater focus both on the brand name and plant in an attempt to assimilate all available information during processing information. The following hypotheses were proposed:
H4a*: Males will have shorter the time to first fixation (TFF) on the branded packaging than females.*

H4b*: Females will have longer total visit duration (TVD) both on the branded packaging and product than males.*

## 2.5 Age

Researchers revealed that older group used the strategies, which required less cognitive processing demands, whereas the patterns of the young group employed compensatory decision rules which had higher processing demands [20] [21]. Dennis and Behe [22] also showed that older consumers purchased more plants compared to younger consumers. However, inconsistent with previous researches mentioned above, Auty and Elliot's [23] study exhibited that youngest age group (age 14-17) exclusively focused on brand image among other attributes of the products than older age groups (age 18-24 and age 15-34).

There are two research questions that will be investigated by this phase of this research. These are:

RQ2: *Would individuals in an older age group be more likely to have their first attention attracted by the branded package compared to an unbranded one?*
RQ3*: Which age group would spend more time in examining information on branded packaging information and branded plant in decision making?*

### 2.6 Visual Attention

Marketing practitioners and academics share the belief that visual attention is a precondition to subsequent processes that eventually lead to choice [24]. Armel and Rangel [25] argued that the probability that an item will be chosen depends on the relative amount of time that consumers fixate on the item during the decision-making process. That is, the amount of time attending to an item can be a predictor of the actual purchase.
The following hypotheses were proposed on the basis of attention-choice relationship:

H5a*: The higher total visit duration on the product area of interest (AOI) will have a positive impact on perceived attractiveness.*
H5b*: The higher total visit duration on an information sign will have a positive impact on perceived attractiveness.*

### 2.7 Attractiveness and Brand

Branded products have been thought to have better profits and more store traffic [26]. Researchers in marketing, retailing have perceived that brand has strong relationship with quality perception and purchase intention [27] [28]. Dodds and Monroe [29] found since consumers tend to perceived branded product had higher quality than unbranded product, they did not mind paying extra for branded products. We proposed a following hypothesis:
H6*: Brand packaging will positively influence consumers' perceived attractiveness.*

## 2.8 Attractiveness and Consumers' Individual Differences

2.8.1 Involvement

There is considerable agreement that high involvement product messages have greater personal relevance and consequences or elicit more personal connections than low involvement messages [30][31]. However, whether the

degree of involvement influences consumers' perceived attractiveness in a positive or negative way was not well understood. Thus we raised another question as follows:
RQ4*: How does consumers' product involvement influence the product's perceived attractiveness?*

2.8.2 Expertise

Zajonc [32] proposed the familiarity effect on attraction based on four assumptions: First, most experience is mildly positive in affective tone, or at least not aversive. Second, familiar stimuli diminish uncertainty and wary reactions [33]. Third, a familiar stimulus tends to be processed cognitively in a more fluent manner, and fluency tends to be experienced in relatively positive and affective ways. Fourth, familiarity or repeated exposure creates opportunity for interaction [34]. The following hypothesis was posed:

H7*: Participants with higher expertise are more likely to be attracted by the product than those with lower expertise.*

2.8.3 Gender and Age

There is considerable agreement that gender is crucial factors in consumption [35] as age is [36]. Regarding age, since the older consumer is more focused on positive features during the evaluation phase, they showed higher satisfaction level that that younger-aged group did [37]. However, it is not entirely clear whether older-aged group perceive the product more attractive than younger-aged group or middle-aged group at the point of purchase. This study raised the following question:

RQ5*: Do gender and age directly influence consumers' perceived attractiveness?*

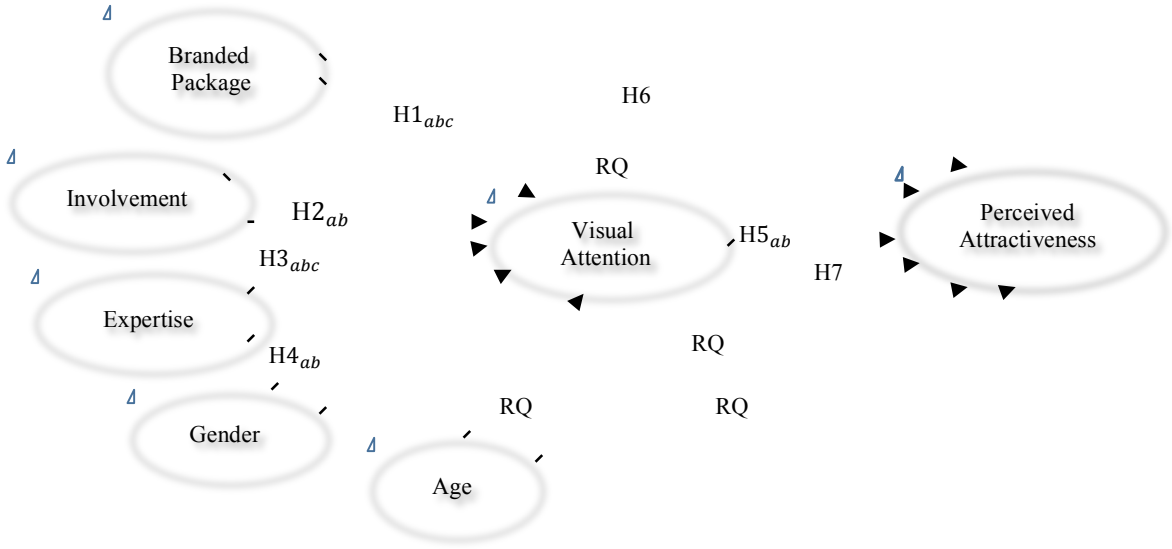



**Figure 1**: Suggested model & hypotheses

## 3. Methods

### 3.1 Participants

Participants ($N$ =108) were recruited through social websites such as Craiglist and Listerv. They received a $30 incentive for participating in this study. Data were collected in Texas and Michigan. 29.6% of participants were age from 18 to 32, 39.0% were 33 to 50 years old and 31.5% were over 50 years old. The majority of participants were female (71.3%) and Caucasian (79%).

### 3.2 Display construction

Flowering plants were selected as the product stimuli as these represent minimally packaged products .We

developed a conjoint design with three plants (rose, hydrangea, and clethra). Images consisted of one display of each of two plant types categorized into two groups: rose (black pot with no brand vs. yellow pot with brand) and hydrangea (black pot with no brand vs. blue pot with brand). Images were manipulated using PowerPoint software. Participants were randomly assigned into 2 conditions (brand vs. no brand). They were seated at the Tobii X1 Light eye-tracking device, and their eye movements were calibrated to the equipment.

Areas of interest (AOIs), or sections within the display images were selected for eye fixation analysis using Tobii Studio 3.0.2.218 licensed through Tobii Technology.

## 3.3 Procedure

Subjects were greeted, provided with an informed consent form, paid a $30 incentive, and provided with the demographic portion of the written survey. Once seated at the eye-tracking device, subjects were calibrated [38] and the eye-tracking portion of the study commenced. Half of the subjects proceeded first to the eye-tracking portion of the study and the other half proceeded to respond to the written survey. After completing the first section, they completed the other section.

For the eye-tracking portion of the study, participants were instructed to verbally respond to each image shown on the computer screen by saying how attractive they found each image, using a 10 point-Likert scale. Subjects were shown a randomized set of five images of 2 branded and 3 unbranded plants. The plants, but not the brands, were used in an earlier portion of the eye-tracking study.

## 3.4 Measurement

### 3.4.1Visual Attention

The length of a fixation is considered as an indication of information processing and thus product choice. To calculate the amount of visual attention, the following measurements were defined and used [39]:
*Time to first fixation* (TFF): The time in seconds from when a stimulus was shown until the start of the first fixation with an area of interest. This TFF indicates where the participants' eyes stop first on the image.
*Total visit duration* (TVD): The total time in milliseconds which is a product of fixation count multiplied by fixation duration and includes any movement in or out of the AOI. TVD indicates how long the product is visually being considered for choice.

### 3.4.2 Involvement

Development of scales to measure consumer product involvement and expertise of minimally packaged woody plants was necessary to explore the hypotheses. We developed 30 questions by adapting them from previous involvement and expertise scales [40]. Since the self-reported item responses are indictors of latent constructs principal factor analysis was used to identify latent constructs and the underlying factor structure using the FACTOR Procedure in SAS® software v. 9.3 [41]. We set prior communality estimates for each variable to its squared multiple correlation with all other variables and extracted the principal factors using the principal-axis factoring method. We used Kaiser's measure of sampling adequacy (MSA) to test the appropriateness of principal factor analysis [42]. Item reduction criteria included examination of Cronbach's alpha and item means and Pearson Correlation Coefficients [43]. Factor reduction included evaluation of the eigenvalues (or commonalities) and the scree test or the average of the prior communality estimates, in this case by SMC [44]. To test a potential scale's reliability, Cronbach coefficient (alpha), was compared to the alpha that would occur if a particular item (variable) or factor were deleted. We found the 2 factors extraction.

Varimax rotation was then applied to the variables and the alpha comparison repeated. Factor loadings > 0.50 were used to assign items to separate factors. No items were cross-loaded. Both scales were subsequently tested for reliability as independent scales. Factor 1 emerged as a 15-item scale and was labeled "expertise."

To measure involvement, participants were asked to circle the number that best reflected their responses in a 5-point Likert-scale. Sample items are: "Outdoor woody plants are important (1) to important (5)," "Outdoor woody plants are of no concern to me (1) to of great concern to me (5) ($\alpha$ = .94, $M$ = 0.00000047, $SD$ = 0.975).

The participants were sorted into the categories of high involvement, moderate and low involvement. The division for high, moderate, and low involvement was determined based on the median score of 0.100300. High involvement was measured by ≥0.100300, and moderate involvement was measured by scores >-0.325830 and <0.100300. Low involvement was determined to be ≤-0.325830. The number of individuals in each group was high (n = 36), moderate (n = 35), and low (n =37) for a total of N=108.

3.4.3 Expertise

Participants indicated how strongly they agreed with the following statements on a 5-pont Likert-scale, ranging from strongly disagree (1) to strongly agree (5). Sample questions are: "I know a lot about outdoor woody plants," "I am an outdoor woody plant expert," "I automatically know which outdoor woody plants to buy" ($\alpha$ = .95, *M* = 0.000000095, *SD* = 0.98). For creating expertise index, we computed individual factor scores to indicate individual's placement on the plant expertise.

The division for high, moderate, and low expertise was determined based on the median score of 0.059930. High expertise was measured by ≥0.550793, and moderate expertise was measured by scores >-0.478920 and <0.550793. Low expertise was determined to be ≤-0.478920. The number of individuals in each group was high (*n* = 36), moderate (*n* = 36), and low (*n* = 36) for a total of N=108.

3.4.4 Product Perceived Attractiveness

A dependent variable perceived attractiveness was measured by asking for participants to rate the object on 10-point scale (1 = very unattractive, 10 = very attractive).

# 4. Results

## 4.1 Hypotheses test

We examined whether the brand, consumers' personal characteristics such as product involvement, expertise as well as their demographic characteristics played a role as an external cue in consumer decision making. In addition, the same independent variables were examined as indicators of consumers' attractiveness.

We desired a single, overall statistical test on the dependent variables instead of performing multiple individual tests, which leads to increased type 1 error. In addition, due to the highly inter-correlated nature of the measures related to dependent variables, a multivariate variance analysis (MANOVA) was conducted by using Windows versions of Statistical Package for Social Sciences [45].

To test the H1, a MANOVA was employed with branded/unbranded as an independent variable, and TFF/ TVD of pot and TFF/ TVD of plant as dependent variables. The multivariate test result showed that there was significant brand effect on visual attention (Wilks' Lambda $F(4,427) = 12.350$, $p = .000$, $\eta^2 = .10$). Interestingly, the results showed that participants gave their first glance at unbranded pot ($M_{pot}$ = .43, *SD* = 1.11; $M_{plant}$= .21, SD = .36) than branded pot ($M_{pot}$= .94, *SD* = 1.18/ $M_{plant}$= .27, SD = .39), $F_{pot}$ (1, 432) = 22.21, $p < .000$, $\eta^2 = .05$, $F_{plant}$ (1, 432) = 3.37, $p = .06$, $\eta^2 = .01$ respectively (see Table 1). These results are not consistent with those of previous researches that perceived brand as an important external cue in drawing consumers' first attention. For $H1_b$, the result marginally supported our hypothesis in that TFF on plant with branded pot was longer than one with unbranded plant $M_{branded\ plant}$= .27, *SD* = .39; $M_{unbranded\ plant}$= .21, SD = .36), , $F_{plant}$ (1, 432) = 3.37, $p = .06$, $\eta^2 = .01$).

However, as we predicted, participants' eye fixation stayed longer on the branded pot and plant ($M_{pot}$ = .55, *SD* = 1.20/ $M_{plant}$= 3.99, SD = 3.04) than unbranded pot and plant ($M_{pot}$ = .07, *SD* = .33/ $M_{plant}$= 3.29, SD = 2.06), $F_{pot}$ (1, 430) = 32.10, $p < .000$, $\eta^2 = .07$, $F_{plant}$ (1, 430) = 7.67, $p < .01$, $\eta^2 = .02$. Therefore, $H1_c$ was supported.

**Table 1:** Means and the Effect of Brand on visual attention

| Visual attention Measure | | Brand | | *F* | *df* | *p* | $\eta^2$ |
|---|---|---|---|---|---|---|---|
| | | Branded M (SD) | Unbranded M (SD) | | | | |
| Plant | TFF | .27(.39) | .21(.36) | 3.37 | 430 | .06 | .01 |
| | TVD | 3.99(3.04) | 3.29(2.06) | 7.67 | 430 | .01** | .02 |
| Pot | TFF | .94(1.18) | .43(1.11) | 22.21 | 430 | .000*** | .05 |
| | TVD | .55(1.20) | .07(.33) | 32.10 | 430 | .000*** | .07 |

Regarding H2, MANOVA was employed with Involvement (high/moderate/low) as an independent variable, and branded/unbranded TFF/ TVD of pot and branded/unbranded TFF/ TVD of plant as dependent variables. The multivariate test result showed that there was significant involvement effect on the pair of dependent variables (Wilks' Lambda = .87, $F(8,422) = 3.82$, $p = .000$, $\eta^2 = .07$).

In the case of $H2_a$, the results did not show a significant difference between groups in terms of TFF on the plant and pot (see Table 2). Indeed, as opposed to the hypothesis, less involved consumers showed shorter

TFF than highly involved consumers. In the similar vein, we proposed $H2_b$ that consumers with higher involvement with a product will show longer TVD on the plant itself than those with lower involvement. As can be seen from the Table 2, the difference between groups in regard to TVD on branded plant are not statistically significant, but consumers with lower involvement showed longer TVD on unbranded plant than those with higher involvement ($M_{low}$ = 3.69, *SD* = 1.59, $M_{high}$= 3.44, *SD* = 1,96). However, group difference in TVD on the branded pot was marginally significant ($F_{pot}$ (1, 429) = 2.80, *p* = .06, $\eta^2 = .01$). The second hypothesis, therefore, was not supported.

**Table 2:** Means and the Effect of Involvement on visual attention

| Visual attention measure | | *Involvement* High *M (SD)* | Moderate *M (SD)* | Low *M(SD)* | *F* | *df* | *p* | $\eta^2$ |
|---|---|---|---|---|---|---|---|---|
| Branded | TFF | .38(.33) | .37(.26) | .33(.18) | 1.47 | 429 | *.231* | .00 |
| Plant | TVD | 4.46(2.76) | 3.98(1.33) | 4.36(1.84) | 2.12 | 429 | .122 | .01 |
| Unbranded | TFF | .45(.51) | .27(.16) | .26(.27) | 13.86 | 429 | .000*** | .06 |
| Plant | TVD | 3.44(1.96) | 3.43(1.11) | 3.69(1.59) | 1.27 | 429 | .282 | .00 |
| Branded | TFF | 1.45(.69) | 1.50(.49) | 1.41(.74) | .72 | 429 | *.489* | .00 |
| Pot | TVD | .74(.74) | .93(1.56) | .64(.59) | 2.80 | 429 | *.062* | .01 |
| Unbranded | TFF | 1.60(.65) | 1.36(.44) | 1.56(.92) | 4.73 | 429 | .009** | .02 |
| Pot | TVD | .12(.17) | .77(.12) | .12(.36) | 1.16 | 429 | .314 | .00 |

Note: **p* < .05, ***p* < .01, ****p* < .001

**Table 3:** Means and the Effect of Expertise on visual attention

| Visual attention Measure | | Expertise High *M (SD)* | Moderate *M (SD)* | Low *M(SD)* | *F* | *df* | *p* | $\eta^2$ |
|---|---|---|---|---|---|---|---|---|
| Branded | TFF | .44(.36) | .34(.16) | .29(.21) | 11.60 | 429 | .000*** | .05 |
| Plant | TVD | 3.77(3.26) | 4.47(2.21) | 4.55(2.26) | 6.38 | 429 | .002** | .03 |
| Unbranded | TFF | .39(.35) | .36(.45) | .23(.19) | 9.02 | 429 | .000*** | .04 |
| Plant | TVD | 3.01(1.24) | 3.65(1.71) | 3.91(1.67) | 12.81 | 429 | .000** | .06 |
| Branded | TFF | 1.56(.67) | 1.35(.50) | 1.44(.75) | 3.96 | 429 | .020* | .02 |
| Pot | TVD | .78 (.90) | .96(1.51) | .56(.38) | 5.61 | 429 | .004** | .03 |
| Unbranded | TFF | 1.55(.60) | 1.35(.89) | 1.62(.57) | 6.02 | 429 | .003** | .03 |
| Pot | TVD | .12(.16) | .16(.38) | .32(.05) | 10.79 | 429 | .000*** | .06 |

Note: **p* < .05, ***p* < .01, ****p* < .001

Regarding H3, the overall multivariate test was significant (*Wilks' Lambda = .78, F*(8,422) = 6.87, *p* < .000, $\eta^2 = .12$). In line with the hypothesis $H3_a$, the moderate-expertise group showed the shortest TFF on the branded pot ($M_{moderate}$ = 1.35, *SD* = .50, $M_{low}$= 1.44, *SD* = .75, $M_{high}$= 1.56, *SD* = .67, *F*(2,429) = 3.96, *p* < .05, $\eta^2 = .02$**)** (see Table 3). In consistent with $H3_b$, the moderate product expertise paid more attention and thus longest TVD on branded pot among groups (($M_{moderate}$ = .96, *SD* = 1.51, $M_{low}$= .56, *SD* = .38, $M_{high}$= .78, *SD* = .90, *F*(2,429) = 5.61, *p* < .01, $\eta^2 = .03$**).** This finding indicates that the moderate group had enough motivation to devote a substantial processing effort in decision making than higher or lower group.

For $H3_{C,}$ the result supported the hypothesis in that individual with higher product expertise would focus less on branded plant than lower or moderate product expertise. ($M_{high}$ = 3.77, *SD* = 3.26, $M_{moderate}$= 4.47, *SD* = 2.21, $M_{low}$= 4.55, *SD* = 2.26, *F*(2,429) = 6.38, *p* < .01, $\eta^2 = .03$**)**.

We employed a MANOVA and examined if interaction between involvement and motivation existed. As predicted, the results showed the interaction effect between involvement and expertise (*F*(8,416) = 4.475, p < .001, $\eta^2$ = .08). We can conclude that involvement and expertise are interdependent each other, so that consumers may be motivated by involvement to focus on information seeking when their knowledge were retrieved from their long-term memory.

To test H4, MANOVA was conducted with gender (male/female) as an independent variable, and Branded/Unbranded TFF/ TVD of pot and Branded/Unbranded TFF/ TVD of plant as dependent variables. The overall multivariate test was significant (*Wilks' Lambda = .93, F*(8,423) = 3.81, *p* < .000, $\eta^2 = .07$). Concerning H4a, the results support the hypothesis that males showed shorter TFF that females ($M_{male\ (branded\ pot)}$ = 1.33, *SD* = .40, $M_{female\ (branded\ pot)}$ = 1.50, *SD* = .72, *F*(1, 430) = 6.10, *p* < .05, $\eta^2$ = .01) (see Table 4). This finding indicates that males utilize heuristic strategies in an attempt to solve problem quickly in information processing.

For H4b, the result exhibited that females demonstrated greater TVD on branded pot as well as branded plant ($M_{female\ (branded\ pot)}$ = .84, *SD* = 1.21, $M_{male\ (branded\ pot)}$ = .59, *SD* = .35, *F*(1, 430) = 5.24, *p* < .05, $\eta^2$ = .02; $M_{female\ (branded\ plant)}$ = 4.44, *SD* = 2.34, $M_{male\ (branded\ plant)}$ = 3.84, *SD* = 1.07, *F*(1, 430) = 7.62, *p* < .01, $\eta^2$ = .02 ). H4 was supported.

**Table 4:** Means and the Effect of Gender on visual attention

| Visual attention measure | | Gender Females *M (SD)* | Males *M (SD)* | *F* | *df* | *p* | $\eta^2$ |
|---|---|---|---|---|---|---|---|
| Plant | Brand TFF | .37(.28) | .32(.28) | 3.57 | 430 | .059 | .01 |
| | Unbrand TFF | .34(.28) | .29(.50) | 1.26 | 430 | .263 | .00 |
| | Brnad TVD | 4.44(2.34) | 3.84(1.07) | 7.62 | 430 | .006** | .02 |
| | Unbrand TVD | 3.49(1.77) | 3.60(1.03) | .43 | 430 | .512 | .00 |
| Pot | Brand TFF | 1.50(.72) | 1.33(.40) | 6.10 | 430 | .014* | .01 |
| | Unbrand TFF | 1.49(.73) | 1.56(.66) | .95 | 430 | .330 | .00 |
| | Brand TVD | .84(1.21) | .59(.35) | 5.24 | 430 | .023* | .02 |
| | Unbrand TVD | .12(.28) | .07(.12) | 2.86 | 430 | .091 | .01 |

Note: *$p$ < .05, **$p$ < .01, ***$p$ < .001

To answer the research question whether older consumers would use a heuristic strategy, thus focusing on branded product at first and would make a quick decision we used a MANOVA. Aged-group was the independent variables and branded/unbranded plant and pot were the dependent variables.

**Table 5:** Means and the Effect of Age on visual attention

| Visual attention measure | | Age Young *M (SD)* | Middle *M (SD)* | Mature *M (SD)* | *F* | *df* | *p* | $\eta^2$ |
|---|---|---|---|---|---|---|---|---|
| Plant | Brand TFF | .44(.40) | .33(.13) | .31(.18) | 10.48 | 429 | .000*** | *.05* |
| | Unbrand TFF | .35(.28) | .30(.25) | .33(.48) | .69 | 429 | .500 | .00 |
| | Brand TVD | 3.92(1.67) | 4.18(2.11) | 4.66(2.30) | 4.83 | 429 | .008** | .02 |
| | Unbrand TVD | 3.46(1.75) | 3.57(1.68) | 3.53(1.36) | .17 | 429 | .171 | .00 |
| Pot | Brand TFF | 1.46(.67) | 1.45(.57) | 1.44(.71) | .03 | 429 | .971 | .00 |
| | Unbrand TFF | 1.44(.62) | 1.56(.78) | 1.53(.71) | 1.05 | 429 | .351 | .00 |
| | Brand TVD | .49(.40) | .77(.60) | 1.02(1.60) | 9.37 | 429 | .000*** | .04 |
| | Unbrand TVD | .05(.07) | .16(.38) | .09(.14) | 7.97 | 429 | .000*** | .04 |

Note: *$p$ < .05, **$p$ < .01, ***$p$ < .001

A significant main effect for age was found (*Wilks lambda* = .859, *F*(8,422) = 4.18, *p* < .000, $\eta^2$ = *.07).* The same trend is shown in Table 5, where the results for the underlying dependent measures used in the MANOVA are displayed. As the researchers predicted, the mature (older) participants showed the shortest TFF on branded plant than middle and youth group ($M_{mature}$ = .31, *SD* = .18, $M_{middle}$ = .33, *SD* = .13, , $M_{youth}$ = .44, *SD* = .40, *F*(2, 429) = 10.48, *p* < .000, $\eta^2$ = .05). The mature group showed the shortest TFF on the branded pot; however, group difference was not statistically significant.

We predicted because the older group would use a heuristic strategy, they would show shorter TVD on branded plant and pot. However, the result showed that among age groups, the mature age group gazed both at branded plant and branded pot for the longest time ($M_{mature(branded\ plant)}$ = 4.66, *SD* = 2.30, $M_{middle(branded\ plant)}$ = 4.18, *SD* = 2.11, , $M_{youth(branded\ plant)}$ = 3.92, *SD* = 1.67, *F*(2, 429) = 4.83, *p* < .01, $\eta^2$ = .02; $M_{mature(branded\ pot)}$ = 1.02, *SD* = 1.60, $M_{middle(branded\ pot)}$ = .77, *SD* = .60, , $M_{youth(branded\ pot)}$ = .49, *SD* = .40, *F*(2, 429) = 9.37, *p* < .000, $\eta^2$ = .04). This result indicates that the search process for older-aged consumers is more comprehensive and they exert greater cognitive effort in information processing.

To test the relationship between total visit duration (TVD) and product attractiveness, a standard multiple regression analysis was conducted to determine how well TVD on pot and TVD on plant predicted perceived attractiveness. The results showed that the amount of time consumers attended to the plant/pot did not significantly predict product attractiveness.

**Table 6:** Regression Predicting Perceived Product Attractiveness

| Model | | Unstandardized Coefficients | | Standardized Coefficients | t | Sig |
|---|---|---|---|---|---|---|
| | | B | SE | Beta | | |
| 1 | (Constant) | 5.732 | .164 | | 34.882 | .000 |
| | PotTVD | -.016 | .109 | -.007 | -.145 | .885 |
| | FoliTVD | .051 | .038 | .067 | 1.340 | .181 |

*Note*: Dependent Variable: Perceived Attractiveness. $R^2$ = .004

A standard multiple regression analysis was employed how well plant/pot TVD, involvement, expertise, age, and gender predicted perceived attractiveness. The results are summarized in the Table 7.

**Table 7:** Regression predicting Perceived Product Attractiveness

| Model | | Unstandardized Coefficients | | Standardized Coefficients | t | Sig |
|---|---|---|---|---|---|---|
| | | B | SE | Beta | | |
| 1 | (Constant) | 4.608 | .373 | | 12.367 | .000*** |
| | Brand | 1.461 | .216 | .308 | 6.767 | .000*** |
| | Gender | .715 | .243 | .136 | 2.937 | .003** |
| | Age | .003 | .007 | .021 | .453 | .651 |
| | Expertise | .130 | .133 | .053 | .972 | .332 |
| | Involvement | .610 | .132 | .248 | 4.628 | .000*** |
| | PlantTVD | .003 | .042 | .003 | .064 | .949 |
| | PotTVD | -.038 | .124 | -.015 | -.308 | .758 |

*Note*: Dependent Variable: Perceived Attractiveness. $R^2$ = .185

*$p$ < .05, **$p$ < .01, ***$p$ < .001

The results showed that brand, involvement and gender were the strongest factors for predicting perceived attractiveness ( $\beta_{brand}$ = 1.46, $p$ = .000, $\beta_{involvement}$ = .61, $p$ = .000; $\beta_{gender}$ = .72, $p$ < .01).

To examine what the best combination of independent variables would be to predict the perceived attractiveness, a stepwise multiple regression was conducted. The results are summarized in the Table 8. This model indicates 18.3 % of the variance of the perceived attractiveness was accounted for by brand, involvement, and gender.

**Table 8:** Regression predicting perceived Attractiveness

| Model | | Unstandardized Coefficients | | Standardized Coefficients | t | Sig |
|---|---|---|---|---|---|---|
| | | B | SE | Beta | | |
| 2 | (Constant) | 5.405 | .167 | | 21.707 | .000 |
| | Brand | 1.444 | 0209 | .305 | 6.979 | .000 |
| | Involvement | .687 | .108 | .279 | 6.367 | .000 |
| | Gender | .701 | .229 | .134 | 3.056 | .002 |

*Note*: Dependent Variable: Perceived Attraction. $R^2$ = .183

## 5. Conclusions

The aim of this study was to examine the role played by brand name as an external cue in consumer information processing. We also investigated whether in-store marketing influences perceived product attractiveness, as assessed with an eye-tracking device. In particular, we analyzed such personal consumer characteristics as product

involvement and expertise and their effects on influencing perceived attractiveness and, thus, product choice. Using the elaboration likelihood model (ELM) and selected model (SM), we considered whether the brand played a role as an external cue.

This study attempted to capture the process of dynamic information seeking by studying how consumers fixed their visual attention while evaluation a product. We also analyzed the influence of individual consumer characteristics (age, gender, involvement, expertise) on how different patterns of responses played out in the information seeking process.

We predicted higher involvement with the product would show shorter TFF and longer TVD on the product compared to those with low involvement with the product. We discovered an overall main effect of involvement on visual attention. However, the univariate analysis did not support our hypotheses. For expertise, we found a main effect on visual attention. In line with our hypotheses, moderate expertise showed the shortest TFF and longest TVD on the branded pot. Higher expertise showed less visual attention to the branded plant. We could conclude that those with higher expertise group might have enough ability, but is not necessarily motivated to process much current information since they could rely on information in memory and their prior experiences. Some scholars argued that separating the effects of involvement and domain knowledge were problematic [46]. We found a main effect of interaction between involvement and expertise on visual attention. So we can conclude that involvement is positively related to domain knowledge.

We predicted that participants would show shorter time to first fixation (TFF) on a branded pot than a non-branded pot. However, surprisingly, the participants reacted to the stimuli in a reverse manner in that individuals first attended to the unbranded pot instead of the branded pot. Since brand has been considered to be an important external cue in drawing consumers' attention, the results are surprising. One possible explanation is that the experimental condition was different from a real-life purchase condition. While participants' first attended to the unbranded pot, they looked longer at the branded pot/plant.

According to the selectivity model (SM) [47], males often do not process all available information cues but instead are highly selective in information processing and use heuristic strategy, whereas females engage in comprehensive and more detailed analysis of specific message content [48][49]. Out findings supported the SM. We found that males showed shorter TFF than females and females paid greater visual attention both to the branded plant and pot than males. This indicates that males use heuristic strategy, while females use comprehensive information seeking strategy.

We found that the older consumers showed not only the shortest TFF on branded plant but also the longest TVD on branded plant and pot. The young group paid the shortest attention to branded pot as well as plant. This indicates that the older consumers processed more available information than the other groups.

The relationship between visual attention and perceived attractiveness was not significant, but the existence of brand name did have an impact on perceived attractiveness.

Limitations of the study include the fact that visual attention was measured with nine slides with similar pictures of plants shown in succession. This may have conjured a learning effect whereby participants were accustomed to the stimuli after viewing the first slide, thus allowing them to make biased assessments of subsequent slide due to the familiarity. Future research could involve using eye-tracking technology for viewing real plants one by one and not fictitious photographs of products, allowing individuals to know they are viewing a completely new item each time. Attractiveness was a one-item measure: using a multi-item scale in future research would increase the measurement properties.

## 6. Implications

This study contributes to information seeking theory by supporting the selectivity model (SM) in that females are more likely to use comprehensive and detailed analysis information processing strategy. Older consumers also have a similar information-seeking pattern to women. In particular, both female and older consumers have a tendency to use brand as a crucial external cue in information processing. Gender and age have been considered critical factors in consumption. That is, consumers' gender and age differences make them different in response to the products' packaging offered by the marketers and retailers. This study proves gender and age can be used critical market segmentation strategies.

Furthermore, the eye-tracking device used in this experiment offers an innovative method to develop an accurate assessment of the process of consumer information acquisition and decision-making. In the highly competitive marketplace, marketers and retailers should know precisely which elements are examined and which ones are ignored by consumers when they make a choice to purchase a product. These factors associated with consumers' personal characteristics can assist in deducing the reasons behind their final purchase decision. This strategy of using eye-tracking device can result in more effective POP merchandising and thus higher profits, strengthening the ability of a brand to survive in today's highly competitive marketplace.

## Acknowledgement

The authors gratefully acknowledge the data collection efforts of Drs. Charlie Hall and Marco Palma (Texas A& M University) and the generous funding from the Horticultural Research Institute.

## References

1. POPAI. (2012). 2012 shopper engagement study: Media topline report. Retrieved from www.popai.com/engage/docs/Media-Topline-Final.pdf.
2. B.K. Behe. J. Zhao. P. Huddleston and S. Minahan, 2013, "Display signs and involvement: The visual path to purchase intention", *The International Review of Retail, Distribution and Consumer Research,* vol. 23, no. 5, pp.1-12.
3. I. Holmberg, 2002, Living trademarks. In Holger, L., & Holmberg, I. (Eds.), *Identity: trademarks, logotypes and symbols*. Stockholm: Raster Forlag.
4. G.A. Miller, 1956, "The magical number seven, plus or minus two: Some limits on our capacity for processing information," *Psychological Review,* vol. 63, pp. 81-97.
5. H. Simon, 1974, "How big is a chunk?", *Science,* vol. 183, pp. 482-488.
6. J. Jacoby. J.C. Olson and R.A. Haddock, 1971, "Price, brand name and product composition characteristics as determinants of perceived quality", *Journal of Applied Psychology*, vol. 55, pp. 570-579.
7. Shiffrin. M. Richard and G.T. Gardner, 1972, "Visual processing capacity and attention control", *Journal of Experimental Psychology*, vol. 93, no. 1, pp. 72-82.
8. R. Howell, 1999, "The effect of product expertise on decision making and search for written and sensory information", *Advances in Consumer Research*, vol. 26, no. 1, pp. 80-89.
9. J.M. Henderson and A. Hollingworth, 1999, "High level scene perception", *Annual Review of Psychology*, vol. 50, pp. 243-271.
10. K. Rayner, 1998, "Eye movement in reading and information processing: 20 years of research", *Psychological Bulletin,* vol. 124, no.3, pp. 372-422.
11. M. Wedel and R. Pieters, 2008, A review of eye-tracking research in marketing. *In Review of Marketing Research,* Vol. 4, N.K. Malhotra (ed.), Armonk, NY: M.E. Sharpe, 123-147.
12. R.E. Petty and J.T. Cacciopo, 1983, Central and peripheral routes to persuasion: Application to advertising. In L. Percy & A.E. Woodside (Eds.), *Advertising and consumer psychology* (pp. 3-23). Lexington, MA: Lexington Books.
13. R.E. Petty. J.T. Cacciopo and D. Schumann, 1983, "Central and peripheral routes to advertising effectiveness: The moderating role of involvement", *Journal of Consumer Research,* vol. 10, pp. 135-145.
14. P. Laaksonen, 1994, *Consumer involvement: concepts and research*. London: Routledge.
15. J.W. Park, 1995, "Effects of involvement on on-line brand evaluation: A strong test of the ELM", *Advances in Consumer Research*, vol. 22, pp. 435-439.
16. J.R. Bettman and W. Park, 1980, "Effects of prior knowledge and experience and phase of the choice process on consumer decision processes: A protocol analysis", *Journal of Consumer Research,* vol. 7, no. 4, pp. 234-248.
17. M. Sujan, 1985, "Consumer knowledge: Effects on evaluation strategies mediating consumer judgments", *Journal of Consumer Research,* vol. 12, no. 2, pp. 31-46.
18. J. Meyers-Levy, 1989, "Elaboration on elaboration: The distinction between relations and item-specific elaboration", *Journal of Consumer Research*, vol. 18, no. 3, pp. 358-367.
19. J. Meyers-Levy and B. Sternthal, 1991, "Gender differences in the use of message cues and judgments", *Journal of Marketing Research*, vol. 28, no.1, pp. 84-96.
20. S.M. Kristi and M.K. Johnson, 1999, "Source memory and eyewitness suggestibility in older adults", *Journal of General Psychology*, vol. 126, no. 1, pp. 74-84.
21. P. Sorce. V. Perotti and S. Widrick, 2005, "Attitude and age differences in online buying", *International Journal of Retail & Distribution Management,* vol. 33, no. 2, pp. 122-132.
22. J.H. Denis and B.K. Behe, 2007, "Evaluating the role of ethnicity on gardening purchases and satisfaction", *HortScience*, vol. 42, no. 2, pp. 262-266.
23. S. Auti and R. Elliot, 1998, "Fashion involvement, self-monitoring and the meaning of brands", *Journal of Product and Brand Management*, vol. 7, pp. 109-123.
24. J.R. Busemeyer and A. Diedrich, 2002, "Survey of decision field theory", *Mathematical Social Science,* vol. 43, pp. 345-370.
25. K.C. Armel and A. Rangel, 2008, "The impact of computation time and experience on decision values", *American Economic Review,* vol. 98, pp. 163-168.
26. W. Dodds. K.B. Monroe and D. Grewal, 1991, "Effects of price, brand, and store information on buyers'

product evaluations", *Journal of Marketing Research,* vol. 28, no. 3, pp. 307-319.
27. A.R. Roa and K.B. Monroe, 1989, "The effect of price, brand name, and store name on buyers' perceptions of product quality: An integrative review", *Journal of Marketing Research*, vol. 26, pp. 351-357.
28. K.B. Monroe and R. Krishnan, 1984, The effect of price on subjective product evaluation, In J. Jacoby and J. Olson (Eds.), *The Perception on Merchandise and store quality*, Lexinton, MA: D.C. Heath.
29. W. Dodds and K.B. Monroe, 1985, "The effect of brand and price information on subjective product evaluations", *Advances in Consumer Research,* vol. 12, no. 1, pp. 85-90.
30. R.E. Petty and J.T. Cacioppo, 1981, *Attitude and persuasion: Classic and contemporary approaches*, Dubuque, IA: William C. Brown.
31. H.E. Krugman, 1965, "The impact of television advertising: Learning without involvement", *Public Opinion Quarterly,* vol. 29, pp. 349-366.
32. R.B. Zajonc, 1968, "Attitudinal effects of mere exposures", *Journal of Personality and Social Psychology*, vol. 9, no. 2, pp. 1-27.
33. P. Winkielman. K.C. Berridge and J.L. Wilbarger. 2003, "Unconscious affective reactions to masked happy versus angry faces influence consumption behavior and judgments of value", *Personality and Social Psychology Bulletin,* vol. 31, no. 1, pp. 121-135.
34. H. Reis M.R. Maniaci. P.W. Eastwick and E.J. Finkel, "Familiarity does indeed promote attraction in live interaction", *Journal of Personality and Social Psychology,* vol.101, no. 3, pp. 557-570.
35. W.K. Darley and R.E. Smith, 1995, "Gender differences in information processing strategies: An empirical test of the selectivity model in advertising response, *Journal of Advertising*, vol. 24, no. 1, pp. 41-56.
36. D. Isaacowitz. H. Wadlinger. D. Goren and H. Wilson, 2006, "Selective preference in visual fixation away from negative images in old age? an eye-tracking study", *Psychology and Aging,* vol. 21, no.1, pp. 40-48.
37. S. Kim. M.K. Healey. D. Goldstein and L. Hasher, 2008, "Age differences in choice satisfaction: A positivity effect in decision making", *Psychology and Aging,* vol. 23, no. 1, pp. 33-38.
38. B.K. Behe. J. Zhao. P. Huddleston and S. Minahan, 2013, "Display signs and involvement: The visual path to purchase intention", *The International Review of Retail, Distribution and Consumer Research,* vol. 23, no. 5, pp.1-12.
39. Tobii Technology (2008). Eye tracking as a tool in package and shelf testing. Retrieved November 2, 2013from http://www.tobii.com/Global/Analysis/Training/WhitePapers/Tobii_EyeTracking_in_Package_and_Shelf_Testing_WhitePaper.pdf
40. G.C. Bruner. K. James and P.J. Hensel, 2001, *Marketing Scales Handbook: A Compilation of Multi-item Measures*, Chicago: AMA.
41. SAS Institute Inc., SAS/STAT® 9.3 User's Guide, Cary, NC, USA. http://support.sas.com/documentation/cdl/en/statug/63962/HTML/default/viewer.htm#statug_factor_sect006.htm.
42. D. Pasta and D. Suhr, 2004, *Creating scales from questionnaires: PROC VARCLUS vs. factor analysis*, In Processings of the twenty-ninth annual SAS Users Group International Conference. Cary, NC: SAS Insitute Inc.
43. SAS Library, 1995, Factor analysis using SAS proc factor. Retrieved October 2013 from http:www.ats.ucla.edu/stat/sas/library/factor_ut.htm.
44. G. Fernandez, 2003, Data mining using SAS applications. Chapman & Hall/CRC (Accessed online Jan 2014, pp. 117-118).
45. IBM SPSS Statistics, SPSS 20 http://www-01.ibm.com/software/analytics/spss/products/statistics/
46. M. Sujan, 1985, "Consumer knowledge: Effects on evaluation strategies mediating consumer judgments", *Journal of Consumer Research,* vol. 12, no. 2, pp. 31-46.
47. J. Meyers-Levy, 1989, "Elaboration on elaboration: The distinction between relations and item-specific elaboration", *Journal of Consumer Research*, vol. 18, no. 3, pp. 358-367.
48. W.K. Darley and R.E. Smith, 1995, "Gender differences in information processing strategies: An empirical test of the selectivity model in advertising response, *Journal of Advertising*, vol. 24, no. 1, pp. 41-56.
49. J. Meyers-Levy and B. Sternthal, 1991, "Gender differences in the use of message cues and judgments", *Journal of Marketing Research*, vol. 28, no.1, pp. 84-96.

# The Design Development of Perforation Rule for Retail Ready Packaging

**Krit Fuangfu and Varna Sudasna***

*Thai Containers Group Co., Ltd., Thailand*

**Corresponding author. Email: varnab@scg.co.th*

**Abstract:** The implementation of Retail Ready Packaging (RRP) is dramatically increasing in the last decade by the cooperation between retailers, brand owners, suppliers, and packaging companies. There are many studies from retailers, packaging suppliers, and consumer organizations on RRP concepts, implementation, and design that have been published and being used as RRP guidelines. Corrugated box with perforation rule is commonly used for RRP because of its compressive strength and display ability, especially smaller flute such as B flute. In addition, the perforation rule on RRP plays an important role to create not only sufficient box strength during transport but also ease of opening with the clean edge on shelf.

Three sets of perforation rule were designed and studied in this research. Each set of perforation has two different rules at the front panel and the flap edge of box. The perforation rules are Set-A Front 8x3(cut x non-cut length) and Flap edge 5x4, Set-B Front 10x4 and Flap edge 6x4, and Set-C Front 10x3 and Flap edge 6x5. The corrugated boards B flute made from white top liner(30% virgin pulp) and brown top liner(100% recycled pulp) were used to manufactured RRP with set of perforation rules for bar soap product. Then, the RRP were measured and evaluated on box compression test, drop resistance, ease of opening, and appearance after opened.

The results showed that different perforation rules on the same position had no significantly effect on compressive strength of box. The shorter cut length of perforation, Set-A, performed better drop resistance than others longer cut length. The easy-to-open and display appearance were resulted in the same direction. The Set-B was scored “easy” and “satisfied” in easy-to-open and display appearance criteria, respectively. Paper board combined with virgin fibers performed better drop resistance. In contrast, it performed “difficult” on easy-to-use and scored “not satisfied” on display appearance aspects.

Base on the results of this study, recommendation guidelines for perforation rule have been developed.

Keywords: retail ready packaging, shelf ready packaging, perforation rule, packaging design.

## 1 Introduction

The increasing of the population and economic growth in Asian counties are pushing Fast Moving Consumer Goods (FMCG) or Consumer Packaged Goods (CPG) companies to expand their production bases to Asian countries. There is a new and growing market with the advantages of lower labor and raw materials cost. Thailand is one of a major production base of many FMCG companies such as Unilever, Johnson & Johnson, Procter & Gamble, Colgate-Palmolive, etc. Most of manufactured products are consumer goods, for example body care and hair care products. These products will be exported worldwide, especially to those developed countries such as United State, Europe, Japan, and Australia.

Recently, the large retailers, such as Walmart, Tesco, Coles, etc. have published their packaging requirements and regulations for products that would be sold in their stores. One of their requirements which is currently a packaging trend is Retail Ready Packaging (RRP). For example, Walmart [1] published RRP Guidelines for North America in 2011. These guidelines provided Walmart suppliers to be more understood on Walmart requirements of RRP. It included the concept of five easies of RRP, merchandising rules and requirements, the preference of gluing and taping on corrugated box, and the graphical and visibility on shelf of the RRP. RRP is becoming a mandatory requirement from retailers, especially for households and foods products.

Benasch [2] from STi Group of packaging company, explained that RRP have been developed to get products from case to shelf. The biggest benefits of RRP are at the retailers on the labor cost saving. However, other business units throughout supply chain also get the advantages from implementing RRP as shown in Figure 1.

For example, the brand owners with the attractive RRP designs will get the benefit of brand image and increased sales volume.




**Figure 1**: Advantage of Shelf Ready Packaging from STI Group

There are many studies and publications from both retailers and packaging suppliers on implementation and design development of RRP. Those studies were included the guidelines that help brand owners and packaging manufacturers to get better understanding and expedite the implementation of RRP. Efficient Consumer Response (ECR) Australasia [3] have first published the RRP toolkit in 2007. It indicated the key driver of RRP which is the improvement of store efficiency through increased speed of replenishment leading to better on-shelf availability and increase sales. The five easies of RRP (easy to identify, easy to open, easy to shelf, easy to shop, and easy to dispose) and prioritization approach of each products were defined as guidelines for retailers, suppliers, wholesalers and packaging companies. The later guidelines from ECR Australasia toolkits [4], [5] determined the implementation process of RRP, types of RRP, and carton design and configuration. Schrijver [6] provided additional evidence that the RRP design plays a significant role in the consumer's purchasing decision. The design elements such as curve, shape, or color of RRP that align with the brand identity could be used as marketing tools to communicate the brand message and distinguish itself from competitor on shelf. On the other hand, the inappropriate or poor RRP design could decrease the brand image and sales.

Roukema [7] cites that creating the RRP is not just adding the perforation on the current packing but there are some conflicting requirements that need to be considered. For example, the box needs to be strong enough not to break during distribution but easy enough to open on shelf at store. Also provided addition consideration elements for RRP on safe and secure through the supply chain, easy and intuitive opening, and optimal appearance. Those including the recommendations of perforation, such as curved perforation are better than straight line in term of load bearing and the difference printing color at the start point of opening can help employee easy to identify and open, etc. Georgia-Pacific Innovation Institute [8] has also developed "Clean and Easy-Perf$^{TM}$" which claimed that it would make the package easier to open with a cleaner edge for superior shelf display.

Corrugated box is commonly used for RRP because of its compressive strength and display ability, especially smaller flute such as B and E flute. The perforation rule on RRP plays an important role to create not only sufficient box strength during transport but also ease of opening with the clean edge on shelf. Unfortunately, there is no data available on perforation rule design, especially for RRP. So, it is challenging to fill this knowledge gap in this study.

The objectives of this research were

- To study the effect of perforation rulings of RRP on difference paper profiles based on compressive strength, drop test performance, open ability and display appearance criteria on the case study of bar soap product.
- To develop packaging design guidelines of perforation rule on RRP.

## 2 Materials and Methods

### 2.1 Test Instrumentation

The Box Compression Tester (BCT) model HT-8506 manufactured by Hung Ta Instrument, Taiwan was used to measure the BCT of the box in this study. The bottom plate is fixed and the top plate is moving downward to

compress the box. The compression area is 100cmx100cm. The maximum compression load is 2,000 kg with the test speed of 13mm/min.

## 2.2 Test Package

Three sets of perforation rules were designed on RRP corrugated box. In each set of perforation rule has two different rules at the front panel and the flap edge of box as shown in Figure 2-4. The first perforation rule is located on the front panel at the starter point for initial opening. The second rule is located on the flap edge of the box as follower lines to fully complete the opening of the box. The three sets of perforation rules are Set-A Front 8x3(cut x non-cut length in millimeter) and Flap edge 5x4, Set-B Front 10x4 and Flap edge 6x4, Set-C Front 10x3 and Flap edge 6x5.

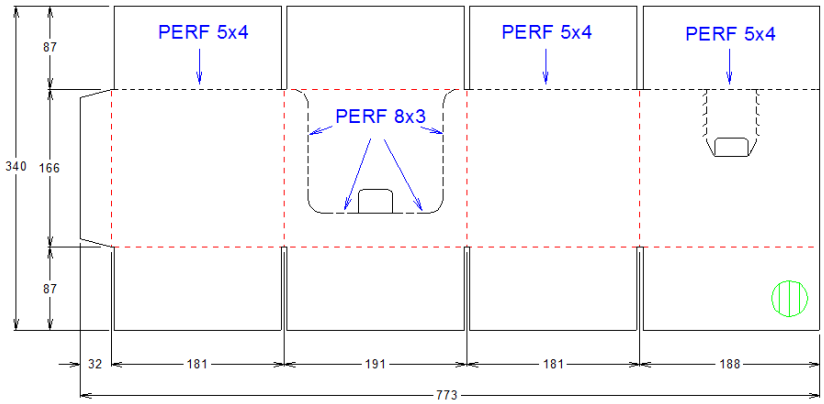



**Figure 2** : Drawing pattern of Set-A perforation rule (Front 8x3, Flap edge 5x4)

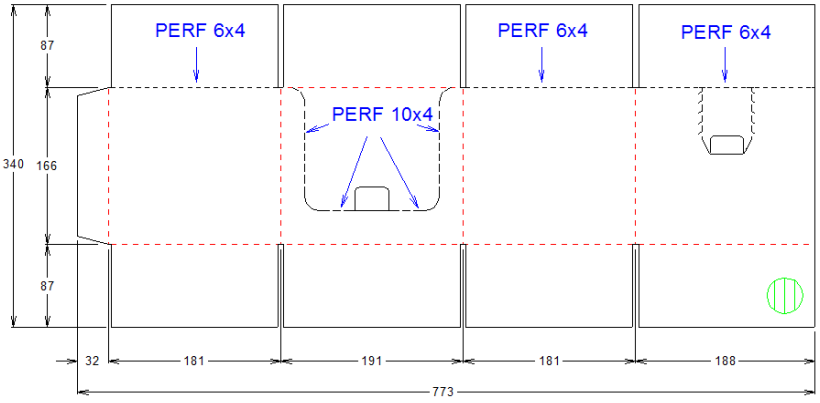



**Figure 3** : Drawing pattern of Set-B perforation rule (Front 10x4, Flap edge 6x4)

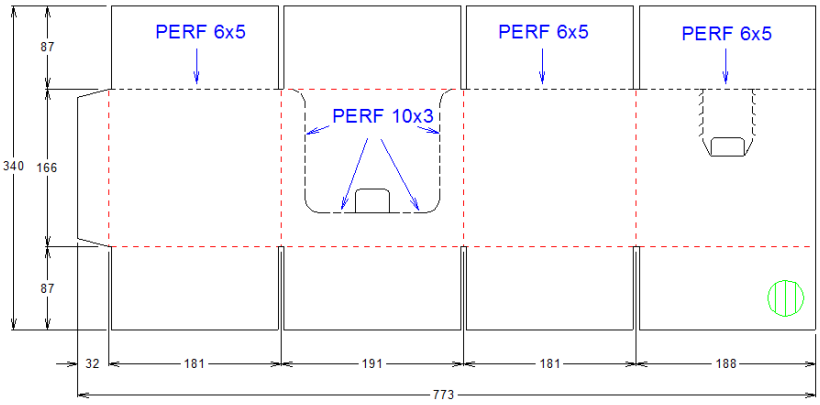



**Figure 4** : Drawing pattern of Set-C perforation rule (Front 10x3, Flap edge 6x5)

The B-flute corrugated boxes with two different liner's profiles and colors were used in this study. The first board combination was KS170/CS110/KT125 (white top test liner, 30%virgin pulp) and the second was KT150/CS110/KT150 (brown top test liner, 100%recycled pulp). The boxes were manufactured from real production without printing, then die-cut and glued. The 30 bars of 100g bar soap were packed into the box and sealed by 2" width plastic sealing tape. The total gross weight is 3.20 kg per box. The total six samples were used in this study as shown in Table 1.

**Table 1 :** The experiment samples in this study

| Sample | Perforation rule (Front , Flap edge) (Cut x Non-cut) | Top liner color | Board Combination | Board Weight (g/sq.m.) | Inside Dimension (mm) (LxWxD) |
|---|---|---|---|---|---|
| 1 | Set-A : 8x3, 5x4 | White | KS170/CS110/KT125-B | 446.8 | 188x178x161 |
| 2 | Set-B : 10x4, 6x4 | White | KS170/CS110/KT125-B | 446.8 | 188x178x161 |
| 3 | Set-C : 10x3, 6x5 | White | KS170/CS110/KT125-B | 446.8 | 188x178x161 |
| 4 | Set-A : 8x3, 5x4 | Brown | KT150/CS110/KT150-B | 451.8 | 188x178x161 |
| 5 | Set-B : 10x4, 6x4 | Brown | KT150/CS110/KT150-B | 451.8 | 188x178x161 |
| 6 | Set-C : 10x3, 6x5 | Brown | KT150/CS110/KT150-B | 451.8 | 188x178x161 |

The test packages were evaluated the performance and appearance by BCT, drop test, easy-to-open, and displaying appearance.

## 2.3 Test Method

### Box Compression Test (BCT)

The samples were evaluated the perforation performance and compression strength of empty box using BCT tester. Thirty boxes of each sample were selected, formed, and sealed with plastic sealing tape for BCT test. Then, the BCT values were averaged and analyzed to determine the compressive resistance and perforation performance.

### Drop Test

The packaged products of each sample were dropped (manually free fall drop) using customer's standard procedure[9] at the height of 1.5 meters. Two boxes per sample are required for drop test. The identification of the faces of the box are shown in Figure 5. The drop sequence and orientation are shown in Table 2. The criteria of drop test evaluation are averaged number of damaged products and overall appearance after dropped. The evaluation were conducted by customer's panel lists (3 persons) and determined the satisfaction score, ranking from 1 to 3 (1 = satisfied, 2 = fair, 3 = not satisfied)

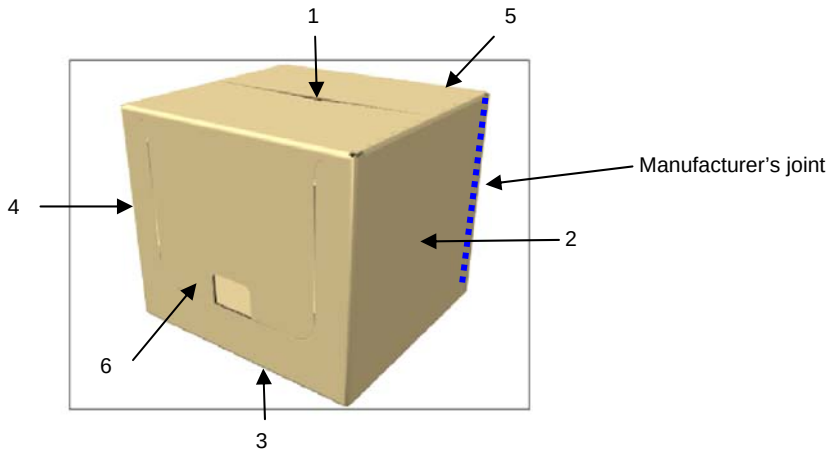



**Figure 5 :** Identify the faces of the box

**Table 2 :** Drop sequence and drop orientation

| Sequence # | Orientation | Specific face |
|---|---|---|
| 1 | Face | Bottom face (Face 3) |
| 2 | Face | Side face, manufacturer's join face (Face 2) |
| 3 | Face | Back face (Face 5) |
| 4 | Face | Side face (Face 4) |
| 5 | Face | Front face (Face 6) |
| 6 | Face | Top face (Face 1) |

### Easy-to-Open

The packaged product of each sample will be torn from starter point at front panel to fully open of the box. Then, the easy-to-open was evaluated based on these criteria; package can be opened without a tool and box could be opened within 10 seconds. The evaluation were conducted by customer's panel lists (3 persons) and determined the satisfaction score, ranking from 1 to 3 (1 = easy to open, 2 = fair, 3 = difficult)

### Display appearance after opening

After evaluated the easy-to-open of the perforation rules, the same packaged product were then evaluated for the appearance on shelf (the cleanliness of the tearing at edge and overall appearance). The evaluation were conducted by customer's panel lists (3 persons) and determined the satisfaction score, ranking from 1 to 3 (1 = satisfied, 2 = fair, 3 = not satisfied)

All the test methods are conducted at Thailand's standard condition at 27C and 65% relative humidity.

## 3 Results and Discussions

The Box Compression Test (BCT) values of each sample were averaged and analyzed. For white top liner (KS170/CS110/KT125), the highest BCT is Set-B(Front 10x4, Flap edge 6x4) 122.2 kg followed by Set-C(Front 10x3, Flap edge 6x5) 119.9 kg. The lowest BCT is Set-A(Front 8x3, Flap edge 5x4) 75.1 kg.

For brown top liner (KT150/CS110/KT150), the highest BCT is Set-C(Front 10x3, Flap edge 6x5) 146.3 kg, followed by Set-B(Front 10x4, Flap edge 6x4) 133.5 kg, and Set-A(Front 8x3, Flap edge 5x4) 127.1 kg, respectively. The results showed in Figure 6.

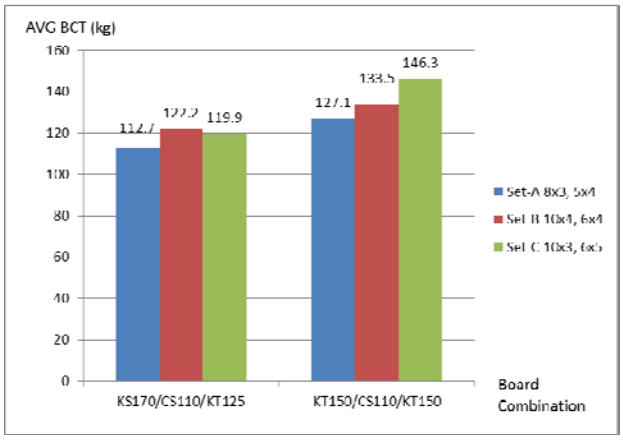



**Figure 6** : The Box Compression Test (BCT) results.

The BCT result showed no significant difference in compressive strength when compared within the same board combination or between board combinations. This is because all samples had the same positions and equal

lengths of perforation lines. So, those would affect the compressive strength in the same manners, even though the perforation rules are difference.

The drop test result showed that Set-A(Front 8x3, Flap edge 5x4) performed the best appearance after dropped for both white and brown top liners as shown in Figure 7. The number of damaged products were found randomly in each sample mostly were minor defects and occurred at the bottom layer of products.

The paper breaking after dropped were found at the front panel of Set-B(Front 10x4, Flap edge 6x4) and Set-C(Front 10x3, Flap edge 6x5). This breaking might be caused from the cut length of perforation rule in Set-B and Set-C are longer than Set-A. So, when boxes were dropped, the perforations were impacted and caused the box to break. The longer cut length of perforation is, the easier the box will be broken when dropped.

The appearances after dropped satisfaction scores were then evaluated. The white top liner showed better appearance than brown top liner as shown in Table 3. Because of the 30%virgin fiber in white top liner, it gives the higher bursting strength and endurance when compared to 100% recycled fiber in brown top liner. So, the white top liner which is more endurance can hold and protect product inside without breaking the perforation during drop.

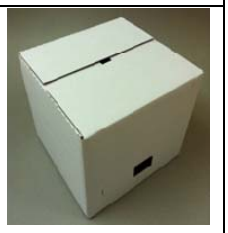
| Top liner color | Perforation rule sets | | |
|---|---|---|---|
| | Set-A : 8x3, 5x4 | Set-B : 10x4, 6x4 | Set-C : 10x3, 6x5 |
| White top |  |  |  |
| Brown top |  |  |  |

**Figure 7 :** Appearance of box after dropped

**Table 3 :** Summarized the satisfaction scores

| Sample | Perforation rule (Front , Flap edge) (Cut x Non-cut) | Top liner color | No. of damaged products after dropped | Average satisfaction score | | |
|---|---|---|---|---|---|---|
| | | | | Appearance after dropped score | Easy-to-open score | Display appearance score |
| 1 | Set-A : 8x3, 5x4 | White | 1 | 1 (satisfied) | 2 (fair) | 2 (fair) |
| 2 | Set-B : 10x4, 6x4 | White | 1 | 2 (fair) | 1 (easy) | 1 (satisfied) |
| 3 | Set-C : 10x3, 6x5 | White | 1 | 2 (fair) | 3 (difficult) | 3 (not satisfied) |
| 4 | Set-A : 8x3, 5x4 | Brown | 1 | 1 (satisfied) | 2 (fair) | 2 (fair) |
| 5 | Set-B : 10x4, 6x4 | Brown | 1 | 3 (not satisfied) | 1 (easy) | 1 (satisfied) |
| 6 | Set-C : 10x3, 6x5 | Brown | 1 | 2 (fair) | 2 (fair) | 2 (fair) |

The easy-to-open result showed in Table 3. The Set-B(Front 10x4, Flap edge 6x4) perforation is the easiest to open on both liners while Set-C scored the difficult to open on white liner. The brown top liner showed the better

easy-to-open score than the white top liner. The percentage of virgin and recycled fibers in paper could affect the open ability and tearing of the box. The paper that consisted of some virgin fibers (long fibers) will has higher tearing resistance than those consisted of short fiber, Caulfield and Gunderson [10].

The cut and non-cut length of the perforation also affect the open ability of the box. The cut and non-cut length of the perforation at the front panel will have less influence on open ability than the perforation at flap edge. Because tearing at the front panel is the tearing along or parallel to the flute direction of box. This tearing requires lower force than tearing across the flute direction at flap edge. So, the longer non-cut length of perforation is, the more difficult the box to be torn.

Then, the display appearance and the cleanliness of the tearing were evaluated and the result showed in Table 3 and Figure 8. The result showed the evaluation scores are in the same direction as easy-to-open scores. The Set-B(Front 10x4, Flap edge 6x4) perforation received the satisfied scores on both white top and brown top liners. The perforation set that received "easy" score in easy-to-open evaluation, will resulted in "satisfied" score in cleanliness of tearing and display appearance.

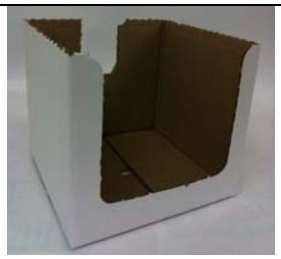
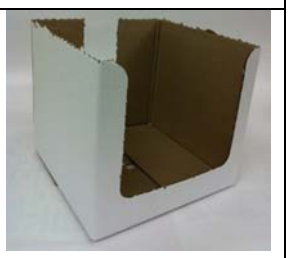
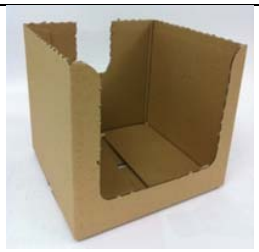
| Top liner color | Perforation rule sets | | |
|---|---|---|---|
| | Set-A : 8x3, 5x4 | Set-B : 10x4, 6x4 | Set-C : 10x3, 6x5 |
| White top |  |  |  |
| Brown top |  |  |  |

**Figure 8 :** Appearance of box after tearing and opening

## 4 Conclusions

This study showed that the different perforation rules (cut and non-cut length), but perforate at the same position of the box, would not affect the compressive strength. The different perforation sets showed no significantly difference in BCT. The shorter cut length of perforation, Set-A(Front 8x3, Flap edge 5x4), performed better drop test resistance than longer cut length, Set-B and Set-C. The results on the easy-to-open and display appearance were resulted in the same direction. The perforation set that was scored "easy" in easy-to-open criteria will be scored "satisfied" in appearance on shelf criteria. The perforation Set-B(Front 10x4, Flap edge 6x4) was scored "easy" and "satisfied" in easy-to-open and display appearance criteria, respectively. However, this study found that the real factor that affects the tearing and appearance is non-cut length of the perforation. The non-cut length between 3-4 mm will give the best performance in them of contain ability, easy-to-open, and appearance on shelf. The non-cut length that shorter than 3mm will be easy to break during transport while the longer than 4 mm will be difficult to tear and create non smooth edge appearance on shelf.

This study also addressed that the paper combination would affect the performance of the box in term of drop resistance and tearing property. The paper combined with virgin fibers performed better drop resistance. In contrast, it performed "difficult" on easy-to-use and scored "not satisfied" on display appearance aspects.

In this study, the perforation Set-B(Front 10x4, Flap edge 6x4) on white top liner was evaluated to be the best of overall performance and recommend to be used for exported bar soap product in this project.

Base on the results of this study, recommendation guidelines for perforation rule have been developed.

## 5 Guiding for perforation rule

5.1 Perforation ruling for corrugated board, the longer cut length of perforation is, the easier the box to be torn and opened. However, the real factor that affects the opening and appearance on shelf is non-cut length of the perforation. The appropriable non-cut length for corrugated board B flute is 3-4mm. With this non-cut length, it will give the best performance for containing product throughout supply chain and display appearance at shelf.

5.2 If the perforation line was designed to be a corner shape, curved perforation line should be used rather than straight line.

5.3 For safety concern, the wave knife should be used along the edge of the blank die-cut sheet to prevent the cutting from the shape edge when employee packing the product into the box.

## Acknowledgements

We would like to express my gratitude to Thai Containers Group Co., Ltd. and Graphic and Pre press Center Ms. Juthamart Sayumpol for helping us on preparing samples and testing. We also would like to gratefully thanks Mr. Pakapol Kittipinyovath for knowledgably supporting this project. Last but not least, special thanks to Packaging Engineer Team from Colgate-Palmolive (Thailand) for supporting us throughout this project.

## References

1. Walmart. (2011). *RRP Guidelines for North America*., Version 1., USA
2. Benasch D. (2013). *Shelf-ready Packaging*. STI Group, Germany. Retrieved from http://www.sti-group.com/en/de/products/packaging/shelf_ready_packaging/shelf_ready_packaging.html
3. ECR Australasia, (2006), *Retail Ready Packaging : A Focus on Shelf Ready Packaging an Industry Toolkit*, ECR Australasia. Australia.
4. ECR Australasia, (2009), *Retail Ready Packaging Edition 2*, ECR Australasia. Australia.
5. ECR Australasia, (2013), *Efficient Consumer Response Australasia Retail Ready Packaging Edition 3*, ECR Australasia. Australia.
6. Schrijver M., (2013), "Retail Ready Packaging and the Importance of design", M.S. Thesis, Department of Communication Science, University of Twente, Netherlands.
7. Roukema M. (2013). *Designing the optimal perforation*. Retrieved from http://www.smurfitkappa.com/vHome/com/Newsroom/PressReleases/Pages/Designing-the-optimal-perforation.aspx
8. Georgia-Pacific Innovation Institute. (2014). *Innovation Products*. Retrieved from http://www.gppackaging.com/InnovationInstitute/Pages/Products.aspx
9. Packaging Test Method, Colgate-Palmolive.
10. D.F. Caulfield and D.E. Gunderson, (1988), "Paper Testing and Strength Characteristics", *TAPPI proceeding of the 1988 paper preservation symposium*, Georgia , USA, TAPPI Press pp. 31-40.

# Is Your Package Pro-LOHAS?

# – Findings of the Finnish LOHASPACK Study 2011-2014

**Virpi M. Korhonen[1*] and Satu O. Jokinen[1]**

[1] *Association of Packaging Technology and Research (PTR), Finland*
[*] *Corresponding author. Email: virpi.korhonen@ptr.fi*

**Abstract:** In recent years, LOHAS (Lifestyles of Health And Sustainability) has emerged as a constantly rising global phenomenon. The LOHAS trend provides major drivers for the package sector, such as a growing interest in personal health and well-being, as well as in ecological, socially responsible and ethical products. Hence, the environmentally-conscious and creative LOHAS consumers can produce valuable insights for packaging research and development. In Finland, one-third of the population are considered as LOHAS consumers.

This paper presents some of the key findings of the Finnish LOHASPACK research project conducted in 2011-2014. The aims of the three-year research project were to (1) increase and spread LOHAS knowledge and understanding in package value networks, (2) study means to resolve how to communicate health, well-being, ecology, as well as ethical and social responsibility through packaging, and (3) develop and test consumer research methods for studying multisensory package concepts.

This paper will focus on the results of the survey and ethnographic research conducted in 2014. The aim of the survey (N=1000) was to identify the major sources of value in packaging for LOHAS consumers, followed by an ethnography (N=10) aimed at validating the main findings of the survey and identifying the role of packaging in LOHAS consumers' everyday decision making processes.

The results indicate that LOHAS consumers set high requirements for packaging. 67% of the LOHAS heavy consumers state that packages have a strong influence on decision making. A majority of the LOHAS consumers experience high value from the environmental, informational, and functional benefits of packaging. Higher value will emerge, if packaging succeeds to contribute to their lifestyle, resulting in delight and commitment. Packaging materials that are safe, more ecological and promote social well-being at a global level, are considered as pro-LOHAS.

Keywords: package, value, LOHAS, consumers, survey, ethnography.

## 1 Introduction

LOHAS (acronym for Lifestyles Of Health And Sustainability) is a global consumer trend that has been spreading from Japan and the USA since the late 1990s. The Cultural Creatives [1] form the basis for the LOHAS segment.

The LOHAS trend represents a new kind of consumer activism, containing major drivers for the package sector, such as an interest in personal development, health and well-being, as well as in ecological, socially responsible and ethical products. Hence, the environmentally-conscious and creative LOHAS consumers can provide packaging manufacturers and packagers with valuable insights. Of adult consumers, 20 % in the USA, 30 % in Japan, 33 % in Europe and 8 % in Australia, are estimated to represent the LOHAS segment [2].

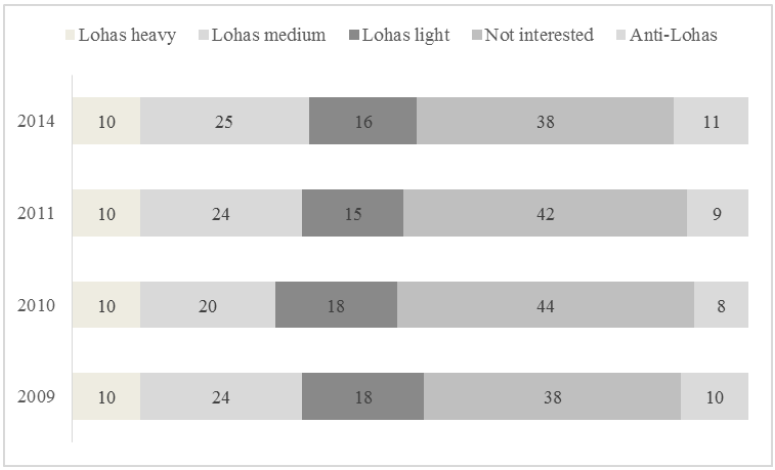
In Finland, 10% of consumers aged 15-75 are considered as LOHAS heavy consumers (Figure 1). Their values are grounded in modern humanism, and they show a strong interest in social responsibility, aesthetics, as well as ecological and ethical products. They consider themselves creative and are satisfied with their lives. Up to 50% of LOHAS heavy consumers produce content in social media.

LOHAS medium consumers account for 25% of LOHAS consumers. They support both modern and traditional humanism. They are equally interested in climate change and nature conservation. They prefer organic and ethical production and also encourage their friends to do so. They consider themselves as ordinary consumers and feel satisfied with their lives.

LOHAS light consumers account for 16 % of LOHAS consumers. They have expressed an interest towards the LOHAS lifestyle, but have not yet applied it in their consumption behavior. The not-interested group (38 %)

shows no interest in LOHAS values, but at the same time they do not feel uncomfortable with such selling arguments. The Anti-LOHAS consumers (11%) are unmotivated by LOHAS values and are unwilling to buy products aimed at this market.

**Figure 1**: LOHAS groups in Finland 2009-2014, % (Tripod Research 2014, www.tripod.fi).




# 2 LOHASPACK research project

## 2.1 Aims of the project

The aims of the three-year LOHASPACK research project were to (1) increase and spread LOHAS knowledge and understanding in package value networks, (2) study means to communicate LOHAS values, i.e. health, wellness, ecology, ethical and social responsibility through packaging, and (3) develop and test consumer research methods for studying multisensory package concepts. The project was funded by the Finnish Funding Agency for Technology and Innovation (TEKES) and fourteen Finnish companies.

This paper will focus on the results of a survey conducted in 2014, followed by an ethnographic research. The focus of the survey (N=1000) was in identifying the major sources of value in packaging for LOHAS consumers. The ethnographic research (N=10) aimed at validating the main findings of the survey and identifying the role of packaging in LOHAS consumers' everyday decision making processes.

## 2.2 Data

2.2.1 LOHAS survey

The LOHAS survey was conducted using an M3 Internet panel in Finland in February 2014. The data were weighted to represent the overall demographics of the Finnish population aged 15-75 years. The respondents were divided into five groups based on the LOHAS classification by Tripod Research described earlier in this paper. The demographics of the LOHAS groups are presented in Table 1, showing that of the LOHAS heavy consumers, 62% are women and 26% have a university degree, and 29% of the group are between 55 to 64 years of age.

**Table 1:** Demographics of LOHAS groups in 2014, N=982-1000 (Chi-Square test).

| Demographics | | LOHAS groups | | | | | |
|---|---|---|---|---|---|---|---|
| | | LOHAS heavy | LOHAS medium | LOHAS light | Not interested | Anti-LOHAS | Total |
| **Gender (%)** | Male | 38 | 45 | 47 | 53 | 67 | 50 |
| **$\chi^2$ =22.1 (df=4); p=0.00** | Female | 62 | 55 | 53 | 47 | 33 | 50 |
| **Age (%)** | 15-24 | 13 | 13 | 17 | 17 | 25 | 16 |
| **$\chi^2$ =76.1 (df=20); p=0.00** | 25-34 | 12 | 12 | 12 | 17 | 33 | 16 |
| | 35-44 | 13 | 16 | 16 | 20 | 18 | 17 |
| | 45-54 | 17 | 20 | 18 | 22 | 8 | 19 |
| | 55-64 | 29 | 21 | 23 | 16 | 8 | 19 |
| | 65-75 | 15 | 19 | 16 | 8 | 7 | 12 |
| **Level of education (%)** | Primary | 11 | 13 | 10 | 17 | 28 | 15 |
| **$\chi^2$ =47.7 (df=12); p=0.00** | Vocational | 42 | 53 | 57 | 56 | 55 | 54 |
| | Bachelor | 21 | 21 | 14 | 18 | 9 | 17 |
| | Master | 26 | 14 | 18 | 9 | 7 | 13 |

Table 2 presents measures describing the differences in pro-environmental behaviors between the LOHAS groups. The behaviors were evaluated on a 7-point scale (1=does not describe me or my actions at all; 7 = describes me or my actions very well).

**Table 2:** LOHAS group ratings for pro-environmental behaviours[1], N=960 (one-way ANOVA).

| | LOHAS groups | | | | | | | |
|---|---|---|---|---|---|---|---|---|
| | LOHAS heavy (N=99) | LOHAS medium (N=248) | LOHAS light (N=159) | Not interested (N=375) | Anti-LOHAS (N=79) | Total (N=960) | F | Sig. |
| I sort household waste carefully. | 6.5 | 6.0 | 5.3 | 4.8 | 3.1 | 5.2 | 73.2 | 0.00 |
| I try to avoid products that are packed in too many packages. | 6.2 | 5.6 | 4.6 | 3.9 | 2.8 | 4.6 | 102.2 | 0.00 |
| When choosing detergents I consider their impact on the environment. | 5.9 | 5.3 | 4.1 | 3.3 | 2.6 | 4.2 | 117.5 | 0.00 |
| I prefer eco-friendly products. | 6.4 | 5.8 | 4.8 | 3.9 | 2.8 | 4.7 | 161.8 | 0.00 |
| I prefer organic products. | 5.8 | 4.8 | 3.8 | 3.1 | 2.6 | 3.9 | 92.6 | 0.00 |
| I prefer local products. | 6.4 | 5.6 | 4.8 | 4.2 | 3.0 | 4.8 | 89.0 | 0.00 |
| I try to avoid unnecessary driving. | 5.8 | 5.1 | 4.5 | 3.9 | 2.8 | 4.4 | 51.0 | 0.00 |
| I recycle empty cans and bottles. | 6.9 | 6.8 | 6.6 | 6.4 | 5.1 | 6.5 | 41.9 | 0.00 |
| I avoid using chemical fertilizers in yard/garden/balcony plants. | 6.3 | 5.5 | 4.5 | 4.0 | 2.8 | 4.6 | 75.0 | 0.00 |
| I avoid flying if possible. | 4.9 | 4.6 | 3.9 | 3.4 | 2.5 | 3.9 | 29.8 | 0.00 |
| I prefer non-toxic products. | 6.4 | 6.0 | 5.3 | 4.6 | 3.1 | 5.1 | 92.7 | 0.00 |
| I only buy products that are not tested on animals. | 5.4 | 4.6 | 3.8 | 3.2 | 2.7 | 3.9 | 52.0 | 0.00 |
| I want the products I buy to be made of recyclable or reusable materials. | 5.9 | 5.0 | 4.2 | 3.5 | 2.8 | 4.2 | 89.3 | 0.00 |
| I prefer energy-efficient appliances. | 6.2 | 6.0 | 5.4 | 4.8 | 3.5 | 5.3 | 72.5 | 0.00 |
| I prefer products whose production and/or use consumes less water. | 5.5 | 4.8 | 4.0 | 3.6 | 2.8 | 4.1 | 59.9 | 0.00 |
| I prefer products made of natural/organic materials. | 6.0 | 5.1 | 4.3 | 3.6 | 2.8 | 4.3 | 91.8 | 0.00 |
| In the shop I compare green and conventional products. | 5.8 | 5.0 | 4.1 | 3.2 | 2.7 | 4.0 | 88.4 | 0.00 |
| I buy green products only if their prices are competitive compared to conventional. | 5.3 | 5.1 | 5.2 | 4.7 | 3.5 | 4.8 | 17.7 | 0.00 |
| In the shop I go directly to the shelf or selection of green products, if available. | 5.0 | 4.0 | 3.1 | 2.4 | 2.3 | 3.2 | 84.9 | 0.00 |
| I see no need for green products. | 2.2 | 2.9 | 3.5 | 3.7 | 4.0 | 3.4 | 21.6 | 0.00 |
| Green products are safer than conventional. | 5.8 | 5.0 | 4.4 | 3.8 | 3.1 | 4.4 | 55.4 | 0.00 |
| Green products are of higher quality than conventional. | 5.6 | 4.9 | 4.2 | 3.7 | 2.9 | 4.2 | 53.4 | 0.00 |
| Green products are healthier than conventional. | 5.9 | 5.2 | 4.6 | 4.0 | 3.1 | 4.5 | 57.8 | 0.00 |
| Green products are readily available. | 4.7 | 4.2 | 4.0 | 3.6 | 3.0 | 3.9 | 20.8 | 0.00 |
| Green products are less expensive than conventional. | 2.9 | 2.7 | 2.4 | 2.2 | 2.3 | 2.5 | 7.9 | 0.00 |

[1)] 1 = does not describe me or my actions at all; 7 = describes me or my actions very well).

2.2.2 Ethnographic research

The ethnographic research was conducted as a combination of accompanied shopping followed by thematic interviews held at participants' homes. The participants were recruited from Research Insight Finland's qualitative panel, qualified either as LOHAS heavy (N=5) or LOHAS light consumers (N=5), applying the Tripod Research's LOHAS screener. All participants lived in the Helsinki metropolitan area. Their ages ranged from 30 to 51 years, and they had at least one child living at home. Each shopping round followed by a home interview lasted approximately 3 hours.

## 2.3 Value measures

A total of 39 attitude statements were constructed for the survey, representing the following dimensions of package value for the consumer: functional, environmental, informational, brand & quality, emotional, instrumental, and price.

All items were presented with 7-point bipolar Likert-type rating scales (1 = strongly disagree; 4 = neither agree nor disagree; 7 = strongly agree). The attitude statements were tested and validated in the previous survey conducted in 2011 [3].

The data were analyzed by statistical multivariate analyses. Principal axis factoring with Varimax rotation was employed for analyzing and validating the value measures. The number of factors was based on the Kaiser rule (eigenvalue greater than one). Individual factor scores for each dimension were created by the regression method. The group differences between the LOHAS groups were tested with one-way ANOVA. Missing data was not replaced in the analyses, resulting in a smaller sample size.

# 3 Findings

## 3.1 Package value for LOHAS consumers

The factor analysis yielded seven factors that were labelled according to the high (above 0.40) loadings on each factor (Table 3). The factors represented the brand & design, environmental, functional, instrumental, price, informational, and aesthetic & emotional value experienced from packaging.

**Table 3:** Factor loadings of value scale variables (Principal axis factoring with Varimax rotation).

| **Rotated Factor Matrix** | | | | | | | |
|---|---|---|---|---|---|---|---|
| | Factor | | | | | | |
| | Brand & Design | Environmental | Functional | Instrumental | Price | Informational | Aesthetic & Emotional |
| I'm willing to pay more for packaging designed by famous designers. | **0.728** | 0.142 | -0.134 | 0.009 | -0.080 | 0.065 | 0.150 |
| I could pay more for individually packaged products. | **0.712** | 0.190 | -0.041 | 0.021 | -0.110 | 0.015 | 0.046 |
| I seldom look at the price tag, if a product has an especially appealing package. | **0.687** | 0.130 | -0.173 | 0.115 | -0.094 | -0.008 | 0.123 |
| I often buy products with packaging that stands out from the others in a positive way. | **0.638** | 0.183 | 0.166 | -0.084 | 0.041 | 0.023 | 0.075 |
| Colorful and impressive packages often persuade me to try out new products. | **0.628** | 0.005 | 0.161 | -0.037 | 0.081 | -0.093 | 0.161 |
| I avoid buying cheap-looking packages. | **0.616** | 0.132 | 0.053 | -0.024 | -0.025 | 0.039 | -0.027 |
| On the street, I easily notice people carrying packages or bags of brands. | **0.616** | 0.076 | -0.011 | -0.020 | 0.112 | 0.045 | 0.090 |
| Good packaging strengthens my brand loyalty. | **0.529** | 0.106 | 0.362 | -0.097 | 0.006 | -0.052 | 0.071 |
| I think that packaging quality also says something about the quality of the actual product. | **0.522** | 0.078 | 0.385 | -0.062 | 0.055 | -0.095 | -0.043 |
| I collect unusual packages. | **0.516** | 0.135 | -0.191 | 0.054 | -0.003 | 0.057 | **0.427** |
| I like to shop in stores where product packages are displayed with thought and attention. | **0.495** | 0.161 | 0.336 | -0.118 | 0.033 | 0.020 | 0.039 |
| I value good design in packaging. | **0.488** | 0.081 | 0.345 | -0.075 | -0.025 | 0.019 | 0.123 |
| I pay attention to packaging when I'm shopping for myself. | **0.488** | 0.220 | 0.295 | -0.156 | -0.028 | 0.075 | 0.108 |

| | Factor | | | | | | |
|---|---|---|---|---|---|---|---|
| | Brand & Design | Environmental | Functional | Instrumental | Price | Informational | Aesthetic & Emotional |
| Environmentally harmful packaging stops me from buying a product. | 0.261 | **0.709** | 0.019 | -0.065 | 0.010 | 0.105 | -0.014 |
| I won't buy products if I think they're over-packaged. | 0.148 | **0.681** | 0.174 | -0.042 | 0.041 | 0.055 | 0.055 |
| I feel guilty buying environmentally harmful packages. | 0.230 | **0.679** | 0.093 | -0.159 | 0.086 | 0.040 | 0.056 |
| I'm willing to pay a higher price per kilo for products with environmentally friendly packaging. | 0.416 | **0.608** | -0.031 | -0.115 | -0.092 | 0.065 | -0.002 |
| I like buying products with recyclable packaging. | 0.036 | **0.571** | 0.395 | -0.178 | 0.211 | 0.045 | 0.050 |
| I always buy non-packaged food, if possible. | 0.137 | **0.563** | 0.026 | 0.023 | 0.044 | 0.130 | 0.060 |
| I value reusable packaging. | -0.026 | **0.446** | 0.393 | -0.112 | 0.234 | 0.008 | 0.066 |
| I always check the producer and country of origin when I buy private label products. | 0.131 | **0.443** | 0.309 | -0.075 | -0.023 | **0.431** | 0.009 |
| I prefer light packaging materials in order to avoid heavy shopping bags. | 0.121 | **0.419** | 0.320 | 0.080 | 0.088 | -0.009 | 0.060 |
| I can think of several packages that I avoid buying because they are too difficult to open. | 0.246 | **0.409** | 0.233 | 0.047 | 0.074 | 0.051 | 0.112 |
| To avoid wasting food, I prefer appropriate package sizes. | -0.074 | 0.265 | **0.595** | 0.019 | 0.066 | 0.076 | -0.036 |
| When I'm shopping for presents, I want top-quality product packaging. | 0.209 | 0.038 | **0.553** | 0.064 | -0.015 | 0.088 | 0.022 |
| I always choose a package from which I can clearly see that no-one has opened it before me. | 0.065 | 0.082 | **0.544** | 0.075 | 0.136 | 0.118 | -0.021 |
| I prefer packages that clearly show the producer and origin of the product. | 0.060 | **0.469** | **0.517** | -0.043 | 0.015 | 0.283 | -0.019 |
| I prefer packages that provide long shelf life. | 0.061 | 0.048 | **0.514** | 0.129 | 0.165 | 0.017 | 0.020 |
| Packages with empty space make me angry. | -0.063 | 0.392 | **0.456** | -0.025 | 0.132 | -0.013 | 0.033 |
| I don't care what material packages are made of. | 0.183 | -0.371 | -0.095 | **0.599** | 0.089 | -0.045 | 0.055 |
| I often throw away packages without paying them any special attention. | -0.019 | -0.119 | 0.045 | **0.566** | -0.018 | -0.109 | -0.099 |
| I only consider packaging as protection for products. | -0.248 | 0.101 | 0.167 | **0.515** | 0.106 | -0.052 | -0.018 |
| The appearance of packaging is not important to me, it's the price that counts. | -0.263 | -0.013 | 0.123 | **0.460** | 0.323 | -0.053 | -0.001 |
| I buy all products based on the cheapest package size available per kilo. | -0.016 | 0.117 | 0.126 | 0.154 | **0.765** | 0.004 | 0.047 |
| With food products, I often prefer the cheapest package sizes, and I preserve/freeze a portion of the food. | 0.026 | 0.149 | 0.246 | 0.058 | **0.601** | 0.021 | 0.053 |
| Before buying, I carefully read product descriptions on packages. | 0.170 | 0.327 | 0.201 | -0.070 | 0.073 | **0.721** | 0.037 |
| I seldom read product descriptions on packages. | 0.242 | -0.079 | -0.106 | 0.369 | 0.045 | **-0.609** | -0.003 |
| I keep some packages because they're pretty. | 0.348 | 0.047 | 0.060 | -0.108 | 0.082 | 0.013 | **0.731** |
| Packages that I keep are often connected with a particular experience or story. | 0.385 | 0.175 | 0.074 | -0.050 | 0.065 | 0.005 | **0.477** |
| Eigenvalue | 9.0 | 4.5 | 2.8 | 1.9 | 1.4 | 1.3 | 1.0 |
| Variance explained (%) after rotation | 14.4 | 10.8 | 8.3 | 4.0 | 3.4 | 3.3 | 2.9 |

Significant differences between groups were found in all value dimensions except for "aesthetic & emotional" (Table 4). The LOHAS heavy segment experienced the highest environmental and informational value from packaging in comparison to the other groups. 67% of the LOHAS heavy consumers agreed that packages have a strong influence on decision making. They also scored high on functional value along with the LOHAS medium

and light segments. The low score in the instrumental value reflects the intense relationship between LOHAS heavy consumers and packaging. Despite of this, the LOHAS heavy group also expressed a strong preference for non-packaged food. As many as 76% of the LOHAS heavy group vs. 41% of the whole sample stated that they always buy non-packaged food, if possible.

**Table 4:** Mean factor scores for LOHAS groups, N=960 (one-way ANOVA).

| Factor | LOHAS heavy (N=99) | LOHAS medium (N=248) | LOHAS light (N=159) | Not interested (N=375) | Anti-LOHAS (N=79) | F | Sig. |
|---|---|---|---|---|---|---|---|
| Brand & Design | 0.03 | 0.01 | -0.06 | -0.08 | 0.31 | 3.77 | 0.01 |
| Environmental | 0.84 | 0.45 | -0.03 | -0.37 | -0.45 | 75.76 | 0.00 |
| Functional | 0.21 | 0.21 | 0.22 | -0.05 | -0.83 | 34.93 | 0.00 |
| Instrumental | -0.29 | -0.12 | 0.00 | 0.11 | 0.15 | 7.09 | 0.00 |
| Price | 0.02 | 0.06 | -0.01 | 0.03 | -0.27 | 3.37 | 0.01 |
| Informational | 0.21 | 0.15 | -0.04 | -0.09 | -0.14 | 5.30 | 0.00 |
| Aesthetic & Emotional | -0.02 | -0.04 | 0.00 | 0.00 | 0.09 | 0.53 | 0.72 |

## 3.2 Results of the ethnographic research

3.2.1 Personal Health & Well-Being

The LOHAS consumers preferred clean and unprocessed foodstuffs. Domestic and/or organic products were often considered as clean and therefore healthy choices. Some consumers also purchased processed foods, and the requirements for clean, domestic or organic characteristics were not emphasized as strongly in this category.

Added sugar was considered as a health risk and avoided by most participants. However, concessions even in this matter generally occurred to appease children, even though their health was placed as the first priority. High sugar content also curbed purchasing of products such as juices.

Similar logic was applied for packaging considerations of health and well-being. In some cases, metal cans were perceived as a health risk and avoided because of permeation of metals and chemicals. Some LOHAS consumers admitted making exceptions with metal cans, but not too often, so that health risks remain low. Two respondents who preferred organic products even chose non-organic products, if the organic product was only available in a metallic can. None of the participants, however, chose a different shop or changed their recipes because of limited packaging alternatives, but rather accepted that they did not have a choice in the matter.

Overall, package markings were considered as an important means of communicating the health benefits of products, such as the product origin and content. As the metal can example shows, a perceived conflict between product and packaging can produce an obstacle to purchase.

3.2.2 Social & Ethical Responsibility

In addition to perceived health benefits, a strong preference for domestic products was often also justified with arguments for social and ethical responsibility. A number of participants stated that buying domestic products was important to maintain domestic jobs. The same applied in packaging; an imported product under a Finnish brand won the debate over competitive imported products perceived to have been packaged elsewhere.

Some participants knew the WWF seafood guide and stated it as a tool for making better and sustainable choices. They also hoped that the markings according to the guide could be printed on fish packaging.

Discrepancies in corporate ethics, political issues and lobbying were well acknowledged among the younger participants, even within the LOHAS light group. They stated that they did not buy certain brands for these reasons.

The social and ethical responsibility of products is mostly linked to the products themselves or the manufacturing companies and therefore communicated through brand or package markings, such as labels of origin. This makes LOHAS heavy consumers also heavy users of package information.

In terms of packaging materials, plastic was perceived as ethically problematic. Most participants felt responsibility and guilt for the use and misuse of plastics. For some LOHAS consumers, these emotions reached a global scale and they referred to the plastic islands found in the Pacific Ocean as a reason for avoiding plastic

packaging. Even though most participants understood the importance of plastic packaging in keeping products fresh, they felt a lack of choice and guilt concerning the western lifestyle that requires use of plastic.

3.2.3 Ecology

Local or domestic products were considered more ecological due to shorter transport distances. The choice of dish detergents revealed a complicated process in which participants weighed risks. The chemicals were perceived as a risk for both health and the environment, but wrecking dishwashers using ecological detergents was also perceived as un-ecological. Most participants also felt guilty for the bulky and large plastic packaging especially used for laundry detergent that "would remain in the landfill forever". Concern was also expressed about micro plastics found in the environment, e.g. in fishes and birds.

Participants with small children experienced environmental guilt over disposable diapers. Some had tried washable nappies but they proved to be too laborious after the first or second child. Some LOHAS consumers had also tried disposable eco-diapers, but children had developed rashes. One parent also mentioned that disposable eco-diapers had to be changed more often, so more waste was created.

In general, the LOHAS heavy participants considered ecological matters and acted more easily on them than LOHAS light consumers while shopping for products in grocery stores. Here again, the behavior of the younger LOHAS light consumers coincided with that of the LOHAS heavy. Some bought the product they considered healthy even when they recognized the accompanying package as un-ecological by their standards.

At product level, ecological value usually resulted from the high informational value of packaging. In contrast, high functional performance created little ecological value on the whole, even though some participants did recognize the value of plastic packaging in protecting the products and the ecological benefits in curbing produce wastage. Overall, the perceived negatives outweighed the positive. Most participants chose not to use plastic bags for fresh produce when purchasing fruits and vegetables singularly and/or with a peel. Some of the LOHAS heavy consumers perceived unpackaged produce as an option to reduce the environmental impact of their consumption, while the LOHAS light simply considered the bags useless for them personally.

3.2.4 Role of Packaging

For LOHAS consumers, packaging becomes an obstacle to choice when it is perceived to pose a risk for either health or the environment. LOHAS consumers will either not buy such products or refrain from buying them too often, in order to diminish the impacts of what they perceive harmful.

In some cases high functional value, e.g. extended shelf life, may create ecological value. Observing actual shopping baskets, it can be seen that especially the LOHAS heavy consume large amounts of fresh produce. This explains why unpackaged fresh products are so strongly supported within the LOHAS consumer groups. Thus, the needs of the logistic systems and retail environments differ greatly from those of the LOHAS consumers. Yet the consumers are often unwilling to spend more time and effort going to the markets for fresh produce.

## 4 Conclusions

The results show that the LOHAS consumers experience value especially from the environmental, informational and functional benefits of packaging. Higher value will emerge, if packaging succeeds to contribute to their lifestyle. LOHAS consumers also experience value from packaging design, and they were delighted to find ecological products with aesthetic packaging, within a reasonable price range.

Personal health and well-being can be supported by safe and clean packaging materials with a low risk of migration or misuse. Packaging technologies enabling low processing of food or less use of additives would be highly appreciated.

For LOHAS consumers, concern for ecological, social and ethical issues is global. Communication about corporate actions regarding these issues must be truthful to avoid strong reactions to brand washing. Transparency is highly appreciated and the role of packaging as a trusted source of information is emphasized.

Effective use of materials, renewable resourcing, material recycling and socially responsible production in packaging results in ecological value for LOHAS consumers. Ease of recycling is also perceived a major source of advantage by LOHAS consumers.

## Acknowledgements

The data presented in this paper were collected as part of the LOHASPACK project funded by The Finnish Funding Agency for Technology and Innovation (TEKES) and a number of companies. In 2011-2014, the companies involved in the LOHASPACK (by PTR and Aalto University) were Anton & Anton, Atria, Coveris Rigid Finland, The Environmental Register of Packaging, Finnish Corrugated Board Association, Kanniston Leipomo, Kuulas Research Agency, HK Ruokatalo, Metsä Board, Myllyn Paras, Saarioinen, Stora Enso, Verman, and Westpak.

## References

[1] Ray, P.H. and Anderson, S.R. "The Cultural Creatives: How 50 Million People Are Changing the World". New York: Harmony Books. 2000.

[2] Harding, A. The Rise and Glory of LOHAS. Green Unplugged. 7th June 2010. http://www.slideshare.net/GreenUnplugged/andrew-harding

[3] Korhonen V. Package Value for LOHAS Consumers—Results of a Finnish Study. In: 18th IAPRI World Packaging Conference, Proceedings. 2012. p. 156.

# Material Identity in a Packaging Context

**Annika Kihlstedt, Siv Lindberg, Annika Lindström, and Sandra Pousette**
*Innventia AB, Stockholm, Sweden,*
*siv.lindberg@innventia.com*

**Abstract:** Package design includes a number of considerations ranging from protecting the content to conveying the brand image. The aim of this study was to gain a deeper understanding on how Swedish consumes perceive product packaging attributes, with a special emphasis on in which way packaging material (carton, paper plastic), and structural design (folding carton, paper bag, standing pouch and plastic bag), have an emotional impact on consumers' evaluation of the product and packaging.

Assessing the appearance and effectiveness of a packaging system is often confounded by branding, why it is important to separate the brand influence from the attributes of the packaging system. Thus, in the experimental part, packaging prototypes of different structural design and materials were manufactured in order to present commercial cereal brands in different types of packaging.

The research involved a combination of qualitative and quantitative methods, comprising (i) focus groups on cereal (muesli) packaging; (ii) a mock-up study of four muesli packaging types: transparent plastic bag, carton box, paper bag, and a resalable stand-up plastic pouch; and (iii) a questionnaire on environmental attitudes to packaging materials. Fourteen respondents participated in the focus groups and 20 in the mock-up study.

Result show that the paper bag and the carton box were perceived to be the most environmentally friendly packaging material. Heavy ink usage on paper bags and carton boxes can however raise concern regarding the environmental impact. Introducing functionality and good print quality can cause preferences to divert to an alternative packaging material. In the mock-up study the standing pouch was the most liked package type regardless of brands. Functional reasons (protect, re-closable etc.) and appearance reasons (nice print, nice colours) was claimed for giving this package high ratings.

Keywords: perception, packaging appearance, material identity.

## 1 Introduction

Successful marketers understand that the package is the product [1]. The shape, graphics, brand, and colour of the package are what are supposed to grab the consumer's attention and stand out on the shelf in competition with other brands. Packaging communicates brand personality via multiple structural and visual elements, including a combination of brand logo, colours, fonts, materials, pictorials, product descriptions, shapes and other elements that provide rich brand association. Underwood, Klein, and Burke [2] argue that the package gives the consumer an impression of the product itself and the quality of the product. This is particularly important when the product is unfamiliar. Underwood suggests that the symbolism generated and/or communicated by the package may include convenience, environmental consciousness, ethnicity, family, health consciousness, national and/or regional authenticity, nostalgia, prestige, value and variations in quality, among others [3].

"People participate in packages, and what they find in them is often far more than what they see. Psychologists know that we hear their unheard music, project ourselves onto the scenes they depict, and are energized by the dynamism we find on them" [4]

Sensory consumer research has confirmed that extrinsic product cues, such as packaging and branding, influence how consumers evaluate food products For example, Schifferstein demonstrated that the sweet taste and liking of soft drinks were impacted by cup material (e.g. glass, ceramics, metal, plastic, cardboard, foam), and Becker et al. that shape curvature of package could affect taste intensity especially among people that have a heightened sensitivity to design [5, 6]. Packaging and brand evaluation has been shown to be the strongest drivers for informed liking of wine whereas grape variety and origin were found to be least important, but consumer segments differ in their information processing strategies in that some consumer segments are more sensitive to design than other [7]. Krishna and Morrin found a perceptual transfer of haptic or touch-related characteristics from product containers to judgments of the products themselves as reflected in some tasters rating of the perceived quality of water as lower when served in a flimsy cup [8]

The extent to which variations in packaging material impact consumers' impression of the soup naturalness was investigated by Labbe, Pineau and Martin [9]. Consumers' expectations of naturalness of a dehydrated soup was significantly impacted by touching or seeing different paper and textile materials.

The majority of research on package design has used either two-dimensional photographs or drawings of package varieties, or on-screen presentations. To our knowledge, very few studies have been made that use physical packages where the material itself and its haptic and tactile properties are varied as a part of the package design

Assessing the appearance and effectiveness of a packaging system is often confounded by branding, why it is important to separate the brand influence from the attributes of the packaging system. Thus, in the experimental part of our study, packaging prototypes of different structural design and materials were manufactured in order to present commercial muesli brands in different types of packaging material.

## 2 Methods and materials

### 2.1 Focus groups

Two consumer focus groups were conducted on the topic of consumers' perception of packaging for muesli products. Focus groups were formed in accordance with guidelines traditionally followed in the marketing research field [10]. Participants were recruited through advertisement in a local newspaper in Stockholm and selected to fit the demographic profiles of muesli purchase. The participants in the focus groups were 40% men and 60 % women to reflect the assumption that still more women than men are responsible for household shopping (see Table 1). Participants were screened to ensure recent use of muesli products.

After sandwiches and drinks upon arrival, the focus groups were seated at a centrally positioned table where a selection of muesli packages not included in the study was displayed. The participants were asked to comment on these in order to set the right frame of mind for the subsequent discussion.

The actual focus group interviews contained an individual part and a group discussion. During the individual part, participants first viewed individual packages, physical packages placed on the table in front of them. Participants were asked to list attributes they felt were relevant for their perception of the packaged products. Secondly in the individual part, participants rated each physical package on one product attribute: *liking* and five packaging attributes: eye-*catching, protects the product, looks tasty, storage ability,* and how *environmentally friendly* the packaging is. The focus group discussions centred around six packages and the participants' perceptions of their attention grabbing features, what they packaging communicated, functionality and the reasons for liking or disliking a certain package. The participants were encouraged to focus on the packaging rather than on the product and on the impression of the product that was given by the packagaging.

**Table 2:** Distribution of participants in the focus group studies

| | Age | Male | Female |
|---|---|---|---|
| Group 1 | 31 - 62 (43) | 2 | 5 |
| Group 2 | 28 – 64 (43) | 3 | 4 |
| | Total | 5= 36 % | 9=64% |

### 2.2 Focus group materials

The muesli packages were chosen to represent carton, paper and plastic: paper bags (5), folding carton (3), transparent plastic bag (1) and stand-up plastic pouch (2). They were all familiar domestic brands except for one foreign brand, not sold on the Swedish market and packed in a folding carton.




**Figure 1**: Focus group discussing packaging types. To the left: standing pouches and transparent plastic bag. To the right: paper bags, and in the back: folding carton boxes.

## 2.3 Mock-up study materials

Packaging prototypes of different structural design and materials were manufactured in order to present commercial cereal brands in different types of packaging. Each brand was presented in each of the four materials: transparent plastic bag carton box, paper bag, and a resalable stand-up plastic pouch. Thus, each product was prototyped and presented in 4 different packaging types; its original package and the packages of the 3 other products, using the products original graphic design in all varieties. The packages were filled with oatmeal and sealed except for the transparent bag which was filled with the product indicated on the respective graphic designs. An example of mock-ups is shown in Figure 1. As assessment of brands was not an aim in this project, thus the images shown in Figure 1 are slightly manipulated. In the tests, the original graphic designs were used.



**Figure 2**: Example of mock-ups. From the left: folding carton box, paper bag, standing plastic pouch with zip lock and transparent plastic bag.

## 2.4 Mock-up study procedure

Twenty respondents were recruited through a recruitment agency, Academic Work. The respondents were recruited to correspond to the age and gender distribution of the focus groups, see Table 2.

**Table 2:** Distribution of participants in the mock-up study.

| Age | Male | Female | Total |
|---|---|---|---|
| 27 - 33 | 6 | 8 | 14 = 70% |
| 34 - 40 | 3 | 3 | 6 = 30 % |
| Total | 9 = 45 % | 11 = 55 % | 20 |

The filled packages were given to respondents to hold and look at. They were rated one at the time using the same attribute as in the individual part of the focus groups on, only in this test the general liking attribute was altered to "*How much do you like the product when looking at this package"*. The five packaging attributes remained the same: *eye-catching, protects the product, looks tasty, storage ability,* and how *environmentally friendly* the packaging is. Comments were also collected. After finishing the test, a short survey on packaging attributes and material was filled in.

The general condition for the evaluations was that the price was not a variable (e.g. all packages had the same price) and they all contained equally much of the product.

# 3 Results

## 3.1 Focus groups

In the first task in the focus groups, the muesli packages were individually rated for six attributes related to package design and material. In addition the liking of the product itself was rated. The ratings from the two focus groups were merged (n=14) and categorized for packaging type, e.g. folding *carton* box (n=3), *paper bag* (n=5), transparent *plastic bag* (n=1), and standing plastic *pouch* (n=2). Mean attribute ratings for each material and analysis of variance (ANOVA) statistics ($\alpha$=0.05) were calculated. The results show that products presented in paper bags were perceived to look significantly tastier than products packed in carton board and standing pouches. For the folding carton boxes, the very low ratings for the foreign brand contribute heavily to the low average ratings for this package type. Paper bags and carton boxes were rated to perform significantly better than the plastic bags on storing the product at home. The carton box and paper bags perform best on protecting the product, differences being significant to plastic bag. Environmental aspects show significant differences between packaging types where paper bags are considered most environmentally friendly, carton boxes second and plastic bags in third place.

In the group discussions, both groups thought it was important to be able to see the product although it was pointed out that some products will crumble and might not look so nice. Muesli was considered a natural product and thus paper was considered the best material for packaging. Matt paper was said to look a bit dull, however, glossy paper and more print was said to give a less environmentally friendly impression. Plastic did not give an impression of environmental friendliness. Two of the paper bags were mentioned as packages that signal environmental friendliness. Also the KRAV label sent and ecological message. In general paper bags were said to be most suitable for this product segment and some said they would be more appealing if they had a shiny finish. In addition a few participants believed that a re-closable plastic pouch could also be suitable. A combination of price and content was said to be decisive for purchase in one group. The other group mentioned ecological product as number one factor, second price and third nutritional aspects.

## 3.2Mock-up study

20 respondents rated the packages on the same five attributes related to the design and material that were used in the focus groups. In addition the variable used for liking of the product was slightly altered to: "*How much do you like the product when looking at is packaging?"* in order to set the respondent's frame of mind on packaging aspects. Data was averaged for each packaging type over all brands, as well as separated for men (n=9) and women (n=11), and analysis of variance (ANOVA) statistics were calculated. Results are shown in Table 3.

**Table 3:** ANOVA table.

| Factor | Like p | Eye-catching p | Protecting p | Tasty p | Storage p | Environment p |
|---|---|---|---|---|---|---|
| Packaging | 0.000** | 0.000** | 0.000** | 0.086* | 0.000** | 0.000** |
| Gender | 0.007** | 0.000** | 0.697 | 0.069* | 0.870 | 0.000** |
| Package*Gender | 0.340 | 0.098* | 0.869 | 0.218 | 0.059* | 0.022* |

**Significant difference at p<0.01 * Significant difference at p<0.1

All attributes presented significant differences between packaging types and materials.

The standing pouch is the most liked package despite brand. The difference is significant to plastic bag and also large to the carton and paper bags although these differences are not significant at the chosen alpha level,

α=0.05. From the comments we found that functional reasons (protection, re-closable by a zip lock seal, etc.), and appearance reasons (nice print, nice colours) was claimed for giving this package high ratings. In addition the pouch is rated as significantly more eye-catching than the plastic and paper bags, but not than the carton boxes.

The functionality of the packaging at home, i.e., protecting and storing the muesli, was evaluated to be equally good for all types except for the transparent plastic bag, which was evaluated significantly lower on these attributes, see Figure 3 and Table 3.

The perceived negative environmental impact of plastic packaging is relatively constant over brands, differences being predominantly between paper and plastic materials. The plastic materials are rated significantly lower than the paper based packaging materials (carton box and paper bag), see Figure 3.

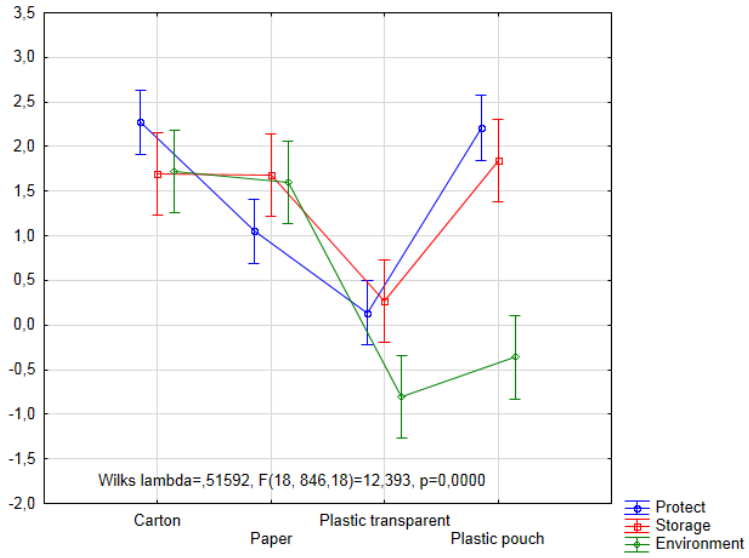



**Figure 3**: Mean ratings *for protect, storage* and *environmental friendliness* for each package type. Vertical bars denote 95 % confidence intervals.

Analysis of variance, ANOVA was performed with gender as a categorical variable and with package types and brands as factors respectively. The significant differences between genders regarding package type (averaged over brands) were:

Men rated the *environmental impact* from packages on average more severe than the women ($p<0.05$).

Women rated the *eye-catching* features of the packages on average more favourable than did the men ($p<0.5$). There was also a tendency that they gave higher ratings for tasty looking ($p<0.1$).

The interaction effects between gender and packaging type were found to be:

Men rated the standing pouch to be less *environmentally friendly* than the women ($p<0.05$) as shown in Figure 4.

There was a tendency that male group rated plastic bag and pouch lower on eye-catchiness than the female group ($p<0.1$), see Figure 4.

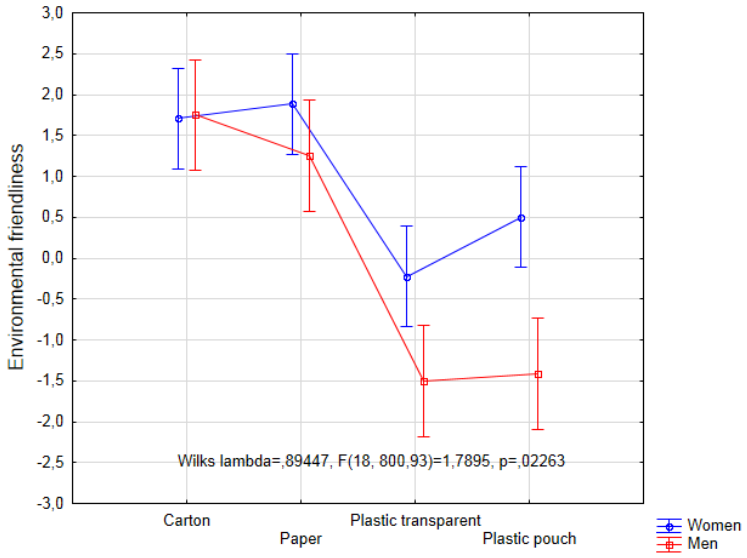



**Figure 4**: Mean ratings for *environmental friendliness* for each package type, separated for men and women. Vertical bars denote 95 % confidence intervals.

### 3.3 Comments from respondents

The comments on brands mostly concerned information issues (pictures, text, health issues) and appearance (colour, design) but also environmental issues (recyclability) and functional issues (re-closure storage). Packages received a higher score if there was a picture of the muesli and a lower score if the respondent did not see information about the content (picture or text). This contributed to the positive remarks for the transparent plastic bag where the content could be seen. The original paper bag product received high ratings because it was perceived as an ecological product. Colour and design was important factors for the other packages and had both positive and negative impact. For the plastic bag, the appearance of the content largely decided the scoring.

The original packages were preferred for the paper bag and the standing pouch. In cases where the products were originally packaged in a carton box and in a plastic bag, the standing pouch was often preferred. Reasons stated by the respondents were e.g., the reclosing function with the zip lock, nice print, tasty looking, easy to waste, refill, environmentally friendly.

Comments also concerned functionality (storage, protection, re-closure), ergonomics (handling) and environmental issues of the package material (paper and carton were perceived as environmental friendly but plastic not) but also appearance (print, colour, appetizing). The amount of ink on the paper bag/carton was commented on for the mock-ups of one design where the design had large printed full tone areas, and concern was expressed that it might not be environmentally friendly. Also the colours on that design (green and yellow) may not have been perceived appealing. In general, across all brands, the standing pooch was preferred, second the paper bag and the carton box, and last the transparent plastic bag.

### 3.4 Survey on attitudes to materials and packaging attributes.

The data is based on 20 respondents. The most appreciated packaging characteristics were related to good readability and environmental aspects such as recyclable and biologically degradable material, minimizing of material and re-closure. These aspects are judged significantly higher in importance than functional aspects such as easy to open and reusability. Low weight was considered to be the least important attribute. Data is shown in Figure 5.

The respondents also rated different packaging materials for how adverse their environmental impact was perceived to be. Plastic and metal was perceived to have the most adverse environmental impact whereas paper and carton was perceived to have the lowest impact on the environment

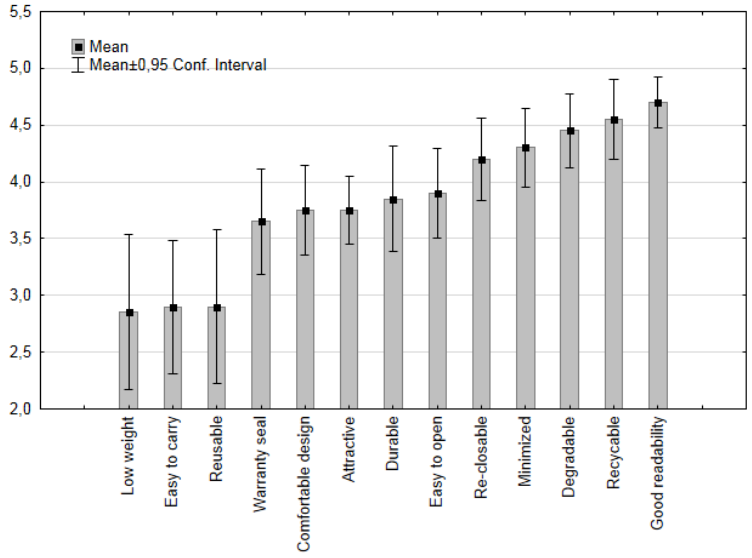



**Figure 5**: Appreciated packaging attributes

## 3 Conclusions

The findings presented indicate that regardless of brand and product, the structure of packaging and the material itself gives an identity and expectation of the product.

- In the focus groups paper bags were rated to be the most environmentally friendly and also said to be suitable for this product type.
- A combination of price and content was said to be decisive for purchase in one focus group whereas the other group mentioned ecological products as the number one factor, second price and third nutritional aspects.
- Introducing functionality and good print quality can cause preferences to divert to an alternative packaging material. In the mock-up study the standing pouch was the most liked package type regardless of brands. Functional reasons (protect, re-closable by a zip lock seal, etc.), and appearance reasons (nice print, nice colours) was claimed for giving this package high ratings.
- A brand with an ecological profile may be less affected by perceptions of negative environmental impact from plastic (standing pouch) if the package has attractive functionalities and attractive appearance.
- Men and women differed in their ratings so that men assessed the environmental impact by plastics to be more severe than did the female respondents and women rated the eye catching features on average than did the male respondents. It shall be noted though that the samples are small in this study and thus, these potential gender differences need to be further explored.
- The paper bag and the folding carton box were rated to be the most environmentally friendly package by all respondents.
- Heavy ink usage on paper bags and carton boxes may raise concern regarding the environmental impact.

The mock-up studies showed some interesting tendencies regarding the impact of the package on how we feel towards a product. In several cases the original package was preferred and as the original package was slightly better than the prototypes, e.g. the original folding carton box had some embossing on the text which the prototypes lacked. It might be advisable in future studies to also prototype the original package in order to get a clearer picture. We also get indications that the brand image (ecological, budget), functionality (zip lock, folding of paper bag) and print/image quality (nice, nice image) affect how attracted we are to a package and how we feel about its environmental impact. Further studies would investigate more in detail how, for example, surface finish (rough, matt, glossy), amount of ink, and material selection would affect brand perception.

## Acknowledgements

This work was part of a consortium project on the visual and interactive functionality of packaging
Financial support from BHS Corrugated, BillerudKorsnäs, Holmen, M-real, and Peterson & Son is gratefully acknowledged.

## References

1. Meyers, H.M. and L.J. Murray, *The Marketers Guide to Sucessful Package design*. 1998, (Chicago) Illinois: NTC Business Books.
2. Underwood, R.L., L.M. Klein, and R.B. Burke, *Packaging communication: attentional effects of product imagery.* The Journal of Product and Brand Management, 2001. **10**(7): p. 403-422.
3. Underwood, R.L., *The communicative power of packaging: creating brand identiy via lived and mediated experience.* Journal of Marketing. Theory and Practice, 2003.
4. Hine, T., *The Total Package: The secret History and Hidden Meanings of Boxes, Bottles, Cans and other Pursuasive Containers*. 1995, Boston, New York, Toronto, London: Back Bay Books, Little Brown and Company.
5. Becker, L., et al., *Tough package, strong taste: The influence of packaging design on taste impressions and product evaluations.* Food Quality and Preference, 2011. **22**(1): p. 17-23.
6. Schifferstein, H.N.J., *The drinking experience: Cup or content?* Food Quality and Preference, 2009. **20**(3): p. 268-276.
7. Mueller, S. and G. Szolnoki, *The relative influence of packaging, labelling, branding and sensory attributes on liking and purchase intent: Consumers differ in their responsiveness.* Food Quality and Preference, 2010. **21**(7): p. 774-783.
8. Krishna, A. and M. Morrin, *Does Touch Affect Taste? The Perceptual Transfer of Product Container Haptic Cues.* Journal of Consumer Research, 2007. **37**: p. 807-818.
9. Labbe, D., N. Pineau, and N. Martin, *Food expected naturalness: Impact of visual, tactile and auditory packaging material properties and role of perceptual interactions.* Food Quality and Preference, 2013. **27**(2): p. 170-178.
10. Bellenger, D.N., J. Goldstucker, L. , and K. Bernhardt, L, *Qualitative research in marketing.* . 1976, Chicago: American Marketing Association.

# Crumpling of paper sheet and packaging

Jean Baptiste NOLOT [(1),] Serge ROHMER[(2)], Vincent FLODERER [(2)], Alain COPINET [(1)], Damien ERRE [(1)]

(1) GRESPI (EA 4694)**, MPSE** (Matériaux, Procédés et Systèmes d'Emballage) de l'Université de Reims Champagne-Ardenne**,** ESIREIMS Esplanade Roland Garros 51630 Reims cedex 2, France.

(2) Centre de Recherches et d'Etudes Interdisciplinaires sur le Développement Durable (CREIDD) Institut Charles Delaunay CNRS STMR 628112 rue Marie curie CS42060 10004 TROYES cedex, France.

Alain.copinet@univ-reims.fr

## Abstract

Crumpling is a new method derived of the origami techniques that transforms a single paper sheet into a three-dimensional structure by a systematic generation of random folds. The resulting crumpled object is an innovative answer to packaging industries that need attractive and dynamic products in a sustainable context. In order to understand the performances of crumpled structures and their applications in the field of packaging. The specific crumpling techniques developed by CRIMP create organized crease patterns very similar to those observed in nature, allowing attractive dynamic objects for packaging applications. In a sustainable context, the expected environmental performances depends on the elasticity property that provides a simplified transportation in a minimum of space, it also depends on the crumpling process that needs no gluing or cutting activities, and also from the agro-resources that constitute the raw material of the paper sheet for a simplified recycling. New investigations based on empirical experiences performed by CRIMP show that crumpled folds networks fall into three main categories: random, parallel, radial..We have shown using cushion curves that both the thickness and the bending mode provided different damping powers. Comparing them to corrugated single flute cardboard b and c, we could note a broader spectrum for less matter. These results are consistent with the values obtained with polyurethane. It is thus possible to associate lightness, environment and protection.

*Keywords: crumpling, eco-design cushioning material.*

## 1 Introduction

Nowadays, plastic materials, which are made from petroleum resources exhibit massive environmental problems, like polystyrene, polyester, polyether and polyolefin. The huge consumption of these non-renewable resources has encouraged researchers to find renewable green materials. So, new trends push companies in designing innovative packaging: competition in the marketplace, customers needs, environmental regulations (1, 2). In a sustainable context, companies develop eco-design strategies to reduce their costs and to improve their environmental impacts (3, 4). The practice of folding sheet based on origami techniques is a good way to achieve booth. It gives to companies the possibility to create attractive packaging for their products. HEXA POT™ for example, is an ultra-light, and 100% biodegradable cookware (5), the product must be unfolded and expanded to make the hexagon pot shape. The ice bucket created by the designer Mathias van de Valle is a foldable package that can be easily transported and stored before and after use. Many examples of foldable packages created from a single sheet can be found. Some of them use origami techniques (6) but in terms of industrial complexity, origami packaging essentially exploit planar and basic curved faces, they are considered as static objects, they do not permit complex shapes. New forces must be required. This article deals with the characterization of dynamic

packaging properties of pads, comparing them to corrugated single flute cardboard b and c such as dynamic cushioning curves, vibration transmissibility and frequency curves. The main feature of article is the evaluation on the dynamic shock cushioning property and vibration transmissibility of Crumpling of paper sheet pads by a series of experimental studies on the drop shock tester and vibration tester, the establishment of experimental formulas of dynamic cushioning curves, and the analysis of resonance frequencies and vibration transmissibility. to create the packages of the future.

## 2 Materials and methods

Crumpling is a method derived of the origami folding techniques that consists in a systematic random generation of folds from a single paper sheet. Inspired by Paul Jackson's definition of basic crumpling methods, this technique has been used since over fifteen years by the CRIMP team to design a wide range of biomimetic models. The basic idea is that crumpled structures bring powerful mechanical and environmental performances to create dynamic three-dimensional structures. The expected performances of such structures are made possible by eliminating cut and glue processes, as well the use of a single raw material for a simplified recycling. A crumpled paper ball is a basic example of crumpled structure. Two Crumpling of papers sheet was tested (figure 1) Sample A: Kraft paper, basis weight: 80 $g.m^{-2}$, thickness 157 µm, crumpling of paper sheet thickness 11 mm and basis weight 275 $g.m^{-2}$. Sample B: sulfurized paper, basis weight 41 $g.m^{-2}$, thickness 70 µm, crumpling of paper sheet thickness 11 mm and basis weight 225 $g.m^{-2}$ .

**Figure 1 :** **A** **B**



The dynamic shock cushioning property describes the capability of absorbing drop shock energy of Crumpling of paper sheet pads, and reflects the relationship between peak acceleration and static stress during drop shock. The peak acceleration is a non-dimension ratio of peak acceleration of the packaged item to gravity acceleration. It is usually presented as a family of dynamic cushioning curves (or peak acceleration and static stress curve), which shows peak acceleration during drop shock for a range of static loads and is constructed for several drop heights. The test system for dynamic shock cushioning property **(Figure 2**) shall consist of a drop shock tester, a signal acquisition & processing device, a set of Data Acquisition & Lansmont (TP3) software, filter of 300Hz was used. The drop shock tester has a drop block and weight (to represent the packaged item) and impact base for dynamic loading of a test specimen to simulate drop shock in handling. The weight is mounted on the drop block. The mass of weight and drop height of the drop block are adjustable. An acceleration sensor is mounted on the drop block, and the signal output from the acceleration sensor is firstly fed into the signal acquisition & processing device, then the drop shock acceleration and time curve may be read and displayed by TP3.

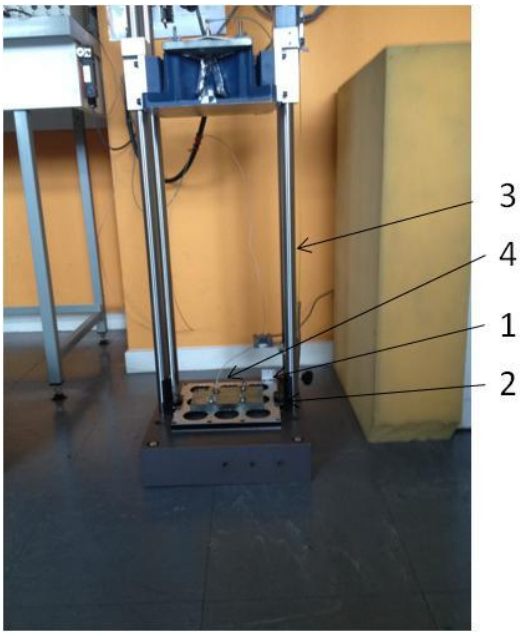
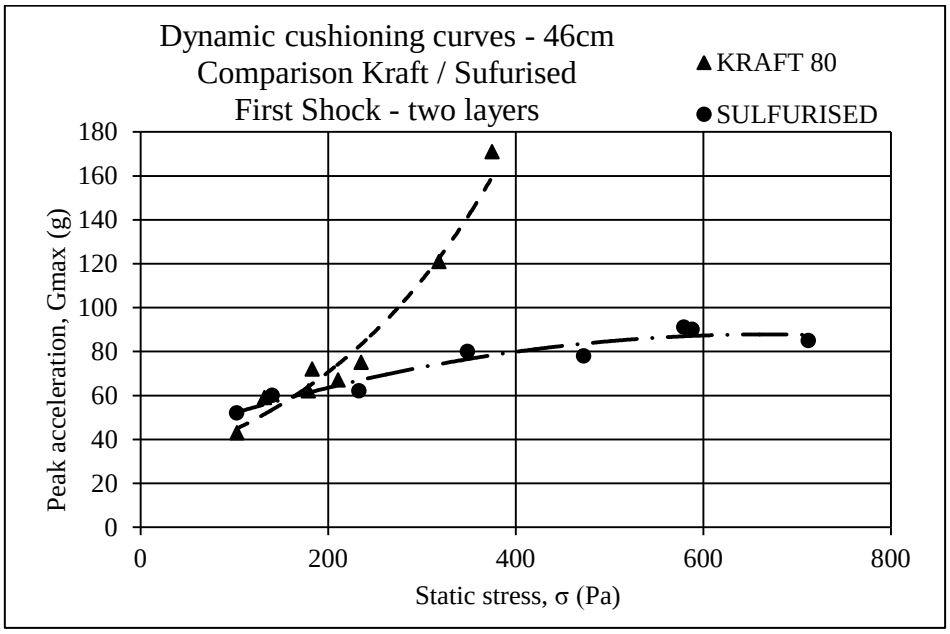



**Figure 2. Test system of dynamic shock cushioning property: 1.Weight; 2.Drop block; 3.Guide column; 4. Acceleration sensor.**

## Results

Dynamic cushioning curves was realised for 46 and 60 cm drop test height on the two materials and for two thicknesses.
Figure 3 shows the dynamic cushioning curves of sample A and B. The drop height was 60 cm. These measures correspond to the first shock.

Figure 3 : Dynamic cushioning curves – 46 cm – sample A & B

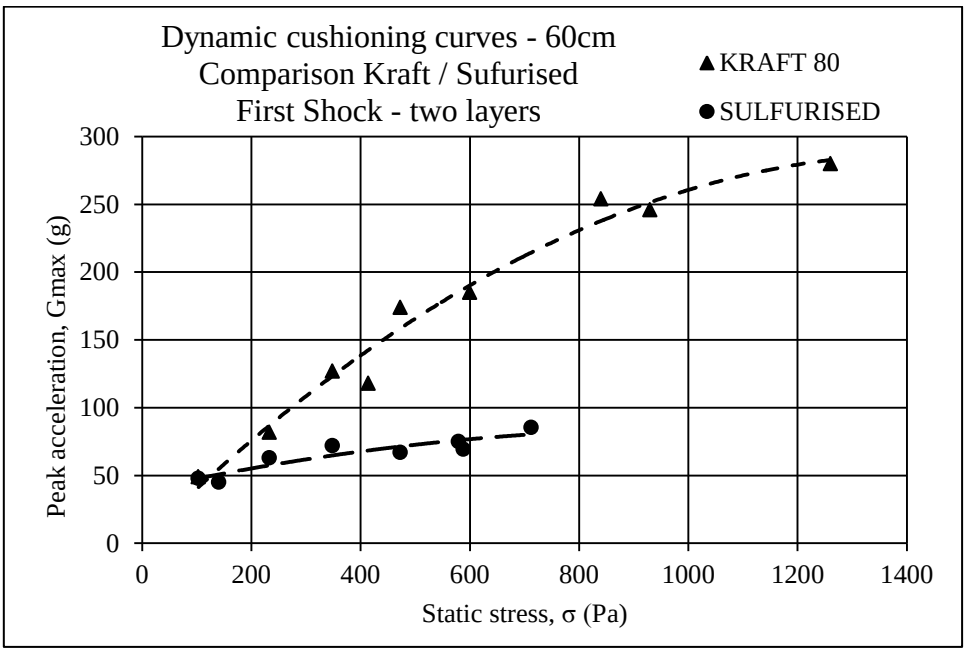



For a static pressure lower than 170 Pa, the two samples show an equivalent shock damping. For upper pressure, the sample B is more shock absorbing than sample A.

For an environmental-friendly development, the sample B is more efficient.

Figure 4 shows the dynamic cushioning curves of the both material A and B. Curves was realised with two different crumpling paper thicknesses. The drop height was 60 cm. These measures correspond to the first shock.

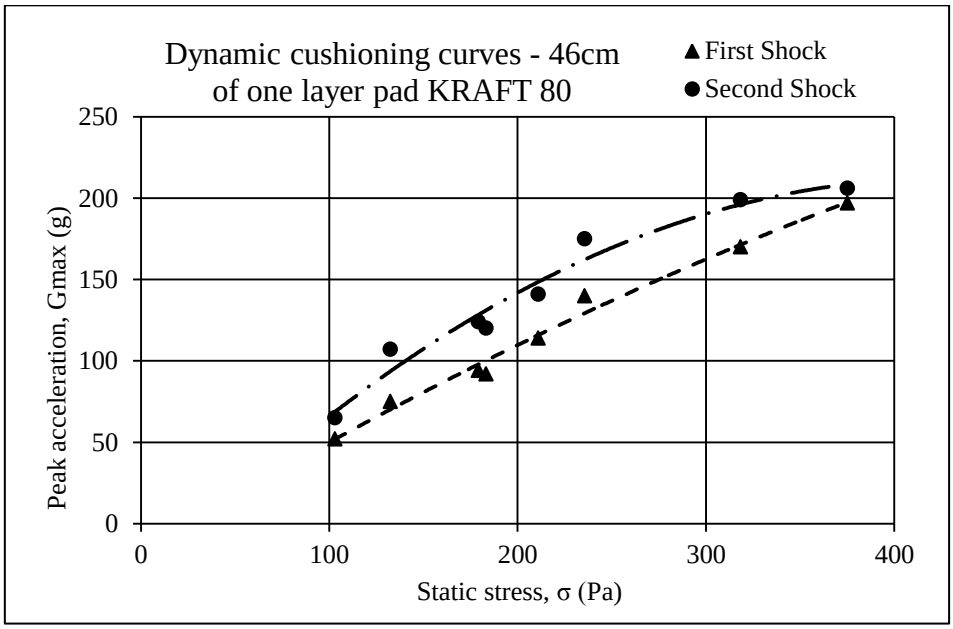
Figure 4 : Dynamic cushioning curves – 60cm - sample A & B




With the rise of the drop test height, the measured acceleration stays in the same order of magnitude until 400 Pa. Damping performances are quite similar for the two heights of drop tests. Sulfurized paper gives a better shock protection.

Figure 5 shows dynamic cushioning curves for sample A and B. The drop height was 46 cm. These measures correspond to the second shock.

Figure 5 : Dynamic cushioning curves – 46cm – Sample A



First shock gives a better shock protection than the second shock. It is important to note that static pressures lower than 100 Pa are difficult to achieve.

## Conclusion

In working on paper cushioning performances, we can do an environmental-friendly conception. Packagings are more lightweight and performer.

For any height of drop test, performances stay equivalent.

Crumpling paper protection is well adapted for lightweight goods. It should be good to wrap the product.

For example:

A smartphone of 120g and standard dimensions (6 x 12 cm) shows a static pressure of 150 Pa. If the product has a threshold of fragility of 80g, so, it can be packed in two crumpling paper layers and be protected for a drop of 46 and 60 cm.

By contrast, with the sample B, the smartphone will break with 46 cm of fall.

## References


1. European Directive 94/62/EC: Packaging and Packaging Waste (1994)
2. Alwael, M. :The impact of product charges and EU directives on the level of packaging waste recycling in Poland. Resources, Conservation and Recycling, vol. 54, issue 10, pp. 609-614 (2010)
3. Restuccia, D., Spizzirri, U.G., Parisi, O.I., Cirillo, G., Curcio, M., Iemma, F., Puoci, F., Vinci, G., Picc, N.: New EU regulation aspects and global market of active and intelligent packaging for food industry applications. Food Control, vol. 21, issue 11, pp. 1425-1435 (2010)
4. Botto, S., Niccolucci, V., Rugani, B., Nicolardi, V., Bastianoni, S., Gaggi, C.: Towards lower caron footprint patterns of consumption: The cas of drinking water in Italy. Environmental Science & Policy, vol. 14, issue 4, pp 388-395 (2011)
5. Pasqualinoa, J., Meneses, M., Castells, F.:The carbon footprint and energy consumption of beverage packaging selection and disposal. Journal of Food Engineering, vol. 103, 357-365 (2011)
6. Yoshizawa A.: Atarashi origami geijutsu. Origami Geijutsu-Sha (1954)

# PACKAGING FOR FOOD & AGRICULTURE

# Migration of Plasticizers from Paper and Board into Food Simulant Tenax and Olive Oil During Microwave Cooking

**J. Cheng[1,3], C.-Y. Hu[2,3 *], Y.-M. Wu[1,3], N. Wang[1,3], J.-W. Wu[1,3], Z.-W. Wang[1,3]**

*[1] Packaging Engineering Institute, Jinan University, Zhuhai, Guangdong 519070, China;*

*[2] Department of Food Science and Engineering, Jinan University, Guangzhou 510632, China;*

*[3] Key Laboratory of Product Packaging and Logistics of Guangdong Higher Education Institutes, Jinan University, Zhuhai, Guangdong 519070, China*

*[*] corresponding author. Email:hucy0000@sina.com*

**Abstract:**Paper and board are one of the most important food packaging materials. Microwave heating is a widely used food heating method. The migration of the phthalates (PAEs) from paper packaging into food simulants during microwave heating was investigated. 13 kinds of local paper samples were treated using accelerated solvent extraction (ASE) and the concentration and type of PAEs in them were determined by GC-MS. The kinetic migration of PAEs from microwave paper to Tenax and olive oil was studied at different microwave power, respectively. At the initial stage, the migration to both simulants followed the same trend. When the migration reached a certain degree, the migration percentage decreased for Tenax, while remained almost the same for olive oil.

Keywords: migration; paper; microwave heating; accelerated solvent extraction; phthalates; GC/MS; olive oil; Tenax

## 1 Introduction

Packaging safety is as important as food safety. Paper and board are widely used in the fast food industry as primary, secondary and tertiary packaging. They are supposed to be safe and harmless to health as they are made of natural wood. However, during the manufacture procedure, several kinds of processing agents were added to make sure the good properties of paper and board. The residue during processing may migrate into the food packed inside the paper and board. Phthalates (PAEs), the most frequently used plasticizers are among the contaminants that are most often present in paperboard packaging. The contamination of foodstuffs with phthalates (PAEs) is closely watched in China for the found of plenty PAEs in several kinds of beverages and foods in Taiwan in the last two years. The PAEs could interfere with the human hormones, and with the endocrine systems[1,2]. In case of avoiding the health problem, PAES were permitted for use in the food contact material under a maximum allowable concentration in many countries[3-5]. There are several studies reported in the literature dealing with migration of the PAES from the food wrapper into foods and food stimulants under conventional heating. B.Aurela studied the distribution of the phthalates in the paper, the source of the phthalates mainly came from the adhesive and the printing[6]. Triantafyllou[7] studied migration of selected model of contaminants from paperboard into Tenax and dry foods with low and intermediate fat content. The modeling of migration from paper into food was also examined, the partition behavior of organic surrogates was studied by Triantafyllou[8]. A. zulch[9] and C-X. Huang[10] studied the migration prediction model from paper to food simulants. But there was no report on the effect of microwave heating on the migration of the PAEs from paper packaging. Fast food was often reheated in microwave oven before sold to the customers. When the food is

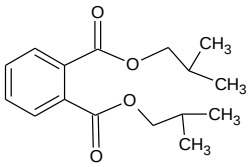
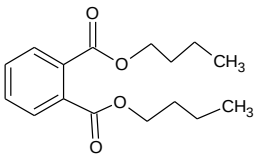
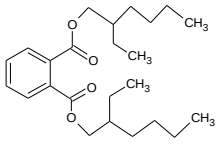
cooked with conventional heating, the heat is transmitted from the surface to the interior, producing a temperature gradient in the foodstuff. In contrast, microwaves penetrate the food to several centimeters thickness similarly, making the polar molecules in motion at the same time, thus the heat is generated quickly and quite uniformly throughout the mass of the foodstuff[11]. The different heating can result in different migration behaviors of the PAEs. Researches[12,13] showed that the rate of migration into the simulant Tenax (modified polyphenyleneoxide) was always greater than into dry foodstuffs. Similarly, the final equilibrium partitioning concentration between P/B and Tenax simulant, was always at least one-order of magnitude less than the partitioning between P/B and foodstuff. Tenax is used as the food simulant in this study for it is more "severe" than food. Olive oil was also chosen as the food simulant. Tenax stands for the solid food while Olive oil stands for the liquid food. Tenax and olive oil was both recommended by the EU as the food simulant. The purpose of this article is to find out the effect of the microwave heating on the migration of PAEs, as a basis for future research of modelling to predict the migration of PAEs during microwave heating.

## 2 Materious and Methods

### 2.1 Reagents and Solutions

Phthalates, i.e. diisobutyl phthalate (DIBP, C16H22O4, CAS No. 84-69-5), dibutyl phthalate (DBP, C16H22O4, CAS No. 84-74-2), bis(2-ethylhexyl) phthalate (DEHP, C24H38O4, CAS No. 117-81-7) were purchased from Sigma-Aldrich(USA). The characteristic of the phthalates were listed in Table1. Methanol solvents were purchased from Merk(Germany). Tenax-TA (60~80mesh) were purchased from Buchembv(Holland) . Olive oil was purchase from Borges (USA).

**Table 1**: The characteristic of the phthalates.

| Substance | Structure | Molecular weight | Boiling point (℃) |
|---|---|---|---|
| DIBP |  | 278.38 | 327 |
| DBP |  | 278.34 | 340 |
| DEHP |  | 390.56 | 385 |

### 2.2 Apparatus

Analysis was performed with an Agilent 7890A gas chromatograph companied with a 5975 mass-spectrometric detector. An accelerated solvent extraction (ASE) (ASE350, Dionex Corporation, USA) was used to extract the initial concentration of the PAEs in the paper. The migration test was placed in a Panasonic microwave oven

equipped with a turntable and 8 FOT-L-SD (FISO, Canada) fiber optic sensors which can test the temperature of the samples. The solution was evaporated using a Concentration Workstation (TurboVap Ⅱ,Caliper Life Sciences,USA).

### 2.3 Samples

The paper samples may encounter a using in the microwave oven was purchased from local Wal-mart store(Zhuhai, China). The samples were selected from applications where there was intended to be contact to the foodstuff. These samples are described in Table 2. S1-S4 were used to package the hamburgers. S5-S8 were disposable paper cups, maybe used as drink holders. S9 was a chipboard box used to package the pizza. S10-S13 were used to package the cakes. All these paper samples may be used in the microwave oven to reheating the foods in China.

**Table 2**: Paper samples collected in Chinese local market.

| Sample code | Type | Grammage ($g/m^2$) | Thickness (μm) | Density ($kg/m^3$) |
|---|---|---|---|---|
| S1 | White kraft | 33 | 144 | 275 |
| S2 | White kraft | 42 | 165 | 348 |
| S3 | White kraft | 37 | 158 | 295 |
| S4 | White kraft | 41 | 152 | 363 |
| S5 | disposable paper cup | 313 | 542 | 743 |
| S6 | disposable paper cup | 386 | 622 | 821 |
| S7 | disposable paper cup | 312 | 583 | 777 |
| S8 | disposable paper cup | 357 | 568 | 692 |
| S9 | chipboard | 358 | 549 | 852 |
| S10 | grease-proof paper | 178 | 234 | 562 |
| S11 | grease-proof paper | 193 | 266 | 641 |
| S12 | grease-proof paper | 234 | 209 | 668 |
| S13 | grease-proof paper | 189 | 215 | 602 |

### 2.4 Determination of Initial PAEs Concentration in Paper Samples

The paper samples were tested to get the initial concentration of the PAEs which may become the potential migrants using the accelerated solvent extraction method. 0.5 g shredded paper samples was taken into a 34 mL stainless steel vessel. The conditions of accelerated solvent extraction (ASE) were as follows: extract solvent-dichloromethane, oven temperature-120℃, static time-5 min, flush volume-60%, purge time-60 s, static cycle twice. The extracts were concentrated to 1 mL by the Concentration Workstation. The 1 mL concentrate was filtered using a 0.45μm pore size PTFE syringe filter, then analyzed by GC-MS. GC-MS analysis was performed with an Agilent 7890A gas chromatograph companied with a 5975 mass-spectrometric detector. Compounds were separated on a 30m*0.25mm internal diameter fused silica capillary HP-5 with a film

thickness of 0.25μm. Injections(1μL) were performed in split mode (split ratio 1∶20) by means of an auto-sampler. The column temperature was held at 60℃ for 3 minutes after injection then raised at 25℃ min-1 to 290℃ and held for 4 minutes. Helium was used as carrier gas at 40 kPa. Injector temperature: 280℃. Mass spectral detection was made in electron impact scanning mode (35 to 500 amu) to enable component identification (Agilent processing software with NIST and Wiley libraries).Concentrations were estimated by comparing the PAEs' quantitative ion peak response to the concentration of the PAEs standard solution. Response factors were considered to be unity so that an estimate of relative amounts could be made.

### 2.5 Fortification of Paper Samples with PAEs

To study the migration behavior of the detected PAEs, paper samples were required containing substances at sufficient levels to allow measurement of migration levels into food. The method used in this study was to fortify the paper samples with PAEs detected from the paper samples in real situation. Strips of the paper samples with approximate dimensions 4 *1 cm were placed in 20mL septum glass vials. The vials were filled with 20mL of contamination solution having mixed PAEs concentration of 200 mg/L. The vials were sealed and left for approximately 2 hr in a horizontal position at 25 ℃, while the paper strips were totally immersed into the contamination solution. The paper strips were then picked out the vials and laid in a glass dish in a ventilated hood at room temperature for drying for 20 minutes. The paper samples were ready for the test of migration. To detect the initial concentration of the plasticizers in the contaminated paper samples, the paper strips were cut into smaller pieces(1*1 cm) and placed in 10 mL vials with 5 mL methanol. Extraction was performed by gentle shaking of the vials for 1h at room temperature. The methanol extracts were analyzed by GC-MS described previously after filtered through a 0.45μm pore size PTFE syringe filter.

### 2.6 Migration Test

To check if the paper could be used as food packaging under microwave heating, migration studies of PAEs detected in paper samples into foods have been performed at different microwave powers. Ner ń[14] studied the migration of DBP and DIBP from thinner paper was easier and more rapid. S2 was chosen to study the migration behavior of the PAEs. The test conditions represent short-term exposures at high powers (rapid testing), or an unfreeze operation frequently done at home for a relatively long time (15-30 minutes) at low powers. It is important to know the transference capacity of these pollutants during microwave heating, which is the process called migration. Kinetic migration studies were carried out with strips of both paper samples contaminated with the phthalate mixture as described previously. Each contaminated strip was laid on the bottom of a petri dish . After covering 0.1g Tenax uniformly on the strips, another petri dish with a hole on the bottom was covered on it reversely. The FISO(Canada) Microwave Work Station equipped with a turntable was performed to measure the sample temperature in the microwave oven with the FISOs fiber optic sensors. The sensors get in the vial through the hole and stayed inside the Tenax to get the temperature while the microwave oven works. The migration of the PAEs from the paper strip to the olive oil was carried out in a 20mL septum glass vial, with 20mL olive oil in it. Five kinds of average power output of the microwave oven was chosen in the migration test. The experimental power output of the microwave oven/time exposure conditions were as follows:

- 100w: 15, 20, 25, 30min;
- 250w: 5, 13, 17, 21, 26, 30min;
- 440w: 3, 5, 7, 9, 11, 13, 15min;

- 600w: 1, 3, 5, 7, 9, 11, min;
- 900w: 20,40,60,90,120,150,180,240,300s;

All the experiments were carried out in triplicate. The extraction of the migrated plasticizers in the Tenax was performed as the following: the food simulants were collected in a 10 mL vials after removing from the respective paper strip. 2 mL methanol was added into the vials. After gentle shaking of the vials for 1.5h at room temperature, the vials were left standing for 0.5hr. The extraction was repeated twice. The combined extracts were concentrated under nitrogen stream. The methanol extracts were analyzed by GC-MS after filtered through a 0.45μm pore size PTFE syringe filter. To extract the PAEs migrated to the olive oil, the paper strip was taken out of the olive oil. After the migration test, 1 mL olive oil was transferred to a conical flask, 15 mL dichloromethane and 2g anhydrous sodium sulfate was added into the conical flask, too. The mixture was filtered and the filtrate was collected into a 50mL volumetric flask. The solution was then analyzed by GC-MS after filtered through a 0.45μm pore size PTFE syringe filter. The concentration of the rest plasticizers in the paper strips was tested as described previously. The recovery of the extraction method after migration was verified by spiking on the olive oil with different levels (0.2mg/L – 2mg/L) in six replicate.

## 3 Results and Discussion

### 3.1 Linearity, Limit of Detection (LOD) and Limit of Quantitation(LOQ)

Stock solutions were prepared by dissolving 250mg of each PAEs in 1 L of methanol and stored in a volumetric flask at 4 ℃. Standard working solutions, at various concentrations, .5 standard solutions with concentrations of 0.32, 0.64, 1.6, 8.0, 16.0 and 32.0 mg/L were prepared by appropriate dilution with methanol. The stock solutions before use were obtained by diluting the stock standard solution with methanol, and filtered using a 0.45μm pore size PTFE syringe filter before analysed by GC-MS. The responses were linear over the concentration ranges tested with correlation coefficients of 0.9999, 0.9949 and 1.0000 for DIBP, DEHP and DIBP, respectively(Table 3).

Validation of the analytical method comprised of the limit of detection (LOD), limit of quantitation(LOQ). The LODs for the PAEs were diluted to the lowest concentrations which gives responses three times of the average of the baseline noise. The LOQ was at the lowest concentration that gives response ten times of the average baseline noise. The data are summarized in Table 3. The recovery of the extraction method after migration turned out to be between 89.3% to 105.8%.

**Table 3:** Linear equation, correlation coefficient, LOD.

| Compound | Linear equation | Correlation coefficient/$R^2$ | quantitative ion | LOD(mg/kg) | LOQ(mg/kg) |
|---|---|---|---|---|---|
| DIBP | y=1341375.76x-176232.93 | 0.9999 | 149.2 | 0.012 | 0.030 |
| DEHP | y=1642543.97x-294854.70 | 0.9949 | 149.2 | 0.075 | 0.214 |
| DBP | y=840197.85x-112442.22 | 1.0000 | 149.2 | 0.014 | 0.039 |

### 3.2 Initial PAEs Concentration in Paper Samples

The initial PAEs concentration in the paper samples was detected using the GC-MS method. Three phthalate esters are present in a total of 13 paper samples. The concentration of these three phthalate esters was listed in

Table 4. According to the detected results, PAEs existed in most of the paper samples are DIBP, DEHP, DBP, thus the migration behavior of DIBP, DEHP, DBP was studied during microwave heating in this paper.

**Table 4**: Concentration of the phthalates in the paper samples (mg/kg).

| | S1 | S2 | S3 | S4 | S5 | S6 | S7 | S8 | S9 | S10 | S11 | S12 | S13 | S14 |
|---|---|---|---|---|---|---|---|---|---|---|---|---|---|---|
| DIBP | 41.21 | 9.63 | 33.51 | 56.92 | 4.12 | 13.04 | 5.23 | 5.83 | 2.45 | 4.05 | 9.81 | 9.97 | 8.59 | 9.12 |
| DEHP | 21.22 | - | 14.65 | 48.93 | - | 10.96 | 4.81 | 5.49 | 11.87 | 1.75 | 5.68 | 3.58 | 3.56 | 2.66 |
| DBP | 8.21 | - | 15.56 | 22.01 | 0.99 | 2.57 | 0.98 | 1.51 | 0.87 | - | - | - | - | - |

### 3.3 Initial PAEs Concentration in the Fortified Paper Samples

The paper strips were fortified using a contamination solution with relatively high concentration (200 mg/L) in order to make sure the initial plasticizers concentration is workable for the migration experiments. Methanol was found to cause complete extraction of absorbed plasticizers from the paper under the experimental conditions described previously. The amounts of the PAEs after the fortification operating was tested. The average concentration of the fortified plasticizers in the paper strips were shown in Table 5.

**Table 5:** The average concentration of the absorbed plasticizers in the paper strips (mg/kg).

| Phthalates | concentration |
|---|---|
| DIBP | 522.1 |
| DEHP | 563.9 |
| DBP | 623.3 |

### 3.4 Temperature——Time Curve underDifferent Microwave Powers

Figure. 1 shows the growth of the temperature under different microwave powers. The temperature grows as time passes, and the temperature growth rate is proportional to the microwave energy. It is obvious that the temperature grew much faster in the first 10 minutes during microwave heating, then the rate of the temperature growth becomes flat. One thing that needs to be noticed is that when heating under 100W, the temperature can only get to about 50 degrees, and the maximum heating time of the microwave oven used in this experiment is 30 minutes.

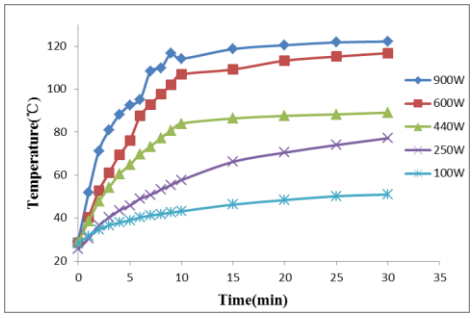
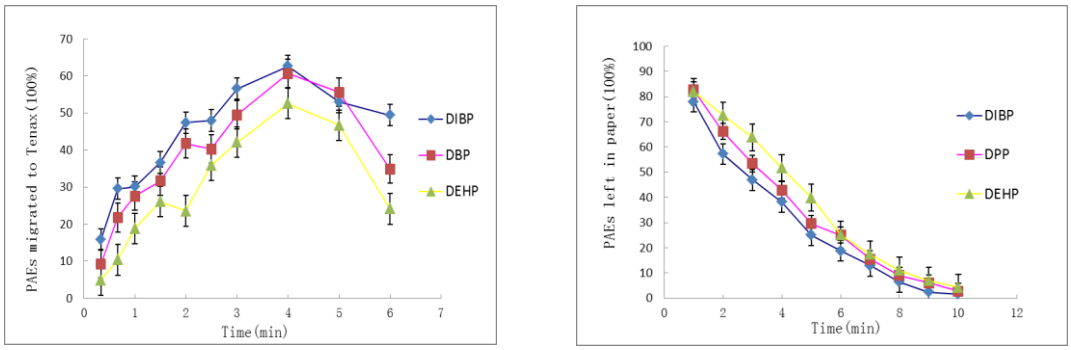


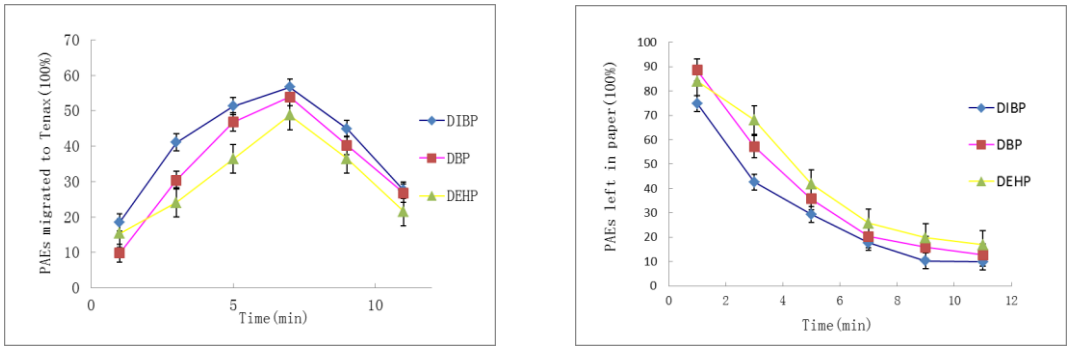

**Figure 1**: Changing temperatures during microwave heating (℃).

### 3.5 Migration of PAEs to Tenax

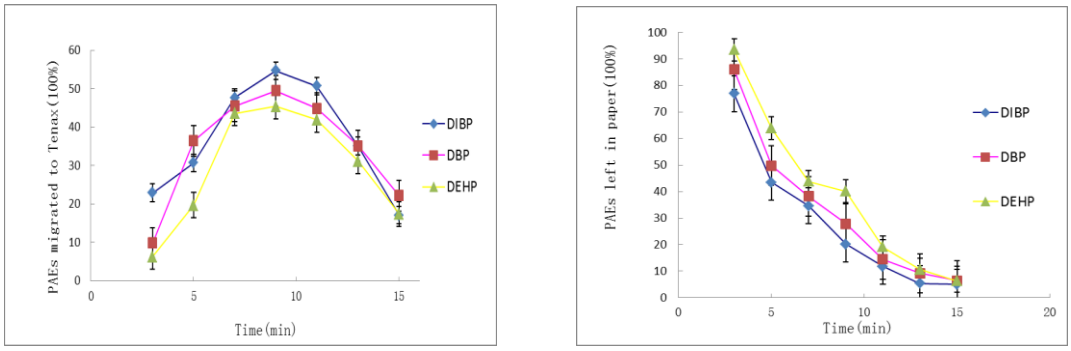
Migration was expressed as percentage of the initial PAEs concentration in the paper. During the microwave heating, the high-frequency oscillation caused by the alternating electromagnetic field made the polar molecules start to motion and rubbed mutual, thus generates heat. The greater the microwave power, the faster the speed and direction of the molecular motion change, thus more heat is generated, accelerated migration occurs. Heated under the higher microwave power, the PAEs had a higher migration percentage as the time passes, as shown in Figure 2. Under experimental conditions, with increasing microwave power, migration of the PAEs into the food simulant has increased. In fact, the microwave power has an intense effect on the migration. Figure 2(a), Figure 2(b), Figure 2(c) showed an increase migration at first, after going through the highest point, and then lasting for a period, then the percentage gradually decreased. Contrast to the temperature data in Figure1, the turning point showed temperature dependence. This decline occurred when the temperature almost rose to 80 ℃. Figure 2(d), Figure 2(e) showed no decrease because the temperature could not reach 80 ℃ at the end during the microwave heating. The heating operation only lasted 30 minutes because the microwave oven could be heated 30 minutes at most.



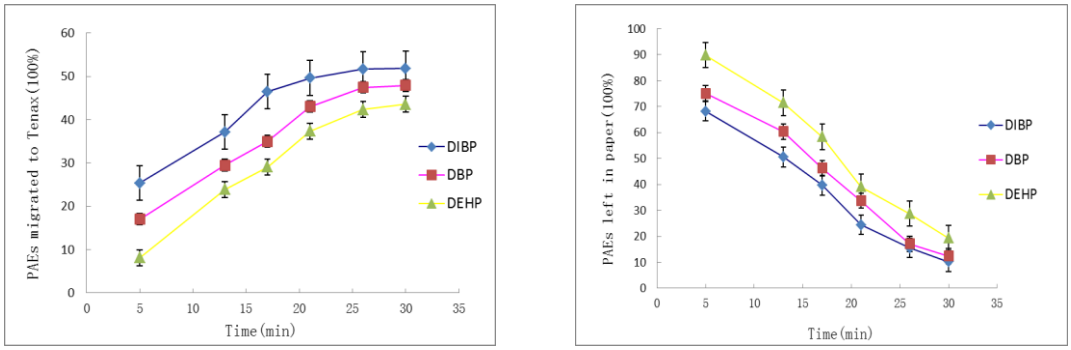

(a) 900W



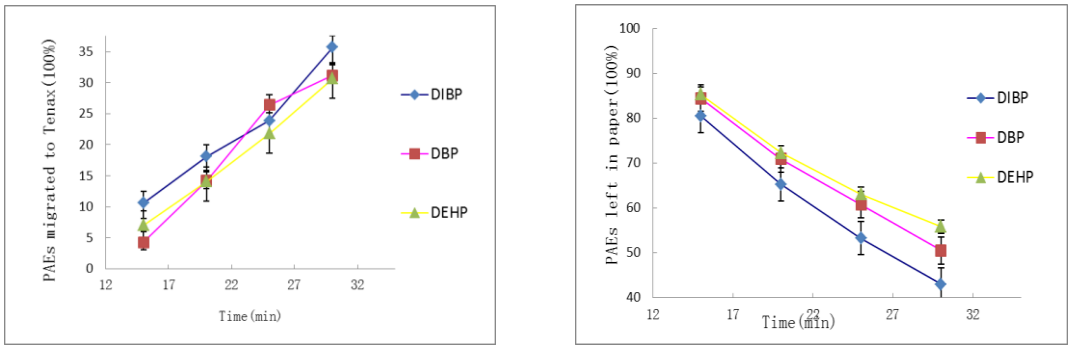

(b) 600w




(c) 440W




(d) 250W




(e) 100W

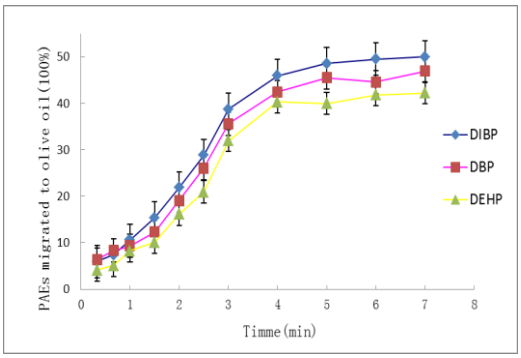
**Figure 2:** Percentage of migrated PAEs from paper into Tenax and PAEs left in paper at microwave power: (a) 900W; (b) 600W; (c) 440W; (d) 250W; (e) 100W, respectively.

The content of the PAEs remaining in the paper after the migration was also examined, they are persistent in the decline, and over the turning point, the total amount of plasticizer remaining in the paper and the plasticizer migrated to Tenax was smaller than the plasticizer content in the fortified paper. This must be caused by the volatilization of the PAEs. After the temperature rose to a certain range about 80℃, either the PAEs stayed in the paper or migrated to the Tenax, started to volatilize into the gas phase. Several migration studies from paper had been carried out under the conventional heating. When the migration of PAEs from paper to food simulants was carried out at high temperature( 70℃ - 100℃), the percentage of PAEs migrated to paper was persistently growing without a decline[15-18]. The migration studies from plastic packaging had also been done during microwave heating, the percentage of PAEs migrated from plastic to food simulants also showed no decline[12,19-20]. During the migration to the solid food simulant, PAEs had to overcome the attraction from

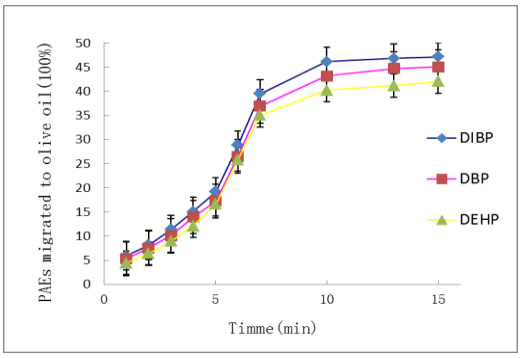
the packaging, and move to the gas gap between packaging and Tenax before moving into Tenax. The porosity of paper is different from the densification of plastic, which means there is a stronger attraction between plastic and PAEs. Tenax reaches a higher temperature when heated under the conventional heating, but its molecule is less attracted to the PAEs under continuous high frequency oscillation.

### 3.6 Migration of PAEs to Olive oil

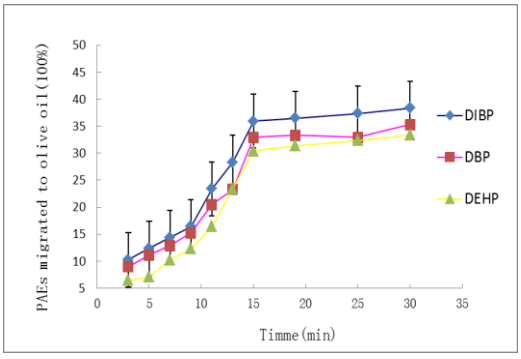
The migration of the PAEs from paper strips to the olive oil is different from the migration of the PAEs to the Tenax. There is no decline of migration percentage with temperature growing during microwave heating. Unlike the conventional heating, in the initial stage, PAEs migration rate is slower, with the increase of time, a rapid growth of the PAEs migration rate can be seen as shown in Figure 3(a), Figure 3(b), Figure 3(c) and Figure 3(d). This is due to the change of temperature while the sample was heated under the microwave heating. Paper has repeat units of glucose residues and is very hydrophilic. Thus, there is a strong attraction between paper and the PAEs. The temperature was low during the first few minutes, most of the PAEs molecules didn't get enough power to run away from the cellulose fiber of the paper. With continuous microwave heating, the temperature increased. The PAEs then got enough power to escape from the attraction of the cellulose fiber of the paper， thus a rapid migration rate was shown. After most of the PAEs near the surface of the paper had moved out, the PAEs in the inner part of the paper had to overcome a stronger force to migrate to the olive oil.



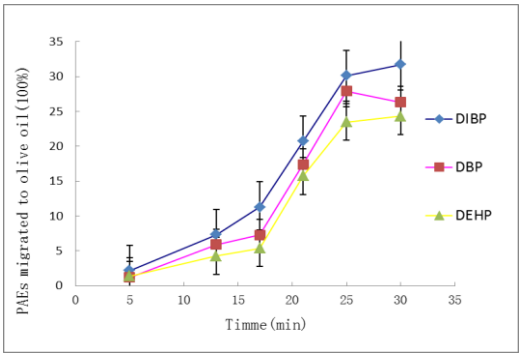

(a) 900W



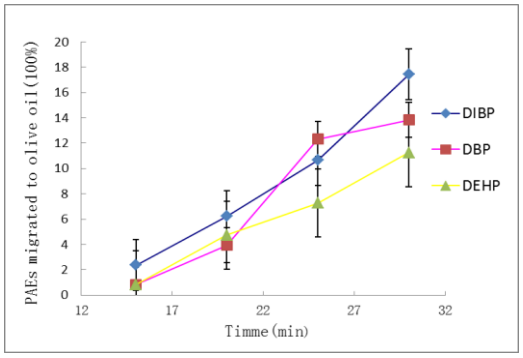

(b) 600w




(c) 440W




(d) 250W

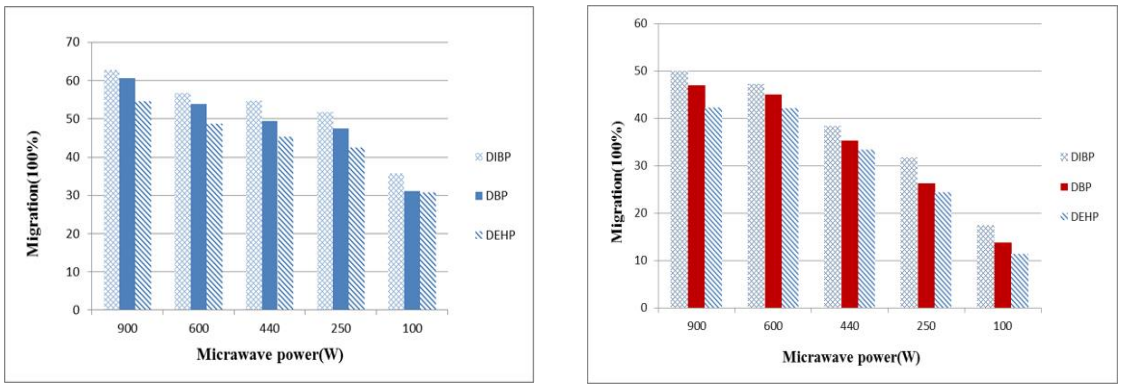



(e) 100W

**Figure 3:** Percentage of migrated PAEs from paper into olive oil at microwave power: (a) 900W; (b) 600W; (c) 440W; (d) 250W; (e) 100W, respectively.

### 3.7 Effect of microwave power in migration test

Figure.4 compared the migration percentage of the three PAEs under different microwave powers when reaching the balance. The PAEs spent less time to get to the balance after migrating under a greater microwave power, but got a higher migration percentage. The migration percentage is lower when heated under 100W due to the very low temperature. DIBP, DEP, DEHP have a similar symmetrical structure with a growing carbon chain which led to a growth in their molecular mass, and the stability showed a corresponding growth. Thus DIBP, DEP, DEHP showed a decline in the migration ability with the growth of the molecular chain length and the molecular mass. DIBP, DBP, DEHP also showed a growth on their polarity, which is another important influencing factor in the migration. Tenax had a weak polarity which made the PAEs have a relatively higher polarity with a lower migration percentage. On the other hand, the high-frequency oscillation movement caused by microwave radiation was proportional to the molecular polarity. Molecules with a higher polarity are more active, thus when migrating to the Tenax, they could lose more during the volatilization. Figure 4 showed the migration of PAEs increases with the microwave power.




(a) Tenax (b)olive oil

**Figure 4:** Migration percentage of phthalates to (a) and (b)olive oil under different microwave powers.

As shown in Table 6, China issued a "food containers, packaging materials used additives health standards" (GB 9685-2008), set a maximum limit of usage and migration of hundreds of species used in plastics, rubber, paper products, additives, including seven common phthalate plasticizers content limiting and migration restrictions. "food containers, packaging materials used additives health standards" only applies to non-fatty food contact materials. EU “food contact plastic materials and products regulations” (10/2011 / EU) has entered into force on

May 1, 2011, new regulations gave a detailed provisions to the amount of food contact materials phthalate plasticizers usage [21, 22].

**Table 6**:Limit of PAEs in food contact material from different countries.

| Country | legislations | Chemicals | Applicable scope | Content restriction | SML |
|---|---|---|---|---|---|
| CHINA | GB9685-2008 | DEHP | Only applicable to food contact materials used in non-fat foods. Shall not be used for infant food contact materials | Appropriate use ccording to production needs | 1.5mg/kg |
| | | DIBP | | 10%（PVC） | — |
| | | DBP | | 10% | 0.3 mg/kg |
| EU | 10/2011/EU | DEHP | Only applicable to food contact materials or tools used in non-fat foods. | 0.1% | 1.5mg/kg |
| | | DBP | | 0.05% | 0.3mg/kg |

While the initial concentration of the PAEs in the paper samples didn't pass the restriction set by China and EU, the amount of the PAEs that migrated to both fatty solid food and fatty liquid food is not negligible during microwave heating, it's necessary to give further details about the safety assessment of the usage of paper used in microwave oven.

## 4 Conclusions

In this paper, three kinds of PAEs were detected in the paper samples collected in local supermarket. Migration of the detected PAEs from paper strip into food simulants under microwave heating was studied. The PAEs in paper samples would migrate into solid food simulant during microwave heating, and showed that the migration percentage increasedas the temperature increased and reached the peak at about 80℃. The migration of PAEs from paper into liquid food simulant during microwave heating showed a relevance to the rate of rise of temperature. The amount of migration mainly depends on the heating time and microwave power.

## Acknowledgements

This research was supported by project 21077045 supported by the National Natural Science Foundation of China and project 21277061 supported by the National Natural Science Foundation of China.

## References

1. A Ishihara, S Sawatsubashi, K Yamauchi, 2003, "Endocrine disrupting chemicals: interference of thyroid hormone binding to transthyretins and to thyroid hormone receptors",Molecular and Cellular Endocrinology, vol. 199, no.1-2, pp.105-177.
2. R Mankidy, S Wiseman, H Ma and J Giesy, 2013, "Biological impact of phthalates", Toxicology Letters, vol.217, no.1, pp. 50-58.
3. J Jurewicz, W Hanke, 2011, "Exposure to phthalates: reproductive outcome and children health. A review of epidemiological studies", International Journal of Occupational Medicine and Environmental Health, vol.24, no.2, pp.115-141.
4. V Pak, L McCauley, J Pinto-Martin, 2011, " Phthalate Exposures and Human Health Concerns A Review and Implications for Practice", AAOHN Journal, vol.59, no.5, pp.228-233.

5. J.Y Lu, 2011, “Plasticizer event in Taiwan”, Journal of Formor Medical Association, vol.110, no.9, pp.553-554.

6. B Aurela, H Kulmala, L Soderhjelm, 1999, “ Phthalates in paper and board packaging and their migration into Tenax and sugar”, Food Additives & Contaminants, vol.16, no.12, pp.571-577.

7. V.I Triantafyllou, K Akrida-Demertzi, P.G Demertzis, “A study on the migration of organic pollutants from recycled paperboard packaging materials to solid food matrices”, Food Chemistry, vol.101, no.4, pp.1768-1795.

8. V.I Triantafyllou, K Akrida-Demertzi, P.G Demertzis, 2002, “Studies on the usability of recycled paper and board packaging materials for direct and /or indirect food contact” 6th International Conference on Protection and Restoration of the Environment. Skiathos isl, Greece, Vol.Grafima Loannis Tsarouchidis, pp.989-996.

9. C.X Huang, D Duan, M Yan and S Wang, 2013, “Migration Prediction Model of Residual Contaminants from Food Packaging Paper and its Experimental Verification”, Packaging Technology and Science. vol.26, no.Supplement 1, pp.59-69.

10. A Zulch, O Piringer, 2010, “Measurement and modelling of migration from paper and board into foodstuffs and dry food simulants”, Food Additives & Contaminants, vol.27, no.9, pp.1306-1324.

11. V Guillard, M Mauricio-Iglesias, N Gontard, 2010, “Effect of Novel Food Processing Methods on Packaging: Structure, Composition, and Migration Properties”, Critical Reviews In Food Science And Nutrition, vol.50, no.10, pp.969-988.

12. C Nerin, D Acosta, 2002, “Behavior of some solid food simulants in contact with several plastics used in microwave ovens”, Journal of Agricultural and Food Chemistry, vol.50, no.25, pp.7488-7492.

13. C Nerin, E Contin, E Asensio, 2007, “Kinetic migration studies using Porapak as solid-food simulant to assess the safety of paper and board as food-packaging materials”, Analytical And Bioanalytical Chemistry, vol.387, no.6, pp.2283-2288.

14. C Nerin, E Asensio, 2004, “Behaviour of organic pollutants in paper and board samples intended to be in contact with food”, Analytica Chimica Acta, vol.508, no.2, pp.185-191.

15. W Summerfield, I Cooper, 2001, “Investigation of migration from paper and board into food - development of methods for rapid testing”, Food Additives & Contaminants, vol.18, no.1, pp.77-88.

16. V.I Triantafyllou, K Akrida-Demertzi, P.G Demertzis, 2005 , “Determination of partition behavior of organic surrogates between paperboard packaging materials and air”, Journal Of Chromatography A, vol.1077, no.1, pp.75-79.

17. V.I Triantafyllou, K Akrida-Demertzi, P.G Demertzis, 2001 , “Migration studies from recycled paper packaging materials: development of an analytical method for rapid testing”, Analytica Chimica Acta. vol.467, no.1-2, pp.253-260.

18. Y.M Wu, C.Y Hu, L Wang, J Cheng, Z.W Wang, Y Zhu, 2010, “Migration of Contaminants from Packaging Materials into Dairy Products”, 17th IAPRI World Conference on Packaging. Tianjin, China, pp.207-211.

19. J Alin, M Hakkarainen, 2012, “Migration from polycarbonate packaging to food simulants during microwave heating”, Polymer Degradation And Stability, vol.97, no.8, pp.1387-1395.

20. S Johns, S Jickells, W Read and L Castle, 2000, “ Studies on functional barriers to migration. 3. Migration of benzophenone and model ink components from cartonboard to food during frozen storage and microwave heating”, Packaging Technology and Science. vol.13, no.3, pp.99-104.

21. European Food Safety Authority. 2011. Commission Regulation(EU) No 10/2011of 14 January 2011 on plastic materials and articles intended to come into contact with food. Available from: http://eur-lex.europa.eu/LexUriServ/LexUriServ.do?uri=OJ:L: 2011:012:0001:0089: EN:PDF.

22. GB 9685—2008.Hygienic standards for uses of additives in food containers and packaging materials. Available from: http://wenku.baidu.com/view/03d5e947a8956b- ec0975e337.html.

# The Effect of Packaging on Consumer Food Quality Perception in Quick-Service Restaurants[#]

**Rupert Hurley[*], Emily Thackston, Chip Tonkin and Kay Cooksey**

*Clemson University, United States*

[*]*Corresponding author. Email: ruperth@g.clemson.edu*

**Abstract:** The majority of menu items available in quick-service restaurants (QSR) are consumed directly from a container or package. The main reasons consumers choose to eat fast food are because it is convenient, prepared quickly, a good value, and inexpensive. Therefore, the packaging becomes an integral part of the food product and from a consumer perspective must be consistent with their expectations and motives for choosing to eat fast food. Prior research has directly linked characteristics of consumer food packaging experience to their perception of its contents. The purpose of this research is to determine if consumer quality perception of food products in quick-service restaurants varies depending on the material properties of the packaging in which the food product is presented. The commonly used foodservice packaging styles and materials selected for testing included: a 14-pt paperboard clamshell, an expanded polystyrene clamshell, an F-flute (micro-flute) corrugated clamshell, and a paper wrap. All materials were tested in a realistic QSR environment. Sensory, functionality, and credence attributes were evaluated by participants. Preference and ranking response data was also collected. A questionnaire was used to measure participant response. Findings from the research indicate that while the sensory attribute ratings did not differ significantly, respondents had significant preference for certain package materials based on functionality and credence attributes, and perceived certain materials as more suitable for certain food products.

Keywords: packaging; food quality perception; quick-service restaurants; fast food.

[#] This is the abstract of a peer-reviewed paper to appear in a Special Edition of Wiley's journal *Packaging Technology and Science* dedicated to the 19th IAPRI World Conference on Packaging 2014 hosted by Victoria University, Melbourne, Australia.

# Determination of Ti in Nano/submicro-$TiO_2$-plastic Composite Food Packaging by Microwave Digestion and Inductively Coupled Plasma Atomic Emission Spectrometry or Inductively Coupled Plasma Mass Spectrometry

**Qin-Bao Lin [1, 2*], He Li[2], Huai-Ning Zhong[3], Quan Zhao[3], Da-Hui Xiao[3] and Zhi-Wei Wang[1]**

[1] *Key Laboratory of Product Packaging and Logistics, Institute of Packaging Engineering, Jinan University, Zhuhai 519070, China;*

[2] *College of Life Science, Shanxi University, Taiyuan 030006, China;*

[3] *Guangdong Border Inspection and Quarantine Technology Center, Guangzhou 518010, China*

** Corresponding author. E-mail: tlinqb@jnu.edu.cn*

**Abstract:** The determination of Ti in nano/submicro-$TiO_2$-plastic food packaging by microwave digestion with inductively coupled plasma atomic emission spectrometry (ICP-AES) and inductively coupled plasma mass spectrometry (ICP-MS) has been studied. Microwave digestion was optimized by trialling different acid mixtures and an acid mixture consisting of 6 mL of $HNO_3$ + 1.5 mL of $H_2O_2$ + 0.5 mL of HF gave the highest digestion efficiency for Ti. Both ICP techniques showed good reproducibility, repeatability and recovery. For ICP-AES analysis, the limit of detection (LOD) was 5.0 mg $kg^{-1}$, the analytical range was 100–5000 μg $L^{-1}$, the average recoveries for blank samples spiked with Ti were in the range of 94.7–100.1%, and the relative standard deviations (RSDs) were from 2.1% to 7.1%. For ICP-MS analysis, the LOD was 0.3 mg $kg^{-1}$, the analytical range was 0.5–200 μg $L^{-1}$, the recoveries were 88.4–96.3% and the RSDs were 6.3–7.4%. These results indicated that proposed methodologies were effective, however, ICP-MS was preferred for trace/ultra-trace determinations of Ti in nano/submicro-plastic food packaging due to its more superior LOD.

Keywords: microwave digestion, food composite packaging, nano/submicro $TiO_2$, inductively coupled plasma atomic emission spectrometry (ICP-AES), inductively coupled plasma mass spectrometry (ICP-MS).

## 1 Introduction

Nanomaterials, the most basic element of nanotechnology, are commonly defined as having a grain size structure of 1–100 nm in at least one dimension [1]. With increasing attention being given to environmental and quality-of-life issues, many scientists, from the perspective of biological safety and environmental assessment, have extended the size range of nanomaterials, recommending that submicro materials with dimensions greater than 100 nm should also be included in the classification [2]. Because of their small size, nano/submicro materials exhibit unique properties, such as quantum size effect, high surface area, short inter-face migration

distance and photoactivity. All of these unique properties result in an enhanced photocatalytic performance [3]. To date, such materials have been used in a wide range of applications [4, 5], including novel products [6], cosmetics [7], environmental protection [8], food additives [9], food packaging [10] and food contact materials [11].

Nano/submicro technology in the food packaging industry is used to extend the shelf life of products. Over the last decades, the use of nano/submicro composite polymers as food packaging materials has increased enormously owing to their advantages over other traditional materials [12, 13]. Many applications of nanotechnology in food packaging and food safety have been researched including use as barrier materials, antimicrobials and sensors [1, 14]. Packagings have been made by incorporating metal, metal oxide, semimetal or clay nano/submicro particles into polymer films. The polymers used for fabrication of nano/submicro composites are typically polyamides, polyethylene, polypropylene, polystyrene, polyurethane, polyethylene terephthalate and epoxy resins [6, 14]. The metal and metal oxide nano/submicro particles used for the composites include Ag, Au, ZnO, $TiO_2$, MgO, CaO, $Al_2O$, $Fe_3O_4$ and $Fe_2O_3$ [10, 15]. The nano semimetals and clays commonly used are $SiO_2$, carbon, kaolin and montmorillonite [16, 17].

Nano $TiO_2$ posses many attributes including high photosensitivity, non-toxic nature, wide availability, strong oxidising power, photocatalytic activity and long-term stability [5]. The Ti nanomaterial is commonly used in packaging because of its photocatalytic antibacterial properties.

Many analytical methods are available for characterisation and analysis of NPs and the host matrix, including field emission scanning electron microscopy, transmission electron microscopy, atomic force microscopy, Fourier transform infrared spectrometry, laser particle size analysis [6, 18], inductively coupled plasma atomic emission spectrometry (ICP-AES) and inductively coupled plasma mass spectrometry (ICP-MS) [19]. The determination of Ag in nano-plastic films [19] and the migration of Ag from nano-plastic films to food simulants [20] have been described by our group. Shaw et al. [21] reported the determination of Ti originating from $TiO_2$ NPs in fish tissue. The traditional approach for determining trace metals in diverse samples such as soils [22], cosmetics and food products [23] is based on acid digestion of the sample and subsequent analysis of dissolved metals by ICP-AES or ICP-MS. However, such conventional methods are ineffective for nano-$TiO_2$-plastic films because of the refractory nature of the polymer matrix and the high strength of the Ti-O bond. To the best of our knowledge, the dissolution of Ti in nano-$TiO_2$ composite plastic food packaging film has not been investigated using modern dissolution techniques such as microwave-assisted acid digestion. This paper aims to develop a novel and highly sensitive method for the determination of Ti in representative samples of nano/submicro-$TiO_2$ polyethylene plastic food packaging. Microwave digestion, employing 6 mL of $HNO_3$, 1.5 mL of $H_2O_2$ and 0.5 mL of HF was used for sample dissolution and resulting digests were analysed by ICP-AES and ICP-MS. Results indicated that ICP-MS was more suited to the trace and ultra-trace determination of Ti in nano/submicro-$TiO_2$-plastic food packaging samples.

## 2 Materials and methods

### 2.1 Instrumentation

A microwave oven (ETHOS CMMWG) equipped with ten polytetrafluoroethylene (PTFE) vessels (Milestone, Bergamo, Italy) was used for sample digestion. Samples were analysed with an ICAP 6000 ICP-AES (Thermo Electron Corporation, Boston, USA), and an Agilent 7500c ICP-MS equipped with an octopole reaction system (Agilent, Palo Alto, USA). The operating conditions of the instruments are shown in Table 1. An ultrasonic bath (KQ-500E, Kunshan Ultrasonic Co., Ltd, Kunshan, China) was used for cleaning of labware. High purity water

was produced by an ultrapure water system (UPHW-I-90T; Chengdu Ultrapure Technology Co., Ltd., Chengdu, China). A micro control digital electric hot plate (Controller P 320, Nabertherm Co., Ltd., Lilienthal, Germany) was used for evaporation of sample digests.

**Table 1:** Operating conditions for ICP-AES and ICP-MS

| ICP-AES | | ICP-MS | |
|---|---|---|---|
| RF Power (W) | 1150 | RF Power (W) | 1500 |
| Plasma gas flow rate (L $min^{-1}$) | 15.0 | Plasma gas flow rate (L $min^{-1}$) | 15.0 |
| Auxiliary gas flow rate (L $min^{-1}$) | 0.8 | Auxiliary gas flow rate (L $min^{-1}$) | 1.00 |
| Atomizing gas flow rate (L $min^{-1}$) | 0.2 | Makeup Gas (L $min^{-1}$) | 1.00 |
| Sample uptake rate (mL $min^{-1}$) | 1.0 | Carrier Gas (L $min^{-1}$) | 1.00 |
| Detection wavelength (nm) | 334.941 | Samplng Depth (mm) | 6.7 |
| Integration time (s) | 30 | Spray chamber temperature (°C) | 2.0 |
| Observation mode | Axial | PeriPump (rps) | 0.1 |

## 2.2 Reagents and chemicals

Concentrated reagents, $HNO_3$, $H_2SO_4$, $H_2O_2$ (≥30.0%) and HF (≥40.0%), were of Guaranteed Reagent grade and were obtained from the Guangzhou Chemical Reagent Co., Ltd. (Guangzhou, China). Reference stock solutions of Ti (1000 μg $mL^{-1}$) were obtained from the National Analysis Center for Non-ferrous Metals and Electronic Materials (Beijing, China) and working standard solutions were prepared from the stock solutions by appropriate dilution with 5% $HNO_3$.

## 2.3 Analytical performance

The limit of detection (LOD) and limit of quantification (LOQ) of the ICP instruments were calculated as three and ten times the standard deviation of the signals for the blank measurements, respectively. Values were calculated based on 11 determinations of the blank samples. The LOD and LOQ were estimated based on the analysis of spiked blank plastic film samples at concentrations of three and ten times the standard deviation of the blank plastic samples, respectively. In fact, it was not valid to estimate LOD values by calculation because of the low concentrations of Ti, which were below the analytical ranges established for ICP-AES and ICP-MS.

In this study, the following procedure was used to measure the LODs. Dilute standard solutions (*a, x* μg $L^{-1}$) were prepared by dilution with 5% $HNO_3$, where *a* is the LOD by calculation and *x* is a value that was in close proximity to *a*. Two standard solutions were analysed by ICP-AES and ICP-MS and the $\overline{A}$ and *y* values were obtained by formulas (1) and (2):

$$\overline{A} = \frac{A_x - A_0}{x} \quad (1)$$

$$y = \frac{A - A_0}{\overline{A}} \quad (2)$$

Where $\overline{A}$ is the signal intensity of unit concentration; $A_x$ is the signal intensity of the standard solution *x*; $A_0$ is the signal intensity of the blank solution (5% $HNO_3$); *A* is the signal intensity of the standard solution *a* and *y* is the theoretical value. Increasing concentrations of *a* were introduced to the ICP instruments until the theoretical value (*y)* equalled *a*.

### 2.3 Samples preparation and digestion

Nano/submicro-$TiO_2$-plastic films designed for food packaging and selected for this study were manufactured by the Kai Gong Plastic Co., Ltd. (Taiyuan, China) and the Guangzhou Jin Fangyuan Machinery and Equipment Manufacturing Co., Ltd. (Guangzhou, China). Table 2 gives basic information on these films. Samples were cleaned using ultrapure water and dried before use.

**Table 2:** Basic information on nano/submicro $TiO_2$-PE composite films

| Sample | 1# | 2# | 3# | 4# |
|---|---|---|---|---|
| Size of $TiO_2$ (nm) | 30 | 200-300 | 100 | 30 |
| Thickness (mm) | 0.053±0.005 | 0.060±0.006 | 0.052±0.003 | 0.055±0.002 |
| Density (g $cm^{-3}$) | 0.85±0.01 | 0.76±0.02 | 0.87±0.02 | 0.91±0.06 |

Sample aliquots (0.1 g) were weighed into a PTFE vessel and 6 mL of $HNO_3$, 1.5 mL of $H_2O_2$ and 0.5 mL of HF were added. The vessels were closed and the samples were digested using the microwave oven. The programme for microwave digestion was as follows: using a power setting of 1000 W, the temperature was raised to 150 °C in 10 min; next, the temperature was raised to 210 °C over the next 10 min and then held at this temperature for 20 min. The vessels were allowed to cool for 1–2 h and then the digests were evaporated to near dryness on a hot plate before making up with 5% $HNO_3$ (100 mL). Samples were then analysed by ICP-AES and ICP-MS.

A traditional ashing method was also used for sample dissolution. Specimens were cut to approximately 1 $cm^2$, weighted accurately in a quartz vial to 2.00 g and then placed in the muffle furnace. The heating programme was as follows: the temperature was raised to 300°C in 1 h, then increased to 500°C over 1 h and held for 3 h at 500°C. The beakers were allowed to cool for 3 h, then 6 mL of $HNO_3$, 1.5 mL of $H_2O_2$ and 0.5 mL of HF were added to the vessels containing the ashed residues. The beakers were next heated on a hot plate and the acid mixture was evaporated to 1–2 mL and then diluted to 100 mL with 5% $HNO_3$. Samples were then analysed by ICP-AES and ICP-MS as above.

### 2.4 Statistical analysis

Statistical analyses were carried out using Minitab 15.0 (Minitab Inc., State College, PA, USA) and Statistical Product and Service Solutions (SPSS) 13.0 (IBM SPSS Inc., New York, NY, USA) analytical software. $P<0.05$ was identified as being statistically significant at the 95% confidence level.

## 3 Results

### 3.1 Analytical performance

For ICP-AES, six standard solutions with concentrations of 100, 200, 500, 1000, 2000 and 5000 mg $L^{-1}$ in 5% $HNO_3$ were measured. For ICP-MS, nine standard solutions with concentrations of 0.50, 1.00, 2.00, 5.00, 10.0, 20.0, 50.0, 100.00 and 200.00 µg $L^{-1}$ in 5% $HNO_3$ were measured. The equations for the line of best fit over the respective concentration ranges, the correlation coefficients, the LODs and the LOQs for both techniques are shown in Table 3.

**Table 3:** Performance parameters for ICP-AES and ICP-MS

| Method | Linear equation | Analytical range (µg $L^{-1}$) | Correlation coefficient/$R^2$ | $LOD^i$ (µg $L^{-1}$) | $LOQ^i$ (µg $L^{-1}$) | $LOD^m$ (mg $kg^{-1}$) | $LOQ^m$ (mg $kg^{-1}$) |
|---|---|---|---|---|---|---|---|
| ICP-AES | $y$=22763.0$x$+47.3 | 100-5000 | 0.9999 | 15 | 50 | 5 | 20 |

| | | | | | | | |
|---|---|---|---|---|---|---|---|
| ICP-MS | $y$=530.4$x$+881.0 | 0.5-10 | 0.9996 | 0.08 | 0.25 | 0.3 | 1.0 |
| | $y$=520.3$x$+761.2 | 10-200 | 0.9999 | | | | |

Note: $LOD^i$, $LOD^m$: the LOD of the instrument and the LOD of the method; $LOQ^i$, $LOQ^m$: the LOQ of the instrument and the LOQ of the method.

### 3.2 Analyte recovery and method repeatability

For ICP-AES analysis, the repeatability of the method was verified by spiking blank film (0.100 g) with three concentrations (50, 100, 200 mg $kg^{-1}$) of Ti standard solutions in six replicate experiments. For ICP-MS analysis, the blank film (0.100 g) was spiked at concentrations of 1.0, 2.0 and 5.0 mg $kg^{-1}$, respectively. In the case of ICP-AES, the recoveries for Ti in the blank film sample were in the range of 94.7–100.1% and the RSDs were 2.1–7.1%, while for ICP-MS, the recoveries were in the range of 88.4–96.3% and the RSDs were 6.3–7.4% (Table 4).

**Table 4:** Analyte recoveries and RSDs for analysis of spiked blank samples (n=6)

| Method | Spike concentration (mg $kg^{-1}$) | Recovery (RSD) (%) |
|---|---|---|
| ICP-AES | 50 | 94.7 (7.1) |
| | 100 | 95.8 (4.8) |
| | 200 | 100.1(2.1) |
| ICP-MS | 1 | 86.9 (6.5) |
| | 2 | 93.9 (7.4) |
| | 5 | 96.3 (6.3) |

### 3.3 Analysis of real samples

Once the methods were established and validated, they were applied to the analysis of four nano/submicro-$TiO_2$-PE composite films used for food packaging. Table 5 shows the results for Ti, which were in the range of 162.40±6.33 to 878.43±3.65 mg $kg^{-1}$.

**Table 5 Concentrations of Ti in 4 composite film samples (n=3)**

| Sample | Content of Ti (mg $kg^{-1}$) | | | |
|---|---|---|---|---|
| | 1# | 2# | 3# | 4# |
| ICP-AES | 250.99±4.82 | 162.40±6.33 | 254.83±1.46 | 867.73±5.10 |
| ICP-MS | 253.15±1.40 | 164.79±3.72 | 261.00±2.95 | 878.43±3.65 |

## 4 Discussion

### 4.1 Comparison of sample preparation methods

Sample preparation is a key step in analytical methods for determination of trace elements in polymer samples. In this study, wet ashing and microwave digestion were performed and the results for sample 1 are shown in Figure 1. Concerning the concentrations of Ti, at the 95% confidence level, the paired t-test did indicate that extraction efficiency was higher for microwave digestion compared with wet ashing (p=0.00). In addition, microwave digestion was less time consuming, so microwave digestion was chosen for the preparation of all subsequent samples.

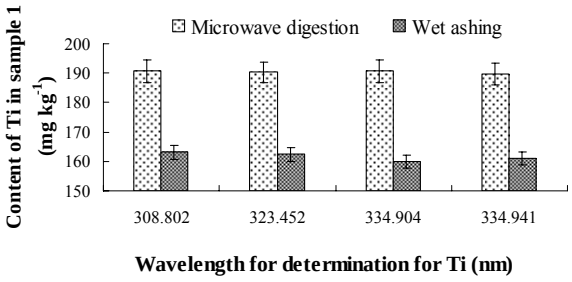



**Figure 1:** Effect of different digestion methods on determination of Ti in sample 1 (n=6)

## 4.2 Selection of acid mixtures for microwave digestion

Different mixtures of acids for the dissolution of composite films by microwave digestion were evaluated. According to previous experience and recent literature [21], the acids evaluated for microwave digestion were 6 mL of $HNO_3$ + 2 mL of $H_2O_2$ (procedure A), 6 mL of $HNO_3$ + 1.5 mL of $H_2O_2$ + 0.5 mL of HF (procedure B), 6 mL of $HNO_3$ + 2 mL of $H_2SO_4$ (procedure C) and 6 mL of $HNO_3$ + 1.5 mL of $H_2SO_4$ + 0.5 mL of HF (procedure D). The digestions were performed on sample 1 and the results are presented in Figure 2. The analysis of variance and multiple comparison studies indicated that procedure B gave a statistically higher digestion efficiency than the other procedures. In addition, $H_2SO_4$ was not recommended for digestion, when using ICP-MS for analysis, because of the molecular interferences of $^{32}S^{15}N$ and $^{32}S^{18}O$ on $^{47}Ti$ and $^{48}Ti$, respectively. Consequently, procedure B was used for digestion in subsequent experiments.

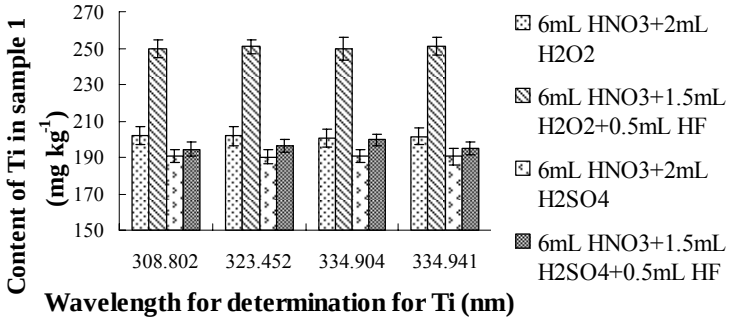



**Figure 2:** Effect of different mixtures of acids for microwave digestion on determination of Ti in sample 1 (n=6)

## 4.3 Matrix effects

Potential matrix effects were checked by analysing standard solutions diluted with 5% $HNO_3$ and spiked into digests of blank plastic film. Figure 3 shows the recoveries for Ti (analysed by ICP-AES, spike levels, 0.2, 0.5, 1.0 mg $L^{-1}$) in the pure solution and the plastic film matrix. There was no significant difference in the analytical values based on the paired t-test ($p=0.399>0.05$). Thus, it was concluded that there were no significant matrix effects.

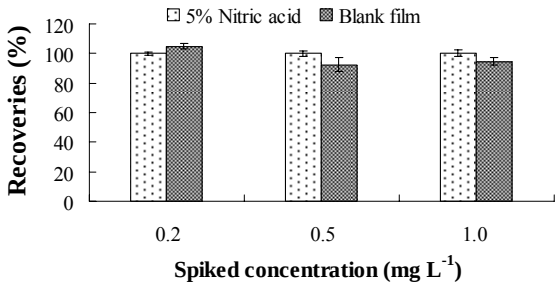



**Figure 3:** Effect of different matrices (5% $HNO_3$ and blank film) on recovery of Ti (n=3)

### 4.4 Comparison of ICP-AES and ICP-MS

ICP-AES and ICP-MS are often used for the determination of trace elements in diverse materials. In the present study, the performance of the two methods were compared in terms of analytical range, LOD, LOQ (Table 3), spike recovery (Table 4) and analysis of real samples (Table 5). The paired t-test ($p=0.124>0.05$) indicated that there was no significant difference in the two methods in terms of the analytical values. However, the LOD for ICP-MS (0.3 mg $kg^{-1}$) was significantly lower than that for ICP-AES (5.0 mg $kg^{-1}$). Given that in ongoing work, the migration of Ti from nano/submicro-plastic films to food simulants and diverse foodstuffs is under investigation, the more sensitive ICP-MS technique is preferred for trace and ultra-trace determinations of Ti.

## 5 Conclusion

Nano/submicro $TiO_2$-plastic films used for food packaging were subjected to microwave digestion and the Ti contents were determined by ICP-AES and ICP-MS. An acid mixture consisting of 6 mL of $HNO_3$ + 1.5 mL of $H_2O_2$ + 0.5 mL of HF gave the highest digestion efficiency for Ti. Spiking of blank samples resulted in high analyte recoveries and good precision and accuracy with respect to the determination of Ti in the composite films. Although both ICP methods were considered reliable, the LOD for ICP-MS was superior to ICP-AES, hence the former technique was preferred for trace/ultra-trace determinations of Ti in nano/submicro-plastic food packaging.

## Acknowledgements

We would like to thank the National Natural Science Foundation of China (21277085 and 21277061), the National Science and Technology Support Program (2011BAK10B05-03) and the Science and Technology Research Project of Shanxi Province (20120313030-3) for supporting this research.

## References

1. T.V. Duncan. 2011, “Applications of nanotechnology in food packaging and food safety: Barrier materials, antimicrobials and sensors”, *Journal of Colloid and Interface Science*, vol. 363, no. 1, pp. 1-24.
2. W. Han. Y.J. Yu. N.T. Li and L.B. Wang. 2011, “Application and safety assessment for nano-composite materials in food packaging”, *Chinese Science Bull*, vol. 56, no. 12, pp. 1216-1225.
3. K. Tiede. A.B.A. Boxall. S.P. Tear. J. Lewis. H. David and M. Hassellov. 2008, “Detection and characterization of engineered nanoparticles in food and the environment”, *Food Additives and Contaminants*, vol. 25, no. 7, pp. 795-821.
4. C.H. Kwon. J.H. Kim. I.S. Jung. H. Shin and K.H. Yoon. 2003, “Preparation and characterization of

$TiO_2$–$SiO_2$ nano-composite thin films", *Ceramics International*, vol. 29, no. 8, pp. 851-856.

5. N. Venkatachalam. M. Palanichamy and V. Murugesan. 2007, "Sol-gel preparation and characterization of nanosize $TiO_2$: Its photocatalytic performance", *Materials Chemistry and Physics*, vol. 104, no. 2-3, pp. 454-459.
6. L. Calzolai. D. Gilliland and F. Rossi. 2012, "Measuring nanopartices size distribution in food and consumer products a review", *Food Additives and Contaminants*, vol. 29, no. 8, pp. 1183-1193.
7. H. Onoda and T. Yamaguchi. 2013, "Preparation of titanium phosphates with additives in hydrothermal process and their powder properties for cosmetics", *International Journal of Cosmetic Science*, vol. 35, no. 2, pp. 196-200.
8. B. Ferreira Da Silva. S. Perez. P. Gardinalli. R.K. Singhal. A.A. Mozeto and D. Barcelo. 2011, "Analytical chemistry of metallic nanoparticles in natural environments", *Trac-Trends in Analytical Chemistry*, vol. 30, no. 3, pp. 528-540.
9. A.P.D.A. David and M.C.I. José. 2010, "Mass transport studies of different additives in polyamide and exfoliated nanocomposite polyamide films for food industry", *Packaging Technology and Science*, vol. 23, pp. 59-68.
10. A. Llorens. E. Lloret. P.A. Picouet. R. Trbojevich and A. Fernandez. 2011, "Metallic-based micro and nanocomposites in food contact materials and active food packaging" , *Trends in Food Science and Technology*, vol. 24, no. 1, pp. 1-11.
11. N.B. Hatzigrigoriou and C.D. Papaspyrides. 2011, "Nanotechnology in plastic food-contact materials", *Journal of Applied Polymer Science*, vol. 122, no. 6, pp. 3720-3739.
12. C. Silvestre. D. Duraccio. S. Cimmino. 2011, "Food packaging based on polymer nanomaterials", *Progress in Polymer Science*, vol. 36, no. 12, pp. 1766-1782.
13. H. Stamm. N. Gibson and E. Anklam. 2012, "Detection of nanomaterials in food and consumer products: bridging the gap from legislation to enforcement", *Food Additives and Contaminants*, vol. **29, no.** 8, pp. 1175-1182.
14. Q. Chaudhry. M. Scotter. J. Blackburn. B. Ross. A. Boxall. L. Castle. R. Aitken and R. Watkins. 2008, "Applications and implications of nanotechnologies for the food sector", *Food Additives and Contaminants*, vol. 25, no. 3, pp. 241-258.
15. I.G. Becerril-Juárez. R.A. Morales-Luckie. F. Ureña-Nuñez. J.A. Arenas-Alatorre. J.P. Hinestroza and V. Sánchez-Mendieta. 2012, "Silver micro-, submicro- and nano-crystals using bovine bone as template. Formation of a silver/bovine bone composite", *Materials Letters,* vol. 85, pp. 157-160.
16. M. Avella. J.J. De Vlieger. M.E. Errico. S. Fischer. P. Vacca and M.G. Volpe. 2005, "Biodegradable starch/clay nanocomposite films for food packaging applications", *Food Chemistry*, vol. 93, no. 3, pp. 467-474.
17. G.X. Li. H.N. Song. Y.C. Zhang and Y.S. Liu. 2011, "Preparation of nano-kaolin/PE and its application to food packaging film", *Modern Plastics Progressing and Applications*, vol. 23, no. 4, pp. 34-37.
18. T. Abdiryim. A. Ubul. R. Jamal. Y.C. Tian. T. Awut and I. Nurulla. 2012, "Solid-state synthesis and

characterization of polyaniline/nano-$TiO_2$ composite", *Journal of Applied Polymer Science*, vol. 126, no. 2, pp. 697-705.

19. Q.B. Lin. B. Li and H. Song. 2011, "Determination of silver in nano-plastic food packaging by microwave digestion coupled with inductively coupled plasma atomic emission spectrometry or inductively coupled plasma mass spectrometry", *Food Additives and Contaminants,* vol. 28, no. 8, pp. 1123-1128.

20. H. Song. B. Li and Q.B. Lin. 2011, "Migration of silver from nano-plastic food packaging to food simulants", *Food Additives and Contaminants*, vol. 28, no. 12, pp. 1758-1762.

21. B.J. Shaw. C.S. Ramsden. A. Turner and R.D. Handy. 2013, "A simplified method for determining titanium from $TiO_2$ nanoparticles in fish tissue with a concomitant multi-element analysis", *Chemosphere,* vol. **92,** no. 9, pp. 1136-1144.

22. V. Sandroni and C.M.M. Smith. 2002, "Microwave digestion of sludge, soil and sediment samples for metal analysis by inductively coupled plasma-atomic emission spectrometry", *Analytical Chimica Acta*, vol. 468, pp. 335-344.

23. D. Beltrami. D. Calestani. M. Maffini. M. Suman. B. Melegari. A. Zappettini. L. Zanotti. U. Casellato. M. Careri and A. Mangia. 2011, "Development of a combined SEM and ICP-MS approach for the qualitative and quantitative analyses of metal microparticles and sub-microparticles in food products". *Analytical and Bioanalytical Chemistry*, vol. 401, no. 4, pp. 1401-1409.

# Determination of Four Types of Hazardous Chemicals in Food Contact Materials by UHPLC-MS/MS

**Qin-Bao Lin[1, 2*], Long-Fei Cai[2], Shao-Jing Wu[3], Xi Yang[3], Zhi-Nan Chen[3], Song-Hua Zhou[2], Zhi-Wei Wang[1]**

[1] *Key Laboratory of Product Packaging and Logistics, Institute of Packaging Engineering, Jinan University, Zhuhai 519070, China*
[2] *College of Life Science, Shanxi University, Taiyuan 030006, China*
[3] *Shenzhen Border Inspection and Quarantine Bureau, Shenzhen, 518010, China*

[*] *Corresponding author. Email: tlinqb@jnu.edu.cn*

**Abstract:** A simple ultrahigh-performance liquid chromatography-tandem mass spectrometric (UHPLC-MS/MS) method for the identification and quantification of two photoinitiators: 4-methylbenzophenone and 2-ethylhexyl-4-dimethylamino benzoate; nine plasticizers including di(2-ethylhexyl) adipate and diisobutyl adipate; three primary aromatic amines: 4-aminobiphenyl, 4-amino-2',3-dimethylazobenzene and bis-(4-aminophenyl) methane; and six bisphenols: bisphenol F diglycidyl ether, bisphenol A diglycidyl ether, bisphenol A (BPA), bisphenol B (BPB), bisphenol E (BPE) and bisphenol F (BPF) in food contact materials has been developed. The chromatographic conditions, pretreatment methods and matrix effects were studied and optimised. For determination of the four bisphenols, BPA, BPB, BPE and BPF, the UHPLC method employed a mobile phase of aqueous ammonia and methanol in binary gradient mode and measurement was based on a triple quadrupole mass spectrometer equipped with an electrospray ionisation (ESI) source operating in negative ion mode. The remaining chemicals were determined using the ESI source in positive ion mode and using the $[M+NH_4]^+$ or $[M+H]^+$ adducts as precursor ions for tandem mass spectrometry. The calibration graphs were linear with correlation coefficients of $\geq 0.995$. Detection limits for the method were in the range of 1–16 μg $kg^{-1}$. Analyte recoveries were in the range of 70–114% and relative standard deviations (RSDs) were 1–14%. Under optimised conditions, the chromatographic separation was performed in 12 min. The validation data indicated that the method was effective for the determination of the four classes of hazardous chemicals in plastic packaging materials or in can lacquers. The optimised method was successfully applied to trace analysis of commercially available food contact materials.

Keywords: food contact materials, composite plastic packaging, cans, ultrahigh-performance liquid chromatography-tandem mass spectrometry, photoinitiators, plasticizers, primary aromatic amines, bisphenols.

## 1 Introduction

With increasing concern on food contamination, the safety of food packaging has attracted considerable attention in recent years. Among the various types of food packaging, plastic products and canned packaging are of particular interest. Plastic products that originate from synthetic resins, as raw material, contain numerous additives including plasticizers, photoinitiators, stabilisers and antioxidants.

Photoinitiators are widely used in printing the external labels of packaging products. Benzophenone-based derivatives, as photoinitiators for ultraviolet-cured inks, have gradually replaced the traditional volatile solvent-based inks because of their strong adhesive properties, low organic solvent residue, low toxicity and low environmental pollution [1]. The photoinitiators, however, are not always completely used or eliminated after the printing process. It has been reported that, 4-methylbenzophenone (MBP), a low-molecular-weight photoinitiator, which is applied on the external surface of food packaging material, might permeate through the printed material and migrate into the food product [2]. The carcinogenicity, reproductive toxicity and skin contact toxicity of MBP were demonstrated in animal testing by [3]. The tolerable daily intake for MBP is 0.01 mg $kg^{-1}$ body weight [4]. Current methods to detect benzophenone-based derivatives are mainly based on GC-MS and high-performance liquid chromatography (HPLC) [1, 4], electrochemical analysis and micellar electrokinetic capillary chromatography [4].

Plasticizers, which are used to improve the flexibility and workability of polymeric materials, are very ubiquitous and can be found in many industrial products such as toys, food packaging, shower curtains, adhesives, detergents and shampoo [5]. Among them, di(2-ethylhexyl) adipate (DEHA) is the most widely used plasticizer in the plastics field owing to its low cost. Because of its noncovalent interaction with plastics, DEHA

readily penetrates the environment and biota including humans [6, 7]. Some studies have indicated that adipates could interfere with hormone secretions and cause deformities, cancer and mutation if they are allowed to accumulate in the body over the long term [8]. Methods for rapid determination of adipate-based plasticizers in packaging products, based on GC-FID [8] and GC-MS [9], have been reported.

Primary aromatic amines (PAAs) are potentially hazardous substances. The presence of PAAs in food contact materials is strictly prohibited by the European Union (EU). Azo colorants are important and widely used as intermediates in the chemical industry and they have been extensively used with some plastics for producing colored material for use in textiles, leathers and food contact materials [10]. Along with azo colorants, PAAs will be decomposed by reaction with residual aromatic isocyanates and hence be in direct contact with food. To the best of our knowledge, detection methods for PAAs are mainly concerned with dye products, so there is an urgent need to develop new methods for the identification and quantification of PAAs in food packaging products. Moreover, the use of UHPLC-MS/MS for such an application has not been reported.

Epoxy-based lacquer materials, which have excellent flexibility, chemical resistance and adhesion, are commonly used for coating the inside of food cans, large storage vessels and food containers to reduce food spoilage and to prevent degradation of the food can [11]. Among these compounds, epoxy-phenolic resin and vinyl resin are the most common. The former coating is mainly derived from BPA and BADGE [12], whereas the latter requires BFDGE and BADGE during its production to neutralise and solidify the hydrochloric acid generated by the reaction to avoid decomposition of the coating. BFDGE is prepared by the condensation of BPF and epichlorohydrin. Owing to the stringent restrictions on the use of BPA, as an alternative, BPE and BPB can be used to produce the resin coating layer [13, 14]. These lacquers are epoxy phenolic resins based on the polymerisation products of bisphenols: BFDGE, BADGE, BPA, BPB, BPE and BPF. If the chemical reaction in the production process of the coating is not complete and the cross linking of materials is not sufficient, residues of bisphenols may form. In addition, the coatings can release the bisphenols, as well as oligomers, which can migrate into the packaged foods during processing, sterilization, jolting during transportation and storage [15, 16]. Such compounds, which can enter the human body through the food chain, may affect human health.

Various methods have been described for the determination of bisphenols in different foods including GC-MS with stir bar sorptive extraction [17, 18] or with liquid-liquid extraction [19], HPLC with liquid-liquid microextraction [20, 21, 22], liquid chromatography coupled to multiple-stage mass spectrometry ($LC/MS^n$) [23], UHPLC-MS with ultrasonic solid-liquid extraction [11, 25], LC-MS/MS based on adducts [24, 26, 27] or with pressurised liquid extraction [28], HPLC-FD [29] and HPLC-UV [30]. However, the GC method would seem to have limited use in the case of BPA, BADGE and BFDGE because of their low volatility [17, 18]. Without an effective barrier, the potentially toxic chemicals could permeate through the packaging materials and migrate to the surrounding media, especially for plasticizers, which can readily diffuse into foods of high fat content and bisphenols, which are known to migrate into canned food when adverse conditions apply [31]. On account of these reasons, the maximum total migration limit for food packaging printing ink in the case of MBP was set at 0.6 mg $kg^{-1}$ by the European Standing Committee of Food Chain and Animal Health (SCFCAH) [32]. The specific migration limit (SML) set by the European Commission for aromatic amines is 0.01 mg $kg^{-1}$ and for DEHA is 18 mg $kg^{-1}$ [33]. The EU has established legislation concerning the SML for BADGE and related compounds in foods [34]. Regarding legislation, the EU has set a maximum SML of 9 mg $kg^{-1}$ for the sum of BADGE. The SML for BPA is 0.6 mg $kg^{-1}$ [20, 35]. The presence of BFDGE in food packaging products has been prohibited since 2005 [26]. Recently, the French Parliament has decreed that the presence of BPA in any food containers will be banned from 1 January 2014 [20].

To control the presence of hazardous chemicals in food contact materials, more rapid and efficient monitoring methods are required. The accuracy and efficiency of detection of hazardous chemicals in food contact materials are particularly important. The objective of this study is to develop a reliable and robust UHPLC-(ESI) MS/MS method for the detection of six bisphenols, nine plasticizers, two photoinitiators and three PAAs, which are in widespread use in canned and plastic food packaging products.

## 2 Materials and Methods

### 2.1 Instrumentation

A Waters Acquity UPLC-MS/MS system (Waters, Milford, PA, USA) equipped with a Turbo Ion Spray electrospray ionisation (ESI) source and triple quadrupole were employed. Waters MassLynx 4.1 software featuring the Quanlynx program was used for data processing. A Waters Acquity UPLC BEH C18 column (50 mm × 2.1 mm i.d., 1.7 µm particle size) was used for separations. Elution was carried out in binary gradient mode. Other equipment used during the experimental procedures included an XW-80A vortex shaker (Troody Technology Co., Ltd, Shanghai, China) and a nitrogen stream evaporator (Zymark Turbo Vap LV; Caliper Co.,

Ltd, USA). A fridge (BCD-206TS) for sample storage was supplied by Haier Co., Ltd (Qingdao, China). An ultrasonic bath (AS10200BT; Tianjin Autoscience Instrument Co., Ltd. Tianjin, China), a rotary evaporator (Hei-VAP, Heidolph, Germany) and a Milli-Q water system (Millipore, Billerica, MA, USA) were used in a sample preparation. Pipettes (10–100 µL, 100–1000 µL, Eppendorf Co., Ltd. Eppendorf, Germany) were used for sample dilution. Millipore filter apparatus (Millipore) and filters of 0.45 µm pore size were used for pretreatment of the mobile phase.

## 2.2 Reagents

Ethyl acetate (HPLC grade, >99.9%, CAS No. 141-78-6) was purchased from the Tedia Company Inc. Co., Ltd. (Fairfield, Connecticut, USA). Methanol (LC-MS grade, >99.9%, CAS No. 67-56-1) was purchased from Oceanpak Alexative Chemical Co., Ltd. (Goteborg, Sweden). Acetonitrile (HPLC grade, >99.9%, CAS No. 75-05-8), dichloromethane (HPLC grade, >99.9%, CAS No. 75-09-2) and tert-butyl methyl ether (HPLC grade, >99.9%, CAS No. 1634-04-4) were purchased from Shanghai Anpel Scientific Instrument Co., Ltd. (Shanghai, China). Ammonium acetate (A. R., ≥98.0%, CAS No. 631-61-8), ammonia solution (25%, A. R., CAS No. 1336-21-6) and formic acid (HPLC grade, >99.9%, CAS No. 64-18-6) were supplied by Xi Long Chemical Co., Ltd. (Shantou, Guangdong, China).

## 2.3 Standards and samples

The sources and detailed information of studied chemicals are presented in Table 1. Individual stock solutions, prepared by dissolving 10 mg of each compound in 10 mL of methanol, were stored in brown glass-stoppered bottles at 4 C. Standard solutions, at various concentrations, were prepared on a daily basis by appropriate dilution of the stock solution with methanol. The samples investigated were three ink-printed plastic composite bags (area ~600cm$^2$) including two OPP/CPP composite films (plastic 1, plastic 2), one PET/VMCPP composite film (plastic 3), one PVC cling film (plastic 4) and three lacquered tin plate cans (can 5, can 6, can 7; volumes ~300, 450 and 1200 mL, respectively). Plastic 1 and plastic 2 were made by the Noodle House Industrial Co., Ltd. (Hong Kong, China); plastic 3 and plastic 4 were purchased at a local foodstuff factory (Hong Kong, China); cans 5, 6 and 7 were purchased from the Kai Bo Food Supermarket (Hong Kong, China), the Tien Chu Co., Ltd (Hong Kong, China) and the Dongguan Wing Wash Cake Shop Ltd (Dongguan, Guangdong, China), respectively.

**Table 1:** Detailed Information of 20 Studied Chemicals.

| Standards Type | Abbreviation | Chemical Name | Mw[a] | CAS No. | SML[b]/ (mg kg$^{-1}$) | Source |
|---|---|---|---|---|---|---|
| Photoinitiator | MBP | 4-methylbenzophenone | 196.24 | 134-84-9 | 0.60 | J & K Chemical, Ltd. (Beijing, China) |
| | EHDAB | 2-Ethylhexyl-4-dimethylamino-benzoate | 276.40 | 21245-02-3 | - | AccuStandard, Inc. (New Haven, USA) |
| Plasticizer | DEHA | Di(2-ethylhexyl) adipate | 370.57 | 103-23-1 | 18.00 | Pure Chemical Analysis Co., Ltd. (Boenew, Belgium) |
| | DIBA | Diisobutyl adipate | 258.35 | 141-04-8 | - | |
| | DEA | Diethyl adipate | 202.25 | 141-28-6 | - | |
| | BBOEA | Bis(2-butoxyethyl) adipate | 346.46 | 141-18-4 | - | |
| | DBA | Dibutyl adipate | 258.35 | 105-99-7 | - | |
| | DIDA | Diisodecyl adipate | 426.67 | 27178-16-1 | - | |
| | DNA | Dinonyl adipate | 398.62 | 151-32-6 | - | |
| | DOA | Dioctyll adipate | 370.57 | 123-79-5 | - | |
| | BBPA | Bis(1-butylpentyl) adipate | 398.62 | 77916-77-9 | - | Fluka Cheme GmbH, Buchs Sigma-Aldrich (Augsburg, Germany) |
| Primary Aromatic Amines | 4-ABP | 4-Aminobiphenyl | 169.22 | 92-67-1 | 0.01 | Dr. Ehrenstorfer GmbH (Augsburg, Germany) |
| | ADEAB | 4-Amino-2',3-dimethylazobenzene | 225.30 | 97-56-3 | 0.01 | |
| | BAPM | Bis-(4-aminophenyl) methane | 198.26 | 101-77-9 | 0.01 | |
| Bisphenols | BFDGE | Bisphenol F diglycidyl ether | 321.40 | 2095-03-6 | 0.00 | Dr. Ehrenstorfer GmbH (Augsburg, Germany) |
| | BADGE | Bisphenol A diglycidyl ether | 340.41 | 1675-54-3 | 9.00 | |
| | BPA | Bisphenol A | 228.29 | 80-05-7 | 0.60 | AccuStandard Inc. (USA) |
| | BPB | Bisphenol B | 242.31 | 77-40-7 | - | |
| | BPE | Bisphenol E | 214.26 | 2081-08-5 | - | Tokyo Chemical Industry Co., Ltd. (Tokyo, Japan) |
| | BPF | Bisphenol F | 200.23 | 620-92-8 | - | AccuStandard Inc. (USA) |

[a] Molecular Weight.

[b] SML: Specific Migration Limit which allowed by Commission Directives 2011/EC.
- No SML allowed by Commission Directives 2011/EC.

## 2.4 Chromatographic Conditions

Column temperature was kept at 35 °C, and the injection volume was 2 µL for mixed standards and samples. The mobile phase in $ESI^+$ mode was 0.1 % formic acid in 5 mM ammonium acetate solution (A) and methanol (B). Before analysis, the column was conditioned for 15 min with A:B (70:30) to obtain a stable baseline. Separation of the 20 hazardous chemicals was carried out on an Acquity UPLC BEH C18 column using gradient elution. The binary gradient program employed in $ESI^+$ mode was the following: 0–1 min, 30 % B; 1–2 min, 30–70 % B; 2–2.5 min, 70 % B was maintained; 2.5–3.5 min, 70–75 % B; 3.5–5 min, 75 % B was maintained; 5–6 min, 75–90 % B; 6-7 min, 90 % B was maintained; 7–7.5 min, 90–95 % B; 7.5–9 min, 95 % B was maintained; 9–11 min, 95–30 % B; 11–12 min, 30 % B was maintained. The flow rate of the mobile phase was 0.2 mL $min^{-1}$. The mobile phase in $ESI^-$ mode was 0.2 % Ammonia solution (A) and methanol (B). The binary gradient program employed in $ESI^-$ mode was the following: 0–0.5 min, 30 % B; 0.5–2 min, 30–70 % B; 2–3.5 min, 70 % B was maintained; 3.5–5 min, 70–30 % B. The flow rate of the mobile phase was 0.2 mL $min^{-1}$.

## 2.5 Mass spectrometry

Mass spectrometry data were acquired and processed using MassLynx 4.1 software. Analytes were detected in multiple reaction monitoring mode (MRM) using ESI in positive or negative ion mode and using a single chromatographic run per sample. Two reaction fragmentations were scanned for each analyte. The MS source parameters were as follows: ion source temperature 120 °C, desolvation temperature 350 °C, desolvation flow rate 750 L $h^{-1}$, cone gas flow rate 50 L $h^{-1}$ and capillary voltage 3.2 kV. The gas used for the mass spectrometer was high purity (99.99 %) nitrogen. Argon was used as collision gas at 1.5 mtorr and the optimum cone voltage (V) and collision energy (eV) selected for each transition are indicated in Table 2.

**Table 2:** Tandem mass spectrometry transitions for MRM.

| Standards Type | Abbreviation | Precursor ion (m/z) | Quantitation Product ions*(m/z) | Cone (V) | Collision (eV) |
|---|---|---|---|---|---|
| Photoinitiator | MBP | 197.0[a] | 105.1; 119.2 | 30 | 15; 15 |
| | EHDAB | 278.3[a] | 150.9; 165.9 | 40 | 30; 20 |
| Plasticizer | DEHA | 388.5[b] | 147.0; 129.2 | 15 | 15; 20 |
| | DIBA | 276.2[b] | 185.2; 129.0 | 15 | 15; 15 |
| | DEA | 220.2[b] | 157.1; 111.0 | 15 | 10; 20 |
| | BBOEA | 364.1[b] | 155.3; 210.9 | 20 | 20; 15 |
| | DBA | 276.2[b] | 185.0; 129.1 | 15 | 10; 15 |
| | DIDA | 427.5[b] | 129.2; 269.1 | 37 | 15; 10 |
| | DNA | 4146.[b] | 255.2; 129.0 | 16 | 15; 15 |
| | DOA | 388.5[b] | 241.2; 128.9 | 17 | 13; 17 |
| | BBPA | 416.4[b] | 147.2; 129. | 13 | 15; 15 |
| Primary Aromatic Amines | 4-ABP | 170.1[a] | 152.2; 127.1 | 35 | 25; 25 |
| | ADEAB | 226.2[a] | 91.0; 121.0 | 34 | 23; 27 |
| | BAPM | 199.1[a] | 105.9; 78.2 | 35 | 25; 25 |
| Bisphenols | BFDGE | 330.3[b] | 163.1; 133.0 | 27 | 15; 15 |
| | BADGE | 358.4[b] | 191.2; 135.2 | 28 | 15; 30 |
| | BPA | 227.2[c] | 211.3; 133.1 | 45 | 20; 20 |
| | BPB | 241.1[c] | 212.2; 226.1 | 38 | 20; 20 |
| | BPE | 213.1[c] | 198.1; 119.0 | 40 | 20; 20 |
| | BPF | 199.1[c] | 93.0; 105.1 | 39 | 20; 20 |

[*] The first ion indicated for each analyte was employed for quantification purposes while the second ion was used for confirmation.
[a] the $[M+H]^+$ adduct as precursor ion; [b] the$[M+NH_4]^+$ adduct as precursor ion; [c] the $[M-H]^-$ adduct as precursor ion.

## 2.6 Sample preparation

Four plastic composite bags and three metal cans were processed using sample treatment procedures described

below.

*Plastic food packaging*

A specimen of each sample was cut into small pieces of approximately 1 $cm^2$, accurately weighed (0.500 g), then placed in a glass bottle (50 mL), soaked in 15 mL of tert-butyl methyl and then ultrasonically extracted (Frequency: 40 KHz; Power: 300 W; 30 °C) for 20 min. The extract was collected in a 100-mL round-bottom flask and the residue was taken up in 5 mL of tert-butyl methyl, this step being repeated three times. The extraction procedure was performed twice and the total combined extract was evaporated to near dryness at 40 °C with a rotary evaporator. The residue was dissolved in methanol and the solution made up to 10 mL. Finally, 1 mL of the solution was passed through a 0.45-µm nylon membrane filter prior to analysis by UHPLC-MS/MS.

*Cans*

Three hundred milliliters of tert-butyl methyl ether was poured into the metal can (can 5, 300 mL) and sealed with aluminum foil, then ultrasonically extracted (frequency: 40 KHz; power: 300 W; 30 °C) for 20 min. Thirty milliliters of the extract was taken and evaporated to near dryness at 40 °C with a rotary evaporator. The remaining steps for sample processing were as described above for the plastic food packaging.

### 2.7 Statistical analysis

Statistical analyses were carried out using Minitab 15.0 (Minitab Inc., State College, PA, USA) and Statistical Product and Service Solutions (SPSS) 13.0 (IBM SPSS Inc., New York, NY, USA) analytical software. $P<0.05$ was identified as being statistically significant at the 95% confidence level.

## 3 Results

### 3.1 Method validation

Validation of the method for the determination of 20 hazardous chemicals in the food packaging materials, involved establishing performance parameters including limit of detection (LOD), limit of quantitation (LOQ), linearity, recovery and repeatability.

*Linearity, LOD and LOQ*

Standard solutions (50, 100, 200, 500 and 1000 µg $L^{-1}$) were obtained by diluting stock standard solutions (10 mg $L^{-1}$) with methanol. LOD and LOQ values corresponded to three and ten times the standard deviation of the signal for blank measurements, respectively. Typically, the values were calculated based on ten determinations of the blank samples. In this study, dilute standard solutions of the analytes were injected until the signal responses coincided with three or ten times the standard deviation of the apparent concentrations of the blanks. Analyte responses were linear over the concentration ranges tested and equations for lines of best fit, correlation coefficients, LODs and LOQ are shown in Table 3.

**Table 3:** The Retention Time, Linearity Equation, Correlation Coefficient, LOD, and LOQ of 20 Chemicals (n=6).

| Standards Type | Abbreviation | Retention Time ±SD(min) | Linearity Range: 50-1000 µg $L^{-1}$ | | Correlation Coefficient/$R^2$ | $LOD^I$, $LOD^M$ (µg $L^{-1}$, µg $kg^{-1}$) | $LOQ^I$, $LOQ^M$ (µg $L^{-1}$, µg $kg^{-1}$) |
|---|---|---|---|---|---|---|---|
| | | | Slope ±SD | Intercept ±SD | | | |
| Photoinitiator | MBP | 4.17±0.005 | 166.71±1.80 | -912.71±52 | 0.9995 | 3.0, 6.0 | 10.0, 20.0 |
| | EHDAB | 7.31±0.008 | 464.53±2.76 | 1738.12±127 | 0.9992 | 0.5, 1.0 | 2.0, 5.0 |
| Plasticizer | DEHA | 8.74±0.008 | 106.44±1.15 | 2330.94±194 | 0.9979 | 1.0, 2.0 | 4.0, 7.0 |
| | DIBA | 5.25±0.005 | 71.50±0.60 | 134.57±13 | 0.9954 | 1.0, 2.0 | 4.0, 7.0 |
| | DEA | 3.30±0.002 | 92.02±0.83 | 1134.82±76 | 0.9979 | 1.0, 2.0 | 4.0, 7.0 |
| | BBOEA | 4.99±0.005 | 124.57±0.80 | 338.39±28 | 0.9996 | 2.0, 5.0 | 7.0, 20.0 |
| | DBA | 5.39±0.010 | 171.29±1.60 | 1104.83±45 | 0.9981 | 0.8, 2.0 | 3.5, 7.0 |
| | DIDA | 9.87±0.017 | 124.88±0.89 | -152.25±11 | 0.9996 | 8.0, 16.0 | 25.0, 45.0 |
| | DNA | 9.68±0.017 | 123.46±0.91 | 5.64±0.18 | 0.9995 | 0.8, 2.0 | 3.5, 7.0 |
| | DOA | 8.97±0.011 | 139.39±1.10 | 368.12±42 | 0.9979 | 2.0, 5.0 | 7.0, 20.0 |
| | BBPA | 9.17±0.015 | 277.41±1.40 | 1226.26±119 | 0.9989 | 2.0, 5.0 | 7.0, 20.0 |
| Primary | 4-ABP | 3.12±0.006 | 50.85±0.53 | -107.17±17 | 0.9995 | 1.5, 3.0 | 5.0, 10.0 |

| | | | | | | | |
|---|---|---|---|---|---|---|---|
| Aromatic Amines | ADEAB | 4.59±0.001 | 153.09±1.00 | 1558.53±154 | 0.9979 | 1.0, 2.0 | 4.0, 7.0 |
| | BAPM | 0.88±0.004 | 87.81±0.39 | -783.41±70 | 0.9990 | 2.0, 5.0 | 7.0, 20.0 |
| Bisphenols | BFDGE | 3.82±0.001 | 28.35±0.63 | -253.77±34 | 0.9978 | 5.0, 10.0 | 15.0, 35.0 |
| | BADGE | 4.32±0.001 | 28.10±0.47 | -283.17±21 | 0.9977 | 8.0, 16.0 | 25.0, 45.0 |
| | BPA | 3.01±0.005 | 2.16±0.09 | 41.39±3.8 | 0.9988 | 1.0, 2.0 | 4.0, 7.0 |
| | BPB | 3.29±0.004 | 2.89±0.12 | 48.85±4.3 | 0.9983 | 1.5, 3.0 | 6.0, 10.0 |
| | BPE | 2.83±0.004 | 4.04±0.11 | 87.57±5.7 | 0.9982 | 1.0, 2.0 | 4.0, 7.0 |
| | BPF | 2.60±0.004 | 1.87±0.09 | 27.16±1.4 | 0.9986 | 1.0, 2.0 | 4.0, 7.0 |

$LOD^I$, $LOD^M$: the LOD of the instrument and the LOD of the method; $LOQ^I$, $LOQ^M$: the LOQ of the instrument and the LOQ of the method.

*Analyte recoveries and method repeatability*

The accuracy of the method was estimated through recovery studies. The repeatability of the method was verified by spiking the processed samples for each packaging material with standard solutions containing the two analytes at three concentration levels (50, 100, 200 µg $kg^{-1}$). The spiking procedure was performed six times. The analyte recoveries were in the range of 70–114 % and the RSDs were in the range of 1–14 % (Table 4). These results indicated that the developed method was fit for purpose and reliable.

**Table 4:** The Recoveries and RSDs of 20 chemicals with 3 spiked concentrations 50, 100, 200 µg L-1 (n=6).

| Standards Type | Abbreviation | Recoveries (RSD) /% | | |
|---|---|---|---|---|
| | | 50 µg $L^{-1}$ | 100 µg $L^{-1}$ | 200 µg $L^{-1}$ |
| Photoinitiator | MBP | 98(3) | 111(3) | 89(3) |
| | EHDAB | 99(4) | 105(1) | 100(4) |
| Plasticizer | DEHA | 114(5) | 103(3) | 97(5) |
| | DIBA | 92(6) | 103(5) | 100(1) |
| | DEA | 70(3) | 95(4) | 73(8) |
| | BBOEA | 101(4) | 111(2) | 103(2) |
| | DBA | 101(1) | 107(4) | 95(3) |
| | DIDA | 105(4) | 102(5) | 99(3) |
| | DNA | 104(3) | 108(2) | 96(3) |
| | DOA | 104(4) | 98(2) | 95(3) |
| | BBPA | 102(2) | 105(1) | 97(4) |
| Primary Aromatic Amines | 4-ABP | 96(1) | 105(6) | 99(4) |
| | ADEAB | 103(6) | 98(4) | 97(3) |
| | BAPM | 95(5) | 98(1) | 92(6) |
| Bisphenols | BFDGE | 101(14) | 105(3) | 93(4) |
| | BADGE | 98(10) | 94(5) | 91(8) |
| | BPA | 107(10) | 101(10) | 98(3) |
| | BPB | 111(6) | 110(7) | 100(2) |
| | BPE | 95(2) | 110(6) | 101(4) |
| | BPF | 104(5) | 99(5) | 101(2) |

## 3.2 Application

The developed method was applied to the analysis of four films and three canned materials used for food packaging. Table 5 lists the four types of additives detected in the samples. Taking into account the relatively large differences in chemical composition (e.g., PVC content) of the individual samples, sample dilution steps were necessary before analysis by UHPLC-MS/MS. The results indicated that DEHA in the food contact materials and BADGE in the canned materials were the predominant chemicals, respectively. The concentrations of DEHA were in the range of 0.010–45459 mg $kg^{-1}$ and that of BADGE were in the range of 0.410–45.811 mg $kg^{-1}$. BPA was present in the can lacquer at concentrations of 0.298–0.468 mg $kg^{-1}$.

**Table 5:** The concentration of 2 photoinitiators, 9 plasticizers, 3 primary aromatic amines and 6 Bisphenols in 4 plastic packaging and 3 metal cans (n=3).

| Standards Type | Abbreviation | Concentration of analytes in samples (Average±SD, mg $kg^{-1}$) | | | | | | |
|---|---|---|---|---|---|---|---|---|
| | | Plastic 1 (composite) | Plastic 2 (composite) | Plastic 3 (composite) | Plastic 4 (PVC film) | Tin can 5 | Tin can 6 | Tin can 7 |

| | | | | | | | | |
|---|---|---|---|---|---|---|---|---|
| Photoinitiator | MBP | n. d. | n. d. | n. d. | n. d. | 0.029±0.00 | 0.03±0.00 | n. d. |
| | EHDAB | n. d. | n. d. | n. d. | n. d. | n. d. | n. d. | n. d. |
| Plasticizer | DEHA | 1.83±0.52 | 0.60±0.16 | 19.27±0.20 | 45459.25±795.86 | 0.08±0.01 | 0.01±0.004 | 0.13±0.05 |
| | DIBA | n. d. | n. d. | n. d. | n. d. | n. d. | n. d. | n. d. |
| | DEA | n. d. | n. d. | n. d. | - | n. d. | n. d. | n. d. |
| | BBOEA | n. d. | n. d. | n. d. | n. d. | n. d. | n. d. | n. d. |
| | DBA | n. d. | n. d. | n. d. | n. d. | n. d. | n. d. | n. d. |
| | DIDA | n. d. | n. d. | n. d. | n. d. | n. d. | n. d. | n. d. |
| | DNA | n. d. | n. d. | n. d. | n. d. | n. d. | n. d. | n. d. |
| | DOA | n. d. | n. d. | n. d. | n. d. | n. d. | n. d. | n. d. |
| | BBPA | n. d. | n. d. | n. d. | n. d. | n. d. | n. d. | n. d. |
| Primary Aromatic Amines | 4-ABP | n. d. | n. d. | n. d. | n. d. | n. d. | n. d. | n. d. |
| | ADEAB | n. d. | n. d. | n. d. | n. d. | n. d. | n. d. | n. d. |
| | BAPM | - | n. d. | n. d. | n. d. | n. d. | n. d. | n. d. |
| Bisphenols | BFDGE | n. d. | n. d. | n. d. | n. d. | n. d. | n. d. | n. d. |
| | BADGE | 19.86±0.25 | 53.96±3.92 | n. d. | n. d. | 0.44±0.06 | 0.41±0.15 | 45.81±2.78 |
| | BPA | - | n. d. | n. d. | n. d. | 0.47±0.07 | 0.30±0.03 | 0.41±0.04 |
| | BPB | n. d. | n. d. | n. d. | n. d. | n. d. | n. d. | n. d. |
| | BPE | n. d. | n. d. | n. d. | n. d. | n. d. | n. d. | n. d. |
| | BPF | n. d. | n. d. | n. d. | n. d. | n. d. | n. d. | n. d. |

n. d.: not detected.
-: have detection but lower than LOQ of this method.

# 4 Discussion

## 4.1 Optimization of chromatographic separation

Various experiments were carried out to establish a suitable composition for the mobile phase. After multiple experiments, a mobile phase comprising 0.1 % formic acid in 5 mM ammonium acetate (A) and methanol (B) was selected as optimum. The use of this mobile phase produced the best response for the parent and product ions selected for ESI. Previously, it had been reported that 0.1% formic acid was beneficial for analyte ionisation [36]. The study also showed that MBP and PAAs readily underwent hydrogenation. In addition, excellent signal responses were obtained using the $[M+NH_4]^+$ adduct for BFDGE, BADGE and the plasticizers. In the case of the remaining bisphenols, experiments showed that a mobile phase containing ammonia could effectively increase the ionisation of hydrogen ions, thus the dehydrogenation mode was chosen. Other mobile phases were evaluated and included mixtures of acetonitrile-water in differing proportions. In these experiments very low analyte responses were obtained, probably owing to tthe fact that quasi-molecular clusters between the analyte and acetonitrile did not undergo efficient ionisation [26]. Therefore, the mobile phase selected for the optimization of chromatographic separation was 0.1 % formic acid in 5 mM ammonium acetate-methanol. This solution was similar to those used in other studies concerning the separation, characterisation and quantification of bisphenols [23, 26, 28]. Although there have been few reports in the literature, results for MBP, plasticizers and PAAs using the above mobile phase were also promising.

The gradient program was optimised to obtain an effective separation of all analytes and with good stability of retention times. As can be seen in Figure 1, employing the binary gradient as described in **Chromatographic Conditions**, effective separation of the 20 analytes was obtained in 12 min. For the bisphenols, however, signal strength was relatively low reflecting, as mentioned above, low ionisation efficiency for this class of compound. In the case of BFDGE, three peaks occurred in the MRM scan signifying the presence of three isoforms.

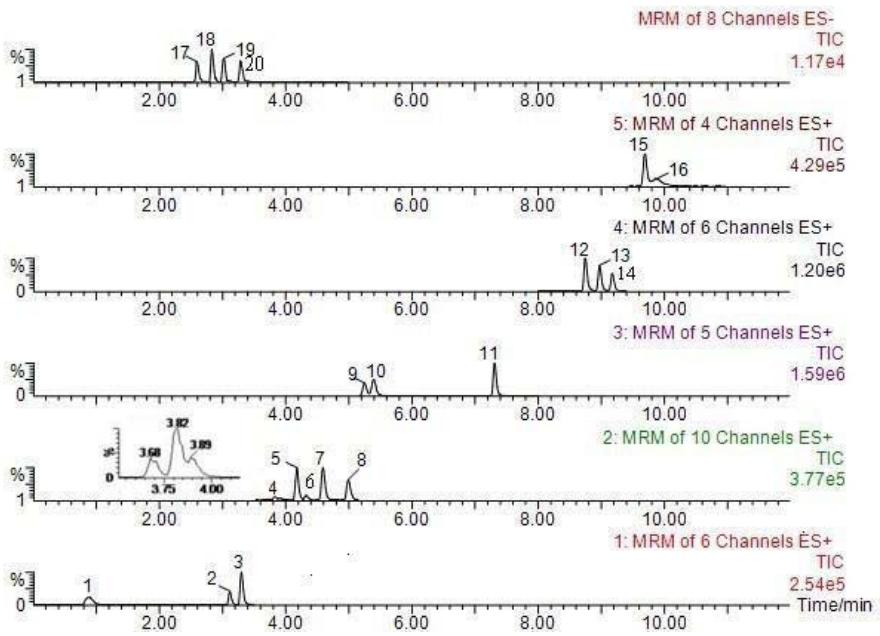



**Figure 1:** UHPLC-MS/MS chromatograms in MRM mode of the 20 studied hazardous chemicals (100 µg $L^{-1}$).

1: BAPM; 2: 4-ABP; 3: DEA; 4: BFDGE; 5: MBP; 6: BADGE; 7: ADEAB; 8: BBOEA; 9: DIBA; 10: DBA; 11: EHDAB; 12: DEHA; 13: DOA; 14: BBPA; 15: DNA; 16: DIDA; 17: BPF; 18: BPE; 19: BPA; 20: BPB.

## 4.2 Selection of extraction solvent

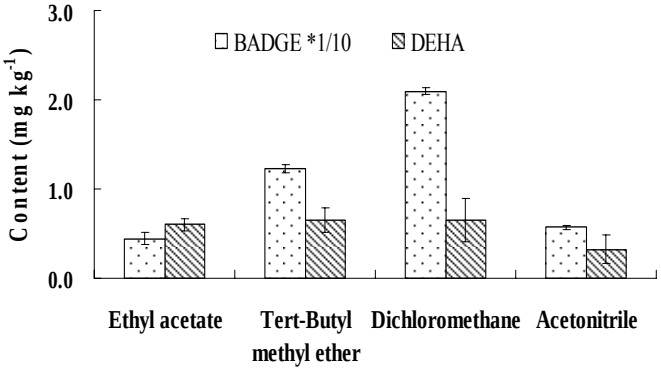



**Figure 2:** Effect of different extraction solvents on the determinated concentration of BADGE and DEHA in plastic 1 (n=3).

In this study, four solvents including ethyl acetate, tert-butyl methyl ether, dichloromethane and acetonitrile were compared to assess their extraction efficiency. The experiments were carried out on plastic composite bag 1 and the results are shown in Figure 2. Analysis of variance (ANOVA) was performed on the amounts of DEHA and BADGE extracted from bag 1 using the four solvents. In the case of BADGE, there was a statistically significant difference (p=0.000) in extraction efficiencies for the four extraction solvents, except acetonitrile and ethyl acetate (p=0.055) (Table 6). For DEHA, there was no significant difference between the extraction efficiencies for the four solvents (p>0.05). The results indicated that the extraction efficiency for dichloromethane was higher than that of the other solvents. However, given that tert-butyl methyl ether was relatively involatile during ultrasonic sample pretreatment and it yielded minimal matrix effects in UPLC-MS/MS, this compound was chosen as the extraction solvent in further studies.

**Table 6:** Analysis of variance (ANOVA) and multiple comparison performed on the extraction amount of BADGE and DEHA from plastic 1.

| Solvent A | Solvent B | P-value (BADGE) | P-value (DEHA) |
|---|---|---|---|

| | | | |
|---|---|---|---|
| Ethyl acetate | Tert-Butyl methyl ether | 0.000 | 0.981 |
| Ethyl acetate | Dichloromethane | 0.000 | 0.981 |
| Ethyl acetate | Acetonitrile | 0.055 | 0.305 |
| Tert-Butyl methyl ether | Dichloromethane | 0.000 | 0.998 |
| Tert-Butyl methyl ether | Acetonitrile | 0.000 | 0.186 |
| Dichloromethane | Acetonitrile | 0.000 | 0.185 |

### 4.3 Effect of solvent volume on extraction of plastic samples

The effect of different volumes of tert-butyl methyl ether (15×1 mL, 15×2 mL, 15×3 mL) on the amount extracted was examined. The experiments were carried out on plastic composite bag 1 and the results, shown in Figure 3, indicated that 15×2 mL of tert-butyl methyl ether was very effective for extraction of the target chemicals. Note that to aid the comparison of the results for BADGE and DEHA, the concentrations of BAGDE, as used in the experiments (Figures 2 and 3), were reduced tenfold.

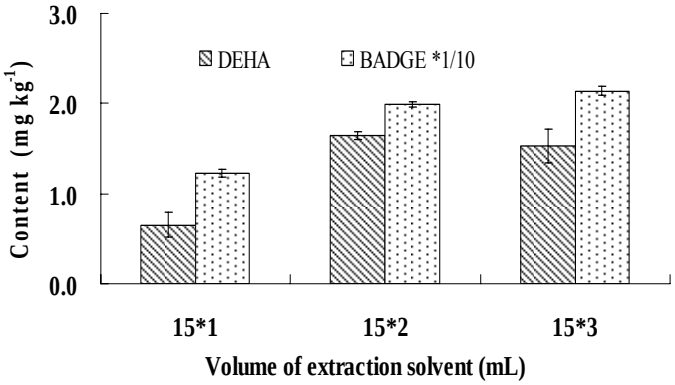



**Figure 3:** Effect of different volume of extracting solvents on the determinated concentration of BADGE and DEHA in plastic 1 (n=3).

### 4.4 Optimization of extraction procedure for cans

Six metal cans (can 5, 300 mL), which had not been in contact with food, were cleaned by Milli-Q water and dried. They were then divided into two groups. For the three cans of group 1, each of them was cut into pieces of approximately 1 $cm^2$, accurately weighed (5.000 g) and extracted with 15 mL of tert-butyl methyl ether, as described earlier for plastic packaging. For group 2, 300 mL of tert-butyl methyl ether was poured into the can (can 5, 300 mL), which was sealed with aluminum foil and then ultrasonically extracted (frequency: 40 KHz; power: 300 W; 30 °C) for 20 min. Thirty milliliters of the extract was then evaporated to near dryness at 40 °C by rotary evaporator. The remaining steps in sample preparation were as described above for the plastic packaging. According to the results, there was no significant difference in extraction amounts between the two groups, hence, for convenience, the procedure as used for group 2 was used in further studies.

### 4.5 Matrix effects

Matrix effects are a common problem in mass spectrometric analysis of organic samples. For the current study, the matrix effect was investigated by comparing the signal responses of the standards in pure solution and in the two matrices, i.e., plastic composite bag 1 and metal can 5. As representative chemicals, the responses for MBP, DEHA, DEA, 4-ABP, BAPM, BFDGE, BADGE and BPA in the pure solution and the matrices are presented in Figure 4. Note that BPA was only present in the lacquer of the metal can. DEHA, as the main plasticizer, exhibited a relatively high standard deviation, perhaps reflecting residual contamination arising during sample processing and analysis. A paired T-test was performed on the responses for the analytes in the matrices. At the 95% confidence level, the results revealed that the optimised method was free from matrix interferences in the case of MBP, DEA, BAPM, BFDGE, BADGE and BPA ($p>0.05$). At the same time, samples corresponding to the plastic composite bag 1 and metal can 5 had slightly weaker signal responses in the case of 4-ABP ($p=0.047<0.05$ for pure solution and plastic composite bag 1, $p=0.029<0.05$ for pure solution and metal can 5), and the response for DEHA was slightly lower for the metal can 5 ($p=0.024<0.05$ for pure solution and metal can 5).

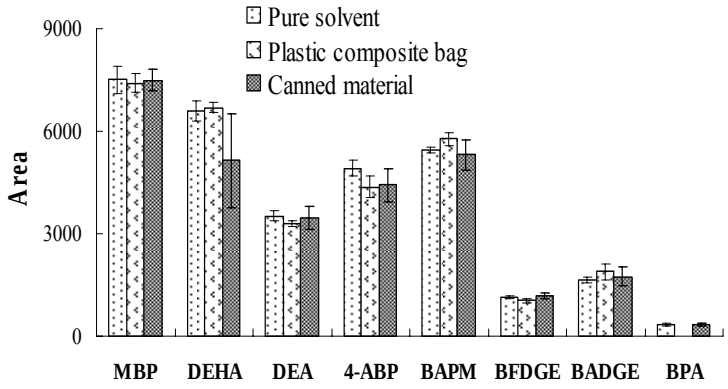



**Figure 4:** Comparision of the standards responses in pure solvent and in the matrix (n=3).

## 5 Conclusions

A UHPLC-MS/MS method has been developed for the identification and quantification of six bisphenols, nine plasticizers, two photoinitiators and three PAAs in food contact materials. The optimised method was validated in terms of analyte recoveries (range, 70–114%) and method reproducibility (RSDs, 1–14%). Method limits of detection for the 20 hazardous chemicals were in the range of 1–16 μg $kg^{-1}$. It is projected that the proposed method can be applied to a wide range of these four classes of hazardous chemicals in food contact materials, especially for bisphenols and plasticizers.

## Acknowledgements

We would like to acknowledge the support of the National Science and Technology Support Program (2011BAK10B05-03), the National Natural Science Foundation of China (21277085 and 21277061) and the Science and Technology Research Project of Shanxi Province (20120313030-3).

## References

1. A. Sanches-Silva. S. Pastorelli. J.M. Cruz. C. Simoneau. I. Castanheira and P. Paseiro-Losada, 2008, "Development of an Analytical Method for the Determination of Photoinitiators Used for Food Packaging Materials with Potential to Migrate into Milk", *Journal of Dairy Science*, vol. 91, no. 3, pp. 900-909.

2. S. Papilloud and D. Baudraz, 2002, "Migration tests for substrates printed with UV ink systems in aqueous simulants", *Progress in Organic Coatings*, vol. 45, no. 2-3, pp. 231-237.

3. M.C. Rhodes. J.R. Bucher. J.C. Peckham. G.E. Kissling. M.R. Hejtmancik and R.S. Chhabra, 2007, "Carcinogenesis studies of benzophenone in rats and mice", *Food and Chemical Toxicology*, vol. 45, no. 5, pp. 843-851.

4. H.D. Li. H.M. Guan. H. Dai. Y.J. Tong. X.N. Zhao. W.J. Qi. S. Majeed and G.B. Xu, 2012, "An amperometric sensor for the determination of benzophenone in food packaging materials based on the electropolymerized molecularly imprinted poly-o-phenylenediamine film", *Talanta*, vol. 99, pp. 811-815.

5. J. Sun and Y. Shi. J. Chen, 2013, "Simultaneous determination of plasticizer di(2-ethylhexyl)phthalate and its metabolite in human urine by temperature controlled ionic liquid dispersive liquid-liquid microextraction combined with high performance liquid chromatography", *Analytical Methods*, vol. 5, no. 6, pp. 1427-1434.

6. E. Fasano. F. Bono-Blay. T. Cirillo. P. Montuori and S. Lacorte, 2012, "Migration of phthalates, alkylphenols, bisphenol A and di(2-ethylhexyl)adipate from food packaging", *Food Control*, vol. 27, no. 1, pp. 132-138.

7. H. Fromme. L. Gruber. M. Schlummer. et al, 2007, "Intake of phthalates and di(2-ethylhexyl)adipate: Results of the Integrated Exposure Assessment Survey based on duplicate diet samples and biomonitoring data", *Environment International*, vol. 33, no. 8, pp. 1012-1020.

8. M. Bonini. E. Errani and G. Zerbinati, 2008, "Extraction and gas chromatographic evaluation of plasticizers content in food packaging films", *Microchemical Journal*, vol. 90, no. 1, pp. 31-36.

9. W. Zhang. C. Wang. L. Liu. et al, 2009, "Determination of Plasticizers in Plastics by Microwave

Extraction and Gas Chromatography-Mass Spectrometry", *Plastics Science and Technology*, vol. 37, pp. 77-91.

10. L.H. Ahlstrom. J. Raab and L. Mathiasson, 2005, "Application of standard addition methodology for the determination of banned azo dyes in different leather types", *Analytical Chimica Acta*, vol. 522, no. 1-2, pp. 76-80.

11. H. Gallart-Ayala. E. Moyano and M.T. Galceran, 2011, "Fast liquid chromatography-tandem mass spectrometry for the analysis of bisphenol A-diglycidyl ether, bisphenol F-diglycidyl ether and their derivatives in canned food and beverages" *Journal of Chromatography A*, vol. 1218, no. 12, pp. 1603-1610.

12. H. Petersen. A. Biereichel and K. Burseg, 2008, "Bisphenol A diglycidyl ether (BADGE) migrating from packaging material 'disappears' in food: reaction with food components", *Food Additives & Contaminants: Part A*, vol. 25, no. 7, pp. 911-920.

13. A. Goodson. W. Summerfield and I. Cooper, 2002, "Survey of bisphenol A and bisphenol F in canned foods", *Food Additives & Contaminants*, vol. 19, no. 8, pp. 796-802.

14. C. Kubwabo. I. Kosarac and B. Stewart, 2009, "Migration of bisphenol A from plastic baby bottles, baby bottle liners and reusable polycarbonate drinking bottles", *Food Additives & Contaminants: Part A*, vol. 26, no. 6, pp. 928-937.

15. E.M. Munguia-Lopez and H. Soto-Valdez, 2001, "Effect of heat processing and storage time on migration of bisphenol a (BPA) and bisphenol A-diglycidyl ether (BADGE) to aqueous food simulant from Mexican can coatings", *Journal of Agricultural and Food*, vol. 49, no. 8, pp. 66-3671.

16. I. Poustkova. J. Dobias. I. Steiner. J. Poustka and M. Voldrich, 2004, "Stability of bisphenol A diglycidylether and bisphenol F diglycidyl ether in water-based food simulants", *European Food Research and Technology*, vol. 219, no. 5, pp. 534-539.

17. J.I. Cacho. N. Campillo. P. Vinas and M. Hernandez-Cordoba, 2012, "Stir bar sorptive extraction coupled to gas chromatography-mass spectrometry for the determination of bisphenols in canned beverages and filling liquids of canned vegetables", *Journal of Chromatography A*, vol. 1247, pp. 146-153.

18. A. Ballesteros-Gomez. S. Rubio and D. Perez-Bendito, 2009, "Analytical methods for the determination of bisphenol A in food", *Journal of Chromatography A*, vol. 1216. no. 3, pp. 449-469.

19. C. Brede. I. Skjevrak and H. Herikstad, 2002, "Improved sample extraction and clean-up for the GC-MS determination of BADGE and BFDGE in vegetable oil", *Food Additives & Contaminants*, vol. 19, no. 5, pp. 483-491.

20. S. Liu. Q. Xie. J.Chen. J. Sun. H. He and X. Zhang, 2013, "Development and comparison of two dispersive liquid-liquid microextraction techniques coupled to high performance liquid chromatography for the rapid analysis of bisphenol A in edible oils", *Journal of Chromatography A*, vol. 1295, pp. 16-23.

21. C. Sun. L.P. Leong. P.J. Barlow. S.H. Chan and B.C. Bloodworth, 2006, "Single laboratory validation of a method for the determination of Bisphenol A, Bisphenol A diglycidyl ether and its derivatives in canned foods by reversed-phase liquid chromatography", *Journal of Chromatography A*, vol. 1129, no. 1, pp. 145-148.

22. T. Yoshida. M. Horie. Y.J. Hoshino and H. Nakazawa, 2001, "Determination of bisphenol A in canned vegetables and fruit by high performance liquid chromatography:, *Food Additives & Contaminants*, vol. 18, no. 1, pp. 69-75.

23. H. Gallart-Ayala. E. Moyano and M.T. Galceran, 2010, "Multiple-stage mass spectrometry analysis of bisphenol A diglycidyl ether, bisphenol F diglycidyl ether and their derivatives", *Rapid Communications in Mass Spectrometry*, vol. 24, no. 23, pp. 469-3477.

24. H. Gallart-Ayala. E. Moyano and M.T. Galceran, 2011, "Analysis of bisphenols in soft drinks by on-line solid phase extraction fast liquid chromatography–tandem mass spectrometry", *Analytica Chimica Acta*, vol. 683, no. 2, pp. 227-233.

25. D. Perez-Palacios. M.A. Fernandez-Recio. C. Moreta and M.T. Tena, 2012, "Determination of bisphenol-typeendocrine disrupting compounds in food-contact recycled-paper materials by focused ultrasonic solid-liquid extraction and ultra performance liquid chromatography-high resolution mass spectrometry", *Talanta*, vol. 99, pp. 167-174.

26. J. Míguez. C. Herrero. I. Quintás. C. Rodríguez. P.G. Gigosos and O.C. Mariz, 2012, "A LC–MS/MS method for the determination of BADGE-related and BFDGE-related compounds in canned fish food samples based on the formation of $[M + NH_4]^+$ aducts", *Food Chemistry*, vol. 135, no. 3, pp. 1310-1315.

27. B. Shao. H. Han. J.Y. Hu. J. Zhao. G.H. Wu. Y. Xue. Y.L. Ma and S.J. Zhang, 2005, "Determination of alkylphenol and bisphenol A in beverages using liquid chromatography / electrospray ionization tandem mass spectrometry", *Analytica Chimica Acta*, vol. 530, no. 2, pp. 245-252.

28. O. Pardo. V. Yusa. N. Leon and A. Pastor, 2006, "Determination of bisphenol diglycidyl ether residues in canned foods by pressurized liquid extraction and liquid chromatography-tandem mass spectrometry", *Journal of Chromatography A*, vol. 1107, no. 1-2, pp. 70-78.

29. N. Leepipatpiboon. O. Sae-Khow and S. Jayanta, 2005, "Simultaneous determination of bisphenol-A-diglycidyl ether, bisphenol-F-diglycidyl ether, and their derivatives in oil-in-water and aqueous-based canned foods by high-performance liquid chromatography with fluorescence detection", *Journal of Chromatography A*, vol. 1073, no. 1-2, pp. 331-339.

30. M. Rezaee. Y. Yamini. S. Shariati S, A. Esrafili and M. Shamsipur, 2009, "Dispersive liquid-liquid microextraction combined with high-performance liquid chromatography-UV detection as a very simple, rapid and sensitive method for the determination of bisphenol A in water samples", *Journal of Chromatography A*, vol. 1216, no. 9, pp. 1511-1514

31. A.G. Cabado. S. Aldea. C. Porro. G. Ojea. J. Lago. C. Sobrado and J.M. Vieites, 2008, "Migration of BADGE (bisphenol A diglycidyl-ether) and BFDGE (bisphenol F diglycidyl-ether) in canned seafood", *Food and Chemical Toxicology*, vol. 46, no. 5, pp. 1674-1680.

32. Directorate-General E C H A. 2009. Standing Committee of Food Chain and Animal Health Section Toxicological Safety, Conclusions of the Meeting of 06 March 2009[S].

33. Commission of the European Communities. Commission Regulation (EU) No 10/2011 of 14 January 2011 on plastic materials and articles intended to come into contact with food[S], 2011.

34. Commission of the European Communities. Commission Regulation (EU) No 1895/2005 of 18 de November 2005 on the restriction of use of certain epoxy derivates in materials and articles intended to come into contact with foodstuffs. *European Communities* 2005: 28-32.

35. Commission of the European Communities. EC/8/2011 amending Directive 2002/72/EC as regards the restriction of use of Bisphenol A in plastic infant feeding bottles[S], 2011.

36. H. Zhang. M. Xue. Y.Y. Zou. Y.Z. Dai and K. Lin, 2010, "Simultaneous determination of NOGE-related and BADGE-related compounds in canned food by ultra-performance liquid chromatography-tandem mass spectrometry", *Analytical and Bioanalytical Chemistry*, vol. 398, no. 7-8, pp. 3165-3174.

# Modelling of Migration from Printing Inks on Paper Packaging and Its Verification[#]

**Zhi-Wei Wang[1*], Song Gao[2], Chang-Ying Hu[1] and Yu-Mei Wu[1]**

[1] *Jinan University, China*
[2] *Jiangnan University, China*

[*]*Corresponding author. Email: wangzw@jnu.edu.cn*

**Abstract:** The migration model of the contaminants from the inks on the paper packaging to the food was developed based on the penetration of the ink in the paper and Fick's diffusion. The printed paper was divided as ink layer and paper layer. At the beginning the distribution of the contaminant in the paper layer was gradual. Mass transfer coefficient hm and partition coefficient KF,P in the interface between food and paper were considered. The model was solved by the method of separation of variables. Mass transfer coefficient of dibutyl phthalate (DBP) at 50˚C was obtained by the model based on the partition coefficient obtained from the experimental data and diffusion coefficient was obtained by Brandsch model. It was assumed that mass transfer coefficient was independent of the temperature. The coefficient hm at 50˚C was used in the model to predict the migration behavior at 70˚C and 100˚C. Because bis(2-ethylhexyl) phthalate (DEHP) and di-n-octyl phthalate (DOP) are isomer, the diffusion coefficients DP obtained from Brandsch model are the same, therefore the difference in their migration behavior cannot be expressed. Proper hm can be chosen to improve the predictive ability of DEHP and DOP. The prediction of the model was investigated at different paper grammage and initial concentration of the contaminant. There was good agreement between the predicted and experimental values, indicating the reliability of this model.

Keywords: printing inks; plasticizers; paper packaging; migration; migration modelling.

[#] This is the abstract of a peer-reviewed paper to appear in a Special Edition of Wiley's journal *Packaging Technology and Science* dedicated to the 19th IAPRI World Conference on Packaging 2014 hosted by Victoria University, Melbourne, Australia.

# Glucoamylase Time-Temperature Indicators Based on Fat Oxidation of Chilled Pork

**Jing Qian[1,2*] Guanglin Zheng[1] and Qin Feng[1]**

[1] *Department of Packaging Engineering, Jiangnan University, China*
[2] *Key Laboratory of Advanced Manufacturing Equipment Technology in Jiangsu, China*

[*] *Corresponding author. Email: qj639@jiangnan.edu.cn*

**Abstract:** The dynamics property of three glucoamylase type TTIs was studied and the activation energies of three kinds of TTIs were achieved. The research on the fat oxidation of chilled pork gives its activation energy and shelf life. According to the activation energy and ending point matching principle between TTI and the perishable, the matching experiments were set up both in constant and variable temperature. One of the glucoamylase TTI was selected to predict the shelf life of chilled pork accurately based on experiments and following calculation.

**Keywords**: time-temperature indicator, glucoamylase, activation energy, chilled pork, fat oxidation.

## 1 Introduction

Thermal damage is a primary concern during the distribution of temperature-sensitive products such as food, pharmaceutical, horticulture and electronic products. Insulating package is one of transport solutions for temperature-sensitive products [1]. In insulating package, various insulated shipping containers and phase change materials are used to maintain product temperatures within acceptable ranges. Time-Temperature Integrator (TTI) has been introduced as a tool for designing and evaluating thermal processes [2].

Time Temperature Integrators with appropriate performance specifications may provide a relatively simple way to meet stringent monitoring requirements. The principle of TTI operation is a mechanical, chemical, electrochemical, enzymatic, or microbiological irreversible change usually expressed as a visible response, in the form of a mechanical deformation, color development or colour movement [3,4]. TTI was identified its effectiveness and reliability on various perishable and refrigerated food products, such as vegetables, mushrooms, seafood, poultry, meat and dairy products [5-10].

In this research, amylase was chosen to prepare TTI for shipping temperature-sensitive products, such as chilled pork, around five days when the storage temperature is 3-4℃. The basic principle of this TTI is the chameleon phenomenon when starch solution meets Iodine. In reaction, the color of solution turns from black blue to deep purple and light pink, and finally turns to colourless.

In line with the matching principle, the dynamic characteristics of TTI and chilled pork are studied. Their activation energy is measured. Test TTI and chilled pork in different constant temperature and non-isothermal condition, and verify the matching attribute on the reaction end of TTI and shelf life of chilled pork.

## 2 Material and method

### 2.1 Material and reagents

Tenderloin (chilled pork): China resources vanguard Co., Ltd.

Glucoamylase (100000U/mL): Jiangsu Yueyang biotechnology Co. Ltd.

Maltodextrin: ROQUETTE (China) Co., Ltd.

Analytically pure of I, KI, $Na_2HPO_4 \cdot 12H_2O$, $NaH_2PO_4 \cdot 2H_2O$: Sinopharm Chemical Reagent Co., Ltd, A.R.

Preparation on maltodetrin solution: take 2.2g $Na_2HPO_4 \cdot 12H_2O$, 6.84g $NaH_2PO_4 \cdot 2H_2O$ and 1L distilled water, mix completely to get the buffer solution whose pH value is 6; put 40g maltodetrin into 1L buffer solution, mix completely to become maltodetrin solution whose concentration is 40g/L.

Preparation on iodine solution: take 0.5g iodine, 1g potassium iodide and 500mL distilled water, mix to particle of iodine melt completely, and get iodine solution whose concentration is 1g/L.

## 2.2 Instrument and equipment

UV-2802 Ultraviolet and Visible Spectrophotometer, Unico (Shanghai) Instrument Co., Ltd

SPX-150B-Z Biochemical Incubator, Shanghai Boxun Industrial Co., Ltd

PQX Multistage Programmable Manual Climatic Box, Ningbo Southeast Instrument Co., Ltd

JYC-21ES10 Induction Cooker, Sun Co., Ltd

HY-4 Speed Governing Vibrator, Jintian Ronghua Instrument Co., Ltd

## 2.3 Test Method

2.3.1 Kinetic study on glucoamylase time-temperature indicator

To satisfy the demand of different products, the research works on kinetic character of three TTIs with different enzyme dosage. Therefore the TTIs could become a TTI series to achieve the request of different transport temperature and time [11]. The enzyme dosage of 1# TTI is 30μL, 2# is 50μL, and 3# is 75μL.

Get 9 test tubes, put into 10mL maltodetrin solution, 3mL iodine solution and different dosage of glucoamylase, each 3 tube become a group, place the tubes in biochemical incubator with different temperature, measure the absorbance value every once in a while, and get the Absorbance value-Time curve of each TTI.

When the Absorbance value-Time curves under different temperature are achieved, fitting the curves by softer ware, the reaction rates of TTIs could be obtained, and then the activation energy of TTI systems could be determined to confirm the application range of TTIs.

2.3.2 Measurement of oxidation kinetics parameter on chilled pork

There are lots of parameters to indicate the freshness of chilled pork, such as Aerobic Bacterial Count, Total Volatile Basic Nitrogen (TVBN), pH value, 2-thio barbituric acid (TBA), etc. These parameters corroborate each other, and could reflect the freshness of chilled pork in a way [12,13]. In this research, the TBA value is selected to evaluate the degree of fat oxidation. The principle of TBA method is that Oxidative decomposition of unsaturated fatty acids yields malondialdehyde and other derivatives, and they could have chromogenic reaction with TBA. Therefore TBA value could be achieved by measuring the absorbance value of reaction product on 532nm and 600nm wave length [14]. While the degree of oxidation intensifies, the oxidation products increase, and the TBA value could be bigger accordingly. The absorbance value of reaction products could indicate the degree of fat oxidation quantificationally.

**Method**：Weight 10g comminuted meat sample; put it into 100mL conical flask with 50mL 7.5g/100mL trichloroacetic acid solution, shaking out 30min in vibrator, filter milk white mixed liquor with double filter paper(to ensure the liquor clean, filter should be repeated) ; remove 5mL filter liquor to 25mL test tube by transfer pipette, add 5mL 0.02mol/L TBA solution into the tube, insert the plug and shake up; put the tube into boiled water 40min, stand out till cooling to room temperature; pick up supernatant to 25mL another test tube, add 5mL chloroform and shake up, stand to layered; suck the supernatant to a cuvette, measure the absorption value under 532nm and 600nm wavelength, respectively; calculate the TBA value on the basis of following equation.

$$\text{TBA Value (mg/kg)} = (A532-A600)/155\times (1/10) \times 72.6\times 100 \quad (1)$$

where A532 and A600 are the absorption value of supernatant under 532nm and 600nm wavelength.

To obtain the fat oxidation rate of chilled pork under different temperature, put the subpackaged chilled pork in different thermotank with different temperature, and get the TBA Value of chilled pork at regular intervals.

## 2.4 The matching principle on TTI and perishable product

Applicability is an important issue to consider whether a TTI can indicate the quality of perishable product or not. A TTI may not apply to all products, researcher must target to choose corresponding indicator for different product.

The TTI may not be applied on corresponding product until it could accord with matching principle. The matching principle of TTI is as following [15].

(1) The difference activity energy value of TTI and perishable product is not more than 25kJ/mol;

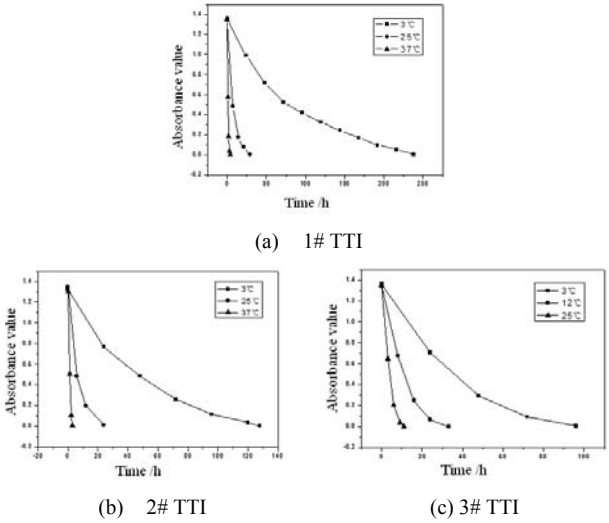
(2) The end of TTI reaction should be matched with the end of perishable product's shelf life.

# 3 Results and analysis

## 3.1 Kinetic study on glucoamylase time-temperature indicator

3.1.1 Determine the reaction rate of TTIs under different temperature

In the research, after measuring the absorbance value of TTI during the reaction of color change, the Absorbance value-Time curve of three different TTIs could be achieved. See Figure 1.




(a) 1# TTI

(b) 2# TTI (c) 3# TTI

**Figure 1**: Relationship curves of the absorbance of TTIs and reaction time at different temperature.

By using data processing software, following exponential function could be fitted by Absorbance value-Time curves.

$$X=a*\exp(-kt)+b$$

where X is absorbance value of TTIs; a, k and b are fitting function parameters, respectively. Therefore the reaction rate (k) of TTI could be achieved in Table 1.

**Table 1: The parameters of fitting curves and the ln*k* value**

| | *T*/K | a | b | *k* | $R^2$ | 1/*T* | ln*k* |
|---|---|---|---|---|---|---|---|
| 1#TTI | 276（3℃） | 1.38600 | -0.04975 | 0.012 | 0.99662 | 0.00362 | -4.423 |
| | 298（25℃） | 1.34646 | -0.00367 | 0.144 | 0.99959 | 0.00336 | -1.938 |
| | 310（37℃） | 1.42412 | -0.06897 | 0.822 | 0.99890 | 0.00323 | -0.196 |
| 2#TTI | 277（3□） | 1.43066 | -0.11779 | 0.019 | 0.99889 | 0.00362 | -3.9792 |
| | 298（25℃） | 1.35024 | -0.00325 | 0.167 | 0.99948 | 0.00336 | -1.7898 |
| | 310（37℃） | 1.42937 | -0.12634 | 0.843 | 0.99856 | 0.00323 | -0.1708 |
| 3#TTI | 276（3℃） | 1.51356 | -0.14747 | 0.025 | 0.99921 | 0.00362 | -3.6969 |
| | 285（12℃） | 1.47432 | -0.11943 | 0.082 | 0.99784 | 0.00351 | -2.4990 |
| | 298（25℃） | 1.50224 | -0.14526 | 0.226 | 0.99777 | 0.00336 | -1.4885 |

From Table 1, all correlation coefficients ($R^2$) of fitted curves in deferent temperature are above 0.99. It shows a good correlation of the curve line.

3.1.2 Determine the activation energy of TTIs

The influence of temperature on the reaction rate during enzyme catalytic reaction will follow the Arrhenius formula as following [16].

$$\ln k = \ln k_0 - \frac{E_a}{R}\frac{1}{T} \qquad (2)$$

where $k$ is the reaction rate of TTI, $k_0$ is a pre-exponential factor (it is a constant for a reaction), $R$ is the molar gas constant ($R$=8.314*J/mol •K*), $T$ is thermodynamic temperature in K, and *Ea* is the activation energy of TTI.

If ln$k$ and 1/$T$ have significant linear relationship, it shows the reaction rate and temperature follow the Arrhenius formula. Therefore the activation energy of TTI *Ea* and pre-exponential factor $k_0$ could be achieved via the Arrhenius formula.

According the data in Table 1, ln*k*-1/*T* curve could be obtained as Figure 2.

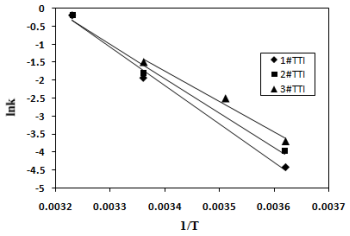



**Figure 2**: The curve of TTIs between ln*k* and 1/*T*

The fitting straight line of each TTI could be achieved via data processing software. All correlation coefficients ($R^2$) of fitted lines are above 0.99. It shows a good correlation of the curve line. So the activation energy of TTI *Ea* and pre-exponential factor $k_0$ could be obtained in Table 2.

**Table 2:** The kinetic parameters of TTIs

| | 1#TTI | 2#TTI | 3#TTI |
|---|---|---|---|
| Fitting straight line | $\ln k = 34.08 - 10655.49\frac{1}{T}$ | $\ln k = 30.327 - 9496.576\frac{1}{T}$ | $\ln k = 34.08 - 10655.49\frac{1}{T}$ |
| $R^2$ | -0.99604 | -0.99536 | -0.99056 |
| $k_0$ （$h^{-1}$） | $6.32\times10^{14}$ | $1.48\times10^{13}$ | $4.27\times10^{11}$ |
| $E_a$ （kJ/mol） | 88.59 | 78.95 | 69.76 |

The research shows when the difference of activation energy between TTI and perishable product is within 25 kJ/mol, the TTI could be applied the perishable product. According to the activation energy of main reaction, which gives rise to food deteriorate (Labuza mentioned[17]), all these three kind of TTIs could be applied to the food, such as grease and meat, whose quality loss are caused by fat oxidation. In this research, chilled pork is selected as a target food. The research will show which TTI could match chilled pork during transportation.

## 3.2 Determination on oxidation kinetics parameter of chilled pork

Chilled pork is a typical sample on deterioration caused by fat oxidation. In a general way, when the TBA Value of chilled pork is over 0.5mg/kg, pork will have peculiar smell and nutrient losses seriously [18,19]. The shelf life of chilled pork is the duration time which the TBA Value of chilled pork reached 0.5mg/kg.

Measuring the TBA Values of chilled pork during metamorphic processing, the TBA Value-Time curve could be achieved in shelf life of chilled pork. Fitting curves via data processing software, as shown in figure 3, the fat oxidation rate of chilled pork in different temperature could be obtained.

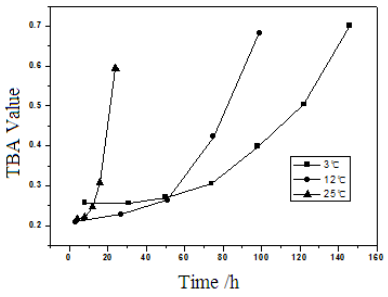



**Figure 3:** Relationship of TBA Value of chilled pork and reaction time at 3℃, 12℃, 25℃

Figure 3 shows TBA Value in different temperature and reaction time have conspicuous exponential relationship. The duration time which TBA Value reaches 0.5mg/kg are shorter while temperature increases. It clears that the fat oxidation rate will be going faster when ambient temperature increases.

From figure 3, correspondence relationship of the fat oxidation rate of chilled pork and the temperature could be obtained in Table 3.

**Table 3:** The ln*k* value under different temperatures of chilled pork

| *T*/K | 1/*T* | ln*k* |
|---|---|---|
| 276（3℃） | 0.00362 | -3.8167 |
| 285（12℃） | 0.00351 | -3.4029 |
| 298（25℃） | 0.00336 | -1.8031 |

The ln$k$ -1/$T$ curve of chilled pork could be achieved from Figure 3. The multiple correlation coefficient of this fitting model is -0.9694, which shows ln$k$ and 1/$T$ of chilled pork is linearity. Thus the activation energy and pre-exponential factor $k_0$ of chilled pork could be found in Arrhenius formula.

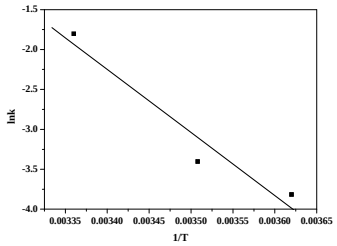



**Figure 4:** The curve of chilled pork between ln$k$ and 1/$T$

The fitting straight line in Figure 4 is $\ln k = 24.63 - 7904.6\frac{1}{T}$, the activation energy and pre-exponential factor $k_0$ of chilled pork are as following.

$$k_0^{chilled\ \ pork} = 4.97\times10^{10}\text{h}^{-1} \quad (3)$$

$$E_a^{chilled\ \ pork} = 65.72\text{kJ/mol} \quad (4)$$

## 3.3 TTI application on indication of chilled pork quality

3.3.1 Activation energy matching

The activation energy of chilled pork is 65.72kJ/mol. According to the matching principle, the activation energy of TTI should be between 40.72 and 90.72 kJ/mol. It clears that all activation energy of these three kinds of TTI is among the range. In another word, three kinds of TTI match the principle.

3.3.2 Reaction endpoint matching in constant temperature

The previous experiments give the indicate time of TTIs and the shelf life of chilled pork in 3℃and 25℃ (Figure 1 and 3). Table 4 shows them together.

**Table 4:** The indicate time of TTIs and shelf life of chilled pork under different constant temperatures

| Constant temperature | Shelf life /h | Indicate time /h | | |
|---|---|---|---|---|
| | Chilled pork | 1#TTI | 2#TTI | 3#TTI |
| 3℃ | 122 | 238 | 128 | 96 |
| 25℃ | 22 | 29 | 24 | 11 |

Table 4 shows the indicator time of 2# TTI is very close to the shelf life of chilled pork both in 3℃ and 25℃.The forecast error is 4.92% and 9.09%, respectively. Therefore the reaction endpoint of 2#TTI matches the shelf life of chilled pork in constant temperature.

3.3.3 Reaction endpoint matching in non-isothermal test

During transport, the ambient temperature of food could be various. So it is necessary to know the matching situation of 2#TTI and chilled pork in non-isothermal test.

The 2#TTI and chilled pork samples are putted into same Multistage Programmable Manual Climatic Box. The non-isothermal temperature is shown in figure 5 [20]. The temperature cycle comprised 12 h at 3℃, 3 h at 23℃, 1 h at 37℃, 5 h at 12℃, and then keep 3℃ till the TBA Value of chilled pork reaches 0.5mg/kg.

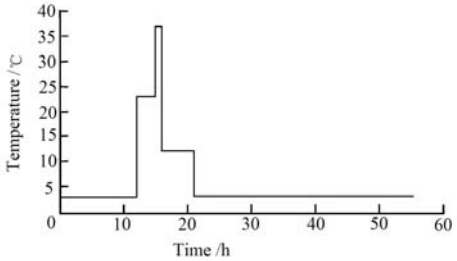



**Figure 5:** The time-temperature history for chilled pork and TTIs in non-isothermal test

Figure 6 shows the change of TBA Value on chilled pork while time extends. During whole non-isothermal test, TBA Value of chilled pork increase little by little. The duration time is about 49 hours while TBA Value is increase from 0.24mg/kg to 0.5mg/kg. It also clears that the change of TBA is slower in 3℃, the fastest change of TBA is happened in 37℃, the change in 12℃ and 23℃ are between them. The rate of change is different under different temperature. The higher temperature, the faster fat oxidation rate is.

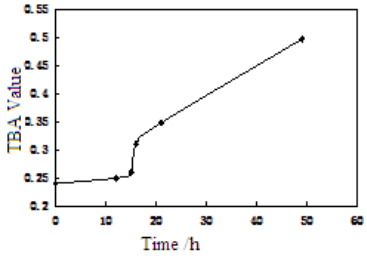



**Figure 6:** The changes of TBA value of chilled pork with time in non-isothermal test

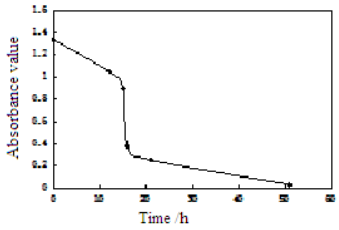



**Figure 7:** The changes of absorbance value of 2#TTI with time in non-isothermal test

The corresponding absorbance value change is shown in Figure 7. It shows the absorbance value of 2#TTI is close to zero on 52nd hour. The color of TTI system turns to colorless, and the reaction reaches end. The decrease of absorbance value is slower in 3℃, and the curve of absorbance value is steep in 37℃. It is same as the change of fat oxidation rate of chilled pork with temperature.

The response function *F(X)* of TTI is the function of effective temperature $T_{eff}^{TTI}$; during food shelf life analysis in non-isothermal test, the quality function *Q(A)* of food could also be expressed in effective temperature $T_{eff}^{food}$.

$$F(X)_t = k_0^{TTI} \exp(-E_a^{TTI} / RT_{eff}^{TTI})t \qquad (5)$$

where *F(X)* is the response function of TTI, $k_o^{TTI}$ is the pre-exponential factor of TTI, $E_a^{TTI}$ is the activation energy of TTI in kJ/mol, $T_{eff}^{TTI}$ is the experienced effective temperature of TTI in K.

$$Q(A)_t = k_0^{food} \exp(-E_a^{food} / RT_{eff}^{food})t \qquad (6)$$

where *Q(A)*is the quality function of food, $k_o^{food}$ is the pre-exponential factor of food, $E_a^{food}$ is the activation energy of food in kJ/mol, $T_{eff}^{food}$ is the experienced effective temperature of food in K.

For the non-isothermal experience like Figure 5, at the end of indication the response function *F(X)* of 2#TTI could be achieved in following equation.

$$F(X)_t = \int_0^t kdt = \int_0^{12} k_3 dt + \int_{12}^{15} k_{23} dt + \int_{15}^{16} k_{37} dt + \int_{16}^{21} k_{12} dt + \int_{21}^{51} k_3 dt \qquad (7)$$

where $k_3$, $k_{12}$, $k_{23}$ and $k_{37}$ are the rate of absorbance value in 3℃、12℃、23℃、37℃, respectively. The range of integration is the beginning and ending time of each constant temperature experience.

Based on equation 2, pre-exponential factor and activation energy of 2#TTI, the expression of reaction rate could be as following.

$$k_{2\#\mathrm{TTI}} = 1.48 \times 10^{13} e^{(-78.95 \times 10^3 / RT)t} \qquad (8)$$

Hence, the reaction rate of 2#TTI in different temperature is as shown in Table 5.

By using the data in Table 5 to Equation 7, the response function *F(X)*of 2#TTI is 2.236. Put this value, pre-exponential factor of 2#TTI $k_o^{2\#TTI}$ ($1.48\times10^{13}h^{-1}$), activation energy of 2#TTI $E_a^{2\#TTI}$ (78.95kJ/mol), and the indicator time *t* (51h) to Equation 5, the equivalent temperature of 2#TTI during this non-isothermal experience could be achieved （$T_{eff}^{2\#TTI}$=284K）.

**Table 5:** The reaction rates of 2#TTI and chilled pork in different temperatures

| Temperature | Reaction rate of 2#TTI | Rate of fat oxidation on chilled pork |
|---|---|---|
| 3℃ | 0.017 | 0.018 |
| 12℃ | 0.050 | 0.045 |
| 23℃ | 0.173 | 0.125 |
| 37℃ | 0.736 | 0.419 |

For the non-isothermal experience like Figure 5, at the end of shelf life the quality function *Q(A)*of chilled pork could be achieved in following equation.

$$Q(A)_t=\int_0^t kdt=\int_0^{12}k_3dt+\int_{12}^{15}k_{23}dt+\int_{15}^{16}k_{37}dt+\int_{16}^{21}k_{12}dt+\int_{21}^{51}k_3dt \qquad (9)$$

where $k_3$, $k_{12}$, $k_{23}$ and $k_{37}$ are the fat oxidation rate of chilled pork in 3℃、12℃、23℃、37℃, respectively. The range of integration is the beginning and ending time of each constant temperature experience.

Based on equation 2, pre-exponential factor and activation energy of 2#TTI, the fat oxidation rate of chilled pork could be expressed as following.

$$k_{chilled\ pork}=4.97\times10^{10}e^{(-65.72\times10^3/RT)t} \qquad (10)$$

Therefore the fat oxidation rate of chilled pork in different temperature is as shown in Table 5.

By using the data in Table 5 to Equation 9, the quality function *Q(A)*of chilled pork is 1.739. Put this value, pre-exponential factor of chilled pork $k_o^{chilled\ \ pork}$ ($4.97\times10^{10}h^{-1}$), activation energy $E_a^{chilled\ \ pork}$ (65.72kJ/mol), and the shelf life *t* (51h) to Equation 6, the equivalent temperature of chilled pork during this non-isothermal experience could be achieved （$T_{eff}^{chilled\ \ pork}$=285K）.

From the above calculation in non-isothermal experience as shown in Figure 5, the equivalent temperature of chilled pork and 2#TTI is 1K, and the prediction error on shelf life is 8.16% which is less than 15%. So the reaction end of shelf life matches the end of chilled pork's shelf life. That is 2#TTI could be applied to monitor the quality of chilled pork during transportation. In practical application, if the color of TTI is deep purple, it shows that chilled pork is in low temperature surrounding and good freshness; if the color of TTI is light pink it means chilled pork is almost degeneration and the nutrition lost seriously.

## 4 Conclusions

Based on experimental research, activation energy of three kinds of TTIs with different enzyme dosage is obtained. Meanwhile the quality change mechanism and kinetics performance of chilled pork are under study. The fat oxidation rate and the activation energy of chilled pork are achieved. By testing TTI and chilled pork in constant temperature and non-isothermal experience, discuss the matching between them. The experiments verify that the glucoamylase TTI with 50μL enzyme dosage could predict the shelf life of chilled pork accurately.

## Acknowledgements

This research was supported in part by the Fundamental Research Funds for the Central Universities and Scientific Research Funds for Returned People from the Ministry of Education of China.

## References

1. S.P. Singh, G. Burgess and J. Singh, 2008, "Performance Comparison of Thermal Insulated Packaging Boxes, Bags and Refrigerants for Single-parcel Shipments", *Pack. Tech. & Sci.*, vol. 21, no. 1, pp.25－35.
2. R. Ahvenainen, 2003, *Novel Food Packaging Techniques*,1st Ed., Woodhead Publishing, England.
3. E. Shimoni, E. Manderson，T. P. Labuza, 2001, "Reliability of Time Temperature Indicators Under Temperature Abuse", *Food Engineering and Physical Properties*, vol. 66, no.9, 1337-1340.

4. H. Reichert, P. Simmendinger and T. Bolle, 2010, “Enzyme-based time temperature indicator”, U.S. Patent 7736866 B2.
5. C. Wanihsuksombat, V. Hongtrakul，P Supparkul, 2010, “Development and characterization of a prototype of a lactic-acid-based time-temperature indicator for monitoring food product quality”, [D].Thailand.
6. Giannakourou MC, Taoukis PS, 2003, “Application of a TTI-based distribution management system for quality optimization offrozen vegetables at the consumer end”, *Journal of Food Science*, vol68, no.1, pp.201–209.
7. Bobelyn E, Hertog M, Nicolai BM, etc., 2006, “Applicability of an enzymatic time temperature integrator as a quality indicator for mushrooms in the distribution chain”, *Postharvest Biology and Technology*, vol. 42, no.1, pp. 104–114.
8. Tsironi T, Stamatiou S, Giannoglou M, etc., 2011, “Predictive modeling and selection of time temperature integrators for monitoring the shelf life of modified atmosphere packed gilthead seabream fillets”, *LWT – Food Scienceand Technology*, vol 44, pp. 1156–1163.
9. Ellouze M, Augustin JC, 2010, “Applicability of biological time temperature integrators as quality and safety indicators for meat products”, *International Journal of Food Microbiology*, vol.138, no.1, pp.119–129.
10. L. Lu, W. Zheng, Z. Lv and Y. Tang, 2013, “Development and Application of Time–temperature Indicators Used on Food during the Cold Chain Logistics”, *Pack. Tech. & Sci.*, vol26, Suppl. 1, pp.80–90.
11. G. Zheng, J. Qian, 2013, “Study on time-temperature indicator reaction system based on glucoamylase”, *Food Science*, vol. 34, no.12, pp.82-85.
12. A. Geng, G. Zheng, H. Qian, 2006, “The detection method of meat freshness”, *Meat Industry*, vol. 37-39.
13. M. Li, Q. Zhang, X. Gao, 2008, “The relationship study on quality index of chilled pork during storage”, *Food and fermentation industry,* vol. 34, no. 7, pp.168-171.
14. Y. Wang, 1999, “the fat oxidation of meat product”, *Meat research*, vol.10, no.1, pp.16-19.
15. Giannakourou MC, Koutsoumanis K, etc., 2005, “Field evaluation of the application of time temperature integrators for monitoring fish quality in the chill chain”. *International Journal of Food Microbiology*, vol. 102, pp. 323–336.
16. Vaikousi H, Biliaderis CG, Koutsoumanis KP, 2009, “Applicability of a microbial time temperature indicator (TTI) for monitoring spoilage of modified atmosphere packed minced meat”, International Journal of Food Microbiology, vol. 133, no. 3,pp.272–278.
17. Labuza, T P, 1982, *Shelf-life dating of foods,*1st Ed., Food and Nutrition Press, Westport, CT.
18. Taoukis P S and Labuza T P. 1989, “Applicability of Time Temperature Indicators as shelf-life monitors of food products”, *Food Science*, vol. 24, no.2, pp.783-788.
19. Sun Y, Cai HW, Zheng LM, Ren FZ, 2004, “Development and characterization of a new amylase type time–temperature indicator”, Food Control, vol.19, pp.315–319.
20. Taoukis P S, Labuza T P, 1989, “Reliability of Time-temperature indicators as food quality monitors under non-isothermal conditions”, *Journal of Food Science,* vol.54, no.4, pp.789-792.

# The Flexible Packaging Line – PickNPack

**Søren R. Østergaard[1*] and Alexander Bardenstein[1]**

[1] *Packaging, Danish Technological Institute, Denmark*

[*] *Corresponding author. Email: sos@dti.dk*

**Abstract:** In the 12 mill. € European Union financed project under FP7 the PickNPack concept offers the food industry the benefits of automation – cost reduction, greater hygiene and more efficient use of resources – combined with the unique ability to adapt to the product and batch size at hand. PickNPack will give the food industry a vital competitive advantage in the rapidly changing marketplace of the future, where customers demand more quality, more choices and more safety at lower prices.

The project will develop three types of modules that can cope with the typical variability of food products and the requirements of the sector regarding hygiene, economics and adaptability, which will be working closely together:

1. A sensing module that assesses quality of the individual or small batch products before or after packaging.
2. A vision controlled robotic handling module that picks up and separates the product from a harvest bin or transport system and places it in the right position in a package.
3. An adaptive packaging module that can accommodate various types of packaging with flexibility in terms of package shape, size, product environment, sealing and printing.

These modules connect to a multi-point framework for flexible integration into a production line that optimally makes use of the capabilities of the modules.

The communication is based on a shared, vendor-independent vocabulary. The combination of modules will be with a user-friendly interface and all modules are equipped with automated cleaning systems to ensure hygiene. All available information in the production chain and the information produced by the sensors in the system is combined, stored and made available to the different modules and both upstream and downstream in the chain. With added intelligence, this will lead to maximum performance in quality, reducing change over time, reducing time for reprogramming, adaptation to operators, reducing waste of food and packaging material and stock. Human intervention will be reduced to a minimum.

The presentation will focus on the adaptive packaging module that can accommodate various types of packaging with flexibility in terms of package shape, size, and product environment, sealing and printing. The scope is to develop an ultimate flexible system able to produce product batches down to 1-100 packs on a batch with almost no need of time to change and reduce lead time from design to production to 5-10 minutes. The system includes an active heating system for heating food in microwave owns.

Keywords: Flexible packaging line, short lead time, small batches, food packaging, flexible decoration, flexible mould.

## 1 Introduction

In 2011 The European Union in it Seventh Framework Programme (FP7) had following call for proposals [1]:

***KBBE.2012.2.3-03: Automation in food packaging systems*** *- Call: FP7-KBBE-2012-6 – single stage*

*The high number of food product varieties and units, as well as packaging types dictated by customer requirements, means the food packaging industry is geared towards short runs and small batch production. The aim of this topic is to develop automated packaging systems to reach standardised operational flexibility in the packaging industry for both fresh and processed food, also ensuring convenience.*

Under the coordination of Wageningen UR 14 organisations applied for this call under the title PickNPack and the 4 year project was financed by EU with the start 1 October 2012. Participants in the project are Wageningen University and Research Centre (NL), Danish Technological Institute (DK), Tecnalia Research and Innovation (SP), Katholieke Universiteit Leuven (BE), University of Manchester together with University of Lincoln (UK),

Fraunhofer AVV (DE), Lacquey BV (NL), ITENE (SP), Spectroscan (FR), Marel (IS), Tecnalia-AZTI (SP), Cam-Tech A/S (DK), XaarJet AB (SE), and Marks & Spencer (UK).

Budget: 11.9 mill. € (18.3 mill. AUD) with finansial support from FP7 of 8.8 mill. € (13.6 mill. AUD)

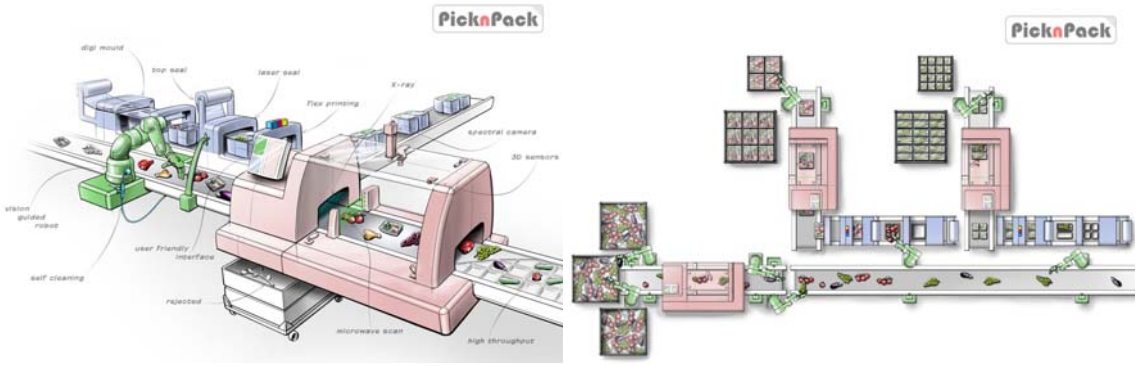



**Figure 1:** Artist impression of PickNPack in the application

## 2 The adaptive packaging line (WP6)

Already in the beginning of PickNPack it was decided to perform following demonstrations in the end of the project:

- Packaging of fruits and vegetables in the Netherlands
- Packaging of ready meals in UK

PickNPack has in the start of the project studied different packaging methods in a number of European countries. But in the following text the data for the demonstration sites will be in focus.



**Figure 2**: Packaging of tomatoes and grapes, and an UK packaging for ready meals



**Figure 3:** Ready meal production in UK

## 2.1 PickNPack in different jobs

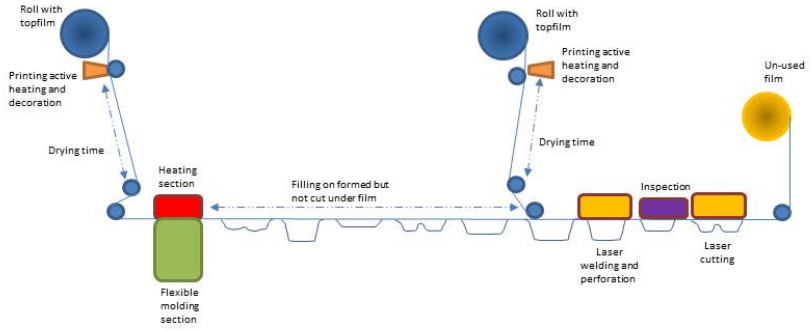



**Figure 4:** General lay-out of packaging line

PickNPack has decided that the packaging line is a flexible tray packaging line with top film. Such a system has a first part where under film is rolled out sometime decorated and then heated up and formed in a mould either with vacuum and/or pressurised air. Next step is a long line of different trays ready for filling. In PickNPack different robots and dispensers filling the trays in a flexible way. Next step is the application of a decorated over film. In PickNPack these two films are welded together with a laser. After inspection of the sealing each tray is cut out of the on-going film.

Each of these jobs has its own challenges. But it is also obvious that these jobs can be solved in different groups.

A. Thermoforming system (Cam-Tech, DTI)
B. Printing of decoration and active heat system (DTI, Xaar)
C. End-of-line-system (KUL, UM/University of Lincoln, DTI)
D. Integration of all these units to PicknPack (All)

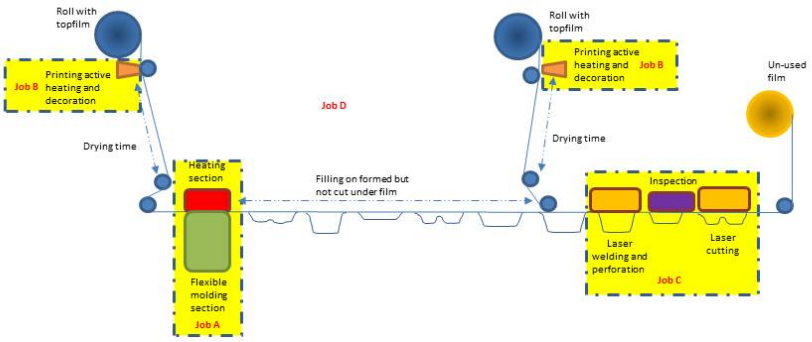



**Figure 5:** General lay-out with 4 jobs and tasks

## 2.2 Job A - Thermoforming system

### 2.2.1 Thermoforming system

PickNPack has decided to rebuild an old thermo former in order to demonstrate that our technology can be implemented into existing packaging lines.



**Figure 6:** Old thermoforming machine from sliced meat production.

### 2.2.2 Flexible mould technologies

#### 2.2.2.1 Moulds with many small pins

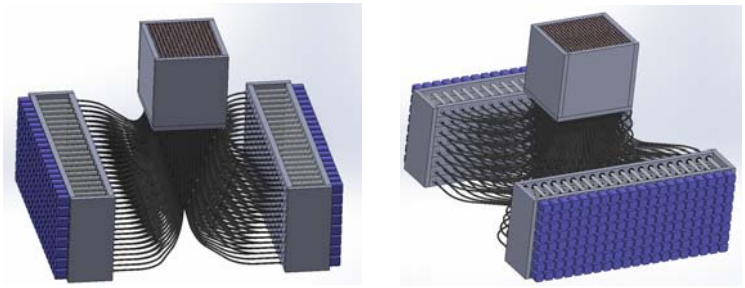


**Figure 7:** Digital mould with many pins operated with cables and servo motors

The mould has a number of pins able to move up and down. PickNPack notes that resolution and quality is a trade-off between price and quality. In a mould of 210x210 mm we need following:

**Table 1:** Resolution and number of pins

| Resolution in mm | Number of pins |
|---|---|
| 10 mm | 441 |
| 6 mm | 1,225 |
| 5 mm | 1,764 |
| 4 mm | 2,756 |
| 3 mm | 4,900 |
| 2 mm | 11,025 |

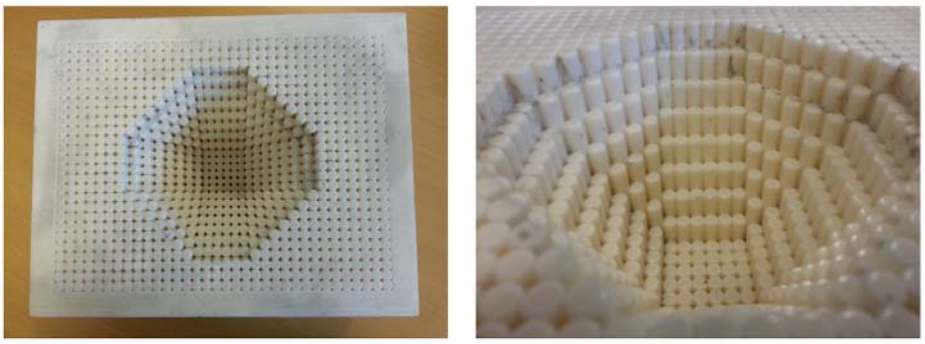


**Figure 8:** Mould with 5 mm pins



**Figure 9:** Tray produced in a mould with 5 mm pins

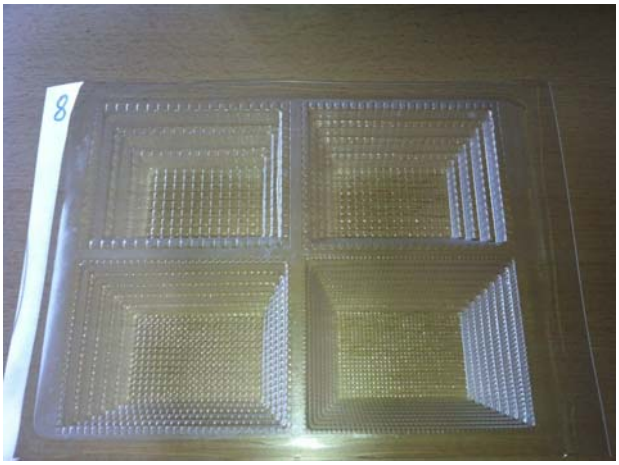


**Figure 10:** Tray produced in a mould with 2, 3, 4 and 5 mm pins

The quality of a tray made in a mould with 5 mm pins is not acceptable. In order to upgrade quality either the pins must be less and/or a flexible layer between the pins and the plastic shall result in a smooth surface.

As a test a mould with 2 mm, 3 mm, 4 mm and 5 mm pins was produced. Still it is doubtful if even the trays made with small pins can be accepted in the packaging industry.

*Welding of trays made in a pin mould*

PickNPack has tested all trays including welding top film on the different trays. Heat welding will always including a mechanical pressure between the two films to be welded. This works perfect. PicknPack are going to use laser welding of two films only laying on each other using gravity. University of Lincoln is responsible for the laser welding. Samples of the moulds have been send to University of Lincoln in order to evaluate the laser welding quality. Conclusion of the tests at University of Lincoln was that pinholes in the laser welding already start if the distance between the two films is more than 50 microns. Pin moulds and laser welding is a challenge we have to find a solution for. We have just noted that the Dutch project OptiMal Forming Solutions (www.optimalforming.com) already has developed a solution very like our idea. The idea is called Flexi Mould. For this reason PicknPack will stop working with the pin solution.

### 2.2.2.2 Off-line digital mould

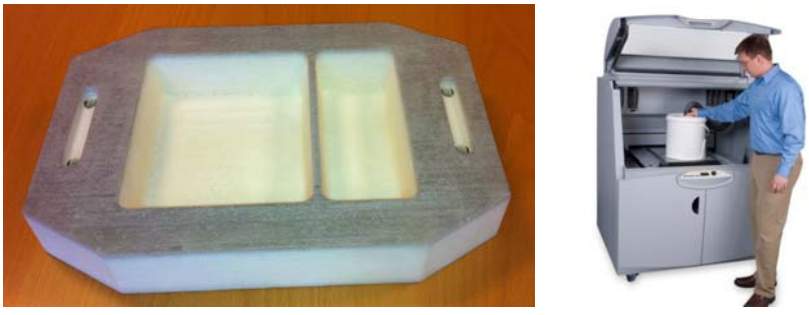


**Figure 11:** Digital produced plaster moulds produced off-line

Based on a standard 3-D printer for prototypes you can produce moulds which are able to produce about 1-3,000 trays and with a surface treatment also more smooth. The moulds will in the off-line system be produced off-line and shall be mounted on the thermo-forming-machine before the production. Off-line moulds can also be produced in simple CNC milling machine. The mould can be made out of a ceramic, concrete or aluminium block of a porous material.

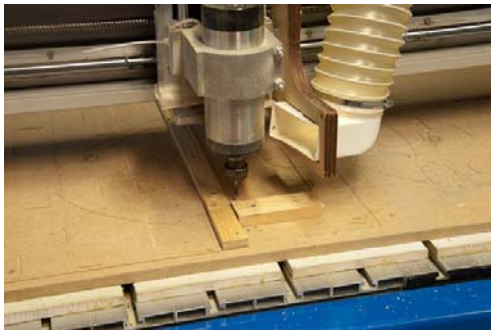


**Figure 12:** CNC milling machine



**Figure 13:** Porous aluminium blocks for CNC-milling to moulds

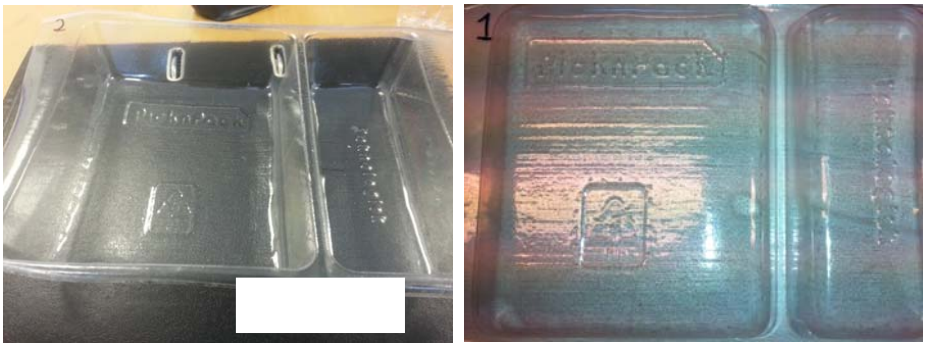


**Figure 14:** Tray made in a plaster mould from a 3-D printer

The plaster/concrete/ceramic/aluminium technology produces flexible moulds able to be used for more than 1,000 items in a very high quality.

Lead time for these technologies is 4-10 hours for 3-D plaster technology and 1-2 hours for CNC milling of concrete moulds. But 3-D modelling is in a fast development these years and is expected to be more efficient, fast and inexpensive within a few years.

#### 2.2.2.3 Moulds in bricks

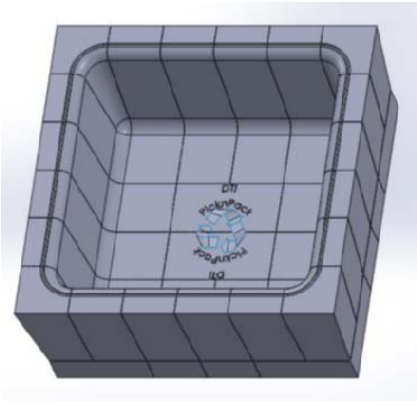


**Figure 15:** Mould in bricks

The idea is to produce the mould in small parts (sections) of aluminium. These parts need to have an interlock system and shall be able to be assembled the final mould fast.

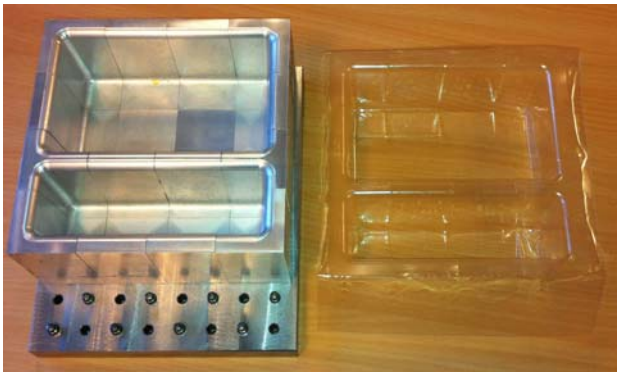
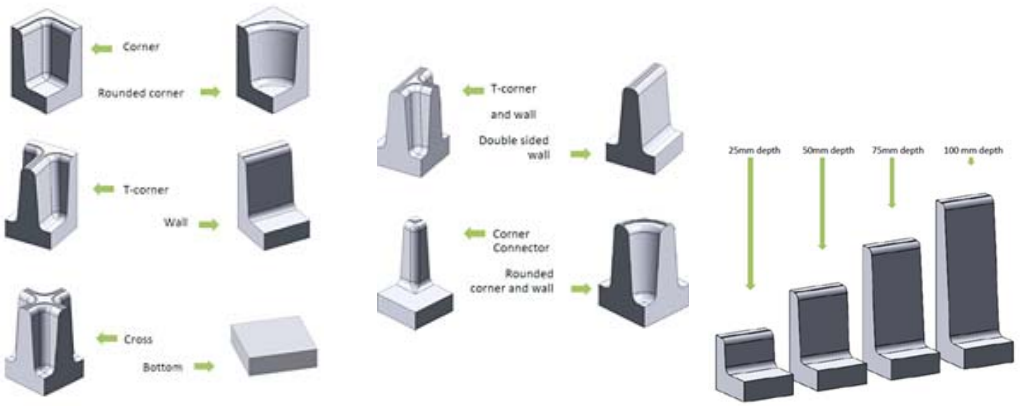


**Figure 16:** Photo of a mould in bricks with a thermoformed plastic tray




*Basic bricks* *Special bricks* *Bricks with different heights*

**Figure 17:** Selection of bricks

A selection of different bricks will give the user many different options to create the mould needed for a specific product. The idea is that the design process can be done with the product next to the designer. And in seconds a new mould is designed and produced. A camera can see the selected bricks and send the information to the control system of PickNPack. The data is needed for the later decoration, welding and cutting.

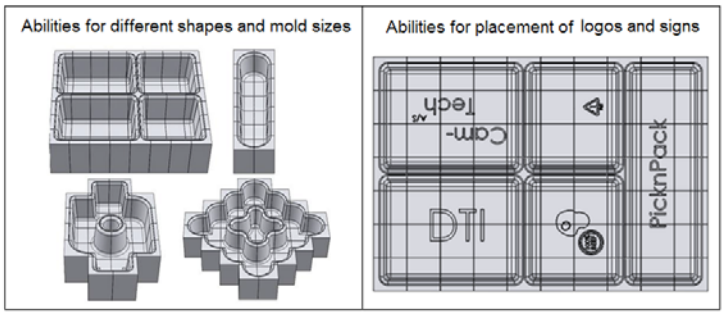



**Figure 18:** Design options for a brick mould system

### 2.2.3 Exchange of moulds in thermoforming unit

After the production of the moulds these can be placed in an exchangeable storage under the thermoforming unit. As the thermoforming process is performed as a stop-and-go-process it is possible to change mould as the under film is moving.

The combination of a brick mould and this exchange system can reduce lead time from the beginning of the design process until the end of production to less than 5 minutes.

## 3.3 Printing

### 3.3.1 Decoration

PickNPack has decided to use inkjet printing technology from Xaar.




**Figure 19:** Xaar 1001 inkjet print head for high quality packaging print

The Xaar 1001 print head, which is the preferable choice for this project, is about 70 mm wide and prints on a substrate that is moved in a distance of 0.5 - 2 mm underneath the print head. It is possible to print onto wider rolls of plastic film by placing several heads side by side. This print head model utilizes a continuous ink-circulation through the print head, which allows very high reliability when printing continuously in a roll-to-roll process.

Each print head only prints one colour of the decorative coating, or the microwave-active coating. For the printing of the active coating other print head models with fewer nozzles, but larger drop volumes might be considered as well, like the Xaar Proton model, which has 382 nozzles and up to 60pL drop volumes, and covering a print width of 53.7 mm per print head.

In PickNPack the print technology is demonstrated with two colours. It is only a matter of print heads to upgrade the quality. Print heads are typically aligned side-by-side in a print bar, in such a way that the single heads can be fine-aligned to each other, and also that the whole print bars can be aligned to each other and to the substrate. Following drawings show some examples for print bar designs. Depending on the number of print heads, similar print bars will be integrated into the demonstrator.

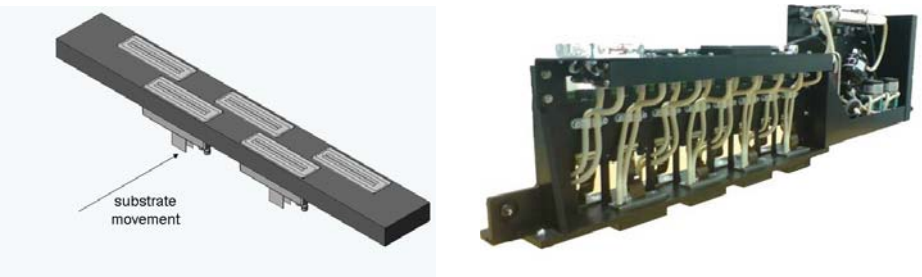



**Figure 20:** Print bar designs with 5 Xaar 1001 print heads, with view from underneath (left), and with 8 Xaar 1001 heads with integrated ink system (right)

Furthermore, suitable drying / sintering tools have to be included after the print bar. For the decoration, low-migration UV-curable inks are currently evaluated, which can be cured with UV-LED lamps; most likely separate UV-lamps are required for white and coloured inks. For the conductive elements, fast sintering methods employing photonic sintering or near-infrared lamps are required.

*Printing speed*

The printers' works best if the film is moved forward under a constant speed. But the packaging processing must happen in steps of different lengths. For this reason we need a buffer between the printing and packaging.

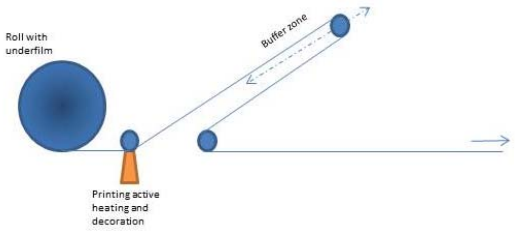



**Figure 21:** Buffer zone after printing

The Xaar 1001 print heads allow a print speed of around 0.4 m/s if printing in grey scale mode and a resolution of 360dpi in print direction. For the deposition of thicker metallic reflector layers, the substrate speed could be slowed down, allowing the printing at lower drop spacing and thus deposition of thicker layers.

For the achievement of high printing quality it will be important to have accurate encoders included close to the print head position, to trigger the printout in relation to the current substrate speed.

### 3.3.2 Active heating system

The challenge in microwave heating is to apply following in a pattern on the packaging substrate:

- Reflector of more than 1-5 microns of metal coating
- Susceptor of about 1-5 nano-meters of metal coating

Normal printing only applies layers just in between these two dimensions.

Tests demonstrate that 6-10 consecutive printed layers with current silver inks works as a reflector. In consequence we hope to find/develop an ink able to apply thicker layers of metal.

For susceptor we have tested the appliance of a reflector in a micro-pattern. Tests indicate some function. If this will be possible we only need to apply one active layer in a pattern on both trays and top film.

PickNPack need to continue with more research to find suitable solutions for both cases.

A special challenge is the change in pattern of the heat system as the film is printed before shaping the film with heat to trays. It is important to focus on this problem.

Research has documented those active coatings of metals before thermoforming is broken up under the forming process with the consequence that the coating is not active after. In order to solve this problem the coating on the tray need to be applied after forming the tray.

*Heating systems in demonstrators*

Over the summer of 2013 we have studied possible demonstrators. In relation to heating systems the situation is:

- Grapes and tomatoes do not need heating system.
- Ready meals need a printed structure of shielding in order to control the heating of multiple components

Ready meals:




**Figure 22:** Heating system for ready meals

- Based on these considerations, it is suggested to split the development of the heating system to:

  a) Research in Flexible Deposition of Microwave Active Patterns, including the evaluation of advanced structured pattern for susceptor layers, and the investigation of other metallic inks as an alternative to silver-nanoparticle based inks.

  b) Development of heating systems for two ready meals as specified above. Here the total reflective (metal foil belt) and susceptor (commercial PET+cardboard materials) elements will be set in the tray by a robotic arm during the meal assembling, while the partially transparent (patterned reflector) elements on the top film and the bottom surface of the tray are aimed to consist of inkjet printed layers. However, the printing process for these elements will be first developed in an offline-fashion, where the printed reflector elements can be inserted during meal assembly as well. In this way the feasibility of printing thick reflector layers in a cost-effective way, as well as further processing parameters like metal layer sintering and deposition of advanced pattern, can be investigated first. The packaging line should be designed in such a way that an inkjet printing station for the heating elements can be implemented into the demonstrator at a later stage, once the process has been developed further and shown to be viable.

## 3.4 End-of-line-system

### 3.4.1 Welding

The laser can both weld and cut the packaging. The top and the under film are mechanical locked together at the same level and moved into the laser machine.

The laser welder and cutter include a controllable mirror system.

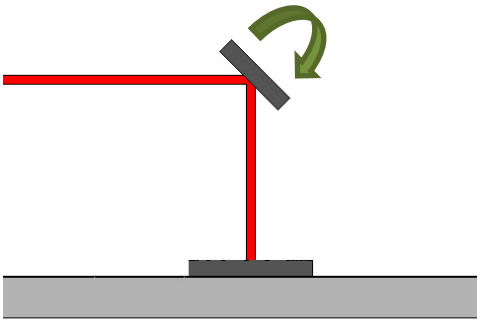


**Figure 23:** The laser with controllable mirror system

The laser must be able to follow this stop-go situation and process as follows:

1. Weld the two films together
2. Perforate to specific needs
3. Cut the trays out from the films

### 3.4.2 Cutting problem

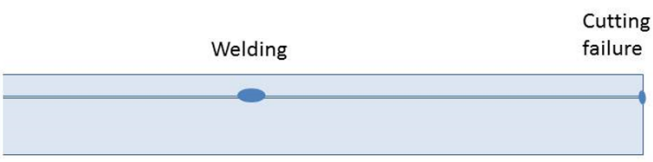



**Figure 24:** Cutting problem

Laser welding is able to weld the two films together and the same laser will also be used for cutting the trays out of the film. The difference is the power settings on the laser. But under cutting the remained two films will be interconnected and make opening difficult.

In order to solve this problem the mould need to have a little shape down in order to avoid this problem.

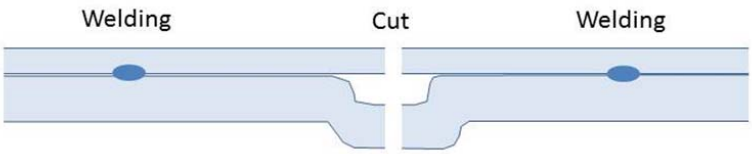



**Figure 25:** Cutting problem solved with a little distance between top and bottom films

### 3.4.3 Level problem under cutting the final trays

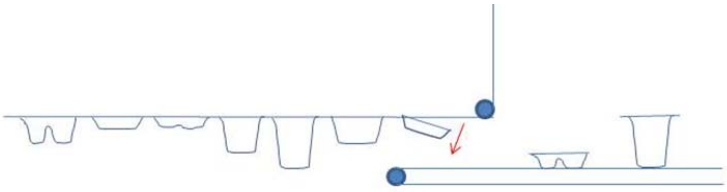


**Figure 26:** Level problems under cutting the final trays

The laser does not cut the final trays out in one cut. The cutter works continuously over the cutting line. This means that some parts of the tray are connected to the basis film and other parts are not. For that reason the tray will swing down to the conveyer transporting the trays to next operation. If the trays have the same height the conveyer can be adjusted, but this is not the case.

We need to develop a system taking care of this problem.

### 3.4.2 Inspection

The inspection will be done by an IR-camera placed about 500 mm above the packaging. The inspection is a scanning of the welding done line-by-line.

## 4 Total adaptive packaging line

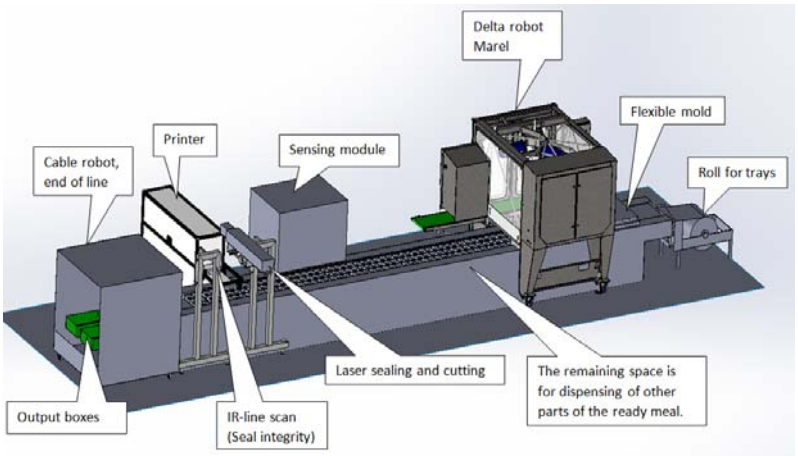



**Figure 27:** Lay-out for WG6 Adaptive packaging line in PickNPack

After the flexible forming section on right a robot will fill the trays with big solid components. In the open space after dispensers can add extra components as bulk, liquids etc. After the sensing module the printed top film will be applied from the side in order to have distance to printing process for food safety reasons. Finally the pack are welded, inspected and cut before a robot is sorting different products to several pallets.

## 5 Conclusions

PickNPack has big ambitions to create an extreme flexible packaging line for food packaging. Over the last 1½ year different partners have investigated many different details in order to fulfil the aim. Over the summer of 2014 PickNPack will build the first prototype expected to be tested in the winter of 2014-15. Partners from PickNPack will later inform about these results.

## Acknowledgements

Authors would like to acknowledge the EU Seventh Framework Programme (FP7-KBBE) for providing financial support for this research that is currently being conducted in the frame of the PickNPack project .

## References

1. WORK PROGRAMME 2012, COOPERATION, THEME 2, FOOD, AGRICULTURE AND FISHERIES, AND BIOTECHNOLOGY (European Commission C(2011)5068 of 19 July 2011)
2. OptiMal Forming Solutions (www.optimalforming.com)

# Sulfide Black in Canned Meat

**Fiorella B. H. Dantas[1*], Sílvia T. Dantas[1], Paula F. J. Bócoli[1], Ana Paula S. Bernardo[2] and Marise Ap. R. Pollonio[2]**

[1] *Packaging Technology Center – CETEA, Brazil*

[2] *University of Campinas – UNICAMP, Brazil*

[*] *Corresponding author. Email:fiorella@ital.sp.gov.br*

**Abstract:** Sulfide black and sulfide staining are generic terms used to define the bleaching occurring inside the cans during food packaging. It occurs due to the reaction between sulfur products and some components of the package, such as tin or iron, forming sulfides of brown, black or purplish color. Although it is not dangerous to human health, not changing flavor, odor or the nutritional value of the product, and does not lead to package failures, sulfide staining changes the appearance of the product and its packaging, causing strong negative impact on packaged products, among which stands out the canned meat.

This study aimed to evaluate sulfide black formation upon different process parameters variations (tin layer, cure of lacquer applied inside, presence or absence of superficial scratches in the lacquer, sterilization time and temperature and filling temperature) by analyzing the composition of the black spots using the techniques of infrared spectroscopy, scanning electron microscopy (SEM) and microanalysis by X-ray dispersive energy (EDX). The characteristics of the steel can exposure through the porosity of the lacquer and the tin layer were also evaluated.

The results of SEM and EDX showed that there was exposure of metallic material and the region of the cans with a higher incidence of black spots was the curvature or radius of the lid in the countersink region and spectral microanalysis showed the presence of P and Cl in the stains, indicating a probable relationship of these elements with the sulfide black reaction. Attenuated total reflectance Fourier transform infrared spectrometry (ATR-FTIR) affords a lot of structural information in order to evaluate the organic part of the different products. It shows that there are differences between regions with and without the presence of sulfide black associated to the carbonyl group bonds characterized by C = O and the center N. In addition, it was possible to conclude that the techniques are suitable tools in the sulfide black evaluation.

Keywords: sulfide black, corned beef, canned meat, metallic packaging, SEM/EDX, ATR – FTIR.

## 1 Introduction

High-protein food such as canned food, poultry, fish and leafy vegetables may be a source for sulfide black. The free hydrogen sulfide released by the degradation of proteins, when in contact with the metal from the packages results in metal sulfides. The formation of tin sulfides (sulfide staining) produces the colors violet and brown, whereas iron sulfides (sulfide black) results in stains or black spots.

Brazil is one of the world's largest exporters of beef either fresh or processed. Corned beef is the processed product obtained exclusively with beef, which is cured, cooked, packaged, hermetically sealed, commercially sterilized and quickly cooled down. Beef, the major ingredient of corned beef, is one of the main products susceptible to the reaction, as it consists of about 3% of sulphurated amino-acids such as cysteine and methionine.

This study aimed to evaluate sulfide black formation upon different process parameters variations (tin layer, cure of lacquer applied inside, presence or absence of superficial scratches in the lacquer, sterilization time and temperature and filling temperature) by analyzing the composition of the black spots using infrared spectroscopy, scanning electron microscopy (SEM) and microanalysis by X-ray dispersive energy (EDX) techniques.

## 2 Material and Methods

### 2.1 Product

The corned beef was produced by using frozen industrialized meat from slaughter-houses under the federal inspection, and by adding liquid fat (approximately 1%) and nitrite solution (0.06%). The meat was previously cooked and then grounded in discs with holes of 4 mm diameter.

The processing consisted of the following stages: cooking, mincing the raw material, formulation and homogenization, packaging, double seaming, thermal treatment and the final product packaging.

### 2.2 Cans

Trapezoidal welded tin cans with easy-open bottoms were used. The production consisted of two stages: preparation of tinplates by cutting coils, lacquering and curing and then the manufacturing of each can component (lid, body, and bottom), as well as double seaming. The variables established for the can lids were the following: 2.8 and 5.6 g/m$^2$ internal tin coating, lids with superficial scratches and normal lids, as well as internal lacquer cure temperature: normal (200 ºC) and supercured (220 ºC). The internal face of the body and bottom were made of 2.8 g/m$^2$ tin layer and the lacquer was epoxy-phenolic with aluminium, cured under normal conditions. Powder lacquer was applied as side stripe.

### 2.3 Characterization of Metal Exposure

The can porosity was determined by the electrochemical method (WACO Enamel Rater Test, Chicago, Illinois, USA) and the iron evaluation value was carried out in a EG&G Model 273A potentiostat/galvanostat system, controlled by a EG&G 354 program (EG&G PARC, Princeton, New Jersey, USA), using three-electrode cell. The method involves measurement of the anodic dissolution current of exposed iron in tinplate cans, this amount is proportional to the current value and its location is detected as deposits of hydrated iron oxide on the iron exposure positions.

### 2.4 SEM Analysis

Test pieces were cut out of the cans and small amount of the product were collected in the regions with and without spots. All the samples were mounted on aluminium stubs, followed by carbon coating using a SCD 050 sputter coater by Balzers. Either secondary or backscattered electron images were obtained with a Zeiss DSM 940A scanning electron microscope with analysis carried out using a Link Isis microanalysis system by Oxford instruments equipped with an Oxford detector to obtain X-ray spectra. X-ray microanalysis was performed at an acceleration voltage of 20 kV, specimen tilt (0º), working distance (25 mm) and emission current (80 µA). Analysis was focused on the specific areas of interest with an appropriate zoom.

### 2.5 Infrared Analysis

The black stains were evaluated by infrared spectroscopy in a Perkin Elmer Model FT-IR Spectrum 100, by direct transmission reading. Each ATR-FTIR spectrum was collected by using 16 scans/sample at 4 cm$^{-1}$ resolution. Before scanning each sample, the background spectrum was taken with an empty ATR crystal and stored in the computer. Each sample was replicated two times.

### 2.6 Statistical Analysis

The averages obtained in the porosity (lacquer and iron) results were compared by Tukey's test, considering 95% confidence level, through Statistica program, version 5.0 (1995)[1].

## 3 Results and Discussion

### 3.1 Characterization of Metal Exposure

Table 1 shows the porosity of the samples identified as normal cure lacquer and supercured lacquer. Figure 1 shows the graph for the iron evaluation value for each batch. Both determinations are directly related to the iron exposure and availability for sulfide black reaction, the object of this study.

According to the results, both batches of normal cure lacquer as supercured lacquer presented similar porosity results (with no significant difference between the results at 95% confidence level). However, it was observed that the coefficient of variation for the supercured-lacquered can is higher (61%) than the coefficient for normal cure lacquered can (56%). Probably, the higher porosity of supercured cans can be due to a higher discontinuity of the lacquer caused by reduced flexibility as compared to the normal cure lacquer. Dantas *et al.* [2] found

porosity in the internal lacquer in pea cans of 63.2 ± 5.3 mA/can, for the lacquer identified as oleoresinous and with suitable cure degree, and for aggressive products such as tomato sauce. Dantas *et al.* [3] found internal porosity of 47.6 ± 13.9 mA/can for the lacquer identified as epoxy phenolic with appropriate cure degree. Considering the similarity of surface area, these results are reasonably equivalent to those found for the cans containing corned beef evaluated in this study.

**Table 1:** Results for porosity tests (mA/can)[(1)].

| | Normal Cure Lacquer | Supercured Lacquer |
|---|---|---|
| Average | 35.4a | 35.2a |
| Standard deviation | 19.9 | 21.6 |
| Variance | 3.5 – 86.5 | 19.3 – 118.5 |

*a, b – means followed by the same letter in the same row do not differ significantly, at 95% confidence level by Tukey's test*

As shown in Figure 1, the batches produced with 2.8 g/m$^2$ tin layer presented similar results, with average IEV values below 15 µA/can, with no statistical difference at 95% confidence level for these samples. Despite the mean values for the batches produced with 5.6 g/m$^2$ tin layer and super cured lacquer were up to 14 times higher than the batches with 2.8 g/m$^2$ tin layer, no statistical difference was observed, probably due to the high coefficient of variation. However, the mean results for the batches produced with 5.6 g/m$^2$ tin layer and normal cure lacquer were statistically different from the other batches at 95% confidence level.

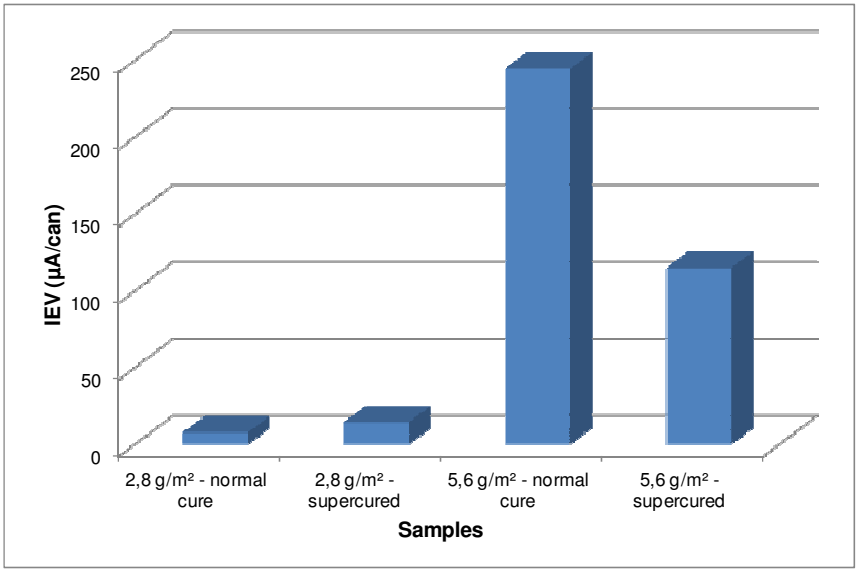



**Figure 1:** Mean results of the iron-exposure value (IEV) for the cans containing corned beef.

The cans produced with tin layers of 5.6 g/m$^2$ exhibited more exposed base metal as compared to the other batches, unlike what was expected, since a higher tin layer provides a better steel covering. However, as the further development of lacquers occurred for smaller layers, there is greater tin layers can lower lacquer adhesion to the metal substrate, which could explain the higher values found for the batches produced with tin layer of 5.6 g/m$^2$. Overall, the IEV values of the present study can be considered low, once Moreno Filho [4] found values of 0.89 mA/cm$^2$ and 1.68 mA/cm$^2$, and 0.62 mA/cm$^2$ and 1.62 mA/cm$^2$ for cylinders with and without expansion, respectively, when studying two tinplate samples with the same thickness (T52 temper, box annealing and T59 temper, continuous annealing) used in the manufacture of expanded cans.

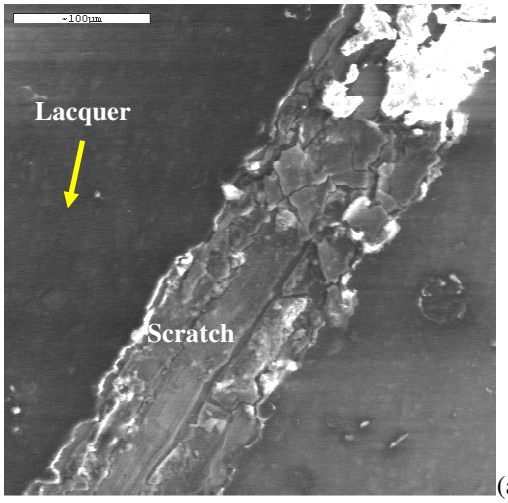
## 3.2 SEM Analysis

Figure 2 shows the micrographs obtained by SEM/EDX for the black stains on the lids of the corned beef cans. The presence of the black deposit was always associated with the metal exposure regardless of whether or not caused intentionally. Figures 2a and 2b show the lid scratches and the black spots, while Figures 2c and 2d show

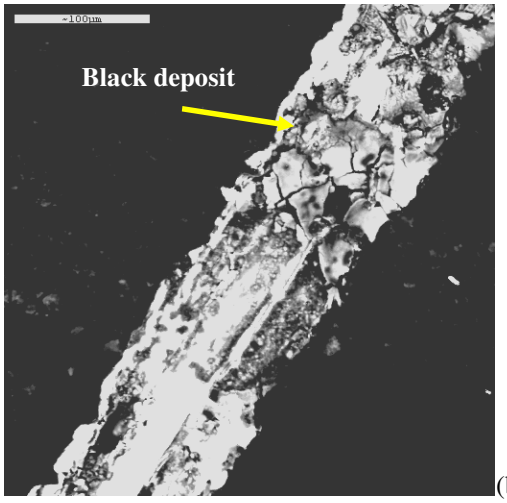
a continuous line of detached lacquer known as depth of the recess near the seaming region. Charbonneau [5] reported the relationship between lacquer failures and the occurrence of sulfide black in cans of minced clams.

Double seam is a necessary step for joining the ends (cover lid or bottom) to the body of the cans, but it involves intense deformation of both the metal as of the lacquer, which may not withstand, thus rupturing and exposing the metal. The metal exposure was also observed in the lids with 5.6 g/m$^2$ tin layer (Figures 2e and 2f), evidencing the effect of the lacquer adhesion failure due to the greater layer.

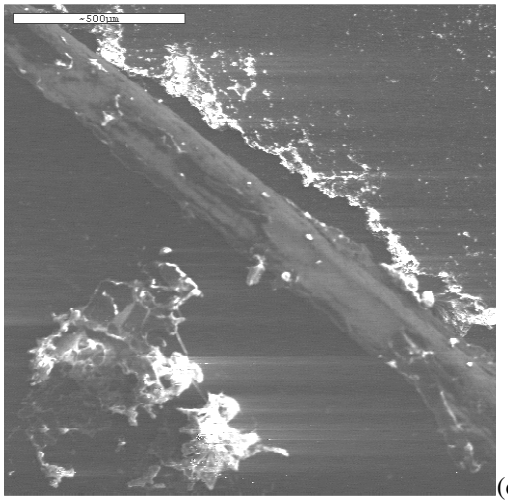
The images also showed the occurrence of corrosion (Figures 2a and 2b, 2e and 2f) and Fe exposure, making it available to react with the S from the product.



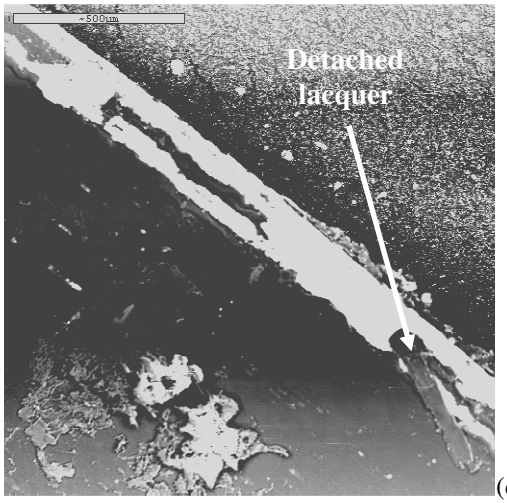
(a)



(b)



(c)



(d)

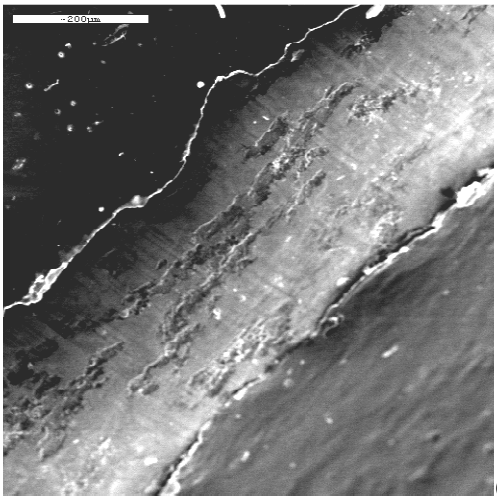
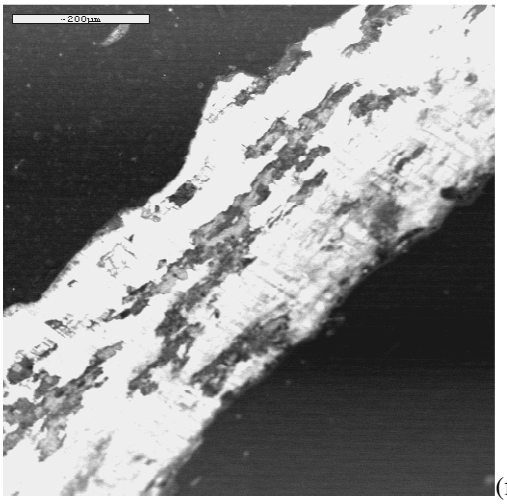

(e)

(f)

**Figure 3:** Photomicrographs of the test pieces showing the lids with black stains, obtained by SEM/EDX system: (a), (b), (c) and (d) lids with 2.8 g/m$^2$ tin layer and normal cure lacquer; (e) and (f) lids with 5.6 g/m$^2$ tin layer and normal cure lacquer. The pictures (a), (c) and (e) were obtained by SE detector, and the pictures (b), (d) and (f) were obtained by BSE detector all at an acceleration voltage of 20 kV, specimen tilt (0º) and 25 mm of working distance.

Table 2 shows the chemical elements found on both the surface of the can lids of corned beef with sulfide black and the product. The elements without number, on the right, have been observed in 100% of the spectra. Values in parentheses correspond to the occurrence of each element, in relative percentage.

**Table 2:** Chemical elements found in both the internal surface of the can lids containing corned beef with sulfide black and in the product

| Region | Majority elements | Other elements |
|---|---|---|
| Stain - Product | Cl | Na (93%), Mg (13%), P, S, K, Ca (27%), Fe (53%) |
| Stain - lid scratch 2.8 g/m$^{2(1)}$ | S | P, Sn, Fe, Si (20%), Cl (40%), Mg (40%), Na (20%), Ca (80%) |
| Stain - lid 2.8 g/m$^2$ | Cl, Fe | Na (50%), S (75%), K (75%), Al (25%), Ca (25%), Si (25%), Ti (25%) |
| Stain - lid 2.8 g/m$^2$ (other can) | Fe | P, S (88%), Cl (88%), Sn (38%) |
| Stain - lid seam 2.8 g/m$^2$ | Ti | S, Ca, Fe, Zn, Al (75%) |
| Stain - lid 5.6 g/m$^2$ | Sn | Fe, S (82%), Cl (45%), Ca (36%), Si (18%) |
| Stain – lid 5.6 g/m$^2$ (other can) | Fe | S, Sn, P (33%), Cl (33%) |
| Lacquer | Al | Sn, Fe |

*Chlorine / Sodium / Magnesium / Phosphorus / Sulfur / Potassium / Calcium / Iron /Tin / Silicon / Aluminum/ Titanium / Zinc*

*(1) intentionally scratched can*

According to the results in Table 2, the spectra of the product have indicated Cl as a major element, and Na, Mg, P, S, K, Ca and Fe as the other elements. The presence of the elements Na, Mg, Cl, Ca and P is related to the product composition (corned beef), while the presence of Fe in most of the spectra is due to both the metallic

(tinplate) package and the iron coming from the product. With respect to the element S, besides derived from the sulfur-containing amino acids of the product, it comprises the sulfide black found in the lids under study. Williams [6] determined the nutritional composition of beef in Australia and found that these chemical elements are present in that meat even at concentrations below 1%. Elements such as Na, Cl and K also constitute the ingredients added in the dry blend, such as salt or curing agents.

Most of the spectra exhibited P and Cl, indicating a probable relationship of these elements with the sulfide black reaction. However, Charbonneau [5] found that despite the black spot can occur without the presence of S, it occurs in the presence of Fe and P, but the study by Kontominas *et al.* [7] found S in fish cans. Charbonneau [5] concluded that the stain may be composed of $Fe_3PO_4$ while Kontominas *et al.* [7] reported it as FeS. Pournaras *et al.* [8] found that the stains on tinplate cans containing octopus in brine presented Sn, Zn, S, Fe and Si and reported that, despite the presence of Fe, tin sulfide was formed, while Zn came from the lacquer and Si from the metal sheet.

In addition, despite Sn was not found in the lids with 2.8 g/m$^2$ tin layer in concentrations above 1%, it was found in the lids with 5.6 g/m$^2$ tin layer, evidencing that the coating thickness had an influence on the Fe exposure.

Figure 4 shows the spectral microanalysis of the stains from the product and from the surface of the can lids of corned beef.

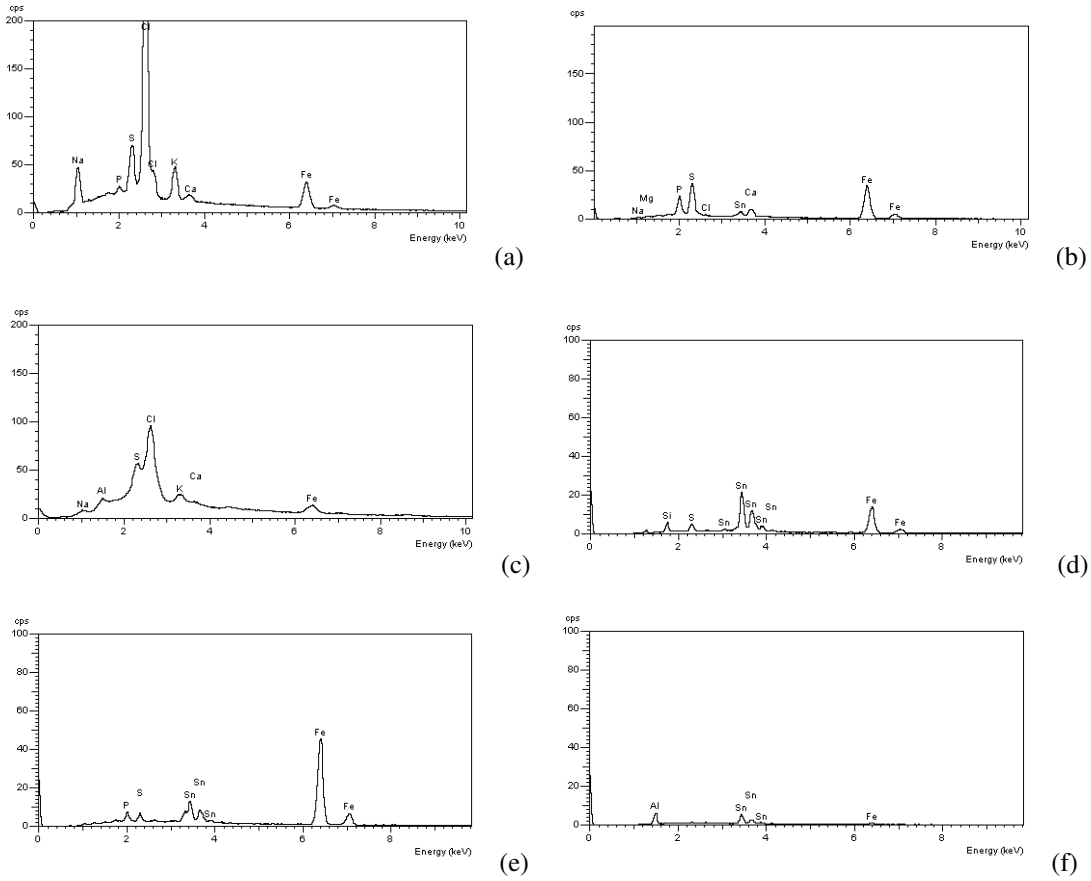



**Figure 4:** Spectral microanalysis of the stains collected from both the product and the surface of the can lids of corned beef by SEM/EDX system operating at 20 kV and working distance of 25 mm: (a) stain collected from the product; (b) stain in the intentionally scratched lid with 2.8 g/m$^2$ tin layer; (c) stain in lid with 2.8 g/m$^2$ tin layer; (d) stain in lid with 5.6 g/m$^2$ tin layer ; (e) stain in another lid sample with 5.6 g/m$^2$ tin layer (f) lacquer.

Except for the intentionally scratched cans, the region with higher incidence of stains was the curvature or cover radius. This result demonstrates that the seam area, where there is greater mechanical stress lacquer, should receive more attention during the steps of lacquer specification, application to the metal substrate, and closing. The results found for iron exposed value evidenced the influence of the tin layer on the metal exposure, but the seam tightness can also damage the lacquer especially when high temperatures of curing reduce the flexibility and the lacquer becomes crumbly. Birkeland *et al.* [9] found that increasing seaming-roller pressure caused a

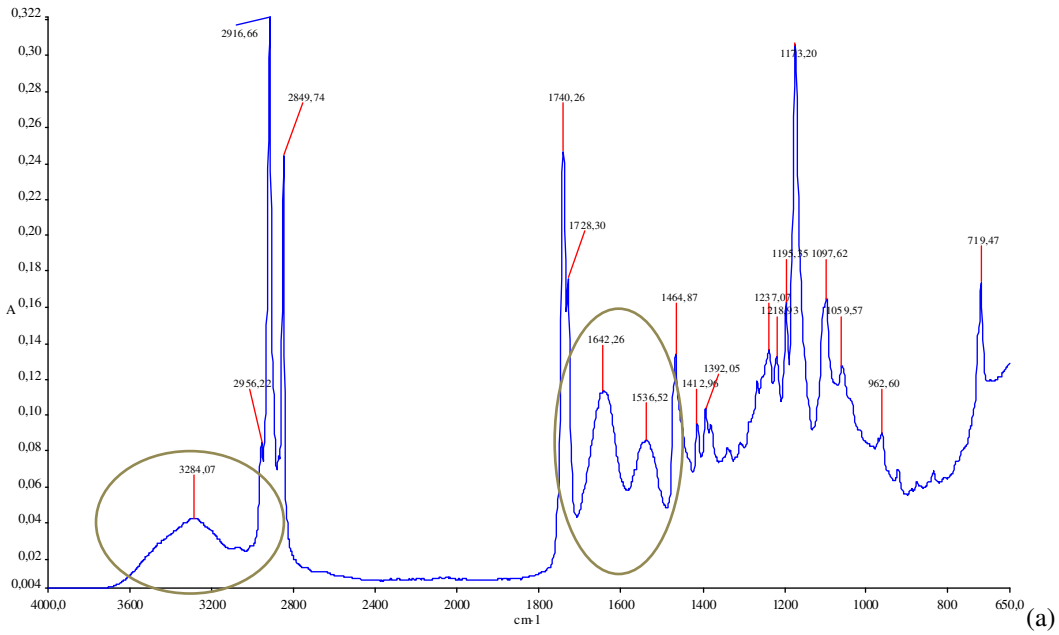
significantly decrease in the double seam thickness, greater compression of the material (tin plate and lacquer) and consequently a greater mechanical stress of the lacquer in the weld seam region.

## 3.3 Infrared Analysis

The spectra obtained from FTIR-ATR showed strong C-H absorption between 3000 and 2850 $cm^{-1}$. Oils also have strong bands at 1749, 1464 and 1165 $cm^{-1}$ that correspond to C=O (ester) stretching, C-H bending (scissoring), and C-O, $CH_2$ stretching, bending, respectively [10]. For the fat samples, these compounds corresponded to the bands at 1740, 1464, and 1172 $cm^{-1}$, respectively. Papadopoulou *et al.* [11] evaluated pork samples and reported the occurrence of a major peak at 1640 $cm^{-1}$, which was related to the moisture content (O-H) and contribution of amide I bands of the proteins. A second peak was observed at 1550 $cm^{-1}$ due to absorption of amide II (C-N stretch), followed by a peak at 1745 $cm^{-1}$ corresponding to fat (C=O ester carbonyl) [11].

The differences between the spectra of the stains observed on fat and the spectra of the fat only (without stains) are mainly found between 1500 and 1700 $cm^{-1}$, whose structural units may be classified as belonging to the carbonyl group, possibly ketones and tertiary amines. The ketones are characterized by C=O bonds, while amines have a central N. Thus, it can be stated that compounds from degraded proteins may be present in the black spot, as well as compounds resulting from the degradation of sodium nitrite added to corned beef, evidencing a reaction between the amino acids coming from meat and Fe from the cans. The presence of C was expected due to the interface between the fat and stain, as well as the presence of O, since the product is characterized by low vacuum packaging and low free-space and the consequent presence of air inside the package. The presence of oxygen should not be desired and controlled using free-space and vacuum since the oxygen depolarizes, accelerating the corrosion process, and consequently, the sulfide black reaction. The lower the oxygen concentration in the storage atmosphere, the lower the peroxidation rate in meat [12]. The authors also verified that during a short period of storage, aerobic packaging (packaging with gas concentration equivalent to the atmospheric air) did not appear to be a critical factor in the development of lipid oxidation in beef, but in the case of metallic packaging there is an additional point that is the acceleration of the corrosion process.

Spectra obtained by ATR-FTIR representing both the spectra of the stains observed on fat and the spectra of the fat only (without stains), with the differences highlighted are presented Figure 5.



(a)

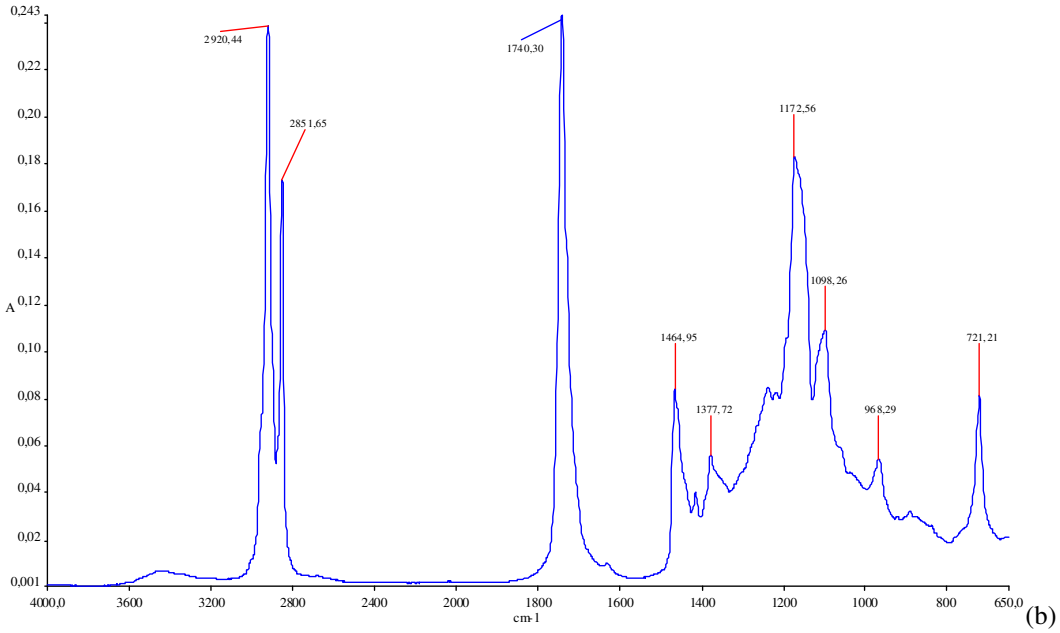



**Figure 5:** Spectra obtained by ATR-FTIR representing both the stains on the fat (a) and fat without stains (b). The circles indicate the differences caused by stains formation.

## 4 Conclusions

Cans produced with lids with 5.6 g/m$^2$ tin layer presented higher metal exposure, indicating that lacquer adhesion is lower in greater tin layers. Furthermore, the present study has shown that the black stain was always associated with the metal exposure, since most of the cans exhibited stains along the double seam lacquer failure. Thus, there was no evidence of $S^{2-}$ ion permeation through the lacquer. The black stains were comprised of amino acids and other components coming from the product, including C and O, showing the effect of the packaging process in the occurrence of sulfide black. In additional, it was possible to conclude that the techniques are suitable tools in the sulfide black evaluation.

## 5 Acknowledgements

The authors thank FAPESP (2011/09717-0) for the financial support for this study, and the company JBS S.A. for providing the materials, cans and processing plant.

## 6 References

1. Statistica (data analysis software system). version 5 StatSoft. Inc.,Tulsa, Oklahoma (USA).
2. S.T. Dantas, J.B. Gatti, E.S. Saron, P.H.M. Kiyataka, F.B.H. Dantas, 2011, “Stability of canned peas in tinplate cans with reduced layer”, *Brazilian Journal of Food Technology*, v. 14, no. 3, pp. 249-257.
3. S.T. Dantas, J.B. Gatti, E.S. Saron, P.H.M. Kiyataka, F.B.H. Dantas, 2012, “Stability of canned tomato sauce in tinplate cans with reduced tin layer”, *Brazilian Journal of Food Technology*, v. 15, no. 2, pp. 110-117.
4. V. Moreno Filho, 2007, “Metal Packaging: evaluation of tinplates used to make cans through the stretching process”, *Instituto Mauá de Tecnologia*, São Caetano do Sul, v. 1, p. 158.
5. J.E. Charbonneau, 2001, “Investigation of corrosion and container integrity in metal food containers using scanning electron microscopy X-ray microanalysis”, *Scanning*, v. 23, no. 3, pp. 198-203.
6. P. Williams, 2007, “Nutritional composition of red meat”, *Nutrition & Dieletic*, v. 64, pp. S113-S119.
7. M.G. Kontominas *et al.*, 2006, “Investigation of fish product–metal container interaction using scanning electron microscopy X-ray microanalysis”, *Food Chemistry*, v. 98, no. 2, pp. 225-230.
8. A.V. Pournaras, M.I. Prodomidis and A.P. Katsoulidis *et al*, 2008, “Evaluation of lacquered tinplated cans containing octopus in brine by employing X-ray microanalysis and electrochemical impedance spectroscopy”, *Journal of Food Engineering*, v. 86, no. 3, pp. 460-464.

9. S. Birkeland, H. Bergslien, A. Strand and M. Sivertsvik, 2005, "Effects of seaming conditions on external and internal double seam characteristics in round metal cans", *Packaging Technology and Science*, v. 18, pp. 279-283.

10. B. Innawon, P. Mallikarjuna, J. Irudayaraj and J.E. Marcy, 2004, "The determination of frying oil quality using Fourier transform infrared attenuated total reflectance", *Lebensm.-Wiss. u.-Technol.* v. 37, pp. 23-29.

11. O. Papadopoulou *et al*, 2011, "Contribution of Fourier transform infrared (FTIR) spectroscopy date on the quantitative determination of minced pork meat spoilage", *Food Research International*, v. 44, pp. 3264-3271.

12. F. Ferioli, P.C. Dutta, PC and M.F. Caboni, 2010, "Cholesterol and lipid oxidation in raw and pan-fried minced beef stored under aerobic packaging", *Journal of the Science of Food and Agriculture*, v. 90 , 1050-1055.

# Packaging for Controlling Texture of Frozen Microwaveable Sandwiches

**Alexander Bardenstein*, Helle Allermann, S. Vikram Singh, and Stanislav Landa**

*Packaging Section, Danish Technological Institute, Denmark*

**Corresponding author. Email: alb@dti.dk*

**Abstract:** A generic packaging concept for frozen microwaveable sandwiches allowing the retaining of the original dual texture of the bread (crispy exterior–soft interior) is proposed and tested. The packaging comprises two main functional components: Internal packaging, which is a perforated cardboard microwave susceptor box with built-in metal film coil that is thick enough to displace the microwave field, and external packaging, which is a heat-insulating box or bag. For instance, this can be a corrugated carton or a paper wrapping with a barrier polymer coating. Each of these inherent components carries a whole number of functions determined by thermal and dielectric properties of the both bread and fillers in the sandwich. Being put together in a packaging unit, they prevent 'water pumping' and staling phenomena in the re-heated bread at the same time achieving homogeneous heating of all sandwich components. This concept has been particularly embodied in tailor-made packaging solutions for several kinds of frozen sandwiches that include top and bottom bread, cheese, bacon, sausage patty or burger, egg patty etc.

Keywords: active microwave packaging, frozen sandwiches, bread texture, heating homogeneity.

## 1 Introduction

In a world that is pressed for time, ready to heat microwaveable buns, sandwiches, hamburgers, and sausage rolls are convenient and are now getting popular both for breakfast and lunch. This is why demand for microwaveable food has increased. Moreover, consumers want to shorten cooking time without compromising with the taste, high nutritional values and indeed the conventional 'home-made' food experience. Often, microwaveable products fall short of providing this. For example, frozen bread products present a challenge in the microwave because of textural changes that occur during heating from frozen. Bread from a traditional oven tastes and looks 'fresh', but when heated in the microwave, loses its texture and flavour. To a large extent, this results from a known phenomenon described e.g. by Schiffman [1] and referred to as 'water pumping'. In the microwave oven, water vapor pressure increases in the product's interior and pumps the vapor rapidly toward its surface, saturating it with moisture. At the same time, air inside the oven remains cold and water vapor therefore condenses and cools the exterior of the re-heated product, resulting in no browning and a soggy surface. Naturally, the interior of the product is simultaneously deprived of its initial moisture content. In the case of frozen bread, this simply means that microwave re-heating leads to loss of its natural dual texture, i.e. crispy crust and soft interior.

Besides the above mentioned trouble with retaining the bread texture in the microwave, it is also difficult to homogeneously heat multicomponent bread-based products, such as sandwiches, hamburgers, and rolls. Food components, i.e. bread and such fillings as burgers, sausages, egg, cheese, bacon, filleted fish etc. heat at different rates due to difference in their dielectric and thermal properties, and also their geometrical shapes. Ryynänen *et al.* [2] thoroughly investigated microwave heating of a hamburger sandwich and concluded that a homogeneous temperature distribution in such a small load is very difficult to achieve, and the heating uniformity cannot be improved by barely modifying a recipe. Furthermore, the temperature of a re-heated product must reach a minimum of 75°C in every component in compliance with, for instance, the Danish Veterinary and Food Administration regulations. It is clear that for example a bun in a hamburger may already be heated up to water vaporization temperature, thereby loosing moisture content and getting stale, while the meat component remains underheated. Thus, deterioration of the bread texture in multicomponent sandwiches may result both from uneven heat caused by their intrinsic heterogeneity and from the 'water pumping' effect discussed above.

This reasoning leads to a sincere conclusion that texture-retaining homogeneous microwave re-heating of frozen sandwiches requires active packaging that controls the electromagnetic field and temperature distributions both inside the product and in its immediate vicinity. In this study we have emphasized the development of such a generic yet practical active packaging concept and performed its experimental validation for several kinds of frozen sandwiches.

## 2 Peculiarities of microwave heating of bread

Keeping in with the aim, comprehensive experimental studies and computer simulations of microwave heating of frozen buns were first carried out in order to identify physical outlines of the packaging concept.

The samples were 50-60 gram wheat-bread buns shaped as cylinders (e.g. so-called Toast Buns and Biscuits) or as compositions of a spherical-segment top on a cylindrical bottom (e.g. classical Hamburger Buns). Microwave heating experiments were carried out using appliances of distinct brands allowing 650-700 W of microwave power output at full-power operation. The microwave power was measured using a standard 'Determination of microwave power output' test as provided by the IEC/EN 60705 standard. Temperature distributions of the heated products were visualized and measured using infrared camera Testo 878 (Testo AG, Germany) and fiber-optic temperature sensors Neoptix T1 connected to the 4-channel data processing unit ReFlex (Neoptix, Inc, Canada). The fiber-optic sensors were also used to perform *in-situ* monitoring of the interior temperature.

Finite-Element Method (FEM) computer simulations of microwave heating were carried out using the COMSOL Multiphysics FEM software environment. Following COMSOL add-on modules have been employed:

- Radio Frequency(RF) Electromagnetics Module to simulate radiation, transmission, reflection and absorption of electromagnetic waves, including radio- and microwaves;
- Heat Transfer Module to simulate heat conduction, convection, and radiation.

The experiments and simulations allowed making the following outline of the physical processes that accompanying microwave re-heating of a frozen bun placed unpacked in an oven on a microwave-transparent plate. In the beginning, frozen bread transmits microwaves nearly lossless from every direction. This is because the energy of microwaves can dissipate in the bread almost solely by thermal motion of water molecules, and their mobility is significantly depressed at low temperatures. Indeed, penetration depth in the ice at –20°C for 2450-MHz microwaves (as used in microwave ovens) is about 12 meters. Nevertheless, dielectric permittivity of the frozen bread is still considerably higher than that of the surrounding air, and microwaves that penetrate from different directions are superimposed ('focused') in the core of the bun. This effect is illustrated in Figure 1 by pictures on the left. Analogous 'focusing' arises in axisymmetric bread components of sandwiches, e.g. in a top bun of a hamburger that has a form of a spherical segment, or in a cylindrical biscuit.

Consequently, the water in the core of a bun thaws up faster than in the subsurface layers. Once thawed, the bread core absorbs microwaves 8 times better (see also Figure 2). Thus a lot of heat is promptly accumulated in the core, and its temperature grows rapidly. This is an excellent example of a runaway heating; as the frozen bread core thaws it absorbs microwaves better, so it heats up quicker. The heating makes absorption of microwaves easier and easier, until the core temperature reaches steam point, as it is shown in Figure 1 (see pictures on the left).

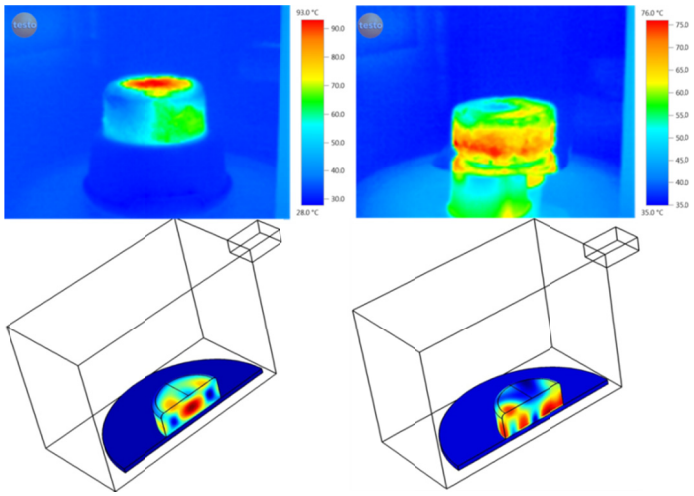


**Figure 1**: Thermal images of the microwaved cylindrical bun (pictures on the top) and results of FEM 3D computer simulation (pictures on the bottom) for microwave transparent (pictures on the left) and reflective (pictures on the right) supporting plates. Microwave output power is 650 W, and the heating time is 30 s.

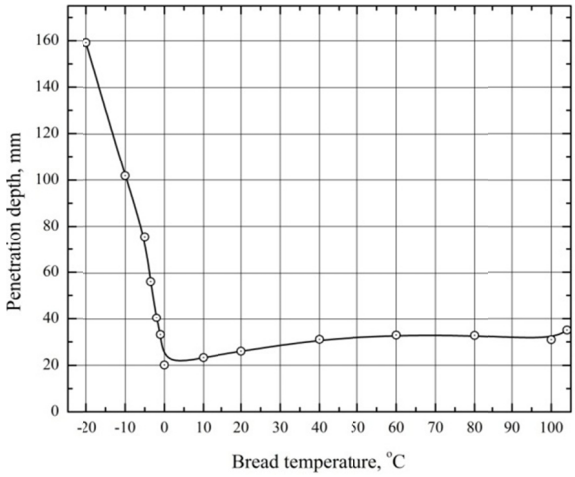



**Figure 2:** Penetration depth of 2450-MHz microwaves in the Standard Nordic White Bread versus temperature. The points resulted from calculations that made use of the data on the bread permittivity at 2450-MHz provided by P. O. Risman, Microtrans AB, Sweden. The permittivity data have been used in COMSOL Multiphysics models for the simulation of microwave heating of frozen bread.

With regard to the bread texture, this moment signifies the beginning of its irreversible change since evaporating water diffuses toward bread crust. It is simply driven by a strong temperature gradient directed outward, as the interior of the oven is still cold and works as a heat sink for the bread surface. Thus, the core dries out, whereas the crust gets soaked. But most importantly, the peak of microwave absorption will now shift from the core to the surface, which, in its turn, also dries out and cracks. The dehydrated bread core then gets hard like wood. Finally, the bun becomes 'crusty, tough and dry and certainly inedible', well known experience among the regular microwave oven users [3].

Now, let us get onto the analysis of re-heating results of exactly the same bun placed on a reflective bottom, which are shown in Figure 1, pictures on the right. It can be seen that the temperature distribution becomes much more homogeneous, and it does not have any pronounced localized maximum in the center of the core. This obviously happens because the microwaves are 'defocused' by means of a 'mirror' placed under the bun. Moreover, the temperature does not exceed 80-90°C in this case, and the bun does therefore not lose any moisture, i.e. the bread interior does not dry out. This is the irrefutable evidence that the softness of the bread interior may be preserved solely by using reflective or partially reflective packaging components. Unfortunately, the sole use of microwave reflectors as active packaging components does not help to make the bread crust crispy.

Such a thorough consideration enabled us in the final analysis to pick out two fundamental indispensable conditions for securing an acceptable quality of the bread prepared in the microwave oven:

1. Microwaves must not superimpose in the frozen bread interior, i.e. it is necessary to shield bread partially.
2. The surrounding air temperature in the vicinity of the bread surface must considerably exceed 100°C in order to avoid the thermo-stimulated water diffusion toward the crust and at the same time toast the bread crust brown and crispy.

## 3 Formulating the packaging concept

Obviously, active packaging that controls microwaves' penetration and heat distribution in a product is required in order to meet the above listed conditions. Moreover, it is inevitable that one of the key elements of the packaging must necessarily be constructed from a microwave *susceptor* that is widely used in microwave packaging for crisping and browning. Note, that a susceptor absorbs microwaves and transforms them into heat [1, 4, 5]. In food packaging practice, a susceptor is a laminate of metalized polyester film and cardboard or paper [4]. Essentially, the thickness of this metal coating should be much less than the skin depth for alternating electrical current at 2450 MHz. For instance, an aluminum layer demonstrates pronounced susceptor properties if it is thinner than approximately 10 nm [4]. The temperature of such a susceptor laminate stabilizes at approximately 220°C in a microwave oven, where it may then heat food by conduction, or convection, or by infrared radiation. Moreover, this material not only absorbs but also reflects and transmits microwaves: Fractions of incident power absorbed, transmitted, and reflected by an aluminum susceptor film at optimal operation conditions are ~ 0.5, ~ 0.25, and ~ 0.25, respectively [4].

Thus, microwave power fractions reflected and transmitted by continuous susceptors are approximately equal. However, if it becomes necessary to accent this equilibrium, e.g. if the susceptor's reflectivity is not high enough to provide for a microwave field configuration resulting in homogeneous re-heating, then, as it has already been concluded above, *reflective* elements must be used and combined with susceptors in order to achieve the desired effect. It has to be recalled that a continuous metallic layer becomes a total reflector if its thickness exceeds triple skin depth, e.g. for the frequency of 2450 MHz this is an aluminum layer, whose thickness is above ~ 3 μm [5].

Interestingly, the opposite situation is also possible, when reflection and/or absorption of susceptors is locally higher than it is necessary. This can be solved by means of implementation of *patterned perforation* in continuous susceptor sheets. As a matter of fact, perforated *reflectors* partially transmitting microwaves have been extensively studied and found their use in different technical and physical applications [6, 7], and this approach may be adopted for reduction of reflectivity of continuous susceptors at 2450 MHz. At the same time, absorptivity of a perforated susceptor sheet gets reduced as against continuous material. Thereby perforated susceptors can be used for *fine optimization* of microwave power losses and heat rating delivered to different surface patches of a packed food product.

Thus, use of perforated susceptors and reflective elements should theoretically allow meeting above derived conditions of texture-retaining microwave heating of bread products. However, experiments and practice of susceptor packaging show that the use of susceptors does not always help against the 'water pumping' phenomenon [1]. We believe that this insufficiency results from two obvious thermodynamic phenomena.

First of all, a significant amount of heat generated in the susceptor simply dissipates in the cold air and never reaches the product. Therefore, the energy, which could otherwise strike a blow for heating and dehydrating the product's crust thereby browning and crisping it, is irretrievably lost.

Secondly, the susceptor and therefore the air surrounding the product, instantly cools down when microwaving is cut off. On the contrary, the product's interior remains hot for a few minutes after termination of heating. Thus, the 'water pump' that does not function when the susceptor is hot, starts squeezing moisture out of the products interior again and swamps the crust with the condensing vapor. Obviously, in order to avoid 'water pumping', the air adjoining the crust must not cool down faster than the interior of the product.

These considerations lead to an apparent solution of having a sufficient thermal insulation around the product that is already packed in a combined susceptor/reflector 'jacket'. Thus this has now become clear that the packaging must comprise two main functional components:

1. Internal 'active' packaging, which is closest to the product and actively interacts with microwaves. The mandatory constructive elements are susceptors that have patterns of perforations in some parts. Besides, it may be necessary to have reflective elements in it.
2. External 'passive' packaging, basically a box or a bag, which is totally transparent to microwaves, has excellent heat-insulating capability, and separated from internal packaging by a tangible air space.

Schematic picture illustrating the devised concept is shown in Figure 3.

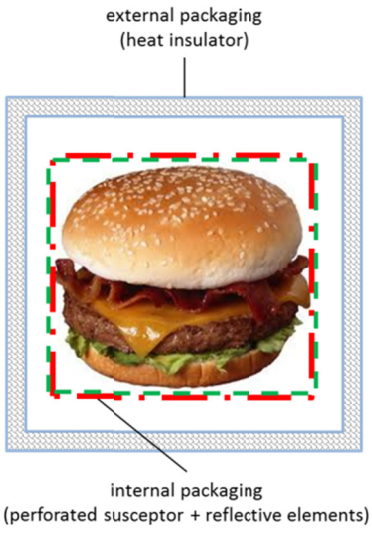



**Figure 3:** Schematic of the two-component packaging concept for microwaving sandwiches.

The packaging components carry the following functional load:

*The internal component*

- redirects and redistributes microwaves thereby providing for more homogeneous heating;
- provides for the crispy crust by radiative and convective heating;
- maintains high temperature of ~ 200°C in the air adjoining the sandwich thereby preventing the interior of the bread from dehydration and staling;
- smooths out microwave intensity gradients and partially transmits leveled microwave radiation toward the sandwich interior.

*The external component*

- restricts heat-release volume thus minimizing heat losses;
- helps to maintain high temperature in the air adjoining the sandwich;
- accelerates heating;
- allows passive afterheating of the sandwich interior when microwaving is ceased, thereby smoothing out temperature gradients;
- works as water vapor condenser preventing moistening of the bread crust;
- and, last but not least, it is also a habitual protective packaging.

## 4 Embodiments of the concept

Both laboratory and commercially viable packaging solutions embodying the above formulated concept have been developed for the following kinds of sandwiches:

- Mini sausage rolls
- Hot dogs
- Snack fish burgers with granary ciabatta bun
- Classic cheeseburgers
- American breakfast sandwiches with biscuits

In order to illustrate all peculiarities of the developed concept, we consider its embodiments for microwaving frozen classic cheeseburgers and breakfast sandwiches.

### 4.1 Classic cheeseburger

The samples were 150-g net weight Classic cheeseburgers (Abbelen Fleischwaren GmbH & Co., Germany) frozen at –20°C. The sandwich is shown in Figure 4 and comprises a Classic hamburger bun (55-60 g), a processed Cheddar cheese slice (10-15 g), and a beef burger (75-80 g).

The implemented packaging design includes:

- Inner packaging is a cylindrical susceptor cage with perforated top and bottom and a continuous side face. Perforation patterns are shown in Figure 5 and the specifics of their geometry is explained below. The used susceptor is a commercial 279 gsm board construction with the Level 3 Safety Susceptor Film (API Laminates Ltd, UK).
- Outer packaging is a carton in FOE (full-depth-tuck-in-top) shape, and the material is a PET-laminated E-grade board flute.

As it will be shown below, it is not necessary to use extra reflective elements in the packaging to provide for homogeneous re-heating of such a cheeseburger: Eigen reflectivity of susceptors and controlled transmission of microwaves through the patterns of perforations in the top and bottom susceptor elements ensure extremely homogeneous temperature distribution in this kind of sandwiches. This statement is illustrated by the typical thermal images shown in Figure 4. The thermal images of the cheeseburger were taken after unpacking and also after bisection of the sandwich. It can be concluded from the figure that the entire sandwich is uniformly heated and the bun's crust is browned. We assume that the physical cause through which it was possible to achieve such a high homogeneity of heating without implementation of strong reconfiguration of microwave field by means of full reflectors is that the moisture content of all three sandwich components is nearly the same, about 40%.

The patterns shown in Figure 5 were optimized using computer simulations and experiments. The perforation pattern in the top susceptor element (shown on the right of Figure 5) comprises several resonant transmission gaps allowing higher absorption of microwaves at the periphery and lower absorption at the center. This is due to the specifics of microwave interaction with a susceptor patch having a slit perforation, where the temperature at

the edges of the gap perforation is much higher than in the middle [4]. This effect enables higher temperature and lower transmission of microwaves at the periphery, and vice versa lower temperature and higher transmission in the center. Since the top part of a hamburger bun has the spherical-segment shape, optimization of both widths and separations of the gaps in the pattern enables higher susceptor temperature where the susceptor-bun separation is the largest and lower temperature where the crust approaches the top susceptor surface. Furthermore, the higher transmission of microwaves in the center of the top susceptor makes this arrangement ideal for achieving homogeneous re-heating of the burger, since it counteracts the well-known effect of preemptive absorption of microwaves at the edges of flat objects and underheating in their centers [5].

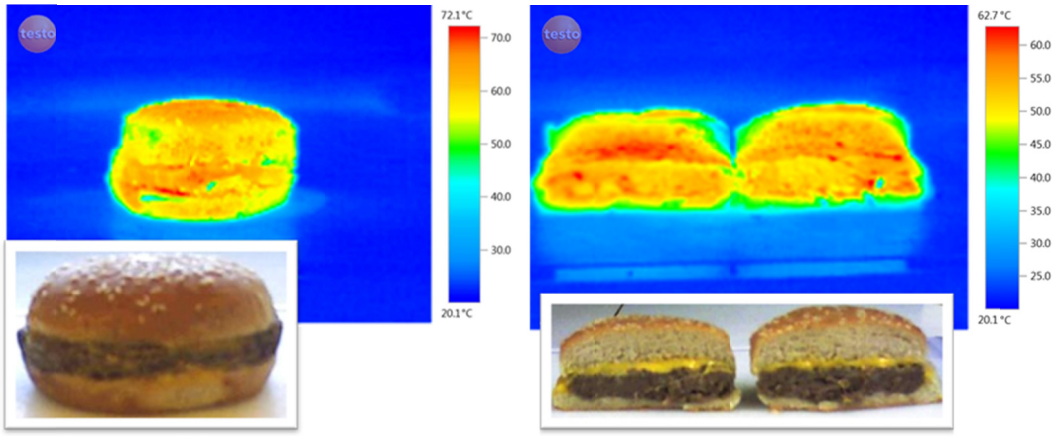



**Figure 4:** Cheeseburger microwaved for 2 min at 650 W electromagnetic power output in the developed packaging: Pictures on the left were taken after a minute of relaxation (meaning the sandwich was unpacked in a minute after the heating completed). Pictures on the right show temperature distribution in the sandwich interior and its cross-section after bisection of the same cheeseburger.

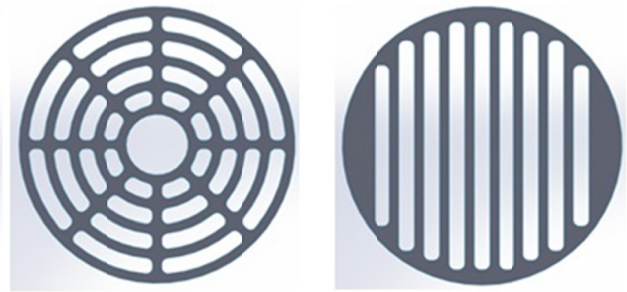


**Figure 5:** Patterns of perforations in the bottom (on the left) and top (on the right) susceptor elements of the cheeseburger packaging.

As for the pattern of perforations in the bottom susceptor element shown on the left of Figure 5, it was shown that its optimum geometry ensures high homogeneity of the temperature distribution along with improved microwave transmission. Since the bottom of the bun is flat, this structure is pertinent here.

### 4.2 Breakfast Sandwich

This class of protein-reach sandwiches counts many kinds of products, which include top and bottom breads, a slice of cheese or fried bacon, a sausage patty or a burger, and without fail an egg patty. The variety of bread sorts includes biscuits, croissants, muffins, bagels etc. These sandwiches are nutritious yet convenient breakfast and lunching options that are popular in many countries, especially in the United States.

The samples of the biscuit-based sandwich with cheese, sausage and egg patties by an undisclosed manufacturer were chosen for the study, since this type seems to be the most conventional, at least in the United States. These sandwiches typically have a 125-135 g net weight and comprise a 50-60 g biscuit, a processed cheese slice (10-15 g), a porcine sausage patty (25-30 g), and an egg patty (25-30 g). A typical frozen sandwich in the manufacturer's packaging is shown in Figure 6.




**Figure 6:** Frozen biscuit sandwich with cheese, sausage and egg patties.

Regarding the microwave heating of this sandwich, the presence of an egg patty is crucial since it results in strongly inhomogeneous distribution of the moisture content in the product. Indeed, bread, cheese, and processed meat have their moisture content of the order of 30-40%, and in the cooked whole egg it is about 70-75%. The immediate corollary of the twofold moisture content is an almost doubled specific heat capacity of the egg in comparison to the other components. Consequently, the egg patty requires much more heat to achieve the necessary temperature than, for instance, the sausage patty does. Thus, it could be *a priori* assumed that the microwave packaging optimized for a sandwich with the egg patty needs reflective elements in order to homogenize the temperature distribution. By other words, extra 'focusing' of microwaves in the core of the egg patty is needed here, and this can be achieved by implementation of reflective shielding [5].

It was easy to confirm this assumption experimentally having the described in the Section 4.1 well performing laboratory packaging prototype for the classic cheeseburger sandwich. The cheeseburger packaging was simply scaled to fit to the overall dimensions of the biscuit sandwich. The frozen sandwich was then re-packed and microwaved for 2 min at 650 W electromagnetic power output. After microwaving, the sandwich stood in the microwave oven for a minute, and after that it was unpacked and bisected, and temperature distributions in the cross-sectional plane were visualized using the infrared camera. Besides the post-microwaving thermal imaging, the *in-situ* temperature monitoring in the sandwich was carried out using the fiber-optic sensors. Since the optical fiber tip is encapsulated in a soft plastic film sleeve, it was not possible to put the sensors in the core of the frozen sandwich components before microwaving. Therefore, the optical fibers were placed between the components, roughly at the vertical axis of the sandwich. The results of the temperature visualization and monitoring are shown in Figure 7.

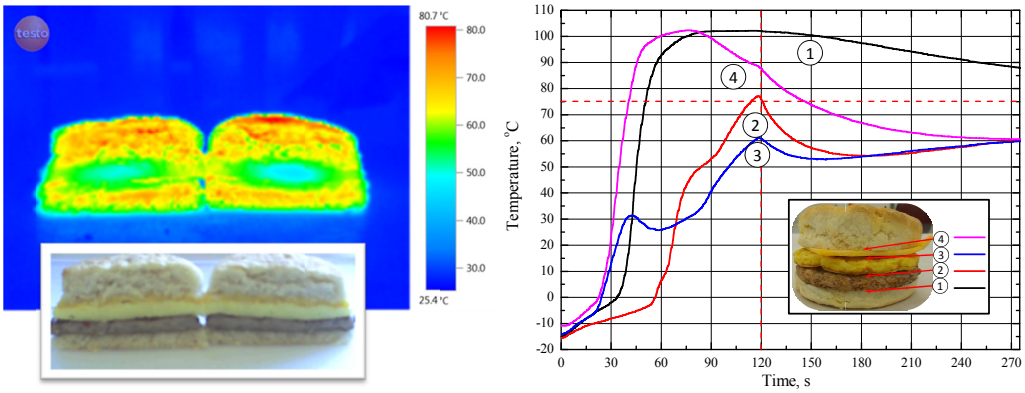



**Figure 7:** Results of post-microwaving visualization (picture on the left) and *in-situ* monitoring of temperature in the sandwich (graph on the right) shown in Figure 6.

The illustrative result of the experiment is first of all that the core of the egg patty had never reached the necessary temperature of 75°C. Furthermore, the effect of preemptive absorption of microwaves at the edges of flat objects that is already mentioned above was pronounced in the egg patty. Based on the temperature monitoring results, it can be concluded that the microwave heating process in the sandwich components was extremely inhomogeneous and ended up with the underheated egg and the overheated biscuit. The exfoliation of the biscuit crust visible in the picture at the left of Figure 7 is the result of the overheating and extensive dehydration in the top half of the biscuit. Thus, the conclusion can be made that the internal 'active' packaging

element made of solely microwave susceptor material was not able to ensure neither homogeneous heating nor acceptable sandwich texture quality.

Therefore, it was decided to introduce a reflective element in the packaging in order to 'focus' microwaves into the core of the egg patty. This reflector, or shield [5], is simply a shading metal film coil; the film must be thick and wide enough to displace the 2450 MHz alternating electric field deeper into the core of the egg patty. Such a film coil made of a 12-μm-thick closed aluminium foil strip was laminated on the inner surface of the cylindrical susceptor cage. The width of the strip was optimized by means of computer simulations and experiments in order to ensure the most homogeneous distribution of the electromagnetic power losses in the sandwich.

Besides the use of the electric shield, the structure of the pattern of perforations in the top susceptor element shown on the right in the Figure 5 was changed in this embodiment of the packaging concept: only four gaps in the center of the pattern were cut out, and their length was reduced down to half-wavelength at 2450 MHz, i.e. approximately 61 mm. This was done in order ensure enhanced microwave transmission through the top susceptor solely into the central circle of the sandwich.

The results of microwaving of a biscuit sandwich in the modified packaging are shown in Figure 8. The experimental procedure here was held the same as is described above.

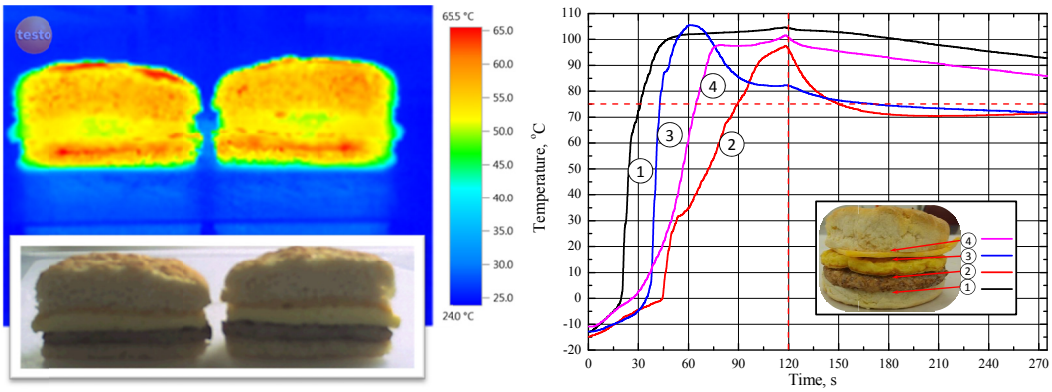



**Figure 8:** Results of post-microwaving visualization (picture on the left) and *in-situ* monitoring of temperature in the sandwich (graph on the right) microwaved in the modified packaging with the built-in electric shield.

The temperature distribution and history shown in Figure 8 speak for themselves: the optimized shield does its work and enables homogeneous and synchronous microwave heating of the sandwich. It is noteworthy that the packaging allows significant heating time reduction as against packaging without the reflector. According to the temperature versus time data presented in Figure 8, microwaving should have been stopped already after the first 90 seconds when temperature in all sandwich components overcomes the necessary level of 75°C.

Thus, it can be concluded that implementation of the microwave-active elements in the packaging enables homogeneous temperature distribution even in the sandwich that comprises components with very different dielectric and thermal properties. However, the electric shield must be thoroughly optimized. Otherwise, the presence of reflector elements may make the heating homogeneity worse. The temperature distribution shown in Figure 9, which is a result of an incorrectly designed shield, is a very good example: The aluminium strip was too wide here, and the electric field was therefore totally displaced from the edges of the egg patty! In our opinion, this illustrates in the best way possible that active microwave packaging is also "...a mixture of art and science, with heavy emphasis on the science." [8].

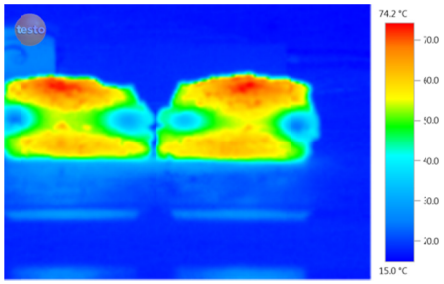



**Figure 9:** The result of erroneous implementation of the reflector: the shielding rim is so wide that the edge of the egg patty is completely shadowed from microwaves and remains cold, and its center warms up.

## 5 Conclusions

Summarizing this development, we want to emphasize one of the key advantages of the proposed packaging designs in connection with the bread texture in the re-heated frozen sandwiches: We have achieved a very reliable insulation of the sandwich bread crust from the moisture that accumulates inside the packaging during microwaving. Indeed, vapor escapes through the perforations in the susceptor/reflector and does not condense while microwaving continues, since the temperature of the air-steam mixture inside the packaging remains well above the dew point. As soon as the microwaving stops, water vapor condensation initiates on the inner surface of the external packaging, since it cools down faster than the internal packaging due to the cold air surrounding the packaging in the oven. Then, as the susceptor cools down, condensation continues also on the outer walls of the susceptor cage. Thus, water vapor does not have any chance to moisten the bread crust. This 'steam trap' functions very well and ensures crispiness of the bread crust.

In conclusion, we would simply like to formulate the principal results of this work:

- The dual-packaging concept for implementation of bread texture retaining homogeneous re-heating of buns and sandwiches has been developed and validated using a number of commercial products.
- The packaging comprises an internal 'active' component, which interacts with microwaves and generates heat, and an external 'passive' component that is totally transparent for microwaves but has excellent heat-insulating capability.
- This approach allows counteracting such fundamental effects as 'water pumping', microwave focusing in axisymmetric objects and edges of flat samples, as well as local overheating (hot spots) due to inhomogeneity of foods' dielectric and thermal properties.
- It has been proven that the developed dual-packaging solutions enable for microwaved sandwiches similar eating experience as from freshly baked products out of a conventional oven.

Finally, we believe that the packaging concepts developed in this work can be implemented for a variety of food products, where a dual texture of a crispy crust and a softer interior is demanded. These can be coated meat and fish, roasted meat and poultry. For instance, it is well known among food engineers that microwavable chicken nuggets and coated 'fish sticks' remain to be sort of 'the Holy Grail of the food technology'. By adapting and embodying the above described dual-packaging concept for these difficult products, we have already achieved satisfactory sensory results at a laboratory level. We will report these results elsewhere soon.

## Acknowledgements

This work was supported by the Danish Ministry of Food, Agriculture and Fisheries through the Innovation Project no. 3414-08-02278 'Packaging for better meals cooked in microwave oven'.

## References

1. Schiffman, R. F. Microwave Technology, a Half-Century of Progress. Food Product Design 5 (1997) 1-15.
2. Ryynänen, S., Risman, P. O., and Ohlsson, T. Hamburger Composition and Microwave Heating Uniformity. Journal of Food Science 69 (7) (2004) 187–196. DOI: 10.1111/j.1365-2621.2004.tb13619.x
3. Parker, K., and Vollmer, M. Bad food and good physics: the development of domestic microwave cookery. Physics Education 39 (1) (2004) 82-90.
4. Perry, M. R., and Lentz, R. R. Susceptors in microwave packaging, in Lorence, M. W. and Pesheck, P. S. (eds.), Development of packaging and products for use in microwave ovens, Boca Raton – Boston – New York – Washington, DC, CRC Press – Woodhead Publishing Limited (2009) 207-235. ISBN 978-1-84569-420-3.
5. Buffler, C. R. Microwave Cooking and Processing. Engineering Fundamentals for the Food Scientist, New York, AVI Book (1993). ISBN 0-442-00867-8.
6. Otoshi, T. Y. A Study of Microwave Transmission Through Perforated Flat Plates. JPL Technical Report 32-1526 (Vol. II) 80-85.
7. Kelly, R. J., Lockyear, M. J., Suckling, J. R., and Sambles, J. R. Enhanced microwave transmission through a patterned metal film. Applied Physics Letters 90 (2007) 223506. DOI:10.1063/1.2745202.
8. Bertrand, K. Microwavable Foods Satisfy Need for Speed and Palatability. Food Technology 59 (1) (2005) 30-34 (http://scentsationaltechnologies.com/news/FoodTechMag0105.pdf)

# Effect of propolis extract on physical and antioxidant properties of chitosan film

**Ubonrat Siripatrawan* and Waranya Vitchayakitti**

*Department of Food Technology, Faculty of Science, Chulalongkorn University, Bangkok 10330, Thailand*

*Corresponding author. Email: ubonratana.s@chula.ac.th*

**Abstract:** This research aimed to study the effect of Thai propolis on physical and antioxidant properties of chitosan based film. Thai propolis extract was prepared by using 60:40 water to ethanol solution. Different concentrations of the propolis extract including 0, 2.5, 5 and 10% (w/v) were added into the chitosan film-forming solution. Chitosan film without propolis extract was used as control. Physical properties including surface color (L*, a*, b*), water vapor permeability (WVP), tensile strength (TS), and elongation at break (%E) were measured. Antioxidant properties including total phenolic content (mg gallic acid equivalent/g) and radical scavenging activity were determined using Folin-Ciocalteau method and 2,2-diphenyl-1-picrylhydrazyl (DPPH) radical scavenging activity, respectively. The results showed that ΔE, TS, %E of the film increased, while %T and WVP decreased with concentration of the propolis. Total phenolic content and DPPH increased with concentration of the propolis.

Keywords: chitosan film, propolis, antioxidant, polyphenol.

## 1. Introduction

Chitosan, a linear polysaccharide of randomly distributed β-(1-4)-linked D-glucosamine and N-acetyl-D-glucosamine, is a deacetylated product of chitin and is considered a biobased environmentally friendly material [1]. Chitosan has potential to be used as alternative resources for active food packaging. Incorporation of antioxidants into packaging materials has become popular since oxidation is a major problem affecting the food quality [2,3].

Propolis, the natural resinous substance collected by honeybees from various plant sources, is considered as a good source of natural antioxidants and antibacteria [4]. Propolis contains a variety of chemical compounds such as polyphenols, sesquiterpene quinines, coumarins, steroids, amino acids and inorganic compounds. The aim of this research was to develop an environmentally friendly active film from chitosan incorporated with Thai propolis as a natural antioxidant.

## 2 Materials and methods

### 2.1 Film preparation

Chitosan with degree of deacetylation of 95% was used to prepare chitosan-based film. Chitosan film forming solution was prepared according to the procedure of Yingyuad *et al*. [5] with slight modification. Thai propolis extract was prepared by using 60:40 water to ethanol solution following the method of Siripatrawan, Vitchayakitti & Sanguandeekul [4]. Different concentrations of the propolis extract including 0, 2.5, 5 and10% (w/v) were added into the chitosan film-forming-solution. Chitosan film without propolis extract was used as control.

### 2.2 Physical properties

Film thickness was measured using a digital micrometer (Mitutoyo Absolute, Tester Sangyo Co., Ltd., Tokyo, Japan). Five replications were conducted for each sample treatment.

Hunter color (*L, a, b*) values were measured using a Minolta Chromameter (Minolta Camera Co., Japan).
Water vapor transmission rate (WVTR) of the films was determined following ASTM [6]. The water vapor permeability coefficient (WVP) of the films was then used to calculate the using Eq (3).

$$WVP = WVTR\frac{x}{\Delta p} \qquad (3)$$

where $x$ is the film thickness, $\Delta p$ is the partial water vapor pressure gradient between the inner ($p_1$) and outer ($p_2$) surface of the film.
Mechanical properties including tensile strength (TS) and percentage of elongation at break (%E) were measured with an Instron Universal Testing Machine (Instron Corporation, Canton, USA) following the ASTM [6].

$$TS = \frac{F_{\max}}{\Phi} \qquad (4)$$

$$\%E = \frac{\Delta l}{l_0}100 \qquad (5)$$

### 2.3 Total phenolic assay

Total phenolic content (TPC) of the chitosan film samples was determined according to the Folin-Ciocalteu method as described by Singleton, Orthofer & Lamuela-Raventos [7] with slight modifications.

### 2.4 Determination of antioxidant activity

The antioxidant activity of the film samples was evaluated using DPPH free radical scavenging assay according to Blois [8] with slight modification. The absorbance was then measured at 517 nm. The DPPH effect was determined using the following equation:

$$\text{DPPH scavenging effect (\%)} = \frac{Abs_{DPPH} - Abs_{extract}}{Abs_{DPPH}}100 \qquad (7)$$

where $Abs_{DPPH}$ is the absorbance value of the methanolic solution of DPPH and $Abs_{extract}$ is the absorbance value for the sample extracts.

## Results and Discussion

The effects of propolis concentration on film color and opacity are shown in Table 1. Adding propolis into chitosan films significantly affected ($p \leq 0.05$) L*, a* and b* values of the film surface. Films without propolis were lighter. L* values of the films decreased, but a* increased (indicator of the tendency towards redness) and b* values increased (indicator of the tendency towards yellowness), as the propolis concentrations increased from 0 to 10 %.

**Table 1** Color values of chitosan film containing propolis

| Propolis concentration (% w/v) | L* | a* | b* |
|---|---|---|---|
| 0 | $87.01^{a}$±1.27 | $-2.30^{d}$±0.51 | $25.40^{c}$±4.38 |
| 2.5 | $79.21^{b}$±2.55 | $0.83^{c}$±1.48 | $31.34^{bc}$±3.85 |
| 5 | $73.97^{c}$±2.18 | $3.92^{b}$±1.77 | $36.42^{ab}$±2.48 |
| 10 | $65.32^{d}$±1.64 | $8.30^{a}$±1.00 | $39.29^{a}$±1.35 |

Different letters in the same column indicate significantly different ($p \leq 0.05$)

Water vapor permeability of the chitosan films incorporated with different concentrations of propolis was examined at 25 °C. The results showed that propolis had a significant effect ($p \leq 0.05$) on WVP and density of the films as shown in Table 2. The permeability coefficient decreased, as the concentration of propolis increased from 0 to 10 %. Incorporation of propolis into chitosan film caused the resulting films to become denser and less water vapor permeability.

**Table 2** WVP of chitosan film containing propolis

| Propolis concentration (% w/v) | WVP (g mm/Pa day $m^2$) |
|---|---|
| 0 | $0.67^{a}$±0.08 |
| 2.5 | $0.52^{b}$±0.03 |
| 5 | $0.56^{b}$±0.02 |
| 10 | $0.55^{b}$±0.06 |

Different letters in the same column indicate significantly different ($p \leq 0.05$)

The mechanical properties including tensile strength (TS) and elongation at break (%E) are shown in Table 3. The mechanical properties of chitosan films incorporated with different propolis concentrations were statistically compared. The results showed that propolis significantly affected ($p \leq 0.05$) the tensile strength of the chitosan-based films. Percent elongation at break significantly increased when propolis concentration increased from 0-5 %, but significantly decreased when propolis concentration increased from 5 to 10 %. The improvement in mechanical properties of the films incorporated with propolis may be attributed to the interaction between chitosan matrix and polyphenolic compounds from propolis.

**Table 3.** TS and % E of chitosan film containing propolis

| Propolis concentration (% w/v) | TS (MPa) | %E |
|---|---|---|
| 0 | $6.23^{e}$±0.71 | $5.41^{e}$±0.58 |
| 2.5 | $16.37^{c}$±0.39 | $11.58^{b}$±0.96 |
| 5 | $18.33^{b}$±0.81 | $12.36^{ab}$±1.05 |
| 10 | $21.47^{a}$±1.00 | $6.93^{d}$±0.41 |

Different letters in the same column indicate significantly different ($p \leq 0.05$)

Phenolic compounds and antioxidant activity are shown in Table 4. The results of TPC showed that total phenolic content in the chitosan films significantly increased ($p \leq 0.05$) with increasing propolis concentration. The results of DPPH activity showed that DPPH scavenging activity of the films significantly increased ($p \leq 0.05$) with increasing propolis concentration. The chitosan films without propolis extract showed some scavenging activity on DPPH. In the films containing propolis, the antioxidant activity increased in relation to the control samples. As the propolis increased in the film formulation, so did the expected antioxidant character of the active film.

**Table 4.** TPC of chitosan film containing propolis

| Propolis concentration (% w/v) | TPC* (mg gallic acid equivalent/g) | DPPH activity (%)* |
|---|---|---|
| 0 | $4.05^{b}$±0.06 | $11.63^{c}$±2.15 |
| 2.5 | $4.36^{b}$±0.45 | $32.34^{b}$±1.51 |
| 5 | $4.90^{a}$±0.17 | $53.86^{a}$±1.88 |
| 10 | $5.52^{a}$±0.06 | $54.85^{a}$±1.34 |

Different letters in the same column indicate significantly different ($p \leq 0.05$)

## 4. Conclusions

This study indicated that an active film from chitosan-based film could be achieved by incorporation with propolis, as a natural antioxidant. Addition of propolis improved mechanical, water vapor barrier and antioxidant properties of the resulting films. These changes could be attributed to the interactions between functional groups of chitosan and propolis polyphenolic compounds. The chitosan film incorporated with propolis shows potential to be used as an active film.

## Acknowledgements

The authors acknowledge the Royal Thai Government for the funding resource under project "Resource management for sustainable development".

## References


1. Fernandez-Saiz, P., Lagaron, J.M., & Ocio, M.J. (2009). Optimization of the biocide properties of chitosan for its application in the design of active films of interest in the food area. *Food Hydrocolloids, 23*, 913-921.
2. Gómez-Estaca, J., Gimnez, B., Montero, P. & Gómez-Guillén, M.C. (2009). Incorporation of antioxidant borage extract into edible films based on sole skin gelatin or a commercial fish gelatin. *Journal of Food Engineering, 92*, 78-85.
3. Siripatrawan, U., and Harte, B. R. 2010. Physical properties and antioxidant activity of an active film from chitosan incorporated with green tea extract. *Food Hydrocolloids,24*, 770-775.
4. Siripatrawanm U., Vitchayakitti,W. & Sanguandeekul, R. (2013). Antioxidant and antimicrobial properties of Thai propolis extracted using ethanol aqueous solution. *International Journal of Food Science and Technology, 48*, 22–27.
5. Yingyuad, S., Ruamsin, S., Leekprokok, T., Douglas, S., Pongamphai, S., & Siripatrawan, U. (2006). Effect of chitosan coating and vacuum packaging on the quality of refrigerated grilled pork. *Packaging Technology and Science*, *19*, 149-157.
6. ASTM. (2003). *Annual Book of ASTM Standards*. Pennsylvania: American Society for Testing and Materials.
7. Singleton, V. L., Orthofer, R., & Lamuela-Raventos, R. M. (1999). Analysis of total phenols and other oxidation substrates and antioxidants by means of Folin-Ciocalteu reagent. *Methods in Enzymology, 299*, 152-178.
8. Blois, M.S. (1958). Antioxidant determinations by the use of a stable free radical, *Nature*, *181*, 1199-1200.

# Effects of in-package atmosphere on temporal changes in the fractionation of oxygen isotopes during respiration in tomatoes

**Yoshio Makino[1*], Shohei Honda[1], Seiichi Oshita[1], Ko Noguchi[2], Satoru Nakao[3]**

[1]*Graduate School of Agricultural and Life Sciences, The University of Tokyo, Japan*
[2] *School of Science, The University of Tokyo, Japan*
[3] *P-Plus Project, Sumitomo Bakelite Co., Ltd., Japan*

[*]*Corresponding author. Email: amakino@mail.ecc.u-tokyo.ac.jp*

**Abstract:** Oxygen molecules that diffuse into biological cells are utilized by mitochondrial enzymes such as cytochrome *c* oxidase (COX). This reaction is required to oxidize the protons produced during oxidative phosphorylation, resulting in the generation of adenosine 5′-triphosphate (ATP), an energy-rich compound. Plant cells utilize an alternative pathway to oxidize protons without generating ATP through the action of alternative oxidase (AOX). This enzyme preferentially acts on $^{32}O_2$ over $^{34}O_2$, and this tendency is stronger than that observed in case of COX. Moreover, AOX activity has been reported to increase with an increase in the respiratory rate. Modified atmosphere packaging (MAP) is a popular method of storing horticultural products by depressing respiratory rate. These findings suggest that AOX activity of products that have been sealed in a pouch is influenced by their respiratory rate. However, there have been no reports describing $O_2$ consumption by AOX during storage under MAP. Therefore, in the present study, the effects of in-package atmosphere on AOX activity of tomatoes that were packaged in pouches were evaluated on the basis of temporal changes in the fractionation of $O_2$ isotopes. Two types of micro-perforated film pouches were prepared to create two levels of in-package $O_2$ concentrations. Two tomatoes were sealed in a micro-perforated film pouch and stored at 15°C or 25°C. Changes in in-package $O_2$ and $CO_2$ concentrations were monitored using a gas analyser. Changes in the fractionation of $O_2$ isotopes were measured using a mass spectrometer. The fractionation of $^{34}O_2$ increased with increasing in-package $O_2$ concentrations, suggesting that AOX activity increases with increasing $O_2$ concentrations.

Keywords: alternative oxidase, modified atmosphere packaging, stable isotope.

## 1 Introduction

Horticultural products, such as fruits and vegetables, are living tissues that are subject to continuous change, even after harvesting. This means that metabolic reactions are active in cells. Furthermore, this phenomenon causes deterioration of products, such as wilting, color changes, nutrient reduction, and so on. The rate of product deterioration is generally proportional to the respiration rate. Robinson *et al.* [1] reported that the shelf-life of products decreased with increasing respiration rate, calculated as $CO_2$ production rate. This suggests that respiration rate is associated with product deterioration.

It is well known that metabolic reactions are depressed by methods employed to reduce enzymatic activity, such as cold storage, controlled atmosphere storage and modified atmosphere packaging (MAP) [2]. The objective of these operations is to slow metabolic activities represented by respiration.

Most $O_2$ molecules taken up by biological cells are consumed in the process of serial electron transportation, performed by enzymes buried in the mitochondrial inner membrane [3]. The enzymes are encoded in nuclear or mitochondrial DNA [4].

The so-called classical electron transport chain (ETC) is composed of four large protein oxidative phosphorylation (OXPHOS) complexes (I, II, III, IV) that interact with each other via the small lipid ubiquinone, and the small protein cytochrome *c* [5]. Complex I, NADH-ubiquinone reductase (E.C. 1.6.99.3), catalyzes the oxidation of NADH to reduce ubiquinone. This complex includes a FMN and FeS proteins to transfer $e^-$. Complex II, succinate dehydrogenase (E.C. 1.3.5.1), is the sole enzyme to exist in the inner membrane of the mitochondrion as a member of the tricarboxylic acid cycle. This enzyme catalyzes the oxidation of succinate to reduce ubiquinone with connecting $FADH_2$. FeS proteins are also part of complex II. Complex III, ubiquinone-cytochrome *c* oxidoreductase (E.C. 1.10.2.2), transports $e^-$ to cytochrome *c*. This complex includes two

cytochrome *b*, a cytochrome $c_1$ and a FeS to transfer $e^-$ to cytochrome *c*. Complex IV, cytochrome *c* oxidase (COX) (E.C. 1.9.3.1) composed of cytochrome *a* and $a_3$, is the terminal enzyme of the ETC. This enzyme catalyzes the reaction consuming $O_2$ for the oxidation of $H^+$ to $H_2O$ [6]. Therefore, the amount and activity of this enzyme is also associated with the external respiration rate of biological tissues. Most studies on this enzyme have been conducted using COX derived from bovine serum, due to the ease of preparing test samples [7, 8]. Conversely, Maeshima and Asahi [9], and Maeshima *et al.* [10] studied the characteristics and activity of COX prepared from sweet potato and cassava roots.

When $H^+$ is oxidized to $H_2O$ by COX, adenosine 5′-triphosphate (ATP), a high-energy compound needed for almost all vital enzymatic reactions, is produced. The OXPHOS complex V, $F_OF_1$-ATP synthase (E.C. 3.6.3.14), catalyzes this reaction. This complex is composed of two units as $F_O$ and $F_1$, and $H^+$ flows from $F_O$ and $F_1$. The $H^+$ flow generates a proton gradient as the driving force to rotate an actin filament connected with the γ-subunit in the $F_1$ unit. ATP is produced by attaching phosphate to adenosine 5′-diphosphate (ADP) using the rotation power [11, 12]. This proton gradient is caused by the decomposition of nutrients as carbohydrates, fatty acids and organic acids. Therefore, $O_2$ consumption in ETC is associated with the deterioration of fruits and vegetables.

Conversely, a number of plants are well known to have an alternative oxidase (AOX), which catalyzes the reaction providing $e^-$ and $H^+$ to $O_2$, as observed for COX [5]. However, this enzyme is not associated with generating ATP; thus, this is a non-phosphorylating (non-energy conserving) respiratory pathway. This reaction is termed cyanide (CN)-resistant respiration because the activity is not inhibited by CN [13]. However, this enzyme is inhibited by salicylhydroxamic acid (SHAM) [14]. It was reported that the contribution of AOX to $O_2$ consumption in plant tissues increased with increasing sugar concentration as the substrate of mitochondrial respiration [15]. This suggests that $O_2$ consumption by AOX, as well as COX, should be associated with the deterioration of fruits and vegetables. As AOX does not contribute to the production of ATP, the ratio of COX/AOX activities may affect the deterioration of the products. AOX consumes $^{32}O_2$ more dominantly than $^{34}O_2$ compared with COX. Therefore, Ribas-Carbo *et al.* [16] evaluated the ratio by measuring the $^{18}O/^{16}O$ ratio in a mitochondrial solution prepared from soybean (Glycine max (L.) Merr.) using a modified aqueous phase on-line mass spectrometry-gas chromatography system. Macfarlane *et al.* [17] estimated ATP production efficiency equivalent to the distribution rate of $e^-$ to AOX by measuring enthalpy conversion efficiency in *Eucalyptus globulus* Labill. seedlings. However, to date, no research has been found concerning an external respiration model that takes into account the influence of AOX. Conversely, AOX reaction does not produce reactive oxygen species, which differs from the COX reaction [18].

## 2 Materials and methods

Tomato (*Solanum lycopersicum* L.) fruits at red stage were harvested in farm in Japan and transported to laboratory to use for the following experiments.

Three kinds of micro-perforated oriented polypropylene film pouches were prepared ($O_2$ permeance: A 5,000; B 8000; C 50000 $mL•m^{-2}•d^{-1}•atm^{-1}$). A high-barrier film pouch ($O_2$ permeance 8 $mL•m^{-2}•d^{-1}•atm^{-1}$) was also prepared.

Two fruits were sealed in a micro-perforated pouch and stored at 15 or 25ºC. The pouches A and C were used for the 15ºC storage. The pouches B and C were used for the 25ºC storage. Changes in in-package $O_2$ and $CO_2$ were measured during storage using the gas analyser (CheckMate 3, Dansensor A/S, Ringsted, Denmark) (Figure 1).




**Figure 1**: Gas analyser (CheckMate 3, Dansensor A/S, Ringsted, Denmark)

After the storage, the micro-perforated pouch was sealed in a high-barrier pouch and stored at the same temperature as before the second round of the sealing. Changes in in-package $O_2$ were measured during storage using CheckMate 3 and 10 mL of in-package gas was sampled through a silicon rubber septum using a gastight syringe during storage for stable isotope analysis.

The sampled gas was introduced in a gaschromatograph with a thermal conductivity detector to extract pure $O_2$. The extracted $O_2$ was introduced in the mass spectrometer (IsoPrime100, JASCO International Co., Ltd., Hachioji, Tokyo) (Figure 2) to determine $^{18}O/^{16}O$ ratio.



**Figure 2**: Mass spectrometer (IsoPrime100, JASCO International Co., Ltd., Hachioji, Tokyo)

According to the O'Leary's theory [19], the following relationship can be derived:

$$\ln\left(\frac{R}{R_O}\right) \bullet 1000 = D \bullet \left(-\ln f\right) \tag{1}$$

where $D$ is the discriminant factor, $f$ is the fraction of the initial concentration of $O_2$ remaining in the high-barrier pouch, $R$ is the $^{18}O/^{16}O$ ratio, the subscript 0 denotes the initial value. Guy *et al.* [20] reported that the $D$ value increased with increasing in AOX activity.

## 3 Results and discussion

Changes in in-package $O_2$ and $CO_2$ were shown in Figure 3. Two levels of $O_2$ concentrations were successfully created around tomato fruits using two kinds of micro-perforated pouches independent of storage temperature. This indicates that $O_2$ uptake rate of tomato fruits is controlled at two levels at each temperature. This may be effective for evaluating the ratio of enzymatic activities of COX and AOX in tomato fruits.

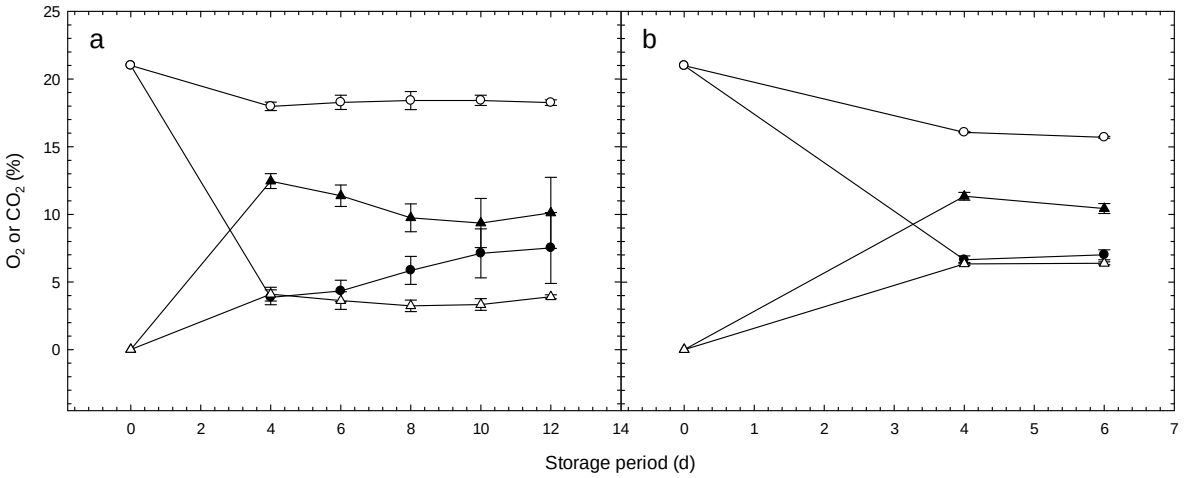



**Figure 3**: Changes in in-package $O_2$ and $CO_2$ during storage at (a) 15 and (b) 25ºC

In figure a, open and closed circles denote the $O_2$ concentrations in micro-perforated pouches C and A, respectively. Open and closed triangles denote the $CO_2$ concentrations in micro-perforated pouches C and A, respectively. In figure b, open and closed circles denote the $O_2$ concentrations in micro-perforated pouches C and B, respectively. Open and closed triangles denote the $CO_2$ concentrations in micro-perforated pouches C and B, respectively.

Typical changes in isotope ratio with the fraction of the initial concentration of $O_2$ remaining in the high-barrier pouch at 25ºC was shown in Figure 4. This measurement was performed using tomato fruits after stored in a micro-perforated pouch C for 7 d. Isotope ratio linearly increased with –ln *f* according to this result. It was confirmed that the Equation 1 is effective for evaluating enzymatic activity ratio between COX and AOX.

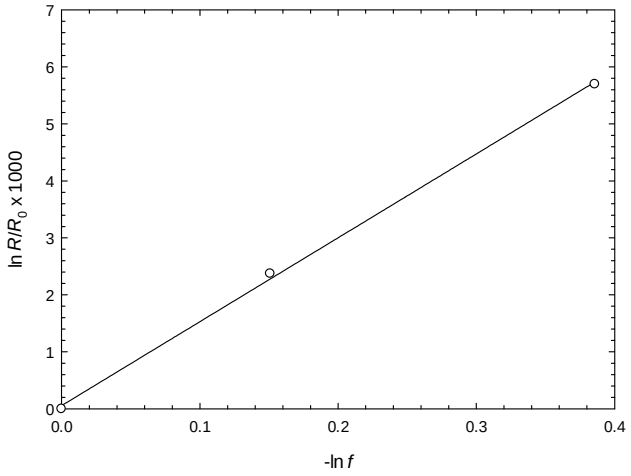



**Figure 4**: Typical changes in isotope ratio with the fraction of the initial concentration of $O_2$ remaining in the high-barrier pouch at 25ºC after stored in a micro-perforated pouch C for 7 d

Open circles and a solid line denote the measured data and the linear regression line (correlation coefficient: 0.999), respectively.

Influence of storage conditions on discrimination factor associated with enzymatic activity ratio between COX and AOX in tomato fruits after storage for 7 d was shown in Figure 5. This result indicated that AOX activity increased with $O_2$ concentration. This suggests that AOX acts to contribute for a large amount of $O_2$ consumption in plant cells as well as COX. However, influence of storage temperature on the activity ratio was not clear. These results suggest that AOX activity is stimulated not by rapid respiration rate but by high $O_2$ concentration around the tomato fruits.

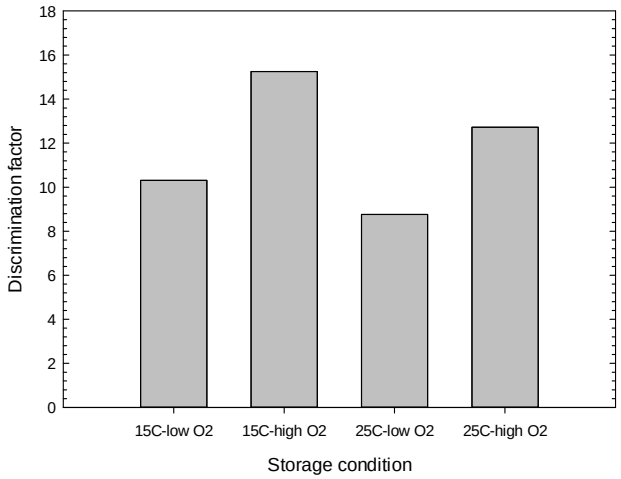



**Figure 5**: Influence of storage conditions on discrimination factor associated with enzymatic activity ratio between cytochrome *c* oxidase and alternative oxidase in tomato fruits after storage for 7 d

## 4 Conclusions

Enzymatic activity ratio between COX and AOX was affected by storage conditions created by MAP. Especially, AOX activity may be stimulated not by rapid respiration rate but by high $O_2$ concentration around the tomato fruits.

## Acknowledgements

This research was partly supported by the Ministry of Education, Science, Sports and Culture, Grant-in-Aid for Scientific Research (A) 25252045.

## References

1. J.E. Robinson, K.M. Brown, W.G. Burton, 1975, "Storage characteristics of some vegetables and soft fruits", *Ann. Appl. Biol.*, vol. 81, pp. 399-408.
2. A.A. Kader, ed., 2002, *Postharvest Technology of Horticultural Crops*, University of California, Oakland.
3. B. Alberts, D. Bray, J. Lewis, M. Raff, K. Roberts, J.D. Watson, 1994, "The respiratory chain and ATP synthase", In: *Molecular Biology of the Cell*, 3rd Ed., Garland Publishing, Inc., New York. pp. 672-683.
4. T.C. McCabe, D. Daley, J. Whelan, 2000, "Regulatory, developmental and tissue aspects of mitochondrial biogenesis in plants", *Plant Biol.*, vol. 2, pp. 121-135.
5. A.H. Millar, J. Whelan, K.L. Soole, D.A. Day, 2011, "Organization and regulation of mitochondrial respiration in plants", *Annu. Rev. Plant Biol.*, vol. 62, pp. 79-104.
6. T. Yonetani, G.S. Ray, 1965, "Studies on cytochrome oxidase VI. Kinetics of the aerobic oxidation of ferrocytochrome c by cytochrome *c* oxidase", *J. Biol. Chem.*, vol. 240, pp. 3392-3398.
7. B. Chance, G.R. Williams, 1956, "The respiratory chain and oxidative phosphorylation", In: F.F. Nord (ed.), *Advances in Enzymology and Related Subjects of Biochemistry*, vol. 17, Interscience publishers, Inc., New York, pp. 65-134.
8. S. Yoshikawa, 2002, "Cytochrome *c* oxidase", *Adv. Protein Chem.*, vol. 60, pp. 341-395.
9. M. Maeshima, T. Asahi, 1978, "Purification and characterization of sweet potato cytochrome *c* oxidase", *Arch. Biochem. Biophys.*, vol. 187, pp. 423-430.
10. M. Maeshima, I. Uritani, T. Asahi, 1980, "Effect of temperature on the activities of cytochrome *c* oxidase and respiration in cassava root mitochondria", *Agr. Biol. Chem.*, vol. 44, pp. 2493-2494.
11. P.D. Boyer, 1993, "The binding change mechanism for ATP synthase-some probabilities and possibilities", *Biochim. Biophys. Acta*, vol. 1140, pp. 215-250.

12. H. Noji, R. Yasuda, M. Yoshida, K. Kinosita, 1997, "Direct observation of the rotation of $F_1$-ATPase", *Nature*, vol. 386, pp. 299-302.

13. K. Yoshida, I. Terashima, K. Noguchi, 2007, "Up-regulation of mitochondrial alternative oxidase concomitant with chloroplast over-regulation by excess light", *Plant Cell Physiol.*, vol. 48, pp. 606-614.

14. K. Yoshida, I. Terashima, K. Noguchi, 2006, "Distinct roles of the cytochrome pathway and alternative oxidase in leaf photosynthesis", *Plant Cell Physiol.*, vol. 47, pp. 23-31.

15. H. Lambers, H., 1985, "Respiration in intact plants and tissues: Its regulation and dependence on environmental factors, metabolism and invaded organisms", In: R. Douce and D.A. Day (eds), *Encyclopedia of Plant Physiology*, vol. 18, Springer-Verlag, Berlin, pp. 418-473.

16. M. Ribas-Carbo, J.A. Berry, D. Yakir, L. Giles, S.A. Robinson, A.M. Lennon, J.N. Siedow, 1995, "Electron partitioning between the cytochrome and alternative pathways in plant mitochondria", *Plant Physiol.*, vol. 109, pp. 829-837.

17. C. Macfarlane, M.A. Adams, L.D. Hansen, 2002, "Application of an enthalpy balance model of the relation between growth and respiration to temperature acclimation of Eucalyptus globulus seedlings", *Proc. R. Soc. Lond. B*, vol. 269, pp. 1499-1507.

18. A.L. Umbach, F. Fiorani, J.N. Siedow, 2005, "Characterization of transformed Arabidopsis with altered alternative oxidase levels and analysis of effects on reactive oxygen species in tissue", *Plant Physiol.*, vol. 139, pp. 1806-1820.

19. M.H. O'Leary, 1981, "Carbon isotope fractionation in plants", *Phytochemistry*, vol. 20, pp. 553-567.

20. R.D. Guy, J.A. Berry, M.L. Fogel and T.C. Hoering, 1989, "Differential fractionation of oxygen isotopes by cyanide-resistant and cyanide-sensitive respiration in plants", *Planta*, vol. 177, pp. 483-491.

# An Innovative Corrugated Shipper to Improve Palletized Load Airflow for Fresh Produce

**R. Kisch[1*] , J. Singh[2]**

[1] Cal Poly State University, California, USA
[2] Cal Poly State University, California, USA

[*] Corresponding author: rgkisch@calpoly.edu

**Abstract:** The best possible quality of any fresh produce exists at the moment of harvest. Beyond this point quality cannot be improved, only maintained. Deterioration of fresh commodities can result from physiological breakdown due to natural ripening processes, water loss, temperature injury, physical damage, or invasion by microorganisms. All of these factors can interact, and all are influenced by temperature. This research studied the effectiveness of an innovative corrugated fiberboard shipper design towards air flow, and hence temperature maintenance, for palletized loads of baby carrots and bananas. Test palletized loads constructed using the new shipper design were compared for temperature performance against control loads constructed of commonly deployed existing shipper styles. All palletized loads were instrumented with temperature monitors and were subjected to field trials in distribution channels from packinghouse to storage to destination markets. The fresh produce was able to maintain better air flow and lower product temperature for the test loads as compared to the control loads.

Keywords: temperature, innovative corrugated shipper, airflow.

## 1. INTRODUCTION

Fresh fruit and vegetable production and distribution systems are one of the most dynamic and challenging marketing systems worldwide. Continuing shifts in product security and contamination concerns are continuously being addressed; often resulting in packaging that restricts airflow and the ability to maintain acceptable temperature control of the produce, which is critical to product quality and shelf life. Being able to ensure that a shipment will remain within a temperature range for an extended period of time comes down largely to the type of primary packaging, the container that is used and the refrigeration method. Factors such as duration of transit, the size of the shipment and the ambient temperatures experienced are important in deciding what type of packaging is required.

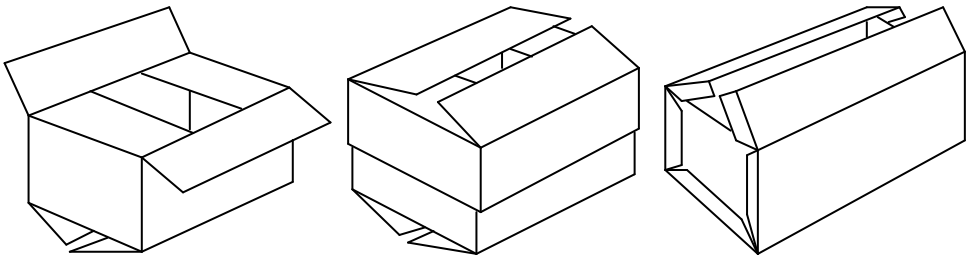
This being said, when it comes to produce and airflow there have been very few changes to the corrugated outer case other than experimenting with the positioning and number of ventilation holes to overcome the density of the product, or the design of primary, or inner packaging which restricts airflow and heat transfer. Examples of this are clamshells for products such as berries and mushrooms, bags for salads and vegetables and many other fresh fruit and vegetables types that are being packaged in some form of primary packing material.

In the case of bananas, temperature control is vital to maintaining product quality. The final quality of bananas is greatly influenced by pulp temperature of the fruit during ripening. Therefore, bananas must be kept refrigerated at a controlled temperature throughout the distribution cycle which calls for both vertical and horizontal airflow at different stages in the journey from pack house to consumer. Also, bananas produce large quantities of heat during the ripening process due to respiration. This heat buildup needs to be removed as it causes premature ripening.

Although produce containers typically include ventilation holes to allow flow of air through the container, a full pallet load of existing shipping containers does not provide for effective air flow. In addition the structural integrity of the box is negatively affected when too many ventilation holes are created in the side and end walls of the box.

The most commonly used style of corrugated boxes used for bagged fresh-produce applications and bananas are (figure 1):

- *Slotted boxes*: generally made from one piece of corrugated or solid fiberboard. E.g. Regular Slotted Containers (FEFCO 0201)
- *Telescoping boxes*: usually consist of separate top or top and bottom that fit over each other or a separate body. E.g. Full Telescope Half Slotted Container (FEFCO 0320)
- *Rigid/Bliss boxes*: the three pieces of this style of box includes two identical end panels and a body that folds to form the two side panels, an unbroken bottom and the top. E.g. Bliss Style Container (FEFCO 0606)



**Regular Slotted Container, FEFCO 201** | **Full Telescope Half Slotted, FEFCO 320** | **Bliss Style Container, FEFCO 606**

**Figure 1: Common Styles of Boxes used for Fresh Produce**

Ventilation holes can be cut into the side or end walls or both, depending on the ventilation requirements.

This research involved redesign of corrugated shippers commonly used for fresh produce and evaluated the temperature profiles between a standard RSCs and boxes with spacers that create gaps between all faces of the adjacent boxes when stacked on a pallet thus allowing air to flow freely between the adjacent faces of the boxes.

Three separate tests were carried out.

## 2. MATERIALS AND METHOD

### 2.1 Corrugated boxes

Both the control and test sample boxes had outer dimensions of 16 inches long by 12 inches wide by 9inches high. The boxes were stacked 7 layers high on a standard 48 inch by 40 inch pallet. Each layer consisted of 10 boxes as depicted in figure 2 and 3. None of the boxes in the test series had ventilation holes. All boxes were constructed using the same corrugated board specification

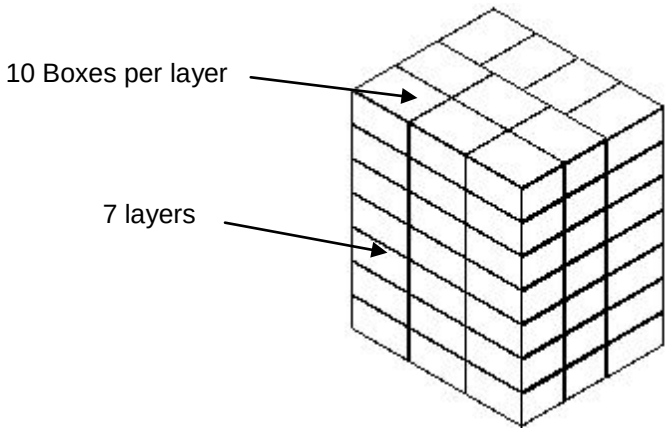



**Figure 2: Pallet Pattern**



**Figure 3: Pallet pattern used for each test series**

## 2.2 Container Designs

The box designs that were evaluated in the study for test 1 and test 2 were standard regular slotted box with no vent holes (control box) and a tray style box with the glue flanges orientated on the outer face of the side walls (test box), thus creating a space between adjacent boxes in the stacked pallet. See figures 4 & 4a.

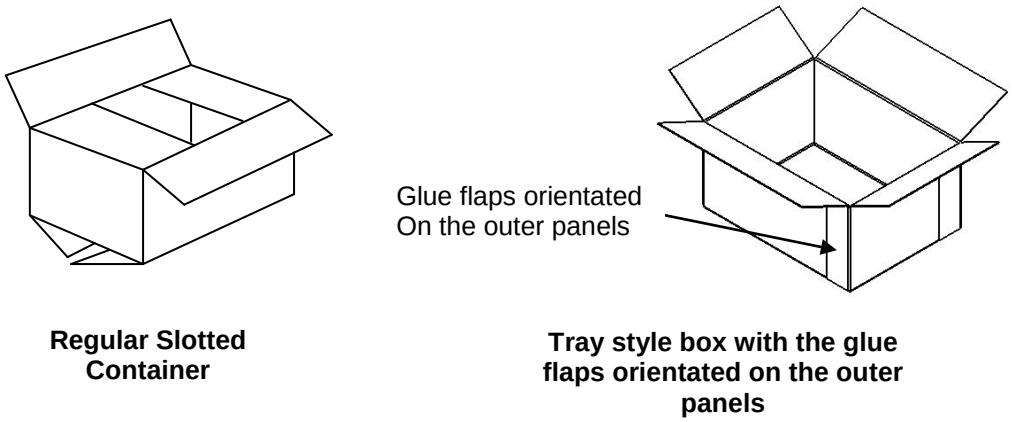



**Figure 4: Box Designs Evaluated in the Study.**

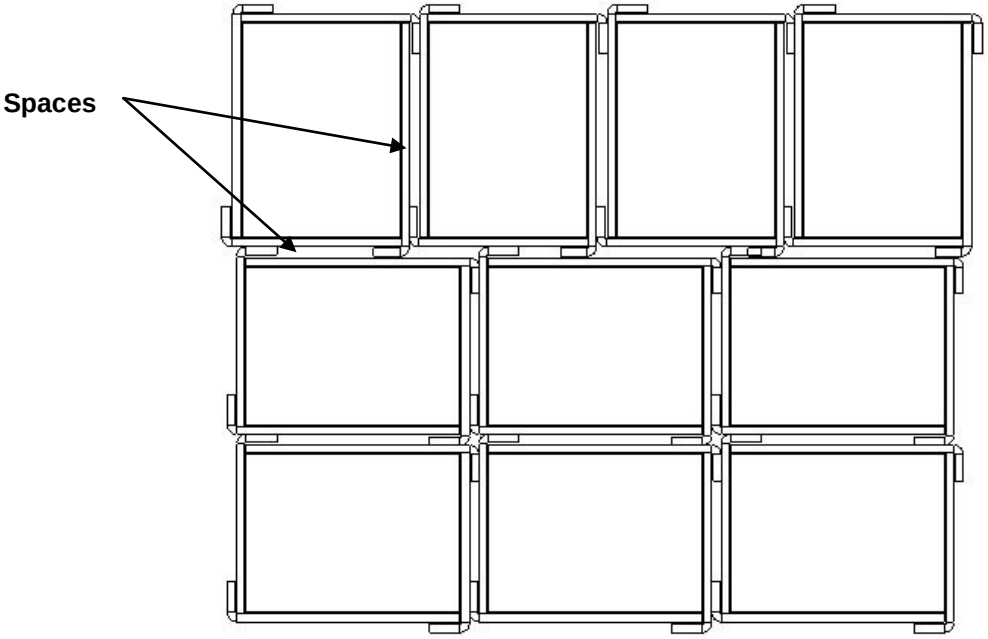



**Figure 4a: Space between adjacent boxes in the stacked pallet.**

For test 3, a box with protrusions on the corners and middle of the box was developed to make sure that possible side bulge was eliminated thus maintaining a uniform space between adjacent boxes. See figure 4, 4a and 4b.

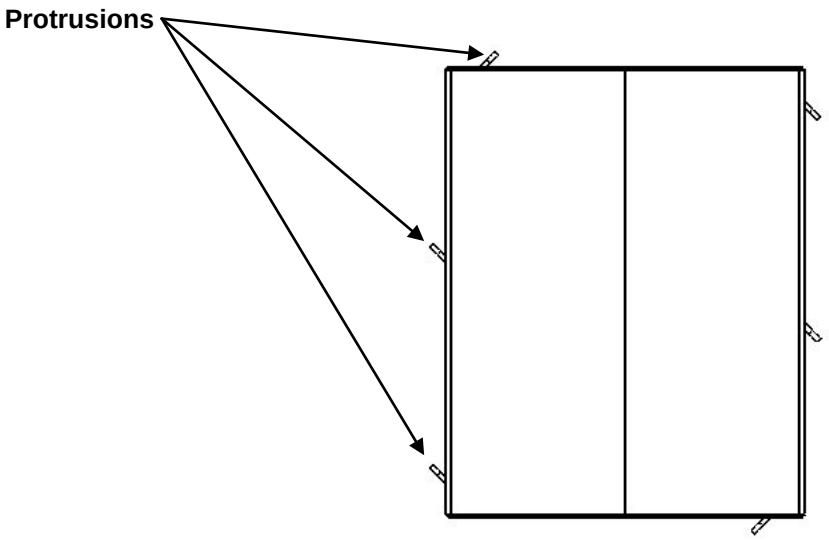



**Figure 4: Protrusions on the corners and middle of the box**

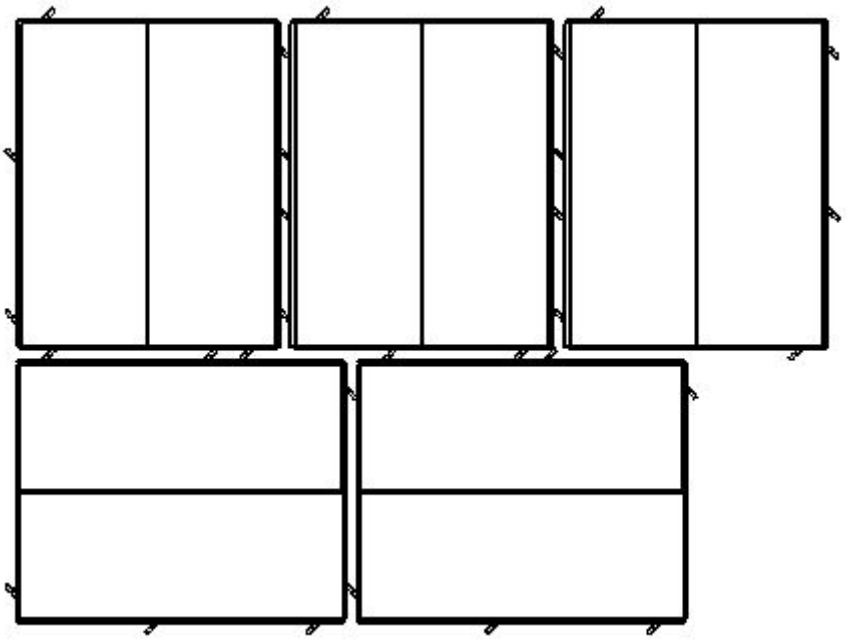


**Figure 4a: Protrusions on the corners and middle of the box create uniform spaces and prevent side bulge closing spaces.**



**Figure 4b: Picture of spaces created by protrusions**

## 2.3 Method

Three separate tests were carried out using Sensitech Temp Tale 4 temperature recorders. The recorders were preset using Sensitech Temp Tale Manager Desk Top 7.2.1 software. The recorders were set to degrees Fahrenheit with readings captured at 5 minute intervals with the manual start option checked. No alarms or temperature limits were activated. The recorders were placed in all 3 tests in the same locations in both the control and test boxes. See figure 5. The recorders were activated and placed in the predetermined positions whilst the pallet was being stacked.

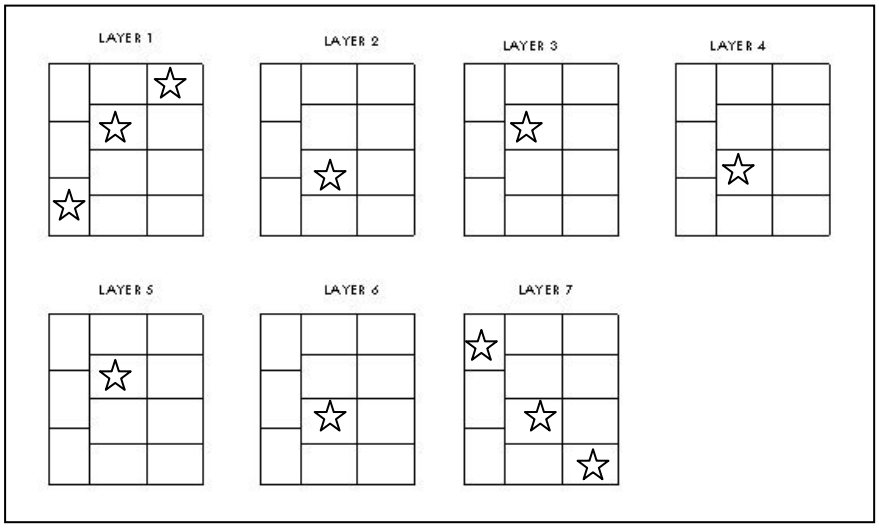



**Figure 5: Temperature Recorder Positioning**

Test 1: The boxes were packed with 6, 5 pounds bags of baby carrots and stacked on a 48 by 40 inch pallet in a 10 per layer configuration 7 layers high. The temperature recorder's probes were placed between the 1st and 2nd layers of the bagged carrots in each box. A plastic bag was placed over the top of the completed pallets. The pallets were then completely manually wrapped with stretch film. This blocked airflow from entering the stack in the horizontal orientations and also blocked through flow of air in the vertical orientation. The completed pallets were placed in a cold room at 37 degrees Fahrenheit for 24 hours then loaded onto a refrigerated trailer with a temperature set to 36 degrees Fahrenheit. The trailer was on the road for 6 days before returning to the cold room where it stood for 12 hours before retrieving the temperature recorders. Total duration of the test was 7.5 days with 1957 data points recorded.

Test 2: The boxes were packed with 6, 5 pounds bags of bagged baby carrots and stacked on a 48 by 40 inch pallet in a 10 per layer configuration 7 layers high. The temperature recorder's probes were placed between the 1st and 2nd layers of the bagged carrots in each box. The completed pallets were secured by means of corner boards placed on each corner of the boxes on the pallet and held in place by 3 straps located the middle of layer 1, the middle of layer 4 and the middle of layer 7 thus allowing air to flow into the stack in both the horizontal and vertical orientations. The completed pallets were placed in a cold room at 37 degrees Fahrenheit for 24 hours then loaded onto a refrigerated trailer with a temperature set to 36 degrees Fahrenheit. The trailer was on the road for 5 days before returning to the cold room where it stood for 12 hours before retrieving the temperature recorders with 1402 data points recorded.

Test 3: Test three was conducted in 2 identical Darwin walk-in environmental chambers. The chamber temperatures were set at 36.5 degrees Fahrenheit. The test and control boxes were packed with bottled water and stacked on a 48 by 40 inch pallet in a 10 per layer configuration 7 layers high. A hole was drilled into the lid of a single water bottle in box containing the temperature recorder. The probe of the recorder was placed through the hole into the water. The completed pallets were loaded into the Darwin walk-in chambers. The temperature recorders were retrieved after 23 hours with 276 data points recorded.

## 3. RESULTS AND DISCUSSION

### 3.1 Temperature Results

Table 1 shows details of the minimum and maximum temperatures of the 11 recorders placed in test series 1 and 2 as well as the average temperatures of the 11 recorders placed in test series 1 and 2. The percentage differences are shown graphically in figure 6a, 6b and 6c between tests 1 and 2. All temperatures are stated in degrees Fahrenheit.

**Table 1: Temperature Test Results for Test 1 & 2**

| | Test 1 | | Test 2 | |
|---|---|---|---|---|
| | **Control Box** | **Test Box** | **Control Box** | **Test Box** |
| **Average Max Temp** | 41.88 | 40.88 | 40.25 | 39.39 |
| **Average Min Temp** | 38.51 | 37.46 | 38.48 | 37.40 |
| **Average Temp of all recorders** | 40.27 | 39.11 | 39.22 | 38.55 |

The difference of 2.45% and 2.18% between the maximum temperatures of the control and test boxes in tests 1and 2 (figure 6a) indicates that the spaces created between the adjacent boxes make a difference in temperature even when airflow is restricted by a plastic pallet cap and shrink wrap. The 2.18% difference in test 2 indicates that the removal of plastic pallet cap and shrink wrap had an effect on the maximum temperature of the control boxes

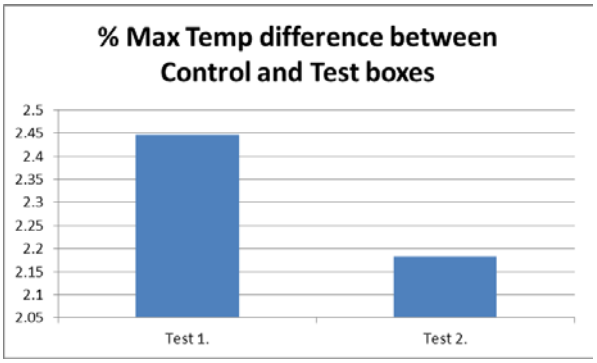



**Figure 6a: Maximum percentage Temperature difference between Control and Test boxes.**

The difference of 2.80% and 2.89% between the maximum temperature of the control and test boxes in test 1and 2 (figure 6b) proves that the spaces created between the adjacent boxes makes a difference in temperature. The removal of the plastic pallet cap and shrink wrap had a marked benefit on the minimum temperature in test 2

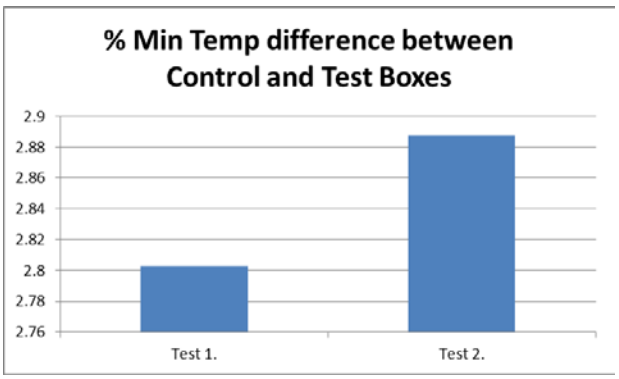



**Figure 6b: Minimum percentage Temperature difference between Control and Test boxes.**

The difference of 2.97% and 1.74% between the average temperatures of the control and test boxes in tests 1and 2 (figure 6c) confirms that the spaces created between the adjacent boxes make a difference in average temperatures and conforms to the comments made related to figure 6a.

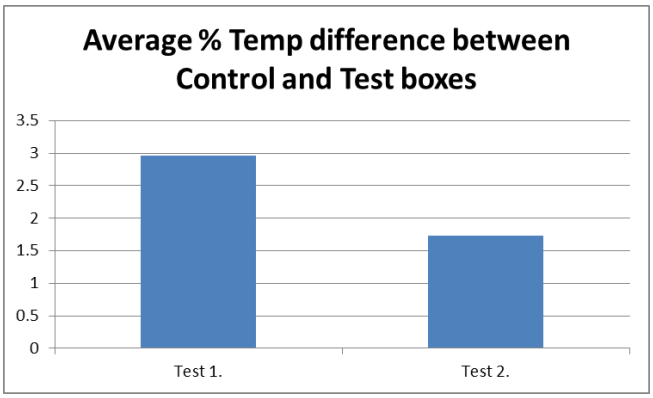



**Figure 6c: Maximum percentage Temperature difference between Control and Test boxes**

The graphs in figure 7 and 8 show the average temperature profiles over the full test periods and confirm the findings in the preceding discussion.

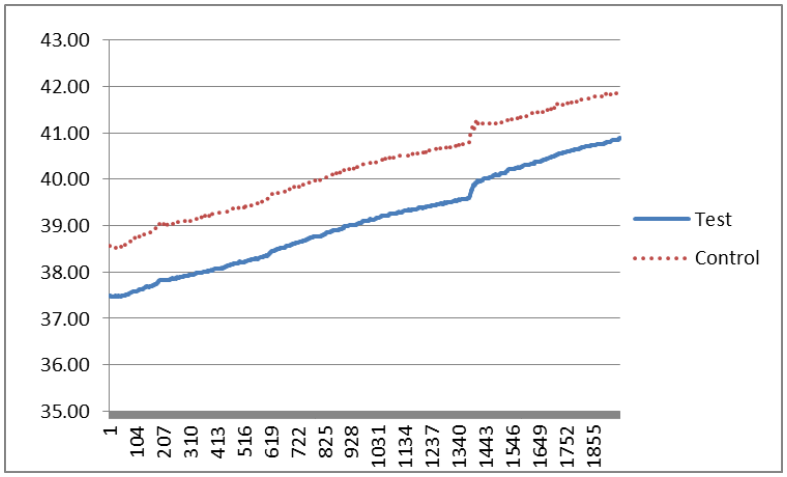



**Figure 7: Average Temperature of all recorders test 1**

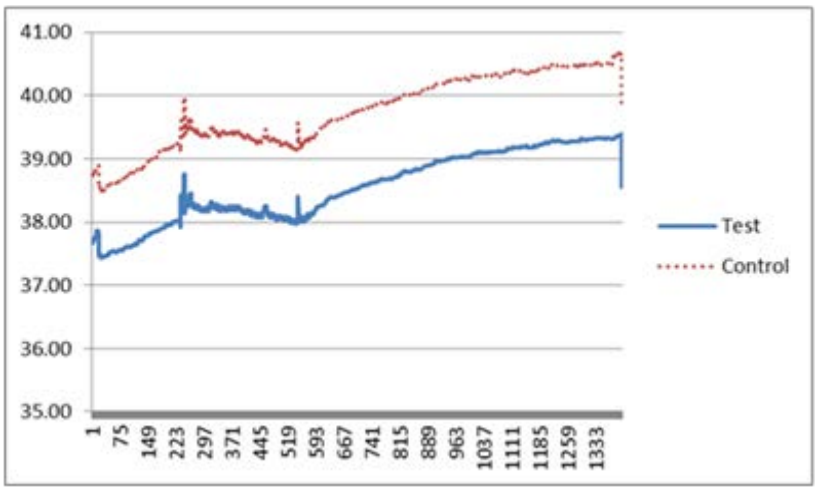



**Figure 8: Average Temperature of all recorders test 2**

Test 3 was initiated to monitor the cooling rate over a fixed period between the control box with no spacers in between adjacent boxes and the test box with spaces between adjacent boxes (See figures 9, and10.) in the controlled temperature of an environmental chamber. Figure 11 shows completed pallet in the Darwin walk-in environmental chamber.



**Figure 9: Boxes with no spaces**



**Figure 10: Boxes with spaces**



**Figure 11: Complete pallet in chamber**

Table 2 shows details of the minimum and maximum temperatures of the 11 recorders placed in test series 3 series as well as the average temperatures of the 11 recorders placed in test series 3. The average temperature difference of 4.24 degrees Fahrenheit across all recorders in a 23 hour period is significant especially when the rate of cooling of fruits such as strawberries is of prime importance. The results of the test are shown graphically in figure 9. All temperatures are stated in degrees Fahrenheit.

**Table 2: Temperature Test results for Test 3**

| | **Test 3** | |
|---|---|---|
| | **Control Box** | **Test Box** |
| **Average Max Temp** | 72.78 | 70.74 |
| **Average Min Temp** | 37.96 | 37.31 |
| **Average Temp of all recorders** | 50.08 | 45.84 |

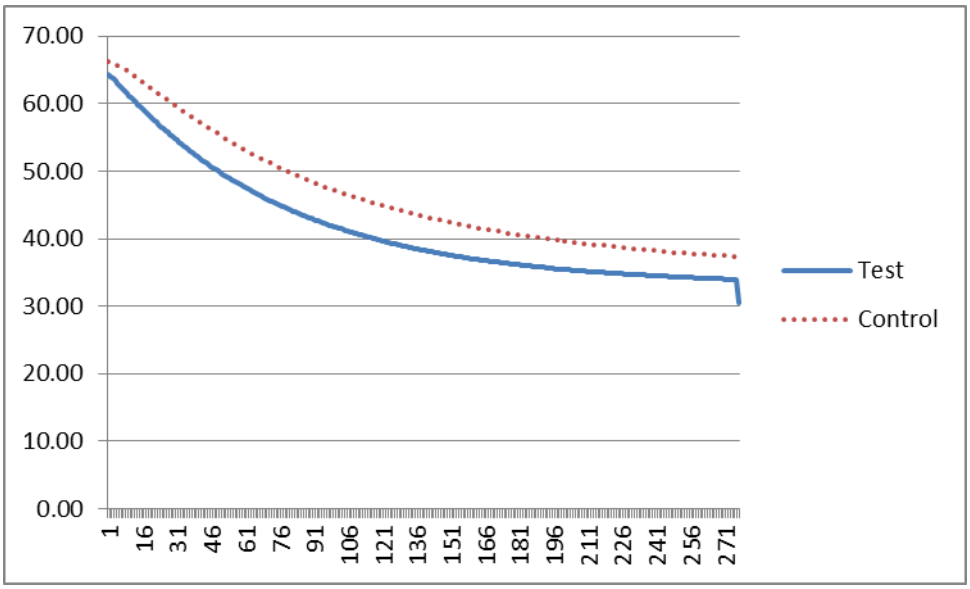



**Figure 9: Average Temperature of all recorders test 3.**

## 4. CONCLUSION

This study shows that the new box designs have a marked effect on the temperature of fresh produce over a typical distribution cycle from the production facility to a central distribution warehouse. The 6 and 5 days quoted in test1 and test 2 respectively is representative of a typical journey of +/- 1800 miles on the refrigerated truck.

The results of test 3 show great potential where accelerated cooling times are required to enhance product quality and shelf life.

Based upon results of this initial study further testing has been initiated and are currently underway.

# Development of a Freshness Indicator for monitoring Chicken meat Freshness

**N.Herranz *, T.Calvo, I.Lorente, S.Aucejo.**

*Packaging, Transport and Logistics Research Institute (ITENE)*
*C/Albert Einstein, 1, 46980 Paterna, (Valencia), Spain.*

**Corresponding author. E-mail: nherranz@itene.com*

**Abstract:** Food waste has acquired dimensions that must be considered as a worldwide problem that affects all the food supply chain from farm to fork. In Europe, total food waste is estimated in 89 million tonnes per year. The Waste and Resources Action Programme (WRAP) found that over a quarter of avoidable food waste was thrown away completely or still in its packaging. One reason is that current product expiry dates are conservatives. That means that to prevent foodborne illness and assure food quality, products show a shorter shelf life than the shelf life that they really have so, hundreds and hundreds of tonnes of safe food are wasted each year.

The development of intelligent packaging solutions could be a tool for reducing it. To be precise, the development of freshness indicators that will inform about the real shelf life of each individual product according to their microbial loads and degree of freshness, will allow printing longer shelf lifes on the products.

A freshness indicator for monitoring chicken meat freshness has been developed in SENSOPACK project. This technology will inform in an easy way about the real shelf life of packed fresh chicken meat products. This indicator uses a solvent-based flexographic ink. This ink is formulated using a reactive indicating compound, instead of common dyes or pigments. The indication compound is a metallic salt, which is allowed to the used in food contact applications. The initial colour of the metallic salt is blue. When sulphur volatile compounds are generated during the chicken breast spoilage, the metallic salt reacts with them and metal sulphide is generated, which colour is brown. As the more spoiled the meat product is, the darker the indicator colour is, so the indicator colour is related to the degree of freshness of the meat product.

Keywords: freshness indicator, metallic salt ink, sulphur volatile compounds.

## 1 Introduction

Consumer demand for mildly preserved, minimally processed, easily prepared and ready – to – eat “fresher” products have created the need of developing accurate, cost – effective, rapid, reliable, non – invasive and non-destructive methods or devices to evaluate real – time freshness of food products [1].

The production of poultry meat and products has increased significantly throughout the work in the last decade. Chicken and poultry products have become popular due to their specific sensory attributes and the increasing tendency of the public to consider white meat as being healthier compared to red meat [2].

Poultry is a highly perishable food and the time it takes to deteriorate varies from 4 to about 10 days after slaughtering [3]. Deterioration also depends on the condition of the poultry carcasses at the time of packaging, among many other factors [4].

Traditionally, the shelf life studies of perishable meat products are carried out by evaluating the microbiological and sensory quality of the product as a function of the storage time. In addition to these traditional methods, chemical metabolites produced in the microbiological deterioration of the food products have also been suggested as quality indicators of meat [5]. In particular, for packaged poultry products, volatile sulphur compounds such as hydrogen sulphide ($H_2S$) are generated in considerable amounts during the ageing of chicken packed storage [6]. Thus, selection of accurate compounds capable to react with these volatile compounds might monitor chicken freshness.

Specifically, metal organic compounds and or metal oxides can react directly and spontaneously with hydrogen sulphide to produce coloured metal sulphides. For example, lead acetate powder is suitable for use as pigments

for paints and inks, which with a low concentration of hydrogen sulphide gas results in a rapid visible change of colour from white to brown [7]. When the metal reacts with hydrogen sulphide or other possible volatile sulphur compounds (i.e. dimethyl sulphide and/or dimethyl disulphide), sulphides are produced. The chemical reaction with the sulphur compound results in a relatively abrupt change in the colour which correlates well with the quantity of the sulphur compound emitted [8].

In line with this behaviour, chicken freshness might be monitored with intelligent packaging solutions such as a freshness indicators applied on packaging materials. Safe and accurate formulations of indicators to be in contact with packaged product atmosphere might inform about freshness state in real time and even more accurately than expiry date.

Following with this solution, the main objective of this study was to develop a freshness indicator based on a metallic salt ink for monitoring chicken meat freshness. Chicken breast packages with different freshness indicators formulations were validated in a packaging trial according to sensory, microbiological and colour analysis at different storage temperatures.

## 2 Materials and methods

### 2.1 Materials and reagents

Metallic salt was purchased from Scharlab S.L. (Barcelona, Spain), cellulose-based varnish was supplied by Chimigraf (Barcelona, Spain) and cardboard substrates (thickness: 0.24 mm, weight: 120 g/m$^2$, L: 95.14, a: 0.28, b: 0.25) were purchased from a local office equipment retailer.

### 2.2 Freshness indicator development

2.2.1. Freshness ink manufacturing

2-10% (w/w) of metallic salt was mixed with 90-98% (w/w) cellulose-based varnish under 1200 rpm stirring during 15 minutes. In order to obtain a homogeneous dispersion, the mixture was milled with zirconia oxide/yttrium microspheres (0.6-1.2 mm of diameter) up to obtain a particle size < 5 µm approximately. A pale greenish-blue dispersion was finally achieved as a freshness ink. Three different formulations were prepared to obtain Indicator A, Indicator B and Indicator C.

2.2.2. Freshness ink application
4 µm draw downs of freshness ink were applied on cardboard substrates using an automatic film applicator (4340 Elcometer, UK). 10 replicates around 1.5 x 1.5 cm were prepared for each indicator.

### 2.3. Freshness indicator validation

2.3.1. Packaging trial

Chicken breast pieces were purchased in a local slaughterhouse. Chicken breast were packaged (SMART 300 Traysealer; ULMA, Spain) in PP / EVOH / PP trays, and a barrier PP / PA film was used as a sealing top. The ratio between the volume of gas and weight of food product (G/P ratio) was 3.5:1 (v/w). Chicken was packaged using 70% $N_2$ – 30% $CO_2$ of MAP conditions. A headspace gas analyser (PBI Dansensor Check Mate II; Denmark) was used to adjust MAP composition during packaging of chicken breast. The indicators with applied freshness ink were adhered in the inner layer of PP/PA film of each packaged tray with an adhesive tape. Samples were stored in a refrigerator at two different constant temperature conditions: 4°C and 15ºC. 10 replicates for each temperature with indicators A, B and C were studied.

2.3.2. Sensory analysis

Quantitative descriptive analysis was used to assess breast chicken inside the trays on different post-packaging days. Odour, colour, visual aspect and lixiviated liquids were the attributes used by a trained sensory panel to conclude a global score of each sample as a sensory quality quantification. The acceptability limit was the score 5 with 3 corresponding to an unacceptable quality (clearly recognizable off-odour and inedible). The samples were tempered during 15 minutes at 25ºC. Furthermore, batches were assessed for colour before opening pouches and for odour just after opening them. A minimum of three samples were evaluated.

2.3.3. Microbiological analysis

Chicken breast samples were removed from the pouches using sterile scalpels and forceps. Two cores of 10 ± 0.1 g, were aseptically removed from each sample and blended with a 90 ml of 1% peptone water (w/v) for 60 s in a Stomacher (BagMixer 400; Interscience, France). Additional dilutions were made in 1% peptone (w/v). Then 1 ml of the undiluted homogenate and of each dilution was spread on duplicate plates. Bacterial numbers were determined form plates bearing 30 – 300 colonies. Counts were obtained as follows: Aerobic plate counts on Plate Count Agar (Scharlab®), incubated at 32º C for 48 h; *Enterobacteriaceae* on Violet Red Bile Glucose Agar (Scharlab®), incubated at 37º C for 24 h and *Salmonella* on Salmonella Shigella Agar (Scharlab®), incubated at 37º C for 24 h. The legal limit was $10^6$ UFC/g (CENAN 1982) [9]. A minimum of three samples were evaluated.

2.3.4. Colour measurement

CIELab coordinates (L*, b* a* values) of freshness indicators applied in each chicken breast packaging were measured using a spectrophotometer (Konica Minolta, model cm-2500d). A circular measurement area (D=8mm) and a calibration with a white standard plate (L=100) was used. ΔE in order to evaluate colour change of tested indicators was calculated according to (1). Data treatment was carried out with SpectraMagic NX software to obtain pseudo-colour of each indicator.

$$\Delta E = \sqrt{(L_{initial} - L)^2 + (a_{initial} - a)^2 + (b_{initial} - b)^2} \quad (1)$$

## 3 Results and discussion

Samples of MAP (70% $N_2$ – 30% $CO_2$) chicken breasts were analysed to validate colour change of freshness indicators based on printing inks. 4ºC and 15ºC storage temperatures allowed to evaluate indicators evolution with two chicken freshness stages.

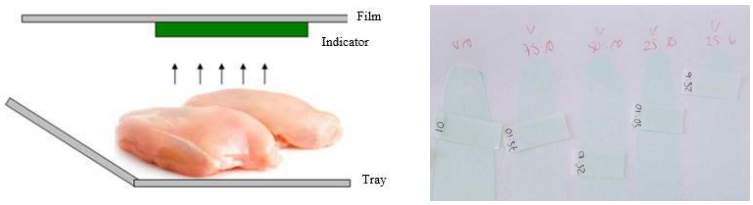



**Figure 1**: (A) Scheme of freshness indicator validation (B) Draw downs and indicators samples

### 3.1. Chicken meat shelf life study

Chicken meat shelf life was inferred with sensory and microbiological analysis. Figure 2 shows the chicken freshness loss according to these two studies.

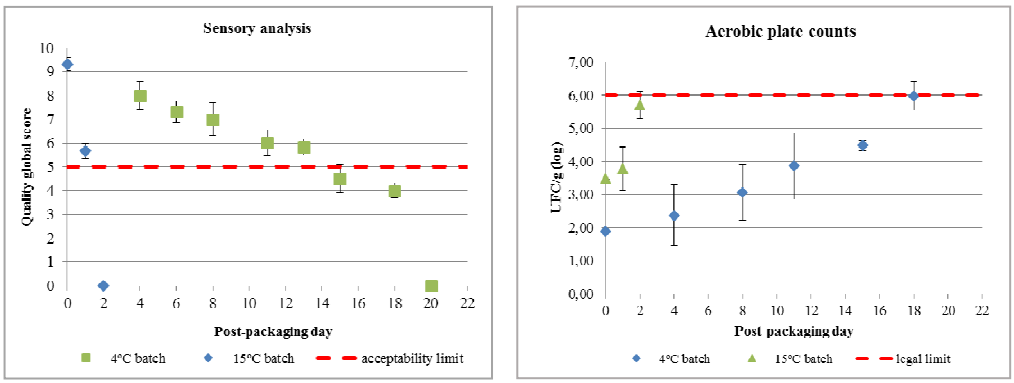



**Figure 2**: Chicken meat shelf life study. (A) Sensory analysis. (B) Microbiological analysis

As shown in Figure 2 (A), trained sensory panel detected chicken freshness variations with time. Furthermore, results were different according to each temperature conditions due to its effect on breast chicken spoilage. The higher temperature is, the faster the deterioration. Hence, sensory analysis concluded between post-packaging day 1 and 2 for 15ºC batch, and for day 15 for 4ºC batch. These days were where the global score of studied samples was less than acceptability limit (score 5).

In terms of microbiological quality as Figure 2 (B) indicates, aerobic plate counts exceeded legal limit ($10^6$ UFC/g) also at different times according to temperature storage conditions. 15ºC batch lingered up to day 2 and 4ºC batch with a slower evolution, reached legal limit in post-packaging day 18. *Enterobacteriaceae* count showed the same result as aerobic plate counts and only in post-packaging day 18 for 4ºC batch there was presence of *Salmonella*.

As a conclusion, in order to obtain a unified parameter of chicken breasts shelf life for comparing the colour change evolution of freshness indicators, according each temperature, an inferred value of shelf life was assumed regarding sensory and microbiological analysis. For each batch, microbiological results were considered prevalent due to its higher objectivity than sensory panel. As Table 1 shows, post-packaging day 2 and 18 for 15ºC and 4ºC batch respectively, were the end of shelf life for analysed packaged chicken breasts.

**Table 1:** Chicken meat shelf life study

| Analysis | Shelf life 15ºC batch (post-packaging days) | Shelf life 4ºC batch (post-packaging days) |
|---|---|---|
| Sensory | 1-2 | 15 |
| Microbiological | 2 | 18 |
| **Inferred shelf life** | 2 | 18 |

## 3.2. Colour evolution of freshness indicators

Freshness indicators with three different ink formulations (Indicator A, B and C) between 2-10% (w/w) of metallic salt and 90-98% (w/w) of cellulose-based varnish were evaluated. Measurements of CIELab coordinates were carried out for each sample from 4ºC and 15ºC batches. Figure 3 shows ΔE evolution calculated with L* a * b * values as equation (1) indicates.

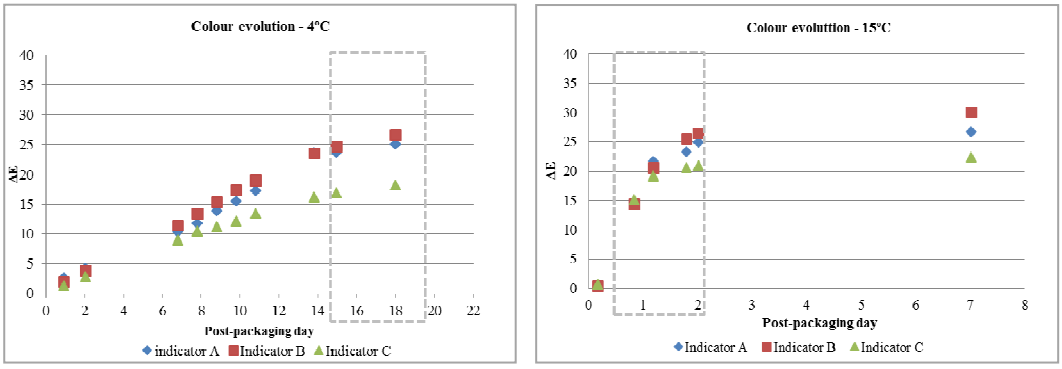



**Figure 3**: Colour evolution. (A) 4ºC Batch. (B) 15ºC Batch.

As Figure 3 shows, an increase of colour change (ΔE) was obtained for each indicator when post-packaging days became higher. Specifically, for 4ºC batch (Figure 3 (A)), the increase were more gradual than for batch 15ºC (Figure 3 (B)) due to the different levels of breast chicken freshness. However, ΔE values reached at the end of shelf life (Figure 3 highlighted area) were similar for two temperature batches and even for each indicator (A, B and C). Thus, tested ink formulations showed similar behaviour and the three indicators were adjusted for each freshness stage (batch 15ºC, batch 4ºC) accurately.

As an example, Table 2 and Table 3 show the correspondence between CIELab coordinates and pseudo colour given by SpectraMagic NX software for one of tested indicators.

**Table 2:** Indicator B. CIELab coordinates and pseudo colour (4ºC Batch)

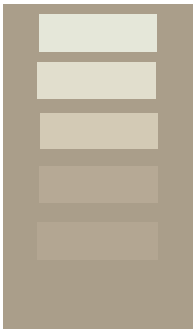
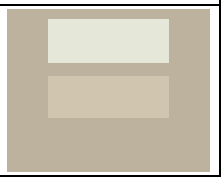
| Post-packaging day | 4ºC batch | | | Pseudo colour |
|---|---|---|---|---|
| | L* | a* | b* | |
| 0 | 91.37 | -2.84 | 5.87 |  |
| 2 | 88.54 | -1.60 | 8.20 | |
| 7 | 81.61 | 0.29 | 10.79 | |
| 14 | 70.12 | 1.54 | 11.66 | |
| 16 | 68.97 | 1.60 | 11.50 | |
| **18 – End of shelf life** | 65.69 | 1.45 | 11.21 | |

**Table 3:** Indicator B. CIELab coordinates and pseudo colour (15ºC Batch)

| Post-packaging day | 15ºC batch | | | Pseudo colour |
|---|---|---|---|---|
| | L* | a* | b* | |
| 0 | 91.37 | -2.84 | 5.87 |  |
| 1 | 80.08 | 0.05 | 12.40 | |
| **2 - End of shelf life** | 73.16 | 0.06 | 11.60 | |

As pseudo colour images shown in Table 2 and Table 3, Indicator B changed its colour gradually in a distinguishable manner from pale greenish-blue to dark brown at the same time chicken breast was spoiled. In addition, according to temperature storage conditions, colour change presented different speed with a faster behaviour for higher temperatures due to a more accelerate freshness loss.

## 4 Conclusions

A freshness indicator based on a metallic salt ink has been validated as a tool for monitoring chicken meat freshness. Ink components are capable to react with generated sulphur volatile compounds from chicken breast spoilage. The interaction generates a gradual colour change of the indicator, which become darker in accordance with freshness packaged product loss. Furthermore, the study of two temperature conditions shows the relation of indicator colour change to different degrees of freshness.

## 5 Acknowledgements

Authors would like to thank the SENSOPACK consortium and the financial support by Spanish Ministry of Economy and Competitiveness (MINECO) and European Commission for the Project SENSOPACK - IPT-020000-2010-014.

## 6 References

1. A Nopwinyuwong, S Trevanich, P Suppakul, 2010, “Development of a novel colorimetric indicator label for monitoring freshness of intermediate – moisture dessert spoilage”, *Talanta*, vol. 81, no. 3, pp. 1126 - 1132
2. C. C. Balamatsia, E. K. Paleologos, M. G. Kontominas, and I. N. Savvaidids, 2006, “Correlation between microbial flora, sensory changes and biogenic amines formation in fresh chicken meat stored aerobically or under modified atmosphere packaging at 4ºC: possible role of biogenic amines as spoilage indicators”, *Springer*.

3. C. Marenzi, 1986, “Proper meat storage prevents spoilage”, *Poultry*, vol. 6, pp. 12 – 15.

4. S. M. Jimenez, M. S. Salsi, M. C. Tiburzi, R. C. Rafaghelli, M. A. Tessi, and V. R: Coutaz, 1997, “Spoilage microflora in fresh chicken breast stored at 4ºC influence of packaging methods”, *Journal of Applied Microbiology*, vol. 83, pp. 613 – 618.

5. R. H. Dainty, 1996, “Chemical / biochemical detection of spoilage”, *International Journal of Food Microbiology*, vol. 33, pp. 19 – 33.

6. M. Smolander, E. Hume, K. Latva-Kala, T. Luoma, H.L. Alakomi, R. Ahvenainen, 2002, “Myoglobin-based indicators for the evaluation of freshness of unmarinated broiler cuts”, *Innovative Food Science & Emerging Technologies*, vol. 3, pp. 279–288.

7. W. Hoagland, D. K. Benson, R. D. Smith 2013, “Hydrogen sulphide indicating pigments”, *US Patent* No 8,574,917 B2.

8. E. Hurme, S. Kivinen, M. Koivisto, M. Smolander, 2004, “Indicator”, *US Patent* No 2007/0087443 A1.

9. M. Moragas, B. De Pablo, 2004, “Recopilación de normas microbiológicas de los alimentos y asimilados y otros parámetro físico-químicos de interés sanitario”, *www.euskadi.net.*

# If At First You Don't Succeed: Older Consumers And Hospital Food & Beverage Packaging – A Matter Of Try, Try And Try Again!

**Alison Bell[1*], Karen Walton[1,] Nicola Westblade[1], Kate Morson[1], Jacqueline Chevis[2], Leire Harries[3] and Alaster Yoxall[4]**

[1] *School of Health Sciences, University of Wollongong, Australia*

[2] *School of Health Sciences, University of Wollongong, Australia*

[3] *Department of Mechanical Engineering, University of Sheffield, UK*

[4] *Art and Design Research Centre, Sheffield Hallam University, UK*

[*] *Corresponding author. Email: abell@uow.ed.eu*

**Abstract:** 'Openability' of food and beverage packaging has been shown to be problematic for older consumers. Pressure on resources has seen the use of packaged food and beverages increase in Hospitals within the NSW region of Australia. Studies at the University of Wollongong have shown that not only is Hospital food & beverage packaging problematic, difficulty opening it was identified as a barrier to nutritional intake.

Given the serious nature of the problem, a series of studies have been undertaken by the University of Wollongong and Sheffield Hallam University, to evaluate the issues surrounding the 'openability' of this packaging in an attempt to understand in detail the issues leading to difficulty in use.

Amongst the poor performing packs were seen to be water bottles, drink cartons and cheese portions. Whilst issues surrounding strength were seen to be linked to accessed to bottled water, all other pack types were significantly affected by dexterity and in particular the fine control needed to pinch and peel tabs or remove drinking straws.

Sound ergonomics indicates that products should be designed for the user population, yet the experience of our consumers indicates that this is not necessarily the case. Work is ongoing to understand in more detail the effects of ageing such a reduced dexterity on packaging 'openability' as well as the effects of age and posture. The eventual aim of this work is to collaborate with packaging designers, manufacturers and brand owners to develop and produce effective and reliable packaging for both the healthcare and retail environments.

Keywords: inclusive design, malnutrition, packaging.

## 1 Introduction

Society is ageing; in 2011 16% of United Kingdom's population was above 65 years of age [1] and is predicted to rise to 19% in 20 years [2]. This is not just a UK phenomenon, the UN predicts the population of over 65's to rise to over 1.5 billion in 2050 from 486 million in 2006 (UN, 2008). A society in which a large proportion of its citizens are aged creates a major public health problem for government, health practitioners and other stakeholders. As we age, the likelihood of living with some form of chronic illness is significant. The prevalence of disability from the US Census in 2005 demonstrates that for individuals over 75, the proportion of people who need assistance was 55.9% rising to 71% for those 80 and over [3].

Health services across the world are under severe pressure due to this increase in longevity and associated likelihood of chronic illness, older people are more likely to visit hospital and stay for longer. However, many of the illnesses previously associated with old age have more recently been attributed to poor diets and there is undisputed evidence that diet and nutrition are directly linked to many of the chronic diseases afflicting older adults [6].

Researchers have estimated that 40% of UK hospital patients were malnourished [7] and further studies have shown that elderly patients are five times more likely to be at risk of malnutrition than younger patients [8,9].

A series of researchers [7,10,11], have identified inability to access food and beverage packaging as a contributing factor to malnutrition among the elderly and disabled in hospitals. Work by Bell et al., [12] looked at the issue of packaging accessibility in hospitals in the NSW region of Australia. This work used a patient and staff questionnaire along with pinch and grip strength measurements to assess reasons surrounding inability to access food and beverage products in the hospital environment. A typical meal tray with packaged items is shown in the Figure 1 below.




**Figure 1:** Typical meal tray in the study by Bell et al., [12]

In the study by Bell et al., [12], approximately 140 participants under took the packaging questionnaire along with 60 staff. The mean age of the sample was 72 years (±15 years); 46% male and 54% female. The patient interviews in this initial study identified five forms of packaging that could not be opened: 23% could not open convenience dinners, 17% water bottles, 17% cereal, 12% tetra packages and 10% condiments (jam). The problematic packaging types are shown in Figure 2.

Of those patients who could open the products, approximately 50% of patients had some difficulty opening the convenience meal, the milk and the cereal pack. Nearly 40% of these patients also had difficulty opening the water bottle and tetra packs. All staff reported that patients ask for help opening food and beverage packaging and 39% of staff reported some difficulty opening certain food and beverage packaging items themselves. Figure 3 below shows that items that participants were unable to open were also those items that took the longest time to open where the item could be opened. The work showed that for water bottles the accessibility issue was related to strength, whereas for the cereal packages and tetra packs the issue appeared to be a problem of both dexterity and strength. Hence it was decided to study the issues surrounding poor openability in further detail using a range of ergonomic techniques and analyse the effect of posture on strength and dexterity.




**Figure 2:** Problematic packaging types

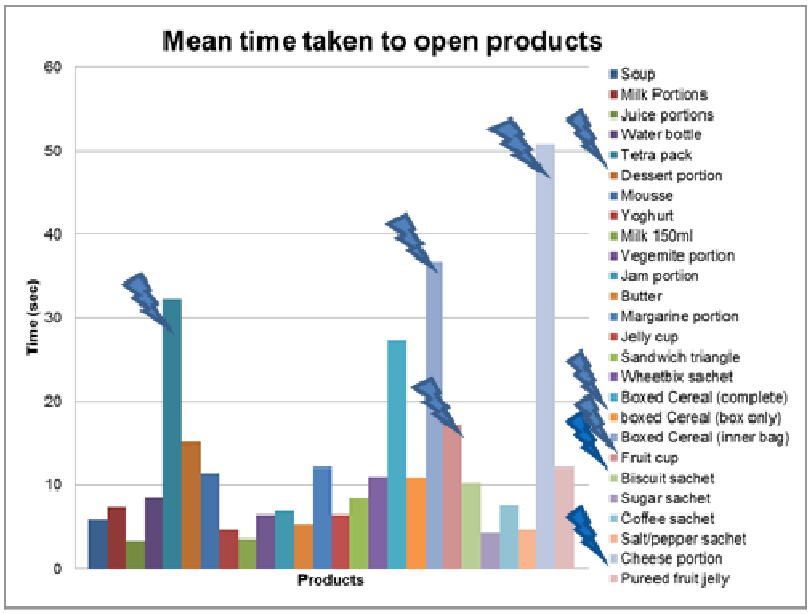



**Figure 3:** Time taken to open various packaging items

## 2 New Studies

A series of studies using a range of ergonomics assessment techniques was undertaken to understand dexterity in more detail and to further analyse the effect of posture on strength and dexterity.

### 2.1 Task Analysis: opening supermarket items

In order to gain a wide insight to the type of tasks needed to access standard packaging products available, the product range of a supermarket was chosen, as they sell many different types and varieties of food products. The supermarket chosen was the UK supermarket Tesco due to their significant presence with more than 3000 stores in the UK [13] and their website has an online grocery section which contains thousands of products, representative of what consumers are expected to open.

Using the images on the website it was possible to identify how certain products were opened. If the images were not detailed enough or unavailable, a store was visited for identification. If the product was not available in

store, its method of opening was left unidentified. This was possible as after identifying the first several hundred products, few new types of packaging were documented, in all likelihood unidentified packaging types will have already been documented.

The process itself involved using a tally chart, for each product that matched a type of packaging a tally was added. The type of packaging was dependent on the design of the packaging and not the method by which it is opened, as the opening techniques vary from one person to another.

### 2.2 Grip and Pinch Strength Testing: well elderly adults in a hospital environment

A total of 37 people (14 male [38%], 23 female [62%]) responded to the invitation, with each being randomly allocated a time slot on one of the two days of testing. Participants were to be over 65 years of age, independently living in the community and considered to be well. Each participant was tested in either the bed or chair first, depending on their allocated time slot. In each position, grip strength, pinch strength and dexterity were measured using validated testing procedures. Grip strength was measured using a Jamar Dynamometer [14]. Participants were tested on their dominant hand first for both the grip and pinch strength measurements. Pinch strength was tested with a Jamar Hydraulic Pinch Gauge [14] using three different tests; tip pinch, three point pinch and a lateral pinch. Both instruments were calibrated for the testing days. Dexterity was tested using the Perdue Pegboard [15], followed by the participants having to identify and open seven packaged items commonly found in the hospital setting.

### 2.3 Dexterity Testing: well elderly adults in a hospital environment

Dexterity of participants was analysed using the Purdue Pegboard Test first proposed by Tiffin in 1948 [15]. The Purdue Pegboard Test can be used for numerous purposes including testing for the presence and/or extent of brain damage, learning disabilities and dyslexia. There are four individual tests that are carried out when using the Purdue Pegboard. Normally, for all of these tests, the participant sits at a table that is at comfortable height and all standard data 'norms' such as those provided by Lafayette Instruments [14] and Desrosiers [16] have previously been measured in this way. However, given that the study by Bell [12] identified that 'fidliness' was a major factor; participants were also tested sitting in a chair and lying in a bed (as per the grip and pinch study described in section 2.2). The pinch, grip and dexterity tests were undertaken in a hospital training facility at The School of Health Sciences at the University of Wollongong, Australia, as shown in Figure 4. An example of a participant undergoing testing is shown in Figure 5.



**Figure 4**: Hospital training environment used to study posture effects



**Figure 5**: Posture analysis for grip strength and dexterity

### 2.3 High Speed Video Analysis of package opening

Participants were also analysed using High Speed Video (HSV) analyses to study finger motion in greater detail. This analyses is able to film at speeds significantly higher than a standard video camera (60 thousand frames a second, a standard camera films at 25 frames per second) using both a 'Phantom' SA3 camera and a pair of Phantom V4.2 cameras (Photron.com). Six participants were analysed opening a range of 'fiddly' packaging and their dexterity videoed and analysed using equations calculating joint motions.



**Figure 6:** participant opening packaging whilst being filmed using HSV

## 3 Results and Discussion

### 3.1 Task Analysis

After studying the packaging items available online and undertaking a task analysis it was found that packaging in general required one, or a combination of the following methods to open:

- Press and Dispense
  - Pressing down on a component allows for release of the product
- Bag

- A pulling apart action allows for the bag to be opened at the seal
- A tearing action produces an opening

- Tab Removal/ Interaction
  - A component that has to be snapped away from the packaging in order to open the packaging, it may also be snapped then peeled
  - A seal of the packaging must be pierced to allow for access
  - A component of the packaging may have to be: bent, pulled apart, unwound or torn away in order to remove it.
- Lid and Cap
  - A lid or cap that has to be twisted and lifted away from the rest of the packaging.
  - A lid that peels away from the rest of the packaging.
- Box and Unwrap
  - A box that is torn to be opened
  - Packaging that must be unfolded with little force as the packaging has no form of seal.

It can be seen from the list that certain forms of packaging facilitate a number of precision actions to open the pack (see Figure 7). The aim here was to attempt to categorise pack formats by tasks needed and to identify pack forms and that actions that may be problematic. Packaging that has multiple functions to open such as a tetra pack, drinks carton or boxed cereal scored badly in the original survey by Bell et al., [12]. By taking a task analysis approach to packaging we can select items that have fewer manipulations to use, for example cereal in pots rather than in boxes with a separate bag.

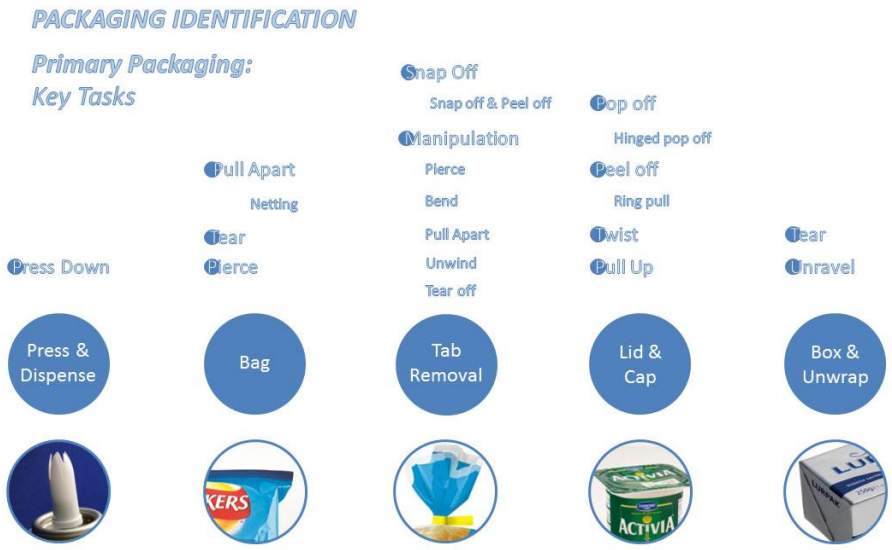



**Figure 7**: packaging identification by task analysis

### 3.2 Grip and Pinch Strength Testing

Given that many hospitalised patients access food in bed or from a chair it was necessary to examine the effect of posture on grip and strength. Using the instrumentation and the methods described in section 2.2 the results of grip and pinch are shown are shown in Table 1 for both the bed and the chair postures, (Mean (standard deviation [SD]) and median (interquartile range [IQR]) grip and pinch strength scores). A Shapiro-Wilk test for normality showed varied distributions for each variable; therefore both the mean and median have been reported.

**Table 1**: Mean (standard deviation) and median (interquartile range) for grip strength test, tip, three point and lateral pinch strength tests in the bed and chair posture.

| | Grip strength | Tip pinch | Three point pinch | Lateral pinch |
|---|---|---|---|---|
| **Bed** | | | | |
| **Mean (SD) R Hand** | **29.2 (10.7)** | **3.8 (1.5)** | **5.4 (2.1)** | **6.8 (2.3)** |
| **Median (IQR) R Hand** | **27.7 (20.9-37.2)** | **4.0 (2.5-5.1)** | **5.3 (3.9-6.5)** | **6.9 (4.9-8.6)** |
| **Mean (SD) L Hand** | **27.4 (11.4)** | **3.8 (1.5)** | **5.4 (1.9)** | **6.2 (2.5)** |
| **Median (IQR) L Hand** | **24.6 (18.9-33.6)** | **3.5 (2.5-4.8)** | **5.3 (3.7-7.1)** | **5.5 (4.4-8.3)** |
| **Chair** | | | | |
| **Mean (SD) R Hand** | **28.8 (10.4)** | **24.3 (1.3)** | **6.2 (2.1)** | **7.3 (2.3)** |
| **Median (IQR) R Hand** | **26.5 (21.4-34.4)** | **4.5 (3.0-5.3)** | **6.0 (4.4-7.8)** | **6.9 (5.5-9.3)** |
| **Mean (SD) L Hand** | **27.4 (10.7)** | **4.2 (1.3)** | **5.9 (1.8)** | **6.7 (2.5)** |
| **Median (IQR) L Hand** | **24.3 (21.1-34.9)** | **4.0 (3.2-4.8)** | **6.0 (4.5-7.1)** | **6.4 (4.8-8.0)** |

Table 2 is a collation of all the significant results found when testing for a correlation between each of different tests and the various food products. As illustration in the table, there was a consistently significant correlation found with both the time and number of attempts to open the bag within the cereal box, as well as the time to open the foil sealed thickened water. The strongest correlations were found between the bed grip left (r=-0.710), bed tip pinch right (r=-0.712), the chair tip pinch right (r=0.889) and the chair three point pinch right (r=0.795) with the time taken to open the foil seal water. No significant correlations were found in relation to the other packaged food products.

**Table 2***:* Significant correlations between grip strength, tip, three point and lateral pinch strength tests for the right and left hands in the bed and chair posture.

| Test | Food Item | Correlation Coefficient | Sig. (2-tailed) | Significant |
|---|---|---|---|---|
| **Bed Grip Right** | **Box cereal – no attempts to open bag** | **-0.352** | **0.044** | **Yes (moderate)** |
| **Bed Grip Left** | **Foil Sealed water – time** | **-0.710** | **0.032** | **Yes (strong)** |
| **Bed Grip Left** | **Box cereal – no attempts to open bag** | **-0.401** | **0.021** | **Yes (moderate)** |
| **Bed Pinch Tip Right** | **Foil sealed water – time to open** | **-0.712** | **0.031** | **Yes (strong)** |
| **Bed Pinch Tip Right** | **Box cereal – attempts to open bag** | **-0.345** | **0.049** | **Yes (moderate)** |
| **Bed Pinch 3 Point Pinch Right** | **Box cereal – attempts to open bag** | **-0.377** | **0.030** | **Yes (moderate** |
| **Bed Pinch3 Point Pinch Left** | **Box cereal – time to open bag** | **-0.345** | **0.049** | **Yes (moderate)** |
| **Bed Pinch 3 Point Pinch Left** | **Box cereal – attempts to open bag** | **-0.410** | **0.018** | **Yes (moderate)** |
| **Chair Pinch Tip Right** | **Foil Sealed water – time** | **0.889** | **-0.001** | **Yes (strong)** |
| **Chair 3 Point Pinch Right** | **Foil Sealed Water – time** | **0.795** | **0.01** | **Yes (strong)** |

Figure 8 illustrates the median, minimum and maximum times taken to open each of the packaged food items in the two postures. No significant differences were found between the two postures, however Figure 8 illustrates that the most problematic packages to open in both postures were the tetra pack, honey sachet, the boxed cereal and the cheese portion.

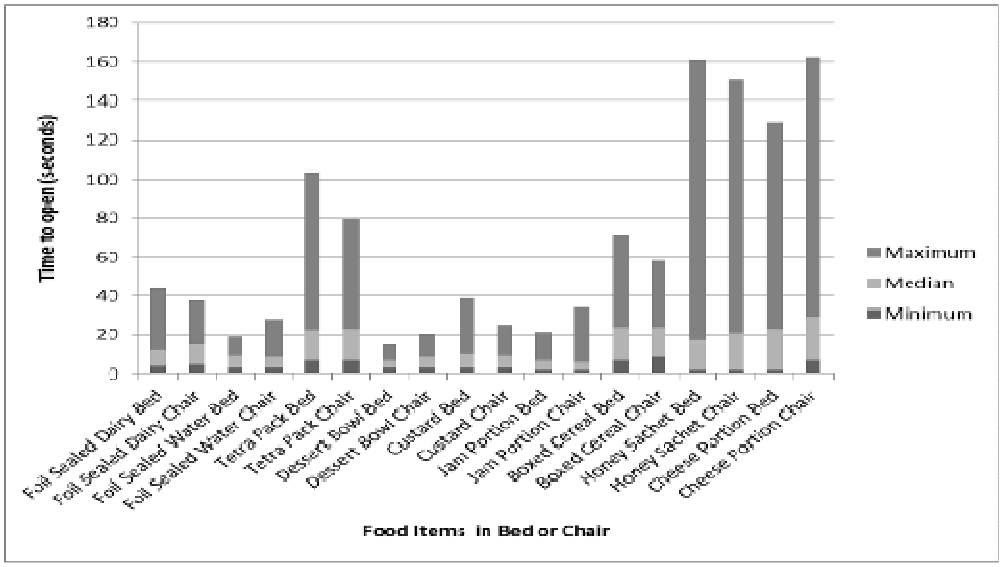



**Figure 8**: Median, minimum and maximum times taken to open food packages in the bed and chair posture strength test, all pinch strength tests were found to be significantly different, with laying down consistently proving to be the more difficult posture.

### 3.3 Dexterity Testing

As for grip and pinch strength testing above, dexterity was measured in both sitting and laying down postures to replicate the hospital environment. Using the instrumentation and the methods described in section 2.3 the results for the effect of posture on dexterity scores (Table 3) as well as the correlation between dexterity, time taken and number of attempts to open a package was determined (Table 4). Both these tables are shown below. This study demonstrated that the laying down posture adversely affected the Subject's dexterity scores. Additionally, there was an inverse correlation between dexterity and time taken to open the tetra-packs, custard (foil sealed cup) and the inner bag of the boxed cereal.

**Table 3***:* Differences in dexterity scores between sitting and laying down postures

| Dexterity measure pair | Mean | Std. Deviation | t or Z score† | Sig. (2-tailed)* | Sig difference?‡ |
|---|---|---|---|---|---|
| **Bed Left- Chair Left** | -.667 | 1.493 | t= -2.565 | .015 | ✓ |
| **Bed both- Chair both** | -.909 | 1.182 | t= -4.417 | .000 | ✓ |
| **Bed right+left+both- Chair right+ left +both** | -3.152 | 3.114 | t= -5.814 | .000 | ✓ |
| **Bed assembly- Chair assembly** | -1.273 | 3.979 | t= -1.838 | .075 | × |
| **Bed right – Chair right** | - | - | Z= - 3.775 | .000 | ✓ |

†- t score for evenly distributed data where t-tests were utilised, and Z score recorded when Wilcoxon Signed Ranks Test was utlised
*- Significant when P value <0.05 (two-tailed)
‡- ✓ indicates there was a statistically significant difference. × indicates there was not a significant difference

**Table 4***:* Significant correlations between time and attempts to open a product and dexterity

| Food Product | Subject Posture/ time or attempts | Dexterity measure | Correlation Coefficient† | Significance | Strength of Correlation‡ |
|---|---|---|---|---|---|
| **Tetra pack** | Bed/time | Both hands | -.369 | .041 | ✓ |
| | | Right+left+ both | -.452 | .010 | ✓✓ |
| | Chair/time | Both hands | -.446 | .011 | ✓✓ |
| | | Right+left+both | -.448 | .010 | ✓✓ |
| **Custard** | Bed/ time | Both hands | -.861 | .000 | ✓✓✓ |
| | | Right+left+both | -.824 | .001 | ✓✓✓ |
| | Chair/time | Both hands | -.812 | .001 | ✓✓✓ |
| | | Right+left+both | -.796 | .001 | ✓✓✓ |
| **Boxed cereal** | Bed/ time | Both hands | -.536 | .002 | ✓✓ |
| | | Right+ left +both | -.446 | .010 | ✓✓ |
| | Chair/time | Both hands | -.463 | .007 | ✓✓ |
| **Boxed cereal-inner packet** | Bed/ Time | Both hands | -.623 | .000 | ✓✓ |
| | | Right+left+both | -.535 | .002 | ✓✓ |
| | Chair/time | Both hands | -.410 | .039 | ✓✓ |
| | Bed/ attempts | Both hands | -.439 | .012 | ✓✓ |
| | | Right+left+both | -.434 | .013 | ✓✓ |
| **Cheese** | Bed/attempts | Both hands | -.363 | .038 | ✓ |
| | Chair/attempts | Both hands | -.360 | .036 | ✓ |
| **honey** | Bed/time | Right+left+both | -.377 | .031 | ✓ |
| | Chair/time | Both hands | -.581 | .000 | ✓✓ |
| | | Right+left+both | -.651 | .000 | ✓✓ |
| **Foil dairy** | Bed/ time | Both hands | -.501 | .029 | ✓✓ |
| | | Right+left+both | -.462 | .047 | ✓✓ |
| **jam** | Bed/ time | Both hands | -.661 | .000 | ✓✓ |
| | | Left+right+both | -.634 | .000 | ✓✓ |

**† - Correlation is significant at the 0.05 level (2-tailed).**
**‡- One tick indicates a weak/small correlation, two ticks indicate moderate correlation, three ticks indicates a strong correlation**

Of particular concern is the finding for Tetra packs as they are used in hospitals to provide high energy, high protein supplements for patients with low appetites, are malnourished or are at risk of becoming malnourished. A previous study by Wilton et al. [17] also identified Tetra packs as the most problematic type of packaging for patients to open.

### 3.4 High Speed Video Analysis

The software Check3D was used for calibration and digitisation of the points of interest on the hand by selecting the points of interest in each frame. This software gives the (x, y, z) coordinates of each point during the opening task. Figure 9 is an image still of the process.

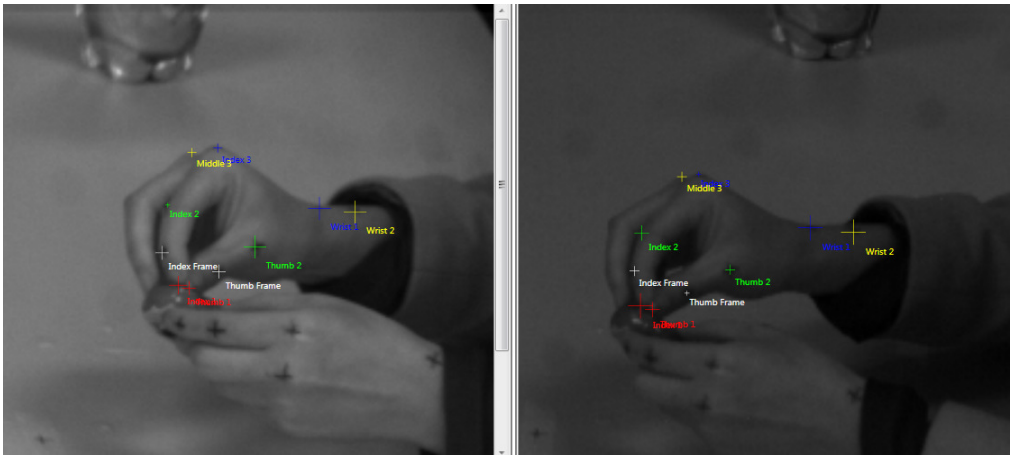



**Figure 9**: A frame from the Check3D software showing the points on the hands for a recording opening the cheese portion.

These points had to be determined. The different variables that were measured using Check3D included the total distance travelled and the angles of the hand. The middle, little and ring finger were not considered. To evaluate the total distance covered three points were chosen: the tip of the index finger, the tip of the thumb and a point on the wrist. The joint angles considered are shown in Figure 10 below.

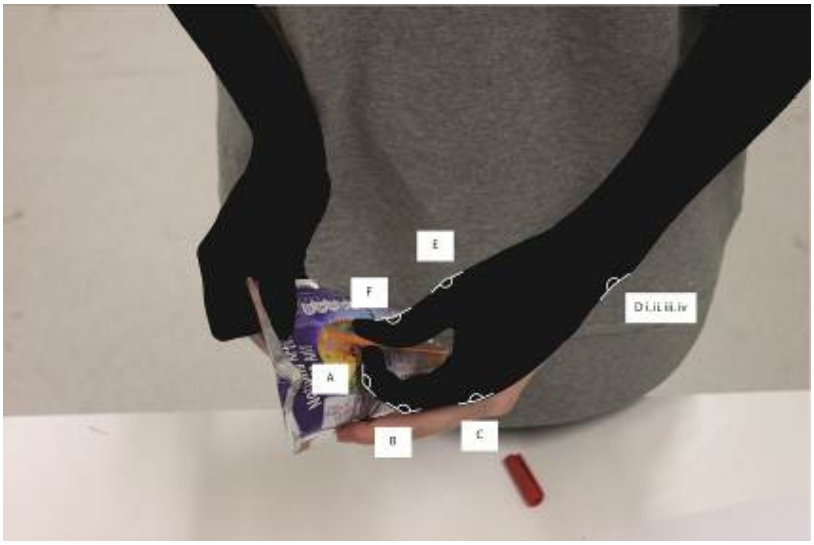



**Figure 10:** Joint angles considered for pack items

Figure 11 below is a graph showing the size of the angles of the index finger for the drinks packaging with a straw. As there was a lot of noise in the data, the moving average was calculated to see clearly the trends of the movement. Information about events occurring have been plotted, with time zones covering areas which are defined by the task description from section 3.1, with key events, shaded and separated by vertical lines. This aids to identify stages of more difficulty.

There are horizontal lines plotted which relate to the Range Of Motion (ROM). Knowing the expected ROM it was believed that proximity to this limit could suggest a difficult position. From this a ROM limit zone was created, where the zone was 75% to 100% of the expected range of motion of the different joints [18]. If the moving average crosses the line of the ROM limit zone, it could suggest an angle of difficulty.

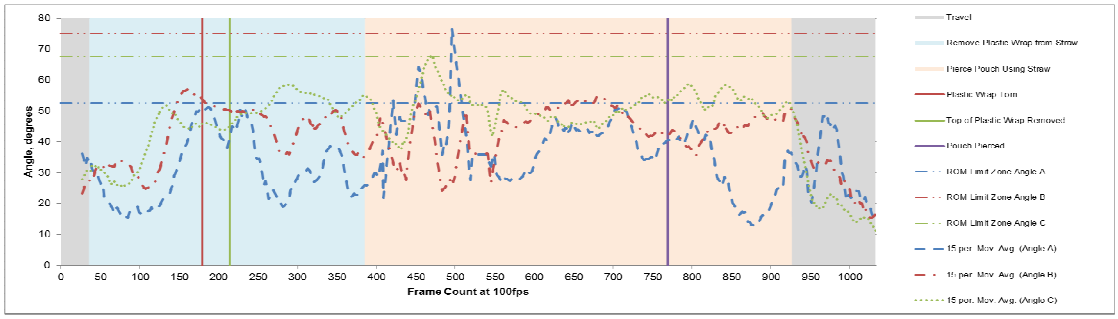



**Figure 11**: The angles of the finger when opening drinks pack with straw

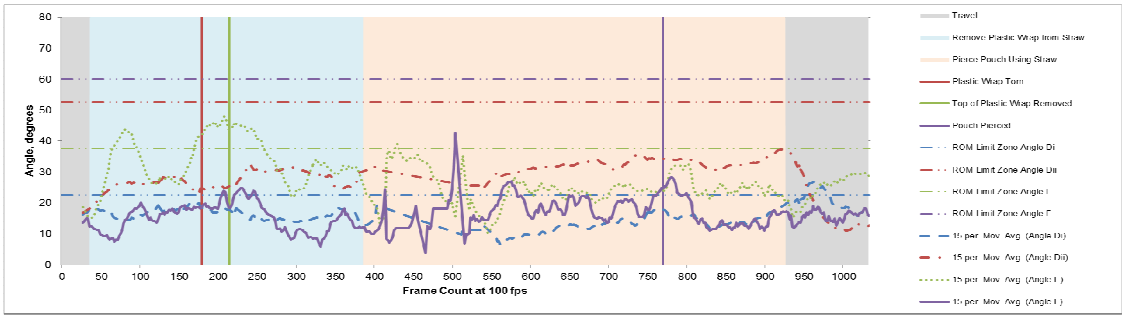



**Figure 12**: The angles of the thumb when opening drinks pack with straw

In studying the ROM of the fingers the authors also calculated the distance travelled between the fingers, i.e. the degree of separation between the index finger and middle finger at any time. Combined with the results from the above Figures we are able to establish whether the 'fidliness' was associated with the amount of joint movement or finger separation. When combined with the task analysis initial results suggest that 'fidliness' is not associated with the amount of movement of the fingers but the development of a precision grip (the fingers moving together) and the amount of tasks need to complete the opening of the pack.

## 3 Conclusions

Several ergonomic techniques have been brought to bear to study and analyse the opening of packaging in detail and in particular to study and understand the elements patients termed in a questionnaire by Bell et al [12] as 'fiddly'.

In measuring grip strength and dexterity it was found that grip strength is affected by posture whilst understanding dexterity was more complex. Initial results suggest that measured dexterity is less effected by posture than grip strength. Further HSV analysis suggests that the issues surrounding 'fidliness' are associated with the number of task involved and the difficulty of forming a precision grip pinch grip.

If we view the design of hospital packaging through the prism of 'inclusive' or 'universal' design whereby the packaging should be assessed against the following principles [19];

- equitable use, provide the same means of access for all users
- flexibility in use, provide alternative means to access
- simple and intuitive to use
- perceptible information
- tolerance for error
- low physical effort
- size and space for approach and use

It can readily be seen that several key themes emerge, current packaging doesn't not facilitate low physical effort or tolerance for error. The formation of precision grips to access tabs and peelable lids causing difficulty to those questioned whilst relatively significant strength is needed to open water or peel the lid once (and if) the grip is formed.

Further, results suggest that posture can affect the degree of pinch strength produced and dexterity leading to issues around the use of packaging in hospitals. This work suggests that either the design of truly inclusive packaging is driven by the hospital environment whereby users will have low strength, or that hospital packaging is designed especially for that environment. The authors would suggest the former since specialist packaging does not meet the inclusive design agenda and would lead to increasing costs for health care services.

## 4 Future Work

It is anticipated to undertake further work on dexterity, strength and posture along with more detailed analysis using HSV.

## Acknowledgements

The authors would like to thank Professor Elena Rodriguez for her help and Daniel Ura, Victor Gonzalez for their assistance with work on the high speed cameras.

## References

1. Office for National Statistics. 2011 Census: Population Estimates for the United Kingdom. 27 March 2011.
2. Table A2-1, Principal Projection- UK Population in Age Groups, 2012-based. 2013.
3. US Census Bureau (2010). Population division 1-886-758-1060. <http://www.census.gov/cgi-bin/broker> Accessed 14.05.14.
6. National Research Council (US), Committee on Diet (1989). Diet and health. Implications for reducing chronic disease risk. Washington: Academy Press.
7. Schenker, S. (2003). Undernutrition in the UK. Nutrition Bulletin, 28(1), 87–120.
8. Lazarus, C., & Hamlyn, J. (2005). Prevalence and documentation of malnutrition in hospitals. A case study in a large private hospital setting. Nutrition & Dietetics, 62(1), 41–47.
9. Vivanti, A., Banks, M., Aliakbari, J., Suter, M., Hannan-Jones, M., & McBride, E. (2008). Meal and food preferences of nutritionally at-risk inpatients admitted to two Australian tertiary teaching hospitals. Nutrition & Dietetics, 65(1), 36–40.
10. Walton, K., Williams, P., & Tapsell, L. (2006). What do stakeholders consider the key issues affecting the quality of foodservice provision for long-stay patients? Journal of Foodservice, 17(5–6), 212–225.
11. Tsang, M. F. (2008). Is there adequate feeding assistance for the hospitalised elderly who are unable to feed themselves? Nutrition & Dietetics, 65(3), 222–228.
12. Bell, A.F., Walton, K., Chevis, J.S., Davies, K., Manson, C., Wypych, A., Yoxall, A., Kirkby, J., Alexander, N. (2013). Accessing packaged food and beverages in hospital. Exploring experiences of patients and staff. Appetite, 60 (1), pp. 231-238.
13. Tesco PLC. Tesco PLC Annual Report and Financial Statements 2013.
14. Desrosiers, J., Hébert, R., Dutil, E., & Bravo, G. (1993). Development and reliability of an upper extremity funtion test for the elderly: The TEMPA. *Canadian Journal of Occupational Therapy , 60*, 9-16.
15. Tiffin, J., Asher, EJ. (1948). The Purdue Pegboard: Norms and Studies of Reliability and Validity. Journal of American Psychology, 1948, Vol. 32.
16. Lafayette Instruments Company, http://lafayetteinstuments.com , Accessed 12/05/2014
17. Wilton A, Burton L, Cavanagh R, Higgins R, McDougall K, Appleton J. Assessing the ability of patients to access their meal trays 22nd National Conference of the Dietitians Association of Australia. Melbourne: Dietitian Association of Australia; 2004.
18. Mulligan, E P. Range of Motion Measurements. *Continuing ED.* [Online]2011.http://www.continuing ed.cc/hsgoniometry/goniometrystandards.pdf. Accessed 14/05/2014
19. The seven principles or Universal design, NC University, The Center for Universal Design http://www.ncsu.edu/ncsu/design/cud/about_ud/udprinciplestext.htm, Accessed 14/05/2014

# Equilibrium Modified Atmosphere Packaging of Longan for Preserving Quality and Extension of Shelf-life

**Chao Sripethdee[1,*], Witchuda Daud[1], Noppadon Kerddonfag[1], Charinee Winotapun[1], Jareenuch Rojsatean[1], Wisaroot Payubnop[1], Vanee Chonhenchob[2] and Wannee Chinsirikul[1]**

[1] *Polymer Research Unit, National Metal and Materials Technology Center, National Science and Technology Development Agency, Pathumthani 12120, Thailand*
[2] *Department of Packaging and Materials Technology, Faculty of Agro-Industry, Kasetsart University, Bangkok 10900, Thailand*

[*] *Corresponding author. Email: chaos@mtec.or.th*

**Abstract:** Longan is non-climacteric which deteriorates rapidly unless proper handling techniques are employed. The major factors reducing the storage-life of longan are microbial decay and pericarp browning. Equilibrium modified atmosphere (EMA) packaging with different oxygen transmission rate (OTR) was developed to create optimum atmosphere inside the package for extending storage-life of longan. Sulfur dioxide ($SO_2$) fumigation was applied to pre-packaged longan for preventing fruit rot. A package size of 18 cm x 25 cm was used for 450 g packed fruit. The type of packages under this study are plastic net bag (Control), polyethylene film with OTR of 2,551 ± 123 $cm^3 \cdot m^{-2} \cdot d^{-1}$ (B2500) and polyethylene film with OTR of 6,056 ± 244 $cm^3 \cdot m^{-2} \cdot d^{-1}$ (B6000). Packaged longan was then stored at 2°C. Different quality attributes such as weight loss, total soluble solids and $SO_2$ residue in both longan pericarp and flesh were determined at regular intervals. Fruit stored at 2°C retained quality up to 15, 20 and 40 d in control bag, B6000 package and B2500 package, respectively. Both EMA packaging of $SO_2$-treated fruits resulted in a reduction of weight loss (0.42 ± 0.05%, as compared with 16.43 ± 1.86% when stored in plastic net (control)) for the same period of time. Prevention of browning and retention of good color were obtained in the EMA packaging. It was also found that the reduction rate of the $SO_2$ in the longan flesh packaged in B2500 packaging was slower than that of the fruit packaged in B6000 bag and control bag (plastic net) resulting in delaying fruit decay and eventually extending the shelf-life of the longan. The humidity level inside the package was shown to differently affect the $SO_2$ residue on the longan flesh.

Keywords: longan, modified atmosphere packaging, storage-life.

## 1 Introduction

Longan (*Dimocarpus longan* Lour.**)** is a tropical fruit tree generally grown in the upper northern region of Thailand. The longan is preferably consumed fresh, and has a delicate and sweet flesh. The official harvesting season for longan runs from June to August. Thailand is a major grower and exporter of longan, in both the fresh fruit and dried longan [1]. Longan shelf-life is limited by a decline in visual appearance, a reduction in sensory properties and the development of disease. Rapid moisture loss from fruit occurs during storage under low humidity conditions where visual appearance declines to an unacceptable level due to skin dehydration and browning. In general, longan can be stored at 1-5°C for about 30 d depending upon the cultivar [2, 3]. Longan is perishable, therefore it is necessary to rely on an appropriate postharvest practice. Postharvest practices must also consider the storage and transportation to prolong the shelf-life of fresh longan. Sulfur dioxide ($SO_2$) fumigation was applied to longan for delaying fruit rot. It was found that sulfur dioxide fumigation of longan pericarp can prevent fungi and pericarp browning [4, 5]. Pericarp browning has been mainly attributed to polyphenol oxidase (PPO) enzymatic oxidation activity which produces "brown colored" quinine. $SO_2$ can prevent browning by a coupled reaction. One reaction is that the chemical will react with quinine and form a stable and colorless quinine-sulphite compound. Another reaction is that the $SO_2$ acts as a competitive inhibitor which alters the reaction between polyphenol and PPO enzyme which limits the browning reaction [6]. Longan fumigated with $SO_2$ gas of 200-300 ml $SO_2 \cdot kg^{-1}$ fruit has $SO_2$ residue of 1,200-3,000 ppm in pericarp immediately after fumigation. However, $SO_2$ residue in the flesh occasionally exceeds national and international acceptable limits. Progress has been made in achieving reduced $SO_2$ residue to 1-30 ppm in flesh [5, 7, 8]. $SO_2$ residue level declines rapidly in the first period of fumigation and with a slower rate after fumigation. $SO_2$ in the longan flesh treated with 5 g sulfur per 11 kg of longan is 3.13 ppm on the first day after fumigation (DAF). It declines to 50% on the 3 DAF and cannot be detected at the 12 DAF. While $SO_2$ in longan flesh treated with 7.5 g sulfur per 11 kg of longan is 89-99 ppm during the first 5 DAF. It declines below 50 ppm within 12 DAF and

reached 5 ppm at 56 DAF. The result has shown that higher level of $SO_2$ fumigation gives a better storage-life, but leaves a higher level of $SO_2$ residue [9]. Obviously, this is considered an important safety issue.

Controlled atmosphere storage (CA) has successfully been used to reduce fruit decay, inhibit polyphenol oxidase (PPO) activity, prevent skin browning, decrease ethylene productions and extend storage-life of longan. Fruit kept in CA of $4\%O_2 + 15\%CO_2$ was reported to retain good taste and quality, without any deterioration or off-flavour development after 60 d of storage at 2°C with approximately 95% relative humidity (RH) [10]. However, the CA system is complicated and expensive.

Modified atmosphere packaging (MAP) is available for the retention of overall quality of the fruits at a low temperature storage with the advantage of low cost and ease of implementation in the commercial scale [11]. MAP has been shown to reduce browning in longan. Longan stored in the 0.03 mm thick polyethylene bags with an initial atmosphere of $3\%O_2$ and $5\%CO_2$ had less browning and higher total soluble solid (TSS, representing, higher sugar content) compared with that stored in air. The storage-life of 35 d at 4°C was reported [12]. Longan packaged in the 0.06 mm thick polyethylene bags, flushed with $N_2$, and stored at 5°C had extended storage-life, better fruit quality and reduced browning, compared with unpackaged fruit [13]. However, no study has yet addressed the effect of equilibrium modified atmosphere packaging on the $SO_2$ residue level in both pericarp and flesh of longan and the quality of the fruit under the storage.

This research aims to study the extension of shelf-life of longan stored at 2°C using different types of packaging materials varying in gas permeabilities, which include (1) plastic net bag (control), (2) polyethylene bag with low oxygen transmission rate (B2500) and (3) polyethylene bag with medium oxygen transmission rate (B6000). The effect of modified atmosphere on the changes of $SO_2$ residue in pericarp and flesh of the longan and the quality of longan during storage is investigated.

## 2 Experimental

***Materials & Methods:*** Longan (*Dimocarpus longan* Lour.) fruit cv. Daw with a maturity in a range of about 85-90% was harvested from Lamphun, the northern province of Thailand in March 2014, and then packaged in a plastic basket containing 11 kg of longan for sulfur dioxide fumigation. The sulfur dioxide fumigation process was conducted in an air-tight room for 1 h as in a commercial practice by burning sulfur with a dosage of 7.0 g per basket in order to produce the fumigant and blow into the room. After that, longan was pre-cooled at a temperature of 2°C for 10 h and then the stalks were cut to about 3-5 mm long. The selected short-stalk longan with uniform size was weighed and packaged (approximately 450 g) into 3 different types of packaging materials, as described in Table 1.

**Table 1:** Sample code, packaging materials and gas transmission properties.

| Sample code | Packaging materials | OTR* ($cm^3 \cdot m^{-2} \cdot d^{-1}$) | WVTR** [$g \cdot m^{-2} \cdot d^{-1}$] |
|---|---|---|---|
| Control | Plastic net bag | N/A | N/A |
| B6000 | Polyehtylene film, thickness = 50 µm package size = 18 cm x 25 cm | 6,056 ± 243 | 11.72 ± 0.88 |
| B2500 | Polyehtylene film, thickness = 80 µm package size = 18 cm x 25 cm | 2,551 ± 123 | 5.39 ± 0.12 |

*Oxygen transmission rate (OTR) was measured at 23°C, 0% RH according to OTR-ASTM D3985 using MOCON OX-TRAN 2/2, USA
**Water vapour transmission rate (WVTR) was measured at 37.8°C, 90% RH according to ASTM Standard E-398 using MOCON PERMATRAN-W 398, USA.

All packages of longan were stored at 2°C for quality analyses (four replicates of each sample) every 5 d. The parameters used to monitor the quality of packaged longan before and after storage were: gases in package, weight loss, total soluble solid (TSS) content, sulfur dioxide residue and the overall appearance of longan flesh.

***In-pack gas concentration measurement:*** $O_2$ and $CO_2$ headspace concentration in the package was measured using portable $O_2/CO_2$ analyzer, PAC CHECK® model 325 (MOCON Portable $O_2/CO_2$ Analyzer, USA). Sampling gas was obtained from head space of the four packages for each treatment. In-pack gas concentration was determined to follow the change of atmospheric compositions throughout the storage period.

***Weight loss measurement:*** Weight loss of longan over the storage period at 2°C was evaluated in this study using a two-decimal precision balance (Mettler Toledo, Switzerland). Data was recorded every 5 d during storage of four replicates for each treatment.

***Total soluble solid measurement:*** Soluble solids are composed of polysaccharides that may be broken down enzymatically into free sugars. Total soluble solid (TSS) was measured in °Brix with refractive index measurements, which represented gram sucrose per 100 g of solution and was assayed by refractometry using a refractometer (ATAGO (0-32 °Brix), Japan). Data was recorded every 5 d during storage of five fruits of each four replicates for each treatment.

***Pericarp color:*** The pericarp color of the longan was analyzed initially and after being storaged for 5, 10, 15, 20, 25, 30, 35 and 40 d. The color was measured on outer side of the fruit using spectrophotometer (MiniScan EZ firmware V.1.00, USA) which provided $L^*$, $a^*$ and $b^*$ values.

***Sulfur dioxide residue analysis:*** Pericarp and flesh of longan samples were separated carefully, to prevent contamination of the sulfur dioxide residue from the pericarp to the flesh of longan. The analysis was carried out at SGS (Thailand) Co., Ltd., a commercial laboratory, having extensively experience with the Monier-Williams method for sulfites approved by Association of Official Analytical Chemists (AOAC International) (AOAC 990.28, 1984), and involved distillation of the sulfur dioxide formed from refluxing with hydrochloric acid. The sulfur dioxide was quantified by titration with sodium hydroxide. Sulfur dioxide results were expressed as part per million (ppm) (or milligram per kilogram) on a fresh mass basis. An average value with standard deviation of three replicates for each treatment was reported. Data was recorded every 5 d during storage.

***The appearance of longan flesh:*** Longan flesh was removed from its pericarp for evaluating the overall appearance by trained persons.

## 3 Results and discussion

As longan was respiring under storage condition, a general change of headspace levels of $O_2$ and $CO_2$ was found inside both B2500 and B6000 in a similar trend: modified atmosphere in package with lower level of oxygen and higher level of carbon dioxide as compared with ambient atmosphere. In the case of B6000 package, the rapidly increasing of $CO_2$ concentration reached the maximum level (about 11.09%) within 24 h (or day 1) and then slowly decreased to the plateau level (about 5.18%) in day 20 of storage period (see Figure 1). On the contrary, the $O_2$ concentration decreased to the minimum value (about 2.88%) and rose to the steady state (about 6.16%) in day 20 of storage period. However, for the B2500 package with lower OTR, the higher $CO_2$ level and lower $O_2$ level were found at steady state for this package. The $CO_2$ and $O_2$ concentration in B2500 package reached the value of 9.45% and 1.34%, respectively. It is interesting to see that the $O_2$ level in the B2500 package reached the steady state with a small variation (about 1.34 ± 0.58%) above zero value which indicating the aerobic respiration of longan along the storage period. The high $CO_2$ level (> 9%) found in B2500 package is similar to the result published by Tian et al. suggesting that the enriched $CO_2$ atmosphere is able to effectively reduce decay and extend shelf-life of longan [14].

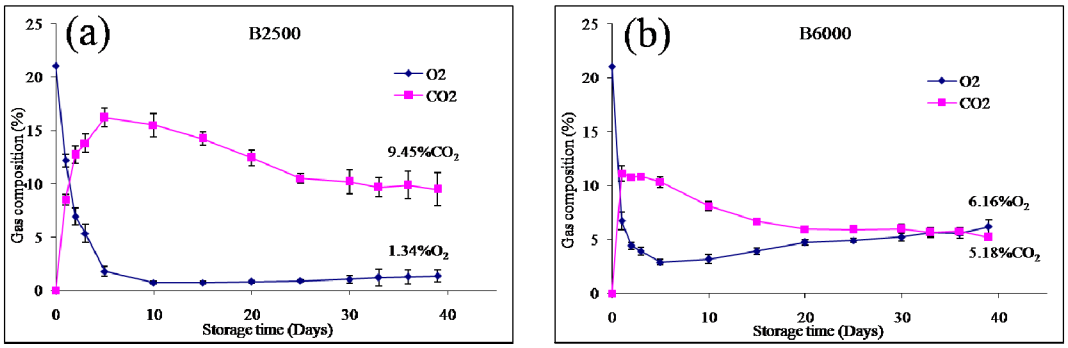



**Figure 1**: In-pack oxygen (♦) and carbon dioxide (■) concentrations of longan in different packaged: (a) B2500 and (b) B6000.

Dehydration is an important indication of the deterioration of longan quality during storage. According to the perception of customers, the appearance of dehydration of longan is easily detected. It generally occurs when longan is stored in ambient or in a refrigerator. Dehydration has a major influence on both the flesh and pericarp of longan as it contributes to the weight loss and dryness of the flesh, and the hardening of the pericarp. As reported, a high percentage of weight loss in a range of 5-10% can cause unacceptable quality of fresh produce [15]. Figure 2 shows weight loss throughout storage period for longan packaged in control and modified atmosphere packages stored at 2ºC. Weight loss progressively increased with storage time for longan packaged in plastic net (control samples) where longan was exposed to air, directly. At the end of the storage time (40 d), control samples exhibited the highest weight loss of about 16.43 ± 1.86%. However, the increasing hardness of

pericarp to the unacceptable level was detected earlier since day 20 of storage period. It was also found that the shrinkage of longan flesh due to dehydration resulting in the separation from its pericarp. On the other hand, weight loss of longan was significantly lower in the B2500 and B6000 packages. The polyethylene film packages were found to possess a relatively low WVTR of about 5.39 ± 0.12 and 11.72 ± 0.88 $g \cdot m^{-2} \cdot d^{-1}$ for B2500 and B6000, respectively. Longan in both polyethylene film packages exhibited a similar weight loss in a range of 0.35 to 0.45%, though WVTR of B6000 film was two times higher than that of B2500 film. In-package relative humidity (RH) of both B2500 and B6000 sample were measured and found to be 100%RH throughout storage period which were higher than the relative humidity in ambient (85-90%RH). It should be noted that the size of the packaging is relatively small compared to the amount of the packaged fruit, resulting in a small headspace; therefore, the in-package RH quickly reached equilibrium and maximum RH of 100%. Apart from the small headspace effect on high humidity development inside the package, the low WVTR characteristic of the polyethylene film could also act as a hindrance of the moisture. Thus, high moisture content was retained in the packages.

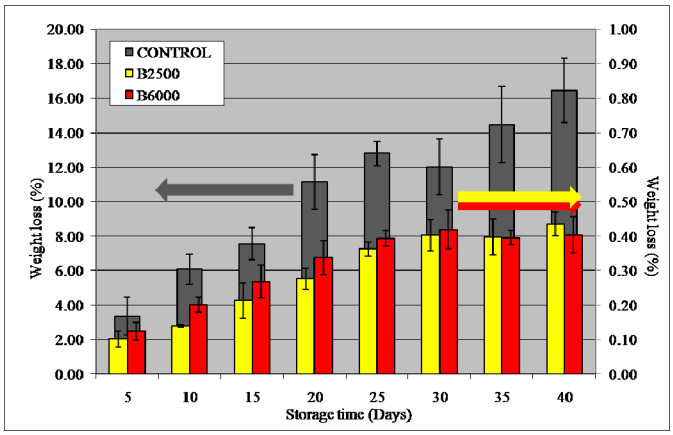



**Figure 2**: Weight loss of longan in different packages.

The longan is a non-climacteric fruit and will not continue to ripe after harvest; therefore, the sugar content remains constant throughout its shelf-life [16]. The consumption quality of longan mainly depends on the sweetness, which is determined by the level of soluble sugars such as glucose, fructose and sucrose. The total soluble solids (TSS) represent both soluble sugars and titratable acids (TA). However, the TA of longan was found to be unchanged throughout the storage period which was in a good agreement with the previous works reported by Rinpol and Rattanapanon [17]. In this study, the total soluble solids (TSS) were used to reflect the consumption quality of longan stored in different packaging. As seen in the Figure 3, the TSS of longan flesh from all packages increased from 17 to 20 °Brix within 5 d after storage. After 5 d of storage, the TSS of longan flesh from control package slightly increased from 19.76 ± 0.35 to 21.76 ± 0.64 °Brix. This result was in good agreement with the study by Dharini and Lise [18] which addressed that the high TSS in $SO_2$ fumigated litchi is due to dehydration during long-term storage. In the case of B2500 and B6000 packages, the sweetness from longan flesh was retained after 5 d of storage, as TSS contents were varied in a small range of 19.60 ± 0.42 and 19.59 ± 0.36 °Brix, respectively. The TSS was stable during the storage period in accordance with Uthairatanakij et al. [19], which reported that polyethylene film packaging significantly reduced the weight loss and also maintained soluble solids content.

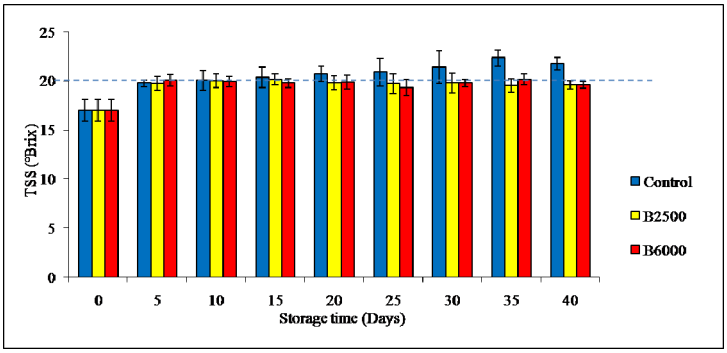



**Figure 3**: Total soluble solid (TSS) of longan in different packages.

$SO_2$ fumigation has been the most effective and practical postharvest treatment in controlling color change and reducing decay of longan. $SO_2$ inhibits browning and bleaches the longan to a bright yellow color [5, 20]. Color is one of the most important visual attributes for longan. The color parameters of the pericarp, including $L^*$, $a^*$ and $b^*$ values representing brightness, red/green color and yellow/blue color, respectively, were measured for longan in all three packaging types throughout the storage period. The values are shown in Table 2. For all samples, the $L^*$ value, representing the brightness, was 55.62 ± 2.75 in the day after $SO_2$ fumigation along with the $a^*$ value of 5.27 ± 0.91 and $b^*$ of 43.81 ± 1.56, indicated that the longan pericarp had bright yellow color. As time passed, it was seen that the $L^*$ value of the pericarp of longan from control sample remained the same for the storage duration; however, the $a^*$ value increased (increased red color) and the $b^*$ value decreased (increased blue-yellowish color). It was observed visually that the browning of the pericarp had occurred. While the color parameters of the pericarp of longan samples from B2500 and B6000 packages were seen to be different from that of the longan from control sample. It was seen that there was a slight increase in the $L^*$ value indicating brightness as the $a^*$ value and $b^*$ value increased which showed an increase in red and yellow colors. It was observed visually that the pericarp of longan remained bright yellow despite slight reddish undertone.

**Table 2:** Effect of $SO_2$ treatment, storage temperature (2ºC) and storage duration on the changes of pericarp color of longan in different packages.

| Sample | Storage time (Days) | Pericarp color parameters | | |
|---|---|---|---|---|
| | | $L^*$ | $a^*$ | $b^*$ |
| Control | 0 | 55.62 ± 2.75 | 5.27 ± 0.91 | 43.81 ± 1.56 |
| | 5 | 54.39 ± 1.68 | 7.70 ± 0.45 | 45.16 ± 0.80 |
| | 10 | 54.27 ± 1.33 | 8.49 ± 0.88 | 44.00 ± 1.62 |
| | 15 | 54.42 ± 1.27 | 8.51 ± 0.17 | 45.61 ± 0.57 |
| | 20 | 54.50 ± 2.12 | 9.01 ± 0.83 | 45.20 ± 1.05 |
| | 25 | 55.43 ± 1.98 | 9.21 ± 0.77 | 44.22 ± 1.40 |
| | 30 | 55.54 ± 0.19 | 9.18 ± 0.52 | 39.22 ± 0.98 |
| | 35 | 54.53 ± 0.39 | 10.08 ± 1.17 | 42.86 ± 1.67 |
| | 40 | 55.50 ± 1.83 | 9.87 ± 0.78 | 36.79 ± 0.80 |
| B6000 | 0 | 55.62 ± 2.75 | 5.27 ± 0.91 | 43.81 ± 1.56 |
| | 5 | 55.36 ± 1.61 | 7.66 ± 0.88 | 44.00 ± 1.27 |
| | 10 | 56.91 ± 2.41 | 7.92 ± 0.50 | 45.10 ± 0.73 |
| | 15 | 56.63 ± 0.82 | 7.84 ± 0.35 | 43.46 ± 0.79 |
| | 20 | 56.61 ± 0.79 | 8.70 ± 0.49 | 44.88 ± 0.97 |
| | 25 | 57.23 ± 1.17 | 8.48 ± 0.58 | 44.47 ± 0.80 |
| | 30 | 57.41 ± 2.09 | 7.99 ± 0.20 | 43.53 ± 0.61 |
| | 35 | 59.24 ± 1.70 | 8.64 ± 0.51 | 39.25 ± 0.92 |
| | 40 | 56.04 ± 0.63 | 9.10 ± 0.66 | 44.93 ± 0.70 |
| B2500 | 0 | 55.62 ± 2.75 | 5.27 ± 0.91 | 43.81 ± 1.56 |
| | 5 | 57.64 ± 1.05 | 7.17 ± 0.61 | 45.39 ± 0.93 |
| | 10 | 57.26 ± 1.19 | 7.46 ± 0.46 | 45.56 ± 1.11 |
| | 15 | 57.73 ± 1.69 | 7.86 ± 0.62 | 44.49 ± 0.90 |
| | 20 | 57.90 ± 1.76 | 8.40 ± 0.64 | 45.45 ± 0.92 |
| | 25 | 57.82 ± 0.74 | 8.46 ± 0.71 | 45.13 ± 0.51 |
| | 30 | 58.22 ± 0.48 | 8.34 ± 0.64 | 44.56 ± 1.42 |
| | 35 | 56.34 ± 0.52 | 8.90 ± 0.55 | 45.16 ± 0.52 |
| | 40 | 57.40 ± 2.63 | 8.54 ± 0.32 | 45.17 ± 1.04 |

Browning of longan pericarp and fruit decay can be prevented by $SO_2$ fumigation; however, $SO_2$ residue on both pericarp and flesh is monitored and controlled closely by the importing countries. Over the limit residue can cause rejection of the shipment or import license being revoked. It was noticed that $SO_2$ residue in the flesh of longan from control package (26.67 ± 0.58 ppm at day 0) declined from 26.67 ± 0.58 ppm on day 0 to 0 ppm as storage time passed. No residue was detected after 5 d of storage. As the longan in control sample was stored in atmospheric conditions, $SO_2$ can easily dissipate from the longan.

In case of the B2500 package, the $SO_2$ residue in longan flesh rose with storage time and peaked at 92.67 ± 0.58 ppm on day 10 of storage period, after that $SO_2$ residue slightly dropped to 64.67 ± 3.79 ppm. As for the B6000 package, the $SO_2$ residue from longan flesh was seen to slightly increase from 26.67 ± 0.58 ppm, on day 0, to 37.67 ± 3.21 ppm, on day 15, and then decline to 12.00 ± 1.00 ppm on day 31 (as shown in Figure 4). It is also noticed that the $SO_2$ residue in longan flesh from the B6000 package was lower than the $SO_2$ residue in longan flesh from the B2500 package throughout the storage period. According to the gas transmission rate of both B2500 and B6000 polyethylene film listed in Table 1, it can be suggested that the low gas transmission rate can prohibit the release of $SO_2$ from the longan pericarp out of the packaging film, thus creating a $SO_2$-rich atmosphere inside the packaging. Therefore, it is possible that $SO_2$ permeates into the longan flesh which gives rise to the $SO_2$ residue level as depicted in Figure 4. The B2500 polyethylene film (OTR of 2,551 ± 123$cm^3 \cdot m^{-2} \cdot d^{-1}$ and WVTR of 5.39 ± 0.12 $g \cdot m^{-2} \cdot d^{-1}$) has a lower gas transmission rate than that of the B6000 polyethylene film (OTR of 6,056 ± 243 $cm^3 \cdot m^{-2} \cdot d^{-1}$ and WVTR of 11.72 ± 0.88 $g \cdot m^{-2} \cdot d^{-1}$), which could be responsible for the higher level of $SO_2$ residue in longan flesh from B2500 package.

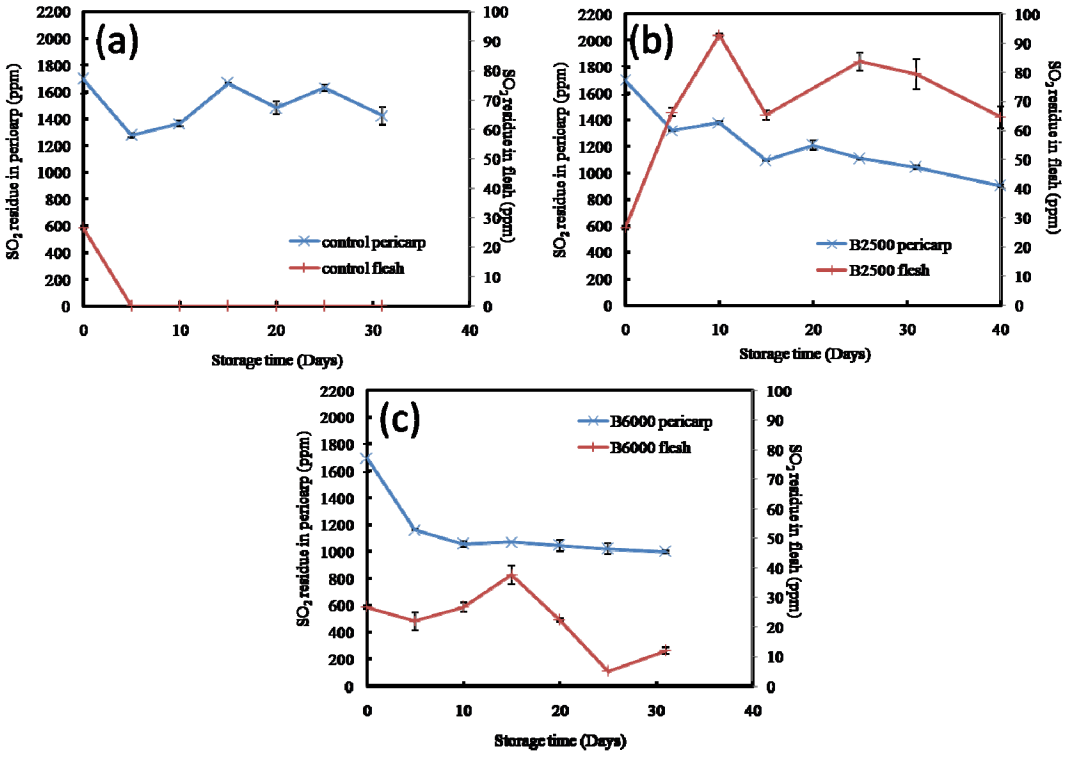



**Figure 4**: $SO_2$ residue of longan pericarp (left axis) and flesh (right axis) in different packaged: (a) control, (b) B2500 and (c) B6000.

In general, longans are rejected when consumption qualities become visually unacceptable. These qualities can range from pericarp browning [21], disease [16] and deterioration of the flesh [22]. In this study, it was found that there were small changes in pericarp color, without any appearance of fungi, and small changes in TSS content among longan in all packaging types throughout the storage duration; hence, the deterioration of longan flesh is the only major factor indicating the longan shelf-life. As for the longan in control package, the deterioration of longan flesh was not observed. However, the longan in control package exhibited the highest level of weight loss (over 10% on day 20) as well as unacceptable visual quality due to flesh shrinkage, browning and pericarp hardening; therefore, shelf-life of longan in control package was limited to 15 d. The longan in B6000 package had shelf-life of 20 d. On day 25 of storage period, it was discovered that the flesh of the longan had deteriorated. It appeared soft and showed sign of pink color around the seed-stalk of the fruit as displayed in Figure 5(d), the fruits were rejected on day 25 indicating that the last acceptable consumption quality was observed on day 20. Therefore, the shelf-life of 20 d was attained for longan in B6000 package. In case of the longan in B2500 package, the deterioration of longan flesh was not detected until day 45. This may be attributed to the high level of $SO_2$ in the package which helps preserving the quality of longan flesh. As a result the shelf-life of longan in B2500 package of 40 d was seen to be the highest in this study.

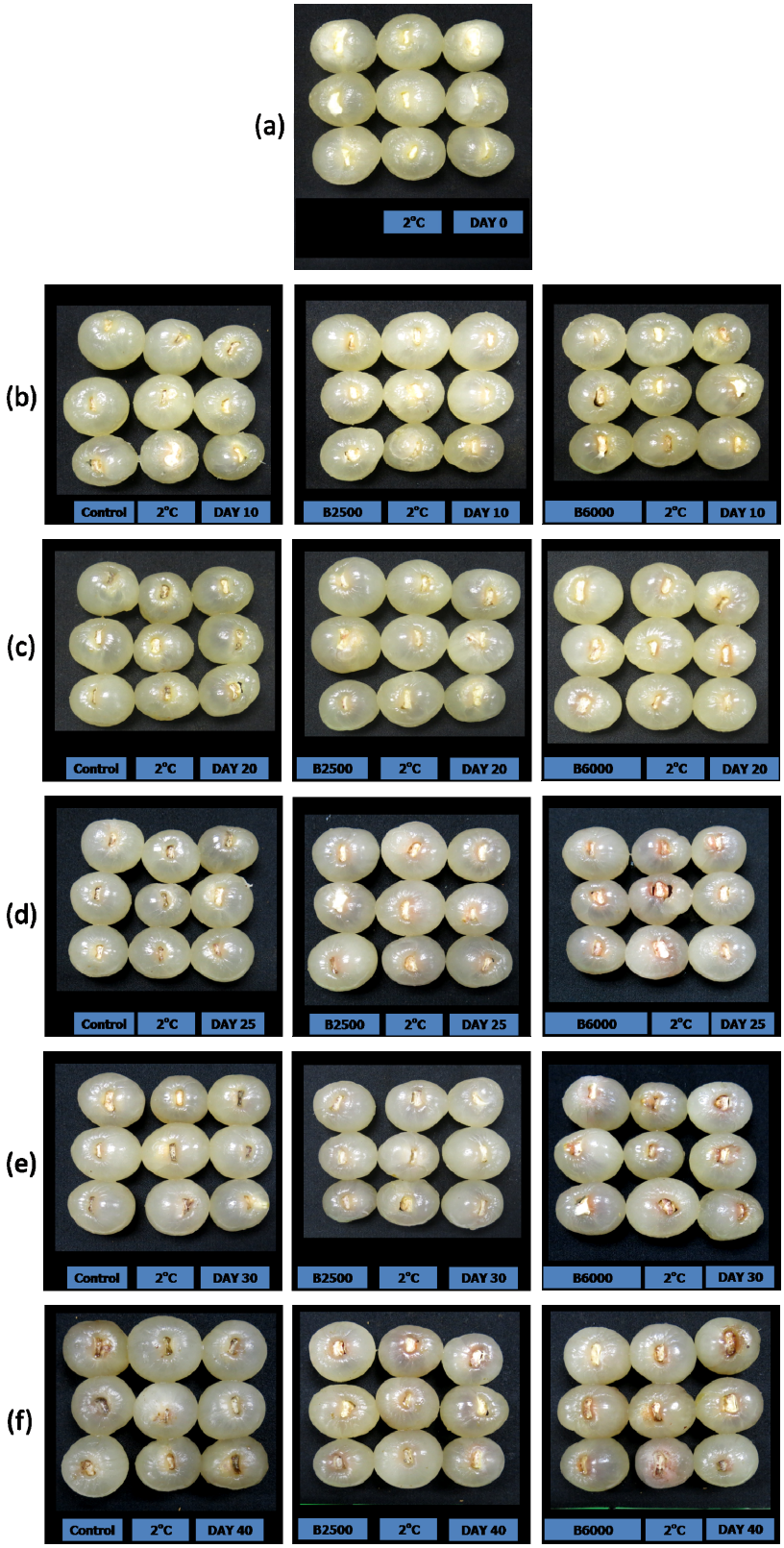



**Figure 5**: The effect of storage time on changing of longan flesh in different packages at 2ºC (a) day 0, (b) day 10, (c) day 20, (d) day 25, (e) day 30 and (f) day 40.

It is suggested that B2500 polyethylene film package can reduce the quality deterioration of longan via maintaining a modified atmosphere environment with elevated $CO_2$ and decreased $O_2$ concentrations. Therefore, when selecting a film type for longan, it is important to select the correct gas permeability in order to achieve the desired modified atmosphere composition that will delay browning, control $SO_2$ residue and maintain fruit quality.

## 4 Conclusions

In conclusion, the shelf-life of the longan can be extended up to 40 d of storage at 2°C when the appropriate equilibrium modified atmosphere (EMA) packaging is selected. EMA packaging is a versatile and economical tool for minimizing weight loss and color deterioration, while retaining excellent eating quality during long term low temperature storage. In addition, it is observed that the low gas transmission rate of the EMA packaging (B2500) could give rise to the $SO_2$ level in the flesh of longan and possibly delay the onset of fruit rot. However, $SO_2$ residue level in the flesh of longan stored in this EMA package exceeds the maximum residue limit (MRL) of international standard (MRL of $SO_2 \leq 50$ ppm, in China). Hence, it is still a challenge to design a proper MA packaging for longan where a correct mixture of the in-pack gas compositions is obtained for quality retention and at the same time the $SO_2$ residue in the longan flesh can be controlled within the acceptable safety limit. This is the area of our further development.

## Acknowledgements

The authors are grateful to the National Science and Technology Development Agency, Ministry of Science and Technology, Royal Thai Government for financial support. Manoch Co., Ltd. and Central World Wide Co., Ltd. are thanked for supplying fruit and plastic films, respectively. The assistance from the staff and students of the Department of Agro-Industrial Technology, Kasetsart University are gratefully appreciated.

## References

1. C. Thirawan and C. Ni-orn, 2010, "Exploring feasibility for production of longan fruit wine as a small scale enterprise in Thailand", *Asian Journal of Food and Agro-Industry*, vol. 3, no.2, pp. 242-247.
2. Y.M. Jiang and Y.B. Li, 2001, "Effects of chitosan coating on postharvest life and quality of longan fruit", *Food Chemistry*, vol. 73, pp. 139-143.
3. D.M. Han. Z.X. Wu. Z.L. Ji and M. Han, 1999, "Effects of $SO_2$ treatment on the oxidation and senescence of longan fruit", *Journal of Fruit Science*, vol. 16, pp. 24-29.
4. S.J.R Underhill. J. Bagshaw. A. Prasad. G. Zauberman. R. Ronen and Y. Fuchs, 1992, "The control of Litchi postharvest skin browning using sulphur dioxide and low pH", *Acta Horticulturae*, vol. 321, pp. 732-741.
5. S.C. Thongdee, 1994, *Sulfur dioxide fumigation in postharvest handling of longan and lychee for export*, In: G.I. Johnson and E. Highley (Eds.), Development of Postharvest Handling Technology for Tropical tree Fruits. ACIAR Canberra, Australia. pp. 186-195.
6. J. J. Macheix. A. Fleuriet and J. Billot, 1990, *Fruit phenolics*, CRC Press, Boca Raton, Florida, pp. 378.
7. Z.L. Ji. D.M. Han and Z.X. Wu, 1999, "Effect of sulphur dioxide fumigation on postharvest longan fruit cv. Shixia and its residues", *Chinese Journal of Tropical Crops*, vol. 20, pp. 36-40.
8. J.M. Liu, 1999, "Studies on abstraction and stability of yellow pigment and color-retenting and fresh keeping of longan fruit", *Journal of Fruit Science*, vol. 16, pp. 30-37.
9. W. Patchara. A. Wittiya and W. Sodshol, 2009, "The Sulfur Dioxide Residues in Fresh Longan at Different Periods after Fumigation", *Thai Agricultural Research Journal*, vol. 1, pp. 26-42.
10. S.P. Tian. Y. Xu. Q.Q. Gong. A.L. Jiang. Y. Wang and Q. Fan, 2001b, "Effects of controlled atmospheres on physiological properties and storability of longan fruit", *Proceedings of a International Symposium on Tropical and Subtropical Fruits*, Cairns, Australia, Nov. 26-Dec. 1, pp. 659-665.
11. F.B. Flores. M.C. Martinez-Madrid. M.B. Amor. J.C. Pech. A. Latche and F.Romojaro, 2004, "Modified atmosphere packaging confers additional chilling tolerance on ethylene inhibited cantaloupe Charentais melon fruit", *European Food Research and Technology*, vol. 219, pp. 431-435.

12. D.L. Zhang and P.C. Quantick, 1997b, “Preliminary study on effects of Modified atmosphere packaging on postharvest storage of longan fruit”, *Proceedings of the Seventh International Controlled Atmosphere Research Conference*, Davis, USA, Jul. 13-18, pp. 90-96.

13. Q. Zhang. J. Xie and S.Q. Xu, 2002, “Modified atmosphere packaging storage of ‘Chike’ longan fruit”, *Food science*, vol. 23, no.4, pp. 118-120.

14. S.P. Tian. Y. Xu. A.L. Jiang and Q.Q. Gong, 2002, “Physiological and quality responses of longan fruit to high O2 or high CO2 atmospheres in storage”, *Postharvest Biology and Technology*, vol. 24, no. 3, pp. 335-340.

15. L. Lee. J. Arult. R. Lenckit and F. Castaigne, 1995, “A Review on Modified Atmosphere Packaging and Preservation of Fresh Fruits and Vegetables: Physiological Basis and Practical Aspects-Part I”, *Packaging Technology and Science*, vol. 8, pp. 315–331.

16. Y.M. Jiang. Z.Q. Zhang. D.C. Joyce and S. Ketsa, 2002, “Postharvest biology and handling of longan fruit (*Dimocarpus longan* Lour.)”, *Postharvest Biology and Technology*, vol. 26, pp. 241-252.

17. A. Rinpol and N. Rattanapanon, 2005, “Effect of storage temperatures on the quality of SO2 -treated longan fruit cv. Daw”, *Proceedings of the Fifth National Horticultural Congress*, Pattaya, Thailand, Apr. 26-29, pp. 251-276.

18. S. Dharini and K. Lise, 2006, “Influence of modified atmosphere packaging and postharvest treatments on quality retention of litchi cv. Mauritius”, *Postharvest Biology and Technology*, vol. 41, pp. 135-142.

19. A. Uthairatanakij. P. Jitareerat. S. Photchanachai and P. Ieamtim, 2010, “Combined treatments of sulfur dioxide and polyethylene bags on the quality and disease incidence in gamma irradiated longan fruit 'Daw'”, *Acta Horticulturae*, vol. 877, pp. 1489-1494.

20. T.J. O’Hare and A. Prasad, 1991b, “Longan storage in conjunction with metabisulphite pads”, *North Queensland Horticultural News*, pp. 55-56.

21. K.J. Scott. B.I. Brown. G.R. Chaplin. M.E. Wilcox and J.M. Bain, 1982, “The control of rotting and browning of litchi fruit by hot benomyl and pkastic film”, *Scientia Horticulturae*, vol. 16, pp. 253-262.

22. C.C. Huang and Y.T. Wang, 1990, “Effect of storage temperature on the color and quality of litchi fruit”, *Acta Horticulturae*, vol. 269, pp. 307.

# Development of Time-Temperature Indicator Based on Polydiacetylene/Silica Nanocomposite for Monitoring Fresh Skinless Chicken Breast Quality

**Atchareeya Nopwinyuwong[1,3], Chompoonoot Rukchon[1], Chanassa Nandhivajrin[1,3], Waraporn Boonsupthip[2,3], Chiravoot Pechyen[1,3] and Panuwat Suppakul[1,3,*]**

[1] *Department of Packaging and Materials Technology, Faculty of Agro-Industry, Kasetsart University, Bangkok, 10900, Thailand*

[2] *Department of Food Science and Technology, Faculty of Agro-Industry, Kasetsart University, Bangkok, 10900, Thailand*

[3] *Center for Advanced Studies in Agriculture and Food, KU Institute for Advanced Studies, Kasetsart University, 10900, Thailand (CASAF, NRU-KU, Thailand)*

[*] *Corresponding author. Email: panuwat.s@ku.ac.th*

**Abstract:** A novel new colorimetric time-temperature indicator (TTI) based on polydiacetylene (PDA) and silica nanoparticles were investigated and developed for monitoring spoilage of fresh skinless chicken breast. An irreversible color change of a PDA/$SiO_2$ nanocomposite as a colorimetric indicator occurs due to temperature change. Temperature which is one of the most critical factors can affect to the quality of food products, especially chilled and frozen foods, during transportation, distribution and storage. PDA is widely known for excellent color transition from blue to red upon temperature and other external stimuli. For an incorporation of silica nanoparticles, a functional group of silica nanoparticles can form a strong ionic interaction with a carboxylic groups head groups of PDA vesicles and can occur the stability of PDA structures. To formulate PDA/$SiO_2$ nanocomposite-based TTI label, a suspension consists of a blue-colored PDA/$SiO_2$ nanocomposite solution, poly(vinyl alcohol) (PVOH) as matrix polymers, and plasticizer. A mixture of Pluronic F127 and poly(ethylene glycol-400) (PEG-400) was used as plasticizer. The PEG-400-added PDA/$SiO_2$ incorporated PVOH film showed initially purple color due to a plasticizer impact upon the stability of PDA structures. The PEG-400-added PDA/$SiO_2$ film was attached on a fresh skinless chicken breast's package and kept at 4 and 10 °C. Carbon dioxide ($CO_2$) was used as spoilage metabolite because the amount of $CO_2$ increased during storage time. Its color changes, in terms of total color difference (TCD or $\Delta E$) indirectly correlated with $CO_2$ levels of skinless chicken breast. At 10 °C, the $CO_2$ levels rapidly increased in the package, in turn, a purple-to-red color change was faster in comparison with the treatment storing at 4 °C. Therefore, this polymer-based TTI prototype could be used as an effective tool for monitoring the quality of fresh skinless chicken breast.

Keywords: time-temperature indicator, polydiacetylene, silica nanoparticle, chicken, $CO_2$.

## 1 Introduction

For a long time, three basic functions of food packaging are traditionally storage, preservation and protection that are still required for better maintenance of quality and handling of foods [1]. Moreover, the need for more effective food quality and safety assurance systems in food packaging can cause the decreased incidence of foodborne disease. The intelligent or smart packaging is a modern quality and safety assurance system which should prevent contamination through the monitoring, recording, and controlling of critical parameters during a food product's entire life cycle, and includes the post processing phase and extends over the time of use by the final consumer [2]. An important indicator for monitoring the quality of packaged food is temperature. Time-temperature indicators (TTIs) as intelligent packaging are used as cost-effective and user-friendly devices to monitor the overall effect of temperature history during storage and transportation, and give indirectly information about food quality [3-6]. It has the ability to track the product, sense the environment outside the package, and communicate with the consumer.

Polydiacetylene (PDA) is a class of conjugated polymers which could induce the color transition from blue to red upon external stimuli such as temperature, pH, biomolecules, solvent and mechanical stress [7-9]. PDA which is one of the most interesting conjugated polymers can be prepared from vesicles of 10,12-pentacosadiynoic acid (PCDA). The structure of PCDA monomers consist of hydrophilic carboxylic group that generally binds with water, and hydrophobic parts which are long hydrocarbon chain. PDAs are formed by 1,4

addition of the PCDA monomers and then has alternating double- and triple-bond groups in the main polymer chain under UV irradiation. They can be assembled in the form of lipid bi-layer vesicles by photopolymerization. PCDA vesicle is initially colorless and change to blue color after UV irradiation. Addition of amphiphilic polymers or plasticizers, it can change from blue to red color exposed to below temperature 60 °C [8,10], as shown in Figure 1. This color transition could be observed by naked eye.



**Figure 1**: The color transition of PDA vesicle.

Fresh skinless chicken breast is a highly perishable poultry meat to spoilage by many microorganisms including bacteria, such as *Pseudomonas* spp., *Shewanella putrefaciens* and yeasts, depending on the initial microbiological quality of the poultry carcasses [11-12]. In air packaged meat system, microorganisms are able to grow during storage and produced metabolites such as $H_2S$ and sulphur based, ammonia-based, methane-based, organic acid-based and others sensorial important organic compounds also [13]. Carbon dioxide ($CO_2$) is generally known to be produced during microbial growth, thus it can be used as a quality indicator of meat product. The objective of this study is to develop PEG-400-added PDA/$SiO_2$ incorporated PVOH film as a time-temperature indicator for monitoring the freshness of skinless chicken breast.

## 2 Materials and methods

### 2.1 Preparation of PDA/silica nanocomposite

PCDA monomer was self-assembly polymerized to obtain PDA with the concentration of 5 mM. Firstly, PCDA monomer was dissolved in an absolute ethanol and ultra-sonicated by sonicator bath at 60-70 °C. After that, it was removed large aggregates using a nylon syringe filter (pore size ~0.45 μm). Five percent of silica nanoparticles (on the basis of PCDA's weight) were pre-dispersed in deionized water by ultrasonication until homogeneous and clear. Then, this silica nanoparticle solution was added into the PCDA solution to self-assembly form PDA/$SiO_2$ nanocomposite and followed by ultra-sonication at 60-70 °C. Next, this lipid suspension was stored at 4 °C for 24 h, then placed at ambient temperature and irradiated by UV-light to obtain a blue-shaded solution.

### 2.2 Preparation of plasticized PDA/$SiO_2$ incorporated PVOH film

Poly(vinyl alcohol) (PVOH) (10 wt.%) was used as a substrate for film formation. It was dissolved in hot deionized water (80-90 ºC). Poly(ethylene glycol-400) (PEG-400) was weighed and easily dissolved into deionized water to obtain PVOH solutions with a plasticizer concentration (30% of solids). The 5% w/v Pluronic F127 was prepared and then mixed with PEG-400, used as plasticizer. Film forming suspension consisted of a blue-colored PDA/$SiO_2$ nanocomposite solution and a plasticized PVOH solution. It was casted onto PP sticker film (130 μm thickness), then dried at room temperature for 24 h. After that it was cut to a small label (1.5×1.5 cm).

### 2.3 Color changes of TTI label for skinless chicken breast spoilage trial

One hundred and thirty-four point five nine grams of skinless chicken breast samples purchased from Betagro Food Company Limited were aseptically placed into sterilized 267.67 mL PE tray, and then heat sealed by nylon/LLDPE film. The PEG-400-added PDA/$SiO_2$ incorporated PVOH film was attached on nylon/LLDPE film in each PE tray. The samples were stored at 4 and 10 ºC using an incubator (I250-S, Thailand), and periodically analyzed for product quality in terms of carbon dioxide ($CO_2$) during storage. Carbon dioxide was analyzed by headspace gas detection, using a headspace sample of 3 mL. All measurements were carried out using a PAC CHECK® model 650 EC headspace analyzer (MOCON, USA). Carbon dioxide produced by microorganisms within packaging was detected and displayed in percentage value (%) during storage time. During this time, the color change of film was measured instrumentally with a Minolta CR-400 spectrophotometer, using *L*, *a*, *b* values to describe the color of the indicator. The index describing the total color difference (TCD) was suggested by Hunt [14]. Color change ($\Delta E$) was given in equation (1).

$$\Delta E = \left[ \left( \Delta L^* \right)^2 + \left( \Delta a^* \right)^2 + \left( \Delta b^* \right)^2 \right]^{1/2} \quad (1)$$

where $\Delta L^*$ is the brightness difference between initiation and each time interval, $\Delta a^*$ is the redness-greenness difference between initiation and each time interval, and $\Delta b^*$ is the yellowness-blueness difference between initiation and each time interval.

## 3 Results and discussion

### 3.1 Film formation of plasticized PDA/$SiO_2$ incorporated PVOH film

PDA/$SiO_2$ nanocomposite solution was prepared by the ultrasonic method. Initially, PCDA monomers and silica nanoparticles were homogeneously dispersed into a deionized water and then irradiated by UV light to obtain a blue-colored solution. Under photopolymerization, self-assembled PCDA monomers were in the form of lipid bilayer vesicles of PDAs. For the incorporation of silica nanoparticles, a functional group of silica nanoparticles strongly interact with PDA vesicles that results due to the interaction between carboxylic head groups and active groups at the silica surface [15], as if silica nanoparticles could move into core-shell of PDA vesicles. The PDA/$SiO_2$ nanocomposite could clearly exhibit stronger color tone than that of pure PDA due to structural stability. PDA vesicles were usually still in the blue-colored form below 50 ºC, and could transit from blue to red color at or above ca. 60 ºC [8]. Amphiphilic polymer could contribute to decrease the color-transition temperature of PDA below 50 ºC. As our previous work [10], the mixture of Pluronic F127 polymers and PEG-400 were used as amphiphilic polymer. However, the insertion of amphiphilic polymer affected to the structure of PDA/$SiO_2$ molecule, thus the solution could cause a significant blue-shift to purple-shift of absorption spectrum [16]. The purple-colored PDA/$SiO_2$ solution was formed film by PVOH solutions which was casted onto PP sticker film, as shown in Figure 2.

(a) (b)

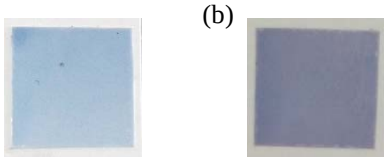


**Figure 2**: The color of plasticizer-free PDA/$SiO_2$ (a) and PEG-400-added PDA/$SiO_2$ (b) film.

### 3.2 Color changes of TTI label during skinless chicken breast spoilage trial

Figure 3 shows carbon dioxide ($CO_2$) levels increased with storage time at 4 and 10 °C. Carbon dioxide produced by microorganisms was released from the food matrix into the headspace within packaging; thus, the levels of $CO_2$ were measured using a headspace analyser. It was markedly detected in skinless chicken breast because a dynamic change in $CO_2$ level could be related to the growth of microorganisms. In addition, Nopwinyuwong *et al*. [17] found a correlation between $CO_2$ concentration and the growth of microorganisms in golden drop. The limit of acceptability was based on the onset of food spoilage, which was considered to be 7.00 log CFU $g^{-1}$ of microorganism in fresh poultry [18,19]. Thus, shelf lives of fresh skinless chicken breast, stored at 4 and 10 °C, were less than 6 d and 3 d, respectively, corresponding to the study by Kontominas *et al*. [20], which found that shelf life of chicken breast fillets stored at 4 °C was 6 d. During storage, the levels of $CO_2$ ranged from 0% (v/v) to 18.96% (v/v) and 0% (v/v) to 21.71% (v/v) at 4 and 10 °C, respectively. TTI labels showed a clear spectrum from deep purple to deep red which could be related to a change in $CO_2$ level during storage time (Figure 3). The changes of $CO_2$ as a result of skinless chicken breast spoilage can be modelled theoretically in accordance with Hong and Park [21]. Polynomial functions give the lines of this curve, represented by equation (2) and (3).

At 4 °C,

$$X = \text{-7E-09}x^4 + \text{1E-05}x^3 - 0.0021x^2 + 0.1555x + 0.6686 \quad (2)$$

At 10 °C,

$$X = \text{-4E-05}x^3 + 0.007x^2 - 0.1116x + 2.1809 \quad (3)$$

The above equation can be rearranged to the desirable form, given in (4) and (5) below.
At 4 °C,

$$F(X) = \frac{1.0996}{\left(1 + \left(\frac{4.8728}{X}\right)^{4.5663}\right)} = kt \quad (4)$$

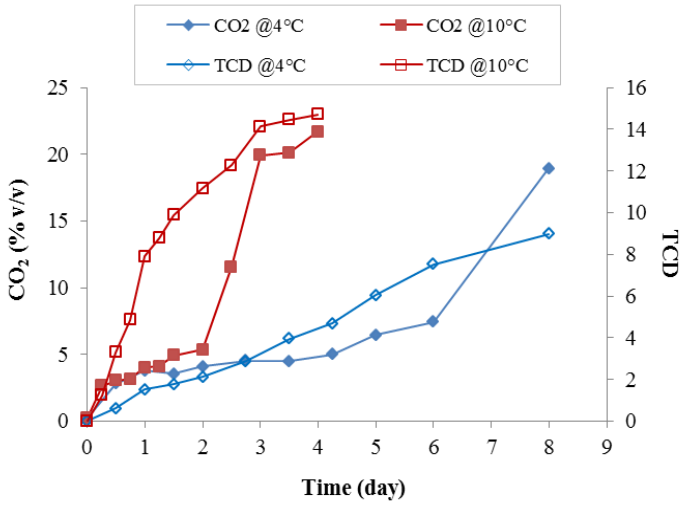



**Figure 3**: Plot of changes in $CO_2$ level in skinless chicken breast and changes in total color difference of PEG-400-added PDA/$SiO_2$ film at 4 and 10 °C.

At 10 °C,

$$F(X) = \frac{57.3837X}{(X + 924.9415)} = kt \tag{5}$$

where $k$ is the reaction or response rate constant, and $t$ is time.

Plotting the function $F(X)$, given by the logarithmic expression in the above equation, versus time gives two straight lines of different slopes at each temperature (Figure 4). The rate constants and the coefficients of determination for $CO_2$ levels of skinless chicken breast at different temperatures are given in Table 1. Based on Arrhenius equation, carbon dioxide formation during skinless chicken breast spoilage yields an activation energy $E_a$ = 86.36 kJ $mol^{-1}$.

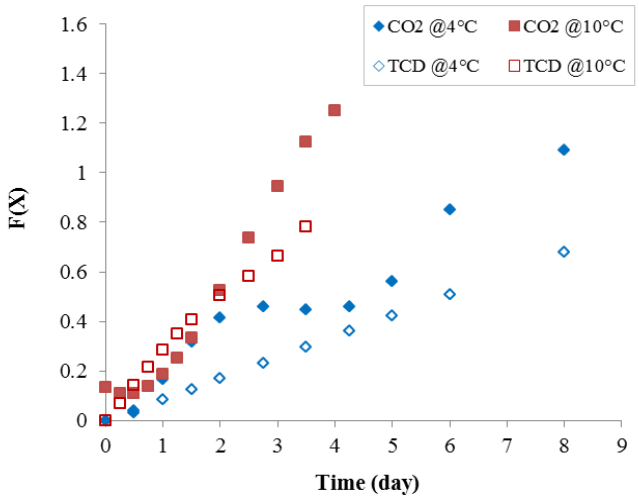



**Figure 4**: Plot of response function $F(X)$ with time for $CO_2$ level in skinless chicken breast and for total color difference in TTI labels.

The TCD value also changed continuously and consistently with the response of the TTI label. TCD values gradually increased with time. The final TCD values were 8.99-14.71. It is generally known that TCD values greater than 5.0 can be easily detected by the unaided eye, and TCD greater than 12.0 indicates a completely different color space [22]. A kinetic approach could be used to model the measurable TCD change of the TTI label because the changes in TCD of the label showed a zero-order behavior. A normalized TCD value, $X$ = TCD, was used as the variable. The indicator response $X$ when plotted against time gives straight lines (Figure

4), if $F(X) = kt$ is defined as the response function. The rate constants and coefficients of determination for TCD of TTI label at different temperatures are given in Table 1. Total color difference of indicator labels resulted in $E_a$ of 114.06 kJ $mol^{-1}$. Packaged skinless chicken breast with TTI label is shown in Figure 5.

**Table 1:** Response rate constants and coefficients of determination[a] for $CO_2$ of skinless chicken breast and for total color difference (TCD) of TTI label at different temperatures.

| Temperature (°C) | $CO_2$ | | TCD | |
|---|---|---|---|---|
| | $k$ ($day^{-1}$) | $r^2$ | $k$ ($day^{-1}$) | $r^2$ |
| 4 | 0.0056 | 0.9325 | 0.0035 | 0.9999 |
| 10 | 0.0124 | 0.9555 | 0.0100 | 0.9837 |

[a] Significance level of $P < 0.05$.



(a) (b)

**Figure 5**: Packaged skinless chicken breast with TTI label. Purple = fresh; Red = spoilage.

## 3 Conclusions

$PDA/SiO_2$ nanocomposite solution was prepared by the ultrasonic method and irradiated by UV light. The blue-colored $PDA/SiO_2$ nanocomposite solution could change purple color after the addition of F127 and PEG-400 plasticizers. The PEG-400-added $PDA/SiO_2$ incorporated PVOH film could clearly show purple color. The results presented in this study indicated that PEG-400-added $PDA/SiO_2$ film is the sensitive detection under cold temperature conditions and indirectly related to spoilage metabolites in skinless chicken breast which can be achieved by a non-invasive colorimetric method when compared with others. The response function of TTI was rather similar to the response function of $CO_2$ in skinless chicken breast, therefore enabling the real-time monitoring of spoilage. Finally, the novel TTI based on plasticized $PDA/SiO_2$ nanocomposites is possibly develop TTI system for chilled food product application.

## Acknowledgements

The authors gratefully acknowledge the financial support from the Department of Packaging and Materials technology, Faculty of Agro-Industry, KU; Center for Advanced Studies in Agriculture and Food, Institute for Advanced Studies, KU; Graduate School Kasetsart University Grant and Kasetsart University Research and Development Institute (KURDI). PP sticker film was supported by UPM Raflatac Co., Ltd.

## References

1. K. Galić. M. Ščetar and M. Kurek, 2011, "The benefits of processing and packaging", *Trends in Food Science & Technology*, vol. 22, pp. 127-137.
2. K. Koutsoumanis. P.S. Taoukis and G.J.E. Nychas, 2005, "Development of a safety monitoring and assurance system for chilled food products", *International Journal of Food Microbiology*, vol. 100, pp. 253-260.
3. P.S. Taoukis and T.P. Labuza 2003, "Time-Temperature Indicators (TTIs)", In: R. Ahvenainen (ed.), *Novel Food Packaging Techniques*, Woodhead Publishing Ltd., England, pp. 103-126.
4. M.C. Giannakourou. K. Koutsoumanis. G.J.E. Nychas and P.S. Taoukis, 2005, "Field evaluation of the application of time temperature integrators for monitoring fish quality in the chill chain", *International Journal of Food Microbiology*, vol. 102, pp. 323-336.

5. J.H. Han. C.H.L. Ho and E.T. Rodrigue 2005, “Intelligent Packaging”, In: J.H. Han (ed.), *Innovation in Food Packaging*, Elsevier academic press, London, pp. 138-155.

6. A. Pacquit. K. Crowley and D. Diamond 2008, “Smart Packaging Technologies for Fish and Seafood Products”, In: J. Kerry and P. Butler (eds.), *Smart Packaging Technologies for Fast Moving Consumer Goods*, John Wiley&Sons, Ltd., England, pp. 75-98.

7. N. Charoenthai. T. Pattanatornchai. S. Wacharasindhu. M. Sukwattanasinitt and R. Traiphol, 2011, “Roles of head group architecture and side chain length on colorimetric response of polydiacetylene vesicles to temperature, ethanol and pH”, *Journal of Colloid and Interface Science*, vol. 360, pp. 565-573.

8. M.L. Gou. G. Guo. J. Zhang. K. Men. J. Song. F. Luo. X. Zhao. Z.Y. Qian and Y.Q. Wei, 2010, “Time-temperature chromatic sensor based on polydiacetylene (PDA) vesicle and amphiphilic copolymer”, *Sensors and Actuators B: Chemical*, vol. 150, pp. 406-411.

9. Y.L. Su. J.R. Li and L. Jiang, 2004, “Effect of amphiphilic molecules upon chromatic transitions of polydiacetylene vesicles in aqueous solutions”, *Colloids and Surfaces B: Biointerfaces*, vol. 39, pp.113-118.

10. A. Nopwinyuwong. W. Boonsupthip. C. Pechyen and P. Suppakul, 2012, “Preparation of polydiaceylene vesicle and amphiphilic polymer as time-temperature indicator”, *Advanced Materials Research*, vol. 506, pp. 552-555.

11. S.M. Russell. D.L. Fletcher and N.A Cox, 1995, “Spoilage bacteria of fresh broiler chicken carcasses”, *Poultry Science*, vol. 74, pp. 2041-2047.

12. A. Hinton Jr. J.A. Cason and K.D. Ingram, 2002, “Enumeration and identification of yeasts associated with commercial poultry processing and spoilage of refrigerated broiler carcasses”, *Journal of Food Protection*, vol. 65, pp. 993-998.

13. T.M. Lovestead and T.J. Bruno, 2010, “Detection of poultry spoilage markers from headspace analysis with cryoadsorption on a short alumina PLOT column”, *Food Chemistry*, vol. 121, pp. 1274-1282.

14. R.W.G. Hunt, 1991, *Measuring Colour*, 2nd Ed., Ellis Horwood Ltd, Chichester, UK.

15. A. Nopwinyuwong. W. Boonsupthip. C. Pechyen and P. Suppakul, 2013, “Formation of polydiaceylene/silica nanocomposite as a colorimetric indicator: effect of time and temperature”, *Advances in Polymer Technology*, vol. 32, pp. E724-E731.

16. A. Nopwinyuwong. T. Kaisone. P. Hanthanon. C. Nandhivajrin. W. Boonsupthip. C. Pechyen and P. Suppakul, 2014, “Effects of nanoparticle concentration and plasticizer type on colorimetric behavior of polydiacetylene/silica nanocomposite as time-temperature indicator”, *Energy Procedia*, In press.

17. A. Nopwinyuwong. S. Trevanich and P. Suppakul, 2010, “Development of a novel colorimetric indicator label for monitoring freshness of intermediate-moisture dessert spoilage”, *Talanta*, vol. 81, pp. 1126-1132.

18. S.D. Senter. J.W. Arnold and V. Chew, 2000, “APC values and volatile compounds formed in commercially processed, raw chicken parts during storage at 4 and 13 °C and under simulated temperature abuse conditions”, *Journal of the Science of Food and Agriculture*, vol. 80, pp. 1559-1564.

19. C.C. Balamatsia. A. Patsias. M.G. Kontominas and I.N. Savvaidis, 2007, “Possible role of volatile amines as quality-indicating metabolites in modified atmosphere packaged chicken fillets: Correlation with microbiological and sensory attributes”, *Food Chemistry*, vol. 104, pp. 1622-1628.

20. A. Khanjari. I.K. Karabagias and M.G. Kontominas, 2013, “Combined effect of N,O-carboxymethyl chitosan and oregano essential oil to extend shelf life and control Listeria monocytogenes in raw chicken meat fillets”, *LWT - Food Science and Technology*, vol. 53, pp. 94-99.

21. S.-I. Hong and W.-S. Park, 2000, “Use of color indicators as an active packaging system for evaluating *kimchi* fermentation”, Journal of Food Engineering, vol. 46, pp. 67-72.

22. F.J. Francis 1983, “Colorimetry of Foods”, In: M. Peleg and E.B. Bagley (eds.), *Physical Properties of Foods*, AVI Publishing, Westport, CT, pp. 105-123.

# Response Modelling of Time-Temperature Indicator Based on Polydiacetylene/Silica Nanocomposite

**Atchareeya Nopwinyuwong[1,3], Chanassa Nandhivajrin[1,3], Waraporn Boonsupthip[2,3], Chiravoot Pechyen[1,3] and Panuwat Suppakul[1,3,*]**

[1] *Department of Packaging and Materials Technology, Faculty of Agro-Industry, Kasetsart University, Bangkok, 10900, Thailand*

[2] *Department of Food Science and Technology, Faculty of Agro-Industry, Kasetsart University, Bangkok, 10900, Thailand*

[3] *Center for Advanced Studies in Agriculture and Food, KU Institute for Advanced Studies, Kasetsart University, 10900, Thailand (CASAF, NRU-KU, Thailand)*

[*] *Corresponding author. Email: panuwat.s@ku.ac.th*

**Abstract:** The development of time-temperature indicator (TTI) based on polydiacetylene (PDA) and silica nanoparticles as an effective tool was investigated. With a time-temperature change, a PDA/$SiO_2$ nanocomposite could irreversible change from blue to red color under a color transition temperature of PDA vesicles (>60 °C). However, the addition of plasticizer into PDA/$SiO_2$ nanocomposite embedded in poly(vinyl alcohol) (PVOH) film does not exclusively increase flexibility during film formation, but it reduces the color transition temperature of PDA/$SiO_2$ films as well, including appropriate the chilled food product application. The plasticizer could insert into a PDA vesicle structure and its mobility was occurred, thus the initial color of plasticized PDA/$SiO_2$ film was shifted from blue to purple. In this research, the different TTIs prepared from three types of plasticizer were poly(ethylene glycol-400), glycerol and sorbitol-added PDA/$SiO_2$ films. A constant temperature profile and dynamic temperature profile were designed in the experiment. The mathematical model of TTI shows the relationships between the changes of time and temperature and the TTI's color changed in terms of total color difference (TCD or $\Delta E$). Higher temperature at isothermal condition was presented in a faster color change from blue to purple, reddish purple and finally red. Moreover, it could be determined Arrhenius kinetics parameters of the TTI system as a function of temperature. For dynamic thermal condition, the recorded data was TTI-response modelled and calculated the effective temperature ($T_{eff}$) and the remaining shelf life ($t_r$) of TTIs. Finally, it showed potentially the applicability and usefulness of TTI for chilled food distribution, and this new polymer-based TTI used as a reliable device could exhibit time-temperature history.

Keywords: time-temperature indicator, polydiacetylene, silica nanoparticle, activation energy, shelf life kinetics.

## 1 Introduction

Time-temperature indicators (TTIs) are defined as simple and inexpensive devices that show an easily measurable, time-temperature dependent change that reflects the temperature history of food products. In the event of temperature abuse, it can monitor, record and control critical parameters during a food product's entire life cycle [1]. Temperature is a critical parameter for monitoring the quality of packaged food, especially chilled food products, due to it mainly determines the rate of microbial activity. Therefore, the TTI can give indirectly information about the product quality and the storage conditions of the package [2,3]. It can show an irreversible color change under abusive conditions during transportation, distribution and storage. Selecting a suitable TTI device requires a previous knowledge of the kinetic characteristics of food deterioration and its dependence on temperature. Generally, the application of TTIs to food products can be considered by the activation energy ($E_a$) of TTI response and the food quality losses, which the activation energy ($E_a$) is based on Arrhenius equation. For kinetic approach, both the $E_a$ values should match for indicating the temperature sensitivity of the TTI response to the shelf life of food products [4,5]. Recently several types of TTIs, mainly chemical or physical systems, are enzymatic TTI based on the reaction between amylase and starch [6], bacterial-based TTI based on the growth and metabolic activity of a *Lactobacillus sakei* strain [7], photochromic-based TTI based on a photochromic solid state reaction under specific temperature conditions [8] and diffusion-based TTI based on the vapor diffusion of lactic acid [9].

Polydiacetylene (PDA) is a class of conjugated polymers which could induce the color transition from blue to red upon external stimuli such as temperature, pH, biomolecules, solvent and mechanical stress [10,11].

Advantages of PDA vesicles are easily prepared in a vesicle form that is homogeneously dispersed in water because of a high polar carboxylic head groups and a nonpolar hydrocarbon chain of PDCA molecules. It appears blue and red color with a maximum absorption at about 640 and 540 nm, respectively. The addition of silica nanoparticles can help increase their strong ionic interaction with functional groups of polymer chain [12] because of the interaction between carboxylic head groups and active groups at the silica surface [13]. At 640 nm, the absorbance intensity of the PDA/$SiO_2$ nanocomposites in aqueous solution increased compared with pure PDA molecules after UV irradiation, because silica nanoparticles could affect to mobility of the PDA side chain. Poly(vinyl alcohol) (PVOH) used as matrix polymers are hydrophilic nature, easily hydrogel film-forming, environmental friendliness and inertness to guest molecules [14]. The objective of this study are to investigate kinetics parameters of the TTI system at isothermal and non-isothermal conditions, and to determine the effective temperature ($T_{eff}$) and the remaining shelf life ($t_r$) of TTIs for monitoring chilled food product quality.

## 2 Materials and methods

### 2.1 Preparation of PDA/silica nanocomposite

PCDA monomer was self-assembly polymerized to obtain PDA with the concentration of 5 mM. Firstly, PCDA monomer was dissolved in an absolute ethanol and ultra-sonicated by sonicator bath at 60-70 °C. After that, it was removed large aggregates using a nylon syringe filter (pore size ~0.45 μm). Five percent of silica nanoparticles (on the basis of PCDA's weight) were pre-dispersed in deionized water by ultrasonication until homogeneous and clear. Then, this silica nanoparticle solution was added into the PCDA solution to self-assembly form PDA/$SiO_2$ nanocomposite and followed by ultra-sonication at 60-70 °C. Next, this lipid suspension was stored at 4 °C for 24 h, then placed at ambient temperature and irradiated by UV-light to obtain a blue-shaded solution.

### 2.2 Preparation of plasticized PDA/$SiO_2$ incorporated PVOH film

Poly(vinyl alcohol) (PVOH) (10 wt.%) was used as a substrate for film formation. It was dissolved in hot deionized water (80-90 ºC). Poly(ethylene glycol-400) (PEG-400) was weighed and easily dissolved into deionized water to obtain PVOH solutions with a plasticizer concentration (30% of solids). The 5% w/v Pluronic F127 was prepared and then mixed with PEG-400, used as plasticizer. Film forming suspension consisted of a blue-colored PDA/$SiO_2$ nanocomposite solution and a plasticized PVOH solution. It was casted onto PP sticker film (130 μm thickness), then dried at room temperature for 24 h. After that it was cut to a small label (1.5×1.5 cm).

### 2.3 Color changes of TTI label under isothermal and non-isothermal conditions

The plasticized PDA/$SiO_2$ films were tested isothermally at different temperatures (4 and 10 ºC) and non-isothermally at two dynamic thermal profiles (Figure 1) using an incubator (I250-S, Thailand). The first profile was periodically alternated 48 h cycle of 24 h at 0 ºC and 24 h at 8 ºC to simulate abrupt changes and sustained abuse periods in the distribution chain. The second profile was periodically alternated 12 h cycle of 3 h at 4 ºC, 3 h at 9 ºC, 3 h at 15 ºC and 3 h at 12 ºC to simulate a gradually and continuously changing storage environment. Films were observed in every 24 h and 4 h for profile 1 and profile 2, respectively. The color change of films corresponding to the value of total color difference (TCD or $\Delta E$) was recorded in each time interval, using a Chroma Meter spectrophotometer (Minolta CR-400, Japan). The TCD was calculated as described by equation (1).

$$\Delta E = \left[ \left( \Delta L^* \right)^2 + \left( \Delta a^* \right)^2 + \left( \Delta b^* \right)^2 \right]^{1/2} \quad (1)$$

where $\Delta L^*$ is the brightness difference between initiation and each time interval, $\Delta a^*$ is the redness-greenness difference between initiation and each time interval, and $\Delta b^*$ is the yellowness-blueness difference between initiation and each time interval [15].

In addition, the value of total color difference (TCD or $\Delta E$) was determined Arrhenius kinetics parameters of the TTI system as a function of temperature and the recorded data was TTI-response modeled [16]. The effective temperature ($T_{eff}$) and the remaining shelf life ($t_r$) of TTIs were calculated by equation (2).

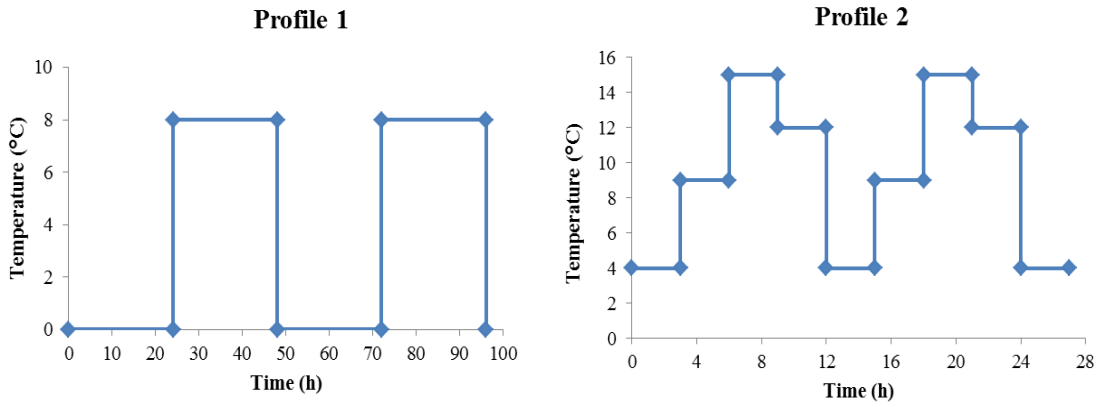



**Figure 1**: Dynamic thermal profiles.

$$F(X) = k_1 t = k_{1,ref} \exp\left[\frac{-E_a}{R}\left(\frac{1}{T_{eff}} - \frac{1}{T_{ref}}\right)\right] t \quad (2)$$

where $F(X)$ is the function of $X$ or TCD, $k_{1,ref}$ is the reaction or response rate constant of TTI at reference temperature ($T_{ref}$), $T_{eff}$ is the effective temperature and $t$ is time.

## 3 Results and discussion

### 3.1 Color change of plasticized PDA/$SiO_2$ incorporated PVOH film under isothermal and non-isothermal conditions

The ultrasonic method was used to prepare silica nanoparticles and PCDA/$SiO_2$ nanocomposite solution. Under UV irradiation, PCDA monomers and silica nanoparticles which were homogeneously dispersed into a deionized water could obtain a blue-colored PDA/$SiO_2$ solution [17]. PDA/$SiO_2$ nanocomposite solution was mixed directly with plasticizers that were fixed ratio between F127 and PEG-400, and PVOH solution during film forming process. This solution revealed purple color as a result of an insertion of plasticizer in lipid monolayer of PDA [11]. The purple-colored solution was casted onto PP sticker film and finally formed a dried purple-colored film at room temperature. The initial color ($L^*$, $a^*$, $b^*$ value) of plasticized PDA/$SiO_2$ incorporated PVOH films were measured and calculated to the total color difference (TCD or $\Delta E$). For isothermal condition, a change of TCDs of PEG-400-added PDA/$SiO_2$ films could gradually increase during storage time. At higher temperature (10 °C), these films underwent fast a purple-to-red color transition in comparison with lower temperature (4 °C). The TCD of these films ranged from 0 to 8.99 for 8 day and 0 to 14.71 for 4 day when kept at 4 and 10 °C, respectively. For non-isothermal condition, the change of TCDs of profile 1 and profile 2 were similar to those of films kept at 4 and 10°C, respectively. Here, the TCD data of profile 1 and profile 2 were recorded within 5 day (TCD = 0-9.28) and 24 h (TCD = 0-5.87), respectively.

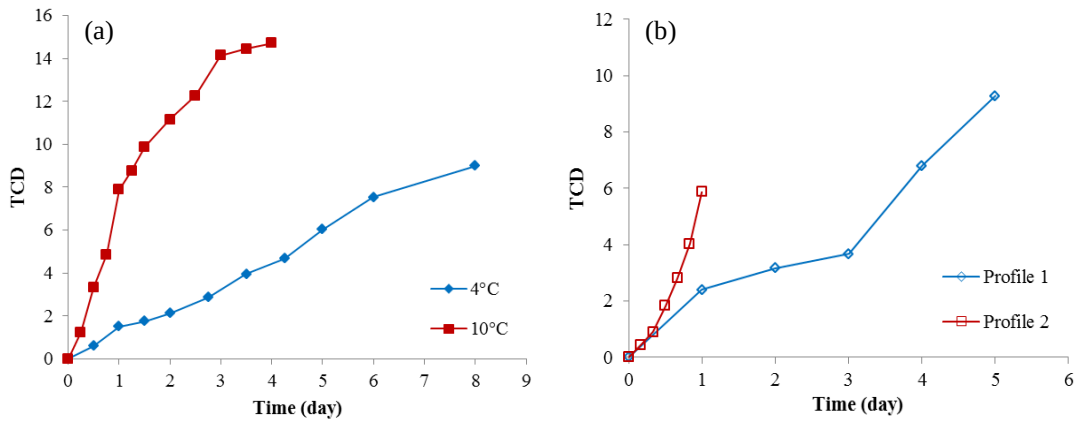



**Figure 2**: Plot of changes in TCD of PEG-400-added PDA/$SiO_2$ incorporated PVOH films under isothermal (a) and non-isothermal (b) conditions.

### 3.2 Time-temperature indicator based on PDA/$SiO_2$ nanocomposite modelling

Time-temperature indicator labels showed a clear spectrum from deep purple to deep red which could be related to the change of the total color difference (TCD or $\Delta E$) during storage time. Under isothermal and non-isothermal conditions, the changes of TCD can be modelled theoretically in accordance with Hong and Park [18]. Polynomial functions give the lines of this curve, represented by (3) and (4) below.

At 4 °C and profile 1,

$$X = \text{-1E-06}x^2 + 0.0485x \tag{3}$$

At 10 °C and profile 2,

$$X = \text{7E-07}x^4 - 0.0001x^3 + 0.003x^2 + 0.2727x \tag{4}$$

The above equation can be rearranged to the desirable form, given in (5) to (8) below.

At 4 °C,

$$F(X) = 0.0004 + 0.0649X = kt \tag{5}$$

At 10 °C,

$$F(X) = 0.0482X = kt \tag{6}$$

For profile 1,

$$F(X) = \frac{51.1180X}{(X + 493.7677)} = kt \tag{7}$$

For profile 2,

$$F(X) = \frac{13.6333X}{(X + 502.1964)} = kt \tag{8}$$

where $k$ is the reaction or response rate constant, and $t$ is time.

Plotting the function $F(X)$, given by the logarithmic expression in the above equation, versus time gives two straight lines of different slopes at each temperature (Figure 3). The TCD value also changed continuously and consistently with the response of the TTI label. TCD values gradually increased with time. It is generally known that TCD values greater than 5.0 can be easily detected by the unaided eye, and TCD greater than 12.0 indicates a completely different color space [21]. A kinetic approach could be used to model the measurable TCD change of the TTI labels because the changes in TCD of the label showed a zero-order behavior. A normalized TCD value, $X$ = TCD, was used as the variable. The indicator response $X$ when plotted against time gives straight lines, if $F(X) = kt$ is defined as the response function. The rate constants and coefficients of determination for TCD of TTI label at different temperatures are given in Table 1. Total color difference of indicator labels resulted in $E_a$ of 114.06 kJ $mol^{-1}$.

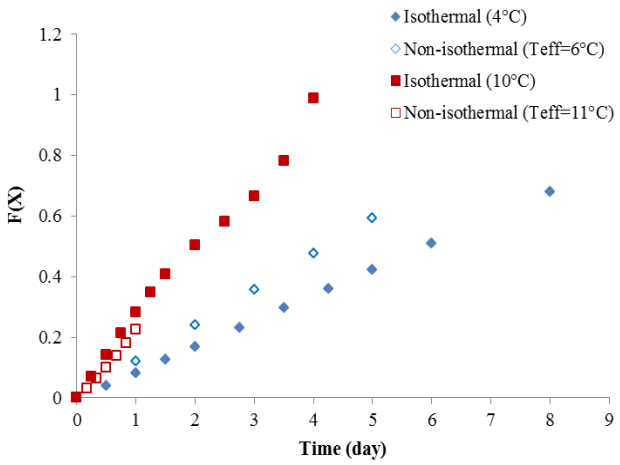



**Figure 3**: Plot of response function $F(X)$ with time for total color difference in TTI labels.

**Table 1:** Response rate constants and coefficients of determination[a] for total color difference (TCD) of TTI label under isothermal and non-isothermal conditions.

| | Isothermal | | | | Non-Isothermal | | | |
|---|---|---|---|---|---|---|---|---|
| | 4 °C | | 10 °C | | Profile 1 | | Profile 2 | |
| | k ($day^{-1}$) | $r^2$ | k ($day^{-1}$) | $r^2$ | k ($day^{-1}$) | $r^2$ | k ($day^{-1}$) | $r^2$ |
| TTI | 0.0035 | 0.9999 | 0.0100 | 0.9837 | 0.005 | 1.000 | 0.0090 | 0.9930 |

[a] Significance level of $P < 0.05$.

For dynamic thermal condition, the $T_{eff}$ of PEG-400-added PDA/$SiO_2$ incorporated PVOH films were 6.04 and 10.97 °C in profile 1 and profile 2, respectively. The provided information of TTIs could be translated to $t_r$ of TTIs for indicating the time of endpoint. The $t_r$ of TTIs were 2.87 and 2.24 day in profile 1 and profile 2, respectively (Table 2).

**Table 2:** Effective temperature ($T_{eff}$) and remaining shelf life ($t_r$) for total color difference (TCD) of TTI label under non-isothermal condition.

| | Non-Isothermal | | | |
|---|---|---|---|---|
| | Profile 1 | | Profile 2 | |
| | $T_{eff}$ (°C) | $t_r$ (day) | $T_{eff}$ (°C) | $t_r$ (day) |
| TTI | 6.04 | 2.87 | 10.97 | 2.24 |

## 3 Conclusions

The ultrasonic method can be used to prepare PDA/$SiO_2$ nanocomposite solution irradiated by UV light. The blue solution of PDA/$SiO_2$ nanocomposite was observed by unaided eyes. For casting method, PDA/$SiO_2$ nanocomposite embedded PVOH films were mixed with fixed ratio plasticizers of F127 and polyol. Plasticizer does not exclusively increase flexibility during film formation, but it reduces the color transition temperature of PDA/$SiO_2$ films as well. Plasticized PDA/$SiO_2$ films could change from purple to red when stored at 4 and 10 °C. The present study showed the systematic approach to be followed for response modelling and selection of appropriate TTI based PDA/$SiO_2$ nanocomposites in order to achieve an effective monitoring of food quality during distribution. Thus the novel TTI based on PDA/$SiO_2$ nanocomposites could be applied to show time-temperature history.

## Acknowledgements

The authors gratefully acknowledge the financial support from the Department of Packaging and Materials technology, Faculty of Agro-Industry, KU; Center for Advanced Studies in Agriculture and Food, Institute for Advanced Studies, KU; Graduate School Kasetsart University Grant and Kasetsart University Research and Development Institute (KURDI). PP sticker film was supported by UPM Raflatac Co., Ltd.

## References

1. K. Koutsoumanis. P.S. Taoukis and G.J.E. Nychas, 2005, "Development of a safety monitoring and assurance system for chilled food products", *International Journal of Food Microbiology*, vol. 100, no. 1-3, pp. 253-260.
2. J.H. Han. C.H.L. Ho and E.T. Rodrigue 2005, "Intelligent packaging", In: J.H. Han (ed.), *Innovation in Food Packaging*, Elsevier academic press, London, pp. 138-155.
3. A. Pacquit. K. Crowley and D. Diamond 2008, "Smart packaging technologies for fish and seafood products", In: J. Kerry and P. Butler (eds.), *Smart Packaging Technologies for Fast Moving Consumer Goods*, John Wiley&Sons, Ltd., England, pp. 75-98.
4. P.S. Taoukis and T.P. Labuza, 1989a, "Applicability of Time Temperature Indicators as shelf life monitors of food products", *Journal of Food Science*, vol. 54, pp. 783-788.
5. P.S. Taoukis and T.P. Labuza, 1989b, "Reliability of Time Temperature Indicators as food quality monitors under non isothermal conditions", *Journal of Food Science*, vol. 54, pp. 789-792.
6. S. Yan. C. Huawei. Z. Limin. R. Fazheng. Z. Luda and Z. Hengtao, 2008, "Development and characterization of a new amylase type time-temperature indicator", *Food Control*, vol. 19, pp. 315-319.

7. H. Vaikousi. C.G. Biliaderis and K.P. Koutsoumanis, 2008, “Development of a microbial time/temperature indicator prototype for monitoring the microbiological quality of chilled foods”, *Applied and Environmental Microbiology*, vol. 74, pp. 3242-3250.

8. J. Kreyenschmidt. H. Christiansen. A. Hubner. V. Raab and B. Petersen, 2010, “A novel photochromic time-temperature indicator to support cold chain management”, *International Journal of Food Science and Technology*, vol. 45, pp. 208-215.

9. C. Wanihsuksombat. V. Hongtrakul and P. Suppakul, 2010, “Development and characterization of a prototype of a lactic acid-based time-temperature indicator for monitoring food product quality”, *Journal of Food Engineering*, vol. 100, pp. 427-434.

10. N. Charoenthai. T. Pattanatornchai. S. Wacharasindhu. M. Sukwattanasinitt and R. Traiphol, 2011, “Roles of head group architecture and side chain length on colorimetric response of polydiacetylene vesicles to temperature, ethanol and pH”, *Journal of Colloid and Interface Science*, vol. 360, no. 2, pp. 565-573.

11. M.L. Gou. G. Guo. J. Zhang. K. Men. J. Song. F. Luo. X. Zhao. Z.Y. Qian and Y.Q. Wei, 2010, “Time-temperature chromatic sensor based on polydiacetylene (PDA) vesicle and amphiphilic copolymer”, *Sensors and Actuators B: Chemical*, vol. 150, pp. 406-411.

12. G. Schmidt and M.M. Malwitz, 2003, “Properties of polymer-nanoparticle composites”, *Current Opinion in Colloid and Interface Science*, vol. 8, pp. 103-108.

13. A. Nopwinyuwong. W. Boonsupthip. C. Pechyen and P. Suppakul, 2013, “Formation of polydiaceylene/silica nanocomposite as a colorimetric indicator: effect of time and temperature”, *Advances in Polymer Technology*, vol. 32, pp. E724-E731.

14. J.M. Kim, Y.B. Lee, S.K. Chae, D.J. Ahn, Patterned color and fluorescent images with polydiacetylene supramolecules embedded in poly(vinyl alcohol) films. Adv Funct Mater, 16 (2006) 2103-2109.

15. F.J. Francis 1983, “Colorimetry of Foods”, In: M. Peleg and E.B. Bagley (eds.), *Physical Properties of Foods*, AVI Publishing, Westport, CT, pp. 105-123.

16. T. Tsironi. A. Stamatiou. M. Giannoglou. E. Velliou and P.S. Taoukis, 2011, “Predictive modelling and selection of Time Temperature Integrators for monitoring the shelf life of modified atmosphere packed gilthead seabream fillets”, *LWT - Food Science and Technology*, vol. 44, pp. 1156-1163.

17. A. Nopwinyuwong. T. Kaisone. P. Hanthanon. C. Nandhivajrin. W. Boonsupthip. C. Pechyen and P. Suppakul, 2014, “Effects of nanoparticle concentration and plasticizer type on colorimetric behavior of polydiacetylene/silica nanocomposite as time-temperature indicator”, *Energy Procedia*, In press.

18. S.-I. Hong and W.-S. Park, 2000, “Use of color indicators as an active packaging system for evaluating *kimchi* fermentation”, Journal of Food Engineering, vol. 46, no. 1, pp. 67-72.

# Development of a Biodegradable Coating Based on Seaweed Extracts and Starch for Food Packaging Applications

**Ana Beltrán*, Luis M. Guardeño, Mercedes Hortal, Teresa Calvo, Susana Aucejo**

Packaging, Transport and Logistic Research Institute (ITENE) C/Albert Einstein, 1, Parque tecnológico, Paterna, 46180 Valencia, Spain.

*Corresponding author. Email: ana.beltran@itene.com

**Abstract:** Paper and cardboard are sustainable food packaging alternatives since they are highly recyclable materials. In order to achieve better barrier properties, there is a high interest in the improvement of their water and oil resistance by the application of coatings based on petrochemical derived waxes and polymers. However, due to the increasing petroleum costs, the packaging sector is looking for alternatives of reliable and sustainable coating products [1] reducing the economic cost of recycling or improving the paper compostability. In this sense, starch and seaweed extracts are friendly biopolymers capable to improve the functional properties of the cellulosic packaging material at the same time they can extend shelf life of the packaging material [2]. However, their poor barrier properties limit its application as food packaging, particularly in the presence of water and grease.

In order to improve the grease properties of paper and paperboard, PLANTPACK project has developed a biodegradable coating based on seaweed extracts combined with starch. The application of these formulations on the substrates is based on the spraying technique avoiding depth wetting of substrate. The spray head is modelled to determine the 'ideal' venturi to create an atomised droplet of between 12 and 100 microns. Coatings based on seaweed extracts and starch resulted in coatings that gave excellent grease resistance. The mechanical behaviour of the paper and cardboard samples and its biodegradability and compostability is not affected by the application of the coating dissolution. From the results obtained, it is important to highlight that this new package will reach conventional synthetic multilayer materials in specific products applications opening a new market opportunity for all the SMEs and RTDs involved in the consortium.

Keywords: paper, paperboard, biodegradable coating, food packaging, grease resistance.

## 1 Introduction

Paper and cardboard are widely used in packaging applications since they are biodegradable and therefore perfectly safe for the environment. Paper consists of a porous cellulose structure made up of microfibrils, which are composed of long-chain cellulose molecules in a crystalline state with amorphous regions regularly disrupting the crystalline structure. The hydrophilic nature of cellulose, due to the -OH sites in the basic unit of cellulose ($C_6H_{10}O_5$) and fiber network porosity, limits the barrier properties of these materials. Paper and cardboard packaging also easily absorb water and grease from the environment or from the food and loses its physical and mechanical strengths. Moisture and grease migration can occur in these materials by diffusion through the void spaces and through the fiber cell walls [3].

Because of the drawbacks of these materials related to barrier and mechanical properties, they are often associated with other materials, such as plastic materials and aluminum, for their good barrier properties that could be advantageously combined as a coating with paper and cardboard. In this sense, polyolefins are generally chosen as coating materials to overcome porosity and hygroscopicity of paper and cardboard. Unfortunately, the obtained material loses its biodegradation and recyclability characteristics due to the addition of synthetic polymer layers.

In order to replace the current synthetic coatings, biopolymer-based packaging materials originated from naturally renewable resources such as polysaccharides, proteins, and lipids or combinations of those components offer favourable environmental advantages of recyclability and reutilization compared to conventional petroleum-based synthetic polymers. Biopolymer films and coatings may also serve as gas and solute barriers and complement other types of packaging by minimizing food quality deterioration and extending the shelf life of foods. Therefore, the importance of accurate methodologies for determining the film performances has been developed [4] highlighting the measurement of the following properties:

### 1.1 Mechanical properties

In many packaging applications, mechanical resistance is required. In general, mechanical properties of coated/laminated films in a composite structure tend to rely strongly on the substrate or base film rather than the coating [5]. The mechanical properties frequently measured to characterize paper/cardboard-based packaging materials are tensile strength (TS), elongation (E), elastic modulus (Young's Modulus) (EM), and tearing resistance (TR). TS is a measure of the ability of a film to resist breaking under tension, which is dependent on the strength of fibers, their surface area, and length, and also the bonding strength between them. E is a quantitative representation of the film's ability to stretch. EM is defined as the ratio of stress to strain in the initial linear part of the stress-strain curve and it is a fundamental measurement of inherent stiffness of the material. TR corresponds to the average force applied during the tearing operation; it is likely that it relates to the fracture stress and/or fracture resistance or toughness of the material [6].

### 1.2 Barrier properties

**Oil resistance.** Grease resistance is an important property of paper packaging materials used for foods containing fats or oils. Limited research has been done on quantifying the oil permeability of packaging materials. Coated paper or paperboard with a good grease barrier is important for packaging used in fast food restaurants, as well as food-packaging applications such as cereal boxes, donut boxes and pizza boxes. Previous studies indicated that the grease resistance of corn zein coated paper was no significantly different in comparison with commercial polyethylene laminated paper [7].

The main objective of this study was to develop a biodegradable and sustainable coating based on starch and seaweed extracts. The effect of the develop coating was tested on the mechanical and barrier properties of coated paper and paperboard samples used for food packaging applications.

## 2 Materials and methods

### 2.1 Materials

In order to formulate the biodegradable coating, a commercial grade of native maize starch was obtained from Roquette (Spain) and seaweed extracts were supplied by Chemcolloids Ltd (United Kingdom). The coating was tested in two different commercial papers and a paperboard commonly used for food packaging applications supplied by KRPA PAPER (Czech Republic).

### 2.2 Coating formulation and application

A coating with a combination of seaweed extract and starch was formulated and applied to paper and paperboard samples. The application of the coating was carried out by using the spraying technique. In order to obtain a homogeneous coating, the spray head was modelled to determine the 'ideal' venturi to create an atomised droplet of between 12 and 100 microns. The Figure 1 shows the scheme of the spraying technique employed in this work.

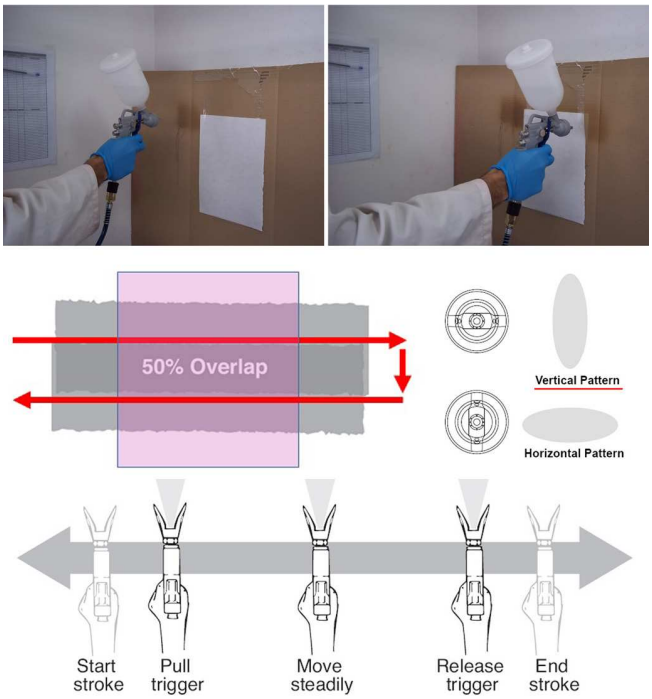



**Figure 1**. Scheme of the spraying technique.

Coated samples were dried based on the Standard UNE EN 20187: 1994 "Paper, board and pulps. Standard atmosphere for conditioning and testing and procedure for monitoring the atmosphere and conditioning of samples". All the developed samples were dried by using a climatic chamber VOTSCH (VC 2020) 56601054 supplied by CALSERVICE HERATEC S.L. and they were maintained at 23ºC, 50 % RH for 24 h following standard method recommendations [8].

## 2.3 Characterization methods

### Thickness (µm) and weight (g $m^{-2}$) measurements

The thickness (µm) of dry paper and cardboard samples was measured using a digital micrometer up to 7.5 mm based on the Standard ISO 534:2012. The set is also composed by a steel support for a block slides rectified, inner face section of 2 $cm^2$ and a drive lever that allows movement of the upper contact probe. The contact pressure is 1 Kg/cm2.

The weight (g $m^{-2}$) measurements of dry paper and cardboard samples was determined based on the Standard ISO 536:2013. Samples of 10x10 $cm^2$ surface were cut and conditioned at 23 ºC and 50% RH before the test weight by using an electronic balance SCALTEC SBC 41 (METROTEC).

### Mechanical properties measurements

Tensile test were carried out by using a TESTOMETRIC universal machine model M350-20kN CT (350-9109) (Figure 2). Samples of known thickness were cut to have a length of 180 mm and a width of 15 mm. The test speed was set at 20 mm/min and tensile tests were carried out based on the Standard method UNE EN ISO 1924-2:2009 to determine the Young's Modulus (GPa) and Elongation at Break (mm).

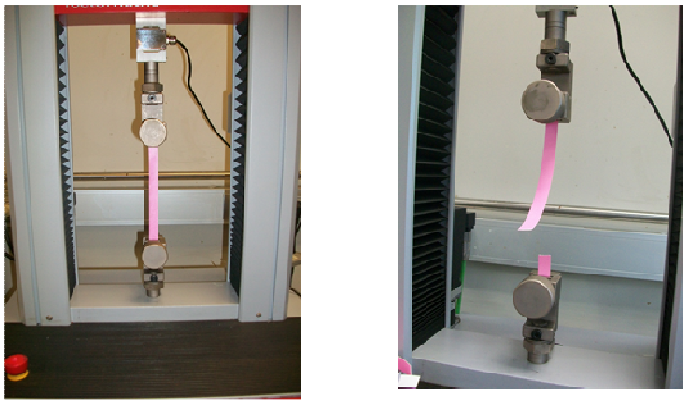


**Figure 2.** Tensile tests carried out using TESTOMETRIC universal machine model M350-20kN CT (350-9109)

**Grease Resistance measurements**

The grease resistance of the coated paper and paperboard samples were assessed using the method described in the TAPPI standard T559cm-129. The method describes a procedure for testing the grease repellency of coated paper and paperboard samples by using solutions with different composition of castor oil, toluene and n-heptane.

The method consists on selecting an intermediate kit number test solution and release a drop onto the surface of the coated sample and start the timer. After 15 s, the excess of solution is quickly removed with a cotton and immediately the test area is examined. A failure is determined by a darkening of the test specimen, even in a small area.

**Scanning electron microscopy (SEM) measurements**

The morphology of both the surface and cross-sectional views of coated paper and paperboard samples was studied by a field emission scanning electron microscope (4100 Scanning Electron Micrograph, Hitachi High-Technologies Corp., Tokyo, Japan).

## 3 Results and Discussion

**Thickness (µm) and weight (g $m^{-2}$) measurements of coated paper and cardboard samples.**

In order to obtain a coated paper and paperboard samples with good grease barrier properties, coatings of 50 µm were applied to paper and paperboard. As it can be seen in Table 1, the higher coating thickness values were obtained for paperboard (ranging between 44.5 and 51.7 µm). On the other hand, the lower values were obtained in samples of Kraft paper (values of coating thickness ranging from 5.3 to 9.4 µm). These differences could be explained in terms of coating absorption. These data reveals that brown paper (Kraft) samples absorbed a higher amount of solution being thinner the superficial coating compared to control samples. In terms of weight of coating, there is no significant differences among the three different substrates which indicates that the application of the coating is a homogeneous process.

**Table 1:** Thickness (µm) and weight (g $m^{-2}$) results for paper and paperboard coated with Starch/Seaweed extracts solution.

| Substrate | Coating | Thickness (UNE EN ISO 534:12) (µm) 20 measurements | Weight (UNE EN ISO 536:13) (g $m^{-2}$) 20 measurements | Coating (µm) | Coating (g $m^{-2}$) |
|---|---|---|---|---|---|
| White paper | Control | 63.5 ± 1.8 | 42.6 ± 0.5 | | |
| White paper | Starch/Seaweed | 74.9 ± 2.7 | 57.5 ± 2.4 | 11.4 | 14.9 |
| Brown paper (Kraft) | Control | 41.1 ± 3.7 | 34.8 ± 0.3 | | |
| Brown paper (Kraft) | Starch/Seaweed | 50.5 ± 1.0 | 45.7 ± 3.3 | 9.4 | 10.9 |
| Paperboard | Control | 384.6 ± 1.9 | 236.0 ± 1.3 | | |
| Paperboard | Starch/Seaweed | 430.3 ± 11.7 | 252.8± 2.0 | 50.1 | 16.8 |

**Grease resistance measurements of coated paper and cardboard samples.**

The values of grease resistance of the developed coatings (Figure 3) were compared with the ones obtained for white paper coated with polyethylene (Figure 4). The obtained results are presented in Tables 3 and 4.

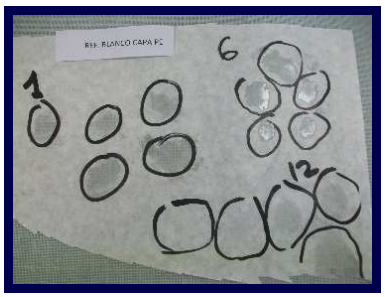



**Figure 3.** Grease resistance measurements of white paper coated with polyethylene

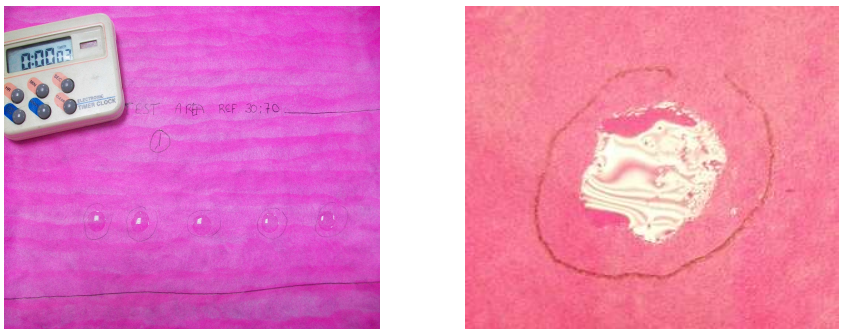


**Figure 4.** Grease resistance measurements of samples coated with Starch/Seaweed extracts

**Table 3:** Grease resistance results for paper and paperboard coated at laboratory scale with Starch/Seaweed extracts.

| | | Kit test solution | | | | | | | | | | | |
|---|---|---|---|---|---|---|---|---|---|---|---|---|---|
| **Substrate** | **Coating** | **1** | **2** | **3** | **4** | **5** | **6** | **7** | **8** | **9** | **10** | **11** | **12** |
| White paper | Control | | | | | | | | | | | | |
| White paper | Polyethylene (PE) | | | | | | | | | | | | |
| White paper | Starch/Seaweed | | | | | | | | | | | | |
| Brown paper (Kraft) | Control | | | | | | | | | | | | |
| Brown paper (Kraft) | Starch/Seaweed | | | | | | | | | | | | |
| Paperboard | Control | | | | | | | | | | | | |
| Paperboard | Starch/Seaweed | | | | | | | | | | | | |

Fail Pass

**Mechanical properties of coated paper and cardboard samples**

Ten different samples of each reference were tested and the averages and standard deviation are shown in Table 4. As expected, the application of the Starch/Seaweed extracts coatings to paper and paperboard samples caused a reduction in the Young's Modulus in comparison with control substrates.

**Table 4:** Young's Modulus (GPa) and Elongation at Break (mm) results for paper and paperboard coated with Starch/Seaweed extracts.

| Substrate | Coating | Young Modulus (GPa) | Elongation at break (mm) |
|---|---|---|---|
| **TRANSVERSAL** | | | |
| White paper | Control | 1.692 ± 0.114 | 5.017 ± 0.546 |
| White paper | Starch/Seaweed | 0.575 ± 0.092 | 13.930 ± 1.437 |
| Brown paper (Kraft) | Control | 3.670 ± 0.244 | 5.538 ± 0.631 |
| Brown paper (Kraft) | Starch/Seaweed | 2.146 ± 0.145 | 9.684 ± 1.304 |
| Paperboard | Control | 1.426 ± 0.034 | 9.918 ± 0.604 |
| Paperboard | Starch/Seaweed | 1.123 ± 0.025 | 12.509 ± 0.742 |
| **LONGITUDINAL** | | | |
| White paper | Control | 4.040 ± 0.39 | 2.560 ± 0.266 |
| White paper | Starch/Seaweed | 1.421 ± 0.191 | 5.213 ± 0.445 |
| Brown paper (Kraft) | Control | 9.886 ± 0.191 | 3.356 ± 0.271 |
| Brown paper (Kraft) | Starch/Seaweed | 5.269 ± 0.741 | 5.156 ± 0.154 |
| Paperboard | Control | 3.326 ± 0.120 | 4.125 ± 0.204 |
| Paperboard | Starch/Seaweed | 2.492 ± 0.065 | 5.314 ± 0.330 |

The values shown in Table 4 indicate a plasticizer effect of the coating that is justified by an increase of the elongation at break values improving the elasticity of the material.

**Scanning Electron Microscopy (SEM) analysis.**

The surface and cross section of the coated paper and paperboard samples were evaluated with a scanning electron microscope in order to study the homogeneity of the coated samples. The SEM micrographs are shown in the Figures 5-6:

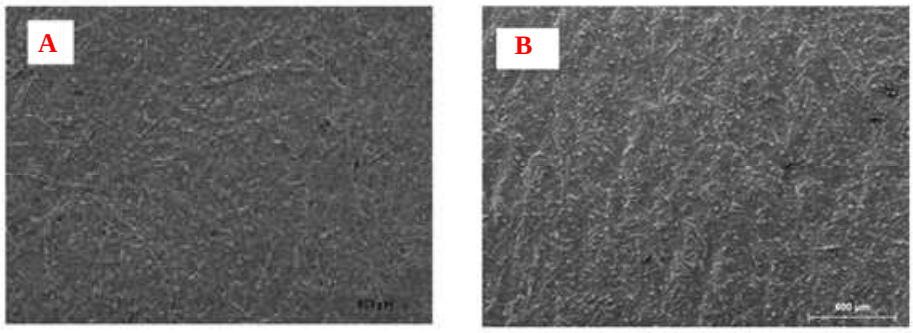



**Figure 5:** SEM micrographs of the surface views of white paper and paperboard coated with Starch: Seaweed Extracts.

The SEM images indicated that the porous fibrous structure of the paper is partially filled with the coating. In the case of white paper and paperboard coated with the Starch:Seaweed extract solution, a very smooth surface was obtained as it can be observed in the SEM images (Figure 5, A-B).

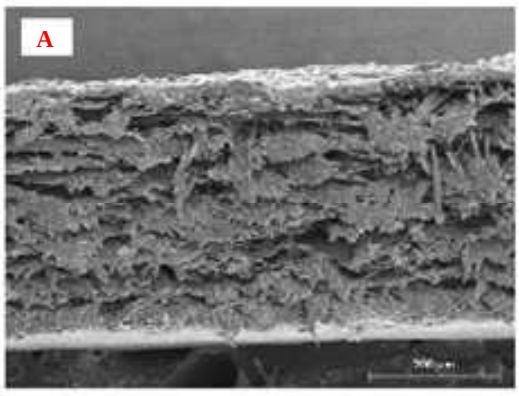



**Figure 6:** SEM micrographs of the cross-sectional view of paperboard coated with Starch: Seaweed Extracts

It is interesting to note that the borderline between coating layer and paperboard shown in the view of Starch:Seaweed extract (Figure 6) is not very clear because of the hydrophilic nature of the coating that is more compatible to the hydrophilic fibers to infiltrate more into the paperboard fiber layers.

## 3 Conclusions

Paper and paperboard samples coated with Starch/Seaweed Extract solutions showed a good grease resistance that is suitable for fatty foods like hamburgers, cheese and jam. In terms of mechanical properties, all the coated samples presented lower values of Young´s modulus (E) indicating a plasticizer effect of the coating that is justified by an increase of the elongation at break values improving the elasticity of the material. In terms of SEM analysis, a homogeneous coatings have been achieved.

## Acknowledgements

Authors would like to thank the PLANTPACK consortium and the finantial support by the European Comission for the Project PLANTPACK (311803) FP7-SME-2012.

## References

1. K. Khwaldia, E. Arab-Tehrany, S. Desobry, 2010, "Biopolymer coatings on paper packaging materials", *Comprehensive Reviews in Food Science and Food Safety*, vol 9, pp. 82-91.

2. J.W. Rhim. 2011, **"**Effect of clay contents on mechanical and water vapour barrier properties of agar-based nanocomposite films". *Carbohydrate Polymers 86*: *691*-699.

3. Bandyopadthay A, Romarao BV, Ramaswamy S. 2002. "Transient moisture diffusion through paperboard materials". *Colloids and Surface A, vol* 206, pp. 455–67.

4. Wihodo, M., Moraru, C.I. 2013, "Physical and chemical methods used to enhance the structure and mechanical properties of protein films: A review". *Journal of Food Engineering*, vol 114 (3), pp. 292-302.

5. Hong SI, Han JH, Krochta JM, 2004, "Optical and surface properties of whey protein isolate coatings on plastic films as influenced by substrate, protein concentration, and plasticizer type". *Journal Applied Polymer Science*, vol 92, pp.335–43.

6. Rabinovitch EB, 2003. "Effect of extrusion melt temperature on properties of flexible PVC". *Journal of Vinyl and Additive Technology*, vol 9, pp.61–4.

7. Trezza TA; Vergano PJ, 2006, "Grease resistance of corn zein coated paper". *Journal of Food Science*, vol 59 (4), pp. 912-915.

8. Standard UNE EN 20187: 1994 "Paper, board and pulps. Standard atmosphere for conditioning and testing and procedure for monitoring the atmosphere and conditioning of samples

9. TAPPI T559cm-12, 2012.Grease resistance test for paper and paperboard.

# PACKAGING MATERIALS

# Evaluation of Static and Dynamic Cushioning Properties of Polyethylene Foam for Determining Its Cushion Curves[#]

**Guang Li[1], Vincent Rouillard[2*] and Michael Sek[2]**

[1] *Tianjin University of Science and Technology, China*
[2] *College of Engineering and Science, Victoria University, Australia*

[*]*Corresponding author. Email: vincent.rouillard@vu.edu.au*

**Abstract:** A comparison of static and dynamic cushioning properties is discussed in this paper. A variable dynamic stress and dynamic factor functions are defined and obtained from the analysis on the experimental data from compression and cushion tests. Then the total instantaneous stress during impacts can be approximated by the static compression data multiplied by the dynamic factor function. This research can assist in determining the accuracy of cushion curves from the dynamic factor function of special cushioning material and compression test data. This new procedure will greatly simplify the experimental process for determining cushion curves.

Keywords: cushion curve; dynamic effect; compression; impact; polyethylene foam.

[#] This is the abstract of a peer-reviewed paper to appear in a Special Edition of Wiley's journal *Packaging Technology and Science* dedicated to the 19th IAPRI World Conference on Packaging 2014 hosted by Victoria University, Melbourne, Australia.

# Outdoor Weathering of HDPE Containers filled with Nitric Acid

**Anja Geburtig[1], Thomas Goedecke[1], and Volker Wachtendorf[1]**

[1] *BAM Federal Institute for Materials Research and Testing, Berlin, Germany*

[*] *Corresponding author. Email: anja.geburtig@bam.de*

**Abstract:** Jerrycans made from three different types of high-density polyethylene (HDPE) were exposed outdoors, for one Berlin summer season. They were filled with a 55 percent nitric acid solution ($HNO_3$), pure water, or air, and half of them were protected from sunlight by an UV absorbing canvas. Thus, the separate effects of UV radiation and nitric acid could be compared to the combined impact. Combined impact was mainly affected by decomposition of nitric acid, resulting in presence of reactive nitrogen oxides, increased oxygen partial pressure, and UV radiation energy, simultaneously in vapour phase.

To investigate the degradation effects after the outdoor exposure, jerrycans were exposed to a so called hydraulic internal pressure test, similar to an approval test for dangerous goods packaging. After combined impact of UV radiation and nitric acid, internal pressure tests showed very fast failures, whereas after separate impacts no remarkable deteriorations were observed, compared to unaged jerrycans.

Thus, the combined exposure was found to be much harder than the sum of the separate UV and nitric acid exposures, revealing synergistic effects.

Due to sensitivity of uncoloured HDPE to combined impact of UV radiation and nitric acid, nitric acid should not be transported and stored in uncoloured HDPE containers.

Keywords: high-density polyethylene HDPE, nitric acid $HNO_3$, outdoor exposure, UV radiation, weathering

## 1 Introduction

Nitric acid is one of the most important raw materials in chemical industry. Thus, safe transport and storage of this dangerous liquid is a basic task in economy and society.

In small amounts, storage often takes place in brown glass bottles. For larger amounts, special steel or plastic containers are used. For economic reasons, HDPE containers are long established, enabling space-saving shapes. However, to guarantee safety and functionality, HDPE's ageing behavior has to be understood and to be made the user familiar with. Relevant precautions have to be taken.

Generally, uncoloured HDPE containers are allowed for transport and storage of dangerous liquids such as nitric acid ($HNO_3$). According to dangerous goods regulations (e.g. [1]), containers must pass specified tests, reflecting mechanical as well as chemical exposures [1, 6.1.5]. These requirements for approval of packages include (among others) passing drop tests at low temperatures, stacking test, leakproofness test as well as hydraulic internal pressure test.

Additionally, the material shall be adequately resistant to ageing and to degradation caused by the substance contained or, where relevant, by UV radiation [1].

As it is not trivial to evaluate this adequacy, critical scenario of outdoor storage of $HNO_3$ filled jerrycans was tested. Due to safety and health protection, container quantity was limited.

Aim of this work was to compare these often separately investigated impacts of UV radiation and nitric acid with their combined impact, at outdoor storage conditions.

## 2 Materials and Methods

### 2.1 Materials

Three different HDPE types were investigated, in the form of 22 litre jerrycans.

Nitric acid ($HNO_3$) was used, in 55 % concentration.

## 2.2 Outdoor exposure

Jerrycans had been exposed outdoors, for one Berlin summer season. They were filled with nitric acid, water or air, with two different filling levels. Half of them were protected from sunlight, by an UV absorbing canvas.

For safety reasons, the exposure area was barred. $HNO_3$ filled containers were arranged on drip pans.

Due to the potential health and safety risk, no duplicates were exposed.



**Figure 1**: Outdoor exposed jerrycans

Yellow and orange colour revealed $HNO_3$ decomposition.

For the filling and emptying, full-body protection was worn, see Figure 2.




**Figure 2**: Due to nitric acids potential health and safety risk, full-body protection was worn.

## 2.3 Hydraulic internal pressure test

The only approval test from [1] that enables ageing stage evaluation from only one component is a hydraulic internal pressure test. Slightly changed to test requirements for packaging [1, 6.1.5.5], this test was carried out for the differently exposed jerrycans.

The water filled jerrycan was fixed on an electronic balance. By further, controlled water inflow, excess pressure was set to constantly 2,15 ±0,02 bar, until leakage occurred [2]. Time dependent mass and pressure was recorded.

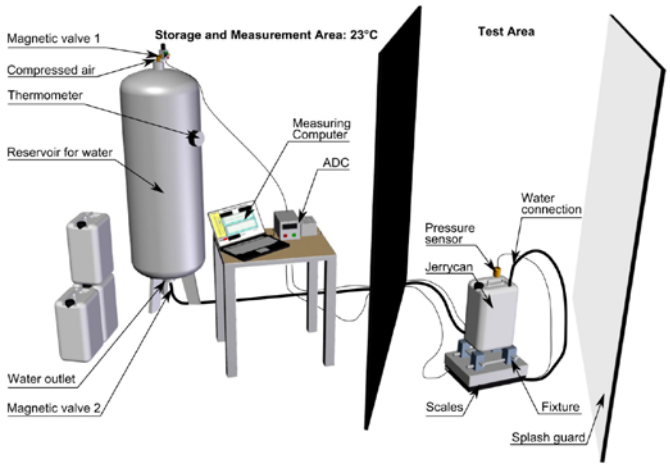



**Figure 3**: Setup of adapted hydraulic internal pressure test [2]

# 3 Results and discussion

For the unaged jerrycans, pressure set point had been hold for about one to two hours, till failure occurred, see black curves in Figure 4 and Figure 5. In temporal mass increase, inflexion points are detectable, indicating plastic flow before failure. This plastic flow was located at the vertical edges, as can be seen in Figure 6.

To evaluate reproducibility, results from two unaged jerrycans are shown. The small jumps in the pressure records at about 0,4 bar are related to the setup, but not to the materials.

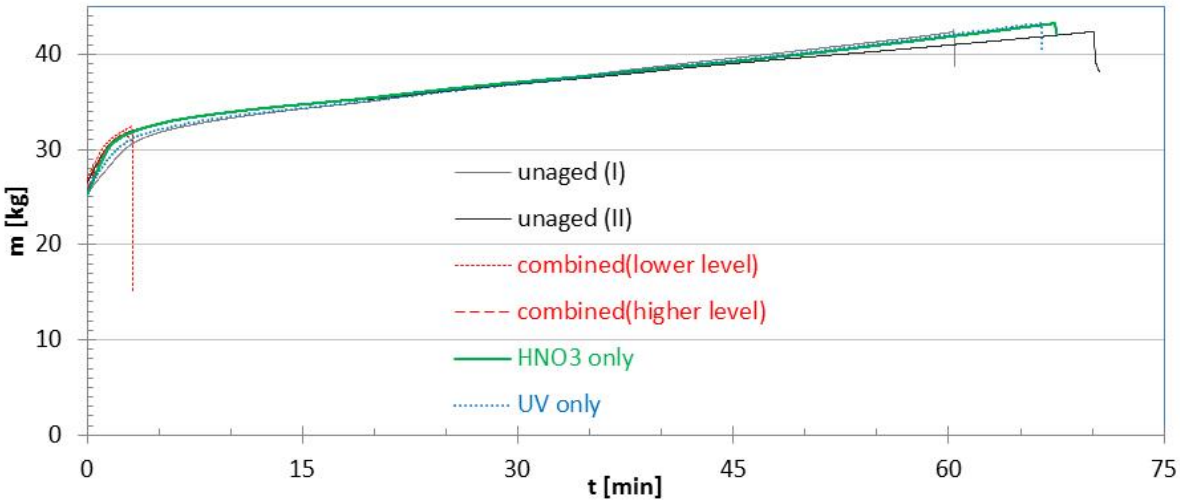



**Figure 4**: Mass increase in hydraulic internal pressure test after different exposures, for one material

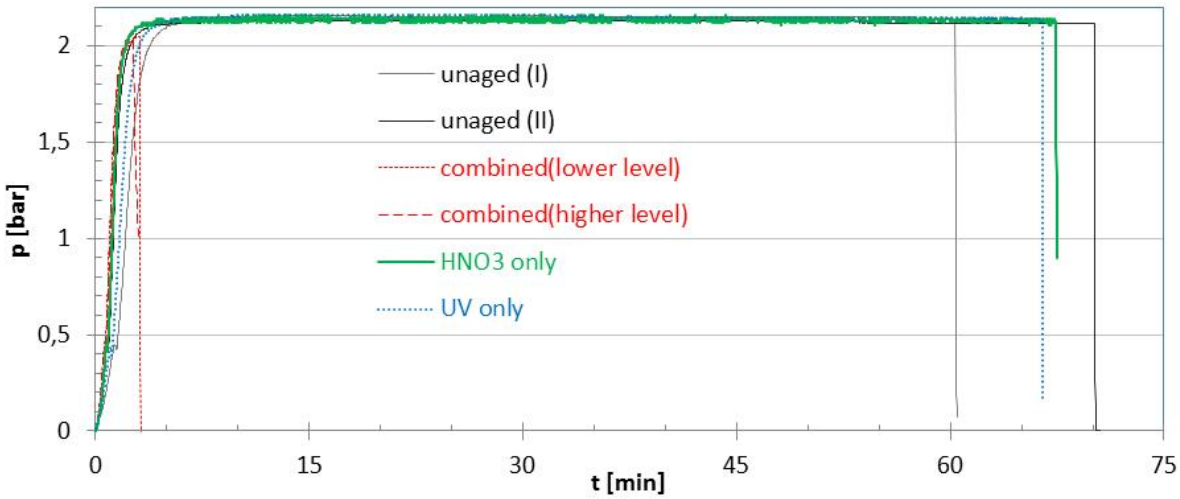



**Figure 5**: Pressure increase in hydraulic internal pressure test after different exposures, for one material



**Figure 6**: Unaged jerrycan after hydraulic internal pressure test

For comparison, mass and pressure records after different exposures are shown in the same Figures, for the same material. Red dashed lines show results after combined exposures, with the two different $HNO_3$ filling levels. Green continuous line shows behaviour after pure nitric acid exposure. Blue dotted line characterizes exposure by UV radiation only.

After separate UV or nitric acid exposure, no relevant deterioration could be found, compared to the unaged state. Both duration at pressure set point and water uptake were similar to the unaged jerrycan. Also plastic flow was detectable, again in the vertical edges.

For combined exposure, hydraulic internal pressure test results base on two jerrycans per material with varied $HNO_3$ filling degree at outdoor exposure. However, influence of filling degree was not detectable, in contrast to the strong deterioration, compared to the unaged or separately $HNO_3$ or UV exposed jerrycans.

None of the jerrycans exposed to both UV radiation and nitric acid could achieve the chosen pressure set point value. Samples failed after about five minutes without reaching 2,15 bar excess pressure. No plastic flow occurred before brittle cracking. Additionally, surface cracks occurred, along regions of higher draw ratio, see Figure 7.



**Figure 7**: Surface cracking after hydraulic internal pressure test and combined exposure

Whereas hydraulic internal pressure test showed no relevant changes after separate UV or nitric acid exposures compared to the unaged state, after combined exposure strong deterioration was detected, revealing synergistic exposure effects.

## 4 Conclusions

Combined UV-$HNO_3$ exposure was compared to both separate exposures, for three different uncoloured HDPE types. Therefore, jerrycans filled with nitric acid, water, or air were exposed outdoors, for one Berlin summer season.

Behaviour in hydraulic internal pressure test extremely worsened, after combined exposure, whereas separate UV or nitric acid exposures did not change the behaviour, compared to unaged state.

Due to sensitivity of uncoloured HDPE to combined UV-$HNO_3$ impact, nitric acid should not be transported and stored in uncoloured HDPE.

## Acknowledgements

We like to thank to our BAM colleagues Mr. Drousch, Mr. Jahnke, Ms. Heinrich, Mr. Nieruch, and Ms. Teutschbein for their proactive support.

## References

1. UNECE: ADR. European Agreement concerning the International Carriage of Dangerous Goods by Road 2011
2. A. Menrad, T. Goedecke, K.-P. Gründer, M. H. Wagner, 2013, “The Internal Pressure Test in Experiment and Simulation—Influence of the Wall Thickness Variation and the Change of the Packaging Behavior after the Impact of Standard Liquids”. *Packaging Technology and Science*, vol. 26, pp. 311-326.

# The Effect of A Vibration Force Field on The Crystallization and Barrier Properties of Polymer Nanocomposites

**Yuejun Liu*, Xiumei Pan, Yiwu Liu**

*Key Laboratory of New Materials and Technology for packaging,*
*Hunan University of Technology, Zhuzhou 412007, China*

** Corresponding authors. Email: yjliu_2005@126.com*

**ABSTRACT:** High-density polyethylene (HDPE)/nano-$SiO_2$ and polypropylene (PP)/nano-$SiO_2$ films have been prepared by two different processing conditions; i.e., under traditional steady state (TSS) and with a vibration force filed (VFF). In this paper, we mainly studied the crystallization and barrier properties of films manufactured under different processing conditions. The results showed that the barrier, crystallization and mechanical properties of the nanocomposites processed under the VFF condition were superior to those processed under the TSS condition. Differential scanning calorimetry (DSC) and scanning electron microscopy (SEM) were used to characterize the crystalline structure and morphology of the films which provided evidence for the explaining the distinct barrier and mechanical properties under the two processing conditions. DSC and SEM results clearly showed that an increase in the degree of crystallinity and orientation of the lamella were found in the nanocomposites prepared under the VFF condition.

Keywords: vibration force field; crystallization; barrier properties; lamella; orientation

## 1 INTRODUCTION

It is well known that well-dispersed nanoparticles and good interfacial interactions between particles and polymers are crucial factors for the preparation of polymer/nano-fillers composites. Some researchers prepared well-exfoliated polymer/layered silicate nanocomposites (PLNs) with improved barrier properties due to the nucleation effect of the clay layers and the growth of crystalline lamellae in a polymer matrix [1-3]; Others have modified polymers in order to improve their microstructure and orientation [4]. Still others have developed barrier technologies, such as blending [5], multilayer compound [6], and surface treatment [7], to improve the barrier properties of the polymer materials. However, these methods either require high-end equipment or the process were difficult to control.

It is clear, however, that the barrier properties of polymer are closely related to crystallization and orientation of the fillers. As reported that melt vibration can be used to control morphology and enhance various of properties of polymers [8]. Deng and Shen prepared HDPE/clay nanocomposite with a high degree of crystallinity and thicker crystal planes, which contribute to the improvement of mechanical properties [9].

In this study, we focused on studying the effect of vibration field on the crystallization and the barrier properties of HDPE/nano-$SiO_2$ and PP/nano-$SiO_2$ composites. Both the traditional steady state (TSS) processing condition

and a vibration force filed (VFF) processing condition were researched. Mechanical properties, barrier properties, crystalline structure and morphology were investigated and compared for the two processing methods.

# 2 EXPERIMENTS

## 2.1 Materials

The high density polyethylene (HDPE) used in this study was supplied by LanZhou Petrochemical Corp. (China). Polypropylene (PP) was produced by DuShanzi Petrochemical Corp. (China). The nanosilicon dioxide (nano-$SiO_2$) particles, with diameter 20-50nm, were purchased from Zhejiang Hongsheng Inc. The industrial grade coupling agents (KH550, KH560) were obtained from DeBang Chemical Materials Corp. of HuBei.

## 2.2 Characterizations

*Fourier Transform Infrared Spectroscopy (FTIR)*

The surface composition of the modified nano-$SiO_2$ was analyzed by FTIR from Thermo Nicolet Corp.

*Scanning Electron Microscopy (SEM)*

SEM images were taken to reveal the crystal morphology of the nanocomposites. Samples were etched by permanganic etching technique developed by Olley and coworkers [10] before the surface was subsequently coated with gold and observed under the QUANTA 200 SEM instrument (FEI Company).

*Differential scanning calorimetry (DSC)*

Calorimetric measurements were conducted on DSC-Q20 machine (TA Instruments). Film sample of 3 to 5 mg were heated from room temperature to 180 ℃ at the rate of 10 ℃/min under a nitrogen atmosphere and kept at this temperature for 5 min. to erase any prior thermal history. The first heating was followed by a subsequent cooling form 180 ℃ to 30 ℃, at which temperature the sample was kept isothermally for 5 min. Finally, the sample was heating again from 30 ℃ to 180 ℃ for the second heating run.

*Tensile property tests*

Following the GB13022-1991 standard, a tensile machine (model XLW (L)) was employed for tensile testing at room temperature and at the extension speed of 100 mm/min.

*Barrier properties tests*

The permeability of nanocomposites was measured based on GB1037-88 (moisture permeation) and GB1038-2000 (oxygen permeation). The moisture permeability machine (model TSY-T3) and oxygen permeability machine (model BTY-B1) were used to complete these tests.

# 3 RESULTS AND DISCUSSION

## 3.1 Surface Modification of Nano-SiO2 and FTIR Analysis

In order to ensure a good dispersion of nano-$SiO_2$ particles in HDPE and PP, two different coupling agents (KH550 and KH560) were used to modify the nano-$SiO_2$. The details are described as follows. First, a moderate amount of KH550 was added into a solution of absolute ethyl alcohol and deionied water. This mixture underwent supersonic treatment for 20min. Next the nano- $SiO_2$ particles were dried in a vacuum oven at 120℃

for 12h before being placed onto a dry round-bottom flask, into which the solution prepared in Step1 was decanted slowly. The reaction was carried out under 80℃ for 3 h. Third, nano-$SiO_2$ particles were collected through filtering and then washed several times by ethyl alcohol until the PH reached 7. Besides, the same steps for nano-$SiO_2$ particles modified by KH560.

IR spectrums of unmodified nano-$SiO_2$ particles, as well as particles modified by KH550 and KH560 are shown in **Figure 1** with all the characteristic peaks labeled. Unmodified nano-$SiO_2$ (cure (a)) display characteristic peaks of at 1100 $cm^{-1}$ (Si—O—Si anti-symmetry stretch), 799 $cm^{-1}$ (Si—O symmetry stretch) and 1637 $cm^{-1}$ and 3438 $cm^{-1}$, which are associated with the vibration of hydroxide as previously reports by other researchers[11]. In contrast to the FTIR spectrum of curve a, The absorption peak at 1556 $cm^{-1}$ on curve (b) is assigned to N—H and the absorption peak at 1323 $cm^{-1}$ on cure (c) is associate with KH560. Therefore these characteristic peaks indicated the modification of nano-$SiO_2$ were successful.

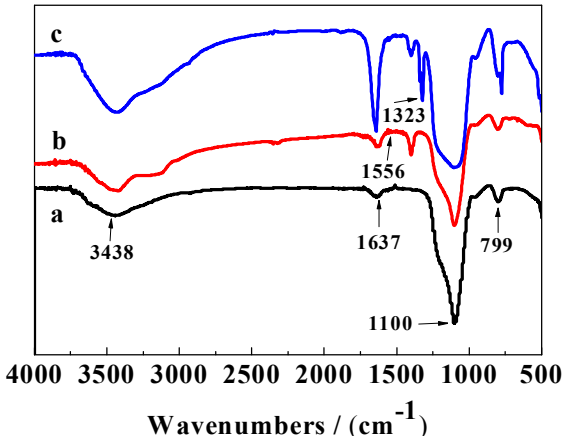



**Figure 1:** Infrared spectra of nano-$SiO_2$ particles.
(a) unmodified, (b) modified by KH550 and (c) modified by KH560

### 3.2 Preparation of Films

HDPE, PP and modified nano-$SiO_2$ were first dried at 80℃ for 12 h in a baking oven. Then, the materials were melt-mixed in a CTE-35 twin-screw extruder (Nanjing Coperion Corp.). Nanocomposites with different nano-$SiO_2$ contents (0 to 5 wt %) were prepared. Finally, films were produced by a single screw extruder with a vibration system (**Figure 2**). The vibration frequency and vibration amplitude were set at 20HZ and 25%, respectively. The extrusion was carried out at 195℃ and 40 rpm. For comparison, the same procedure and process parameters were also employed in preparing common nanocomposites (i.e., without using the vibration system).

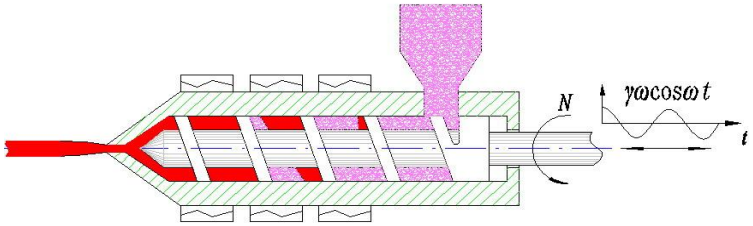



**Figure 2:** Sketch of a single-screw extruder with a vibration system.

### 3.3 SEM Analysis

SEM images were shown in **Figure 3**, with images (a) and (c) for films made under the TSS condition, and images (b) and (d) for films made under the VFF condition. It is obvious that with the application of the vibration force field, the lamella structure was formed and orientated not only along the melt flow direction but also other directions as showed in **Figure 3** (b) and (d). The formation and orientation of the lamellas under the VFF condition changed the material's microstructure and enhance the crystallization of the nanocomposites, leading to improvements in various aspects of performances of the nanocomposites.

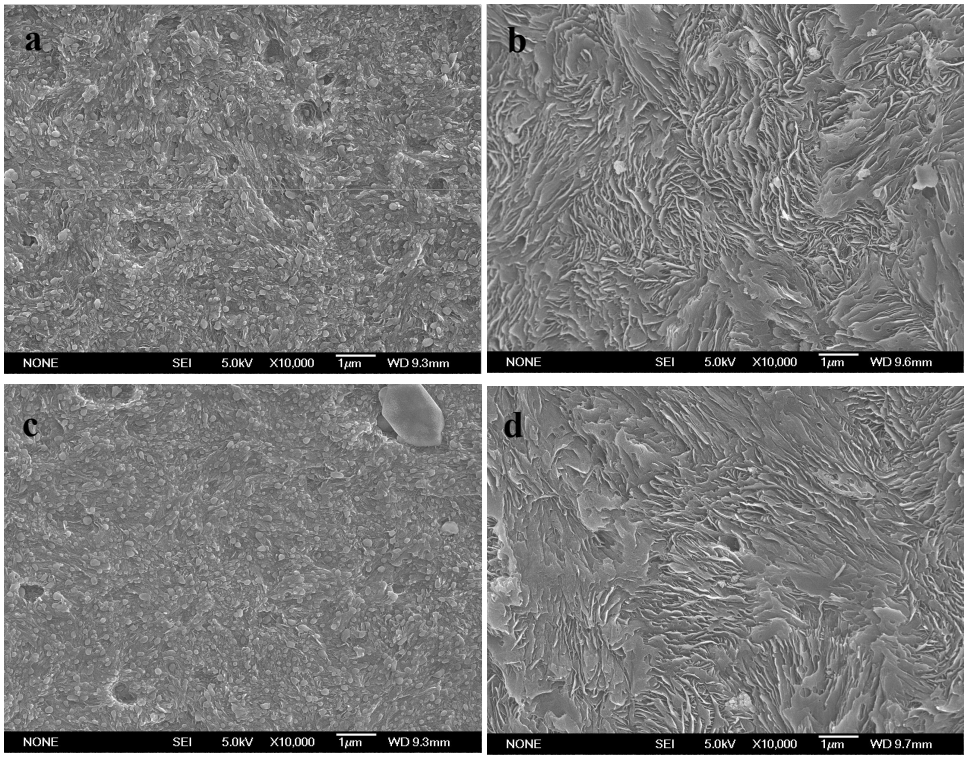



**Figure 3:** SEM images of the nanocomposites.
(a) TSS, HDPE/$SiO_2$, (b) VFF, HDPE/$SiO_2$, (c) TSS, PP/$SiO_2$, (d) VFF, PP/$SiO_2$

### 3.4 DSC Analysis

DSC was used to characterize the crystallization behavior of HDPE/nano-$SiO_2$ and PP/nano-$SiO_2$ composites with two different processing technologies (TSS and VFF). **Figure 4 and 5** are the DSC curves of HDPE/nano-$SiO_2$ and PP/nano-$SiO_2$ composites, respectively, with the DSC data tabulated in **Tables 1 and 2**, respectively. In the tables, *Tc* is crystallization temperature of the nanocomposites, $\triangle T$ is the degree of subcooling, which can characterize the crystallization rate of a material (i.e., the smaller of the value of the $\triangle T$, the closer the crystallization temperature is to the melting temperature and the faster the crystallite rate), $T_{d1/2}$ is the width at half height of the crystallite peak, which indicate the size distribution of the micro crystals (i.e., the smaller the $T_{d1/2}$, the narrower the crystallite peek and more homogeneity the microcrystal size distribution), *Hc* is the crystallization enthalpy, and *C* is the degree of crystallinity.

From **Figure 4 and 5**, it can be seen that the onset and peak points of crystallization of the two nano-composites shift to higher temperature under VFF condition compared to those under the TSS condition. Furthermore, as for the data in the tables, the $\triangle T$ and $T_{d1/2}$ of the nanocomposites processed under the VFF condition clearly

decreased as compared to those under the TSS condition at the same nano-$SiO_2$ content , which means the improvement of the nanocomposites' crystallization rate and homogeneity of the microcrystallite size distribution. Furthermore, the degree of crystallinity of the nanocomposites increased under the VFF condition. These results suggest that the vibration force field is helpful for the macromolecule chains elongation and orientation, which is of great benefit to crystallization, and consequently, improves the structure of the nanocomposites. In addition, the nano-$SiO_2$ particles dispersed better under the VFF condition and the heterogeneous nucleation effects of the nano-$SiO_2$ particles were more profound in the nanocomposites. Therefore, the formation of microcrystal is easier and faster, and the microcrystal size contribution is narrower and more homogeneous. Thus, it can be concluded that the vibration force field is beneficial to molecule chain orientation and improve nanocomposite structure.

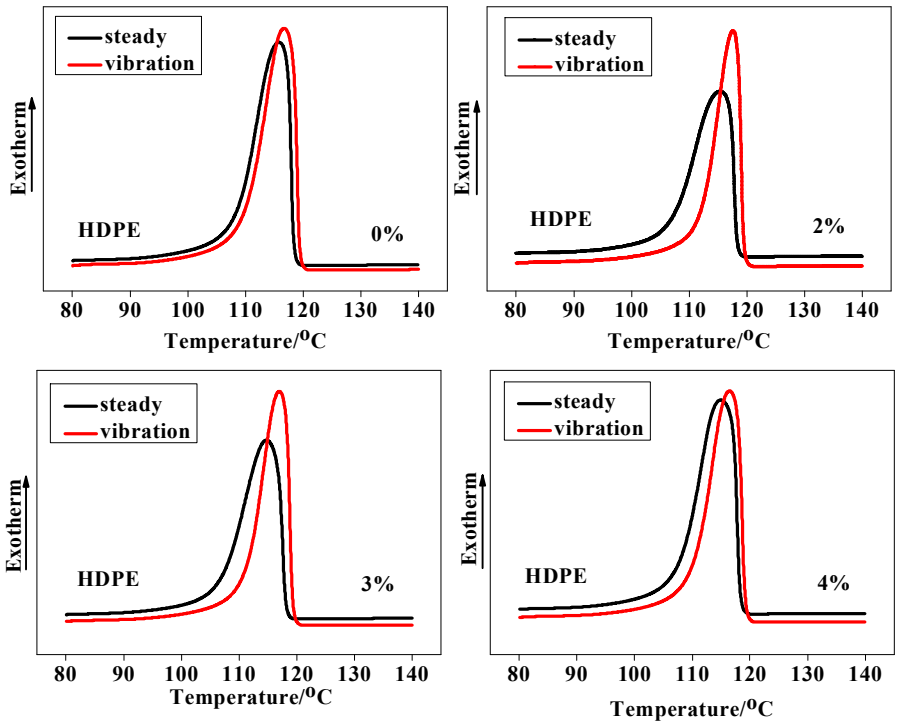



**Figure 4:** DSC curves of HDPE and HDPE/nano-$SiO_2$ (0, 2, 3, 4 wt% $SiO_2$) composites under TSS and VFF.

**Table 1:** DSC data of HDPE and HDPE/nano-$SiO_2$ (0, 2, 3, 4 wt% $SiO_2$) composites under TSS (S) and VFF (V)

| *Wt% $SiO_2$* | | *Tm/℃* | *Tc/℃* | *△T/℃* | *$T_{d1/2}$/℃* | *Hc/$Jg^{-1}$* | *C/%* |
|---|---|---|---|---|---|---|---|
| 0% | S | 122.70 | 118.32 | 4.38 | 6.87 | 182.9 | 62.3 |
| | V | 124.08 | 120.34 | 4.04 | 6.52 | 183.8 | 62.6 |
| 2% | S | 124.73 | 120.81 | 3.92 | 7.79 | 180.5 | 62.7 |
| | V | 126.34 | 122.68 | 3.66 | 4.85 | 182.4 | 63.4 |
| 3% | S | 124.99 | 121.07 | 3.92 | 7.59 | 174.8 | 61.4 |
| | V | 126.05 | 122.47 | 3.58 | 5.46 | 181.3 | 63.7 |
| 4% | S | 124.51 | 121.53 | 2.98 | 7.39 | 182.9 | 64.9 |
| | V | 125.42 | 122.57 | 2.85 | 6.19 | 183.7 | 65.2 |

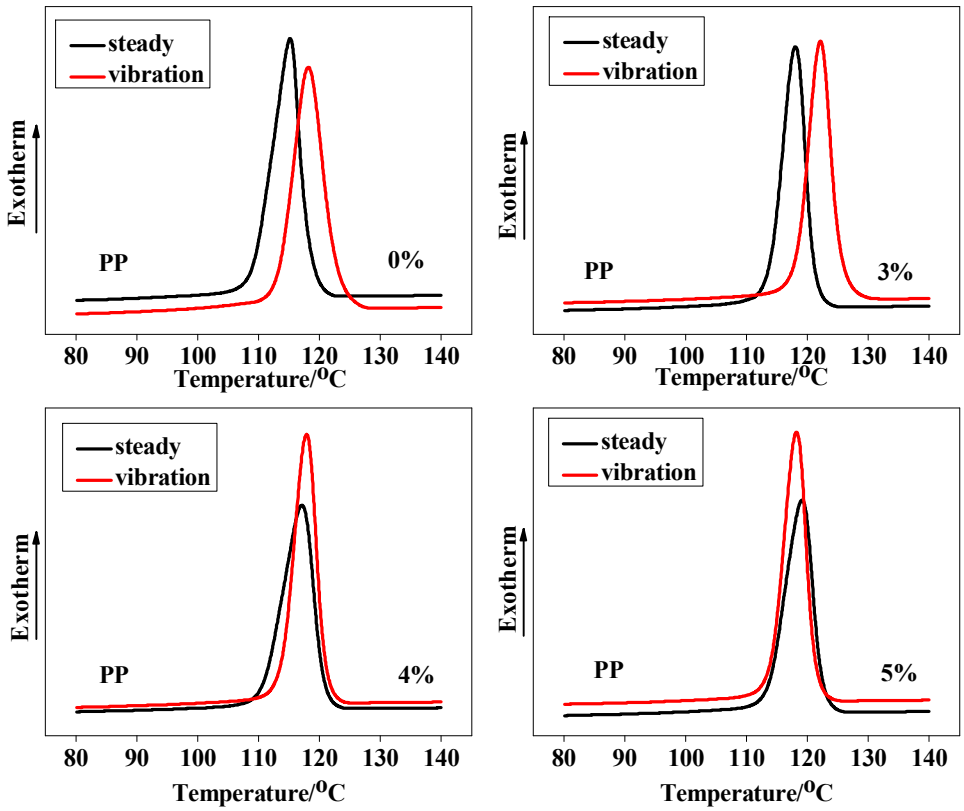



**Figure 5:** DSC curves of PP and PP/nano-$SiO_2$ (0, 3, 4, 5wt% $SiO_2$) composites under TSS and VFF.

**Table 2:** DSC data of PP and PP/nano-$SiO_2$ (0, 3, 4, 5wt% $SiO_2$) composites under TSS (S) and VFF (V)

| *Wt% $SiO_2$* | | *Tm/℃* | *Tc/℃* | *△T/℃* | *$T_{d1/2}$/℃* | *Hc/$Jg^{-1}$* | *C/%* |
|---|---|---|---|---|---|---|---|
| 0% | S | 152.86 | 118.75 | 34.11 | 5.15 | 91.04 | 44 |
| | V | 154.94 | 121.90 | 33.04 | 5.09 | 92.54 | 46.4 |
| 3% | S | 154.19 | 121.09 | 33.10 | 4.30 | 93.99 | 46.8 |
| | V | 157.01 | 125.94 | 31.07 | 3.95 | 95.97 | 47.8 |
| 4% | S | 153.75 | 120.64 | 33.11 | 5.72 | 92.55 | 46.6 |
| | V | 156.94 | 124.77 | 32.17 | 4.19 | 93.32 | 46.9 |
| 5% | S | 157.41 | 122.37 | 35.04 | 5.15 | 88 | 44.7 |
| | V | 157.12 | 124.84 | 32.28 | 4.21 | 94 | 47.8 |

### 3.5 Barrier Properties Analysis

**Figure 6 and 7** show the barrier properties curves containing the oxygen permeability coefficient and the moisture permeability coefficient with different contents of nano-$SiO_2$ of HDPE/ nano-$SiO_2$ and PP/nano-$SiO_2$ composites processed by two different methods. From **Figure 6**, it can be seen that both the oxygen permeability coefficient and the moisture permeability coefficient of HDPE/nano-$SiO_2$ composite processed under VFF are lower than those under the TSS condition. Meanwhile the two coefficients decrease with increasing nano-$SiO_2$ at low nano-$SiO_2$ content (1 %~2 %) and then increase in a higher nano-$SiO_2$ content (3 %~5 %). Compared with pure HDPE, the increment of oxygen barrier properties and moisture barrier properties of HDPE/nano-$SiO_2$

composite were 34.1 % and 42.4 %, respectively, under the vibration force field condition, versus 21.03 % and 29.4 % under the TSS condition with an optimum content of nano-$SiO_2$ (2%). The results might be attributed to following reasons. Due to the vibration force field, which contributed to the orientation of the macromolecule chains and formation of obvious lamellar structures, the microstructures of nanocomposites was improved and the barrier properties were enhanced comparing with nanocomposites under the TSS condition. Furthermore, the nano-$SiO_2$ particles dispersed better under the vibration field and induced heterogeneous nucleation, which made HDPE more apt to crystallize and the crystal grains to become smaller and more homogeneous, thus refining the structure of the nanocomposites and improving the barrier properties. Unfortunately, excess nano-$SiO_2$ particles were difficult to disperse and led to aggregation in the polymer matrix, which then cause defects in the HDPE. That's why the barrier properties of HDPE/nano-$SiO_2$ decreased when the content of nano-$SiO_2$ exceeded 2%.

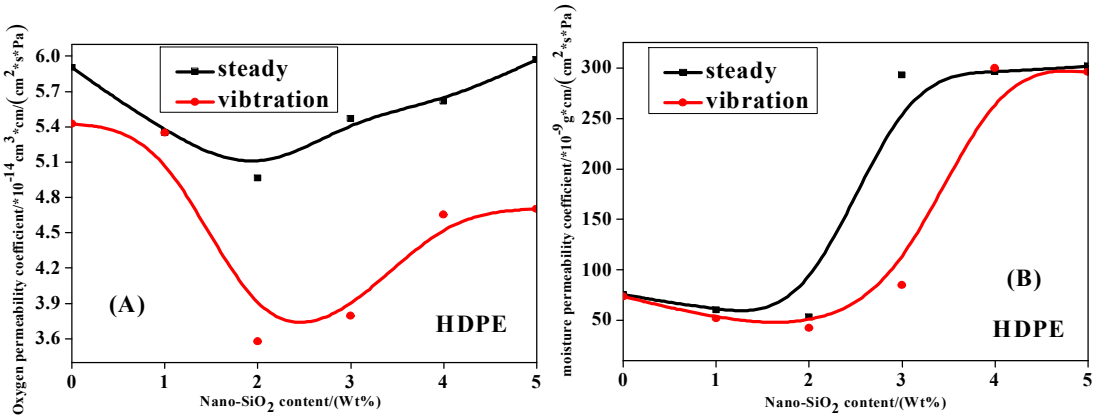



**Figure 6:** Effects of nano-$SiO_2$ content on the oxygen permeability coefficient and moisture permeability coefficient of HDPE/nano-$SiO_2$ composites under the TSS and VFF condition.

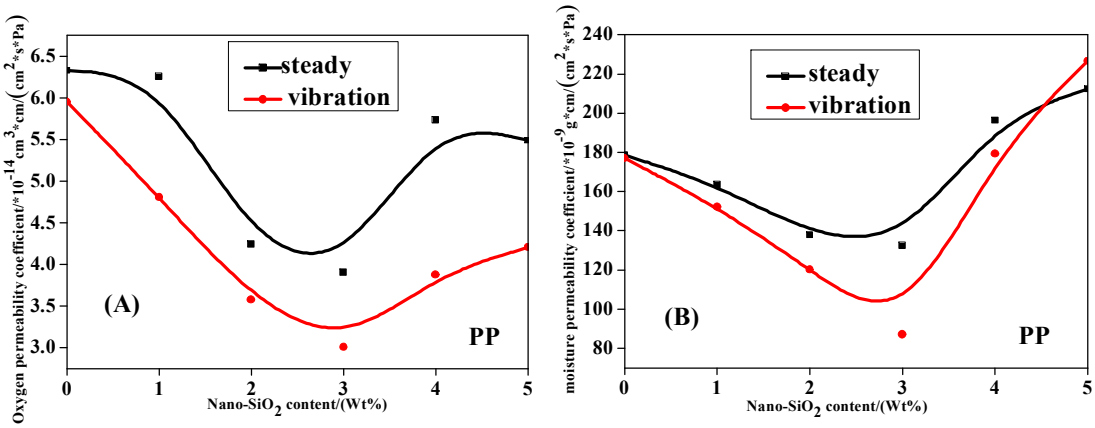



**Figure 7:** Effects of nano-$SiO_2$ content on the oxygen permeability coefficient and moisture permeability coefficient of PP/nano-$SiO_2$ composites under the TSS and VFF condition.

As for the PP/nano-$SiO_2$ composites shown in **Figure 7**, the barrier properties of PP/nano-$SiO_2$ composites under VFF were better than under TSS. In addition, the barrier properties improve initially, and then decreased with any further increase of nano-$SiO_2$ content. The oxygen and moisture barrier properties of PP/nano-$SiO_2$

increased by 49.5% and 50.8%, respectively, with an optimal content of nano-$SiO_2$ (3%) under VFF, and by 38.4% and 25.9% under TSS. The reason for this phenomenon can be ascribed to the formation and orientation of the lamellar structures associated with VFF condition, as shown in the SEM pictures above. Likewise, the enhanced heterogeneous nucleation effects of the nano-$SiO_2$ particles in the nanocomposites when processing under VFF condition showed the same trend as the HDPE/nano-$SiO_2$ composites.

### 3.6 Mechanical Properties of Nano-composites

**Figure 8** presents the tensile test cures for the two kinds of films (HDPE/nano-$SiO_2$, PP/nano-$SiO_2$) processing under TSS and VFF conditions. It can be seen that as the content of modified nano-$SiO_2$ increases, the tensile strength increase in the low content range from 1 % to 3 %. Meanwhile, the tensile strength exhibited a decreasing trend in the high content range form 4 % to 5 %. This indicates that the nano-$SiO_2$ particles modified by KH550 and KH560 were well-dispersed in HDPE and PP matrices, thereby improving the interfaces and interactions between the nanofiller and the polymer matrix. Consequently, the mechanic property of the two nano-composites have been raised about 24.8 % (HDPE/nano-$SiO_2$) and 6.4 % (PP/nano-$SiO_2$) compared with neat HDPE and PP without any nano-$SiO_2$under TSS condition. In addition, it should be pointed out that nano-$SiO_2$ particles played a role in the physical entanglement and increased the crosslinking density of the nanocomposites. Thus, the tensile strength increased. However, the tensile strength of nanocomposites decreased with a higher content (4% to 5%) of nano-$SiO_2$. This was due to the formation of nano-$SiO_2$ agglomerates at a high nano-$SiO_2$ content. Worse, these aggregate particles became surface defects and stress concentration points for the nanocomposites. Therefore, the mechanical property of the composites decreased with a higher content of nano-$SiO_2$.

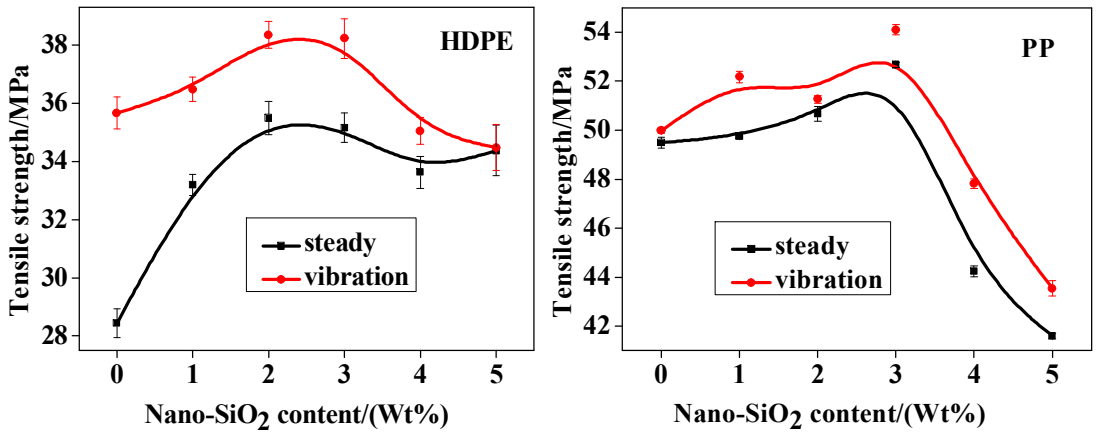



**Figure 8:** Effects of nano-$SiO_2$ content on the mechanical properties of HDPE/nano-$SiO_2$. (a) and PP/nano-$SiO_2$ ; (b) composites processing under TSS and VFF condition

Moreover, as the curves showed in **Figure 8**, compared with nanocomposites processing under the TSS condition, the tensile strength of the nanocomposites processing under the VFF condition were higher. The tensile strength of HDPE/nano-$SiO_2$ and PP/nano-$SiO_2$ composites were increased by 34.8% and 9.3% with an optimal content of nano-$SiO_2$ (3%) under VFF condition compared with neat HPDE and PP under TSS condition, respectively. This indicates that vibration was favorable to the orientation of the macromolecular chains such that

the crystalline grains became finer, thereby, improving the microstructure of the nanocomposites. Furthermore, nano-$SiO_2$ particles could be dispersed effectively under the vibration condition, thereby making full use of the reinforcing effects to improve the properties of the nanocomposites. From the above discussions, a conclusion can be drawn that, in order to obtain better mechanic properties of HDPE/nano-$SiO_2$ and PP/ nano-$SiO_2$ composites, the best choice would be adding the proper amount of nano-$SiO_2$ particles (about 2 % to 3 %) and processing them under the VFF condition.

### 3.7 Barrier Mechanism Analysis

As SEM images (**Figure 3**) shows the lamella structure are formed and orientated in the nanocomposites processed under the VFF condition. That's because different nano-$SiO_2$ particles obtained different instantaneous impulse in the vibration shear field and that can changed the nano-$SiO_2$ particles' motor direction continually, then formed motor speed difference and collisions between the particles. Finally, the nano-$SiO_2$ agglomerates broke and the size of the nano-$SiO_2$ particles were smaller meanwhile the distribution was more uniform in the polymers. Furthermore, the melt polymer chain with similar conformation much easier to march orderly in one direction in the sinusoidal periodic vibration force field, and with more and more polymer chain arranged in the crystal lattice of the crystal nucleus, the lamellas were formed gradually and orientation in a way. It is just because of the lamellas existence, the permeation molecule must steer clear of the lamellas for their transmission in the nanocomposites. So this structure can extend the path of permeation molecule through material effectively, therefore the barrier properties of the composites were improved. The barrier mechanical model shows in **Figure 9**.

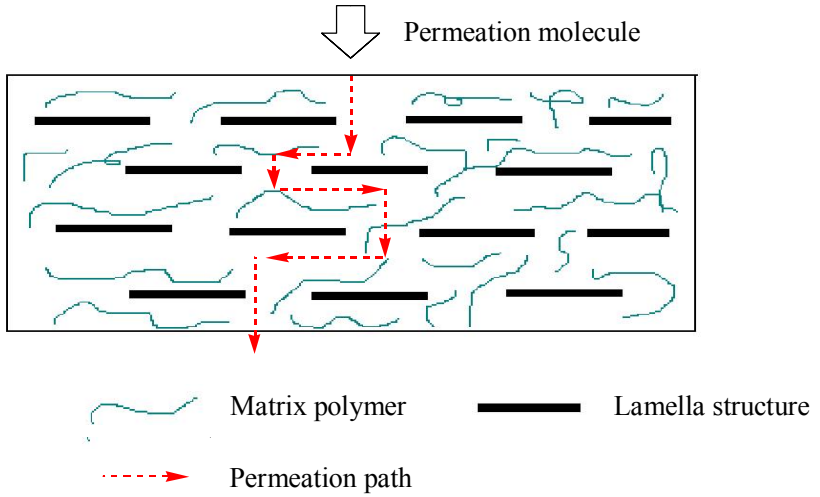



**Figure 9:** Diffusion model of molecules through polymer/$SiO_2$ composites processed under VFF.

## 4 CONCLUSIONS

This paper compares the effects of two processing methods (traditional steady state (TSS) and vibration force field (VFF)) on the crystallization and barrier properties of the HDPE/nano-$SiO_2$ and PP/nano-$SiO_2$ composites. It is shown that the mechanical and barrier properties, as well as the microstructure, were very different. According to the results and analysis above, the conclusions of this research can be summarized as follows.

(1) With a vibration force field, lamella structure were formed and orientated not only along the melt flow direction but also in other directions in the nanocomposites, which was confirmed by the SEM images.

(2) As the DSC curves indicated, the degree of crystallinity of the nanocomposites was enhanced due to the heterogeneous nucleation effects of the nano-$SiO_2$ particles, especially under the vibration force field (VFF) condition.

(3) The barrier properties of the composites under the VFF condition were superior to those under the TSS condition due to the formation of different microstructures under the different processing conditions.

(4) The improvement of barrier properties of the nanocomposites is based on the theory of the transmission path extension.

## ACKNOWLEDGEMENTS

The present study was supported by the National Natural Science Foundation of China (No. 11372108), the New Century Excellent Talent of the Ministry of Education of China (No. NCET-10-0161), the Natural Science Foundation of Hunan Province (No. 14JJ5021) and the University Innovation Platform Development Fund of Hunan Province (No. 13K098).

## REFERENCES

1. Reddy Chaganti Srinivasa, Ratna Debdatta, and Das Chapal Kumar, 2008, “Polyethylene nanocomposites by gas-phase polymerization of ethylene in the presence of a nanosilica-supported zirconocene catalyst system”, *Polymer International*, Vol. 57, No. 2, pp. 282-291.
2. Qizheng Dou, Xiaomin Zhu, Karin Peter, Dan E. Demco, Martin. Möller, and Claudiu Melian, 2008, “Preparation of polypropylene/silica composites by in-situ sol-gel processing using hyperbranched polyethoxysiloxxance”, *Sol-Gel Science Technology*, Vol. 48, pp. 51-60.
3. Qi Zhou, Erik Malm, Helena Nilsson, and Per Tomas Larsson, 2009, “Nanostructured biocomposites based on bacterial cellulosic nanofibers compartmentalized by a soft hydroxyethylcellulose matrix coating”, *Soft Matter*, No. 5, pp. 4124-4130.
4. Seo Jongchul, Jeon Jongho, Gun Shul Yong, and Han Haksoo, 2000, “Water sorption and activation energy in polyimide thin films”, *Journal of Polymer Science Part B: Polymer Physics*, Vol. 38, No. 21, pp. 2714-2720.
5. Dukjoon Kim, and Seong Woo Kim, 2003, “Barrier property and morphology of polypropylene/polyamide blend film”, *Korean Journal of Chemical Engineering*, Vol. 20, No. 4, pp. 776-782.
6. R. Leaversuch, 2003, “Barrier PET bottles: No breakthrough in beer, but juice and soda surge ahead”, *Plastics Technology*, Vol. 49, No. 3, pp. 48-60.
7. Kjellgren Henrik, Gällstedt Mikael, and Engström Gunnar, 2006, “Barrier and surface properties of chitosan-coated greaseproof paper”, *Carbohydrate Polymers*, Vol. 65, No. 4, pp. 453-460.
8. Gűrhan Kalay, and Michael J. Bevis, 1997, “Processing and physical relationships in injection-molded isotactic polypropylene. 2. morphology and crystallinity”, *Journal of Polymer Science Park B: Polymer*

*Physics*, Vol. 35, No. 2, pp. 265-291.

9. Cong Dend, Xueqin Gao, Zhanchun Chen, Shan Xue, and Kaizhi Shen, 2010, "Study of the effect of organic clay in the shear-induced crystallization of high-density polyethylene through dynamic-packing injection molding", *Polymer International*, Vol. 59, No. 12, pp. 1660-1664.
10. D.C. Bassett, and R.H. Olley, 1984, "On the lamellar morphology of isotactic polypropylene spherulites", *Polymer*, Vol. 25, pp. 935-943.
11. F. Schlottig, and M. Texor, 1999, "Template synthesis of $SiO_2$ nanostructures", *Mater Sci. Lett.*, Vol. 18, No. 8, pp. 599-601.

# The Effect of Heating Speed on the Expression of Heat Seal Strength in Plastics Packaging Materials[#]

**Kazuo Hishinuma**[*]

*Hishinuma Consulting Engineer Office, Japan*

[*]*Corresponding author. Email: rxp10620@nifty.com*

**Abstract:** Heat sealing is an indispensable technique for the use of plastic packaging materials. Heat seal bonding can be easily completed by heating and cooling. It has been believed for the past half century that "heat sealing strength" can be adjusted in two dimensions by adjusting "heating temperature".
Based on this “conventional wisdom, the author also believed that proper heating is indispensable to effective heat sealing for the past two decades. The “MTMS" method that measures the temperature on the bonding layer directly was developed. [1] Although development of accurate heat sealing was attempted, the lack of agreement for data on expression of heat sealing strength was not resolved.
The results of application of high precision temperature measurements to precise control of heating temperature has shown that "heating speed" greatly influences heat sealing strength. It was shown that this phenomenon is common to polyolefin materials.
A detailed analysis of the measurement method, details of the phenomenon and heating speed is presented in this paper. It has been shown by these analyses that heat sealing is a three dimensional phenomenon of melting surface temperature, heating time and heat sealing strength. And, the phenomenon was distinctly expressed within the range of regularly used speeds. It has been shown that the measurement of the melting surface temperature response including speed information will be indispensable in the evaluation of the heat seal phenomenon in the future. This phenomenon was named the “Hishinuma Effect".
The mechanistic analysis of the expression phenomenon has not been completed. However, it has been inferred that distribution of molecular weights in the material is involved from experimental data.
This discovery provides information that will contribute to improvement in the field of packaging machinery technology and material technology that depend on heat sealing technology.

Keywords: heat sealing; heat sealing strength; openability; closability; peel sealing; heating speed; mtms; cut; "hishinuma effect"; astm; minute sensor.

[#] This is the abstract of a peer-reviewed paper to appear in a Special Edition of Wiley's journal *Packaging Technology and Science* dedicated to the 19th IAPRI World Conference on Packaging 2014 hosted by Victoria University, Melbourne, Australia.

# Maximum Gauge Pressure in Dangerous Goods Packaging under Normal Conditions of Carriage - Comparison of Direct Measurement and Calculations[#]

**Eva Schlick-Hasper[1*], John Bethke[1], Wolfgang Jahnke[1], Björn Drousch[1], Thomas Goedecke[1] and Matthias Kraume[2]**

[1] *BAM Federal Institute for Materials Research and Testing, Germany*
[2] *Technical University Berlin, Germany*

[*]*Corresponding author. Email: eva.schlick-hasper@bam.de*

**Abstract:** The aim of this experimental work was the measuring of the maximum gauge pressure in the vapour phase above the liquid in different design types of dangerous goods packaging under normal conditions of carriage. The scenario of intercontinental transport of dangerous goods packaging in freight containers was assumed as normal conditions of carriage. The design types investigated were steel and plastics packaging with a volume of approximately 6 litres.
Dichloromethane was used as a filling substance because it belongs to the most important transported substances relating to their quantitative amount and has a relatively high vapour pressure.
The pressure inside the packaging filled with dichloromethane was directly measured using data loggers in the vapour phase. The test was performed under simulated conditions of carriage (degree of filling: 90 %; filling temperature: 15 °C; temperature during storage: 31 °C).
The maximum measured gauge pressures inside the packaging were between 89 mbar for a light plastic jerrican and 336 mbar for a steel drum. The calculated value for a rigid receptacle is 553.5 mbar for the same scenario.
The results show that the gauge pressures which can occur during normal conditions of carriage can be above the level for the leakproofness test of dangerous goods packaging prescribed by the international UN Model Regulations article 6.1.5.4 (200 mbar for packaging group II and III; 300 mbar for packaging group I). They are covered by the level prescribed for the internal pressure (hydraulic) test according to UN Model Regulations article 6.1.5.5.4 b) which requires a test pressure of 150 kPa (1500 mbar) for dichloromethane.

Keywords: dangerous goods packaging; gauge pressure; overpressure; dichloromethane; data loggers; normal conditions of carriage.

[#] This is the abstract of a peer-reviewed paper to appear in a Special Edition of Wiley's journal *Packaging Technology and Science* dedicated to the 19th IAPRI World Conference on Packaging 2014 hosted by Victoria University, Melbourne, Australia.

# Preparation and Characterization of Low Methoxyl Pectin/Carboxymethyl Cellulose-based MMT Composite Films

Zhi-Wei Wang,[1,2,4*] Wen-Xi Yu[1] and Chang-Ying Hu[3,4]

[1]*Department of Packaging Engineering, Jiangnan University, Wuxi 214122, China*

[2]*Packaging Engineering Institute, Jinan University, Zhuhai 519070, China*

[3]*Department of Food Science and Engineering, Jinan University, Guangzhou 510632, China*

[4]*Key Laboratory of Product Packaging and Logistics of Guangdong Higher Education Institutes, Jinan University, Zhuhai 519070, China*

[*]*Corresponding author. Email: wangzw@jnu.edu.cn*

**Abstract:** Recently, there is an increasing interest of using biodegradable, renewable and edible materials to prepare food packaging films. Pectin and Carboxymethyl Cellulose (CMC) have been used to prepare edible/biodegradable films and coating. However, their using is limited due to the poor mechanical properties of pectin and lower water barrier property of CMC. The aim of this study to improve the mechanical properties of pectin and water barrier property of CMC and by preparing the Low Methoxyl Pectin/CMC-based nano-montmorillonite (LMP/CMC-MMT) composite films with different proportion of LMP and CMC and different content MMT (0-8%). The mechanical properties (e.g. tensile strength (TS) and elongation at break (EAB)), color, transparency and water vapor permeability (WVP) of LMP/CMC- MMT composite films were investigated. The maximum of TS of the composite films was 252% of that of the pure LMP film due to the formation of hydrogen bonds proved by fourier transform infrared spectroscopy (FTIR). With the addition of CMC and nano-MMT to the pure LMP film, the EAB decreased slightly. The maximum reduction of WVP of the composite films was 333% of that of the pure CMC film because of the tortuosity effect of the nanoclay platelets. Fourier transform infrared spectroscopy (FTIR) and morphological characteristics of x-ray diffraction (XRD) and scanning electron microscopy (SEM) were also studied.

Keywords: food packaging, composite films, pectin, carbomethoxy cellulose, nano-montmorillonite.

## 1 Introduction

Biopolymer/biodegradable films and coatings have recently received an increasing amount of research attention, and potential sources of biopolymers have been reviewed [1]. Natural biopolymers have the advantage of being biodegradable, renewable and often edible. A large number of researchers have carried out to study properties of films made of a single hydrocolloid component: polysaccharide or protein. The most frequently utilized polysaccharides are cellulose and starch (and their derivatives), seaweed extracts (carrageenans and alginates), exudate gums (arabic, tragacanth and karaya), seed gums (locust bean and guar), pectin and chitosan [2]. The most commonly used proteins are soy isolated protein, zein, wheat protein isolated, casein and gelatin. Wherein, chitosan [3], cellulose [4, 5], zein [6] and protein [7, 8] also have been proposed to prepare antimicrobial films with antimicrobial agents.

Pectin and carboxymethyl cellulose, both belonging to the group of polyuronates, are two characteristic examples of natural ionic polysaccharides. Pectin is a complex anionic polysaccharide composed of β-1, 4-linked D-galacturonic acid residues, wherein carboxyl groups of uronic acid are either fully (HMP, high methoxyl pectin, DE > 50%) or partially (LMP, low methoxyl pectin, DE < 50%) methyl esterified [9]. Many food processors and pectin ingredient suppliers need to confirm pectin content to control the quality of their products [10]. In earlier research, pectin often was used as controlled release drug carriers [11, 12] and was prepared edible/biodegradable films and coating with sodium alginate [9, 13] and chitosan [14] to improve its mechanical proporties. Carbomethoxy cellulose (CMC), one of the most important derivatives of cellulose, is a typical anionic polysaccharide that has been widely used as a stabilizer in food. CMC is one of the natural water-soluble

cellulose derivatives with β-(1→4) glucopyranose residues that have no harmful effects on human health. Due to its non-toxicity, biocompatibility, biodegradability, hydrophilicity and good film-forming ability, CMC has been used in a high number of edible film formulations [15]. Furthermore, CMC contains a hydrophobic polysaccharide backbone and many hydrophilic carboxyl groups, and hence shows amphiphilic characteristics.

Amounts of montmorillonite clay were used as reinforcement in most of the published studies on polymer clay nanocomposites. Alves *et al* [16] prepared pectin/k-carrageenan-based nanoclays biodegradable composite films and found that water vapor permeability was decreased by the addition of nanoclays. Films barrier properties may be further improved by enhancing the particles dispersion and exfoliation degree. Nanoclay also can be used to improve the mechanical properties of films [17].

The objective of this study to improve the mechanical properties of LMP and water barrier property of LMP by preparing the LMP/CMC-MMT composite films with different content MMT (0-8%).
This template contains the styles and formatting required IAPRI 2014 papers. The paper must be A4, use single column format and have the following margins: top 3cm, left/right/bottom 2.5cm. All text, figures and tables are to be kept within the margins.

# 2 Materials and methods

## 2.1 Materials

LMP (Apple pectin) was obtained from Henan Yuzhong Biological Science and Technology Co., Ltd (Henan, China). CMC was obtained from Damao Chemical Reagent Factory (Tianjin, China). Ultrapure water was prepared using an EPED purification system (Nanjin, China). Glycerol and calcium chloride were supplied by Damao Chemical Reagent Factory (Tianjin, China). MMT (specific surface area 240 $m^2$) was obtained from Aladdin (Shanghai, China).

## 2.2 Film preparation

***LMP/CMC composite films***
The paper must be arranged in the following order: title, authors, affiliation, corresponding author, abstract,
Film forming solutions of biopolymer (2.0 g/150 ml) were prepared by dissolving CMC and LMP into 150 ml of distilled water at the proportions in Table 1. Powdered $CaCl_2$ was used at 2% as a crosslink and glycerol as a plasticizer at 25% (w/w of polysaccharides). Then solutions were mixed 30 min at room temperature, and then heated with mixing up to 70℃ and maintained 60 min. The solutions were degassed under a vacuum for 30 min and then cast on a series of glass plates (15×25 $cm^2$). Films were dried at 45℃ in Electric Heated Thermostatic Air Dry Oven (Fuma Instrument Co.Ltd, shanghai, China) for 12 h. Dried films were peeled-off and conditioned at 50 ±1% RH and 25 ±1℃ in temperature and humidity chamber (Chengcheng Instrument Co.Ltd, Guagnzhou, China) for 2 days prior to testing.
***LMP/CMC-based MMT nanocomposite films***
For the preparation of LMP/CMC-based MMT composite films, a pre-determined amount of MMT (1, 2, 4 and 8%, w/w of polysaccharides) was dispersed in the solvent by vigorous stirring for 12 h using a magnetic stirrer, followed by sonication for 30 min at room temperature using a High Intensity Ultrasonic Processor (Labuy-10LHT, Hangzhou, China). Then the MMT solutions were mixed with the previously prepared LMP/CMC solution for 30 min. After that time solutions were heated with mixing up to 70℃ and maintained 60 min. The solutions were degassed under a vacuum for 30 min and then cast on a series of glass plate (15×25 $cm^2$). Films were dried at 45℃for 12 h. Dried films were peeled-off and conditioned at 50 ±1% RH and 25 ±1℃ for 2 days prior to testing.

**Table 1:** The films based on LMP/CMC films composite films with different content MMT.

| Sample LCM0 | LMP/CMC (w/w) -MTT (0%) | Sample LCM1 | LMP/CMC (w/w) -MTT (1%) | Sample LCM2 | LMP/CMC (w/w) -MTT (2%) | Sample LCM4 | LMP/CMC (w/w) -MTT (4%) | Sample LCM8 | LMP/CMC (w/w) -MTT (8%) |
|---|---|---|---|---|---|---|---|---|---|
| LCM01 | 10:0 | LCM11 | 10:0 | LCM21 | 10:0 | LCM41 | 10:0 | LCM81 | 10:0 |
| LCM02 | 9:1 | LCM12 | 9:1 | LCM22 | 9:1 | LCM42 | 9:1 | LCM82 | 9:1 |
| LCM03 | 8:2 | LCM13 | 8:2 | LCM23 | 8:2 | LCM43 | 8:2 | LCM83 | 8:2 |
| LCM04 | 7:3 | LCM14 | 7:3 | LCM24 | 7:3 | LCM44 | 7:3 | LCM84 | 7:3 |
| LCM05 | 6:4 | LCM15 | 6:4 | LCM25 | 6:4 | LCM45 | 6:4 | LCM85 | 6:4 |
| LCM06 | 5:5 | LCM16 | 5:5 | LCM26 | 5:5 | LCM46 | 5:5 | LCM86 | 5:5 |
| LCM07 | 4:6 | LCM17 | 4:6 | LCM27 | 4:6 | LCM47 | 4:6 | LCM87 | 4:6 |
| LCM08 | 3:7 | LCM18 | 3:7 | LCM28 | 3:7 | LCM48 | 3:7 | LCM88 | 3:7 |
| LCM09 | 0:10 | LCM19 | 0:10 | LCM29 | 0:10 | LCM49 | 0:10 | LCM89 | 0:10 |

The “LCM0”, “LCM1”, “LCM2”, “LCM4” and “LCM8”represent LMP/CMC-MMT composite films with 0, 1, 2, 4 and 8% MMT, respectively.
The “10:0” to “0:1” represent the proportion of LMP and CMC.
The “LCM01” to “LCM 09” represent LMP/CMC films composite films with the proportion of LMP and CMC from “10:0” to “0:1” and 0% content MMT, respectively.
The “LCM11” to “LCM 19” represent LMP/CMC films composite films with the proportion of LMP and CMC from “10:0” to “0:1” and 1% content MMT, respectively.
The “LCM21” to “LCM 29” represent LMP/CMC films composite films with the proportion of LMP and CMC from “10:0” to “0:1” and 2% content MMT, respectively.
The “LCM41” to “LCM 49” represent LMP/CMC films composite films with the proportion of LMP and CMC from “10:0” to “0:1” and 4% content MMT, respectively.
The “LCM81” to “LCM 89” represent LMP/CMC films composite films with the proportion of LMP and CMC from “10:0” to “0:1” and 4% content MMT, respectively.

## 2.3 Film characteristics

***Film thickness***

Film thickness was measured by a DRK204A electric thickness meter (Deruike Instrument Co. Ltd, Jinan, China) with an accuracy of 0.0001 mm. The average thickness of three analysed samples was adopted as the thickness of the film, after at least eight random locations of each sample were measured.

***Color and transparency***

The color of films was measured using Pires method [18] with a portable sphere spectrophotometer (x-Rite SP64, America). The films were applied on the surface of a white standard plate ($L^*$ = 94.87, $a^*$ = -1.41, $b^*$ = -0.93) and the color of the films was expressed as $L^*$-value (lightness), $a^*$-value (greenness/redness), $b^*$-value (blueness/yellowness) and total difference of color ($\Delta E$), which was calculated as follows:

$$\Delta E = \sqrt{\left(\Delta L^*\right)^2 + \left(\Delta a^*\right)^2 + \left(\Delta b^*\right)^2}$$

where $\Delta L^*$, $\Delta a^*$, $\Delta b^*$ are the differentials between the color parameter of the samples and the white standard used as the film background.

The transparency value of the films was calculated by the equation as reported by Han and Floros [19]. Film samples were cut into rectangles (1.0×1.5 $cm^2$) and placed on the UV–9600 spectrophotometer (Rayleigh, China) cell. The relative transparency was measured by transmittance (%) at 600 nm.

Transparency value = $A_{600}$ /x

Where $A_{600}$ is the absorbance at 600 nm and x is film thickness (mm). According to this equation, higher transparency values indicate lower transparency of film.

Color tests were made at least in four different positions of four different films and transparency tests were made at least eight different films.

***Water vapor permeability (WVP)***

The water vapor transmission rate (WVTR) was measured using a Mocon Permatran-3/33 (MOCON Inc., USA) at 25℃ and 50% RH according to ASTM F 1249-90 [20] and other methods [21]. The specimens (two replicates of each sample) were tightly sandwiched between two steel plates, providing a 5 $cm^2$ exposure area. Permeability values are reported as WVP coefficient (×$10^{-12}$ g·$m^{-1}$ $s^{-1}$·$Pa^{-1}$).

$$WVTR = \frac{\Delta m}{t \times A}$$

$$WVP = \frac{WVTR \times L_p}{\Delta p}$$

$L_p$---film thickness(mm)； A--- films area (m)； t---time interval(d)； $\Delta m$---t water vapor permeance mass (g)； $\Delta p$---water vapor pressure difference of film two sides (Pa).

***X-ray diffraction (XRD) characterization***

X-ray diffraction patterns were obtained by XRD (Bruker AXS D8, Germany) at 40kV, 40 mA for Cu Kα radiation of wavelength 0.1542 nm in the 2θ range 5 - 40°at 2 °·$min^{-1}$ scan rate.

***Fourier transform infrared spectroscopy (FTIR)***

FTIR spectra of the dried samples were obtained using an Equinox 55 IR spectrometer (Bruker, Germany). Scanning was carried out in the range 400 - 4000 $cm^{-1}$.

***Scanning electron microscopy (SEM)***

Morphology of the films was examined by field-emission SEM ultra 55 (Zeiss, Germany) with an accelerating voltage of 3 kV. The samples were gently and randomly broken and fixed upon a cupper cylinder using a double-sided electric tape, and then the cylinder with films were coated with gold.

## 2.4 Statistical analyses

One–way analysis of variance (ANOVA) was used to determine statistically significant differences among averages using the SPSS 13.0. Differences with the probability value of <0.05 were considered significant and all the data were reported in the form of mean ± SD.

# 3 Results and discussion

*Color and transparency*

Color parameters of film samples with the different ratio of LMP and CMC and different MMT are shown in Table 2. As the proportion of CMC increased, lower $b^*$- and $\Delta E^*$- values were observed in LMP/CMC films with the concomitant higher $L^*$ -values ($p < 0.05$). Among all film samples, those incorporated with the MMT had the higher $b^*$- and $\Delta E^*$-values ($p < 0.05$) compared with LMP/CMC films without MTT. However, higher

MMT resulted in the opposite results for $L^*$ -values ($p < 0.05$). This result suggested that the color of MMT directly affected the color of resulting film. Based on transparency value (Table 2), films incorporated with higher MMT had the higher transparency value than the LMP/CMC films ($p < 0.05$). And as the levels of CMC increased, lower transparency was obtained in films ($p < 0.05$). The result indicated that the LCM/CMC –MMT films became less transparent as at higher MMT content was incorporated.

*Water vapour permeability*

Permeability depends on the solubility and diffusivity of the water in the polymeric matrix. According to the XRD and FTIR spectra, the greatest interaction between MMT and LMP, CMC, LMP/CMC hinders the path of water molecules through the film. Figure 1 shows the effect of ratio of LMP/CMC (10:0, 7:3, 5:5, 4:6 and 0:10) and different MMT (1, 2, 4, 8%) contents on the WVP of films. CMC showed higher WVP due to many hydrophilic carboxyl groups. When the ratio of CMC to the composite films was decreased, the WVP of LMP/CMC films decreased. Films incorporated with MMT (from 1 to 4%) showed lower WVP compared with LMP/CMC films, especially with increasing amount of MMT, the WVP of films were decreased in the same ratio LMP/CMC. This behaviour was associated with the tortuous path caused by nanoclay incorporation. Slavutsky [17] obtained similar results with MMT in brea gum /MMT films, and attributed the decrease in WVP to the strong interaction of MMT with brea gum and to the formation of a tortuous path. The same behaviour was reported by Mangiacapra *et al* [23] in films based on pectin and MMT. However, films incorporated with MMT (8%) showed the highest WVP. It may be the high content of the MTT aggregate in films. This result can be proved by the highest peak intensity in Figure 5 (d).

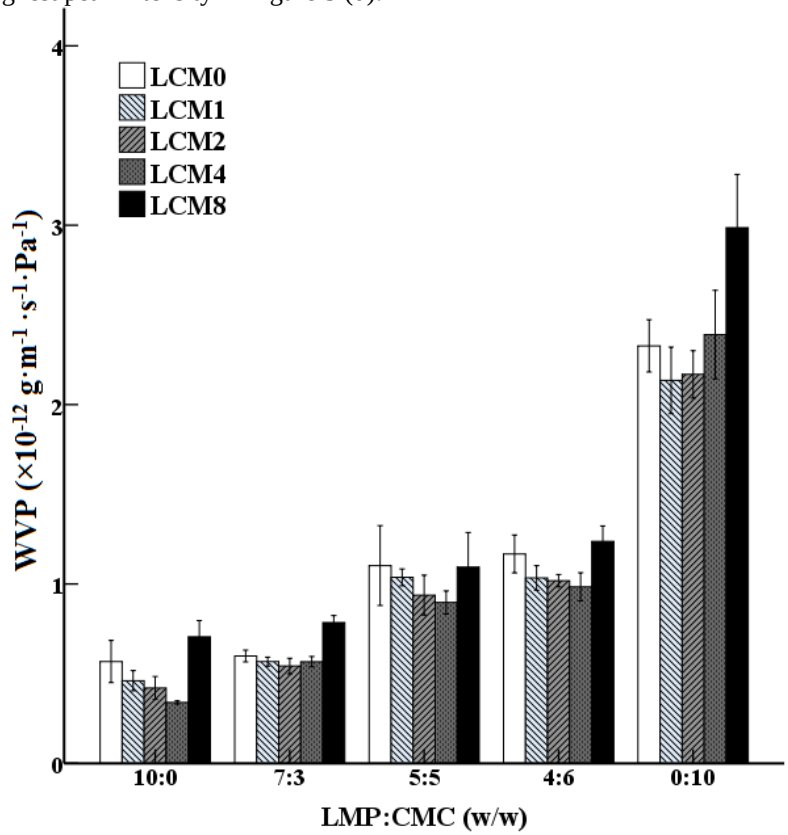



**Figure 1:** Water vapour permeability (WVP) of LMP/CMC films with different content MMT.

**Table 2:** Color and transparency of LMP/CMC composite films with different content MMT.

| Sample | *L** | *a** | *b** | ΔE* | Transparency |
|---|---|---|---|---|---|
| LCM01 | 91.48 ±0.11$^{i}$ | -1.32 ±0.02$^{n}$ | 3.84 ±0.09$^{n}$ | 5.85 ±0.13$^{n}$ | 2.98 ±0.17$^{stu}$ |
| LCM02 | 91.79 ±0.11$^{k}$ | -1.32 ±0.01$^{n}$ | 3.41 ±0.16$^{l}$ | 5.32 ±0.20$^{m}$ | 2.47 ±0.22$^{mno}$ |
| LCM03 | 92.41 ±0.13$^{o}$ | -1.18 ±0.67$^{o}$ | 2.39 ±0.16$^{i}$ | 4.19 ±0.28$^{j}$ | 2.11 ±0.17$^{ghij}$ |
| LCM04 | 92.74 ±0.11$^{pq}$ | -1.40 ±0.02$^{mn}$ | 2.33 ±0.14$^{i}$ | 3.89 ±0.17$^{i}$ | 2.07 ±0.12$^{fghi}$ |
| LCM05 | 92.90 ±0.11$^{r}$ | -1.42 ±0.01$^{jklmn}$ | 1.88 ±0.18$^{gh}$ | 3.43 ±021$^{h}$ | 1.93 ±0.18$^{f}$ |
| LCM06 | 93.04 ±0.29$^{st}$ | -1.42 ±0.01$^{klmn}$ | 1.67 ±0.15$^{f}$ | 3.18 ±0.27$^{g}$ | 1.69 ±0.16$^{e}$ |
| LCM07 | 93.38 ±0.06$^{v}$ | -1.43 ±0.01$^{ijklmn}$ | 1.43 ±0.83$^{e}$ | 2.63 ±0.11$^{e}$ | 1.46 ±0.07$^{d}$ |
| LCM08 | 93.70 ±0.04$^{w}$ | -1.41 ±0.01$^{lmn}$ | 0.71 ±0.04$^{d}$ | 2.01 ±0.06$^{d}$ | 1.29 ±0.12$^{c}$ |
| LCM09 | 94.64 ±0.07$^{z}$ | -1.38 ±0.01$^{n}$ | -0.55 ±0.02$^{a}$ | 0.45 ±0.04$^{a}$ | 0.95 ±0.07$^{a}$ |
| LCM11 | 90.47 ±0.11$^{d}$ | -1.94 ±0.02$^{a}$ | 7.65 ±0.23$^{w}$ | 9.65 ±0.30$^{x}$ | 2.78 ±0.07$^{st}$ |
| LCM12 | 91.63 ±0.14$^{j}$ | -1.61 ±0.03b$^{cdefg}$ | 4.46 ±0.20$^{p}$ | 6.29 ±0.24$^{pq}$ | 2.28 ±0.08$^{qr}$ |
| LCM13 | 91.82 ±0.08$^{k}$ | -1.60 ±0.04$^{cdefg}$ | 4.07 ±0.04$^{o}$ | 5.86 ±0.06$^{n}$ | 2.27 ±0.08$^{kl}$ |
| LCM14 | 92.23 ±0.14$^{mn}$ | -1.56 ±0.01$^{cdefg}$ | 3.43 ±0.18$^{l}$ | 5.10 ±0.23$^{l}$ | 2.40 ±0.19$^{lm}$ |
| LCM15 | 92.43 ±0.09$^{o}$ | -1.56 ±0.02$^{defg}$ | 2.96 ±0.24$^{k}$ | 4.65 ±0.28$^{k}$ | 2.01 ±0.06$^{fgh}$ |
| LCM16 | 92.95 ±0.11$^{rs}$ | -1.53 ±0.01$^{defghij}$ | 2.23 ±0.18$^{i}$ | 3.70 ±0.22$^{i}$ | 1.97 ±0.12$^{fg}$ |
| LCM17 | 93.09 ±0.04$^{tu}$ | -1.54 ±0.03$^{defghi}$ | 1.98 ±0.11$^{h}$ | 3.41 ±0.11$^{h}$ | 1.51 ±0.06$^{d}$ |
| LCM18 | 93.36 ±0.04$^{v}$ | -1.52 ±0.01$^{fghijkl}$ | 1.57 ±0.07$^{ef}$ | 2.92 ±0.08$^{f}$ | 1.48 ±0.06$^{d}$ |
| LCM19 | 94.41 ±0.04$^{y}$ | -1.40 ±0.01$^{mn}$ | -0.32 ±0.20$^{b}$ | 0.77 ±0.18$^{b}$ | 1.07 ±0.05$^{b}$ |
| LCM21 | 90.87 ±0.14$^{f}$ | -1.64 ±0.02$^{bcdefg}$ | 6.17 ±0.21$^{u}$ | 8.15 ±0.25$^{u}$ | 3.51 ±0.11$^{w}$ |
| LCM22 | 90.83 ±0.15$^{f}$ | -1.63 ±0.02$^{bcdefg}$ | 6.20 ±0.29$^{u}$ | 8.20 ±0.32$^{u}$ | 2.54 ±0.06$^{mnop}$ |
| LCM23 | 91.10 ±0.31$^{g}$ | -1.64 ±0.02$^{bcdef}$ | 5.35 ±0.52$^{s}$ | 7.32 ±0.61$^{s}$ | 2.52 ±0.04$^{mnop}$ |
| LCM24 | 91.48 ±0.16$^{i}$ | -1.56 ±0.02$^{defg}$ | 4.86 ±0.24$^{q}$ | 6.71 ±0.29$^{r}$ | 2.24 ±0.07$^{ijk}$ |
| LCM25 | 91.65 ±0.09$^{j}$ | -1.56 ±0.02$^{defg}$ | 4.36 ±0.12$^{p}$ | 6.19 ±0.14$^{op}$ | 2.07 ±0.07$^{fghii}$ |
| LCM26 | 92.29 ±0.08$^{n}$ | -1.60 ±0.04$^{bcdefg}$ | 3.78 ±0.20$^{n}$ | 5.38 ±0.20$^{m}$ | 1.89 ±0.08$^{f}$ |
| LCM27 | 92.76 ±0.28$^{pq}$ | -1.61 ±0.02$^{bcdefg}$ | 2.69 ±0.26$^{j}$ | 4.19 ±0.31$^{j}$ | 1.93 ±0.10$^{f}$ |
| LCM28 | 93.03 ±0.07$^{st}$ | -1.58 ±0.02$^{cdefg}$ | 2.15 ±0.15$^{h}$ | 3.50 ±0.37$^{h}$ | 1.44 ±0.06$^{d}$ |
| LCM29 | 94.30 ±0.07$^{x}$ | -1.40 ±0.01$^{mn}$ | -0.34 ±0.19$^{ab}$ | 0.78 ±0.07$^{b}$ | 1.28 ±0.12$^{c}$ |
| LCM41 | 90.14 ±0.09$^{b}$ | -1.65 ±0.03$^{bcde}$ | 8.00 ±0.18$^{x}$ | 10.11 ±0.20$^{y}$ | 3.40 ±0.22$^{vw}$ |
| LCM42 | 90.36 ±0.19$^{cd}$ | -1.51 ±0.02$^{ghijklm}$ | 7.00 ±0.27$^{v}$ | 9.12 ±0.32$^{w}$ | 3.27 ±0.16$^{v}$ |
| LCM43 | 90.91 ±0.09$^{f}$ | -1.44 ±0.01$^{hijklmn}$ | 5.13 ±0.13$^{r}$ | 7.23 ±0.16$^{s}$ | 2.58 ±0.05$^{nop}$ |
| LCM44 | 91.85 ±0.20$^{k}$ | -1.72 ±0.01$^{b}$ | 4.29 ±0.28$^{p}$ | 6.04 ±0.34$^{no}$ | 2.62 ±0.16$^{opq}$ |
| LCM45 | 92.14 ±0.07$^{m}$ | -1.69 ±0.01$^{bc}$ | 3.66 ±0.09$^{mn}$ | 5.35 ±0.11$^{m}$ | 2.62 ±0.10$^{jklopq}$ |
| LCM46 | 92.22 ±0.15$^{mn}$ | -1.66 ±0.01$^{bcd}$ | 3.41 ±0.22$^{l}$ | 5.09 ±0.26$^{l}$ | 2.26 ±0.05$^{jkl}$ |
| LCM47 | 92.84 ±0.09$^{qr}$ | -1.61 ±0.02$^{bcdefg}$ | 2.44 ±0.16$^{i}$ | 3.94 ±0.18$^{i}$ | 2.25 ±0.09$^{jk}$ |
| LCM48 | 93.19 ±0.06$^{u}$ | -1.55 ±0.01$^{defgh}$ | 1.71 ±0.09$^{fg}$ | 3.13 ±0.11$^{g}$ | 2.14 ±0.11$^{ghijk}$ |
| LCM49 | 94.20 ±0.06$^{x}$ | -1.40 ±0.01$^{mn}$ | -0.26 ±0.04$^{b}$ | 0.95 ±0.06$^{b}$ | 1.46 ±0.07$^{d}$ |
| LCM81 | 89.72 ±0.25$^{a}$ | -1.66 ±0.03$^{bcde}$ | 8.33 ±0.42$^{y}$ | 10.59 ±0.47$^{z}$ | 4.62 ±0.12$^{x}$ |
| LCM82 | 90.28 ±0.27$^{c}$ | -1.56 ±0.01$^{defg}$ | 6.29 ±0.35$^{u}$ | 8.55 ±0.41$^{v}$ | 3.32 ±0.15$^{v}$ |
| LCM83 | 90.36 ±0.19$^{cd}$ | -1.57 ±0.01$^{cdefg}$ | 6.48 ±0.29$^{u}$ | 8.68 ±0.34$^{v}$ | 3.10 ±0.29$^{u}$ |
| LCM84 | 90.61 ±0.25$^{e}$ | -1.53 ±0.02$^{efghijk}$ | 5.72 ±0.33$^{t}$ | 7.90 ±0.41$^{t}$ | 3.05 ±0.10$^{tu}$ |
| LCM85 | 91.29 ±0.14$^{h}$ | -1.56 ±0.02$^{cdefg}$ | 4.83 ±0.26$^{q}$ | 6.78 ±0.29$^{r}$ | 2.88 ±0.04$^{rs}$ |
| LCM86 | 91.78 ±0.22$^{k}$ | -1.63 ±0.05$^{bcdefg}$ | 4.72 ±0.39$^{q}$ | 6.44 ±0.40$^{q}$ | 2.67 ±0.10$^{pq}$ |
| LCM87 | 91.99 ±0.05$^{l}$ | -1.53 ±0.01$^{defghijk}$ | 3.55 ±0.07$^{lm}$ | 5.33 ±0.08$^{m}$ | 2.68 ±0.03$^{pq}$ |
| LCM88 | 92.64 ±0.09$^{p}$ | -1.55 ±0.02$^{defg}$ | 2.68 ±0.16$^{j}$ | 4.25 ±0.16$^{j}$ | 2.42 ±0.11$^{lmn}$ |
| LCM89 | 93.95 ±0.04$^{w}$ | -1.42 ±0.01$^{klmn}$ | 0.09 ±0.03$^{c}$ | 1.37 ±0.05$^{c}$ | 2.18 ±0.08$^{hijk}$ |

[A] a–z indicate significant differences ($p < 0.05$) within column *L**.
[B] a–o indicate significant differences ($p < 0.05$) within column *a**.
[C] a–y indicate significant differences ($p < 0.05$) within column *b**.
[D] a–z indicate significant differences ($p < 0.05$) within column *ΔE**.
[E] a–x indicate significant differences ($p < 0.05$) within column Transparency.

*Mechanical properties*

Mechanical properties of film samples incorporated with different proportion of LMP/CMC and four different contents of MMT are shown in Figure 2. For pure LMP films, TS values reported in literature were higher than those obtained in the present work, and this may be attributed to LMP composition, presence of plasticizer and method of film preparation. Several factors, such as the source of LMP, the viscosity and the experimental conditions can explain the observed differences. The presence of hydroxyl groups in CMC has been confirmed, and LMP contain polar groups such as carboxyl [9]. Thus, the strengthening of TS may be attributed to the formation of intra-molecular hydrogen bonds between the LMP and CMC, as well as the compact structure of composite films. Among the LMP/CMC films, the LMP/CMC films showed the higher TS ($p < 0.05$), compared with pure LMP films and as the levels of CMC increasing, higher TS were observed ($p < 0.05$). Films incorporated with MMT (from 1 to 4%) showed higher TS compared with LMP/CMC films and TS increased with the content of MMT. Especially, TS increased from 15.83 ± 1.38 to 39.85 ± 2.51 MPa, with the addition of 4% of MMT. However, as the content of MTT increased, the MTT disperse irregularly in the matrix and agglomeration, which can be observed in Figure 5. The highest peak intensity (Figure 5(d)) was observed with the addition of 8% of MMT and this did not generate a significant improvement in the TS. The EAB of composite films was less than the LMP film. And the EAB of LMP/CMC-MMT composite films as a whole slightly below LMP/CMC composite films.

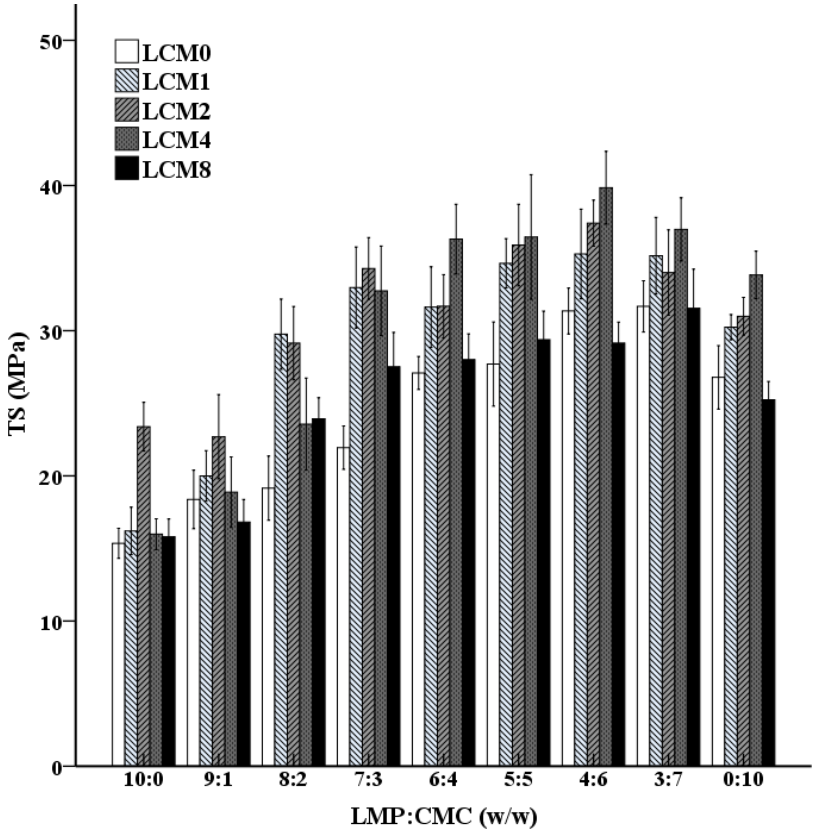



**Figure 2:** Tensile strength (TS) of LMP/CMC composite films with different content MMT.

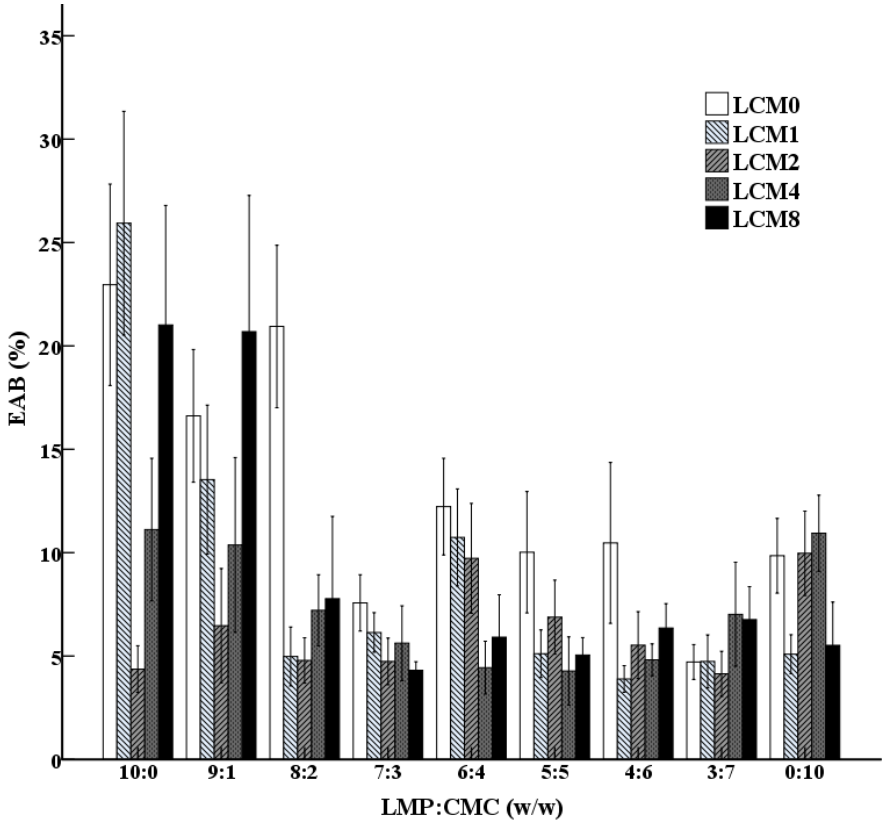



**Figure 3:** Elongation at break (EAB) of LMP/CMC composite films with different content MMT.

*Fourier transform infrared spectroscopy (FTIR)*

In the FTIR spectrum of MMT, the broad band centered near 3429 $cm^{-1}$ was due to the -OH stretching mode of the interlayer water. The overlaid absorption peak in the region of 1634 $cm^{-1}$ was assigned to the –OH bending mode of adsorbed water. The band at 1058 $cm^{-1}$ was assigned to the Si–O–Si stretching vibration for layered silicates. The band in the region of 798 $cm^{-1}$ was due to the Si–O–Al stretching mode for MMT. The FTIR peaks at 529 $cm^{-1}$ and 471 $cm^{-1}$ were assigned to the Si–O–Al and Si–O–Si bending vibration, respectively [24].
In the FTIR spectrum of LMP, the peak of 3282 $cm^{-1}$ was due to single bond –OH stretching vibration and 2923 $cm^{-1}$ was due to the stretching vibration of methyl group of methyl ester. The carbonyl absorption bands shown at 1644 $cm^{-1}$ was from free (COO–) groups. Asymmetric modes of stretching vibration of carboxylic groups were observed at 1415 $cm^{-1}$. The absorption bands at 1147 and 1018 $cm^{-1}$ corresponded to ether (R–O–R) and C–C bond in the ring structure of pectin molecules [25].
In the FTIR spectrum of CMC, the peak at 3317 $cm^{-1}$ was due to single bond –OH stretching vibrations and 2922 $cm^{-1}$ due to the methylene. Symmetric and asymmetric modes of stretching vibration of carboxylic groups were observed at 1589 and 1413 $cm^{-1}$. The band in the range of 1000-1166 $cm^{-1}$ was assigned to the ether bonds [24, 25].
Compared the FTIR spectrum of LCM07 and LCM47 composite films, the relative rate of the band in the 3000-3500 $cm^{-1}$ and the band in 1000-1640 $cm^{-1}$ of LCM07 film was obviously higher than that of the LCM47 film. The higher may be caused by the hydrogen bonds interaction between MMT and LMP/CMC. This indicates that in the LCM/CMC-MMT composite, hydrogen bonds between the hydroxyl groups of MMT and hydroxyl groups of LMP and CMC chains.

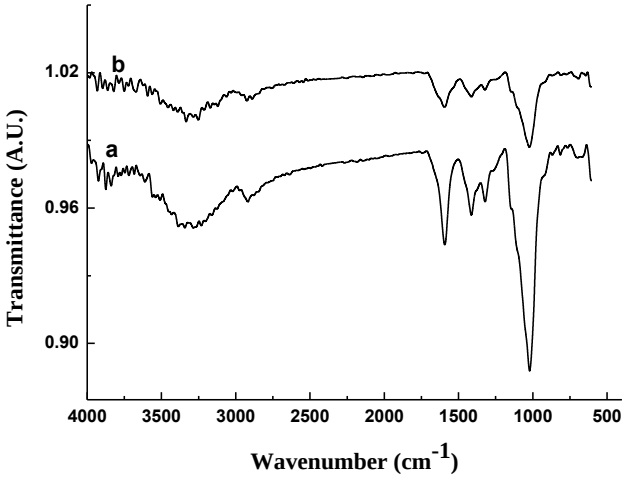



**Figure 4:** FTIR spectra of (a) LCM07 and (b) LCM47 films.

*X-ray diffraction*

X-ray diffractograms were performed on LCM/CMC-MMT (0, 1, 4 and 8%) composite films (Figure 5). X-ray analyses were carried out on the composite films to investigate the dispersion feature of MMT layers. Figure 5 (b) shows that the peak in LCM17 (1% MMT) is very low. The peak is raised to higher level with the increasing of MMT. The low peak intensity observed for LCM17 is caused by the low MMT concentration and an increase in the diffraction peak intensity is due to the increase in MMT concentration [26]. In addition, some exfoliation structures resulting from the lower clay content might be formed in LCM17, which will also decrease the peak intensity. It is noteworthy that the diffraction peak in LCM87 (8% MMT) changes dramatically in comparison with LCM17 and LCM47, which is owing to the higher content and aggregated MMT. These results can further interpreted the lower TS and higher WVP.

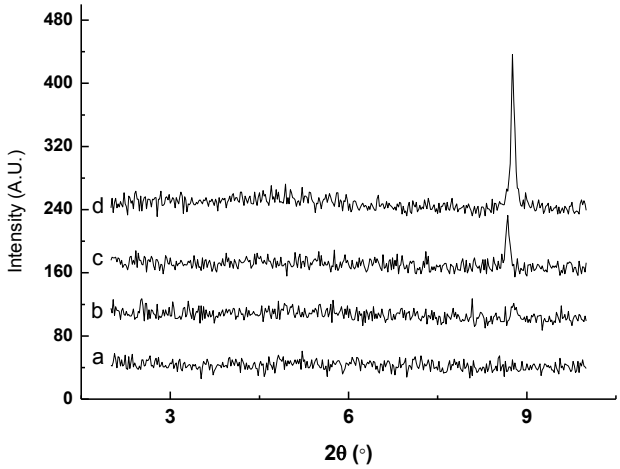



**Figure 5:** XRD patterns of (a) LCM07, (b) LCM17, (c) LCM47 and (d) LCM87.

*Scanning electron microscopy*

Neat CMC and LMP/CMC films without and with MMT were flexible and homogenous. The film samples also had smooth surfaces without pores and cracks visible to the naked eye. They were easily detached from the casting. However, pure LPM film showed poor smooth compared with others. The morphological characteristics of LMP, LCM07, LCM17, LCM47, LCM87 and CMC films are shown in Figure 6. The figure 6 (a) and (f) shows the microstructures of LMP and CMC film. We can observe the smooth surface of CMC film and poor LMP film surface. Figure 6 (b) shows the smooth and flat appearance of surface of the LMP/CMC film, and seems to indicate the mixture of LMP, glycerol and CMC is homogenous. The figure 6 (c) and (c') also showed that MMT (1%) was approximately well dispersed in the LMP/CMC matrix. In contrast to figure 6 (c), slight aggregation can be seen in the compostie film LCM47 containing higher content (4%) of MMT (figure 6(d)).

Figure 4e shows high aggregation of LCM47 containing the highest content (8%) of MMT, which can further interpreted the decreasing of TS and increasing of WVP of LCM/CMC-MMT (8%).

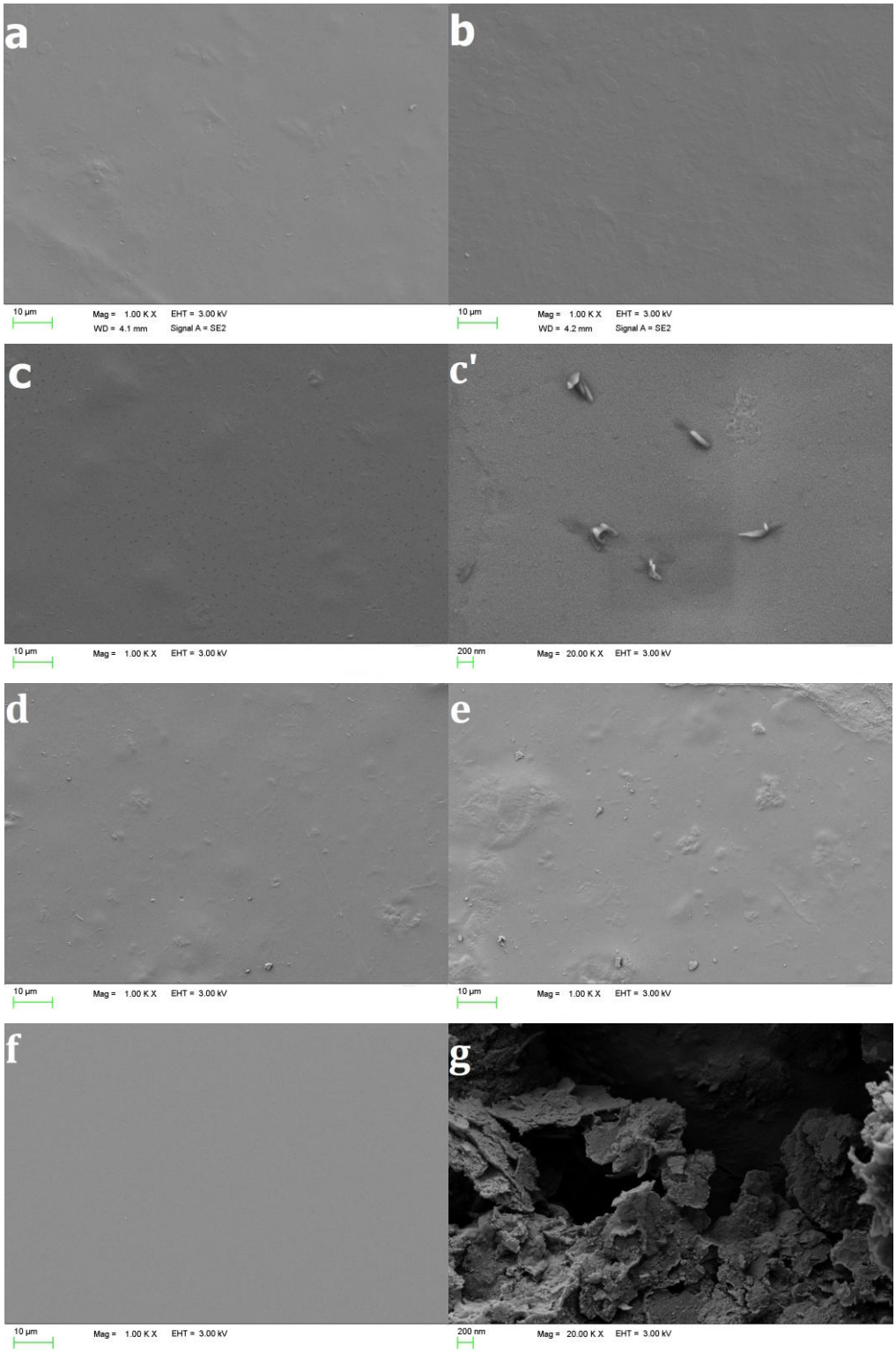



**Figure 6:** SEM micrographs of the surface of (a) LMP, (b) LCM07, (c and c') LCM17, (d) LCM47, (e) LCM87, (f) CMC films and (g) MMT.

## 4 Conclusions

Among the LMP/CMC-based MMT (0, 1, 2, 4 and 8%) composite films prepared in this study, the incorporation of MMT in film forming solution indicated a strong interaction between LMP/CMC and MMT. The decrease in

WVP with MMT (1-4%) content confirms that a strong interaction between hydrophilic groups of MMT and LPM/CMC exists and that water molecules move through a tortuous path when diffuse across the polymer matrix. MMT incorporation affects mechanical properties of LPM/CMC-MMT films. The strengthening of TS with MMT (1-4%) may be attributed to the formation of intra-molecular hydrogen bonds between the LMP, CMC and MMT. The FTIR, XRD and SEM results suggested that the improved water barrier property and tensile property of films is due to dispersion of clay platelets. Film transparency value increases with MMT addition. The LPM/CMC-MMT composite films with improved water vapour and mechanical properties could be potentially used as environmentally friendly food packaging materials.

## Acknowledgements

The authors gratefully acknowledge the financial support of this study by projects 21277061, 21077045 and 21277085 supported by the National Natural Science Foundation of China.

## References

1. H.J. Bae, H.J. Park, D.O. Darby, R.M. Kimmel and W.S. Whiteside, 2009, "Development and Characterization of PET/Fish Gelatin-Nanoclay Composite/LDPE Laminate", *Packaging Technology and Science*, vol. 22, no. 2, pp. 371-383.

2. C.A. Campos, L.N. Gerschenson and S.K. Flores, 2011, "Development of Edible Films and Coatings with Antimicrobial Activity". *Food and Bioprocess Technology*, vol. 4, no. 6, pp. 849-875.

3. I. Lecetaa, P. Guerreroa, I. Ibarburub, M.T. Duenasb, K. de la Cabaa, 2013, "Characterization and antimicrobial analysis of chitosan-based films", *Journal of Food Engineering*, vol. 116, no. 4, pp. 889-899.

4. I.M. Jipa, A. Stoica-Guzun and M. Stroescu, 2012, "Controlled release of sorbic acid from bacterial cellulose based mono and multilayer antimicrobial films", *Lwt-Food Science and Technology*, vol. 47, no. 2, pp. 400-406.

5. M. Uz and S.A. Altinkaya, 2011, "Development of mono and multilayer antimicrobial food packaging materials for controlled release of potassium sorbate", *Lwt-Food Science and Technology*, vol. 44, no. 10, pp. 2302-2309.

6. M.A. Del Nobile, A.Conte, A.L. Incoronato and O. Panza, 2008, "Antimicrobial efficacy and release kinetics of thymol from zein films", *Journal of Food Engineer*ing, vol. 89, no. 1, pp. 57-63.

7. C.Y. Hu, M. Chen and Z.W. Wang, 2012, "Release of Thymol, Cinnamaldehyde and Vanillin from Soy Protein Isolate Films into Olive Oil", *Packaging Technology and Science*, vol. 25, no. 2, pp. 97-106.

8. M. Chen, Z.W. Wang, C.Y Hu and J.L. Wang, 2012, "Effects of Temperature on Release of Eugenol and Isoeugenol from Soy Protein Isolate Films into Simulated Fatty Food", *Packaging Technology and Science*, vol. 25, no. 8, pp. 485-492.

9. S. Galus and A. Lenart, 2013, "Development and characterization of composite edible films based on sodium alginate and pectin", *Journal of Food Engineering*, vol. 115, no. 4, pp. 459-46.

10. M.A. Monsoor, U. Kalapathy and A. Proctor, 2001, "Determination of polygalacturonic acid content in pectin extracts by diffuse reflectance Fourier transform infrared spectroscopy", *Food Chemistry*, vol. 74, no. 2, pp. 233-238.

11. G.S. Macleod, J.T. Fell and J.H. Collett, 1997, "Studies on the physical properties of mixed pectin/ethylcellulose films intended for colonic drug delivery", *International Journal of Pharmaceutics*, vol. 157, no. 1, pp. 53-60.

**12.** Z. Wakerly, J.T. Fell, D. Attwood and D. Parkins, 1997, "Studies on drug release from pectin/ethylcellulose film-coated tablets: a potential colonic delivery system", *International Journal of Pharmaceutics*, vol. 153, no. 2, pp. 219-224.

13. M.A.D. Silva, A.C.K. Bierhalz and T.G. Kieckbusch, 2009, "Alginate and pectin composite films crosslinked with $Ca^{2+}$ ions: Effect of the plasticizer concentration", *Carbohydrate Polymers, vol.* 77, no. 4, pp. 736-742.

14. B.G. de S. Medeiros, A.C. Pinheiro, M.G. Carneiro-da-Cunha and A.A.Vicente, 2012, "Development and characterization of a nanomultilayer coating of pectin and chitosan – Evaluation of its gas barrier properties and application on 'Tommy Atkins' mangoes", *Journal of Food Engineering*, vol. 110, no. 3, pp. 457-464.

15. H. Togrul and N. Arslan, 2004, "Extending shelf-life of peach and pear by using CMC from sugar beet pulp cellulose as a hydrophilic polymer in emulsions", *Food Hydrocolloids*, vol. 18, no. 2, pp. 215-226.

16. V.D. Alves, R. Castelló, A.R. Ferreira, N. Costa, I.M. Fonseca and I.M. Coelhoso, 2011, "Barrier properties of carrageenan/pectin biodegradable composite films", *Procedia Food Science*, vol. 1, pp. 240-245.

17. A.M. Slavutsky, M.A. Bertuzzi, M. Armada, M.G. Garcia and N.A. Ochoa, 2014, "Preparation and characterization of montmorillonite/brea gum nanocomposites films", *Food Hydrocolloids*, vol. 35, pp. 270-278.

18. P. Tongnuanchan, S. Benjakul and T. Prodpran, 2013, "Physico-chemical properties, morphology and antioxidant activity of film from fish skin gelatin incorporated with root essential oils", *Journal of Food Engineerin*g, vol. 117, no. 3, pp. 350-360.

19. J.H. Han and J.D. Floros, 1997, "Casting antimicrobial packaging films and measuring their physical properties and antimicrobial activity", *Journal of Plastic Film and Sheeting*, vol. 13, no. 4, pp. 287-298.

20. ASTM F, 1249-90, 1995, "Standard test method for water vapor transssion rate through plastic film and sheeting using a modulated infrared sensor", *In annual book of ASTM standards*, ASTM: Philadelphia, Pennsylvania, pp. 1137-1141.

21. S. Mali, L.B. Karam, L.P. Ramos, M.V. Grossmann, 2004, "Relationships among the composition and physicochemical properties of starches with the characteristics of their films", *Journal of Agricultural and Food Chemistry*, vol. 52, no.25, pp. 7720-7725.

22. ASTM D 882-02, 2002, "Standard test method for tensile properties of thin Plastic sheeting", *In annual book of ASTM standards*, ASTM: Philadelphia, Pennsylvania, pp. 1-9.

23. P. Mangiacapra, G. Gorrasi, A. Sorrentino and V. Vittoria, "Biodegradable nanocomposites obtained by ball milling of pectin and montmorillonites", *Carbohydrate Polymers*, vol. 64, no. 4, pp. 516-523.

24. Y. Bao, J.Z. Ma and N. Li, 2011, "Synthesis and swelling behaviors of sodium carboxymethyl cellulose-g-poly(AA-co-AM-co-AMPS)/MMT superabsorbent hydrogel", *Carbohydrate Polymers*, vol. 84, no. 1, pp. 76-82.

25. N. Ninan, M. Muthiah, I. Park, A. Elain, S. Thomas and Y. Grohens, 2013, "Pectin/carboxymethyl cellulose/microfibrillated cellulose composite scaffolds for tissue engineering", *Carbohydrate Polymers*, vol. 98,no. 1, pp. 1879-1344.

26. J. Guo, X. Li, C. Mu, H. Zhang, P. Qin and D. Li, 2013, "Freezing–thawing effects on the properties of dialdehyde carboxymethyl cellulose crosslinked gelatin-MMT composite films", *Food Hydrocolloids*, vol.33, no. 2, pp. 273-279.

# New Bio-Based Plastics, from a Non-Edible Plant Oil Side-Stream, for Film Extrusion

**Hannah Rasel[1], Mikael S. Hedenqvist[2], Therese Johansson[1], William R. Newson[3], Eva Johansson[3] and Mikael Gällstedt[1*]**

[1] *Packaging Solutions, Innventia, Sweden*
[2] *Department of Fibre and Polymer Technology, Royal Institute of Technology, Sweden*
[3] *Department of Plant Breeding, The Swedish University of Agricultural Sciences, Sweden*

[*] *Corresponding author. Email: mikael.gallstedt@innventia.com*

**Abstract:** Renewable sourced PET, PA, PE, starch blends, etc, are fastly growing due to the processability and final performance, that is similar to their petroleum derived options. A bit in the shadow of the development of these plastics, development is ongoing on another group of plastics, made directly of the side-streams of agricultural products: oil plant residues and proteins. They can be used in edible applications but not all of them are suitable for food or forage.

Industrial oilseed meal from crambe abyssinica contains relatively high levels of protein that is not suitable for human or animal consumption due to the presence of anti-nutritional compounds.

This paper presents research on crambe meal as a base for new plastics, developed to extrude continuous, flexible plastic films based on crambe meal, blended with vital wheat gluten as an elastic component and urea as a protein denaturant.

The effect of process parameters, such as screw speed, die temperature and pressure, and the effect of components were studied with regards to the final performance of the film extrudates. E.g. mechanical properties, oxygen permeability and moisture content were determined and surface and cross-section morphologies were examined with electron microscopy.

The results showed that crambe-based blends can be extruded as continuous, flexible plastic films, which exhibit barrier properties towards oxygen. Recipes and methods for pelletizing of master batches for post-converting (e.g. extrusion or compression molding) were successfully developed. Addition of a renewable plasticizer improved the extrusion performance and resulted in less hygroscopic films, which further showed the overall highest tensile strength while the extensibility was nearly unaffected. The results provide a first basis to further develop the process and the blend towards potential industrial applications, for example as packaging materials to trays, pots and similar type of packages.

Keywords: oxygen barrier, renewable plastics, crambe, wheat gluten, extrusion.

## 1 Introduction

Packaging is one of the major applications for plastic materials. Besides providing an selling appearance, transport enhancer, information display, etc, packaging has the important function to protect its content. Especially with regards to food packaging, the barrier properties to e.g. oxygen, grease and water are often crucial for fulfilling this demand. Today, these functions are exceptionally provided by non-biodegradable polymers derived from petroleum, either used as mono- or multilayers.

However, increasing environmental concerns and uncertain future petroleum prices have drawn the attention to the development of bio-based plastics. The market has seen a great increase in number of “green” plastics, the last years and the development seems to proceed faster and faster. The background of these plastics, their different definitions, which to be selected for which market and products, their properties, etc, can be found in

the literature. This paper focuses on thermoformed plastic composites of gluten proteins and crambe meal. Wheat gluten is edible but not crambe meal, and the entire composite is thus not edible. This composite is recently developed, still in "the researchers lab", but approaches up scaled processing trials.

Wheat gluten is the proteins in wheat flour. The other major component in wheat flour is the wheat starch which is believed increase in production volume as the production of bio-ethanol fuel is increasing.

Defatted crambe meal, is an interesting side stream material from seed oil extraction. It is rich in protein and crude fibers but unsuitable as animal feedstock due to its high level of glycosinolates.

## 2 Materials and processing

### Wheat gluten

The term vital wheat gluten (WG) is referred to the protein-rich fraction of wheat, which is obtained by removing the water-soluble components such as mainly starch, from the wheat dough.

The barrier and mechanical properties of protein films are principally dependent on the processing technique and the processing parameters (especially temperature), as well as on the choice and amount of plasticizer. Furthermore, relative humidity plays a large role. Because the films are susceptible to the uptake of moisture, which acts as a plasticizer, permeability and extensibility usually increase with humidity, whereas tensile strength is reduced [1].

Wheat gluten is an amorphous system that undergoes a glass transition, the transformation from the glassy to the viscous–rubbery state as the temperature is raised through the glass transition temperature [2]. Due to their extensive hydrogen-bonding pattern, protein-based materials are generally brittle and there- fore require a plasticizer in order to introduce flexibility. Besides positive effects, a plasticizer usually increases the permeability of a plastic film as an effect of the extended structure [3].

### Crambe abyssinica

Crambe abyssinica is an annual herbal plant that belongs to the cruciferae family. Since crambe plants have only few demands on their growing conditions, they can be cultivated in many varied soils.

From an industrial point of view, crambe has gained increasing interest as an alternative raw material source for oil production, especially because their seed oil is very rich in the valuable erucic acid. The oil content of crambe seed is reported to be ca. 36 wt%, the proteins 20-26 wt%, crude fibers 14-18 wt% and it contains ca. 5 wt% ash [4,5]. Crambe meal is the residue of the crambe seed, which is left after pressing and solvent extraction. It is known to contain a relatively high amount of proteins, but it is also rich in crude fiber.

### Extrusion

The most common processing method of plastics, in terms of annual production volume, is the extrusion. Despite its simple principle, extrusion is a sophisticated process and the quality of the extrudates depends largely on the optimal interplay between material, extruder configuration (screw elements, die shape, screw-length to diameter ratio) and process parameters. Important process parameters, which are adjustable during extrusion, are the temperature profile along the barrel, die temperature, feeding rate and screw speed. Responding parameters are melt temperature, residence time in the barrel, die pressure, torque, specific mechanical energy input and the degree of screw fill [6].

### Wheat gluten during thermoplastic processing

Lagrain et al. [7] have reviewed the physical and chemical changes of gluten proteins during thermal processing and under the influence of additional shear; conditions to which polymers are generally subjected during standard industrial processing methods, such as extrusion.

As plasticized WG is exposed to elevated temperature up to 130 °C, a significant increase in viscosity can be observed as the result of network formation via disulfide crosslinks [7]. On a molecular level, thermal treatment initially causes unfolding of the WG proteins and the disruption of hydrogen bonding between glutenin and gliadin. Those conformational changes make previously unavailable SH-groups accessible for reactions. Below 100 °C, glutenin proteins crosslink via disulphide bridges, as a result of the oxidation of SH-groups. Above 90 °C, SH/SS exchange reactions enable the covalent bonding between glutenin and gliadin, while creating a free SH-group on gliadin, which can react further [7].

Additional shear strain drastically reduces the activation energy for the crosslinking reactions from 170 kJ/mole during thermal treatment, to 33.7 kJ/mole. It is supposed that shear strain promotes the mechanical scission of

disulfide bonds and thus the creation of reactive thiyl radicals, which quickly interact by creating additional intermolecular disulphide bonds in the gluten network [7,8].

## Enlarging the processing window of wheat gluten using protein denaturants

Due to the crosslinking reactions when subjected to thermal treatment, WG is known to have a very narrow processing window. When it comes to industrial large-scale applications, a narrow processing window could be an obstacle for the commercial use.

Thus, attempts have been made to extend the upper processing limits of plasticized wheat gluten by incorporating substances, which delay or limit the onset of disulphide crosslinking, a technique inspired by the use of scotch retarders in the rubber industry [9].

Ullsten et al [9] succeeded in significantly enhancing the extrudability of WG films, by adding 1 wt% salicylic acid (SA) to the recipe. The presence of SA decreased the degree of protein aggregation due to radical scavenging and consequently, the die temperature could be increased from 90 °C to 135 °C, without interfering with the mechanical properties of the extruded films [9]. A less aggregated protein net- work impairs the oxygen barrier properties, though [10].

In further studies by Ullsten et al [11], it was shown that the use of alkaline ammonium hydroxide ($NH_4OH$) in addition to 1.5 wt% SA, considerably improved the extrudate quality in terms of smoothness, homogeneity, oxygen permeability and strength. Oxygen permeability values comparable to oriented polyethylene and polyamide 66 could be obtained, whereas the modulus was competitive to that of plasticized polyvinylchloride.

Due to its alkaline character, $NH_4OH$ obviously favors the initial protein denaturation followed by extensive polymerization via intermolecular disulphide bonds, leading to an highly aggregated network with the corresponding improvement in properties. At the same time, the presence of SA enabled the extrudability at 120°C die temperature, by delaying the onset for crosslinking and by reducing the intermolecular friction in the extruder barrel [11].

Although the semi-dry process with $NH_4OH$/SA produces high quality films, it is from an industrial and economic perspective more desired to implement solvent free extrusion processes. Prior to the studies with NH4OH, the attempt has been made to incorporate sodium hydroxide (NaOH) in combination with SA into the formulation [10]. Even though enabling a solvent free extrusion, the use of NaOH is rather undesired, due to its toxic and corroding character and due to the inferior extrudate quality compared to $NH_4OH$. This has driven the research motivation of Ture et al [12], who was the first extruding plasticized WG in a solvent free process, using urea as a protein denaturant.

## Urea

Urea is generally known to be an effective protein denaturant. It promotes the unfolding of proteins by screening intermolecular hydrogen bonds and by minimizing the hydrophobic effect [13]. In the context of soybean films, it also showed to have beneficial effects on the ageing properties [14].

The study of Ture et al [12], performed on a single screw extruder, succeeded in improving the extrudability in the presence of 10-20 wt% urea, allowing die temperatures up to 130 °C. Very good oxygen barrier properties were obtained, similar to those achieved with $NH_4OH$, which was correlated to the highly aggregated protein structure, caused by the large denaturation effect of urea. It was furthermore proposed that urea also introduces plasticization, since the strength and stiffness were significantly reduced compared to WG and the films produced by Ullsten et al [9,10,11], and further decreased with increasing urea content. At the same time, extensibility increased. A following up study, related those results to the swelling of the hexagonal closed packed (HCP) supramolecular structure that was observed with increasing urea content, describing urea as an internal plasticizer [15]. Increasing WVP and OP with increasing urea content, was, besides due to plasticization, attributed to the hydrophilic character of urea [12].

## Thermoplastic processing and properties of crambe plastics

The research interest to use crambe as a raw material source is very new and therefore, not many studies have been performed on this material yet. Johansson [16] showed that it is generally possible to compression mold and to extrude crambe, using 15 % glycerol as a plasticizer and a processing temperature of 100 °C.

The work on crambe meal was continued by Henne [17]. By comparing pressing temperatures of 100 °C and 130 °C, it was observed that with 130 °C, significantly lower water absorption and higher tensile strength was obtained, due to a larger extent of protein crosslinking. The findings by Henne [17] were in accordance with the

study of Newson et al [18], who investigated the changes that occur in plasticized crambe meal (20–30 % glycerol) when compression molded at different temperatures, ranging from 100 °C – 180 °C.

### The combination of crambe and wheat gluten

The first experiments were performed crambe meal extrusion by Henne (2011) on a twin screw extruder. In order to improve the rather brittle character of compression molded films and extrudates of crambe meal, it was blended with wheat gluten, exploiting the well-known viscoelastic properties of this material. Furthermore, urea as a protein denaturant was incorporated to the formulation, delaying the onset of crosslinking as experienced with wheat gluten processing.

To investigate the effect of urea on crambe meal, extrudates were produced containing different amounts of urea and glycerol (without WG). The processing window was determined to be between 130 °C and 180 °C, higher temperatures leading to more brittle material. As with wheat gluten, urea accounts for flexibility in crambe meal extrudates. Increasing the urea amount from 10 wt% to 20 wt% almost doubled the strain at break, while Young's modulus and maximum stress were significantly reduced.

By introducing wheat gluten to the recipe, flexibility was significantly enhanced, while the processing window was found to be narrower and lower. At 130 °C, ruptured extrudates with inhomogeneity and surface cracks were obtained. Decreasing the temperature to 100 °C–105 °C resulted in more homogeneous, flexible and elastic samples. The higher the ratio wheat gluten to crambe, at constant glycerol and urea levels, the higher was the strain at break and the lower was the Young's modulus.

## 3 Conclusions

Glycerol plasticized crambe meal, blended with wheat gluten as an elastic component and with urea as a protein denaturant, can successfully be extruded as continuous, flexible plastic films, which exhibit barrier properties towards oxygen.

The blends of crambe meal and wheat gluten show the potential to be processed in a continuous, master-batch like manner. Granules, produced by pelletizing pre-extruded strands, could be fed automatically into the extruder by using a volumetric feeder, and then be extruded to films.

## Acknowledgements

The authors acknowledge the EC FP7 project ICON for their support of this work. Richard Andersson, Michaela Salajkova (Dept. of Fibre and Polymer Department, KTH) and Göran Flodberg (Innventia) are thanked for experimental assistance.

## References

1. N. Gontard. H. Agellier-Coussy. P. Chalier. E. Gastaldi. V. Guillard and C. Guillaume, 2011, "Food Packaging Applications of Biopolymer-Based Films", In D. Plackett (ed), *Biopolymers - New Materials for Sustainable Films and Coatings*, John Wiley & Sons, New York, pp. 211-232.
2. N. Gontard and S. Ring, 1996, "Edible Wheat Gluten Film: Influence of Water Content on Glass Transition Temperature", *Journal of Agricultural Food Chemistry*, 3474-3478.
3. M. Pouplin. A. Redl and N. Gontard, 1999, "Glass Transition of Wheat Gluten Plasticized with Water, Glycerol, or Sorbitol", *Journal of Agricultural Food Chemistry*, pp. 538-543.
4. K.D. Carlson and H. L. Tookey, 1983, "Crambe Meal as a Protein Source for Feeds", *Journal of the American Oil Chemists Society*, Vol 60, No. 12, pp. 1979-1985.
5. L. Lazzeri. O. Leoni. L.S. Conte and S. Palmieri, 1994, "Some technological characteristics and potential uses of Crambe abyssinica products", *Industrial Crops and Products*, Vol. 3, pp. 103-112.
6. V.M. Hernandez-Izquierdo and J.M. Krochta, 2008, "Thermoplastic Processing of Proteins for Film Formation", *Journal of Food Science*, Vol. 73, pp. 30-39.
7. B. Lagrain. B. Goderis. K. Brijs and J.A. Delcour, 2010, "Molecular Basis of Processing Wheat Gluten towards Biobased Materials", *Biomacromolecules*, Vol. 11, 533-541.
8. M. Pommet. A. Redl. M.-H. Morel. S. Domenek and S. Guilbert, 2003, "Thermoplastic Processing of Protein-Based Bioplastics: Chemical Engineering Aspects of Mixing, Extrusion and Hot Molding", *Macromolecular Symposia*, Vol. 197, No. 1, pp. 207-217.

9. N.H. Ullsten. M. Gällstedt. E. Johansson. A. Gräslund and M.S. Hedenqvist, 2006, “Enlarged Processing Window of Plasticized Wheat Gluten Using Salicylic Acid”, *Biomacromolecules*, Vol. 7, No. 3, pp. 771-776.

10. N.H. Ullsten. S.-W. Cho. G. Spencer. M. Gällstedt. E. Johansson and M.S. Hedenqvist, 2009, “Properties of Extruded Vital Wheat Gluten Sheets with Sodium Hydroxide and Salicylic Acid”, *Biomacromolecules*, Vol. 10, 479– 488.

11. N.H. Ullsten. M. Gällstedt. G. Spencer. E. Johansson. S. Marttila. R. Ignell, 2010, “Extruded High Quality Materials From Wheat Gluten”, *Polymers from Renewable Sources*, Vol. 1, No. 4, pp. 173-186.

12. H. Türe. M. Gällstedt. R. Kuktaite. E. Johansson and M. Hedenqvist, 2011. “Protein network structure and properties of wheat gluten extrudates using a novel solvent-free approach with urea as a combined denaturant and plasticizer”, *Soft Matter*, Vol. 7, pp. 9416-9423.

13. B.J. Bennion and V. Daggett, 2003. “The molecular basis for the chemical denaturation of proteins by urea”. *Proceedings of the National Academy of the Sciences of the United States of America*, USA, April, Vol. 100, No. 9, pp. 5142-5147.

14. X. Mo and X. Sun, 2003, “Effects of Storage Time on Properties of Soybean Protein-based Plastics”, *Journal of Polymers and the Environment*, Vol. 11, pp. 15-22.

15. R. Kuktaite. T.S. Plivelic. H. Ture. M.S. Hedenqvist. M. Gällstedt. S. Marttila and E. Johansson, 2012, “Changes in the hierarchical protein polymer structure: urea and temperature effects on wheat gluten films”, *RSC Advances*, Vol. 2, pp. 11908-11914.

16. T. Johansson, 2010, “Development of bioplastics from oil plant by- products”, Master Thesis Report, Innventia, Sweden.

17. S. Henne, 2011, “Green Packaging Plastics of Crambe and Gluten” , Bachelor Thesis Report, Innventia, Sweden.

18. W.R. Newson. R. Kuktaite. M.S. Hedenqvist. M. Gällstedt and E. Johansson, 2013, “Oilseed Meal Based Plastics from Plasticized Crambe Abyssinica and Brassicia Carinta Residuals”, Journal of the American Oil Chemists' Society, Vol. 90, No. 8, pp. 1229-1237.

# Degradation of Steel Packages in Tropical Environments – Results After 10 Years of Discarding

**J.L.C. Santos[1], J.A.B. Gatti[2*], S.T. Dantas[2], W. R. Santos[1]**

[1] *Research Center, Companhia Siderúrgica Nacional – CSN, Brazil*
[2]*Packaging Technology Center – CETEA, Institute of Food Technology – ITAL, Brasil*

[*]*Corresponding author. Email: jozeti@ital.sp.gov.br*

**Abstract:** The performance of steel cans and other packages in the environment is mentioned in several publications, including infantile education books. In spite of this, just a few scientific data are available. A study considering Brazilian environmental conditions was carried out aiming to the development of data on the metal packaging performance when discarded in different natural conditions instead of an adequate disposal. The behavior of steel packages in four local tropical environments during the time of 10 years was studied: on the ground at an industrial site, on the seashore, buried in the ground and immersed in a riverbed. Four different kinds of steel cans were used (plain powdered milk and soybean oil three piece tinplate cans and lacquered soft drink DWI tinplate can and tomato sauce tinplate three piece cans). Alternative packages containing the same products - PET bottles for soybean oil, aluminum cans for soft drinks, laminated plastic bags for powdered milk and carton based multilayer packaging for tomato sauce - were used as control. Annually, samples of all packages were removed from the studied sites and visually analyzed. Powdered milk and soybean oil cans were completely degraded in the industrial and marine environments between 6 and 7 years. Tomato sauce can sample was totally degraded between 7 and 8 years in the industrial environment. However, although some important surface damage was observed, none of the studied types of steel cans was completely degraded in both conditions: buried in the ground and immersed in a riverbed during the 10 years of study. Alternative packaging showed smaller alteration than steel cans in the studied period and conditions.

Key words: steel can, degradation, tropical environments, environment

## 1 Introduction

In 2012, according to CEMPRE (2014), a total of 47% of steel packaging consumed was recycled in Brazil, although the country already had installed capacity to absorb 100% of this form of scrap. Around 300,000 tons of post-consumption steel cans were returned for the process of recycling in the country. This rate has been rising thanks to the expansion of the programs of selective waste collection, environmental education and there is a trend towards significant growth following the implementation of the National Solid Waste Policy, forecast for 2014. The difficulties, however, lie in the structuring of the recycling chain due to various factors affecting the return of this packaging for a new cycle of production, such as the low rate of selective collection or collection on an economically appropriate scale and low prices in comparison with other materials. Moreover, the logistics of this process, which are fundamental, are something of a challenge as a result of the geographical expanse of the country and the various social, cultural, political and economic differences, where the regional profiles, in terms of waste generation and management, are still quite trenchant (FERREIRA, 2003).

When steel packaging is incorrectly disposed of in the environment, its metal constituents present significant potential for degradation, reverting to the chemical forms in which they are to be found in nature, though not in the original conditions, as they cannot be reused as if they had just come out of the mines. This ultimately represents a dissipation of natural resources. Furthermore, it is necessary to understand the environmental impact of the indiscriminate release of the other components of the packaging, besides the metals. However, the timeframes for these reactions are not well quantified. The information published by the media is contradictory and without scientific vindication. Bromander[(1)]conducted a study in Norway with the aim of surveying the degradation time of this form of packaging when disposed into the environment, however the climatic conditions of that country are very specific and completely different from those to be found in a tropical country like Brazil. Accordingly, CSN, the national tinplate and chromium plate producer, in conjunction with CETEA Packaging Technology Center, conducted a study in order to gather information on the average degradation time of several types of packaging under specific, tropical environmental conditions. In addition to steel cans, a number of packages produced from other materials were placed in the same experimental fields, to be used as benchmarks. The packaging was left in the experimental fields from 2002 to 2012.

The packaging was placed on a riverbed, in marine and industrial environments as well as being buried in the soil. The aim of this study is to present the results obtained after 10 years of exposure of the samples in the various environments. This approach did not include an investigation into the effect of the degraded material on the environment, which should be the focus of consideration in future studies.

## 2 Methodology

### 2.1 Materials

The following items of steel packaging were analyzed:

- Steel can for 400 g powdered milk, unused, without its fitted lid and with a non-varnished material
- Steel can for 350 ml soft drinks, unused, closed with stay on tab easy-open aluminum end
- Steel can for packing tomato products (350 g purée or 340 g sauce), unused, with seamed lid opened, tomato sauce with easy-open lid and tomato purée with a conventional lid opened using a household can opener
- Steel can for 900 ml soybean oil, unused, with seamed lid opened with a household can opener

In addition to the steel cans, some packaging manufactured from other materials was placed in the same experimental fields to be used as a benchmark, namely:

- Laminated plastic bag for 400 g modified powdered milk, used, empty and unwashed.
- Carton packaging for 520 g tomato paste, used, empty and unwashed.
- PET bottle for 900 ml soybean oil, used, empty and unwashed.
- Two-piece aluminum cans, for packing 350 ml soft drinks, used, empty and unwashed.

The specifications of the materials used in the steel packaging being studied, according to manufacturer's information, are described in Santos et al. (2005) and Santos et al. (2010).

### 2.2 Monitored fields and methodology for exposure of samples

2.2.1 Soil – Soil close to the CSN Research Center in Volta Redonda, Rio de Janeiro, Brazil

2.2.2 Open-air industrial environment – experimental station located at the "Presidente Vargas" plant close to the coke production unit in Volta Redonda, Rio de Janeiro, Brazil

2.2.3 Open-air marine environment– experimental station located at the Restinga da Marambaia beach in Rio de Janeiro, Brazil

2.2.4 Riverbed – experimental station (floating boathouse) built on the Paraíba do Sul River, where it cuts across the property of the "Presidente Vargas" plant in Volta Redonda, Rio de Janeiro, Brazil

The methodology employed in this study is described in detail in Santos et al. (2005) and Santos et al. (2010).

### 2.3 Description of the parameters monitored in each testing environment

For each testing environment, some parameters were selected for analysis, to physically and chemically characterize the conditions to which the samples would be exposed. These parameters are described below:

a) Soil: organic matter, pH, phosphorus, potassium, calcium, magnesium, sulfur, electrical conductivity and chlorides. These analyses were made only once, in the beginning of the study;

b) Open air, industrial environment: temperature, relative humidity, rain fall, total particles in suspension, sulfur dioxide, nitrogen dioxide and solar radiation (monthly monitoring);

c) Open air, marine environment: temperature, relative humidity, rain fall and chlorides (monthly monitoring);

d) River water: temperature, magnesium, calcium, chemical oxygen demand (COD), total alkalinity, electrical conductivity, pH, chlorides and organic matter (monthly monitoring).

The methodology employed in this study is described in detail in Santos et al. (2005) and Santos et al. (2010).

## 3 Results and Discussion

Soil analysis was performed in the beginning of the study and the results are described in Table 1:

**Table 1.** Characteristic parameters of the soil in the CSN Research Center.

| Parameter | Value measured |
|---|---|
| Organic matter | 32 g/dm$^3$ |
| pH | 6.8 |
| Phosphorus | 61 mg/dm$^3$ |
| Potassium | 2.5 mmol/dm$^3$ |
| Calcium | 118 mmol/dm$^3$ |
| Magnesium | 22 mmol/dm$^3$ |
| Sulfur | 9 mg/dm$^3$ |
| Electrical condutivity | 170 μS/cm |
| Chloride | 18.5 mg/dm$^3$ |

Table 2 presents the results obtained by monthly monitoring of the characteristic parameters of the air in the industrial environment where the packagings were exposed for the ten years.

**Table 2.** Parameters obtained while monitoring the air in the industrial environment during the ten years exposition of the samples.

| Parameter | General Mean | MonthlyMinimum Mean | Monthly Maximum Mean |
|---|---|---|---|
| Temperature ($^0$C)$^{(1)}$ | 22.7 | 14.8 | 27.8 |
| Relative Humidity$^{(2)}$ | 77.8 | 61.0 | 93.0 |
| Sulfur Dioxide (μg/m$^3$)$^{(3)}$ | 11.9 | 1.9 | 58.1 |
| Nitrogen Dioxide (μg/m$^3$)$^{(4)}$ | 18.9 | 5.6 | 36.2 |
| Total particles in suspension (μg/m$^3$)$^{(5)}$ | 55.8 | 32.5 | 85.7 |
| Solar Radiation (W/m$^2$)$^{(6)}$ | 164.9 | 69.1 | 268.6 |
| Rainfall Accumulated Monthly (mm)$^{(7)}$ | 121.8 | 0.5 | 482.6 |

*(1) Results of 102 determinations*
*(2) Results of 96 determinations*
*(3) Results of 98 determinations*
*(4) Results of 106 determinations*
*(5) Results of 109 determinations*
*(6) Results of 73 determinations*
*(7) Results of 91 determinations*

Table 3 presents the atmospheric parameters monitored on the Marambaia Beach, RJ (*Restinga da Marambaia*) during the 7 years the samples were exposed.

**Table 3.** Parameters obtained by monitoring the marine air during the seven years the samples were exposed.

| Parameter | Mean | Minimum Value | Maximum Value |
|---|---|---|---|
| Temperature ($^0$C)$^{(1)}$ | 23.0 | 19.6 | 27.6 |
| Relative Humidity (%)$^{(2)}$ | 82.0 | 70.0 | 94.1 |
| Chlorides (mg/m$^2$/dia)$^{(4)}$ | 141.9 | 45.7 | 264.1 |
| Rainfall Accumulated Monthly(mm)$^{(3)}$ | 88.2 | 1.4 | 472.4 |

*(1) Results of 80 determinations*
*(2) Results of 64 determinations*
*(3) Results of 79 determinations*
*(4) Results of 52 determinations*

Table 4 presents the characteristic parameter values of the Paraíba do Sul River water where the samples were exposed, obtained by monthly sampling and analysis.

**Table 4.** Parameters obtained by monitoring Paraíba do Sul River water for the ten years the samples were exposed.

| Parameter | Mean in the study period | Annual Minimum Mean | Annual Maximum Mean |
|---|---|---|---|
| Magnesium (ppm)[(1)] | 1.07 | 0.75 | 1.24 |
| Calcium (ppm)[(1)] | 3.45 | 1.07 | 4.52 |
| Chemical oxygen demand - COD (mg/l)[(2)] | 11.83 | 7.54 | 17.67 |
| pH[(3)] | 6.70 | 6.23 | 6.89 |
| Electrical Conductivity (µS/cm)[(3)] | 82.22 | 66.63 | 99.95 |
| Total Alkalinity (% $CaCO_3$)[(3)] | 0.01 | 0.00 | 0.05 |
| Chlorides (ppm)[(3)] | 6.31 | 4.64 | 7.58 |
| Temperature ($^0$ C)[(4)] | 22.95 | 22.10 | 23.69 |
| Organic Matter[(5)] | 3.56 | 2.49 | 4.89 |

*(1) Results of 73 determinations*
*(2) Results of 72determinations*
*(3) Results of 78 determinations*
*(4) Results of 77 determinations*
*(5) Results of 58 determinations*

Figures 1 to 16 display photographs illustrating the evolution of the degradation of cans buried in the soil and placed on the riverbed, in an industrial and a marine environment, respectively, for a period of 10 years.

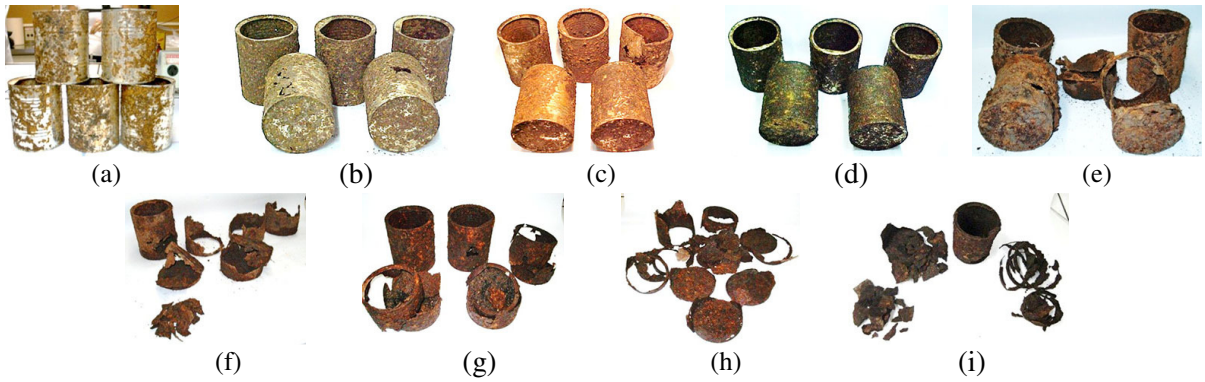
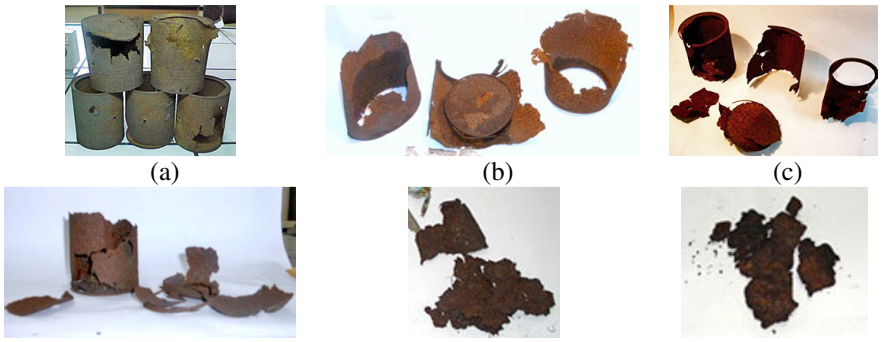



**Figure 1.** Powdered milk cans buried in the ground: (a) after one year exposition, (b) after two years exposition, (c) after three years exposition, (d) after four years exposition, (e) after five years exposition, (f) after six years exposition, (g) after seven years exposition, (h) after eight years exposition and (i) after ten years exposition.

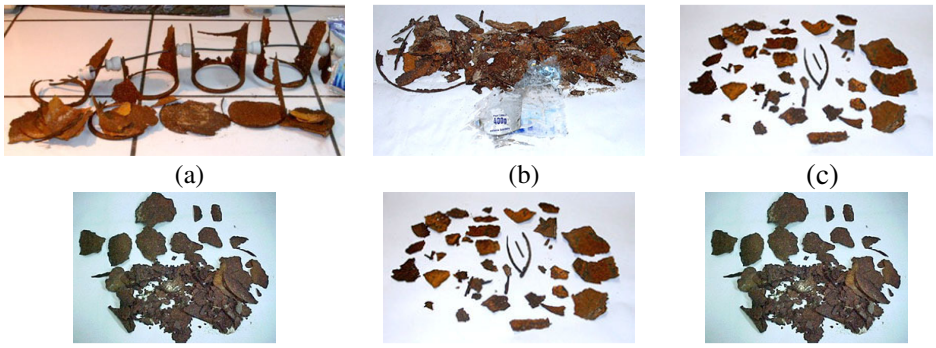



**Figure 2.** Powdered milk cans immersed in the river: (a) after one year exposition, (b) after two years exposition, (c) after three years exposition, (d) after four years exposition, (e) after five years exposition, (f) after eight years exposition and (g) after ten years exposition.



(a) (b) (c) (d) (e) (f)

**Figure 3.** Powdered milk cans discarded in the open air, in an industrial environment: (a) after one year exposition, (b) after two years exposition, (c) after three years exposition, (d) after four years exposition, (e) after five years exposition and (f) after six years exposition.



(a) (b) (c) (d) (e) (f)

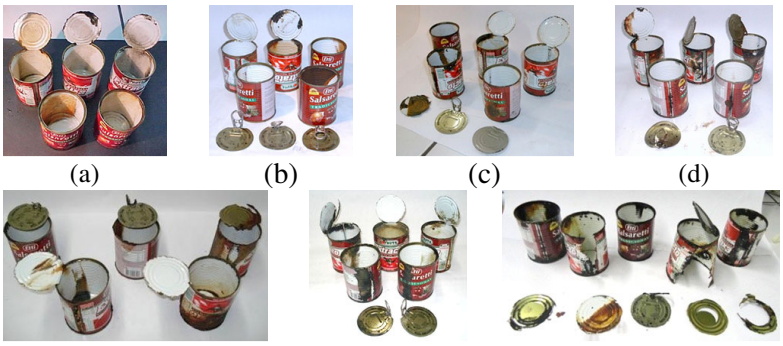
**Figure 4.** Powdered milk cans discarded in open air, in a marine environment: (a) after one year exposition, (b) after two years exposition, (c) after three years exposition, (d) after four years exposition, (e) after five years exposition and (f) after six years exposition.

According to the photographs in Figures 1 to 4, an evolution can be seen in the degradation of the powdered milk cans buried in the soil, though they did not end up fully integrating into the environment in which they were enveloped. Ten years after placement, fragments were recovered of the body and/or base and the seaming with part of the material from the body and the base; one of the cans still preserved the body attached to the base. An evolution of the degradation was also observed with the cans of powdered milk when placed on the riverbed. However, after 10 years, one of the cans exhibited the base and approximately ¾ of the body still attached, although of the other cans, only fragments of seaming and the body/base had been located. In the industrial and marine environments, the evolution of the degradation of these cans occurred more quickly when compared to the cans placed in the soil and in the river, since 6 years after placement, only scattered fragments could be found in the areas where they had been placed.



(a) (b) (c) (d) (e) (f) (g) (h) (i)

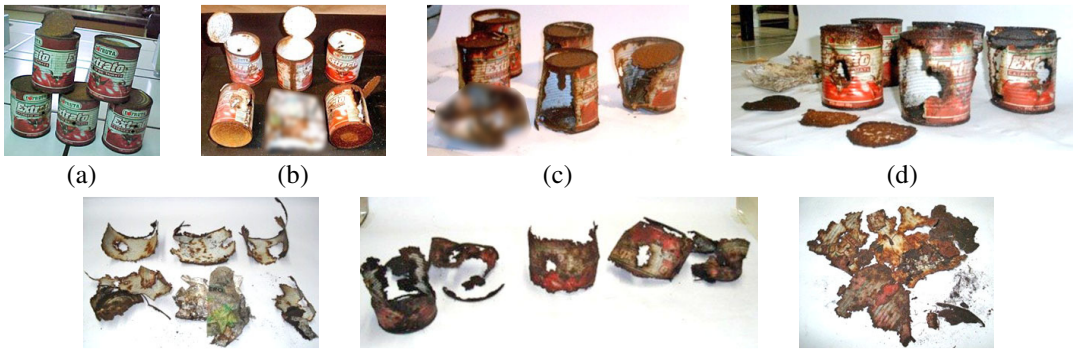
**Figure 5.**Tomato product cans buried in the ground: (a) after one year exposition, (b) after two years exposition, (c) after three years exposition, (d) after four years exposition, (e) after five years exposition, (f) after six years exposition, (g) after seven years exposition, (h) after eight years exposition and (i) after ten years exposition.



(a) (b) (c) (d)

(e) (f) (g)

**Figure 6.** Tomato product cans immerse in the river: (a) after one year exposition, (b) after two years exposition, (c) after three years exposition, (d) after four years exposition, (e) after five years exposition, (f) after eight years exposition and (g) after ten years exposition.



(a) (b) (c) (d)

(e) (f) (g)

**Figure 7.** Tomato product cans discarded in the open air, in an industrial environment: (a) after one year exposition, (b) after two years exposition, (c) after three years exposition, (d) after four years exposition, (e) after five years exposition, (f) after six years exposition and (g) after seven years exposition.



(a) (b) (c) (d)

(e) (f) (g)

**Figure 8.**Tomato product cans discarded in open air, in a marine environment: (a) after one year exposition, (b) after two years exposition, (c) after three years exposition, (d) after four years exposition, (e) after five years exposition, (f) after six years exposition and (g) after seven years exposition.

Observing the photographs in Figures 5 to 8, it was found that the evolution of the degradation of the cans of tomato products, when placed in the soil, is the slowest of the four environments studied, followed by cans placed on the riverbed, the industrial environment and the marine environment. Ten years after placement, the cans of tomato products placed in the soil had slightly discolored outer printing and were without their lids; they had corrosion on the seams, the welds, the body and the base, both outside and inside, as well as dirt stuck to them, however none of the welds was completely opened; all the cans placed in the river had corrosion on the body and the base and two of them had the side seam ruptured due to corrosion; one of the cans still had its lid attached to the body but there was no base, which was separated from the body of the can. It was also noted that, on two of the lids that were loose, the center had come apart from the remainder of the material; fragments of the cans of tomato products placed in industrial and marine environments were found and it was still possible to observe the outer printing, after 7 years.



(a) (b) (c) (d) (e)

(f) (g) (h) (i)

**Figure 9.** Soybean oil cans buried in the ground: (a) after one year exposition, (b) after two years exposition, (c) after three years exposition, (d) after four years exposition, (e) after five years exposition, (f) after six years exposition, (g) after seven years exposition, (h) after eight years exposition and (i) after ten years exposition.



(a) (b) (c) (d)

(e) (f) (g)

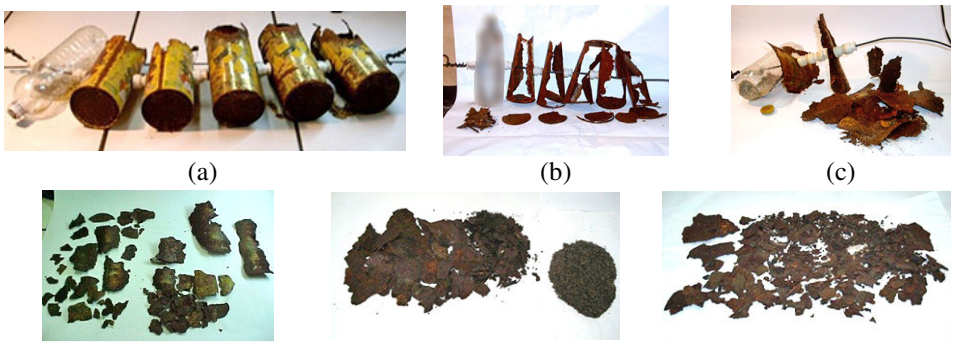
**Figure 10.** Soybean oil cans immersed in the river: (a) after one year exposition, (b) after two years exposition, (c) after three years exposition, (d) after four years exposition, (e) after five years exposition, (f) after eight years exposition and (g) after ten years exposition.



(a) (b) (c) (d)

(e) (f)

**Figure 11.** Soybean oil cans discarded in the open air, in an industrial environment: (a) after one year exposition, (b) after two years exposition, (c) after three years exposition, (d) after four years exposition, (e) after five years exposition and (f) after six years exposition.



(a) (b) (c)

(d) (e) (f)

**Figure 12.** Soybean oil cans discarded in open air, in a marine environment: (a) after one year exposition, (b) after two years exposition, (c) after three years exposition, (d) after four years exposition, (e) after five years exposition and (f) after six years exposition.

Observing Figures 9 to 12, it was found that all the units of cans of oil buried in the soil still had their base while two units still had the lid attached to the body. It was still possible to identify the outer printing on the cans, although the corrosion was quite intensive and the body was already missing some parts after 10 years. Two of the cans placed on the riverbed still had larger parts of the body intact, while only fragments of the other cans could be found after 10 years. As for the cans placed in marine and industrial environments, after 6 years only fragments could be found spread out across the adjacent areas, but it was possible to identify two fragments of seam attached to the parts at the base of the cans of oil in the industrial environment; after 7 years these fragments could no longer be located.



(a) (b) (c) (d) (e)

(f) (g) (h) (i)

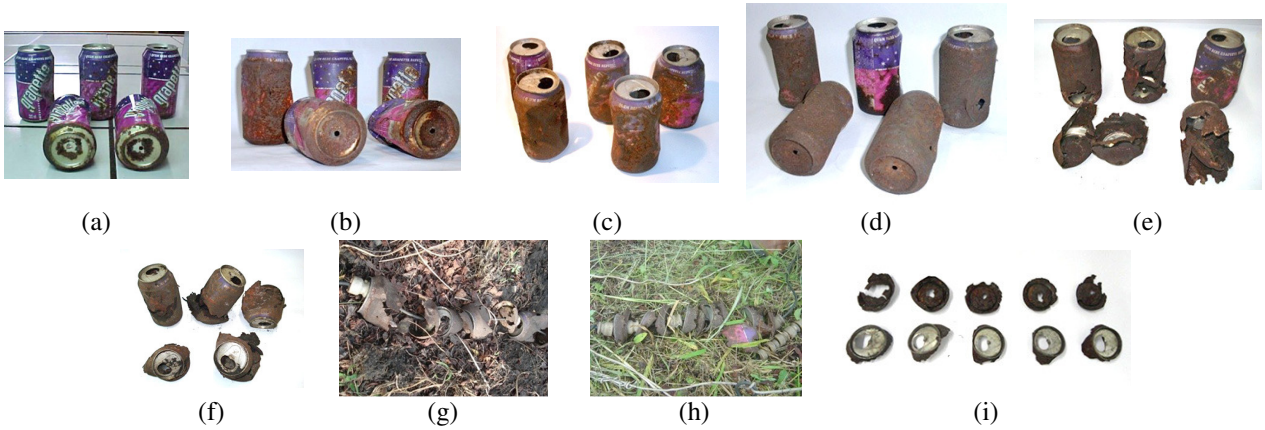
**Figure 13.** Steel DWI cans for soft drinks buried in the ground: (a) after one year exposition, (b) after two years exposition, (c) after three years exposition, (d) after four years exposition, (e) after five years exposition, (f) after six years exposition, (g) after seven years exposition, (h) after eight years exposition and (i) after ten years exposition.



(a) (b) (c) (d)

(e) (f) (g)

**Figure 14.** Steel DWI cans for soft drinks immersed in the river: (a) after one year exposition, (b) after two years exposition, (c) after three years exposition, (d) after four years exposition, (e) after five years exposition, (f) after eight years exposition and (g) after ten years exposition.



(a) (b) (c) (d) (e)

(f) (g) (h) (i)

**Figure 15.** Steel DWI cans for soft drinks discarded in the open air, in an industrial environment: (a) after one year exposition, (b) after two years exposition, (c) after three years exposition, (d) after four years exposition, (e) after five years exposition, (f) after six years exposition, (g) after seven years exposition, (h) after eight years exposition and (i) after ten years exposition.



(a) (b) (c) (d)

(e) (f) (g)

**Figure 16.** Steel DWI cans for soft drinks discarded in open air, in a marine environment: (a) after one year exposition, (b) after two years exposition, (c) after three years exposition, (d) after four years exposition, (e) after five years exposition, (f) after six years exposition and (g) after seven years exposition.

Observing Figures 13 to 16, after 10 years it was found that 5 cans placed in the soil showed external printing with little discoloration and all the lids still had their hatches, though without the easy-open ring-pull tab. There were areas with corrosion over the entire body and less intensive corrosion on the base, mainly in the area of the dome. The module with 5 units of DWI steel cans had already been removed from the soil during a previous collection, as one of the cans was open. Intensive corrosion was observed in the open can as well as perforations in the body; the incidence of corrosion was also found on the base and the lid. All of the DWI steel cans placed in the river, after 10 years, still had their aluminum lid hatches and, on two of them, the base was separated from the body as a result of the intensive corrosion, while on another unit only a part of the body remained maintaining the join with the base, and the corrosion was less intensive in the other two units. The cans placed in the industrial environment were heavily oxidized, with lid and base separated and both were still attached to the small part of the body. No body fragments were found in the experimental field after 10 years. In the marine environment, after 7 years, the cans had fragmented bases and bodies, and it was not possible to identify any printing. Some fragments were scattered in the soil. The aluminum lids exhibited some rust stains and still had their flaps.




(a) (b) (c) (d)

**Figure 17.** Packages produced with other materials buried in the ground after ten years exposition: (a) laminated plastic bag for powdered milk, (b) aluminum DWI cans for soft drinks, (c) carton package for tomato paste (d) PET bottle for soybean oil.

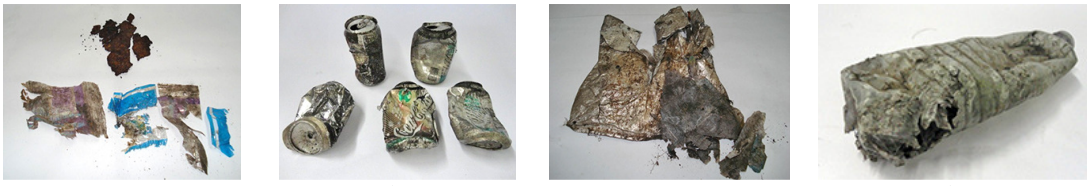
Observing the photographs in Figure 17, it was found that the plastic bag for the powdered milk remained intact after being buried in the soil for 10 years, the module with 5 units of DWI aluminum cans had already been removed from the soil at the time of a previous collection, so one of the cans was open, the outer printing was a little discolored and three of the lids still had their flaps, though without the easy-open ring-pull tab.The external part of all the cans had some form of stain on the body, lid and base and heavy staining was noted on the base with the occurrence of surface corrosion, but without perforation. Inside the open can, small regions were found with the incidence of corrosion spread out over the body, lid and base, but without perforation. The carton packaging of the tomato pulp exhibited delamination with exposure of the aluminum in some areas, intense discoloration, however the most part of the three materials constituting this package was preserved. The PET packaging for the soybean oil was intact, with cap, although the label had become separated.




(a) (b) (c) (d)

**Figure 18.** Packages produced with other materials immersed in the river after ten years exposition: (a) laminated plastic bag for powdered milk, (b) aluminum DWI cans for soft drinks, (c) carton package for tomato paste (d) PET bottle for soybean oil.

Observing the photographs in Figure 18, it can be seen that the plastic bag for powdered milk remained intact, the printing on the aluminum cans showed little discoloration, though did have some corrosion and a presence of dark blotches all over; inside the body of the open can there were areas with corrosion and perforation, as well as some points with corrosion at the base: all lids still had their flaps. The carton packaging for tomato pulp had its plastic material separated from the structure of cellulose material with aluminum and there was no discoloration of the printing on the cap or the label on the PET bottle; both were stained but intact, 10 years after being placed on the riverbed.



(a) (b) (c) (d)

**Figure 19.** Packages produced with other materials discarded in the open air, in an industrial environment: (a) laminated plastic bag for powdered milk, after six years exposition, (b) aluminum DWI cans for soft drinks, after ten years exposition, (c) carton package for tomato paste, after seven years exposition, (d) PET bottle for soybean oil, after ten years exposition.

Observing the photographs in Figure 19, it can be seen that, as regards the laminated bag for powdered milk, only fragments of the plastic layer remained, practically without any metal coating and with the printing discolored, 6 years after being placed in the industrial environment. The aluminum cans had discolored outer printing and corrosion over the whole surface, and perforations, but all the parts were still connected, 10 years after placement in this environment. The remaining portion of the carton packaging for tomato pulp was

composed of a plastic and aluminum material and did not exhibit any printing nor did it have its layer of cellulose material after 7 years and the PET bottle for soybean oil was without its cap and label and, in addition, had parts of its base and body missing, after 10 years.



(a) (b) (c) (d)

**Figure 20**. Packages produced with other materials discarded in open air, in a marine environment: (a) laminated plastic bag for powdered milk, after two years exposition (b) aluminum DWI cans for soft drinks, after seven years exposition, (c) carton package for tomato paste, after seven years exposition, (d) PET bottle for soybean oil, after seven years exposition.

The photograph displayed in Figure 20a is of the plastic bag for powdered milk, two years after being placed in the marine environment. After this period, only fragments of this packaging could be located and they were not photographed.

After 7 years, the printing on the aluminum cans, shown in Figure 20b,was somewhat discolored, two units still had their easy-open ring-pull tab and all the lids still had their flaps. The outer surfaces of the cans were very rough, probably as a result of generalized corrosion. Inside the open can there was some corrosion on the lid and the base, but it was mostly found on the body, however no perforations could be observed. Figure 20c displays a photograph of part of the carton packaging found after 7 years, still with fragments of paper, the majority being made up of aluminum foil and plastic already with delamination. After 7 years, the PET bottle for soybean oil (Figure 20d) did not have its label and the cap was found in the vicinity. It should be pointed out that the marine environment was decommissioned after this sample collection (after 7 years of exposure).

Table 5 shows a summary of the estimated degradation time of the steel packaging placed in the 4 experimental fields studied over a period of up to 10 years.

**Table 5.** Estimate of degradation time (years) of packaging placed in 4 experimental fields studied over a 10 years period.

| Packaging | Estimate of degradation time (years) | | | |
|---|---|---|---|---|
| | Experimental field | | | |
| | Marine(1) | Industrial(2) | Riverbed(3) | Soil(3) |
| Powdered milk (steel can) | 6< t <7 | 6< t <7 | >10 | >10 |
| Tomato products (steel can) | >7 | 7< t<8 | >10 | >10 |
| DWI (steel can) | >7 | >10 | >10 | >10 |
| DWI (aluminum can) | >7 | >10 | >10 | >10 |
| Soybean oil (steel can) | 6< t <7 | 6< t <7 | >10 | >10 |
| Soybean oil in PET bottle | >7 | >10 | >10 | >10 |
| Tomato products in carton packaging | >7 | >7 | >10 | >10 |
| Powdered milk in laminated plastic bag | >6 | >7 | >10 | >10 |

*(1) The marine environment was deactivated after the 7th evaluation as it was not possible to estimate the degradation time of the DWI steel and aluminum cans and the tomato products cans. Of the cans of tomato products, several fragments still remained with a part of the outer printing still visible, enabling us to make the assumption that the degradation time of this packaging was no greater than 7 years. Around 1/3 of the carton packaging was also removed, still with fragments of paper, the majority being represented by the aluminum foil and plastic already with delamination. The PET bottle for soybean oil was without its label and its cap and did not demonstrate any significant alteration. The cap was found in the vicinity. The plastic bag for powdered milk was not located;*

*(2) At the time of the 7th evaluation, pieces related to the aluminum foil and plastic film of the carton packaging were found and the bag for powdered milk showed intense delamination, some parts were missing and there was also discoloring; both sets of packaging were removed from the experimental station. After 10 years, the DWI aluminum cans, a part of the DWI steel cans and the PET bottle still remained.*

*(3) On the riverbed and in the soil, none of the packaging had fully degraded over the period of 10 years.*

## 4 Conclusions

Considering as the criterion for the determination of packaging degradation time the inability to distinguish the fragments found in the experimental fields, by virtue of their appearance, after ten years of exposure to the different environments, it was found that:

- The order of aggressiveness of the four tropical environments used as the experimental fields may be established as follows: marine atmosphere >industrial atmosphere > riverbed >soil;
- The steel packaging placed in marine and industrial environments already showed an intense level of degradation in the early years of exposure;
- The steel packaging for powdered milk and soybean oil, placed in marine and industrial environments, was considered to be completely degraded within a period of 6 to 7 years;
- The steel packaging for tomato products, placed in the industrial environment, was considered to be completely degraded within a period of 7 to 8 years;
- None of the steel packaging buried in the soil or submersed on the riverbed was completely degraded within the period of 10 years;
- Amongst the packaging manufactured from other materials, PET bottles and aluminum cans of beverages were the ones that demonstrated the fewest alterations in the 4 test environments. Laminated plastic bags and carton packaging presented greater fragmentation, especially in marine and industrial environments. This fragmentation occurred ostensibly through the physical action of the environment.

## Acknowledgements

The authors would like to thank the entire technical team at CSN involved in the project, the companies Companhia Metalúrgica Prada, Nestlé Brasil Ltda. And Companhia Metalic do Nordeste for supplying the steel packaging used in the study, professor Isabel Cristina Pereira Margarit (COPPE/UFRJ), Thaís Fagury (ABEAÇO), Marcos Sérgio de Souza, Cristina Hitoe Makino and Verônica Pascoarelli for their participation in several of the project phases.

## References

1 BROMANDER, A. L.; “Self-destruction” of metal containers: results from a 20 year long environmetal test run ; The Canmaker, West Sussex, , v. 2, p. 17-19, 1989.

2 SANTOS, J. L. C.; ARAUJO, I.; SANTOS, W. R.; SÁ, T. F.; GATTI, J. A. B.; DANTAS, S. T.; Average time estimate for the degradation of steel packagings in tropical environments; 22nd IAPRI Symposium, Campinas, Brazil, 2005.

3 FERREIRA, L. S. **Reciclagem das latas de aço**. Monografia do curso de Especialização em Engenharia de Embalagem. Escola de Engenharia Mauá, São Paulo, 2003. 29p.

4 CEMPRE – COMPROMISSO EMPRESARIAL PARA A RECICLAGEM. **Latas de aço**: O mercado para a reciclagem. Fichas técnicas. São Paulo Disponível em: < http://www.cempre.org.br/ft_latas_aco.php>. Acesso em: 27 fev. 2014.

5 SANTOS, J. L. C.; SANTOS, W. R.; GERMANO, R. L. S. et al. Estimativa do tempo médio de degradação das embalagens de aço em ambientes tropicais.In: CONGRESSO ANUAL DA ASSOCIAÇÃO BRASILEIRA DE METALURGIA, MATERIAIS E MINERAÇÃO, 65., 2010, Rio de Janeiro, RJ. **Anais...** São Paulo, SP: ABM, 2010. 17 p.

# Characteristics of Active Natural Fibre Reinforced Poly(lactic acid) Composites

**Intan S. M. A. Tawakkal[1], Marlene J. Cran[2*] and Stephen W. Bigger[1]**

[1] *College of Engineering and Science, Victoria University, PO Box 14428, Melbourne, 8001, Australia.*
[2] *Institute for Sustainability and Innovation, Victoria University, PO Box 14428, Melbourne, 8001, Australia*

[*] *Corresponding author. Email: marlene.cran@vu.edu.au*

**Abstract:** The use of bio-based polymers as alternatives to synthetic polymers has increased extensively in recent years for a wide range of applications. Food packaging, in particular, has seen a growth in the use of materials derived from natural and renewable resources such as poly(lactic acid) (PLA). In many cases, however, the initial costs associated with new technologies to produce biopolymers that rival synthetically derived materials are typically high so new techniques must be sought to reduce costs without compromising material properties. Naturally sourced fibres such as kenaf are often used as cost-reducing fillers for PLA. In some cases the fibres can be treated by alkalization to improve the compatibility with the polymer matrix. This work explores the thermal and mechanical properties of PLA composites incorporated with treated or untreated kenaf fibres (kenaf) together with the addition of thymol, a natural antimicrobial substance. Composites of PLA incorporated with 30% w/w kenaf and 10% w/w thymol were prepared and compared with control systems containing either no kenaf or no thymol. The composites containing treated kenaf had significantly higher tensile strength than composites prepared with untreated fibres. Micrograph images of the fracture surface revealed better adhesion between the treated fibres and the matrix was achieved resulting in improved reinforcement of the composite. In addition, composites containing thymol demonstrated lower tensile strength than those without thymol suggesting a possible plasticizing effect in the presence of the additive. Thermal analysis by differential scanning calorimetry showed similar trends for composites containing treated and untreated fibres with decreases in the glass transition temperature, cold crystalline temperature, melting temperature and melting enthalpy with the addition of thymol. The results suggest that composites containing treated kenaf in particular have a potential for the development of food packaging materials.

Keywords: poly(lactic acid), kenaf fibre, antimicrobial, composites, tensile properties.

## 1 Introduction

Growing environmental awareness among consumers and plastics manufacturers has driven research in the development of biodegradable packaging materials. The synthesis of bio-based polymers from naturally derived products such as polysaccharides, proteins and lipids is one of the many crucial strategies to minimise the usage of traditional plastics made from petrochemical sources. Poly(lactic acid) (PLA) can be synthesized from renewable resources such as starch and is one of the more promising bio-based polymers available in the market [1]. For packaging applications, this polymer provides good strength, compostability and easy processability and has therefore gained attention as an alternative to petroleum-based plastics such as polystyrene (PS). Although the potential of PLA for use in packaging applications has been established [2], there are some inherent limitations of this material. In addition to the high production costs, PLA has poor water vapour and gas barrier properties and high brittleness that limits its widespread application in packaging.

The use of natural fibres as a filler/reinforcement is a simple and effective approach to modify polymer material properties and reduce overall material costs. The incorporation of natural fibres such as wood flour, kenaf, flax and ramie into bio-based polymer matrices has recently gained attention in order to reduce costs, improve compatibility and mechanical properties as well as enhance biodegradability. Kenaf (*Hibiscus cannabinus* L.) with approximately 53.4% cellulose content has demonstrated good mechanical properties that enable it to be used as reinforcement in polymer composites as an alternative to glass fibres [3]. There are several well-established and recommended pre-treatments of kenaf fibres including graft copolymerisation, the use of coupling agents as well as alkali chemical treatment. In addition to the use of fibres, the use of some naturally derived additives can also provide additional functional properties of PLA packaging materials. One example is the use of antimicrobial (AM) agents to extend the shelf life of packaged food products by minimizing the growth of microorganisms on food surfaces. Thymol, for example, is an essential oil extract obtained from several plant species and is a well-established natural AM agent [4].

The compatibility between the main elements in a composite system comprised of a PLA matrix, kenaf and natural AM substances could potentially contribute to the biodegradability and sustainability of the system as a whole. The aim of the present study is to explore the mechanical, thermal and morphological properties of PLA composites incorporated with treated and untreated kenaf-containing thymol.

## 2 Materials and Methods

### 2.1 Materials

Poly(lactic acid) (7001D Ingeo$^{TM}$) with a specific gravity of 1.24 and melting temperature range from 145 to 160°C was used in this study and was purchased from NatureWorks LLC, USA. The kenaf bast fibre was purchased from Ecofibre Industries, Australia and thymol (T0501) of 99.5% purity was purchased from Sigma Aldrich Pty. Ltd., Australia. Chemicals for fibre treatment such as sodium hydroxide and acetic acid were purchased from Merck Chemicals, Australia.

### 2.2 Preparation of Composites

Surface treatment of the kenaf fibres was performed by immersing them in 5% w/v NaOH for 2 h at room temperature. Acetic acid was used to adjust the pH during the washing and rinsing of the fibres with distilled water. Kenaf fibres were taken out of the solution and dried overnight in an air oven at 105°C. Prior to mixing with the PLA resin the fibres were dried in an oven at 60°C overnight before blending with thymol at 10% w/w of the latter. Polylactic acid/kenaf composites (with and without thymol) were compounded using an internal mixer (Haake PolyLab OS, Germany) at 50 rpm and 155°C for 8 min. Films and slabs of 0.3 and 3 mm in thickness respectively were prepared using a laboratory press (L0003, IDM Instrument Pty. Ltd., Australia). The composites were preheated at 150°C for 2 min and pressed at the same temperature for 3 min under a pressure of 50 kN before quench cooling to 30°C under pressure. A hand-held micrometer (Hahn & Kolb, Stuttugart, Germany) was used for measuring film thickness.

### 2.3 Tensile Testing

Samples for tensile testing were prepared and tests were performed using a Model 4301 Instron Universal Testing Machine with a load cell of 1 kN. Each tensile test was conducted at a cross-head speed of 5 mm min$^{-1}$ on dumbbell-shaped specimens in accordance with ASTM D638 Type V until tensile failure was detected. The average tensile strength, tensile modulus and percentage extension at break were calculated from the stress-strain curves. A total of six replicates were tested.

### 2.4 Thermal Analyses

A differential scanning calorimetry (DSC) instrument (Mettler Toledo DSC1) under an inert nitrogen gas was used to obtain the thermal properties of the PLA and composites. The samples of *ca.* 8-9 mg each were weighed and sealed in aluminium pans. The heating was performed from 30 to 300°C at a rate of 10°C min$^{-1}$ and with a nitrogen flow rate of 20 mL min$^{-1}$. The glass transition temperature ($T_g$), cold crystallisation temperature ($T_{cc}$), melting temperature ($T_m$) and melting enthalpy ($\Delta H_m$) were obtained from the DSC thermogram curves. The degree of crystallinity ($\%X_c$) of each sample was determined from the ratio between the melting enthalpy of the sample and that of a 100% crystalline PLA assumed to be 93.1 J g$^{-1}$ [5].

### 2.5 Imaging of Composites

To observe the morphology of untreated and treated kenaf as well as the tensile fracture surface of composites scanning electron microscopy (SEM) was performed using a JOEL NeoScope (JCM-5000) scanning electron microscope instrument. All samples were coated with a thin layer of gold (6 nm) using a NeoCoater (MP19020NCTR) under high vacuum and using an accelerating voltage of 10 kV in order to eliminate charging effects.

## 3 Result and Discussion

### 3.1 Morphology of Kenaf and Composites

Micrographs of untreated and treated kenaf fibres obtained using SEM are shown in Figures 1(a) and (b). It is evident that there are differences between the surface topography of these samples with the treated kenaf (Figure 1(a)) showing a slightly rougher fibre surface that is observed when the microfibrils are partially revealed following alkaline treatment. Increasing the surface roughness provides better fibre-matrix interface

adhesion due to the improved mechanical interlocking and thus, increases the mechanical properties [6]. Figures 1(c) and (d) show SEM micrographs of a tensile fracture surface of PLA/kenaf composites. For both of these composites, it appears that the kenaf fibres are well dispersed throughout the polymer matrix. For the PLA/kenaf composite containing no thymol (Figure 1(c)), the treated kenaf fibres appear to be more tightly bound to the matrix compared to the composite in which thymol is present (Figure 1(d)). The presence of thymol in the matrix appears to act as a lubricant or plasticizer that facilitates the slippage of the fibres out of the matrix during fracture and this is shown in Figure 1(d) with the presence of more protruding fibres at the matrix surface. The smooth surfaces of some of the fibres, as well as the voids, suggests that there is weaker adhesion between the fibres and the PLA matrix when thymol is present in the formulation.

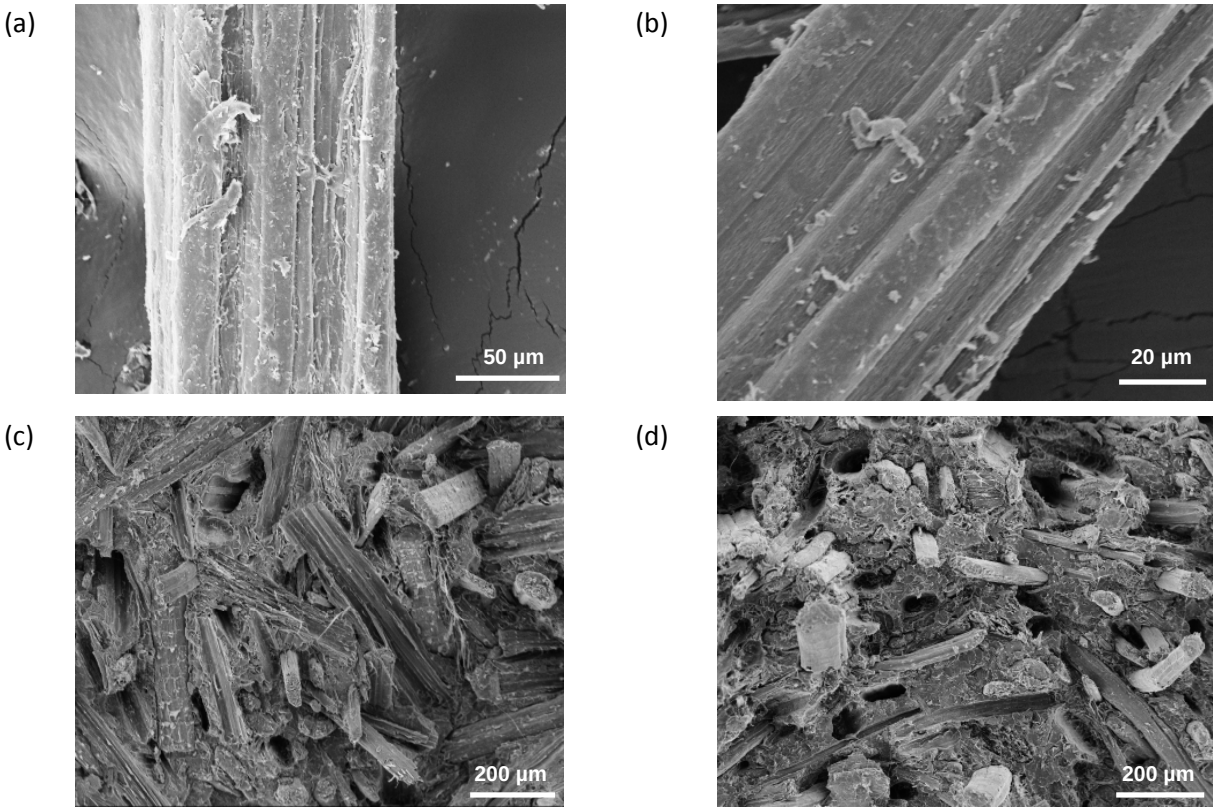



**Figure 1**. Scanning electron micrographs of: (a) untreated kenaf at 50× magnification, (b) treated kenaf at 20× magnification, (c) PLA containing treated kenaf at 200× magnification and (d) PLA containing treated kenaf and 10% w/w thymol at 200× magnification.

### 3.2 Tensile Properties

Figure 2 shows the effect of untreated and treated kenaf fibre composites on the tensile properties of composites containing zero and 10% w/w thymol. The results show that the tensile strength of PLA filled with treated kenaf and containing no thymol was slightly higher than the untreated kenaf composites as well as the neat PLA (see Figure 2(a)). This result suggests that the treated kenaf acts as a reinforcement that provides an approximately 8% increase in the tensile strength. The slight improvement in the tensile strength is possibly due to better interfacial adhesion between the PLA matrix and the treated kenaf. The alkaline treatment of the fibres enhances the fibre surface roughness, leads to fibre fibrillation and improves fibre-matrix adhesion. No significant changes in the tensile strength of the neat PLA and the untreated kenaf composite were observed.

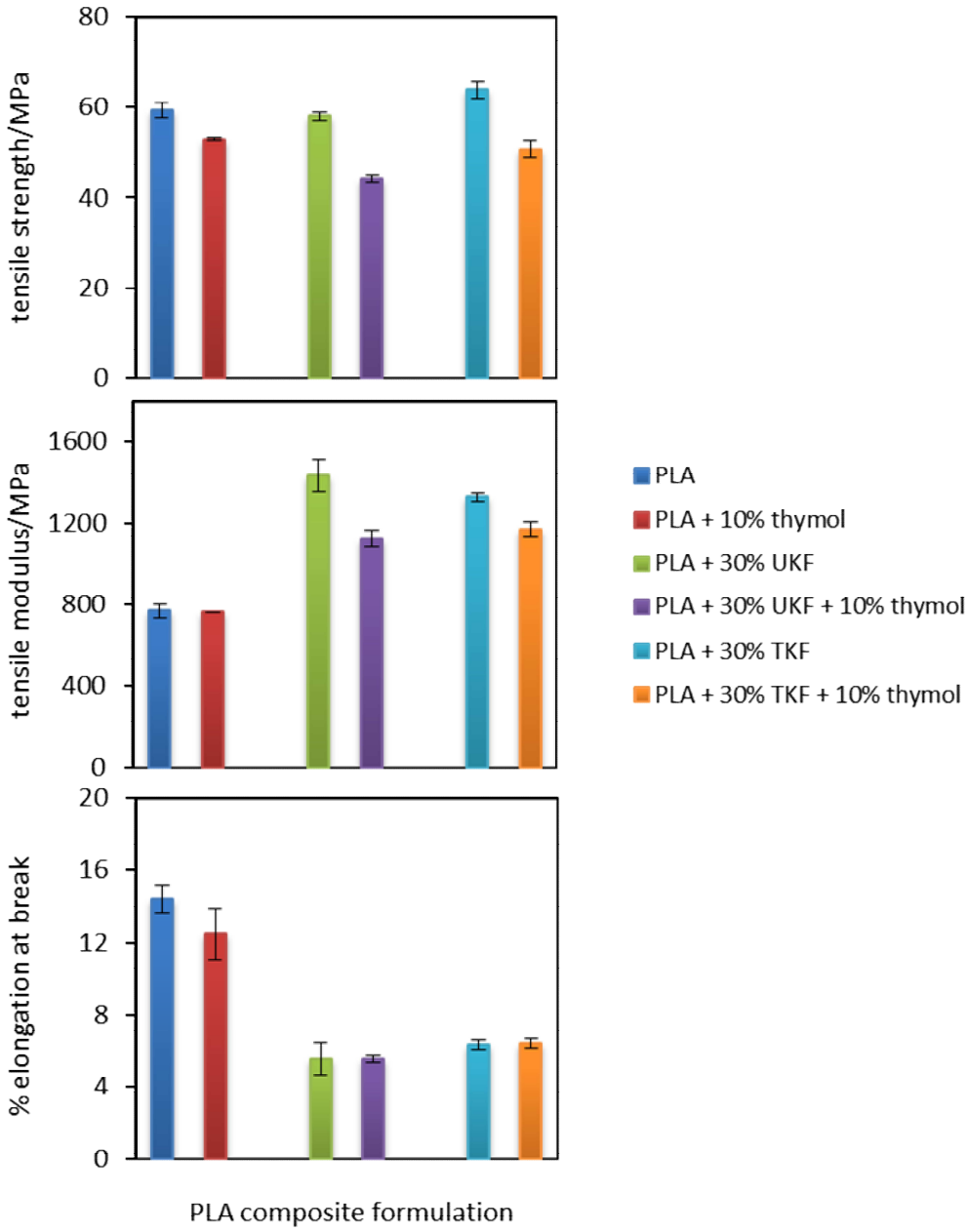



**Figure 2**. Tensile properties of PLA formulations containing zero and 10% w/w thymol: (a) tensile strength, (b) tensile modulus and (c) % elongation at break.

The addition of 10% w/w thymol into the neat PLA and the PLA/kenaf composites containing untreated and treated kenaf caused a significant reduction in tensile strength compared with those formulations without thymol. The reduction in the tensile strength was found to be 11%, 24% and 21% for neat PLA, untreated and treated kenaf composites respectively. This may be due to the plasticizing effect of thymol within the PLA matrix where the additive interferes with the interaction between the PLA matrix and the kenaf during the applied stress. This finding is consistent with the observations made in assessing the SEM micrograph image in Figure 1(b). In addition, the composites containing fibre and 10% w/w thymol demonstrated lower tensile strength than the neat PLA containing only 10% w/w thymol.

The effect of untreated and treated kenaf composites on the tensile modulus and elongation at break containing zero and 10% w/w thymol is also shown in Figure 2. The tensile modulus of the untreated and treated kenaf composites significantly increases over that of the neat PLA by *ca*. 80% (see Figure 2(b)). This may be due to the presence of the kenaf, an inherently high stiffness material, and is in agreement with the work of Sujaritjun *et al.* [7] who incorporated PLA with 30% w/w bamboo fibres and found an increase in the tensile

modulus of *ca.*17%. Figure 2(b) also shows the reduction in tensile modulus that occurs upon the addition of 10% w/w thymol. No significant changes in tensile modulus of neat PLA containing 10% w/w thymol were observed in the present study. For the PLA/kenaf composites containing 10% w/w thymol, there was no significant difference between the treated and untreated fibre surface on the tensile modulus. This may also be due to the decrease in the stiffness of the material due to the plasticizing effect of adding the thymol into the PLA/kenaf composites as evidenced in Figure 2(a).

Figure 2(c) shows the effect of untreated and treated kenaf fibres on the elongation at break of composites containing zero and 10% w/w thymol. In general, the elongation at break of both of these composites containing decreases with the addition of kenaf fibres. This is consistent with the notion that the presence of the kenaf does not contribute to the elasticity or the final composite flexibility and this observation is likely to be related to the high stiffness of the composites as indicated by the results in Figure 3(a). No significant changes in the elongation at break of any of the composites containing kenaf fibre were observed upon the addition of 10% w/w thymol. The samples of neat PLA containing 10% w/w thymol exhibited slightly lower values of the elongation at break compared with the neat PLA without thymol. This finding is similar to that reported by Liu *et al.* [8] who incorporated 5% w/w loadings of both Nisaplin and EDTA into plasticized PLA/glycerol triacetate films and observed a significant reduction of the elongation at break from 108.5 to 62.5% compared to the plasticized PLA.

### 3.3 Thermal Analysis

Table 1 shows a summary of the key findings from the DSC thermograms of PLA and PLA containing untreated and treated kenaf fibres with zero and 10% w/w thymol. Neat PLA exhibited an onset $T_g$ at 59.5°C and $T_{cc}$ at 92.2°C. The onset $T_m$ was observed to be 141.7°C which is in the typical range for this polymer [9]. The incorporation of untreated kenaf into the PLA matrix resulted in no significant changes to the $T_g$ value whereas a slight decrease in the $T_g$ was observed for the treated kenaf composite. No significant changes were observed for the onset $T_{cc}$, $T_{m1}$ and $T_{m2}$ of the PLA composites containing untreated and treated kenaf however, these values for both composites were slightly lower than that of neat PLA. The degree of crystallinity of the composites containing treated kenaf was slightly higher than neat PLA and this finding is in agreement with the work of Du *et al.* [10] who investigated PLA containing 30% w/w pulp fibres from hardwood, softwood and bleached kraft wood. This suggests that the alkaline surface treatment enhances the crystallinity of the resulting composites.

**Table 1**. Thermal analysis data obtained from DSC thermograms of neat PLA, and composites of PLA/kenaf and PLA/kenaf/thymol.

| PLA formulation | Thymol content %w/w | $T_g$ /°C | $T_{cc}$ /°C | $T_{m1}$/°C | $T_{m2}$/°C | $\Delta H_m$/ J g$^{-1}$ | $X_c$/% |
|---|---|---|---|---|---|---|---|
| PLA | 0 | 59.5 | 92.2 | 141.7[a] | 150.5 | 26.1 | 28.0 |
| | 10 | 41.3 | 85.3 | 124.1 | 137.5 | 22.2 | 26.5 |
| PLA/UKF | 0 | 59.7 | 92.6 | 137.1 | 145.0 | 17.5 | 26.6 |
| | 10 | 27.7 | 75.2 | 113.2 | 126.7 | 14.8 | 26.3 |
| PLA/TKF | 0 | 58.7 | 92.1 | 136.9 | 145.1 | 19.1 | 29.1 |
| | 10 | 31.4 | 77.4 | 115.0 | 128.7 | 15.1 | 26.9 |

a. Shoulder on main DSC peak.

The thermogram of the Neat PLA presents a double melting peak with the dominant peak at higher temperature (data not shown). With the addition of kenaf, the double melting peaks became quite distinct. The appearance of these dual melting peaks is in accordance with other reports where the addition of fibres resulted in the development of a small melting peak that shifted to a lower temperature upon further addition of fibres [10, 11]. The minor peak may be due to either a different PLA crystal type formed only in presence of the fibres and/or the melting of the transcrystalline zone [12]. Thermal analysis of neat PLA and PLA composites loaded with 30% w/w untreated and treated kenaf containing 10% w/w thymol showed that in general, the addition of 10% w/w thymol in neat PLA and PLA/kenaf composites resulted a decrease in $T_g$ and $T_{cc}$ (Table 1). This may be due to the plasticising effect of thymol that reduces the $T_g$ value. The observed plasticising effect reflected in the $T_g$ values is consistent with the findings from the morphology images and tensile properties of neat PLA and PLA kenaf composites containing thymol (see Figures 1 and 2).

## 4 Conclusions

The results of this study indicate that the tensile properties and thermal stability of PLA are affected by the addition of chemically treated kenaf fibres. The presence of the treated kenaf fibres increases the tensile strength and tensile modulus of PLA as well as the thermal stability at the maximum degradation temperature. However, some deterioration of the tensile properties in the presence thymol was observed due to the reduced compatibility between the fibres and PLA in the presence of this agent. Compared to untreated kenaf fibres, the treated kenaf when combined with PLA and thymol results in significant improvement in the overall properties of the material and this composite has the potential to be used as an active bio-based packaging material.

## Acknowledgements

The authors would like to gratefully acknowledge technical staff from Royal Melbourne Institute Technology (RMIT) for the preparation of the composites samples.

## References

[1] M. Jamshidian, E. A. Tehrany, M. Imran, M. Jacquot, and S. Desobry, Poly-lactic acid: Production, applications, nanocomposites, and release studies, Comprehensive Review Food Science and Food Safety (2010) 9 552-571.

[2] M. Jamshidian, E. A. Tehrany, and S. Desobry, Antioxidants release from solvent-cast PLA film: Investigation of PLA antioxidant-active packaging, Food Bioprocess Technology (2013) 6 1450-1463.

[3] H. P. S. Abdul Khalil, A. F. I. Yusra, A. H. Bhat, and M. Jawaid, Cell wall ultrastructure, anatomy, lignin distribution, and chemical composition of Malaysian cultivated kenaf fiber, Industrial Crops and Products (2010) 31 113-121.

[4] P. Falcone, B. Speranza, M. A. Del Nobile, M. R. Corbo, and M. Sinigaglia, A study on the antimicrobial activity of thymol intended as a natural preservative, Journal of Food Protection (2005) 68 1664-1670.

[5] D. E. Henton, P. Gruber, J. Lunt, and J. Randall, *Polylactic acid technology*, in *Natural fibers, biopolymers and biocomposites*, A.K. Mohanty, M. Misra, and L.T. Drzal, Eds. 2005, CRC Press London. p. 527-577.

[6] M. S. Huda, L. T. Drzal, A. K. Mohanty, and M. Misra, Effect of fiber surface-treatments on the properties of laminated biocomposites from poly(lactic acid) (PLA) and kenaf fibers, Composites Science and Technology (2008) 68 424-432.

[7] W. Sujaritjun, P. Uawongsuwan, W. Pivsa-Art, and H. Hamada, Mechanical Property of Surface Modified Natural Fiber Reinforced PLA Biocomposites, Energy Procedia (2013) 34 664-672.

[8] L. S. Liu, T. Jin, D. R. Coffin, C. K. Liu, and K. B. Hicks, Poly(lactic acid) membranes containing bacteriocins and EDTA for inhibition of the surface growth of gram-negative bacteria, Journal of Applied Polymer Science (2010) 117 486-492.

[9] Y. Byun, Y. T. Kim, and S. Whiteside, Characterization of an antioxidant polylactic acid (PLA) film prepared with α-tocopherol, BHT and polyethylene glycol using film cast extruder, Journal of Food Engineering (2010) 100 239-244.

[10] Y. Du, T. Wu, N. Yan, M. T. Kortschot, and R. Farnood, Fabrication and characterization of fully biodegradable natural fiber-reinforced poly(lactic acid) composites, Composites Part B: Engineering (2014) 56 717-723.

[11] C. Prapruddivongs and N. Sombatsompop, Roles and evidence of wood flour as an antibacterial promoter for triclosan-filled poly(lactic acid), Composites Part B: Engineering (2012) 43 2730-2737.

[12] A. A. Yussuf, I. Massoumi, and A. Hassan, Comparison of polylactic acid/kenaf and polylactic acid/rise husk composites: The influence of the natural fibers on the mechanical, thermal and biodegradability properties, Journal of Polymers and the Environment (2010) 18 422-429.

# Properties of Corrugated Liner Made from Musa Sapientum Linn Banana Pulp and Recycled Kraft Pulp

**Nucharin Luangsa-Ard[1*] and Komsant Wiwatchaimaneee[2]**

[1] *Department of Printing and Packaging Technology, King Mongkut's University of Technology Thonburi, Thailand*

[2] *Department of Printing and Packaging Technology, King Mongkut's University of Technology Thonburi, Thailand*

[*] *Email: nucharin.lua@kmutt.ac.th*

**Abstract:** This research was aimed to examine and compare physical and mechanical properties of corrugated liner made of banana pulp mixed with recycled kraft pulp and virgin kraft pulp mixed with recycled kraft pulp as well as to estimate the production cost of banana pulp, and to compare with the cost of imported virgin kraft pulp. Initially, banana pulp was cooked in a closed system with the use of Sodium Hydroxide, then handsheets of 125 grams were produced by mixing recycled kraft pulp with banana fiber at 10, 20, 30, 40 and 50 percent (on oven dry weight). Later, their physical and mechanical properties were measured. The results showed that the optimal condition for cooking banana pulp was with the use of 20 percent Sodium Hydroxide, and its yield was 29.2 percent. It was found that the samples made of banana pulp mixed with recycled kraft pulp at 50:50 had the optimal physical and mechanical properties. The results also indicated that the virgin kraft pulp mixed with recycled kraft pulp samples yielded higher tearing strength, tensile strength and bending resistance than the banana pulp mixed with recycled kraft pulp samples. However, banana pulp mixed with recycled kraft pulp samples performed better with respect to ring crush resistance and bursting strength. Lastly, the production cost of banana pulp was 23,058 Baht/ton and the import cost of virgin kraft pulp was 24,000 baht /ton.

Keywords: Banana Pulp, Recycle kraft Pulp, Corrugated Liner.

## 1 Introduction

Paper is an important material in the implementation of human activities such as office document, publication printing, packaging and etc. Currently, the role of paper using is increasing steadily especially in packaging industries. Corrugated board is widely used as packaging paper since it has suitable properties such as durability, lightweight, economical and environmentally friendly and etc. Therefore, corrugated board is counted as an essential and highly desirable packaging material.

Paper is consisted of many compositions such as short fiber, long fiber, and some chemicals that mixed and formed into a sheet of paper. These compositions can be divided into two major parts which are fibrous and non-fibrous materials. Fibrous material is formed into structure of the paper and non fibrous materials are additives that added to improve paper properties in order to meet the purposes of the use of each type of paper [1].

Basically, paper has 70-95% of fibrous material and the amount of fibrous material is depended on each type of produced paper. In general, fibrous material or fiber in paper is a mixture of long fiber and short fiber. At present, pulp manufacturing in Thailand can produce only short fiber which comes from local plants such as bagasse, bamboo, rice straw and eucalyptus. For long fibers which produced from softwood such as pine, cedar and spruce however, Thailand does not have enough softwood for pulp manufacturing. Therefore, pulping and papermaking industries in Thailand have to import long fiber pulp from overseas countries [2].

In general, long fibers have average fiber length around 3-5 mm. and long fibers also provide good fiber-bonding within paper. These long fibers will enhance better mechanical properties such as tensile strength, tear strength as well as better runnability to the paper. Since long fibers are vital raw material for packaging papermaking therefore Thailand has to import them from abroad. In addition, old corrugated containers (OCC) are also imported from the US. to use as recycled kraft pulp while virgin long fibers are mostly ordered from Canada (Alberni fiber), Switzerland (Spring wood fiber) and Sweden (Frovifors and Billerund fiber) [2].

Musa Sapientum Linn banana is one of popular banana specie that can be planted in all weather conditions in Thailand. Generally, bananas are very easy to grow and their stem and leaves can be used in many ways. When all bananas are first harvested, farmers will usually cut the stems down since newly planted banana trees will

give better quality bananas than old banana trees. Later, all eliminated banana trees will cause some environmental problems such as air pollution and waste. This rotten waste eventually will become a source of pathogens and habitats of some poisonous animals or insects [3]. Therefore, in order to minimize the problems from abundant of unwanted banana trees, the researchers were interested in using these banana trees to produce paper pulp. Since banana fiber is categorized as long fiber, then the researchers tried to use banana pulp for corrugated liner production by mixing it with recycled kraft pulp or mixing it with virgin long fiber pulp. Later, physical and mechanical properties of all produced samples were examined and compared. Furthermore, the estimating cost of banana pulping manufacturing was also compared with the cost of imported virgin long fiber pulp from overseas countries.

## 2 Materials and Methods

In this research, banana trees average age of 6 months, from Nueng Sua district, Prathumthani province, were cut. The banana stems then were cut into pieces around 3x1 inch and they were air dried. Dry matter content (DMC) of banana chips was calculated according to ISO 638:1978. Recycled kraft pulp (OCC pulp) and virgin kraft pulp were sponsored by SCG paper groups, Thailand.

For banana pulping, the banana chips were cooked in the autoclave digester (CRS, Reactor Engineering, Italy) by the use of Sodium hydroxide (NaOH) under cooking condition as shown in table 1.

**Table 1**: Cooking condition of banana pulp (closed system)

| | **Cooking Condition** |
|---|---|
| Banana chip (g) | 200 |
| NaOH charge (%) | 20 |
| Cooking Temperature (°C) | 170 |
| Cooking time (min.) | 120 |
| Wood : Liquid ratio | 1:6 |

The first set of handsheets were made at 125 grams by mixing banana pulp with recycled kraft pulp at different ratio of 10:90,20:80,30:70,40:60 and 50:50 on oven dried weight (OD. weight). The second set of handsheet were made by mixing virgin kraft pulp with recycled kraft pulp at ratio 30:70 (the ratio used for KI making; one type of kraft paper from SCG paper groups, Thailand)[4]. Consequently, both set of produced samples were measured for grammage, thickness, air permeability, tearing strength, tensile strength, bending strength, water absorbency, ring crush resistance and bursting strength according to SCAN –P6, SCAN –P7, SCAN –P60, SCAN –P11, SCAN –P11, SCAN –P67, SCAN –P29, SCAN –P12, SCAN –P34 and SCAN –P24, respectively. Consequently, chose the best ratio from the first set handsheet (which gave the best results in both physical and mechanical properties) for further study in the next part [5].

For the second set of handsheet, the banana pulp was refined in PFI mill (Mark VI Hemjern Maskin Hamar, Norway) at three levels; 3,000, 6,000, and 9,000 rpm to make handsheet at ratio 50:50 of banana pulp mixed with recycled kraft pulp. Later, all the handsheets were tested by the same procedures as previous part. Finally, the assessment cost of banana pulping were assessed by calculating all processes including raw materials preparation, chemicals, energy and water consumption, as well as maintenance costs and then compared the cost of imported virgin kraft pulp with banana pulping production cost

## 3 Results and Discussion

### 3.1 Production of banana pulp for corrugated liner making

From the experiment, it was found that at the cooking condition of 20% NaOH charged, temperature at 170 °C, cooking time of 120 mins., and wood : liquid ratio at 1:6, was the optimal condition for banana pulping and the cooking yield was 29.2%. Consequently, the banana pulp was mixed with recycled kraft pulp to form handsheet at different ratio and the data of physical and mechanical properties was showed in table 2 and 3.

### 3.2 Physical and mechanical properties of handsheets

**Table 2:** Physical and mechanical Properties of the Banana pulp mixed with recycled kraft pulp handsheets and virgin kraft pulp mixed with recycled kraft pulp handsheets.

| Test | Banana pulp : OCC pulp | | | | | Virgin Kraft pulp : OCC pulp |
|---|---|---|---|---|---|---|
| | 10:90 $\bar{x}$ ± std. | 20:80 $\bar{x}$ ± std. | 30:70 $\bar{x}$ ± std. | 40:60 $\bar{x}$ ± std. | 50:50 $\bar{x}$ ± std. | $\bar{x}$ ± std. |
| Basis Weight (grammage) | 128± 2.78 | 128± 1.38 | 129± 1.22 | 129 ± 0.75 | 130 ± 1.09 | 126± 1.12 |
| Thickness (micron) | 264 ± 12.6 | 262 ±5.77 | 274 ±3.34 | 280 ± 7.18 | 273 ± 9.81 | 264 ± 3.34 |
| Air permeability (ml/min) | 1136 ±6.29 | 866 ± 6.40 | 535 ± 4.52 | 419 ± 4.41 | 327 ± 3.88 | 2214 ± 10.17 |
| Tear strength index (mN/g/m$^2$) | 7.69± 0.72 | 11.0± 0.99 | 12.0± 0.85 | 12.3± 0.63 | 13.4± 0.79 | 14.3± 0.99 |
| Tensile strength Index (Nm/g) | 23.4± 0.84 | 23.7± 1.67 | 24.0± 0.94 | 25.2± 1.52 | 25.4 ± 1.35 | 25.7 ± 0.85 |
| Bending resistance (mN) | 56.8± 1.26 | 1.43 ± 56.6 | 55.9± 1.09 | 55.7± 1.47 | 54.5± 0.89 | 60.2± 1.27 |
| Water Absorbency)g/m$^2$) | 242± 4.43 | 242 ± 3.82 | 243± 5.79 | 243± 5.60 | 243± 5.98 | 298± 6.63 |
| Ring Crush Resistance (N) | 100± 1.58 | 102± 1.26 | 104± 1.19 | 117± 1.41 | 136± 1.49 | 90.3± 1.33 |
| Burst Resistance (kg/cm$^2$) | 2.67± 0.09 | 2.89± 0.08 | 3.15± 0.10 | 3.30 ± 0.06 | 3.42± 0.07 | 2.75± 0.11 |

The data from table 2 indicated that the samples produced from virgin kraft pulp mixed with recycled kraft pulp had basis weight of 126 gram while the samples made from banana pulp mixed with recycled kraft pulp had basis weight around 128-130 gram. Though, the target basis weight of the samples in this experiment was 125 gram, but all the produced samples were around 126-130 gram. This variances or errors might be from some experimental errors that occurred during the handsheets forming. Likewise, thickness of the samples made from virgin kraft pulp mixed with recycled kraft pulp (264 micron) was thinner than thickness of all the samples made from banana pulp mixed with recycled kraft pulp (262-280 micron). Normally, banana fiber is bulkier than virgin kraft fiber therefore the samples made from banana fibers would have higher thickness than the samples made from virgin kraft pulp [6,7].

For air permeability aspect, the dada showed that the sample made from virgin kraft pulp mixed with recycled kraft pulp had higher air permeability (2,214 mL./min.) than all the samples made from banana pulp mixed with recycled kraft pulp (327 – 1,136 mL./min.). It could be summarized that banana fibers gave a better fiber-to-fiber bonding than virgin kraft fibers, therefore the air could not easily flow through the virgin kraft samples [6].

According to the data from table 2, it was indicated that tear and tensile strength index as well as bending resistance of the samples made from virgin kraft pulp mixed with recycled kraft pulp were higher than tear and tensile strength index and bending resistance of the sample made from banana pulp mixed with recycled kraft pulp. Theoretically, virgin kraft fiber length is 3-4 mm. and banana fiber length is 3.13 mm.. The longer fiber length will provide higher tearing and tensile strength index as well as bending resistance to the paper; therefore the samples made from virgin kraft pulp should have better tearing and tensile strength as well as bending resistance. Moreover, virgin kraft fibers also has better fiber to fiber bonding than banana fibers therefore, the samples made from virgin kraft pulp were eventually stiffer or tougher than all the samples made from banana pulp [8].

For water absorbency aspect, it was found that the samples made from virgin kraft pulp mixed with recycled kraft pulp was higher than water absorbency of all the samples made from banana pulp mixed with recycled kraft pulp. It could be implied that banana fibers might have more lignin content (which was hydrophobic) therefore its water absorbency was much lower than virgin kraft fibers.

For both ring crush resistance and burst resistance, the data showed that the samples made from virgin kraft pulp mixed with recycled kraft pulp had lower ring crush and burst resistance than all the samples made from banana pulp mixed with recycled kraft pulp. Basically, banana fiber length was shorter than virgin kraft fiber length therefore banana fibers would have better fiber-to-fiber bonding within sheet of paper then the banana fibers would enhance much more ring crush and burst resistance to the paper [8].

**Table 3:** Physical and mechanical Properties of the Banana pulp mixed with recycled kraft pulp @ ratio of 50: 50 handsheets.

| Test | Banana pulp: Recycled OCC pulp @ ratio50 : 50 | | | |
|---|---|---|---|---|
| | refine 3000 rpm $\bar{x}$ ± std. | refine 6000 rpm $\bar{x}$ ± std. | refine 9000 rpm $\bar{x}$ ± std. | Without refining $\bar{x}$ ± std. |
| Basis Weight (grammage) | 129± 1.57 | 128 1.53± | 128± 1.75 | 130± 1.09 |
| Thickness (micron) | 195± 6.49 | 195± 1.23 | 191± 6.73 | 273± 9.81 |
| Air permeability (ml/min) | ± 35.6 4.08 | 1.18 ± 29.9 | 1.41 ± 26.6 | 3.88 ± 327 |
| Tear strength index(mN/g/m$^2$) | 10.7± 0.59 | 10.5± 0.31 | 9.63± 0.34 | 13.4± 0.79 |
| Tensile strength Index (Nm/g) | 56.2± 1.32 | 63.4± 0.72 | 65.7± 0.37 | 25.4± 1.35 |
| Bending resistance (mN) | 65.6± 1.02 | 72.3± 1.07 | 74.8± 0.95 | 54.5± 0.89 |
| Water Absorbency)g/m$^2$) | 150± 3.11 | 148± 1.38 | 109± 1.85 | 243± 5.98 |
| Ring Crush Resistance (N) | 152 0.99± | 163 ± 1.08 | 165 1.03± | 136± 1.49 |
| Burst Resistance (kg/cm$^2$) | 6.70 ± 0.40 | 6.520.13± | 6.42± 0.11 | 3.42± 0.07 |

From table 2, the data showed that when banana pulp was more refined the thickness and air permeability of the samples were lower. Normally, when fiber was refined its fiber length will be shorter and the fiber will have more fibrils then fiber will be easily collapsed during web pressing process. Therefore, the paper that made from refined fiber will have lower thickness (bulkiness) and air permeability [2]. Likewise, when banana pulp was

refined its fiber length was shortened then its tear strength was also decreased. Furthermore, when the refining period was longer, the samples would have lower tear strength.

However, the refined fibers could also promote fiber to fiber bonding inside sheet of paper, and then these fibers would make the paper much tougher and stronger. Therefore, tensile strength index and bending resistance of refined banana pulp mixed with recycled pulp samples were increased when compared with the samples made from no refined banana pulp. Moreover, the increasing of refining period also increased tensile strength index and bending resistance of the samples [8].

In a way, when banana pulp was refined, water absorbency of all the samples was decreased and it was also indicated that the longer refining period, the lower of water absorbency of the samples was occured. Theoretically, after refining the fibrillation of fiber would be increased and the fibers were easily to compress. Therefore the samples with refined pulp could absorb less water since there were fewer gaps between each fiber inside the sheet as well as the surface of the paper would be more compacted [7]. For ring crush resistance and burst resistance aspects, it was found that ring crush resistance and burst resistance were significantly increased when banana pulp was refined. Since when banana pulp was refined the more fibrils would occur. These fibrils provide better fibers bonding and then the samples would be more flexible and tougher therefore their ring crush resistance and burst resistance were increased.

### 3.3 Estimation of the cost of pulping production.

According to the data from SCG paper groups (Thailand), the imported virgin kraft pulp cost was 24,000 Baht/ton while the total cost of banana pulping production was around 23,058 Baht/ton (including raw material preparation and pulping production). According to the general regulations from Thai Industrial Standards Institude (TISI) standard No.170 for corrugated liner making, paper manufacturers have to use recycled pulp and/or pulp that produced from agricultural waste at least 50 % by weight. Therefore, banana pulp could be one of good choices to be used as raw materials in corrugated liner production in Thailand since the production cost was lower than the import virgin kraft pulp cost.

## 4. Conclusions

This research was just a preliminary to show that the waste from banana trees could be used as an alternative raw material in corrugated liner production. All the obtained values indicated that the properties of the paper made from banana pulp mixed with recycled kraft pulp were not significantly different from the paper made from virgin kraft pulp mixed with recycled kraft pulp. However, some more researches should be done especially in the area of adding some additives into paper to enhance its physical and mechanical properties. In addition, all the results in this research were only in laboratory scale which may not applicable to plant scale. Some procedures might have to be adjusted and further researches should be done to make it usable in industrial scale.

## Acknowledgements

The researcher would like to express their gratitude to SCG paper groups (Thailand) for providing virgin kraft pulp and recycled kraft pulp and all staff from Pulp and Paper Program at Asian Institute of Technology for providing laboratory instruments and department of printing and packaging technology, King Mongkut's University of Technology Thonburi for some financial support.

## References

1. R. Wattanawong, 1996, "Studying materials for printing materials (chapter 9)", Sukhothai Thammathirat University Press, Nonthaburi, Thailand, pp.19-24.
2. T. Tungwichachan, 1996, "Elements of Paper" Sukhothai Thammathirat University Press, Nonthaburi, Thailand, pp.14-25.
3. Banana [Online]. Available : http://thailand.gen.in/node/722 [2011, January 18]
4. Siam Kraft, "Type of kraft paper" [Online]. Available : http ://www.thaipaperbox.com/about-paper.php [2010, July 11]
5. SCAN TEST, 1995, SCANDINAVIAN PULP, PAPER AND BOARD TESTING COMMITTEE, Paper and board testing SCAN - P7 P11 P12 P24 P29 P34 P60 P67, Sweden.

6. R. Wattanawong, 2004, “Studying materials for printing materials”, Sukhothai Thammathirat University Press, Nonthaburi, Thailand, pp.44-47
7. S. Kunkaew , et.al., 2010, “The Study of Papermaking for Handicraft from Banana Trees” Senior Project , Printing Technology Program, Faculty of Mass Communication Technology, Rajamangala University of Technology Thanyaburi.
8. T. Aunchaleewittayakul, 2003, “Papermaking from Banana Trees and its Usage”, Master of Art thesis, Economics for Community Development Program, Faculty of Education, Ramkhamhaeng University.

# Effect of Compatibilizer on Physical and Rheological Properties of PLLA/PPC Binary Blends

**Sung Wook Hwang, Dong Ho Park, In Sub Yun, Tae Young Park and Jin Kie Shim***

*Korea Packaging Center, Korea Institute of Industrial Technology, Bucheon, South Korea*

**Corresponding author. Email: jkshim@kitech.re.kr*

**Abstract**: Poly(L-lactic acid) (PLLA)/Poly(propylene carbonate)(PPC) binary blend was prepared with/without the maleic anhydride (MA) as compatibilizer in an internal mixer under the presence of radical initiator in reactive compatibilization process. The properties - structure relationship of PLLA/PPC binary blends was observed, and the effect of compatibilization on physical, mechanical, and morphological properties of PLLA/PPC blends was also assessed. The $T_g$ of PLLA decreased indicating that the addition of PPC resulted in increasing the molecular chain mobility of PLLA in the binary blend. It was also found that the addition of PPC had a significant effect on reducing the onset decomposition temperature of PLLA indicating the thermal stability of the PLLA greatly decreased while the reactive compatibilization of PLLA/PPC 80/20 (weight percent) blend showed little effect on the thermal stability of the blends. The tensile strength revealed the decrease tendency with addition of ductile PPC, and the cavities and clear edges from morphological observation showed the poor interfacial adhesion between PLLA and PPC. The PPC effect on the oxygen barrier property was observed, and the compatibilizd PLLA/PPC blend showed the better oxygen barrier than neat PLLA/PPC binary blend.

Keywords: PLLA, PPC, Blending, Compatibilization, Maleic anhydride

## 1. Introduction

Poly(lactic acid) (PLA) is one of the well-known biodegradable polymers, and it has been intensively researched due to its good mechanical properties comparable to polystyrene (PS) and poly(ethylene terephthalate) (PET). It is currently being used a single deposal items such as a cup, tray, plastic bag, and so on. [1] However, the brittleness of the PLA still gave a limitation for various industrial applications.

Blending two polymers is well known to be the cost effective technique to enhance mutual physical or mechanical properties of both polymers, [2] and the blending PLA with other biodegradable polymers were intensively investigated since it provides the improved physical and mechanical properties without compromising the biodegradability. Sheth *et al.* studied PLA/polyethylene glycol (PEG) blends and reported that the blend was found to be miscible blend at less than 50/50 blend ratio. The modulus of blends was found to decrease while the strain was found to increase with addition of PEG. [3] Iannace *et al*. investigated the PLA/Poly(3-hydroxybutyrate-co-3-hydroxyvalerate)(PHBV) blends prepared by the solvent casting technique and reported that the blends showed partial molecular interaction with phase separation indicating that the blends were not compatible. [4] Ke *et al*. studied PLA/starch blends having above 50% amylose and reported that water resistance of PLA/starch blends was profoundly improved without compromising the mechanical properties. [5]

It was widely known that most polymer/polymer blends are an immiscible system due to their poor interfacial adhesion between two polymers; therefore reactive compatibilization process is often introduced to improve compatibility of polymers, and this could be done by a chemical reaction of two polymers during their blending since the polymers containing a functional group such as –COOH, –OH, and $–NH_2$ in the polymer chain could chemically reacted with reactive polymers such as maleic anhydride (MA). [6] Our previous study also investigated that PLLA/corn starch blends with enhanced interfacial adhesion between PLLA and starch due to the reactive compatibilization effect of MA grafted onto PLLA and starch blends. [7]

Poly(propylene carbonate)(PPC) synthesized from carbon dioxide ($CO_2$) and PPO has gained a great attention due to its biodegradability and excellent properties such as ductility, compatibility, and impact strength, oxygen barrier properties, but the thermal stability and low $T_g$ are still need to be improved. Many researchers has investigated to improve these properties, and Tao *et al*. did a research with the PPC/PHBV blends prepared by the solution casting, and they found that the addition of PHBV on the blend improves the thermal stability of PPC. [8] Yao *et al.* investigated the PLA/PPC/MA blends, and found that the toughness was improved by 1355% while the strength is remained constant with a addition of very low content of MA in the

blends. [9]

In this study, PLLA/PPC binary blends were prepared with a melt compounding process, and the physical, mechanical, and barrier properties of PLLA/PPC blends were assessed to evaluate the compatibility of the blends for potential packaging applications.

## 2. Experimental

### 2.1 Materials

PLLA resin, 4032D extrusion grade (98% L-lactic acid), was obtained from NatureWorks LLC, MN, USA. The PPC were purchased from EMPOWER Materials Inc. (New Castle, DE, USA). The radical initiator, 2,5-Bis(tert-butyl-peroxy)-2,5-dimethylhexane (Luperox® 101) (L101) and Maleic anhydride (MA) were purchased from Sigma-Aldrich (St. Louis, MO, USA). PLLA and PPC were vacuum dried at 60℃ for 24hrs prior to use, and L101 and MA were used as they received without further purification.

### 2.2 Sample preparation

The PLLA/PPC binary blends with various compositions were prepared by mixing them with a Plasti-Corder® Rheometer equipped with a three-piece mixing head (Brabender, Duisburg, Germany) at 190 ℃ with 50 rpm of rotor speed. Total mixing time was fixed for 8 min. The blend composition is given in Table 1. The blended sample melts were cooled to room temperature, and then compression molded to a film with a thickness of 150 ~ 200 μm by an automatic hydraulic laboratory press, model QM900A (QMESYS, Gyangmyung, South Korea) at 200 ℃. All samples were dried in vacuum oven prior to use. The test specimens were prepared with the DSM microinjection moulder (DSM Xplore, Netherlands) at 200 ℃.

**Table 1**: The blend composition of PLLA/PPC binary blends

| Samples | PLLA, wt% | PPC, wt% | L101, phr | MA, phr |
|---|---|---|---|---|
| PLLA-neat | 100 | 0 | 0 | 0 |
| 82-neat | 80 | 20 | 0 | 0 |
| 82-L0.1 | 80 | 20 | 0.1 | 0 |
| 82-L0.1M1 | 80 | 20 | 0.1 | 1 |
| 82-L0.1M2 | 80 | 20 | 0.1 | 2 |
| 82-L0.1M3 | 80 | 20 | 0.1 | 3 |
| 82-L0.1M4 | 80 | 20 | 0.1 | 4 |
| 82-L0.1M5 | 80 | 20 | 0.1 | 5 |
| 82-L0.2 | 80 | 20 | 0.2 | 0 |
| 82-L0.2M1 | 80 | 20 | 0.2 | 1 |
| 82-L0.2M2 | 80 | 20 | 0.2 | 2 |
| 82-L0.2M3 | 80 | 20 | 0.2 | 3 |
| 82-L0.2M4 | 80 | 20 | 0.2 | 4 |
| 82-L0.2M5 | 80 | 20 | 0.2 | 5 |
| PPC-neat | 0 | 100 | 0 | 0 |

### 2.3 Sample characterizations

The thermal properties such as the glass transition temperature ($T_g$), melting temperature ($T_m$), and percent crystallinity ($X_c$) were determined with a Diamond™ DSC (Perkin-Elmer, Waltham, MA, USA). The measurements were carried out under nitrogen atmosphere with a temperature range from 20 to 220 ℃ at a heating rate of 10 ℃/min, and the Diamond Analysis software was used for data analysis. 93.1 J/g of the heat of fusion for 100% PLA [10] was applied to determine the $X_c$ by the following equation (1).

$$x_c(\%) = \frac{\Delta H_m - \Delta H_c}{\Delta H_m^c (1 - x)} \times 100 \qquad (1)$$

Where $\Delta H_m$ is enthalpy of fusion, $\Delta H_c$ is the enthalpy of cold crystallization, $\Delta H^c_m$ is enthalpy of fusion of pure crystalline PLA; $\Delta H^c_m$ = 93.1 J/g, $x$ is the weight fraction of PPC. Thermal stability of the PLLA/PPC binary

blends was analyzed by the thermal gravimetric analysis (TGA), Q600 (TA Instruments, New Castle, DE, USA). The measurements were carried out under a nitrogen atmosphere up to 800 ℃ with a heating rate of 10 ℃/min.

The mechanical properties such as tensile strength, Young's modulus, and elongation at break were evaluated with the Universal Test Machine (UTM), Instron 4465 (Instron, Canton, MA) according to ASTM D 882-02. The injection molded specimens were conditioned at 23 ℃ and 50 %RH for at least 24 hrs. The specimens were tested at a crosshead speed of 10 mm·min$^{-1}$. At least five specimens were tested for each composition. Dynamic mechanical analysis (DMA) of the PLLA/PPC binary blend samples was performed with a Solid Analyzer, RSA-G2 (TA Instruments, New Castle, DE, USA). Samples with a width of 6.0 ± 0.5 mm and a length of 10 ± 0.5 mm were tested in the tension mode. The storage modulus, E′ and loss modulus, E″ were determined at a heating rate of 5 ℃/min and a temperature range of -20 to 180 ℃ with a frequency of 1 Hz.

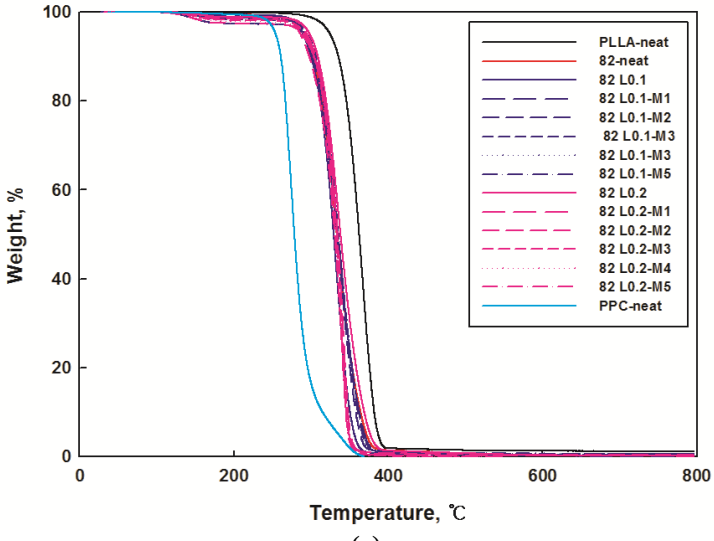
The rheological properties of PLLA and PLLA/PPC binary blends were assessed using a rotational rheometer, MCR302 (Anton Paar GmbH, Graz, Austria) using a 25 mm parallel plate. All the samples were vacuum dried at 50℃ for 8 hrs before testing. Tests were carried out at 190℃. A dynamic frequency sweep test over a frequency range of 0.1 ~ 100 rad$^{-1}$ was applied.

Oxygen permeability ($O_2$) of the PLLA/PPC binary blends were measured with a MOCON OX-TRAN 702 (MOCON Inc. MN, USA), and the tests were performed in accordance with ASTM 3985. The morphological observation of the PLLA/PPC binary blends was performed using a field emission scanning electron microscope (FE-SEM), SU8020 (HITACHI, Tokyo, Japan). The molded samples were fractured after freezing in liquid nitrogen to prevent deformation during fracture.

## 3 Results and discussions

### 3.1 Thermal properties

The TGA thermograms of PLLA, PPC, and PLLA/PPC blends are presented in Figure 2. The addition of PPC had a profound effect on decreasing onset decomposition temperature of PLLA due to the lower thermal stability of PPC as compared to neat PLLA. It was well known that the PPC molecular chain is easily decomposed to cyclic carbonate at elevated temperature, and Lai *et al*. reported that the MA end-capping to PPC enhanced the thermal stability avoiding the unzipping degradation and chain scission.[11] The compatibilization of MA between PLLA and PPC seemed have little effect on thermal stability of PLLA/PPC 80/20 (weight percent) binary blends.




(a)

**Figure 1**. TGA thermogram of PLLA, PPC, and PLLA/PPC binary blends

Table 2 summarizes the thermal properties such as $T_g$, $T_m$, and $X_c$ of PLLA, PPC and PLLA/PPC binary blends obtained from the first heating scan. It is interesting that the both $T_{g1}$ ($T_g$ of PPC) and $T_{g2}$ ($T_g$ of PLLA) move toward each other indicating this PLLA/PPC binary blend is partially miscible. MA *et al*. also observed the compatibility of PLA/PPC blend, and reported that PLA and PPC are partially miscible.[12] The addition of ductile PPC on the blends results in slight decrease on $T_{g2}$ due to increasing chain flexibility, and it was found

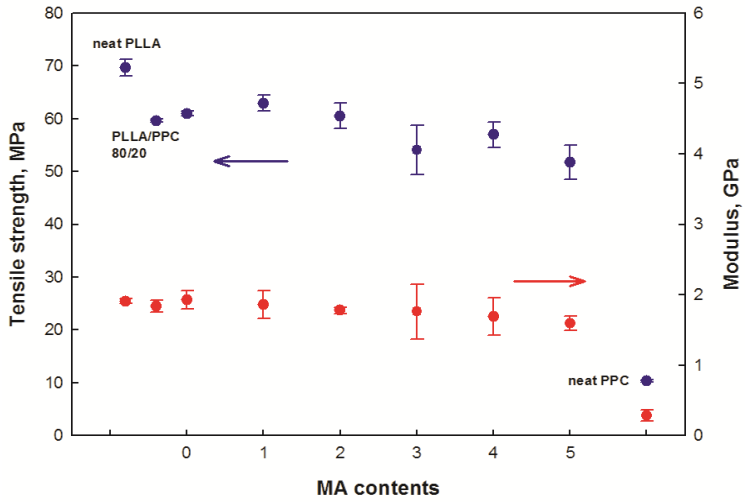
that the radical initiator, L101 did have little effect on $T_{g2}$ while it had a great effect on $T_{g1}$. It could be assumed that the free radical reaction would be predominantly occurred at PPC as compared to PLLA affecting the reduction of $T_{g2}$. The addition of MA on the blend results in the further decrease in both $T_{g1}$ and $T_{g2}$ due to plasticizing effect of MA with increased chain mobility. It was also found that the reduction magnitude of $T_{g1}$ is much higher than $T_{g2}$, and this can be seen that the grafting reaction of MA on PPC dominates than that of MA on PLLA. Therefore, it can be concluded that the plasticized PPC could act as a plasticizer for PLLA. The percent crystallinity, $X_c$ increased considerably due to higher chain mobility.

**Table 2**. DSC results of PLLA, PPC, and PLLA/PPC binary blends

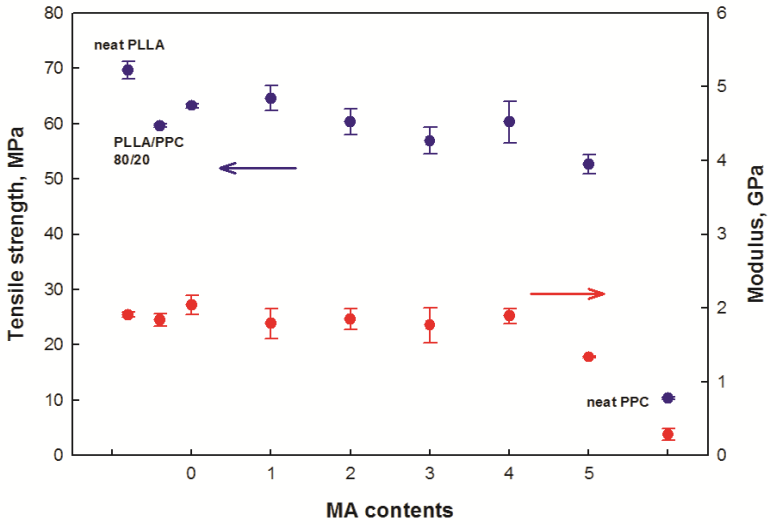
| ***Sample*** | $T_m$, ℃ | $T_{g1}$, ℃ | $T_{g2}$, ℃ | $X_c$, % |
|---|---|---|---|---|
| PLLA-neat | 170.76 | - | 64.57 | 6.47 |
| 82-neat | 169.57 | 34.79 | 59.28 | 12.70 |
| 82 L0.1 | 167.40 | 29.71 | 58.89 | 28.14 |
| 82 L0.1-M1 | 167.31 | 27.83 | 58.13 | 35.24 |
| 82 L0.1-M2 | 160.20 | 17.94 | 52.34 | 36.01 |
| 82 L0.1-M3 | 162.70 | 16.24 | 50.45 | 36.80 |
| 82 L0.1-M4 | 159.68 | 13.24 | 47.46 | 38.21 |
| 82 L0.1-M5 | 163.20 | 12.39 | 47.22 | 35.08 |
| 82 L0.2 | 164.19 | 11.09 | 58.50 | 41.03 |
| 82 L0.2-M1 | 164.27 | 17.23 | 53.24 | 38.59 |
| 82 L0.2-M2 | 166.19 | 15.35 | 53.86 | 40.08 |
| 82 L0.2-M3 | 159.73 | 15.62 | 50.22 | 38.99 |
| 82 L0.2-M4 | 162.48 | 18.49 | 52.79 | 39.26 |
| 82 L0.2-M5 | 162.40 | 8.88 | 45.30 | 35.79 |
| PPC-neat | n/a | 25.65 | - | n/a |

### 3.2 Mechanical properties

The mechanical properties such as tensile strength, modulus, and elongation at break were shown in Figure 2. The decrease of the tensile strength with addition of 20wt% of PPC in the PLLA was found in PLLA/PPC binary blends. It could be seen that the ductile PPC have an effect on giving the flexibility of the blend. The compatibilization effect of MA was found up to 2.0 phr of MA, and excess MA in the blends results in reduction of tensile strength, and this could be attributed to the plasticizing effect of MA in the blend. The modulus was found to remain the constant.




(a) 0.1 phr of L101




(b) 0.2 phr of L101

**Figure 2**. Tensile strength and modulus of PLLA, PPC, and PLLA/PPC binary blends

Figure 3 shows the elongation at break of PLLA, PPC, and PLLA/PPC binary blends. The addition of 20 wt% of PPC enhances about 700% as compared to neat PLLA (7.8%). It was also found that the addition of L101 only to PLLA/PPC blend results in reduction of elongation at break due to chain scission from the radical reaction. The elongation at break increase again after the introduction of MA in the blend indicating that the interfacial adhesion between PLLA and PPC was significantly improved with reactive compatibilization.

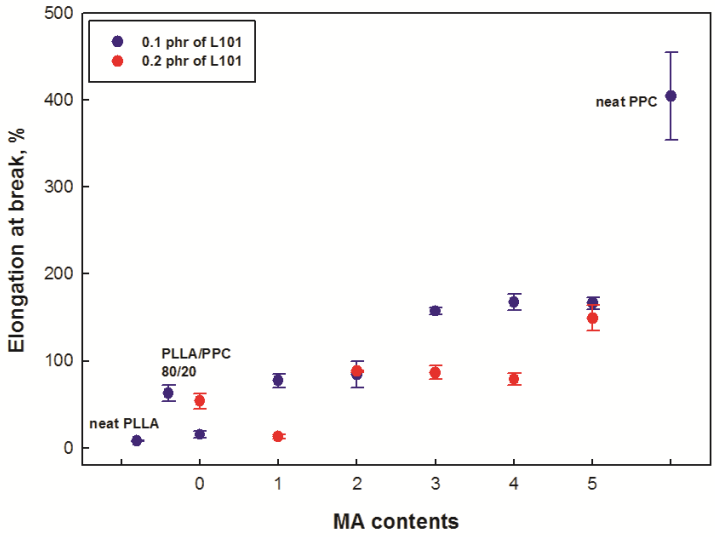



**Figure 3**. Elongation at break of PLLA, PPC, and PLLA/PPC binary blends

### 3.3 Dynamic mechanical analysis

Figure 4 presents the dynamic storage modulus (*E'*) of neat PLLA, PPC, and PLLA/PPC binary blend. It is noted that the addition of 20 wt% of PPC in the blend gives a reinforcing effect increasing *E'* before $T_g$ of PPC, and E' gradually decreases after $T_g$. This increase could be attributed to the high elastic property of PPC. The *E'* shows decrease tendency as MA is introduced to the blend, and this could be due to excess of MA indicating that the plasticizing effect of MA reduces the elastic modulus of PLLA/PPC blend. It can be seen that plasticizing effect

dominantly occur in the higher MA contents in the blend. Yao *et al.* also investigated the PLA/PPC blend with MA, and found that elastic properties and thermo-mechanical stability of the blend is reduced by additional PPC. [9]

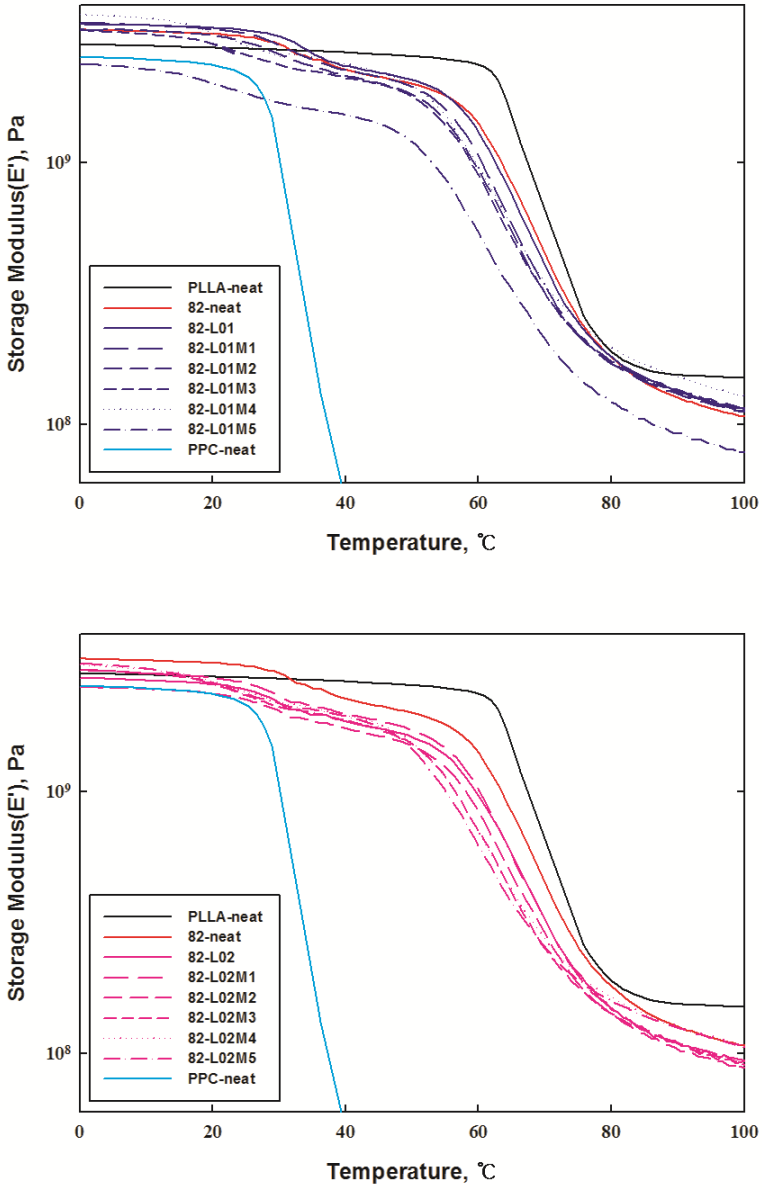



**Figure 4**. Storage modulus, E' of PLLA, PPC, and PLLA/PPC binary blends

### 3.4 Rheological properties

In narrow molecular weight ($M_w$) distribution homo polymer melts, the shear storage modulus, $G'(\omega)$ curve lines with a slope of 2 at a terminal region (low frequencies region), and this is expressed by a power law of $G'(\omega) \propto \omega^2$. [13] The $G'(\omega)$ of the PLLA and PLLA/PPC blends was presented in Figure 5. The slopes of $G'(\omega)$ of neat PLLA are near 2, and the addition of PPC considerably lowers the slope which means PLLA/PPC binary blend is weakly dependent at low frequencies, and they shows a solid-like behavior. It was found that the addition of L101 in the blend has little effect on $G'(\omega)$. The addition of MA did not have significant effect on the solid-like behavior, and the MA contents up to 2.0 phr in the blend increases $G'(\omega)$ due to reinforcing effect from improved interfacial adhesion, and it decreases with over 3.0 phr of MA contents. This could be due to plasticizing effect of MA in the blend as proven in the DSC and DMA results.

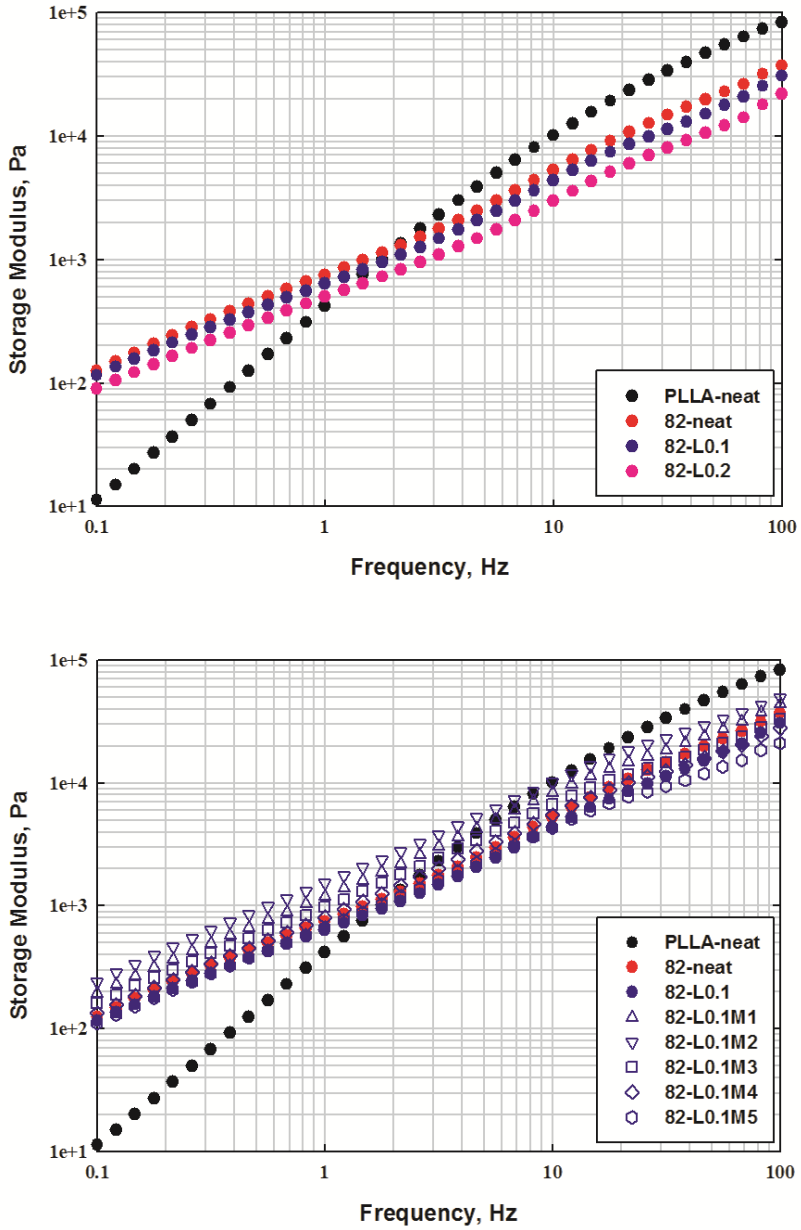



**Figure 5**. Shear storage modulus, *G'(ω)* of PLLA, PPC, and PLLA/PPC binary blends

### 3.5 Oxygen permeability

The oxygen ($O_2$) permeabilty of PLLA, PPC, and PLLA/PPC binary blends was given in Figure 6. It has been widely known that the PPC has an excellent $O_2$ barrier (0.45 ~ 0.6 cc·mm/cm$^2$·day·atm). [14] In this study, neat PPC shows the 5.4 ± 0.3 cc·mm/cm$^2$·day·atm of oxygen permeability value that is one order magnitude higher than reported value. There are a variety parameters that influence the permeability such as polymer structure, molecular weight, crystallinity, chain entanglement, processing techniques, and so on. The samples in this study were compression molded and morphological structure could be differentiated from that of extrusion casting film. In addition, thermal degradation of PPC could be another factor decreasing the $O_2$ barrier property of neat PPC. The addition of PPC in the PLLA seemed to have an effect on reducing the permeability due to the PPC effect, and the L101 and MA would not have much effect on the permeability. However, under excess of MA in case of 0.1 phr of L101, increase tendency in permeability was observed, and this could be attributed to increase free volume from MA branching and chain scission of PPC. PLLA is relatively low $O_2$ barrier polymer, and the

combination of PLLA with this PPC, a high $O_2$ barrier polymer with 100% biodegradable would increase the potential for various industrial applications.

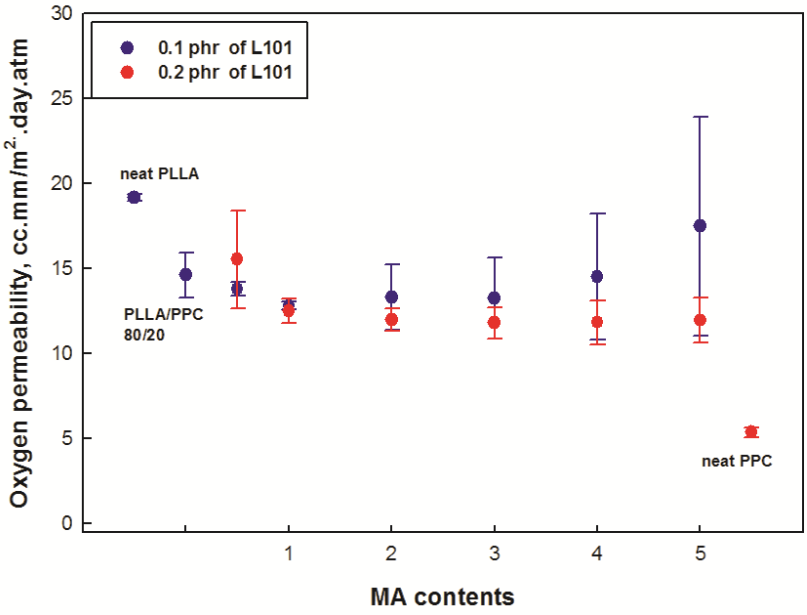
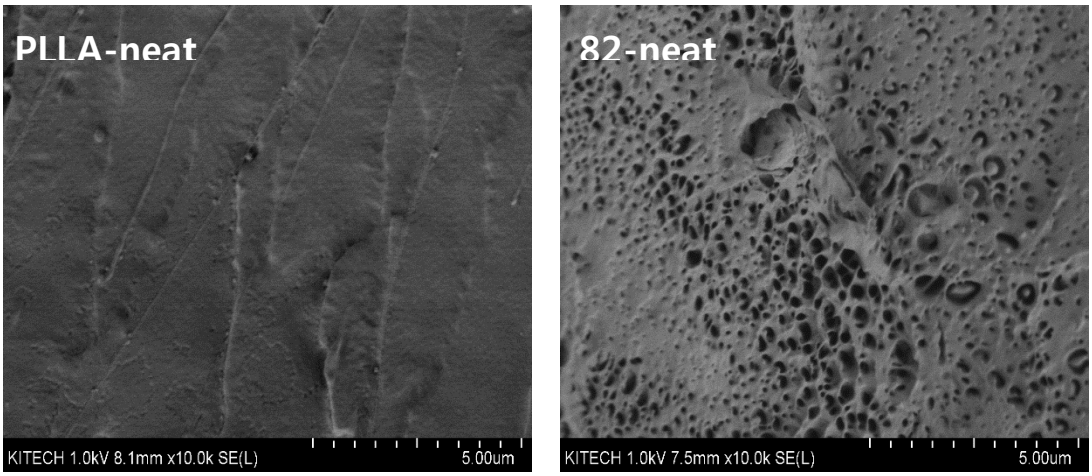



**Figure 6**. Oxygen permeability of PLLA, PPC, PLLA/PPC binary blends

### 3.6 Morphological observation

In the polymer blend, the mechanical properties are dependent on the internal morphological structure. As given in Figure 7, the PPC domains were formed in PLLA matrix, and cavities were founded between the PLLA and PPC indicating the poor interfacial adhesion between them. However, the addition of MA up to 3.0 phr in the PLLA/PPC blends shows relatively rough surface morphology with no clear differentiation indicating the improved interfacial adhesion between the PLLA and PPC phases, and the interfacial adhesion was found to be decreased again from the addition of 4.0 phr of MA in the blend showing smoother surface morphology. This could be attributed to greater plasticizing effect of excess MA in the blend. These results are consistent with the mechanical behavior of the PLLA/PPC blend.



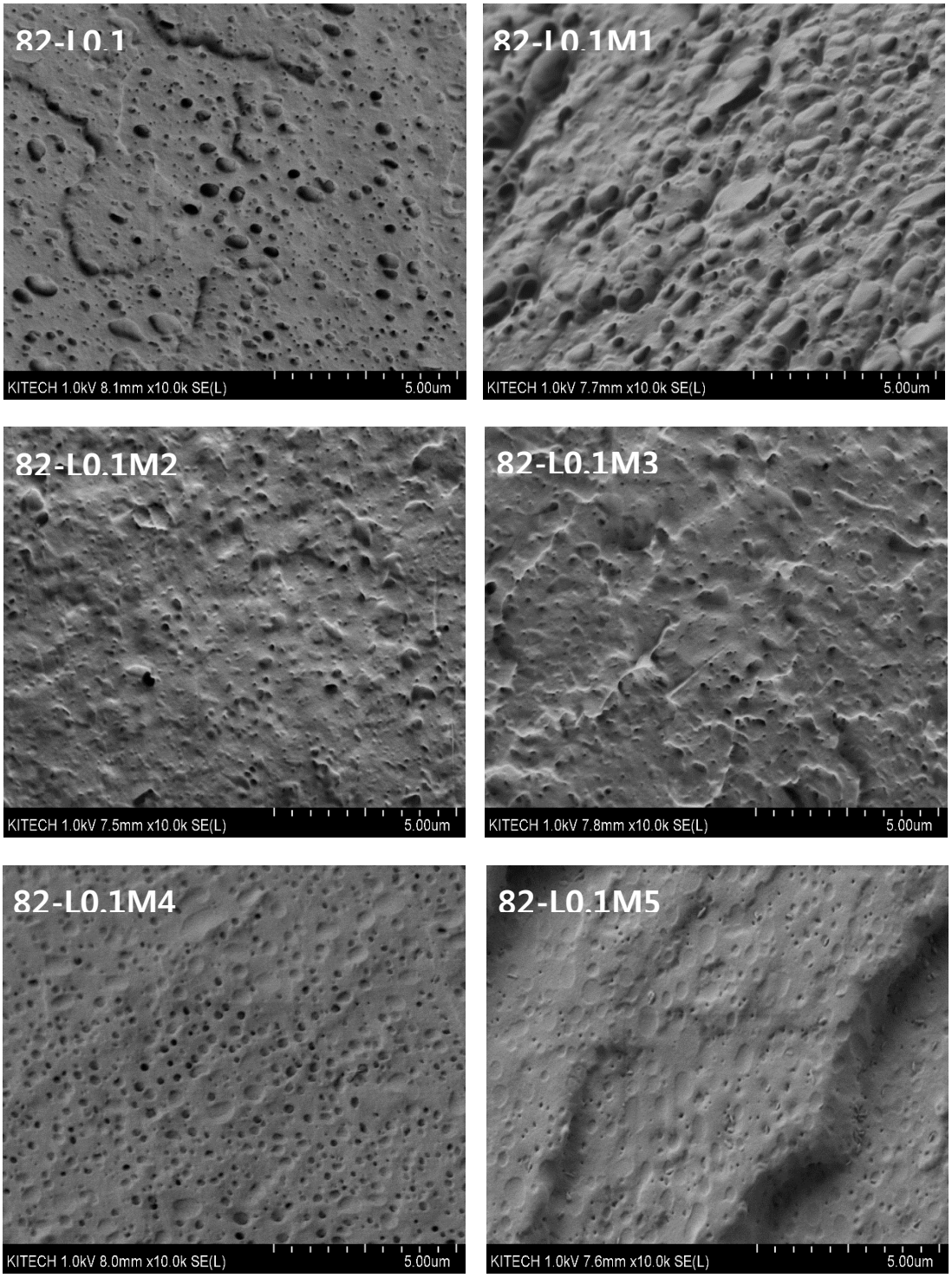



**Figure 7**. SEM micrographs of PLLA/PPC blend samples

## 4 Conclusions

PLLA/PPC binary blends were prepared with/without a reactive compatibilization of MA. It was found that the reactive compatibilization decreased $T_g$ of the PLLA/PPC, and had little effect on the thermal stability. The addition of 20 wt% of PPC profoundly improved elongation at break about 700% as compared to neat PLLA (7.8%), and decreased the tensile strength. A reactive compatibilization up to 2.0 phr of MA increased tensile strength again due to improved interfacial adhesion. It was also found that excess MA acted as a plasticizer in the

blend. The MA contents up to 2.0 phr in the blend increased *G'(ω)* due to the reinforcing effect from improved interfacial adhesion as confirmed in morphology. The $O_2$ barrier property showed increase tendency, and further investigation would be needed to improve the barrier property for packaging application.

**References**


1. R. Auras., B. Harte, and S. Selke, 2004, "An Overview of Polylactides as Packaging Materials", *Macromolecular Bioscience*, vol. 4, no. 9, pp. 835-864.
2. Y. Nishio, 2006, *Polysaccharides II*, Springer Berlin Heidelberg. pp. 97-151.
3. M. Sheth, et al., 1997, "Biodegradable polymer blends of poly(lactic acid) and poly(ethylene glycol)" *Journal of Applied Polymer Science*, vol.66, no. 8, pp. 1495-1505.
4. S. Iannace, et al., 1994, "Poly(3-hydroxybutyrate)-co-(3-hydroxyvalerate)/Poly-L-lactide blends: Thermal and mechanical properties", *Journal of Applied Polymer Science*, vol. 54, no. 10, pp. 1525-1535.
5. T. Ke, S.X. Sun, and P. Seib, 2003, "Blending of poly(lactic acid) and starches containing varying amylose content", *Journal of Applied Polymer Science*, vol. 89, no. 13, pp. 3639-3646.
6. S.J. Kim, et al., 2001, "Reactive compatibilization of the PBT/EVA blend by maleic anhydride", *Polymer*, vol 42, no. 9, pp. 4073-4080.
7. S.W. Hwang, et al., 2013, "Effect of Maleic-Anhydride Grafting on the Physical and Mechanical Properties of Poly(L-lactic acid)/Starch Blends", *Macromolecular Materials and Engineering*, vol. 298, no. 6, pp. 624-633.
8. J. Tao, et al., 2009, "Thermal properties and degradability of poly(propylene carbonate)/poly(β-hydroxybutyrate-co-β-hydroxyvalerate) (PPC/PHBV) blends", *Polymer Degradation and Stability*, vol. 94, no. 4, pp. 575-583.
9. M. Yao, et al., 2011, "Modification of poly(lactic acid)/poly(propylene carbonate) blends through melt compounding with maleic anhydride", *Express Polymer Letters*, vol. 5, no. 11, pp. 937-949.
10. E.W. Fischer, H. Sterzel, and G. Wegner, 1973, "Investigation of the structure of solution grown crystals of lactide copolymers by means of chemical reactions", *Kolloid-Zeitschrift und Zeitschrift für Polymere*, vol. 251, no. 11, pp. 980-990.
11. M.F. Lai, J. Li, and J.J. Liu, 2005, "Thermal and dynamic mechanical properties of poly(propylene carbonate)", *Journal of Thermal Analysis and Calorimetry*, vol. 82, no. 2, pp. 293-298.
12. X. Ma, J. Yu, and N. Wang, 2006, "Compatibility characterization of poly(lactic acid)/poly(propylene carbonate) blends", *Journal of Polymer Science Part B: Polymer Physics*, vol. 44, no. 1, pp. 94-101.
13. S. Sinha Ray, et al., 2003, "New polylactide-layered silicate nanocomposites. 2. Concurrent improvements of material properties, biodegradability and melt rheology", *Polymer*, vol. 44, no. 3, pp. 857-866.
14. *Empower Materials Inc. (2010) QPAC poly(alkylene carbonate) copolymers.* http://www.empowermaterials.com *Assessed Novembr.* 2013.

# Influence of reprocessing on mechanical properties of virgin SAN (stryrene-stat-acrylonitryle) copolymer by injection molding

**Touria ACHTIOUI[1*], Catherine LACOSTE[1,2], Marie LE BAILLIF[1,2,], Damien ERRE[1,2]**

[1]*University of Reims Champagne-Ardenne (URCA), GRESPI, F-51100, Reims, France*
[2]*ESIReims, Esplanade Roland Garros, B.P 1029, F51686 Reims Cedex 2, France*

[*]*Corresponding author. Email: achtioui.touria@gmail.com*

**Abstract :** This study was focused on the influence of the reprocessing of virgin SAN copolymer in injection molding on its mechanical properties in order to understand its structure-property relations. This would help manufacturers to control and limit the degradation of SAN during processing and therefore it would make the recycling of SAN packaging possible without significantly reducing its properties. SAN copolymer was reprocessed up to fifteen times. The effect of temperature (190°C and 250°C) and reprocessing cycles were evaluated by mechanical tests and by the yellowness indexes. It was found that the yellowness index increased according to an exponential law and saturation was reached twice faster at high temperature. Average molecular weights determined by Gel Permeation Chromatography (GPC) were found to decrease with injection cycle number. However, the effect of temperature on mechanical properties was not significant up to fifteen recycling even if the Young modulus and tensile strength were slightly modified. Strain at break stayed unchanged.

Keywords: reprocessing, copolymer, mechanical properties, styrene-*stat*-acrylonitrile, injection molding.

## 1 Introduction

As plastic wastes increase, packaging companies should now develop a strategy of sustainable development with a good management efficiency. As the price of raw plastic material is directly linked to petroleum costs, reducing the volume of their waste remains their major cause of concern. Thus they have to better consider the recycling of their sprues and undelivered packages. Among plastic packaging, one could find the styrene-acrylonitrile copolymer (SAN). This amorphous copolymer based on statistical distribution of styrene and acrylonitrile monomer appeared to be interesting for cosmetic packaging because of its good balance of properties, toughness/strength coupled with high quality surface finish and ease of processing. Nevertheless, the performance of products made from recycled polymers will differ from products made from virgin polymers [1-4]. As SAN is sensitive to thermo-oxidation, it could be degraded during repeated processing cycles. The thermo-mechanical degradation would affect the molecular weight of the material by chain scissions and therefore its mechanical properties [2-4]. Therefore, the goal of this study was to understand on the influence of the number of cycles and of the temperature on mechanical properties of virgin SAN copolymer in injection molding, in order to establish a structure-property relation.

## 2. Experimental

### 2.1 Material

The studied virgin SAN were an injection-molding grade (Kostil®B366) supplied by Polimeri Europa (Melt Volume Flow Rate 220°C/10 kg = 30 $cm^3$/10 min). This material is used for cosmetic packagings.

### 2.2 Injection molding

A mass of 7 kilos of granules were dried at 80°C in a hopper for 3h before processing in order to avoid the bubbles effect of moisture. Fifteen injection molding cycles were carried out in a Krauss-Maffei injection molding machine with a grinder to obtain flakes at each injection cycles according to the ISO 527-2 standard. The operating gradient temperature of injection was between 45°C to 190°C and to 45°C to 250°C (190°C and 250°C being commonly used in industries), the injection screw speed was fixed at 30 $mm.s^{-1}$, the time of injection was of 0.88 s and the time of one cycle was 19.2 s. Several samples were taken for mechanical properties.

## 2.4 Optical properties

The coloration of the polymer was measured on polymer plates of comparable thicknesses (~2mm) with spectrophotometer (observation angle = 10°, illumination D65). The results were expressed using a yellowness index (YI). Yellowness Index is a number calculated according to ASTM E313 from spectrophotometric data that describes the change in color of a sample from white through to yellow for positive values.

## 2.3 Gel Permeation Chromatography

Average molecular weight was measured by Gel Permeation Chromatography (GPC) on a Varian 390-LC. It was equipped with two columns packed with polystyrene gel PLgel 5 microns MIXED-D 300 * 7.5 mm (length*diameter of columns), a Varian 290-LC pump, an injector, a refractive index (RI) detector used in this study. Chloroform was used as eluant at a flow rate of 1 $mL.min^{-1}$ at 30°C for a test time of 30 minutes. The injection volume was 100 µL. The calibration was performed using polystyrene standards and the results were given in polystyrene equivalents. 4 mg of pellets were dissolved in 2 mL of chloroform for 24 h. The solutions were then filtered with a PTFE filter porosity of 0.45 µm before injection.

## 3. Results and discuss

The Influence of reprocessing and the effect of temperature on the optical and mechanical properties and weight average molecular weight of virgin SAN were investigated. Coloration of virgin SAN that was regrinded after each injection cycle at two temperatures was studied and showed that samples have changed color during reprocessing. The yellowness indexes of all samples were measured and it appears that the reprocessing tended to obtain highly colored polymers for higher temperature. If we compared experiments that were carried out at lower temperatures, coloration characteristics were lower. For both cases, yellowness increased as an exponential law. Saturation was reached two time faster at higher temperatures than at low temperatures. It reveals that thermo-mechanical degradation induced by viscous dissipation during processing led to the formation of chromophore species. Those are most probably due to the consumption of antioxidation stabilizers during repeated cycles which implied a less protected material [13,16-18]. From the polymer molecular mass measurements, it can be observed that chain scission was probably more controlled by processing than temperature. The decreasing of weight average molecular weight of SAN processed at the higher temperature was the same that at low temperature. This could be explained by the fact that the values of energy are lower than the energy that is required to imply chain scissions of material because of a low residence time during process. On the other hand, the results of mechanical properties showed that the Young modulus slightly decreased with the number of cycles whereas that weight average molecular weight obtained by GPC analysis was slightly more significantly. The tensile strength was found to be two times superior at low temperature. Strain at break remained constant. It indicates that breaks in the polymer chain were responsible of slightly loss of the Young modulus and the tensile stress whereas the strain at break remained unchanged.
It is therefore believed that SAN materials can be recycled without decreasing its properties additives were added.

## Acknowledgements

The authors would like to thanks Albea group for graciously supplying ABS polymers. The present work would not have been possible without the Thalia 2 project and Champagne-Ardenne council who financially supported this study. We are also thankful to Dr Serge ODOF for his help on colorimeter tests during this study.

## References

1. J. M. Pérez, J. L. Vilas, J. M. Laza, S. Arnáiz, F. Mijangos, E. Bilbao, et L. M. León, mars 2010 « Effect of Reprocessing and Accelerated Weathering on ABS Properties », *J Polym Environ*, vol. 18, n° 1, p. 71‑78.
2. J. Pérez, J. Vilas, J. Laza, S. Arnáiz, F. Mijangos, E. Bilbao, et L. León, 2010 « Effect of Reprocessing and Accelerated Weathering on ABS Properties », *Journal of Polymers and the Environment*, vol. 18, n° 1, p. 71‑78.
3. R. Balart, J. López, D. García, et M. Dolores Salvador, sept. 2005 « Recycling of ABS and PC from electrical and electronic waste. Effect of miscibility and previous degradation on final performance of industrial blends », *European Polymer Journal*, vol. 41, n° 9, p. 2150‑2160,

4. N. Grassie et D. R. Bain, 1970 « Thermal degradation of copolymers of styrene and acrylonitrile. I. Preliminary investigation of changes in molecular weight and the formation of volatile products », *Journal of Polymer Science Part A-1: Polymer Chemistry*, vol. 8, n° 9, p. 2653–2664.

# Development of biodegradable Starch-Based Cushions with high shock absorption

**Georges ABINADER[1*], Catherine LACOSTE[1], Marie LE BAILLIF[1], Damien ERRE[1] and Alain COPINET[1]**

[1] *Laboratory of Science Engineering (GRESPI), Department of Materiel Process and Packaging System (MPSE), Reims Engineering school (ESIReims), Université de Reims Champagne-Ardenne (URCA), Reims, France*

[*] *Corresponding author. Email: georges.abinader@etudiant.univ-reims.fr*

**Abstract:** Biodegradable starch-based foam cushion sheets were developed with a Clextral BC21 co-rotating twin-screw extruder machine. An experimental study was developed to identify the effect of natural fibers, biopolymers and other additives on the structural and mechanical properties of the starch based foams. Several characterization tests were performed on the extruded materials: bulk expansion, cellular structure and mechanical tests. In addition, a dropping test was performed on a product protected by the starch-based foam material. The impact absorption of the foams was registered and the level of the protection provided for the products was identified. The results showed that the cushion materials were affected by the foam's formulation. The cell density of the foam remarkably increased and the cell size average highly decreased at high level of calcium carbonate content. Foams with high level of polylactic acid, had good mechanical properties with high hydrophobic properties. While foams with long linter fiber size had low expansion ratio and high water sensibility. The extruded materials revealed their suitability for cushioning use, by having good shock absorption performances in comparison to the commercial petroleum plastic foams such as the ones made of polyethylene. The products were considerably better protected by the starch-based foams after a series of dropping tests. Current efforts are about optimizing the shape, the aspect and the aging stability of the foams, which would expand their use in the packaging market.

Keywords: Starch, biopolymers, fibers, foams, cushions, packaging, biodegradable, shock absorption

## 1 Introduction

Plastic foam materials exhibit an environmental problem because petroleum-based foams are hard and expensive to recycle. This induces opportunities for biodegradable or renewable polymers and a lot of efforts has been made to improve the development of biodegradable foams[1–5]. The purpose of this study was to optimize the development of biodegradable cushion foams previously published and presented at the 26th IAPRI Symposium and the 4th Biofoams international conference [6–8]. Biopolymers, natural fibers and other additives were added to the starch formulation, to provide more strength and stability to the extruded starch-based foam materials.

## 2 Experimental

Starch and gluten were conditioned and then mixed with glycerol in order to prepare the pre-mixture of [starch-gluten-glycerol]. Sodium bicarbonate was added to the conditioned blends immediately prior extrusion. Two contents of calcium carbonate ($CaCO_3$), low [L] and high [H], of Polylactic acid (PLA), low [L] and high [H], and linter fiber sizes, short [L] and long [H] were used in the experimental study. The foams were compounded using a Clextral BC21 co-rotating twin-screw extruder machine. The extruded ribbons were cut into 15 cm length and 2 cm width strips, identified and conditioned for one week at 23±2°C and 50±10% relative humidity according to NF EN ISO 7214 prior characterization. Commercial expandable polyethylene foams (EPE) with high and low densities (EPE220: 35 kg/m$^3$ and EPE400: 58kg/m$^3$) were purchased and used for comparison with the resulted starch-based foams (SBF).

Several characterization tests were performed on the conditioned foams to determine the following properties:

- Bulk expansion: bulk density; expansion ratio (ER)
- Cellular structure: cell density; cell size average; moisture content (MC)
- Mechanical characteristics: dynamic cushion curves; dropping test

## 3 Results and discussion

The effect of PLA, $CaCO_3$ and linter fibers content on the bulk density, the ER, the cell size, the cell density and the MC of the foams, were studied. The results showed that the ER decreased with increasing PLA, $CaCO_3$ content

and linter fibers size. It was observed that the bulk density of the foams increased in the presence of low and high level of PLA contents, but decreased at high level of $CaCO_3$ and long linter fibers. The maximum increase of bulk density was obtained at high level of PLA content. This can be explained by the decrease of the melt viscosity of the thermoplastic starch at high level of PLA, which induced a lower expansion. As for the cellular structure, the cell density of the foam increased with the increase of PLA, $CaCO_3$ content and linter fiber size but it remarkably increased at high level of $CaCO_3$ content. This can be explained by the effect of $CaCO_3$ on promoting nucleation sites, which increased the generation of small bubbles. This induced a decrease in the cell size area of the foams with the increase of $CaCO_3$ content. As for the water sensibility of the foams, $CaCO_3$ had no effect on the water absorption of the foam at 23°C and 50% normal relative humidity conditions. While long linter fibers size increased slightly the water retention in the foam. However, PLA increased the hydrophobic structure of the foam by decreasing its MC.

Mechanical and morphological test were performed on commercial EPE plastic foams to compare and evaluate their characteristics with the SBF. Figure 1, shows the dynamic cushion curves of SBF with different additives and the two commercial EPE foams. SBF cushion curves indicated comparable deceleration peak with the commercial polyethylene plastic foams. High level of PLA made the foam denser, which made them more appropriate to protect heavy rugged products with high static load range. While foams with high level of $CaCO_3$ made the foam softer. Their cushion curves were comparable to the pure SBF, which make them appropriate to protect light product with low static load range. The pure SBF had the lowest deceleration peak of 95G, which is better than EPE foams. This indicates that the SBF sheets would provide enough protection for a large range of light moderately rugged to rugged heavy products with a fragility level greater than 95G.

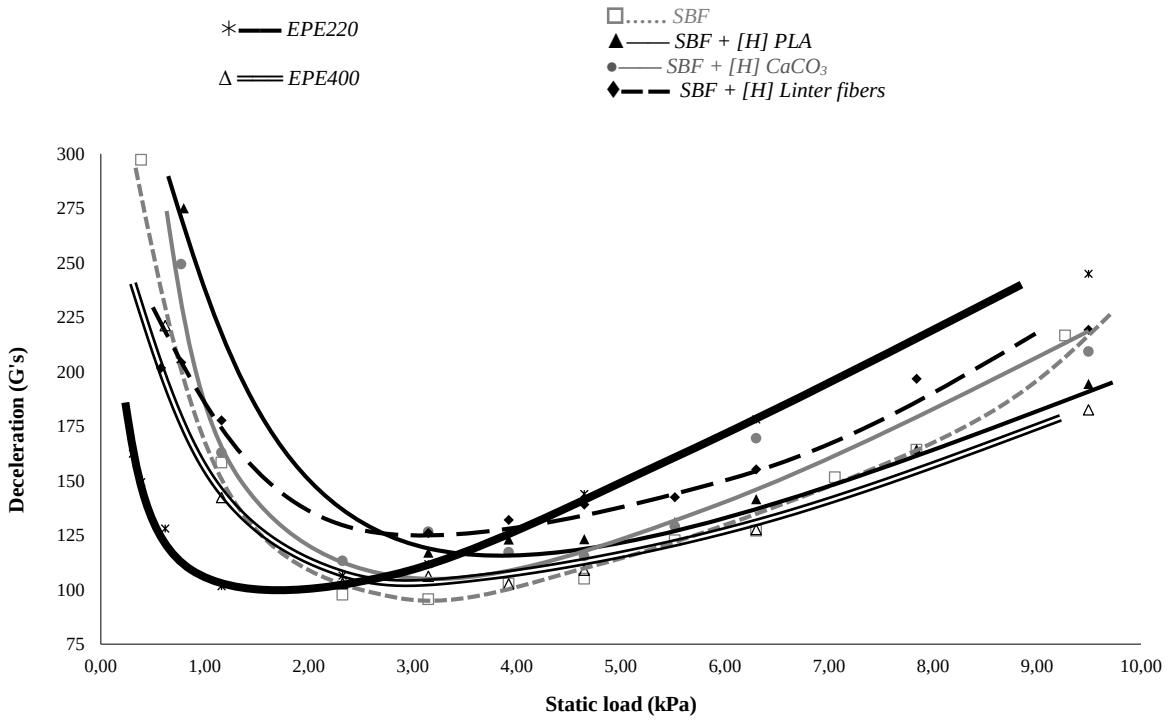



**Figure 1**. Dynamic cushion curves of 10mm thick SBF with different high level of PLA and $CaCO_3$ content and high size of linter fibers versus EPE220 and EPE440, at a drop height of 46cm

To validate the previous cushion curve results, a dropping test was performed on a glass sheet of approximately 200G-product fragility. The glass was protected separately with the same portion of 10mm thick SBF, EPE220 and EPE400 foams. The shock absorption of the different foams was registered during the impact of the [glass + foam] at 46cm drop height. The level of protection provided by the SBF to the products was better than for the EPE foams. This test showed the pertinence of the previous cushion curve results, and confirmed the high shock absorption of the SBF.

## Conclusions

The biodegradable starch based foam sheets materials were affected by the foam's formulation. Foams with high level of $CaCO_3$ content had higher number of small and uniform cells, which provided them good mechanical properties in term of cushioning and elasticity. The additives and the biopolymers affected the strength and the hydrophobic properties of the starch-based foams. PLA content decreased the moisture content of the foams. This induced better strength and hydrophobic stability. $CaCO_3$ had no significant effect on the moisture content of the material but its presence increased the cell density and decreased the cell size bubble in the foams. While long linter fiber size increased the water sensibility of the foam. Finally, the biodegradable starch based foam sheet materials revealed their suitability for cushioning use by having comparable physical properties with the commercial plastic foams. The dropping test indicated that the SBF sheets provided high shock absorption properties. They had lower deceleration peak value than the expandable polyethylene plastic foams and they considerably better protected the glass sheet after the dropping test.

## Acknowledgements

This research paper was a contribution of Reims Engineering School (ESIReims). The study was partially financed by the INTERREG IV program and with the collaboration of Celabor society. The authors would like to thank the ESIReims technical staff for helping in the mechanical tests. The authors are grateful to Chamtor and A.R.D society for graciously supplying the raw materials.

## References

1. Y. Nabar, R. Narayan, M. Schindler, 2006, "Twin-screw extrusion production and characterization of starch foam products for use in cushioning and insulation applications", *Journal of Polymer Engineering and Science*, vol. 46, no. 4, pp. 438–451.

2. Y. Nabar, D. Draybuck, R. Narayan, 2006, "Physicomechanical and hydrophobic properties of starch foams extruded with different biodegradable polymers", *Journal of Applied Polymer Science*, vol. 102, no. 1, pp. 58–68.

3. HA. Pushpadass, GS. Babu, RW. Weber, MA. Hanna, 2008, "Extrusion of starch-based loose-fill packaging foams: effects of temperature, moisture and talc on physical properties", *Journal of Packaging Technology Science*, vol. 21, no. 3, pp. 171–183.

4. J-C. Bénézet, A. Stanojlovic-Davidovic, A. Bergeret, L. Ferry, A. Crespy, 2012, "Mechanical and physical properties of expanded starch, reinforced by natural fibres", *Journal of Industrial Crops Products*, vol. 37, no.2, pp.435–440.

5. SY Lee, KM. Eskridge, WY. Koh, MA. Hanna, 2009, "Evaluation of ingredient effects on extruded starch-based foams using a supersaturated split-plot design", *Journal of Industrial Crops Prod*ucts, vol.29, pp. 427–436.

6. G. Abinader, C. Lacoste, M. Le Baillif, D. Erre, A. Copinet, 2014, "Effect of the formulation of starch-based foam cushions on the morphology and mechanical properties", *Journal of Cellular Plastics*, vol. 50, no. 3, pp. 1-14

7. G. Abinader, C. Lacoste, M. Le Baillif, D. Erre, 2013, "Biodegradable starch-based foams for cushioning use", *Proceedings of the 26th IAPRI Symposium on Packaging*, Espoo, Finland; Jun. 10-13, pp.139

8. G. Abinader, C. Lacoste, M. Le Baillif, D. Erre, A. Copinet, 2013, "Extrusion of starch-based foam sheets for cushioning use", *Proceedings of the 4th BIOFOAMS conference*, Toronto, Canada; Aug. 27-29, pp.104-107

# Evaluating the Dynamic Characteristics of Inexpensive Biodegradable Packaging

**Justin J. Milverton[1], Matthew J. Lamb[2*] and Vincent Rouillard[3].**

[1,2,3] *College of Engineering and Science, Victoria University, Australia*

[*] *Corresponding author. Email: matthew.lamb@vu.edu.au*

**Abstract:** In line with a global trend to minimise packaging waste, concerns related to the environmental impact of many traditional protective packaging materials have been raised. As a result, the use of environmentally friendly alternatives is increasing. However, the performance of many such materials is not well established. This paper focuses on the evaluation of the dynamic characteristics of a biodegradable, starch based loose-fill cushioning material, Envirofill™. The mechanical characteristics pertinent to cushion design were investigated experimentally under a broad range of environmental conditions including extremes in temperature and relative humidity. These characteristics include compression, shock and vibration. Results reveal measurable differences in performance of the material over the range of environmental conditions. Compression tests show that prolonged exposure at high temperature and low humidity results in a slight increase in compression stiffness. However, the material has the ability to re-absorb moisture over time and fully recover its original compression characteristics. In terms of cushion curves, results show that the environmental conditions do not have a significant influence on the shock absorbing characteristics of the material for the first drop. However, when the material is subjected to extreme heat and dry conditions, its cushioning performance was reduced for sequent drops. This is attributed to the brittle nature of the dry beads which become damaged. Furthermore, an increase in moisture content appears to have some improvement on the long term cushioning performance (repeated shocks) of the material. Vibration tests show that the material's dynamic characteristics remain consistent across the environmental conditions used. The results of this study provide a valuable reference for the use of biodegradable, starch based loose-fill as a protective packaging material. They can also be used to assist in optimising the design of cushioning systems using loose-fill material.

Keywords: Enviro-fill, bio-degradable packaging, cushion curves, frequency response function.

## 1 Introduction

During the distribution process, products are continuously exposed to dynamic hazards caused from vehicle vibrations as well as drops and shocks from various types of handling. In order to reduce the effect of such loads on products during this process, protective packaging materials (cushions) are used. In the past, cushioning materials have generally been made from petroleum based sources due to their low cost, ease of manufacture and well established mechanical properties. Examples of petroleum based cushioning materials include expanded polystyrene (EPS) and polyurethane foams. The environmental impact of these protective packaging materials has received significant attention in the last two decades, leading to the development and use of biodegradable cushioning materials. If these biodegradable materials are to be used for cushioning purposes, their ability to retain their mechanic function when subjected to the hazards of the distribution environment must be evaluated.

This paper focusses on the evaluation of the dynamic characteristics of a biodegradable, starch based loose-fill cushioning material, Envirofill™, and how such characteristics are affected by environmental conditions. The results of this study will contribute to the protective packaging design procedure and provide a valuable reference for the use of biodegradable, starch based loose-fill as a protective packaging material.

## 2 Material

Envirofill™ is a protective loose-fill packaging made predominantly from Australian wheat starch. It is fully biodegradable, water soluble and is not known to present any hazards in its diluted form. The beads are manufactured using a patented system which mixes and extrudes the wheat starch into small log forms. Using gravimetric and thermo-gravimetric analysis (TGA), the beads were found to have an average moisture content of 7.57% ±0.17%, with the remaining composition consisting of approximately 79.5% starch and 12.9% inorganic filler (Silica, Si). The effect of these inorganic fillers may present opportunities for further research in chemical and environmental fields. Scanning Electron Microscope images demonstrating the microstructure of the starch beads are shown in Figure 1.

(a) (b)

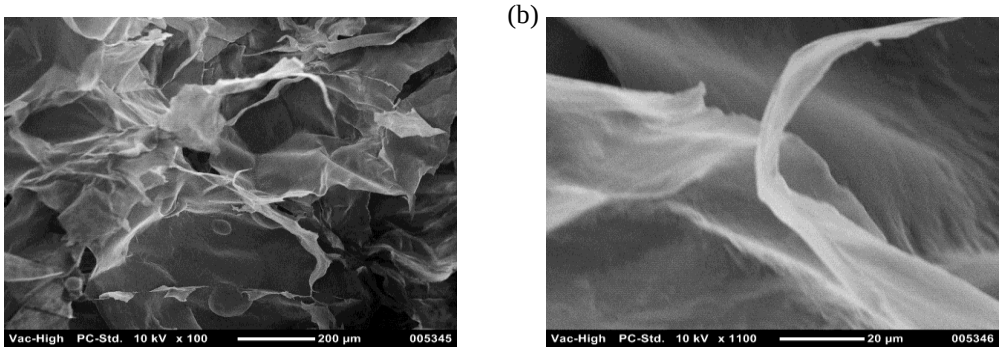



**Figure 1:** Starch bead microstructure (a) 100 time magnification (b) 1100 time magnification.

## 3 Experimental Design

As products can be shipped around the globe, it is important that the protective packaging retains its ability to protect the product when exposed to the various climatic conditions of alternative environments. To simulate such atmospheric hazards, the samples were subjected to climatic conditions in a programmable environmental chamber prior to testing.

The dynamic performance of the loose fill starch was evaluated for three climatic conditions. The conditions were selected to allow for a comparative evaluation for climates ranging from extreme humidity to extreme dry conditions that are relevant to Australian exports into the Asian markets. The International Safe Transit Association (ISTA) [1] provides a set of standard test conditions and these were used as the basis for the experiments. The standard conditions used are outlined in Table 1.

**Table 1:** Conditioning Table [1].

| Standard Conditions | Min. Time (hrs) | Temperature (°C ±2°C) | Relative Humidity (%) |
|---|---|---|---|
| Standard room | 72 | 23 | 50 |
| Hot Humid | 72 | 38 | 85 |
| Extreme Heat, Dry | 72 | 60 | 15 |

For the duration of each test the temperature and humidity inside the chamber was continually recorded using a temperature/humidity sensor connected to a data acquisition box and a PC with specially developed data acquisition software installed.

After conditioning the beads were subject to a series of compression, shock and vibration tests in order to estimate the performance of the beads for each set of conditions. Specific details for each test are provided in sections 3.1 to 3.3.

For each test the beads required containment. This was achieved using a small, engineered PVC pipe section with an internal diameter of 146.5 mm. As can be seen in Figure 2, the PVC section had a number of equally spaced holes drilled in its walls in order to avoid pneumatic compression and suction. The beads were stacked two rows high (1.5 inches, approximately 38 mm) with effort concentrated around the placement of the beads to aid in the repeatability of the experiments. Nevertheless, the ability to consistently pack the containers at a constant density was restricted by variations in bead dimensions and human judgement.

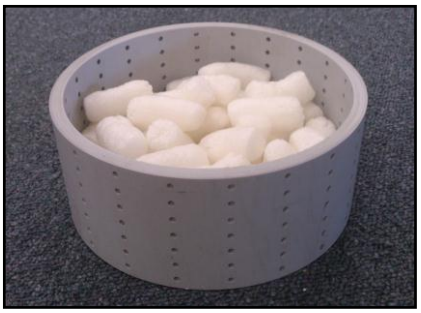


**Figure 2:** Containment method for compression, shock and vibration testing.

### 3.1 Compression Tests

To investigate the compressive resistance of the beads when subjected to alternative environmental conditions, a series of static and dynamic compression tests were performed using an Instron 8501 Universal Testing Machine. Quasi-static compression tests were performed at 0.5 mm/s to simulate static compression. Dynamic tests were performed at 1 mm/s, 10 mm/s, 100 mm/sec and 200 mm/s. Samples were compressed to 90% of their original free height. Each of the compression tests were performed using a circular piston with a diameter of 143 mm.

### 3.2 Shock Tests

A series of shock tests were performed using a solid wooden cylinder (143 mm diameter) of known mass attached to a guided platen which was dropped from a set height of 12 inches (approximately 300 mm). During impact between the cylinder and the beads the deceleration of the platen was recorded using an attached accelerometer and remote data acquisition system. Five equally spaced static stresses ranging from 1 kPa to 2.5 kPa were used.

Full cushion curves were predicted during post-processing using the numerical prediction methods presented by Sek and Kirkpatrick [2], and Sek *et al.* [3]. These methods make use of the data obtained during the compression tests as well as the results obtained from the five static stresses and significantly reduce the number of experiments required to develop a full cushion curve.

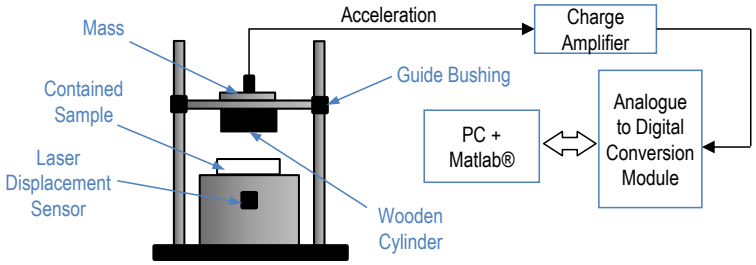



**Figure 3:** Experimental arrangement for shock testing.

### 3.3 Vibration Tests

Multiple samples of the starch beads were subjected to Band Limited White Noise (BLWN) vibration (3-50Hz) using the Vibration Test Systems ((VTS), Aurora, Ohio, USA) model 500 electro-dynamic shaker in conjunction with the configuration shown in Figure 4. The apparatus consists of a guide rod housed within an air bearing. At the bottom of the rod is a circular end plate (142 mm in diameter) on which a mass is placed. The shaker was controlled using SIGNALCALC® software (Data Physics, San Jose, CA, USA). The root-mean-squared (RMS) excitation was set at 1.5m/s$^2$ to avoid inducing damage to the beads whilst providing sufficient deflection to allow the system's modal characteristics to be established.

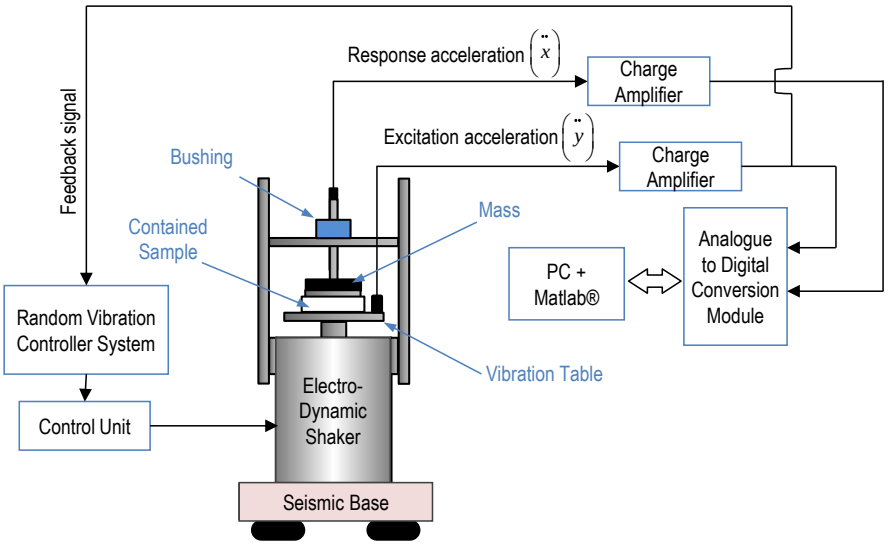



**Figure 4:** Experimental arrangement for vibration testing.

During post-processing the natural frequency and damping ratio of the system was estimated using a least mean-squared curve-fit of its frequency response function (FRF). The system's FRF was determined using the Fourier transform with a sub-record length of 5 s, 500 averages and 88% averaging overlap, which required 5 minutes of temporal data to be recorded. Specific details on the analysis technique and the influence of each analysis parameter can be found in Lamb [4].

In addition to the 5 minutes of temporal data required for post-processing, the system was allowed 2 minutes of settling time, resulting in 7 minutes of total exposure to the laboratory environment (approximately 20°C and 45% relative humidity).

## 4 Compression Test Results

The quasi-static compression curves for each conditioning profile are shown in Figure 5. The most prominent differences between each profile are seen throughout the central regions of the curves, particularly when comparing profiles at standard room and extreme heat dry conditions. Prolonged exposure at high temperature and low humidity has resulted in a loss of moisture content. This loss is believed to have increased the brittleness and compressive resistance of the starch beads. Inspection of the beads during testing supported this theory, with the visual difference between beads conditioned at extreme heat dry and standard room conditions displayed in Figure 6. Figure 6 shows that extreme heat and low humidity causes the beads to dry and become brittle, resulting in cracking and distortion of the beads structure.

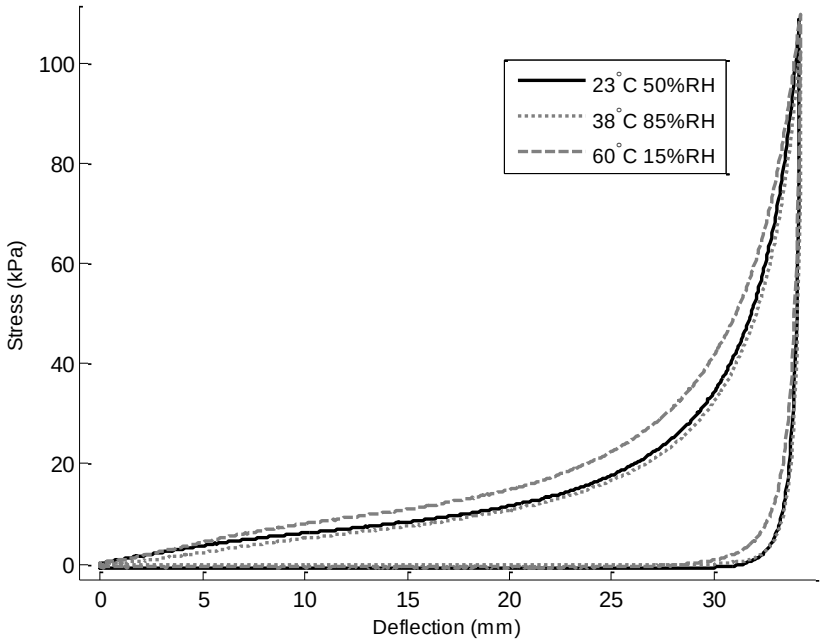



**Figure 5:** Quasi-static compression curves of each conditioning profile.

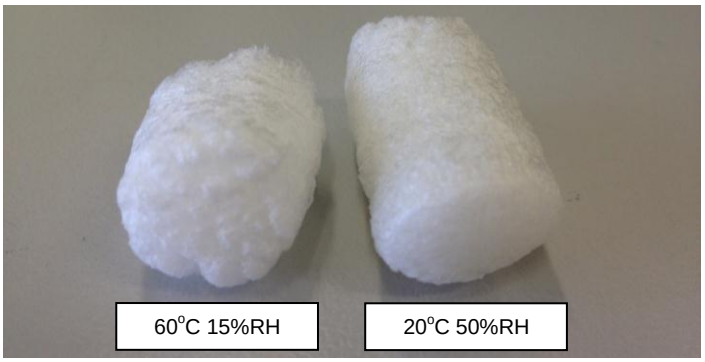



**Figure 6:** Starch bead embrittlement resulting from extreme heat dry conditioning**.**

The untested beads that were subjected to extreme heat dry conditioning were allowed to 'recover' at 23°C 50% relative humidity for approximately 48 hours to investigate the materials ability to re-absorb moisture. Compression tests were performed on these beads with the results compared in Figure 7. These results suggest that the beads can in fact recover, with their compressive resistance returning back to that at controlled conditions.

The compression curves as a result of dynamic compression at various rates under standard room conditions are displayed in Figure 8. As expected, the maximum compressive stress increases at the higher compression rates (100 and 200 mm/sec) due to the increased velocity change experienced. The higher rates also cause the beads to 'stick' to the testing apparatus during rebound, shown by the small dips in the compression curves at high deflection and low stress values.

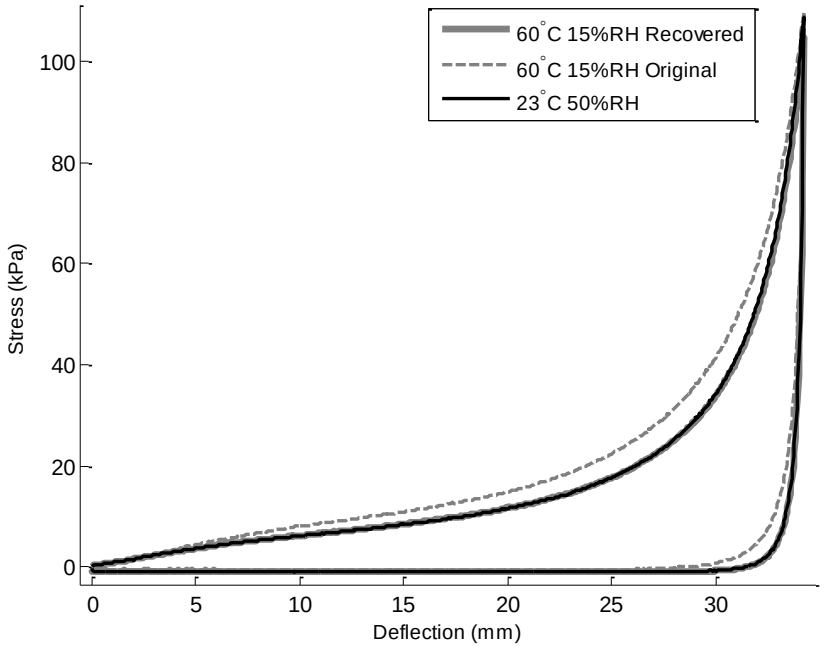



**Figure 7:** Recovery of embrittled starch beads after conditioning at 23°C 50% relative humidity for 48hrs.

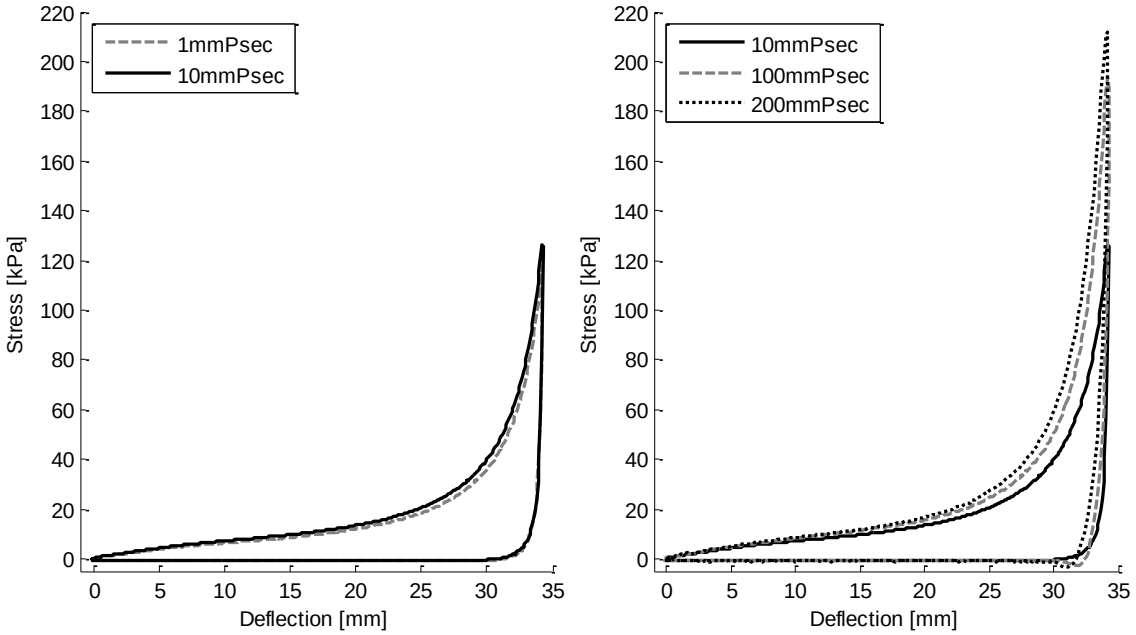



**Figure 8:** Dynamic compression curves for starch beads conditioned at 23°C 50% relative humidity.

## 5 Shock Test Results

This section of the paper presents the results, in the form of cushion curves, obtained from the shock tests. The predicted cushion curves presented were all validated by fitting the curve to the average peak acceleration data obtained from the physical shock tests. An example of this validation is shown in Figure 9 for the data from the samples conditioned at standard room. The results suggest that the technique presented by Sek *et al.* [3] is capable of predicting cushion curves for the first drop.

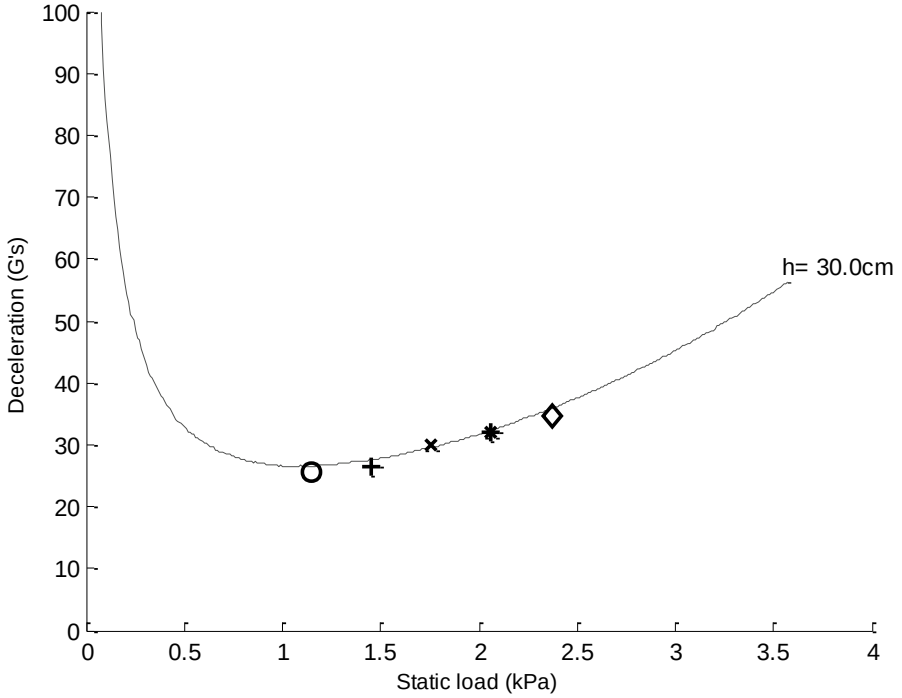



**Figure 9:** Typical results for cushion curve prediction versus physical results for first drop.

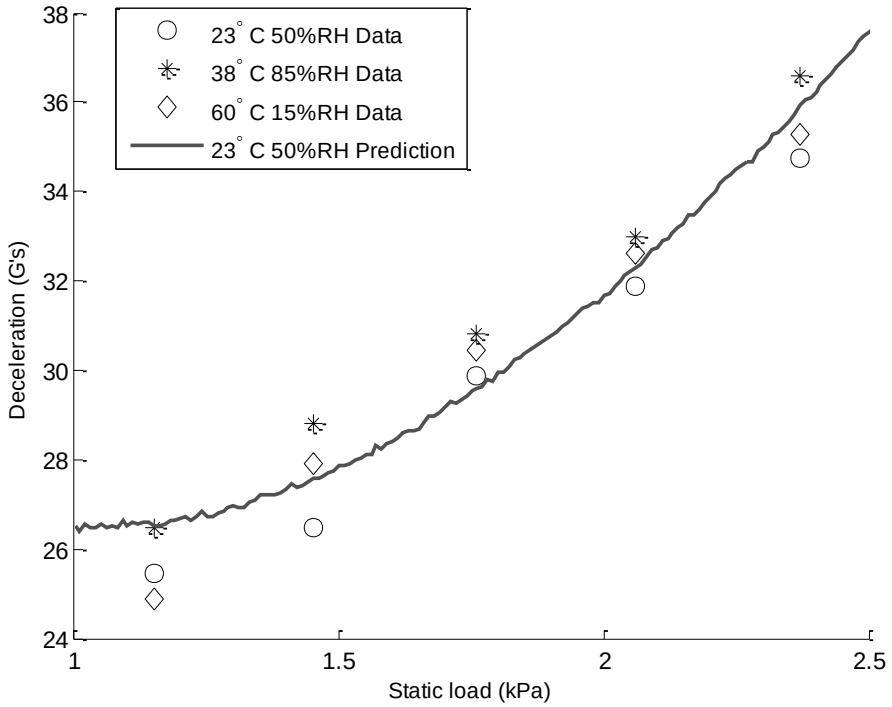



**Figure 10:** Cushion curve results for first drop.

To evaluate the effect of environmental conditions on the cushioning characteristics of the Envirofill™, the experimental data for each profile is plotted in Figure 10. In addition, the predicted cushion curve for standard room conditions is plotted as a reference.

The decrease in moisture content in the material does not have a significant influence onto the cushion curve. However, increase moisture content does result in a marginal but consistent increase in transmitted deceleration levels for the initial drop suggesting that increased moisture content resulted in a loss of cushioning performance for first drop condition.

Figure 11 shows a comparison of the predicted cushion curves for each environmental condition, demonstrating the effect of conditioning on the estimated cushioning performance of the beads. Figure 11 reflects the results discussed earlier, that is, the increased moisture content appears have reduced the capability of the beads to cushion the initial impact of the falling mass. The effect of extreme heat and low RH becomes evident at higher static stresses where the transmitted acceleration is marginally lower.

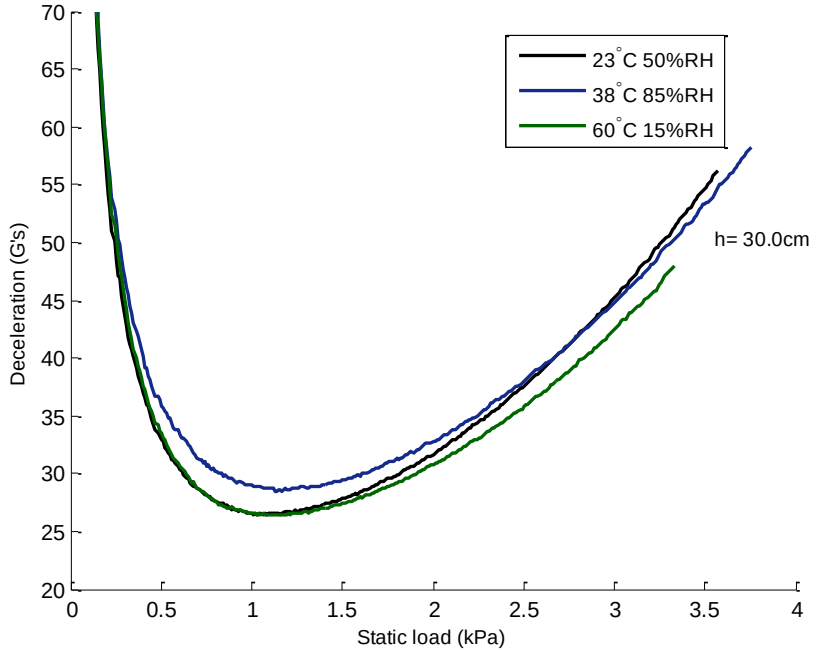



**Figure 11:** Predicted cushion curve results for all conditions.

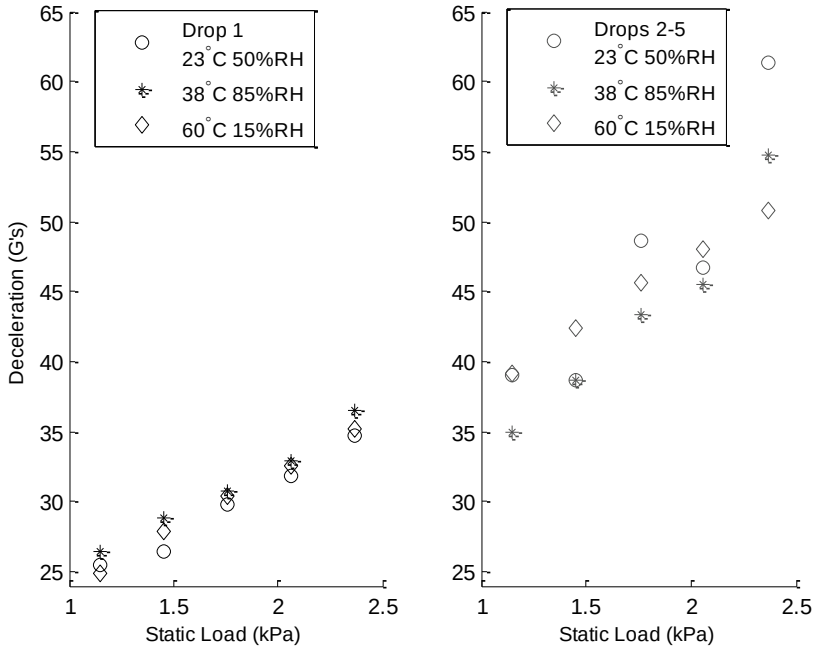



**Figure 12:** Comparison of cushion curve results for first drop and averages 2-5.

Results for initial impact and the average of drops 2-5 are shown in Figure 12. For drops 2-5, the cushioning performance of the beads containing lower moisture content was reduced. This is attributed to the brittle nature of the beads which become damaged after the first drop. Conversely, an increase in moisture content appears to improve the long term cushioning performance, with the beads conditioned at hot humid conditions showing the lowest transmitted acceleration on average.

## 6 Vibration Test Results

During the vibration testing, some variation in estimates of the FRF were noticed. This was attributed to additional friction on the guiding mechanism for the dead load due to the loose-fill nature of the material. Consequently, experiments for each static load (mass) and conditioning profile were repeated a number of times.

The FRF at each conditioning profile for the respective masses is displayed in Figure 13. Both increased and decreased moisture content appeared to affect the stiffness of the beads. This is reflected by a small decrease in natural frequency for hot humid and extreme heat dry conditions at 1.51 kg. The variation for the other static loads are smaller. This is attributed to the compacting effect on the loose-fill material by the higher loads. The decreased natural frequency for extreme heat dry conditioning may be explained by the embrittlement of the beads combined with the increase static load. The beads are believed to have quickly damaged (lost stiffness) as a result of vibration, causing the natural frequency to decrease. Overall, the FRF of the material (including self-damping) appears consistent over a range of static load and environmental conditions.

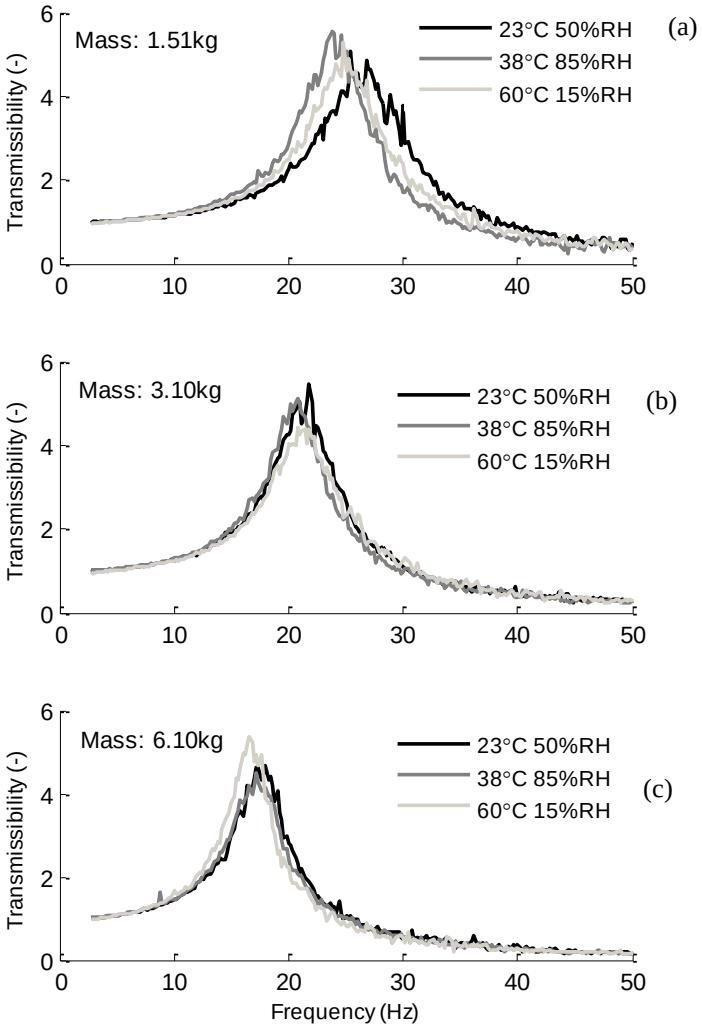



**Figure 13:** FRF for each conditioning profile for static loads (a) 1.51 kg, (b) 3.10kg and (c) 6.10kg.

## 7 Conclusions

The environmental impact of protective packaging materials such as expanded polystyrene is resulting in increasing reliance on more environmentally friendly alternatives. In order to enable optimised protective packaging (cushion) design using such materials, it is essential that their mechanical properties be characterised. Especially, their ability to retain their mechanical function when subjected to a range of environments must be evaluated. This paper focussed on the evaluation of the dynamic characteristics of a biodegradable, starch based loose-fill cushioning material, Envirofill™.

Compression tests reveal that prolonged exposure at high temperature and low humidity results in a slight increase in compression stiffness but no noticeable change in the hysteretic behaviour of the material. However, the material has the ability to re-absorb moisture over time and fully recover its original compression characteristics.

In terms of cushion curves, results show that the environmental conditions do not have a significant influence on the shock absorbing characteristics of the material for the first drop. However, when the material is subjected to extreme heat and dry conditions, its cushioning performance was reduced for sequent drops. This is attributed to the brittle nature of the dry beads which become damaged. Furthermore, an increase in moisture content appears to have some improvement on the long term cushioning performance (repeated shocks) of the material. Vibration tests show that the material's dynamic characteristics remain consistent across the environmental conditions used.

The results of this study provide a valuable reference for the use of biodegradable, starch based loose-fill as a protective packaging material. They can also be used to assist in optimising the design of cushioning systems using loose-fill material.

This study will lead to similar investigations which evaluate the performance of a range of protective materials for a variety of climatic conditions.

## Acknowledgements

The authors would like to thank like to thank Dr Marlene Cran and Mr Michael Long of Victoria University for the time and effort they contributed to this study.

## References

1. International Safe Transit Association, 2011, "ISTA Procedure 2A 11-11: Packaged-Products 150lb (68kg) or Less", p. 6.
2. M. Sek. J. Kirkpatrick, 1997, "Prediction of the Cushioning Properties of Corrugated Fibreboard from Static and Quasi-dynamic Compression Data", *Journal of Packaging Technology and Science*, vol. 10, pp. 87-94.
3. M. Sek. M. Minett. V. Rouillard and B. Bruscella, 2000, "A New Method for the Determination of Cushion Curves", *Journal of Packaging Technology and Science*, vol. 13, pp. 249-255.
4. M. Lamb, 2011, *Monitoring the Structural Integrity of Packaging Materials Subjected to Sustained Random Loads*, PhD thesis, Victoria University, Melbourne, Australia.

# Designing polypropylene lidding film with combined peelable and antifogging properties for food packaging

**Charinee Winotapun*, Pitcha Liewchirakorn, Wisaroot Payubnop, Witchuda Daud and Wannee Chinsirikul**

*Polymer Research Unit, National Metal and Materials Technology Center, National Science and Technology Development Agency, Pathumthani 12120, Thailand*

*Corresponding author. Email: charinew@mtec.or.th*

**Abstract:** In general, fresh produce and ready-meal products packaged and stored at cold temperature would require packaging film with effective easy peel and antifogging performance for convenience and display reason. Structuring plastic film having a minor phase dispersed in the polymer matrix is one route in tailoring bond strength when sealed with a substrate and to produce desirable peelable property. Based on this principle and polymer blending, metallocene catalyzed linear low density polyethylene (mPE) was selected and incorporated into polypropylene (PP) in this study. Some early investigations revealed improved processability of this blend; however, published data on the peel-seal property of this particular blend have not been found. In addition to the desired peelable performance, selecting a suitable antifogging (AF) additive was also considered. Two-layer films with thickness of 40 µm were produced by co-extrusion. Sealant and antifogging function were designed in the thin inner layer with a thickness of 8 µm where the outer layer of 32 µm was neat PP. The mPE and AF additive were blended with PP in various compositions (10 to 40 wt% of mPE and 3 to 9 wt% of AF). The fabricated film was then sealed with PP sheet having thickness of approximately 300 µm, at 150°C and 1 bar. Peel force was measured using I-peel method. Low measured peel force was achieved within a commonly known easy peel range of 2.70 - 7.95 $N.15cm^{-1}$. Findings revealed that the peelable films could be obtained through an incorporation of at least 20 wt% of mPE (peel force of 3.31 ± 0.11 $N.15cm^{-1}$). Antifogging performance of lidding films was analyzed by cold fog test. Using 3 wt% of AF additive could result in clear film with no discrete water droplets for 20 d. Results of easy peel, antifog and possible failure mechanism upon peeling the PP blend films from the thick PP substrate were included.

Keywords: easy peel, antifogging property, multilayer PP film.

## Introduction

In food packaging, retail packages of fresh-cut fruit and ready to eat products have been increasing in the supermarkets. These products are normally packaged in containers or trays with desirable easy-opening or peelable lidding film. The development of peelable film is essential for customer's convenience. It is required that the lidding film is not only easy to peel but also effectively protects the content inside as it is transported along the distribution chain. Designing a plastic film having minor phase dispersed in the polymer matrix is one route in tailoring bond strength when sealed with a substrate and to produce desirable peelable property [1-3]. Such structure with a minor phase enabling an easy-peel function is normally incompatible with the polymer matrix. Nase et.al [1, 2] reported the peelable low density polyethylene (LDPE) film system. The LDPE film containing a minor phase of isotactic polybutene-1 (iPB-1) ( up to 20wt%) can provide easy opening property based on the incompatibility of the two parts. They found that the easy-opening of LDPE/iPB-1 film occurred based on the very low adhesive strength between polymer matrix and minor phase. The higher the iPB-1 content, the lower the peel force was. Manias et.al studied peelable PE film with ethylene vinyl acetate (EVA) and montmorillonite (MMT). They designed a hermetic seals with an easy-open character across the broadest possible range of sealing temperature. The combination of EVA and MMT provides favorable interactions for nanocomposite formation and maintain the sealant intergrity, but weak enough at the interfacial adhesion to promote peelable film. However, from the literature review [1-3], most previous studies have involved peelable PE film, and the development on the peelable polypropylene (PP) lidding film is very limited. Various attractive properties of PP, such as stiffness, heat resistance and low cost, are desired for food packaging [4]. Therefore, based on the polymer blend principle, metallocene catalyzed linear low density polyethylene (mPE) was selected and incorporated into PP to develop peelable PP lidding film. Some early investigations revealed improved processability of this blend [4process]; however, published data on the peel-seal property of this particular blend have not been found.

In addition to a challenge for packaging design on a balanced between seal and peel property of the lidding film, antifogging property is another required attribute when products should be visible during on-shelf display. During cold storage of food with high water content such as fresh fruits and vegetables, the lidding film can be foggy due to moisture condensation. The condensation of moisture or water vapor on the film surface can generate discrete water droplets due to a difference between surface tension of water and film. This phenomenon leads to the undesirable effects and reducing the consumer's ability to see the products inside the package. In addition, in some applications, fogging can deteriorate the food quality. To solve this problem, one approach is to improve the wettability of the polymer surface [5]. Antifogging additives can modify the wettability of the film surface. Antifogging agent is commonly blended with the host polymer using extrusion. The antifogging additive migrates to the surface of the polymer and increases the surface tension of the polymer. Another role of the antifogging agent is to decrease the surface tension of water by being dissolved into the water With these mechanisms, the surface tensions of the polymer and water become more or less equal and the water droplet is spread into a thin continuous layer on the polymer surface. To achieve an effective antifogging property, a suitable type and optimum quantity of the additive are critical factors in controlling its migration behavior from the bulk to the film surface and the resulting antifog performance.

Thus, an attempt in this present work is to develop the peelable PP lidding film with combined antifogging properties by designing material formulation and multilayer film structure. Since peelable and antifogging property should be effective only in the sealant layer of the lidding film. Therefore, only a small amount of antifogging agent is incorporated in the sealant layer where the easy peel function from the blend of mPE/PP is also present.

## Materials and Method

### Materials and Blends Preparation

Polypropylene homopolymer resin (PP) used was Moplen HP420J with a density of 0.904 $g.cm^{-3}$, provided by HMC Polymers Company Limited. The melt flow index of PP measured at 230$^{o}$C with a load of 2.16 kg is 3.0 g (10 $min^{-1}$). Metallocene catalyzed linear low density polyethylene (mPE) used was AFFINITY™ PT 1450G1 with a density of 0.904 $g.cm^{-3}$, supplied by Dow Chemical Company. The melt flow index of mPE measured at 190$^{o}$C with a load of 2.16 kg is 7.5 g (10 $min^{-1}$). Antifogging agent for cast polypropylene films used was Accurel ® GA332 (polyglycerol ester 60%w/w in porous PP), provided by Membrana GmbH.

In order to study the effects of blending, the mPE and PP were blended by two methods: dry blending and twin-screw blending. In the case of dry blending, mPE was physically mixed with PP to different mixing

ratios (10/90, 20/80, 30/70 and 40/60 wt%) before being fed into the co-extrusion cast film line. Regarding twin-screw blending, mPE and PP were mixed in a co-rotating twin-screw extruder (LABTECH, THAILAND) with a screw diameter of 20 mm and L/D ratio of 32 at 210$^{o}$C. The extruder screw was designed to provide distributive and dispersive functions during mixing. The screw speed and feed rate was set at 140 rpm and 2.5 kg.h$^{-1}$, respectively. The melt-extruded blends of mPE/PP passing through the rod die were pelletized. Resulting blends in pellet form were used for film fabrication.

## Cast Film Extrusion

All cast film samples were produced on a laboratory-scale co-extrusion cast film line (Dr. Collin, GERMANY). This line was equipped with three extruders for producing three layer films. Each extruder had a 20 mm diameter single screw, 25 L/D ratio, a mixing section at the end (2.5 D), and a compression ratio of 3:1. The blended materials (mPE/PP) were extruded into one layer component (inner layer, A) of the co-extruded film where PP was present as the outer layer (B) with A/B configuration. Cast films were extruded through T-die with a die gap of 0.3 mm. Optimum barrel (zones 1 - 4), adapter (zone 5) and die set temperatures (zone 6 - 7) were approximately 60, 180, 190, 200, 210, 230 and 230 °C, respectively. Cooling was performed on a chilled roll at the temperature of 25 $^{o}$C. These parameters were kept constant for all films production. Resulting two layer films had thickness of ~ 40 ± 5 μm. All film samples were produced at a screw speed of 60 RPM (for each extruder) or about 4 kg.h$^{-1}$ output rate. After film processing, the films were sealed with PP substrate (thickness of 300 ± 25 μm) at a temperature of 150°C, pressure of 1 bar and dwell time of 3 s. The sealed films were subsequently cooled to ambient temperature.

## Peeling Measurement

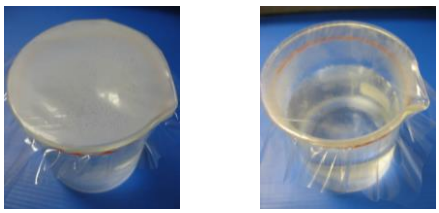
All peel tests were performed on a universal testing machine, or Instron 5943 (Instron, USA), according to ASTM F88-00. Samples of 25 mm gauge length and 15 mm width were tested at a crosshead speed of 200 mm.min$^{-1}$, using a 100 N load cell. The peel force-elongation curves were recorded for five specimens. The average peel force for each specimen was determined between 40% and 80% of the elongation in the peel force curve (or a plateau-like region). Five specimens per set were tested and averaged.

## Cold Fog Test

The antifogging performance of the film samples was evaluated by a cold fog test according to the method described by U.S. Patent No. 6726968 [6]. The film sample covered the top of a beaker containing 200 cm$^{3}$ of water. The beaker was then placed in a temperature-controlled cabinet at 4°C. The film appearance was observed for a period of 30 d. The effectiveness of the antifogging performance was evaluated by visual inspection of water condensed on the inner film surface using ratings from 0 to 10, as described in Table 1. Rating 10 indicates the desirable antifogged film that there is no visible trace of water on the film. In contrast, rating 0 indicates foggy films or 100% small discrete water droplets on the film surface. This test was performed to mimic the application of films containing antifogging agent under chilled storage of food products.

Table 1 Appearance ratings of antifogging performance [6]

| Rating | Antifog Performance |
|---|---|
| 0 | Fine fog across entire surface<br>Difficult to view product |
| 2 | Small droplets (1-2 mm diameter)<br>Product somewhat obscured |
| 4 | Medium droplets (2-4 mm diameter) |
| 6 | Large droplets (>4 mm diameter) |
| 8 | Moisture visible but fairly uniform with some texture or large droplets |
| 10 | Indistinguishable from dry film over entire package |



(a) (b)

Fig. 1 Pictures of foggy film versus desirable antifog film

(a) Foggy film, rating 0

(b) Antifog film, rating 10

## Results and Discussion

### Effect of mPE content in inner layer on peel property

The mPE was physically blended with PP using different mixing ratios (10/90, 20/80, 30/70 and 40/60 wt%) and were extruded into one layer component as the inner layer (A) where neat PP was presented in the thick outer layer (B) with A/B configuration (two-layer film). The fabricated two-layer films (considered as the lidding films) were sealed with another PP substrate (thickness of 300 ± 25 μm) at a temperature of 150°Cfor a constant pressure of 1 bar and dwell time of 3 s. Fig. 2 illustrates the peel force curves of the two-layer PP films containing mPE of 10, 20, 30, and 40 wt% in the inner layer. The averages of peel force were calculated between 40% and 80% of elongation (in the range of peel propagation or plateau-like region). From this figure, it is observed that films with higher amount of mPE show lower peel force. When the mPE content in the inner film increased to 30 and 40%, the measured peel forces of the two films are almost the same.

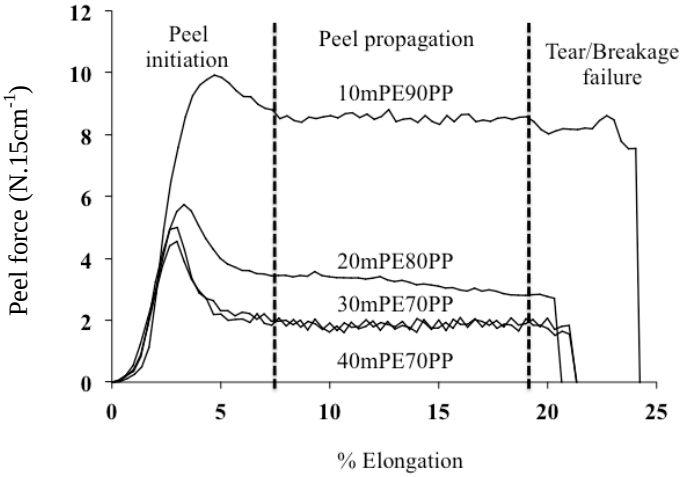



Fig. 2 Peel force curve between the mPE/PP blend films (with various mPE content in the inner layer) and the PP substrate.

Fig.3 represents the peel forces as a function of the mPE content in the inner layer. It can be seen that the peel force tended to decrease with increasing the mPE content. The peel force of PP film with 10, 20, 30 and 40 wt% mPE in the innerlayer sealed with PP substrate are 8.45 ± 0.34, 3.31 ± 0.1, 1.87 ± 0.07 and 1.89 ± 0.07 N.15cm$^{-1}$, respectively. Note that the peel force of 0.77 N.15cm$^{-1}$ is considered as the onset of the hermetic seal formation where the peel force in the range of 2.70 - 7.95 N.15cm$^{-1}$ is considered as peelable (easy-open) [3]. However, the peel force of PP film with 10 wt% mPE in the inner layer (sealant layer) is higher than the easy-open range while the peel force of PP film with 20, 30 and 40 wt% mPE in the inner layer are in the easy-peel range. Therefore, an incorporation of at least 20 wt% mPE in the PP inner layer could produce peelable PP films. This may be attributable to the resulting heterogeneous structure of the two phases of PP and mPE. Blends of mPE/PP show phase-separation, revealed by SEM. For instance, SEM image showing cross-sectional area of the 30mPE/70PP blend film (fig.4) reveals that the mPE component is present as a minor phase dispersed in PP matrix. This structure may introduce a number of weak bonds between mPE and PP. Therefore, easy-open ability between the mPE/PP film and the PP substrate was obtained.

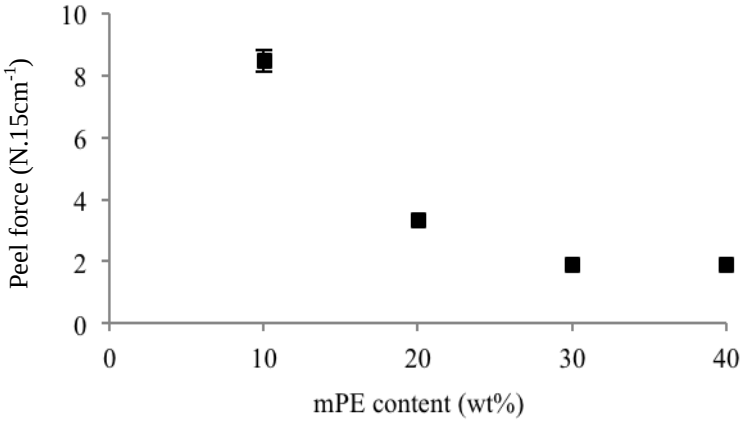



Fig. 3 Peel force versus mPE content for the mPE/PP blend films and the PP substrate.

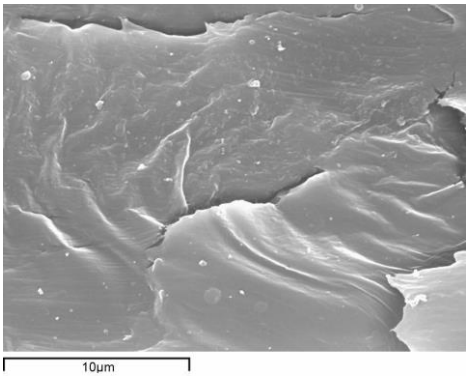



Fig. 4 Scanning electron micrograph of cross-section area of 30mPE/70PP film along the machine direction (MD) produced from dry blend, at magnification of 5,000x.

## Effect of dry blending and twin-screw blending of mPE in PP inner layer

By keeping the co-extruded structure, blending of mPE/PP inner layers (or sealant layer) were either dry blending or melt-compounding via a twin-screw extruder. The PP with 20 wt% mPE (the lowest mPE content showing easy peel property) in the sealant layer was selected for a comparison. The PP with 20 %wt mPE blends from the two different blending process were fed through the co-extrusion cast film line to produce the two-layer film structure, the inner (sealant) layer was the mPE/PP blend and the core layer was neat PP. The sealing temperature of 150°C, pressure of 1 bar and dwell time of 3 s were used. Fig.5 shows a comparison of SEM images of the PP substrates after peeling off the the films when the sealant layer of the two samples are different,((a) using dry blend of mPE/PP and (b) twin-screw blend). It was found that the samples having the sealant layer based on the twin-screw blend of mPE/PP showed less amount of coarse fibrils on the peeled PP substrate as compared to films using dry blend at the sealant layer. Observed fibrils on the twin-screw blend of the sealant layer appear to be finer in diameter. This may suggest that when mPE was blended with PP by co-rotating twin-screw extruder, mPE phase size can be reduced as compared to the dry blend system. It is generally known that an intensive mixing with high shear in the twin-screw extrusion can also provide a good dispersion and distribution of the blends. In this series of study, we are convinced that twin-screw blends of mPE/PP can help reduce "strings or angle hair" left over on the peeled surface. The "angel hair or string" (thin pieces of film that remain attached to the container) that may fall into the packaged food products, which seems unacceptable for consumer [7]. In terms of peel force, it was observed that the PP with 20 wt% mPE, prepared by twin-screw mixing, possessed a slightly higher peel force, as compared to dry blends-sealant layer sample. The peel force of dry blend and twin-screw blend of mPE/PP sealant layer samples are 3.31 ± 0.11 and 3.37 ± 0.07 $N.15cm^{-1}$, respectively.

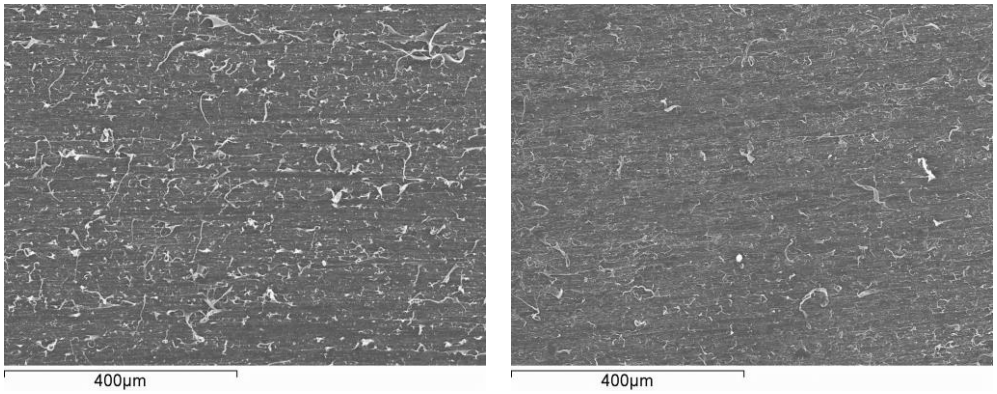



Fig. 5 Scanning electron micrographs showing the peeled surfaces for PP substrates sealed with films having the sealant layer prepared from dry blend and twin-screw blend, at a magnification of 200x.

### Antifogging performance of PP peelable films

The lidding films with easy-opening and antifogging properties are considered for food packaging. Good sealant and antifogging function could be designed by multilayer film structure, by placing the layer with these specific functions at the inner/sealant layer. From the peel test, it was found that the easy-peelable films were obtainable through an incorporation of at least 20 wt% of mPE in to the PP. By a twin-screw blending method, another advantage of the mPE/PP selant layer was a reduction of strings or angle hairs on the peeled surfaces (both on the substrate and film side) and peel force obtained ($3.37 \pm 0.07$ N.15cm$^{-1}$) was well in an easy-peel range) Therefore, antifogging agent from 0 to 9 wt% was incorporated in the blend system of 20mPE/80PP by twin-screw extruder. Antifogging performance of the antifogged mPE/PP inner layer films were evaluated by cold fog test. The antifogging performance of the films containing antifogging agent of 3, 6 and 9 wt% are illustrated in Table 2. This justification was based on the cold fog test demonstrating a good antifogging performance at 4°C condition. It was found that antifogging performance of mPE/PP films were improved when the amount of antifogging agent increased from 0 to 9 wt%. This was indicated by clearly uniform water layer without discrete droplets. The better antifogging performance was observed as increasing storage time after film production. The effective antifogging performance of the films with 3 and 6 wt% antifogging agents were 20 d (Rating 8 - 10) of storage time. Moreover, the mPE/PP films containing 9 wt% antifogging agents have good antifogging performance (Rating 8-10) within 15 d after film production. This can be explained by the function of antifogging agent that helps spread the liquid water into a clear thin layer, instead of being discrete droplets [5, 8].

Table2 Antifogging performance of antifogged mPE/PP films by "cold-fog" test.

| Storage Time (days) | Antifogging performance of [20mPE/80PP] film (Rating from 0-10) | | | |
|---|---|---|---|---|
| | 0%AF | 3%AF | 6%AF | 9%AF |
| 1 | 0 | 0 | 0 | 0 |
| 7 | 0 | 0 | 0-2 | 2 |
| 10 | 0 | 2 | 4 | 6 |
| 15 | 0 | 4-6 | 6-8 | 8-10 |
| 20 | 0 | 8-10 | 10 | 10 |
| 30 | 0 | 10 | 10 | 10 |

The amount of antifogging agent used in the 20mPE/80PP inner layer film could be 3 to 6 wt% to achieve an effective antifogging performance, depending upon the required storage time before film usage. Too much antifogging additives used may bring about an undesirable surface blooming. Surface blooming can cause seal problem between the film and the substrate (or the lid film and the tray rim for common food packaging). Consequently, using the least amount of antifogging agent is necessary not only to avoid surface blooming but also to reduce the cost of additive. Nevertheless, further investigation has also been underway to establish a better understanding on the migration of antifogging agent in the selected blend films.

## Conclusions

In this paper, the designed material formulation and two-layer film structure could be successfully developed for the PP lidding film to provide an easy peel with effective antifogging properties. Study revealed that the peelable films were obtainable through an incorporation of at least 20 wt% of mPE into the PP by twin-screw extruder. This blend acted as a sealant layer and offered easy-peel performance at the same time (peel force was $3.37 \pm 0.07$ N.15cm$^{-1}$). Blending the mPE and PP using twin-screw extruder also provided another advantage over the dry blend process in reducing the remaining strings on the peeled surfaces. Antifogging performance of lidding films was analyzed by cold fog test. Using 3 wt% of AF could result in clear film with no discrete water droplets by 20 d (Rating 8-10). Clearly, targeted properties of packaging films required for a variety of fresh produce or foods can be optimized and tailored through integrated concept based on material formulation and multilayer film structure.

## Acknowledgements

The authors gratefully acknowledge financial support of this study from National Metal and Materials Technology Center (MTEC), National Science and Technology Development Agency (NSTDA), Ministry of Science and Technology, Thailand.

## References

1. M. Nase, A. Zankel, B. Langer, H.J. Bauman, W. Grellmann, P. Poelt, 2008, "Investigation of the peel behavior of polyethylene/polybuthylene-1 peel films using in situ peel tests with environmental scanning electron microscopy", *Polymer*, vol. 49, pp. 5458-5466.
2. M. Nase, B. Langer, W. Grellmann, 2008, "Fracture mechnics on polyethylene/polybutene-1 peel films" *Polymer Testing*, vol. 27, pp. 1017-1025.
3. E. Manias, J. Zhang, J.Y. Huh, K. Manokrung, P.Songtiya, MD.M Jimenez-Gasco, 2009, "Polyethylene nanocomposite heat-sealant s with a versatile peelable character", *Macromolecule Rapid Communications*, vol. 30, pp.17-23.
4. K. Ono, H.Ogita, K. Okamoto, M.Yamaguchi, 2009, " Processability and mechniacalproperties for binary blends of PP and LLDPE produced by metallocene catalyst", *Journal Applied Polymer Science*, vol. 113 pp. 3368-3375.
5. C.Winotapun, U. Watcharosin, P. Panitanta , W.Chinsirikul, 2010, "Migration Analysis of Antifogging Agent in Polyethylene Films by FTIR-ATR and Cold Fog Tests ", *Proceedings of Polymer Conference*, Thailand, Oct. 7-9, pp. 130-135.
6. SJ. Porter, 2004, "Antifog/barrier laminate for use in meat packaging", *U.S. Patent No. 6726968*. April 27.
7. M. Baker, 2009, "Analysis of Peelable Film in Food packaging", *2008-09 Italian Packaging Technology Awards Program*, pp.1-15.
8. L. Irusta, A. Gonzalez, M. J. Fernandez-Berridi, J.J. Iruin, J.M. Asua, I.Albizu, A. Ibarzabal, A.Salmeron, E.Espi, A. Fontecha, Y. Garcia, A.I.Real, 2009, "Migration of Antifog Additives in Agricultural Films of Low-Density Polyethylene and Ethylene-Vinyl Acetate Copolymer", *Journal of applied Polymer Science*, vol. 111, pp. 2299-2307.

# Microperforation of Three Common Plastic Films by Laser and Their Enhanced Oxygen Transmission for Fresh Produce Packaging[#]

**Wannee Chinsirikul[1], Charinee Winotapun[1*], Noppadon Kerddonfag[1], Pramote Kumsang[1], Bongkot Hararak[1], Vanee Chonhenchob[2] and Teerapon Yamwong[1]**

*[1] National Metal and Materials Technology Center, Thailand*
*[2] Department of Packaging and Materials Technology, Kasetsart University, Thailand*

*[*]Corresponding author. Email: wcharinee@hotmail.com*

**Abstract:** This paper described the use of Nd-YAG laser to perforate three plastic films including biaxially-oriented polypropylene (BOPP), biaxially-oriented polyethylene terephthalate (BOPET) and low density polyethylene (LDPE). The films were perforated under various pulse energies of 50, 150 and 250 mJ and with pulse duration of ~10 ns and pulse repetition of 1 Hz. It was found that perforation diameters of all films increased with increasing pulse energies. Observed perforations were different among the three film types. Explanation was contributed to material inherent property and its interaction with laser. Incorporation of an inorganic filler (i.e. silica based anti-blocking agent used in packaging film) of 0.5 wt% into the LDPE films (0.5Si-LDPE) could improve perforation performance for LDPE. This was attributed to an increased thermal diffusivity of the 0.5Si-LDPE film. Commercial BOPET and BOPP films containing 97 microholes.$m^{-2}$ (hole diameter of ~100 µm) showed an improvement in oxygen transmission rate (OTR) of 18 and 5 times, respectively, that of the regular films. In the case of perforated film of 0.5Si-LDPE having similar perforation quantity of 97 microholes.$m^{-2}$ and perforation diameter of 100 µm, a two-fold increase of OTR was obtained. Gas transmission rates of the microperforated films were measured based on the static method. Measured OTR and CO2TR values of the three films with varying perforation diameters in a range of ~40 - 300 µm were compared and discussed. Overall results clearly indicate that perforation by laser is an effective process in developing breathable films with tailored oxygen transmission property for fresh produce packaging.

Keywords: microperforation; oxygen transmission rate; modified atmosphere packaging.

[#] This is the abstract of a peer-reviewed paper to appear in a Special Edition of Wiley's journal *Packaging Technology and Science* dedicated to the 19th IAPRI World Conference on Packaging 2014 hosted by Victoria University, Melbourne, Australia.

# PACKAGING PRINTING & GRAPHICS

# Qualitative Analysis of Coverage Value Transfer in Modern Packaging Printing Workflow

**Tamara Tomašegović[1], Sanja Mahović Poljaček[1*] and Diana Milčić[2]**

[1] *Department of printing plates, University of Zagreb, Faculty of Graphic Arts, Croatia*
[2] *Department of graphic machines, University of Zagreb, Faculty of Graphic Arts, Croatia*

[*] *Email: smahovic@grf.hr*

**Abstract:** Modern packaging printing workflow has been nowadays directed to flexographic printing technique. It requires a usage of a number standardised processing procedures in order to create an attractive and consumer appealing packaging. With constantly increasing number of brands on the market, new qualitative requirements are present for flexography. The aim of this research was to evaluate two different types of modern flexographic workflow systems (LAMS and TIL technology). The hypothesis was that the standardised different workflows should give a product of similar technical and visual appearance quality. Measured parameters were: the formation and structure of the image elements on the printing plates, transfer of the printing ink to the printing substrate, dot gain on the printing substrate and visual evaluation of the imprints. Obtained results revealed the differences in formation of image elements on the printing plates as well as the difference in coverage values transfer from the printing plate to the printing substrate. Differences were detected in specific coverage areas (highlights, shadows), where the surface structures of the printing plates were significantly different. Addition analysis in form of visual evaluation of images, specific colours and tone gradients has been made and gave different results. They indicated that highlights and realistic colour on the imprint have been better reproduced by LAMS printing plate, despite the fact that better transition of tones through the whole tone range was measured on reproductions with TIL printing plate. This research has proved that technically correct printing plate and imprint can give a reproduction of lower visual appearance quality. Results have shown that reproduction of each packaging product should be considered individually in a closed reproduction workflow. Visual impression should be considered as a relevant parameter used in planning and production of packaging in order to satisfy the appealing and creative design requirements in packaging.

Keywords: flexography, LAMS, TIL, coverage value, dot gain, visual evaluation.

## 1 Introduction

The appearance of packaging is one of the most important factors for consumer in the decision making process when purchasing a product. Special colours, design and creative printing of high quality enhance the effect of the packaging and provide a positive impact on the customer. Therefore, with increased number of different brands of particular product present on the market nowadays, the features of the packaging design and the print quality became essential [1]. The question arising from that is weather and how the idea that comes from packaging designer can be reproduced in order to fulfil the purpose of packaging.
The most common printing technique for packaging is flexography. It is a direct printing technique which means that printing ink has to be transferred from the anilox roller to the printing plate and from the printing plate directly to the printing substrate (Figure 1) [2]. The imprint in flexography is based on the geometrical difference between the image and non image areas on the printing plate (Figure 2) [2]. Flexographic printing plates are mainly made of photopolymer material and are used to transfer the image from the original digital file to the printing substrate (paper, foil, etc.).

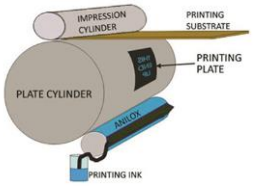



**Figure 1**: Principle of flexography.

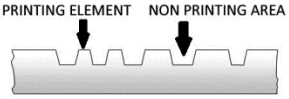



**Figure 2**: Image and non image areas on flexographic printing plate.

The main advantage of the flexographic printing plate is its flexibility. It enables printing on a wide range of materials, such as paper, paperboard, corrugated board, films, laminates, foils and metal. On the other hand, due to its flexibility, the transferred images can be deformed and changed in the printing process because of the straining of the printing plate and the pressure on the substrate [3]. However, with new formulations of photopolymers in flexography and improved digital workflow of the printing plate production, the deformations of the printing elements can be minimized and high quality of printed products can be achieved [1, 4]. Photopolymer material used for flexographic printing plates is mostly made of composition that includes monomers, copolymers, photoinitiators, UV stabilizers, and plasticizers. In the printing plate workflow photopolymer material has to be exposed to UVA radiation which will, in the areas which have been exposed, initiate photopolymerization [5,6]. Polymerized areas of the printing plate become insoluble in the defined developing solution (organic solutions or water), and after rinsing, geometrical difference between printing and non printing areas is achieved. However, oxygen disables the photopolymerization, reacting with the surface of the photopolymer, which results with an incomplete and poor formation of the small printing elements [7]. Therefore, in most workflows, corrections of the digital image must be performed, where the highlight areas have to be *bumped up* in order to make those printing areas reproducible, and to adjust the dimension of the printing elements to the anilox roller cell. After the *bump curve*, other correction should be performed in order to adjust the image to the printing workflow. It is defined as a *compensation curve*. The purpose of that correction is to decrease the surface coverage in the whole tone reproduction area, from the smaller coverage values to the shadows. It should be made in order to compensate the dot gain in printing, which occurs because of the pressure in the printing process and the interaction between printing ink and printing substrate [1,8].
Computer to Plate (CtP) workflows provide the complete control of the printing plate production processes and enable those corrections in a digital file. Two modern technologies, Laser Ablation Mask Layer (LAMS) and Thermal Imaging Layer (TIL), have been implemented in the flexographic printing plate production in the last decade. Process phases of those printing plates can be seen in the Figure 3 and Figure 4. The main difference in LAMS and TIL technology is in the process of formation of the image in the mask layer. Photopolymer material is in LAMS technology covered with LAMS mask which has to be ablated after the back exposure. In TIL technology the laser ablation of the mask layer is made separately from the photopolymer material. After ablation, mask layer has to be laminated on the photopolymer material before the UV exposures. Unlike the LAMS technology, the barrier layer in TIL technology disables the oxidation of the photopolymer material. This difference can result with a flat top of printing element on the printing plate and could enhance the reproduction ability of the highlights and the optimal tone transfer in the whole tone range area [9].

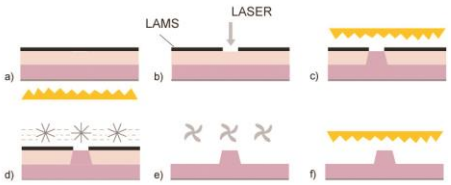



**Figure 3:** LAMS printing plate production: a) ablation of LAMS, b) back exposure, c) main exposure, d) rinsing, e) drying, f) post treatment (UVA + UVC).

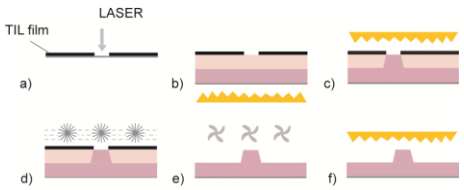



**Figure 4:** TIL printing plate production: a) ablation of TIL, b) lamination of TIL to the printing plate and back exposure, c) main exposure, d) rinsing, e) drying, f) post treatment (UVA + UVC).

## 2 Experimental settings

In this research, properties of the imprints made by LAMS and TIL printing plates have been studied. Sample 1 was the printing plate based on LAMS technology, while Sample 2 was the printing plate based on TIL technology. Digital file was prepared with the aim of obtaining the similar visual appearance of the imprints reproduced with LAMS and TIL printing plates. Nevertheless, the hypothesis was that the quality of the printing elements of Sample 2 will provide the correct transfer of the printing ink to the substrate in the whole coverage area and exceed the quality of the imprint produced by means of Sample 1 printing plate.
The bump up curve was applied on the sample produced by means of the LAMS technology (Sample 1) in order to ensure the optimal reproduction of the highlights and to adjust the dimensions of the minimal printing

element. As it was shown in previous publications [8, 9], the reproduction of highlights with this type of plates is possible by using a bump up curve. On Sample 2, produced by means of the TIL technology, the bump up curve was not applied, concerning the manufacturer recommendations.
In order to define the compensation curves, in the first step, the hardness of the finished printing plates was measured. It was similar for both printing plates (69-71 Shore A) and after the adjustment of the printing workflow, printing plate samples were tested in the same reproduction workflow and compensation curves were calculated and created. Besides mentioned, one other improvement was implemented in the workflow. On the surface of the Sample 2 printing plate digitally was defined the application of a fine texture pattern by forming of the micro-screening in the whole reproduction area. It was made in order to ensure the correct transfer of the printing ink onto the substrate. On the other hand, on Sample 1 a micro-roughness was applied as well, but only in the areas from 90% to 100% coverage value. Previous publications [9,10] proved that applying of a specific texture pattern to the shadow areas has a mayor influence on ink transfer process of this printing plate type. The reason for this is based on the fact that increased roughness on the printing element surface enables better adsorption of the printing ink, due to enhanced specific surface. This kind of pattern ensures the greater amount of the printing ink to be transferred to the printing substrate, resulting in more vivid colours on the imprint.
The printing substrate was the foil and the screen ruling was 54 $lcm^{-1}$. Polyester foil was used because it is one of the most common substrate used in packaging industry. Any other substrate would require a similar but new one adjustment of digital file in packaging printing workflow. In order to get insight into a reproduction of a whole tone range a control wedge with measuring fields of surface coverage for process colours (CMYK) was made. Results are presented in figures where tone reproduction curves have been shown.
Coverage values on the samples were measured by VipFlex – device for measuring of film, imprint and flexographic printing plate. VipFlex can capture the images of printing plate, film, and imprint, in order to calculate the screen ruling, screen angle and coverage values of obtained images. However, the transparency and micro-structure on the surface of the examined samples can cause the reflection of the light and inaccurate calculation of the coverage values. Therefore, the open-source software for image analysis, ImageJ, was used in this research to obtain correct analysis of the coverage values. Previous research [10, 11] proved ImageJ as an optimal substitute to conventional printing plate surface analysis program support. Images of the printing plate surfaces of the Sample 1 and Sample 2, and corresponding imprints, were captured by VipFlex and imported in ImageJ. After the corrections of the light distribution on the images and removal of the noise, images were transferred to bitmap, and coverage values were calculated and tone reproduction curves were made.
In addition, printing elements of different coverage values were visually monitored and captured by Olympus Metallurgical Microscope BX51. Olympus BX51 is a microscope with the ability of capturing images of magnification up to 1500x, with program support for image adjustment and analysis. After processing the obtained results, the visual analysis of the imprints was performed. Visual evaluation of the imprints was performed as a questionnaire among 35 students of graphic design technology who are familiar with the elements relevant for imprint evaluation. The observed testing photos had specific colours: human skin, image with prevailing highlights, image with prevailing shadows and image with colourful motives of fruit.

## 3 Results and discussion

### 3.1 Printing plates

Figure 5 and Figure 6 presents the surface coverage measured on the printing plates made with LAMS and TIL. The results are presented through calculated and nominal values of coverage with detailed preview of printing elements in highlight and shadows areas. Black and magenta were chosen among the similar obtained results.

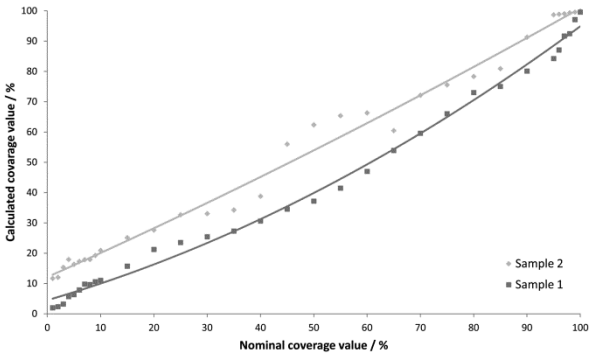



**Figure 5**: Coverage values of black Sample 1 and Sample 2 printing plates.

One can see on Sample 1 (LAMS) that bump up curve is applied, and that the minimal values of coverage have been increased. There has been a certain change in coverage values in shadows as a consequence of applying a micro-texture in the area from 90% - 100% coverage value. Sample 2 (TIL) shows better reproduction of the coverage values in highlight and shadow areas. Deviation in calculation of middle coverage values for black can be seen (Figure 5) which is probably the consequence of remained printing ink on the printing plate.

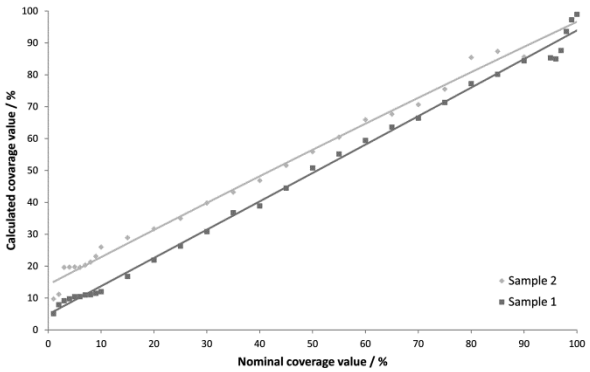
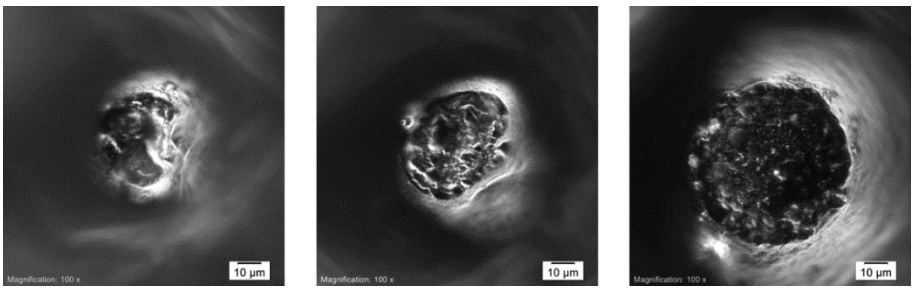


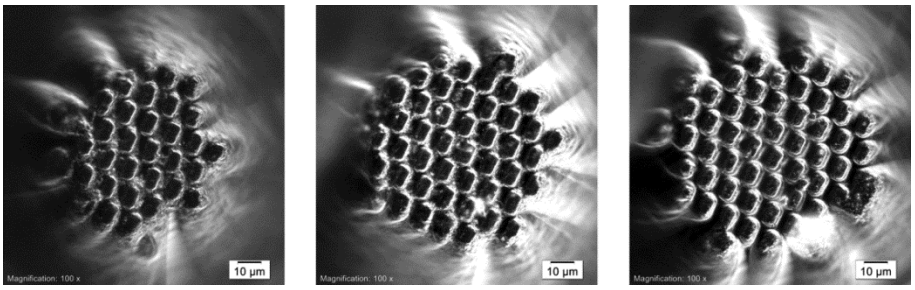

**Figure 6**: Coverage values of magenta on Sample 1 and Sample 2 printing plates.

For detail observation of the printing plate surfaces a microscopic images have been captured. In Figure 7 and 8 one can see the printing elements on Sample 1 and Sample 2 under magnification of 1000x. It is visible in Figures 7a and 7b that printing elements in Sample 1 have not been regularly formed. The surfaces of 1% and 3% coverage value have round top which can result, due to pressure in the printing process, with uneven formation of raster elements on imprints. Figure 7c represents a surface coverage of 10%. The printing element has circular shape but the top of an element has not been correctly formed. On the other hand, it is visible that printing elements on Sample 2 (Figure 8) have been regularly shaped and have a flat top surface. They are formed by application of fine micro-texture which should enhance the transfer of the printing ink to the printing substrate.




a) b) c)

**Figure 7**: Images of printing elements on Sample 1 printing plate
a) 1% coverage value, b) 3% coverage value, c) 10% coverage value.




a) b) c)

**Figure 8**: Images of printing elements on Sample 2 printing plate

a) 1% coverage value, b) 3% coverage value and c) 10% coverage value.

Figure 9 and 10 present the measuring of the coverage values of black and magenta printing plate in shadow areas (70% - 100%). Those areas are separated in order to see the transfer of coverage values by usage of micro-texture pattern on both printing plate samples. It is visible in Figure 9 that deviations and increased values are present on both samples. Certain regularity can be detected on printing plate Sample 1 where the coverage

transfer is gradually better than it is measured on Sample 2. In Figure 10 one can see the results of coverage values of magenta printing plate. Sample 1 shows better gradual transfer and Sample 2 similar increase as on black sample. The reason for this is the usage of different correction curves for Sample 2 printing plates as it was seen in Figures 5 and 6. Microscopic preview of plate's surface structure can be seen in Figures 11-13.

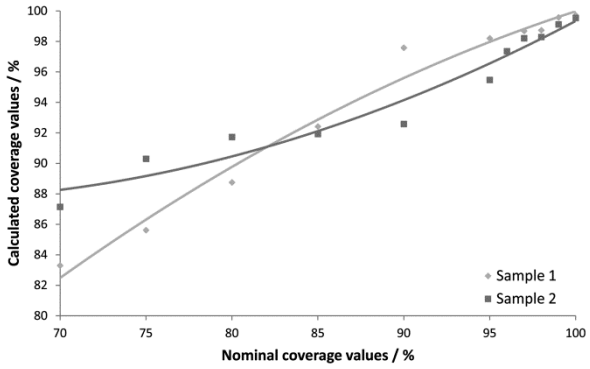



**Figure 9**: Coverage values of black on printing plates Sample 1 and Sample 2 in shadows.

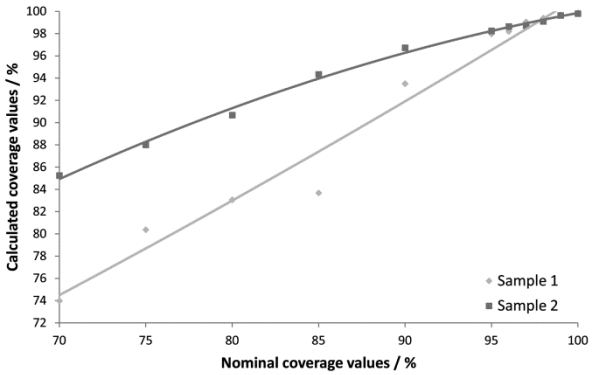
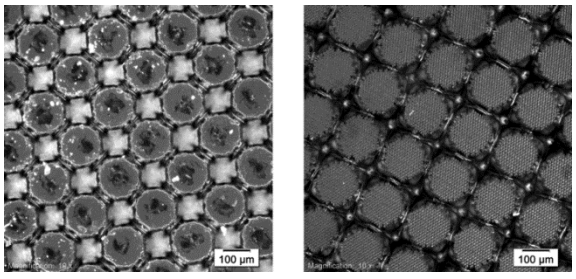



**Figure 10**: Coverage values of magenta on printing plates Sample 1 and Sample 2 in shadows.

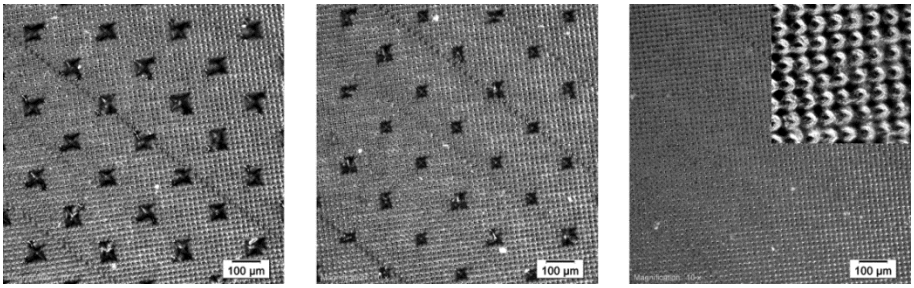
Figure 11 presents printing elements of 50% coverage value of both printing plate samples under the magnification of 100x. The shapes of the printing elements are correct on both samples and the micro-texture surface structure of printing elements on Sample 2 can be seen.
In order to get the detail information about the shape of printing elements in shadows, the microscopic images of those surfaces were captured and presented in Figures 12 and 13 under the magnification of 100x. The images of 90%, 95% and 100% coverage value can be seen.




a) b)

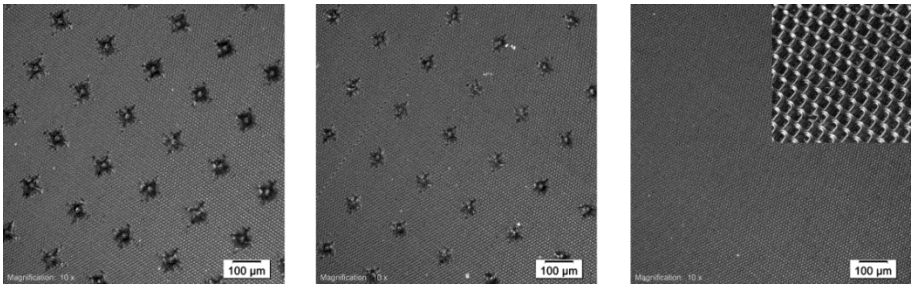
**Figure 11**: Printing elements of 50% coverage value on a) Sample 1 and b) Sample 2.

It is visible that Sample 2 has a surface structure with smaller micro elements (Figure 13), and therefore larger specific surface compared to Sample 1 (Figure 12). Enhancement of the printing element's specific surface can cause adsorption of the larger amount of the printing ink on the printing plate, resulting with more uniform and increased transfer of the printing ink to the printing substrate, as well [12]. This is particularly visible on the expressed increase of the coverage values of 90% on Sample 1, compared to the coverage value of 95% (Figure 12). Figures 12c and 13c show segments of the printing elements of 100% captured under magnification of 1000x.




a) b) c)

**Figure 12**: Surface structure of the printing elements on Sample 1 printing plate: a) 90% coverage value, b) 95% coverage value, c) 100% coverage value.




a) b) c)

**Figure 13**: Surface structure of the printing elements on Sample 2 printing plate: a) 90% coverage value, b) 95% coverage value and c) 100% coverage value.

## 3.2. Imprints

After obtaining the results of coverage value calculations of printing plate samples and the imprints, dot gain on the imprints for black colour and magenta was calculated and presented in Figures 14 and 15. Figure 14 presents the dot gain on the imprints compared to their corresponding printing plate sample. It can be seen that the printing plate produced by means of the LAMS technology (Imprint 1) causes greater dot gain in the printing process, especially in the mid-tone area, which is common for any printing process (Figure 14) [13,14]. The reason for this is an inadequate adsorption of the printing ink on the surface which results with irregular transfer of the printing ink on the foil substrate. On the other hand, the shape and functional properties of the printing elements on the plates can cause the difference as well. Greater dot gain obtained with Sample 1 printing plate is obviously caused by the deformation of the printing elements due to their incorrect formation during the production process (influence of the oxygen) resulting with round top elements (Figures 7 and 11). In the printing process, the pressure causes deformation of screen elements, increasing its values and finally, higher coverage values on the imprint.

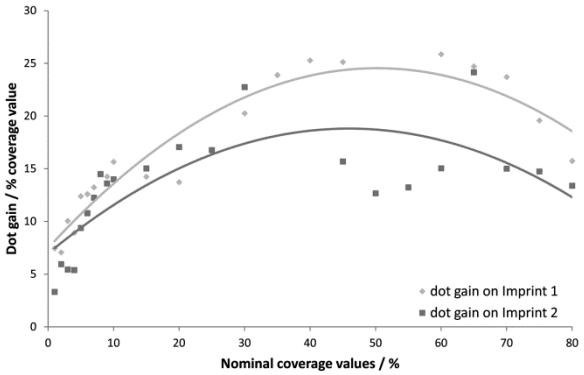



**Figure 14**: Dot gain of black colour on Imprint 1 and Imprint 2.

Similar results are visible for magenta imprints in Figure 15. However, the compensation curve for each process printing colour is different because of the sensitivity of the human eye to different wavelengths and the representation of colours on the reproduced image. Therefore, the dot gain for magenta is higher on the Sample 2

in coverage area over 45%. The final visual impression of the imprint is obtained after the proofing, and the additional corrections of the compensation curves can often be required [15, 16].

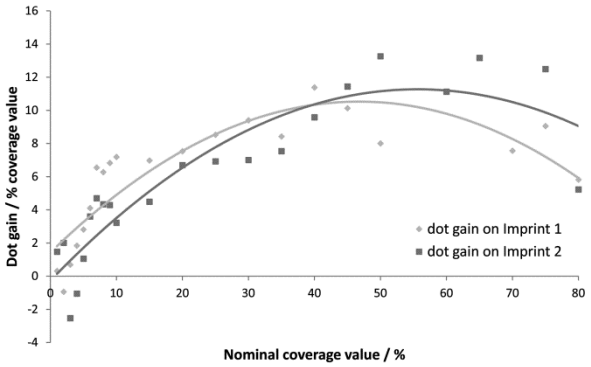
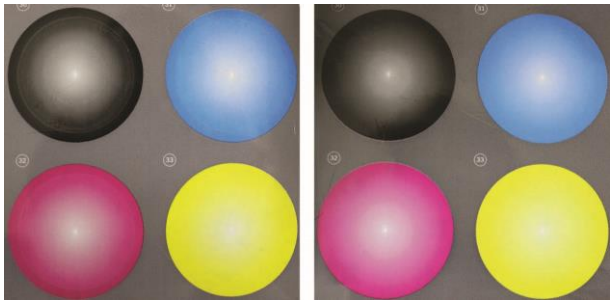



**Figure 15**: Dot gain of magenta on Imprint 1 and Imprint 2.

In order to get inside the formation of gradient on the imprints, the circular test elements with gradient from highlights to shadows were observed. Figure 16 presents the circular gradient on cyan, magenta, yellow and black imprints produced with Sample 1 (LAMS) and Sample 2 (TIL) printing plates. Flat top printing elements and uniformity of the printing ink transfer on Sample 2 provide the smooth gradient on the imprint (Figure 16b). Compared to imprint produced by means of the Sample 1, the superiority of the colour transition is obvious. The reason for the unsmooth tone transition in high coverage value area on the imprint produced with Sample 1 (the light ring inside the gradient of all colours in Figure 16a is caused by the change of printing element's surface structure between 85% and 90% coverage value - implementation of micro-texture on Sample 1 only in the shadows).



a) b)

**Figure 16**: Colour circular gradient on the imprints produced by means of a) Sample 1 and b) Sample 2.

It is obvious that micro-roughness of the printing element's surface enhances the transfer of the printing ink in the graphic reproduction process. Such surface structure, as on the Sample 2, applied to the whole coverage area (1% - 100%), will ensure the greater amount of the printing ink is being transferred to the printing substrate [17]. However, in spite of the lower dot gain on the imprints with flat top elements (Figures 14 and 15), and adequate transfer of the printing ink when applying surface micro-texture to the printing plate, the final visual impression of the imprint can differ from the expected [18].

## 3.3. Visual evaluation

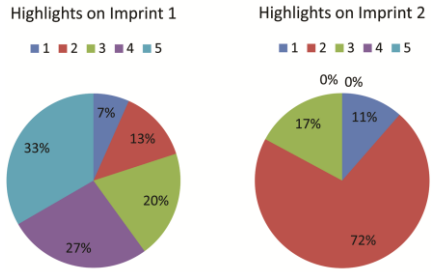
For final observation of the imprints the visual evaluation of imprints was made. In reproduction process, visual evaluation it is often the only mean to evaluate and confirm the final impression of the imprint. Since the characteristics of the printing elements on the flexographic printing plate and raster elements on the imprints are not clearly visible to the human eye without the expensive equipment, the fastest and also reliable way to evaluate the imprint is the visual method. Human eye, especially when the expert is the observer, is sensitive to disturbances in the fluent tone transition, noise, natural colour reproduction; and hue, saturation of the colour, brightness and the contrast in general.



a) b)

**Figure 17**: Images for the visual evaluation produced by means of a) Sample 1 printing plate, b) Sample 2 printing plate.

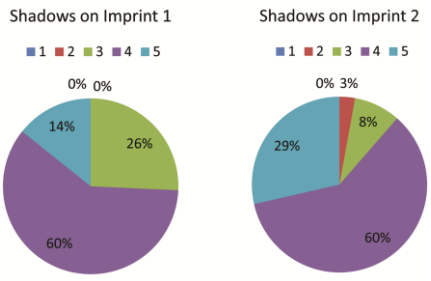
For this research, a questionnaire about the quality of the imprints produced by Sample 1 and Sample 2 printing plates among 35 students was performed. Students were involved in Graphic design course on Faculty of Graphic Arts, and were therefore able to recognize the relevant quality properties of the observed motives. The motive used for the visual evaluation can be seen in Figure 17. It is constituted of the images with predominantly highlight, as well as shadow area. Human skin and the area with vivid colours (fruit) are also represented. Light conditions for the observation of the imprint were constant, under the D50 light source.




a) b)

**Figure 18**: Visual evaluation of highlights on the imprints produced by means of a) Sample 1 printing plate, b) Sample 2 printing plate.

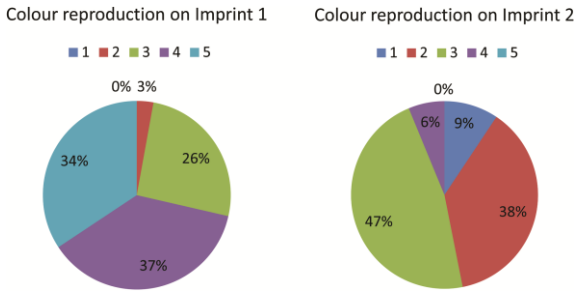
Results of the questionnaire are presented in Figure 18 to 20, as a pie diagram with distribution of grades from 1(bad) to 5(excellent). One can see that the average better grade is assigned to Sample 1, which is, if observing only the data obtained by means of image analysis program support and microscope, not expected. Despite the deformed printing elements in highlight area, the average grade for highlight area on imprint corresponding to Sample 1 is 3.66, while the imprint corresponding to Sample 2 was graded with 2.06 in average (Figure 18).




a) b)

**Figure 19**: Visual evaluation of shadows on the imprints produced by means of a) Sample 1 printing plate, b) Sample 2 printing plate.

According to the visual evaluation of shadows on imprints (Figure 19), Sample 1 and Sample 2 are of almost similar quality. The average grade for the shadow area for imprint from Sample 1 is 3.89, while 4.15 for Sample 2. This result indicates that the finer surface structure on Sample 2 printing plate provides more adequate transfer of the printing ink to the foil, overcoming the potential problem of uneven transfer of the dark tones to some polymer surfaces.




a) b)

**Figure 20**: Visual evaluation of colour reproduction on the imprints produced by means of a) Sample 1 printing plate, b) Sample 2 printing plate.

The average grade for colour reproduction obtained by evaluation of an image with colourful motives of fruit and image of human skin is presented in Figure 20. Mostly realistic impression of the reproduction is 4.02 for the imprint produced by printing plate Sample 1, and 2.5 for the imprint produced by printing plate Sample 2.
After conducted visual evaluation, and obtained results, it is obvious that the quality of the surface micro structure on the printing plate produced with TIL technology and eliminated influence of the oxygen resulting in flat top printing elements, does not necessary assure superior visual impression than the other type of high-quality flexographic printing plate production system. Although the correction in form of the bump curve is not necessary in TIL prepress workflow, detailed compensation should nevertheless be applied to the printing plate in order to reproduce highlights correctly (the improved transfer of the printing ink must not cause visually too vivid, even unnatural highlights, and too dark reproduction of tones mid-tone area) [19]. At the same time, the application of micro structure to the printing elements only in high coverage area, like on Sample 1, causes sharp transition in high coverage value area, and will result with poor quality of the imprint with a gradient or the fluent tone transition in the shadow area. Surface of the printing element without the applied micro-roughness will result with the decreased amount of the printing ink transferred to the printing substrate, especially foil, therefore giving a poor quality of the imprint with a motive where vivid colours should be expressed [20].

## 4 Conclusions

The aim of this research was to evaluate two different types of modern flexographic workflow systems by analysing the samples of the printing plates and corresponding images printed on frequently used printing substrate in flexography – the foil. The first type of printing plate was produced by means of LAMS technology, while other used the black mask with oxygen-blocking barrier layer, ablated separately from the printing plate and then laminated to it (TIL technology).
The results obtained from the coverage value calculations on the printing plates and the imprints, and microscopic visual analysis of the printing elements of the samples indicated that both printing plate types were technically correct in terms of the reproduction of whole coverage area. However, printing plate with separately ablated black mask proved as qualitatively superior with lower dot gain, fluent tonal transitions and correct shape of the smallest printing element (1% coverage value). However, visual evaluation in form of the questionnaire about the quality of the imprints showed different results. Results of the questionnaire indicated that highlights and realistic colour reproduction are better on the imprint produced by printing plate with LAMS technology.
One can conclude that the adjustments of the coverage values on the high quality flexographic printing plate should overcome the technical corrections, such as the minimal reproducible printing element, dimension of the anilox cell and the compensation of the dot gain itself. Visual assessment proved that the usage of compensation curves and colour management in closed reproduction process should anticipate not only technical, but also visual inaccuracies inclined to appear. Printing plate produced by LAMS technology has obviously a weakness in form of the oxygen influence on the photopolymer material and incorrect formation of smallest printing elements, as well as the round top dots in lower and middle coverage areas. This has resulted in greater dot gain due to the deformation on the printing elements in the printing process and less vivid colour reproduction. However, the human eye is accustomed to less vivid imprints on some packaging products, and since flexography has the limitation in the reproduction area of highlights, formed, but not completely correct printing element which transfers the smaller amount of the printing ink to the printing substrate may seem more natural than a vivid reproduction in the highlight area produced by flat top printing element with additionally roughened surface. On the other hand, motives with solid tones, on which the printing ink should be uniformly covered, can be achieved obviously only by application of the fine surface micro-texture on the photopolymer material which ensures the elimination of the oxygen influence during the printing plate production procedure. Surface micro-texture (fine pattern applied to the surface of the printing element) should therefore be used just in the

selected part of the coverage area, or applied to the whole scale of coverage values, depending on the reproduced motive, as well. Therefore, with development of flexographic technology and improvements in the printing plate production workflow in particular, additional reproduction image quality parameters should be considered. This research has proved that technically correct printing plates and imprints can give reproductions of lower visual appearance quality. This means that visual impression should be taken into consideration as a relevant parameter used in planning and production of packaging in order to satisfy the appealing and creative design requirements in packaging.

## References


1. O. Brajnović, 2011, "Adjustment of the photopolymer printing forms to match new qualitative requirements", Master thesis, Faculty of Graphic Arts, University of Zagreb.
2. H. Kipphan, 2001, *Handbook of Print Media*, Springer, Berlin, Germany, ISBN 3-540-67326-1.
3. J. Page Crouch, 2005, *Flexography Primer*, 2nd edition, PIA/GATF Press, Pittsburgh, ISBN 0-883622-04-1.
4. Esko-Graphics, n.d. "HD Flexo: a new standard for flexographic printing plates" [online]Available at: <http://www.esko.com/en/Products/Overview/hdflexo/Overview >[Accessed 22 November 2013]
5. T. Matsubara, R. Oda, 2011, "Block copolymer composition for flexographic printing plates", Pat. 20,110,308,412.
6. R. Knoll, 2002, "Photopolymerizable flexographic printing elements comprising SIS/SBS mixtures as binder for the production of flexographic printing plates", Pat. US 6,531,263 B2.
7. T.Y. Lee, C.A. Guymon, E. Sonny Jönsson, C.E. Hoyle, 2004, "The effect of monomer structure on oxygen inhibition of (meth)acrylates photopolymerisation", *Polymer*, vol. 45, Issue 18, Elsevier, ISSN 0032-3861, pp. 6155–6162.
8. T. Tomašegović, S. Mahović Poljaček, T. Cigula, 2013, "Impact of screen ruling on the formation of the printing elements on the flexographic printing plate", *Acta Graphica*, no. 1-2/13, pp. 1-12.
9. S. Mahović Poljaček, T. Cigula, T. Tomašegović, 2012, "Meeting the quality requirements in flexographic plate making process", *IC2012*, Budapest, Hungary.
10. T. Hudika, T. Tomašegović, S. Mahović Poljaček, 2012, "Offset printing plates: alternative method for quality control", *GRID 2012 Proceedings*, Novaković, Dragoljub (ed.), Novi Sad: Faculty of Technical Science, Department of Graphic Engineering and Design,. pp. 129-133.
11. T. Tomašegović, T. Cigula, S. Mahović Poljaček, M. Gojo, 2011, "Comparison of different measuring systems for printing plate's coverage values evaluation", *Printing future days proceedings 2011*, Reinhard R. Baumann (ed.), Chemnitz : VWB - Verlag für Wissenschaft und Bildung, pp. 39-44.
12. D.K. Owens and R.C. Wendt, 1969, "Estimation of the surface free energy of polymers", *Journal of Applied Polymer Science*, vol. 13, Issue 8, pp. 1741-1747.
13. G.L. Laurent, 2006, "Measurement and prediction procedures for printability in flexography", Doctoral thesis, Royal Institute of Technology, Stockholm.
14. ISO standard 12647-6, 2006, "Graphic technology - Process control for the production of half-tone colour separations, proofs and production prints -Flexographic printing".
15. M. Rentzhog, 2004, "Characterisation of Water-Based Flexographic Inks and their Interactions with Polymer-Coated Board", Licentiate Thesis, Royal Institute of Technology, Institute for Surface Chemistry, Sweden.
16. D. J. Lanska, 2007, "Common-Sense Flexography, A User's Guide to Improved Pressroom Productivity", Printing Industries Press, Pittsburgh.
17. J. Johnson, 2003, "The Influence of Moisture, Temperature, Pulse Pressure, and Substrate on Print Quality in Flexographic Printing", Karlstad University, Sweden.
18. G. L. Laurent, 2001, "Analysis of the Correlation Between the Print Quality Required in Flexography and the Tolerances in Materials and Paper Manufacturing in Terms of Printability", Royal Institute of technology, Department of Numerical Analysis and Computer Science, Sweden.
19. D.E. Bisset, 1979, *The printing ink manual*, 3rd Ed., Northwood Books, London.
20. *FIRST - Flexographic Image Reproduction Specifications & Tolerance - 3rd edition*, 2003, Foundation of Flexographic Technical Association, Inc., USA.

# A Method for General Printing Anti-counterfeiting by Moiré Patterns

**Yunfei Zhong[1*], Yaojian Hu[2] and Xianghua Gu[1]**

[1] *School of Packaging and Materials Engineering, Hunan University of Technology, China*
[2] *The People's Printing Plant of Guangzhou Co., LTD., China*

[*] *Corresponding author. Email: maczone@163.com*

**Abstract:** Moiré security is a type of information hiding technology based on optics. The generation and principle of moiré pattern anti-countfeiting were analysed. The mobile terminals unlock technologies of moiré pattern security for general printing was discussed in depth. According to the structure of the LCD screen, the feasibility of the mobile terminal screen decoding implementation is analysed. Graphic design software was used to design a special information implied in moiré patterns, and apply it to the security design, proofing and verify the effect of the mobile terminal screen decoding. The results show that the security documents which were applied by moiré anti-counterfeiting technology can reveal hiding information pre-designed using a mobile terminal screen to decoding, and a certain authentication effect can be obtained. Finally, the design elements for mobile terminal screen to decode the moiré pattern application and implementation process are given.

Keywords: moiré, information hiding, optical security, printing anti-counterfeiting, mobile terminal decoding.

## 1 Introduction

The current anti-counterfeiting methods for civil application are low cost and easy to identify, but they are easily forged with poor security effect. The authentication by moiré patterns is high reliable, exclusive with simple techniques and low cost. Moiré-based methods offer an interesting solution to counterfeiting of security documents such as banknotes, checks, certificates, packaging for valuable products etc., which can be easily incorporated in the document or product production process without incurring additional production costs[1-3]. Moiré security elements are usually designed and printed as part of the document itself, it is more important that they can be also incorporated in independent security elements such as holograms, special inks, etc. Hu[4] argued that holograms should be integrated with moiré patterns in order to enhance the anti-countfeiting performance. Wang[5] presented a design method of pattern-controllable dynamic moiré holograms that the strip moving and shapes changing can be pre-determined, which is feasible and practical, and the anti-countfeiting capacity can be dramatically enhanced and the hologram is easy distinguished. Qiu[6] proposed to use the ratio of mesh count and screening frequency to generate moiré patterns so as to achieve special effects for printing anti-countfeiting. The method is relatively adapted for monochrome printing but not for colour printing, which can affect printing quality because of screening angle interference in colour printing. Wang[7] summarized the current anti-countfeiting technique by moiré patterns was mainly applying the new spot-colour channel, adjusting the screening frequency and mesh count to design security pattern, but the designed moiré pattern is not predictable.

Currently, most applications in the process of moiré pattern anti-countfeiting need a decoding chip in order to reveal hidden information successfully, which will certainly increase the cost of the anti-countfeiting and it is a certain degree of inconvenience. In the following sections we present an anti-countfeiting method by moiré patterns based on general printing using mobile terminal screen decoding technology. With the flow chart given the security design in the prepress process, printing moiré achieve security in the general printing methods, the mobile terminal screen moiré pattern unlock feasibility was discussed, and gives a reasonable printing implementations

## 2 Principle of anti-countfeiting by moiré patterns

### 2.1 Moiré phenomenon

The moiré effect is a well-known phenomenon which occurs when repetitive structures (such as screens, grids or gratings) are superposed or viewed against each other. It consists of a new pattern of alternating dark and bright areas which is clearly observed at the superposition, although it does not appear in any of the original structures [8]. The moiré effect occurs due to an interaction between the overlaid structures. It results from the geometric distribution of dark and bright areas in the superposition: areas where dark elements of the original

structures fall on top of each other appear brighter than areas in which dark elements fall between each other and fill the spaces better (see Figure 1).

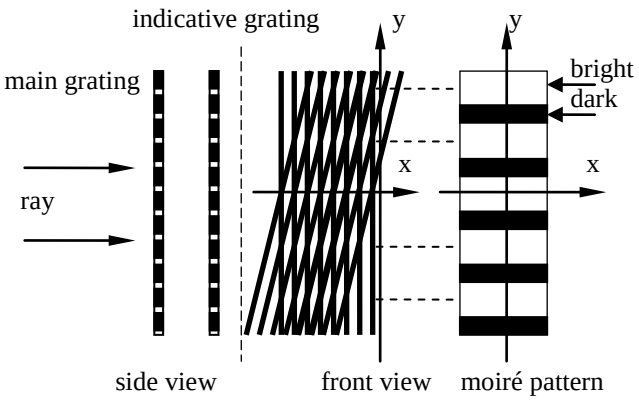



**Figure 1**: Generation of moiré pattern.

### 2.2 Anti-countfeiting by moiré patterns

The method of anti-countfeiting by moiré patterns is to use computer aided graphics design software to produce two similar period images based on the moiré principle as shown in Figure 2. Latent image A is a coding part with the hiding information, B is a decoding part to interpret the hidden information. Image A can be put into a special position of a certain product packaging. After the packaging with latent image A was printed out, we can put the image B above A with little different distance or angle, the image C can be observed which is different from A and B. C is the moiré pattern with hiding information after decoding and the anti-countfeiting effect can be achieved.

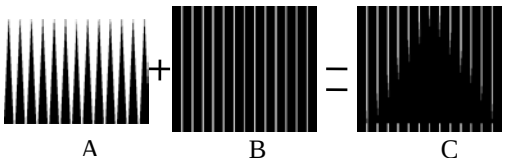



**Figure 2**: Principle of anti-countfeiting by moiré patterns.

## 3 Mobile terminal-based anti-countfeiting by moiré patterns

### 3.1 Process of using mobile terminal means

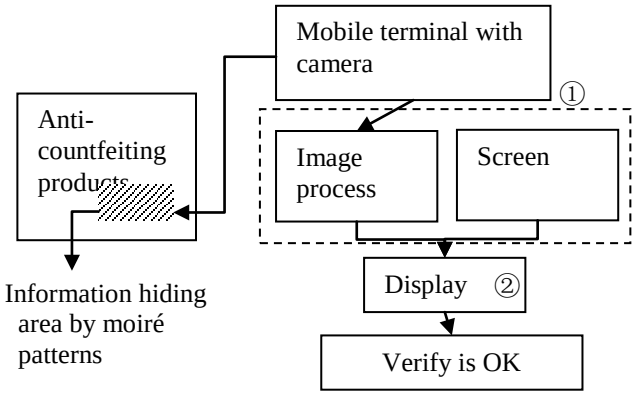



**Figure 3**: Flow chart of mobile terminal decoding.

As shown in Figure 3, in the decoding process of mobile terminal-based anti-countfeiting by moiré patterns, we only need have a clear photo with the camera of mobile terminal, and then the hiding information can be seen from the screen under the decoding matching image processing procedures.

### 3.2 The structure of LCD

A liquid-crystal display (LCD) is a flat panel display, electronic visual display, or video display that uses the light modulating properties of liquid crystals and liquid crystals do not emit light directly. Each pixel of an LCD typically consists of a layer of molecules aligned between two transparent electrodes, and two polarizing filters (parallel and perpendicular), the axes of transmission of which are (in most of the cases) perpendicular to each other. Without the liquid crystal between the polarizing filters, light passing through the first filter would be blocked by the second (crossed) polarizer. Thin-film transistor liquid-crystal displays (TFT-LCDs) are a variant of LCDs that offer improved image quality[9]. TFT-LCDs have a sandwich-like structure with liquid crystal filled between two transparent glass electrode plates coated with indium tin oxide (ITO) as shown in Figure 4. The TFT-LCD panel has TFTs, liquid crystal, pixel electrodes, storage capacitors andcolour filter. The colour filter has a colourresin film containing three primary colour pigments (red, green and blue). An active-matrix LCD uses a separate transistor for each unit pixel. This allows the pixels to stay 'on' longer and thus produce a brighter image.Therefore active-matrix LCDs are used in computer monitors, laptops,TVs, mobile screens, etc.

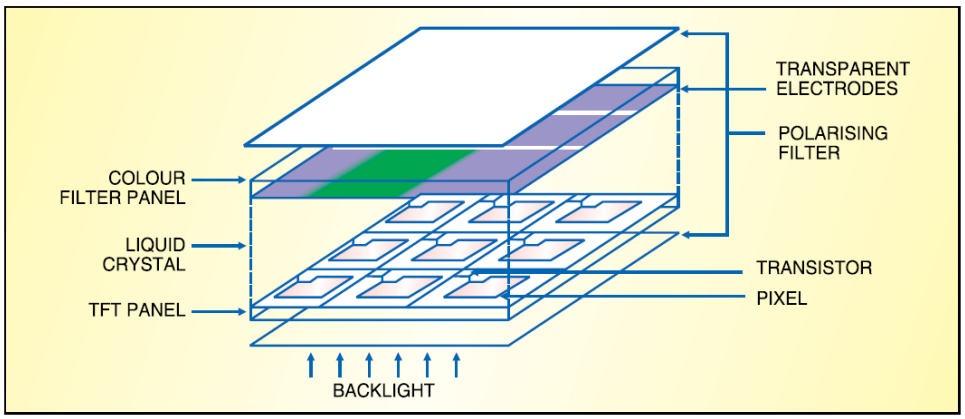



**Figure 4**: TFT-LCD structure.

### 3.3 Screen decoding

To achieve the moiré pattern unlock screen mobile terminal authentication, the mobile terminal must have two essential conditions: camera and screen. Mobile phone is just a mobile terminal along with these two necessary conditions and also plays a essential role of people's daily life. Camera'pixel amounts of mobile phone is an important factor affecting image clarity and it is also an important factor to be taken to distinguish the impact of the original details of the capabilities. If the camera is lack of the ability to distinguish the difference between the original details, which seriously affects the decoding to verify the effect of the screen phone.

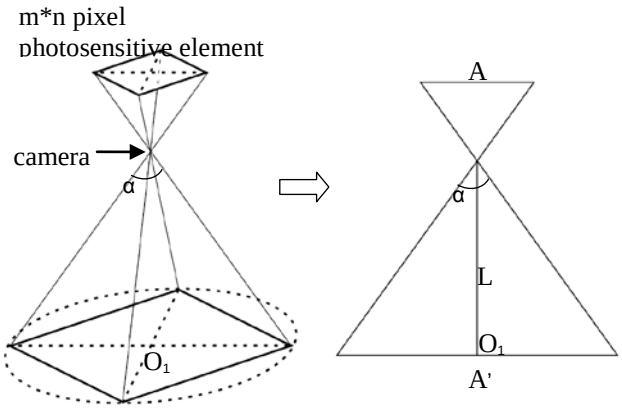



**Figure 5**: Simplified model taking a photo by mobile phone.

Mobile phone present the subject in the form of digital images on the phone screen, which requires a very important element - photosensitive element. A photosensitive element change the light signal into a electric signal, an AD converter change the electric signal into a digital signal. The number of pixels on the photographic camera photosensitive element densely arranged determines the final image pixel camera that can shoot. The

simplified model of the mobile phone when taking a photo as shown in Figure 5. Assuming that D is the shooting width, α is shooting angle, and N(ppi) is shooting distance to describe pixel density of the original details, then

$$\mathrm{N}=\frac{\mathrm{A}'}{\mathrm{D}}, \quad D = 2 \cdot L \cdot \tan\frac{\alpha}{2}, \quad A' = \sqrt{m^2 + n^2}, \tag{1}$$

and we can get:

$$N = \frac{\sqrt{m^2 + n^2}}{2 \cdot L \cdot \tan\frac{\alpha}{2}}. \tag{2}$$

It is obviously, the shooting distance is farther, the pixel density values capacity of the captured original to describe the details is smaller. The ability to capture the details of the original is inversely proportional to shooting distance L. If the areas shooting in distance L are $a \times a$ pixel, we can get equation (3):

$$a = \frac{\sqrt{2} \cdot L \cdot \tan\frac{\alpha}{2}}{\sqrt{m^2 + n^2}}. \tag{3}$$

When we have a further discussion on the biconvex lens image theory, we can get the rage of L as described in equation (4) and (5).

$$L_{\min} = \frac{A \cdot f}{A - 2 \cdot f \cdot \tan\frac{\alpha}{2}} \tag{4}$$

$$L_{\max} = \frac{b \cdot \sqrt{m^2 + n^2}}{\sqrt{2} \cdot \tan\frac{\alpha}{2}}. \tag{5}$$

## 4 Experiment result and Discussion

### 4.1 The printing process of moiré patterns

The flow chart of printing process using moiré patterns design to anti-countfeiting is shown in Figure 6. The parameters of moiré pattern design are corresponding with the specific graphic's size of product packaging in order to meet with anti-countfeiting requirement. It's very important to optimize the parameters of coding and decoding to obtain the best suitable coding and decoding, which can bring us the greatest visual result. The detail will be discussed in another paper in the future. And of course, any other anti-countfeating technology need to be combined with moiré patterns in the real application.

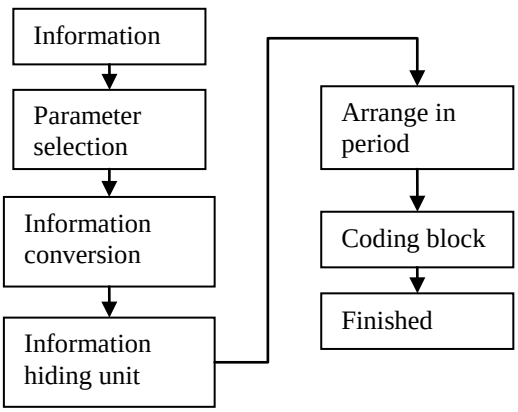



**Figure 6**: Moiré patterns design flow chart.

### 4.2 LCD screen decoding

In the experiment, the arrangement density of moiré patterns coding is range of 50 to 100 lpi and the printing type is offsetp rinting. The disturbing backgrounding is printed by HP Indigo 5600. We choose two brand mobile phone in order to have a decoding test, and the parameter are shown in Table 1. The distance L is 100, 150 and 200mm. We use the mobile phone to have a picture on the coding block and then check the decoding effects by LCD screen, shown as in Figure 7. The test data is shown as in Table 2 when distance L is 100mm. The zoom

rate from the test result is very close to calculating result in theory, but the disturbing background is affect the decoding results slightly. With the same method, we can compare the test result with the calculating result in the distance L is 150 and 200mm. The zoom rate is not affected by the distance L, but the clarity of decoding block will be influenced. The clarity of moiré patterns decoded descends when the distance L increases. So the suggestion distance L is the neraest shooting distance.

**Table 1:** Parameters of two brand mobile phone.

| Brand | Screen | | Camera | |
|---|---|---|---|---|
| | Size(inch) | Density(ppi) | Pixel(M) | Focal length(mm) |
| 1 | 5.5 | 200 | 5 | 4 |
| | 5.5 | 267 | 13 | 4 |
| 2 | 4 | 326 | 8 | 4 |

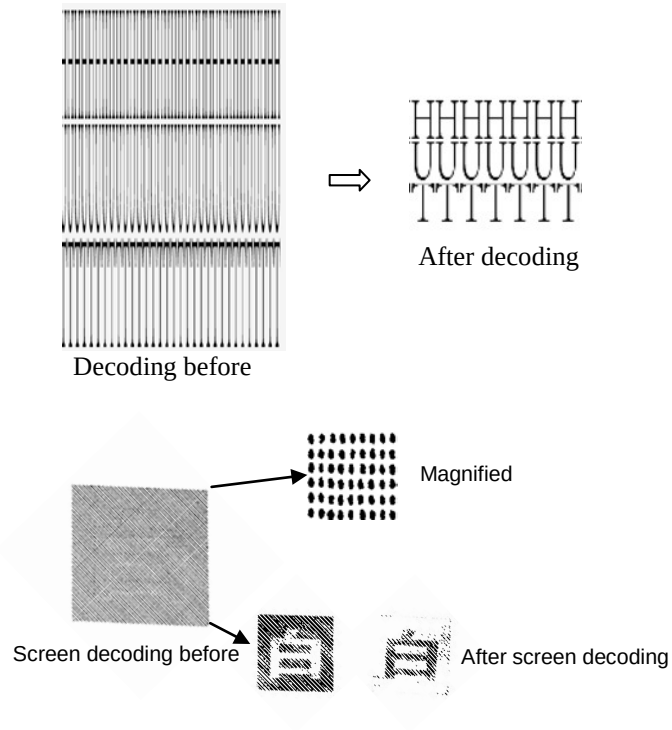



**Figure 7**: The verify process and effcets

**Table 2:** Zoom rate in distance L=100mm.

| | 50 | 60 | 70 | 80 | 90 | 100 | background |
|---|---|---|---|---|---|---|---|
| 200 | 0.243 | 0.310 | 0.357 | 0.408 | 0.443 | 0.486 | no |
| 267 | 0.193 | 0.228 | 0.265 | 0.303 | 0.342 | 0.379 | no |
| 326 | 0.157 | 0.186 | 0.221 | 0.242 | 0.284 | 0.314 | no |
| 200 | 0.246 | 0.305 | 0.348 | 0.410 | 0.439 | 0.493 | yes |
| 267 | 0.193 | 0.227 | 0.267 | 0.307 | 0.342 | 0.379 | yes |
| 326 | 0.157 | 0.185 | 0.221 | 0.243 | 0.284 | 0.313 | yes |

## 5 Conclusions

Many different methods by moiré patterns for the protection of products have been introduced over the years. In this paper we discuss the moiré patterns-based anti-countfeiting technique by general printing. We review the theory of the moiré phenomenon, design the moiré patterns and give a new decoding method by LCD screen. The test result is satisfied with calculating result in theory. The most advantage using the mobile terminal to decoding is simple and convenient because almost every consumer carry a mobile phone with him and he can verify the goods' genuine. The decoding block is not being needed in this method presented in this paper.

## Acknowledgements

Project is supported by Natural Science Foundation of Hunan Province (Grant No. 12JJ9043), National College Students Research Learning and Innovative Experiment Plan Project (Grant No. [2013]102), College Students Research Learning and Innovative Experiment Plan Project of Hunan Province (Grant No. [2013]191) and College Students Research Learning and Innovative Experiment Plan Project of Hunan University of Technology (Grant No. [2013]9).

## References

1. I. Amidror, S. Chosson, R.D. Hersch, 2007, "Moiré methods for the protection of documents an products: A short survey", *Journal of Physics: Conference Series*, pp.77.
2. S. Chosson, 2006, "Synthse d' Images Moiré", Switzerland: Ecole polytechnique fédérale de Lausanne.
3. R.D. Hersch, S. Chosson. Authentication of documents and articles by moire patterns. *US Patent No.7194105*.
4. C.W. Hu, 2004, "Moiré Theory Used in Holograph Anti-Counterfeit", *Printing Field*, no. 12, pp. 11-12.
5. X.L. Wang, J.F. Zhang, J. Zhu and etc., 2002, "Pattern-controllable Dynamic Moiré Holograms", *Optical Technique*, vol. 28, no. 5, pp. 427-428.
6. W. Qiu, 2007, "Application of Moiré Effect in Anti-false Screen Printing", *Screen Printing*, pp. 19-20.
7. Y.Q. Wang, 2004, "Purposefully set Moiré in Normal Printing for Anti-Counterfeit Purpose", *Printing Field*, no. 12, pp. 13-14.
8. S. Liu, J.Z. Chen, P. Chen, 1999, "Study on Moiré Concealed Codes", *Optical Technique.* vol. 25, no. 1, pp. 14-15.
9. A. F. Daniel, R. P. Harshal, 2010, "TFT-LCD Panel Fundamentals", *Electronics for You*, no. 3, pp. 113-116.

# The Study on Symbol Contrast of Inks and Paper Liners for Barcode Printing on Corrugated Box

**Daojai Sukhato[1*] and Pronthip Sinjarernpokai[2]**

[1] *Graphic and Prepress Center, Thai Containers Group Co., Ltd., Thailand*
[2] *Trainee at Graphic and Prepress Center, Thai Containers Group Co., Ltd., Thailand*

[*] *Corresponding author. Email: daojaisu@scg.co.th*

**Abstract:** Barcode's primary function is to carry data from the point at which it is originated to the point that the data has to be captured. So barcode is a vital link in data communication chain of any applications. If it fails, the chain will break. A barcode which cannot be scanned causes more problems to trading partners than no symbol at all. As a result, barcode readability becomes one of the top serious concerns in packaging industry, especially for corrugated packaging. Although most of the times barcode defects found are related to the print quality, there are other factors that make barcode unreadable. One among those factors is color combination of inks (the printed bars) and substrates (the spaces). It is widely known that the best color combination for barcode is black bars on a white background. Though other combinations can be used, not all are functional; especially in flexographic printing where the cooperation of ink pigments, printing methods, and substrates critically results in color limitations.

This research addresses the limitation of barcode color combinations on corrugated packaging by conducting an experiment, based on GS1 General Specifications, to identify scope of materials to be practically used. In this experiment, the Symbol Contrast between ink colors (using 3 color-groups: cold, medium, and warm) and corrugated liners (using 4 different colored-liners: white (KS), light brown (KI), golden yellow (KA), and dark brown (KT)) were graded using Axicon 6015 barcode verifier. The results showed that the group of cold colors (dark blue, light blue, green, and black) on white liner (KS) had the highest Symbol Contrast (B grade), followed by those colors on KI and KA (C grade), and on KT (D grade). The group of medium colors (purple, pink, dark brown, and grey) received C grade on KS and D grade on the rest liners. For the group of warm colors (white, yellow, red, and orange), the Symbol Contrast was D grade for all liners. The collected data were then analysed and developed to be a guideline for barcode readability improvement in the real production.

Keywords: barcode readability, barcode verification, symbol contrast, flexographic printing.

## 1 Introduction

Scannability of printed barcodes on corrugated is a challenge due to the low reflectance value of the corrugated materials as a scanner read a barcode by identifying the difference between bars and spaces. Nowadays it is even more difficult for printers to make barcodes scannable since recycled materials tend to be more popularly used in the industry. For barcode printing, the right color combination is a very important factor to make barcode being recognisable by a scanner. According to GS1[1] – an international organization that develops and maintains standards for supply and demand chains, there are seven parameters to be measured to verify readability of barcode, including Decode, Minimum Reflectance, Symbol Contrast, Minimum Edge Contrast, Modulation, Defect, and Decodability; and verification grade for each barcode will be the lowest grade of any one of these seven parameters. The parameter to be considered for adequate color combinations is Symbol Contrast. Stated in GS1 guideline, Symbol Contrast is a parameter governed by the reflectance of substrate and ink, calculated by finding the difference between the minimum and maximum reflectance value. If the contrast value gets too low, the scanner will not be able to differentiate between bars and spaces and thus makes the barcode appear invisible for the scanner. Symbol Contrast is graded A through F. A low contrast grade indicates that either the bars are too light or the background is to dark or both. Because the measurement uses red light, it is generally recommended white or one of the warm colors (red, orange, or yellow) as the background (spaces) and black, brown, and cool colors like blue or green as the bars. Figure 1 shows the samples of good and poor contrast of the color combination.




**Figure 1**: Samples of good and poor print contrast of barcode. [2]

### 1.1 Symbol Contrast

Symbol Contrast (SC) is a graded parameter – A to F, advised by John Nachtrieb [3]. It is a straight subtraction of the minimum reflectance value (Rmin) from the light reflectance value (Rmax), while Rmin is the colors of the bars and Rmax is the color of background. Then the value will be calculated into percentage. The reflectance of the bars must be equal to or less than half the reflectance of the background. In general the target is to achieve ANSI/ISO C grade or above; but for corrugated packaging, which is basically printed on bare Kraft, test liners, or recycle materials, the target can be as low as D grade. Here below is how Symbol Contrast is grading.

A grade = SC of greater than or equal to 70%

B grade = SC of greater than or equal to 55%

C grade = SC of greater than or equal to 40%

D grade = SC of greater than or equal to 20%

F grade = SC of less than 20%

Basically barcode scanner uses 660nm red light to scan, warm colors like red, yellow, or orange are not recommended for the bars. From Bar Code Graphics, Inc. website [4], the following charts (figure 2) suggest some scanable and non-scanable color combinations.

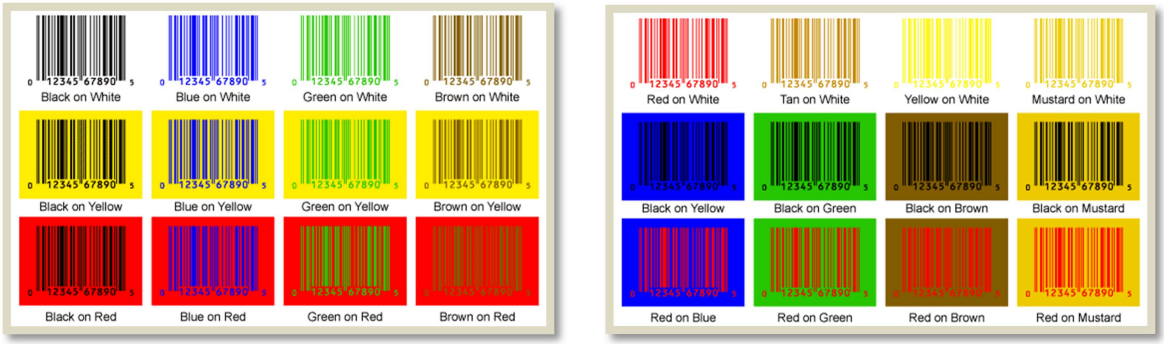



**Figure 2:** Scannable color combinations (left) and Non-scannable color combinations (right).

### 2.1 Objective of the Study

This study was done at Graphic and Prepress Center, Thai Containers Group, since 2012. The Center mainly supplies flexographic printing plates and printing technical supports to Thai Containers' corrugated manufactures – 13 plants in Thailand and 4 plants in regional countries. With long experience in corrugated industry, our technicians know exactly how serious the problem is when printed barcodes cannot be read. Our team, thus, came up with this experiment to get an understanding on scope of color combinations that make the printed barcodes work on corrugated substrates based on inks and paper materials available in our productions. This study was to identify functional and non-functional color combinations from our ink-shade and paper liner lists. At the end, the results were intended to be used as a practical guideline of barcode color selection for both the company and the customers purposefully direct to the barcode defects reduction.

## 2 The Experiment of Symbol Contrast of Inks / Paper Liners for Barcode on Corrugated

### 2.1 Methodology and Testing Materials

In this experiment, the values of Symbol Contrast between printed barcodes (using flexographic inks grouped into three groups: cold, medium, and warm colors) and printing substrates (the four different corrugated liners: white (KS), light brown (KI), golden yellow (KA), and dark brown (KT)) were measure using Axicon 6015 barcode verifier (Figure 3). Both the inks and the liners are printing materials commercially used. Figure 4 shows the corrugated liners and the printed inks on corrugated liners used for the experiment, respectively.



**Figure 3:** Axicon 6015 barcode verifier



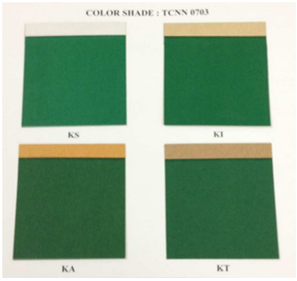



**Figure 4:** Samples of KS, KI, KA, and KI (left) and printed inks on liner papers (right).

The corrugated liners – KS, KI, KA, and KI – are test-liners produced by paper mills in SCG Paper group. These four liners represent the major substrates used at Thai Containers Group.

KS – White top liners: 30% bleached, colored virgin pulp on top layer

KI – Natural brown top liners: 30% bleached, non-colored virgin pulp on top layer

KA – Golden yellow top liners: 30% bleached, colored virgin pulp on top layer

KT – Recycled brown liners: 100% recycled liner

For each ink shade, the four liner samples (one of each kind) were printed using lab-scale ink applicator. Each printed sample will then be measured aside by the same color liner as shown in Figure 5.

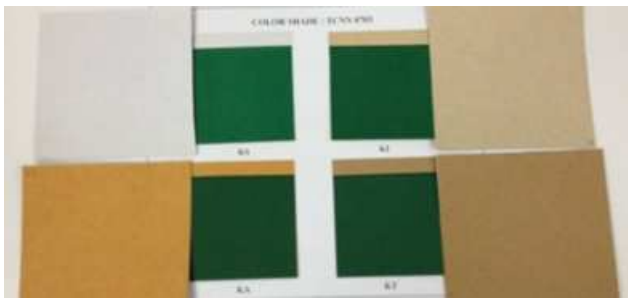





**Figure 5:** How the samples were measured.

As there are many plants in our group, we selected the color list from 7 main plants for this study and classified all colors into 3 major groups, which were cold color, medium color, and warm color. Then in each major group, the colors were separated into 3 or 4 minor groups with the member of similar shades. The ink-color classification for this experiment is described below.

| | |
|---|---|
| #1 Cold Color (354 colors): | Dark blue (131 shades), Light blue (100 shades), Green (109 shades), and Black (14 shades) |
| #2 Medium Color (159 colors): | Violet (56 shades), Pink (43 shades), Brown (43 shades), and Grey (17 shades) |
| #3 Warm Color (186 colors): | Red (106 shades), Yellow (40 shades), and Orange (40 shades) |

From above classification, there were 699 sets of samples to be measured. One set was composed of 1 ink shade on 4 different substrates. Once each sample was scanned the Axicon verifier software then verified its Symbol Contrast value. The result was shown as graph and percentage on Scan Reflectance Profile window (Figure 6).

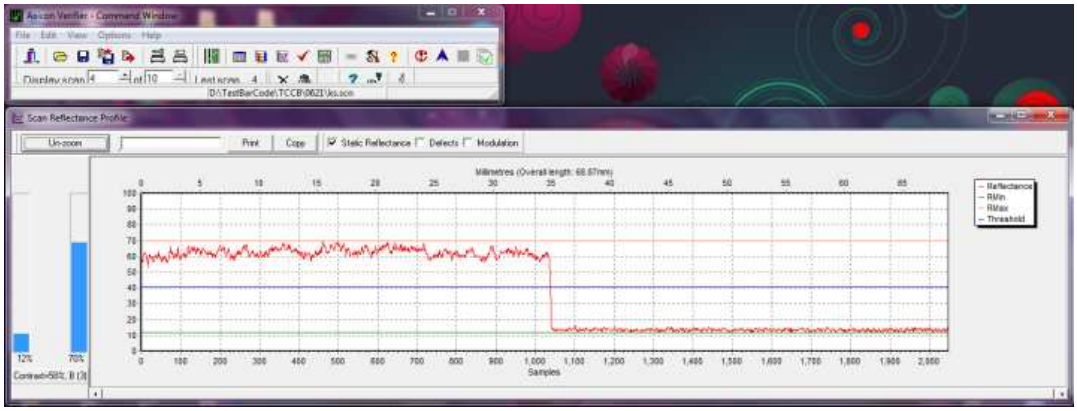


**Figure 6:** Symbol Contrast result shown in graph and percentage by Axicon verifier software.

Those results were collected in designed datasheet as the samples presented in Figures 5 and 6.

| No. | color mode | KI | | KT | | KA | | KS | | |
|---|---|---|---|---|---|---|---|---|---|---|
| | | Symbol Contrast (%) | Grade | Symbol Contrast (%) | Grade | Symbol Contrast (%) | Grade | Symbol Contrast (%) | Grade | |
| 1 | TCNK 0101 | 23 | D | 27 | D | 27 | D | 42 | C | |
| 2 | TCNK 0105 | 36 | D | 26 | D | 35 | D | 47 | C | |
| 3 | TCNK 0109 | 35 | D | 32 | D | 38 | D | 37 | D | |
| 4 | TCNK 0110 | 34 | D | 33 | D | 25 | D | 37 | D | |
| 5 | TCNK 0112 | 36 | D | 31 | D | 37 | D | 40 | C | |
| 6 | TCNK 0113 | 31 | D | 35 | D | 36 | D | 42 | C | |
| 7 | TCNK0126 | 30 | D | 33 | D | 37 | D | 39 | D | |
| 8 | TCNK 0127 | 39 | D | 31 | D | 36 | D | 38 | D | |
| 9 | TCNK 0130 | 29 | D | 23 | D | 35 | D | 49 | C | |
| 10 | TCNK 0137 | 38 | D | 32 | D | 37 | D | 39 | D | |
| 11 | TCNK 0150 | 33 | D | 39 | D | 31 | D | 46 | C | |

**Figure 7:** Samples of the datasheet for TCNK Plant-Red shades.

| No. | color mode | KI | | KT | | KA | | KS | | |
|---|---|---|---|---|---|---|---|---|---|---|
| | | Symbol Contrast (%) | Grade | Symbol Contrast (%) | Grade | Symbol Contrast (%) | Grade | Symbol Contrast (%) | Grade | |
| 26 | TCNK 0501 | 47 | C | 35 | D | 42 | C | 58 | B | |
| 27 | TCNK 0502 | 46 | C | 39 | D | 43 | C | 59 | B | |
| 28 | TCNK 0503 | 47 | C | 39 | D | 41 | C | 60 | B | |
| 29 | TCNK 0504 | 46 | C | 36 | D | 41 | C | 59 | B | |
| 46 | TCNK 0627 | 46 | C | 36 | D | 40 | C | 59 | B | |
| 47 | TCNK 0628 | 43 | C | 32 | D | 39 | D | 56 | B | |
| 48 | TCNK 0639 | 44 | C | 34 | D | 36 | D | 56 | B | |
| 49 | TCNK 0644 | 43 | C | 32 | D | 37 | D | 55 | B | |
| 60 | TCNK 0726 | 45 | C | 36 | D | 42 | C | 61 | B | |
| 61 | TCNK 0727 | 44 | C | 33 | D | 43 | C | 56 | B | |
| 63 | TCNK 0759 | 46 | C | 33 | D | 38 | D | 55 | B | |
| 64 | TCNK 0762 | 45 | C | 34 | D | 40 | C | 57 | B | |
| 76 | TCNK 1001 | 45 | C | 34 | D | 45 | C | 60 | B | |
| 77 | TCNK 1092 | 47 | C | 38 | D | 44 | C | 62 | B | |

**Figure 8:** Samples of the datasheet for TCNK Plant-Dark blue, -Light blue, -Green, and -Black shades.

## 2.2 Measurement Results

Actually from these results we collected and analysed additional data, and then created a manual of "Color-combination Guideline for Barcode Readability" for each plant. However for conceptual understanding in this study, the results were also calculated to find an average Symbol Contrast and grade of each color, focusing minor-group level, as presenting in Table 3.

**Table 1:** Average Symbol Contrast and grades calculated from the results.

| Color | KS | KI | KA | KT |
|---|---|---|---|---|
| | % Symbol Contrast [Grade] | | | |
| #1-Dark Blue | 61 [B] | 47 [C] | 43 [C] | 33 [D] |
| #1-Light Blue | 59 [B] | 46 [C] | 40 [C] | 36 [D] |
| #1-Green | 61 [B] | 47 [C] | 42 [C] | 38 [D] |
| #1-Black | 62 [B] | 47 [C] | 44 [C] | 38 [D] |
| #2-Violet | 46 [C] | 38 [D] | 33 [D] | 27 [D] |
| #2-Pink | 47 [C] | 39 [D] | 37 [D] | 34 [D] |
| #2-Brown | 51 [C] | 38 [D] | 33 [D] | 30 [D] |
| #2-Grey | 44 [C] | 33 [D] | 35 [D] | 32 [D] |
| #3-Red | 39 [D] | 30 [D] | 37 [D] | 33 [D] |
| #3-Yellow | 38 [D] | 33 [D] | 32 [D] | 28 [D] |
| #3-Orange | 37 [D] | 33 [D] | 23 [D] | 28 [D] |

*#1 Cold Color, #2 Medium Color, #3 Warm Color*

The results showed that, in average, the group of cold-color (#1) on KS (white top) had the highest Symbol Contrast (59-62% – B grade), followed by the same group on KI (natural brown top) and KA (golden yellow top) at 40-47% – C grade, and that on KT (recycled paper) at 33-38% – D grade. For the group of medium-color (#2), the Symbol Contrasts in average were 44-51% – C grade for only when printed on KS, and were 27-39% – D grade when printed on the other three substrates. The last group, warm-color (#3), all combinations had the average results at 23-39% – D grade at most.

## 3 Discussions and Conclusions

### 3.1 Discussion

From the result, the group of cold-color tends to have higher potential for feasible barcode which is matched to the suggestions from national and international standards like ANSI, ISO, and GS1, although its performance on corrugated liners that we tested is not so high (colored liners got only C grade). As same as the group of warm-color, suggested not to be used for barcode, the results show in the same direction as we expected, all got "D". However for the medium-color, the results are a little underestimated. Although the overall results are better than those of warm colors, the Symbol Contrast values are not much higher.

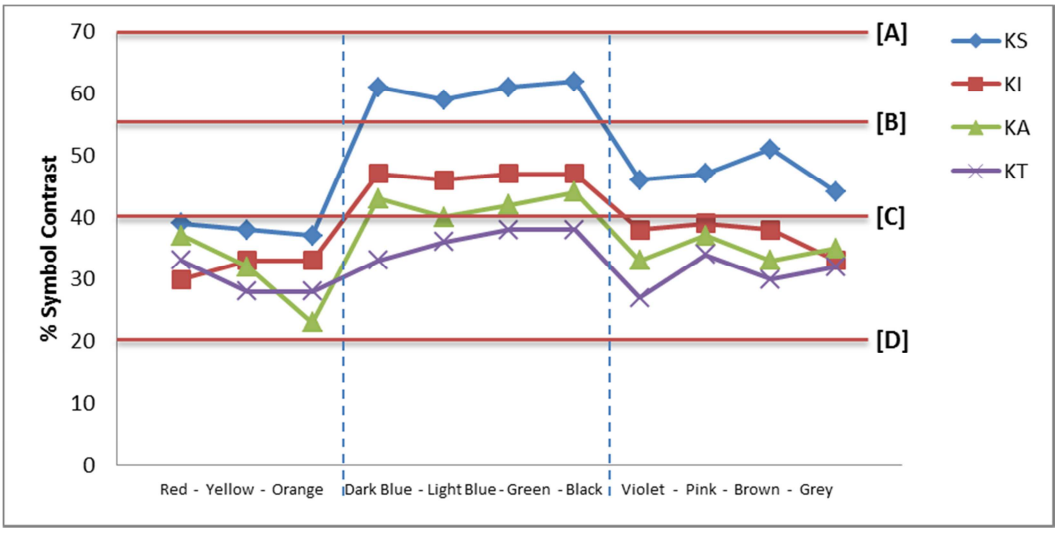



**Figure 9:** Graph of Symbol Contrast results focusing on ink colors.

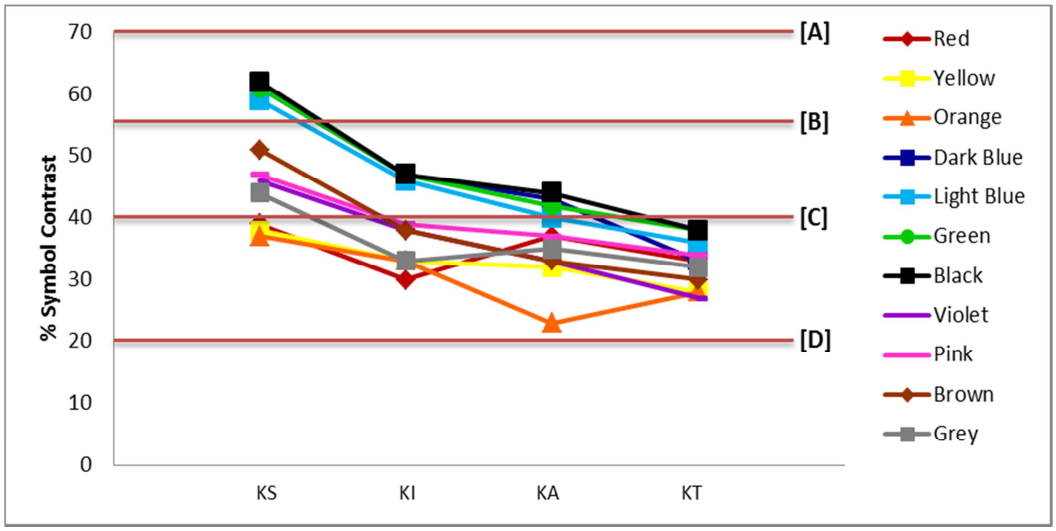



**Figure 10:** Graph of Symbol Contrast results focusing on substrates.

After analysing the measurement results, the finding tends to be a little different from what assumed at the first place. The designers and the printers certainly considered more on ink color selection when trying to make any barcode readable with less regard on the substrates characteristics like shade and surface roughness. Look at the graphs of Symbol Contrast results in Figure 7 and 8 plotted in the opposite aspect of each other. Although the ink color plays an important part for readability of barcodes, the different substrates show critical impact on the readability as well. From both graphs (figures 7 and 8), it is obvious that the printed on different liners (different colors and properties) always gave the different level of readability no matter what ink colors were used. As shown in the graphs, the prints on KS got higher Symbol Contrast than those on KI, KA, and KT respectively (except orange on KA, they are similar shades).

### 3.2 Conclusion

Although the study results in convincing the general suggestions on readable color-combinations for barcode that easily found from published information. The printing substrates to be used are also important factors to be concerned. Additionally different companies always used different inks and substrates in their productions. Therefore it should be more practical to have own guideline for ink selection on each substrate. Done by this study, now we have the color-combination guideline manual for our team to improve quality of printed barcodes such as for packaging designers to select suitable barcode colors for new jobs, and for printers/technician to assure scannability of barcodes on finished jobs. The guideline is helpful not only to significantly reduce the number of defects from unreadable barcodes but also to increase customer trust by acknowledging them to understand this limitation.

Additionally it should not be forgotten that even though the average Symbol Contrast values resulted in this test show all passes (equal to or above D grade), it doesn't mean that every individual values are really passed. Also this results represent just one parameter out of seven, and especially this parameter is of material issue not production issue which has more risk for readbility. So the Symbol Contrast data is only a primary helper to prevent defects.

## Acknowledgements

We would like to thanks to Ms.Juthamart Sayampol, Thai Containers Group, for her help, advice, and also the discussions about the research. We also thanks to Mr.Pakapol Kittipinyovath and Ms.Jirapa Daeberitz, Thai Containers Group, for guiding our research and for their kindness on co-operation with printers and designer to understand about color-combination for barcode readability. Finally we thanks to Mr.Chonnatad Prasertsom, MM&NN CO.,LTD., for training and consulting on Axicon verifier usage and standard barcode principal.

## References

1. GS1 UK, 2008, *GS1 barcode validation and verification guideline*, GS1 UK, UK, pp. 4-11.
2. Bar Code Graphics, Inc. (2014). *Printing Tips.* Retrieved from http://www.barcode-us.com/upc/printingTips.html
3. John Nachtrieb, 2012, "Barcode Colors – What Works and What Doesn't?", *Barcode Tutorial*, BARCODE-TEST, USA.
4. Bar Code Graphics, Inc.(2014). *Color Selection for Barcode Symbols*. Retrieved from http://www.barcode-us.com/ upc/upcColorChart.html

# PACKAGING SUSTAINABILITY

# Implementing Packaging Sustainability Metrics in a Developing Economy

**Prasad Balan Iyer, Sagar S. Shejwalkar and Siddhant R. Dwivedee***

*Department of Printing and Packaging Technology, SIES Graduate School of Technology, Navi Mumbai, India*

*Corresponding author. Email: dwivedee.siddhant@siesgst.ac.in*

**Abstract:** The objective of this paper is to study the feasibility and challenges associated with implementing various sustainability metrics and guidelines prescribed by International Standard for Sustainable Packaging (ISO TC122/SC4), (SPC) Sustainable Packaging Coalition (SP Metrics Framework) and Australian Packaging Covenant (APC) in a developing economy where the mind set of stakeholders and consumers at various levels differs in their interpretation and expectation of the definition of what may be classified as truly sustainable from the rest of the world. The focus of the paper is on the Indian Economic model. The paper highlights through real life examples from the industry the scope for processes and designs to become more sustainable via source reduction, technological advancement and managing the requirements of packaging without compromising on quality. There exists a gap between what may be considered a truly sustainable organization in a developing economy and a developed economy. Even though global organizations such as Walmart expect the same standards world over, this gap cannot be ignored. By setting different benchmarks while implementing metrics and guidelines, this gap can be bridged without having to negotiate on the primary functions of packaging. Sustainability in a developing economy can be achieved alongside economic development and economic development need not be a precursor to it. In this lies a tremendous opportunity for economic progress to reflect not only in terms of GDP (gross domestic product) but also in terms of sustainability. By implementing metrics and setting realistic targets, this could turn into a reality.

Keywords: sustainability, sustainable packaging, metrics, green packaging, developing economy, life cycle assessment, sustainable development product, sustainable profit ratio

## 1 Introduction

The global market for sustainable packaging is projected to reach $142.42 billion by 2015 (Global Industry Analysts (GIA) [1]. The global packaging industry is conservatively estimated at $417 billion and employs more than five million people all over the world. These numbers indicate a tremendous opportunity but the packaging industry also enjoys the dubious distinction of being responsible for a major chunk of the solid waste generated every day. Here arises the need for Sustainable packaging. The SPC defines Sustainable packaging as:

i. Beneficial, safe and healthy for individuals and communities throughout its life cycle.
ii. Able to meet market criteria for performance and cost.
iii. Sourced, manufactured, transported and recycled using renewable energy.
iv. Able to maximize the use of renewable or recycled source materials.
v. Manufactured using clean production technologies and best practices.
vi. Made from materials healthy in all probable end-of-life scenarios.
vii. Physically designed to optimize materials and energy.
viii. Effectively recovered and utilized in biological and/or industrial cradle-to-cradle cycles.

By implementing cradle-to-cradle methodology, the landscape of sustainability can be changed. “The industrial application of cradle-to-cradle design creates a cycle for industrial materials. Like the earth’s nutrient cycles, the flow of materials eliminate the concept of waste” [2].

For a long time, sustainability has been a vague, subjective concept that is largely open to interpretation. This has led to companies making false claims regarding the sustainability of their products and practices and misrepresenting themselves as “green” organizations. Metrics and indicators serve to challenge these claims and evaluate at different stages, the sustainability performance. In a developing economy, the scope for making false claims is further incentivized because of:

i. Lack of education among consumers & absence of active consumer rights forums.

ii. Purely profit oriented businesses at grassroots level with few supervising authorities and infrequent audits.
iii. Absence of the recognition of the need for inculcating sustainable practices.
iv. Lack of Life Cycle Assessment tools and support.

Sustainability is often referred to the triple bottom line. The triple bottom line means juxta-positioning of parameters evaluating economic, ecological and social success of an organization. This serves to highlight that the economic success may be independent of the ecological success as seen in the case of Big Oil corporations in the US back in the 90s. The SPC believes that through intelligent packaging and system design, it is possible to "design out" the potential negative impact of packaging on the environment and societies.

Sustainable packaging can be evaluated on a rudimentary basis by classifying it into two key aspects: Design Sustainability (DS) and Process Sustainability (PS).

## 2 Design Sustainability (DS)

Realizing Design Sustainability provides ample opportunities for designers and manufacturers to get creative. The criteria are not necessarily new; some simply extend existing considerations. As they stand now, conventional definitions of design quality are typically limited to cost, technical performance, appearance, and, in certain cases, regulatory compliance. However, when sustainability is added to the mix, it introduces an expanded set of criteria which may include optimizing resources, responsible sourcing, material health, and resource recovery. This means the ability to design packaging that strives for a whole new level of design quality [2].

What this means is that we need to really just make new connections between old ideas. The human mind is the connection machine. Since 1950 alone, the world's people have consumed more goods and services than the combined total of all humans who ever walked the planet before us. The scope for creativity in design is perhaps at an all-time high and the need for it is direr than ever. According to Albert Einstein; creativity is the residue of wasted time. Developments ignored the sustainability aspects of design from a very long time. Creativity in design has been limited to finding new ways to attract more consumers and tap fresh markets. In a developing economy, several designers and consumers, particularly in non-urban zones carry the belief that an over packaged product is a superior product. That, if a particular product is packaged like fort Knox, its contents must be worth more. These misconceptions are misused by organizations to increase the market share of their product at expense of a more sustainable design. While a heavily packaged or at times over packaged product does marginally bring down wastage throughout the supply chain, the overall impact of this paradigm is harmful for the environment. This is compounded by the fact that even though the packaging cost rises for such a product every stock keeping unit (SKU), it is more than made up for by the heavy markup levied to justify the over packaging and further propagate the myth of a superior product. Such a company can claim that by reducing food losses because of the added packaging features, they are implementing a brand of sustainable packaging but this is where priorities must be identified.

### 2.1 Case Study on Design Sustainability (DS)




**Figure 1**: ITC Sunfeast's Delishus cookies pack (Source: ITC Portal)

A good example to explain this is that of ITC's Sunfeast Delishus cookies, priced at almost twice the mark-up for similar biscuits and cookies in that range, where 6 individual cookies are packed in 3-side sealed flexible laminate pouches inside a lined carton. This is a perfect example of an over packaged, unsustainable design that achieves nothing in terms of packaging efficiency or enhancing protection for the product. The cookies are no more susceptible to crumbling, cracking or chipping around the edges as they would in a thermoformed tray inside a single three side sealed pouch (which is the standard accepted design for alternatives available in the market). In fact, the thermoformed trays are much more effective in providing a degree of cushioning and since they are directly in contact with the perimeter of the biscuits, it is a much more closely spaced design, restricting movement within the pack, assisting overall protection against vibrations and mechanical damage. Additionally,

the trays are made of a single material and are easily separated from the rest of the package which increases their recyclability as compared to multi-layer pouches where individual layers cannot be delaminated and hence they cannot be recycled effectively. Biscuit and cookie packs are discarded immediately after being opened so their potential for reuse is minimal. Thus, the need is for their packaging to be minimal as well.




**Figure 2**: The more sustainable packaging alternative (Source: ITC Portal)

Even if Sunfeast argues fewer losses accounted for by wastage and returns due to damaged units, the overall hyperextended use of packaging machinery, packaging materials, energy and shelf space is not justified, a classic case of projecting an illusion that an over packaged product is superior. It must also be noted here that ITC is one of India's leading food conglomerates.

This example also highlights the mentality of the consumers in this scenario. A large number of consumers still believe that nitrogen flushing inside potato chips and fried snacks pouches is air and the purpose it serves is to reduce the actual quantity of chips provided. They are unaware of the cushioning and modified atmosphere functions that assist in improving the shelf life. Nitrogen flushing in the packaging of potato chips is an extremely sustainable packaging methodology since it i) improves shelf life of the product – longer lasting products add to packaging sustainability, ii) It provides cushioning, a must for a product like chips that break easily, thereby losing their appeal iii) nitrogen is readily available, being the largest component of atmospheric air, which reduces strain on materials that would have otherwise been used as cushioning and their processing. This indicates that consumers lack education about the functions of packaging and why a technology that is being implemented is ultimately in their interests. Sadly instead of taking the initiative and starting campaigns to educate and create awareness among consumers, companies conveniently choose to ignore the big picture and turn a blind eye toward long term sustainability goals. This is one of the biggest challenges in implementing sustainability metrics in a developing economy.

Therefore, DS can be expressed as **the most minimalistic design that can practically as well as economically exist without compromising any one of the primary packaging functions.**

"The industry has a responsibility to review and optimize the environmental performance of the packaging it uses with respect to all relevant life cycle stages. But this analysis of impacts must be done in the round. It must include the impact of product losses that may result from the use of **too little** packaging as well the impact of using **too much**.

Finding the balance between under-packaging and over-packaging is the aim"

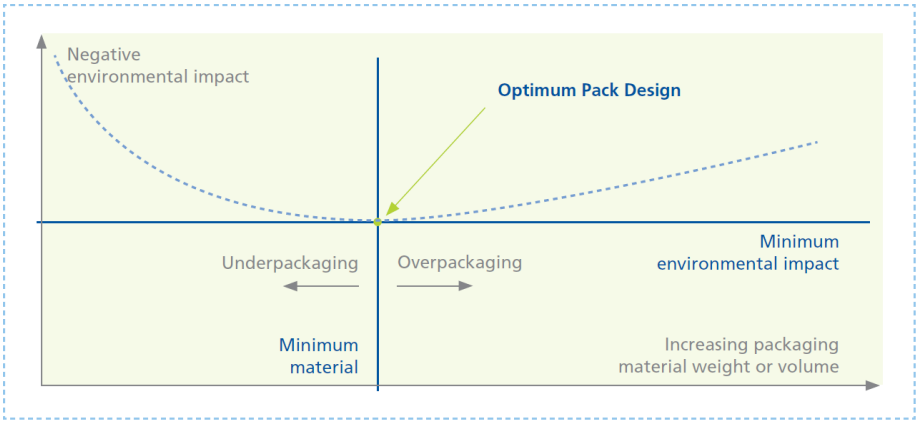



**Figure 3**: The Innventia AB model

Optimum Packaging: The Innventia AB model shows that the environmental consequences of product losses caused by excessive packaging reduction are far greater than guaranteeing adequate protection through an incremental excess of packaging [3]

## 3 Process Sustainability (PS)

In dealing with the second aspect of Sustainability or Process Sustainability, there are several factors to be considered by the Company's policy makers. A few of these have been listed by the SPC and are as follows:

i. Are there local sources of packaging materials?
ii. Does the approved supplier have a proven environmental commitment (e.g., Ceres Principles, Corporate Social Responsibility reporting)?
iii. Do the suppliers understand why human and environmental health is important to me?
iv. Does the approved supplier have internal goals to minimize the number of hazardous substances in their production processes?
v. What other measures is the supplier using to enhance their sustainability performance?
vi. Does the approved supplier have any programs that go beyond compliance?
vii. What base materials were used in the packaging? What substances have been added to the base material?
viii. What is the chemistry of any auxiliaries?
ix. Is there potential to release known or potentially toxic substances?
x. Are there safer/healthier alternatives to use in the package?

### 3.1 The Twelve Principles of Green Packaging

Though the basic concept of sustainability remains the same, it was found that the definition for sustainable/green packaging differs from company to company depending on their product, packaging material or process of conversion. This has led the authors of The Twelve Principles of Green Packaging [4] to standardize the twelve principles which can be applied by every packaging industry to the process in their own possible way and also know where they stand in terms of sustainable packaging as shown in Figure 4.

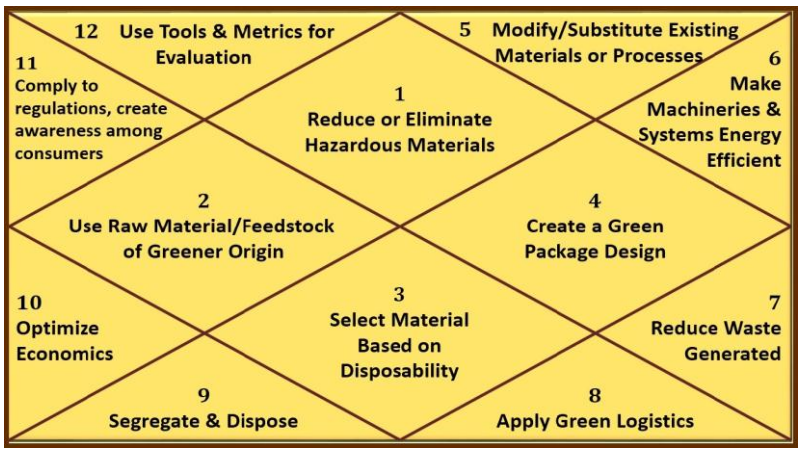



**Figure 4**: Twelve House Diagram for Principles of Green Packaging

1. **Reduce / Eliminate Hazardous Substances in the Packaging Material.** Manufacturers and consumers need to be educated about the hazardous additives that packaging materials contain and their harmful effects. With low levels of literacy, this knowledge is difficult to spread.
2. **Use Raw Material / Feedstock of Greener Origin.** Again, the challenge here lies in convincing the consumers and other stakeholders in the life cycle to trace back the packaging materials to their origins. Without proper knowledge and awareness, this is difficult to implement.
3. **Select Packaging Material Based on its Disposability.** Without proper disposal and recycling systems in place, the selection is almost rarely based on disposability.
4. **Create a Green Package Design**. While basic segregation goes on at the rag picker level, individual components like label and closure from the container are left intact. This makes their recycling even more tedious. Thus, a green design that uses the same material for all components can be implemented.
5. **Modify / Substitute existing Packaging Material or Process.** This is illustrated in Case Study 2 whereby simple modifications in the process can help make the overall process much more sustainable.

6. **Make Packaging Machineries and Systems Energy Efficient.** This can be achieved by reducing the number of unnecessary displays, frequent quality checks and timely servicing of machine and electrical components.
7. **Reduce Waste Generated during Processing, Conversion and Packing Operations.** A simple example of this is reusing or recycling wasted lots instead of discarding it away.
8. **Apply Green Logistics.** Environmental concerns and stringent government regulations have led organizations to shift towards sustainable or green logistics which begin with cutting down $CO_2$ emissions. Green logistics comprise of carbon auditing of supply chains, transferring freight to "greener" transport modes, reducing the environmental impact of warehousing, improving fuel efficiency in freight transport, making city logistics more environmentally sustainable and reverse logistics for the management of waste and the role of the government in promoting sustainable logistics [5].
9. **Segregate and Dispose of the Waste.** By applying cradle-to-cradle approaches, better systems to segregate and dispose waste will evolve.
10. **Optimize Packaging Economics.** Striking a right balance between all levels of packaging costs right from material selection to waste disposal/utilization is essential for sustainable development.
11. **Comply with Regulations and Create Awareness among Consumers.** This is of critical importance in developing economies. The packaging materials, processes and machineries should be compliant with the existing regulations and standards laid down by different countries and international organisations like ASTM, FDA, ISO etc. Some of these regulations relate to packaging recyclability, compostability and biodegradability. Quality and environment management systems as per ISO assist in improving quality and environmental performance. New standards are now under development by ASTM for "packaging and environment"
12. **Use Suitable Packaging Metrics & Tools to evaluate Sustainable Packaging.** For instance, adopting the Sustainable Development Product (SDP) Model rather than Gross Domestic Product (GDP) Model for economic growth.

An important aspect of Process Sustainability (PS) is source reduction included in Principle No.7. While source reduction may seem to be in the interest of the manufacturer more than the consumer, when it comes to practically implementing effective source reduction, manufacturers and convertors often fall short. A simple example is demonstrated in the case study below:

## 3.2 Case Study on Process Sustainability (PS)

**Profile of Company F:** Company F is one of the largest retail chains in India and manufactures hundreds of products under their brand available exclusively at their retail outlets. One such product is a dish wash concentrated gel liquid, manufactured ex situ, and packaging for the same is outsourced. A label manufacturing set up, Company S, has been contracted for supplying the labels for the Glycol modified Polyethylene Terephthalate (PETG) containers varying in size as per volume. The art work for the label is prepared in advance and sent to company S.

**Profile of Company S:** Company S uses an 8 colour web fed flexographic printing unit to print on substrate having front: Biaxially Oriented Polypropylene (BOPP) Silver metal film; back: Polypropylene (PP) (White) and 62-65 GSM silicon/mirror-coat release paper using hot melt adhesive. Punching operations are performed in house at Company S while platemaking operations are outsourced. For achieving perfect color matching, Company S first printed an entire web of substrate by taking trials, stopping to observe intermittently and continuing in this manner. Nearly 2-3 large rolls of web were consumed till the perfect color match was accomplished. This is the normal accepted methodology at Company S.

A simple technological addition to the process would be to include a spectrophotometer, a simple device that instantly provides color density across the tonal range of a particular color patch. By comparing each printed label with the spectrophotometer reading of the original a perfect color match can be obtained much faster and more accurate results are possible. The spectrophotometer readings provides the machine operator with information about the quantity of the ink (i.e the three primaries C, M, Y) to be added. The optical density of the ink can also be evaluated. This is a small instrument that would make a useful addition to the process and since the flexographic press used is a sophisticated 8 color machine capable of reverse printing with a preinstalled stroboscope (web viewing device), the absence of a spectrophotometer can only perhaps be attributed to lack of awareness at Company S. Their decision to waste rolls of expensive label stock, printing ink, power used for running the press for nearly one hour till the color match is obtained each time is a highly non-sustainable option considering the simple solution. Company F, that contracts Company S is bound to be aware of this but for

reasons known only to them, do not bother to intervene. This can be owed to the general lack of concern and low priority status for adopting a sustainable approach. Company F has a greater responsibility since it is a bigger corporate entity.

The suggested solution complies with as many as three of the principles of green packaging listed below namely,
5 – Modify/Substitute Existing Materials or Processes,
6 – Make Machineries & Systems Energy Efficient, and
7 – Reduce waste generated.

There is an element of unavoidable wastage with labels and stickers. Silicone paper is scraped as it is unfit for recycling. The multi-layer polypropylene material also contributes to post consumer wastage. The most effective method of tackling the problem of post-consumer waste is source reduction. The PETG bottle is unsuitable for reuse there is an aversion towards reusing detergent and soap containers for food applications. While this is justified, reusing the container for a refill pack is practiced by a small percentage of consumers. Proper recycling facilities for any of the components in the package are not available. Like ITC, company F is a large organization that chooses to turn a blind eye towards a sustainable future and makes no effort to increase consumer awareness or reduce the burden on the environment.

In addition, the SPC has provided guidelines on how material health and safety can be implemented to make processes more sustainable:

i. Take a proactive stance on the safety and environmental impact of packaging by understanding the chemistry of the materials that are used.
ii. Develop an internal list of substances of concern or identify external lists that a company could adopt.
iii. Ask the suppliers to identify the chemicals used in packaging materials and auxiliaries, ideally down to 100 ppm.
iv. If confidentiality is a concern, ask the suppliers to (1) sign a confidentiality agreement, (2) use a third party certifier, or (3) self-certify that their materials do not contain any of your listed substances of concern (in some cases, it may be necessary or advisable to specify precise, nonzero concentration thresholds). Compare the constituents of the materials against internal or other substances-of-concern lists.
v. Carefully select and specify the materials that meet performance requirements but are also safe in their likely end-of-life scenarios.
vi. Continuously monitor materials bans, restricted substances lists, and legislation prohibiting the use of certain substances within packaging.
vii. Develop or adopt tools and methodologies to assess material health to allow more transparent communication of material characteristics throughout the value chain. [2]

## 4 Life Cycle Assessment

Rising demands from customers and regulators for improved environmental performance and increased transparency are driving a surge in interest life cycle assessment (LCA) as a tool for continuous improvement and innovation and a way of improving environmental performance while avoiding burden shifting and unintended consequences.

### 4.1 Applications of LCA Range from Efficiency to Innovation to Marketing

LCA is a pliable tool and with multiple applications. Savvy organizations apply it to a range of opportunities. Examples [6]:

**Production processes.** Companies can use LCA to identify the part of a production process that has the greatest environmental impact so they can focus optimization efforts on that part. Or process engineers can compare two alternative production processes with LCA to select the process with overall superior environmental performance. AkzoNobel has implemented this.

**Waste management.** LCA can be used to select among multiple waste management approaches. Recycling may not always be superior to incineration, for example. An LCA can reveal if this is the case.

**Product and packaging development.** Companies draw on LCA methods in product and packaging design. It can help them select materials with lower environmental impacts. It can guide the development of designs that have lower impacts in the use phase or are easier to recycle. Stonyfield Farm has used LCA to select packaging for its yogurt.

**Sustainability goals.** A company with internal or public sustainability goals can use LCA to understand the impact of a new process on its ability to achieve those goals. This can give it advance notice that it may need to adjust some internal goals as a consequence of launching a new product or process. AkzoNobel uses LCA in this way.

**Green marketing.** LCA has communication applications. A rigorous, science-based analysis, conducted in compliance with international standards, provides a sound basis for communicating with customers about environmental performance and progress. LCAs are the basis of environmental product declarations, a communication tool of growing importance.

**Strategy and risk management.** Some companies use LCA to get a better understanding of their dependence on critical raw materials, the availability of alternative sources and the impacts of those sources, and their exposure to interruptions in supply.

Incorporating Life cycle assessment tools represents more than one challenge in a developing economy. The foremost being apprehensive approach due to lack of adequate awareness and the perception of it being an added constraint. Companies that do not have the resources are unwilling to add another variable to the mix and companies that do in fact have the resources and should be raising the bar by setting a precedent seemingly do not care beyond their role in the life cycle. Their approach is more cradle-to-grave and lacks vision among other things to see the greater picture. In the above example stated, A far sighted executive at Company S should understand that with each wasted roll of label stock that is not recycled, the strain on resources increases, even if it seems negligible for one roll of stock for one print run. This strain on resources compounds each time wasteful practices like this are followed. This eventually causes the price of label stock to increase and in due time, procuring of label stock becomes more expensive for Company S. To account for this, Company S charges Company F a higher price per SKU but Company F has deep pockets so the fractional increase in price per label goes unnoticed or is ignored.

Similarly, competitors to Sunfeast's Delishus cookies will try to tap into the market created by consumers' with the mindset "Over-packaged is better" and the likely result of this is re-launching their product counterparts with similar packaging, because a new precedent has now been set. This multiplies the strain on resources which, once again cannot be effectively recycled and will inevitably cause material prices to increase sooner or later. The overall net effect is about the same. A wrong precedent anywhere in the life cycle can do as much damage as a healthy one can do good.

The sustainability agenda often gains traction at companies when they pursue relatively easy projects that offer cost savings and reduction in environmental impacts, such as energy-saving lighting retrofits. But once the low-hanging fruit are picked, companies are faced with more challenging questions about how to improve their environmental performance. LCA is increasingly recognized as a tool that enables companies to understand the environmental tradeoffs associated with various courses of action and equips them to make rational decisions after the easy choices are made [6].

It is here that a retail chain like Company F must draw an example from a global enterprise like Walmart. The company has had an undeniable influence in championing the business case for sustainability practices. The numbers alone tell a convincing story: since making a public commitment to sustainability in 2005, Walmart has increased sales from $315 billion to $444 billion and built 3,000 stores overseas [6]. This is discussed in greater detail in the subsequent section.

## 5 The Indian Sustainability Scenario

The World Business Council for Sustainable Development (WBCSD), a global grouping of prominent CEOs is encouraging the sustainable development agenda and also simultaneously working on altering the existing frameworks and drivers of the corporate world to level the playing field.

Presently, there is no reward for companies that are more sustainable than others as financial markets remain obsessed with purely financial returns and short-term performance. For example, Unilever has battled this short term orientation over the past few years.

Sporting goods manufacturer Puma has reported EP&L (environmental profit and loss) for a while and is even fine-tuning a social P&L to be announced in 2015. Yet, it is not perceived any differently from other companies. This puts no pressure on companies like ITC and Company F that don't address the externalities of doing business.

Several Indian companies already follow GRI and Global Reporting Initiative (GRI) guidelines. A few, including Tata Steel, are also participating in the International Integrated Reporting Council (IIRC) reporting pilot.

The Sustainability Accounting Standards Board (SASB) has been making quiet inroads by designing standards for disclosure in 'mandatory' filings to the US Securities and Exchange Commission. In India, capital market regulator Securities and Exchange board of India (SEBI) has mandated rudimentary business responsibility reports for the top listed companies. The excess of reporting requirements has inevitably lead to the 'disclosure overload' question. The WBCSD is trying to simplify and harmonize standards.

The concept of 'materiality' is rapidly gaining resonance. Materiality, in simple terms, means the most critical, or the most relevant issues, that impact a company and its ability to create or erode value in the sustainability context. For instance, obesity would be material to Coke or PepsiCo; carbon emission to energy utilities.

SASB has devised a materiality map that lists over 40 sustainability issues and analyses them in importance for 80 industries in 10 sectors. SASB standards are expected to catalyze improved performance of about 13,000 firms, with $16 trillion in funds, on environmental, social and governance issues.

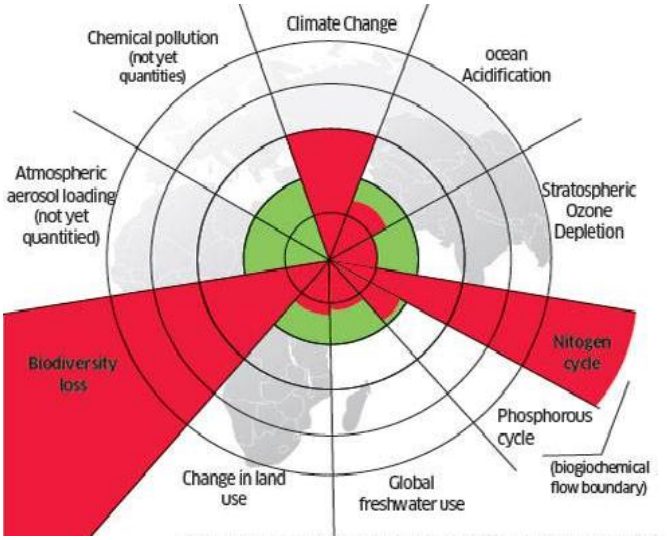



**Figure 5**: Green is the acceptable boundary and the world has crossed in three areas (Source: Stockholm Resilience Centre)

Tinkering with corporate social responsibility or CSR, therefore, as is happening in India, will not do. It is compliance-driven, and is not harnessed to the dire needs of the times. The 2% CSR spend mandated recently by the government hasn't impressed the international community; it is, at best, seen as a first step, but inadequate. [8]

## 6 Walmart's Prospects in India

As of April 2014, Walmart has invested Rs 1328 crore in its India unit and currently has 20 Best Price Modern Wholesale stores located at places such as Amritsar, Zirakpur, Jalandhar, Kota, Bhopal, Ludhiana, Raipur, Indore, Vijayawada, Agra, Meerut, Lucknow and Jammu. Walmart India, a new company it registered in January, issued and allotted more than 81 crore equity shares at Rs 16.35 each to its Bentonville-based parent as share application money worth Rs 1,328 crore, according to a board resolution passed recently. [9]

Krish Iyer, the chief executive of its India unit, will be responsible for leading the growth and success of the India operations while also continuing to develop Walmart's future retail strategy there. The prospects of Walmart ultimately depends on the government's stance by the end of 2014.

Bharti and Walmart reached an agreement to independently own and operate separate business formats in India and discontinue their franchise agreement in the retail business. The US retail giant has been pitching for relaxing local sourcing norms under the foreign direct investment policy for multi-brand retail. The Indian government has no plans to relax the mandatory 30 per cent local sourcing norms for foreign players in the sector [8].

India is allowed 51 per cent investment in multi-brand retailing in September 2012, but no foreign retailer has so far applied to enter the country. The Indian Government feels that Walmart will be a speck in India's retail market which is driven by millions of standalone stores and that India's retail market has been strengthened by Indian retail chains. There could be bright future for Walmart in India if they are able to stay in the fight long enough for a change in the political scenario or policy change, in which case they will dominate a chunk of the Sustainable Development market. If Walmart achieves their Packaging Neutral target on time, other retail chains like Company F and ITC may have to follow suit to keep up with market demands. Given Walmart's demands from suppliers in their Packaging Scorecard as shown in Figure 6, it could boost modifications to make more processes sustainable across the country. The next two years are critical in this regard.




**Figure 6**: Walmart's Scorecard Metrics (Source: Walmart Inc.)

## 7 Beyond GDP – Defining a New Metric

Owing to the continued deterioration of the environment, rapidly diminishing natural resources, increase in instances of terminal illnesses & frequency of natural disasters and loss of biodiversity, several debates have been going on regarding the efficiency of GDP (Gross Domestic Product) as an indicator of the well-being and prosperity of humans and the general population. It is time we take a few steps to look beyond GDP when it comes to evaluating economic growth and take into account the indispensable element of sustainable growth. While GDP as a measure of economic growth and progress has its merits and its use dates back to several decades, this data and drawing conclusions from GDP alone has its flaws.

For a more effective and inclusive method of evaluating economic progress in the 21st century, a sustainability factor must be included to indicate the strain on the environment while economic growth was seen. Because the GDP of developing economies is likely to grow, there is an opportunity to express this growth in terms of environment-friendliness and compare it with growth measure purely in terms of GDP.

### 7.1 Sustainable Development Product (SDP)

A simple and effective way of evaluating this is to cite GDP as a ratio of percentage growth vs. percentage sustainable growth. Since GDP is a percentage, we can calculate the percentage of economic growth that was sustainable and express the two as a ratio, giving Sustainable Development Product or SDP, a more tangible indicator of economic growth.

For example: if the GDP of an economy is 8% and 40% of this growth was estimated as sustainable (i.e. portion of growth contributed by sustainable organizations or Sustainable Growth Portion (SGP)) then the Sustainable Development Product (SDP) is expressed as 8:40.

Hence, **SDP = GDP : SGP**

By comparing this to the world average, a better insight into the priority of sustainability in an economy can be gained. It will also give developing economies clear targets by comparing their SDP with those of developed economies.

### 7.2 Sustainable Profit Ratio (SPR)

As an extension of this idea, the formula can be used by individual companies to estimate their profit percentage in terms of Sustainable Growth. But this is likely to be less objective as the details of sustainable profits can be vague and methods to evaluate will vary from company to company.

Hence, **SPR = Net Profit : Sustainable Profit**

## 8 Conclusions

In summation, we've discussed the existing ideas of sustainability and frameworks for metrics. The case studies have helped establish that while metrics are easy to quantify it's in their implementation where the real challenge lies. To address this challenge, mathematical models across the packaging supply chain need to be developed that focuses on the impact of potential failures at points along the supply chain. With the advent of digital technology in India it is now possible to transfer awareness about the sustainable metrics through various communication networks available across the country as compared to a decade ago where there were rampant power cuts and limited network facilities. India is on the brink of development and the time is right to focus on sustainability so that a better example can be set for underdeveloped countries.

To realize this opportunity, we have simplified the idea of sustainability from a vague, rather subjective concept to a combination of two key ideas: Design Sustainability (DS) and Process Sustainability (PS). In the end, new metrics have been defined for expressing sustainable development and economic growth as a simple formula for Sustainable Development Product (SDP) and Sustainable Profit Ratio (SPR) as an attempt to look beyond GDP when studying economic growth.

## References


1. Global Sustainable Packaging Market to Reach Nearly $143B by 2015, published on August10, 2010, www.environmentalleader.com [accessed on November 20, 2013].
2. Sustainable Packaging Coalition Report: Design Guidelines for Sustainable Packaging, Ver. 1.0, December 2006.
3. The Consumer Goods Forum, A Global Language for Packaging and Sustainability, Revised Edition, September 2011.
4. S.S. Shejwalkar and P. Iyer, 2012, "Twelve Principles of Green Packaging", *Proceedings of IAPRI 2012 World Packaging Conference, San Louis Obispo, California, USA*, June 17-21, pp.312-320.
5. A.C. McKinnon. S. Cullinane. M. Browne. A. Whiteing, 2010 *Green Logistics: Improving the Environmental Sustainability of Logistics*, 1st Ed., Kogan Page Publishers, pp. 05-15.
6. PE International, Whitepaper on Life Cycle Assessment An Executive Overview of Applications, Market Drivers and Business Benefits, July 2011.
7. B. King, Walmart Explains Introduction of Sustainability Scorecards for Product Categories, published on 02 May, 2010 in www.sustainablebrands.com [accessed on November 22, 2013].
8. News Article, Walmart will be a spec in India's retail market published on 14 October, 2013 in articles.economictimes.indiatimes.com [accessed on November 12, 2013].
9. News Article, Walmart bets Rs 1,328 crore on India after recent break-up with Bharti published on 7 April, 2014 in http://articles.economictimes.indiatimes.com/2014-04-07/news/48939577_1_bharti-enterprises-modern-wholesale-walmart-india [accessed on April 18, 2014].

# ULab© Cloud Testing System for Flexible Plastic Packages

**Xin Chen[1*], Haimo Jiang[1], Yunzhong Jiang[1], Yuan Su[2]**

[1] *Labthink Instruments, Co., Ltd., China*
[2] *International Office, Hunan University of Technology , China*

[*] *Corresponding author. Email:sdjndxcx@163.com*

**Abstract:** There are over 20 conventional testing items for flexible package and even more if we need a comprehensive test. It is costly and not efficient to purchase instruments and perform tests in one laboratory. The test results are isolated and not sharable. Statistical analysis based on mega data is unavailable.

To comply with the trend "Green Package and Resource Sharing", ULab© Cloud Testing System is proposed by Labthink, supported by the company's advanced testing instruments and leading technologies.

ULab© Cloud Testing System for flexible plastic packages is a powerful and convenient testing platform, which is developed on the basis of Internet of Things, cloud computation technology and multiple testing instruments with automatic data uploading function. It will be widely used to provide flexible plastic manufacturers and customers with reliable, highly efficient and cost effective automatic testing services. The customers do not need to establish their own laboratories, thus saving numerous investments and social resources.

ULab© Cloud Testing System is composed of a remote laboratory data management system and a site testing data management system, which could collect and analyze online test data and then generate testing report and analysis report automatically. Customers only need to register an account and log in the system to get reports for the materials tested. Testing items in ULab© cover the overall properties of flexible plastic packages. The site testing instruments could test the product packages in production line so that unqualified packages could be identified.

ULab© could also be used to provide various industries with quality diagnosis and precautionary of packaging material in different links. With optimization of resource allocation and information system, ULab© provides its customers with the tons of test data tracing, management and statistical analysis services throughout the quality control process.

This article introduces basic concept, structure and applications of ULab©.

Keywords: ULab Cloud Testing System, Flexible Plastic Package, Optimize Resource, Resource Saving and Sharing, Green Package.

## 1 Introduction

Without self-operated laboratories or advanced testing instruments, most of manufacturers and users (factories) have to request third party inspection institutions to perform the tests of their packaging materials. However, third party test is usually high in cost but low in efficiency, which can not satisfy the requirements for frequent

quality control in daily production. Only testing data is obtained in self-operated laboratories or from third party inspection institutions, and no guidance is given on the improvement of processing craft and selection of packaging materials. As a result, it is difficult for manufacturers or users (factories) to establish an effective data system for quality control.

Labthink ULab Cloud Testing System is developed on the basis of Internet of Things and cloud computation, which combines the wireless communication technology and software platform. ULab Cloud Testing System includes Testing Center Data Management System and Factory Test Data Management System, which realizes mega data storage and analysis as well as diagnosis and quality control of packaging materials from multiple aspects. ULab Cloud Testing System is a revolutionary invention which is cluster management and reduces testing costs by optimization of resource. Labthink creates a new type packaging testing laboratory with ULab Cloud Testing System which is uniform in service mode with a high testing efficiency.

## 2 Internet of Things & Cloud Computing Technology

Integrating with Internet of Things and cloud computing technology, Labthink creates a new type service mode for flexible packaging testing, ULab Cloud Testing System. With Internet of Things function, signal sent by the sensor equipped in testing instruments can be shown to operator on the monitor and transferred to data receiving module i.e. data acquisition server through wireless data transfer modules such as Zigbee, Bluetooth and WIFI, etc., which are also embedded in testing instruments. The signal received by data acquisition server is converted to readable data, which is reported to cloud computing center. Eventually the data is stored and processed in cloud computing center and then sent to users of Testing Center Data Management System or Factory Data Management System, displayed in test reports. Please refer to Figure 1 to see how data is transferred with the functions of Internet of Things.

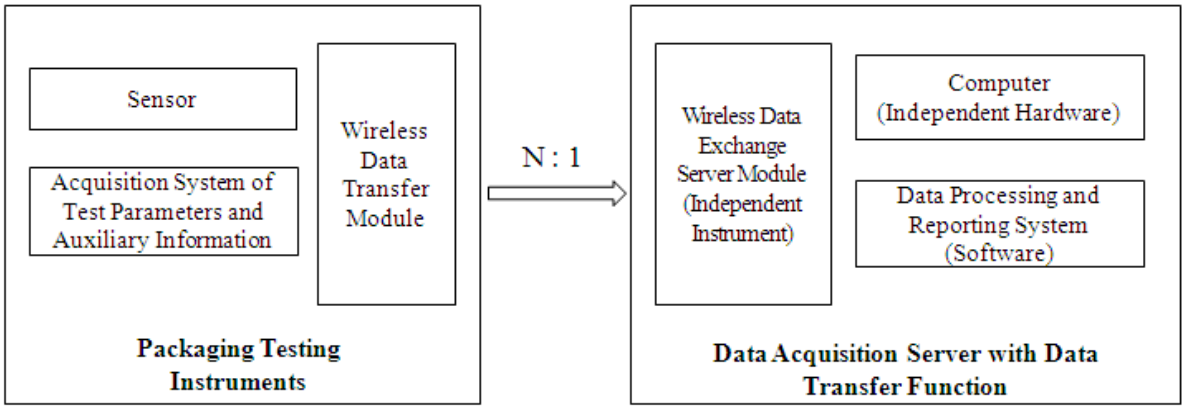



**Figure 1**: Internet of Things Function & Wireless Data Communication.

Wireless communication of test data can minimize the errors caused by manual operation and guarantee the accuracy of test results. Additionally one data acquisition server can be used to communicate with multiple testing instruments. Through internet, data communication between multiple remote laboratories at different locations can be realized easily.

## 3 ULab Cloud Testing System

### 3.1 Framework of Labthink ULab Cloud Testing System

Process and test data can be transmitted by on-site testing instruments and regular testing instruments with data transmission function automatically or by the other instruments without such function though data interface. The

data mentions above is stored, converted and extracted in local database of ULab Cloud Testing System and then managed by the application management platform. Eventually the data is applied in the two sectors of the ULab Cloud Testing System i.e. Testing Center Data Management System and Factory Test Data Management System. The framework of ULab Cloud Testing System is shown in Figure 2.

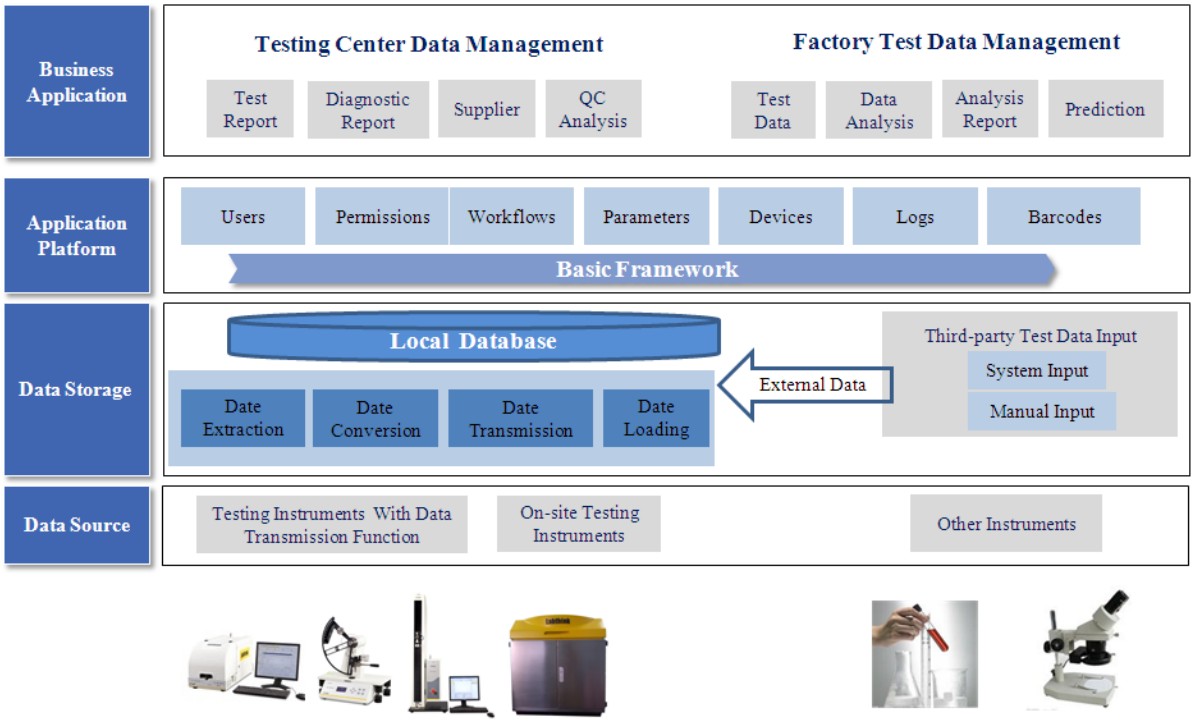



**Figure 2**: Framework of ULab Cloud Testing System.

### 3.2 Testing Center Data Management System

Testing Center Data Management System, which saves the costs of labor force, investment in lab establishment and management or the service fee charged by third party inspection institutions, includes there software modules. In the service module, users can manage remote laboratories, test requests, test reports and the whole testing process. Labthink i.e. the remote laboratory receives and handles test requests in this module and manages lab information and user information. The system is equipped with modules for data acquisition, data storage and management so that original data and business data can be saved, managed, synchronized and parsed. In the test reports generated automatically module, test data is processed according to users' requirements and test reports or analysis reports are generated and sent to the service module of the system. Please refer to Figure 3 for the detailed functions of Testing Center Data Management System.

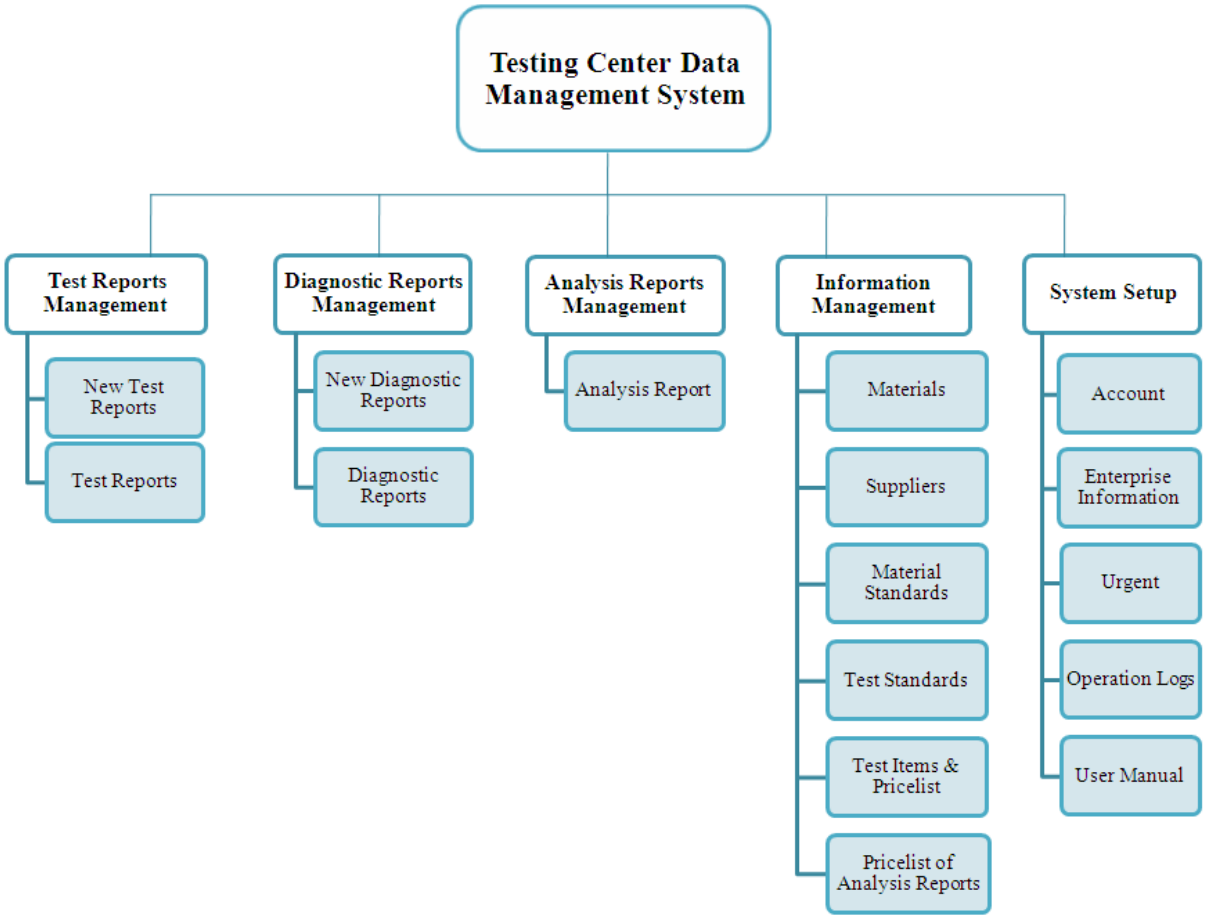



**Figure 3**: Structural Diagram of Testing Center Data Management System.

Testing of packaging materials, quality diagnosis and historical data specific analysis can be realized respectively through test reports management, diagnostic reports management and analysis reports management according to users' requirements, which is helpful to long-term quality control of packaging materials. In information management section, users can search testing standard and information about sending packaging materials, so that packaging materials can be managed systematically on an information-based system.

The workflow of Testing Center Data Management System is shown in Figure 4.

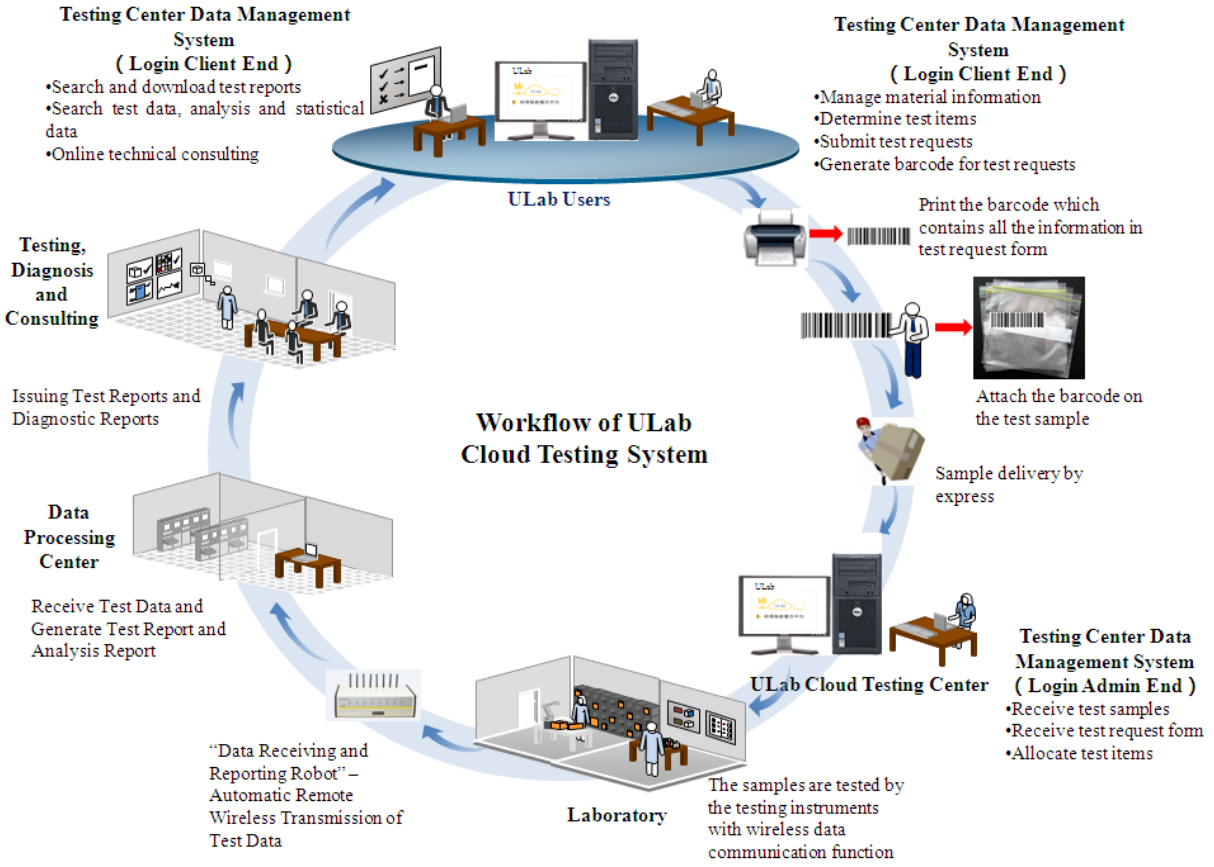



**Figure 4**: Workflow of Testing Center Data Management System.

### 3.3 Factory Test Data Management System

Test data and information from laboratories and on-site testing instrument can be automatically collected, integrated and processed by Factory Test Data Management System. With this system, enterprises can realize automatic testing procedure, process data tracking, data management and data analysis. Additionally the management and quality control capacity of packaging can be improved.

According to the variety of data sources and test phases, the Factory Test Data Management can be classified into on-site test data management, testing center data management and third-party test data management. On-site test data management refers to the management of test data obtained at production site (Please refer to Figure 5 for On-site Testing Procedures). Testing center data management refers to the management of test data obtained from testing instruments with data transfer function, which includes the functions of test data searching, analysis and management, settings of test parameters and specimen information as well as management of test reports. Third-party test data can be imported from the instruments without automatic data transmission function to the Factory Test Data Management System so that all test data can be managed uniformly.

In addition to the functions mentioned above, the instrument management, background management and connection port management of remote laboratories are also available in this management system.

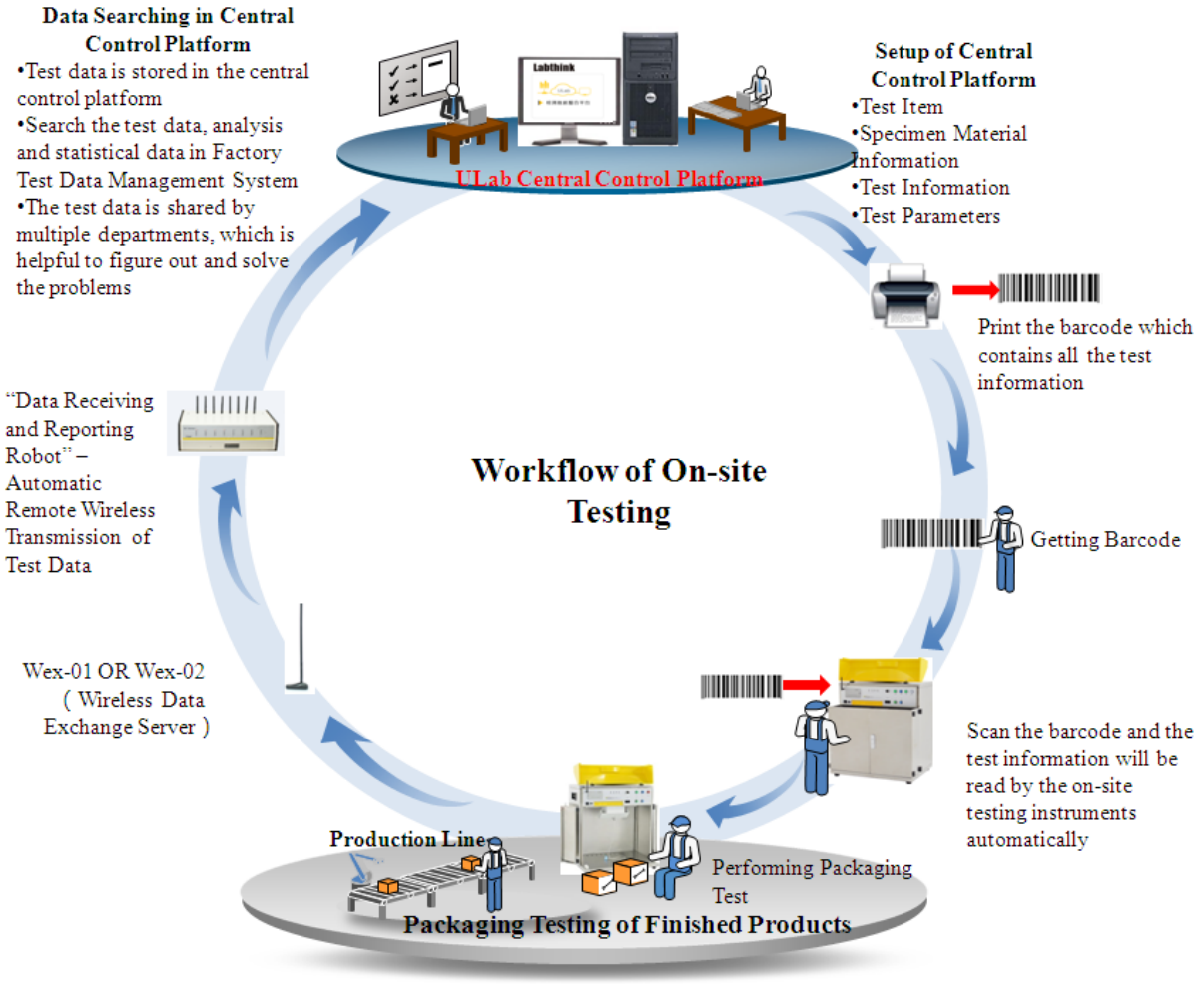



**Figure 5**: On-site Testing Procedures.

# 4 Application of ULab Cloud Testing System

## 4.1 Classical Application

Testing Instruments and Test Items: Testing instruments used in ULab Cloud Testing System are all developed by Labthink Instruments Co., Ltd. The testing instruments are applicable in permeability tests, physical and mechanical property tests as well as chemical and sanitary performance tests of flexible plastic packaging materials. The physical and mechanical properties include anti-elongation, impact resistance, flex durability, frictional property and heat shrinkage property, etc. Additionally the heat seal performance, leak and seal performance, high temperature resistance of package as well as oxygen residual of vacuum package can also be tested. i-PROCESS series instruments are designed for on-site testing of finished package in production line. The i-PROCESS series instruments can be used in torque test, leak and seal test, headspace gas analysis, volume and weight analysis, etc. in quality control of the finished products.

**Quality Control Solution**: ULab Cloud Testing System can provide professional analysis reports of historical test data including analysis reports for supplier management and analysis reports for production management. Diagnostic reports that contain improvement and performance index value of packaging are given to users on the basis of test data and the characteristics of contents inside the package. Additionally ULab Cloud Testing System can also provide quality control solution in which effective means of regulating packaging materials are

recommended to help users with the quality control of packaging materials and prevent potential risks caused by packaging problems.

To meet the requirement for tests of increasing types of packaging materials in various packaging patterns and the increasing market demands, more and more testing instruments and software functions are introduced into ULab Cloud Testing System.

### 4.2 ULab Testing Solution

Testing Center Data Management System and Factory Test Data Management System of ULab Cloud Testing System can satisfy various requirements of users for quality control of packaging materials. With the testing instruments, ULab can provide comprehensive service to enterprises. The basic functions and general procedures of ULab Cloud Testing Service are shown in Figure 6 and Figure 7.

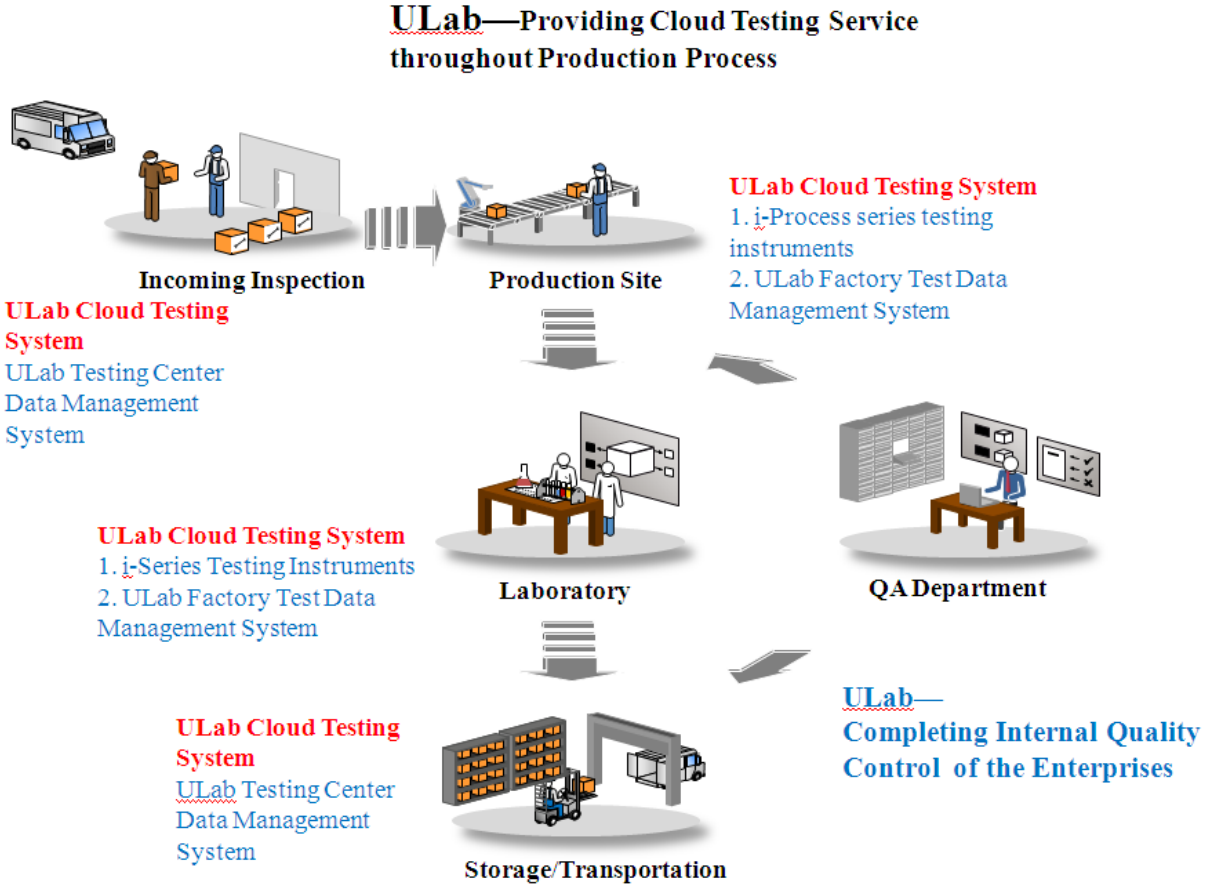



**Figure 6**: Basic Functions of ULab Cloud Testing System.

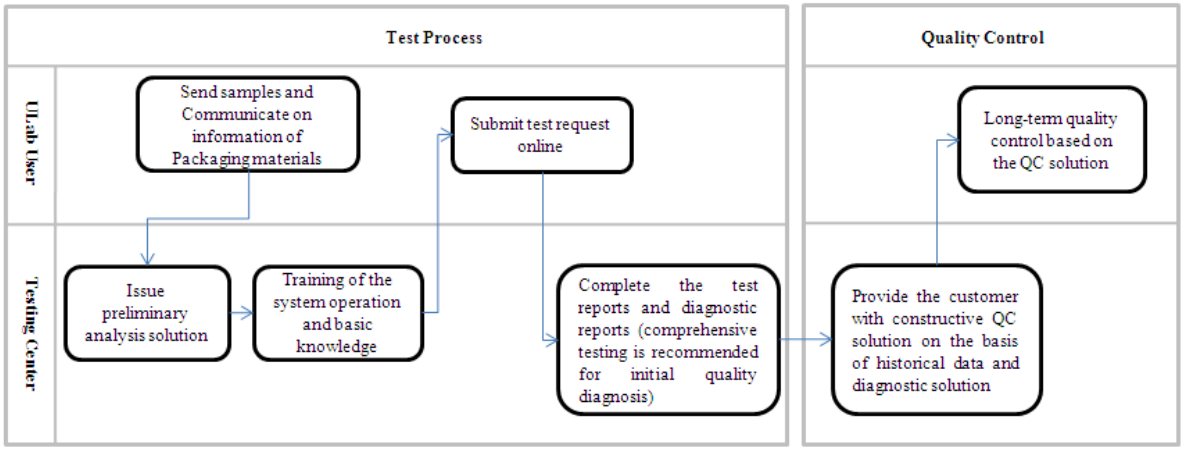



**Figure 7**: General Procedures of ULab Cloud Testing Service.

Take large-scale enterprises with the requirement of packing materials quality control in the flexible package application industry for an example, a summary of comprehensive testing solutions with ULab Cloud Testing System is shown in Table 1.

**Table 1:** Application of Ulab Cloud Testing System in Flexible Packaging Industry.

| Department | Process | Configuration of ULab Cloud Testing System | |
|---|---|---|---|
| Manufacturing Department | On-site Finished Package | Factory Test Data Management System | On-site Testing Instruments<br>On-site Test Data Management |
| QA Department | Purchase & Selection of Packaging Materials<br>Inspection of Finished Package | Testing Center Data Management System | Preliminary Analysis Solution<br>Testing Service & Test Report<br>Analysis report on Historical Data<br>Diagnostic Solution<br>Quality Control Solution |
| | | Factory Test Data Management System | i-Series Testing Instruments<br>Testing Center Data Management<br>Third Party Test Data Management<br>Instrument Management |

The multi-angle solutions mentioned above aim at users with high material quality control requirements. Users can select the optimal solution in practical application according to actual requirements.

## 5 Conclusions

Internet of Things technology makes it possible to link real-time information generated by the sensors to cloud computing center with an intelligent lab management system (user end) processing test data automatically. Additionally the remote labs packaging testing service is available to target customers in SaaS (Software-as-a-Service) mode which optimizes resource sharing so that users can even complete the quality control of packaging materials at home. ULab Cloud Testing System is a renovation of traditional testing mode, which brings up a uniform, integrated, cost-effective and high-efficiency packaging testing service. In contrast to traditional laboratories, the consumption of paper and occupation of space is reduced. ULab Could Testing System is a revolutionary invention in the field of green testing technology.

Distinguished from third party testing laboratories, ULab Cloud Testing System is featured with tons of data storage and infinite computing capability, especially when testing data is from multiple testing instruments or many laboratories. With ULab Cloud Testing System, data accumulation and data comparison can be realized, which provides valuable reference for users to evaluate the validity of packaging. Additionally a comprehensive quality control solution can help users to monitor the quality of packaging materials effectively.

# Green Fibre Bottles

**Søren R. Østergaard[1*] , Dr. S. Vikram Singh[1] and Jesper Servé[2*]**

[1] *Packaging Section, Danish Technological Institute, Denmark*
[2] *EcoXpac, Denmark*

[*]*Corresponding authors. Email: sos@dti.dk; js@ecoxpac.eu*

**Abstract:** In the Danish project: Green Fibre Bottles, EcoXpac and Danish Technological Institute has an on-going development project with the purpose of creating an environment friendly bottle that is biodegradable and can replace glass and plastic bottles and also cans for both carbonised and non-carbonised liquids.

The bottle has several environmental and commercial advantages.

- Bottles can be designed with either screw cap or single-use seal.
- Packing can be produced in order to fit in with any existing filling plants.
- Raw material can be all kinds of paper pulp – a sustainable material.
- New patented production technology guarantees high level of energy saving - up until 80% compared with conventional moulded pulp production.
- After use the bottle can enter into recycling systems on equal terms with cardboard and paper, or decompose directly in nature.
- The production unit is small and compact, thus it can be transported and set up wherever in the world the bottles are to be filled.
- The bottle quality is very convincing with a surface as writing paper.
- The surface coating is based on a natural sustainable applied very thin.
- The total barrier performance will be almost as perfect as glass bottles and metal cans.
- Production costs are lower than similar packaging.

The development project is carried out in collaboration between a number of experts including the Danish Technological Institute. The project budget is funded by the Business Innovation Fund in Denmark.

The presentation will include a presentation of the background of this on-going project and a description of the innovative production method. Also samples of fibre based bottles will be presented to the audience. The coating strategy for the fibre bottle will be presented by Dr. S. Vikram Singh in another presentation.

Keywords: Sustainable packaging, bottle, paper, liquid packaging, moulded paper packaging.

## 1 Introduction

Environment and sustainability has been in focus for both consumers, in policy, and in business for the last decades. This has a big impact on all stakeholders purchasing behaviour. All are looking for more sustainable packaging but not always these sustainable packaging are sustainable in reality. Many packaging give consumers an impression to be sustainable although LCA studies document different.

Liquid packaging is approx. 30-35 % of all packaging used. Based on this the sales value in the World of liquid packaging is about 80 billion € or 125 billion AUD. The annual production worldwide is 900-1,200 billion bottles. Typical liquid packaging is gable tops in paper/polymer, glass bottles, cans, blown plastic packaging etc.

For different reasons many stakeholders are looking for bio-based packaging. But liquid packaging is difficult to produce as the water is a natural component in the bio-degradation process. Most bio-packaging either has a short shelf life or use an oil-based polymer to have food contact.

## 2 Project background

In 2010 EcoXpac and Danish Technological Institute (DTI) worked together in another project. Under the breaks we started a debate about a new product EcoXpac started to produce based on a concept from UK.

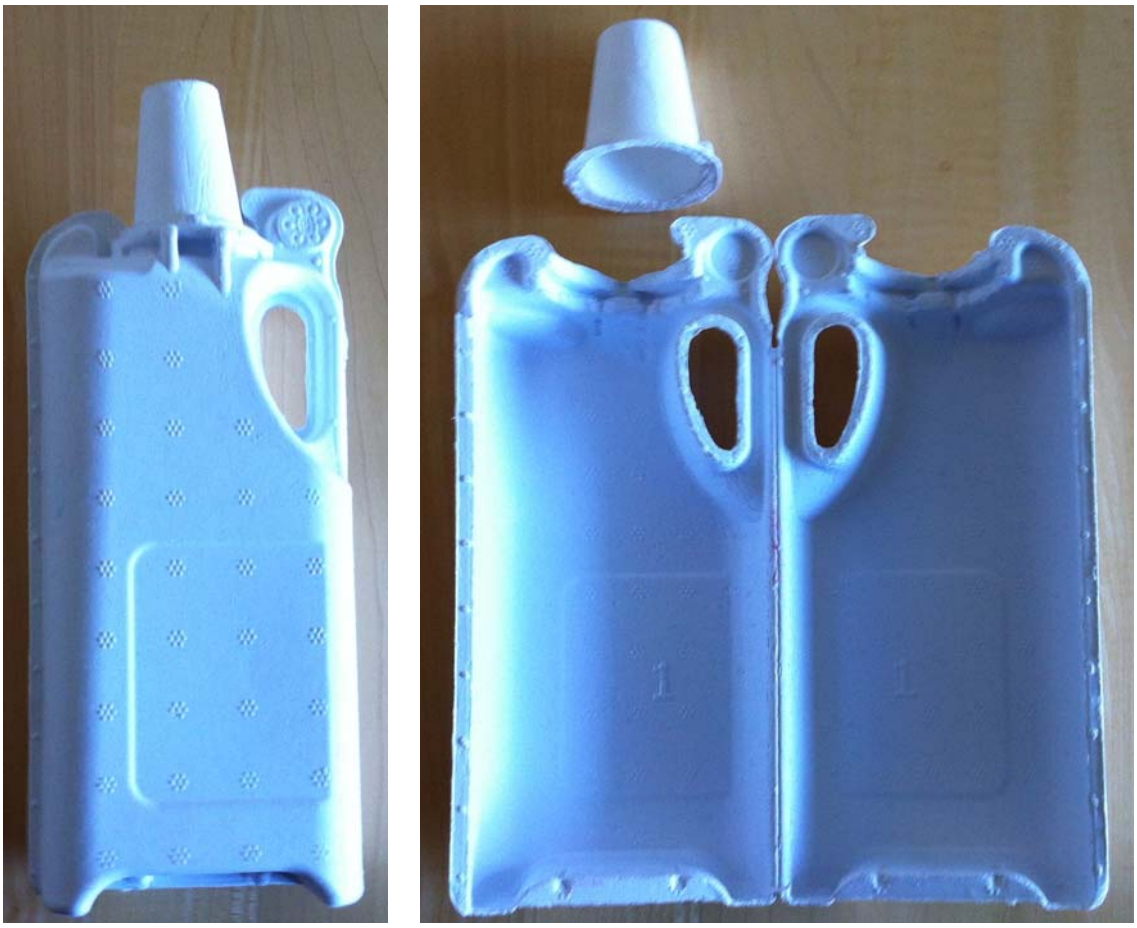


**Figure 1**: Moulded fibre based bottle produced in 3 parts

The technology is just as many moulded paper bottles on the market today based on two half parts glued together with a top part integrated with a polymer bag in order to have liquid contact and protection to fibres of on known origin.

Many of the fibre based bottles on the market today are produced in traditional paper moulding technology. The pulp is then sprayed on a fine metallic net in order to separate the 98-99 % water in the pulp from the 1-2 % paper fibres. Then the wet product is placed in another mould for after pressing before the rest water in the still wet product is dried in a hot oven. The heat drying process will in many cases use more oil for heating than if the bottle is made of 100 % plastic.

EcoXpac did already in 2010 use a more energy efficient method. EcoXpac produce moulded paper packaging for cushion of industrial products and electronics. These packaging is produced with a vacuum technology formed in an aluminium mould with many small holes. The pulp was also sprayed in the mould. But the separation is done with the vacuum only. After the processing the product is very stable and only need a short

time in atmospheric air for the final drying. This production method save the energy consuming drying on a hot oven and 70-80 % of the energy and environmental impact is reduced.

But even worse these types of bottles need different filling machines. And as I all the food industry the investments in the packaging lines are larger than in food processing. For this reason EcoXpac had big trouble selling the fibre bottles.

We all realised that fibre bottles need to be filled in traditional filling equipment in order to be implemented in the liquid food and drink industry.

## 2 Project aims

Already we got national founds for developing a Green Fibre Bottle by the Danish Ministry of Industry with following aims:

- Development of a paper based bottle made in one unit
- Design option better than PET bottles
- Development of screw led in paper
- Bottle and lid shall be sealing water, moisture, oxygen, $CO_2$ (carbonized drinks) etc.
- Able to be produced full or partly of recycled fibres incl. a barrier between food and recycled fibres
- The used fibre bottles shall be able to be:
    - Re-used
    - Recycled
    - Incinerated with positive energy production
    - Biodegradable
- Printing direct on bottles
- Filling in traditional and existing plastic bottle filling equipment
- Production costs and environmental impact dramatically reduced compared with other liquid packaging

As we are using paper it was not expected to create transparent packaging.



**Figure 2**: Filling station for PET bottles

# 3 Fibre bottle productions

## 3.1 Production method

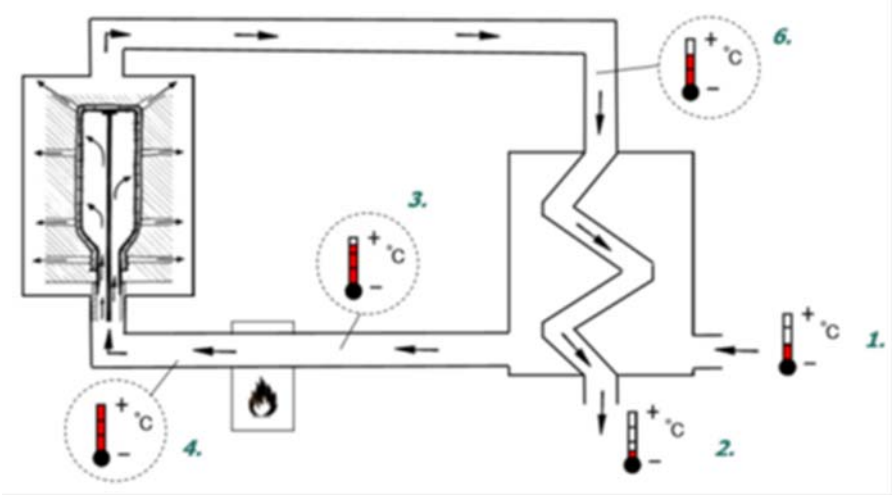



**Figure 3**: Production with overheated pulp

We realised that the bottle need to be produced on only one unit to be able to full fill all these requirements. For this reason traditional paper moulding technology was impossible. It was needed to process the fibres in something like blow moulding of polymers in order to have a big container and a little led. First we believed it was possible to use vacuum moulding as EcoXpac already was using for packaging cushion. Pulp can easy be sprayed in the inside of the mould using a pipe. The first tests demonstrated a soft wall design even worse than normal moulded paper. In some way we had a need to compact the fibre more dense together. We also wanted to reduce the energy consumption. EcoXpac came up with an innovative and now patent pending technology using over-heated pulp.

Pulp (water and paper fibres) is heated up under pressure to a temperature much higher than boiling temperature in atmospheric conditions ($100^0$C). The pulp is led into the mould in a pipe. When the valve open this overheated pulp is under normal pressure the liquid water intermediately becomes steam and this create an explosion sending the wet fibres up against the walls of the mould. The vacuum on the mould remove the steam/water to be recycled both as energy and process water.

In this way we get compact fibres and reduce the energy use even more than vacuum moulding. We expect to reduce energy up to 90 %. We still need optimisation of the process.

## 3.2 After pressure



**Figure 4**: Double forming sections

After the first forming on a traditional vacuum mould the bottle is removed and placed in another mould with the same shape but with many small holes. With vacuum and pressure from the inside the last water is removed and the bottle is ready for coating. Both steps in the process can be done in 6 seconds. So each set of moulds can produce 10 bottles per minute. The forms can be doubled up several times to the correct capacity with a marginal extra use of space.

### 3.3 Paper bottle performance

The bottles we produce are about half the weight of normal PET bottles but more ridged and stiff.



**Figure 5**: Bottle with 1-2 mm thin walls

The material is very compact and only 1-2 mm thick. Calculations indicate that the production costs and the environmental impact is more than half of gable tops and plastic bottles.

But the method is not ready for implementation.



**Figure 6**: Bottle design



**Figure 7:** Screw cap will also be in paper




**Figure 8**: Different kind of materials, Virgin paper, recycled paper and corrugated




**Figure 9**: Fibre bottles produced in different colours

## 4 Coatings

Paper and fibres will always be a hygroscopic material designed at many small nets added together. We started with traditional varnish coatings but these coatings do not work.

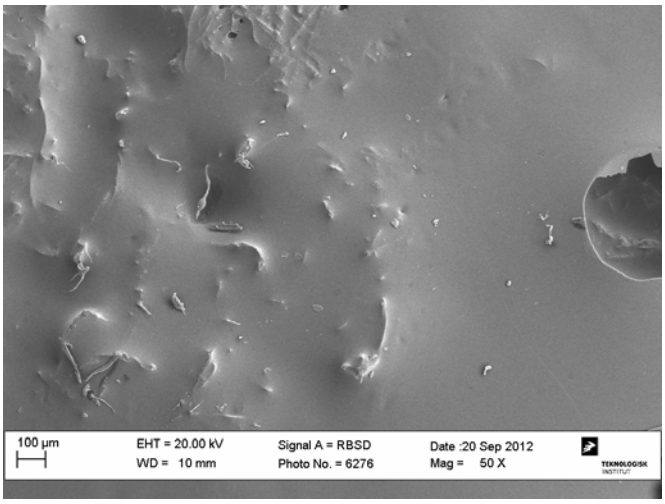



**Figure 10**: Microscope photo of traditional paint and varnish coating of fibre bottles

Even when a lot a varnish is used we still have big pin holes in the surface and fibres sticking out of the substrate. The material is not able to be recycled as the coating will flat together with the fibres almost half in to the paper substrate.

We are just now working with different options for coatings:

1. Thin polymer paint system only coating the surface. The coating can perform perfect. But we do not have a full recycling system.
2. Plasma coating with $SiO_2$ or $SiO_x$. See the presentation made by Dr. S. Vikram Singh, DTI.
3. AKD treated paper work perfect as a water barrier but all gasses have free access through the bottle. Cannot use recycled paper due to food contact and the bottle do not perform optimal when recycled.
4. Coating and treatments with different bio-polymers are in progress.

## 5 Local production units

Transport of empty packaging is expensive as the packaging has a big volume and a little weight. And also the value is low. For this reason empty packaging cannot be transported over long distances.

For these reasons we have designed the production equipment as a container like turn-key-unit able to be installed next to the filling line. The raw materials you need are then only compact balled paper fibres and coating materials. Also in this way we save resources.

## 6 The technology used for other packaging formats

We expect to upgrade this technology for other packaging formats and systems. It is expected the technology can be transformed to the production of:

- Trays
- Jars
- Cans
- Etc.

But transparency we never expect.

# 7 Conclusions

EcoXpac and DTI are still working on the project and expect to have a final product ready on the market next year. The results just now are promising as you can evaluate by studying the samples we have with us today. Fibre bottles have already with success be filled on existing plastic bottling filling lines. These filling lines only needed minor upgrades to operate.

We also know now that we can reduce the production costs and environmental impact even using virgin fibres. We also have a challenge to produce the bottles of recycled fibres in order to reduce costs even more and have the used bottles into a circular material flow.

EcoXpac and DTI hope to present the further development over the following years.

# Acknowledgements

EcoXpac and DTI would like to acknowledge the Danish Ministry of Industry for the big financial support in this project.

# Plasma Enhanced Surfaces for Sustainable Fiber Based Packaging

**S. Vikram Singh[1*], Steffen Sønderby[1], Soren R Østergaard[1] and Jesper Servé[2]**

[1]*Packaging and Logistics, Danish Technological Institute, Denmark*
[2]*EcoXpack, Denmark*

[*]*Corresponding author. Email: shas@teknologisk.dk*

**Abstract:** The recent trends of packaging materials and technology have been highly oriented towards sustainability along with search for novel applicability areas. In this connection, sustainable biodegradable fibrous material such as tree based new fibers, recycled fibers, etc., are excellent raw materials. Packaging made by utilizing such materials has already appeared in the market in one form or the other. However, packaging produced from such materials often suffers from poor gas and liquid diffusion barrier; hence external additive materials are introduced to improve such barrier properties. To keep the sustainability of the packaging, the external additives/intrusions/treatments/fillings have been tried to keep minimal, and limited to the surfaces of the packaging. Moreover, these introduced materials often dictate the nature of the packaging in terms of its sustainability.

Plasma based surface processing have emerged as a potential candidate to enhance gas and liquid barrier properties, printability, hydrophobicity, etc., of a surface. Note that few microns thick plasma coating (even <2% of the original material) can be enough to achieve desired material properties. Here an atmospheric pressure plasma enhanced chemical vapor deposition was utilized to deposit $SiO_x$-like (where x = 1-2) thin film coatings on highly porous paper substrates to enhance gas and liquid barrier properties. The thin films were deposited by controlling hexamethyldisiloxane (HMDSO) and $O_2$ plasma chemistry in the ambiance of He, Ar or $N_2$ discharge. The coated paper samples have excellent barrier properties against water; moreover, the coated surfaces are also investigated for their barrier properties against other liquid along with gases like $O_2$, $CO_2$, etc. We also studied influence of distinct discharges on packaging surfaces to obtain improved hydrophobicity, adhesion and printability. All these plasma induced surface processing were performed using radiofrequency capacitively coupled plasma, where the substrate temperature was kept at room temperature.

Keywords: sustainable fiber based packaging, $SiO_x$-like plasma coating, surface modification of packaging material.

## 1 Introduction

Plasma processing is regarded as a crucial technology in a large number of industries, where surface modification are involved, such as microelectronics, lighting, solar cells, bio-compatible implants, display panels, packaging, etc., [1-6]. Surface modification by plasma processing is performed utilizing low-temperature plasmas, which are generally partially ionized [7]. Depending on the precursor gas used, the plasma chemistry could be tuned to be active for the dedicated process. Such processing is carried out by the plasma species like electrons, ions, radicals, and excited atoms/molecules. Plasma has ability to generate surface modifications like fine and controlled etched surfaces and thin film coatings and chemical activation (by adding or activating the surface molecules) on material surfaces. Plasma processed coatings have immense potential in using as a protective coating and gas barrier coatings. Processing plasma chemistry can be easily and finely tuned to generate thin film coatings with distinct surface properties- very hard, gas barrier, hydrophobic, hydrophilic, passivation layers, optical selectivity, self-cleaning, etc., coatings.

Plasma induced barrier coatings are well known in the packaging world [4, 6]. Moreover, the recent trends of packaging materials and technology have been highly oriented towards sustainable biodegradable fibrous material such as tree based new fibers, recycled fibers, etc., (e.g., [8]). Although packaging made by utilizing such sustainable fiber based materials has already appeared in the market in one form or the other, but packaging produced from such materials often suffers from poor gas and liquid diffusion barrier. In this connection, plasma coatings have great potential to replace the existing external additive (non-sustainable) materials used to improve such barrier properties. Very thin coating, e.g., $SiO_x$-like coating on the compacted fibrous substrate can be sufficient to generate gas and liquid barrier properties. Hence, large amount of non-sustainable external

additives/intrusions/treatments/fillings can be removed or minimised from green packaging. Over and above such plasma treatments are mostly limited to the surfaces of the packaging.

In this work we have tried to induce surface barrier properties by adding SiOx-like thin film coating on a paper base packaging substrate. Here we have utilized low temperature radiofrequency (rf) plasma at moderately high pressure.

## 2 Experimental setup and results

### 2.1 Plasma setup

The used experimental setup is described in details elsewhere [9-10]. Briefly, a Gaseous Electronic Conference (GEC) rf reference cell was utilized to perform these plasma depositions. Here, the rf power was coupled capacitively, also known as Capacitively Coupled Plasma (CCP). The upper electrode was a showerhead electrode where the power was coupled and through which the gas was discharged in the vessel. The lower electrode and the rest of the vessel were grounded. The inter-electrode spacing is fixed at 25.4 mm and the diameter of the electrodes are 10.2 cm. Ground shields surround the insulators and extend from the electrode mounting flange to the plane of the electrode. A RF generator (Dressler, Cesar 1312) with a frequency of 13.56 MHz was used which can provide RF power up to 300 W. The power was coupled through an automatic matching network (Dressler, VM 150 W-CCP) with some alterations, to adapt to high pressure operations.

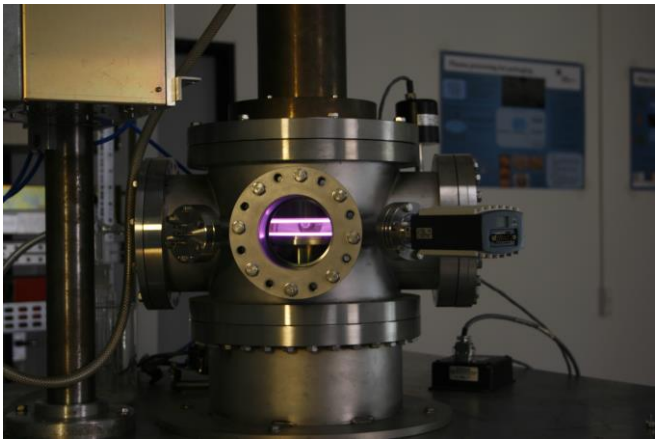


**Figure 1**: CCP source, where plasma emission can be seen between the electrodes.

Good qualities of $SiO_x$-like coatings have been successfully deposited at a gas pressure between 50 to upto 500 mbar. However, here we present the results on the depositions obtained at around 100 mbar. The depositions were successfully performed on paper based substrates of diameter around 7 cm. Some of the samples had a cup-shape of same base diameter, but with the wall height of just about 2 cm. The coatings are water tight and some of the samples are under water barrier test since several months.

### 2.2 Plasma chemistry

All the depositions were performed under helium plasma using Hexamethyldisiloxane (HMDSO) and $O_2$ chemistry [5, 11]. Helium and $O_2$ were injected via the upper showerhead electrode, whereas the HMDSO was injected via an injection ring. Around 11 cm diameter injection ring is made-up of a copper tube (of outer diameter 6 mm). The ring was placed parallel to the upper electrodes face. We assume that the precursor vapour was injected in a laminar flow, during the depositions. Note that the by-products of this processing are He, $H_2O$, CO, $CO_2$ and $H_xC_y$ which are pumped out thorough a roughing pump.

### 2.3 Material properties

The results on $SiO_x$-like coatings, presented in this section, were performed at distinct powers, namely, 20 W, 30 W, 35 W, and 40 W. All the coatings were performed at room temperature. The coatings were performed to see the influence of $SiO_x$ matrix at distinct powers deposited on the substrates (Ø = 1 cm), which were cut from the state-of-the-art virgin paper bottles. The paper bottle project is elaborately described in another presentation by Østergaard *et al*. [12]. (Note that this work is performed under an ongoing commercial research project.) Earlier, as a proof-of-concept the water tight $SiO_x$ coatings were deposited on flat virgin samples at 35 W and are water tight since 20 June 2013. However, even at 30 W and 40 W water tight coatings have been produced on the flat samples but with a very low success rate, they were relatively bad films. Under these conditions, the coated flat samples leaked water after several hours or some could hold water for few days.

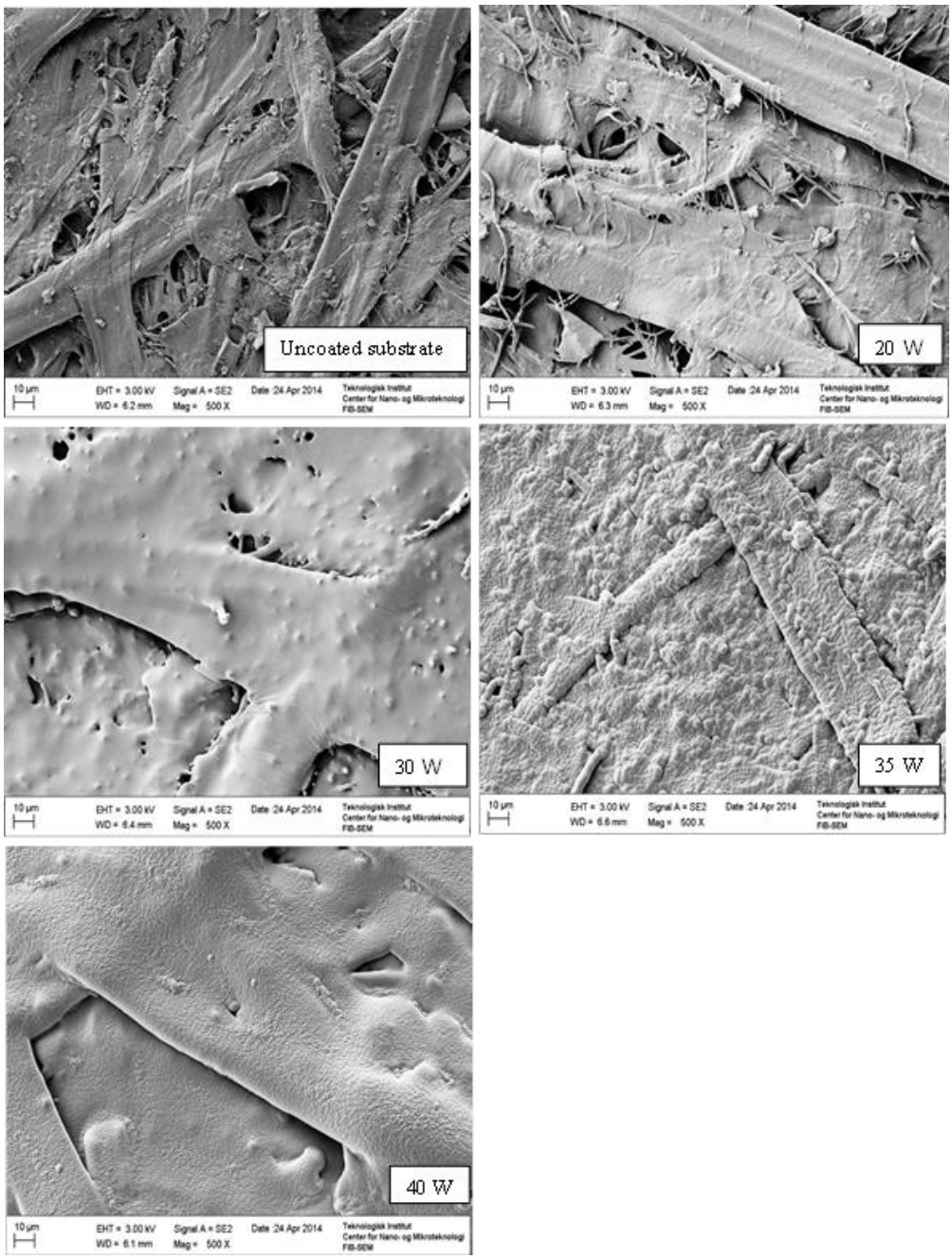



**Figure 2**: 500 x SEM image showing evolution from polymeric smooth surface to rough granular surface, with increasing applied rf power.

We believe that the coatings at lower powers like 20 W and 30 W are soft with polymeric organosilican (Si-$C_xH_yO_z$) scattered sites which were weak or dissolvable, hence could not hold the water longer. However, at the 40 W and above the coatings are highly stressed which we believe have a large probability of developing stressed-cracks.

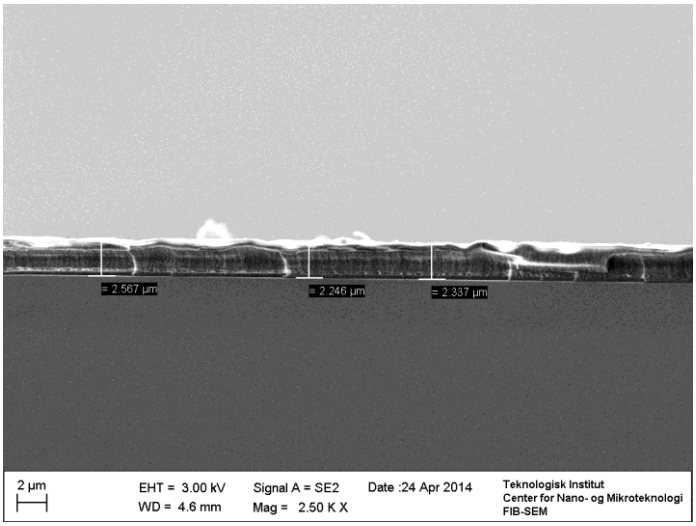



Figure 3: SEM cross-section of the film on a c-Si substrate. Two-layer structure shows the two distinct deposition conditions with one (bottom-layer) normal deposition and the other (top-layer) due to stopping process. Note that the third starting layer is not that obvious.

The structure of the coating can be assumed based on the surface morphology, see Fig. 2. The coating at 20 W and at 30 W have smooth surface with a signature of polymeric coating. Whereas, at 35 W and at 40 W the coatings have a columnar structure inheriting rough and granular surface morphology. The columnar structure can also be seen in Fig. 3, deposited on c-Si wafer. This cross-section image also gives an estimate of deposition rate (0.5 micron/min), which was deposited at 35 W.

## 3 Conclusions

At this stage we have been able to produce good water barrier $SiO_x$-like coatings on paper substrate. The spectroscopic ellipsometry measurement on $SiO_x$ deposited at 35 W reveals refractive index of 1.45 for the material. The coated paper samples are well intact under water barrier test since June 2013. Below 1 micro meter coated material has been able to provide water barrier to paper substrates. These depositions were performed at moderately high pressure and at room temperature. Presently, these coatings have been deposited at around 0.5 micron/min, which we believe can be improved by tuning the plasma chemistry and gas delivery.

## Acknowledgements

EcoXpac and DTI would like to acknowledge the Danish Ministry of Industry for the big financial support in this project. Prof. Dr. H. Soltwisch of Ruhr-University Bochum, Germany is also gratefully acknowledged for borrowing us the plasma setup used in this work.

## References

1. N.H. Lin, M. Kim, G.T. Lewis and Y. Cohen, 2010, "Polymer surface nano-structuring of reverse osmosis membranes for fouling resistance and improved flux performance" *J. Mater. Chem.* vol. 20, pp. 4642-4652.
2. S.V. Singh, T. Zaharia, M. Creatore, R. Groenen, K. Van Hege, and M.C.M. van de Sanden, 2010, "Hard Graphitelike hydrogenated amorphous carbon grown at high rates by remote plasma", *J. Appl. Phys.*, vol. 107, pp. 13305-01-10.
3. A.P. Roberts, B.M. Henry, A.P. Sutton, C.R.M. Grovenor, G.A.D. Briggs, T. Miyamoto, M. Kano, Y. Tsukahara, M. Yanaka, 2002, "Gas permeation in siliconoxide/polymer (SiOx/PET) barrier films: role of the oxide lattice, nano-defects and macro-defects", *J. Membr. Sci.*, vol. 208, pp. 75-88.
4. D. Pappas, 2011, "Status and potential of atmospheric plasma processing of materials", *J. Vac. Sci. Technol. A*, vol. 29, pp. 020801-01-17.

5. F. Palumbo, R. d'Agostino, F. Fracassi, S. Laera, A. Milella, E. Angelini, and S. Grassini, 2009, "On low pressure plasma processing for metal protection", *Plasma Processes and Polymers*, vol. 6, pp. S684-S689.
6. A.M. Coclite, A. Milella, R. d'Agostino, and F. Palumbo, 2010, "On the relationship between the structure and the barrier performance of plasma deposited silicon dioxide-like films", *Surface & Coatings Technology*, vol. 204, pp. 4012-4017.
7. M.A. Liberman and A.J. Lichtenberg, 2005, "Principles of Plasma Discharges and Materials Processing", Wiley.
8. http://pffc-online.com/coat-lam/coatings/8832-siox-barrier-benefits-1001.
9. S.V. Singh and C. Pargmann, 2008, "Electrical characterization of an inductively coupled gaseous electronics conference reference cell", *J. Appl. Phys.*, vol. 104, pp. 083303-01-11.
10. J.K. Olthoff and K.E. Greenberg, 1995, "The gaseous electronics conference RF reference cell - an introduction", *J. Res. Natl. Inst. Stand. Techno.*, vol. 100, pp. 327-339.
11. P.A. Premkumar, S.A. Starostin, M. Creatore, H. de Vries, R.M. J. Paffen, P.M. Koenraad and M.C.M. van de Sanden, 2010, "Smooth and Self-Similar $SiO_2$-like Films on Polymers Synthesized in Roll-to-Roll Atmospheric Pressure-PECVD for Gas Diffusion Barrier Applications", *Plasma Processes and Polymers*, vol. 7, pp. 635-639.
12. S.R. Østergaard, S.V. Singh and J. Servé, 2014, "Green Fiber Bottle", on going *19th IAPRI World Conference on Packaging*, Melbourne, Australia.

# The Greenhouse Gas Profile of a "Hungry Planet"; Quantifying the Impacts of the Weekly Food Purchases Including Associated Packaging and Food Waste of Three Families

**Karli Verghese[1*], Enda Crossin[1], Stephen Clune[2], Simon Lockrey[1], Helen Williams[3], Maud Rio[1] and Fredrik Wikstrom[3]**

[1] *Centre for Design and Society, School of Architecture and Design, RMIT University, Australia*
[2] *ImaginationLancaster, Lancaster University, UK*
[3] *Karlstad University, Sweden*

[*] *Corresponding author.* Karli.Verghese@rmit.edu.au

**Abstract:** The United Nations Food and Agricultural Organisation (FAO) have estimated that 1.3 billion tonnes of food is wasted across the supply chain, while food security emerges as one of the leading challenges facing a growing global population. Life cycle assessment (LCA) can illustrate the environmental implications of food production, consumption and waste. In 2005, Peter Menzel and Faith D'Aluisio presented a photographic study in "Hungry Planet – What the World Eats" documenting what thirty families across twenty-four countries ate during the course of one week. The weekly food purchasing inventories of three of these families have been combined with LCA data to report the greenhouse gas intensity of these food purchases. The greenhouse gas emission profile including those of 128 varieties of fresh food, along with data on packaging material production and household food waste, have been used in the calculations. The paper will present the findings illustrating the contribution each component has: food, packaging and food waste; and will also discuss the implications for food packaging design.

Keywords: food packaging design, food purchases, greenhouse gas, life cycle assessment, LCA, packaging.

## 1 Introduction

Packaging LCA's have historically been completed in isolation of the food stuff they aim to protect, however there is a need to broaden this understanding of the environmental impacts to include those associated with food production, and food waste. This is appropriate due to packaging's potential causal relationship to food waste. In 2001 using five food categories, Packforsk documented with the use of LCA, the contribution of energy to food production and consumption and the packaging materials. It was reported that packaging's contribution was less than 10% (Erlov et al., 2000). This was further supported by INCPEN in 2009 with the release of their publication *Table for One* that expanded upon food categories and documented the energy contribution across the whole supply chain. For an average European's weekly food consumption over 50% of the life cycle energy impacts are associated with farm operations, home storage and cooking contributing 31% and packaging 10% (INCPEN, 2009).

In recent years there has been significant activity to document and report food loss and waste through the global supply chain (Gunders, 2012, Gustavsson et al., 2011, Institution of Mechanical Engineers, 2013, Quested et al., 2013b, Lipinski et al., 2013). This has been estimated to be in the range of 1.3 billion tonnes globally (FAO, 2013). In developed nations the majority of the loss occurs between farm and sale due mainly to inadequate infrastructure and packaging (Kummu et al., 2012), while in developed nations the majority is at retail and consumption (Institution of Mechanical Engineers, 2013, Kummu et al., 2012) due to factors including excessive consumption.

Everyday across the world households consume and waste food that has crossed local neighbourhoods, states and countries as it moves from the farm or sea, through to processing and manufacturing, distribution, retail, purchase, storage, preparation and cooking and eventually into our stomachs, or partly disposed of into landfill, incinerators or compost. There are however, stark differences amongst households in what they purchase, how much they purchase, how the food is packaged, how much they cook and consume, and how much they waste. These differences were captured on film by Peter Menzel and Faith D'Aluisio in their 2005 photographic study

*Hungry Planet – What the World Eats* that documented what thirty families across twenty-four countries ate during the course of one week (Menzel and D'Aluisio, 2005). The images are powerful as they depict the abundance of food and beverages overflowing on tables of households in developed western countries compared with counterparts in developing countries where a sack of rice and a couple of other staples are all that can be purchased.

The aim of this paper is to explore the relational complexity and environmental impacts of diet, food waste and packaging. We are curious to find out what food, packaging and waste configurations contribute to a household's weekly greenhouse gas (GHG) profile. We propose to study three family's GHG profile from three different countries and discuss the implication of the findings for food packaging design.

In this paper we take the food and packaging inventory of three families from *Hungry Planet* – the Molloys from Australia, the Manzos from Italy and the Baintons from the United Kingdom, and combine these with LCA GHG emission profiles for the production of the food and packaging materials. These LCA values are combined with household food waste statistics to arrive at a profile illustrating the contribution of each component: food, packaging and food waste. The LCA waste treatment used in the model assumes similar landfilled treatment of food waste for each family; however, the transport and infrastructure impacts are calculated specifically for each country's energy grid. Considering the LCA results for each family, the paper then discusses the implications and directions for packaging designers to ameliorate the impacts via food packaging design, in accord with the intent of this conference.

# 2 Background

In this section we provide a background on the three main data sources: (i) LCA of food and packaging materials, (ii) household food waste statistics and (iii) the family food and packaging inventories.

## 2.1 LCA of food and packaging materials

GHG inventories for the production of dairy, fresh fruits, vegetables, nuts, grains, other starchy foods, meat, fish and eggs were estimated by coupling the mass and type of food to GHG profiles for the individual food types. The GHG profiles were adopted from data from Clune et al. (under review 2014), which are averages based on approximately 100 life cycle assessment studies. The system boundary of the studies underpinning Clune et al. varied, but always included farming operations. Inventories for beverages, condiments, prepared food, snacks and deserts were based on input-output modelling, which relate economic flows to environmental flows. The input-output databases were modified to exclude impacts from packaging. The Australian Input Output 2008-09 GHG (Grant, 2013a) and the EU & DK Input Output 2003 LCA databases were used. Prices were adjusted to the year of the original publication year by applying inflation factors, based on Australian (ABS, 2014) and European Union (EC, 2014) averages. Great British pound prices were converted to Euro prices based on historical exchange rate data from www.oanda.com. The impacts of packaging production was estimated by determining or approximating the mass and type of packaging used for each food item, and then coupling this data with existing life cycle inventories for packaging materials from ecoinvent 2.2 (Hischier, 2007, Hischier, 2004), PlasticsEurope (Boustead, 2005), and the Australasian Unit Process Life Cycle Inventory (AUPLCI, Grant, 2013b).

The end of life for all *wasted* food and beverages was assumed to be landfill. Degradation of food and paper/board waste in landfill was determined by calculating the dry mass from moisture contents for each flow. Moisture contents were from the United States Department of Agriculture's National Nutrient Database. The dry mass was then modelled using default values from IPCC waste landfill models (IPCC, 2006), which accounts for the generation of biogenic carbon dioxide and methane through anaerobic and aerobic degradation. The fate of landfill methane was based on region-specific rates for fugitive emissions, flaring and energy capture. No credits were applied for avoided electricity or heat generation, as these were assumed to be part of the next life cycle.

The end of life of packaging waste was split between landfill and recycling. Recycling rates for Italy and the United Kingdom were based on historical recycling rates (EC, 2014), while Australian recycling rates were linearly interpolated from 2003 and 2011 data (APC, 2011). Landfill and recycling models for packaging were adopted from AUPLCI (Grant, 2013b) with energy inputs modified to account for the different regions. Credits for avoided production stemming from recycling were excluded from the assessment. Inventories for the collection and transportation of waste (recycled and landfill) was adopted from AUPLCI (Grant, 2013b), with energy inputs modified to account for the different regions. Energy models for the United Kingdom and Italy were taken from ecoinvent 2.2 (Frischknecht et al., 2007).

Life cycle impact assessment (LCIA) was undertaken using global warming potentials from the IPCC Fourth Assessment report for a 100 year time horizon (IPCC, 2007). The global warming potential for biogenic methane was adjusted to account for carbon sequestered within methane. Carbon uptake and sequestration in soil were excluded from the assessment. GHG was selected as the focus of this paper, as this is the most common environmental impact category where consistent data is available across food types, packaging and end of life. Other environmental indicators, such as water use and eutrophication, can also be of importance, but available impact data on this is often inconsistent on impact assessment methodology.

## 2.2 Household food waste statistics

The number of studies regarding food waste has increased in recent years. They include studies that have been experimentally or statistically achieved (Sibrián et al., 2006, Lebersorger and Schneider, 2011, Knudsen, 2009, Hall et al., 2009, Monier et al., 2010), documenting the reasons for household food waste (Evans, 2011, Baker et al., 2009) or with both amounts and reasons (Koivupuro et al., 2012, Williams et al., 2012, Ventour, 2008). In industrialized countries more than 40% of the food waste occurs in retail and households (Gustavsson et al., 2011). Of this 40%, the per capita waste in North America and Oceania has been estimated at 115kg/a, compared with the per capita figures from sub-Saharan Africa and South/Southeast Asia at 6-11 kg/a. In the EU, the average household waste is 76 kg/capita/a, in Italy it is 46 kg/capita/a and in the UK 49 kg/capita/a (Monier et al., 2010). Australian households waste an estimated $239/capita/a worth of food (Baker et al., 2009). However methods on how to calculate and interpret food waste data between studies is still ambiguous (Lebersorger and Schneider, 2011).

There are various studies that have quantified food waste percentages and Figure 1 presents a graphical perspective of key food categories and their associated waste percentages (combining results from two studies). Vegetables, prepared food, dairy, fruit and berries and breads and grains are the key food categories that have the highest waste percentages.

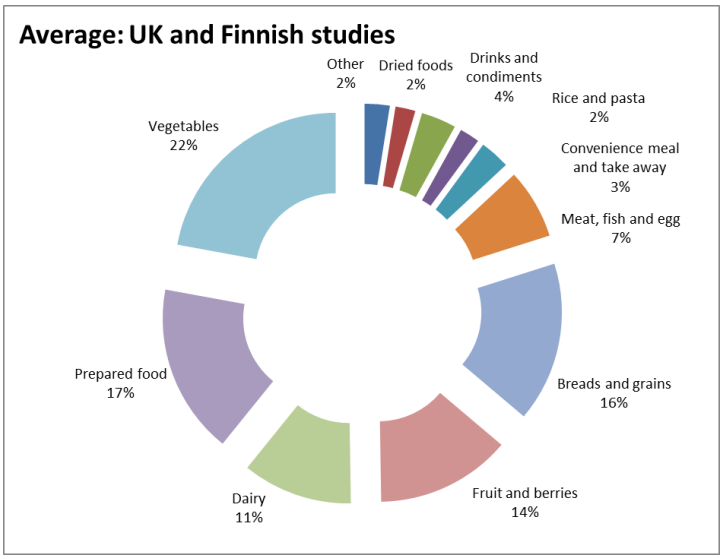



Figure 1 An example of what food categories are wasted (combining findings from the UK and Finland)

Notes: Study 1: 2138 UK households with collection and sorting of waste from waste bins +interviews with 2715 households. 70 kg/capita of avoidable food waste (Ventour, 2008). (Avoidable waste means food that at some point prior to disposal was edible; not peals and bones). Study 2: 380 Finish households filling in food waste diary with weighting and questionnaire, 23 kg/capita of avoidable food waste (Katajajuuri et al., 2012).

In this paper, food waste figures for Australia were aggregated from FAO figures (Gustavsson et al., 2011) and proxy data sourced from the UK's Waste Resource and Action Programme (WRAP) publications on *Household Food and Drink Waste* (Quested and Johnson, 2009, Quested et al., 2013a); for the UK it came in a disaggregated form (Quested and Johnson, 2009, Quested et al., 2013a), where given inputs for food waste data was on single products within a group of foods; while data for Italy was in an aggregated form on the summarized level presented in this study e.g one single data for meat, fish and egg (BCFN, 2012). Assumptions for food waste percentages for each food type and region are presented in Table 1.

Table 1: Regional food waste assumptions (%)

| Food type | Region | | |
|---|---|---|---|
| | Australia | United Kingdom | Italy |
| Grains and starchy foods | 27.8 | 17.7 | 10.7 |
| Dairy | 15 | 6.5 | 35.0 |
| Meat | 18.2 | 10.4 | 18.3 |
| Fruit and vegetables | 26.3 | 17.6 | 10.6 |
| Condiments | 13.3 (Proxy – UK data) | 13.3 | 13.3 (Proxy – UK data) |
| Snacks and deserts | 8.8 (Proxy – UK data) | 8.8 | 8.8 (Proxy – UK data) |
| Prepared foods | 22.7 (Proxy – UK data) | 22.7 | 22.7 (Proxy – UK data) |
| Beverages | 7.6 (Proxy – UK data) | 7.6 | 7.6 (Proxy – UK data) |
| Data sources: (BCFN, 2012, Gustavsson et al., 2011, Quested and Parry, 2011, Quested et al., 2013b) | | | |

Household's food practices and routines are many, separated in space and time and therefore complex (Quested et al., 2013b). The main reasons for wasting food include food left on plate or cooking too much, food that has passed its best before or use by dates or spoiled (Ventour, 2008). Household planning and shopping routines are important for the amount of food waste (Stefan et al., 2013). Households who shop more regularly for smaller amounts of food waste significantly less than households that shop once a week (Williams et al., 2012). Food safety issues are also important to households and uncertainty about date labels contribute to food waste (Cox and Downing, 2007, Evans, 2011, Broad Leib et al., 2013). In a Swedish study, packaging that was too large or difficult to empty contributed to 10% of the food waste (Williams et al., 2012). Studies also reveal a lack of knowledge about how to store food at home leading to incorrect or inappropriate food storage may cause the shelf-life of food to be reduced (WRAP, 2007, Plumb et al., 2013).

## 2.3 The families

The *Hungry Planet* (Menzel and D'Aluisio, 2005) families provide a rich and diverse inventory of food and packaging items from 24 countries. Inventory items in *Hungry Planet* are more detailed than the generic data that can be extrapolated from national databases such as the Household Expenditure (ABS, 2008) and National Nutrition Surveys, in that specific food types, brands and packaging amounts can be estimated.

Three families were selected and modelled for this paper from Australia, the United Kingdom and Italy. The composition of each household varied slightly. The Molloys from Australia were composed of three adults and a child, the Manzos from Italy two adults and three young children, while the Baintons from the United Kingdom had two adults and two teenagers. The selection of families for this paper was based on countries where sound consumer food waste data was available in a disaggregated form. The co-location of authors to the selected countries also enabled packaging to be weighed accurately. Recycling data from the selected countries was also readily available (Quested and Johnson, 2009, Quested et al., 2013a).

The food each family purchased when converted to US dollars was of a similar quantum (see Table 2). However the diet of each family had subtle differences. A detailed overview of the diet of each family is provided in Table 2. The key differences between the families are:

- The Bainton family (UK) consumed by far the largest amount of dairy products 21.0kg compared to 12.3kg in the Molloy household (AU) and 6.5kg in the Manzos (IT), as well as the highest amount of beverages (15L).
- The Bainton family (UK) consumed the least amount of fruit and vegetables. 12.1kg of fruit and vegetables in comparison to 17.0-17.3kg for the Molloy's and Manzos respectively.
- The Molloy household (AU) had the highest amount of meat consumed at 8.9kg, the Manzo household 3.6kg, and the Bainton household 3.4kg. The percentage of ruminant meat (beef and lamb) consumed in the Molloy household was also higher.
- The Molloy household also purchased the least amount of snacks and desserts by weight (2.4kg in comparison to 5.2-5.4kg for the Manzos and Bainton households).

Table 2: The weekly food inventories of the Australian (Molloy), United Kingdom (Bainton) and Italian (Manzo) households

| THE MOLLOYS (Australia) | THE BAINTONS (Great Britain) | THE MANZO (Italy) |
|---|---|---|
| **Grains and Other Starchy Foods** | | |
| White russet variety potatoes; white bread; sliced, 2 loaves; bread rolls, 10; *Dick Smith Bush* foods breakfast cereal; *San Remo* spaghetti*; San Remo* penne; white rice; sweet chili twist (savory bread). | White potatoes; *Kingsmill Gold* soft white bread, slices, 2 loaves; *Hovis* crusty white bread; *Weetabix* whole-grain cereal; new (young) potatoes; *McDougall's* self-raising flour; *Saxby* puff pastry; *Seeds of Change* tagliatelle; *Waitrose* porridge oats; *Kellogg's* Coco Pops; *Waitrose* corn flakes; *Waitrose* garlic baguette, organic; *Jacob's* TUC crackers | *Poiatti* spaghetti, rotini, orzo, margherite, macaroni; bread; bread crumbs; white potatoes; *Kellogg's* Frosties Chocos cereal; *Mulino Bianco* fette biscottate, 1 loaf; *Mulino Bianco* white bread, sliced, 1 loaf; white flour |
| **Dairy** | | |
| *Pura* Light Start milk, *Pauls* milk, whole, cheese, *Pauls* Greek yoghurt, natural set, *Pauls* thickened cream, *Woolworths* sour cream, butter<br><br>*Dairy purchased = 21.0kg* | Semi-skim milk; full cream milk (whole); *Waitrose* strawberry yoghurt; *Muller Corner* strawberry yoghurt; *Waitrose* custard mild English cheddar; *Philadelphia* cream cheese; *Waitrose* rhubarb yoghurt; *Waitrose* toffee yoghurt; *Country Life* butter; *Cropwell Bishop* cheese: *Dairy purchased = 12.3kg* | *Granarolo* whole milk; *Da Cucina* cooking cream; *Galbi* yoghurts; *Grandi Pascoli* butter; parmesan cheese, grated<br><br>*Dairy purchased = 6.5kg* |
| **Meat, Fish and Eggs** | | |
| Chicken, whole; tuna, canned; *Woolworths* beef; *Woolworths* chicken breast; *Woolworths* lamb; sea perch; *Woolworths* pork; eggs; ham; salami: *Meat, Fish and Eggs purchased = 8.9kg* | *Waitrose* British pork; *Waitrose* eggs (12); *Waitrose* pork escalopes; *Waitrose* tuna, canned in brine; honey roasted ham; *Waitrose* unsmoked British bacon; *Waitrose* large prawns, frozen: *Meat, Fish and Eggs purchased = 3.6kg* | Fish sticks, frozen; sometimes a fresh fish; eggs (12); beef, ground; sausage; veal *involtini* (meat rolls); clams; tuna; wurstel (German hot dog); ham and cheese, sliced; anchovies: *Meat, Fish and Eggs purchased = 3.4kg* |
| **Fruits, Vegetables and Nuts** | | |
| Watermelon, seedless; *Sundowner* variety apples; oranges; yellow bananas; plums; green grapes; lemons; nectarines; *Heinz* baked beans; avocados; *Iceberg* lettuce, 2 heads; cucumbers; *Val Verde* peeled tomatoes, canned; tomatoes; white onions; carrots; sweet corn, 4 ears; asparagus; Silverbeet; celery; *Master Foods* tomato sauce; mushrooms; broccoli; beetroot, canned; Italian flat beans; tomato paste; snow peas; red bell peppers; garlic | *Coxes* variety apples; *Braeburn* variety apples; yellow bananas; oranges; *Granny Smith* variety apples; green grapes, seedless; *Del Monte* pineapple chunks, canned; *Heinz* baked beans, canned; *Waitrose* Brussel sprouts, fresh; *Birds Eye* garden peas, frozen; white cabbage, organic, 1 head; white mushrooms; cauliflower, 1 head; carrots; parsnips; iceberg lettuce, 1 head; tomatoes; broccoli; cucumber; red onion; runner beans; mange tout peas (snow peas); sugar snap peas | Red grapes; yellow bananas; lemons; pears; persimmons; *Vitale* crushed tomatoes, canned; *Star* tomato sauce, bottled; broccoflower (hybrid of broccoli and cauliflower), 1 head; chard; peas, frozen; tomatoes; *Comal* olives; corn, canned; garlic |
| **Prepared Food** | | |
| *Heinz* spaghetti, canned; beef Stroganoff mix | *New Covent Garden Food Co* vegetable and lentil soup; *Waitrose* five cheese and pepperoni pizza; *Loyd Grossman* four cheese pasta sauce; *Heinz* cream of tomato soup, canned; *Waitrose* cheese and onion flan; *Waitrose* chicken and mushroom flan; *Dairylea* ham Lunchables; *Bisto* granules gravy mix, roast vegetable flavoured; *Waitrose* carbonara sauce | *Star* Gran ragù sauce; *Star* vegetable bouillon cubes; school lunch, lasagne or pasta and juice, 6 days for two children |

Table 2 continued

| THE MOLLOYS (Australia) | THE BAINTONS (Great Britain) | THE MANZO (Italy) |
|---|---|---|
| **Condiments** | | |
| Coconut milk; peanut butter; *Kikkoman* less salt soy sauce; *Lea & Perrins Worcestershire* sauce; *Master Foods* BBQ sauce; *Nutella* chocolate spread; *Master Foods* seeded mustard sauce; *Viva* olive oil; red chili peppers; basil; ginger; *Capilano* honey; parsley, 1 small bunch; balsamic vinegar; coriander (cilantro), 1 small brunch; *Master Foods* horseradish; jam; Mayonnaise; *Master Foods* tomato and chili pickle (salsa); mint, 1 small bunch; oregano; *Tonkatsu* sauce; *Vegemite*; cumin; mustard seeds; rosemary, 4 sprigs; turmeric; black pepper; curry leaves (20); salt; thyme, 1 small bunch;Bay leaves (5) | *I Can't Believe It's Not Butter* spread; *Heinz* ketchup; *Hartley's Best* raspberry jam; *Heinz* salad cream; *Hellmann's Real* mayonnaise; *Waitrose* smooth peanut butter, organic; *Waitrose* blend olive oil; *Tate Lyle* white sugar; *Waitrose* dark-brown muscovado sugar; waldorf salad topping; paprika; black pepper; *Maldon* sea salt; *Saxa* table salt; basil, 1 bunch; parsley, 1 bunch; *Sweetex sweetener*, 80 tablets (they are very small) | *Tevere* vegetable oil; olive oil; white wine, used only for cooking; *Bonanno* white vinegar; mayonnaise; cherry jam; pine nuts and raisins; Italia white sugar; salt; tomato paste, 1 tube; bicarbonate of soda (baking soda); pepper |
| **Snacks and Desserts** | | |
| Ice blocks (popsicles), 24 pk; sultana raisins; *Cadbury* Milk chocolate bar; *Uncle Tobys* strawberry muesli bars; *Uncle Tobys* fruit twists; *SAKATA* crackers; *Arnott's* shortbread cream biscuits; *Smith's* chicken flavoured potato crisps | *McCain* oven chips, frozen; *Mars* candy bars, multipacks; *Waitrose* savory wedges, frozen; *Waitrose* milk chocolate digestive biscuits; *Waitrose* treacle tart; *Cadbury* twirls; *Trebor* softmints; *Haribo* Maoam Stripes; *Waitrose* rich tea biscuits; *Golden Wonder* Nik Naks; *Walker's* BBQ crisps; *Walker's* prawn cocktail crisps; *Waitrose* caramel surprise; *Waitrose* chocolate surprise; *Onken* chocolate hazelnut mousse; strawberry laces; *Waitrose* mini jelly babies; *Dairylea* Double Dunker nachos; Flying Saucers candy | *Kinder* milk chocolate; biscotti; *Nutella* chocolate spread; *Kinder* paradiso chocolate; *Buondí* (packaged cream cakes); baby biscuits; *Kinder* Brioss (packaged cream cakes); *Mulino Bianco* flauti (packaged cream cakes with chocolate); *Pavesini* biscuits; candies, assorted |
| **Homemade food** | | |
| | Savoury pancakes, made with flour, milk and eggs, listed above | |
| **Beverages** | | |
| Water; fruit juice; red wine, 3 bottles (each); *Just* juice poppers (juice boxes); *Mateus* rose wine; *Cascade* light beer, 6 bottles (each); *Nescafe* gold blend coffee; *Nestle* milo (instant chocolate drink); *Twinings* of London English breakfast tea, 10 teabags | *Capri Sun* fruit juice, 12 6.8 fl oz pkg; *Somerfield Pennine Valley* Water; *Wadworth* beer, 12 16.9 fl oz cans; *Waitrose* pineapple juice; *Waitrose* press apple juice; *Waitrose* pure orange juice; *Tesco* mountain spring water; *Cadbury* drinking chocolate; *James Herrick* red wine; *Douwe Egberts Continental Gold* Coffee; *PG Tips* tea, 40 teabags; tap water, for drinking and cooking | *Pepsi*, 2 bottles (each); ginger soda; peach juice, 12 mini bottles (each); *San Benedetto* iced tea; *Spuma* (light cola drink); *Top* cola; *Espresso Bar* coffee; tap water for drinking and cooking |

Table 2 continued

| THE MOLLOYS (Australia) | THE BAINTONS (Great Britain) | THE MANZO (Italy) |
|---|---|---|
| **Total weight of food purchased** | | |
| 40.6 kg solid food<br>25.3 kg liquid (milk and beverages) | 38.6 kg solid food<br>33.2 kg liquid (milk and beverages) | 50.42 kg solid food<br>12.92 kg liquid (milk and beverages) |
| **Food expenditure for one week (excluding medicines, tobacco and pet food)** | | |
| AU$387.73, equivalent to US$303.37 | £138.59, equivalent to €208.62/ US$225.55 | €164.44, equivalent to US$199.44 |
| Notes: Family food purchases were captured during the period of 2001-2004, and subsequently published in 2005. Input output modelling for the United Kingdom was based on Euro prices | | |
| Source: (Menzel and D'Aluisio, 2005) | | |

# 3 Results

The central focus of this paper is on the relationship between purchased food type, packaging and food waste. The GHG profile related to food purchases of each household is not the focus of comparison. The differing number of family members renders that comparison inconsistent; however for completeness the total GHG profile for the weekly food purchases was 158.9 kg $CO_{2\text{-eq}}$ for the Molloy household, 169.0 kg $CO_{2\text{-eq}}$ for the Manzo household and 178.1 kg $CO_{2\text{-eq}}$ for the Bainton household. The remainder of the results are presented as broken down percentages of the above result, to show the relationship between food types, packaging and food waste.

## 3.1 Consumed food

The GHG profile of the consumed food, as a percentage of the total amount of food purchased in one week, for each food category for the Molloy, Bainton and Manzo families over one week is presented in Figure 2.

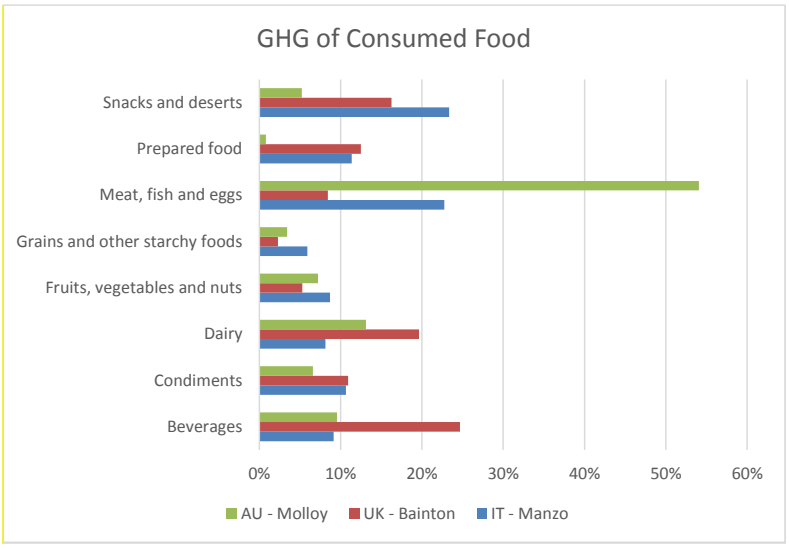



**Figure 2:** The greenhouse profile, as a percentage, of the Australian (Molloys), United Kingdom (Bainton), and Italian (Manzo) households

The GHG results illustrate distinct differences amongst the three households, for example the higher meat, fish and eggs consumption of the Molloy household; high dairy and beverages in the Bainton household; and high snacks and desserts in the Manzo household. The results track the variation of products highlighted in the previous section, and presented in Table 2.

The majority of the GHG profile of the weekly purchased food, food waste and packaging for the Molloy household is associated with the embedded GHG of the purchased food and beverages (73%). This is followed by 15% associated with the wasted food component, while packaging materials contributed 10%.

The following sections will present values for the Molloy (Australian) household for the four top food categories, based upon the GHG profile for the consumed food: meat, fish and eggs; dairy; beverages; and fruits, vegetables and nuts.

## 3.2 Meat, fish and eggs (Molloy – Australian household)

The GHG profile of the meat, fish and egg category for the Molloy (Australian) household is presented in Figure 3 where the majority is associated with the embedded GHG of the meat, fish and eggs (80%), followed by 18% or 14 kg $CO_{2\text{-eq}}$ associated with the wasted food component, while packaging materials only contribute 2%.

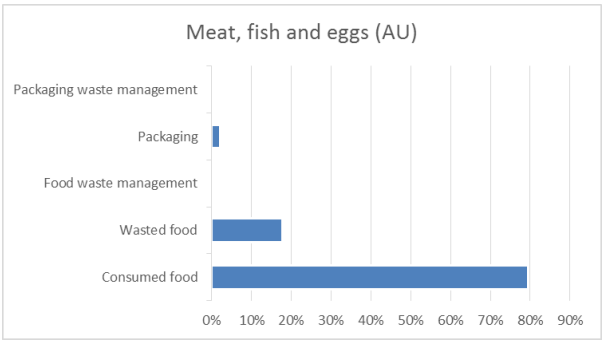



**Figure 3:** The greenhouse profile for meat, fish and eggs for the Molloys – Australian household

## 3.3 Dairy (Molloy – Australian household)

The GHG profile of the dairy category for the Molloy (Australian) household is presented in Figure 4, where the majority is associated with the embedded GHG of the dairy products (75%), followed by 13%, or 2.6 kg $CO_{2\text{-eq}}$ associated with the wasted food component, while packaging materials contribute 10%.

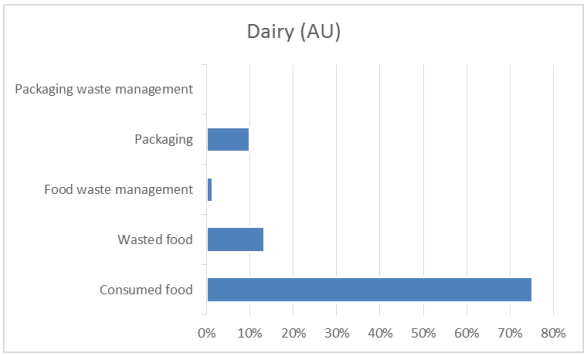



**Figure 4:** The greenhouse profile for dairy for the Molloys – Australian household

## 3.4 Beverages (Molloy – Australian household)

The GHG profile of the beverages category for the Molloy (Australian) household is presented in Figure 5, where majority is associated with the embedded GHG of the beverages (56%), followed by 38% associated with the packaging materials (dominated by glass) and the wasted beverage component only contributes 5% or 1 kg $CO_{2\text{-eq}}$.

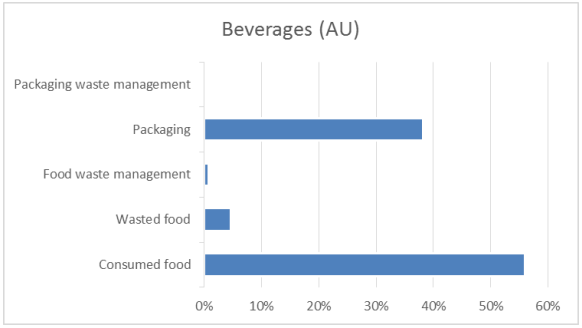



**Figure 5:** The greenhouse profile for beverages for the Molloys – Australian household

## 3.5 Fruit, vegetables and nuts (Molloy – Australian household)

The GHG profile of the fruit, vegetables and nuts category for the Molloy (Australian) household is presented in

Figure **6**, where the majority is associated with the embedded GHG of the fruits, vegetables and nuts (62%), followed by 22% associated with the wasted food component, while packaging materials only contribute 12%.

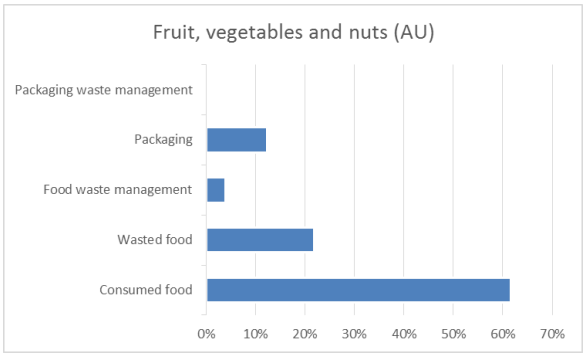



**Figure 6:** The greenhouse profile for fruit, vegetables and nuts for the Molloys – Australian household

# 4 Discussion

In this section we discuss the results in relation to the role of packaging design for efficient food containment and protection while minimizing food waste.

## 4.1 Food waste

The Love Food Hate Waste fact sheet provided by the New South Wales (NSW) Environment Protection Authority in Australia (DECCW, 2009, p.2) highlights a number of broad reasons why food is wasted by households (percentages refer to the proportion of respondents who indicated each cause): (i) Buying: I think I need more than I do (61%) and I'm tempted by special offers (44%); (ii) Cooking: I prefer to serve too much rather than too little (48%) and I find it hard to estimate how much to cook per person (32%); and (iii) Storing: I'm unsure about the best way to store different types of food (60%) and I forget about leftovers (63%)

Within the causes of waste identified above, the perishable food groups of meat, fish, eggs, dairy, fruit and vegetables, food waste contributes between 13-22% of weekly greenhouse gas impacts. The climate impact of wasted meat, fish and eggs are higher than the impact of all purchased fruit and vegetables.

Helping consumers buy and cook the correct amount of food by designing and selling a larger diversity of packaging sizes at retail is one possible development in tackling food waste. Other packaging attributes that need to be considered include: containing the desired quantity; mechanical protection; resealability; accessibility including easy to open, grip, dosing and emptying; containing the correct quantity; food safety/freshness information and facilitating sorting of household waste (Wikstrom et al., 2014). Smarter packaging with better atmospheres and coatings aimed at elongating shelf life may also assist to reduce this food waste (Verghese et al., 2013).

The UK has made a broad, considered effort to reduce food waste, from industry through to consumers. For packaging designers, the WRAP packaging design and food waste checklist suggests resealable/ recloseable packaging, portion packaging, shelf life extension packaging and better on-pack consumer communication as a means to address food waste (WRAP, 2009). They have also implemented initiatives between packaging designers and retailers, for example "WRAP, The Co-operative and VionFoods (UK), Giraffe Innovation Ltd who investigated the opportunity to reduce meat waste through a packaging solution" (Holdway, 2011, p.1). The partnership resulted in packaging that separated individual portions to facilitate freezing. WRAP has indicated that since the launch of the program, food waste within the UK has declined (Quested et al., 2013b), however it is not possible to establish efficacy of each program initiative to this decline.

## 4.2 Packaging design

These reasons for food waste listed in Section 4.1, provide insights where packaging design can contribute to overcoming food waste. Opportunities for packaging design to reduce or eliminate food waste can include better facilitation or communication around portioning, special offers that link to appropriate food requirements rather than bulk sales, assistance in per person cooking requirements, expiry date/ best before extension or better clarification, and left over storage solutions.

Moreover, focusing packaging designs on waste reduction for areas of particularly high food category waste impacts can also be a strategy of climate impact reduction. In the case of the Molloys, solutions to reduce the waste for either high climate impact foods per kg (and subsequently relatively high total waste impacts for

related food waste) such as wasted meat, fish and eggs, or high climate impact foods for total waste (not necessarily high climate impact foods per kg, however relatively high climate impact when accumulated waste is considered for related food waste) such as fruit and vegetables, could start to address the impacts of food waste.

The relationship between packaging, product and waste impacts should also be part of any strategy to reduce waste impacts of product-packaging systems. As an example of a particular food category for the Molloys, the beverage category results reveal that packaging has more than 7 times higher climate impact than of food waste. This indicates a challenge for industry when these products with low environmental impacts are to be packed. For this specific Australian family the impact from beverage packaging has half the climate impact from wasting meat, fish and eggs, the drivers of food waste impacts. The high impact is driven by the use of glass packaging for that particular beverage (based upon the photographic image from Hungry Planet), though this needs to be put into context and also compared against the other packaging attributes this type of packaging material delivers in the containment and protection of the product to the consumer. Packaging material selection and design needs to focus upon appropriate material use, not just light weighting, whereby the right combination of the amount of and appropriate choice of material is used, ensuring packaging integrity and stability through the supply chain – that it is 'fit-for-purpose'.

The variations evident across the food categories in Section 3 illustrates that the contribution of product and packaging are always different and that the relationship between packaging and product impacts is not a one size fits all approach. Detailed investigations within food categories and packaging formats is required to understand the implications for various combinations of product and packaging, linked to consumer preferences and use. This research, along with attention to packaging attributes listed above in Section 4.1 will ensure that each product-packaging system is designed to minimise food waste and packaging impacts, while catering for consumer preferences, and the requirement to protect and preserve products in the process.

### 4.3 Data assumptions

Food waste figures for the UK were calculated using data from the UK's WRAP publications on Household Food and Drink Waste (Quested and Johnson, 2009, Quested et al., 2013a). Waste percentages from 2012 were used where possible, with more comprehensive data from 2007 being utilised to complete the waste estimates.

There are some differences in how aggregated data was used for food waste among the three countries. Packaging data was compiled with estimates and direct measurement of packaging formats and combined with existing LCA data. This data aggregation derived from observations of the *Hungry Planet* family photos and food purchasing lists. Packaging recycling data is derived from information governments collect for different materials which is often transparent and coherent.

It is important to remember that the data used in this study are estimates of three families in three different regions, and that it does not apply to the broader population. Also we have taken food waste figures and assumed these were directly applicable for the three families, while this may not have been the case. The research is aimed at understanding the difference between environmental impacts of food type, packaging and food waste in particular case contexts, rather than a generalizable set of results. This is made in order to inform the direction of further research that may indeed start to broaden the scope of this new knowledge to a constituent, national or global level.

## 5 Conclusions

Brandowners and packaging manufacturers have a critical role to play in reducing food waste and thus the GHG emission profile of consumers such as the three families from *Hungry Planet* explored in this paper. Although these three families had similar absolute GHG emissions from their weekly food shop, differences amongst food GHG emission impact, packaging and food waste are clear from the results generated. Data are complex and no single rule for waste reduction can be used in all types of food categories. However, it is important to minimise waste from food items with high GHG emission impacts, or from food items that may have lower GHG emission intensity per kg yet are wasted in high amounts leading to a large absolute GHG emissions.

Packaging designs can help to facilitate this saving of resources. Further research is required to understand the role packaging may play from a functional perspective. This could involve ethnographic and action research tracking the uptake or success of designed packaging instruments aligned to the themes in the discussion section of this paper. The current paper could also be expanded upon to investigate the trends and differences across all three families in regards to similarities and differences between packaging and food waste contributions to GHG emissions for all food item categories. An assessment on a larger population could inform more comprehensively packaging design in relation to reducing waste for particular food types. Primarily, this interaction between packaging and product in saving food, and where the sweet spot lies in this phenomenon at a food item level,

provides researchers with an opportunity to articulate how packaging design can contribute to a more sustainable supply chain.

## References


ABS 2008. 6535.0.55.001 - Household Expenditure Survey, Australia: Detailed Expenditure Items, 2003-04 (Reissue). Canberra: Australian Bureu of Statistics.

ABS 2014. 6401.0 - Consumer Price Index, Australia. Australian Bureau of Statistics.

APC 2011. The National Packaging Covenant: 2010 Annual Report. Australian Packaging Covenant Council.

BAKER, D., FEAR, J. & DENNISS, R. 2009. What a Waste. An Analysis of Household Expenditure on Food. Banbury UK: The Australian Institute.

BCFN 2012. Food waste: causes, impacts and proposals. Barilla Food Center for Food & Nutrition.

BOUSTEAD, I. 2005. Eco-profiles of the European Plastics Industry. Brussels: PlasticsEurope.

BROAD LEIB, E., GUNDERS, D., FERRO, J., NIELSEN, A., NOSEK, G. & QU, J. 2013. The Dating Game: How Confusing Food Date Labels Lead to Food Waste in America. New York: Natural Resources Defense Council.

CLUNE, S., CROSSIN, E. & VERGHESE, K. under review 2014. Analysis of greenhouse gas emissions for different fresh food categories: a review. *Journal of Cleaner Production*.

COX, J. & DOWNING, P. 2007. Food Behaviour Consumer Research: Quantitative Phase. Banbury UK: Waste & Resources Action Programme.

DECCW. 2009. *Food Waste Avoidance Benchmark Study 2009* [Online]. Sydney: Department of Environment, Climate Change and Water NSW. Available: http://www.lovefoodhatewaste.nsw.gov.au/portals/0/kit/print/10242FWAFactsheetCMYK_print.pdf [Accessed 12/10/2010 2010].

EC. 2014. *eurostat: http://ec.europa.eu/eurostat* [Online]. Brussels: European Commission. [Accessed 23/04/2014.

ERLOV, L., LOFGREN, C. & SORAS, A. 2000. PACKAGING - a tool for the prevention of environmental impact. Kista, Sweden: Packforsk.

EVANS, D. 2011. Beyond the Throwaway Society: Ordinary Domestic Practice and a Sociological Approach to Household Food Waste. *Sociology*, 46**,** 1841-56.

FAO 2013. Food wastage footprint. Impacts on natural resources. Summary Report. Rome: Food and Agriculture Organisation of the United Nations.

FRISCHKNECHT, R., TUCHSCHMID, N., FAIST EMMENEER, M., BAUER, C. & DONES, R. 2007. Strommix und Stromnetz. In: Sachbilanzen von Energisystemen: Grundlagen fuer die oekolischen Vergleich von Energiesystemen und den Einbezug von Energiesystemen in Oeobilanzen fuer die Schweiz (ed. Dines, R.). ecoinvent report No. 6 v2.0. Villigen and Duebendorf: Paul Scherrer Institut and Swiss Life Cycle Centre for Life Cycle Inventories.

GRANT, T. 2013a. Australian Input Output 2008-09 GHG database. Published by Life Cycle Strategies Pty Ltd, Melbourne.

GRANT, T. 2013b. Australasian Unit Process Life Cycle Inventory. Published by Life Cycle Strategies Pty Ltd, Melbourne.

GUNDERS, D. 2012. Wasted: How America is Losing up to 40 Percent of its Food from Farm to Fork to Landfill. New York: Natural Resources Defense Council.

GUSTAVSSON, J., CEDERBERG, C. & SONESSON, U. 2011. Global food losses and food waste: extent, causes and prevention. Rome: Swedish Institute for Food and Biotechnology for the Food and Agriculture Organization of the United Nations.

HALL, K. D., GUO, J., DORE, M. & CHOW, C. C. 2009. The pro- gressive increase of food waste in America and its environmental impact. PLoS ONE 4.

HISCHIER, R. 2004. Life Cycle Inventories of Packagings and Graphical Papers. ecoinvent-Report No. 11. Part III Paper and Board. Dübendorf: Swiss Centre for Life Cycle Inventories.

HISCHIER, R. 2007. Life Cycle Inventories of Packaging and Graphical Papers. ecoinvent-Report No. 11. Part II, Plastics. Duebendorf: Swiss Centre for Life Cycle Inventories.

HOLDWAY, R. 2011. Final report: Packaging design to reduce household meat waste. Oxon: WRAP and Giraffe Innovation.

INCPEN 2009. Table for one. Reading: The Industry Council for Packaging and the Environment.

INSTITUTION OF MECHANICAL ENGINEERS 2013. Global food waste not want not. London.

IPCC 2006. 2006 IPCC Guidelines for National Greenhouse Gas Inventories. Volume 5. Waste. *In:* EGGLESTON, S., BUENDIA, L., MIWA, K., NGARA, T. & TANABE, K. (eds.). Kanagawa: Intergovernmental Panel on Climate Change.

IPCC 2007. *Climate Change 2007: The Physical Science Basis*, Cambridge, Cambridge University Press.

KATAJAJUURI, J. M., SILVENNOINEN, K. H., HARTIKAINEN, H., JALKANEN, L., KOIVUPURO, H. K. & REINIKAINEN, A. Food waste in the food chain and related climate change impacts. LCA Food, 2012 St Malo

KNUDSEN, M. L. C. 2009. In Danish: Affaldsforebyggelse i husholdninger - muligheder og barrierer for Danmark. Roskilde University: Roskilde University.

KOIVUPURO, H. K., HARTIKAINEN, H., SILVENNOINEN, K., KATAJAJUURI, J.-M., HEIKINTALO, N., REINIKAINEN, A. & JALKANEN, L. 2012. Influence of socio-demographical, behavioural and attitudinal factors on the amount of avoidable food waste generated in Finnish households. *International Journal of Consumer Studies,* 36**,** 183-191.

KUMMU, M., DE MOEL, H., PORKKA, M., SIEBERT, S., VARIS, O. & WARD, P. 2012. Lost food, wasted resources: Global food supply chain losses and their impact on freshwater, cropland and fertiliser use. *Science of the Total Environment,* 438**,** 477-489.

LEBERSORGER, S. & SCHNEIDER, F. 2011. Discussion on the methodology for determining food waste in household waste composition studies. *Waste management* 31**,** 1924-33.

LIPINSKI, B., HANSON, C., LOMAX, J., KITINOJA, L., WAITE, R. & SEARCHINGER, T. 2013. Reducing Food Loss and Waste. Working Paper, Installment 2 of Creating a Sustainable Food Future. Washington DC: World Resources Institute.

MENZEL, P. & D'ALUISIO, F. 2005. *Hungry planet - what the world eats,* New York, Random House Inc.

MONIER, V., MUDGAL, S., ESCALON, V., O'CONNOR, C., ANDERSON, G., MONTOUX, H., REISINGER, H., DOLLEY, P., OGILVIE, S. & GARETH MORTON, G. 2010. Preparatory study on food waste across the EU 27. Final report. *In:* C-INDUSTRY, D. (ed.). European Commission (DG ENV).

PLUMB, A., DOWNING, P. & PARRY, A. 2013. Consumer Attitudes to Food Waste and Food Packaging.

QUESTED, T., INGLE, R. & PARRY, A. 2013a. Final Report Household Food and Drink Waste in the United Kingdom 2012. Oxon: Waste & Resources Action Programme.

QUESTED, T. & JOHNSON, H. 2009. Household Food and Drink Waste in the UK. *Final Report.* Oxon: Waste & Resources Action Programme.

QUESTED, T. & PARRY, A. D. 2011. New estimates for household food and drink waste in the UK : A report presenting updated estimates of food and drink waste from UK. Oxon: Waste & Resources Action Programme.

QUESTED, T. E., MARSH, E., STUNELL, D. & PARRY, A. D. 2013b. Spaghetti soup: The complex world of food waste behaviours. *Resources, Conservation and Recycling,* 79**,** 43-51.

SIBRIÁN, R., KOMOROWSKA, J. & MERNIES, J. 2006. Estimating household and institutional food wastage and losses in the context of measuring food deprivation and food excess in the total population. *Working Paper Series.* Rome, Italy: Statistics Division.

STEFAN, V., VAN HERPEN, E., TUDORAN, A. A. & LÄHTEENMÄKI, L. 2013. Avoiding food waste by Romanian consumers: The importance of planning and shopping routines. *Food Quality and Preference,* 28**,** 375-381.

VENTOUR, L. 2008. *The Food We Waste,* Banbury UK, WRAP.

VERGHESE, K., LEWIS, H., LOCKREY, S. & WILLIAMS, H. 2013. The role of packaging in minimsing food waste in the supply chain of the future. Sydney: CHEP Australia and RMIT University.

WIKSTROM, F., WILLIAMS, H., VERGHESE, K. & CLUNE, S. 2014. The influence of packaging attributes on consumer behaviour in food-packaging LCA studies - a neglected topic. *Journal of Cleaner Production.*

WILLIAMS, H., WIKSTRÖM, F., OTTERBRING, T., LÖFGREN, M. & GUSTAFSSON, A. 2012. Reasons for household food waste with special attention to packaging. *Journal of Cleaner Production,* 24**,** 141-148.

WRAP 2007. Food Storage and Packaging. Retail Programme-Food Waste: Final Report. Banbury UK: Waste & Resources Action Programme.

WRAP 2009. Packaging design & food waste checklist. Oxon: Waste & Resources Action Programme.

# Film performance of Poly(lactic acid) blends for packaging applications

**Carlos A. Diaz[1*], Hsun Yi Pao[2], Sungyoung Kim[2]**

[1] *Department of Packaging Science, Rochester Institute of Technology, USA*
[2] *College of Applied Science & Technology, Rochester Institute of Technology, USA*

[*] *Corresponding author. Email: cdamet@rit.edu*

**Abstract:** Poly(lactic acid) (PLA), a biodegradable thermoplastic derived from renewable resources, stands out as a substitute to petroleum-based plastics. PLA based films for food packaging has been an area of both industrial and research interest within the context of sustainability. In spite of its excellent properties, packaging applications have been limited because PLA is more brittle than traditional oil-based plastics. Because of this, films display low tear and impact resistance and produce a loud crackling sound when manipulated. Although many studies address the toughening of PLA in the bulk, little attention has been placed on the film performance. The present study is aimed at providing a survey of binary PLA based blends with other biodegradable and non-biodegradable plastics. Acrylic impact modifier (AIM, 5 wt. %), ethylene vinyl acetate (EVA, 20 wt.%), Polyhydroxyalkanoate (PHA, 10 wt.%) and polycaprolactone (PCL, 30 wt.%) were each blended with PLA through single-screw extrusion and converted into films via the blown-film process. Tear resistance, impact resistance, heat seal strength, and noise level were measured. AIM improved the heat seal strength (2x) and impact resistance (2.5x), but reduced the tear resistance. When blended with another resin, the tear resistance improved regardless of the resin used, with EVA having the highest effect (>2x). This may be due to the dispersed phase in the blend which provided resistance to the crack propagation. PHA showed a marked effect in increasing the heat seal strength followed by AIM. Conversely, EVA did not show a significant effect in increasing heat seal strength. All blends showed a modest increase in impact resistance with AIM having the highest effect (i.e. 2.4x improvement). Significant noise reduction was achieved in films containing EVA and PCL. These results will be used to select blend systems for the further study of specific properties.

## 1 Introduction

The past decade has witnessed a steady growth for the market of bio-based and biodegradable resins [1], [2]. Plastics are being approached in a more responsible and holistic way, taking into account the sources from which they are derived as well as the ultimate fate of the materials. As the technology evolves, suppliers are able to tailor the polymer to specific applications by controlling the molecular weight and molecular architecture. As a result, new and improved grades of bioplastics resins are continuously being introduced in the market.

Polylactic acid (PLA) is at the forefront of commercially available bioplastics. PLA is derived from renewable resources and biodegradable. PLA based films for food packaging has been an area of both industrial and research interest within the context of sustainability [3]. In spite of its excellent properties, packaging applications have been limited because PLA's brittle behavior. Because of this, films display low tear and impact resistance, low elongation, and produce a loud crackling sound when manipulated.

Different approaches have been proposed to overcome the brittleness of PLA including copolymerization, plasticization and blending with other polymers [4]. Copolymerization is not economically viable unless produced in a large industrial scale. Plasticization requires large amounts of plasticizers to achieve flexibility and has leaching issues after the material is manufactured [5]. On the other hand, blending with other polymers is a convenient way to modify the properties. Polyhydroxybutyrate (PHB) [6], Popycaprolactone [7], poly(ethylene-co-vinyl acetate) (EVA) [8], have been blended with PLA to improve toughness. Ma and coworkers found that the compatibility between PLA and EVA could be adjusted by varying the vinyl acetate (VA) content on EVA. Copolymers with 50 wt.% VA content showed the highest improvement in elongation at break, over 300% compared with <10% for pure PLA [8].

Although some studies have addressed the toughening of PLA through blending, the sample manufacturing and characterization has focused on thick samples such as dog-bone shape and thick bars for flexural and impact test. Little attention has been placed on the film performance. The present study is aimed at providing a survey of binary PLA based blends with other biodegradable and non-biodegradable plastics with the ultimate goal of identifying blend systems with the potential for property improvement targeting specific applications. The

material selection focused on newer resins with high molecular weight intended for thermoplastic applications. The manufactured films were evaluated in terms of tensile properties, tear resistance, heat seal strength and impact resistance. Additionally, noise level was recorded and analyzed. Future studies will include modelling and optimization of specific blend systems.

# 2 Experimental

## 2.1 Materials

Table 1 lists the materials used in this study as well as the blend compositions. Polylactic acid, Ingeo 4043 D, was purchased from Natureworks, LLC. Acrylic impact modifier (AIM), Paraloid BPM 515, was obtained from DOW Chemical Company. Ethylene-vinyl acetate copolymer, Levamelt 500, was supplied by Lanxess. The copolymer contains 50 wt % vinyl acetate. Polyhydroxyalkanoate, M-vera B5008, was supplied by Metabolix. Polycaprolactone (PCL), CAPA FB 100, was kindly supplied by Perstorp. CAPA FB 100 has a slightly crossed-linked structure with a molecular weight of 100,000 Daltons. Blend compositions were selected based on a literature review and suppliers recommendations for the case of AIM.

**Table 1:** Blend formulations information. MFI measured at 210°C and 2.16 kg

| Blends | MFI (g/10min) | Ratio by mass | Additive Full Name | Supplier's name |
|---|---|---|---|---|
| PLA | 5.2 | 100:00 | | Natureworks 4043D |
| PLA/AIM | 6.1 | 95:05 | Acrylic Impact Modifier | PARALOID BPM-515 |
| PLA/EVA | 6.4 | 80:20 | Ethylene co-vinyl acetate | Lanxess Levamelt 500 |
| PLA/PHA | 7.5 | 90:10 | Polyhydroxyalkanoate | Metabolix Mirel P5001 |
| PLA/PCL | 9.3 | 70:30 | Polycaprolactone | Perstrop CAPA FB 100 |

## 2.2 Melt mixing and film manufacturing

Melt mixing of the components was carried out on a single-screw extruder (Wayne Machine & Die Co.) followed by pelletizing. The temperature profile used, from die to feed throat, was 390, 390, 380, 375, 375, 355, and 320 °F. Only for the PLA/EVA blend the profile was adjusted to 335, 335, 330, 310, 280, 250, and 120 °F.

Films were manufactured in a LabTech blown film laboratory line (390 to 360 °F). Blown film conditions (i.e., blow up ratio, rotational screw speed) was adjusted targeting a nominal thickness of 1.5 mils. All the materials were pre-dried before mixing and blown film process.

## 2.3 Testing

Tensile testing of all samples was performed on an Instron 4301, 43K1 tensile tester with 5 kN load cell and pneumatic grips. The initial gauge length was set to five inches and a crosshead speed of 0.5 inch/min was used according to ASTM D 882-02. Specimens were carefully selected and cut to 1" x 6" strips with the machine direction.

Tear resistance was determined according to ASTM D 1922 standard using an Elmendorf-type tester (200g pendulum). Test specimens in both machine direction and cross direction were cut to 2.5" x 3" with a template such that the direction of the tear would be parallel to the 2.5" side. A machine direction specimen is defined such that the direction of the tear is normal to the machine direction.

The potential of using PLA and PLA blends as heat seal layers was investigated by determining the heat seal strength (ASTM F88-06). Fin seals were produced on a Sencorp Bar Heat Sealer 24 AS/1 using temperatures ranging from 120 to 140 °C for 1 second.

Impact resistance of the films was measured according to ASTM D1709 method A on a TMI 43-26 Falling Dart Impact Tester. The drop height of the dart was modified from 26 to 2 inches because of the low impact resistance of the films.

PLA films are known for producing a loud noise upon manipulation, which is highly undesirable in certain packaging applications. 9.5 by 9.5 inch squares were cut from each sample for noise characterization. Four replicates of each sample were tested. Manual manipulation of the films was done in a recording studio at RIT

(reverberation time is about 0.3 sec at 500 Hz). Noise was recorded with a condenser microphone with cardioid directivity facing the sound source (AKG 414) at an approximate distance between the microphones and sound source of 40 cm. The noises were recorded to a digital audio workstation (Pro Tools HD) with sampling frequency of 48 kHz and 24 quantization bit. We chose a 3-seconds long segment having a relatively constant noise pattern from each recorded signal. Subsequently the edited segments were analyzed using Matlab for comparing various physical characteristics including the RMS value and the spectral energy ratio between high and low frequency.

## 3. Results and Discussion

Table 1 shows the modulus of elasticity, tensile strength, elongation at break and impact resistance of the samples. All the blends decreased the modulus of elasticity but only the changes produced by EVA and PCL were statistically significant. The results were anticipated because PLC and EVA are flexible and rubberlike (low modulus) imparting flexibility to the blends as the content increase. Similarly, a decrease in tensile strength was observed in the PLA/PCL blend.

**Table 2:** Tensile properties of PLA and PLA blends. Groups that have the same letters are not statistically significant ($p > 0.05$)

| | Tensile Strength (MPa) | Modulus of Elasticity (GPa) | Elongation at break | Average thickness (mil) | Dart drop impact (g) |
|---|---|---|---|---|---|
| PLA | 41.6±5.0A | 2.28±0.23A | 2.5-3.2% | 1.45 | 83 |
| PLA/AIM | 38.7±6.5A | 2.11±0.34AB | 3.1-6.4% | 1.52 | 204 |
| PLA/EVA | 37.3±3.3AB | 1.87±0.17BC | 3.0-12% | 1.52 | 175 |
| PLA/PHA | 42.3±3.7A | 2.17±0.12A | 3.1-5.2% | 1.58 | 100 |
| PLA/PCL | 32.3±4.4B | 1.76±0.17C | 4.5-20% | 1.89 | 111 |

None of the blends showed a significant increase in the elongation at break, which is usually an indicator of toughening. Ma and coworkers prepared PLA/EVA blends with the same composition and VA content and found a significant decrease in the tensile strength and a dramatic increase in the elongation at break (>300%) [8]. The thickness of the samples may have had an effect on the observed elongation when comparing the two studies. The cross section of Ma's samples was 2 x 0.8 mm compared to 25.4 x 0.03 mm in this study. The results in Table 2 suggest that the thickness of the samples could play an important role in determining the deformation mechanisms, since the films only had a moderate increase in elongation.

Dart drop test results show a 210% and a 245% increase in impact strength for the PLA/EVA and PLA/AIM samples respectively and a slight increase for PHA and PCL. The moderate increase in impact resistance in the PLA/PCL blends could be an indication of poor interaction between the PCL and PLA phases. Semba and coworkers found an improvement of 3.5 times in Izod impact strength when using peroxide as compatibilizer imparting the ductile nature of PCL to PLA [9].

Tear resistance measures the energy to propagate a crack in plastics films. Figure 2 shows the tear resistance of the samples. Only the AIM had a negative effect on the tear resistance while the other samples showed an improvement compared to neat PLA. PLA/EVA showed the highest improvement. This may be due to the EVA domains because as the crack propagates it encounters the more flexible EVA domains (see Figure 2). The elastomeric nature of the EVA can dissipate more energy, thus increasing the overall tear resistance.

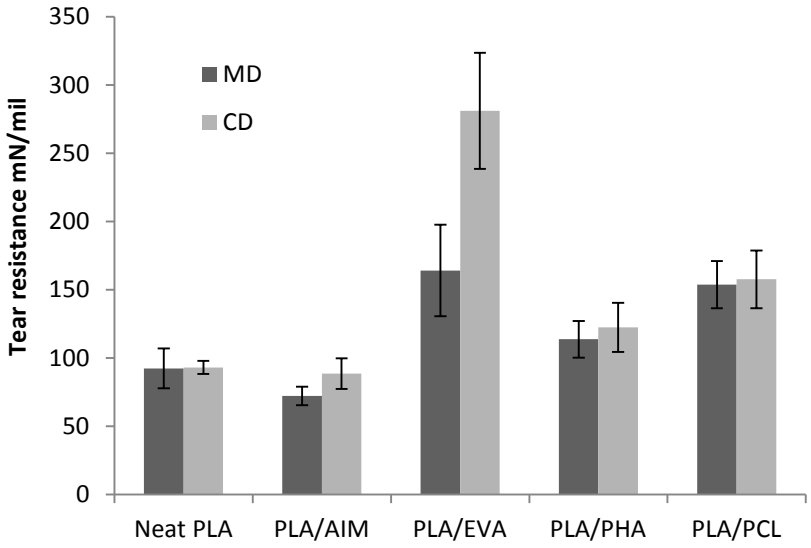



**Figure 1:** Tear resistance of film samples

Figure 2 is a transmission electron micrograph showing the morphology of the PLA/EVA blends. The lighter background is the PLA matrix and the dark spots are the EVA domains. The two-phase morphology and the particle size aided the rubber toughening of the material. The results agree with those of Ma and coworkers [8].

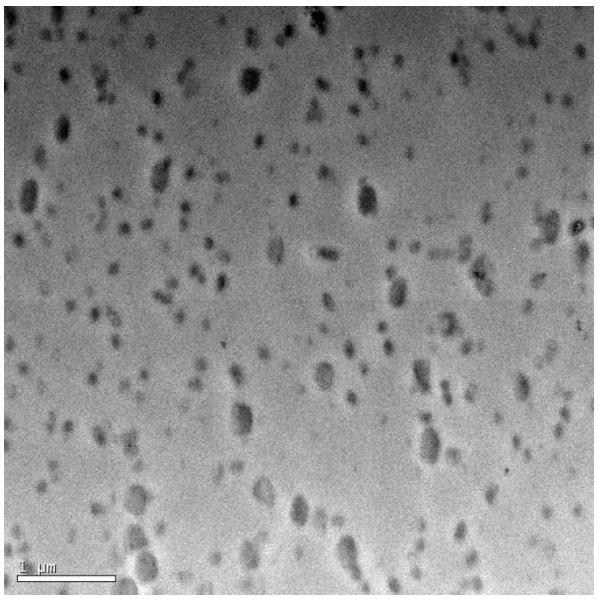


**Figure 2:** TEM micrograph of PLA/EVA

The heat sealing ability of the blends was investigated in the range of 120 to 140 °C. EVA showed a moderate increase in the heat seal strength while PHA and AIM showed a two-fold increase. In PVC formulations, acrylic impact modifiers can lower the melt temperature of the resin and increase fusion times [10]. A similar effect could have taken place when the additive was dispersed in the PLA matrix allowing the interface to melt during heat sealing resulting in higher seal strengths.

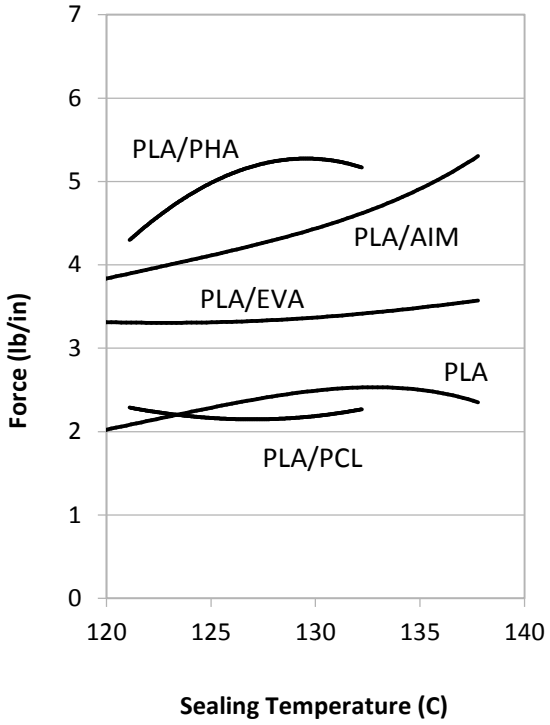



**Figure 3:** Heat Seal strength of PLA and PLA blends

In the case of the PLA/PHA blend, PHA disperses in small domains which remained amorphous at low concentrations [11] facilitating the softening of the material upon heat sealing. The observed increase in seal strength could also be an indication of less crystalline PLA in the blend compared to the films of neat PLA. Potential in using PHA as a dispersed phase to tailor the heat sealing properties of PLA exist.

Since the heat seal was studied in a fixed range, optimum heat seal temperatures of some of the blends may fall out of this range. This may be the case for the blend with EVA. Another interesting observation is that PLA/EVA and PLA/PCL created peelable seals whereas PLA formed fused seals. Therefore, blends with EVA and PLC could be used in packaging applications with easy-open peelable features which have a seal strength of 1 to 2.5 lb/in [12].

One issue that came to the surface upon commercialization of PLA was the noise produced from the manipulation of the films. Noise became a concern for PLA films since consumers complained how laud chip bags can be. Part of the reason has to do with the glass transition temperature of PLA which is just above room temperature. The sound has been described as "crispy and crunchy"[1]. In this study a quantitative analysis is proposed for the characterization of the sound.

Figure 4 and 5 show the physical characteristics of the noise produced by the films when manually crumpled in terms of RMS value and spectral RMS ratio, respectively. The RMS gives an average of the overall intensity of the sound, higher RMS value is known to have a high correlation with a perceptual loudness. Blends with EVA and PCL showed a significant decrease in the RMS value. The results suggest that the rubbery nature of the disperse phase had an attenuating effect in the noise produced by the films.

[1] Plastics News. The problem with PLA: chip bags that are really loud. Retrieved April 3 2014 from: http://www.plasticsnews.com/article/20100818/BLOG01/308189996/

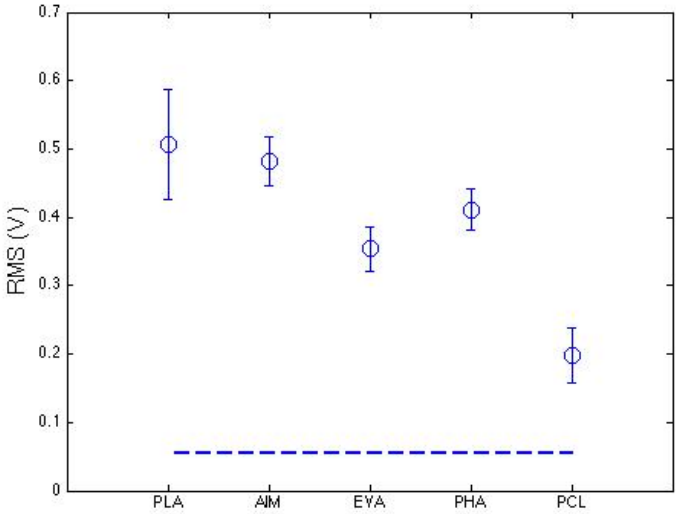



**Figure 4:** Measured RMS values of five tested films. The dashed line represents the RMS level of a reference LDPE bag.

The spectral RMS ratio relates the low frequency component compared with the high frequency component. The reference film (LDPE, dashed line in Figure 5), contain more low frequency components relative to high frequency. In the case of PLA and the blends, this parameter shows a low value indicating that the sound has more high frequency components relative to low frequency. High frequency noises are perceived as annoying, irritating and consequently loud.

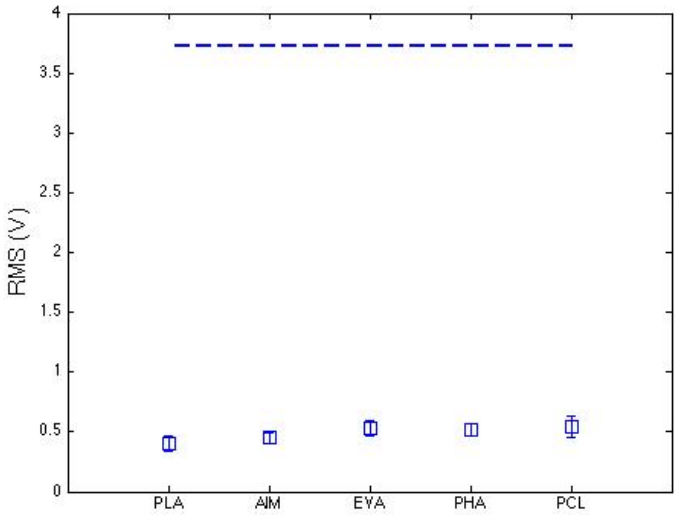



**Figure 5:** Measured spectral RMS ratio (between low and high frequency). The cutoff frequency was 1.5kHz. The dashed line represents the spectral RMS ratio of a reference LDPE bag, which implies that the LDPE contained more of low frequency components.

## 4 Conclusions

This study investigated film properties of PLA and PLA binary blends. Property improvement was observed for the different blends compared to neat PLA in terms of tear resistance, heat seal strength, impact resistance and noise level. However, selection of the best blend system is dependent on specific properties. For instance, the acrylic impact modifier (AIM) improved the impact resistance and heat seal strength but reduced the tear resistance.

PLA blended with EVA showed significant improvement in both tear and impact strength. PHA showed a marked effect in increasing the heat seal strength. Potential in using PHA as a dispersed phase to tailor the heat sealing properties of PLA exist. Significant noise reduction was achieved in films containing EVA and PCL.

It is interesting to see how some of the results obtained for the film differ from reported data for materials with similar compositions, as in the case of EVA. The results point out that the bulk properties usually measured in thick samples may not reflect the film performance.

The results show the potential of melt blending to improve the film properties of PLA. Further studies should focus on modeling and optimization of particular blend systems. For blends such as PLA/PCL, property improvement could be hindered by poor interaction among the components, thus a compatibilizer should be considered.

## References


1. TechNavio, "Global Bioplastics Market 2011-2015," 2012. [Online]. Available: http://www.technavio.com/report/global-bioplastics-market-2011-2015. [Accessed: 17-Mar-2014].
2. Plastics News, "World bioplastics demand (2005-15)," 2012. [Online]. Available: http://www.plasticsnews.com/article/20120203/FYI/302039972. [Accessed: 27-Mar-2014].
3. I. Armentano, N. Bitinis, E. Fortunati, S. Mattioli, N. Rescignano, R. Verdejo, M. A. Lopez-Manchado, and J. M. Kenny, "Multifunctional nanostructured PLA materials for packaging and tissue engineering," Prog. Polym. Sci., vol. 38, no. 10–11, pp. 1720–1747, Oct. 2013.
4. H. Liu and J. Zhang, "Research progress in toughening modification of poly(lactic acid)," J. Polym. Sci. Part B Polym. Phys., vol. 49, no. 15, pp. 1051–1083, Aug. 2011.
5. T. Mekonnen, P. Mussone, H. Khalil, and D. Bressler, "Progress in bio-based plastics and plasticizing modifications," J. Mater. Chem. A, vol. 1, no. 43, p. 13379, Oct. 2013.
6. M. Zhang and N. Thomas, "Blending polylactic acid with polyhydroxybutyrate: The effect on thermal, mechanical, and biodegradation properties," Adv. Polym. Technol., vol. 30, no. 2, pp. 67–79, 2011.
7. C. L. Simões, J. C. Viana, and A. M. Cunha, "Mechanical properties of poly(ε-caprolactone) and poly(lactic acid) blends," J. Appl. Polym. Sci., vol. 112, no. 1, pp. 345–352, Apr. 2009.
8. P. Ma, D. G. Hristova-Bogaerds, J. G. P. Goossens, A. B. Spoelstra, Y. Zhang, and P. J. Lemstra, "Toughening of poly(lactic acid) by ethylene-co-vinyl acetate copolymer with different vinyl acetate contents," Eur. Polym. J., vol. 48, no. 1, pp. 146–154, Jan. 2012.
9. T. Semba, K. Kitagawa, U. S. Ishiaku, M. Kotaki, and H. Hamada, "Effect of compounding procedure on mechanical properties and dispersed phase morphology of poly(lactic acid)/polycaprolactone blends containing peroxide," J. Appl. Polym. Sci., vol. 103, no. 2, pp. 1066–1074, Jan. 2007.
10. A. Abu Bakar, A. Hassan, and A. F. Mohd Yusof, "Study of processability of poly(vinyl chloride): Effects of acrylic and chlorinated polyethylene impact modifiers, oil palm empty fruit bunch fiber, and mixing temperature," J. Vinyl Addit. Technol., vol. 14, no. 4, pp. 204–210, Dec. 2008.
11. P. Ma, A. B. Spoelstra, P. Schmit, and P. J. Lemstra, "Toughening of poly (lactic acid) by poly (β-hydroxybutyrate-co-β-hydroxyvalerate) with high β-hydroxyvalerate content," Eur. Polym. J., vol. 49, no. 6, pp. 1523–1531, Jun. 2013.
12. J. Zhang, E. Manias, G. Polizos, J.-Y. Huh, A. Ophir, P. Songtipya, and M. del M. Jimenez-Gasco, "Tailored Polyethylene Nanocomposite Sealants: Broad-Range Peelable Heat-Seals Through Designed Filler/Polymer Interfaces," J. Adhes. Sci. Technol., vol. 23, no. 5, pp. 709–737, Jan. 2009.

# Trends and drivers influencing papermaking and its products towards the future

**Paul Krochak and Marco F.C. Lucisano***

*Innventia AB, Stockholm, Sweden*

**Corresponding author. Email: marco.lucisano@innventia.com*

**Abstract:** "Papermaking towards the future" is a project investigating the current state and future of global paper manufacture. The project is a critical investigation into the most important questions for the industry today and into the future. What changes can be observed and are currently taking place? What are the challenges at present, and how will they manifest themselves going forward? In which areas is the outlook most promising for the paper industry and how are we going to get there?

Through a combination of expert interviews, workshops, a Dephi survey with respondents in 21 different countries, a student survey, and months of our own research, we have identified what we believe are the most important drivers for global change and the most important growing trends in the paper and packaging industry going forward 20 years. Projecting the information collected throughout this project forward in time, we see a high likelihood that the paper and packaging industry will shift into one centred around bio-refining, where a broad range of forest based products will be produced to support a bio-based world. The future products creating the greatest return on investment will include bio-plastics, bio-chemicals, bio-energy, cellulose textiles, and paper-based packaging materials, where everything produced will be sustainably sourced and everything recycled. However, it is critical that the paper and packaging industry strategize today for this promising future of tomorrow, through investments in marketing, organization, and new product innovation. Moreover, it is important that the industry capitalize on their strong position within this potential bio-based world, by exploiting their fibre processing infrastructure, knowledge, and experience with producing sustainable and recycling products from the forest.

Keywords: paper, papermaking, trends, drivers, packaging materials.

## 1 Introduction

The paper industry is at a transformational point. This is an industry that has been synonymous with printing paper for over 200 years but is now shifting towards one aimed at packaging and bio-based products. "Paper" is becoming more about something that keeps our food safe, something that helps sell a product by creating an image or feeling. It is something with unique touch, looks, and feel. And it is something that is sustainable and recyclable.

Papermaking, like any industry, is part of a larger context. In order to better understand the most likely future developments for the industry it is important to understand this larger context in society. The key external forces such as global economy, people's values and behaviour, technology, demography and the environment are the factors that contribute to shaping the future of society and business, and drive global change. In recent years, associations and confederations connected to the forest-based sector have presented a number of initiatives aimed at discussing how the path towards the future might look like for the papermaking industry. As an example, CEPI, the Confederation of the European Paper Industry, recently presented its 2050 roadmap to a low-carbon bio-economy [1] and the outcome of an ambitious initiative to identify the most promising breakthrough technologies to cut the carbon footprint of pulp and papermaking [2]. Also in Europe, the European Technology Platform for the Forest-based Sector, revised its Strategic Research Agenda [3] and vision for 2030 [4]. Similar initiatives have been promoted by the American Forest & Paper Association in the U.S., by the Forest Products Association of Canada (FPAC) as well as by other major national and regional actors in the business.

In our background research we identified five drivers, which we believe to be essential for the development of the papermaking industry. These five drivers accompany the global drivers of change which we identified in an earlier report on the evolution of packaging towards 2020 [5]. Having searched specifically for drivers of development we chose to label them with names which underline the component of change: (i) from separate companies to ecosystems, (ii) from efficient production to life-cycle sustainability, (iii) from one world to regionalization, (iv) from static to smart, and (v) from western consumers to a global urban middle class.

From separate companies to ecosystems relates to the affiliations among companies, based entirely on close business relationships. The term 'business-ecosystem' has become popular in the business life since it was introduced in the early 1990's. Brundenburger and Nalebuff popularised the term 'co-petition', a situation which occurs when companies with common interests interact to achieve a higher value production compared to one created without cooperation [6]. Considering the potential for new cellulose-based products, the forest product industry is well positioned to develop its own ecosystems. Niche paper-based products, bio-based plastics and chemicals, processes driven by energy derived from biomass and material recycling business can all be notable contributors to an integrated business system.

From efficient production to life-cycle sustainability is a driver connected to the observation that process efficiency alone is no longer the mark of an environmentally conscious business. It is now essential to broaden the scope to consider the origin and extraction of raw materials, the manufacture of the product, the distribution, use, re-use and end of life. On top of this, the resilience of the entire production process and value chain is becoming as important as the process itself.

From one world to regionalisation points towards the balance between thinking globally and acting locally. The global trend towards nearshoring is getting more and more evident in most businesses. Indeed statistics from CEPI and FAO suggest that already today there is an almost perfect match between total production and total consumption of paper and board products, when the world is segmented in macro-regions [7, 8].

From static to smart is a result of the intersection of modern information and communication technology with the consumers' demand for interactivity, personalization and intelligent media. In the world of 2014, the largest part of all digital data collected daily still originates from humans, having intentionally typed, photographed, filmed, recorded, and scanned information. The development of the internet of things is expected to change this balance in a dramatic way and objects will leave digital footprints with no human intervention.

From western consumers to a global urban middle class relates to the effects of the economic progress in Asia, where masses of highly educated people are experiencing the effect of the growing Asian economy. Recent data from the World Economic Forum show that the United States still tops the GDP ranking at 19% of the world total. China's GDP accounts for 14%, which is far ahead of the rest of the region; India follows with 5.6% [8]. The UK, France, Germany and Japan, countries that once ruled the global markets, are today falling behind the BRIC and Next11 countries.

## 2 Methods

Understanding and analysing the trends and drivers which are shaping the future of the papermaking industry is a multidisciplinary exercise which requires a variety of methods, techniques and sources of information. Valuable input to the project has been gathered interacting with hundreds of people, whose field of activity and expertise is connected to the forest-based industry in its wider sense. In our study and for the purpose of this paper, we will refer to them as experts, with no further specification. This group includes scientists, applied researchers, business leaders and CEO's, research directors, papermakers, business analysts, investors, futurists, representatives from N.G.O.s, delegates at scientific and technical conferences, development teams from businesses which are dependent on the products of the paper industry, larger retailers and media houses. In a separate group of interviews, we surveyed 80 second year university students in science and technology from KTH (The Royal Institute of Technology, Stockholm, Sweden).

The process we followed comprised four methods of interaction: (i) one-on-one expert interviews, (ii) research and meta-analysis of published information and data, (iii) workshops and (iv) a Delphi-survey (Figure 1). All stages of this investigation were carried out between August 2013 and January 2014.

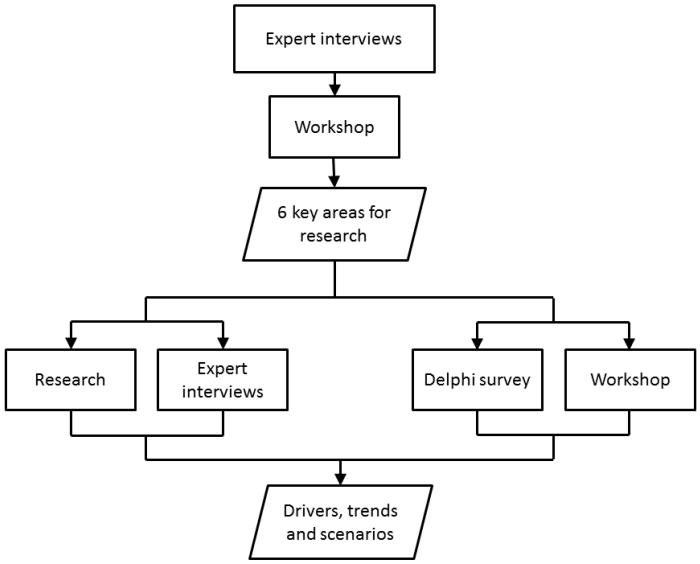



**Figure 1**: Workflow of the global outlook project "Papermaking towards the future".

The project started with a first round of one-on-one expert interviews with the purpose of identifying the themes, questions and uncertainties which are top-of-mind for the people who influence and are influenced by the papermaking industry. We identified six key areas for further research, on which our results and conclusions are based:

1. The ongoing evolution towards a bio-based economy and bio-based industry.
2. The product spectrum and performance of all commercially available materials associated with paper.
3. The processes of industrial papermaking and their foreseeable development, particularly as to resource efficiency.
4. Legislation and regulatory matters.
5. Business organization and value creation in industrial ecosystems.
6. Sustainability, its challenges and possibilities.

Having identified these six focus areas, we continued our expert interviews in parallel with research and meta-analysis of published information and data, including business news and recent strategic decisions of the most important stake-holders in the industry. The research materialized in five major drivers for global change and nine most significant growing trends influencing the pulp and paper business towards 2020 and beyond.

Having identified the key issues for the industry globally, the following step was to quantify the identified key questions and areas. We implemented the methodology known as a Delphi survey, i.e. a survey where the experts are involved in first identifying the questions and then answering them. The methodology, originally described by Linstone and Turoff [9] is used when trying to establish as objectively as possible a consensus on a complex problem, in circumstances where accurate information does not exist or is impossible to obtain. Here we implemented the Delphi method as an electronic survey, which was distributed on-line to 200 participants from 25 countries. The results are based on 140 answers from 21 countries, which corresponds to a response rate of 70%, which we considered as very satisfactory for the purpose of our investigation. On top of the technical questions, the survey included demographical questions aimed at investigating if the answers could be sorted and explained depending on the profession, geographical origin, experience or field of activity of the respondent. Since no such correlations could be identified among the results, we report data for all respondents who completed the survey in its entirety.

In order to interpret the results from the different modes of data acquisition, we organized two full-day workshops with 50 experts from the pulp and paper industry, invited to analyse, discuss and prioritize among the findings. We jointly discussed the historic development of society and the industry, prioritized the trends and elaborated on the potential disruptions and possible futures for the papermaking industry towards the future. The complete set of results of this investigation are presented as an Innventia Global Outlook Report [10].

## 3 Results and discussion

Our analysis of the key drivers and trends influencing the papermaking industry moving towards the future is based on the quantitative results of a Delphi survey, completed by 140 respondents from 21 countries. One crucial question which we focused on at the beginning of our study related to setting the time frame for our definition of the future. Therefore we asked the experts to evaluate the rate of development for twenty phenomena and trends which can be observed in society in connection to our six key areas of research. In each case experts where asked to decide at which point in time a statement can be expected to become true on a scale ranging from "It is already the case" through to "It will never be the case". Figure 2 exemplifies the answers for a subset of the survey questions. The study of the data showed that the large majority of experts consider that the industry will be substantially renewed within 20 years from the start of the project. Therefore we decided to set the timeframe of our investigation to extend to 2030.

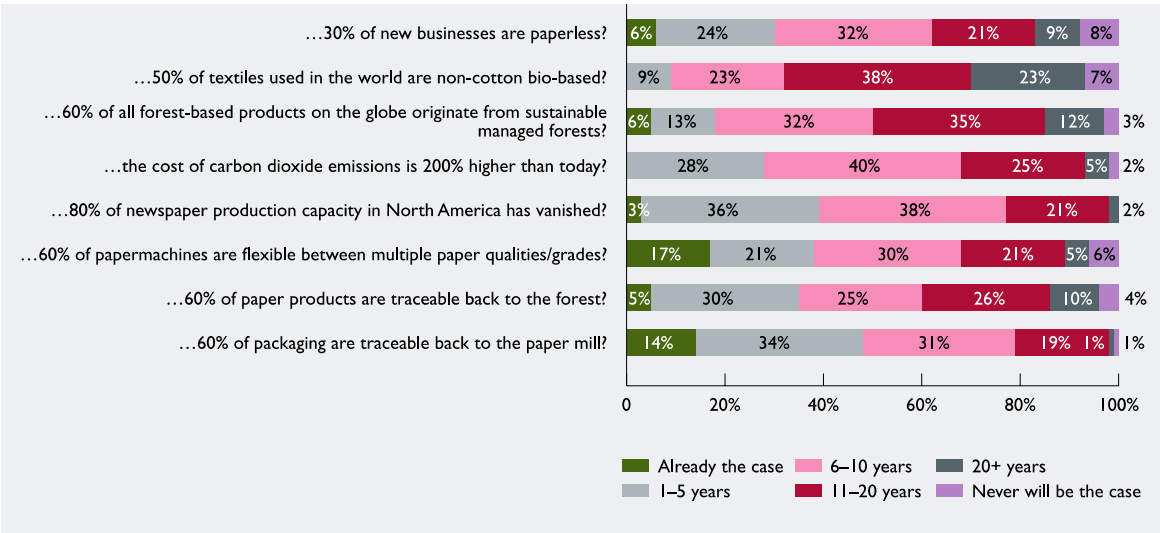



**Figure 2**: Selection of questions from the Delphi survey with focus on the rate of development for phenomena and trends connected to the evolution of papermaking and its products.

### 3.1 The evolution of market segments as a result of the declining demand of paper grades for printing and writing.

Newspaper production has served as the foundation on which the paper- and pulp industry was built, and its success enabled expansion into other areas for fibre-based materials including packaging materials. The past decade, however, has seen a dramatic reduction in demand for newspaper and traditional printing and writing grades, particularly in the western world. In our expert survey, 64% considered board and packaging materials to be the most important product segment for the industry over the coming ten years. In comparison, only 5% deemed printing and writing grades to be of significance, Figure 3.

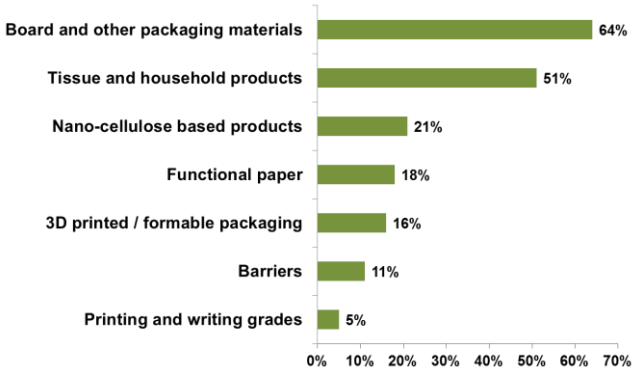



**Figure 3**: Delphi survey results to the questions 'Over the coming ten years, which of the following paper-based products will be of greatest importance to the pulp and paper industry?' Multiple answers were possible.

It is interesting to note that the experts, as a group, attributed much larger credibility to the importance of comparably traditional products, whereas all novel applications ranked lower. The group of alternatives which included nano-cellulose based products, papers with an engineered or designed functionality, 3D-printed materials and formable packaging materials and barrier solutions, was favoured only by 10 to 20% or respondents. This result can be interpreted as a contradiction with respect to the outcome of Figure 2, where the expert group appeared to be very confident in a future which is significantly different from the world of today.

As to the two dominant segments, board/packaging materials and tissue/household products, the opinions expressed by the experts follows the trends on the world market. For the European Union, Andersson [10] reports a decrease in newsprint consumption by 27% and of office paper by 19% as compared to the historical maximum points in the early 2000's. Statistics for the U.S. market are even more dramatic, with a 65% reduction in newsprint and 37% for office paper [11]. However, packaging materials are still showing steady growth. At present, 255 million tonnes of board and packaging grades are consumed each year, with processed foods accounting for the single largest market segment. Estimates by Smithers Pira suggest a steady annual increase by 4.5% in packaging consumption [12]. A growing population and heightened economic standard ensures an increasing demand on food packaging, where a net growth in production of 2.4% was observed for this market segment in 2012 [13]. Yet another driving force for the increase in demand for packaging materials is the increase in online trade. Worldwide product shipments call for high-quality secondary packaging, as well as sustainable solutions for environmental preservation [4]. An example of the outcome of this trend on the industrial scene is the acquisition of Boise Inc. by the Packaging Corporation of America (PCA) for which business analysts cited the possibility to strengthen the position in packaging for Internet-based sales as one main driver.

## 3.2 Diminishing Pool of Skilled Labour

The declining use of print paper grades has resulted in paper machine curtail and mill closures, with subsequent unemployment. Between the years 2000 and 2010, nearly 120 mills have closed in the United States, while over 400 mills have been closed in Europe in the last 20 years [14]. As an example of the effect this has had on employment, the Canadian forest sector, the world's largest exporter, has gone from 260 000 employees in 2003 to 150 000 in 2012 [15]. Therefore, as part of our expert survey, we asked which resource can be expected to be in short supply in the pulp and paper industry over the coming ten years. Here, 'skilled labour' ranked highest, see Figure 4. It is interesting to observe that this concern is not an issue for the paper industry alone. In a global CEO survey, pwc reports that 63% of CEO are concerned with the availability of skilled labour [16].

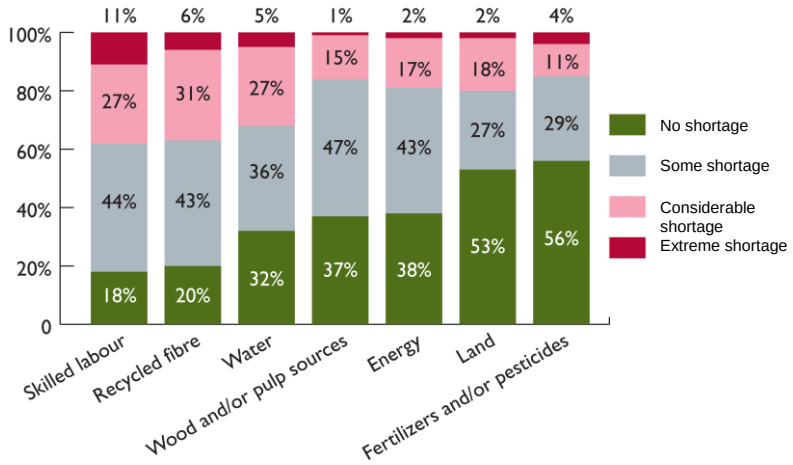



**Figure 4**: Delphi survey results to the questions 'Over the coming ten years, to what extent will the following resources be in short supply'.

## 3.3 Increasing interest for recycled fibre

A second interesting result of the expert survey questions aiming at identifying potential future shortage of supply, was the concerns related to the availability of recycled fibres, which reached the second place, Figure 4. We suggest that this answer shall be considered together corresponding data for virgin fibre sources, for which the expert group showed much lower concerns.

The subject of recycling and the availability of recycled fibres is an often discussed theme in Europe, presently the leading region in terms of recycling rate, followed by North America. In 2011, the European Recovered Paper Council (ERPC) published the 'European Declaration on Paper Recycling', an initiative to increase the recycling rate in Europe to 70% by 2015 [17]. The rationale for this specific target was the fact that, on average 19% of paper and board products are either not collectable (e.g. archive and library material) or recyclable (e.g. sanitary papers). This goal was achieved little more than one year later, as the European recycling rate reached 71.7% in 2012. In total, recycled paper amounted to just under 58 million tonnes, which is an 18 million or 45% increase since 1998 [17, 18]. The US paper industry made a similar effort in 2003 by setting a goal of a 55% recycling rate to be achieved by 2012 [19, 20]. Today, the demand for recycled fibre is in especially high demand in Asia, with China being the largest importer.

Yet another interesting result from the Delphi survey, which can be connected to recycling and recycled fibres, is the fact that recyclability ranked at the third place when experts were asked to express an opinion on the most attractive features of paper products over the next 10 years, Figure 5.

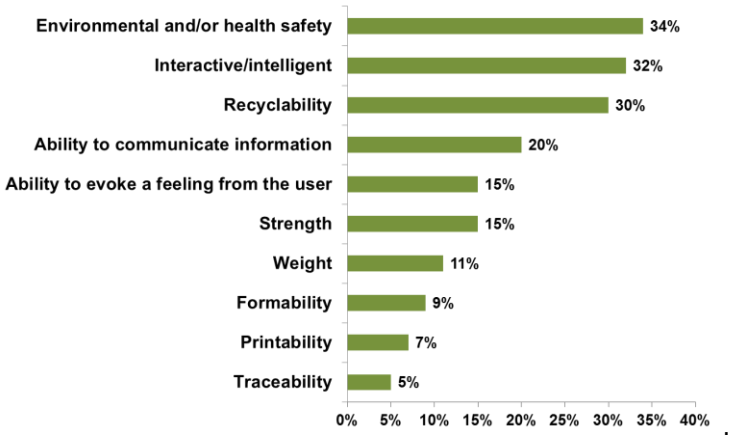



**Figure 5**: Delphi survey results to the questions 'Over the next ten years, what feature of paper-based products will be most desirable?' Multiple answers were possible.

## 3.4 Product safety as the most desirable feature of paper-based products

When looking at the future of the papermaking business from a technology-based perspective, it is interesting to evaluate which properties and features are attractive for tomorrow's use of fibre-based products. We asked the experts to rank the attractiveness of features ranging from the typical physical properties traditionally discussed by papermakers to sustainability and material identity. In our expert survey, 34% considered environmental and health safety to be the most important feature of paper products over the coming ten years, the highest-ranked feature of all, see Figure 5.

The importance of product safety among the feature of materials is not surprising and it can be related to the product safety directives and legislation regarding composition and handling of items in contact with food. No components of the packaging material should be hazardous to human health, and can have no effect on the contents, smell or taste of the associated food. Products that have proved dangerous to humans or the environment are banned, while the use of those that have not yet been confirmed as harmless is effectively limited. Among the recent cases which have attracted large interest both within the packaging and papermaking industry and the public at large, bisphenol A (BPA) and mineral oils in recycled fibres are two excellent examples of today's attention to safety issues. BPA has been identified as an endocrine disrupter, i.e. its capacity to alter the functions of the endocrine system can cause health effects not only for us, but also for yet unborn generations to come [21, 22]. In the case of mineral oils from printing inks, their presence in food packaging is presently being scrutinized by European heath authorities, as it is possibly associated with cancerogenous effects [23, 24].

## 3.5 Resource Efficient Processes

The production of paper and packaging is resource intensive and it requires large amounts of fibre raw material, energy, and water. Therefore we asked the experts to rank different approaches according to the greatest potential to reduce the resource demand of the production processes, Figure 6.

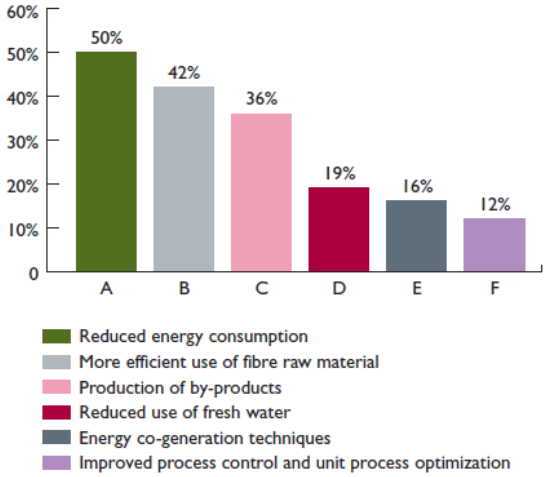



**Figure 6**: Delphi survey results to the questions 'Which of the following measures has the greatest potential to reduce the resource demands associated with paper production?' Multiple answers were possible.

The two options which ranked the highest were reduction of energy consumption and more efficient use of fibre raw materials, being selected by 50% and 42% of participants (multiple answers were possible). Indeed optimizing processes and products to save energy and minimise the use of raw materials is top-of-mind for the entire process industry. Form a technical and scientific point of view, this result is not surprising as it has recently been shown that production costs are proportional to the amount of fibre used [25]. This stems from the fact that water and energy are required to process and prepare fibres in suspension prior to usage, with pumping and processing equipment being driven by electric energy. The largest amount of energy is consumed by removing the water bound within the fibres. The most effective way to reduce energy and fresh water consumption is therefore to reduce the fibre content of the product, without deteriorating product quality. Moreover, a lower energy demand generally results in reduced greenhouse gas emission, while lighter-weight paper products contribute to reducing transport costs.

The total energy expenditures for production today account for 17% of the total papermaking costs [26]. During production, the dryer is the unit process consuming the greatest amount of energy. Efficient water removal reduces the load on the drying section and is therefore essential to decreasing energy consumption. It has been shown that as much as five times as much energy is needed to remove water in the dryer section compared with mechanical water removal in, e.g. the press section [27]. Thus, the energy benefits of removing as much water prior to the dryer section are self-evident. Other strategies could include advanced/improved dryer controls, optimizing pocket ventilation temperature and air flow within the dryer section, and the recovers of waste heat. The importance of energy efficient drying is understood to be so important that it has recently become the central focus of the recent CEPI 2-team projects – an initiative aimed at revolutionizing resource efficiency in the production of paper and board products through the development of new technologies [28].

### 3.6 Paper to pulp to bio-business

While demand for printing grades diminishes, pulp consumption has grown steadily over the past ten years [11]. With a diversified markets dominated largely by package materials, demands on high-quality raw pulp have increased. In many Asian countries and China in particular, paper and packaging production is still in an expansive phase. However, fibre resources are limited and imported pulp is essential for local production.

As part of our expert survey, we asked what application of cellulose has the potential to generate the most profit for the cellulose-based industry over the next 20 years. The results from this survey question are shown in Figure 7. It is interesting to observe that here, where the expert could choose one option only, respondents were evenly divided among the five alternatives: (i) novel paper and board products, (ii) biobased plastics, (iii) biobased chemicals, (iv) biobased energy and (v) biobased textiles. Indeed, exactly one fifth of the responds believed that the future potential for profit lies in new and innovative versions of the materials we today associate with the concepts of paper and board. Biobased products made from non-fossil biological material, e.g. wood and agriculture products, are currently receiving increased attention. The emergence of biobased materials is driven by two major factors: limited availability and increasing costs of fossil resources on one hand, and an increased awareness and focus on sustainability on the other. Material for bio-based textiles, plastics and chemicals can be efficiently produced in biorefineries.

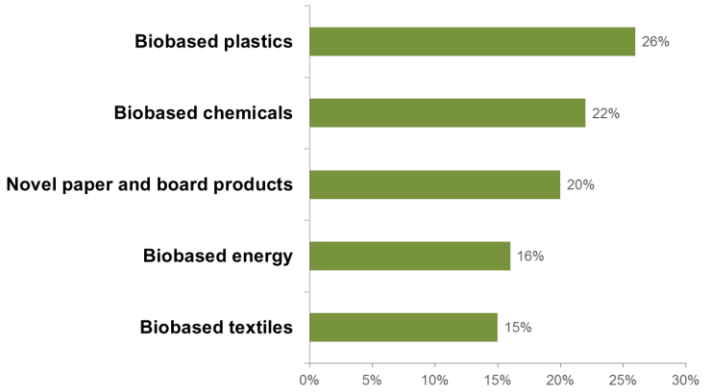



**Figure 7**: Expert survey results to the questions 'Over the coming 20 years, which of the following applications of cellulose has the potential to generate the most profit for the cellulose industry?'

This result from our expert survey should be seen in context of the global market situation for the bio-based economy. Forestry waste and cellulose constitute a huge potential source of biomass for chemical or plastic production. According to estimates, 20% of the chemical market will be bio-based by 2025, compared to a current 4 – 10% [29]. Bio-based plastic production is also increasing, rising from 0.25 million tonnes in 2009 to 1.16 million in 2011. By 2016, global production capacity of bio-based plastics is estimated to have reached 5.8 million tonnes [30].

Global energy consumption is increasing steadily and reached 540 EJ in 2010. Bio-based energy accounted for 12% of total consumption [31]. Wood-based fuels are sustainable alternatives to fossil fuels and provides increased savings over time. By 2020, the EU intends for 20% of all energy produced to be derived from renewable materials. The world's highest consumption for year 2050 has been predicted to 1040 EJ [31]. Depending on the set of assumptions, the total bioenergy production potential is estimated to reach levels in excess of 1500 EJ, thereby far surpassing total global energy demands. As biomass can be extracted from surplus forest growth and forestry residues, this represents a vast potential market for the forest industry.

Textiles constitute yet another area which can be expected to be a key component of tomorrow's bio-based economy. Between 1992 and 2010, global textile consumption increased from 39 to 70 million tonnes, and is predicted to continue to grow by 4% annually [32]. In 2010, non-cotton cellulosic fibres accounted for 5%, or 3.5 million tonnes. With a 7% increase over the recent years, cellulosic-based fibre production has the fastest growth rate of all textile fibres; in comparison, production of synthetic fibre increased by 5% and cotton by 2%, respectively. Today, cotton production accounts for almost 40% of all textiles. From an environmental perspective, however, cultivation of cotton is an unsustainable process. As much as 29 000 litres of water may be required to produce 1 kg cotton [33]. Due to freshwater shortage, non-cotton alternatives are much sought after. In a possible future scenario with restrictions on cotton in effect, wood-derived cellulosic fibres and dissolving pulp would have a large growth potential on the textile market.

## 4 Conclusions

The paper/paper-packaging industry is at a transformational point. This is an industry that has been synonymous with printing paper for over 200 years but is now shifting towards one aimed at packaging and bio-based products. "Paper" is becoming more about something that keeps our food safe, something that helps sell a product by creating an image or feeling. It is something with unique touch, looks, and feel. And it is something that is sustainable and recyclable.

Technological developments in recent years have resulted in a number of novel product solutions that are now becoming a reality. Barriers made from nano-cellulose are being exploited for use in food packaging, while interactive packaging can be used to monitor shelf life and freshness of food products, or to display information on quality and safety precautions relating to their contents. Paper-based packaging equipped with sensory technology can react to different stimuli, for example decaying food, moisture, or temperature, and can even be used as interactive displays.

We are also witnessing changes in company strategy, where innovation in industrial organisation and business practices, whether internal or external, are becoming increasingly important. An example of this is the linking of several stakeholders with similar or compatible expertise, allowing suppliers of equipment and chemicals,

producers of raw materials and end products, as well as distributors and support areas to work closely together to meet the new challenges. In addition, companies with otherwise unrelated products are combining to add value to existing products by expanding the range of product functionality, as in the case of electronic applications for packaging.

And perhaps most exciting, is that we are seeing a shift in industrial thinking towards consumer demand driven innovation. Here we see the industry is conceptualizing and developing new and unique paper and packaging solutions – by themselves – and selling them directly to the consumers and brand owners, positioning themselves at the top of the value chain and creating increased profits. This once traditional industry is now learning to take and manage risk more effectively, expanding on existing market segments and even creating new ones.

Through a combination of expert interviews, workshops, a Dephi survey, a student survey, and months of our own research, we have identified what we believe are the most important drivers for global change and the most important growing trends in the paper and packaging industry going forward 20 years. Projecting the information collected throughout this project forward in time, we see a high likelihood that the paper and packaging industry will shift into one centred around bio-refining, where a broad range of forest based products will be produced to support a bio-based world. The future products creating the greatest return on investment will include bio-plastics, bio-chemicals, bio-energy, cellulose textiles, and paper-based packaging materials, where everything produced will be sustainably sourced and everything recycled. However, it is critical that the paper and packaging industry strategize today for this promising future of tomorrow, through investments in marketing, organization, and new product innovation. Moreover, it is important that the industry capitalize on their strong position within this potential bio-based world, by exploiting their fibre processing infrastructure, knowledge, and experience with producing sustainable and recycling products from the forest. Otherwise, the industry's role in creating this bio-economy may be far less significant than we hope.

## Acknowledgements

RISE Research Institutes of Sweden is gratefully acknowledged for financing this study.

## References

1. CEPI, 2011, The Forest Fibre Industry 2050 Roadmap to a low-carbon bio-economy, CEPI.
2. CEPI, 2013, Unfold the future, Two-Team project, CEPI.
3. FTP, 2013, Strategic Research and Innovation Agenda, Forest-based Sector Technology Platform.
4. FTP, 2013, Horizons – Vision 2030 for the European forest-based sector, Forest-based Sector Technology Platform.
5. Innventia, 2013, Packaging 2020, Innventia Global Outlook Report, Innventia.
6. A.M. Brandenburger and B.J. Nalebuff, 1997, Co-opetition, Currency Doubleday.
7. FAO, 2012, Yearbook of Forest Products 2010, Food and Agriculture Organization of the United Nations.
8. K. Schwab, 2012, The global competitiveness report 2012-2013, Full data edition, World Economic Forum.
9. H.A. Linstone, and M. Turoff (eds.), 1975, The Delphi method: techniques and applications, Addison Wesley.
10. Innventia, 2014, Papermaking towards the future, Innventia Global Outlook Report, Innventia.
11. S. Anderson, 2013, Paper markets in transformation', Nordea Report.
12. Smithers Pira, 2011, The future of global markets for corrugated board packaging to 2017, Smithers Pira.
13. Skogsindustrierna, 2012, Skogsindustrinen faktasamling - 2012 års branschstatistik, Skogsindustrierna (In Swedish).
14. N.A. Basbanes, 2013, On paper, The everything of its two-thousand-year history, Knopf.
15. Forest Products Association of Canada, 2011, Renewing Canada's greenest workforce – A labour market intelligence report.
16. P.K. Cheah, A. Lang, S. Snowden and S. Watts (eds.), 2013, Fit for the future – Capitalising on global trends, 17th Annual Global CEO Survey, pwc.
17. European Recovered Paper Council, 2011, European declaration on paper recycling 2011 – 2015.

18. European Recovered Paper Council, 2013, Paper recycling, Monitoring report.

19. S. Bratkovich, J. Bowyer, K. Fernholz and J. Howe, 2008, Paper recycling in the United States of America and beyond: an update, Dovetail Partners.

20. AF&PA, 2012, Sustainability report, American Forest & Paper Association.

21. L.N. Vandenberg, M.V. Maffini, C. Sonnenschein, B.S. Rubin and A. M. Soto, 2009, Bisphenol-A and the great divide: A review of controversies in the field of endocrine disruption, Endocrine Reviews, Vol 30, No. 1, pp. 75 – 95.

22. EFSA, 2006, Opinion of the scientific panel on food additives, flavourings, processing aids and materials in contact with food on a request from the Commission related to 2,2-BIS(4-HYDROXYPHENYL)PROPANE (Bisphenol A), Question number EFSA-Q-2005-100, EFSA Journal, Vol. 428.

23. M. Biedermann and K. Grob, 2009, Is recycled newspaper suitable for food contact materials? Technical grade mineral oils from printing inks, Eur Food Res Technol, vol. 230, pp. 785–796.

24. ESFA panel on contaminants in the food chain (CONTAM), 2013, Scientific opinion on mineral oil hydrocarbons in food, ESFA.

25. C. Ottestam, 2009, ECOTARGET – New and innovative processes for radical changes in the European pulp and paper industry, Final Activity report, NMP2-CT-2004-500345, STFI-Packforsk.

26. CEPI, 2013, European paper industry – Advancing the bioeconomy, Sustainability report, CEPI.

27. K.J. Kramer, E. Masanet, T. Xu, and E. Worrell, 2009, An ENERGY STAR® guide for energy and plant managers, Contract No. DEAC02-05CH11231, U.S. Department of Energy.

28. CEPI, 2013, Key statistics 2012 – European pulp and paper industry, CEPI.

29. Bio, 2010, Biobased chemicals and products, A driver of U.S. economic development and green jobs, Biotechnology Industry Organization.

30. European Bioplastics, 2013, Bioplastics – Facts and figures, European Bioplastics.

31. S. Ladanai and J. Vinterbäck, 2009, Global potential of sustainable biomass for energy, Report 013, Swedish University of Agricultural Sciences, Department of Energy and Technology.

32. FAO, 2013, World apparel fiber consumption survey, FAO/ICAC.

33. WWF, 2005, Bomull – en ren naturprodukt?, WWF (In Swedish).

# Author Index


Abinader, G., 628
Achtioui, T., 625
Ahmedov, A., 53
Ainalis, D., 109
Alcaraz-Llorca, J., 213
Allermann, H., 476
Almenar, E., 80
Antvorskov, H., 347
Aucejo Romero, S., 506, 545

Babader, A., 321
Bae, M., 368
Balaguer, M.P., 80
Baptista, C., 249
Bardenstein, A., 258, 358, 455, 476
Batt, G., 110
Behe, B., 368
Bell, A., 512
Beltran Sanahuja, A., 545
Bernardo, A.P.S., 467
Bethke, J., 573
Bigger, S., 60, 72, 603
Bix, L., 322
Boonnattakorn, R., 3
Boonsupthip, W., 88, 533, 539
Brockhurst, M., 153
Brockhurst, R., 153
Bronlund, J., 323
Buddeejeen, J., 335
Burgess, G., 322
Bush, R., 284
Bush, T., 322
Bócoli, P.F.J., 467

Calvo Vilanova, T., 506, 545
Candore, J-C., 203, 237, 243
Chalier, P., 80
Chen, X., 687
Cheng, J., 411
Chevis, J., 512
Chinsirikul, W., 524, 640, 648
Chonhenchob, V., 3, 144, 145, 524, 648
Church, E., 112
Cinelli, P., 358
Clune, S., 709
Cooksey, K., 0, 424
Copinet, A., 237, 243, 404, 628
Cran, M., 60, 72, 603
Crossin, E., 709

Dantas, F.B.H., 467
Dantas, S., 467, 591
Daqaq, M., 110
Daud, W., 524, 640
de la Fuente, J., 322
Delloque, P., 237, 243
Diaz, C., 721
Dongmei, W., 0
Drousch, B., 573
Dunwoody, G., 358
Dwivedee, S., 677

Eriksson, D., 172
Erre, D., 203, 237, 243, 404, 625, 628

Fayolle, B., 65
Feng, Q., 447
Floderer, V., 404
Foltynowicz, Z., 40, 295
Fuangfu, K., 380

Gao, S., 446
Garcia, A., 65
Garcia-Romeu, M., 213
Gatti, J.B., 591
Gavara, R., 60, 80
Ge, C., 30, 153, 231
Geburtig, A., 556
Gibert, J., 110
Goedecke, T., 556, 573
Gontard, N., 80
Goodwin, D., 231
Graefe, C., 213
Grimaldi, A.S., 153
Gruber, A.J., 112
Gu, X., 661
Guangjun, H., 167
GuardeÑo, L., 545
Guo, H., 263
Gwiazdowska, D., 295
Gällstedt, M., 586

Han, T., 30
Hararak, B., 648
Harries, L., 512
Hedenqvist, M., 586
Hernández-Muñoz, P., 60, 80
Herranz Solana, N., 506
Higashiyama, A., 183
Hishinuma, K., 309, 572
Holck, A.L., 4
Honda, S., 490
Hongge, G., 0
Hortal, M., 545
Horvath, L., 284
Hu, C-Y., 446, 574
Hu, C., 411
Hu, Y., 661
Huart, V., 203, 237, 243
Huddleston, P.T., 368
Hurley, R., 0, 424
Hwang, S.W., 615

Ishikawa, Y., 195
Iyer, P., 677

Jahnke, W., 573
Jiang, H., 687
Jiang, Y., 687
Johansson, E., 586
Johansson, T., 586
Jokinen, S., 388

Kaikkonen, O., 0
Kamaruddin, S., 53
Kausch, T., 231
Kengpol, A., 335
Kerddonfag, N., 524, 648
Khankaew, S., 88
Kihlstedt, A., 396
Kim, S., 721
Kisch, R., 496
Kitazawa, H., 195
Kittipinyovath, P., 380, 667
Knochenmuss, D., 118
Kones, K., 321
Korhonen, V., 388
Korin, C., 172
Kozak, W., 40
Krajka, N., 203, 243
Kraume, M., 573
Krochak, P., 728
Kubota, K., 0, 0, 301
Kumar Nadar, S., 153
Kumsang, P., 648
Kurniawan, M.P., 144

Lacoste, C., 625, 628
Lamb, M., 111, 631
Le Baillif, M., 625, 628
Li, G., 555
Liao, Q., 263
Liewchirakorn, P., 640
Lim, T.C., 165
Lin, Q-B., 425, 434
Lindberg, S., 396
Lindström, A., 396
Liu, Y., 561, 561
Lockrey, S., 709
Lorente Gómez, I., 506
Louvier, D., 14
Lu, B., 271
Lu, L-X., 0, 30, 165
Luangsa-Ard, N., 0, 609
Lucisano, M., 728

Mahović Poljaček, S., 651
Makino, Y., 490
Maltais, A., 23
Martine, E., 14
Martinez Hermosilla, G.A., 323
Medina, J., 65
Mesic, B., 323
Milverton, J., 631
Milčić, D., 651
Mingvanish, W., 98
Mizoguchi, M., 0
Mizoguti, M., 0
Moen, M.H., 4
Mohd Adzahan, N., 53
Mohd Nor, M.Z., 53
Morson, K., 512
Murata, M., 0, 0, 49, 301
Muriel-Galet, V., 60

Nakao, S., 490
Nandhivajrin, C., 88, 533, 539
Narktubtim, R., 0
Newson, W.R., 586
Noguchi, K., 490
Nolot, J-B., 203, 237, 243, 404
Nopwinyuwong, A., 533, 539

Odof, S., 203, 237, 243
Oshita, S., 490
Ostergaard, S., 258, 347, 455, 696, 704
Othman, Z., 53

Pan, X., 561
Pao, H., 721
Park, D.H., 615
Park, J., 284
Park, T.Y., 615
Parker, A., 111
Payubnop, W., 524, 640
Pechyen, C., 88, 533, 539
Pedersen, M., 258
Pellot, J., 203, 237
Pettersen, M.K., 4
Piao, M., 183
Pollonio, M.A.R., 467
Pousette, S., 396

Qian, J., 447

Rasel, H., 586
Ren, J., 321
Renke, N., 43
Rio, M., 709
Rodewald, D., 295
Rohmer, S., 404
Rojsatean, J., 524
Rouillard, V., 109, 555, 631
Rukchon, C., 533

Sadamoto, K., 0, 0, 49, 301
Sadamoto, T., 0, 301
Sage, L., 368
Saha, K., 145, 166, 249
Saito, K., 183, 195
Santos, J.L.C., 591
Santos, W.R., 591
Sayampol, J., 667
Schlick-Hasper, E., 573
Sek, M., 109, 555
Servé, J., 696
Shamsudin, R., 53
Shejwalkar, S., 677
Shim, J.K., 615
Siddiq, M., 3
Singh, J., 145, 166, 249, 496
Singh, S.P., 3, 144, 145
Singh, S.V., 258, 476, 696, 704
Sinjarernpokai, P., 667
Siripatrawan, U., 485
Sittipod, S., 144
Snyder, E., 0
Sorheim, O., 4
Sripethdee, C., 524
Su, Y., 687
Sudasna, V., 380
Sukhato, D., 667
Sun, G-H., 165
Suppakul, P., 88, 533, 539
Suwannawatanamatee, K., 98

Takahashi, A., 183
Takamori, H., 49
Takeda, M., 0, 301
Tang, Y., 30
Tanprasert, K., 98
Tawakkal, I.S.M.A., 72, 603
Thackston, E., 424
Thuvander, F., 172
Tomašegović, T., 651
Tonkin, C., 0, 424
Twede, D., 257

Verdu, J., 65
Verghese, K., 709
Vitchayakitti, W., 485

Wachtendorf, V., 556
Walton, K., 512
Wang, D., 263
Wang, J., 0, 165
Wang, N., 411
Wang, Z-W., 0, 132, 411, 425, 434, 446, 574
Westblade, N., 512
Wikstrom, F., 709
Williams, H., 709
Winotapun, C., 524, 640, 648
Wiwatchaimanee, K., 609
Wu, J., 411
Wu, Y-M., 411, 446

Xiaohong, G., 0
Xu, W., 271

Yamwong, T., 648
Yiangkamolsing, C., 98, 309
Yildirim, S., 43
Yong, X., 167
Yoxall, A., 512
Yu, W-X., 574
Yun, I.S., 615

Zabaleta, J., 80
Zhang, Y-B., 132
Zhao, Y., 271
Zheng, G., 447
Zhong, Y., 661
Zitouni, M., 23